

**NOT MEASUREMENT
SENSITIVE**

MIL-HDBK-17-3F
Volume 3 of 5
17 JUNE 2002

Superseding
MIL-HDBK-17-3E
23 JANUARY 1997

**DEPARTMENT OF DEFENSE
HANDBOOK**

COMPOSITE MATERIALS HANDBOOK

**VOLUME 3. POLYMER MATRIX COMPOSITES
MATERIALS USAGE, DESIGN, AND ANALYSIS**



This handbook is for guidance only. Do not cite this document as a requirement.

AMSC N/A

AREA CMPS

DISTRIBUTION STATEMENT A. Approved for public release; distribution unlimited.

FOREWORD

1. This Composite Materials Handbook Series, MIL-HDBK-17, are approved for use by all Departments and Agencies of the Department of Defense.
2. This handbook is for guidance only. This handbook cannot be cited as a requirement. If it is, the contractor does not have to comply. This mandate is a DoD requirement only; it is not applicable to the Federal Aviation Administration (FAA) or other government agencies.
3. Every effort has been made to reflect the latest information on polymer (organic), metal, and ceramic composites. The handbook is continually reviewed and revised to ensure its completeness and currentness. Documentation for the secretariat should be directed to: Materials Sciences Corporation, MIL-HDBK-17 Secretariat, 500 Office Center Drive, Suite 250, Fort Washington, PA 19034.
4. MIL-HDBK-17 provides guidelines and material properties for polymer (organic), metal, and ceramic matrix composite materials. The first three volumes of this handbook currently focus on, but are not limited to, polymeric composites intended for aircraft and aerospace vehicles. Metal matrix composites (MMC) and ceramic matrix composites (CMC), including carbon-carbon composites (C-C) are covered in Volume 4 and Volume 5, respectively.
5. This standardization handbook has been developed and is being maintained as a joint effort of the Department of Defense and the Federal Aviation Administration.
6. The information contained in this handbook was obtained from materials producers, industry, reports on Government sponsored research, the open literature, and by contact with research laboratories and those who participate in the MIL-HDBK-17 coordination activity.
7. All information and data contained in this handbook have been coordinated with industry and the U.S. Army, Navy, Air Force, NASA, and Federal Aviation Administration prior to publication.
8. Copies of this document and revisions thereto may be obtained from the Document Automation and Production Service (DAPS), Bldg. 4D (DODSSP/ASSIST), 700 Robbins Avenue, Philadelphia, PA 19111-5094.
9. Beneficial comments (recommendations, additions, deletions) and any pertinent data which may be of use in improving this document should be addressed to: U.S. Army Research Laboratory, Weapons and Materials Research Directorate, Attn: AMSRL-WM-MA, Aberdeen Proving Ground, MD 21005-5069, by using the Standardization Document Improvement Proposal (DD Form 1426) appearing at the end of this document or by letter.

CONTENTS

Foreword	ii
----------------	----

Summary of Changes	xvii
--------------------------	------

CHAPTER 1 GENERAL INFORMATION 1

1.1 INTRODUCTION.....	1
1.2 PURPOSE, SCOPE, AND ORGANIZATION OF VOLUME 3.....	1
1.3 SYMBOLS, ABBREVIATIONS, AND SYSTEMS OF UNITS.....	2
1.3.1 Symbols and abbreviations.....	2
1.3.1.1 Constituent properties.....	7
1.3.1.2 Laminae and laminates	8
1.3.1.3 Subscripts	9
1.3.1.4 Superscripts	10
1.3.1.5 Acronyms.....	10
1.3.2 System of units	12
1.4 DEFINITIONS.....	13

CHAPTER 2 MATERIALS AND PROCESSES - THE EFFECTS OF VARIABILITY ON COMPOSITE PROPERTIES 1

2.1 INTRODUCTION.....	1
2.2 PURPOSE.....	1
2.3 SCOPE	1
2.4 CONSTITUENT MATERIALS	1
2.4.1 Fibers	1
2.4.1.1 Carbon and graphite fibers	1
2.4.1.1.1 Carbon vs. graphite.....	2
2.4.1.1.2 General material description	4
2.4.1.1.3 Processing	4
2.4.1.1.4 Typical properties.....	6
2.4.1.2 Aramid	6
2.4.1.3 Glass.....	8
2.4.1.3.1 Chemical description.....	8
2.4.1.3.2 Physical forms available	9
2.4.1.3.3 Advantages and disadvantages.....	12
2.4.1.3.4 Common manufacture methods and variable.....	14
2.4.1.4 Boron	15
2.4.1.5 Alumina.....	17
2.4.1.6 Silicon carbide	19
2.4.1.7 Quartz.....	21
2.4.1.8 Ultrahigh molecular weight polyethylene.....	26
2.4.2 Resins	29
2.4.2.1 Overview.....	29
2.4.2.2 Epoxy.....	30
2.4.2.3 Polyester (thermosetting)	30
2.4.2.4 Phenolic	30
2.4.2.4.1 Resoles	31
2.4.2.4.2 Novolacs	31
2.4.2.5 Bismaleimide	31
2.4.2.6 Polyimides	32
2.4.2.7 Thermoplastic materials	32

Volume 3, Foreword / Table of Contents

2.4.2.7.1	Semi-crystalline	32
2.4.2.7.2	Amorphous	34
2.4.2.8	Specialty and emerging resin systems	36
2.4.2.8.1	Silicone	36
2.5	PROCESSING OF PRODUCT FORMS	36
2.5.1	Fabrics and preforms	36
2.5.1.1	Woven fabrics	36
2.5.1.1.1	Conventional woven fabrics	36
2.5.1.1.2	Stitched or knitted fabrics	38
2.5.1.1.3	Specialty fabrics	38
2.5.2	Preimpregnated forms	38
2.5.2.1	Prepreg roving	38
2.5.2.2	Prepreg tape	38
2.5.2.2.1	Conventional unidirectional tapes	38
2.5.2.2.2	Two-step unidirectional tapes	39
2.5.2.2.3	Supported unidirectional tapes	39
2.5.2.2.4	Coated unidirectional tapes	39
2.5.2.2.5	Preplied unidirectional tapes	39
2.5.2.3	Prepreg fabric	39
2.5.2.4	Preconsolidated thermoplastic sheet	39
2.6	SHIPPING AND STORAGE PROCESSES	40
2.6.1	Packaging	40
2.6.2	Shipping	40
2.6.3	Unpackaging and storage	40
2.7	CONSTRUCTION PROCESSES	40
2.7.1	Hand lay-up	40
2.7.2	Automated tape placement/automated tape lamination	41
2.7.2.1	Background	41
2.7.2.2	Benefits/capabilities	41
2.7.2.3	Sources of variability	41
2.7.3	Automated tow placement/fiber placement	42
2.7.3.1	Background	42
2.7.3.2	Fiber placement process flow	43
2.7.3.3	Benefits/capabilities	43
2.7.3.4	Material product forms	44
2.7.3.5	Special considerations	45
2.7.4	Braiding	47
2.7.5	Filament winding	48
2.7.6	Pultrusion	49
2.7.7	Sandwich construction	49
2.7.8	Adhesive bonding	50
2.7.9	Prebond moisture	52
2.8	CURE AND CONSOLIDATION PROCESSES	52
2.8.1	Vacuum bag molding	52
2.8.2	Oven cure	53
2.8.3	Autoclave curing processing	53
2.8.3.1	General description	53
2.8.3.2	Sources of variability	54
2.8.4	Press molding	54
2.8.5	Integrally heated tooling	54
2.8.6	Pultrusion die cure and consolidation	55
2.8.7	Resin transfer molding (RTM)	55
2.8.8	Thermoforming	58
2.9	ASSEMBLY PROCESSES	58
2.10	PROCESS CONTROL	59
2.10.1	Common process control schemes	59

2.10.1.1	Empirical methods	59
2.10.1.2	Active sensor-based control	59
2.10.1.3	Passive model-based control	59
2.10.2	Example - autoclave cure of a thermoset composite	59
2.10.2.1	Degree of cure	60
2.10.2.2	Viscosity	60
2.10.2.3	Resin pressure	62
2.10.2.4	Void prevention	63
2.10.2.5	Flow	63
2.11	PREPARING MATERIAL AND PROCESSING SPECIFICATIONS	64
2.11.1	Types of specifications	64
2.11.1.1	Material specifications	64
2.11.1.2	Process specs - controls end product	64
2.11.2	Format for specifications	64
2.11.2.1	Scope	64
2.11.2.2	Applicable documents	64
2.11.2.3	Technical requirements/process controls	65
2.11.2.4	Receiving inspection and qualification testing	65
2.11.2.5	Delivery	65
2.11.2.6	Notes	65
2.11.2.7	Approved sources and other	65
2.11.3	Specification examples	66
2.11.3.1	Industry	66
2.11.3.2	Military	66
2.11.4	Configuration management	66
CHAPTER 3	QUALITY CONTROL OF PRODUCTION MATERIALS AND PROCESSES	1
3.1	INTRODUCTION	1
3.2	MATERIAL PROCUREMENT QUALITY ASSURANCE PROCEDURES	1
3.2.1	Specifications and documentation	1
3.2.2	Receiving inspection	1
3.3	PART FABRICATION VERIFICATION	2
3.3.1	Process verification	2
3.3.2	Nondestructive inspection	5
3.3.3	Destructive tests	6
3.3.3.1	Background	6
3.3.3.2	Usage	6
3.3.3.3	Destructive test approaches	7
3.3.3.4	Implementation guidelines	7
3.3.3.5	Test types	8
3.4	STATISTICAL PROCESS CONTROL	8
3.4.1	Introduction	8
3.4.2	Quality tools	8
3.4.3	Gathering and plotting data	8
3.4.4	Control charts	8
3.4.5	Process capability	9
3.4.6	Troubleshooting and improvement	9
3.4.6.1	Process feedback adjustment	9
3.4.6.2	Design of experiments	11
3.4.6.3	Taguchi	20
3.4.7	Lot acceptance	20
3.5	MANAGING CHANGE IN MATERIALS AND PROCESSES	20
3.5.1	Introduction	20
3.5.2	Qualification of new materials or processes	20
3.5.2.1	Problem statement	20

3.5.2.2	Business case.....	22
3.5.2.3	Divergence and risk.....	22
3.5.2.4	Technical acceptability.....	22
3.5.2.5	Allowables development and equivalency validation.....	22
3.5.2.6	Production readiness.....	22
3.5.2.7	Lessons learned.....	22
3.5.3	Divergence and risk.....	22
3.5.3.1	Divergence.....	24
3.5.3.2	Risk assessment.....	25
3.5.3.3	Risk analysis.....	26
3.5.4	Production readiness.....	26
CHAPTER 4	BUILDING BLOCK APPROACH FOR COMPOSITE STRUCTURES.....	1
4.1	INTRODUCTION AND PHILOSOPHY.....	1
4.2	RATIONALE AND ASSUMPTIONS.....	4
4.3	METHODOLOGY.....	5
4.3.1	General approach.....	5
4.4	CONSIDERATIONS FOR SPECIFIC APPLICATIONS.....	6
4.4.1	Aircraft for prototypes.....	6
4.4.1.1	PMC composite allowables generation for DOD/NASA prototype aircraft structure.....	6
4.4.1.2	PMC composites building block structural development for DOD/NASA prototype aircraft.....	10
4.4.1.3	Summary of allowables and building block test efforts for DOD/NASA prototype composite aircraft structure.....	15
4.4.2	Aircraft for EMD and production.....	15
4.4.2.1	PMC composite allowables generation for DOD/NASA EMD and production aircraft structure.....	15
4.4.2.2	PMC composite building block structural development for DOD/NASA EMD and production aircraft.....	19
4.4.2.3	Summary of allowables and building block test efforts for DOD/NASA EMD and production composite aircraft structure.....	24
4.4.3	Commercial aircraft.....	24
4.4.3.1	Introduction.....	24
4.4.3.2	The building block approach.....	24
4.4.3.2.1	Certification approaches.....	25
4.4.3.2.2	Allowables versus design values.....	26
4.4.3.2.3	Lamina vs. laminate derived allowables for predicting strength.....	26
4.4.3.2.4	Product development.....	27
4.4.3.3	Composite road map.....	27
4.4.3.3.1	Criteria.....	28
4.4.3.3.2	Regulations.....	28
4.4.3.4	Commercial building block approach.....	29
4.4.3.5	Group A, material property development.....	29
4.4.3.5.1	Block 1 - material screening and selection.....	30
4.4.3.5.2	Block 2 - material and process specification development.....	30
4.4.3.5.3	Block 3 - allowables development.....	30
4.4.3.6	Group B, design-value development.....	31
4.4.3.6.1	Block 4 - structural element tests.....	31
4.4.3.6.2	Block 5 - subcomponent tests.....	33
4.4.3.7	Group C, analysis verification.....	33
4.4.3.7.1	Block 6 - component test.....	34
4.4.3.8	Boeing 777 aircraft composite primary structure building block approach.....	34
4.4.3.8.1	Introduction.....	34

4.4.3.8.2	Coupons and elements	35
4.4.3.8.3	Subcomponents	36
4.4.3.8.4	Components	38
4.4.3.8.5	777 pre-production horizontal stabilizer test	38
4.4.3.8.6	Fin root attachment test	40
4.4.3.8.7	777 horizontal stabilizer tests	40
4.4.3.8.8	777 vertical stabilizer test	41
4.4.3.8.9	Future programs	41
4.4.4	Business and private aircraft	41
4.4.4.1	High performance	41
4.4.4.1.1	Introduction	41
4.4.4.1.2	Typical building block program	42
4.4.4.2	Lightweight and kit	46
4.4.5	Rotorcraft	46
4.4.5.1	Design allowables testing	48
4.4.5.1.1	Airframe	48
4.4.5.1.2	Rotor system	48
4.4.5.1.3	Drive system	49
4.4.5.2	Design development testing	50
4.4.5.2.1	Airframe	50
4.4.5.2.2	Rotor system	51
4.4.5.2.3	Drive system	51
4.4.5.3	Full scale substantiation testing	52
4.4.5.3.1	Airframe	53
4.4.5.3.2	Rotor system	53
4.4.5.3.3	Drive system	54
4.4.6	Spacecraft	55
4.5	SPECIAL CONSIDERATION AND VARIANCES FOR SPECIFIC PROCESSES AND MATERIAL FORMS	55
4.5.1	Room Temperature	55
CHAPTER 5	DESIGN AND ANALYSIS	1
5.1	INTRODUCTION	1
5.2	BASIC LAMINA PROPERTIES AND MICROMECHANICS	1
5.2.1	Assumptions	2
5.2.1.1	Material homogeneity	2
5.2.1.2	Material orthotropy	2
5.2.1.3	Material linearity	2
5.2.1.4	Residual stresses	2
5.2.2	Fiber composites: physical properties	2
5.2.2.1	Elastic properties	3
5.2.2.2	Viscoelastic properties	7
5.2.2.3	Thermal expansion and moisture swelling	9
5.2.2.4	Thermal conduction and moisture diffusion	12
5.2.3	Fiber composites: strength and failure	13
5.2.3.1	Axial tensile strength	14
5.2.3.1.1	Weakest link failure	14
5.2.3.1.2	Cumulative weakening failure	14
5.2.3.1.3	Fiber break propagation failure	15
5.2.3.1.4	Cumulative group mode failure	15
5.2.3.2	Axial compressive strength	15
5.2.3.3	Matrix mode strength	17
5.2.4	Strength under combined stress	17
5.2.5	Summary	21
5.3	ANALYSIS OF LAMINATES	21

Volume 3, Foreword / Table of Contents

5.3.1	Lamina stress-strain relations	21
5.3.2	Lamination theory	27
5.3.3	Laminate properties	31
5.3.3.1	Membrane stresses	31
5.3.3.2	Bending	34
5.3.3.3	Thermal expansion	37
5.3.3.4	Moisture expansion	40
5.3.3.5	Conductivity	40
5.3.4	Thermal and hygroscopic analysis	41
5.3.4.1	Symmetric laminates	42
5.3.4.2	Unsymmetric laminates	43
5.3.5	Laminate stress analysis	43
5.3.5.1	Stresses due to mechanical loads	43
5.3.5.2	Stresses due to temperature and moisture	44
5.3.5.3	Netting analysis	45
5.3.5.3.1	Netting analysis for design of filament wound pressure vessels	46
5.3.5.4	Interlaminar stresses	49
5.3.5.5	Nonlinear stress analysis	49
5.3.6	Summary	49
5.4	LAMINATE STRENGTH AND FAILURE	50
5.4.1	Sequential ply failure approach	50
5.4.1.1	Initial ply	50
5.4.1.2	Subsequent failures	53
5.4.2	Fiber failure approach (laminate level failure)	53
5.4.3	Laminate design	55
5.4.4	Stress concentrations	56
5.4.5	Delamination	59
5.4.5.1	Compression	60
5.4.6	Damage and failure modes	61
5.4.6.1	Tension	61
5.4.6.1.1	Matrix cracks	62
5.4.6.2	Compression	63
5.4.7	Summary	64
5.5	COMPLEX LOADS	65
5.5.1	Biaxial in-plane loads	65
5.5.2	Out-of-plane loads	65
5.6	LAMINA TO LAMINATE CONSIDERATIONS	65
5.6.1	Residual stresses and strains	65
5.6.2	Thickness effects	65
5.6.3	Edge effects	66
5.6.4	Effects of transverse tensile properties in unidirectional tape	67
5.6.5	Laminate stacking sequence effects	68
5.6.5.1	Introduction	68
5.6.5.2	Design guidelines	68
5.6.5.2.1	Strong recommendations	69
5.6.5.2.2	Recommendations	70
5.6.6	Lamina-to-laminate statistics	71
5.6.7	Summary	71
5.7	COMPRESSIVE BUCKLING AND CRIPPLING	71
5.7.1	Plate buckling and crippling	71
5.7.1.1	Introduction	71
5.7.1.2	Initial buckling	72
5.7.1.3	Uniaxial loading - long plate with all sides simply supported	72
5.7.1.4	Uniaxial loading - long plate with all sides fixed	74
5.7.1.5	Uniaxial loading - long plate with three sides simply supported and one unloaded edge free	75

5.7.1.6	Uniaxial and biaxial loading - plate with all sides simply supported	75
5.7.1.7	Uniaxial loading - plate with loaded edges simply supported and unloaded edges fixed.....	76
5.7.1.8	Stacking sequence effects in buckling	76
5.7.2	Compressive postbuckling and crippling	79
5.7.2.1	Analytical models.....	86
5.7.2.2	Fatigue effects	88
5.7.2.3	Crippling curve determination	89
5.7.2.4	Stiffener crippling strength determination	89
5.7.2.5	Effects of corner radii and fillets.....	92
5.7.2.6	Slenderness correction	93
5.7.3	Summary.....	93
5.8	CARPET PLOTS	93
5.9	CREEP AND RELAXATION	93
5.10	FATIGUE	94
5.11	VIBRATION	94
5.11.1	Introduction	94
5.11.2	Stacking sequence effects	94
5.12	OTHER STRUCTURAL PROPERTIES	94
5.13	COMPUTER PROGRAMS.....	94
5.14	CERTIFICATION REQUIREMENTS	94
CHAPTER 6	STRUCTURAL BEHAVIOR OF JOINTS	1
6.1	INTRODUCTION.....	1
6.2	ADHESIVE JOINTS	2
6.2.1	Introduction	2
6.2.2	Joint design considerations	3
6.2.2.1	Effects of adherend thickness: adherend failures vs. bond failures	3
6.2.2.2	Joint geometry effects.....	4
6.2.2.3	Effects of adherend stiffness unbalance.....	5
6.2.2.4	Effects of ductile adhesive response	5
6.2.2.5	Behavior of composite adherends	7
6.2.2.6	Effects of bond defects	8
6.2.2.7	Durability of adhesive joints	9
6.2.3	Stresses and structural behavior of adhesive joints	11
6.2.3.1	General	11
6.2.3.2	Adhesive shear stresses	12
6.2.3.3	Peel stresses	17
6.2.3.4	Single and double lap joints with uniform adherend thickness.....	19
6.2.3.4.1	Joint behavior with elastic response of the bond layer	19
6.2.3.4.2	Thermal stress effects.....	29
6.2.3.4.3	Effect of ductility on joint stresses.....	31
6.2.3.4.4	Transverse shear and stacking sequence effects in composite adherends	34
6.2.3.5	Tapered and multi-step adherends	36
6.2.3.6	Finite element modeling	46
6.2.4	Mechanical response of adhesives	48
6.2.5	Mechanical response of composite adherends	49
6.2.6	Adhesive joint conclusions.....	49
6.3	MECHANICALLY FASTENED JOINTS.....	49
6.3.1	Introduction	49
6.3.2	Structural analysis.....	49
6.3.2.1	Load sharing in a joint.....	49

6.3.2.2	Analysis of local failure in bolted joints	51
6.3.2.3	Failure criteria	59
6.3.3	Design considerations	60
6.3.3.1	Geometry	60
6.3.3.2	Lay-up and stacking sequence	60
6.3.3.3	Fastener selection	60
6.3.4	Fatigue	61
6.3.4.1	Influence of loading mode	62
6.3.4.2	Influence of joint geometry	62
6.3.4.3	Influence of attachment details	63
6.3.4.4	Influence of laminate lay-up	63
6.3.4.5	Influence of environment	63
6.3.4.6	Influence of specimen thickness	63
6.3.4.7	Residual strength	63
6.3.5	Test verification	64
CHAPTER 7	DAMAGE RESISTANCE, DURABILITY, AND DAMAGE TOLERANCE	1
7.1	OVERVIEW AND GENERAL GUIDELINES	1
7.1.1	Principles	1
7.1.2	Composite-related issues	1
7.1.3	General guidelines	2
7.1.4	Section organization	4
7.2	AIRCRAFT DAMAGE TOLERANCE	4
7.2.1	Evolving military and civil aviation requirements	5
7.2.2	Methods of compliance to aviation regulations	10
7.2.2.1	Compliance with static strength requirements (civil aviation)	11
7.2.2.2	Compliance with damage tolerance requirements (civil aviation)	12
7.2.2.3	Deterministic compliance method (civil aviation example)	15
7.2.2.4	Probabilistic or semi-probabilistic compliance methods (civil aviation)	19
7.2.2.5	Comparison of deterministic and probabilistic methods	24
7.2.2.6	Full-scale tests for proof of structure (civil aviation)	25
7.3	TYPES, CHARACTERISTICS, AND SOURCES OF DAMAGE	26
7.3.1	Damages characterized by stage of occurrence	27
7.3.1.1	Manufacturing	27
7.3.1.2	Service	27
7.3.2	Damages characterized by physical imperfection	28
7.3.3	Realistic impact energy threats to aircraft	30
7.4	INSPECTION FOR DAMAGE	33
7.4.1	Aircraft inspection programs	33
7.4.2	Recommendations for damage inspection data development	34
7.4.2.1	Goals	35
7.4.2.2	Inspection techniques	35
7.5	DAMAGE RESISTANCE	36
7.5.1	Influencing factors	36
7.5.1.1	Summary of results from previous impact studies	37
7.5.1.2	Through-penetration impacts	38
7.5.1.3	Material type and form effects	41
7.5.1.4	Depth of damage	43
7.5.1.5	Laminate thickness effects	43
7.5.1.6	Structural size effects	46
7.5.1.7	Sandwich structure	48
7.5.2	Design issues and guidelines	50
7.5.2.1	Use of impact surveys for establishing critical damages	50
7.5.2.2	Structural arrangement and design details	50

7.5.2.3	Ground hail	51
7.5.2.4	Lightning	51
7.5.2.5	Handling and step loads	52
7.5.2.6	Exposed edges	52
7.5.3	Test issues	52
7.5.4	Analysis methods - description and assessment.....	52
7.6	DURABILITY (DAMAGE INITIATION)	52
7.6.1	Introduction	52
7.6.2	Life factor approach	53
7.6.3	Load enhancement factor approach.....	55
7.6.4	Ultimate strength approach.....	56
7.6.5	Spectrum truncation.....	57
7.6.6	Durability certification.....	57
7.6.7	Influencing factors.....	57
7.6.8	Design issues and guidelines	57
7.6.9	Test issues	58
7.6.10	Analysis methods - description and assessment.....	58
7.7	DAMAGE GROWTH UNDER CYCLIC LOADING.....	58
7.7.1	Influencing factors.....	58
7.7.2	Design issues and guidelines	60
7.7.3	Test issues	60
7.7.4	Analysis methods - description and assessment.....	60
7.7.4.1	Large through-penetration damage	60
7.7.4.2	Single delaminations and disbonds	60
7.7.4.2.1	Delamination growth	60
7.7.4.3	Impact damages	60
7.7.4.4	Cuts and gouges.....	60
7.8	RESIDUAL STRENGTH.....	61
7.8.1	Influencing Factors	61
7.8.1.1	Relationships between damage resistance and residual strength	61
7.8.1.2	Structure with impact damage	61
7.8.1.2.1	Material effects	61
7.8.1.2.2	Interlaminar toughness effects	62
7.8.1.2.3	Stacking sequence effects	62
7.8.1.2.4	Laminate thickness effects.....	64
7.8.1.2.5	Through-thickness stitching	64
7.8.1.2.6	Sandwich structure	64
7.8.1.2.7	Impact characteristic damage states	64
7.8.1.2.8	Residual strength - compressive/shear loads.....	68
7.8.1.2.9	Residual strength - tensile loads.....	69
7.8.1.2.10	Stiffened panels.....	69
7.8.1.3	Structure with through-penetration damage	71
7.8.1.3.1	Stitched skin/stiffener panels	82
7.8.2	Design issues and guidelines	82
7.8.2.1	Stacking sequences.....	82
7.8.2.2	Sandwich structure	82
7.8.3	Test issues	83
7.8.3.1	Impact tests on coupons.....	83
7.8.3.2	Impact tests on stiffened panels	83
7.8.3.3	Impact tests on sandwich panels.....	83
7.8.3.4	Tests for large through-penetration damage to stiffened panels	84
7.8.3.5	Tests for large through-penetration damage to sandwich panels.....	84
7.8.4	Analysis methods - description and assessment.....	84
7.8.4.1	Large through-penetration damage	84
7.8.4.1.1	Reduced singularity (Mar-Lin) model.....	92
7.8.4.1.2	Strain softening laws	103

7.8.4.1.3	LEFM - based methods.....	109
7.8.4.1.4	R-curves.....	110
7.8.4.2	Single delaminations and disbonds.....	113
7.8.4.2.1	Fracture mechanics approaches.....	114
7.8.4.2.2	Sublaminar buckling methods.....	114
7.8.4.3	Impact damages.....	115
7.8.4.3.1	Sublaminar buckling methods.....	115
7.8.4.3.2	Strain softening methods.....	119
7.8.4.4	Cuts and gouges.....	121
7.9	APPLICATIONS/EXAMPLES.....	121
7.9.1	Rotorcraft (Sikorsky).....	122
7.9.1.1	Damage.....	122
7.9.1.2	Environment.....	122
7.9.1.3	Test loading conditions related to critical failure modes.....	122
7.9.1.4	Test loads - load enhancement factor (LEF).....	122
7.9.1.5	Spectrum - truncation.....	123
7.9.1.6	Residual strength test.....	124
7.9.2	Commercial aircraft (Boeing 777 empennage torque boxes).....	124
7.9.2.1	Durability - environmental.....	124
7.9.2.2	Durability - mechanical loads.....	125
7.9.2.3	Damage.....	125
7.9.2.4	Damage tolerance - "no growth" tests.....	125
7.9.2.5	Damage tolerance - residual strength.....	127
7.9.2.6	Inspection plan.....	127
7.9.3	General aviation (Raytheon Starship).....	127
7.9.3.1	Introduction.....	127
7.9.3.2	Damage tolerance evaluation.....	128
7.9.3.2.1	Regulatory basis.....	128
7.9.3.2.2	Typical damage scenarios and related requirements.....	128
7.9.3.2.3	Damage source and modes.....	128
7.9.3.2.4	Element testing.....	129
7.9.3.2.5	Test results.....	130
7.9.3.2.6	Full scale tests.....	134
7.9.3.2.7	Continued airworthiness inspections.....	135
7.9.3.3	Service experience.....	135
7.9.3.4	Conclusions.....	136
7.9.4	Military aircraft.....	136
CHAPTER 8	SUPPORTABILITY.....	1
8.1	INTRODUCTION.....	1
8.2	DESIGN FOR SUPPORTABILITY.....	2
8.2.1	In-service experience.....	2
8.2.2	Inspectability.....	5
8.2.2.1	General design guidelines.....	5
8.2.2.2	Accessibility for inspection.....	7
8.2.3	Material selection.....	7
8.2.3.1	Introduction.....	7
8.2.3.2	Resins and fibers.....	7
8.2.3.3	Product forms.....	9
8.2.3.4	Adhesives.....	9
8.2.3.5	Supportability issues.....	9
8.2.3.6	Environmental concerns.....	9
8.2.4	Damage resistance, damage tolerance, and durability.....	11
8.2.4.1	Damage resistance.....	11
8.2.4.2	Damage tolerance.....	12

8.2.4.3	Durability.....	12
8.2.5	Environmental compliance.....	13
8.2.5.1	Elimination/reduction of heavy metals.....	13
8.2.5.2	Consideration of paint removal requirements.....	13
8.2.5.3	Shelf life and storage stability of repair materials.....	13
8.2.5.4	Cleaning requirements.....	14
8.2.5.5	Non-destructive inspection requirements.....	14
8.2.5.6	End of life disposal considerations.....	14
8.2.6	Reliability and maintainability.....	14
8.2.7	Interchangeability and replaceability.....	15
8.2.8	Accessibility.....	15
8.2.9	Repairability.....	15
8.2.9.1	General design approach.....	16
8.2.9.2	Repair design issues.....	19
8.3	SUPPORT IMPLEMENTATION.....	20
8.3.1	Part Inspection.....	20
8.3.1.1	Visual.....	21
8.3.1.2	Tap testing.....	22
8.3.1.3	Ultrasonics.....	22
8.3.1.4	Radiography.....	24
8.3.1.5	Shearography.....	25
8.3.1.6	Thermography.....	25
8.3.2	Damage assessment for composite repairs.....	26
8.3.2.1	General.....	26
8.3.2.2	Mandate of the assessor.....	27
8.3.2.3	Qualification of the assessor.....	27
8.3.2.4	Information for damage assessment.....	27
8.3.2.5	Dependence on repair location.....	28
8.3.3	Repair design criteria.....	29
8.3.3.1	Part stiffness.....	30
8.3.3.2	Static strength and stability.....	30
8.3.3.3	Durability.....	31
8.3.3.4	Damage tolerance.....	31
8.3.3.5	Related aircraft systems.....	31
8.3.3.6	Aerodynamic smoothness.....	32
8.3.3.7	Weight and balance.....	32
8.3.3.8	Operating temperatures.....	32
8.3.3.9	Environment.....	32
8.3.3.10	Surrounding structure.....	33
8.3.3.11	Temporary repair.....	33
8.3.4	Repair of composite structures.....	34
8.3.4.1	Introduction.....	34
8.3.4.2	Damage removal and site preparation.....	34
8.3.4.3	Bolted repairs.....	35
8.3.4.3.1	Repair concepts.....	35
8.3.4.3.2	Repair materials.....	37
8.3.4.3.3	Repair analysis.....	37
8.3.4.3.4	Repair procedures.....	38
8.3.4.3.5	Example of a bolted repair.....	39
8.3.4.4	Bonded repairs.....	39
8.3.4.4.1	Repair concepts.....	39
8.3.4.4.2	Repair materials.....	41
8.3.4.4.3	Repair analysis.....	42
8.3.4.4.4	Repair procedures.....	43
8.3.4.4.5	Bonded repair examples.....	46
8.3.4.5	Sandwich (honeycomb) repairs.....	47

8.3.4.5.1	Repair concepts	47
8.3.4.5.2	Core restoration	48
8.3.4.5.3	Repair procedures.....	50
8.3.4.5.4	Sandwich repair example.....	50
8.3.4.6	Repair inspection	51
8.3.4.6.1	In-process quality control	51
8.3.4.6.2	Post-process inspection	51
8.3.4.7	Repair validation	51
8.4	COMPOSITE REPAIR OF METAL STRUCTURE (CRMS)	52
8.5	LOGISTICS REQUIREMENTS	53
8.5.1	Training	53
8.5.2	Spares	54
8.5.3	Materials	54
8.5.4	Facilities	55
8.5.5	Technical data	56
8.5.6	Support equipment	56
8.5.6.1	Curing equipment	56
8.5.6.2	Cold storage rooms	57
8.5.6.3	Sanding/grinding booths.....	58
8.5.6.4	NDI equipment.....	58
CHAPTER 9	STRUCTURAL RELIABILITY	1
9.1	INTRODUCTION.....	1
9.2	FACTORS AFFECTING STRUCTURAL RELIABILITY	1
9.2.1	Static strength	1
9.2.2	Environmental effects	2
9.2.3	Fatigue	2
9.2.4	Damage tolerance	3
9.3	RELIABILITY ENGINEERING.....	3
9.4	RELIABILITY DESIGN CONSIDERATIONS.....	4
9.5	RELIABILITY ASSESSMENT AND DESIGN	5
9.5.1	Background.....	5
9.5.2	Deterministic vs. Probabilistic Design Approach	6
9.5.3	Probabilistic Design Methodology	7
9.5.4	Data Requirements.....	8
9.5.5	Summary.....	8
9.6	RELIABILITY BASED STRUCTURAL QUALIFICATION	10
9.6.1	Analysis.....	10
9.6.2	Testing.....	10
9.7	LIFE CYCLE REALIZATION	10
9.7.1	Manufacturing	10
9.7.2	Operational	10
CHAPTER 10	THICK-SECTION COMPOSITES	1
10.1	INTRODUCTION AND DEFINITION OF THICK-SECTION.....	1
10.2	MECHANICAL PROPERTIES REQUIRED FOR THICK-SECTION COMPOSITE THREE-DIMENSIONAL ANALYSIS	2
10.2.1	2-D composite analysis.....	3
10.2.2	3-D composite analysis.....	3
10.2.2.1	Unidirectional lamina 3-D properties	4
10.2.2.2	Oriented orthotropic laminate 3-D properties	4
10.2.3	Experimental property determination.....	5
10.2.3.1	Uniaxial tests	6
10.2.3.2	Multiaxial tests	16

10.2.3.2.1	Lineal test specimens/techniques	19
10.2.3.2.2	Cylindrical test specimens/techniques	20
10.2.4	Theoretical property determination	21
10.2.4.1	3-D lamina property determination	21
10.2.4.2	3-D laminate property determination	22
10.2.5	Test specimen design considerations	29
10.3	STRUCTURAL ANALYSIS METHODS FOR THICK-SECTION COMPOSITES	29
10.4	PHYSICAL PROPERTY ANALYSIS REQUIRED FOR THICK-SECTION COMPOSITE THREE-DIMENSIONAL ANALYSIS	29
10.5	PROCESS ANALYSIS METHODS FOR THICK-SECTION COMPOSITES	29
10.6	FAILURE CRITERIA	29
10.7	FACTORS INFLUENCING THICK-SECTION ALLOWABLES (I.E., SAFETY MARGINS)	29
10.8	THICK LAMINATE DEMONSTRATION PROBLEM	29
CHAPTER 11	ENVIRONMENTAL MANAGEMENT	1
11.1	INTRODUCTION	1
11.1.1	Scope	1
11.1.2	Glossary of recycling terms	1
11.2	RECYCLING INFRASTRUCTURE	4
11.2.1	Recycling infrastructure development models	4
11.2.2	Infrastructure needs	4
11.2.3	Recycling education	5
11.3	ECONOMICS OF COMPOSITE RECYCLING	5
11.4	COMPOSITE WASTE STREAMS	6
11.4.1	Process waste	7
11.4.2	Post consumer composite waste	8
11.5	COMPOSITE WASTE STREAM SOURCE REDUCTION	8
11.5.1	Just-in-time and just enough material delivery	8
11.5.2	Electronic commerce acquisition management	9
11.5.3	Waste minimization guidelines	9
11.5.3.1	Prepreg	9
11.5.3.2	Resin	9
11.5.3.3	Fiber	9
11.5.3.4	Curing agents	9
11.5.3.5	Autoclaving materials	9
11.5.3.6	Packaging materials	10
11.5.4	Lightweighting	10
11.6	REUSE OF COMPOSITE COMPONENTS AND MATERIALS	10
11.6.1	Reuse of composite components	10
11.6.2	Machining to smaller components	10
11.7	MATERIALS EXCHANGE	10
11.7.1	Reallocation of precursors	11
11.7.2	Composite materials exchange services	11
11.7.2.1	Care of unused materials	11
11.7.2.2	Packaging	11
11.7.2.3	Documentation of care	11
11.7.2.4	Description of unused materials	11
11.7.2.5	DOD resale restrictions	11
11.8	RECYCLING OF COMPOSITE MATERIALS	12
11.8.1	Design for disassembly and recycling	12
11.8.1.1	Fasteners	12
11.8.1.2	Adhesives	12
11.8.1.3	Hybrid composites	12
11.8.2	Recycling logistics	12
11.8.2.1	Collection and transportation	13

11.8.2.2	Identification of fibers and matrices	13
11.8.2.2.1	Fourier transform infrared spectroscopy	13
11.8.2.2.2	Densitometry	13
11.8.2.2.3	Coding of components	14
11.8.2.2.4	Routing of waste streams	14
11.8.3	Processing of composite recyclate	14
11.8.3.1	Size reduction	14
11.8.3.2	Matrix removal	14
11.8.3.3	Fiber reuse	15
11.8.3.4	Products of matrix removal	15
11.8.3.5	Other recycling and processing methods	15
11.8.4	Recycling of waste prepreg	16
CHAPTER 12	LESSONS LEARNED	1
12.1	INTRODUCTION	1
12.2	UNIQUE ISSUES FOR COMPOSITES	1
12.2.1	Elastic properties	1
12.2.2	Tailored properties and out-of-plane loads	2
12.2.3	Damage tolerance	4
12.2.4	Durability	4
12.2.5	Environmental sensitivity	5
12.2.6	Joints	6
12.2.6.1	Mechanically-fastened joints	6
12.2.6.2	Problems associated with adhesive bonding to peel-ply composite surfaces	6
12.2.7	Design	8
12.2.8	Handling and storage	9
12.2.9	Processing and fabrication	9
12.2.9.1	Quality control	10
12.3	LESSONS LEARNED	11
12.3.1	Design and analysis	11
12.3.1.1	Sandwich design	14
12.3.1.2	Bolted joints	15
12.3.1.3	Bonded joints	18
12.3.1.4	Composite to metal splice joints	20
12.3.1.5	Composite to metal continuous joints	21
12.3.1.6	Composite to composite splice joints	21
12.3.2	Materials and processes	21
12.3.3	Fabrication and assembly	22
12.3.4	Quality control	24
12.3.5	Testing	25
12.3.6	Certification	26
12.3.7	In-service and repair	26
INDEX	I-1	

SUMMARY OF CHANGES

Chapter	Section	Title	Change type
All	All	The entire volume has been reorganized	revision
1	1.1	Introduction	revision
2	2.4.1.1.	Carbon Fibers	new
2	2.4.1.8	Ultrahigh Molecular Weight Polyethylene	new
2	2.7.1	Automated Tape Placement	new
2	2.7.2	Fiber Placement/Automated Tow Placement	new
2	2.7.8	Adhesive Bonding	revision
2	2.8.7	Resin Transfer molding	revision
3	3.4	Statistical Process Control	revision
	3.5	Managing Change in Materials and Processes	new
4	All sections	Design and Analysis (Rev E), Building Block Approach for Composite Structures (Rev F)	Now is Chapter 5, with new and revised material
5	All sections	Structural Behavior of Joints (Rev E) Design and Analysis (Rev F)	Now is Chapter 6, with new and revised material
6	All sections	Structural Reliability (Rev E) Structural Behavior of Joints (Rev F)	Now is Chapter 9, with new and revised material
7	All sections	Thick Section Composites(Rev E) Damage Resistance, Durability, and Damage Tolerance (Rev F)	Now is Chapter 10, with new and revised material
8	All sections	Supportability	revised
9	All sections	Lessons Learned (Rev E) Structural Reliability (Rev F)	Now is Chapter 12, with new and revised material
10	All sections	Thick Section Composites	Refer to Chap 7 entry
11	All sections	Environmental Management	new
12	All sections	Lessons Learned	Refer to Chap 9 entry

This page intentionally left blank

CHAPTER 1 GENERAL INFORMATION

1.1 INTRODUCTION

This standardization handbook has been developed and is maintained as a joint effort of the Department of Defense and the Federal Aviation Administration, with considerable participation and input from industry, academia and other government agencies. It is oriented toward the standardization of 1) methods used to develop, analyze and publish mechanical property data for composite materials, 2) procedures to allow design organizations to effectively use the property data published in Volume 2 of this Handbook and other similar databases, and 3) general procedures for designing, analyzing and testing composite structures. In many cases, the standardization is intended to address the needs and requirements of the customer and regulatory agencies, while providing efficient engineering practices.

The standardization of a statistically-based mechanical property data base, procedures used, and overall guidelines for the characterization and use of composite material systems is recognized as being beneficial to both manufacturers and government agencies. A complete characterization of the capabilities of any engineering material system depends on the inherent material physical and chemical composition, which are independent of specific applications. Therefore, at the material system characterization level, the data and guidelines contained in this handbook apply to military and commercial products and provide the technical basis for establishing statistically valid design values acceptable to certifying or procuring agencies.

1.2 PURPOSE, SCOPE, AND ORGANIZATION OF VOLUME 3

For Department of Defense purposes, this handbook is for guidance only. This handbook cannot be cited as a requirement. If it is, the contractor does not have to comply. This mandate is a DoD requirement only; it is not applicable to the Federal Aviation Administration (FAA) or other government agencies.

Volume 3 of MIL-HDBK-17 provides methodologies and lessons learned for the design, analysis, manufacture, and field support of fiber-reinforced, polymeric-matrix composite structures. It also provides guidance on material and process specifications and procedures for utilization of the material data presented in Volume 2. The information provided is consistent with the guidance provided in Volume 1 and intended to be an extensive compilation of the current "best knowledge and practices" of composite materials and structures engineers and scientists from industry, government, and academia. This volume will be continually updated as the "state-of-the-art" of composites technology advances.

Volume 3 contains the following chapters, which are arranged in an order, which approximately follows the traditional "building-block" development approach:

Chapter 2, Materials and Processes, defines major material systems and processing methods. Effects of various processing parameters on final composite product performance are emphasized.

Chapter 3, Quality Control of Production Materials, reviews important issues related to quality control in the production of composite materials. It reviews recommended manufacturing inspection procedures and techniques for material property verification and statistical quality control.

Chapter 4, Building Block Approach, outlines the rationale for the traditional multi-level testing and analysis development approach used for many metallic and composite structures programs, particularly in the aerospace industry. It also contains guidance and example building block test programs for various applications, including DoD/NASA prototype and production aircraft, commercial transport aircraft, business and private aircraft and rotorcraft.

Chapter 5, Design and Analysis, addresses the basic design and analysis of composite laminates. The chapter provides an overview of the current techniques and describes how the various constituent properties contained in Volume 2 are used in the design and analysis of a composite structure. It presents standard analyses to provide a common nomenclature and methodology basis for users of MIL-HDBK-17. The analyses cover lamina and laminate stiffness and strength prediction, and compression buckling methods.

Chapter 6, Design and Analysis of Structural Joints, describes accepted design procedures and analytical methods for determining stresses and deformations in structural bonded and mechanically fastened joints for composite structures.

Chapter 7, Damage Resistance, Durability and Damage Tolerance, provides an extensive discussion of these three broad topics, which in general terms relate to the ability of a structure to perform the design functions over the life of the structure. Aircraft damage tolerance requirements and compliance approaches, types of damages and damage inspection are covered in the first sections of the chapter. Following these sections, in each of the three main areas, influencing factors, design issues and guidelines, testing issues, and analysis methods are covered in detail. Most of the information was developed and is applicable to the aircraft industry, but the general guidelines and basic data provided have application to many other industries.

Chapter 8, Supportability, considers the design for and the design of repairs in composite structures based on maintainability and reliability issues. It provides guidelines to the designer of new structures for considering supportability/maintainability issues, provides information relevant to the design of cost-effective repair procedures, and provides information related to logistical requirements for supporting and repairing composite structures.

Chapter 9, Structural Reliability, discusses some of the important factors affecting composite structure reliability including static strength, environmental effects, fatigue, and damage tolerance. It briefly discusses deterministic versus probabilistic design approaches.

Chapter 10, Thick-Section Composites, details methods of thick-section laminate analysis, thick-section structural analysis techniques, physical property requirements for three-dimensional analysis, experimental property determination techniques, and fabrication process simulation techniques and models for thick laminates.

Chapter 11, Environmental Management, provides guidance for issues related to recycling and re-use of composite materials and structures.

Chapter 12, Lessons Learned, documents a variety of issues related to earlier topics in this volume and provides a depository of knowledge gained from a number of involved companies, agencies, and universities.

1.3 SYMBOLS, ABBREVIATIONS, AND SYSTEMS OF UNITS

This section defines the symbols and abbreviations which are used within MIL-HDBK-17 and describes the system of units which is maintained. Common usage is maintained where possible. References 1.3(a), 1.3(b), and 1.3(c) served as primary sources for this information.

1.3.1 Symbols and abbreviations

The symbols and abbreviations used in this document are defined in this section with the exception of statistical symbols. These latter symbols are defined in Chapter 8. The lamina/laminate coordinate axes used for all properties and a summary of the mechanical property notation are shown in Figure 1.3.1.

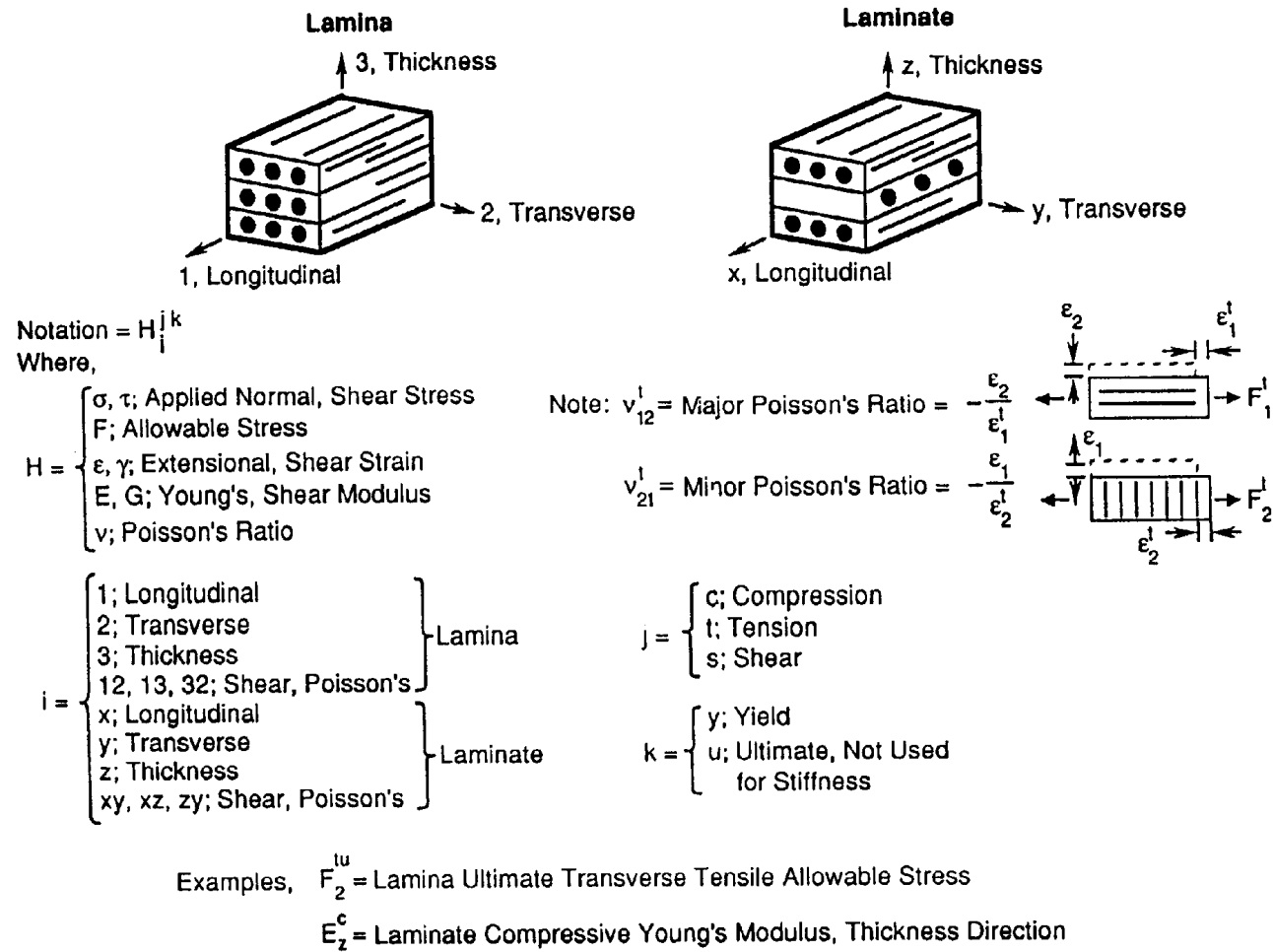


FIGURE 1.3.1 Mechanical property notation.

Volume 3, Chapter 1 General Information

- The symbols f and m , when used as either subscripts or superscripts, always denote fiber and matrix, respectively.
- The type of stress (for example, c_y - compressive yield) is always used in the superscript position.
- Direction indicators (for example, $x, y, z, 1, 2, 3$, etc.) are always used in the subscript position.
- Ordinal indicators of laminae sequence (e.g., 1, 2, 3, etc.) are used in the superscript position and must be parenthesized to distinguish them from mathematical exponents.
- Other indicators may be used in either subscript or superscript position, as appropriate for clarity.
- Compound symbols (such as, basic symbols plus indicators) which deviate from these rules are shown in their specific form in the following list.

The following general symbols and abbreviations are considered standard for use in MIL-HDBK-17. Where exceptions are made, they are noted in the text and tables.

A	- (1) area (m^2, in^2) - (2) ratio of alternating stress to mean stress - (3) A-basis for mechanical property values
a	- (1) length dimension (mm,in) - (2) acceleration ($m/sec^2, ft/sec^2$) - (3) amplitude - (4) crack or flaw dimension (mm,in)
B	- (1) B-basis for mechanical property values - (2) biaxial ratio
Btu	- British thermal unit(s)
b	- width dimension (mm,in), e.g., the width of a bearing or compression panel normal to load, or breadth of beam cross-section
C	- (1) specific heat ($kJ/kg\ ^\circ C, Btu/lb\ ^\circ F$) - (2) Celsius
CF	- centrifugal force (N,lbf)
CPF	- crossply factor
CPT	- cured ply thickness (mm, in.)
CG	- (1) center of mass, "center of gravity" - (2) area or volume centroid
\bar{C}	- centerline
c	- column buckling end-fixity coefficient
\bar{c}	- honeycomb sandwich core depth (mm,in)
cpm	- cycles per minute
D	- (1) diameter (mm,in) - (2) hole or fastener diameter (mm,in) - (3) plate stiffness (N-m,lbf-in)
d	- mathematical operator denoting differential
E	- modulus of elasticity in tension, average ratio of stress to strain for stress below proportional limit (GPa,Msi)
E'	- storage modulus (GPa,Msi)
E''	- loss modulus (GPa,Msi)
E _c	- modulus of elasticity in compression, average ratio of stress to strain for stress below proportional limit (GPa,Msi)
E _c '	- modulus of elasticity of honeycomb core normal to sandwich plane (GPa,Msi)
E ^{sec}	- secant modulus (GPa,Msi)
E ^{tan}	- tangent modulus (GPa,Msi)
e	- minimum distance from a hole center to the edge of the sheet (mm,in)

Volume 3, Chapter 1 General Information

e/D	- ratio of edge distance to hole diameter (bearing strength)
F	- (1) stress (MPa,ksi) - (2) Fahrenheit
F ^b	- bending stress (MPa,ksi)
F ^{ccr}	- crushing or crippling stress (upper limit of column stress for failure) (MPa,ksi)
F ^{su}	- ultimate stress in pure shear (this value represents the average shear stress over the cross-section) (MPa,ksi)
FAW	- fiber areal weight (g/m ² , lb/in ²)
FV	- fiber volume (%)
f	- (1) internal (or calculated) stress (MPa,ksi) - (2) stress applied to the gross flawed section (MPa,ksi) - (3) creep stress (MPa,ksi)
f ^c	- internal (or calculated) compressive stress (MPa,ksi)
f _c	- (1) maximum stress at fracture (MPa,ksi) - (2) gross stress limit (for screening elastic fracture data (MPa,ksi)
ft	- foot, feet
G	- modulus of rigidity (shear modulus) (GPa,Msi)
GPa	- gigapascal(s)
g	- (1) gram(s) - (2) acceleration due to gravity (m/s ² ,ft/s ²)
H/C	- honeycomb (sandwich)
h	- height dimension (mm,in) e.g. the height of a beam cross-section
hr	- hour(s)
I	- area moment of inertia (mm ⁴ ,in ⁴)
i	- slope (due to bending) of neutral plane in a beam, in radians
in.	- inch(es)
J	- (1) torsion constant (= I _p for round tubes) (m ⁴ ,in ⁴) - (2) Joule
K	- (1) Kelvin - (2) stress intensity factor (MPa/m,ksi/in) - (3) coefficient of thermal conductivity (W/m °C, Btu/ft ² /hr/in/°F) - (4) correction factor - (5) dielectric constant
K _{app}	- apparent plane strain fracture toughness or residual strength (MPa/m,ksi/in)
K _c	- critical plane strain fracture toughness, a measure of fracture toughness at point of crack growth instability (MPa/m,ksi/in)
K _{Ic}	- plane strain fracture toughness (MPa/m,ksi/in)
K _N	- empirically calculated fatigue notch factor
K _s	- plate or cylinder shear buckling coefficient
K _t	- (1) theoretical elastic stress concentration factor - (2) t _w /c ratio in H/C sandwich
K _v	- dielectric strength (KV/mm, V/mil)
K _x ,K _y	- plate or cylinder compression buckling coefficient
k	- strain at unit stress (m/m,in/in)
L	- cylinder, beam, or column length (mm,in)
L'	- effective column length (mm,in)
lb	- pound
M	- applied moment or couple (N-m,in-lbf)
Mg	- megagram(s)
MPa	- megapascal(s)
MS	- military standard
M.S.	- margin of safety
MW	- molecular weight
MWD	- molecular weight distribution

Volume 3, Chapter 1 General Information

m	- (1) mass (kg,lb) - (2) number of half wave lengths - (3) metre - (4) slope
N	- (1) number of fatigue cycles to failure - (2) number of laminae in a laminate - (3) distributed in-plane forces on a panel (lbf/in) - (4) Newton - (5) normalized
NA	- neutral axis
n	- (1) number of times in a set - (2) number of half or total wavelengths - (3) number of fatigue cycles endured
P	- (1) applied load (N,lbf) - (2) exposure parameter - (3) probability - (4) specific resistance (Ω)
P ^u	- test ultimate load, (N,lb per fastener)
P ^y	- test yield load, (N,lb per fastener)
p	- normal pressure (Pa,psi)
psi	- pounds per square inch
Q	- area static moment of a cross-section (mm ³ ,in ³)
q	- shear flow (N/m,lbf/in)
R	- (1) algebraic ratio of minimum load to maximum load in cyclic loading - (2) reduced ratio
RA	- reduction of area
R.H.	- relative humidity
RMS	- root-mean-square
RT	- room temperature
r	- (1) radius (mm,in) - (2) root radius (mm,in) - (3) reduced ratio (regression analysis)
S	- (1) shear force (N,lbf) - (2) nominal stress in fatigue (MPa,ksi) - (3) S-basis for mechanical property values
S _a	- stress amplitude in fatigue (MPa,ksi)
S _e	- fatigue limit (MPa,ksi)
S _m	- mean stress in fatigue (MPa,ksi)
S _{max}	- highest algebraic value of stress in the stress cycle (MPa,ksi)
S _{min}	- lowest algebraic value of stress in the stress cycle (MPa,ksi)
S _R	- algebraic difference between the minimum and maximum stresses in one cycle (MPa,ksi)
S.F.	- safety factor
s	- (1) arc length (mm,in) - (2) H/C sandwich cell size (mm,in)
T	- (1) temperature (°C,°F) - (2) applied torsional moment (N-m,in-lbf)
T _d	- thermal decomposition temperature (°C,°F)
T _F	- exposure temperature (°C,°F)
T _g	- glass transition temperature (°C,°F)
T _m	- melting temperature (°C,°F)
t	- (1) thickness (mm,in) - (2) exposure time (s) - (3) elapsed time (s)
V	- (1) volume (mm ³ ,in ³) - (2) shear force (N,lbf)

Volume 3, Chapter 1 General Information

W	- (1) weight (N,lbf) - (2) width (mm,in) - (3) Watt
x	- distance along a coordinate axis
Y	- nondimensional factor relating component geometry and flaw size
y	- (1) deflection (due to bending) of elastic curve of a beam (mm,in) - (2) distance from neutral axis to given point - (3) distance along a coordinate axis
Z	- section modulus, I/y (mm^3, in^3)
α	- coefficient of thermal expansion ($\text{m/m}/^\circ\text{C}, \text{in/in}/^\circ\text{F}$)
γ	- shear strain ($\text{m/m}, \text{in/in}$)
Δ	- difference (used as prefix to quantitative symbols)
δ	- elongation or deflection (mm,in)
ϵ	- strain ($\text{m/m}, \text{in/in}$)
ϵ^e	- elastic strain ($\text{m/m}, \text{in/in}$)
ϵ^p	- plastic strain ($\text{m/m}, \text{in/in}$)
μ	- permeability
η	- plasticity reduction factor
$[\eta]$	- intrinsic viscosity
η^*	- dynamic complex viscosity
ν	- Poisson's ratio
ρ	- (1) density ($\text{kg/m}^3, \text{lb/in}^3$) - (2) radius of gyration (mm,in)
ρ_c	- H/C sandwich core density ($\text{kg/m}^3, \text{lb/in}^3$)
Σ	- total, summation
σ	- standard deviation
σ_{ij}, τ_{ij}	- stress in j direction on surface whose outer normal is in i direction ($i, j = 1, 2, 3$ or x, y, z) (MPa,ksi)
T	- applied shear stress (MPa,ksi)
ω	- angular velocity (radians/s)
∞	- infinity

1.3.1.1 Constituent properties

The following symbols apply specifically to the constituent properties of a typical composite material.

E^f	- Young's modulus of filament material (MPa,ksi)
E^m	- Young's modulus of matrix material (MPa,ksi)
$E_{\bar{x}}^g$	- Young's modulus of impregnated glass scrim cloth in the filament direction or in the warp direction of a fabric (MPa,ksi)
$E_{\bar{y}}^g$	- Young's modulus of impregnated glass scrim cloth transverse to the filament direction or to the warp direction in a fabric (MPa,ksi)
G^f	- shear modulus of filament material (MPa,ksi)
G^m	- shear modulus of matrix (MPa,ksi)
$G_{\bar{x}y}^g$	- shear modulus of impregnated glass scrim cloth (MPa,ksi)
G_{cx}	- shear modulus of sandwich core along X-axis (MPa,ksi)
G_{cy}	- shear modulus of sandwich core along Y-axis (MPa,ksi)
ℓ	- filament length (mm,in)
α^f	- coefficient of thermal expansion for filament material ($\text{m/m}/^\circ\text{C}, \text{in/in}/^\circ\text{F}$)
α^m	- coefficient of thermal expansion for matrix material ($\text{m/m}/^\circ\text{C}, \text{in/in}/^\circ\text{F}$)

Volume 3, Chapter 1 General Information

- α_x^g - coefficient of thermal expansion of impregnated glass scrim cloth in the filament direction or in the warp direction of a fabric (m/m/°C,in/in/°F)
- α_y^g - coefficient of thermal expansion of impregnated glass scrim cloth transverse to the filament direction or to the warp direction in a fabric (m/m/°C,in/in/°F)
- ν^f - Poisson's ratio of filament material
- ν^m - Poisson's ratio of matrix material
- ν_{xy}^g - glass scrim cloth Poisson's ratio relating to contraction in the transverse (or fill) direction as a result of extension in the longitudinal (or warp) direction
- ν_{yx}^g - glass scrim cloth Poisson's ratio relating to contraction in the longitudinal (or warp) direction as a result of extension in the transverse (or fill) direction
- σ - applied axial stress at a point, as used in micromechanics analysis (MPa,ksi)
- τ - applied shear stress at a point, as used in micromechanics analysis (MPa,ksi)

1.3.1.2 Laminae and laminates

The following symbols, abbreviations, and notations apply to composite laminae and laminates. At the present time the focus in MIL-HDBK-17 is on laminae properties. However, commonly used nomenclature for both laminae and laminates are included here to avoid potential confusion.

- A_{ij} (i,j = 1,2,6) - extensional rigidities (N/m,lbf/in)
- B_{ij} (i,j = 1,2,6) - coupling matrix (N,lbf)
- C_{ij} (i,j = 1,2,6) - elements of stiffness matrix (Pa,psi)
- D_x, D_y - flexural rigidities (N-m,lbf-in)
- D_{xy} - twisting rigidity (N-m,lbf-in)
- D_{ij} (i,j = 1,2,6) - flexural rigidities (N-m,lbf-in)
- E_1 - Young's modulus of lamina parallel to filament or warp direction (GPa,Msi)
- E_2 - Young's modulus of lamina transverse to filament or warp direction (GPa,Msi)
- E_x - Young's modulus of laminate along x reference axis (GPa,Msi)
- E_y - Young's modulus of laminate along y reference axis (GPa,Msi)
- G_{12} - shear modulus of lamina in 12 plane (GPa,Msi)
- G_{xy} - shear modulus of laminate in xy reference plane (GPa,Msi)
- h_i - thickness of i^{th} ply or lamina (mm,in)
- M_x, M_y, M_{xy} - bending and twisting moment components (N-m/m, in-lbf/in in plate and shell analysis)
- n_f - number of filaments per unit length per lamina
- Q_x, Q_y - shear force parallel to z axis of sections of a plate perpendicular to x and y axes, respectively (N/m,lbf/in)
- Q_{ij} (i,j = 1,2,6) - reduced stiffness matrix (Pa,psi)
- u_x, u_y, u_z - components of the displacement vector (mm,in)
- u_x^0, u_y^0, u_z^0 - components of the displacement vector at the laminate's midsurface (mm,in)
- V_v - void content (% by volume)
- V_f - filament content or fiber volume (% by volume)
- V_g - glass scrim cloth content (% by volume)
- V_m - matrix content (% by volume)
- V_x, V_y - edge or support shear force (N/m,lbf/in)
- W_f - filament content (% by weight)
- W_g - glass scrim cloth content (% by weight)
- W_m - matrix content (% by weight)
- W_s - weight of laminate per unit surface area (N/m²,lbf/in²)
- α_1 - lamina coefficient of thermal expansion along 1 axis (m/m/°C,in/in/°F)
- α_2 - lamina coefficient of thermal expansion along 2 axis (m/m/°C,in/in/°F)

Volume 3, Chapter 1 General Information

α_x	- laminate coefficient of thermal expansion along general reference x axis (m/m/°C, in/in/°F)
α_y	- laminate coefficient of thermal expansion along general reference y axis (m/m/°C, in/in/°F)
α_{xy}	- laminate shear distortion coefficient of thermal expansion (m/m/°C, in/in/°F)
θ	- angular orientation of a lamina in a laminate, i.e., angle between 1 and x axes (°)
λ_{xy}	- product of ν_{xy} and ν_{yx}
ν_{12}	- Poisson's ratio relating contraction in the 2 direction as a result of extension in the 1 direction ¹
ν_{21}	- Poisson's ratio relating contraction in the 1 direction as a result of extension in the 2 direction ¹
ν_{xy}	- Poisson's ratio relating contraction in the y direction as a result of extension in the x direction ¹
ν_{yx}	- Poisson's ratio relating contraction in the x direction as a result of extension in the y direction ¹
ρ_c	- density of a single lamina (kg/m ³ , lb/in ³)
$\bar{\rho}_c$	- density of a laminate (kg/m ³ , lb/in ³)
ϕ	- (1) general angular coordinate, (°) - (2) angle between x and load axes in off-axis loading (°)

1.3.1.3 Subscripts

The following subscript notations are considered standard in MIL-HDBK-17.

1, 2, 3	- laminae natural orthogonal coordinates (1 is filament or warp direction)
A	- axial
a	- (1) adhesive - (2) alternating
app	- apparent
byp	- bypass
c	- composite system, specific filament/matrix composition. Composite as a whole, contrasted to individual constituents. Also, sandwich core when used in conjunction with prime (') - (4) critical
cf	- centrifugal force
e	- fatigue or endurance
eff	- effective
eq	- equivalent
f	- filament
g	- glass scrim cloth
H	- hoop
i	- i th position in a sequence
L	- lateral
m	- (1) matrix - (2) mean
max	- maximum
min	- minimum
n	- (1) n th (last) position in a sequence - (2) normal
p	- polar
s	- symmetric
st	- stiffener
T	- transverse

¹The convention for Poisson's ratio should be checked before comparing different sources as different conventions are used.

Volume 3, Chapter 1 General Information

- t - value of parameter at time t
- x, y, z - general coordinate system
- Σ - total, or summation
- o - initial or reference datum
- () - format for indicating specific, temperature associated with term in parentheses. RT - room temperature (21°C,70°F); all other temperatures in °F unless specified.

1.3.1.4 *Superscripts*

The following superscript notations are considered standard in MIL-HDBK-17.

- b - bending
- br - bearing
- c - (1) compression
- (2) creep
- cc - compressive crippling
- cr - compressive buckling
- e - elastic
- f - filament
- g - glass scrim cloth
- is - interlaminar shear
- (i) - ith ply or lamina
- lim - limit, used to indicate limit loading
- m - matrix
- ohc - open hole compression
- oht - open hole tension
- p - plastic
- pl - proportional limit
- rup - rupture
- s - shear
- scr - shear buckling
- sec - secant (modulus)
- so - offset shear
- T - temperature or thermal
- t - tension
- tan - tangent (modulus)
- u - ultimate
- y - yield
- ' - secondary (modulus), or denotes properties of H/C core when used with subscript c
- CAI - compression after impact

1.3.1.5 *Acronyms*

The following acronyms are used in MIL-HDBK-17.

- AA - atomic absorption
- AES - Auger electron spectroscopy
- AIA - Aerospace Industries Association
- ANOVA - analysis of variance
- ARL - US Army Research Laboratory
- ASTM - American Society for Testing and Materials
- BMI - bismaleimide
- BVID - barely visible impact damage
- CAI - compression after impact
- CCA - composite cylinder assemblage
- CFRP - carbon fiber reinforced plastic

Volume 3, Chapter 1 General Information

CLS	- crack lap shear
CMCS	- Composite Motorcase Subcommittee (JANNAF)
CPT	- cured ply thickness
CTA	- cold temperature ambient
CTD	- cold temperature dry
CTE	- coefficient of thermal expansion
CV	- coefficient of variation
CVD	- chemical vapor deposition
DCB	- double cantilever beam
DDA	- dynamic dielectric analysis
DLL	- design limit load
DMA	- dynamic mechanical analysis
DOD	- Department of Defense
DSC	- differential scanning calorimetry
DTA	- differential thermal analysis
DTRC	- David Taylor Research Center
ENF	- end notched flexure
EOL	- end-of-life
ESCA	- electron spectroscopy for chemical analysis
ESR	- electron spin resonance
ETW	- elevated temperature wet
FAA	- Federal Aviation Administration
FFF	- field flow fractionation
FGRP	- fiberglass reinforced plastic
FMECA	- Failure Modes Effects Criticality Analysis
FOD	- foreign object damage
FTIR	- Fourier transform infrared spectroscopy
FWC	- finite width correction factor
GC	- gas chromatography
GSCS	- Generalized Self Consistent Scheme
HDT	- heat distortion temperature
HPLC	- high performance liquid chromatography
ICAP	- inductively coupled plasma emission
IITRI	- Illinois Institute of Technology Research Institute
IR	- infrared spectroscopy
ISS	- ion scattering spectroscopy
JANNAF	- Joint Army, Navy, NASA, and Air Force
LC	- liquid chromatography
LPT	- laminate plate theory
LSS	- laminate stacking sequence
MMB	- mixed mode bending
MOL	- material operational limit
MS	- mass spectroscopy
MSDS	- material safety data sheet
MTBF	- Mean Time Between Failure
NAS	- National Aerospace Standard
NASA	- National Aeronautics and Space Administration
NDI	- nondestructive inspection
NMR	- nuclear magnetic resonance
PEEK	- polyether ether ketone
RDS	- rheological dynamic spectroscopy
RH	- relative humidity
RT	- room temperature
RTA	- room temperature ambient
RTD	- room temperature dry
RTM	- resin transfer molding

Volume 3, Chapter 1 General Information

SACMA	- Suppliers of Advanced Composite Materials Association
SAE	- Society of Automotive Engineers
SANS	- small-angle neutron scattering spectroscopy
SEC	- size-exclusion chromatography
SEM	- scanning electron microscopy
SFC	- supercritical fluid chromatography
SI	- International System of Units (Le Système International d'Unités)
SIMS	- secondary ion mass spectroscopy
TBA	- torsional braid analysis
TEM	- transmission electron microscopy
TGA	- thermogravimetric analysis
TLC	- thin-layer chromatography
TMA	- thermal mechanical analysis
TOS	- thermal oxidative stability
TVM	- transverse microcrack
UDC	- unidirectional fiber composite
VNB	- V-notched beam
XPS	- X-ray photoelectron spectroscopy

1.3.2 System of units

To comply with Department of Defense Instructive 5000.2, Part 6, Section M, "Use of the Metric System," dated February 23, 1991, the data in MIL-HDBK-17 are generally presented in both the International System of Units (SI units) and the U. S. Customary (English) system of units. ASTM E-380, Standard for Metric Practice, provides guidance for the application for SI units which are intended as a basis for worldwide standardization of measurement units (Reference 1.3.2(a)). Further guidelines on the use of the SI system of units and conversion factors are contained in the following publications (References 1.3.2(b) - (e)):

- (1) DARCOM P 706-470, *Engineering Design Handbook: Metric Conversion Guide*, July 1976.
- (2) NBS Special Publication 330, "The International System of Units (SI)," National Bureau of Standards, 1986 edition.
- (3) NBS Letter Circular LC 1035, "Units and Systems of Weights and Measures, Their Origin, Development, and Present Status," National Bureau of Standards, November 1985.
- (4) NASA Special Publication 7012, "The International System of Units Physical Constants and Conversion Factors", 1964.

English to SI conversion factors pertinent to MIL-HDBK-17 data are contained in Table 1.3.2.

TABLE 1.3.2 *English to SI conversion factors.*

To convert from	to	Multiply by
Btu (thermochemical)/in ² -s	watt/meter ² (W/m ²)	1.634 246 E+06
Btu-in/(s-ft ² -°F)	W/(m K)	5.192 204 E+02
degree Fahrenheit	degree Celsius (°C)	T = (T - 32)/1.8
degree Fahrenheit	kelvin (K)	T = (T + 459.67)/1.8
foot	meter (m)	3.048 000 E-01
ft ²	m ²	9.290 304 E-02
foot/second	meter/second (m/s)	3.048 000 E-01
ft/s ²	m/s ²	3.048 000 E-01
inch	meter (m)	2.540 000 E-02
in. ²	meter ² (m ²)	6.451 600 E-04
in. ³	m ³	1.638 706 E-05
kilogram-force (kgf)	newton (N)	9.806 650 E+00
kgf/m ²	pascal (Pa)	9.806 650 E+00
kip (1000 lbf)	newton (N)	4.448 222 E+03
ksi (kip/in ²)	MPa	6.894 757 E+00
lbf-in	N-m	1.129 848 E-01
lbf-ft	N-m	1.355 818 E+00
lbf/in ² (psi)	pascal (Pa)	6.894 757 E+03
lb/in ²	gm/m ²	7.030 696 E+05
lb/in ³	kg/m ³	2.767 990 E+04
Msi (10 ⁶ psi)	GPa	6.894 757 E+00
pound-force (lbf)	newton (N)	4.488 222 E+00
pound-mass (lb avoirdupois)	kilogram (kg)	4.535 924 E-01
torr	pascal (Pa)	1.333 22 E+02

* The letter "E" following the conversion factor stands for exponent and the two digits after the letter "E" indicate the power of 10 by which the number is to be multiplied.

1.4 DEFINITIONS

The following definitions are used within MIL-HDBK-17. This glossary of terms is not totally comprehensive but it does represent nearly all commonly used terms. Where exceptions are made, they are noted in the text and tables. For ease of identification the definitions have been organized alphabetically.

A-Basis (or A-Value) -- A statistically-based material property; a 95% lower confidence bound on the first percentile of a specified population of measurements. Also a 95% lower tolerance bound for the upper 99% of a specified population.

A-Stage -- An early stage in the reaction of thermosetting resins in which the material is still soluble in certain liquids and may be liquid or capable of becoming liquid upon heating. (Sometimes referred to as **resol**.)

Absorption -- A process in which one material (the absorbent) takes in or absorbs another (the absorbate).

Accelerator -- A material which, when mixed with a catalyzed resin, will speed up the chemical reaction between the catalyst and the resin.

Accuracy -- The degree of conformity of a measured or calculated value to some recognized standard or specified value. Accuracy involves the systematic error of an operation.

Addition Polymerization -- Polymerization by a repeated addition process in which monomers are linked together to form a polymer without splitting off of water or other simple molecules.

Adhesion -- The state in which two surfaces are held together at an interface by forces or interlocking action or both.

Adhesive -- A substance capable of holding two materials together by surface attachment. In the handbook, the term is used specifically to designate structural adhesives, those which produce attachments capable of transmitting significant structural loads.

ADK -- Notation used for the k-sample Anderson-Darling statistic, which is used to test the hypothesis that k batches have the same distribution.

Aliquot -- A small, representative portion of a larger sample.

Aging -- The effect, on materials, of exposure to an environment for a period of time; the process of exposing materials to an environment for an interval of time.

Ambient -- The surrounding environmental conditions such as pressure or temperature.

Anelasticity -- A characteristic exhibited by certain materials in which strain is a function of both stress and time, such that, while no permanent deformations are involved, a finite time is required to establish equilibrium between stress and strain in both the loading and unloading directions.

Angleply -- Same as **Crossply**.

Anisotropic -- Not isotropic; having mechanical and/or physical properties which vary with direction relative to natural reference axes inherent in the material.

Aramid -- A manufactured fiber in which the fiber-forming substance consisting of a long-chain synthetic aromatic polyamide in which at least 85% of the amide (-CONH-) linkages are attached directly to two aromatic rings.

Areal Weight of Fiber -- The weight of fiber per unit area of prepreg. This is often expressed as grams per square meter. See Table 1.6.2 for conversion factors.

Artificial Weathering -- Exposure to laboratory conditions which may be cyclic, involving changes in temperature, relative humidity, radiant energy and any other elements found in the atmosphere in various geographical areas.

Aspect Ratio -- In an essentially two-dimensional rectangular structure (e.g., a panel), the ratio of the long dimension to the short dimension. However, in compressive loading, it is sometimes considered to be the ratio of the load direction dimension to the transverse dimension. Also, in fiber micro-mechanics, it is referred to as the ratio of length to diameter.

Autoclave -- A closed vessel for producing an environment of fluid pressure, with or without heat, to an enclosed object which is undergoing a chemical reaction or other operation.

Autoclave Molding -- A process similar to the pressure bag technique. The lay-up is covered by a pressure bag, and the entire assembly is placed in an autoclave capable of providing heat and pressure for curing the part. The pressure bag is normally vented to the outside.

Axis of Braiding -- The direction in which the braided form progresses.

B-Basis (or B-Value) -- A statistically-based material property; a 95% lower confidence bound on the tenth percentile of a specified population of measurements. Also a 95% lower tolerance bound for the upper 90% of a specified population. (See Volume 1, Section 8.1.4)

B-Stage -- An intermediate stage in the reaction of a thermosetting resin in which the material softens when heated and swells when in contact with certain liquids but does not entirely fuse or dissolve. Materials are usually precured to this stage to facilitate handling and processing prior to final cure. (Sometimes referred to as **resitol**.)

Bag Molding -- A method of molding or laminating which involves the application of fluid pressure to a flexible material which transmits the pressure to the material being molded or bonded. Fluid pressure usually is applied by means of air, steam, water or vacuum.

Balanced Laminate -- A composite laminate in which all identical laminae at angles other than 0 degrees and 90 degrees occur only in \pm pairs (not necessarily adjacent).

Batch (or Lot) -- For fibers and resins, a quantity of material formed during the same process and having identical characteristics throughout. For prepregs, laminae, and laminates, material made from one batch of fiber and one batch of resin.

Bearing Area -- The product of the pin diameter and the specimen thickness.

Bearing Load -- A compressive load on an interface.

Bearing Yield Strength -- The bearing stress at which a material exhibits a specified limiting deviation from the proportionality of bearing stress to bearing strain.

Bend Test -- A test of ductility by bending or folding, usually with steadily applied forces. In some instances the test may involve blows to a specimen having a cross section that is essentially uniform over a length several times as great as the largest dimension of the cross section.

Binder -- A bonding resin used to hold strands together in a mat or preform during manufacture of a molded object.

Binomial Random Variable -- The number of successes in independent trials where the probability of success is the same for each trial.

Birefringence -- The difference between the two principal refractive indices (of a fiber) or the ratio between the retardation and thickness of a material at a given point.

Bleeder Cloth -- A nonstructural layer of material used in the manufacture of composite parts to allow the escape of excess gas and resin during cure. The bleeder cloth is removed after the curing process and is not part of the final composite.

Bobbin -- A cylinder or slightly tapered barrel, with or without flanges, for holding tows, rovings, or yarns.

Volume 3, Chapter 1 General Information

Bond -- The adhesion of one surface to another, with or without the use of an adhesive as a bonding agent.

Braid -- A system of three or more yarns which are interwoven in such a way that no two yarns are twisted around each other.

Braid Angle -- The acute angle measured from the axis of braiding.

Braid, Biaxial -- Braided fabric with two-yarn systems, one running in the $+\theta$ direction, the other in the $-\theta$ direction as measured from the axis of braiding.

Braid Count -- The number of braiding yarn crossings per inch measured along the axis of a braided fabric.

Braid, Diamond -- Braided fabric with an over one, under one weave pattern, (1 x 1).

Braid, Flat -- A narrow bias woven tape wherein each yarn is continuous and is intertwined with every other yarn in the system without being intertwined with itself.

Braid, Hercules -- A braided fabric with an over three, under three weave pattern, (3 x 3).

Braid, Jacquard -- A braided design made with the aid of a jacquard machine, which is a shedding mechanism by means of which a large number of ends may be controlled independently and complicated patterns produced.

Braid, Regular -- A braided fabric with an over two, under two weave pattern (2 x 2).

Braid, Square -- A braided pattern in which the yarns are formed into a square pattern.

Braid, Two-Dimensional -- Braided fabric with no braiding yarns in the through thickness direction.

Braid, Three-Dimensional -- Braided fabric with one or more braiding yarns in the through thickness direction.

Braid, Triaxial -- A biaxial braided fabric with laid in yarns running in the axis of braiding.

Braiding -- A textile process where two or more strands, yarns or tapes are intertwined in the bias direction to form an integrated structure.

Broadgoods -- A term loosely applied to prepreg material greater than about 12 inches in width, usually furnished by suppliers in continuous rolls. The term is currently used to designate both collimated uniaxial tape and woven fabric prepreps.

Buckling (Composite) -- A mode of structural response characterized by an out-of-plane material deflection due to compressive action on the structural element involved. In advanced composites, buckling may take the form not only of conventional general instability and local instability but also a micro-instability of individual fibers.

Bundle -- A general term for a collection of essentially parallel filaments or fibers.

C-Stage -- The final stage of the curing reaction of a thermosetting resin in which the material has become practically infusible and insoluble. (Normally considered fully cured and sometimes referred to as **resite**.)

Capstan -- A friction type take-up device which moves braided fabric away from the fell. The speed of which determines the braid angle.

Carbon Fibers -- Fibers produced by the pyrolysis of organic precursor fibers such as rayon, polyacrylonitrile (PAN), and pitch in an inert atmosphere. The term is often used interchangeably with "graphite"; however, carbon fibers and graphite fibers differ in the temperature at which the fibers are made and heat-treated, and the amount of carbon produced. Carbon fibers typically are carbonized at about 2400°F (1300°C) and assay at 93 to 95% carbon, while graphite fibers are graphitized at 3450 to 5450°F (1900 to 3000°C) and assay at more than 99% elemental carbon.

Carrier -- A mechanism for carrying a package of yarn through the braid weaving motion. A typical carrier consists of a bobbin spindle, a track follower, and a tensioning device.

Caul Plates -- Smooth metal plates, free of surface defects, the same size and shape as a composite lay-up, used immediately in contact with the lay-up during the curing process to transmit normal pressure and to provide a smooth surface on the finished laminate.

Censoring -- Data is right (left) censored at M, if, whenever an observation is less than or equal to M (greater than or equal to M), the actual value of the observation is recorded. If the observation exceeds (is less than) M, the observation is recorded as M.

Chain-Growth Polymerization -- One of the two principal polymerization mechanisms. In chain-growth polymerization, the reactive groups are continuously regenerated during the growth process. Once started, the polymer molecule grows rapidly by a chain of reactions emanating from a particular reactive initiator which may be a free radical, cation or anion.

Chromatogram -- A plot of detector response against peak volume of solution (eluate) emerging from the system for each of the constituents which have been separated.

Circuit -- One complete traverse of the fiber feed mechanism of a winding machine; one complete traverse of a winding band from one arbitrary point along the winding path to another point on a plane through the starting point and perpendicular to the axis.

Cocuring -- The act of curing a composite laminate and simultaneously bonding it to some other prepared surface during the same cure cycle (see **Secondary Bonding**).

Coefficient of Linear Thermal Expansion -- The change in length per unit length resulting from a one-degree rise in temperature.

Coefficient of Variation -- The ratio of the population (or sample) standard deviation to the population (or sample) mean.

Collimated -- Rendered parallel.

Compatible -- The ability of different resin systems to be processed in contact with each other without degradation of end product properties. (See **Compatible**, Volume 1, Section 8.1.4)

Composite Class -- As used in the handbook, a major subdivision of composite construction in which the class is defined by the fiber system and the matrix class, e.g., organic-matrix filamentary laminate.

Composite Material -- Composites are considered to be combinations of materials differing in composition or form on a macroscale. The constituents retain their identities in the composite; that is, they do not dissolve or otherwise merge completely into each other although they act in concert. Normally, the components can be physically identified and exhibit an interface between one another.

Compound -- An intimate mixture of polymer or polymers with all the materials necessary for the finished product.

Condensation Polymerization -- This is a special type of step-growth polymerization characterized by the formation of water or other simple molecules during the stepwise addition of reactive groups.

Confidence Coefficient -- See **Confidence Interval**.

Confidence Interval -- A confidence interval is defined by a statement of one of the following forms:

- (1) $P\{a < \theta\} \leq 1 - \alpha$
- (2) $P\{\theta < b\} \leq 1 - \alpha$
- (3) $P\{a < \theta < b\} \leq 1 - \alpha$

where $1 - \alpha$ is called the confidence coefficient. A statement of type (1) or (2) is called a one-sided confidence interval and a statement of type (3) is called a two-sided confidence interval. In (1) a is a lower confidence limit and in (2) b is an upper confidence limit. With probability at least $1 - \alpha$, the confidence interval will contain the parameter θ .

Constituent -- In general, an element of a larger grouping. In advanced composites, the principal constituents are the fibers and the matrix.

Continuous Filament -- A yarn or strand in which the individual filaments are substantially the same length as the strand.

Coupling Agent -- Any chemical substance designed to react with both the reinforcement and matrix phases of a composite material to form or promote a stronger bond at the interface. Coupling agents are applied to the reinforcement phase from an aqueous or organic solution or from a gas phase, or added to the matrix as an integral blend.

Coverage -- The measure of the fraction of surface area covered by the braid.

Crazing -- Apparent fine cracks at or under the surface of an organic matrix.

Creel -- A framework arranged to hold tows, rovings, or yarns so that many ends can be withdrawn smoothly and evenly without tangling.

Creep -- The time dependent part of strain resulting from an applied stress.

Creep, Rate Of -- The slope of the creep-time curve at a given time.

Crimp -- The undulations induced into a braided fabric via the braiding process.

Crimp Angle -- The maximum acute angle of a single braided yarn's direction measured from the average axis of tow.

Crimp Exchange -- The process by which a system of braided yarns reaches equilibrium when put under tension or compression.

Critical Value(s) -- When testing a one-sided statistical hypothesis, a critical value is the value such that, if the test statistic is greater than (less than) the critical value, the hypothesis is rejected. When testing a two-sided statistical hypothesis, two critical values are determined. If the test statistic is either less than the smaller critical value or greater than the larger critical value, then the hypothesis is rejected. In both cases, the critical value chosen depends on the desired risk (often 0.05) of rejecting the hypothesis when it is true.

Crossply -- Any filamentary laminate which is not uniaxial. Same as Angleply. In some references, the term crossply is used to designate only those laminates in which the laminae are at right angles to

one another, while the term angleply is used for all others. In the handbook, the two terms are used synonymously. The reservation of a separate terminology for only one of several basic orientations is unwarranted because a laminate orientation code is used.

Cumulative Distribution Function -- See Volume 1, Section 8.1.4.

Cure -- To change the properties of a thermosetting resin irreversibly by chemical reaction, i.e., condensation, ring closure, or addition. Cure may be accomplished by addition of curing (cross-linking) agents, with or without catalyst, and with or without heat. Cure may occur also by addition, such as occurs with anhydride cures for epoxy resin systems.

Cure Cycle -- The schedule of time periods at specified conditions to which a reacting thermosetting material is subjected in order to reach a specified property level.

Cure Stress -- A residual internal stress produced during the curing cycle of composite structures. Normally, these stresses originate when different components of a lay-up have different thermal coefficients of expansion.

Debond -- A deliberate separation of a bonded joint or interface, usually for repair or rework purposes. (See **Disbond**, **Unbond**).

Deformation -- The change in shape of a specimen caused by the application of a load or force.

Degradation -- A deleterious change in chemical structure, physical properties or appearance.

Delamination -- The separation of the layers of material in a laminate. This may be local or may cover a large area of the laminate. It may occur at any time in the cure or subsequent life of the laminate and may arise from a wide variety of causes.

Denier -- A direct numbering system for expressing linear density, equal to the mass in grams per 9000 meters of yarn, filament, fiber, or other textile strand.

Density -- The mass per unit volume.

Desorption -- A process in which an absorbed or adsorbed material is released from another material. Desorption is the reverse of absorption, adsorption, or both.

Deviation -- Variation from a specified dimension or requirement, usually defining the upper and lower limits.

Dielectric Constant -- The ratio of the capacity of a condenser having a dielectric constant between the plates to that of the same condenser when the dielectric is replaced by a vacuum; a measure of the electrical charge stored per unit volume at unit potential.

Dielectric Strength -- The average potential per unit thickness at which failure of the dielectric material occurs.

Disbond -- An area within a bonded interface between two adherends in which an adhesion failure or separation has occurred. It may occur at any time during the life of the structure and may arise from a wide variety of causes. Also, colloquially, an area of separation between two laminae in the finished laminate (in this case the term "delamination" is normally preferred.) (See **Debond**, **Unbond**, **Delamination**.)

Distribution -- A formula which gives the probability that a value will fall within prescribed limits. (See **Normal**, **Weibull**, and **Lognormal Distributions**, also Volume 1, Section 8.1.4).

Volume 3, Chapter 1 General Information

Dry -- a material condition of moisture equilibrium with a surrounding environment at 5% or lower relative humidity.

Dry Fiber Area -- Area of fiber not totally encapsulated by resin.

Ductility -- The ability of a material to deform plastically before fracturing.

Elasticity -- The property of a material which allows it to recover its original size and shape immediately after removal of the force causing deformation.

Elongation -- The increase in gage length or extension of a specimen during a tension test, usually expressed as a percentage of the original gage length.

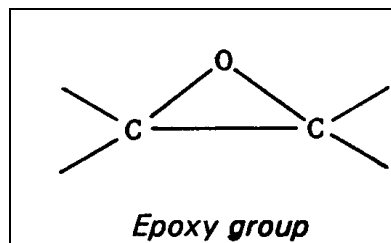
Eluate -- The liquid emerging from a column (in liquid chromatography).

Eluent -- The mobile phase used to sweep or elute the sample (solute) components into, through, and out of the column.

End -- A single fiber, strand, roving or yarn being or already incorporated into a product. An end may be an individual warp yarn or cord in a woven fabric. In referring to aramid and glass fibers, an end is usually an untwisted bundle of continuous filaments.

Epoxy Equivalent Weight -- The number of grams of resin which contain one chemical equivalent of the epoxy group.

Epoxy Resin -- Resins which may be of widely different structures but are characterized by the presence of the epoxy group. (The epoxy or epoxide group is usually present as a glycidyl ether, glycidyl amine, or as part of an aliphatic ring system. The aromatic type epoxy resins are normally used in composites.)



Extensometer -- A device for measuring linear strain.

F-Distribution -- See Volume 1, Section 8.1.4.

Fabric, Nonwoven -- A textile structure produced by bonding or interlocking of fibers, or both, accomplished by mechanical, chemical, thermal, or solvent means, and combinations thereof.

Fabric, Woven -- A generic material construction consisting of interlaced yarns or fibers, usually a planar structure. Specifically, as used in this handbook, a cloth woven in an established weave pattern from advanced fiber yarns and used as the fibrous constituent in an advanced composite lamina. In a fabric lamina, the warp direction is considered the longitudinal direction, analogous to the filament direction in a filamentary lamina.

Fell -- The point of braid formation, which is defined as the point at which the yarns in a braid system cease movement relative to each other.

Fiber -- A general term used to refer to filamentary materials. Often, fiber is used synonymously with filament. It is a general term for a filament of finite length. A unit of matter, either natural or manmade, which forms the basic element of fabrics and other textile structures.

Fiber Content -- The amount of fiber present in a composite. This is usually expressed as a percentage volume fraction or weight fraction of the composite.

Fiber Count -- The number of fibers per unit width of ply present in a specified section of a composite.

Fiber Direction -- The orientation or alignment of the longitudinal axis of the fiber with respect to a stated reference axis.

Fiber System -- The type and arrangement of fibrous material which comprises the fiber constituent of an advanced composite. Examples of fiber systems are collimated filaments or filament yarns, woven fabric, randomly oriented short-fiber ribbons, random fiber mats, whiskers, etc.

Fiber Volume (Fraction) -- See fiber content.

Filament -- The smallest unit of a fibrous material. The basic units formed during spinning and which are gathered into strands of fiber, (for use in composites). Filaments usually are of extreme length and of very small diameter. Filaments normally are not used individually. Some textile filaments can function as a yarn when they are of sufficient strength and flexibility.

Filamentary Composite -- A composite material reinforced with continuous fibers.

Filament winding -- See **Winding**.

Filament Wound -- Pertaining to an object created by the filament winding method of fabrication.

Fill (Filling) -- In a woven fabric, the yarn running from selvage to selvage at right angles to the warp.

Filler -- A relatively inert substance added to a material to alter its physical, mechanical, thermal, electrical, and other properties or to lower cost. Sometimes the term is used specifically to mean particulate additives.

Finish (or Size System) -- A material, with which filaments are treated, which contains a coupling agent to improve the bond between the filament surface and the resin matrix in a composite material. In addition, finishes often contain ingredients which provide lubricity to the filament surface, preventing abrasive damage during handling, and a binder which promotes strand integrity and facilitates packing of the filaments.

Fixed Effect -- A systematic shift in a measured quantity due to a particular level change of a treatment or condition. (See Volume 1, Section 8.1.4.)

Flash -- Excess material which forms at the parting line of a mold or die, or which is extruded from a closed mold.

Former Plate -- A die attached to a braiding machine which helps to locate the fell.

Fracture Ductility -- The true plastic strain at fracture.

Gage Length -- the original length of that portion of the specimen over which strain or change of length is determined.

Gel -- The initial jelly-like solid phase that develops during formation of a resin from a liquid. Also, a semi-solid system consisting of a network of solid aggregates in which liquid is held.

Gel Coat -- A quick-setting resin used in molding processes to provide an improved surface for the composite; it is the first resin applied to the mold after the mold-release agent.

Gel Point -- The stage at which a liquid begins to exhibit pseudo-elastic properties. (This can be seen from the inflection point on a viscosity-time plot.)

Gel Time -- The period of time from a pre-determined starting point to the onset of gelation (gel point) as defined by a specific test method.

Glass -- An inorganic product of fusion which has cooled to a rigid condition without crystallizing. In the handbook, all reference to glass will be to the fibrous form as used in filaments, woven fabric, yarns, mats, chopped fibers, etc.

Glass Cloth -- Conventionally-woven glass fiber material (see **Scrim**).

Glass Fibers -- A fiber spun from an inorganic product of fusion which has cooled to a rigid condition without crystallizing.

Glass Transition -- The reversible change in an amorphous polymer or in amorphous regions of a partially crystalline polymer from (or to) a viscous or rubbery condition to (or from) a hard and relatively brittle one.

Glass Transition Temperature -- The approximate midpoint of the temperature range over which the glass transition takes place.

Graphite Fibers -- See **Carbon Fibers**.

Greige -- Fabric that has received no finish.

Hand Lay-up -- A process in which components are applied either to a mold or a working surface, and the successive plies are built up and worked by hand.

Hardness -- Resistance to deformation; usually measured by indentation. Types of standard tests include Brinell, Rockwell, Knoop, and Vickers.

Heat Cleaned -- Glass or other fibers which have been exposed to elevated temperatures to remove preliminary sizings or binders which are not compatible with the resin system to be applied.

Heterogeneous -- Descriptive term for a material consisting of dissimilar constituents separately identifiable; a medium consisting of regions of unlike properties separated by internal boundaries. (Note that all nonhomogeneous materials are not necessarily heterogeneous).

Homogeneous -- Descriptive term for a material of uniform composition throughout; a medium which has no internal physical boundaries; a material whose properties are constant at every point, in other words, constant with respect to spatial coordinates (but not necessarily with respect to directional coordinates).

Horizontal Shear -- Sometimes used to indicate interlaminar shear. This is not an approved term for use in this handbook.

Humidity, Relative -- The ratio of the pressure of water vapor present to the pressure of saturated water vapor at the same temperature.

Hybrid -- A composite laminate comprised of laminae of two or more composite material systems. Or, a combination of two or more different fibers such as carbon and glass or carbon and aramid into a structure (tapes, fabrics and other forms may be combined).

Hygroscopic -- Capable of absorbing and retaining atmospheric moisture.

Hysteresis -- The energy absorbed in a complete cycle of loading and unloading.

Inclusion -- A physical and mechanical discontinuity occurring within a material or part, usually consisting of solid, encapsulated foreign material. Inclusions are often capable of transmitting some structural stresses and energy fields, but in a noticeably different manner from the parent material.

Integral Composite Structure -- Composite structure in which several structural elements, which would conventionally be assembled by bonding or with mechanical fasteners after separate fabrication, are instead laid up and cured as a single, complex, continuous structure; e.g., spars, ribs, and one stiffened cover of a wing box fabricated as a single integral part. The term is sometimes applied more loosely to any composite structure not assembled by mechanical fasteners.

Interface -- The boundary between the individual, physically distinguishable constituents of a composite.

Interlaminar -- Between the laminae of a laminate.

Discussion: describing objects (e.g., voids), events (e.g., fracture), or fields (e.g., stress).

Interlaminar Shear -- Shearing force tending to produce a relative displacement between two laminae in a laminate along the plane of their interface.

Intermediate Bearing Stress -- The bearing stress at the point on the bearing load-deformation curve where the tangent is equal to the bearing stress divided by a designated percentage (usually 4%) of the original hole diameter.

Intralaminar -- Within the laminae of a laminate.

Discussion: describing objects (for example, voids), event (for example, fracture), or fields (for example, stress).

Isotropic -- Having uniform properties in all directions. The measured properties of an isotropic material are independent of the axis of testing.

Jammed State -- The state of a braided fabric under tension or compression where the deformation of the fabric is dominated by the deformation properties of the yarn.

Knitting -- A method of constructing fabric by interlocking series of loops of one or more yarns.

Knuckle Area -- The area of transition between sections of different geometry in a filament wound part.

k-Sample Data -- A collection of data consisting of values observed when sampling from k batches.

Laid-In Yarns -- A system of longitudinal yarns in a triaxial braid which are inserted between the bias yarns.

Lamina -- A single ply or layer in a laminate.

Discussion: For filament winding, a lamina is a layer.

Laminae -- Plural of lamina.

Laminate -- for fiber-reinforced composites, a consolidated collection of laminae (plies) with one or more orientations with respect to some reference direction.

Laminate Orientation -- The configuration of a crossplied composite laminate with regard to the angles of crossplying, the number of laminae at each angle, and the exact sequence of the lamina lay-up.

Lattice Pattern -- A pattern of filament winding with a fixed arrangement of open voids.

Lay-up -- A process of fabrication involving the assembly of successive layers of resin-impregnated material.

Lognormal Distribution -- A probability distribution for which the probability that an observation selected at random from this population falls between a and b ($0 < a < b < B$) is given by the area under the normal distribution between $\log a$ and $\log b$. The common (base 10) or the natural (base e) logarithm may be used. (See Volume 1, Section 8.1.4.)

Lower Confidence Bound -- See **Confidence Interval**.

Macro -- In relation to composites, denotes the gross properties of a composite as a structural element but does not consider the individual properties or identity of the constituents.

Macrostrain -- The mean strain over any finite gage length of measurement which is large in comparison to the material's interatomic distance.

Mandrel -- A form fixture or male mold used for the base in the production of a part by lay-up, filament winding or braiding.

Mat -- A fibrous material consisting of randomly oriented chopped or swirled filaments loosely held together with a binder.

Material Acceptance -- The testing of incoming material to ensure that it meets requirements.

Material Qualification -- The procedures used to accept a material by a company or organization for production use.

Material System -- A specific composite material made from specifically identified constituents in specific geometric proportions and arrangements and possessed of numerically defined properties.

Material System Class -- As used in this handbook, a group consisting of material systems categorized by the same generic constituent materials, but without defining the constituents uniquely; e.g., the carbon/epoxy class.

Material Variability -- A source of variability due to the spatial and consistency variations of the material itself and due to variation in its processing. (See Volume 1, Section 8.1.4.)

Matrix -- The essentially homogeneous material in which the fiber system of a composite is embedded.

Matrix Content -- The amount of matrix present in a composite expressed either as percent by weight or percent by volume. Discussion: For polymer matrix composites this is called resin content, which is usually expressed as percent by weight

Mean -- See **Sample Mean** and **Population Mean**.

Mechanical Properties -- The properties of a material that are associated with elastic and inelastic reaction when force is applied, or the properties involving the relationship between stress and strain.

Median -- See **Sample Median** and **Population Median**.

Micro -- In relation to composites, denotes the properties of the constituents, i.e., matrix and reinforcement and interface only, as well as their effects on the composite properties.

Microstrain -- The strain over a gage length comparable to the material's interatomic distance.

Modulus, Chord -- The slope of the chord drawn between any two specified points on the stress-strain curve.

Modulus, initial -- The slope of the initial straight portion of a stress-strain curve.

Modulus, Secant -- The slope of the secant drawn from the origin to any specified point on the stress-strain curve.

Modulus, Tangent -- The ratio of change in stress to change in strain derived from the tangent to any point on a stress-strain curve.

Modulus, Young's -- The ratio of change in stress to change in strain below the elastic limit of a material. (Applicable to tension and compression).

Modulus of Rigidity (also Shear Modulus or Torsional Modulus) -- The ratio of stress to strain below the proportional limit for shear or torsional stress.

Modulus of Rupture, in Bending -- The maximum tensile or compressive stress (whichever causes failure) value in the extreme fiber of a beam loaded to failure in bending. The value is computed from the flexure equation:

$$F^b = \frac{Mc}{I} \quad 1.4(a)$$

where M = maximum bending moment computed from the maximum load and the original moment arm,
 c = initial distance from the neutral axis to the extreme fiber where failure occurs,
 I = the initial moment of inertia of the cross section about its neutral axis.

Modulus of Rupture, in Torsion -- The maximum shear stress in the extreme fiber of a member of circular cross section loaded to failure in torsion calculated from the equation:

$$F^s = \frac{Tr}{J} \quad 1.4(b)$$

where T = maximum twisting moment,
 r = original outer radius,
 J = polar moment of inertia of the original cross section.

Moisture Content -- The amount of moisture in a material determined under prescribed condition and expressed as a percentage of the mass of the moist specimen, i.e., the mass of the dry substance plus the moisture present.

Moisture Equilibrium -- The condition reached by a sample when it no longer takes up moisture from, or gives up moisture to, the surrounding environment.

Mold Release Agent -- A lubricant applied to mold surfaces to facilitate release of the molded article.

Molded Edge -- An edge which is not physically altered after molding for use in final form and particularly one which does not have fiber ends along its length.

Molding -- The forming of a polymer or composite into a solid mass of prescribed shape and size by the application of pressure and heat.

Monolayer -- The basic laminate unit from which crossplied or other laminates are constructed.

Volume 3, Chapter 1 General Information

Monomer -- A compound consisting of molecules each of which can provide one or more constitutional units.

NDE -- Nondestructive evaluation. Broadly considered synonymous with NDI.

NDI -- Nondestructive inspection. A process or procedure for determining the quality or characteristics of a material, part, or assembly without permanently altering the subject or its properties.

NDT -- Nondestructive testing. Broadly considered synonymous with NDI.

Necking -- A localized reduction in cross-sectional area which may occur in a material under tensile stress.

Negatively Skewed -- A distribution is said to be negatively skewed if the distribution is not symmetric and the longest tail is on the left.

Nominal Specimen Thickness -- The nominal ply thickness multiplied by the number of plies.

Nominal Value -- A value assigned for the purpose of a convenient designation. A nominal value exists in name only.

Normal Distribution -- A two parameter (μ, σ) family of probability distributions for which the probability that an observation will fall between a and b is given by the area under the curve

$$f(x) = \frac{1}{\sigma\sqrt{2\pi}} \exp\left[-\frac{(x-\mu)^2}{2\sigma^2}\right] \quad 1.4(c)$$

between a and b. (See Volume 1, Section 8.1.4.)

Normalization -- A mathematical procedure for adjusting raw test values for fiber-dominated properties to a single (specified) fiber volume content.

Normalized Stress -- Stress value adjusted to a specified fiber volume content by multiplying the measured stress value by the ratio of specimen fiber volume to the specified fiber volume. This ratio may be obtained directly by experimentally measuring fiber volume, or indirectly by calculation using specimen thickness and fiber areal weight.

Observed Significance Level (OSL) -- The probability of observing a more extreme value of the test statistic when the null hypotheses is true.

Offset Shear Strength --- (from valid execution of a material property shear response test) the value of shear stress at the intersection between a line parallel to the shear chord modulus of elasticity and the shear stress/strain curve, where the line has been offset along the shear strain axis from the origin by a specified strain offset value.

Oligomer -- A polymer consisting of only a few monomer units such as a dimer, trimer, etc., or their mixtures.

One-Sided Tolerance Limit Factor -- See **Tolerance Limit Factor**.

Orthotropic -- Having three mutually perpendicular planes of elastic symmetry.

Oven Dry -- The condition of a material that has been heated under prescribed conditions of temperature and humidity until there is no further significant change in its mass.

PAN Fibers -- Reinforcement fiber derived from the controlled pyrolysis of poly(acrylonitrile) fiber.

Parallel Laminate -- A laminate of woven fabric in which the plies are aligned in the same position as originally aligned in the fabric roll.

Parallel Wound -- A term used to describe yarn or other material wound into a flanged spool.

Peel Ply -- A layer of resin free material used to protect a laminate for later secondary bonding.

pH -- A measure of acidity or alkalinity of a solution, with neutrality represented by a value of 7, with increasing acidity corresponding to progressively smaller values, and increasing alkalinity corresponding to progressively higher values.

Pick Count -- The number of filling yarns per inch or per centimeter of woven fabric.

Pitch Fibers -- Reinforcement fiber derived from petroleum or coal tar pitch.

Plastic -- A material that contains one or more organic polymers of large molecular weight, is solid in its finished state, and, at some state in its manufacture or processing into finished articles, can be shaped by flow.

Plasticizer -- A material of lower molecular weight added to a polymer to separate the molecular chains. This results in a depression of the glass transition temperature, reduced stiffness and brittleness, and improved processability. (Note, many polymeric materials do not need a plasticizer.)

Plied Yarn -- A yarn formed by twisting together two or more single yarns in one operation.

Poisson's Ratio -- The absolute value of the ratio of transverse strain to the corresponding axial strain resulting from uniformly distributed axial stress below the proportional limit of the material.

Polymer -- An organic material composed of molecules characterized by the repetition of one or more types of monomeric units.

Polymerization -- A chemical reaction in which the molecules of monomers are linked together to form polymers via two principal reaction mechanisms. Addition polymerizations proceed by chain growth and most condensation polymerizations through step growth.

Population -- The set of measurements about which inferences are to be made or the totality of possible measurements which might be obtained in a given testing situation. For example, "all possible ultimate tensile strength measurements for carbon/epoxy system A, conditioned at 95% relative humidity and room temperature". In order to make inferences about a population, it is often necessary to make assumptions about its distributional form. The assumed distributional form may also be referred to as the population. (See Volume 1, Section 8.1.4.)

Population Mean -- The average of all potential measurements in a given population weighted by their relative frequencies in the population. (See Volume 1, Section 8.1.4.)

Population Median -- That value in the population such that the probability of exceeding it is 0.5 and the probability of being less than it is 0.5. (See Volume 1, Section 8.1.4.)

Population Variance -- A measure of dispersion in the population.

Porosity -- A condition of trapped pockets of air, gas, or vacuum within a solid material, usually expressed as a percentage of the total nonsolid volume to the total volume (solid plus nonsolid) of a unit quantity of material.

Positively Skewed -- A distribution is said to be positively skewed if the distribution is not symmetric and the longest tail is on the right.

Postcure -- Additional elevated temperature cure, usually without pressure, to increase the glass transition temperature, to improve final properties, or to complete the cure.

Pot Life -- The period of time during which a reacting thermosetting composition remains suitable for its intended processing after mixing with a reaction initiating agent.

Precision -- The degree of agreement within a set of observations or test results obtained. Precision involves repeatability and reproducibility.

Precursor (for Carbon or Graphite Fiber) -- Either the PAN or pitch fibers from which carbon and graphite fibers are derived.

Preform -- An assembly of dry fabric and fibers which has been prepared for one of several different wet resin injection processes. A preform may be stitched or stabilized in some other way to hold its A shape. A commingled preform may contain thermoplastic fibers and may be consolidated by elevated temperature and pressure without resin injection.

Preply -- Layers of prepreg material, which have been assembled according to a user specified stacking sequence.

Prepreg -- Ready to mold or cure material in sheet form which may be tow, tape, cloth, or mat impregnated with resin. It may be stored before use.

Pressure -- The force or load per unit area.

Probability Density Function -- See Volume 1, Section 8.1.4.

Proportional Limit -- The maximum stress that a material is capable of sustaining without any deviation from the proportionality of stress to strain (also known as Hooke's law).

Quasi-Isotropic Laminate -- A balanced and symmetric laminate for which a constitutive property of interest, at a given point, displays isotropic behavior in the plane of the laminate.

Discussion: Common quasi-isotropic laminates are $(0/\pm 60)_s$ and $(0/\pm 45/90)_s$.

Random Effect -- A shift in a measured quantity due to a particular level change of an external, usually uncontrollable, factor. (See Volume 1, Section 8.1.4.)

Random Error -- That part of the data variation that is due to unknown or uncontrolled factors and that affects each observation independently and unpredictably. (See Volume 1, Section 8.1.4.)

Reduction of Area -- The difference between the original cross sectional area of a tension test specimen and the area of its smallest cross section, usually expressed as a percentage of the original area.

Refractive Index - The ratio of the velocity of light (of specified wavelength) in air to its velocity in the substance under examination. Also defined as the sine of the angle of incidence divided by the sine of the angle of refraction as light passes from air into the substance.

Reinforced Plastic -- A plastic with relatively high stiffness or very high strength fibers embedded in the composition. This improves some mechanical properties over that of the base resin.

Release Agent -- See **Mold Release Agent**.

Resilience -- A property of a material which is able to do work against restraining forces during return from a deformed condition.

Resin -- An organic polymer or prepolymer used as a matrix to contain the fibrous reinforcement in a composite material or as an adhesive. This organic matrix may be a thermoset or a thermoplastic, and may contain a wide variety of components or additives to influence; handleability, processing behavior and ultimate properties.

Resin Content -- See **Matrix content**.

Resin Starved Area -- Area of composite part where the resin has a non-continuous smooth coverage of the fiber.

Resin System -- A mixture of resin, with ingredients such as catalyst, initiator, diluents, etc. required for the intended processing and final product.

Room Temperature Ambient (RTA) -- 1) an environmental condition of $73\pm 5^{\circ}\text{F}$ ($23\pm 3^{\circ}\text{C}$) at ambient laboratory relative humidity; 2) a material condition where, immediately following consolidation/cure, the material is stored at $73\pm 5^{\circ}\text{F}$ ($23\pm 3^{\circ}\text{C}$) and at a maximum relative humidity of 60%.

Roving -- A number of strands, tows, or ends collected into a parallel bundle with little or no twist. In spun yarn production, an intermediate state between sliver and yarn.

S-Basis (or S-Value) -- The mechanical property value which is usually the specified minimum value of the appropriate government specification or SAE Aerospace Material Specification for this material.

Sample -- A small portion of a material or product intended to be representative of the whole. Statistically, a sample is the collection of measurements taken from a specified population. (See Volume 1, Section 8.1.4.)

Sample Mean -- The arithmetic average of the measurements in a sample. The sample mean is an estimator of the population mean. (See Volume 1, Section 8.1.4.)

Sample Median -- Order the observation from smallest to largest. Then the sample median is the value of the middle observation if the sample size is odd; the average of the two central observations if n is even. If the population is symmetric about its mean, the sample median is also an estimator of the population mean. (See Volume 1, Section 8.1.4.)

Sample Standard Deviation -- The square root of the sample variance. (See Volume 1, Section 8.1.4.)

Sample Variance -- The sum of the squared deviations from the sample mean, divided by $n-1$. (See Volume 1, Section 8.1.4.)

Sandwich Construction -- A structural panel concept consisting in its simplest form of two relatively thin, parallel sheets of structural material bonded to, and separated by, a relatively thick, light-weight core.

Saturation -- An equilibrium condition in which the net rate of absorption under prescribed conditions falls essentially to zero.

Scrim (also called **Glass Cloth, Carrier**) -- A low cost fabric woven into an open mesh construction, used in the processing of tape or other B-stage material to facilitate handling.

Secondary Bonding -- The joining together, by the process of adhesive bonding, of two or more already-cured composite parts, during which the only chemical or thermal reaction occurring is the curing of the adhesive itself.

Selvage or Selvedge -- The woven edge portion of a fabric parallel to the warp.

Set -- The strain remaining after complete release of the force producing the deformation.

Shear Fracture (for crystalline type materials) -- A mode of fracture resulting from translation along slip planes which are preferentially oriented in the direction of the shearing stress.

Shelf Life -- The length of time a material, substance, product, or reagent can be stored under specified environmental conditions and continue to meet all applicable specification requirements and/or remain suitable for its intended function.

Short Beam Strength (SBS) -- a test result from valid execution of ASTM test method D 2344.

Significant -- Statistically, the value of a test statistic is significant if the probability of a value at least as extreme is less than or equal to a predetermined number called the significance level of the test.

Significant Digit -- Any digit that is necessary to define a value or quantity.

Size System -- See **Finish**.

Sizing -- A generic term for compounds which are applied to yarns to bind the fiber together and stiffen the yarn to provide abrasion-resistance during weaving. Starch, gelatin, oil, wax, and man-made polymers such as polyvinyl alcohol, polystyrene, polyacrylic acid, and polyacetates are employed.

Skewness -- See **Positively Skewed, Negatively Skewed**.

Sleeving -- A common name for tubular braided fabric.

Slenderness Ratio -- The unsupported effective length of a uniform column divided by the least radius of gyration of the cross-sectional area.

Sliver -- A continuous strand of loosely assembled fiber that is approximately uniform in cross-sectional area and has no twist.

Solute -- The dissolved material.

Specific Gravity -- The ratio of the weight of any volume of a substance to the weight of an equal volume of another substance taken as standard at a constant or stated temperature. Solids and liquids are usually compared with water at 39°F (4°C).

Specific Heat -- The quantity of heat required to raise the temperature of a unit mass of a substance one degree under specified conditions.

Specimen -- A piece or portion of a sample or other material taken to be tested. Specimens normally are prepared to conform with the applicable test method.

Spindle -- A slender upright rotation rod on a spinning frame, roving frame, twister or similar machine.

Standard Deviation -- See **Sample Standard Deviation**.

Staple -- Either naturally occurring fibers or lengths cut from filaments.

Step-Growth Polymerization -- One of the two principal polymerization mechanisms. In step-growth polymerization, the reaction grows by combination of monomer, oligomer, or polymer molecules through the consumption of reactive groups. Since average molecular weight increases with monomer consumption, high molecular weight polymers are formed only at high degrees of conversion.

Strain -- the per unit change, due to force, in the size or shape of a body referred to its original size or shape. Strain is a nondimensional quantity, but it is frequently expressed in inches per inch, meters per meter, or percent.

Strand -- Normally an untwisted bundle or assembly of continuous filaments used as a unit, including slivers, tow, ends, yarn, etc. Sometimes a single fiber or filament is called a strand.

Strength -- the maximum stress which a material is capable of sustaining.

Stress -- The intensity at a point in a body of the forces or components of forces that act on a given plane through the point. Stress is expressed in force per unit area (pounds-force per square inch, megapascals, etc.).

Stress Relaxation -- The time dependent decrease in stress in a solid under given constraint conditions.

Stress-Strain Curve (Diagram) -- A graphical representation showing the relationship between the change in dimension of the specimen in the direction of the externally applied stress and the magnitude of the applied stress. Values of stress usually are plotted as ordinates (vertically) and strain values as abscissa (horizontally).

Structural Element -- a generic element of a more complex structural member (for example, skin, stringer, shear panels, sandwich panels, joints, or splices).

Structured Data -- See Volume 1, Section 8.1.4.

Surfacing Mat -- A thin mat of fine fibers used primarily to produce a smooth surface on an organic matrix composite.

Symmetrical Laminate -- A composite laminate in which the sequence of plies below the laminate midplane is a mirror image of the stacking sequence above the midplane.

Tack -- Stickiness of the prepreg.

Tape -- Prepreg fabricated in widths up to 12 inches wide for carbon and 3 inches for boron. Cross stitched carbon tapes up to 60 inches wide are available commercially in some cases.

Tenacity -- The tensile stress expressed as force per unit linear density of the unstrained specimen i.e., grams-force per denier or grams-force per tex.

Tex -- A unit for expressing linear density equal to the mass or weight in grams of 1000 meters of filament, fiber, yarn or other textile strand.

Thermal Conductivity -- Ability of a material to conduct heat. The physical constant for quantity of heat that passes through unit cube of a substance in unit time when the difference in temperature of two faces is one degree.

Thermoplastic -- A plastic that repeatedly can be softened by heating and hardened by cooling through a temperature range characteristic of the plastic, and when in the softened stage, can be shaped by flow into articles by molding or extrusion.

Thermoset -- A class of polymers that, when cured using heat, chemical, or other means, changes into a substantially infusible and insoluble material.

Tolerance -- The total amount by which a quantity is allowed to vary.

Tolerance Limit -- A lower (upper) confidence limit on a specified percentile of a distribution. For example, the B-basis value is a 95% lower confidence limit on the tenth percentile of a distribution.

Tolerance Limit Factor -- The factor which is multiplied by the estimate of variability in computing the tolerance limit.

Toughness -- A measure of a material's ability to absorb work, or the actual work per unit volume or unit mass of material that is required to rupture it. Toughness is proportional to the area under the load-elongation curve from the origin to the breaking point.

Tow -- An untwisted bundle of continuous filaments. Commonly used in referring to man-made fibers, particularly carbon and graphite fibers, in the composites industry.

Transformation -- A transformation of data values is a change in the units of measurement accomplished by applying a mathematical function to all data values. For example, if the data is given by x , then $y = x + 1$, x , $1/x$, $\log x$, and $\cos x$ are transformations.

Transition, First Order -- A change of state associated with crystallization or melting in a polymer.

Transversely Isotropic -- Descriptive term for a material exhibiting a special case of orthotropy in which properties are identical in two orthotropic dimensions, but not the third; having identical properties in both transverse directions but not the longitudinal direction.

Traveller -- A small piece of the same product (panel, tube, etc.) as the test specimen, used for example to measure moisture content as a result of conditioning.

Twist -- The number of turns about its axis per unit of length in a yarn or other textile strand. It may be expressed as turns per inch (tpi) or turns per centimeter (tpcm).

Twist, Direction of -- The direction of twist in yarns and other textile strands is indicated by the capital letters S and Z. Yarn has S twist if, when held in a vertical position, the visible spirals or helices around its central axis are in the direction of slope of the central portion of the letter S, and Z twist is in the other direction.

Twist multiplier -- The ratio of turns per inch to the square root of the cotton count.

Typical Basis -- A typical property value is a sample mean. Note that the typical value is defined as the simple arithmetic mean which has a statistical connotation of 50% reliability with a 50% confidence.

Unbond -- An area within a bonded interface between two adherends in which the intended bonding action failed to take place. Also used to denote specific areas deliberately prevented from bonding in order to simulate a defective bond, such as in the generation of quality standards specimens. (See **Disbond**, **Debond**).

Unidirectional Fiber-Reinforced Composite -- Any fiber-reinforced composite with all fibers aligned in a single direction.

Unit Cell -- The term applied to the path of a yarn in a braided fabric representing a unit cell of a repeating geometric pattern. The smallest element representative of the braided structure.

Unstructured Data -- See Volume 1, Section 8.1.4.

Upper Confidence Limit -- See **Confidence Interval**.

Vacuum Bag Molding -- A process in which the lay-up is cured under pressure generated by drawing a vacuum in the space between the lay-up and a flexible sheet placed over it and sealed at the edges.

Variance -- See **Sample Variance**.

Viscosity -- The property of resistance to flow exhibited within the body of a material.

Void - Any pocket of enclosed gas or near-vacuum within a composite.

Warp -- The longitudinally oriented yarn in a woven fabric (see **Fill**); a group of yarns in long lengths and approximately parallel.

Wet Lay-up -- A method of making a reinforced product by applying a liquid resin system while or after the reinforcement is put in place.

Weibull Distribution (Two - Parameter) -- A probability distribution for which the probability that a randomly selected observation from this population lies between a and b ($0 < a < b < \infty$) is given by Equation 1.7(d) where α is called the scale parameter and β is called the shape parameter. (See Volume 1, Section 8.1.4.)

$$\exp\left[-\left(\frac{a}{\alpha}\right)^\beta\right] - \exp\left[-\left(\frac{b}{\alpha}\right)^\beta\right] \quad 1.4(d)$$

Wet Lay-up -- A method of making a reinforced product by applying a liquid resin system while the reinforcement is put in place.

Wet Strength -- The strength of an organic matrix composite when the matrix resin is saturated with absorbed moisture. (See **Saturation**).

Wet Winding -- A method of filament winding in which the fiber reinforcement is coated with the resin system as a liquid just prior to wrapping on a mandrel.

Whisker -- A short single crystal fiber or filament. Whisker diameters range from 1 to 25 microns, with aspect ratios between 100 and 15,000.

Winding -- A process in which continuous material is applied under controlled tension to a form in a predetermined geometric relationship to make a structure.

Discussion: A matrix material to bind the fibers together may be added before, during or after winding. Filament winding is the most common type.

Work Life -- The period during which a compound, after mixing with a catalyst, solvent, or other compounding ingredient, remains suitable for its intended use.

Woven Fabric Composite -- A major form of advanced composites in which the fiber constituent consists of woven fabric. A woven fabric composite normally is a laminate comprised of a number of laminae, each of which consists of one layer of fabric embedded in the selected matrix material. Individual fabric laminae are directionally oriented and combined into specific multiaxial laminates for application to specific envelopes of strength and stiffness requirements.

Volume 3, Chapter 1 General Information

Yarn -- A generic term for strands or bundles of continuous filaments or fibers, usually twisted and suitable for making textile fabric.

Yarn, Plied -- Yarns made by collecting two or more single yarns together. Normally, the yarns are twisted together though sometimes they are collected without twist.

Yield Strength -- The stress at which a material exhibits a specified limiting deviation from the proportionality of stress to strain. (The deviation is expressed in terms of strain such as 0.2 percent for the Offset Method or 0.5 percent for the Total Extension Under Load Method.)

X-Axis -- In composite laminates, an axis in the plane of the laminate which is used as the 0 degree reference for designating the angle of a lamina.

X-Y Plane -- In composite laminates, the reference plane parallel to the plane of the laminate.

Y-Axis -- In composite laminates, the axis in the plane of the laminate which is perpendicular to the x-axis.

Z-Axis -- In composite laminates, the reference axis normal to the plane of the laminate.

REFERENCES

- 1.3(a) Military Standardization Handbook, *"Metallic Materials and Elements for Aerospace Vehicle Structures,"* MIL-HDBK-5F, 1 November 1990.
- 1.3(b) *DOD/NASA Advanced Composites Design Guide*, Air Force Wright Aeronautical Laboratories, Dayton, OH, prepared by Rockwell International Corporation, 1983 (distribution limited).
- 1.3(c) ASTM E 206, "Definitions of Terms Relating to Fatigue Testing and the Statistical Analysis of Fatigue Data," *1984 Annual Book of ASTM Standards*, Vol 3.01, ASTM, Philadelphia, PA, 1984.
- 1.3.2(a) ASTM E 380, "Standard for Metric Practice," *1984 Annual Book of ASTM Standards*, Vol 14.01, ASTM, Philadelphia, PA, 1984.
- 1.3.2(b) *Engineering Design Handbook: Metric Conversion Guide*, DARCOM P 706-470, July 1976.
- 1.3.2(c) *The International System of Units (SI)*, NBS Special Publication 330, National Bureau of Standards, 1986 edition.
- 1.3.2(d) *Units and Systems of Weights and Measures, Their Origin, Development, and Present Status*, NBS Letter Circular LC 1035, National Bureau of Standards, November 1985.
- 1.3.2(e) *The International System of Units Physical Constants and Conversion Factors*, NASA Special Publication 7012, 1964.

This page intentionally left blank

CHAPTER 2 MATERIALS AND PROCESSES - THE EFFECTS OF VARIABILITY ON COMPOSITE PROPERTIES

2.1 INTRODUCTION

The properties of organic matrix composites are, in general, cure and process dependent. This may result in variations of glass transition (service temperature), corrosion stability, susceptibility to micro-cracking, general strength, or fatigue and service life. In addition, in most cases these materials or structural elements constructed from them are the products of complex multi-step materials processes. Figures 2.1(a) and (b) illustrate the nature of the processing pipeline from raw materials to composite end item. Each rectangle in Figure 2.1(b) represents a process during which additional variability may be introduced into the material. Utilization of a standard composite material property database necessitates an understanding of the dependency of the measured material properties on the characteristics and variability associated with the constituent materials and the sequence of processes used to combine these materials into end products. As a result, development and application of processing controls are essential to achieve the desired mechanical and physical properties for composite structures.

2.2 PURPOSE

The purpose of this chapter is to provide an understanding of the origins and nature of process-induced variability in these materials in the context of an overview of types of composite materials and the associated material processing methodologies. It also seeks to address various approaches to minimizing variability, including implementation of process control, and the use of materials and processing specifications.

2.3 SCOPE

This chapter includes descriptions of composite materials from the perspective of their introduction into the material pipeline as the constituent raw material, subsequent conversion of raw materials into intermediate product forms such as prepregs, and finally the utilization of these intermediate product forms by fabricators to process the materials further to form completed composite structures. Emphasis is placed on the cumulative effects that each processing phase in the pipeline contributes to the final products general quality as well as physical, chemical, and mechanical properties. Finally it includes an overview of common process control schemes and discusses preparation of materials and processing specifications.

2.4 CONSTITUENT MATERIALS

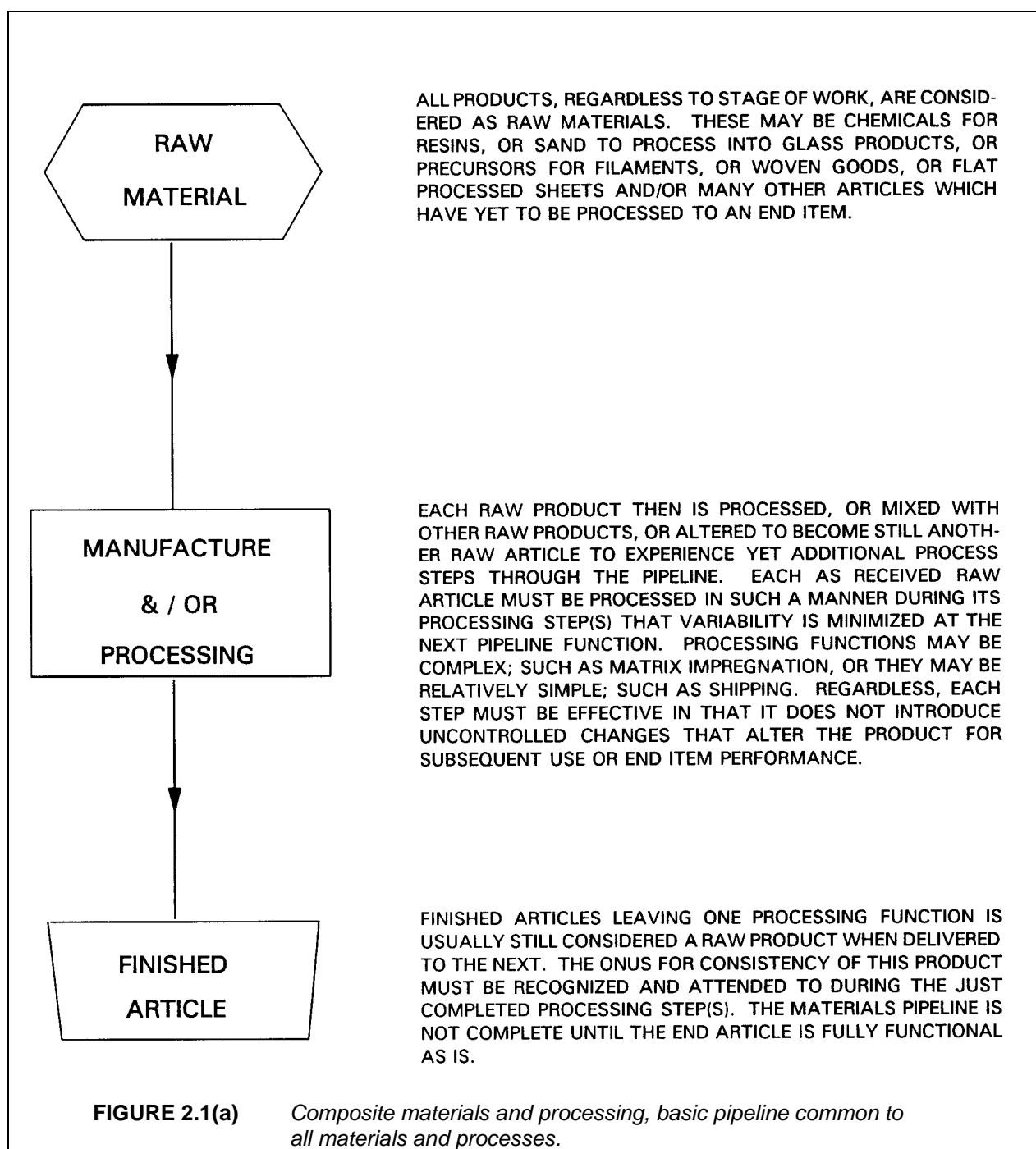
2.4.1 Fibers

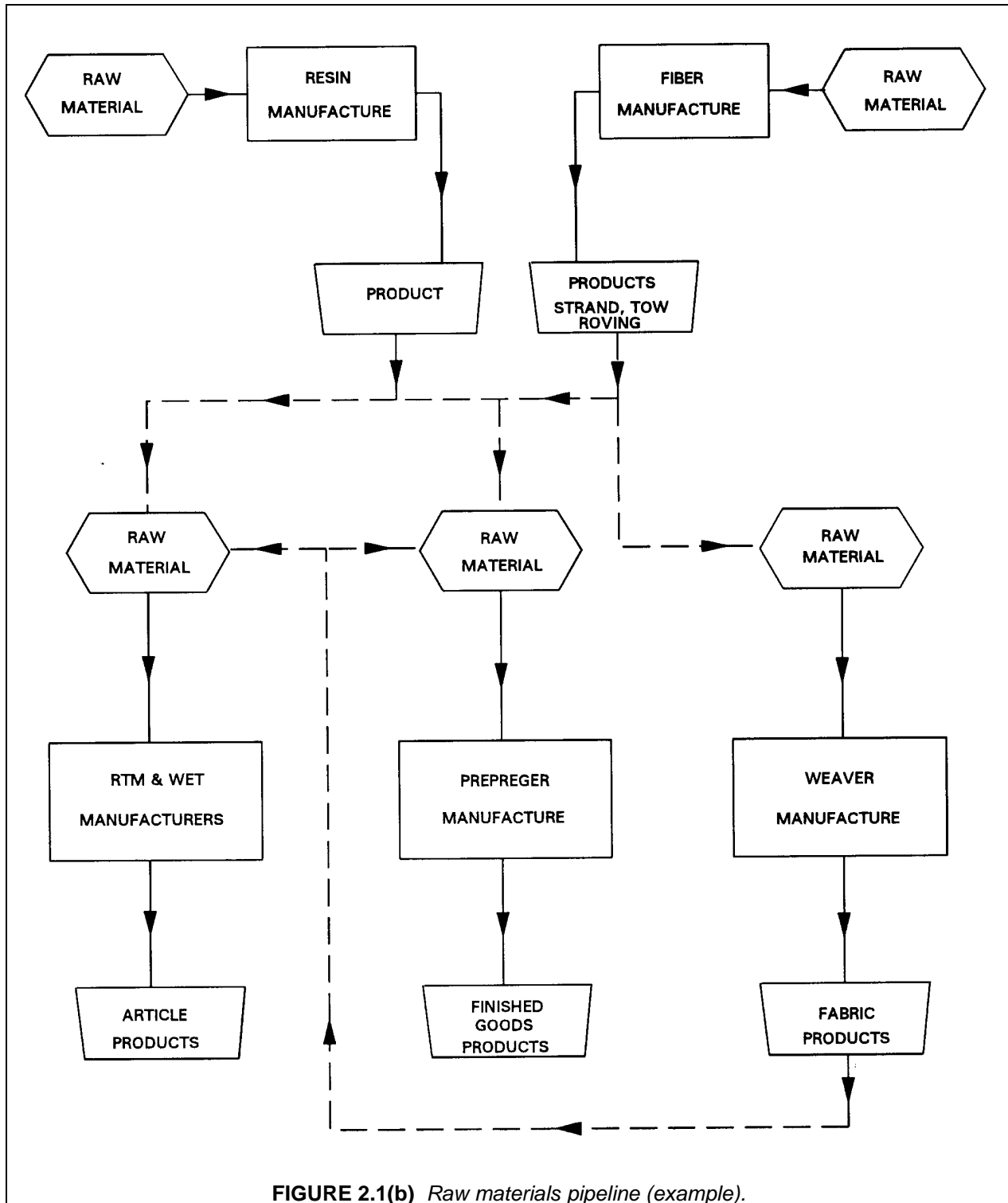
2.4.1.1 Carbon and graphite fibers

Carbon and graphite have substantial capability as reinforcing fibers, with great flexibility in the properties that can be provided. Primary characteristics for reinforcing fibers in polymer matrix composites are high stiffness and strength. The fibers must maintain these characteristics in hostile environments such as elevated temperatures, exposure to common solvents and fluids, and environmental moisture. To be used as part of a primary structure material it should also be available as continuous fiber (Reference 2.4.1.1). These characteristics and requirements have substantial implications for the physical, chemical and mechanical properties of the fiber, which in turn implies processing and acceptance parameters.

2.4.1.1.1 Carbon vs. graphite

Interest in carbon fibers for structural materials was initiated in the late 1950s when synthesized ray-
ons in textile form were carbonized to produce carbon fibers for high temperature missile applications
(Reference 2.4.1.1.1). One of the first distinctions to be made is the difference between carbon and
graphite fibers, although the terms are frequently used interchangeably. Background information for these
differences is contained in the following sections. The primary purpose of making this distinction here is to
alert the reader that users may mean different things when referring to graphite versus carbon fibers.





Carbon and graphite fibers are both based on graphene (hexagonal) layer networks present in carbon. If the graphene layers or planes stack with three dimensional order the material is defined as graphite (Reference 2.4.1.1.1). Usually extended time and temperature processing is required to form this order, making graphite fibers more expensive. Because the bonding between planes is weak, disorder frequently occurs such that only the two dimensional ordering within the layers is present. This material is

defined as carbon (Reference 2.4.1.1.1). With this distinction made, it should be understood that while some differences are implied, there is not a single condition which strictly separates carbon from graphite fibers, and even graphite fibers retain some disorder in their structure.

2.4.1.1.2 General material description

Three different precursor materials are commonly used at present to produce carbon fibers: rayon, polyacrylonitrile (PAN), and isotropic and liquid crystalline pitches (Reference 2.4.1.1.1). Carbon fibers are made predominately from carbonization of PAN. The fibers consist of intermingled fibrils of turbostratic graphite with basal planes tending to align along the fiber axis. This forms an internal structure reminiscent of an onion skin. Pitch fibers may have a different internal structure, more like sheafs or spokes (Reference 2.4.1.1).

The highly anisotropic morphology gives rise to moduli in the range of 200-750 GPa parallel to the fiber long axis, and around 20 GPa in the normal direction. For comparison, single crystal (whisker) of graphite is about 1060 and 3 GPa, respectively, but these properties are not attainable in fiber form. Ultra high modulus fibers can be prepared from liquid-crystalline mesophase pitch; the higher degree of orientation in the precursor translates through to the final carbonized fiber leading to larger and more oriented graphite crystallites.

2.4.1.1.3 Processing

High stiffness and strength implies strong interatomic and intermolecular bonds and few strength limiting flaws (Reference 2.4.1.1). Carbon fiber properties are dependent on the fiber microstructure, which is extremely process dependent, such that properties of fibers with the same precursor but different processing can be dramatically different. The precursor itself can also change these properties. The processing may be optimized for high modulus or strength, or traded off with economics.

2.4.1.1.3.1 Manufacture

The manufacturing process for carbon fiber described below is for the PAN variant, which is one of the most common. Some differences between PAN processing and the pitch and rayon precursors are then described afterwards. The manufacture of PAN based carbon fiber can be broken down into the white fiber and black fiber stages. Most manufacturers consider the details of these processes proprietary.

2.4.1.1.3.1.1 White fiber

Production of PAN precursor, or white fiber, is a technology in itself. Fairly conventional fiber processes are performed: polymerization, spinning, drawing, and washing. Additional drawing stages may be added in the process. Characteristics of the white fiber influence the processing and results for the black fiber processing.

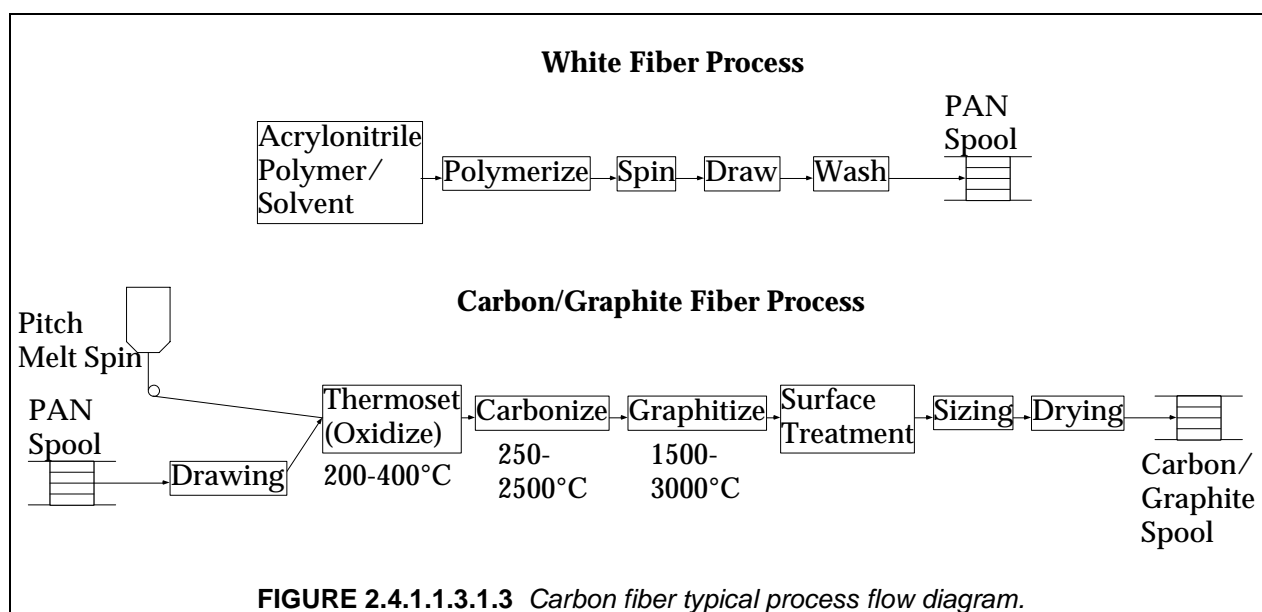
2.4.1.1.3.1.2 Black fiber

The black fiber process consists of several steps: oxidation (or thermosetting), pyrolysis (or carbonizing), surface treatment, and sizing. In the oxidation process the PAN fiber is converted to a thermoset from a thermoplastic. For this oxidation process the fiber diameter is limited by waste gas diffusion. In the pyrolysis process, which is performed under an inert atmosphere, most of the non-carbon material is expelled, forming ribbons of carbon aligned with the fiber axis.

In the surface treatment step the fiber may be etched in either gas or liquid phase by oxidizing agents such as chlorine, bromine, nitric acid or chlorates. This improves the wettability for the resin and encourages formation of a strong, durable bond. Some additional improvement through removal of surface flaws may also be realized. This process can be electrolytic. The carbon fibers are often treated with solution of unmodified epoxy resin and/or other products as a size. The sizing prevents fiber abrasion, improves handling, and can provide an epoxy matrix compatible surface.

2.4.1.1.3.1.3 Carbon fiber differences due to pitch/PAN/rayon precursors

As a rule PAN precursor can provide higher strength carbon fibers, while pitch can provide higher moduli. Rayon based fibers tend to be less expensive but lower performance. Pitch fiber composites have been prepared with elastic moduli superior to steel, and electrical conductivity higher than copper conductor. The shear strengths and impact resistance are degraded, however (Reference 2.4.1.1.3.1.3). Yield for PAN is approximately 50%, but for pitch can be as high as 90%.



2.4.1.1.3.2 Processing to microstructure

Carbon fiber properties are driven by the type and extent of defects, orientation of the fiber, and the degree of crystallinity. The precursor makeup and heat treatment can affect the crystallinity and orientation. The defect content can be driven by contaminants and processing. Orientation is also greatly affected by the drawing process which may be repeated many times in the processing of the fibers.

2.4.1.1.3.3 Microstructure to properties

The strength of a brittle material is frequently controlled by presence of flaws, their number and magnitude. The probability of finding a flaw is volume dependent, thus a fiber with a lower volume per unit length appears stronger. Elimination of defects drives tensile strength up, and also improves thermal and electrical conductivity, and oxidation resistance. However, increasing crystallinity too far can degrade fiber strength and modulus.

2.4.1.1.3.4 Testing

As with most composite material properties, the values obtained are greatly dependent on the testing performed. Determination of fiber modulus can be especially controversial. The stress/strain response can be nonlinear, so where and how measurements are taken can greatly influence the results. As a result, fibers which may appear to be substantially different in the literature may have little or no difference in modulus. Reported differences may be entirely the result of test and calculation differences. Chapter 3 in Volume I can be referenced for more information of fiber test methods.

2.4.1.1.4 Typical properties

Typically limitations on the end use for carbon fibers in composite structure depend more on the resin matrix than the fiber. Some exceptions to this are present, however, in which case the oxidative stability, thermal conductivity, coefficient of thermal expansion, or other properties of the fiber must be taken into account. Some key properties for carbon fiber, including cost, are listed in Table 2.4.1.1.4. Typical values for glass, aramid, and boron are shown for comparison. While some carbon fiber properties are fairly universal, different products from different manufacturers can have substantially different properties. Three of the major manufacturers for the US are Amoco, Hercules and Toray. It should be noted that translation of fiber properties to composite properties is dependent on many factors in addition to rule of mixtures.

TABLE 2.4.1.1.4 Comparison of carbon and other fiber properties.

	Tensile Modulus, Msi	Tensile Strength, ksi	Density, g/cm ³	Fiber Diameter, micron	Cost, \$/#
Carbon (PAN)	30-50	350-1000	1.75-1.90	4-8	20-100
Carbon (Pitch)	25-110	200-450	1.90-2.15	8-11	40-200
Carbon (Rayon)	6	150	1.6	8-9	5-25
Glass	10-12.5	440-670	2.48-2.62	30	5-40
Aramid	20	410	1.44	--	25-75
Boron	58	730-1000	2.3-2.6	100-200	100-250

2.4.1.2 Aramid

In the early 1970's, Du Pont Company introduced Kevlar™ aramid, an organic fiber with high specific tensile modulus and strength. This was the first organic fiber to be used as a reinforcement in advanced composites. Today this fiber is used in various structural parts including reinforced plastics, ballistics, tires, ropes, cables, asbestos replacement, coated fabrics, and protective apparel. Aramid fiber is manufactured by extruding a polymer solution through a spinneret. Major forms available from Du Pont are continuous filament yarns, rovings, chopped fiber, pulp, spun-laced sheet, wet-laid papers, thermoplastic-impregnated tows, and thermoformable composite sheets.

Important generic properties of aramid fibers are: low density, high tensile strength, high tensile stiffness, low compressive properties (nonlinear), and exceptional toughness characteristics. The density of aramid is 0.052 lb/in³ (1.44 gm/cm³). This is about 40% lower than glass and about 20% lower than commonly used carbon. Aramids do not melt and they decompose at about 900°F (500°C). Tensile strength of yarn, measured in twisted configuration, can be varied from 500 - 600 ksi (3.4 - 4.1 GPa) by choosing different types of aramids. The nominal coefficient of thermal expansion is 3×10^{-6} in/in/°F (-5×10^{-6} m/m/°C) in the axial direction. Aramid fibers, being aromatic polyamide polymers, have high thermal stability and dielectric and chemical properties. Excellent ballistic performance and general damage tolerance is derived from fiber toughness. Aramid is used, in fabric or composite form, to achieve ballistic protection for humans, armored tanks, military aircraft, and so on.

Composite systems, reinforced with aramid, have excellent vibration-damping characteristics. They resist shattering upon impact. Temperature of use, in composite form with polymer matrix, range from -33 to 390°F (-36 - 200°C). The nominal tensile properties of composites reinforced with aramid are listed in Table 2.4.1.2(a) - in thermoset (Reference 2.4.1.2(a)) and thermoplastic (Reference 2.4.1.2(b)) resin matrix. At 60% fiber volume fraction, composites of epoxy reinforced with aramid fibers have nominal tensile

strength (room temperature) of 200 ksi (1.4 GPa) and nominal tensile modulus of 11 Msi (76 GPa). These composites are ductile under compression and flexure. Ultimate strength, under compression or flexure, is lower than glass or carbon composites. Composite systems, reinforced with aramid, are resistant to fatigue and stress rupture. In the system of epoxy reinforced with aramid, under tension/tension fatigue, unidirectional specimens ($V_f \sim 60\%$) survive 3,000,000 cycles at 50% of their ultimate stress (Reference 2.4.1.2(a)). Recently, thermoplastic resin composites reinforced with aramid have been developed. These thermoplastic composite systems have exhibited equivalent mechanical properties compared to similar thermoset systems (Reference 2.4.1.2(b)). In addition, thermoplastic systems provide potential advantages in economical processing (Reference 2.4.1.2(c)), bonding, and repair. A unique thermoformable sheet product, in thermoplastic matrix reinforced with aramid fibers, is available (Reference 2.4.1.2(d)). These composite systems are also used to achieve low coefficient of thermal expansion or high wear resistance. They are non-conductive and exhibit no galvanic reaction with metals. Aramid fibers are available in several forms with different fiber modulus (Table 2.4.1.2(b)). Kevlar™29 has the lowest modulus and highest toughness (strain to failure $\sim 4\%$). These fibers are used mostly in ballistics and other soft composite systems such as cut- and slash- resistance protective apparel, ropes, coated fabric, asbestos replacement, pneumatic tires, etc. These are also used for composites where maximum impact and damage tolerance is critical and stiffness is less important. Kevlar™49 is predominantly used in reinforced plastics - both in thermoplastic and thermoset resin systems. It is also used in soft composites like core of fiber optic cable and mechanical rubber good systems (e.g., high pressure flexible hose, radiator hose, power transmission belts, conveyor belts, etc.). An ultra-high modulus Type 149 has been made available recently. It has 40% higher modulus than Kevlar™49. Kevlar™29 is available in fiber yarn sizes and two rovings sizes. Kevlar™49 is available in six yarn and two rovings sizes. Kevlar™149 is available in three yarn sizes. Yarn sizes range from the very fine 55 denier (30 filaments) to 3000 denier (1300 filaments). Rovings are 4560 denier (3072 filaments) and 7100 denier (5000 filaments). Composite thermoplastic tows, several types of melt-impregnated thermoplastic reinforced with different Kevlar™ yarns and deniers, are also available.

TABLE 2.4.1.2(a) *Nominal composite properties reinforced with aramid fiber ($V_f \sim 60\%$).*

Tensile Property	Units	Thermoset (epoxy)		Thermoplastic (J2)	
		unidirectional	fabric ¹	unidirectional	fabric ¹
Modulus	Msi (GPa)	11 (68.5)	6 (41)	10.5-11.5 (73-79)	5.1-5.8 (35-40)
Strength	ksi (GPa)	200 (1.4)	82 (0.56)	180-200 (1.2-1.4)	77-83 (0.53-0.57)

¹ Normalized from $V_f = 40\%$; fabric style S285

Aramid composites were first adopted in applications where weight savings were critical - for example, aircraft components, helicopters, space vehicles, and missiles. Armor applications resulted from the superior ballistic and structural performance. In marine recreational industries, light weight, stiffness, vibration damping, and damage tolerance are valued. Composites reinforced with aramids are used in the hulls of canoes, kayaks, and sail and power boats. These same composite attributes have led to use in sports equipment. Composite applications of aramid continue to grow as systems are developed to capitalize on other properties. The stability and frictional properties of aramids at high temperatures have led to brake, clutch, and gasket uses; low coefficient of thermal expansion is being used in printed wiring boards; and exceptional wear resistance is being engineered into injection-molded thermoplastic industrial parts. Melt-impregnated thermoplastic composites, reinforced with aramids, offer unique processing advantages - e.g., in-situ consolidation of filament-wound parts. These can be used for manufacturing thick parts where processing is otherwise very difficult (Reference 2.4.1.2(e)).

TABLE 2.4.1.2(b) *Nominal properties of aramid fiber.*

Tensile Property	Units	Type of Kevlar™		
		29	49	149
Modulus	Msi (GPa)	12 (83)	18 (124)	25 (173)
Strength	ksi (GPa)	525 (3.6)	525-600 (3.6-4.1)	500 (3.4)

Aramid fiber is relatively flexible and tough. Thus it can be combined with resins and processed into composites by most of the methods established for glass. Yarns and rovings are used in filament winding, prepreg tape, and in pultrusion. Woven fabric prepreg is the major form used in thermoset composites. Aramid fiber is available in various weights, weave patterns, and constructions; from very thin (0.0002 in., 0.005mm) lightweight (275 gm/m²) to thick (0.026 in., 0.66 mm) heavy (2.8 gm/m²) woven roving. Thermoplastic-impregnated tows can be woven into various types of fabrics to form prepregs. These composites demonstrate good property retention under hot and humid conditions (Reference 2.4.1.2(f)). Chopped aramid fiber is available in lengths from 6 mm to 100 mm. The shorter lengths are used to reinforce thermoset, thermoplastic, and elastomeric resins in automotive brake and clutch linings, gaskets, and electrical parts. Needle-punched felts and spun yarns for asbestos replacement applications are made from longer fiber staple. A unique very short fiber (0.08 - 0.16 in., 2 - 4 mm) with many attached fibrils is available (aramid pulp). It can provide efficient reinforcement in asbestos replacement uses. Aramid short fibers can be processed into spun-laced and wet-laid papers. These are useful for surfacing veil, thin-printed wiring boards, and gasket material. Uniform dispersion of aramid short fiber in resin formulations is achieved through special mixing methods and equipment. Inherent fiber toughness necessitates special types of tools for cutting fabrics and machining aramid composites.

2.4.1.3 Glass

Glass in the forms used in commerce has been produced by many cultures since the early Etruscan civilization. Glass as a structural material was introduced early in the seventeenth century and became widely used during the twentieth century as the technology for flat pane was perfected. Glass fibrous usage for reinforcement was pioneered in replacement of metals and used for both commercial and military uses with the advent of formulation control and molten material which is die or bushing pulled into continuous filaments. These events lead to a wide range of aerospace and commercial high performance structural applications still in use today.

2.4.1.3.1 Chemical description

Glass is derived from one of our most abundant natural resources--sand. Other than for, possibly, transport and the melting process, it is not petro-chemical dependent. For purposes of this handbook the typical glass compositions are for electrical/Grade "E" glass, a calcium aluminoborosilica composition with an alkali content of less than 2%, chemical resistant "C" glass composed of soda-lime-borsilicates and high strength S-2 glass which is a low-alkali magnesi-alumina-silicate composition (See Table 2.4.1.3.1). Surface treatments (binders/sizing) can be applied directly to the filaments during the pulling step. Organic binders, such as starch oil, are applied to provide optimum weaving and strand protection during weaving of fabrics or "greige goods". These type binders are then washed and heat cleaned off the fabrics for finishing or sizing at the weaver with coupling agents to improve compatibility with resins. (See

Figure 2.4.1.3.1) The exception to this process for fabrics is when they are heat treated or "caramelized", which converts the starch to carbon (0.2 - 0.5%). Glass roving products (untwisted) type yarns are most often directly finished with the final coupling agents during the filament manufacturing step. Therefore, the products will be identified with the glass manufacturer's product codes and the desizing step is not necessary as common with fabric "greige goods" forms. Heat cleaned products are also available where the product is essentially pure glass. These products, which are subject to damage, are commonly utilized for silicone laminates. Another finish designation is applicable to the heat cleaned product when it is followed with a demineralized water wash (neutral pH). More common for structural applications are the coupling agents which are applied for use with standard organic polymers. During the 1940's Volan¹ finishes were introduced. Since then, many variations/improvements identified with various company designations have appeared. Perhaps the most recognized is Volan A. This finish provides good wet and dry strength properties in use with polyester, epoxy, and phenolic resins. Prior to the application of this finish the clean(ed) glass is saturated with methacrylate chromic chloride so that the chrome content of the finish is between 0.03% and 0.06%. This addition enhances wet-out of the resin during cure. Perhaps more typically called out for use, but not limited to, with epoxy are the silane finishes. Most all are formulated to enhance laminate wet-out. Some also produce high laminate clarity or good composite properties in aqueous environments. Others improve high-pressure laminating, or resist adverse environment or chemical exposures. Although other finishes are used in combination with matrix materials other than epoxy, finishes may have proprietary formulations or varied designations relative to the particular glass manufacturer or weaver, it is believed the compositions are readily available to the resin compounders (prepreggers) to determine compatibility and end use purposes. Note that, non-compatible finishes are purposely applied for ornament applications.

2.4.1.3.2 *Physical forms available*

Due to the high quantity of commercial applications for glass products, there are many product forms available. For purposes of this publication glass forms will be limited to continuous filament product forms. These forms fall into four major categories. They are continuous rovings, yarn for fabrics or braiding, mats, and chopped strand. (See Figure 2.4.1.3.2 and ASTM Specification D 579, Reference 2.4.1.3.2(a) for information on glass fabrics. Further discussion of fabrics may be found in Section 2.5.1 on fabrics and preforms.) They are available with a variety of physical surface treatments and finishes. Most structural applications utilize fabric, roving, or rovings converted to unidirectional tapes. Perhaps the most versatile fiber type to produce glass product forms is "E" glass. "E" glass is identified as such for electrical applications. This type or grade of glass has eight or more standardized filament diameters available. These range from 1.4 to 5.1 mils (3.5 to 13 micrometers). (See Table I, ASTM Specification D 578, Reference 2.4.1.3.2(b).) This facilitates very thin product forms. The "S" glasses are identified as such to signify high strength. The S-2 type glasses are available with but one filament diameter. This does not limit the availability of basic structural fabric styles for S-2 glass however. Although there are more "E" roving products, as to yields, available, this has not noticeably restricted the use of S-2 type roving products or roving for unidirectional tape. S-2 type rovings are available in yields of 250, 750, and 1250 yards per lb (500, 1500, and 2500 m/kg). Although woven rovings may be considered a fabric product form it should be noted for its importance for military applications. Also, there are glass product forms which could be considered as complimentary products for advanced structures. These would include milled fibers and chopped strand.

¹E. I. Du Pont de Nemours

TABLE 2.4.1.3.1 *Typical chemical compositions of glass fiber.*

	% (wt)	E-Glass	S-2 Glass (Nominals)	H _R Glass (B)
Silicon Dioxide (SiO ₂)		52-56 (A)	65	63.5 - 65.0
Aluminum Oxide (Al ₂ O ₃)		12-16 (A)	25	24.0 - 25.5
Boron Oxide (B ₂ O ₃)		5-10 (A)		
Calcium Oxide (CaO)		16-25 (A)		<0.5
Magnesium Oxide (MgO)		0-5 (A)	10	9.5 - 10.5
Lithium Oxide (Li ₂ O)				
Potassium Oxide (K ₂ O)	O.C.	0.0-0.2		
Sodium Oxide (Na ₂ O)	O.C.	0-2		
Titanium Oxide (TiO ₂)	O.C.	0-1.5		
Cerium Oxide (CeO ₂)				
Zirconium Oxide (Zr ₂ O ₂)				
Beryllium Oxide (BeO)				
Iron Oxide (Fe ₂ O ₃)	O.C.	0.0-0.8		
Fluorine (F ₂)	O.C.	0.0-0.1		
Sulfate (SO ₂)				
Alkaline Oxides	PPG	0.5-1.5		
Calcium Fluoride (CAF)	PPG	0.0-0.8		
Finishes/Binders		0.5/3.0		

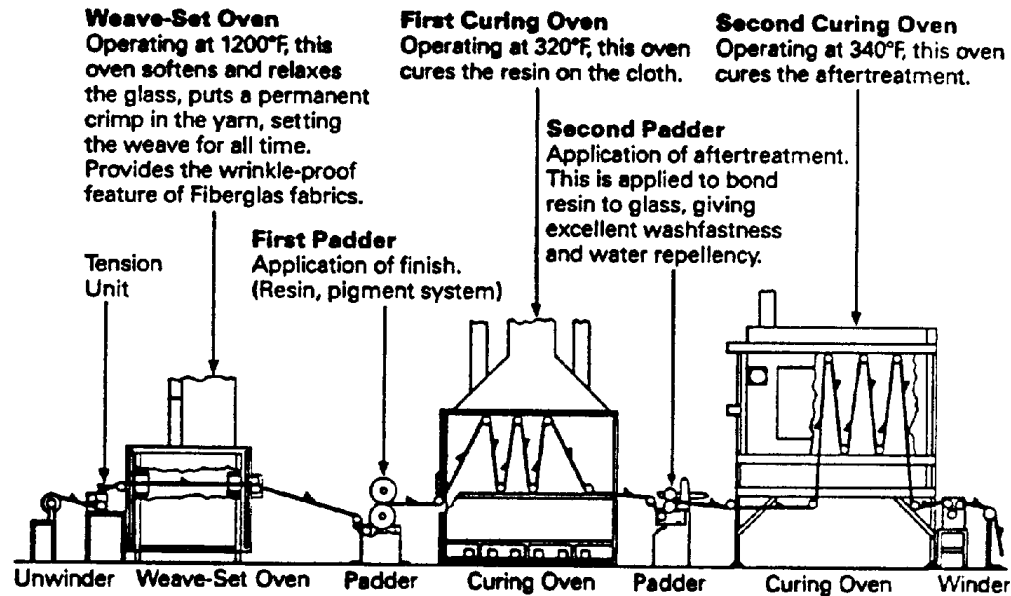


FIGURE 2.4.1.3.1 Fabric finishing (Reference 2.4.1.3.1(c)).

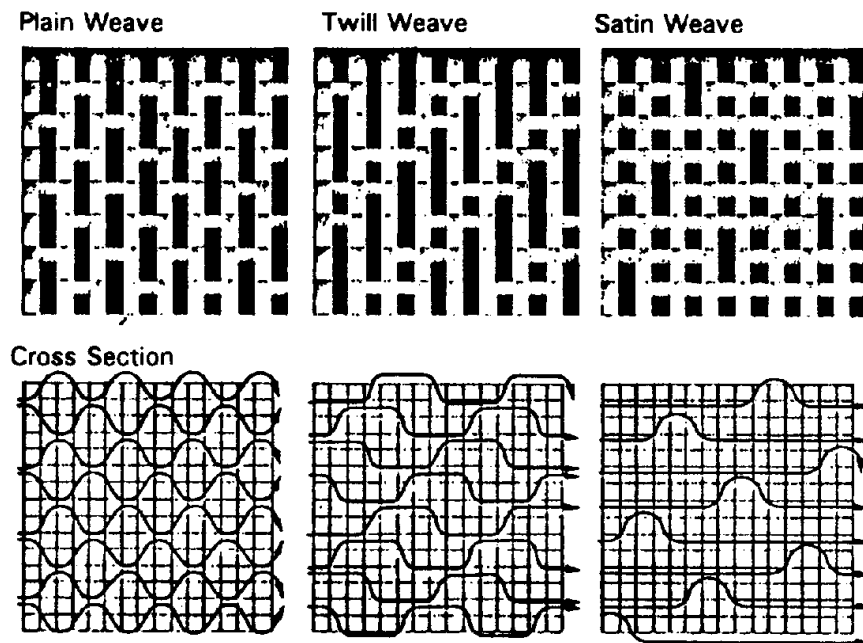


FIGURE 2.4.1.3.2 Common types of weaves for glass fabrics (Reference 2.4.1.3.1(c)).

2.4.1.3.3 Advantages and disadvantages

For many years glass composites have had a distinct strength to weight advantage. Although the rapid evolution of carbon and aramid fibers have gained advantages, glass composite products have still prevailed in certain applications. Cost per weight or volume, certain armament applications, chemical or galvanic corrosion resistance, electrical properties, and availability of many product forms remain as examples of advantage. Coefficient of thermal expansion and modulus properties compared to carbon composites may be considered as typical disadvantages. When compared to aramid composites, glass has a disadvantage as to tensile properties but an advantage as to ultimate compression, shear properties, and moisture pick-up.

Commercial uses for glass products are many-fold. These include filtration devices, thermal and electrical insulation, pressure and fluid vessels, and structural products for automotive and recreation vehicles. Many uses are applicable to military and aerospace products as well. A partial listing would include: asbestos replacement, circuitry, optical devices, radomes, helicopter rotor blades, and ballistic applications. Because of the many product forms, structural applications are limitless to fabricate. If there are limitations, compared to other fibers, they may include low thermal and electrical conductivity or perhaps melting temperatures when compared to carbon fibers.

Typical properties for glass fibers and composite materials reinforced with continuous glass fibers are shown in Tables 2.4.1.3.3(a)-(d).

TABLE 2.4.1.3.3(a) Typical glass fiber electrical properties.

	E	S-2	H _R
Density			
lb/in ³	0.094	0.089	0.090
g/cm ³	2.59	2.46	2.49
Tensile Strength			
ksi	500	665	665
MPa	34,450	45,818	45,818
Modulus of Elasticity			
Msi	10.5	12.6	12.6
GPa	72.35	86.81	86.81
% Ult. Elongation	4.8	5.4	5.4
Dielectric Constant			
73°F (23°C) @ 1 MHZ	6.3-6.7	4.9-5.3	NA

Unburdened costs vary pending product forms and glass types. Typical yield certified "E" glass rovings cost \$1.40 per lb., whereas certified S-2 type 750 yield rovings average \$6.30 per lb. Lower costing for rovings are experienced with rail car purchases. Typical unburdened fabric costs also vary by weave and fiber type. "E" glass 120 style averages \$13.10 per lb., 7781 averages \$4.35 per lb., S-2 type 6781 style is \$8.40 per lb.

TABLE 2.4.1.3.3(b) *Typical glass fiber thermal properties.*

	E	S-2	S _R
Coeff. Thermal Expan. 10 ⁶			
in/in/F°	2.8	1.3	
m/m/C°	5.1	2.6	
Softening Point °F (°C)	1530 (832)	1810 (988)	1778 (970.)
Annealing Point °F (°C)	1210 (654)	1510 (821)	1490 (810.)

TABLE 2.4.1.3.3(c) *Typical corrosion resistance of glass fibers (Wt. Loss %).*

Fluid	E	S-2	S _R
10% H ₂ SO ₄	42	6.8	NA
10% HCL	43	4.4	NA
10% HNO ₃	43	3.8	NA
H ₂ O (Distilled)	0.7	0.7	NA
10% Na OH	29	66	NA
10% KOH	23	66	NA

Conditions: 200°F (96°C) - one week immersion

TABLE 2.4.1.3.3(d) *Typical cured epoxy/glass mechanical properties.*

E Glass, Woven 7781 Style	Standard Structural	Dual Purpose Structural/Adhesive
Tensile Strength, ksi (MPa)	63 (430)	48 (330)
Tensile Modulus, Msi (GPa)	3.8 (36)	2.8 (19)
Compressive Strength, ksi (MPa)	60. (410)	50. (340)
Compressive Modulus, Msi (GPa)	3.6 (25)	3.2 (22)
Flexural Strength ksi, (MPa)	80. (550)	65 (450)
Flexural Modulus Msi, (GPa)	3.7 (26)	3.3 (23)
Interlaminar Shear ksi, (MPa)	2.6 (18)	3.8 (26)
Sandwich Peel, lb/in width (N/m width)	N.A.	30. (3.4)
Metal-to-Metal Peel, lb/lin. in. (N/lin. m)	N.A.	55 (6.3)
Specific Gravity gm/cm ³ (lb/in ³)	1.8 (0.065)	1.6 (0.058)
Cured Resin Content % Wt.	33	48

Reference: Fabric MIL-C-9084, VIII B
 Resin MIL-R-9300, Ty I MIL-A-25463, Ty I, C1 2

2.4.1.3.4 Common manufacture methods and variable

Most often raw products (and/additives) are mixed and are premelted into marbles. This form facilitates sampling for analysis but, more important, presents a raw product form for automated feeding to the individual melt furnaces. Another method is to feed, via hoppers, dried raw products directly to batch cans. Regardless of the raw form, the material is fed into furnaces to become molten at approximately 2800°F (1500°C). The molten mass flows onto plates which contain many bushings with small orifices from which the individual filaments are drawn. In some cases the individual bushings are heat controlled within <1F° (0.6C°). The diameter of the filaments is controlled by the viscosity of the glass melt and the rate of extrusion. Cooling or solidification occurs rapidly as the glass leaves the bushings in filament form under ambient conditions. Cooling is often added by water spray and/or application of the binders. The individual untwisted filaments are gathered and high speed wound on tubes or "cakes". Sometimes finishes are applied after the strands are wound on the tubes then conditioned (dried). For products common to this document the strands are "C" (continuous) filaments--not "S" (staple) filament. To produce rovings the strands are then creeled, unwound and gathered again to form ends or multiple untwisted strands. (See Table 2.4.1.3.4(a).) This process of gathering or combining is again repeated to form rovings of desired yields (yards per pound). For weaving of fabrics and braiding, the strands are twisted to form yarns. (See Table 2.4.1.3.4(b).) Single yarns are composed of single strands twisted by itself. Two (etc.) strand construction is two strands twisted to produce a single yarn. Plied yarns are made from twisting two or more yarns together. Twisting and plying is often referred to as "throwing". A variable in processing "C" filament products is the repeated tensioning required during the numerous product forms fabrication. Tensioning devices are used--such as: disc-type or "whirls", gate-type, tension bars or "S" bars, and compensating rolls in the delivery from the creels. Humidity is another controlled variable in the

twisting, plying, braiding, warping, slashing, gulling and weaving areas. These operations are facilitated to maintain a relative humidity of 60 to 70 percent range. During the glass processing operations surface abrasion is a factor which must be monitored. The many devices such as: guide eyes, spacer bars, rollers and such are subject to wear and must be maintained. Wear could also affect tensioning. These contact devices are manufactured from materials including: stainless steel, chromium plating, and ceramics.

Additional information can be found in References 2.4.1.3.4(a) - (c).

TABLE 2.4.1.3.4(a) Basic strand fiber designations and strand counts (Reference 2.4.1.3.1(c)).

Filament Diameter Designation		Strand Count (Number)		
SI (μm)	U.S. Customary (Letter)	TEX g/km	U.S. Customary	
			100 Yd. Cuts/Lb.	Yds./Lb.
5	D	11	450	45,000
7	E	22	225	22,500
9	G	733	150	15,000
10	H	45	110	11,000
13	K	66	75	7,500

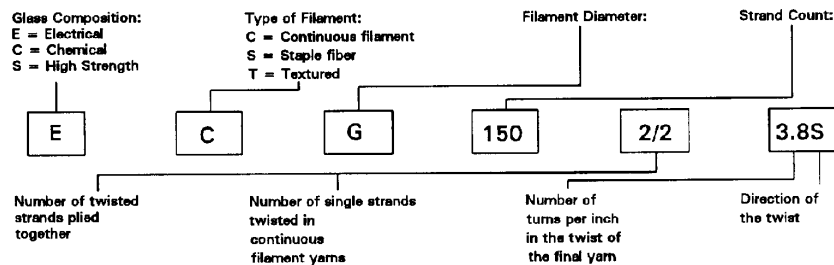
2.4.1.4 Boron

Elemental boron fiber is formed as a deposition reaction on a hot tungsten wire which is continuously drawn through a reactor containing BCl_3 and H_2 . The tungsten wire substrate also reacts to form tungsten boride in the core. The crystalline structure of the deposited boron is considered amorphous due to its small size (20\AA). Boron is available as a cylindrical fiber in two nominal diameters, 4- and 5.6-mil (0.10 and 0.14 mm), which have a density of 2.57 and 2.49 g/cm^3 (0.0929 and 0.0900 lb/in^3), respectively. Chemical etching of the fiber surface produces a higher strength, but the process is not used commercially.

Boron fiber is unmatched for its combination of strength, stiffness, and density. The tensile modulus and strength of boron fiber are 60×10^6 psi and 0.52×10^6 psi (40 GPa and 3600 MPa). Thermal conductivity and thermal expansion are both low, with a coefficient of thermal expansion of $2.5\text{-}3.0 \times 10^{-6}/^\circ\text{F}$ ($4.5\text{-}5.4 \times 10^{-6}/^\circ\text{C}$). Typical end-use properties are shown in Table 2.4.1.4. Currently, the cost of boron fiber is approximately an order of magnitude higher than standard carbon fiber.

TABLE 2.4.1.3.4(b) Typical yarn nomenclature (Reference 2.4.1.3.1(c)).

Filament Designation	Nominal Filament Diameter, inches (mm)	Strand Count (x100 = yds/lb) (g/km)	Approximate Number of Filaments
D	0.00021 (0.053)	1800 (2.8)	51
D	0.00021 (0.053)	900 (5.5)	102
B	0.00015 (0.0038)	450 (11)	408
D	0.00021 (0.053)	450 (11)	204
D	0.00021 (0.053)	225 (22)	408
E	0.00029 (0.0074)	225 (22)	204
B	0.00015 (0.0038)	150 (33)	1224
C	0.00019 (0.0048)	150 (33)	750
DE	0.00025 (0.0064)	150 (33)	408
G	0.00036 (0.0091)	150 (33)	204
H	0.00043 (0.011)	110 (45)	204
C	0.00019 (0.0048)	75 (66)	1500
DE	0.00025 (0.0064)	75 (66)	816
G	0.00036 (0.0091)	75 (66)	408
K	0.00053 (0.014)	75 (66)	204
H	0.00043 (0.011)	55 (90)	408
DE	0.00025 (0.0064)	37 (130)	1632
G	0.00036 (0.0091)	37 (130)	816
K	0.00053 (0.014)	37 (130)	408
H	0.00043 (0.011)	25 (200)	816
K	0.00053 (0.014)	18 (275)	816
G	0.00036 (0.0091)	15 (330)	2052



Available almost exclusively in filament or epoxy matrix prepreg form, boron fiber has been used for aerospace applications requiring high strength and/or stiffness, and for selective reinforcement in sporting goods. The most notable use of this fiber is the stabilizer sections of the F-14 and F-15 military aircraft, dorsal longeron of the B-1B bomber, and the repair of metallic airframe structures. High modulus (HM) or high strength (HS) carbon/epoxy composites can match either the tensile modulus or strength of boron composites at a more economical price, but boron/epoxy composites offer twice the composite strength. Additional information can be found in References 2.4.1.4(a) through (g).

TABLE 2.4.1.4 *Typical end-use properties of a unidirectional boron/epoxy laminate ($V_f = 0.5$).*

	Value, ksi (MPa)
Moduli	
Tensile, longitudinal	30 (207)
Tensile, transverse	2.7 (19)
Strength	
Tensile, longitudinal	192 (1323)
Tensile, transverse	10.4 (72)
Compressive, longitudinal	353 (2432)

2.4.1.5 Alumina

Continuous polycrystalline alumina fiber is ideally suited for the reinforcement of a variety of materials including plastics, metals, and ceramics. Alumina is prepared in the form of continuous yarn containing a nominal 200 filaments. It is supplied in bobbins containing continuous filament yarn, and alumina/aluminum and alumina/magnesium plates. Alumina staple is also available for short fiber reinforcement.

Fibers that are more than 99% purity α alumina have excellent chemical resistance, and have higher modulus and temperature capabilities than ceramic fibers containing silica. The high modulus of 55 Msi (380 GPa) is comparable to that of boron and carbon. The average filament tensile strength is 200 ksi (1.4 GPa) minimum. Since alumina is a good insulator, it can be used in applications where conducting fibers cannot. Nominal properties of alumina are listed in Table 2.4.1.5(a). Cost projections for alumina are competitive with carbon.

Alumina, in continuous form, offers many advantages for composite fabrication including ease of handling, the ability to align fibers in desired directions, and filament winding capability. The fact that alumina is an electrical insulator combined with its high modulus and compressive strength make it of interest for polymer matrix composite applications. For example, alumina/epoxy and aramid/epoxy hybrid composites reinforced with alumina and aramid fibers have been fabricated and are of potential interest for radar transparent structures, circuit boards, and antenna supports. Typical properties of unidirectional composites are listed in Table 2.4.1.5(b).

TABLE 2.4.1.5(a) *Nominal properties of alumina.*

Composition	> 99% α -Al ₂ O ₃	Filaments/yarn	200, nominal
Melting Point	3713°F (2045°C)	Tensile Modulus	55 Msi (385 GPa)
Filament Diameter	0.8x10 ⁻³ in. (20μm)	Tensile Strength	200 ksi (1.4 GPa) minimum
Length/Weight	(~4.7 m/gm)	Density	0.14 lb/in ³ (3.9 gm/cc)

TABLE 2.4.1.5(b) *Nominal properties of alumina composite ($V_f \sim 50$ -55%).*

Moduli		
Tensile, axial		30-32 Msi (210-220 GPa)
Tensile, transverse		20-22 Msi (140-150 GPa)
Shear		7 Msi (50 GPa)
Strength		
Tensile, axial		80 ksi (600 MPa)
Tensile, transverse		26-30 ksi (130-210 MPa)
Shear		12-17 ksi (85-120 GPa)
Fatigue - Axial Endurance Limit		10 ⁷ cycles at 75% of static ultimate (tension-tension, R=0.1, and rotating-bending)
Average Thermal Expansion		
Axial		4.0 μin/in/F° (7.2 μm/m/C°)
Transverse		11 μin/in/F° (20 μm/m/C°)
Thermal Conductivity	68-750° (20-400°C)	22-29 Btu/hr-ft-°F (38-50 J/m-s-°C)
Specific Heat	68-750° (20-400°C)	0.19-0.12 Btu/lbm-°F (0.8-0.5 J/gm-°C)
Density		0.12 lbm/in ³ (3.3 gm/cm ³)

2.4.1.6 Silicon carbide

Various super-refractory fibers were first produced in the early 1950's based upon work by the Arthur D. Little Co. by various production methods. The primary of these based upon:

1. Evaporation for polycrystalline fiber process.
2. HITCO continuous process for polycrystalline fibers.
3. Vapor deposition of aluminum oxide single crystals (Reference 2.4.1.6(a)).

The most recent advances in the CVD type process in use by AVCO consist of substrate wires drawn through glass reaction tubes at high temperature.

Silicon carbide fibers are produced with a nominal 0.0055 in. (140 μm) filament diameter and are characteristically found to have high strength, modulus and density. Fiber forms are oriented toward the strengthening of aluminum or titanium alloys for both longitudinal and transverse properties. Additional forms are also produced as polycrystalline fiber whiskers of varying length and diameters (Reference 2.4.1.6(b)).

Several systems for describing the material morphology exist, the alpha and beta forms designated by Thibault and Lindquist being the most common (Reference 2.4.1.6(c)).

Practically all silicon carbide monofilament fibers are currently produced for metal composite reinforcement. Alloys employing aluminum, titanium, and molybdenum have been produced (Reference 2.4.1.6(b)).

General processing for epoxy, bisimide, and polyimide resin can be either via a solvated or solvent-less film impregnation process, with cure cycles equivalent to those provided for carbon or glass reinforced products. Organic matrix silicon carbide impregnated products may be press, autoclave, or vacuum bag oven cured. Lay-up on tooling proceeds as with carbon or glass composite products with all bleeding, damming, and venting as required for part fabrication. General temperature and pressure ranges for the cure of the selected matrix resins used in silicon carbide products will not adversely affect the fiber morphology.

Silicon carbide ceramic composites engineered to provide high service temperatures (in excess of 2640°F or 1450°C) are unique in several thermal properties. The overall thermal resistance is determined by the through conductivity, thermal expansion, thermal shock and creep resistance. Thermal conductivities of silicon carbide ceramics have a range in Btu-in/s-ft²-°F of 0.12 at room temperature to 0.09 at 1470°F (W/m·K of 60 at room temperature to 48 at 800°C). Expansion values range, in percentage of original dimension, from 0.05 at 390°F (200°C) to 1470°F (0.30% at 800°C). The creep resistance of the silicon carbide ceramic will vary as the percentage of intra-granular silicon phase increases. In general, the creep rate is very low when compared to aluminum oxide or zirconium oxide materials.

Mechanical properties of silicon carbide materials are shown in Table 2.4.1.6(a). Fracture toughness as measured by double torsion analysis has reported literature values for K_{Ic} ranging from 0.55 ksi Jm (0.6 MPa $\sqrt{\text{m}}$) for monocrystalline SiC/Si to 5.5 ksi Jm (6.0 MPa Jm) for hot pressed SiC ceramics (Reference 2.4.1.6(g)). Corrosion resistance, of consideration in advanced structural material design, has been evaluated with a variety of mineral acids on the basis of corrosive weight loss as shown in Table 2.4.1.6(b).

General cost ranges for the CVD processed fibers are currently in the \$100.00 per lb., with the control in crystalline form requiring additional expense (Reference 2.4.1.6(e)).

TABLE 2.4.1.6(a) *Material properties of silicon carbide materials.*

Property	Reported Values (ksi) (MPa)		Reference Information
FLEXURAL STRENGTH	100-1000	700-7000	single crystal, 99+% purity (1)
	10-60	70-400	polycrystalline materials, 78-99% purity, with < 12+% free silicon, sintered (1)
	5-8	30-60	sintered SiC - graphite composites - epoxy, imide, polyimide matrix. (2)
COMPRESSIVE STRENGTH	500-1000	3000-7000	single crystal, 99+% purity (1)
	10-25	70-170	polycrystalline materials, 78-99% purity, with < 12+% free silicon, sintered.(2)
	14-60	97-400	Sintered SiC - graphite composites - epoxy, imide, polyimide matrix. (2)
TENSILE STRENGTH	~20	~140	single crystal, 99+% purity (1)
	5-20	30-140	polycrystalline materials, 78-99% purity, with < 12+% free silicon, sintered.(2)
	2.5-25	17-170	sintered SiC - graphite composites - epoxy, imide, polyimide matrix. (2)
MODULUS OF ELASTICITY	~9.5	~66	single crystal, 99+% purity (1)
	~7.0	~48	Polycrystalline materials, 78-99% purity, with < 12+% free silicon, sintered.(2)

(1) Reference 2.4.1.6(b)

(2) Reference 2.4.1.6(d)

TABLE 2.4.1.6(b) *Corrosive weight loss at 212°F (100°C) (Reference 2.4.1.6(e)).*

TEST REAGENT	Si/SiC COMPOSITES 12% Si <i>mg/cm²·yr</i>	SiC - NO FREE Si <i>mg/cm²·yr</i>
98% Sulfuric Acid	55	1.8
50% Sodium Hydroxide	complete within days	2.5
53% Hydrofluoric Acid	7.9	< 0.2
70% Nitric Acid	0.5	< 0.2
25% Hydrochloric Acid	0.9	< 0.2

2.4.1.7 Quartz

Quartz fiber is very pure (99.95%) fused silica glass fiber. Typical fiber properties are shown in Table 2.4.1.7(a). Quartz is produced as continuous strands consisting of 120 or 240 individual filaments of 9 micron nominal diameter. These single strands are twisted and plied into heavier yarns. Quartz fibers are generally coated with an organic binder containing a silane coupling agent which is compatible with many resin systems. Strands for rovings are combined into multiple ends without applied twist. These strands are coated with a "direct size" which is compatible with many resins. Woven fabrics may be used as woven or may be "scoured" (washed) to remove the nonfunctional components of the binder and some, but not all, of the silane coupling agent. Following scouring, the fabric may be finished with a variety of silane coupling agent finishes having specific resin compatibility.

Quartz fiber nomenclature is the same as that for E or S glass fibers except that the glass composition is designated by the letter Q as shown in Table 2.4.1.7(b). Commonly used quartz fabrics are listed in Table 2.4.1.7(c). Quartz rovings are continuous reinforcements formed by combining a number of 300 2/0 zero twist strands. End counts of 8, 12, and 20 are available having yields from 750 to 1875 yards per pound (660 to 264 g/km). Quartz fibers are also available in the form of chopped fiber in cut lengths from 1/8 inch to 2 inches (3 to 50 mm).

Quartz fibers with a filament tensile strength of 850 ksi (5,900 MPa) have the highest strength-to-weight ratio, virtually exceeding all other high temperature materials. The quartz fibers can be used at temperatures much higher than "E" glass or "S" glass fiber with service temperatures up to 1920°F (1050°C) possible. Quartz fibers do not melt or vaporize until the temperature exceeds 3000°F (1650°C), providing potential in ablative applications. Additionally, these fibers retain virtually all of the characteristics and properties of solid quartz.

The quartz fibers are chemically stable. They are not affected by halogens or common acids in the liquid or gaseous state with the exception of hydrofluoric and hot phosphoric acids. Quartz fibers should not be used in environments where strong concentrations of alkalis are present.

Quartz fibers, when combined with certain matrix systems, offer potential advantages in stealth application due to their high electrical resistivity properties. Quartz does not form paramagnetic centers, nor does it capture neutrons in high energy applications. These fibers offer a low dielectric constant and loss tangent providing excellent properties as electrical insulators. Typical properties for quartz fibers combined with three different polymer matrix systems are shown in Tables 2.4.1.7(d) - (f). Quartz products are relatively expensive compared to "E" or "S-2" glass products, with prices ranging from \$45 to \$150 per pound. Additional information can be found in Reference 2.4.1.7

Table 2.4.1.7(a) *Properties of quartz fiber.*

Specific gravity	2.20
Density, lb/in ³	0.0795
g/cm ³	2.20
Tensile strength	
Monofilament, ksi	870
GPa	6.0
Roving, ASTM D2343 Impregnated	
Strand Test -	
Astroquartz II 9779, ksi	530.5
GPa	3.6
Modulus, Msi	10.0
GPa	72.0
Elongation, percent	
<u>Monofilament Tensile Strength x 100</u>	8.7
Modulus	
Thermal	
Coefficient of expansion	
10 ⁻⁶ in/in/°F	0.3
10 ⁻⁶ cm/cm/°C	0.54
Thermal conductivity	
Cal/sec/cm/°C	0.0033
Btu/hr/ft/°F	0.80
Btu/hr/sq ft/in/°F	9.5
Specific heat	
Joules/Kg/°C	7500
Btu/lb/°F	1.80
Electrical	
Dielectric constant, 10 GHz, 75°F (24°C)	3.78
Loss tangent, 10 GHz, 75°F (24°C)	0.0001

TABLE 2.4.1.7(b) *Quartz continuous strands.*

Strand Number	Number of filaments	Strand Count		Filament Diameter	
		yds/lb	g/km	10 ⁻⁵ in.	μm
QCG 300 1/0	119 ^a	30,000	6.5	45	1.1
QCG 300 2/0	240 ^b	15,000	33	35	0.89
QCG 300 1/2	240 ^a	15,000	33	35	0.89
QCG 300 2/2	480 ^a	7,500	66	35	0.89
QCG 300 2/8	1920 ^a	1,875	264	35	0.89

^aUsed for fabric yarns.^bUsed for roving and fabric yarns.**TABLE 2.4.1.7(c)** *Construction of woven fabrics for aerospace applications.*

Style	Count	Warp Fill	Fill Yarn	Weave	Weight Oz/Sq.Yd.
503	50x50	300 1/2	300 1/2	plain	3.5
507	27x25	300 1/2	300 1/2	plain	2.0
525	50x 50	300 1/0	300 1/0	plain	2.0
527	42x32	300 2/2	300 2/2	plain	5.6
531	68x65	300 1/2	300 1/2	8HS	5.1
557	57x31	300 2/2	300 1/0	crowfoot	5.0
570	38x24	300 2/8	300 2/8	5HS	19.3
572	17x16	300 2/8	300 2/8	plain	9.9
581	57x54	300 2/2	300 2/2	8HS	8.4
593	49x46	300 2/2	300 2/2	5HS	7.5

TABLE 2.4.1.7(d) *Typical properties for quartz/epoxy.*

PROPERTY	Room Temperature		1/2 hr at 350°F (180°C)	
	U.S.	SI	U.S.	SI
Tensile Strength (ksi, MPa)	74.9 - 104	516 - 717	65.4 - 92.2	451 - 636
Tensile Modulus (Msi, GPa)	3.14 - 4.09	21.7 - 28.2	2.83 - 3.67	19.5 - 25.3
Flexural Strength (ksi, MPa)	95.5 - 98.9	658 - 682	53.9 - 75.9	372 - 523
Flexural Modulus (Msi, GPa)	3.27- 3.46	22.5 - 23.8	2.78 - 3.08	19.2 - 21.2
Compressive Strength (ksi, MPa)	66.4 - 72.4	458 - 499	42.6 - 49.9	294 - 344
Compressive Modulus (Msi, GPa)	3.43 - 3.75	23.6 - 25.9	3.10 - 3.40	21.4 - 23.4
Laminate Resin Content (wt%)	33.5 - 32.0			
Specific Gravity (g/cm ³)	1.73 - 1.77			

TABLE 2.4.1.7(e) *Typical properties for quartz/toughened epoxy.*

PROPERTY	Room Temperature		180°F (82°C)	
	U.S.	SI	U.S.	SI
Flexural Strength (ksi,MPa)	129.0	889	111.7	770
Flexural Modulus (Msi,GPa)	4.0	27.6	3.9	26.9
Compressive Strength (ksi,MPa)	88.2	608	77.5	534
Compressive Strength, Wet (ksi,MPa)	76.6	528	70.8	488
Compressive Modulus (Msi,GPa)	4.2	29.0	3.8	26.2
Compressive Modulus, Wet (Msi,GPa)	3.7	25.5	4.0	27.6
Short Beam Strength (ksi,MPa)	13.2	91.0	11.8	81.4
Short Beam Strength, Wet (ksi,MPa)	9.2	63.4	9.3	64.1
Resin Content (wt%)	32.0			
Ply Thickness (in,mm)	0.009	0.23		

TABLE 2.4.1.7(f) *Typical properties for quartz/polyimide.*

PROPERTY	Room Temperature		1/2 Hour at 350°F (177°C)	
	U.S.	SI	U.S.	SI
Tensile Strength (ksi,MPa)	79.1 - 105	545 - 724		
Tensile Modulus (Msi,GPa)	3.9	27		
Flexural Strength (ksi,MPa)	93.7 - 102	646 - 703	62.4 - 68.3	430 - 471
Flexural Modulus (Msi,GPa)	3.2	22	2.6 - 2.8	18 - 19
Compressive Strength (ksi,MPa)	67.0 - 67.4	462 - 465	38.6 - 45.2	266 - 312
Compressive Modulus (Msi,GPa)	3.5 - 3.7	24 - 26	2.8	19
Laminate Resin Content (wt%)	36.2 - 36.2			

2.4.1.8 Ultrahigh molecular weight polyethylene.

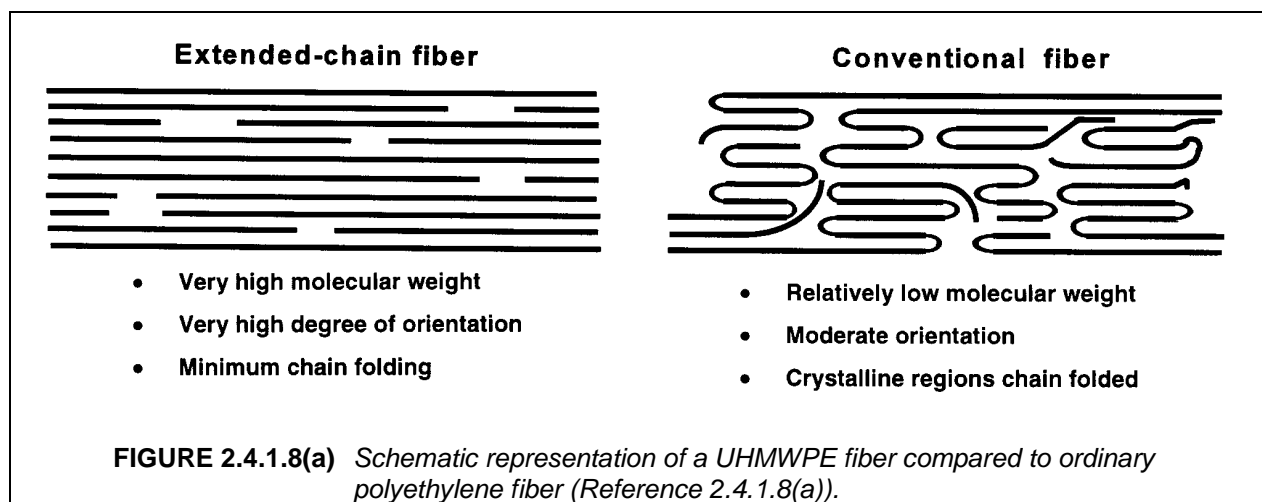
Material Description

Ultrahigh molecular weight polyethylene fiber (UHMWPE) is the generic name for a high performance fiber which is more widely known today by the trade name Spectra[®], assigned by the major marketer of UHMWPE fiber, Allied Signal Inc. Non-oriented UHMWPE was first synthesized in the mid 1950s. A number of academic and commercial institutions in the United States and Europe worked to develop oriented UHMWPE fiber. Allied developed Spectra[®] fiber in the 1970s and it was first offered as a commercial product in 1985.

The generally accepted definition of what constitutes "ultrahigh molecular weight" is a molecular weight greater than 3,000,000. The properties of polyethylene depend strongly on the molecular weight and the degree of branching. UHMWPE fiber is a linear polymer and its molecular weight typically varies between 3,000,000 and 6,000,000. This fiber is highly oriented axially and the chains form a highly crystalline structure, between 95-99%, but the crystallinity is not in the form of folded chains as is typically found in thermoplastics. Instead, the chains are fully extended (Figure 2.4.1.8(a)).

The fiber is formed by a gel-spinning process where the polymer is dissolved in order to disentangle the polymer chains. From solution the fibers are then drawn and the molecules become axially aligned to an extremely high degree. The resulting fiber diameter is rather large at 27 microns (for Spectra[®] 1000) compared to other high performance fibers (typical aramid fiber diameter is 12 microns; S-2 glass, 7; carbon fibers, 7).

The cost of UHMWPE relative to other high performance fibers is competitive, ranging from \$16/lb. for lower performance, high denier Spectra® 900 products to as much as \$80/lb. for high performance, low denier forms of Spectra® 1000.



Advantages and Limitations

The main drawback to UHMWPE is poor temperature performance. The fiber melting point is 300°F (149°C) and the typical maximum service temperature is 230°F (110°C). Temperature is always a consideration when combining UHMWPE with a thermosetting matrix to form a composite by curing, post curing and/or molding. The upper processing limit of UHMWPE (250°F, 121°C) coincides with the recommended cure temperature of many commercially popular structural resin system. 350°F (177°C) cures are not possible. For all practical purposes UHMWPE can not be used in a high performance thermoplastic matrix due to the required high processing temperatures.

Creep is also a problem, even at room temperature (Figure 2.4.1.8(b)). For this reason design for long-term constant-load-bearing applications should be carefully considered. Load bearing at elevated temperature will lead to serious creep problems.

When used in a composite UHMWPE bonds poorly to most matrix resins. This is due to its chemical inertness and poor wettability (low surface energy). To improve bonding, gas plasma treatments are often used to modify the fiber surface to make it more compatible with the various resins.

Although its temperature and creep limitations are severe, UHMWPE still has many applications. Outstanding impact strength, even at cold temperatures, combined with a 33% weight reduction over aramid make it an appealing choice in applications where temperature is not an issue.

Ballistic protection is one of its major uses. The fiber is commercially successful in ballistic applications, particularly lightweight body armor and riot shield applications for military and law enforcement personnel. The U.S. Army is studying it as an alternative to aramid in the standard issue soldier helmet. Two other ballistic applications are ground vehicle mine blast shields and ultra-lightweight armor for aircraft. For example, the AC-130H Spectre Gunship, flown by the Air Force Special Operations Command, uses UHMWPE armor as its attack mode calls for low altitude (500 feet (150m)) flight.

UHMWPE is also used in radomes, which take advantage of a low dielectric constant (2.2) and loss tangent (0.0002). Other applications include cut-resistant fabrics, heavy lift cargo cables, snow and water skis and other sporting goods, and high-wear applications.

Mechanical properties of composites reinforced with UHMWPE fiber are generally quite good. Tensile strength and modulus, elongation, and toughness compare favorably with other fiber types, especially when normalized on a weight basis (although compression and shear properties do not compare as well).

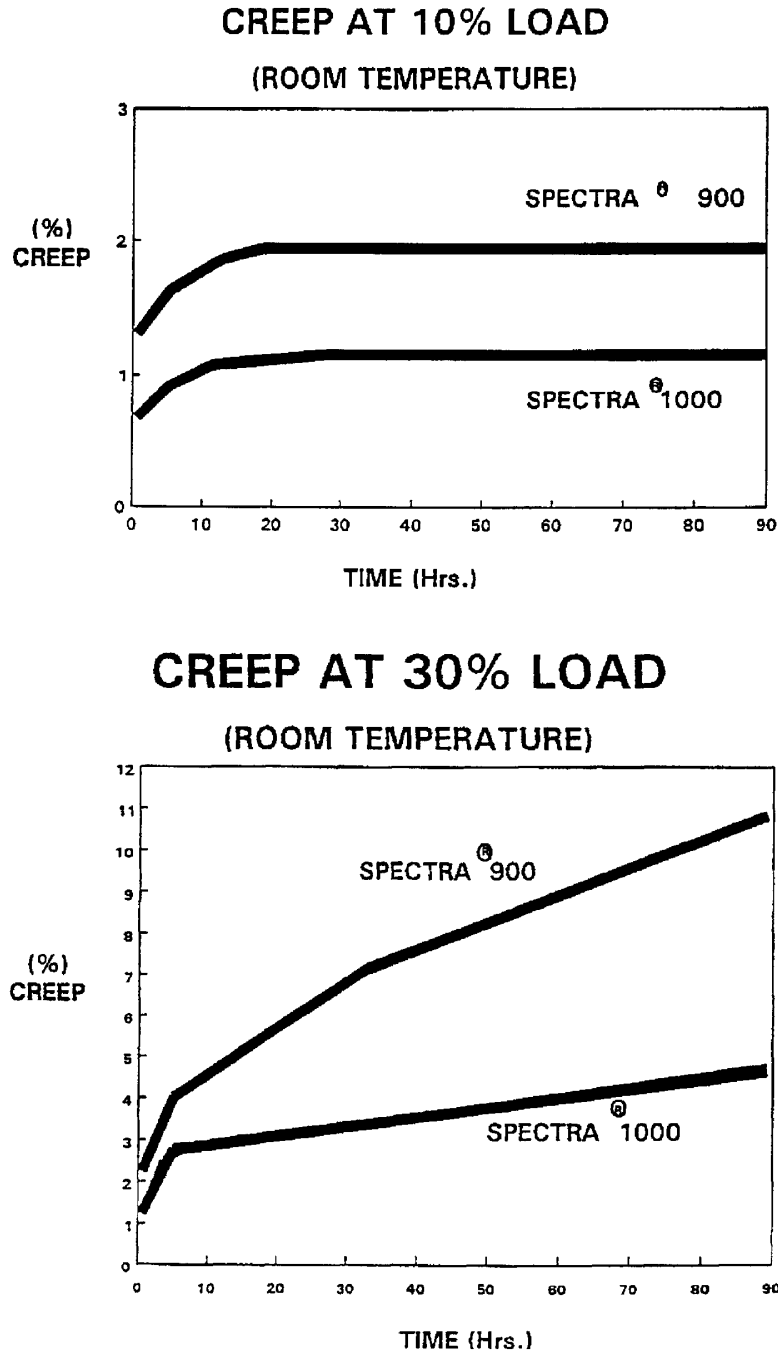


FIGURE 2.4.1.8(b) Room temperature creep properties of Spectra® fiber at 10% and 30% loading (Reference 2.4.1.8(a)).

UHMWPE is a hydrophobic material and is extremely resistant to moisture effects. In fact, with the exception of its poor high temperature performance, UHMWPE stands up well to the environment, including prolonged exposure to sunlight. It has superior solvent resistance (chemical inertness) even to strong acids and bases. Its stability is outstanding in common solvents such as water, gasoline, hydraulic oil and cleaning solvents. The fiber also exhibits good abrasion resistance and self-lubricating properties.

One feature unique to UHMWPE among high performance fibers is that it floats on water. Of the four common high performance fibers, UHMWPE is by far the lightest with a density of 0.97 g/cm^3 (0.035 lb/in^3) (the density of aramid is 1.4 g/cm^3 (0.051 lb/in^3); carbon is 1.8 g/cm^3 (0.065 lb/in^3); S-2 glass is 2.5 g/cm^3 (0.091 lb/in^3)). UHMWPE is most often compared to aramid fibers. The strength and modulus of this fiber are about the same as aramid, but due to a lower density its specific strength and modulus are higher, reaching nearly as high as today's high modulus carbon fibers on a weight basis.

Machining UHMWPE is difficult without special equipment. Generally, the machining requirements of UHMWPE are the same as those of aramid, except that, due to its low melting temperature, UHMWPE can also be cut with a hot knife. Table 2.4.1.8 lists some key properties of two grades of Spectra[®] fiber. Additional information can be found in References 2.4.1.8(b) - (e).

TABLE 2.4.1.8 *Properties of Spectra[®] 900 and Spectra[®] 1000 Fibers (Reference 2.4.1.8(a)).*

Property	Spectra [®] 900	Spectra [®] 1000
Filament Diameter, microns(mils)	38(1.5)	27(1.1)
Density, g/cm^3 (lb/in^3)	0.97(0.035)	0.97(0.035)
Tensile Strength, ksi(MPa)	375(2.58)	435(3.00)
Tensile Modulus, Msi(MPa)	17.4(120)	24.8(171)
Spec. Tensile Strength, M-in(M-m)	10.7(0.272)	12.4(0.315)
Spec. Tensile Modulus, M-in(M-m)	486(12.3)	714(18.1)
Elongation, %	3.5	2.7
Dielectric Constant	2.2	2.2
Loss Tangent	0.0002	0.0002

2.4.2 Resins

2.4.2.1 Overview

Resin is a generic term used to designate the polymer, polymer precursor material, and/or mixture or formulation thereof with various additives or chemically reactive components. The resin, its chemical composition and physical properties, fundamentally affect the processing, fabrication and ultimate properties of composite materials. Variations in the composition, physical state, or morphology of a resin and the presence of impurities or contaminants in a resin may affect handleability and processability, lamina/laminate properties, and composite material performance and long-term durability. This section describes resin materials used in polymer matrix composites and adhesives, and considers possible

sources and consequences of variations in resin chemistry and composition, as well as the effects of impurities and contaminants, on resin processing characteristics and on resin and composite properties.

2.4.2.2 Epoxy

The term epoxy is a general description of a family of polymers which are based on molecules that contain epoxide groups. An epoxide group is an oxirane structure, a three-member ring with one oxygen and two carbon atoms. Epoxies are polymerizable thermosetting resins containing one or more epoxide groups curable by reaction with amines, acids, amides, alcohols, phenols, acid anhydrides, or mercaptans. The polymers are available in a variety of viscosities from liquid to solid.

Epoxies are used widely in resins for prepregs and structural adhesives. The advantages of epoxies are high strength and modulus, low levels of volatiles, excellent adhesion, low shrinkage, good chemical resistance, and ease of processing. Their major disadvantages are brittleness and the reduction of properties in the presence of moisture. The processing or curing of epoxies is slower than polyester resins. The cost of the resin is also higher than the polyesters. Processing techniques include autoclave molding, filament winding, press molding, vacuum bag molding, resin transfer molding, and pultrusion. Curing temperatures vary from room temperature to approximately 350°F (180°C). The most common cure temperatures range between 250° and 350°F (120° and 180°C). The use temperatures of the cured structure will also vary with the cure temperature. Higher temperature cures generally yield greater temperature resistance. Cure pressures are generally considered as low pressure molding from vacuum to approximately 100 psi (700 kPa).

2.4.2.3 Polyester (*thermosetting*)

The term thermosetting polyester resin is a general term used for orthophthalic polyester resin or isophthalic polyester resin. Polyester resins are relatively inexpensive and fast processing resins used generally for low-cost applications. In combination with certain fillers, they can exhibit resistance to breakdown under electrical arc and tracking conditions. Isophthalic polyester resins exhibit higher thermal stability, dimensional stability, and creep resistance. In general, for a fiber-reinforced resin system, the advantage of a polyester is its low cost and its ability to be processed quickly.

Fiber-reinforced polyesters can be processed by many methods. Common processing methods include matched metal molding, wet lay-up, press (vacuum bag) molding, injection molding, filament winding, pultrusion, and autoclaving. Polyesters can be formulated to cure more rapidly than do phenolics during the thermoset molding process. While phenolic processing, for example, is dependent on a time/temperature relationship, polyester processing is primarily dependent on temperature. Depending on the formulation, polyesters can be processed from room temperature to 350°F (180°C). If the proper temperature is applied, a quick cure will occur. Without sufficient heat, the resin/catalyst system will remain plasticized. Compared to epoxies, polyesters process more easily and are much tougher, whereas phenolics are more difficult to process and brittle, but have higher service temperatures.

2.4.2.4 Phenolic

Phenol-formaldehyde resins and their direct precursors were first produced commercially in the early 1900's for use in the commercial market. Ureaformaldehyde and melamine-formaldehyde appeared in the 1920 - 1930's as a less expensive alternative for lower temperature use. Phenolics, in general, cure by a condensation route with the off-gassing of water. The resulting matrix is characterized by both chemical and thermal resistance as well as hardness, and low smoke and toxic degradation products.

The phenolic polymers, often called either phenolic resole or novolacs resins, are condensation polymers based upon either a reaction of excess formaldehyde with a base catalyst and phenol (resole), or a reaction of excess phenol with an acidic catalyst and formaldehyde (novolac). The basic difference between resoles and novolacs consist of no methylol groups in the novolacs and the resulting need for an extension agent of paraformaldehyde, hexamethylenetetraamine, or additional formaldehyde as a curative. These resins have higher molecular weights and viscosities than either parent material. Conse-

quently, they are optimal for processing parts of unusual conformations and complex curvature. The resins allow either press or autoclave cure and allow relatively high temperature free-standing postcures.

2.4.2.4.1 *Resoles*

The reaction of phenol and excess formaldehyde in the presence of base is characterized by low-molecular-weight prepolymers that are soluble in base and contain a large degree of methylol groups ($-\text{CH}_2\text{OH}$). These prepolymers are processed to a workable viscosity (resites) and then cured to an intractable solid of high crosslink density. Water is lost as a volatile (as much as 10-12% of the resin by weight).

2.4.2.4.2 *Novolacs*

The second type of phenolic consists of excess phenol reacted in the presence of an acid catalyst with formaldehyde. These prepolymer resins are complex mixtures of low molecular weight materials slightly soluble in acids and exhibiting random methylene ($-\text{CH}_2$) at the ortho-, para-, and ortho-para-positions on the aromatic ring. Unless a large excess of phenol is present, the material will form an infusible resin. The excess phenol used to moderate the processing viscosity can be varied as the application requires. Both water and formaldehyde are volatile products.

2.4.2.5 *Bismaleimide*

Bismaleimides are a class of thermosetting resins only recently available commercially in prepreg tapes, fabrics, rovings, and sheet molding compound (SMC). Bismaleimide resins, as the term implies, are the maleimide formed from the reaction of a diamine and maleic anhydride. Typically the diamine is aromatic, with methylenedianiline (MDA), the most common by far.

Bismaleimides form useful polymers by homopolymerization or by polymerization with diamines, epoxies, or unsaturated compounds, singular or in mixtures. A wide range of materials like allyl-, vinyl-, acrylate-, epoxy-, and polyester-, and phenolic-type reactive diluents and resins can be used to tailor the properties of the bismaleimide system. However, attention to the specific components is required for useful polymers.

The physical form of the bismaleimide resin depends on the requirement of the final application. The form can vary from a solid to a pourable liquid at room temperature. For aerospace prepregs, sticky resins are required resulting in proprietary specific formulations.

The advantages of BMI resins are best discussed in the relation to epoxy resins. Emerging data suggests that BMI's are versatile resins with many applications in the electronic and aerospace industries. Their primary advantage over epoxy resins is their high glass transition temperature, in the 500-600°F range (260-320°C). Glass transition temperatures for high temperature epoxies are generally less than 500°F (260°C). The second advantage of BMI resins is high elongation with the corresponding high service temperature capabilities. While the high temperature epoxies have approximately one percent elongation when cured with diaminodiphenylsulfone (DDS), BMI's can have two-three percent elongation. Thus, bismaleimide resins deliver higher temperature capability and higher toughness providing excellent performance at ambient and elevated temperatures.

The processing of bismaleimide resins are essentially like that of epoxy resins. BMI's are suitable for standard autoclave processing, injection molding, resin transfer molding, and SMC, among others. The processing time of BMI's are similar to epoxies, except that for the additional higher service temperature, a free-standing post-cure is required. The only limitation is that room temperature curing BMI's have not yet been developed.

The cost of current BMI's is generally higher than the high temperature epoxies. The main disadvantage of bismaleimide resins is their recent commercial introduction. This results in few literature sources

or authoritative reviews. Additionally, the suppliers are as limited as the types of BMI's. This latter disadvantage is partially offset by the wide variety of suitable co-monomers.

2.4.2.6 Polyimides

The polyimide resin family comprises a diverse number of polymers all of which contain an aromatic heterocyclic ring structure. The bismaleimides discussed in Section 2.4.2.5 are a subset of this family. Other polyimides are synthesized from a variety of cyclic anhydrides or their diacid derivatives through reaction with a diamine. This reaction forms a polyamic acid which then undergoes condensation by the removal of water and/or alcohol.

Polyimide matrix composites excel in high temperature environments where their thermal resistance, oxidative stability, low coefficient of thermal expansion and solvent resistance benefit the design. Their primary uses are circuit boards and hot engine and aerospace structures.

A polyimide may be either a thermoset resin or a thermoplastic. The thermoplastic varieties are discussed in Section 2.4.2.7.2. Thermosetting polyimides characteristically have crosslinkable end-caps and/or a rigid polymer backbone. A few thermoplastic polyimides can become thermoset polymers if a sufficiently high postcure temperature is employed during part processing. Alternately, partially cured thermoset polyimides containing residual plasticizing solvents can exhibit thermoplastic behavior. Thus, it is difficult to state with certainty that a particular polyimide is indeed a thermoset or thermoplastic. Polyimides, therefore, represent a transition between these two polymer classifications.

Polyimide properties, such as toughness and thermal resistance, are influenced by the degree of crosslinking and chain extension. Molecular weight and crosslink density are determined by the specific end cap group and by the stoichiometry of the anhydride:amine mixture which produces the polyamic acid by stepwise chain growth, after which the polyamic acid is recycled by continued thermal cure to form the final polymer structure. The choice of solvent employed in the resin formulation has a significant impact on crosslinking and chain extension. Solvents such as N-methyl 2-pyrrolidone (NMP), promote chain extension by increasing resin flow, chain mobility and molecular weight prior to formation of a substantial crosslink network. From a practical standpoint, these solvents are beneficial to polymerization, but they are detrimental to part manufacture because of their tendency to cause ply delaminations.

Most polyimide resin monomers are powders. Some bismaleimides are an exception. As a result, solvents are also added to the resin to enable impregnation of unidirectional fiber and woven fabrics. Commonly, a 50:50 by weight mixture is used for fabrics, and a 90:10 by weight high solids mixture is used to produce a film for unidirectional fiber and low areal weight fabric prepregs. Solvents are further used to control prepreg handling qualities, such as tack and drape. Most of the solvents are removed in a drying process during impregnation, but total prepreg volatiles contents typically range between 2 and 8% by weight. This includes all volatiles, including those produced by the condensation cure reactions.

Polyimides require high cure temperatures, usually in excess of 550°F (~90°C). Consequently, normal epoxy composite consumable materials are not usable, and steel tooling becomes a necessity. Polyimide bagging and release films, such as Kapton and Upilex, replace the lower cost nylon bagging and polytetrafluoroethylene (PTFE) release films common to epoxy composite processing. Fiberglass fabrics must be used for bleeder and breather materials instead of polyester mat materials.

2.4.2.7 Thermoplastic materials

2.4.2.7.1 Semi-crystalline

Semi-crystalline thermoplastics are so named because a percentage of their volume consists of a crystalline morphology. The remaining volume has a random molecular orientation termed amorphous, the name given to thermoplastics containing no crystalline structure. The total percentage of volume which can become crystalline depends on the polymer. Low density polyethylene, for example, can be as high as 70% crystalline (Reference 2.4.2.7.1(a)). Semi-crystalline thermoplastics are characterized by the ability of their molecules to form three-dimensionally ordered arrays (Reference 2.4.2.7.1(b)). This is in

contrast to amorphous polymers that contain molecules which are unable to pack in an ordered crystalline structure. A partial list of semi-crystalline thermoplastics includes polyethylene, polypropylene, polyamides, polyphenylene sulfide, polyetheretherketone, (polyetherketoneketone) and polyarylketone.

Semi-crystalline thermoplastics can be converted into several physical forms, including films, powders and filaments. Combined with reinforcing fibers, they are available in injection molding compounds, compression-moldable random sheets, unidirectional tapes, towpregs, and woven prepregs. Fibers impregnated include carbon, nickel-coated carbon, aramid, glass, quartz, and others.

Semi-crystalline thermoplastics reinforced with short fibers have been used for over two decades in the injection molding industry. The inherent speed of processing, ability to produce complicated, detailed parts, excellent thermal stability, and corrosion resistance have enabled them to become established in the automotive, electronic, and chemical processing industries (Reference 2.4.2.7.1(c)).

The combination of long and continuous fibers with higher performance semi-crystalline thermoplastics is a recent development, but these composites have already shown several advantages over existing materials. The chemical stability of the materials provides for unlimited shelf life. Pot life problems and the need for cold storage are eliminated. The semi-crystalline materials usually possess better corrosion and solvent resistance than amorphous polymers, exceeding that of thermosets in some cases (Reference 2.4.2.7.1(c)). This corrosion resistance is exploited in chemical processing industry equipment. Another benefit of the crystal structure is retention of properties above the glass transition temperature (T_g) of the material. These materials may be used in applications above their T_g depending on loading requirements. One example is down-hole oil field sucker rod guides (Reference 2.4.2.7.1(d)).

Some semi-crystalline thermoplastics possess properties of inherent flame resistance, superior toughness, good mechanical properties at elevated temperatures and after impact, and low moisture absorption which have led to their use in the aerospace industry in secondary and primary structures (References 2.4.2.7.1(e)-(f)). Inherent flame resistance has made these materials good candidates for aircraft interiors and for ship and submarine applications. The superior toughness makes them viable candidates for aircraft leading edges and doors where impact damage resistance is required (Reference 2.4.2.7.1(g)). Low moisture absorption and low outgassing has stimulated interest in space structures where moisture swelling is a problem (Reference 2.4.2.7.1(h)). Also nickel-coated carbon/thermoplastic systems are finding uses in EMI shielding applications.

The primary disadvantages of semi-crystalline thermoplastic composites are lack of a design data base, 0° compression properties that are lower than those of 350°F (180°C) epoxy systems, and creep resistance (Reference 2.4.2.7.1(c)). The creep resistance of semi-crystalline thermoplastics is superior to that of amorphous thermoplastics. Creep resistance in the fiber direction of a laminate is not expected to be a problem.

Processing speed is the primary advantage of thermoplastic materials. Chemical curing of the material does not take place during processing. Therefore, reduced cycle times compared to thermoset composites are experienced (References 2.4.2.7.1(i) and (j)). However, thermoplastic prepregs are typically boardy and do not exhibit the tack and drape of thermosets. Forms are available that consist of thermoplastic and reinforcing fibers interlaced together, known as commingled which are drapeable. The present costs of high performance engineering thermoplastic materials are slightly higher than equivalent performance epoxies, and tooling costs may be higher. However, final part cost may be reduced, due to the decreased processing time. The ability to postform or reprocess molded parts also offers cost saving advantages.

A wide variety of methods and techniques are available for processing semi-crystalline thermoplastics, including stamp molding, thermoforming, autoclave molding, diaphragm forming, roll forming, filament winding, and pultrusion. Semi-crystalline thermoplastics differ from amorphous ones in that the morphology can change based on the time/temperature history of the material during molding. Therefore, the degree of crystallinity can be controlled by controlling the cooling rate. The material must be processed above its melt temperature, which requires temperatures ranging from 500 to 700°F (260 -

370°C) for the higher performance materials. Thermal expansion differences between the tool and the thermoplastic material should be addressed, due to the high processing temperature. The actual pressure required varies with the process, but can be as high as 5000 psi (34 MPa) for stamp molding and as low as 100 psi (0.7 MPa) for thermoforming. Once formed, semi-crystalline thermoplastics can be joined by a variety of methods, including ultrasonic welding, infrared heating, vibration, hot air and gas, resistance heating, and conventional adhesives.

2.4.2.7.2 *Amorphous*

The majority of thermoplastic polymers are composed of a random molecular orientation and are termed amorphous. The molecules are unable to align themselves in an ordered manner, since they are non-uniform or composed of units which have large side groups. In contrast, semi-crystalline thermoplastics have molecules that form ordered three-dimensional arrays (Reference 2.4.2.7.1(b)). Some amorphous thermoplastics include polysulfone, polyamide-imide, polyphenylsulfone, polyphenylene sulfide sulfone, polyether sulfone, polystyrene, polyetherimide, and polyarylate.

Amorphous thermoplastics are available in several physical forms, including films, filaments, and powders. Combined with reinforcing fibers, they are also available in injection molding compounds, compressive moldable random sheets, unidirectional tapes, woven preregs, etc. The fibers used are primarily carbon, aramid, and glass.

Amorphous thermoplastics are used in many applications; the specific use depends on the polymer of interest. Their applications are well established in the medical, communication, transportation, chemical processing, electronic, and aerospace industries. The majority of applications use the unfilled and short fiber form. Some uses for the unfilled polymers include cookware, power tools, business machines, corrosion resistant piping, medical instruments, and aircraft canopies. Uses for short-fiber-reinforced forms include printed circuit boards, transmission parts, under-the-hood automotive applications, electrical connections, and jet engine components (Reference 2.4.2.7.2(a)).

The use of amorphous thermoplastics as matrix materials for continuous fiber reinforced composites is a recent development. The properties of composites have led to their consideration for primary and secondary aircraft structures, including interior components, flooring, fairings, wing skins, and fuselage sections (References 2.4.2.7.2(b) and (c)).

The specific advantages of amorphous thermoplastics depend upon the polymer. Typically, the resins are noted for their processing ease and speed, high temperature capability, good mechanical properties, excellent toughness and impact strength, and chemical stability. The stability results in unlimited shelf life, eliminating the cold storage requirements of thermoset preregs. Several amorphous thermoplastics also have good electrical properties, low flammability and smoke emission, long term thermal stability, and hydrolytic stability (Reference 2.4.2.7.2(a)).

Amorphous thermoplastics generally have higher temperature capabilities than semi-crystalline thermoplastics. Polymers with glass transition temperatures as high as 500°F (260°C) are available. Also, processing is simplified, because the formation of a crystalline structure is avoided, resulting in less shrinkage due to their lower melt viscosities. Amorphous polymers generally have lower solvent and creep resistances and less property retention above the glass transition temperature than semi-crystalline thermoplastics (Reference 2.4.2.7.1(f)).

The primary advantages of amorphous thermoplastics in continuous fiber reinforced composites are potential low cost process at high production rates, high temperature capability, good mechanical properties before and after impact, and chemical stability. High temperature capability and retention of mechanical properties after impact have made amorphous thermoplastics attractive to the aerospace industry. A service temperature of 350°F and toughness two to three times that of conventional thermoset polymers are typical (Reference 2.4.2.7.1(f)). The most significant advantage of thermoplastics is the speed of processing, resulting in lower costs. Typically, cycle times in production are less than for thermosets since no chemical reaction occurs during the forming process (References 2.4.2.7.1(i) and (j)).

Amorphous thermoplastics share many of the disadvantages of semi-crystalline thermoplastics, such as a lack of an extensive database and reduced 0° compression properties compared to 350°F (180°C) cure thermosets. Solvent resistance, which is good for semi-crystalline thermoplastics, is a concern for most amorphous ones. They can be attacked to varying degrees, depending on the polymers and solvents of interest. The creep resistance of the polymer is a concern, but should be good for composite forms loaded in the fiber direction. The materials do not have tack and drape as thermosets do; however, some amorphous thermoplastics are available in commingled forms, which are drapable.

The costs of amorphous thermoplastics prepreg used for advanced composites are higher than equivalent performance epoxies. Finished part costs may be lower due to the processing advantages discussed above. Reprocessability of material results in reduced scrap rates, translating into additional cost savings. For example, the same sheet laminate can be thermoformed several times until the desired configuration is achieved. In addition, certain forms can be recycled.

The processes used with continuous reinforced composites include stamp molding, thermoforming, autoclave molding, diaphragm forming, roll forming, filament winding, and pultrusion. The high melting temperatures require process temperatures ranging from 500°F to 700°F (260 to 370°C). Thermal expansion differences between the tool and the thermoplastic material should be addressed due to the high processing temperatures. Forming pressures range from 100 psi (0.7 MPa) for thermoforming to 5000 psi (35 MPa) for stamp molding. Several amorphous thermoplastics that are hygroscopic must be dried before processing. Hot molds are also recommended to increase material flow. The materials can be joined by several methods, including common adhesives, or fusion bonding such as; ultrasonic welding, infrared heating, hot air and gas, and resistance heating. Surface preparation techniques for using adhesives can be different from those for thermosets. Solvent bonding techniques can be used for joining amorphous thermoplastics but not most semi-crystalline thermoplastics.

One important class of amorphous thermoplastic matrices is the condensation cure polyimides. Examples include polyamideimides, such as Torlon, and polyimides having more flexible backbones, such as AvimidR K3B, NR 150B2 and the LaRC polymers developed by NASA. As stated in Section 2.4.2.1.6, polyimides represent a transition between thermoset and thermoplastic polymers. Thus, these thermoplastics also have many characteristics typical of epoxy and phenolic thermoset polymers (e.g., excellent solvent resistance and high maximum operating temperature limits).

Due to negligible crosslink density, these polymers impart some toughness to composite laminates and permit limited flow during processing, although this flow is more like the high creep rates exhibited by superplastic metals. Unlike other thermoplastics, these polymers do not produce liquid flows, even under high consolidation pressures. Typical processing conditions for the condensation cure thermoplastics are 550°F (290°C) and greater temperatures with consolidation pressures starting at 200 psi (1.4 MPa).

Many of these thermoplastic polymers have been developed with the intent to rapidly stamp or compression mold structural composites parts at low cost. However, this potential has yet to be realized because of low production volumes, high capital equipment and tooling costs as well as excessive fiber distortion in the formed part. The most successful structural applications of these polymers have utilized autoclave processing to reduce tooling costs and fiber distortion. Other polymers in this class have been developed for use in circuit boards because of their low dielectric constant, low moisture absorption and low coefficient of thermal expansion. In these applications, compression molding had been found to be advantageous and cost effective.

Compared to other thermoplastic polymers, the condensation cure thermoplastics have not found a wide variety of applications. Their processability is very similar to the thermosetting polyimides, and this has been a limiting factor. Volatiles are produced by the condensation reaction, and they cause laminate porosity unless consolidation pressures are high enough to suppress void nucleation and growth. Costly high temperature tooling and consumable materials (e.g., vacuum bags and release films) are also required for part processing. While the toughness and processability of many of these condensation cured thermoplastic polyimides are slightly better than those of competing thermosetting polyimides, their

maximum operation temperature limit is somewhat lower. For the present, these thermoplastic polymers are limited to special niche markets which take advantage of their unique performance capabilities.

2.4.2.8 Specialty and emerging resin systems

2.4.2.8.1 Silicone

The silicones are a synthetic resin, composed primarily of organosilicon. The term silicone resin is a general term used for high temperature poly methyl siloxane. Silicone resins are available from a low viscosity liquid to a solid friable resin.

The silicone resin is used where high temperature stability, weatherability, good electrical properties and moisture resistance are required. These excellent properties have allowed the silicone resin to be used in laminates, varnishes, mineral filled molding compounds, and long glass fiber molding compounds. The silicone resin has been used as an impregnant for mica paper, flexible glass tape, glass cloth, and mica products. The molding compounds may be processed by conventional methods: injection, compression, and transfer molding. The cure temperature varies from 250°F to 450°F (120°C to 230°C). The cure time varies from 30 minutes to 24 hours, depending upon cure temperature, wall thickness of molded part, and the desired cured properties. In some applications, additional post cure will be required.

2.5 PROCESSING OF PRODUCT FORMS

2.5.1 Fabrics and preforms

2.5.1.1 Woven fabrics

Woven or knitted fabric product forms, unlike tapes and rovings, are in most circumstances produced prior to the resin impregnation step. Therefore, these product forms, in most part, offer product continuity or retention of fiber placement prior to, during, and after the impregnation step. Most fabric constructions offer more flexibility for lay-up of complex shapes than straight unidirectional tapes offer. Fabrics offer the option for resin impregnation either by solution or the hot melt process. Generally, fabrics used for structural applications use like fibers or strands of the same weight or yield in both the warp (longitudinal) and fill (transverse) directions. However, this is not a set rule as the number of combinations of reinforcement fibers and weave styles are essentially unlimited for custom applications. Also some fabrics are produced which incorporate thermoplastic strands that then become the resin matrix when the fabric is processed to its final state.

Woven fabric selections for structural applications have several parameters which may be considered. These variables are strand weight, tow or strand count, weave pattern, and fabric finish. The variables for glass fabrics are considerably greater than carbon fabrics due to the availability of a greater range of yarn weights. The availability of carbon tow weights or filament count tows are few in comparison. Generally, the lighter or thinner the fabric, the greater the fabric cost. Also factored into the cost is the complexity of the weave pattern or machine output for heavy fabrics. For aerospace structures, tightly woven fabrics are usually the choice for areal weight considerations, minimizing resin void size, and maintaining fiber orientation during the fabrication process.

2.5.1.1.1 Conventional woven fabrics

Woven structural fabrics are usually constructed with reinforcement tows, strands, or yarns interlocking upon themselves with over/under placement during the weaving process. The more common fabrics are plain or satin weaves. The plain weave construction results from each fiber alternating over and then under each intersecting strand (tow, bundle, or yarn). With the common satin weaves, such as 5 harness or 8 harness, the fiber bundles traverse both in warp and fill directions changing over/under position less frequently. (See Figures 2.5.1.1.1(a) and (b).)

These satin weaves have less crimp and are easier to distort than a plain weave. With plain weave fabrics and most 5 or 8 harness woven fabrics the fiber strand count is equal in both warp and fill directions. Example: 3K plain weave often has an additional designation such as 12 x 12, meaning there are twelve tows per inch in each direction. This count designation can be varied to increase or decrease fabric areal weight or to accommodate different fibers of varying weight.

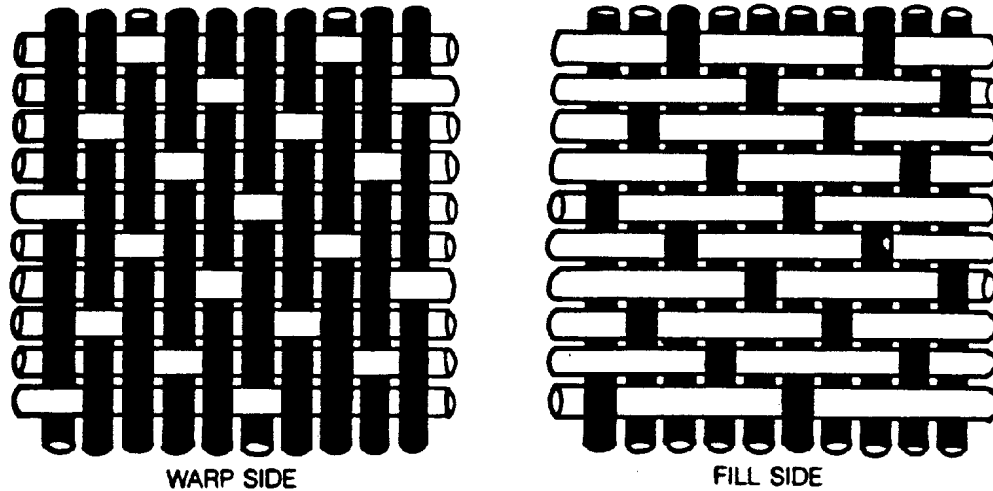


FIGURE 2.5.1.1.1(a) 5 Harness satin weave construction. In this weave construction each yarn goes over 4 and under 1 yarn in both directions.

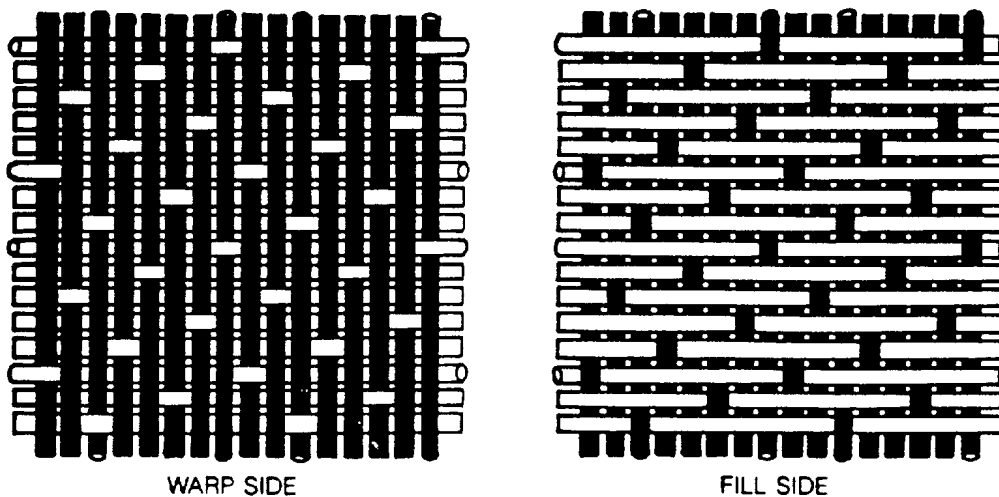


FIGURE 2.5.1.1.1(b) 8 Harness satin weave construction. In this weave construction each yarn goes over 7 and under 1 yarn in both directions.

2.5.1.1.2 *Stitched or knitted fabrics*

These fabrics can offer many of the mechanical advantages of unidirectional tapes. Fiber placement can be straight or unidirectional without the over/under turns of woven fabrics. The fibers are held in place by stitching with fine yarns or threads, after preselected orientations or one or more layers of dry plies. This product form, much like preplied unidirectional tapes, offers a wide range of multi-ply orientations. Although there may be some added weight penalties or loss of some ultimate reinforcement fiber properties, some gain of interlaminar shear and toughness properties may be realized. Some common stitching yarns are polyester, aramid, or thermoplastics.

2.5.1.1.3 *Specialty fabrics*

To list all the possible woven or knitted fabric forms would require space beyond the scope of this document. As an example, there are in excess of one hundred glass fabrics listed in a standard weaver's handbook. These fabrics vary in weight from 0.55 oz./square yard (18.65 gm/m²) to 53 oz./square yard (1796 gm/m²) and vary in thickness from 0.0012 in (0.0305 mm) to 0.0450 in (1.143 mm). Such an industrial listing is limited to but a few basic patterns such as plain, basket, Leno, harness, and twill weaves. There are many other fabrics such as triaxial, orthogonal, knitted bidirectional, stitched multilayer, and angle interlock, to name a few. From these also arise combinations and three-dimensional weaves.

2.5.2 **Preimpregnated forms**

2.5.2.1 *Prepreg roving*

This impregnated product form generally applies to a single grouping of filament or fiber ends, such as 20 end or 60 end glass rovings. Carbon rovings are usually identified as 3K, 6K, or 12K rovings. Other counts are available. It is possible, preferably during the resin impregnation step, to combine two or more counts or filaments or ends to increase the rovings weight, width, etc. per linear length. For mechanical testing purposes individual rovings are usually wound, side by side, to form single ply tapes and processed as such. The roving product form, with its packaging on individual spools, offers the means for automated fiber placement during the manufacture of parts. The rovings can be placed in a unidirectional pattern, like tapes, or to generate a crossover interlocking effect. Most applications for roving products utilize mandrels for filament winding and then resin cure to final configuration. In addition, this product form is used for efficient build-up of oriented filaments to create preforms. The preforms are combined with other lay-ups or processed individually in closed tools rather than the conventional mandrel cure process. Most rovings are supplied untwisted, in nearly flat continuous bands. Band widths can be controlled to a degree during the impregnation step. Compared to tapes or fabrics, roving areal weights for individual plies or wraps are more dependent on the winding process than the impregnation step. However, resin control of the preimpregnated rovings shares a like degree of accuracy.

2.5.2.2 *Prepreg tape*

All product forms generally begin with spooled unidirectional raw fibers packaged as continuous strands. Normally, untwisted tows or ends are specified for unidirectional product forms to obtain ultimate fiber properties. This particular product form depends on the proper fiber wet-out and the tenacity of the uncured resin to maintain proper fiber placement until the tape reaches the curing procedure.

2.5.2.2.1 *Conventional unidirectional tapes*

This particular form has been the standard within the user industry for many years and is common with thermosetting resins. The most common method of manufacture is to draw collimated raw (dry) strands into the impregnation machine where hot melted resins are combined with the strands using heat and pressure. The combination of fibers and resin usually travels through the machine between coated carrier papers or films for ease of release. The tapes are usually trimmed to specified widths in line. One side of the carrier is usually removed prior to the roll-up position to facilitate continuous visual inspection. The remaining carrier is usually left in place with the tape to serve as a separator on the roll and as a

processing aid for fabrication purposes. The tape manufacturing process is continuous within the linear limits of the raw strands created to the machine or specified lot size or availability of resin. Most impregnation machines are designed to permit in-line change over to new rolls (take-ups) without interruption. Raw strand collimation is adjusted to control specified areal weight (dry weight/area). Resin filming for tape machine operations is often done as a separate controlled operation. Some machines accommodate in-line filming that permit resin content adjustments during the impregnation process. Tapes as wide as 60 inches (1.5 m) are commercially available.

2.5.2.2.2 *Two-step unidirectional tapes*

Although not a general practice within the prepreg industry, there are unidirectional tapes manufactured from preimpregnated rovings. The collimation of these rovings to make tapes allow the use of solution impregnated resins, rather than hot melt systems. Although the product form may be similar to conventional tapes, thin uniform flat tapes may be difficult to produce.

2.5.2.2.3 *Supported unidirectional tapes*

To enhance specific mechanical properties or part manufacturing handling operations, it is sometimes advantageous to add product form during the manufacture of unidirectional tapes. Generally, these added fibrous forms are lightweight to be accommodated during the normal tape manufacture operation. The added form may be combined in the machine dry or preimpregnated prior to the tape production. More common added forms are lightweight mats or scrim fabrics of the same or unlike fiber type. The added product form will affect material properties compared to tapes without the supporting material.

2.5.2.2.4 *Coated unidirectional tapes*

Some tape suppliers offer the option of added tape surface coating. These resinous coatings of films are usually of different rheology or viscosities from the fiber impregnation resin to remain as distinct boundaries between plies of the cured tapes. As with supported unidirectional tapes, the added layer may be combined during the tape manufacturing operation.

2.5.2.2.5 *Preplied unidirectional tapes*

These tapes originate as any of the above-described tape forms in single-ply form. Then through a process of stacking, two or more layers of individual tapes are oriented at predetermined angles in relation to the centerline of the new progressively generated tape or broadgoods form. The original individual tapes are located side to side in each angled layer to form a continuous linear form. The original single-ply tapes are usually precut in segments at angles to correspond to the new product form's edges. The progressive stacking sequence usually takes place on a continuous carrier (paper or film) atop a flat surface much like the fabrication process. The carrier, with the preplied form in place, is utilized to take up the preplied tapes onto a shipping/handling core. The predetermined length of the individual precut segments will generally regulate the width of the preplied tapes. However, a final trim of both edges to control specified widths can be incorporated during the take-up step. For economic purposes the preplying operation usually is done in widths of approximately 24 inches (0.6 m) or greater. Should narrow widths be required, they can be accommodated with a secondary slitting operation. To some extent the retention of this product form's continuity is, like single ply tapes, dependent on the tack or tenacity of the uncured resin.

2.5.2.3 *Prepreg fabric*

This section is reserved for future use.

2.5.2.4 *Preconsolidated thermoplastic sheet*

This section is reserved for future use.

2.6 SHIPPING AND STORAGE PROCESSES

Composite precursor materials and adhesives can be very sensitive to how they are stored and shipped. Contamination must be avoided, as it will invariably reduce properties. Materials that have been preimpregnated (prepreg), film adhesives, and other resins are temperature variation sensitive. They can also be very sensitive to moisture and humidity before they are cured. As a result, these materials need special handling and storage in order to provide desired results.

2.6.1 Packaging

Prepreg and film adhesive should be supported on cardboard rolls, or in some other manner. They should be sealed in moisture-proof bags, with desiccant packages if possible. Once packaged, they should be stored in conditions as recommended by the manufacturer, usually at or below 0°F (-18°C) for a shelf life of six months or longer. Since the cure of thermoset materials continues to progress at room temperature, and even these lower storage temperatures, a record must be kept of the time exposed at room and storage temperatures. This record will be used to establish the useful life of the material and to determine when retesting is required. The time that material can be at room temperature and still usable, known as the out-time, can range from minutes to thirty days or longer. For some materials the processing characteristics can change dramatically depending on how much storage and out-time they have experienced.

2.6.2 Shipping

Since these materials require a carefully controlled environment, maintaining that environment while shipping the product can be challenging. Usually the material, still in its moisture-proof sealed bag, is placed in a shipping container approved for use with dry ice. Enough dry ice is placed in the container to allow some to be remaining upon the scheduled arrival, plus about 24 hours. Chemically based temperature sensitive materials, or electronic temperature recording devices can be placed in the container to assure material integrity upon delivery.

2.6.3 Unpackaging and storage

Upon receipt the material should be placed in a freezer to maintain the recommended storage temperature. Any time during shipping where the material temperature has exceeded this storage temperature is deducted from the out-time for the material. When the material is needed for use it needs to be allowed to reach room temperature before the moisture-proof bag is opened. If this is not done moisture will condense on the cool material, and may result in prebond moisture problems with the material.

2.7 CONSTRUCTION PROCESSES

Construction processes are those used to bring various forms of fiber and fabric reinforcement together to produce the reinforcement pattern desired for a given composite part or end item. The resin may or may not be in its final chemical or physical form during placement of the reinforcement. Construction processes include both manual and automated methods of fiber placement, as well as adhesive bonding and sandwich construction.

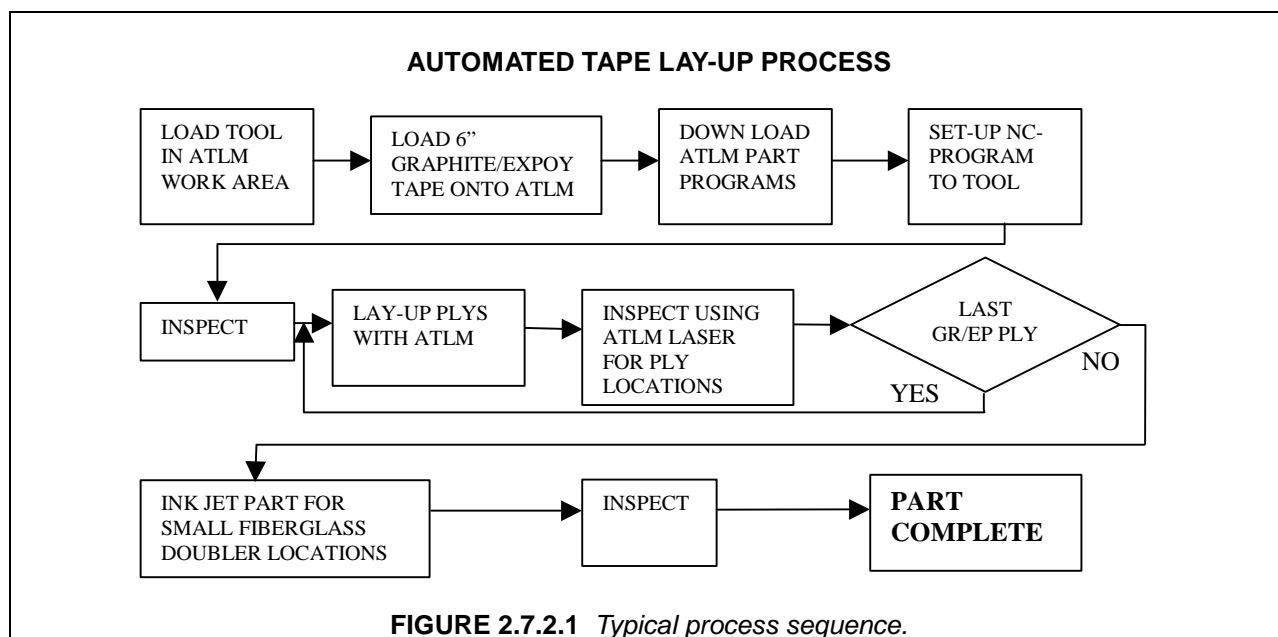
2.7.1 Hand lay-up

This section is reserved for future use.

2.7.2 Automated tape placement/automated tape lamination

2.7.2.1 Background

Composite tape lamination machines have been in use in industry for about 20 years. The early developmental machines were usually custom made for the aerospace industry in small machine shops under the guidance of developmental engineers. Once the technology was proven in the laboratory, commercial machine tool manufacturers began producing and further developing tape laying machines for industrial applications.



2.7.2.2 Benefits/capabilities

The use of automated tape lamination machine allows lay-up of unidirectional composite tape in 3", 6" and 12" (7.62 cm, 15.24 cm, and 30.48 cm) widths. The machines are able to lay-up 10-20 lbs./hr, compared to 2-3 lbs./hr for typical hand lay-up operations. Automated tape laying enables fabrication of large composite components using a minimum of manual labor without the ergonomic problems associated with personnel climbing onto large tools to lay-up parts. Material utilization is increased by at least 50% when compared to historical manual lay-up data. The process can be used on flat or contoured parts, the current commercial heads have a contour limit of 30° out of a horizontal plane. Typical applications in the aerospace industry are for wing and empennage components as well as control surfaces with mild contours. If more contour is required, a custom machine would be required.

2.7.2.3 Sources of variability

Material Tack: The machine performance is dependent on the characteristics of the composite material that is being laid. The development of the material must include manufacturing trials on a tape laminating machine. The relationship between the tack of the prepreg to the backing paper and the adhesion of the prepreg to itself is critical for efficient lamination with a machine. The laminating machine has continuous paths for the backing paper, that is the supply roll will have prepreg and backing paper and the take up roll will only have backing paper. The machine relies on the backing paper/prepreg adherence to deliver the prepreg to the head and the prepreg/prepreg tack to laminate it to the part and release it from the backing paper. These relationships need to be consistent over the range of temperature and humidity

variations that occur in the clean room environment. Tack is also affected by material outtime. In the manufacturing environment the material outtime needs to be closely monitored. For machine lay-up, the handling life of the prepreg is typically half that of hand lay-up materials.

Backing Paper: The backing paper used for the prepreg is coated with a release agent to ensure the level of adhesion to the prepreg is consistent. It also must be very consistent in thickness and not have a propensity to rip when scored with a knife. The reason the material thickness is critical is because of the use of stylus or ultrasonic cutters. The cutter cuts the prepreg against an anvil with the backing paper in between, the cutter depth must be set as to always cut through the prepreg but not cut the backing paper. The cutters are set at depths such that the backing paper gets scored during cutting and is in tension from the machine, therefore, a high notch sensitivity property is required in the release paper.

Impregnation Level: The impregnation level of the prepreg needs to be sufficient to allow removal of prepreg from the release paper with required stiffness to facilitate placement. Additionally, the impregnation level will allow prepreg cutting without tow separation and possess the required surface tack.

Width Tolerances: The prepreg width tolerances must be maintained to achieve required gap and overlap requirements established for the process/application.

Natural Path Part Programming: The tape lamination machines use natural path part programming to define tape paths. The tape paths are defined to minimize the laps and gaps associated with the part contour. On heavily contoured parts, the natural path may result in excessive laps and gaps that will require engineering coverage.

Automated tape lamination has proven to be a very efficient and cost effective manufacturing process for large contoured composite parts. For maximum efficiency of the machines, engineers tailor the part design to the machine capabilities. This tailoring results in reduced scrap lays, minimizes manual operations, and ensures an affordable manufacturing process.

2.7.3 Automated tow placement/fiber placement

2.7.3.1 Background

Fiber placement is an automated machine process utilizing narrow strips of composite material (pre-impregnated tows or slit prepreg tape) taken from multiple spools. The machine collimates the material into a band up to 6 inches wide which is a function of the individual tow width, the number of tows a particular machine can process, and/or the width that the part geometry can accommodate and laminates the material onto a work surface (tool). As each band is placed, some machine heads are capable of adding or dropping individual tows to either widen or narrow the bandwidth accordingly. This capability, allowing a true fiber orientation to be maintained on a contoured surface, is unique to the fiber placement process. The process allows material to be placed only where needed thereby greatly reducing material scrap factors. The uniqueness of the machine process requires a unique manufacturing and design approach. In addition to machine operation and fiber placement specific knowledge, manufacturing personnel must pay close attention to off-machine preparation steps within the work cell and designers must incorporate the physical operating limits of the machine into the component design. These factors are critical to maintaining an efficient process, to maximizing machine capacity, and to ensuring that the component will meet the engineering requirements.

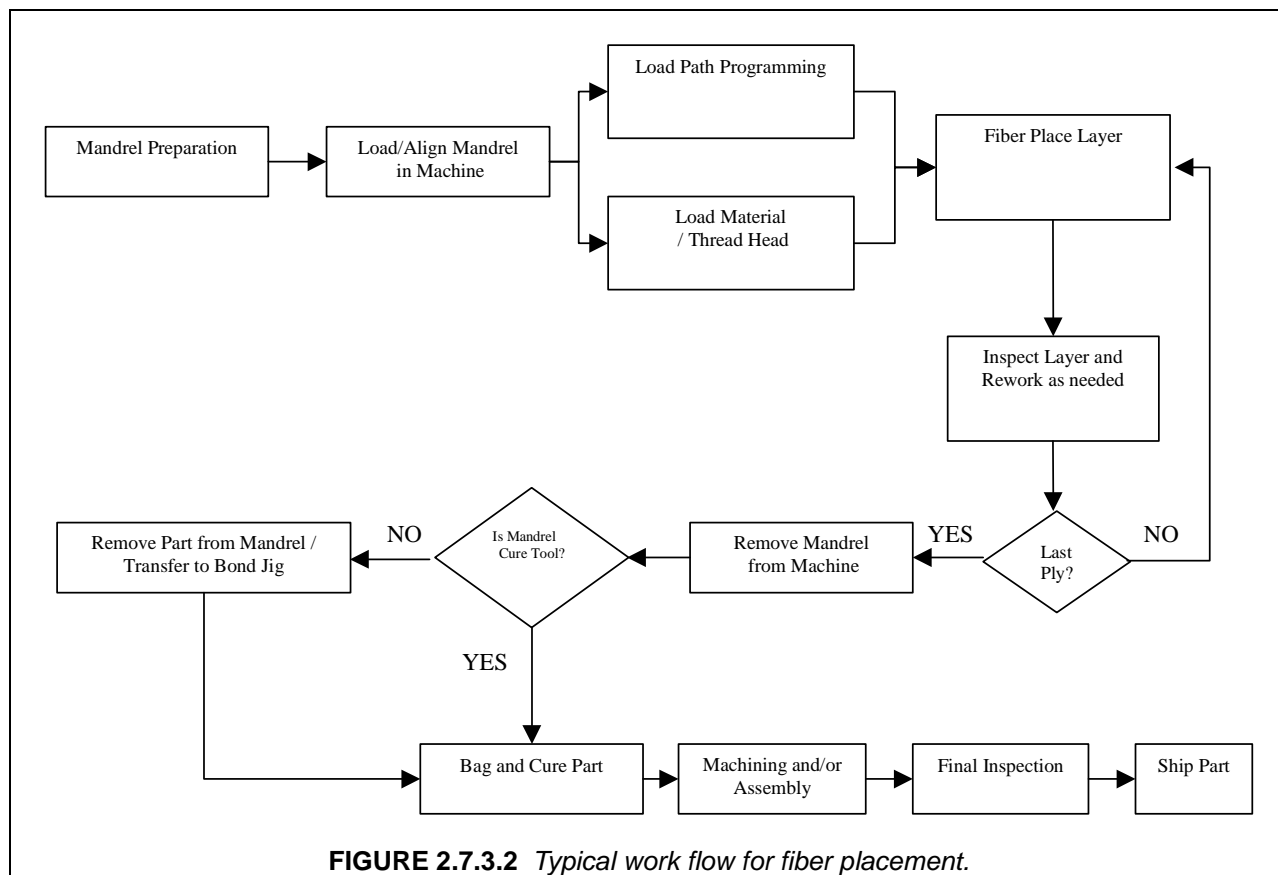
Automated tow placement or fiber placement was first conceived in the early 1980's. Early machines were developed by Hercules Aerospace (now Alliant Techsystems) and Cincinnati Milacron (now Cincinnati Machine). Production programs, mainly military aircraft systems such as the V-22 Osprey, F/A-18E/F Super Hornet, and F-22 Raptor, began using fiber placement for the fabrication of composite parts in the early 1990's. By the mid-nineties business jet manufacturers, most notably Raytheon, began using fiber placement for fuselage sections. Today fiber placement is an accepted production process and a preferred approach for the manufacture of many mild-complex contoured composite parts. With over twenty

production capable machines available worldwide, fiber placement operations can be found on the factory floors of most major aerospace contractors and composite part suppliers.

2.7.3.2 Fiber placement process flow

The typical work flow for fiber placement is shown in Figure 2.7.3.2 and generally consists of: (1) preparation of the tool or mandrel surface that the material will be applied to; (2) loading and aligning the mandrel into the fiber placement machine; (3) preparation of the machine by loading material, threading the tows (tapes) through the delivery system, and loading the computer path programs for the part being built, which have been generated offline; (4) machine collation or automated fiber placement of the tows (tapes) included in a particular ply or layer; (5) inspecting/reworking defects after each ply is placed; (6) continuation of machine collation until all plies are placed; (7) Preparing the part for cure; and (8) bagging/curing the part. Some parts are cured right on the placement tool and other may require transferring the part to a cure tool.

After cure, the part is unbagged and removed from the tool. The bagging, cure, part removal and finishing steps are identical to those required for hand collated parts. This workflow may vary depending on the application. For example, some parts have other materials introduced during fabrication, such as core or alternate fibers, and interim compaction steps may occur.



2.7.3.3 Benefits/capabilities

The use of a fiber placement machine allows the precise control of individual unidirectional composite tows. The ability to control the speed, feed, and tension in each individual tow allows the composite to be steered over complex contours as it's being laid into position. The fiber placement deposition head can

accommodate anywhere between 1 to 32 individual tows. The width of the tow is typically 0.125" (.317 cm) (although other tow sizes such as 0.128", 0.157" and 0.182" (.325 cm, .398 cm .462 cm) are also used) which results in lay down widths ranging between 0.125" and 6" (.317 and 15.24 cm). The equipment is also capable of varying the width of the material band by dropping and adding tows as it goes along during the course of placing a layer. The use of fiber placement to collate and compact the material also minimizes the need for intermediate debulk operations, which are typically done every 3-5 plies for fabric hand lay-up, 5-10 plies for prepreg tape hand lay-up, but only every 10+ plies for fiber placement.

The lay down rates and cost savings achieved with automate fiber placement are very part dependent. On a complex contoured part, labor savings can be as high as 50% while for flat or mildly contoured surfaces as little as 10%. For most parts that are good candidates for fiber placement labor savings are in the neighborhood of 25%. Additional savings are possible through reduced material scrap factors. Fiber placement usually results in material utilization factors in the 1.05-1.20 range, far less than manual operations which can be as high as 2.25. The lower material utilization is somewhat offset by the higher price of the unidirectional tow/slit tape material required for fiber placement which can cost 10-15% more than conventional prepreg material. This price differential is reducing, however, as the use of tow/slit tape material increases. Typical applications in the aerospace industry are: inlet ducts, contoured fuselage panels, full fuselage barrel sections, contoured fairings, nacelle skins, payload shrouds/adapters, and structural shafts (straight and contoured).

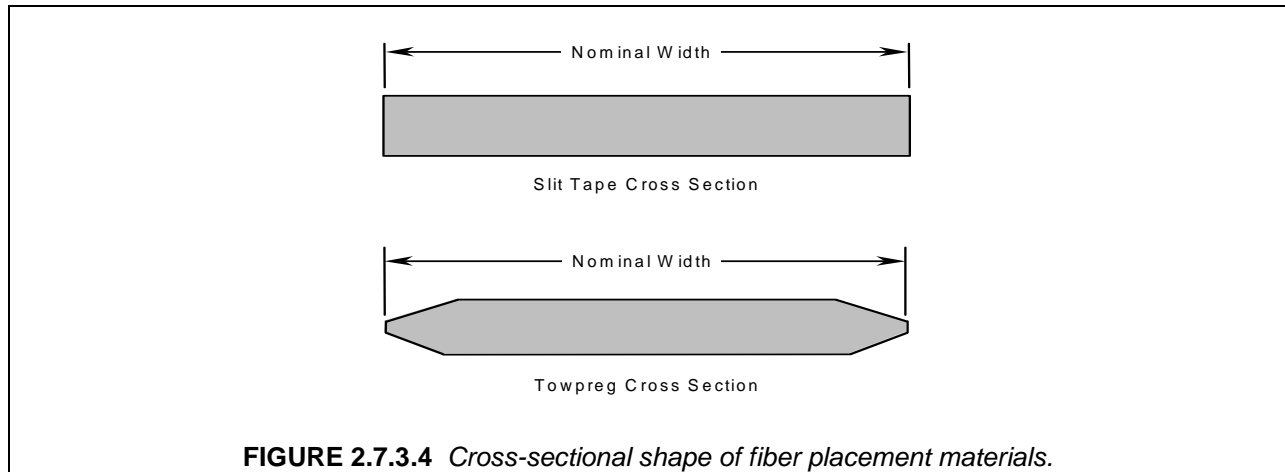
2.7.3.4 Material product forms

Fiber placement material is available in two product forms, slit tape and prepreg tow (towpreg). Both product forms are wound onto a core, which is 11 inches (27.94 cm) long and can vary between 3 to 6 inches (7.62 cm to 15.24 cm) in diameter. The towpreg is generally wound in an open helical winding pattern without any separation films. The slit tape is generally spiraled on in a tight helix pattern with a separation film introduced to keep the tape from sticking to the underlying layer.

The prepreg tow or towpreg manufacturing process involves unspooling a dry fiber spool, impregnating it with the proper resin content, shaping it to the specified width and thickness and respooling it as a prepreg tow or towpreg spool. The impregnation can be either a hot melt process or a solvent process. The process often involves first making parent tape, generally 6 to 12 inches (15.24 to 30.48 cm) wide, impregnating it with resin using normal unidirectional tape technology, then separating it back into individual tows again with a predetermined width based on the tray size of the fiber placement machine. Because the width is set to a specific dimension, the thickness of the towpreg is dependent on the size of the fiber bundles used during prepregging. Towpreg typically is not respooled with any kind of backing film or separator sheet. The process is continuous from the point of unspooling the dry fiber to spooling the towpreg in its final condition. Precise width control is the biggest challenge for the prepreg tow suppliers. Prepreg tow has the potential to be less expensive because it does not use a separation film and does not require a secondary slitting process.

Slit tape is first manufactured in the form of 6-48 inch (15-122 cm) wide unidirectional tape (broadgoods) which are then cut into multi-sected rolls. These multi-sected rolls are then slit to the final width, which is specified for the individual fiber placement machine (most common is 0.125 inches (.317 cm)). Slit tape typically has a 0.002 inch thick polyethylene interleaf or backing sheet which is 0.5 inches (1.27 cm) wide and centered over the tow in order to facilitate spooling and unspooling of the slit tape without damaging the material. This backing sheet is removed during the fiber placement process using vacuum tubes, which are part of the fiber placement machine. Once the blades are set for slitting the multi-sected rolls, the process yields a tow with a very precise width along the tow length. One of the advantages of slit tape is the ability to deliver a tow width that matches existing fiber placement machines at a variety of thicknesses. The thickness of the slit tape is primarily dependent on the fiber areal weight and uncured resin content of the original un-slit tape on the master roll. In cases where fiber placement efficiency can be improved by using thicker material, the master roll may consist of multiple layers of prepplied unidirectional tape.

Another difference between the product forms is the cross-sectional shape of the material. The tow-preg operation, which generally involves peeling individual tows off the parent tape, will yield a tow with a tapered cross-sectional shape. Some prepreg tow suppliers are using dies to shape the tow before spooling, but there still will be some widening of the tow at the turnarounds. Slit tape will have a more rectangular shape. Figure 2.7.3.4 illustrates this difference. If the width of the towpreg tows is a little over nominal size, the tapered shape allows each individual tow to overlap within a course band. This individual overlapping reduces the occurrence and severity of band to band overlaps. The rectangular shape of slit tape and their more precise width allows them to stack nicely together, but does not facilitate individual tow overlapping within a band if the tows are oversize. If the tows are oversize each tow butts up against an adjacent tow within the band or stacks on the one next to it at full band thickness. If they butt side to side it can spread out the overall bandwidth, and will increase the occurrence of band to band overlaps within a part.



2.7.3.5 Special considerations

The machine performance is dependent on the characteristics of the composite material that is being placed. The development of the material must include manufacturing trials on a fiber placement machine. When developing and qualifying a material for fiber placement several factors to be considered are:

Material Tack: The relationship between the tack of the prepreg to the backing paper (in the case of slit tape) and the adhesion of the prepreg to itself (in the case of prepreg tow and general adhesion) is critical for efficient lamination with a machine. These relationships need to be consistent over the range of temperature and humidity variations that occur in the clean room environment. Although "CTLM (Contoured Tape Lamination Machine) grade" material typically works best for fiber placement, the process is less sensitive to tack level than contoured tape laminating machines. However materials with too much tack will tend to gum up the machine and greatly reduce efficiency. Tack is also affected by material out time. While fiber placement machines have environmentally controlled creels for use during material collection, the out time is still important and needs to be monitored. It is important for the material to stiffen-up and have very low tack when it is cooled (the delivery head components are cooled to reduce resin build-up and let the material slide through with little friction, while at the same time making the tow stiff so it can be fed back out during adds) and have good tack to itself when gently heated at the lay-down point.

Impregnation Level: If tow materials are not completely impregnated with resin, dry fibers tend to fray and the edges of the tow will become fuzzy. This problem is mainly seen in slit tape. Early in the development of the slit tape product form, it was believed that prepreg manufactured for hand lay-up operations could simply be slit and used for fiber placement. However, broadgoods for hand lay-up are commonly fabricated with the center (through the thickness) fairly dry. This allows more resin on the surface of the prepreg, which will increase the tack and aid in debulking. It is after these hand lay-up

broadgood rolls are slit that the dry center section is exposed. As the tow begins to fray the fuzziness will accumulate along the fiber path. Whenever tow material that is extremely fuzzy is used, it requires increased maintenance to keep the fiber paths clear. The fuzz will eventually build-up enough to prevent tows from freely moving through the head and the machine operators will have to stop and clean the machine head. This problem can be greatly reduced by ensuring that the parent tape fibers are fully impregnated through the thickness. Broadgoods fabricated for hand collation will have a higher degree of fuzziness than those specifically made to be slit. It is recommended that prepreg material be purchased specifically for slit tape use, and that standard hand collation material not be used for fiber placement.

Width Tolerances: Width control and tolerance of the material is one of the most important parameters to consider. Width tolerances must be maintained to achieve required gap and overlap requirements established for the process/application. Slit tape will have much less variation in the tow width than towpreg. When the tow width deviates from the nominal value, a part fabricated with this material will have either gaps or overlaps. Gaps and overlaps must be repaired on a ply-by-ply basis, which can be costly and labor intensive. Since the tow guide trays in the fiber placement machines are set to a constant width, material that is too wide (out of tolerance) will not smoothly move through the head. In some cases the tow will become stuck in the head and the part fabrication process has to be stopped while the tow is removed. For part quality and possible effects on mechanical performance, the width standard deviation is an important parameter to control. Slit tape will typically have a lower standard deviation than towpreg. To get good parts, typical expectations for slit tape and towpreg are as follows:

Tow Width	Slit Tape Tolerance	Towpreg Tolerance
0.125-0.128 (3.18-3.25 mm)	±.005" (0.127 mm)	±.007" (0.178 mm)
0.157 (3.98 mm)	±.005" (0.127 mm)	±.007" (0.178 mm)
0.182 (4.62 mm)	±.007" (0.178 mm)	±.009" (0.228 mm)

Materials outside these specs have been used successfully, but generally more downtime is involved, and/or part quality is reduced, and the potential implications on mechanical properties must be thoroughly evaluated. Depending on the application, using a lower standard material at a lower cost may still be acceptable.

Material Handling: When using slit tape, the spools of material can be stored and handled according to the same specifications used for broadgoods; however, some towpreg systems require special handling procedures. These special handling procedures are required at room temperature because if a towpreg spool is allowed to sit and come up to room temperature, the resin will creep and flow causing the tows to fuse together on the roll. During despooling, the tow being pulled from the spool will stick to the material still wrapped around the spool causing the tow to bend back on itself. The fibers then kink and break or snap free and cause undesirable tension spikes. This sticking action will occur even if the towpreg (that has already been exposed to room temperature for too long) is re-refrigerated or despoiled in an environmentally controlled creel. Accumulated room temperature exposure should be minimized - limited to eight hours for most epoxy products. Towpreg spools should never be stored with their weight on the prepreg (don't lay them on their side). The spools should be stored with the weight on the cardboard core whenever possible. This is not as critical if the material is at 0°F, but as it warms up, the added contact pressure will cause the tows to fuse even quicker and tighter.

In addition to tow sticking, stringers may develop when using towpreg. Stringers are caused when part of the tow frays off and remains wrapped around the spool during despooling. It will eventually create a ring and will cut the tow in half or fault out the tensioner on the machine. Tow sticking and stringers are not commonly seen in slit tape because the spools have a backing sheet.

Mechanical Properties: In many cases it is desirable to utilize existing material databases/allowables when designing fiber-placed parts. Typically these allowables were generated from hand lay-up coupons/elements. Laminates produced using the fiber placement process are capable of delivering mechanical properties equivalent to hand lay-up. However, the ability to do so depends upon carefully setting and controlling several parameters, the most important of which are lap/gap criteria. The frequency, location, and size of the laps/gaps is influenced by several factors including raw material width variability, path programming settings (when to drop/add tows, convergence settings), and part geometry. It is recommended that a limited test series be conducted to demonstrate the equivalency of fiber-placed laminates to hand lay-up.

Mandrel Tool Design: Tooling coordination is essential to the successful fabrication of a fiber placed part. As in all tooling programs, proper coordination must exist between the “as designed” part, the “as fabricated” part, NC programming, hard tooling, soft tooling, and inspection aids. The tool-to-machine interface is critical to fiber placement accuracy. The introduction of misalignment, play, or non-repeatability, especially at the headstock end, can translate to positioning errors on the tool surface. Fiber placement collation tools must meet minimum strength and stiffness requirements. Tool size, tool weight, part weight, and head compaction force all affect the tool design. Fiber placement tooling structure should be designed to be as light and rigid as possible. It must not sustain any permanent deformations due to part weight and compaction forces. These deformations can be in bending and in torsion. Torsional rigidity is an important design consideration that is often overlooked. It must be remembered that the point of application of these forces can be dimensionally far from the axis of rotation and that the tailstock is free to rotate.

Part Path Programming: Fiber placement machines are capable of several path programming schemes including fixed fiber angle, band offset, and limited parallel (a combination of the other two). The best method selected depends on the geometry of the part, the desired tolerance control of the fiber orientation, and the allowable laps/gaps. Many features exist in the offline programming software that controls both on-part and off-part motions of the machine. Time well spent in offline programming will pay dividends during fiber placement.

2.7.4 Braiding

The braiding process fabricates a preform or final shape at the same time that it generates the woven form. This product form is a unique fiber reinforcement which can use preimpregnated yarn as well as dry fibers. The main advantage of the braiding process is its ability to conform to odd shapes and maintain fiber continuity while developing high damage tolerance compared to unidirectional and laminated products. This allows formation of square, oval, and other constant cross-section shapes. The three-dimensional form of braiding has evolved to the point of allowing the non-uniform cross-sections to be fabricated while maintaining weaving in all three planes.

The uses of braiding have varied during its development. The best known example of braided structure is the fiberglass and carbon fishing rods that became popular in the 1980's. Braiding has also found uses in pressurized piping and complex ducting. A demonstration of its versatility is the open-wheel race car body which was fabricated by braiding. The process has also been used in rocket applications for motorcases and launchers.

In biaxial and triaxial braiding, a mandrel is usually used to form the braid. The mandrel also acts as the mold for the final product. The braiding machine controls the rate of feed of the mandrel and the rotational speed of the carriers. The combination of these parameters and the size of the mandrel controls the braid angle. The braid angle, along with the effective yarn, tape, or tow width (width of the specific size yarn, tape, or tow on the mandrel as placed by the braiding process), ultimately controls the coverage of the braid on the surface of the fabricated form. As the braid angle increases, the maximum size of the mandrel which can be covered with a specific yarn, tape, or tow size decreases. For complicated forms, expendable mandrels may be used. These include mandrels made from low melting temperature metal alloys and water-dissolvable casting materials, and collapsible mandrels.

In three-dimensional (3D) braiding, the weaving process itself is used to control the shape of the fabricated product. The typical 3D braiding process involves a bed of cops, or weaving loops, which are moved in a systematic manner. This systematic movement creates an interwoven product in the x-y plane. As the yarns, tapes, or tows are pulled into the weaving process, the z-direction is also intertwined. The resulting product is essentially self-supporting due to interweaving in three directions. For precision exterior dimension, matched metal molds can be used during the resin matrix curing process. The following are the general steps involved in the braiding process:

1. Set the feed speed, cop speed, and weave pattern (3D braiding).
2. Run the braiding machine until the product is finished.
3. If prepreg material is not being used, use an appropriate resin impregnation process - RTM, wet resin impregnation, etc.
4. Cure according to the appropriate process determined by the impregnation method - autoclave cure, vacuum bag, RTM, etc.
5. Remove the part from the mold or mandrel.

2.7.5 Filament winding

Filament winding is an automated process in which a continuous fiber bundle (or tape), either preimpregnated or wet impregnated with resin, is wound on a removable mandrel in a pattern. The filament winding process consists of winding onto a male mandrel that is rotating while the winding head moves along the mandrel. The speed of the winding head as it moves along the mandrel in relation to the rotation of the mandrel controls the angular orientation of the fiber reinforcement. Filament winding can be done using wet resin winding, preimpregnated yarns and tapes. The following general steps are used for filament winding:

The construction of the mandrel is critical to the process and the materials of choice are dependent upon the use and geometry of the finished part. The mandrel must be capable of withstanding the applied winding tension, retaining sufficient strength during intermediate vacuum compaction procedures. In addition, if the outer surface of the part is dimensionally critical, the part is generally transferred from the male winding mandrel to a female tool for cure. If the internal surface of the part is dimensionally critical, the part is usually cured using the male winding mandrel as the cure tool. Metal is used in segmented collapsible mandrels or in cases where the domes are removed to leave a cylindrical part. Other mandrel material choices are low melt alloys, soluble or frangible plaster, eutectic salts, sand and inflatables.

The following general steps are used for filament winding:

1. The winder is programmed to provide correct winding pattern.
2. The required number of dry fiber or prepreg roving/slit tape spools for the specified band width are installed on the winding machine
3. When wet winding, the fiber bundle is pulled through the resin bath.
4. The fiber bundle is pulled through the eye, attached to the mandrel, the winding tension is set and the winding program is initiated..
5. When winding is complete, the mandrel is disassembled as required and removed from the part if the part is to be cured on a female tool., otherwise the part is trimmed and prepared for cure on the male mandrel.
6. Elevated temperature cure of thermosets resin parts is usually performed in an oven or autoclave, room temperature cure resin parts are usually placed under vacuum to provide compaction during cure. During cure the male mandrel or female tool is often rotated to maintain resin distribution.
7. After cure the mandrel is removed from the part (for male tooled parts)

Cured product characteristics can be affected by both the winding process and design features such as:

1. Uniformity of the fiber to resin ratio (primarily wet winding)
2. Wind angle
3. Layer sequence

4. Effective fiber bandwidth (tight fiber weave or loose/open fiber weave pattern)
5. End closure.

The cure cycle and compaction procedure affects such cured product characteristics as described in the applicable cure and consolidation process section - 2.8.1 (for vacuum bag molding for room temperature cure resins), 2.8.2 (for oven cure), or 2.8.3 (for autoclave cure).

2.7.6 Pultrusion

The pultrusion process consists of passing a continuous resin-impregnated fiber bundle through a heated die for part shape and cure. This process is limited to constant cross-sections such as rods, tubes, I-beams, and channels. The pultrusion process works well with quick-curing resins and is a very low-cost method for high-production parts with constant cross-sections. For a discussion of cure and consolidation during pultrusion, see Section 2.8.6 below.

2.7.7 Sandwich construction

Sandwich construction, as applied to polymer matrix composites, is a structural panel concept consisting in its simplest form of two relatively thin, parallel sheets of structural laminated materials bonded to and separated by a relatively thick, lightweight core. The following information is limited to non-metallic sandwich construction used for structural applications. Sandwich construction provides a method to obtain high bending stiffness at minimal weight in comparison to monolithic laminate construction. This advantage must be weighed against the risk of increased processing difficulty that can increase production costs over monolithic construction. Damage tolerance and ease of repair should also be considered when selecting sandwich panel or monolithic laminate construction. Good structural practice requires selection of skin, core and adhesive materials to be strategically based on overall part quality considerations including:

1. Surface quality (pinholes, mark-off, etc.)
2. Skin quality (porosity, consolidation, waviness, resin loss)
3. Adhesive bond and fillet quality (strength, fillet size)
4. Core strength, cell size, bonding preparation
5. Resistance to moisture ingress

Polymer matrix composite sandwich construction is most often fabricated using autoclave cure, press cure or vacuum bag cure. Skin laminates may be pre-cured and subsequently bonded to core, co-cured to core in one operation, or a combination of the two methods. Pre-cured skin sandwich construction insures a high quality surface, but adequate fit-up to core must be addressed. Co-curing often results in poor panel surface quality which is prevented by using a secondary surfacing material co-cured in the standard cure cycle or a subsequent "fill-and-fair" operation. Co-cured skins may also have poorer mechanical properties, and this may require the use of reduced design values.

Cure cycles can be developed to reliably produce good quality sandwich panels. For co-cured sandwich construction, this is essential. Some primary cure cycle considerations are transport of volatiles, core evacuation and/or pressurization, adhesive and prepreg resin viscosity profiles, and compatibility to monolithic structure co-cured with the sandwich structure.

Skin materials for co-cure processing have a "low flow" resin material system that prevents resin running down the cell walls into the core. A compatible adhesive must be selected that develops an adequate fillet bond to the selected core whether co-cured or secondarily bonded. For co-cured construction, prepreg resin to adhesive compatibility must be demonstrated.

Core should be selected according to the required characteristics of the application often including surface quality, shear stiffness and strength, compressive strength, weight, water absorption, and damage tolerance. Currently available core materials include metallic and non-metallic honeycomb core and a variety of non-metallic foams. Honeycomb core selection can be made from a range of common carbon,

glass or aramid fiber reinforced matrix materials including phenolics, epoxies, polyimides, or thermoplastics.

Additional information may be found in References 2.7.7(a)-(d).

2.7.8 Adhesive bonding

Three types of adhesive bonding are commonly employed with composite structures. These are co-curing, secondary bonding and cobonding. A typical cocure application is the simultaneous cure of a stiffener and a skin. Adhesive film is frequently placed into the interface between the stiffener and the skin to increase fatigue and peel resistance. Principal advantages derived from the cocure process are excellent fit between bonded components and guaranteed surface cleanliness.

Secondary bonding utilizes precured composite detail parts. Honeycomb sandwich assemblies commonly use a secondary bonding process to ensure optimal structural performance. Laminates cocured over honeycomb core may have distorted plies which have dipped into the core cells. As a result, compressive stiffness and strength can be reduced as much as 10 and 20 percent, respectively. While secondary bonding avoids this performance loss, care must be exercised prior to bonding in order to ensure proper fit and surface cleanliness. In some applications, aluminum foil layers or an adhesive sandwiched between two layers of polyester release film is placed into the bonded joint. The assembly is then bagged and run through a simulated bonding cycle using the same temperatures and pressures as those in the actual cycle. The foil or film is removed, and its thickness is measured. Based upon these measurements, additional adhesive can be added to the bondline to ensure proper fit; or detail parts can be reworked to eliminate interference fits.

Precured laminates undergoing secondary bonding usually have a thin nylon or fiberglass peel ply cured onto the bonding surfaces. While the peel ply sometimes hampers nondestructive inspection of the precured laminate, it has been found to be the most effective means of ensuring surface cleanliness prior to bonding. When the peel ply is stripped away, a pristine surface becomes available. Light scuff sanding removes high resin peak impressions, produced by the peel ply weave which, if they fracture, create cracks in the bondline.

In-service secondary bond failures are usually interfacial, with all of the adhesive on one side of the interface and all of the resin on the other. One well-known cause of this condition is transfer of silicone from released peel plies. Another cause of this weakness, which cannot be detected by ultrasonic inspections, is pre-bond moisture. Adhesion relies on the surface energy of the substrate being higher than that of the uncured adhesive. Water at the interface lowers the surface energy of the substrate, making it more difficult or even impossible for the glue to adhere. As little as 0.2 percent pre-bond moisture in undried reinforced epoxy laminates has been found to reduce the shear strength of the bond by as much as 80 percent. The moisture is driven to the interface by the heat applied to cure the adhesive and is prevented from escaping by the typical ridged texture left by removal of even uncoated peel plies. Pre-bond moisture can also be present as the result of the hygroscopic nature of adhesive films left too long in an ambient environment. Condensate on adhesive that had not been properly stored in a sealed bag in the refrigerator has also resulted in kissing bonds that separate because of close to zero peel strength. The mechanical interlock achieved by filling the cavities in peel ply surfaces creates a 'Velcro'-type bond with sufficient strength to pass initial inspections, but without the durability to last in service.

In a particularly illuminating series of tests, using a peel ply known to be free of release agents, the first panel tested failed prematurely because of condensate on the adhesive film that not been properly stored. When the tests were repeated with no change other than to have stored the adhesive properly, the test specimens failed interlaminarly, in the resin between the interface and the nearest fibers in the top ply. In neither case were the adherends abraded. The change was clearly the result of the presence or absence of pre-bond moisture at the interface. The series production program with which these tests were associated has a requirement to severely restrict the out time of the components between curing and bonding to a matter of only hours, instead of days or weeks, and there have been no in-service fail-

ures. An interruption to the manufacturing process would require thorough drying of the cured details before bonding.

Another relevant incident involved metal bonding, with condensate known to be on the adhesive film prior to bonding. In one tool, the molded rubber bag on one side of the bonded assembly prevented any of the moisture from escaping; the stiffeners were held on by only the fillet of adhesive squeezed out along the edges. There was intimate contact but absolutely no adhesion on the faying surfaces. On another tool, using beady balls to simplify bagging, the moisture was easily able to escape through the cavities between the beady balls, and none of these bonds were found to be defective, despite the known presence of moisture before bonding. The difference between these two cases was simply the opposite ends of the spectrum in terms of venting of volatiles during cure. The moisture was able to escape when it had to migrate less than an inch to a huge vent path, but unable to escape when it would need to travel as much as three feet, escaping past as many as six knife-edge rubber seals.

There are not yet any tests in which composite bond surfaces have been grit-blasted, to remove the peel-ply texture to facilitate venting, in combination with the deliberate introduction of moisture to see if it could escape during the cure cycle. These are planned, however.

Experience with adhesive bonding of composite structures has made it clear that pre-bond moisture that is unable to escape easily during the cure has a disastrous effect on the strength and durability of the bonds. It is most important to dry composite laminates made sufficiently long before bonding that they could have absorbed even a small amount of moisture. It is also important to keep moisture away from uncured adhesive films. It is also clear that good venting can increase the tolerance of the bonding process to any pre-bond moisture that may occur accidentally.

Peel plies are generally not useful for thermoplastic composite laminates. Instead, plasma technologies such as flame spray are employed to remove minor amounts of contaminants and to increase surface reactivity. Thermosetting adhesives are sometimes used with pre-consolidated thermoplastic composites, but more commonly melt fusible thermoplastic films are utilized. Amorphous thermoplastics (e.g., polyetherimide) are superior choices for an adhesive film because of their wide processing latitude. In some instances, nichrome wire or ferromagnetic particles are placed into the film to resistively heat the film and effect flow within the bondline. Reference 2.7.8(a) provides an excellent overview of this technology.

Cobonding is a combination of secondary bonding and cocuring in which one detail part, usually a skin or spar web, is precured. Adhesive is placed into the bondline and additional composite plies for another detail part (e.g., a blade or hat stiffener) are laid up over the adhesive. The adhesive and composite plies are then concurrently cured together. The cobonding process has the advantage of avoiding expensive matched metal tooling that may be required for a cocured integrally stiffened composite part having the same geometry.

Whether cobonded joints develop the same structural performance levels as cocured joints is a matter of conjecture. The high cost of matched metal tooling has made conclusive testing prohibitive. Presently, there is no proof that cobonding is inferior to cocuring.

Historically, secondary bonding has been very susceptible to bondline failure as a result of improper cleaning and contamination (e.g., silicones). Cocured joints have demonstrated significantly less susceptibility to shop contaminants; therefore, it is anticipated that cobonding will be somewhat less susceptible to improper surface preparation than secondary bonding.

In many applications, composites are secondarily bonded or cocured with metals. Common examples are stepped lap splices and closure ribs and spars. Special attention must be given to minimizing thermal mismatch in composite to metal bonding. Carbon/epoxy and aluminum have been successfully bonded using adhesives which cure at 250°F (121°C) or less. With 350°F (177°C) curing adhesives, titanium is recommended because its coefficient of thermal expansion more closely matches that of carbon fiber composites.

Surface cleanliness is more critical for metals than composites in a bonded assembly. Aluminum, stainless steel and titanium detail parts require solvent vapor degreasing, alkaline cleaning and acid etch to produce an oxide layer with a controlled thickness and reactivity. The Forest Products Laboratory (FPL) etch, phosphoric acid anodize and chromic acid anodize processes are commonly employed as aluminum surface pre-treatments. Titanium pre-treatments include chromic acid anodize or chromated hydrofluoric acid etch processes. Phosphate solutions have proven successful in pretreating stainless steel surfaces.

In all instances, metal surfaces must be sprayed with a thin coat of adhesive bonding primer within few hours of pre-treatment. For best environmental resistance and bondline durability, a chromated epoxy primer is recommended. However, environmental regulations will restrict both the usage of chromium containing compounds and the application of primers with high volatile solvent contents. The challenge then for the coming decade is to develop environmentally friendly pre-treatment processes and primers while retaining or improving bondline durability under adverse environmental conditions and cyclic loading.

Additional information on joint design, adhesive materials selection processing, testing and quality assurance may be found in MIL-HDBK-691, Adhesive Bonding (Reference 2.7.8(b)).

2.7.9 Prebond moisture

This section is reserved for future use.

2.8 CURE AND CONSOLIDATION PROCESSES

Resin consolidation and cure processes are required to ensure that the individual sections or layers of a composite part are properly bonded, and that the matrix is intact and capable of maintaining the placement of the fibrous reinforcement which will carry the loads applied to the part. These processes are among the most sensitive in the materials processing pipeline. As a thermosetting composite part is formed during cure, the material is undergoing extensive chemical and morphological change. As a result, there are many actions occurring simultaneously. Some of these actions can be controlled directly, others only indirectly, and some of them interact. Such actions as evolution of voids or shifting of reinforcing fibers during matrix flow may result in large changes in properties of the cured composite.

In the case of a thermoplastic matrix composite, the matrix is not intended to undergo chemical change, during consolidation, but changes such as chain scissions resulting in production of volatiles may occur inadvertently. In addition, resin flow is required for consolidation, and semicrystalline thermoplastics may undergo morphological changes such as changes in the degree of crystallinity upon melting, flow and recrystallization, particularly in the fiber/matrix interphase. These changes can cause significant changes in mechanical and physical properties of the consolidated composite. In amorphous thermoplastics, segregation of varying molecular weight materials in the interphase may also result in changes in composite properties.

2.8.1 Vacuum bag molding

Vacuum bag molding is a process in which the lay-up is cured under pressure generated by drawing a vacuum in the space between the lay-up and a flexible sheet placed over it and sealed at the edges. In the vacuum bag molding process, the reinforcement is generally placed in the mold by hand lay-up using prepreg or wet resin. High flow resins are preferred for vacuum bag molding. The following steps are used in vacuum bag molding:

1. Place composite material for part into mold.
2. Install bleeder and breather material.
3. Place vacuum bag over part.
4. Seal bag and check for leaks.

5. Place tool and part in oven and cure as required at elevated temperature.
6. Remove part from mold.

Parts fabricated using vacuum bag oven cure have lower fiber volumes and higher void contents. Vacuum bag molding is a low-cost method of fabrication and uses low-cost tooling for short production runs.

2.8.2 Oven cure

Composite material can be cured in ovens using various pressure application methods. Vacuum bagging, as described in the above section, can be used to remove volatiles and trapped air, and utilize atmospheric pressure for consolidation. Another method of pressure application for oven cures is the use of shrink wrapping or shrink tape. This method is commonly used with parts that have been filament wound, because some of the same rules for application apply. The tape is wrapped around the completed lay-up, usually with only a layer of release material between the tape and the lay-up. Heat is applied to the tape, usually using a heat gun, to make the tape shrink, and can apply a tremendous amount of pressure to the lay-up. After shrinking the part is placed in the oven for cure. High quality parts can be made inexpensively using shrink tape, with a couple of caveats. First, the part must be of a configuration where the tape can apply pressure at all points. Second, flow of the resin during cure must be limited, because the tape will not continue to shrink in the oven. If the resin flows excessively, the pressure applied by the shrink tape will be reduced substantially.

2.8.3 Autoclave curing processing

2.8.3.1 General description

Autoclave curing is the process of curing materials using relatively high heat and high pressure in an autoclave. An autoclave is a heated pressure vessel typically capable of 300 psi (2 MPa) internal pressure and temperatures up to 700°F (370°C). Thermoset composite materials are generally processed at less than 100 psi and at temperatures ranging from 250 to 400°F (120 to 200°C). Thermoplastic composites may require higher temperatures and pressures. Due to the high temperatures in the autoclave during processing, the atmosphere within the vessel is generally purged of oxygen using an inert gas, such as nitrogen, to displace the oxygen thereby preventing thermal combustion or charring of the materials being cured.

Materials that are to be cured in an autoclave are located onto tooling providing the eventual shape of the cured material. The tooling, frequently referred to as the mold, may be comprised of an assembly of mandrels or tool details to accommodate complex geometry. The mold may also include features such as locating devices, tooling tabs or net-molding details to enhance the subsequent processing of the final product or material. Typically, an impervious layer of bagging film or a reusable elastic bladder is located over the material being cured and sealed against the mold. Vacuum is applied between the bagging material and the material being cured such that the plies of material are compressed through the thickness against the mold. In some instances, an autoclave or oven is used to apply heat and pressure to only a portion of the material being cured as an interim debulk step to enhance the quality of the finished product through improved consolidation. As the temperature in the autoclave is raised, the viscosity of the curing material is generally lowered to a fluid state and the gasses within and between the layers escape as the material consolidates. A porous "bleeder" layer and/or a "breather" in the form of sheet, strips or strands may be utilized under the bagging material to help enable the evacuation of gasses. Surface films or in-mold coatings may also be included against the tool surface to improve the surface finish of the cured material. Rigid caul plates or intensifiers may also be incorporated under the bagging material to locally control the thickness and quality of the finished product. In some cases, pre-cured or stage-cured components may be co-cured or co-bonded with the material being cured in the autoclave. For issues regarding specific resins, refer to Volume 3, Section 2.4.2. Also, see Volume 3, Section 2.10 for process control during autoclave curing.

2.8.3.2 Sources of variability

The primary sources of variability in the autoclave curing process are listed below:

- Tooling or mold surface finish; poor surface finish will transfer to finished product.
- Tooling materials, density, and spacing of tools in the autoclave; more, denser tools closer together will act as a heat sink and affect degree of cure.
- Part geometry; the more complex the geometry the more difficult to achieve uniform consolidation and avoid wrinkling.
- Lay-up symmetry; non-symmetrical geometry and/or lay-up cause part warpage or springback.
- Material location and alignment tolerances; non-symmetrical lay-up causes part warpage.
- Bagging technique and bagging materials including bleeder materials and cauls, etc.; vacuum bagging material movement or restriction from complete contact against curing material (i.e., bridging) causes non-uniformity in material compaction and resin flow affecting the quality of the finished product.
- Number of interim debulk cycles and debulk time, temperature and pressure (vacuum); insufficient debulking causes thickness and surface finish variability as well as wrinkles in the finished part.
- Raw material variability (including batch-to-batch variability) and material shelf life; materials are typically time and temperature dependent.
- Moisture content of materials being cured or processed; moisture in material affects laminate quality causing porosity as it turns to steam during cure.
- Number of vacuum ports, location of vacuum ports, and vacuum integrity during cure cycles; materials are consolidated through the thickness during cure as the resin flows and gels. Vacuum integrity affects the level of compaction.
- Autoclave temperature, pressure and time; variations in cure cycle affect the resin flow prior to cure, level of cure, and finished product thickness.
- Part thickness variations; thickness variations may affect consolidation and curing uniformity.

For special issues with respect to thick composites, see Volume 3, Chapter 7. For processing concerns with respect to sandwich construction, see Volume 3, Sections 2.7.7 and 2.7.8.

2.8.4 Press molding

Press curing uses heated platens to apply both pressure and heat to the part. Presses, in general, operate at 20 - 1000 psi (140 - 7000 kPa) and up to 600°F (320°C). Press curing is very economical for flat parts and high production rates. Tooling requires matched die molds for contoured parts. The following steps are used in press molding:

1. Composite material is placed in the mold cavity.
2. Cure monitoring devices are installed.
3. Parts are placed into press and cured. Pressure, temperature, and time are monitored during the cure cycle to ensure curing parameters are met.

Press curing produces high quality parts with low void content.

2.8.5 Integrally heated tooling

With integrally heated tooling the heat required for cure is provided through the tool itself, rather than through the use of external heating in an oven or autoclave. This can be used to make high quality parts without using an autoclave if matched mold tools are used. The heat is usually provided by imbedding electrical resistance elements or hot oil circulation channels within the tool. This can result in hot and cold spots within the tool. Heat surveys are necessary to ensure that all parts of the tool perform with a heat profile that allows the part to be cured completely and with high quality.

2.8.6 Pultrusion die cure and consolidation

Pultrusion is an automated process for the continuous manufacture of composites with a constant cross-sectional area. A continuous reinforcing fiber is integral to the process and the finished product. Pultrusion can be dry, employing prepreg thermosets or thermoplastics, or wet, where the continuous fiber bundle is resin-impregnated in a resin bath. The wet resin process was developed around the rapid addition reaction chemistry exhibited by thermoset polyester resins, although advances in resin and catalyst systems has made the use of epoxy systems commonplace.

In pultrusion the material is cured in a continuous process that can provide large quantities of high quality cured shapes. The material is drawn through a heated die that is specially designed for the shape being made. The tool is designed such that the volume of the cavity for cure causes the resin pressure to build, allowing consolidation of the material to occur. This cure cavity pressure is built up against the cured material that is downstream of it, and induced by the new material upstream which is continuously being drawn into the cavity. As a result this process can be very sensitive to variation in the tow and rate used for pultrusion.

The resins used for pultrusion are also very specialized. There is little time for volatile removal, consolidation, and other activities that can take considerably longer using other cure processes. The resin must be able to cure very rapidly, sometimes in less than a second, when exposed to the proper temperature. The resin must also be very consistent. Disruptions to this process can be very time consuming and expensive. Like most continuous processes, much of the operating expenses are associated with starting up and stopping the line.

The key elements in the process consist of a reinforcement delivery platform, resin bath (for wet pultrusion), preform dies, a heated curing die, a pulling system and a cut-off station. A wide range of solid and hollow profiles can be produced by the process and stitched fabrics, random mats and bidirectional reinforcements can be used in the process. The die employs a bell section opening to help reduce hydraulic resin pressures which build up in the die. The die is also plated to help eliminate die wall adhesion as well as hardened to counteract the abrasive action of the fibers.

In general the following process is used:

1. The reinforcements are threaded through the reinforcement delivery station.
2. The fiber bundle is pulled through the resin bath (if using a wet process) and die preforms.
3. A strap is used to initiate the process by pulling the resin impregnated bundle through the preheated die.
4. As the impregnated fiber bundle is pulled through the heated die, the die temperature and pulling rate are controlled such that the cure of the product (for thermosets) is completed prior to exiting the heated die.
5. The composite parts are cut off by the saw at the desired length as the continuous pultruded product exits the heated die.

The most critical process variable in pultrusion is the temperature control of the product which is a function of the temperature profile of the heated die and the line speed. Temperature control is critical because the product must achieve full cure just prior to exiting the pultrusion die. Other variables which affect cured properties are fiber tension which directly influences the fiber alignment of the final product, and resin bath viscosity which contributes to the completeness of fiber wet-out and the uniformity of the fiber to resin ratio of the final product.

2.8.7 Resin transfer molding (RTM)

RTM is a process which combines a dry fibrous reinforcement material or mixture of materials, generally referred to as a "preform", with liquid resin during the molding process, whereby the combined materials are cured to produce a 3-dimensional component. RTM is a term which is broadly applied to describe a number of variations of this general manufacturing approach throughout the aerospace and non-

aerospace industries with extremely different results in terms of the quality of the end product. The conventional RTM process employs closed "hard" tooling, similar to that used for injection molding, which completely encloses the preform and precisely controls all surfaces of the component. A variation of the conventional RTM process is vacuum assisted RTM (VARTM), which employs a single-sided tooling approach with a flexible film barrier (vacuum bag) to define the "non-tooled" surface. Likewise, some variations may loosely define the preform as simple ply shapes which are placed onto the molding tool surface with little regard to orientation or location control, while others employ additional materials, tools and interim processing steps to precisely control these features of the preform. Components used in critical structural applications generally warrant a more sophisticated and well controlled version of the RTM process in order to obtain a repeatable and reliable end product. It is important that the designer or end user of an RTM component have an appreciation of these variations, as the applicability or validity of material allowables generated for RTM material combinations, and furthermore, the ability to "certify" the component for critical applications is heavily influenced by the degree of control or sophistication employed in the manufacture of the component.

RTM is applied as a cost effective means by which to produce a component due to its use of constituent materials in their simplest, and thus least expensive forms by the producer of the component. Furthermore, in conventional closed mold RTM, due to the nature of the process, extremely complex shapes and 3-dimensional load paths can be obtained, enabling the designer to combine what would otherwise be numerous individual components produced by alternative processes, thereby reducing overall part count, and therefore minimizing the cost of the end product. Unlike conventional RTM which has the capability to produce very complex part details, VARTM produces part details similar to open molding techniques since similar one-sided tools are used. Since the VARTM process usually does not require elevated pressure or heat greater than 200°F, tooling costs are far lower than for autoclave cured open molding or conventional RTM. Probably the most well-known VARTM process is SCRIMP™ (Seemann Composites Resin Infusion Molding Process) which has successfully been applied to numerous marine structures, primarily pleasure boat hulls. Other proprietary VARTM processes include the Marco Method, Paddle Lite, Prestovac, Resin Injection Recirculation Molding (RIRM), and Ultraviolet (UV) VARTM. Careful consideration must be given, however, when designing the component or specifying the RTM process, to determine those features which are necessary for the application so as not to misuse the fabrication approach when an alternative or variation may be more cost effective.

The conventional RTM process begins with the fabrication of the preform whereby the fibrous reinforcement material or materials are formed and/or assembled to produce the geometry and load paths warranted by the application. These fibrous materials may be woven into broadgoods, braided into tubular goods or applied directly onto tooling, or otherwise combined and/or processed with additional materials such as binders or tackifiers which will define the geometry of the reinforcement in the end product. Likewise, 3-dimensional reinforcement may be incorporated into the preform as part of the weaving or braiding process, or as secondary processes such as stitching or alternative fiber insertion techniques. The preform is then located onto the tooling or into the mold and impregnated with the liquid resin, and subsequently cured while contained within the tooling to produce the as-molded geometry of the end product. Depending on the resin being utilized and the desired end product material properties, the cure cycle may require the application of elevated temperatures to produce the final cure state of the product. The cured component must then be removed from the tooling for trimming, machining, finishing and final inspection as applicable. The following general steps are employed for any RTM process:

1. Produce the fibrous reinforcement preform (weaving, braiding, cutting, forming, assembling).
2. Locate the preform onto the tooling or into the mold (this may also entail further assembly of preforms or reinforcement materials).
3. Impregnate the preform with liquid resin (this may require preheating of the assembled tooling and preform, heating of the resin, application of vacuum and/or pressure).
4. Cure (room temperature, elevated temperature, or alternative cure techniques).
5. Remove cured component from tooling for further processing.
6. Post cure (if required).

Variations of (or processes which resemble) the RTM process are Vacuum Assisted RTM (VARTM) and Resin Film Infusion (RFI), in that they incorporate the basic philosophy of combining the dry reinforcement preform and the resin during the molding process which produces the final cured component geometry. An almost endless variety of reinforcement materials, resins and combinations thereof may be employed in the RTM process, offering a large degree of freedom to the designer.

In the VARTM process, the preform is usually fabricated directly onto the tool. Each layer of reinforcement is applied and held in place using a binder or tackifier. Resin inlet tubes are positioned above the part in optimum locations to enable the resin to fully wet out the part prior to the resin gel. Vacuum tubes connected to a vacuum manifold are positioned around the perimeter of the part. The part is vacuum bagged with conventional nylon vacuum bagging film and sealant tape, allowing the resin and vacuum lines to penetrate the bag along its edges. Vacuum is applied to the part, the bag is positioned so as to prevent bridging, and a leak test is performed. The resin lines are inserted into an open container of mixed liquid resin. When the lines are opened the resin is forced through the part by the pressure differential between the resin and the vacuum bag. After it is fully wetted out, the part is allowed to initially cure at room temperature or at an elevated temperature in a convection oven. Alternate methods of cure including ultraviolet, electron beam and microwave have also been employed. The part is then removed from the tool, the process materials are removed, the part is post cured (if required), and finally trimmed.

RFI is a type of RTM in which resin infusion is accomplished by placing resin against the preform. Resin form and placement vary with the resin and tool. Parts have been fabricated using resin in the form of tiles, films, and liquid, with placement either above or below the preform. Resin flows through the preform during cure and vent holes are located at the high points of the tool. Any gaps in the tooling will allow resin leakage that will produce localized dry areas. Generally, parts are bagged and cured using procedures similar to the autoclave cure process.

The benefit of RFI over other resin transfer processes is lower tooling cost because matched metal tooling is not needed. Also, resin is transferred relatively short distances (essentially through the thickness), so part size is not dependent on resin flow capacity and very large parts can be produced. The short transfer distance also increases the number of potential resins, including higher performance resins. Another potential advantage of the process is improved damage tolerance due to the capability to produce unitized structure using stitched preforms. Continuous fiber volume is typically 55-60% by weight and, therefore, other mechanical properties such as tension and compression, are close to those achieved with hand lay-up.

The RFI process has been demonstrated with a variety of resins including epoxies (Hexcel 3501-6, Fiberite 977-3), bismaleimide (Cytec 5250-4RTM) and versions of Dupont K3Bresins. Unitized panels have been successfully fabricated with blade, "J," and hat stiffeners with the above resins. A wing stub box, 1220 pounds and 12 foot long, has been fabricated and tested by NASA to validate the process.

The degree of control of the following variables within the RTM process and how they may affect the end product are as follows:

1. Constituent materials from suppliers - affect laminate strength, stiffness, processability, porosity, surface finish.
2. Reinforcement materials production (weaving, braiding, etc.) - affect laminate strength, stiffness due to fiber orientation, fiber damage, areal weight/fiber volume.
3. Reinforcement materials processing (application of binders or tackifiers and other materials) - affect ability to form materials/define shapes, ability to form multiple layers simultaneously, permeability changes which affect ability to impregnate preform, could affect laminate structural properties if materials are incompatible with each other.
4. Cutting and stacking of plies - affect orientation of materials or lay-up sequence which establishes structural properties, ply drop-offs within the component which define local fiber volumes.
5. Forming of shapes/preforming - affect ply orientation, ply drop-offs, local fiber volumes.
6. Assembly of preforms/tooling - affect ply/fiber orientation and alignment, ply drop-offs, fiber volumes, part geometry, ability to flow resin and impregnate preform.

7. Liquid resin processing/cure parameters (time/temperature profile, vacuum, pressure, flow rate, viscosity of resin) - affect laminate porosity level, glass transition temperature (T_g), laminate surface finish quality.
8. Demolding and tool cleaning (removing part from tooling) - affect laminate integrity due to possible delamination, surface finish (scratches, gouges).
9. Tooling design and tooling materials selection (coefficient of thermal expansion (CTE) considerations) - affect tool life, part surface finish, part integrity (which could be affected by CTE mismatch causing laminate damage), and processability.

2.8.8 Thermoforming

Thermoforming fiber-reinforced thermoplastics. The thermoforming process, as applied to thermoplastic composite materials, is generally divided into two categories: melt-phase forming (MPF) and solid-phase forming (SPF). Thermoforming capitalizes on the rapid processing characteristics of thermoplastics. The composite thermoforming process can be broken down to four basic steps:

1. The material is heated to its processing temperature external to the forming tool. This can be accomplished with radiant heat.
2. The oven-heated material is rapidly and accurately transferred to the forming tool.
3. The heated material is pressure-formed with matched die set tooling into desired shape.
4. The formed laminate is cooled and its shape is set by sinking the heat into the tooling.

MPF is performed at the melting point of the thermoplastic matrix and requires sufficient pressure and/or vacuum application during the forming process to provide complete consolidation. The MPF process is preferred when sharp contour changes requiring some level of resin flow are a characteristic of the part geometry.

SPF is generally performed at temperatures between the onset of crystallization and below the peak melting point. This temperature range provides sufficient formability while the material remains in a solid form. SPF allows forming of preconsolidated sheet to be performed without a consolidation phase, but it is limited to part geometries exhibiting gentle curvatures.

The processing time for thermoforming is governed by the rates at which heat can be added to the material and then removed. This is primarily a function of the material thermal properties, material thickness, forming temperature, and tooling temperature. The pressures required to shape the material are dependent on various factors including part geometry, material thickness, and formability. The general deformability behavior of thermoplastics also depends on the strain-rate used during forming and the thermal history of the thermoplastic matrix. The forming process can affect such final properties as:

1. Degree of crystallinity,
2. Glass transition temperature,
3. Fiber orientation/alignment,
4. Uniformity of the fiber to resin ratio,
5. Residual stress,
6. Dimensional tolerances, and
7. Mechanical Properties.

The forming process has a significant effect on the quality of the finished part. High quality parts with predictable engineering properties require that a well controlled thermoforming process developed for specific applications be utilized.

2.9 ASSEMBLY PROCESSES

Assembly processes are not conventionally covered within composite material characterization, but can have a profound influence on the properties obtained in service. As seen with test coupons, edge

and hole quality can dramatically affect the results obtained. While these effects are not usually covered as material properties, it should be noted that there is an engineering trade-off between part performance and the time and effort expended toward edge and hole quality. These effects need to be considered along with the base material properties.

2.10 PROCESS CONTROL

Composite structures have the potential to provide higher performance in many applications. In order for this potential to be fulfilled, it must be possible to cost effectively manufacture parts of high, uniform quality. During cure of composite parts, the material is being made at the same time as the part. As a result, there are many actions happening at the same time. Some of these actions can be controlled directly, others only indirectly, and some of them interact. Process control is one of the methods used to manage the variability associated with composites.

2.10.1 Common process control schemes

Process control is used to attempt to direct these many changes during cure to reach many objectives. The manufacture of high quality parts is one objective. Others include exotherm avoidance, minimization of cure times, and addressing part specific manufacturing problems. Several different approaches to process control can be pursued: empirical, active, and passive. The most common is empirical, or trial and error. Many different sets of cure conditions are attempted, with the cure conditions providing the best results being picked for manufacturing. The second is active, or real-time process control. Here data is acquired during the cure from the part in question. Data that can be acquired includes temperature, pressure, resin viscosity, resin chemical characteristics (degree of cure), and average ply thickness. An expert system is used to analyze the cure information, and direct the autoclave how to proceed with the cure. The third is passive, or off-line process control. Here mathematical models are used to predict the response of the part during cure. Many different cure approaches can be simulated, and the one that best meets the needs at hand are applied.

Each of these process control approaches benefit from an understanding of the effects and interrelationships that are occurring during the cure of the resin. This understanding is referred to as a process control model. The model remains the same regardless of which particular type of process control is attempted for a particular application.

2.10.1.1 Empirical methods

This section is reserved for future use.

2.10.1.2 Active sensor-based control

This section is reserved for future use.

2.10.1.3 Passive model-based control

This section is reserved for future use.

2.10.2 Example - autoclave cure of a thermoset composite

A generic process control model can be used to evaluate and develop composite cures that produce high quality parts. When the resin is heated and has begun to flow, the system can be divided into gas (volatiles or trapped air), liquid (resin), and solid (reinforcement) phases. All void producing gas phase material should be either eliminated or absorbed by the liquid phase. The liquid phase should be uniformly distributed throughout the part, maintaining or producing the desired resin content. The solid phase should maintain its selected orientation. There are several initial factors that must be determined in order to cure parts, and which are used as input for the process model. These initial factors have been broken

down into the following categories: resin, time, heat, applied pressure, process materials, design, and reinforcement. It is well known that different resins, even within the same general material family, do not always provide equivalent results when processed in the same manner. The cure times and temperatures, including dwell(s) and heat up rates, usually control heat flow. For thick structures heat from resin exotherm can be dominant. The pressure to be used during cure must be determined, and may be changed substantially during the cure. Vacuum bagging or other process materials may be used to perform actions such as resin bleed, but can also have other effects, especially when they fail. Design choices such as the use of sandwich construction and radii affect the results obtained with the cure. Finally, although the reinforcement is usually intended to just maintain its orientation, it does influence gas and liquid flow, and picks up some of the applied pressure.

The number of initial factors alone makes composite processing difficult. What makes it even more complicated is that these initial factors affect the desired results and interact with each other in complex, non-linear relationships. Because of this, adjusting one factor in a seemingly logical fashion often does not obtain the desired results. A diagram of such a process model is shown in Figure 2.10.2. This particular model was designed for autoclave cure of thermoset composites. However, this model would also be largely applicable to most other composite and adhesive cure processes with slight modification. The initial factors are shown at the top of the figure, and the desired output at the bottom. The center area between the initial factors and the desired outputs represents the process interactions. These process interactions are: degree of cure, viscosity, resin pressure, void prevention, and flow. By using this model, cure process changes and optimization can be performed in a logical progression rather than a hit-or-miss fashion. Each of these process interactions is discussed in turn.

2.10.2.1 Degree of cure

The resin degree of cure acts primarily as an input to the viscosity interaction. Determining the rate of change of degree of cure for a resin requires a knowledge of the particular response for the individual resin and the temperature history for the resin. The resin heat of reaction is used as an index of degree of cure. The rate of change of degree of cure is then calculated as a function of the current degree of cure and the temperature. The rate of change of degree of cure is often not linear, which is why it is difficult to estimate the response of a resin to a new temperature profile without a model. In addition, in thick structures the heat of reaction may contribute significantly to the temperature of the resin, in turn affecting the degree of cure, and the viscosity. After the resin has gelled, the glass transition temperature is often used as an index of degree of cure.

2.10.2.2 Viscosity

The resin viscosity is a function of the resin degree of cure and temperature. The resin viscosity response function does vary from resin to resin. Thermoplastic resins do not chemically react during the fabrication process ("cure"), but do flow upon melting of the resin. Because the chemical makeup of the resin is not changing, the viscosity of a thermoplastic resin is strictly a function of the temperature. In other words, the viscosity effects are entirely physical, and no chemical interactions come into play. However, two different thermoplastic resins may have different viscosities at the same temperature due to chain length or other chemical differences.

A thermoset resin does react, so its chemical makeup is constantly changing during cure. Because of increases in chain length and crosslink density, the viscosity of the resin at a given temperature will increase over time. This is because there is increased interaction between the chains, and they become increasingly entangled with each other. Once chain extension and cross-linking have extended sufficiently, a thermoset resin will gel. The reason that viscosity effects for thermoset resins are much more difficult to predict than for thermoplastics is this continuous, sometimes rapid, change in the chemical makeup of the system.

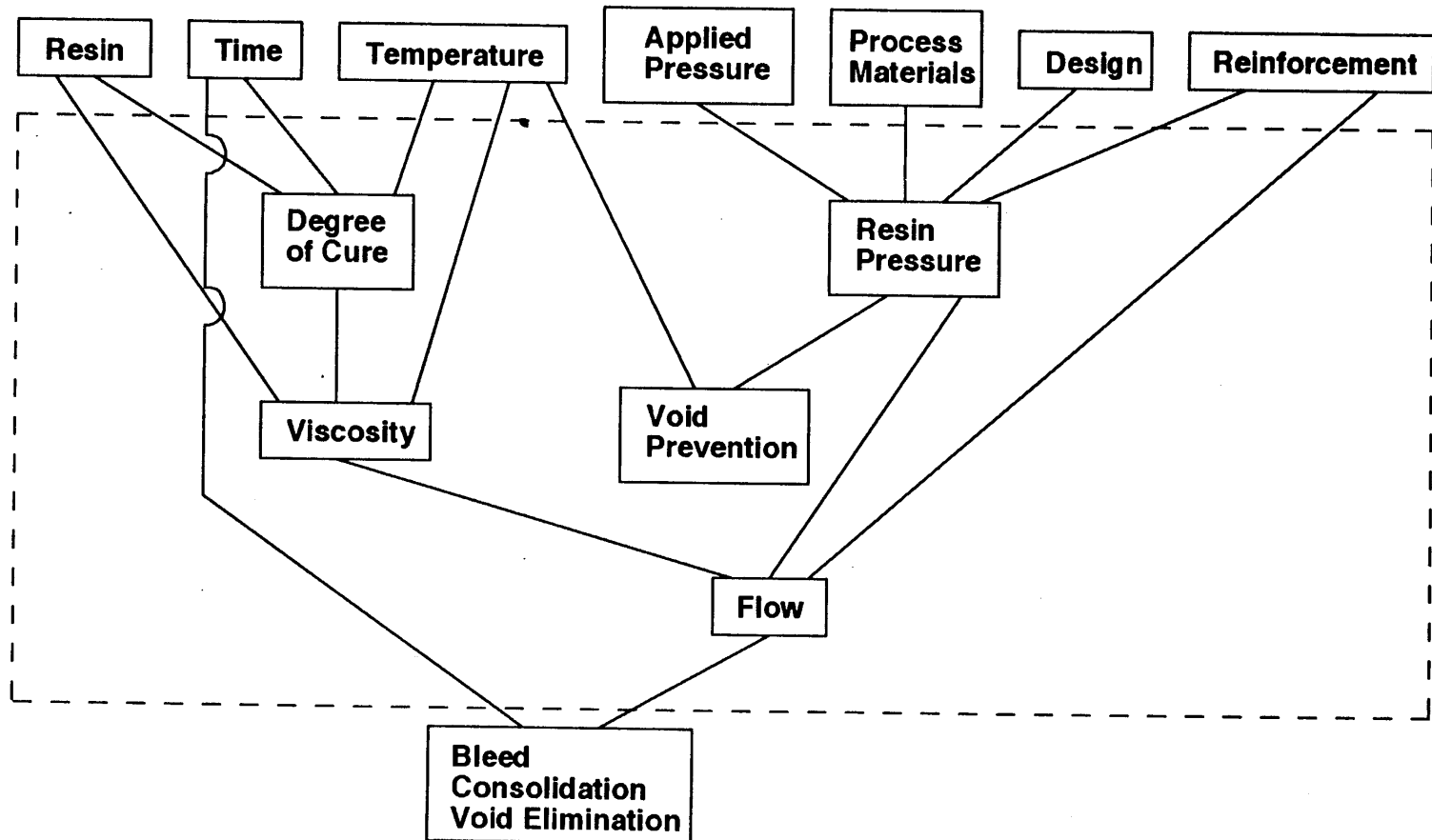
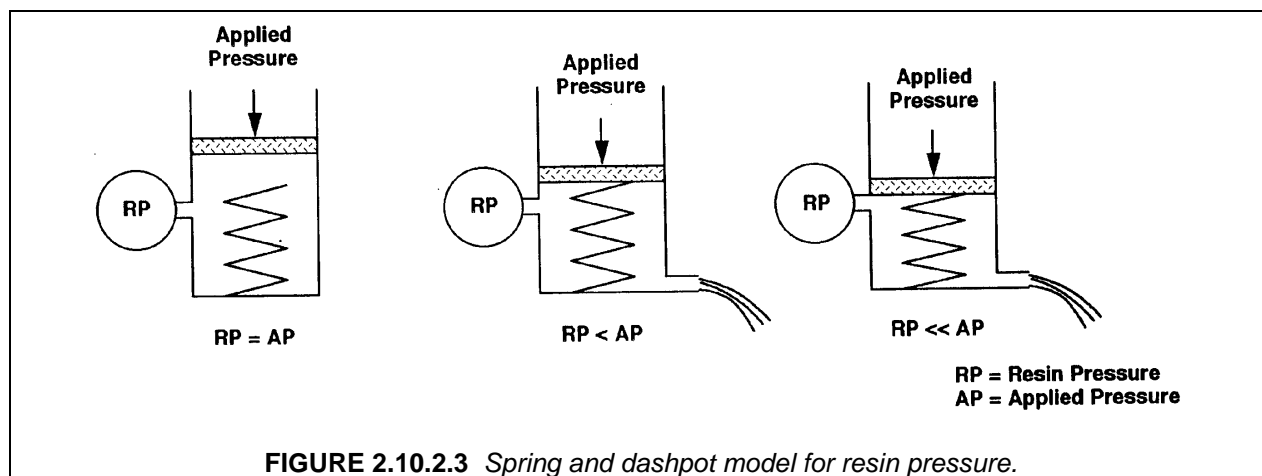


FIGURE 2.10.2 Composite cure process model.

2.10.2.3 Resin pressure

The pressure applied to a laminate is usually not the same as that which is experienced by the resin, referred to as resin pressure. The concept of resin pressure is frequently conceptualized with a spring and dashpot type model, with resin as the fluid, and the fiber pack as the spring. If the spring is completely surrounded by the fluid, it cannot pick up any of the applied load. If there is not enough resin to surround the spring, due perhaps to resin bleed, the spring (fiber pack) will pick up an increasing percentage of the load. The resin loses the corresponding amount of pressure. A diagram of this model can be seen in Figure 2.10.2.3.



Resin pressure is important because it is the driving force for moving resin and gas phase material from one place to another, and because it helps prevent formation of voids. Resin pressure is a function of the applied pressure, how and what process materials are used for cure, the design, and the reinforcement. If there is not sufficient resin to completely surround the reinforcement, then the reinforcement will pick up some or all of the load.

Just as the reinforcement can pick up applied pressure, so can the other process materials, especially the breather and bleeder. These items act as additional springs in the dashpot/spring model, and can absorb a significant amount of the applied pressure, especially for lower pressure cures. One of the design factors affecting the resin pressure is the use of materials such as honeycomb and some types of foam core. With co-cured skins, if a force is applied to the tool or bag side of the skin, resin pressure will be created, but all the resin has to do is flow slightly into the cell to relieve this pressure. This results in quality problems with honeycomb parts, especially if the skins are fairly thin, such as less than five plies. If the skins are fairly thick, then through the thickness resin pressure variations could be present. This would allow the surface of the parts at the tools surface to be under appreciable resin pressure, while at the honeycomb side the resin pressure would be near zero. Given an infinite amount of time, these pressures would equalize, but not in the time frame for many cures. When the skins are thin, the resin pressure is near zero. Thus the skins on thin skin honeycomb are cured with near zero resin pressure, essentially a contact lay-up, and the quality of the skins is often reduced. Because of the resistance that the reinforcement provides, some interesting resin pressure effects can be noted, along with their consequences on part quality. Just as through the thickness variations in resin pressure can be established, they can also be present in the plane of the reinforcement. This helps explain why widely different laminate quality can be present on the same part cured at the same time. Consider the bridging of the fiber reinforcement in a tight corner. Unless the plies can slide past each other to contact the tool in this corner, the reinforcement is, by definition, picking up all of the pressure applied by the autoclave, and the resin pressure is zero. At the location of bridges it can often be seen that increased porosity has occurred,

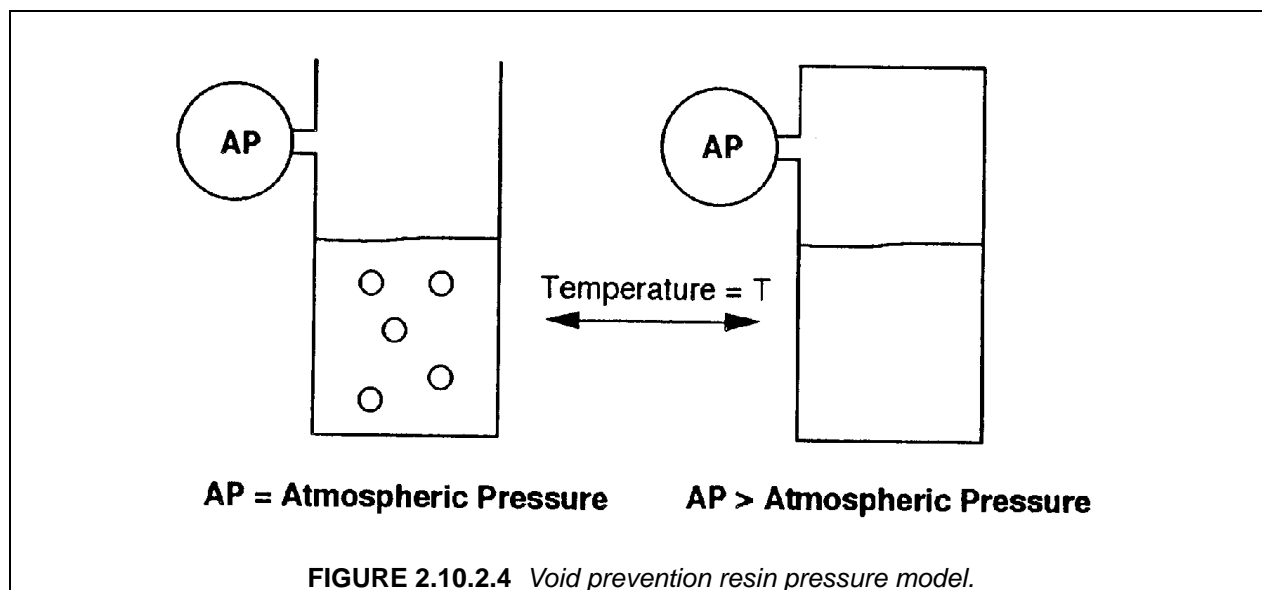
voids at the tool interface are present, and excess resin has built up. These are all due to the fact that the resin pressure in this location is near zero.

Areas surrounding this bridging may have adequate resin pressure. A series of experiments on honeycomb panels revealed that while the resin pressure in the skins (co-cured) was near zero, the resin pressure in the edge band (laminate) was significantly higher. The quality of the laminate in the edge band area was significantly higher even though the two points were only inches apart. This demonstrates the concept of differing resin pressures in close proximity.

2.10.2.4 Void prevention

Some resin systems, especially the higher temperature systems such as polyimides and phenolics, produce volatiles as a part of the cure reaction chemistry. While these byproducts are being evolved, the applied pressure should be minimal, and vacuum applied. As soon as all the volatiles have been created, then resin pressure can be used to drive out any volatile products remaining prior to gel. Once the resin has gelled, flow of the resin has been completed, and issues such as resin content, bleed, volatile content have been settled. The continuing cure advances the cure of the resin, but the physical configuration of the resin is locked in.

Some volatiles may be present in the prepreg, the most common being absorbed moisture. If resin pressure is maintained above the volatile vapor pressure until gel, these compounds cannot volatilize, increasing their volume many-fold, and forming additional voids and/or porosity. This functions in the same manner as a car radiator, as diagramed in Figure 2.10.2.4.



2.10.2.5 Flow

The viscosity, resin pressure and reinforcement factors feed into the flow factor. The viscosity and reinforcement can be thought of as resistances to flow, while the resin pressure can be thought of as the driving force for flow. The amount of flow that occurs due to these factors is then a function of time. This is consistent with experience. If the resin is more viscous, less flow would be expected with the same resin pressure and reinforcement. If the reinforcement is changed, perhaps to a tighter weave, then the resistance to resin and gas phase flow is increased. Once these flow characteristics have been established, then they and the time available for flow determine how bleed of the laminate takes place, how the laminate is consolidated, and the elimination of voids present in the lay-up or formed during the cure.

2.11 PREPARING MATERIAL AND PROCESSING SPECIFICATIONS

Requirements for materials and processes are frequently so specific and extensive, a special type of engineering drawing format was developed. Material and process specifications are one of the ways used to control composite material variability. Specifications are usually E-sized engineering drawings (see MIL-STD-961D (Reference 2.11)). They are part of the engineering package that defines a particular product, whether an airplane or a golf club.

2.11.1 Types of specifications

Material and process specifications are similar but do have some differing requirements.

2.11.1.1 *Material specifications*

The primary purpose of material specifications is to control the purchase of critical materials. The properties and values contained in the specification will relate to, but not necessarily be identical to, the properties used for activities such as design and structure testing. The properties and values contained in the specification are used to assure that the material does not change substantially with time. This is especially critical for materials used in primary applications, and which have undergone expensive qualifications. Material specifications are included in relevant contracts, and are part of the purchase order requirements to purchase material.

2.11.1.2 *Process specs - controls end product*

Process specifications establish the procedures that are required to control the end product. The more process dependent the materials and/or end product are, the more detailed and complex the process requirements. On the other hand, if there is a wide window of acceptable product produced by the process, the requirements may be minimal. Composite and adhesive bonding processing specifications are usually detailed because the materials are very sensitive to process variations, and the aerospace end item requirements are usually very stringent.

2.11.2 Format for specifications

Most specifications follow a similar format, based on guidelines contained in documents such as MIL-STD-961D (Reference 2.11). The sections of a material or process specification are generally as follows: scope, applicable documents, technical requirements or process controls, receiving inspection and quality control, delivery, notes, and approved sources and other. Each is covered in more detail in the following sections.

2.11.2.1 *Scope*

The first section is the scope, which generally describes the materials or processes covered by the specification in a few sentences. Also covered in this first section are any types, classes, or forms, of the materials that are governed by the specification. Another method for handling different material configurations is the use of slash sheets. These slash sheets are part of the base document, but provide the additional information that is specific to that particular material. For example, one material specification may cover several different thicknesses of the same film adhesive, each thickness being a different class. The scope section establishes the shorthand terminology, or callout, which is used to identify the material on other engineering and procurement documents. A process specification may cover multiple processes, such as anodizing, with minor process variations based on the type of alloy being processed.

2.11.2.2 *Applicable documents*

The second section identifies all the other documents that are referenced within the specification. Testing procedures, and other material and process specifications may be called out. A trade-off is made

between a specification being self contained, and redundancy between multiple specifications for similar materials or processes. For example, if a change to a testing procedure is required, only a change to the referenced testing specification is required. If the specifications are all self contained, the test procedure within each specification must be revised. The time and expense associated with changes to common materials and procedures can be substantial. However, when only a limited amount of information is required, the modular approach can bring along a great deal of unused information. These configuration management issues are discussed in more detail in a following section.

2.11.2.3 Technical requirements/process controls

The third section covers the technical requirements for the material or controls for the process. For a materials specification, these requirements can include physical, chemical, mechanical, shelf and work life, toxicity, environmental stability, and many other characteristics. The requirements can be minimum values, maximum values, and/or ranges. Sometimes it is only required that the data obtained from the test be submitted. Only the test result requirements are contained in this section. The test procedure used to obtain this result is covered in the next section. For a process specification, the controls required to ensure the product produced is consistent are specified.

2.11.2.4 Receiving inspection and qualification testing

The fourth section covers testing. Receiving inspection testing is that which is performed each time a quantity of the material is purchased, or a lot of product is processed. Although it is required that all the requirements of the specification be met at all times, only a fraction of the tests are performed routinely. Qualification testing usually involves testing to all of the requirements of the specification to insure that the supplier or processor is capable of meeting the requirements, and is performed only once unless there is cause.

Responsibility for the testing required is also delineated. The manufacturer may do all their receiving inspection testing, or the user may perform additional testing upon receipt of the material. Required reports are defined, as well as requirements for resampling and retesting if a requirement is initially failed.

Sampling and the specific test procedures to be used to determine conformance to the technical requirements are contained in this section. Testing procedures can be critical. In most cases, the value obtained cannot be used unless the specific test used to generate the value is documented. Test results can change when test procedures change, even though the material being tested has not changed itself. Also important is the preparation of the test specimens. Test results can vary widely depending on the configuration and condition of the test specimens. The conditions under which the test is performed can dramatically change the results. Preconditioning of the specimen prior to test is also important, such as exposure to elevated temperature and humidity prior to test.

2.11.2.5 Delivery

Delivery requirements are covered in the fifth section. Issues such as packaging and identification, storage, shipping and documentation must be established. Packaging is especially critical for temperature sensitive materials such as prepreg and film adhesive.

2.11.2.6 Notes

The sixth section is usually notes, although sixth and later section formats can vary substantially. Notes are additional information for reference, and are not requirements unless specifically stated in the requirements section.

2.11.2.7 Approved sources and other

Seventh and additional sections can include information such as what materials are qualified to the specification. This section may reference a separate document that lists the qualified materials. Because

of the substantial expense that can be experienced as a result of qualification, normally only materials that are currently qualified are used for production applications.

2.11.3 Specification examples

Specifications in common use are generally released by industry associations or the military. Industry associations common to composite and adhesive bonded structure are SAE, ASTM, and SACMA. In addition, companies may develop their own internal specifications for materials or processes that are not adequately covered by industry/military specifications, or to protect proprietary information. Company specifications may be similar in style and content to industry and military specifications, but can vary widely in approach and level of control. Each has advantages and disadvantages.

2.11.3.1 Industry

Examples of industry specifications are as follows:

AMS 3897	Cloth, Carbon Fiber, Resin Impregnated
AMS 3894	Carbon Fiber Tape and Sheet, Epoxy Resin Impregnated

AMS specifications are available from SAE, 400 Commonwealth Drive, Warrendale, PA 15096-001.

2.11.3.2 Military

Examples of military specifications are as follows.

MIL-A-83377	Adhesive Bonding (Structural) for Aerospace and Other Systems, Requirements for
MIL-P-9400	Plastic Laminate and Sandwich Construction Parts and Assembly, Aircraft Structural, Process Specification Requirements
MIL-T-29586	Thermosetting Polymer Matrix, Unidirectional Carbon Fiber Reinforced Prepreg Tape (Widths up to 60 Inches), General Specification for

Military specifications are available from DODSSP, Standardization Document Order Desk, 700 Robbins Ave., Bldg. 4D, Philadelphia, PA 19111-5094.

2.11.4 Configuration management

Most major aerospace companies use many materials and process specifications to control and define their products, and those made by their subcontractors. Many companies prefer to have a company controlled specification for some materials and processes, even when equivalent industry or military specifications are available. Industry and military specifications are, by definition, consensus documents. Reaching this consensus can take a good deal of time, and may conflict with a specific company's objectives. With company control, tailoring of the specification to company requirements can be relatively easily effected. Company specifications do allow tailoring, but at the cost of standardization. Company specific tests and procedures incur additional expense. There may be many specifications that govern essentially the same material. Sometimes this is because different specifications offer different levels of control (testing). The amount and complexity of testing required for procurement of material can soon account for a large percentage of the total cost of the material. If only minor changes to the specification are made, amendments or supplements can be released. Some specification changes may only be in effect for limited periods of time, or restricted to certain facilities. Control of the current and prior versions of specifications is an important issue. Specification changes can have a great influence on manufacturing operations, and if additional expenses are associated with the changes in the revision, prices and timing for implementation may have to be negotiated. Not all operations and subcontractors may start work per a new revision of a specification at the same time. In addition, confusion frequently arises from different parties unintentionally using different revisions, or versions, of the same specification.

REFERENCES

- 2.4.1.1 Multicomponent Polymer Systems, I. Miles and S. Rostami ed., Longmore Scientific and Technical, 1992.
- 2.4.1.1.1 Engineered Material Handbook Volume 1: Composites, ASM International, 1987.
- 2.4.1.1.3.1.3 Technology of Carbon and Graphite Fiber Composites, J. Delmonte, Krieger, 1987.
- 2.4.1.2(a) *Data Manual for Kevlar™49 Aramid*, E.I. Du Pont de Nemours & Co., Wilmington, DE 1989.
- 2.4.1.2(b) Krueger, W.H., et al., "High Performance Composites of J2 Thermoplastic Matrix Reinforced with Kevlar™ Aramid Fiber," *Proceedings of the 33rd International SAMPE Symposium*, March 1988, pp. 181-193.
- 2.4.1.2(c) Gruber, M.B., "Thermoplastic Tape Laydown and Consolidation," SME Technical Paper EM86-590.
- 2.4.1.2(d) Okine, R.K., et al., "Properties and Formability of a Novel Advanced Thermoplastic Composite Sheet Product," *Proceedings of the 32nd International SAMPE Symposium*, April 1987, pp. 1413-1425.
- 2.4.1.2(e) Egerton, M.W. and Gruber, M.B., "Thermoplastic Filament Winding Demonstrating Economics and Properties via In-Situ Consolidation," *Proceedings of the 33rd International SAMPE Symposium*, March 1988, pp. 35-46.
- 2.4.1.2(f) Khan, S., "Environmental Effects on Woven Thermoplastic Composites," *Proceedings, Materials Week™, 87*, ASM International, Cincinnati, OH, October 10-15, 1987.
- 2.4.1.3.1(a) "PPG Fiber Glass Yarn Products/Handbook," PPG Industries, Inc., 1984
- 2.4.1.3.1(b) *Engineered Materials Handbook*, ASM, International, Metals Park, Ohio, 1987, pp. 107-100.
- 2.4.1.3.1(c) "Textile Fibers for Industry," Owens-Corning Fiberglas Corporation, Pub. No. 5-TOD-8285-C, September 1985.
- 2.4.1.3.2(a) ASTM Specification D 579, "Greige Woven Glass Fabrics Fiber Yarns," Annual Book of ASTM Standards, Vol 7.01, American Society for Testing and Materials, West Conshohocken, PA.
- 2.4.1.3.2(b) ASTM Specification D 578, "Glass Fiber Yarns," Annual Book of ASTM Standards, Vol 7.01, American Society for Testing and Materials, West Conshohocken, PA.
- 2.4.1.3.4(a) "Discover S-2 Glass Fiber," Owens-Corning Fiberglas Corp., Pub. No. 5-ASP-13101-A, 1986.
- 2.4.1.3.4(b) "Industrial Fabrics," Clark - Schwebel Fiber Glass Corp.
- 2.4.1.3.4(c) "Product Bulletin," Stratifils H_R/P109.
- 2.4.1.4(a) Shoenberg, T., "Boron and Silicon Carbide Fibers," *Engineered Materials Handbook, Volume 1, Composites*, ASM International, Metals Park, Ohio, 1987, pp. 58-59.

- 2.4.1.4(b) Bascom, W.D., "Other Continuous Fiber," *Engineered Materials Handbook, Volume 1, Composites*, ASM International, Metals Park, Ohio, 1987, pp. 117-118.
- 2.4.1.4(c) Krukonis, V., "Boron Filaments," *Handbook of Fillers and Reinforcements for Plastics*, H. Katz and J. Milewski, eds., Van Nostrand Reinhold, Co., 1978.
- 2.4.1.4(d) DeBolt, H.E., "Boron and Other High Strength, High Modulus Low-Density Filamentary Reinforcing Agents," *Handbook of Composites*, G. Lubin, ed., Van Nostrand Reinhold Co., 1982, pp. 171-195.
- 2.4.1.4(e) MIL-HDBK-727, *Design Guide for Producibility*, Chapter 6.
- 2.4.1.4(f) "Boron Monofilament, Continuous, Vapor Deposited," MIL-B-83353.
- 2.4.1.4(g) "Filaments, Boron - Tungsten Substrate, Continuous," AMS 3865B.
- 2.4.1.6(a) *Advanced Materials*, Carrol-Porczynski, Chemical Publishing, 1962, pp. 117,118.
- 2.4.1.6(b) *Engineered Materials Handbook*, ASM International, Vol I, Metals Park, Ohio, 1987, p.58-59.
- 2.4.1.6(c) Lynch, et al., "Engineered Properties of Selected Ceramic Materials," *Journal of American Ceramic Society*, 1966, pp. 5.2.3-5.2.6.
- 2.4.1.6(d) *Advanced Materials and Processes*, "Guide to Selected Engineered Materials," Vol 2, No 1, June 1987, pp. 42-114.
- 2.4.1.6(e) BP Chemical, Advanced Materials Division, Carborundum.
- 2.4.1.7 "Quartz Yarn of High Purity," AMS 3846A.
- 2.4.1.8(a) Spectra[®] fiber properties product data of Allied Signal Inc., Petersburg, VA, May 1996.
- 2.4.1.8(b) Strong, A.B., *Fundamentals of Composites Manufacturing: Materials, Methods, and Applications*, SME, Dearborn, Michigan, 1989.
- 2.4.1.8(c) Billmeyer, Jr., F.W., *Textbook of Polymer Science*, 3rd Ed., John Wiley & Sons, New York, 1984.
- 2.4.1.8(d) Ladizesky, N.H., and Ward, I.M., "A Study of the Adhesion of Drawn Polyethylene Fibre/ Polymeric Resin System," *Journal of Material Science*, Vol. 18, 1983, pp. 533-544.
- 2.4.1.8(e) Adams, D.F., Zimmerman, R.S., and Chang, H.-W., "Properties of a Polymer-Matrix Composite Incorporating Allied A-900 Polyethylene Fiber," *SAMPE Journal*, September/October 1985.
- 2.4.2.7.1(a) Hertzberg, R.W., *Deformation and Fracture Mechanics of Engineering Materials*, John Wiley & Sons, New York, 1976 p. 190.
- 2.4.2.7.1(b) Kaufman, H.S., "Introduction to Polymer Science and Technology," Lecture Notes.
- 2.4.2.7.1(c) "The Place for Thermoplastics in Structural Components," Contract MDA 903-86-K0220, pp. 1-2, 20, 29.

- 2.4.2.7.1(d) Murtha, T.P., Pirtle, J., Beaulieu, W.B., Waldrop, J.R., Wood, H.D., "New High Performance Field Installed Sucker Rod Guides," *62 Annual Technical Conference and Exhibition of SPE*, Dallas, Texas, September 1987, pp. 423-429.
- 2.4.2.7.1(e) Brown, J.E., Loftus, J.J., Dipert, R.A., "Fire Characteristics of Composite Materials - a Review of the Literature," NAVSEA 05R25, Washington, DC, August 1986.
- 2.4.2.7.1(f) "The Place for Thermoplastics in Structural Compounds," contract MOA 903-86-K-0Z20, Table 3-5, p. 1.
- 2.4.2.7.1(g) Horton, R.E., McCarty, J.E., "Damage Tolerance of Composites," *Engineered Materials Handbook*, Volume 1, Composites, ASTM International, 1987, pp. 256-267.
- 2.4.2.7.1(h) Silverman, E.M., Griese, R.A., Wright, W.F., "Graphite and Kevlar Thermoplastic Composites for Space Craft Applications," *Technical Proceedings, 34th International SAMPE Symposium*, May 8-11, 1989, pp. 770-779.
- 2.4.2.7.1(i) Shahwan, E.J., Fletcher, P.N., Sims, D.F., "The Design, Manufacture, and Test of One-Piece Thermoplastic Wing Rib for a Tiltrotor Aircraft," *Seventh Industry/Government Review of Thermoplastic Matrix Composites*, San Diego, California, February 26-March 2, 1991, pp. III-C-1 - III-C-19.
- 2.4.2.7.1(j) Lower Leading Edge Fairing to AH-64A Apache Helicopter-Phillips 66-McDonnell Douglas Helicopter Prototype Program.
- 2.4.2.7.2(a) *Modern Plastics Encyclopedia*, Materials, McGraw-Hill, 1986-1987, p. 6-112.
- 2.4.2.7.2(b) Koch, S., Bernal, R., "Design and Manufacture of Advanced Thermoplastic Structures," *Seventh Industry/Government Review of Thermoplastic Matrix Composites Review*, San Diego, California, February 26-March 1, 1991, pp. II-F1 - II-F-22.
- 2.4.2.7.2(c) Stone, R.H., Paul, M.L., Gersten, H.E., "Manufacturing Science of Complex Shape Thermoplastics," *Eighth Thermoplastic Matrix Composites Review*, San Diego, California, January 29-31, 1991, pp. I-B-1 - I-B-20.
- 2.7.7(a) Lubin, G., *Handbook of Composites*, Van Nostrand Reinhold, 1982, Chapter 21, "Sandwich Construction".
- 2.7.7(b) MIL-P-9400C, *Plastic Laminate and Sandwich Construction, Parts and Assembly, Aircraft Structural, Process Specification Requirements*.
- 2.7.7(c) MIL-HDBK-23 (Canceled), *Structural Sandwich Construction*.
- 2.7.7(d) MIL-STD-401, *Sandwich Constructions and Core Materials: General Test Methods*.
- 2.7.8(a) Kinloch, A.J., Kodokian, G.K.A., and Watts, J.F., "The Adhesion of Thermoplastic Fiber Composites," *Phil. Trans. Royal Soc: London A*, Vol. 338, pp. 83-112, 1992.
- 2.7.8(b) MIL-HDBK-691B, *Adhesive Bonding*, Defense Automation and Production Service, Philadelphia, PA, 1987.
- 2.11 MIL-STD-961D(1), DoD Standard Practice, Defense Specification, Executive Agent for the Defense Standardization Program, Falls Church, 1995.

This page intentionally left blank

CHAPTER 3 QUALITY CONTROL OF PRODUCTION MATERIALS AND PROCESSES

3.1 INTRODUCTION

Quality conformance tests are needed to assure the continued integrity of a previously characterized material system. The tests performed must be able to characterize each batch/lot of material so a proper assessment of critical properties of a material system can be made. These critical properties provide information on the integrity of a material system with regard to material properties, fabrication capability, and usage. Additionally, the test matrix must be designed to economically and quickly evaluate a material system.

Quality control in a production environment involves inspection and testing of composites in all stages of prepreg manufacture and part fabrication. Tests must be performed by the material supplier on the fiber and resin as separate materials, as well as on the composite prepreg material. The user of the prepreg must perform receiving inspection and revalidation tests, in-process control tests, and nondestructive inspection tests on finished parts. These tests are described in the following sections and normal industry practice is discussed.

3.2 MATERIAL PROCUREMENT QUALITY ASSURANCE PROCEDURES

3.2.1 Specifications and documentation

The specification for materials, fabrication processes, and material testing techniques must ensure compliance with the engineering requirements.

Chapters 3, 4, and 6 in Volume 1 of this handbook describe acceptance test methods for characterizing fiber, matrix, and resin-impregnated fiber materials by their chemical, physical, and mechanical properties. Sections 3.3 and 3.4 of this volume provide information on variable statistical sampling plans that are based on MIL-STD-414 (Reference 3.2.1(a)). These plans control the frequency and extent of material property verification testing to achieve targeted quality levels.

The specifications for destructive and nondestructive test equipment and test methods should contain test and evaluation procedures. These procedures need to describe the means by which the equipment will be calibrated to maintain the required accuracy and repeatability; they should also establish the calibration frequency. Information on the standards to be used in the calibration of chemical analysis equipment will be found in preceding sections of this handbook which deal with the particular test technique.

The standards for quality control documentation requirements are found in military and federal specifications such as the Federal Aviation Regulation Part 21 "Certification Procedures for Products and Parts" used by the Federal Aviation Administration production approval holders (Reference 3.2.1(b)).

3.2.2 Receiving inspection

The composite material user typically prepares material specifications which define incoming material inspection procedures and supplier controls that ensure the materials used in composite construction will meet the engineering requirements. These specifications are based on material allowables generated by allowables development programs. The acceptance criteria for mechanical tests must be specified to assure that production parts will be fabricated with materials that have properties equivalent to the materials used to develop the allowables.

The user material specifications typically require the suppliers to provide evidence that each production lot of material in each shipment meets the material specification requirements. This evidence will in-

clude test data, certification, affidavits, etc., depending upon the user quality assurance plan and purchase contract requirements for a particular material. The test reports contain data to verify the conformance of material properties to user specifications and acceptance standards.

Acceptance test requirements may vary from user to user. However, the tests must be sufficient to assure the material will meet or exceed the engineering requirements. A typical example of acceptance tests required for carbon/epoxy unidirectional tape is shown in Table 3.2.2. Note that Table 3.2.2 is divided into two parts. The first part concerns uncured prepreg properties. The purpose of these tests is to assure that the resin and fibers materials are within acceptable limits. The second part involves tests on cured laminates or laminae. The mechanical property tests should be selected to reflect important design properties. They can be direct tests of a property or a basic test that correlates with critical design properties. The 90°/0° tension test evaluates the fiber strength and modulus. The 90°/0° compression test evaluates the reinforced fiber/resin combination. The compression testing also includes hot dry tests since one resin-dependent mechanical property should include elevated temperature tests to ensure the material's temperature capability. A shear test should be run as a resin evaluation. The short beam shear test or the ±45° tension test should be used depending on the end product's emphasis on interlaminar or in-plane properties.

Receiving inspection test requirements should address test frequency and, in the event of initial failure to satisfy these requirements, retest criteria. Test frequency is a function of the quantity of material (weight and rolls) in a batch. Typical testing may include specimens from first, last and random rolls. A retest criteria should be included for the cured lamina tests so that the material is not rejected because of testing anomalies. If a material fails a test, a new panel from the same suspect roll of material should be fabricated and used to rerun that specific test. If a batch has multiple rolls, that test should run on material from the roll before and after the suspect roll in order to isolate the potential problem. If the material fails the retest, the entire batch should be reviewed by material engineering. As use and confidence increase, the receiving inspection procedure can be modified. For example, the test frequency can be decreased or certain tests can be phased out.

3.3 PART FABRICATION VERIFICATION

3.3.1 Process verification

The quality assurance department for the user generally has the responsibility for verifying that the fabrication processes are carried out according to engineering process specification requirements. The wide range of activities to control the fabrication process are described below.

Material Control: The user process specifications must set the material control for the following items as a minimum.

1. Materials are properly identified by name and specification.
2. Materials are stored and packaged to preclude damage and contamination.
3. Perishable materials, prepreps and adhesives, are within the allowable storage life at the time of release from storage and the allowed work life at time of cure.
4. Prepackaged kits are properly identified and inspected.
5. Acceptance and reverification tests are identified.

Materials Storage and Handling: The user material and process specifications set procedures and requirements for storage of prepreps, resin systems and adhesives to maintain acceptable material quality. Storing these materials at low temperatures, usually 0°F or below, retards the reaction of the resin materials and extends their useful life. Negotiations between the supplier and user result in an agreement on how long the supplier will guarantee the use of these perishable materials when stored under these conditions. This agreed to time is incorporated as one of the requirements in the user material specification.

TABLE 3.2.2 *Typical acceptance and revalidation tests required for suppliers and users.*

PROPERTY	TESTING REQUIRED			SPECIMENS REQUIRED PER SAMPLE
	PRODUCTION ACCEPTANCE (SUPPLIER)(3)	PRODUCTION ACCEPTANCE (USER)(3)	REVALIDATION (USER)(3)	
Prepreg Properties				
Visual & Dimensional	X	X		-
Volatile Content	X	X		3
Moisture Content	X	X	X	3
Gel Time	X	X	X	3
Resin Flow	X	X	X	2
Tack	X	X	X	1
Resin Content	X	X		3
Fiber Areal Weight	X	X		3
Infrared Analysis	X			1
Liquid Chromatograph	X	X	X	2
Differential Scanning Calorimetry	X	X	X	2
Lamina Properties				
Density	X			3
Fiber Volume	X			3
Resin Volume	X			3
Void Content	X			3
Per Ply Thickness	X	X	X	1
Glass Transition Temp	X	X	X	3
SBS or $\pm 45^\circ$ Tension	X(2)	X(2)	X(2)	6
90°/0° Compression Strength	X(1)	X(1)	X(2)	6
90°/0° Tension Strength & Modulus	X(2)	X(2)	X(2)	6

(1) Tests should be conducted at RT/Ambient and Maximum Temperature/Ambient (See Volume I, Section 2.2.2).

(2) Tests should be conducted RT/Ambient.

(3) Supplier is defined as the prepreg supplier. User is defined as the composite part fabricator. Production acceptance tests are defined as tests to be performed by the supplier or user for initial acceptance. Revalidation tests are tests performed by the user at the end of guaranteed storage life or room temperature out time to provide for additional use of the material after expiration of the normal storage or out time life.

Materials are generally stored in sealed plastic bags or containers to prevent moisture from condensing on the cold material and migrating into the polymer when it is removed from the freezer and allowed to warm up to ambient temperature. The time interval between material removal from the freezer and when the material bag or container may be opened is generally empirically determined. Physical characteristics such as material roll, stacking height thickness, or material type (e.g., tape vs broadgoods) are considered when determining this time interval. Therefore, the user should have procedures that prevent premature removal of materials from storage bags or containers before material temperature stabilization occurs.

Tooling: The tooling (molds) to be used for lay-up are subject to tool proofing/qualification procedures. This demonstrates that the tooling is capable of producing parts that conform to drawing and specification requirements, when used with the specified materials, lay-up and bagging methods, and cure profile. Also, cured material specimens made from the tool should be tested to ensure they meet specified mechanical and physical properties. Tool surfaces must be inspected before each use to ensure the tool surface is clean and free of conditions which could contaminate or damage a part.

Facilities and Equipment: The user will establish requirements to control the composite work area environment. These requirements are a part of the user's process specifications. The requirements should be commensurate with the susceptibility of materials to contamination by the shop environment. Inspection and calibration requirements for autoclaves and ovens must be defined.

Contamination restrictions in environmentally-controlled areas typically prohibit the use of uncontrolled sprays (e.g., silicon contamination), exposure to dust, handling contamination, fumes, oily vapors, and the presence of other particulate or chemical matter which may affect the manufacturing process. Conditions under which operators may handle materials should also be defined. Lay-up and clean room air filtrations and pressurization systems should be capable of providing a slight positive overpressure.

In-Process Control: During lay-up of composite parts, certain critical steps or operations must be closely controlled. Requirements and limits for these critical items are stated in the user process specifications. Some of the steps and operations to be controlled are listed below:

1. Verification that the release agent has been applied and cured on a clean tool surface.
2. Verification that perishable materials incorporated into the part comply with the applicable material specifications.
3. Inspection of prepreg lay-ups to assure engineering drawing requirements for number of plies and orientation are met.
4. Inspection of honeycomb core installation, if applicable, and verification that positioning meets the engineering drawing requirements.
5. The user paperwork should contain the following information.
 - a. Material supplier, date of manufacturer, batch number, roll number, and total accumulated hours of working life.
 - b. Autoclave or oven pressure, part temperatures, and times.
 - c. Autoclave or oven load number.
 - d. Part and serial number.

Part Cure: Requirements must be defined in user process specifications for the operating parameters for autoclaves and ovens used for curing parts. These include heat rise rates, times at temperature,

cool-down rates, temperature and pressure tolerances, and temperature uniformity surveys in the autoclave or ovens.

Process Control Specimens: Many manufacturers require special test panels to be laid up and cured along with production parts. After cure, these panels are tested for physical and mechanical properties to verify the parts they represent meet the engineering properties.

The requirements for physical and mechanical testing are frequently defined by drawing notes which designate a type or class for each part. Non-critical or secondary structure may require no test specimens and no testing. Critical or safety-of-flight parts may require complete physical and mechanical testing.

During early composite material production, most users required tests for 0° flexure strength and modulus and short beam shear strength. However, in recent years these tests have been changed by many manufacturers to require glass transition temperature, per ply thickness, fiber volume, void content, and ply count on samples taken from designated areas on the production part.

3.3.2 Nondestructive inspection

Having assured in-process control, the detail composite parts must also be inspected for conformance to dimensional and workmanship requirements and nondestructively inspected for processing-induced defects and damage.

Assembly Inspection: Laminates are prone to particular types of defects unless they are machined and drilled properly. Workmanship standards, required by manufacturer's process specifications, are needed to control the quality of trimmed edges and drilled holes. These standards establish visual acceptance/rejection limits for the following typical defects: splintering, delamination, loose surface fibers, overheating, surface finish, off-axis holes, and surface cratering. Typical defects in the drilling operations are delaminations and broken fibers which start at the hole boundary. Since these defects are internal in nature, an evaluation of the seriousness of the flaws is not possible by visual inspection alone. It should be backed up by nondestructive inspection techniques. Internal defect acceptance and rejection limits must be established for nondestructive inspection.

The extent of nondestructive (NDI) inspection on composite parts is dependent on whether the parts are primary structure, safety-of-flight or secondary structure, non-safety-of-flight. The type or class of part is usually defined on the engineering drawing. The engineering drawing also references a process specification which defines the NDI tests and the accept/reject criteria. The NDI tests are used to find flaws and damage such as voids, delaminations, inclusions, and micro-cracks in the matrix.

NDI techniques commonly used in production include visual, ultrasonic and X-ray inspection. Other methods, such as infrared, holographic, and acoustic inspection are being developed and may be used in production applications in the future.

Visual inspection is an NDI technique involving checks to assure the parts meet drawing requirements and to evaluate the surface and appearance of the part. The inspection includes examination for blisters, depressions, foreign material inclusions, ply distortions and folds, surface roughness, surface porosity, and wrinkles. Accept/reject criteria for such defects are given in the manufacturer's process specifications.

The most widely used nondestructive inspection technique for composites production is ultrasonic thru-transmission C-scan inspection, followed by ultrasonic pulse echo A-scan inspection. Since the subject is so broad, the engineering requirements and criteria are usually contained in a document that is referenced in the user's process specification. The principal defects evaluated by ultrasonics are internal voids, delaminations, and porosity. These inspections require fabrication of standards with built-in known defects. The output is in the form of charts which show the sound attenuation variations over the entire part. The charts are compared to the part to show the locations of the sound attenuation variations. If defects are found outside the limits allowed by the specification, the parts are rejected and dispositioned

by Engineering. Parts may be dispositioned 1) acceptable as is, 2) subjected to further rework or repair to make the part acceptable or 3), scrapped.

X-ray inspection is frequently used in NDI testing to evaluate bonding of inserts in laminate panels and honeycomb core to facesheet bonds in sandwich panels. The extent of testing required is designated on the engineering drawing by type or class of inspection. The type or class is usually defined in a separate document that is referenced in the manufacturer's process specification. As with ultrasonic inspection, standards with built-in defects are usually required to evaluate the radiographic film properly.

3.3.3 Destructive tests

3.3.3.1 Background

Destructive tests are often used to ensure the structural integrity of a component whenever assurance cannot be gained by nondestructive techniques alone. These tests include periodic dissection of the part to examine the interior of complex structures and mechanical testing of specimens cut from excess parts of the component (Figure 3.3.3.1).

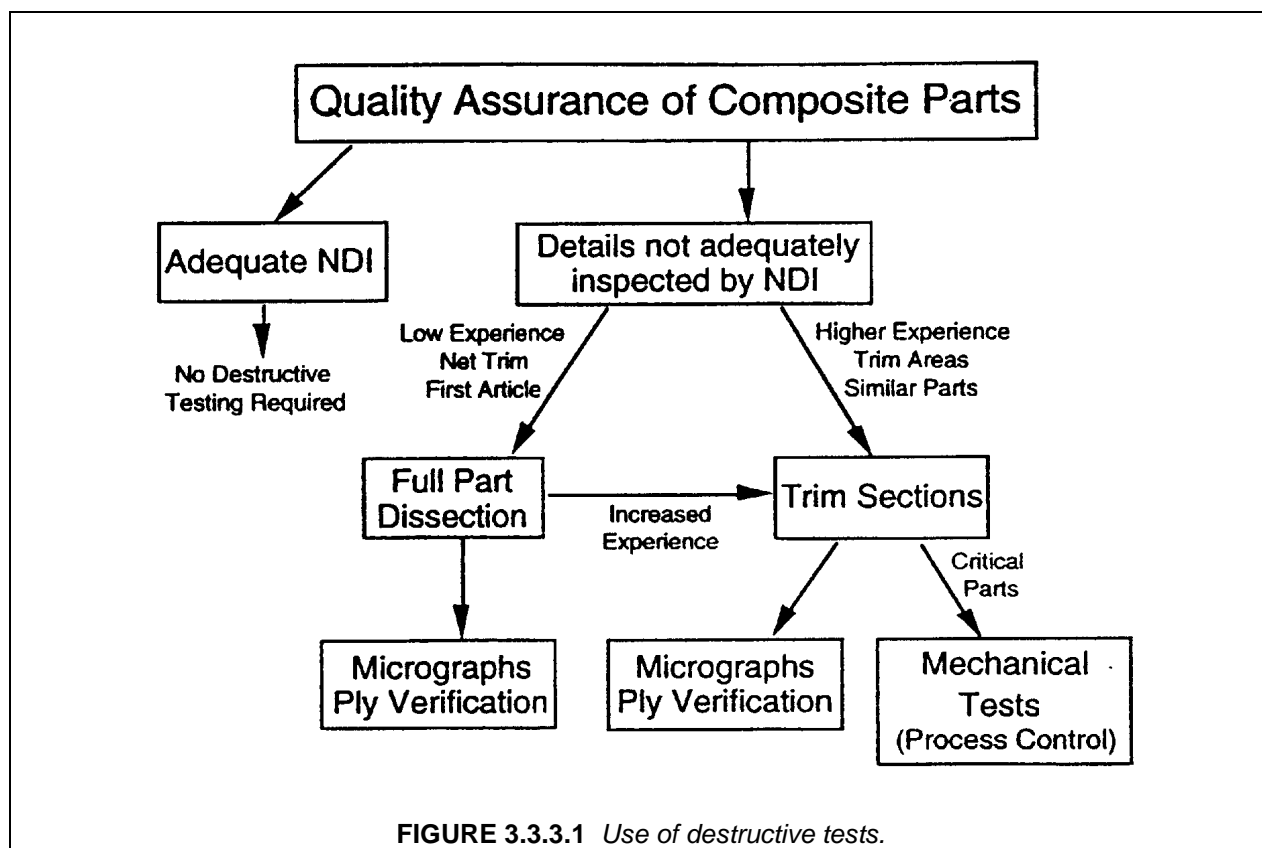


FIGURE 3.3.3.1 Use of destructive tests.

3.3.3.2 Usage

Destructive tests are often used to ensure the structural integrity of a component whenever assurance cannot be gained by nondestructive techniques alone. These tests include periodic dissection of the part to examine the interior of complex structures and mechanical testing of coupons cut from excess parts of the component.

3.3.3.3 *Destructive test approaches*

There are two primary categories of destructive tests: dissection of the full part or examination of trim sections of the part. Full dissection, generally done for the first part from a new tool, gives a complete examination of the part, but is expensive to perform. Examination of excess trim sections is the preferable approach whenever possible. The part is not destroyed, structural details can still be examined and mechanical test specimens can be obtained.

Full Part Dissection: Full part dissection is the approach often envisioned when the term "destructive testing" is mentioned. Since it prevents future use of the part, full part dissection should be reserved for parts that meet the following criteria:

- Areas cannot be adequately inspected by NDI
- Part is complex *and* there is a low experience level for working with the structural configuration or fabrication process
- Part is net trim; detail areas of interest cannot be examined using excess trim areas or part extensions.

Trim Sections: Examination and testing of trim sections offers a balance of quality assurance and cost. Trim sections can be part extensions that are intentionally designed to go beyond the trim line or can be taken from cutout areas inside the part. Section cuts from detail areas can be examined for discrepancies. Test coupons can be machined from the sections and mechanically tested to ensure the structural capability of the part and verify the quality of the fabrication process. Using coupons in this way can satisfy destructive testing requirements and process control requirements (Ref. Section 3.2.2).

3.3.3.4 *Implementation guidelines*

The frequency of destructive tests are dependent on part type and experience. If the producer has significant fabrication experience, complex parts may not require periodic destructive testing, but only a first article dissection. For low experience with complex parts, periodic inspection with increasing intervals may be preferable. Critical (safety of flight) parts warrant consideration for destructive testing.

Examination and testing of trim sections can be carried out on a more frequent basis and at less cost than full part dissection. Quality assurance can be enhanced by using more frequent and less elaborate trim section examinations.

Destructive tests should be conducted before the part leaves the factory. Periodic destructive tests monitor the manufacturing processes to assure the quality of parts. If a problem does occur, the periodic inspections bracket the number of suspect parts. Not every part series needs to be examined. If many parts reflect the same type of configurations and complexity, they can be pooled together for sampling purposes. Parts made on tools fabricated from one master splash can also be grouped together.

Sampling: A typical sampling plan might include first article full part dissection followed by periodic inspections employing dissection of trim sections. The periodic inspection intervals can vary depending on success rate. After a few successful destructive tests, the interval can be increased. If nonconforming areas are found in destructive tests, the inspection interval can be tightened up. If problems are found in service, additional components from the same production series can be dissected to assure that the problem was isolated.

For the trim section approach, periodic destructive tests can be conducted at smaller intervals since the cost is much less. Small intervals may be especially desirable in the case of critical parts.

For first article inspection, one of the first few articles may be chosen to represent first article. Some of the reasons for not stipulating the very first structure built are: (1) it may not be as representative of the production run because of lessons learned and special handling; and (2) another part with processing problems or discrepancies may reveal far more information.

Potential areas: Potential areas and items to examine include:

- Primary load paths within the part,
- Areas that showed indications from non-destructive inspection,
- Tool markoff near cocured details,
- Ply drop offs at a taper,
- Ply wrinkles,
- Resin starved and resin rich areas,
- Corner radii and cocured details,
- Core to face sheet fillets,
- Tapered core areas.

3.3.3.5 *Test types*

Both full part dissection and trim sections involve examination of detail areas. After machining the detail areas, photomicrographs can be obtained to examine the microstructure. Another type of destructive testing is ply verification. Only a small section is need to perform a deply or grind down to verify that the plies are laid up in the correct stacking sequence and orientation. For machine lay-up, this procedure should not be necessary after initial validation. To investigate items such as ply lay-up, potential ply wrinkles and porosity, initial core plugs can be taken at fastener hole locations and photomicrographs can be developed.

When mechanically testing specimens that were machined from trim sections, the coupons should be tested for the critical failure mode for that part or that area of the part. Tests addressing typical failure modes are unnotched compression, open hole compression and interlaminar tension and shear.

3.4 STATISTICAL PROCESS CONTROL

3.4.1 Introduction

Since composites exhibit a strong capacity for variability, the tools used to identify, assess, and hopefully control variability become critical. Statistical process control is a term used to tie together several different aspects of statistical and other quality methods.

3.4.2 Quality tools

There are several methods which form the bulk of SPC efforts. They range from fairly simple methodologies for gathering and evaluating data, to sophisticated statistical techniques for answering very specific questions. What is described in the following sections should not be construed as a comprehensive evaluation. There are many other techniques, or variants on the techniques discussed, which can be reviewed in the literature.

3.4.3 Gathering and plotting data

One of the first concepts in evaluating data is to collect them in a rigorous manner. Once the data have been gathered, the data should almost always be plotted in some fashion. It can be very difficult to discern even moderate trends in tabular data. This can be true with even just a handful of data points. In many cases, the same data can and should be plotted in several different manners, looking for patterns and relationships between factors, or trends over time.

3.4.4 Control charts

One of the specific ways that data can be plotted is as a part of a control chart. With control charts, variability in a process output is measured. The sources of variation are partitioned into chance or com-

mon cause, and assignable variation. Data are plotted as it is generated by a process, and a simple set of rules can be used to determine if an assignable cause should be pursued. With proper application, issues can be identified and addressed prior to reaching rejectable levels.

3.4.5 Process capability

A fundamental question for a manufacturing process is given the variability present, what percentage of product would meet specification requirements. Numbers representing this concept are termed measures of process capability. The process variability, represented by the standard deviation, is used to establish tolerance limits which describe where almost all of the product should fall. For one measure of process capability the range between these limits is compared to the specification range.

The lower the quantity of product produced outside the specification limits, the more capable the process. Various ratios can be used to assess process capability. An important issue is whether the process mean is centered between the specification limits, and the implications if it is not.

3.4.6 Troubleshooting and improvement

Many times a new process requires characterization and development, or improvements become necessary for an established process. A process that was once in control may not be any longer for reasons which are not well understood. In situations such as these, tools for troubleshooting established processes, and making improvements to new or established process become valuable. Three common methods are described below.

3.4.6.1 Process feedback adjustment

Introduction

Process control is achieved through both process monitoring and adjustment. Process monitoring is accomplished through Statistical Process Control (SPC), including tools such as process control (or Shewhart) charts and cumulative sum (Cusum) charts. These are used to interrogate the process or system to determine its stability. Process adjustment is used to bring a process back from drifting and is usually termed Engineering Process Control (EPC). SPC and EPC do not compete but can work together.

They can be adapted for environments where an appreciable cost is associated with making a change to the system or taking the measurement. These look at minimizing the overall cost of controlling the system using also the cost of being off the process target. EPC can also implement bounded adjustment charts that will dictate both the necessity and magnitude for an adjustment to the process. Finally, the monitoring of a process that is undergoing feedback control is covered.

The stable, stationary state, which is the environment under which traditional Statistical Process Control (SPC) is supposed to take place, is actually very difficult to attain and maintain. While the more familiar technique of process monitoring through the use of control charts can help achieve this control, frequently processes require adjustment of parameters to attain the desired output. While some of the tools and procedures are similar to those for process monitoring, the intent and approach is actually quite different.

Process monitoring is defined as the use of control charts that are used to continuously interrogate the stability of the process being investigated. When unusual behavior is detected, assignable causes as the source of the behavior are searched for, and if possible, eliminated. This technique has been widely used in the standard parts industry as SPC.

Process adjustment utilizes feedback control of some variable related to the desired output in order to keep the process as close as possible to a desired target. The origins of this procedure are in the process industry, which is termed Engineering Process Control (EPC).

Control Charts

Control charts that are used to observe frequencies and proportions are covered in the Section 3.4.4.

Different types of charts are used for monitoring of measurement data. These look at a sample average and range and are known as X bar and R charts. Some of the useful simplifications used for frequency and proportion data are not applicable for measurement type data. The same general terminology is used except as noted.

Several rules, some of which are industry or even company specific, can be applied to these control charts. The most widely known set of rules is the Western Electric rules that are applied to the control chart to determine if a deviation warrants the search for an assignable cause to be eliminated.

There are assumptions made for the application of these control charts. While some mild violation of these assumptions is not usually catastrophic, an unstable system can result in inappropriate warning and action limits.

Process Adjustment

In the process regulation the object is not to test hypotheses about the likelihood of a set of data indicating special cause, but rather statistical estimation of a disturbance to the system which is then compensated for in various manners.

As an indication of the differences between the objectives between process monitoring and process adjustment, waiting to implement a process adjustment until the process monitoring indicates a statistically significant deviation as a control strategy would usually lead to excessive process output variation.

For many processes acceptable control may not be achievable without process adjustment at some interval. These adjustments must not be made in an arbitrary fashion for consistent results. Important concepts in implementing process adjustment are the processes resistance to change, termed inertia, and the use of models to predict the future output of the process.

A unit change in the adjustment variable will not most likely result in a unit change of the process output. The relationship between these factors is termed the system gain. In attempting to predict the output of the process, it is useful to split the response in the categories of the white noise, and the system drift.

It is important to note that many processes, if left alone, will continuously drift away from a target value. Because of this drift, a low value is more likely to be followed by another low value, termed autocorrelation. These changes may be in the form of step changes, spikes, or changes in slope. With process adjustment, it is attempted to estimate the direction of the process, and then adjust the process, compensating to keep the process directed toward the target value.

The types of disturbances that induce this drift can be environmental changes such as temperature and humidity, or changes in the composition of the input materials. Whether or not these variables have been identified, some sort of feedback control may be necessary to compensate for their effect, allowing the process output to return to the target value. These feedback adjustment procedures have a direct relation to the types of automatic control methods used in the process industry.

While some sort of alteration of the process based on SPC input is frequently employed, a consistent methodology is seldom implemented. By using some sort of feedback adjustment scheme, the variation in the process output can be reduced several-fold in many applications.

What has allowed feedback adjustment the opportunity for more widespread application outside the traditional chemical process industries is the determination that substantial errors in modeling the system, and even significant errors in applying the feedback adjustment result in minimal effects on the process output variability.

Some processes do not experience the full effect of the process adjustment in one interval. These processes are termed to have inertia. Modified processes are required to adapt to these process characteristics.

Another goal for the process adjustment is to minimize the number of adjustments to the process required. This is especially important when there is an appreciable cost associated with the adjustment process. While constraining the adjustment does have the effect of inflating the process output variability, it has been experienced that dramatic reductions in process adjustment frequency can be implemented with only modest increases in process output variability over the theoretical minimum.

Some of these processes include the use of a dead band about the target value. Process output predictions in this dead band do not result in any process adjustment. Another process is the bounded adjustment.

Another point of concern is the inadvertent use of process adjustment to a process that is already in a state of perfect control. It has been determined that implementation on such a process would only result in an increase of about 5% in the process output variability. Weighed against this potential is the likelihood that most processes violate the assumptions required to achieve a perfect state of control.

Another aspect of concern of feedback adjustment is the potential for costs associated with observing and/or adjusting a process, weighed against the cost of drifting from the target value. Modifications to the feedback adjustment process have been made to minimize the overall cost associated with these areas.

The question of how often a process should be observed is also present, along with the associated costs. Costs associated with reading a process can be weighed against costs from adjusting the process and increased process variability or deviation from the target value.

3.4.6.2 Design of experiments

Background

While the statistical analysis of data generated by manufacturing processes has become commonplace, the layout or structure of the data generated has largely resisted a consistent methodology. Rules of thumb, historical precedent, or simply availability dominate data gathering efforts, although some statistically based analyses of composite bolted joints have been performed. There is a frequent perception that such a methodology would somehow remove control from the technical process expert, or that it has little additional to offer compared with recognized precedents. One of the most established tenets of conventional data layout carried through most programs is that only one data factor is ever intentionally changed at one time in an experimental program. While without an appropriate approach this may be prudent, there is a message that has been lost. With a proper methodology changing more than one variable at a time can be performed efficiently and effectively, providing information that is impossible to obtain when only one factor is changed at a time. Often the uncovered hidden relationships dominate the process results.

The general name for such a methodology is Design of Experiments (DOE). Another term is Designed eXperiments (Dx). Through DOE a great number of factors which could potentially influence an output of interest can be efficiently screened, establishing statistically with a linear model whether they truly influence the process output. Building on this data, interactions between significant factors can be determined, but only by violating the rule about changing only one factor at a time.

Another technique builds upon DOE to form nonlinear models, such as quadratic models, allowing process optimization to be performed. This approach is known as Response Surface Methodology (RSM). As the name implies, the desired output is usually a multi-factor nonlinear relationship.

DOE and RSM are used serially in a process known as sequential experimentation. In this method initial experiments are used to screen for significant factors. If a factor being adjusted is not actually significant, this data is not wasted but becomes replicates or duplicates for other significant factors, providing

additional information on process variance. Additional data can be added to pursue indications of significant interactions. The model also provides signs on whether nonlinear relationships should be further pursued. Additional points added through RSM are used to establish these nonlinear (quadratic) characteristics. The models use all the data generated for one or more purposes, providing for very efficient experimentation.

There are in the literature applications of designed experiments used for determining composite elastic properties, and a few were found used for determining composite mechanical properties such as bolted joint strength. Use of this efficient methodology can allow serious evaluation of processes previously considered too complicated for full experimental investigation. As a result, typically in the past only a few established areas of interest would have been tested, with a pick-the-winner approach. Rarely was it established that there was even a statistical difference between the “winner” and the discarded options, much less that any kind of optimum had been achieved. But application of DOE and RSM experimental methods can provide these tools and options.

One Factor Models – Linear and Quadratic

Fitting a line or linear equation to data is a fairly routine process, as shown in Figure 3.4.6.2(a). The line represents the trend of the data, but rarely do all the data points fall directly on the line. At a given value along the horizontal or X-axis, the data is frequently normally distributed about some average value represented by that point on the line. This can be seen in the figure for one point. The same distribution should hold for all the points on the line.

One of the important considerations in fitting an equation to data is the spacing of the data. If an equation is to be fit for a result as a function of one factor, the data may be closely spaced, as seen in Figures 3.4.6.2(b) and (c). In Figure 3.4.6.2(b), the normal distribution of data at two given points, representing a large sample of data, is shown. In Figure 3.4.6.2(c) a relationship is present, but only a small sampling of data (three points) is indicated. What Figure 3.4.6.2(c) shows is that with a small sample at two closely spaced points a significant relationship can be missed. The farther the data are spread towards the edges of interest or practical experimentation, the more likely to detect a statistically significant relationship with a minimum of data, as seen in Figure 3.4.6.2(d). Frequently only a single data point is gathered at the ends, especially early in a screening program.

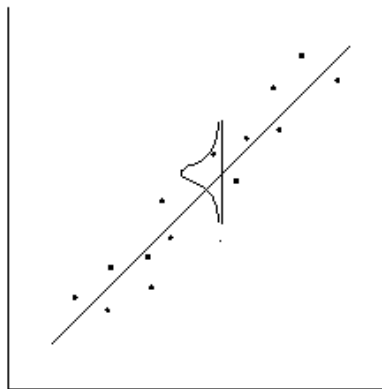


FIGURE 3.4.6.2(a) *Fit of linear equation to data (normal distribution of data about line shown).*

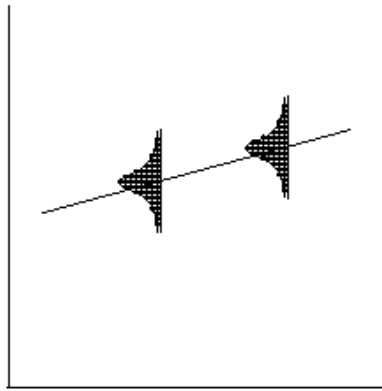


FIGURE 3.4.6.2(b) *True relationship established with large data sample with closely spaced points.*

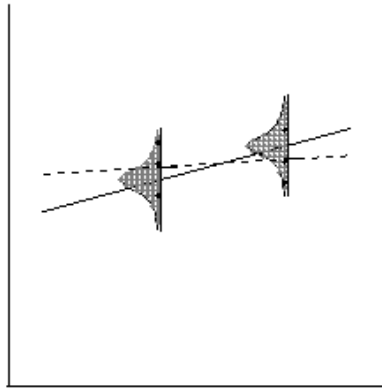


FIGURE 3.4.6.2(c) *True relationship missed with small data sample and closely spaced points.*

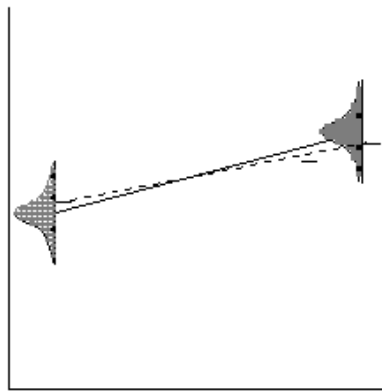
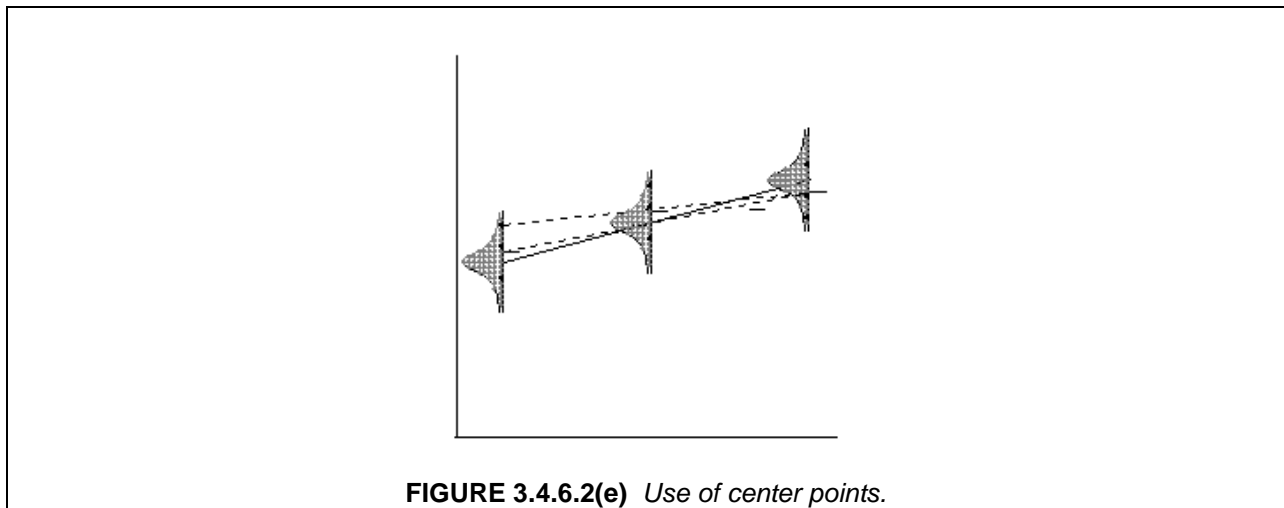


Figure 3.4.6.2(d) *True relationship identified with small sample and widely spread points.*

For linear models, which are typically used for identifying significant factors, this means minimizing the number of points between these edges or end points. Some data points can be used at the midpoint between these edges to replicate data. The estimate of variability derived from the replicate data is used to judge whether differences seen between the ends are statistically significant or not.

The form of a linear equation is the familiar " $y = a + bx$ ". The " x " represents the independent variable that can be manipulated. The " b " which is multiplied by " x " represents the slope of the line. The " a " is the intercept value of " y " when " $x = 0$ ". If the equation is nonlinear, for example a quadratic equation, then an additional term is added. The form of the equation then becomes " $y = a + bx + cx^2$ ". The quadratic term brings the ability to match the curvature seen in the data.

If the relationship is linear, then the average of the data at the center point should be roughly the average between the two end points, as seen in Figure 3.4.6.2(e). If the center point average deviates significantly from this average of the endpoints, it is an indication of a nonlinear relationship.



Certainly one reason for closely spacing the points within the region of interest is that within the spacing the relationship will appear linear, which is much more commonly applied. A nonlinear relationship without proper experimental techniques can be difficult to economically characterize, and typically is avoided if possible. However, if the relationship is truly nonlinear, as shown in Figure 3.4.6.2(f), and there is a reasonable chance that the process may proceed outside the currently established limits, then this is of interest and value, and should not be overlooked.

If the relationship is strong enough and the end points are far enough apart, then a single data point at each of the ends may be sufficient to identify a significant relationship. Some assessment of variability must still be made or assumed. These multiple data points can also be generated at the center point, and much more efficiently than replication at each of the end points. The variability is then assumed to be comparable across the range.

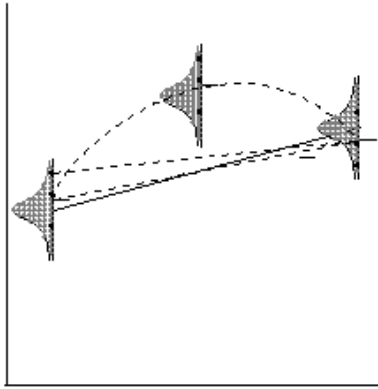


FIGURE 3.4.6.2(f) *Nonlinear relationship identified with center points.*

Two Factor Models – Linear and Quadratic

The same rationale and methodology can then be extended to fitting an equation for some process output as a function of more than one factor. The same ideas about spacing of the data collection levels hold true, as shown in Figure 3.4.6.2(g). The idea is to spread these to the edges as far as possible without changing the basic relationship of the fundamental measurement of interest. Also, the same advantages of center points still hold true, but for continuous factors the center points may serve for both factors. For two factors the equation which is developed can be plotted to create a response surface, a graph with the appearance of a topographical map. This can be looked at as a series of single factor equation lines or curves evenly spaced as a function of the second factor.

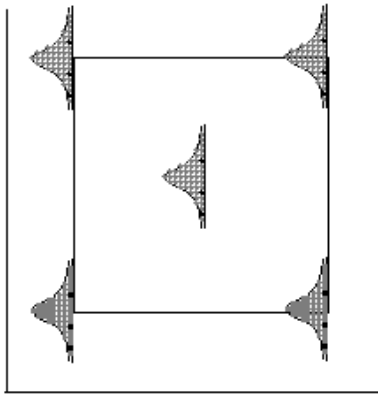


FIGURE 3.4.6.2(g) *Data spacing for two factors.*

If the relationship is strong enough and the end points are far enough apart, then a single data point at each of the ends may be sufficient to identify a significant relationship. Some assessment of variability must still be made or assumed. These multiple data points can also be generated at the center point, and much more efficiently than replication at each of the end points. The variability is then assumed to be comparable across the range.

For a linear model this will create a plane cutting through the four corners of the square. The form of the equation would then be " $y = ax + by + c$ ". It is a natural extension of the single factor linear equation,

although perhaps more difficult to visualize. An example can be seen in Figure 3.4.6.2(h). If there is an interaction between the two factors there can be a twist to the surface, giving the appearance of a nonlinear equation. The interaction term in the equation is the product of the two independent variables multiplied by a coefficient. The form of the equation would then be " $y = ax + by + cxy + d$ ".

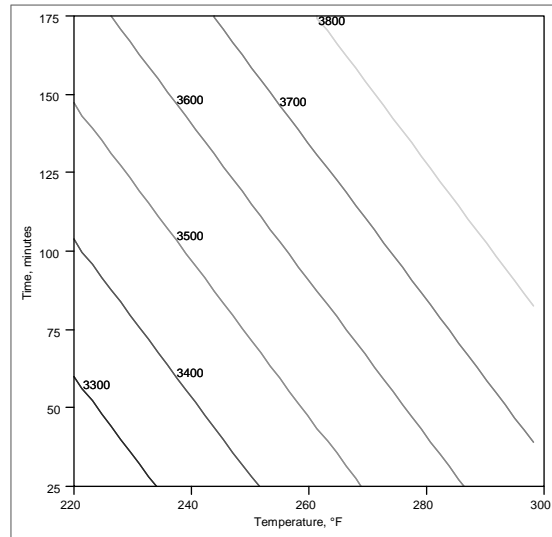


FIGURE 3.4.6.2(h) Example of linear response surface (adhesive lap shear strength in psi as a function of cure final dwell time and temperature).

The center points function in the same manner as for the single factor. If the center points fall reasonably close to the surface of the plane, then there is not an indication of a nonlinear relationship. If the center points do not fall reasonably close to the plane, then there is an indication of nonlinearity.

Here Response Surface Methodology can be introduced to complement Design of Experiments. RSM builds on the data and linear model from the DOE, supplementing with some additional data in the optimal manner which allows generation of a nonlinear model to fit the relationship. The form of the equation would then be " $y = ax + by + c + dxy + ex^2 + fy^2$ ". The data layout can be seen in Figure 3.4.6.2(i).

Here the concept of an interaction comes into play. An interaction means that the level of one factor influences the effect of a second factor. A simple example of this that is a common manufacturing experience is curing a thermosetting plastic. If a plastic is cured at 325°F, then perhaps it takes 100 minutes to optimally cure. If the oven is at 350°F, then perhaps it only takes 50 minutes. The temperature of the oven affects the time it takes to cure; one cannot be optimally set independently from the other. If at 350°F the plastic is left to cure 100 minutes, it may become oxidized, warp, or provide reduced properties. The effect that 50 minutes curing has on the plastic depends on the oven temperature.

The conventional way to handle this type of problem is to attempt to not allow the temperature to change. All but one factor is held fixed. The one factor is varied, and the effect is measured. Without DOE tools this may be the only approach available, but with these tools a more accurate relationship can be developed. These additional RSM points are called "star points", as seen in Figure 3.4.6.2(i). They allow the nonlinearity to be assessed while still using all the data generated in the attempt to create a linear model. The proper placement of these points is the basis of RSM. An example of the response surface generated from a quadratic model can be seen in Figure 3.4.6.2(j).

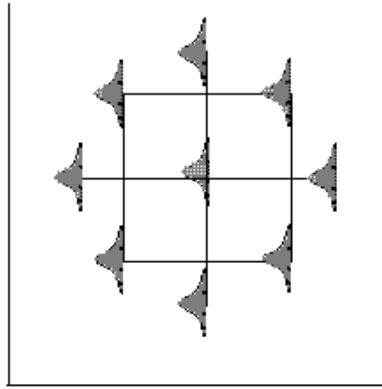


FIGURE 3.4.6.2(i) *Placement of star points outside of square.*

Multiple Factor Models – Linear and Quadratic

Again this method can be extended to three or more factors. Instead of a square the placement of points now extends to a cube, where the vertices of the cube represent the various combinations of high and low values for the three different factors being evaluated, as seen in Figure 3.4.6.2(k).

The fitting of the equation follows the very same methodology, although it is now more difficult to plot the output for all three factors. With one factor fixed, the other two can be plotted in the same manner as seen for two factors above. The center points have also been used in the same manner for all three continuous factors. Because they are being shared for all three factors now, the efficiency of their use has increased even more. The extension to a nonlinear model follows the same basic pattern as well, as shown in Figure 3.4.6.2(l).

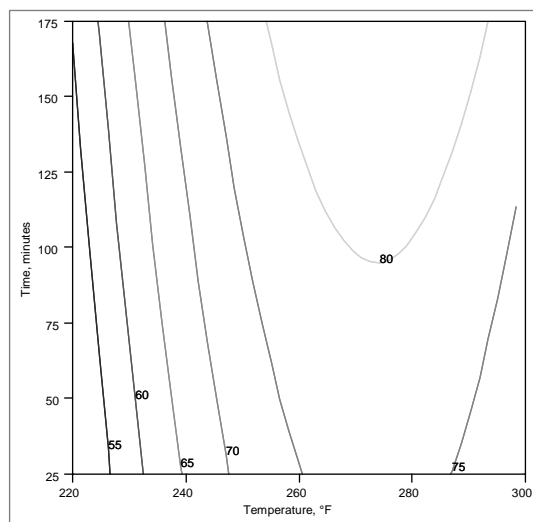


FIGURE 3.4.6.2(j) *Example of quadratic response surface (adhesive peel strength in psi as a function of cure final dwell time and temperature).*

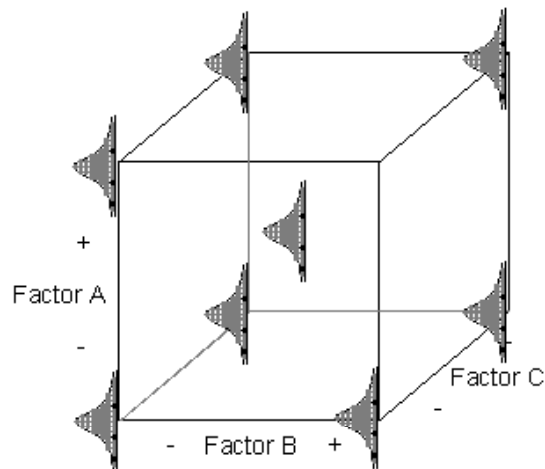


FIGURE 3.4.6.2(k) *Three-factor experimental design.*

One of the superlative features of DOE is the ability to determine effective models without data at all of the points. For the three-factor model, this would mean testing only half of the corners of the box, although in a very specific manner as shown in Figure 3.4.6.2(m). This would allow the generation of a linear model but no interactions. Since there would be four data points, this leaves three degrees of freedom, one for each factor's linear component or main effect. No interactions could be represented, although the alternate data could be generated at a later time. This is termed a fractional factorial. Fractional factorial DOE can also be used with RSM in the same manner as shown above for placing the star points as seen in Figure 3.4.6.2(l).

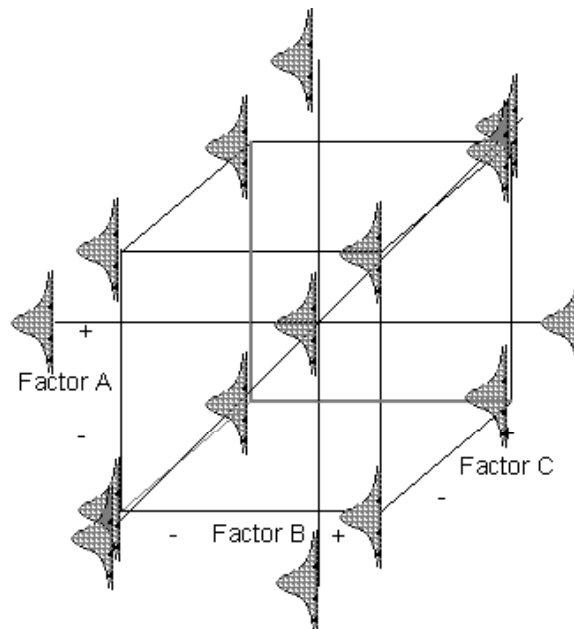


FIGURE 3.4.6.2(l) *Star points outside cube for three-factor design.*

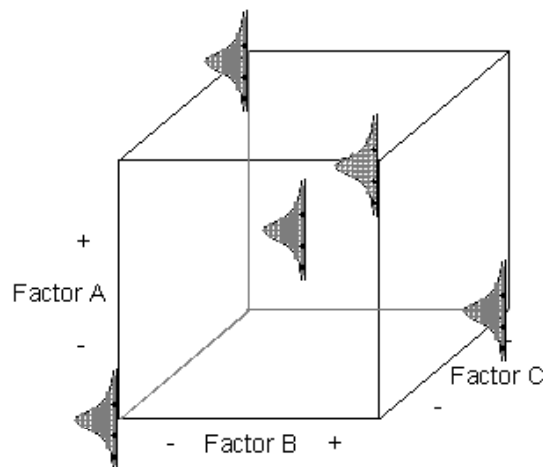


FIGURE 3.4.6.2(m) Half-fraction (2^{3-1}) for three-factor design.

Sequential Experimentation

Sequential experimentation is another important aspect of experimental design. At the beginning of the experimental program, little may be known about the relationships involved. DOE can be used to screen through a great number of potential factors to find significant ones. Once these have been found, the data representing non-significant factors can be treated as replicates for those factors that were determined to be significant. Additional data can then be generated, still using prior data, to confirm linear models and identify interactions.

If the center points indicate nonlinearity, then additional data can be generated at the star points identified to support creation of a quadratic model, again still using the previous generated screening and linear model data. This is the most efficient method possible for creation of experimental models for complex phenomena.

Model Checking

Once any model has been fit to a set of data, each assumption used in creation of the model should be checked to see if it was valid. One of the first model checking parameters that can be examined is the R^2 . This number gives an assessment of how much variability seen in the data is represented by the model that has been fit. Adding more factors to the equation can always increase this number, whether or not they are statistically significant, so to counter this an adjusted R^2 is also calculated. This number will actually decrease if a statistically insignificant factor is added to the model.

Another confirmation of the model is examination of the residuals for the presence of patterns. The residuals are the differences between the actual value and the model-predicted value for each data point. If the model has picked up all the nonrandom patterns in the data, then the residuals should appear random. Thus patterns in the residuals can provide additional useful information on relationships not currently included in the model.

One of the assumptions for using the regression methodology for fitting a model is that the distribution of the data is normal. Whether or not the residuals are normally distributed can check this assumption. The value of the normalized residual for each data point should usually be within two standard errors, or else it is identified as an outlier. This may indicate some error in generating or collecting the data, or may be indicating an effect that is not well represented by the model.

The Cook's distance is a measure of the relative influence of each of the data points on the model that is being evaluated. If the Cook's distance number is calculated as above one, then it indicates that this data point is very influential in determining the form of model. While this is not inherently undesirable,

any error in this data point will result in proportionally greater error in the model compared to other error introduced by data points with distances of less than one.

3.4.6.3 Taguchi

Several ideas have been promoted in an attempt to quantify the cost incurred as a result of poor quality. Taguchi has suggested the use of a quadratic function for departures from the optimum level. In addition, he has promoted the use of experimental designs that can be much easier to implement in a production environment.

3.4.7 Lot acceptance

This section is reserved for future use.

3.5 MANAGING CHANGE IN MATERIALS AND PROCESSES

3.5.1 Introduction

The need to employ alternate material or process may occur during the course of any program. It is essential to the success of the program that these changes be managed in a systematic and cost effective manner. Although materials and processing changes must be dealt with on a case by case basis, generalized methods or protocols have been developed which may be used to guide the process. The section below details an approach to managing materials and processing change. Critical issues that must be addressed and resolved are identified and described.

3.5.2 Qualification of new materials or processes

Qualification evaluations typically exhibit progressive cost escalations from coupon tests, to elements, to components, to parts, and eventually to aircraft. This progression is commonly known as the "building block" approach to qualification. Chapter 4 of Volume 3 deals with this subject in detail. It is important to conduct initial planning to align and coordinate multiple sources, product forms, and processes early in the qualification effort. This planning allows better utilization of the existing expensive large scale tests by incorporating various considerations in left hand/right hand or upper/lower portions of the test items.

Alternate materials or processes can be evaluated for specific applications as required, allowing for a partial replacement of the baseline material. It should be noted that if a partial replacement is considered, the cost of multiple drawing changes required to maintain a distinction between two materials must be considered. In addition, some cost must be allocated for analysis review to determine which application can withstand material properties that are not equivalent or are better than the baseline properties.

When a material or process-related change is identified, or a material or process-related problem requires remediation, the stakeholders may use the protocol described here to develop a solution. The elements and sequential stages of this material and process qualification protocol are illustrated in Figure 3.5.2. Two elements, Divergence and Risk, and Production Readiness are particularly critical to a successful materials or process change, and are covered at greater length below.

3.5.2.1 Problem statement

The problem statement bounds the qualification program by providing a clear statement of the desired outcome and success criteria. It delineates responsibilities for the aspects of the program to the material supplier, processor, prime contractor, test house, or customer. It becomes the cornerstone for other decisions and serves as the basis of the business case as well as divergence and risk analyses on which the technical acceptability test matrix is built. When the problem statement is found (1) to be lacking specificity, (2) to be so specific as to limit approaches, or (3) to have a clear technical error, modifications may be made with the agreement of the qualification participants and stakeholders.

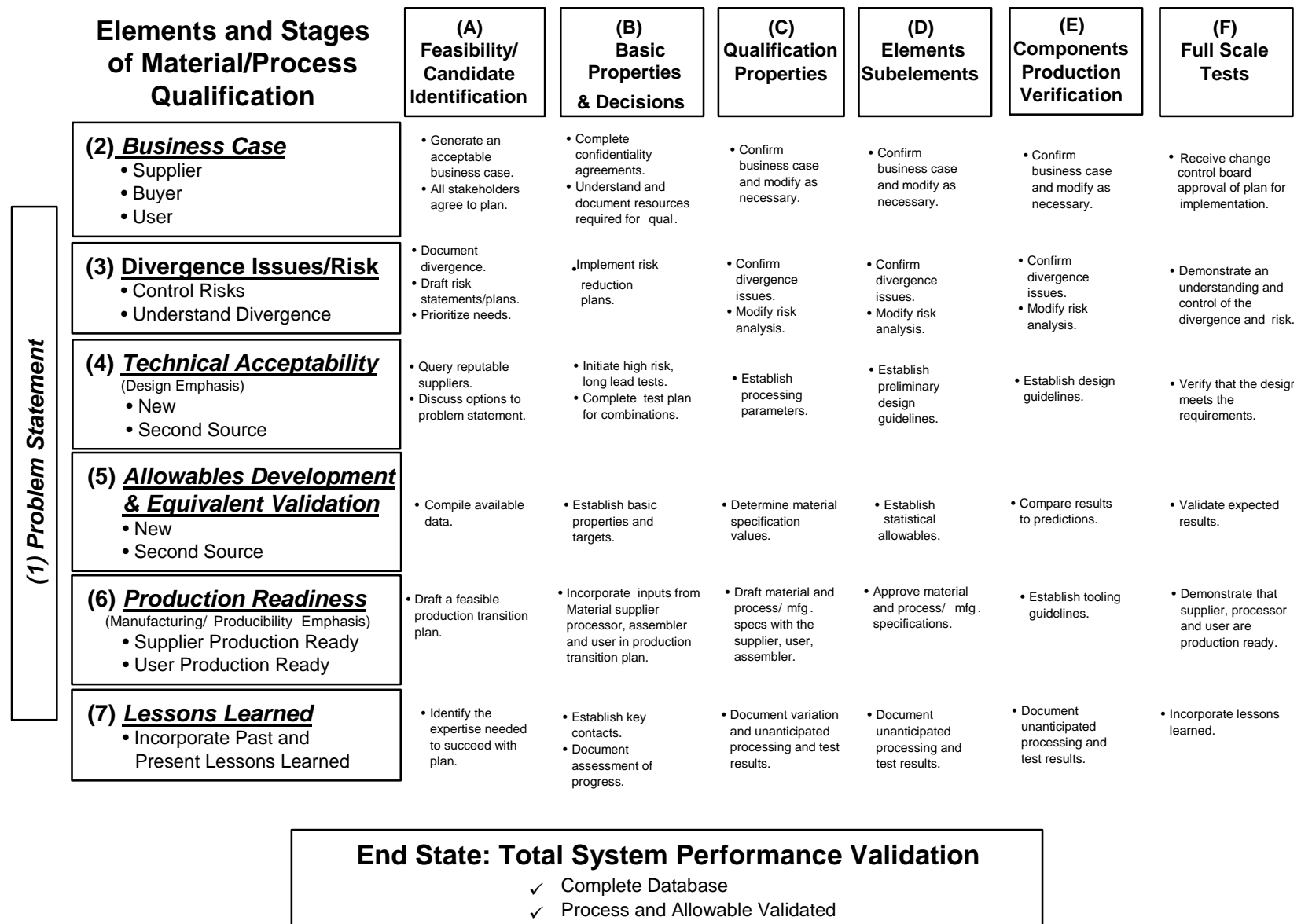


FIGURE 3.5.2 Elements and stages of material or process qualification.

3.5.2.2 *Business case*

Following development of the problem statement, a business case is developed (1) to clarify responsibilities, (2) to show the clear benefit of the qualification to all participants and stakeholders, and (3) to obtain and allocate resources for the qualification effort.

3.5.2.3 *Divergence and risk*

Divergence and risk analyses are conducted to provide the most affordable, streamlined qualification program while addressing risks associated with using related data, point design qualifications, and so forth. The divergence analysis assists the qualification participants in determining how similar or how different the new material or process is from the known and understood materials or processes. Risk analysis is performed to determine the consequence of reduced testing, sequencing testing and so forth.

3.5.2.4 *Technical acceptability*

Technical acceptability is achieved by fulfilling the objectives included in the problem statement, answering technical questions based on historic knowledge and practices, and by showing through test, analysis, and the results of the divergence/risk analyses that the material or process system is understood. Its strengths and weaknesses are then identified and communicated through design and analysis guidelines.

3.5.2.5 *Allowables development and equivalency validation*

The allowables development and equivalency validation focuses on the quantitative aspects of the qualification.

3.5.2.6 *Production readiness*

In the past, qualification programs have often fallen short because they ended with the quantitative aspects of design databases. However, a successful qualification program must include the transition needed to assure production readiness. Production readiness includes raw material suppliers, formulators, fiber suppliers, preformers, processors, quality conformance testing, adequate documentation, and other areas. Again, this protocol methodology does not provide all the answers for specific qualifications. Instead, it provides discussion to stimulate thought by the qualification participants and prompts appropriate planning based on the problem statement, business case, divergence or risk analyses, and technical acceptability testing established for the particular case by knowledgeable stakeholders.

3.5.2.7 *Lessons learned*

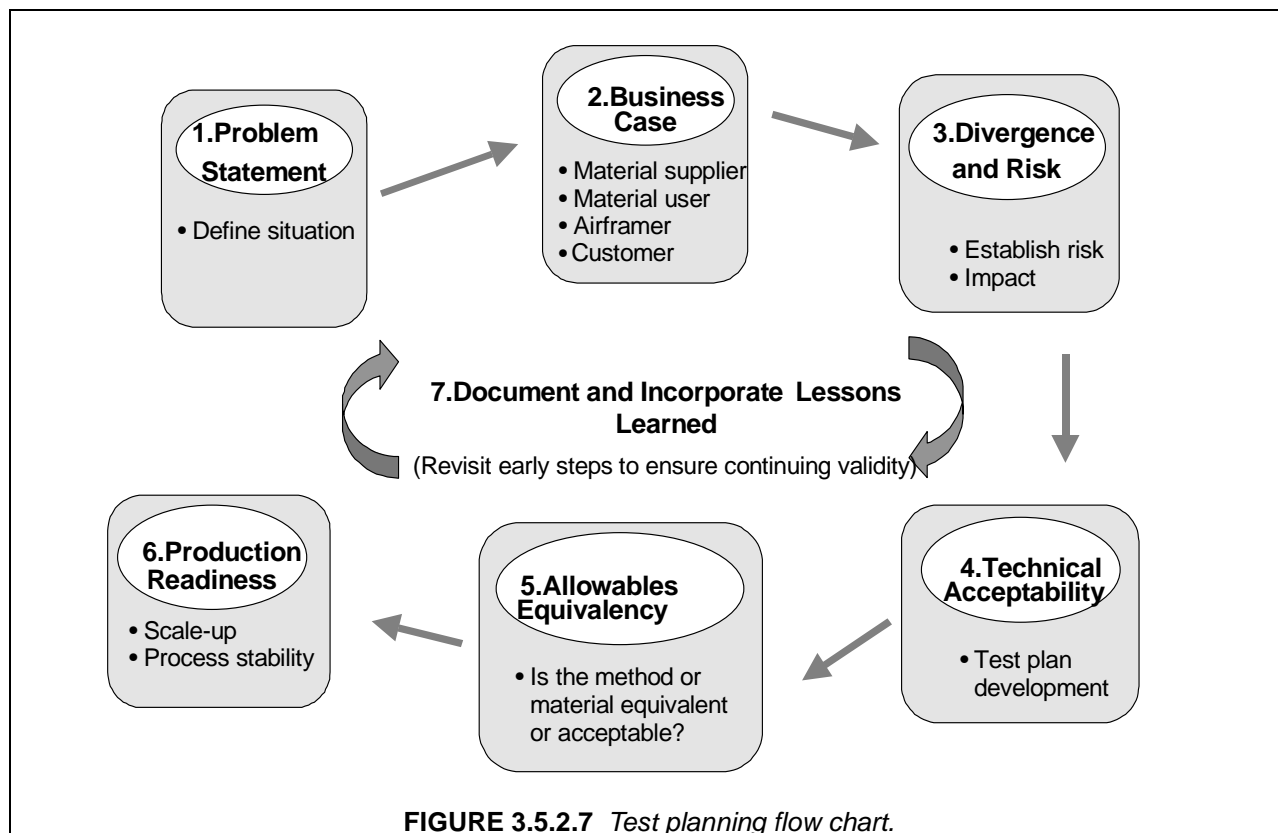
Finally, the methodology admits that no qualification is perfect. Lessons learned from the past should be incorporated into the plan as soon as the tie is identified in the divergence or risk analyses. In addition, lessons learned from the current qualification should be documented and acted upon throughout the qualification.

This methodology requires the qualification participants to revisit each qualification element and make modifications as necessary throughout the sequential stages of qualification. Figure 3.5.2.7 provides a flowchart of the composite material and process qualification procedure.

3.5.3 **Divergence and risk**

Divergence and risk analyses are conducted to provide the most affordable, streamlined qualification program while addressing risks associated with using related data, point design qualifications, and so forth. The divergence analysis assists the qualification participants in determining how similar or how dif-

ferent the new material or process is from the known and understood materials or processes. Risk analysis is also performed to determine the consequence of reduced testing, sequencing testing and so forth.



The level of divergence of a qualification program is determined by assessing how similar or how different the "new" or "modified" material/process is from that used in the baseline, in past experience, or in the general history of composite material and process usage. It is an acknowledgment of those areas of similarity to common knowledge versus those areas that are a departure from common knowledge and experience.

Risk can be defined as an undesirable situation which has a probability of occurring with attendant negative impacts on the success of the effort. An obvious undesirable situation in the context of a material qualification effort is a failure in the alternate material when it is implemented. Areas of failure could include processing difficulties, a structural failure of the component itself, or any other event or development that adversely impacts cost or schedule.

There is always some level of risk associated with the qualification of composite materials. The risk level for a second or alternate source is related to the divergence between the baseline material or process and the alternative material or process. The highest risk is the case where a new material system or process is being qualified as part of a new production program. For this situation there is no baseline material or process, and thus divergence is at its greatest. Although most of the same considerations apply, this case is not addressed in this protocol.

This section discusses the impact of material divergence on the qualification test program. Guidelines are provided on how to establish the level of divergence, assess risk, establish the qualification plan, establish the test sample size, and select test methodologies. It is recommended that all the stakeholders participate in the process defining the level of divergence.

3.5.3.1 Divergence

The first effort in establishing the level of risk is to define the magnitude of divergence between the baseline and the alternate material or process. This is done by listing all the properties, characteristics, descriptors, and attributes associated with the baseline composite materials and processes, then assessing the differences for each of the items on the list.

The list may be top level or detail in nature. Divergence criteria may include: (1) a change in the raw material source; (2) a change in the processing site or equipment; (3) a change in fiber sizing; (4) a change in fabric style; or (5) a change in resin. The difference could also include a change in the part fabrication process, such as going from hand collation to fiber placement, or from hand collation to resin transfer molding. There could be a material change associated with the fabrication process change or there could be no changes in the material. There may also be equipment changes within the fabrication process. The magnitude of divergence between the material and process combinations defines the starting level of risk.

For example, one of the items on the list may be "resin". In one case, the baseline material is a 350°F curing epoxy. To be rated as "no divergence", the alternate material need only be a 350°F curing epoxy resin. In another situation, however, the definition of "no divergence" is an alternate resin mixed at an alternate site, but chemically equivalent to the baseline.

An assessment is made for each item on the list to determine the level of divergence between the baseline material and alternative material. By definition there will be acceptable levels of divergence for some items (such as the qualification of a new prepreg line) and there will be some items where no divergence is allowed (for example, the resin formulation for qualification of a licensed resin).

Relevant testing requirements are defined and identified with respect to these areas of divergence. At times the testing is used to validate that the divergence does not negatively impact the material or the end use of the material, while at other times testing is used to validate that there is no divergence.

A key element of the divergence assessment is to define the accept/reject criteria to be used in analyzing the test data, audit findings, and processing trials. Establishment of criteria requires a clear understanding of the divergence requirements: equivalent versus equal, similar versus identical, statistically based versus typical values, and so forth.

Representative areas of divergence are listed below:

- **Resin**
 - Raw material sources
 - Mixing equipment
 - Mixing parameters
 - Filming equipment
 - Filming parameters
- **Fiber**
 - Precursor source
 - Fiber line
 - Fiber processing parameters
 - Sizing type
 - Sizing source
 - Fiber tow size (filament count)
 - Fabric style for fiber preforms
 - Weaving source for fiber preforms (location)
- **Prepreg Manufacture**
 - Impregnation line
 - Impregnation parameters
 - Auxiliary processing
- **Component Fabrication**
 - Collation method
 - Tooling concept
 - Cure cycle
 - Bagging procedures

This list is intended as a guideline and is not all-inclusive. It references divergence areas that have been commonly seen in past qualifications, but future qualifications will present new and unique areas of divergence that are as yet unknown.

Sample Generation of Divergence Assessment List

In this example, the qualification objective is to qualify a second impregnation line which has been altered to increase fiber wet-out. There is no change in the fiber or resin, including resin mixing.

<i>Potential Impregnation Line Changes</i>	<i>Divergence between Lines</i>
line width	same
fiber creel arrangement	same
fiber tensioning method	same
fiber path	changed
fiber spreading method	changed
resin application method	same
impregnation method	changed
impregnation parameters	changed
chill plate method	same
prepreg slitting	same
prepreg roll-up	same
carrier papers	same

In this example, the objective of qualifying the new impregnation line is resultant equipment that will yield prepreg that is better suited for slitting into narrow tape for a fiber placement process. The two key areas where the change is being affected are: (1) fiber spreading/collimation and (2) impregnation. The intention of the changes is to improve fiber collimation and increase the level of fiber wet-out.

Once the divergence has been defined, the next step is to assess the risk associated with each area of change.

3.5.3.2 Risk assessment

Risk is directly associated with the uncertainties that stem from the level of divergence. The objective is to manage the risk and reduce it to an acceptable level by effectively structuring and conducting the qualification program. The qualification program focuses on the testing of the alternate material, but risk is also reduced through other activities such as audits, processing trials, and drawing on previous experience.

Risk assessments may be subjective. What is viewed as high risk to one person may be viewed as a medium risk to another. Past experiences and familiarity with the new material or process will influence a person's perception of the risk level. For these reasons, it is important that the level of material or process divergence be quantified and that a systematic risk assessment process be documented.

Risk assessment builds on the defined differences so that the risk can be fully defined. When the, "What can go wrong?" question is asked, it is important to apply the question at the correct level within the program. It is not meant to be a global question. ("What can go wrong if the new material is not qualified?") At this stage an assessment is being made for each individual area of divergence.

Continuing with our sample qualification, a risk assessment for each area of divergence follows:

- Fiber path - The change in fiber path has the potential of damaging the fibers. The qualification plan should include tests that are sensitive to fiber damage.

- Fiber spreading method - As with the change in fiber path, a new fiber spreading method also has the potential of damaging the fibers. This is especially true if the intent of the change is to increase the fiber tension. Again, tests that are sensitive to fiber damage are warranted for the qualification test plan.
- Impregnation method and parameters - The change in the method of impregnation and associated parameters has the potential of changing the level of resin advancement and the physical configuration of the prepreg (with less resin on the surface). These changes could result in loss of tack, shortened out-time, reduced resin flow, and elimination of volatile escape paths. They will also help in the formation of a clean edge during the slitting process (the goal of the changes).

The qualification plan should then include tests or evaluations that address fiber damage, changes in potential resin advancement, and handling properties. The plan should also include an assessment that validates what the changes in the impregnation line do to improve the slitting and fiber placement processes.

3.5.3.3 Risk analysis

In this step, the risk is analyzed to determine its magnitude. What is the likelihood of the risk developing? What are the possible consequences of the risk? What category does the risk fit into: cost, schedule, or technical?

The likelihood or probability that a risk will develop can range from not likely to near certainty, depending on the approach being taken to mitigate the risk. If a risk develops, impacts of various magnitudes will result. These magnitudes need to be defined from no impact to unacceptable, so that the qualification plan can be structured to address the identified risks. The risks are then minimized through performance of the qualification plan.

A typical risk analysis spread sheet is shown in Figure 3.5.3.3. This particular spreadsheet is generic to programmatic risk analysis but applicable across a wide range of other risk analysis. The user must assign new definitions to the levels of likelihood and consequence wherever those shown are not appropriate.

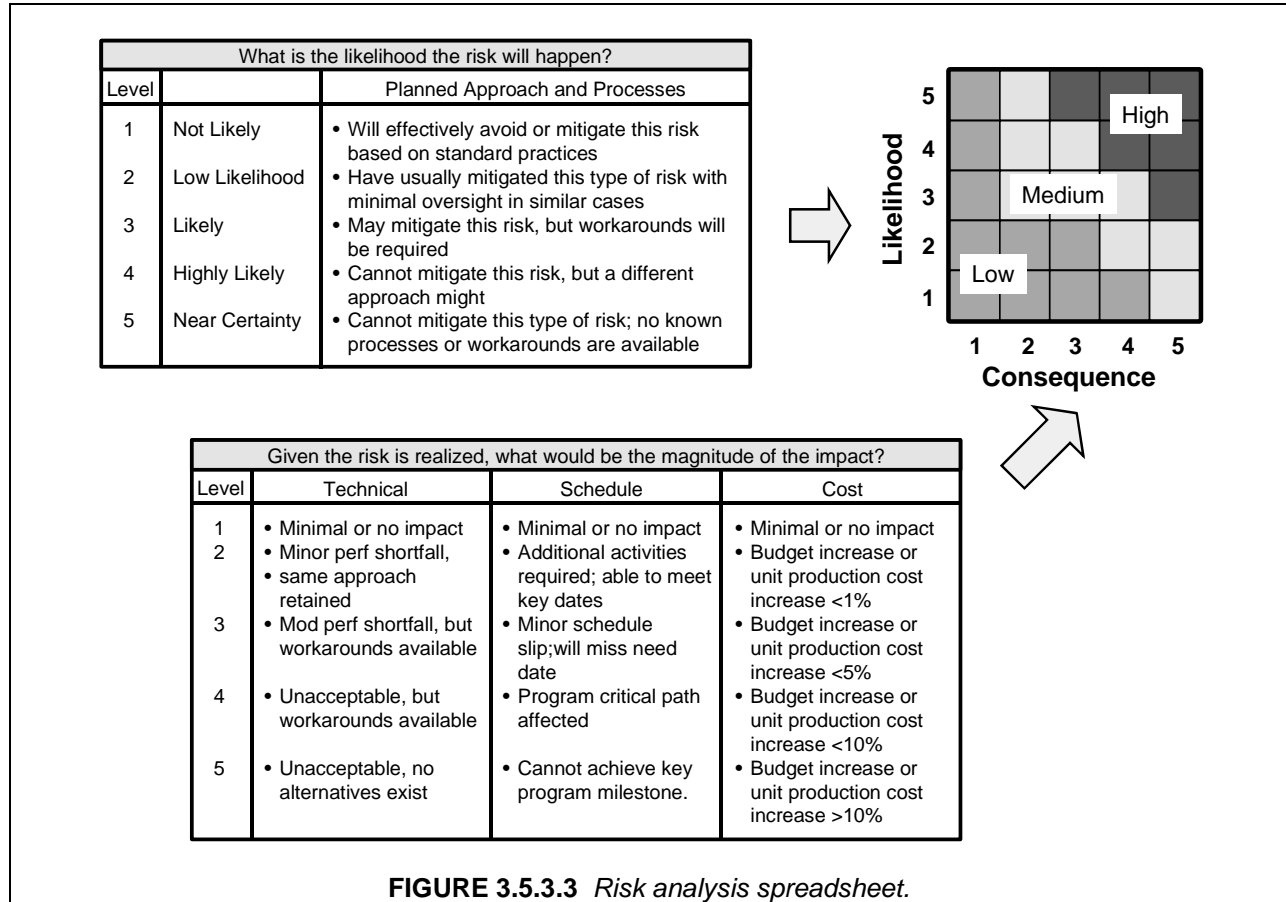
3.5.4 Production readiness

Production readiness assessment must address the ability of each of the following to adhere to appropriately documented processes and to adequately record all pertinent information for traceability:

- The suppliers of the constituent materials
- The formulator/processor/prepregger
- The part fabricator
- The assembly facility
- Any subcontractors, intermediate suppliers, processors, inspectors, etc.

Production readiness is a key consideration in the risk reduction process to assure control of cost, schedule, and technical acceptability of the end product. It is necessary to start at the earliest point of change, because one initial change can often affect processing and documentation at subsequent points in the path to the final product. The necessary documentation takes two forms: 1) that required to delineate procedures and 2) that used for traceability or for stating what has actually occurred, specific to a particular run or final part.

Often, the qualification testing is performed in a pre-production environment. However, scale-up traditionally has had the greatest impact on cost, schedule, or technical parameters in production. For this reason, it is essential to plan batches, processing runs, and part trials which represent processing boundaries in the overall definition and demonstration of production capability. Results must be systematically documented because these will become part of the history file for this process.



When there is a change in production rate/usage, shop characteristics become important and sometimes require change. These aspects need to be understood and stabilized as early as possible. Capital equipment needs and calibration/certification, personnel training, and process flow are some of the typical elements which must be addressed.

The following paperwork must be put in place for production processing: procurement documents, specifications, process instructions (planning including work orders, travelers and the like), quality techniques, etc.

A thorough production readiness review should assess the capability/readiness of the raw material supplier, prepreg supplier, resin supplier, weaver, preformer, and part fabricator (including all subcontractors). Qualify only those materials/processes that are production ready or have a clear path to production.

Readiness should be evaluated at the lowest practical level. Any changes during or after the qualification will have an impact which needs to be checked against the protocol.

If several processors will be utilized, be sure to evaluate each with production-like conditions at this time.

ISO 9000 methodologies should be used throughout the qualification process. It is important to establish a product dependability program. ISO 9000-4 explains what a product dependability program is and how it should be managed. The effort begins by defining a policy, which explains what is meant by product dependability and specifies dependability characteristics. Product dependability requirements are defined by researching customer needs. Resources and organizational functions are defined, tools put in

place, needed documents are defined, an information tracking system is put in place, and review procedures are established. A program dependability plan is implemented which includes requirements, activities, practices and resources. Included in this effort are procedures to analyze, predict and review the dependability of the products and also the purchased materials. Estimates of life cycle costs and cost savings are important. A product improvement plan should be established, and a feedback system from the customer must be in place. Once this is accomplished, then requirements can be established for purchased materials, equipment and facilities, procedures and processes, and quality, all of which will enable meeting the product dependability requirements.

REFERENCES

- 3.2.1(a) MIL-STD-414, *Sampling Procedures and Tables for Inspection by Variables for Percent Defective*, Change Notice 1, 8 May 1968.
- 3.2.1(b) Federal Aviation Regulation Part 21 "Certification Procedures for Products and Parts".

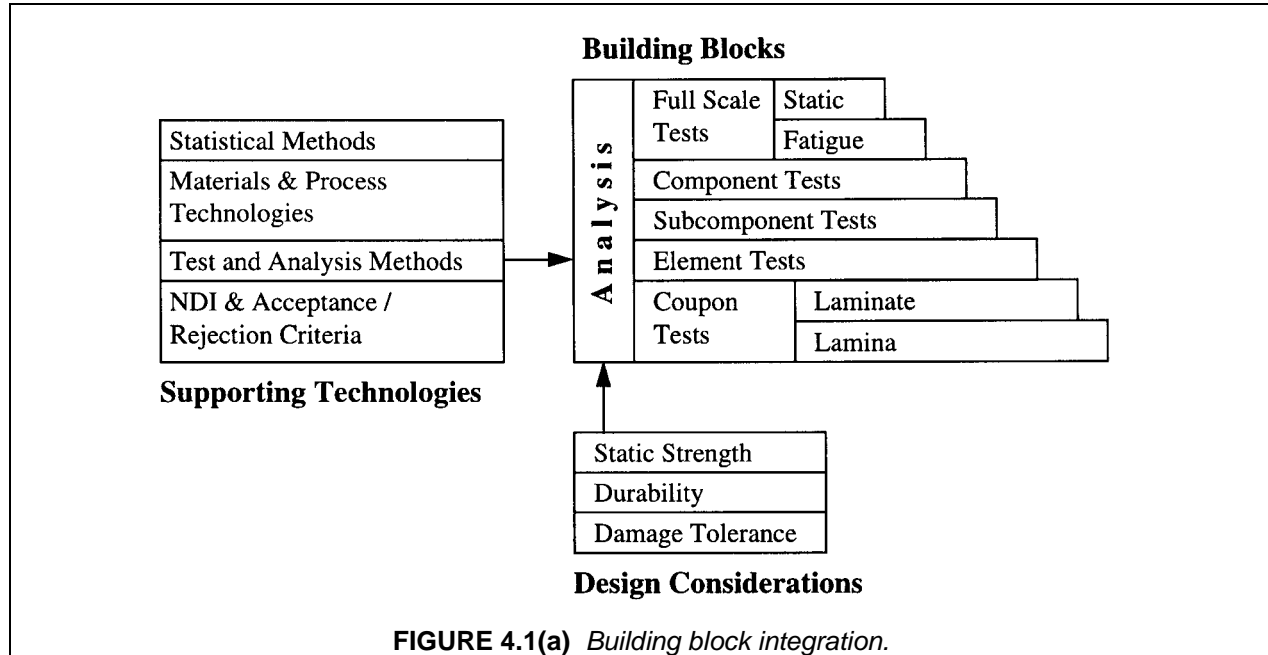
This page intentionally left blank

CHAPTER 4 BUILDING BLOCK APPROACH FOR COMPOSITE STRUCTURES

4.1 INTRODUCTION AND PHILOSOPHY

When composites are to be used in structural components, a design development program is generally initiated during which the performance of the structure is assessed prior to use. This process of substantiating the structural performance and durability of composite components generally consists of a complex mix of testing and analysis. Testing alone can be prohibitively expensive because of the number of specimens needed to verify every geometry, loading, environment, and failure mode. Analysis techniques alone are usually not sophisticated enough to adequately predict results under every set of conditions. By combining testing and analysis, analytical predictions are verified by test, test plans are guided by analysis, and the cost of the overall effort is reduced while reliability is increased.

An extension of this synergistic analysis/test approach is to conduct analysis and associated tests at various levels of structural complexity, often beginning with small specimens and progressing through structural elements and details, sub-components, components, and finally the complete full scale product. Each level builds on knowledge gained at previous, less complex levels. This substantiation process, using both testing and analysis in a program of increasingly complex levels, has become known as the "Building Block" approach. The building blocks are integrated with supporting technologies and design considerations as depicted in Figure 4.1(a). One major purpose of employing this approach is to reduce program cost and risk while meeting all technical, regulatory, and customer requirements. The philosophy is to make the design development process more effective in assessing technology risks early in a program schedule. Cost efficiency is achieved by designing a program in which greater numbers of less expensive small specimens are tested and fewer of the more expensive component and full scale articles are required. Using analyses in place of tests where possible also tends to reduce cost.



Although the concept of the Building Block approach is widely acknowledged in the composites industry, it is applied with varying degrees of rigor, and details are far from universal. In its simplest form, it represents a method of risk mitigation (both technical and financial) in that testing at the various levels reduces the probability that significant surprises will materialize near the end of a program. In a more

elaborate implementation it can be a highly structured and carefully planned effort which addresses many factors in detail, and which may attempt to quantify statistical reliability associated with the process.

Regardless of the details of a specific Building Block program, each level or block takes the general form idealized in Figure 4.1(b) (except for the lowest level). Knowledge gained from analyses and tests in a previous level is combined with structural requirements and used to define and perform the next level of design and analysis. If an acceptable analytical result is not obtained, a structural redesign and/or analysis modification is made until the result is favorable. Once an acceptable analytical result is achieved, it is verified by test. If the test results do not meet the expectations predicted by analysis, the test may be re-designed if an erroneous mode was detected, or the design and/or analytic method may be modified. Additionally, tests or analyses in a previous level may be repeated for verification. The appropriate actions are taken until test results verify an acceptable analytical prediction. When this has been accomplished, the program has advanced to the next level of complexity. It is important to recognize that, since different programs have varying needs, requirements, and constraints, not all building block approaches use the same number of complexity levels or define these levels in the same way.

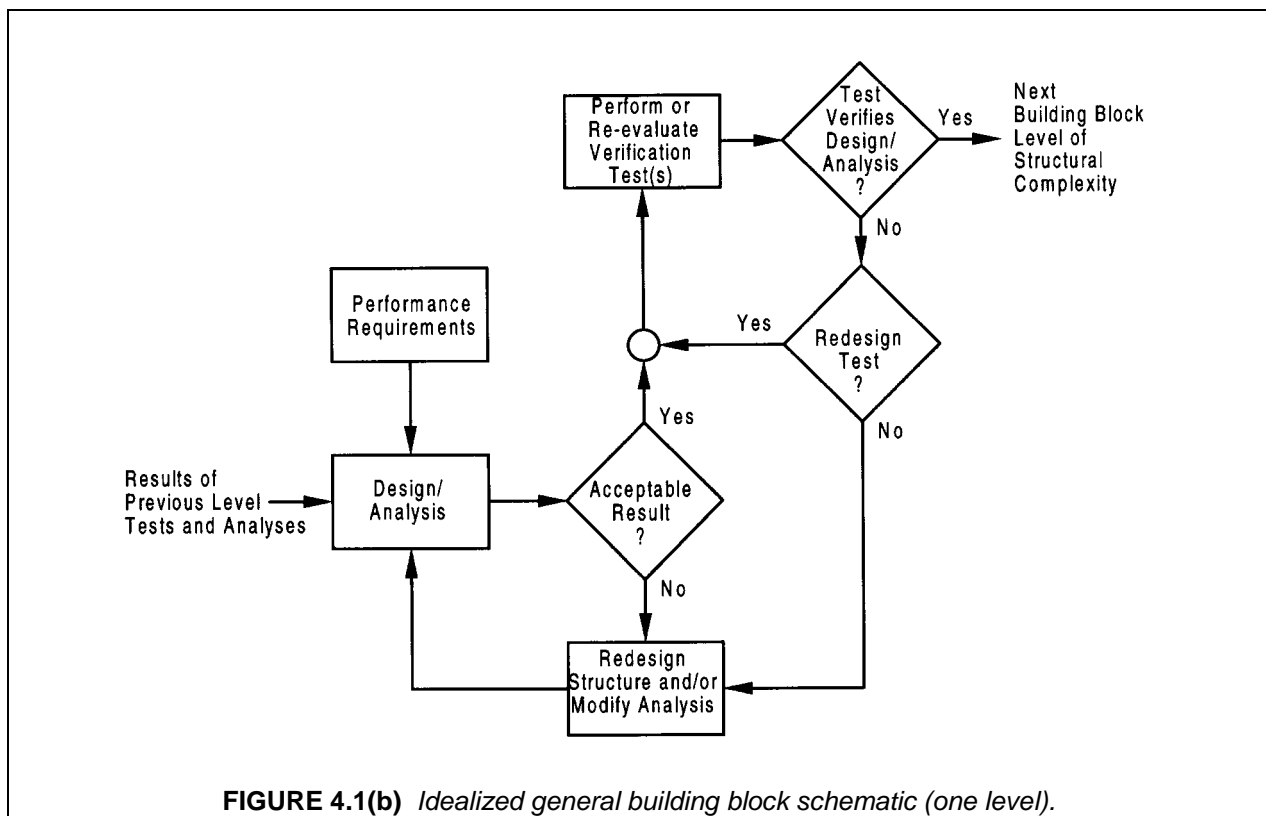
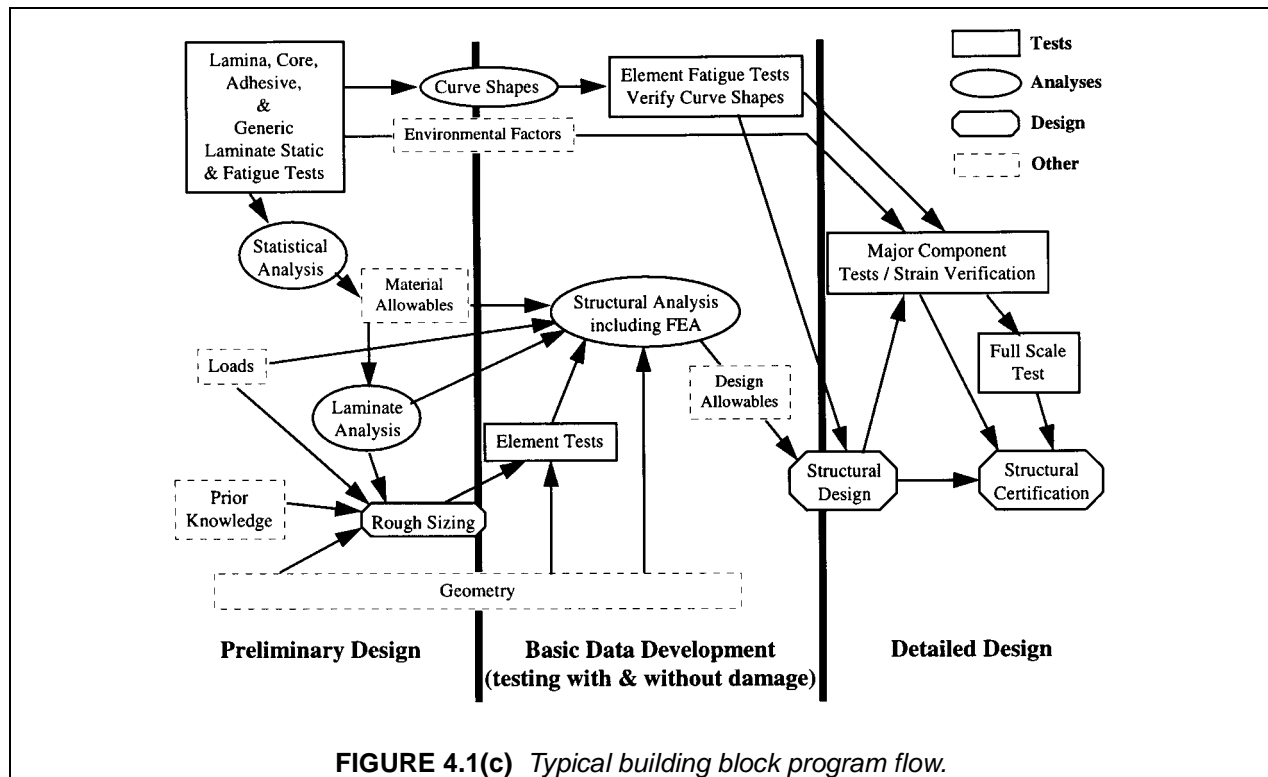


FIGURE 4.1(b) Idealized general building block schematic (one level).

Figures 4.1(a) and 4.1(b) and related discussions convey the idea that the Building Block process is a series of steps that progress neatly in order from one block to the next. While this is a convenient way to idealize the Building Block concept, the process is not quite so linear in practice. In reality, program schedules and availability of resources may be such that portions of various blocks overlap in time, and may even occur in parallel. Figure 4.1(c) shows one example of a typical Building Block program flow. The discussion of Building Block levels that follows relates to the idealized model for simplicity.

At the lowest Building Block level, small specimen and element tests are most widely used to characterize basic unnotched static material properties, generic notch sensitivity, environmental factors, material operational limit (MOL – see Volume 1, Chapter 2, Section 2.2.8), and laminate fatigue response. In the case of this first level, testing is used for starting the Building Block process by providing data for first it-

eration design and analysis. Analysis at this level generally consists of developing material scatter factors and material allowables, evaluation of specimen failure modes, and preliminary laminate analysis. At the same time, external loads for the structure are being defined and initial sizing is being performed.



Analysis in the second level uses the basic information obtained at the first level to calculate internal loads, identify critical areas, and predict critical failure modes. More complex element and sub-component tests are designed to isolate single failure modes and verify analysis predictions. At subsequent levels, even more complex static and fatigue loadings are analyzed and verified, with particular attention directed toward assessing out-of-plane loads and identifying unanticipated failure modes. Variabilities introduced by scale-up and response of the structure as a whole are also addressed. The final Building Block level involves full scale static and fatigue testing (as required). This testing validates predicted internal loads, deflections, and failure modes of the entire structure. It also serves to verify that no significant unpredicted secondary loads have appeared.

During the entire Building Block process, manufacturing quality is continually monitored to assure that properties developed early in the program remain valid. One aspect of this activity might include process cycle surveys to verify that larger components experience process histories similar to those of smaller elements and specimens. Also, non-destructive inspections, such as ultrasonic testing, are generally used to assess laminate quality with respect to porosity and voids. Destructive tests might also be used to verify fiber volumes, fiber alignment, and the like.

As noted earlier, the details of applying the Building Block approach are not standardized. While relationships between numbers of specimens and material basis values are well defined for specimen tests at the lowest level (see Volume 1, Chapter 2, Section 2.2.5), the numbers of specimens used at higher levels of complexity are somewhat arbitrary and largely based on historical experience, structural criticality, engineering judgment, and economics. Thus, there is currently no standardized methodology for statistically validating each level of the process, though some attempts have been made to develop models that relate specimen quantities to overall reliability (Reference 4.1). Also, there is no universal approach to

the types of analyses or tests, as these may be highly dependent upon particular design details, loadings, and structural criticality.

While it is certainly desirable to standardize the Building Block approach and to develop methods for assigning statistical reliability to the process, these goals are viewed as fairly long term, given the current body of work and diversity of individual approaches. The purpose of this chapter is to summarize the most prevalent and widely accepted methodology, and to present examples of Building Block programs for various applications and material forms.

This section has presented an introduction to the concept of a building block approach. The rationale and assumptions required in developing a building block approach are described in Section 4.2. The general methodology of such an approach is described in Section 4.3. An example describing the use of the building block approach for EMD and production aircraft, processed using autoclave cure of prepreg, is presented in detail in Section 4.4. Section 4.5 includes the use of the building block approach for other applications with general descriptions and references to the more detailed example. The implications of using other types of processing and material forms are discussed in the final section.

4.2 RATIONALE AND ASSUMPTIONS

The Building Block approach has been used in aircraft structures development programs long before the application of composites. However, this approach is more crucial for the certification of composite structures because of issues such as sensitivity to out-of-plane loads, their multiplicity of potential failure modes, and their sensitivity to operating environment. The combination of these issues and an inherent defect sensitivity of the composites, which are best classified as quasi-brittle, has resulted in a lack of analytical tools to predict the behavior of full-scale structure from the lowest level material properties.

The multiplicity of potential failure modes is perhaps the main reason that the Building Block approach is essential in the development of composite structural substantiation. The many failure modes in composite structures are mainly due to the defect, environmental and out-of-plane sensitivities of the materials.

The low interlaminar strength of composites makes them sensitive to out-of-plane loads. Out-of-plane loads can arise directly or be induced from in-plane loads. The most difficult loads to design and analyze for are those loads which arise insidiously in full-scale built-up structures. Analysis tools currently available for structural engineers often assume these loads as secondary loads and they are usually simulated with lower degrees of accuracy. Therefore, it is very important to simulate all potential out-of-plane failure modes and obtain experimental data through a well planned Building Block testing program.

Simulation of the correct failure modes plays an important role in a Building Block testing program. Since failure modes are frequently dependent on the test environment and defects present (manufacturing, bad design detail, or accidental damage), it is important to carefully select the correct test specimens that will simulate the desired failure modes. Special attention should be given to matrix sensitive failure modes. Following selection of the critical failure modes, a series of specimens is designed, each one to simulate a single failure mode. These specimens will generally be lower complexity specimens.

Ideally, if structural analysis tools are fully developed and the failure criteria fully established, the structural behavior would be predictable from the constituent properties. Unfortunately, the capability of the state-of-the-art analysis methods are limited. Thus, lower level test data can not always be used to accurately predict the behavior of structural elements and components with higher levels of complexity. The accuracy of the analytical results are further complicated by the material property variability, the inclusion of defects, and the structural scale-up effects. Therefore, step-by-step building block testings are required to:

- 1 Uncover failure modes which do not occur at a lower level tests.

- 2 Verify or modify analysis methods which has been already verified at a lower level.
- 3 Allow inclusion of the defects in configured structure, which often do not take the same form in specimens and elements (e.g., accidental damage caused by impact).

This approach is based on the assumption that the structural/material response to applied load in test specimens with lower levels of complexity is directly transferable to specimens at higher levels of complexity. For example, fiber strength at the specimen level is the same as the fiber strength in the component. It is also implied that their variability is transferable upward. Thus, a statistical knockdown determined from coupon tests (allowables) provides the same level of confidence at the structural component level.

In a successful Building Block testing program, therefore, specimens can be designed so that failure modes at the lower level of structural complexity would be eliminated at the more complex specimens, by using verified design/analysis methods. Thus, the new failure modes at the next higher level of structural complexity can be isolated. The results of the more complex tests would be used to further modify/verify the analysis methods. Finally, an adequate analysis of methodology is verified and final design can be achieved.

4.3 METHODOLOGY

In Section 4.1, Introduction and Philosophy, the Building Block Approach is introduced and the philosophical framework behind it are discussed, whereas, the Rationale and Assumptions in Section 4.2 provide a logical framework to guide the use of this approach while providing the key assumptions used. However, the Methodology used in performing a building block composite structure development program can spell success or failure in the effort. This section will discuss such Methodology, providing guidelines for its selection and use. The following discussion will present and discuss the methodology used in "building block composite structures development" for various vehicle applications. While there are some differences in methodology among these vehicle types, much of it is similar.

4.3.1 General approach

The methodology used is shown in a generally logical, chronological order, but, during an actual vehicle "building block composite structure development" program, the start and completion of the methodology stages may overlap or not be in the order discussed herein. In such development programs in the real world, preliminary design/analysis of parts and elements and subcomponents may be accomplished using preliminary or estimated allowables. Element and/or subcomponent testing may be started or completed before "design-to" allowables are available. But, "design-to" allowables should be completed before full-scale component testing starts.

The first step is to plan and initiate a suitable composite materials design allowables specimen test program on each composite material to be used. The number of material lots and the number of replicates required per type and environment will depend on whether the vehicle being developed is a prototype, intermediate development (EMD), or production. In addition, the vehicle's structure criticality within its vehicle category (for instance, Aircraft, Spacecraft, Helicopter, Ground Vehicle, etc.) will affect the number of material lots and specimen replicates per test type and environment.

The materials receiving inspection and acceptance requirements and the Materials & Processes specification requirements will be a function of the structure criticality of the various parts of the selected vehicle. The number and kind of physical, mechanical, thermal, chemical, electrical and process properties tests on the composite material will be a function of this structure criticality.

The amount and level of quality assurance required on the test elements and subcomponents, as well as on the actual parts for the vehicle, is a function of the structure criticality of those parts and defect con-

siderations for structural substantiation and maintenance. In addition the type of tests selected, the number of replicates, and instrumentation needed is a function of the part's structure criticality.

Customer requirements and costs as well as safety and durability concerns may dictate the full scale testing requirements in addition to analytical prediction verification. Such full-scale testing could be proof loading to critical design limit load at RTD conditions, proof loading at various environmental conditions, static test to Design Limit Load (DLL) and Design Ultimate Load (DUL) at RT with or without load enhancement factors to simulate elevated temperatures, and of course static loading to failure, in some cases. In addition, damage tolerance testing is often required to ensure safety for flight critical structure. Durability (fatigue) testing is sometimes required in severe environments and may be required to prove-out long term acceptable economic lifetimes.

The individual methodologies discussed above are, in many cases, available within the companies doing the development work, or, are readily available at a specialty subcontractor. It is usually a matter of organizing such methodologies in a rational manner to achieve an acceptable vehicle composite structure building block development program. Such methodologies are defined and organized in more detail in the individual vehicle type subsections listed below.

4.4 CONSIDERATIONS FOR SPECIFIC APPLICATIONS

4.4.1 Aircraft for prototypes

A detailed description of the allowables and building block test effort needed for acceptable risk and cost effective DOD/NASA prototype composite aircraft structure is presented in the following sections. Section 4.4.1.1 presents the PMC composite allowables generation for DOD/NASA prototype aircraft structure. In Section 4.4.1.2, the PMC composites building block structural development for DOD/NASA prototype aircraft is detailed. And, finally, a summary of allowables and building block test efforts for DOD/NASA prototype composite aircraft structure is given in Section 4.4.1.3.

4.4.1.1 *PMC composite allowables generation for DOD/NASA prototype aircraft structure*

Allowables generation is needed to support the building block test program depicted in Figure 4.4.1.1, Part A consists of five steps:

1. Experimentally generate ply level static strength and stiffness properties including the testing of 0° or 1-axis tension and compression, 90° or 2-axis tension and compression and 0° or 12-axis in-plane shear specimens with stress/strain curves utilizing, to the extent possible, ASTM D 3039, D 3410, and D 3518.
2. Experimentally generate quasi-isotropic laminate level, static strength and stiffness properties including the testing of x-axis plain and open hole tension, compression, and in-plane shear specimens and tension and compression loaded double shear bearing specimens per ASTM D 3039 for tension and compression and bearing specimens per other standards, respectively, that are currently under development in the ASTM D-30 Committee.
3. The test data generated will be reduced, statistically, to obtain allowable type values using the B-basis value (90% probability, 95% confidence) approach or the 85% of mean value approach if the test scatter is too high. The higher of the two values should be used. This approach was first presented by Grimes in Reference 4.4.1.1.
4. Develop input ply allowables for use in analytical methods that are used in design/analysis. In general the lower of the ultimate or 1.5 x yield strength reduced value should be used for tension, compression, and in-plane shear strength critical allowables. When in-plane shear strength is not critical the reduced ultimate shear strength (a high value) should be used.

5. Laminate design should be fiber-dominated by definition, i.e., a minimum of 10% of the plies should be in each of the 0° , $+45^\circ$, -45° , and 90° directions. For tape and fabric laminates, always input the 0° or 1-axis strength allowable values in both the 1- and 2-axis slots in the analytical methods for tensile and compressive loads. Shear inputs will be as described above. This approach will ensure fiber dominated failure and was first presented by Grimes in Reference 4.4.1.1. All laminates should be balanced and symmetric.

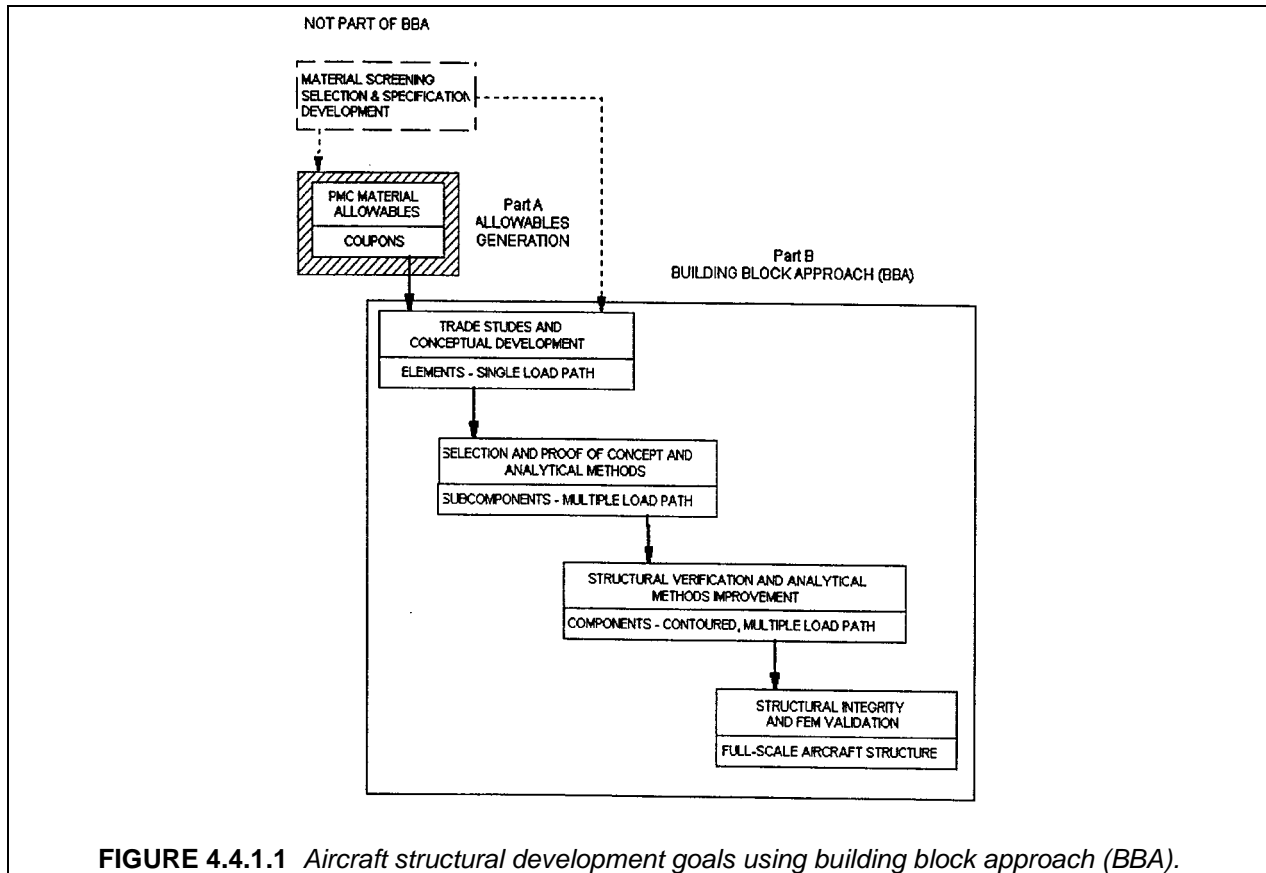


FIGURE 4.4.1.1 Aircraft structural development goals using building block approach (BBA).

A structure classification/allowables chart which defines the relationship between aircraft structure criticality and the allowables requirements for prototypes is presented in Table 4.4.1.1(a). In Table 4.4.1.1(b) structural classification vs. physical defect maximum requirements are given so that the acceptable physical defect size parameter varies indirectly with the aircraft structure criticality. Thus, aircraft structure criticality controls the reliability of the data (allowables) and the material and parts quality that are necessary to support it.

TABLE 4.4.1.1(a) *DOD/NASA aircraft structure classification vs. PMC allowables data requirements for prototypes (Reference 4.4.1.1).***PART A**
(From Figure 4.4.1.1)

Aircraft Structure Classification		Allowable Data Requirements for Prototype Design	
Classification	Description	Preliminary (Tape/Fabric)	Final (Tape/Fabric)
<u>PRIMARY</u>	CARRIES PRIMARY AIR LOADS	Based on	
<ul style="list-style-type: none"> Fracture critical (F/C) 	<ul style="list-style-type: none"> Failure will cause loss of vehicle 	1. Estimates using data on similar materials and experience	1 - lot materials testing: 5 to 8 replicates per test type (static)
<ul style="list-style-type: none"> Noncritical (N/C) 	<ul style="list-style-type: none"> Failure will <u>not</u> cause loss of vehicle 	2. Vendor Data 3. Journals, magazines and books	1 - lot materials testing: 4 to 6 replicates per test type (static)
<u>SECONDARY</u>	CARRIES SECONDARY AIR & OTHER LOADS	Based on	
<ul style="list-style-type: none"> Fatigue critical (FA/C) & economic life critical (EL/C) 	<ul style="list-style-type: none"> Failure will <u>not</u> cause loss of vehicle but may cause cost critical parts replacements 	1. Estimates using data on same or similar materials	1 - lot materials testing: 3 to 4 replicates per test type (static) plus fatigue testing
<ul style="list-style-type: none"> Noncritical (N/C) 	<ul style="list-style-type: none"> Failure will <u>not</u> cause loss of vehicle No cost or fatigue critical parts 	2. Vendor data 3. Journals, magazines and books	Use legitimate, verified data bases
<u>NONSTRUCTURAL</u>	NON- OR MINOR LOAD BEARING	Based on	
<ul style="list-style-type: none"> Noncritical (N/C) 	<ul style="list-style-type: none"> Failure replacement of parts causing minor inconvenience, not cost critical 	1. Estimates using data on similar materials, or 2. Vendor data, or 3. Journals, magazines and books	Estimates using data on similar materials, or Vendor data, or Journals, magazines and books

TABLE 4.4.1.1(b) *DOD/NASA aircraft structure classification vs. PMC physical defect minimum requirements for prototypes (Reference 4.4.1.1).***PART A AND B**
(From Figure 4.4.1.1)

Aircraft Structure		Physical Defect Maximum Requirements for Parts: Carbon or Glass Reinforced PMC Example	
Classification	Description	Tape	Fabric
<u>PRIMARY</u> <ul style="list-style-type: none"> Fracture critical (F/C) Noncritical (N/C) 	CARRIES PRIMARY AIR LOADS <ul style="list-style-type: none"> Failure will cause loss of vehicle 	$\leq 3\%$ porosity over $\leq 10\%$ of area. Delaminations over $\leq 1\%$ of area. No edge delaminations allowed (including holes).	$\leq 5\%$ porosity over $\leq 10\%$ of area. Delaminations over $\leq 1\%$ of area. No edge delaminations allowed (including holes).
	<ul style="list-style-type: none"> Failure will <u>not</u> cause loss of vehicle 		
<u>SECONDARY</u> <ul style="list-style-type: none"> Fatigue critical (FA/C) & economic life critical (EL/C) Noncritical (N/C) 	CARRIES SECONDARY AIR & OTHER LOADS <ul style="list-style-type: none"> Failure will <u>not</u> cause loss of vehicle but may cause cost critical parts replacements 	$\leq 3\%$ porosity over $\leq 15\%$ of area. Delaminations over $\leq 2\%$ of area. No edge delaminations allowed (including holes).	$\leq 5\%$ porosity over $\leq 15\%$ of area. Delaminations over $\leq 2\%$ of area. No edge delaminations allowed (including holes).
	<ul style="list-style-type: none"> Failure will <u>not</u> cause loss of vehicle No cost or fatigue critical parts 		
<u>NONSTRUCTURAL</u> <ul style="list-style-type: none"> Noncritical (N/C) 	NON- OR MINOR LOAD BEARING <ul style="list-style-type: none"> Failure replacement of parts causing minor inconvenience, not cost critical 	$\leq 4\%$ porosity over $\leq 20\%$ of area. Delaminations over $\leq 3\%$ of area. Repaired edge delaminations $\leq 10\%$ of edge length or hole circumference are allowed.	$\leq 4\%$ porosity over $\leq 20\%$ of area. Delaminations over $\leq 3\%$ of area. Repaired edge delaminations $\leq 10\%$ of edge length or hole circumference are allowed.

4.4.1.2 PMC composites building block structural development for DOD/NASA prototype aircraft

Part B of the flowchart in Figure 4.4.1.1 defines the building block test effort in the general categories of:

1. Trade studies and concept development (element-single load path),
2. Selection, proof of concept, and analytical methods verification (sub-component-multiple load paths),
3. Structural verification and analytical methods improvement (contoured composite-multiple load path), and
4. Structural integrity and FEM validation (full-scale aircraft structure testing).

The allowables shown in Figure 4.4.1.1 Part A and in Table 4.4.1.1 (a) logically flow into Part B, building block testing. Table 4.4.1.1(b) on physical defect requirements applies to both Parts A and B. The Part B building block test effort is delineated in Table 4.4.1.2(a) in accordance with the part's structural classification. The four categories, above, are defined in detail for each structural classification, with the higher the structural classification, the more testing and analysis required. The key point here is that these are guidelines for structural development testing. The actual structural testing needed for a specific classification of structure could be more or less, depending on the vehicle's mission and whether it is manned or unmanned. Knowing the structural part classification, the aircraft's purpose and mission, risk analysis can be applied to minimize testing cost and risk. FEM and closed form composite analysis methods utilizing proper mechanical and physical properties and allowables input data will be necessary every step of the way. Failure modes and loads (stresses) as well as strain and deflection readings must be monitored and correlated with predictions to assure low risk. The use of FEM or other analysis methods alone (without testing) or with inadequate testing that does not properly interrogate failure modes, stresses (strains), and deflections for comparison with predictions can create high risk situations that should not be tolerated.

Another risk issue for composite structure is quality assurance (QA), a subject that applies to both Parts A and B. Table 4.4.1.2(b) presents the nominal QA requirements for the categories of

1. Material and process selection, screening, and material specification qualification,
2. Receiving inspection/acceptance testing,
3. In-process inspection,
4. Non-destructive inspection (NDI),
5. Destructive testing (DT), and
6. Traceability

The QA requirements in each of these categories vary with the structural classification, with the higher the classification, the more quality assurance required. By following the procedure outlined in this table, the amount of QA necessary to keep risk at an acceptable level can be ascertained. Again the amount of QA needed and the risk taken will be a function of the aircraft type and mission and whether it is manned or unmanned. Risk and cost are inversely proportional to each other for composite structural parts in each classification, so the determination of acceptable risk is necessary to this building block test program for prototypes.

TABLE 4.4.1.2(a) DOD/NASA aircraft structure classification and goals vs. PMC building block development tests for prototypes
(Reference 4.4.1.1) (continued on next page).

PART B (From Figure 4.4.1.1)

Aircraft Structure		Building Block Structural Development Test Effort	
Aircraft Structure Development Goals		Trade Studies and Conceptual Development Analysis	Selection and Proof of Concept Testing and Analytical Methods Development
Classification	Description	Element - Single Load Path	Sub-Component - Multiple Load Paths (Including Joints)
<u>PRIMARY</u>	CARRIES PRIMARY AIR LOADS	Concept and analytical methods development - static and fatigue test (optional)	Proof of concept and analytical methods - static and fatigue test (residual strength)
<ul style="list-style-type: none"> Fracture critical (F/C) 	<ul style="list-style-type: none"> Failure will cause loss of vehicle 	3 - each stiffening configuration 3 - each joint configuration	1 box beam/cylinder: static ultimate 1 box beam cylinder: fatigue and residual strength
<ul style="list-style-type: none"> Noncritical (N/C) 	<ul style="list-style-type: none"> Failure will <u>not</u> cause loss of vehicle 	1 - each stiffening configuration 1 - each joint configuration	1 box beam/cylinder: static ultimate
<u>SECONDARY</u>	CARRIES SECONDARY AIR & OTHER LOADS	Concept and analytical methods development - static and fatigue test	Proof of concept and analytical methods - static (DLL/fatigue/residual strength test)
<ul style="list-style-type: none"> Fatigue critical (FA/C) & economic life critical (EL/C) 	<ul style="list-style-type: none"> Failure will <u>not</u> cause loss of vehicle but may cause cost critical parts replacements 	2 - each stiffening configuration 2 - each joint configuration	2 box beam/cylinder: static (DLL/fatigue/residual strength test)
<ul style="list-style-type: none"> Noncritical (N/C) 	<ul style="list-style-type: none"> Failure will <u>not</u> cause loss of vehicle No cost or fatigue critical parts 	1 - each stiffening configuration 1 - each joint configuration	No testing required - proved by element tests
<u>NONSTRUCTURAL</u>	NON- OR MINOR LOAD BEARING	Concept development/static test/analytical methods check	Proof of concept: element testing plus analysis
<ul style="list-style-type: none"> Noncritical (N/C) 	<ul style="list-style-type: none"> Failure/replacement of parts causing minor inconvenience, not cost critical 	1 - each most critical configuration	No testing required - proved by element tests and analysis

TABLE 4.4.1.2(a) *DOD/NASA aircraft structure classification and goals vs. PMC building block development tests for prototypes (Reference 4.4.1.1) (concluded).***PART B**

Aircraft Structure		Building Block Structural Development Test Effort	
Aircraft Structure Development Goals		Structural Verification Testing for Analytical Methods	Structural Integrity testing for FEM Validation
Classification	Description	Component with True Contours - Multiple Load Paths	Full Scale Aircraft Structure: Simulated Air Loads & Load Paths
<u>PRIMARY</u>	CARRIES PRIMARY AIR LOADS	Structural verification: static and durability and damage tolerance tests	Structural integrity validation - static strain survey & proof test; static test to DUL/failure or fatigue test depending on budget and schedule requirements
• Fracture critical (F/C)	• Failure will cause loss of vehicle	1 large structural section: static damage tolerance to DUL/failure 1 large structural section: damage tolerance and durability plus residual strength	1 proof test - critical flight load condition: strain/deflection survey and fatigue and residual strength to DLL, to DUL and failure if required
• Noncritical (N/C)	• Failure will <u>not</u> cause loss of vehicle	1 large structural section: static and durability critical damage tolerance to DLL, then take to DUL/failure for residual strength test	1 proof test - critical flight load condition: strain/deflection survey and static test to DLL, durability testing and static residual strength to DUL and failure if required
<u>SECONDARY</u>	CARRIES SECONDARY AIR & OTHER LOADS	Structural verification and analytical methods improvement: static and durability and damage tolerance tests (DUL/failure)	Structural integrity validation - static strain survey & proof test; static test to DUL and failure if required
• Fatigue critical (FA/C) & economic life critical (EL/C)	• Failure will <u>not</u> cause loss of vehicle but may cause cost critical parts replacements	1 large structural section: static damage tolerance to DUL/failure	1 proof test: - critical flight load condition: strain/deflection survey and static test to DLL, to DUL if required
• Noncritical (N/C)	• Failure will <u>not</u> cause loss of vehicle • No cost or fatigue critical parts	No testing required - proved by element tests and analysis	No testing required – proved by element tests
<u>NONSTRUCTURAL</u>	NON- OR MINOR LOAD BEARING	Structural verification by proof test/analysis	Structural integrity validation by previous tests and analysis

TABLE 4.4.1.2(b) DOD/NASA aircraft structure classification vs. PMC quality assurance requirements for prototypes
(Reference 4.4.1.1) (continued on next page).

PART A and B

Aircraft Structure		Quality Assurance Requirements		
Classification	Description	M&P Selection, Screening, and Qualification	Receiving Inspection/Acceptance Testing*	In-Process Inspection
<u>PRIMARY</u>	CARRIES PRIMARY AIR LOADS	Preliminary physical, mechanical, & process variable evaluation & 1-sheet specification development; record evaluate, select & store test data	Per preliminary 1-sheet M&P specifications - minimum physical, mechanical, & process property requirements - test for acceptability; engineering accept/reject decision; store test data	Per preliminary 1-sheet process specification & drawing - inspect/record for conformance & use engineering judgment for accept/reject decision; store test data
	<ul style="list-style-type: none"> Fracture critical (F/C) Noncritical (N/C) 			
<u>SECONDARY</u>	CARRIES SECONDARY AIR & OTHER LOADS	Preliminary, but limited, physical, mechanical, & process variable evaluation & 1-sheet specification development; record, evaluate, select & store test data	Per preliminary, but limited, 1-sheet M&P specifications - minimum physical, mechanical, & process property requirements - minimal tests for acceptability; engineering accept/reject decision; store test data	Per preliminary, but limited, 1-sheet process specification & drawing - inspect/record for conformance and use engineering judgment for accept/reject decision; store test data
	<ul style="list-style-type: none"> Fatigue critical (FA/C) & economic life critical (EL/C) Noncritical (N/C) 			
<u>NONSTRUCTURAL</u>	NON- OR MINOR LOAD BEARING	Limited physical property tests; use vendor recommended process; store data	Vendor certification	Worker self-inspection per vendor process
	<ul style="list-style-type: none"> Noncritical (N/C) 			

* May be done at material vendors plant to 1-sheet specification after M&P approval.

TABLE 4.4.1.2(b) DOD/NASA aircraft structure classification vs. PMC quality assurance requirements for prototypes (Reference 4.4.1.1) (concluded).**PART A and B**

Aircraft Structure		Quality Assurance Requirements		
Classification	Description	Non-Destructive Inspection (NDI)	Destructive Testing (DI)	Traceability
<u>PRIMARY</u> <ul style="list-style-type: none"> Fracture critical (F/C) Noncritical (N/C) 	CARRIES PRIMARY AIR LOADS <ul style="list-style-type: none"> Failure will cause loss of vehicle Failure will <u>not</u> cause loss of vehicle 	100% area; engineering accept/reject decision based on defect standard (defect panel or lead tape); store data	Preliminary physical and mechanical property testing on non-integral process control panel; engineering accept/reject decision; store test data	Keep files on all receiving, in-process, & non-destructive inspection & destructive test records for each vehicle
<u>SECONDARY</u> <ul style="list-style-type: none"> Fatigue critical (FA/C) & economic life critical (EL/C) Noncritical (N/C) 	CARRIES SECONDARY AIR & OTHER LOADS <ul style="list-style-type: none"> Failure will <u>not</u> cause loss of vehicle but may cause cost critical parts replacements Failure will <u>not</u> cause loss of vehicle No cost or fatigue critical parts 	90% area; engineering accept/reject decision based on defect standard (defect panel or lead tape); store data	Preliminary, but limited, physical and mechanical testing on non-integral process control panel; engineering accept/reject decision; store test data	Keep files on all receiving, in-process, & non-destructive inspection & destructive test records for each vehicle
<u>NONSTRUCTURAL</u> <ul style="list-style-type: none"> Noncritical (N/C) 	NON- OR MINOR LOAD BEARING <ul style="list-style-type: none"> Failure replacement of parts causing minor inconvenience, not cost critical 	None	None	None

4.4.1.3 Summary of allowables and building block test efforts for DOD/NASA prototype composite aircraft structure

In the above sections, composite material allowables development needed for prototype aircraft is detailed along with the related building block test effort required for such structure development. Both allowables requirements and building block structural test requirements are related to aircraft structure part criticality classifications and then each is related to the test/evaluation/analysis categories that need to be interrogated to study the risk involved. For allowables the categories are preliminary and final values and physical defect minimum requirements in each classification. For the building block structures development test effort categories, the procedure used is the progressive scale up of the size of the test parts along with going from single to multiple load paths and adding joints to the test structure as it gets bigger. And, finally, the relationship of the quality assurance requirements from those required for design allowables for flat panels to those required for major structural components to those required for full size structure are presented for the six QA needs categories for each structural classification of the parts to be built.

The Part A allowables effort will provide for acceptable risk and cost effective allowables for composite structure prototypes. The Part B building block structures test development effort will satisfy the goals of:

1. Appropriate conceptual development,
2. Proof of concept and analytical methods development,
3. Structural verification testing for analytical methods, and
4. Structural integrity testing and FEM validations.

Once these goals are achieved, the user will have acceptable risk, cost effective prototype composite aircraft structure that will have the necessary integrity and reliability needed for the specific aircraft being developed.

4.4.2 Aircraft for EMD and production

A detailed description of the allowables and building block test effort needed for acceptable risk and cost effective DOD/NASA engineering and manufacturing development (EMD) and production composite aircraft structure is presented in the following sections. Section 4.4.2.1 presents the PMC composite allowables generation for DOD/NASA EMD and production aircraft structure. In Section 4.4.2.2, the PMC composites building block structural development for DOD/NASA EMD production aircraft is detailed. And finally, a summary of allowables and building block test efforts for DOD/NASA EMD and production composite aircraft structure is given in Section 4.4.2.3.

4.4.2.1 PMC composite allowables generation for DOD/NASA EMD and production aircraft structure

Allowables generation is needed to support the building block test program depicted in Figure 4.4.2.1, Part A consists of five steps:

1. Experimentally generate ply level static strength and stiffness properties including the testing of 0° or 1-axis tension and compression, 90° or 2-axis tension and compression and $0^\circ/90^\circ$ or 12-axis edgewise shear specimens with stress/strain curves utilizing, to the extent possible, ASTM D 3039, D 3410, and D 3518.
2. Experimentally generate quasi-isotropic laminate level, static strength and stiffness properties including the testing of x-axis plain and open hole tension and compression specimens and tension loaded double shear bearing specimens per ASTM D 3039 for tension and compression and bearing specimens per other standards, respectively, that are currently under development in the ASTM D-30 Committee.

3. The test data generated will be reduced, statistically, to obtain allowable type values using the B-basis value (90% probability, 95% confidence) approach. For EMD prototypes use the guidelines in Section 4.4.1.1.
4. Develop input ply allowables for use in analytical methods that can be used in design/analysis. In general the lower of the ultimate or 1.5 x yield strength reduced values should be used for tension and compression. Edgewise shear strength ultimate values should be used for allowables when edgewise shear strength is not critical. The reduced (1.5 x yield) ultimate edgewise shear strength should be used when edgewise shear loads are critical.
5. Laminate design should be fiber-dominated by definition, i.e., a minimum of 10% of the plies should be in each of the 0° , $+45^\circ$, -45° , and 90° directions. For tape and fabric laminates, always input the 0° or 1-axis strength allowable values in both the 1- and 2-axis slots in the analytical methods for tensile and compressive loads. Shear inputs will be as described above. This approach was first presented by Grimes in Reference 4.4.1.1. All laminates should be balanced and symmetric.

A structure classification/allowables chart which defines the relationship between aircraft structure criticality and the allowables requirements for EMD and production is presented in Table 4.4.2.1(a). In Table 4.4.2.1(b) structural classification vs. physical defect maximum requirements are given so that the physical defect size parameter varies indirectly with the aircraft structure criticality. Thus, aircraft structure criticality controls the reliability of the data (allowables) and the material quality that are necessary to support it.

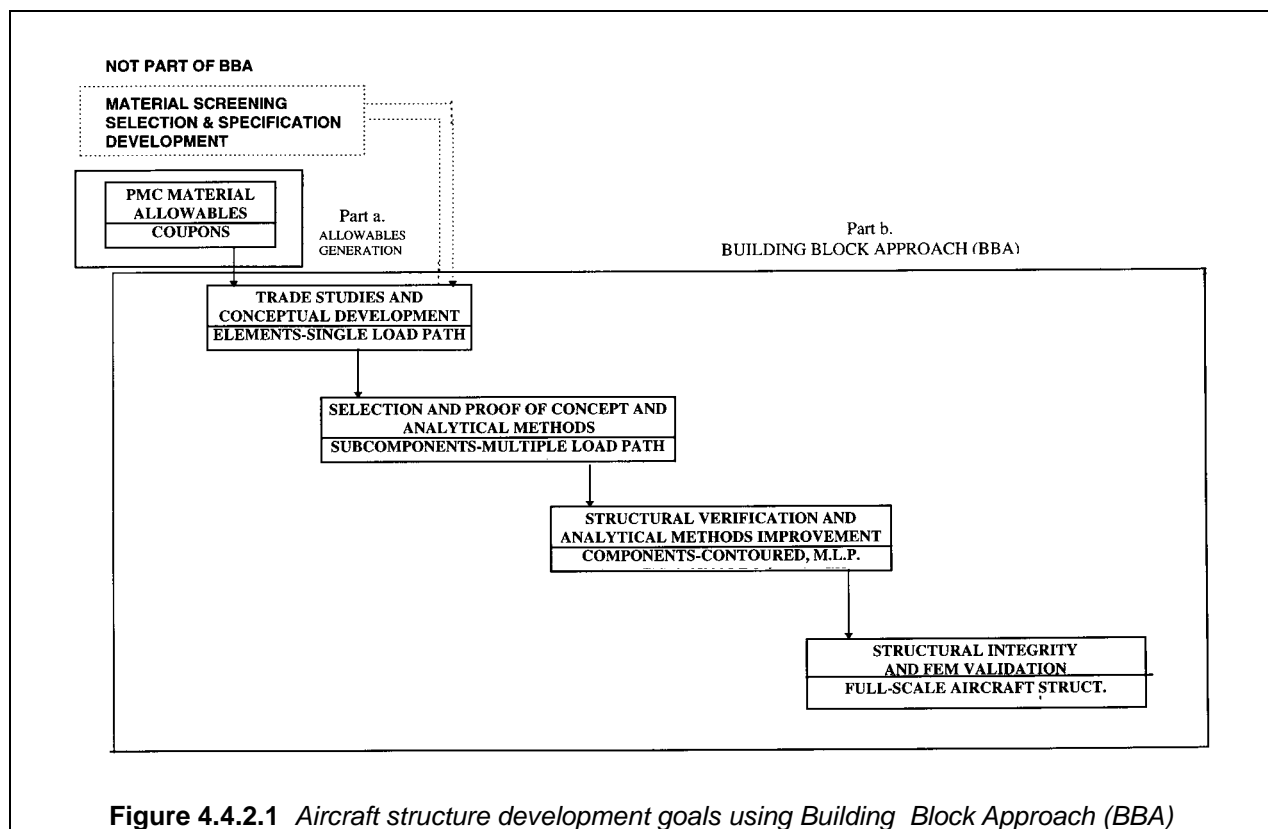


TABLE 4.4.2.1(a) DOD/NASA aircraft structure classification vs. PMC allowables data requirements for EMD* and production**PART A**
(Reference Figure 4.4.2.1)

Aircraft Structure Classification		Allowable Data Requirements for EMD and Production* Design	
Classification	Description	EMD* (Tape/Fabric)	Production (Tape/Fabric)
<u>PRIMARY</u>	CARRIES PRIMARY AIR LOADS	1-lot materials testing 8-replicates per test type	Based on: 5-lots of materials testing 8-replicates per test type
<ul style="list-style-type: none"> Fracture critical (F/C) 	<ul style="list-style-type: none"> Failure will cause loss of vehicle 		
<ul style="list-style-type: none"> Noncritical (N/C) 	<ul style="list-style-type: none"> Failure will not cause loss of vehicle, cost critical replacement or repair 	1-lot materials testing 6-replicates per test type	4-lots of materials testing 6-replicates per test type
<u>SECONDARY</u>	CARRIES SECONDARY AIR AND OTHER LOADS	1-lot materials testing 4-replicates per test type plus fatigue testing	3-lots of materials testing 5-replicates per test type plus fatigue testing
<ul style="list-style-type: none"> Fatigue critical (FA/C) and economic life critical (EL/C) 	<ul style="list-style-type: none"> Failure will not cause loss of vehicle, cost critical replacement or repair 		
<ul style="list-style-type: none"> Noncritical (N/C) 	<ul style="list-style-type: none"> Failure will not cause loss of vehicle Not cost or fatigue critical 	N/A	2-lots of materials testing 4-replicates per test type
<u>NONSTRUCTURAL</u>	NON- OR MINOR LOAD BEARING	Based on 1. Estimates using data on similar materials, or 2. Vendor data, or 3. Journals, magazines and books	1-lot of materials testing 3-replicates per test type
<ul style="list-style-type: none"> Noncritical (N/C) 	<ul style="list-style-type: none"> Failure/replacement minor inconvenience, not cost critical 		

*For EMD, use procedure given for prototypes in Section 4.4.1

TABLE 4.4.2.1(b) *DOD/NASA aircraft structure classification vs. PMC physical defect minimum requirements for EMD* and production*

PARTS A AND B
(Reference Figure 4.4.2.1)

Aircraft Structure		Physical Defect Maximum Requirements for Parts: Carbon or Glass Reinforced PMC Example	
Classification	Description	Tape	Fabric
<u>PRIMARY</u> <ul style="list-style-type: none"> Fracture critical (F/C) Noncritical (N/C) 	CARRIES PRIMARY AIR LOADS <ul style="list-style-type: none"> Failure will cause loss of vehicle Failure will not cause loss of vehicle, cost critical replacement or repair. 	$\leq 2\%$ porosity over $\leq 5\%$ of area. No delaminations allowed. No edge delaminations allowed (including holes).	$\leq 3\%$ porosity over $\leq 5\%$ of area. No delaminations allowed. No edge delaminations allowed (including holes).
<u>SECONDARY</u> <ul style="list-style-type: none"> Fatigue critical (FA/C) Noncritical (N/C) 	CARRIES SECONDARY AIR & OTHER LOADS <ul style="list-style-type: none"> Failure will not cause loss of vehicle, cost critical replacement Failure will not cause loss of vehicle Not cost or fatigue critical 	$\leq 2\%$ porosity over $\leq 10\%$ of area. No delaminations. No edge delaminations allowed (including holes).	$\leq 3\%$ porosity over $\leq 10\%$ of area. No delaminations. No edge delaminations allowed (including holes).
<u>NONSTRUCTURAL</u> <ul style="list-style-type: none"> Noncritical (N/C) 	NON- OR MINOR LOAD BEARING <ul style="list-style-type: none"> Failure/replacement minor inconvenience, not cost critical 	$\leq 3\%$ porosity over $\leq 10\%$ of area. Delaminations over $\leq 2\%$ of area. Repaired edge delaminations $\leq 4\%$ of edge length or hole circumference are allowed.	$\leq 4\%$ porosity over $\leq 15\%$ of area. Delaminations over $\leq 2\%$ of area. Repaired edge delaminations $\leq 4\%$ of edge length or hole circumference are allowed.

*For EMD, use procedure given for prototype in Section 4.4.1

4.4.2.2 *PMC composite building block structural development for DOD/NASA EMD and production aircraft*

Part B of the flowchart in Figure 4.4.2.1 defines the building block test effort in the general categories of:

1. Trade studies (element-single load path),
2. Selection, proof of concept, and analytical methods (sub-component-multiple load paths),
3. Structural verification and analytical methods improvement (contoured composite-multiple load path), and
4. Structural integrity and FEM validation (full-scale aircraft structure testing).

The allowables shown in Figure 4.4.2.1 Part A and in Table 4.4.2.1(a) logically flow into Part B, building block testing. Table 4.4.2.1(b) on physical defect requirements applies to both Parts A and B. The Part B building block test effort is delineated in Table 4.4.2.2(a) in accordance with the part's structural classification. The four categories above are defined in detail for each structural classification, with the higher structural classification requiring more testing and analysis. The key point here is that these are guidelines for structural development testing. The actual structural testing needed for a specific classification of structure could be more or less, depending on the vehicle's mission and whether it is manned or unmanned. Knowing the structural part classification, the aircraft's purpose and mission, risk analysis can be applied to minimize testing cost and risk. FEM and closed form composite analysis methods utilizing proper mechanical and physical properties and allowables input data will be necessary every step of the way. Failure modes and loads (stresses) as well as strain and deflection readings must be monitored and correlated with predictions to assure low risk. The use of FEM or other analysis methods alone (without testing) or with inadequate testing that does not properly interrogate failure modes, stresses (strains), and deflections for comparison with predictions can create high risk situations that should not be tolerated.

Another risk issue for composite structure is quality assurance (QA), a subject that applies to both Parts A and B. Table 4.4.2.2(b) presents the nominal QA requirements for the categories of

1. Material and process selection, screening, and materials specification qualification,
2. Receiving inspection/acceptance testing,
3. In-process inspection,
4. Non-Destructive inspection (NDI),
5. Destructive testing (DT), and
6. Traceability.

The QA requirements in each of these categories vary with the structural classification, with the higher classification requiring more quality assurance. By following the procedure outlined in this table, the amount of QA necessary to keep risk at an acceptable level can be ascertained. Again the amount of QA needed and the risk taken will be a function of the aircraft type and mission and whether it is manned or unmanned. Risk and cost are inversely proportional to each other for composite structural parts in each classification, so the determination of acceptable risk is necessary to this building block test program for EMD and production.

TABLE 4.4.2.2(a) *DOD/NASA aircraft structure classification and goals vs. PMC building block development tests for EMD* and production, (continued on next page).***PART B** (Reference Figure 4.4.2.1)

Aircraft Structure		Building Block Structural Development Test Effort	
Aircraft Structure Development Goals		Trade Studies and Conceptual Development Analysis	Selection and Proof of Concept Testing and Analytical Methods Development
Classification	Description	Element - Single Load Path	Sub-Component - Multiple Load Paths (Including Joints)
PRIMARY	CARRIES PRIMARY AIR LOADS	Concept and analytical methods development - static and fatigue test (mandatory)	Proof of concept and analytical methods - static and fatigue test (residual strength)
<ul style="list-style-type: none"> Fracture critical (F/C) 	<ul style="list-style-type: none"> Failure will cause loss of vehicle 	6-each stiffening configuration 6-each joint configuration	4-box beam/cylinder static ultimate 6-box beam/cylinder: fatigue and residual strength
<ul style="list-style-type: none"> Noncritical (N/C) 	<ul style="list-style-type: none"> Failure will not cause loss of vehicle, cost critical replacement or repair 	4-each stiffening configuration 4-each joint configuration	3-box beam/cylinder: static ultimate 1-fatigue, residual strength
SECONDARY	CARRIES SECONDARY AIR & OTHER LOADS	Concept and analytical methods development - static and fatigue test (mandatory)	Proof of concept and analytical methods - static (DLL/fatigue/residual strength test)
<ul style="list-style-type: none"> Fatigue critical (FA/C) & economic life critical (EL/C) 	<ul style="list-style-type: none"> Failure will not cause loss of vehicle, cost critical replacement 	3-each stiffening configuration 3-each joint configuration	3-box beam/cylinder: static (DLL/fatigue/residual strength test)
<ul style="list-style-type: none"> Noncritical (N/C) 	<ul style="list-style-type: none"> Failure will not cause loss of vehicle Not cost or fatigue critical 	2-each stiffening configuration 2-each joint configuration	2-fatigue residual strength required
NONSTRUCTURAL	NON- OR MINOR LOAD BEARING	Concept development/static test/analytical methods check	Proof of concept: element testing plus analysis
<ul style="list-style-type: none"> Noncritical (N/C) 	<ul style="list-style-type: none"> Failure/replacement minor inconvenience, not cost critical 	1-each most critical configuration	1-fatigue, residual strength

*For EMD, use procedure given to prototypes in Section 4.4.1

TABLE 4.4.2.2(a) *DOD/NASA aircraft structure classification and goals vs. PMC building block development tests for EMD* and production, concluded***PART B** (Reference Figure 4.4.2.1)

Aircraft Structure		Building Block Structural Development Test Effort	
Aircraft Structure Development Goals		Structural Verification Testing for Analytical Methods	Structural Integrity Testing for FEM Validation
Classification	Description	Component With True Contours - Multiple Load Paths	Full Scale Aircraft Structure: Simulated Air Loads & Load Paths
<u>PRIMARY</u>	CARRIES PRIMARY AIR LOADS	Structural verification: static and durability and damage tolerance tests	Structural integrity validation - static strain survey & proof test; static test to DUL/failure or fatigue test depending on budget and schedule requirements
<ul style="list-style-type: none"> Fracture critical (F/C) 	<ul style="list-style-type: none"> Failure will cause loss of vehicle 	3-different large structural sections: static damage tolerance to DUL/failure 6-large structural sections: damage tolerance and durability plus residual strength (3 configurations)	3-different proof tests - critical flight load condition: strain/deflection survey and fatigue and residual strength to DLL, to DUL and failure if required
<ul style="list-style-type: none"> Noncritical (N/C) 	<ul style="list-style-type: none"> Failure will not cause loss of vehicle, repair or replacement cost critical 	2-large structural section: static and durability critical damage tolerance to DLL, then take to DUL/failure for residual strength test	2-proof tests - critical flight load condition: strain/deflection survey and static test to DLL, durability testing and static residual strength to DUL and failure if required
<u>SECONDARY</u>	CARRIES SECONDARY AIR & OTHER LOADS	Structural verification and analytical methods improvement: static and durability and damage tolerance tests (DUL/failure)	Structural integrity validation - static strain survey & proof test; static test to DUL and failure if required
<ul style="list-style-type: none"> Fatigue critical (FA/C) & economic life critical (EL/C) 	<ul style="list-style-type: none"> Failure will not cause loss of vehicle, cost critical replacement 	3-large structural sections: static damage tolerance to DUL/failure	1 proof test - critical flight load condition: strain/deflection survey and static test to DLL, to DUL if required
<ul style="list-style-type: none"> Noncritical (N/C) 	<ul style="list-style-type: none"> Failure will not cause loss of vehicle Not cost or fatigue critical 	No testing required - proved by element tests and analysis	No testing required - proved by element test
<u>NONSTRUCTURAL</u>	NON- OR MINOR LOAD BEARING	Structural verification by proof test/analysis	Structural integrity validation by previous tests and analysis
<ul style="list-style-type: none"> Noncritical (N/C) 	<ul style="list-style-type: none"> Failure/replacement, inconvenient, not cost critical 	No testing required - verification by element testing	No testing required - validation by subcomponent testing

*For EMD, use procedure given to prototypes in Section 4.4.1

TABLE 4.4.2.2(b) *DOD/NASA aircraft structure classification vs. PMC quality assurance requirements for EMD* and production, (continued on next page).*

PARTS A and B (Reference Figure 4.4.2.1)

Aircraft Structure		Quality Assurance Requirements		
Classification	Description	M&P Selection, Screening, & Qualification	Receiving Inspection/ Acceptance Testing*	In-Process Inspection
<u>PRIMARY</u> <ul style="list-style-type: none"> Fracture critical (F/C) Noncritical (N/C) 	CARRIES PRIMARY AIR LOADS <ul style="list-style-type: none"> Failure will cause loss of vehicle 	Physical, mechanical, & process variable evaluation & complete specification development; Record,	Per complete M&P specifications - minimum physical, mechanical, & process property requirements - test for acceptability; engineering	Per complete process specification & drawings - inspect/record for conformance & use
	<ul style="list-style-type: none"> Failure will not cause loss of vehicle, repair or replacement cost critical 	evaluate, select & store test data	accept/reject decision; store test data	engineering judgment for accept/reject decision; store test data
<u>SECONDARY</u> <ul style="list-style-type: none"> Fatigue critical (FA/C) & economic life critical (EL/C) Noncritical (N/C) 	CARRIES SECONDARY AIR & OTHER LOADS <ul style="list-style-type: none"> Failure will not cause loss of vehicle, cost critical replacement 	Complete physical, mechanical, & process variable evaluation & complete specification development; Record, evaluate, select & store test data	Per complete M&P specification - minimum physical, mechanical & process property requirements - maximum tests for acceptability; engineering accept/reject decisions and store test data	Per complete process specifications & drawings - inspect/record for conformance & use engineering judgment for accept/reject decisions; store test data
	<ul style="list-style-type: none"> Failure will not cause loss of vehicle Not cost or fatigue critical 			
<u>NONSTRUCTURAL</u> <ul style="list-style-type: none"> Noncritical (N/C) 	NON- OR MINOR LOAD BEARING <ul style="list-style-type: none"> Failure/replacement minor inconvenience, not cost critical 	Limited physical property tests; use vendor recommended process; store data	Vendor certification	Worker self-inspection per vendor process

*For EMD, use procedure given for prototypes in Section 4.4.1

TABLE 4.4.2.2(b) *DOD/NASA aircraft structure classification vs. PMC quality assurance requirements for EMD* and production, (concluded).***PARTS A and B** (Reference Figure 4.4.2.1)

Aircraft Structure		Quality Assurance Requirements		
Classification	Description	Non-Destructive Inspection (NDI)	Destructive Testing (DT)	Traceability
<u>PRIMARY</u> <ul style="list-style-type: none"> Fracture critical (F/C) 	CARRIES PRIMARY AIR LOADS <ul style="list-style-type: none"> Failure will cause loss of vehicle 	100% area; Engineering accept/reject decision based on defect standard (defect panel); store data	Physical and mechanical property testing on integral process control panel; engineering accept/reject decision; store test data	Keep files on all receiving, in-process, & non-destructive inspection and destructive test records for each vehicle
	<ul style="list-style-type: none"> Noncritical (N/C) 			
<u>SECONDARY</u> <ul style="list-style-type: none"> Fatigue critical (FA/C) & economic life critical (EL/C) 	CARRIES SECONDARY AIR & OTHER LOADS <ul style="list-style-type: none"> Failure will not cause loss of vehicle, cost critical replacement 	100% area; Engineering accept/reject decision based on defect standard (defect panel); store data	Physical and mechanical property testing on nonintegral process control panel; engineering accept/reject decision; store test data	Keep files on all receiving, in-process, & non-destructive inspection & destructive test records for each vehicle
	<ul style="list-style-type: none"> Noncritical (N/C) 			
<u>NONSTRUCTURAL</u> <ul style="list-style-type: none"> Noncritical (N/C) 	NON- OR MINOR LOAD BEARING <ul style="list-style-type: none"> Failure/replacement minor inconvenience, not cost critical 	Visual, dimensional	None	Keep materials receiving inspection records.

*For EMD, use procedure given for prototypes in Section 4.4.1

4.4.2.3 Summary of allowables and building block test efforts for DOD/NASA EMD and production composite aircraft structure.

In the above sections, composite material allowables development needed for prototype aircraft is detailed along with the related building block test effort required for such structure development. Both allowables requirements and building block structural test requirements are related to aircraft structure part criticality classifications and then each is related to the test/evaluation/analysis categories that need to be interrogated to study the risk involved. For allowables, the categories are preliminary and final values and physical defect minimum requirements in each classification. For the building block structures development test effort categories, the procedure used is to progressively scale up the size of the test parts, along with going from single to multiple load paths and adding joints to the test structure as it gets bigger. And, finally, the relationship of the quality assurance requirements from those required for design allowables for flat panels to those required for major structural components to those required for full size structure are presented for the six QA needs categories for each structural classification of the parts to be built.

The Part A allowables effort will provide for acceptable risk and cost effective allowables for EMD and production composite structures. The Part B building block structures test development effort will satisfy the goals of:

1. Appropriate conceptual development,
2. Proof of concept and analytical methods development,
3. Structural verification testing for analytical methods, and
4. Structural integrity testing and FEM validations.

Once these goals are achieved the user will have acceptable risk, cost effective EMD and production composite aircraft structure that will have the necessary integrity and reliability needed for the specific aircraft being developed.

4.4.3 Commercial aircraft

4.4.3.1 Introduction

This section describes an (commercial) approach to determining and verifying material allowables and design values for commercial aircraft composite structures. The approach provides a systematic method of dealing with composite materials, from initial materials screening to the final certification of actual structure.

The focus of this section describes the use of the building block approach to derive and validate material allowables and design values for structures fabricated using advanced composite material laminates. How the building block approach was used on the Boeing 777 commercial aircraft is described in Section 4.4.3.8 for an example.

4.4.3.2 The building block approach

To accommodate the unique features of composites, a method for determining relevant design properties has been devised. This is the "building block approach." This method provides a systematic way of treating composite materials to obtain design information. The life cycle of composite structure, from when a candidate material is first screened, to the final production part, is broken down into a number of different blocks. To complete a structure each block, with its essential information, needs to be built and understood. This method is illustrated in Figure 4.4.3.2, and is described in Section 4.4.3.8 for application to the Boeing 777.

This results from the extensive experience gained from certification of many different structures. Typically commercial aircraft structures certify by analysis supported by tests. It should be noted that this approach does not imply that each block is performed only after the lower one is completed, in fact some

level of structural element and sub-component testing should be performed as early in the design cycle as possible to reduce risks and to validate design concepts.

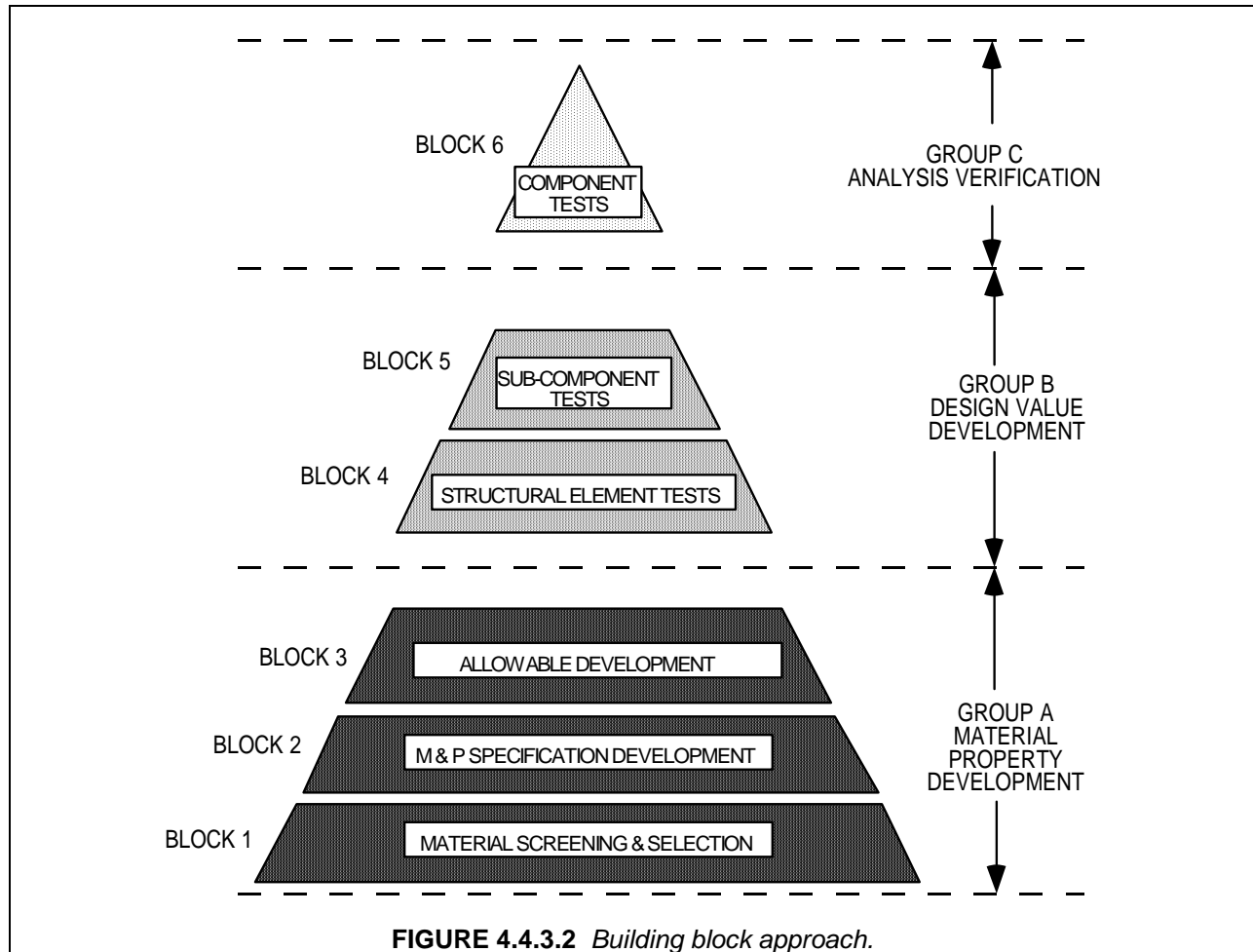


FIGURE 4.4.3.2 Building block approach.

4.4.3.2.1 Certification approaches

The approach taken to certify a structure impacts both the methods of analysis and allowable requirements used. There are two approaches that can be taken: certify by test or certify by analysis. While each has many features in common, emphasis is on different points of the design process. It is also possible to use a combination of these approaches to satisfy the unique needs of individual aircraft.

For a certify-by-test approach, (point design testing), the final basis for certification is testing the complete structure. The allowables and analysis methods are used for sizing, but final proof is by testing the full-scale structure. The amount of effort to develop material properties and validate analysis methods depends on the degree of risk a program chooses to assume. While this approach may drastically lower the cost of the program, it may not reveal design flaws until late in the project, or to mitigate the risk a weight penalty would result. In addition the cost of individual complex tests are much higher while being much more limited in their application. Also, the information gained over the course of the program may be of no practical use to other programs. So the next project would not benefit from their experience.

The other validation approach, certifying by analysis, assumes that the behavior of the structure can be predicted through analysis. This approach makes use of approved allowables and analysis methods.

The initial costs of this approach may be greater than the certify-by-test approach, but the results may be relevant to other programs and long-range cost may be greatly reduced. This method also enables the program to better analyze problems associated with liaison work, design changes, fleet support and air-plane derivatives.

Regardless of which approach is taken, or mixture of approaches, sufficient testing of representative structure must be conducted to validate that approach. In the case of the analytical certification approach, there may be sufficient information from past history from either identical designs or research and development activities to reduce the program-specific element tests. However, this requires the use of validated configurations and analysis tools.

4.4.3.2.2 Allowables versus design values

In common practice, the terms “allowable” and “design value” are often misunderstood as being interchangeable. While both terms are related, they do not have the same meaning. The following definitions are used:

- a. Allowable - A material property value (e.g., modulus, maximum stress level, maximum strain level) that is statistically derived from test data.
- b. Design Value - A material property or load value that takes into consideration program requirements (e.g., fitting and scaling factors, cutoff levels) and that has been approved for use in the design and analysis of structure.

4.4.3.2.3 Lamina vs. laminate derived allowables for predicting strength

The aerospace industry has two general approaches to analyzing composite laminate strength. Both approaches use laminated plate theory for stiffness calculations using ply moduli values. Both approaches calculate the ply level strains at a point in the laminate using the applied loads on the structure. A failure criterion is applied to each ply of the laminate. The difference in the approaches is in the failure theories and the test data used in conjunction with the failure criteria.

The first approach is the lamina (or ply) failure theory approach. This method uses allowables established for the individual plies of the material using unidirectional or cross-ply laminate tests. These values are tailored for use as the inputs to a lamina failure -theory model. In most cases, correction or modification factors must be applied to either the ply design values or elsewhere in the analysis. This is to account for lamination or structural load path effects which are not reflected in the lamina specimen tests used to obtain the allowables. To obtain these factors, tests of the actual laminates and structure must be conducted.

The advantage of using this approach is that, initially, allowables are only needed at the ply level. This means that the allowables testing can be done on a small number of specimens, and often the same test data as used for material qualification can be used as part of the allowables database. Unfortunately, failure theories using lamina level test data have not been shown to correlate well over the range of potential failure modes. Therefore, unless very conservative lamina values are used, laminate-level tests are required to verify the predicted failures or to create the modification factors. Additional testing or factors may also be needed to account for the production methods used to fabricate parts.

The second approach uses allowables and design values derived from tests on representative laminates. Ply-level information is generally only collected to obtain moduli. The allowables are based on linearized laminate failure strains (calculated using nominal moduli and ply thickness). They are used in a maximum strain failure criteria evaluated on a ply-by-ply basis at a given point in the laminate. The key difference from the lamina approach is that the strain allowables are a function of the specific laminate ply percentages and stacking sequence for the ply being analyzed. This approach has the advantage of interrogating the variables that may impact the performance of actual structure. Variables such as stacking sequence and processing irregularities may be included in the testing from which the allowables are sta-

tistically derived. Additional correction factors to account for laminate effects are not required. Disadvantages include somewhat larger test specimens, the increased numbers of test specimens to cover the numerous lay-ups that are representative of the structure, and the restrictions that may have to be placed on the design. To reduce the number of variables, design criteria that limit the permitted fiber orientation and stacking sequences are established. An advantage of this approach is that laminate test specimens have been shown to be less sensitive to test variables and irregularities, thereby reducing data scatter and resulting in more accurate material properties.

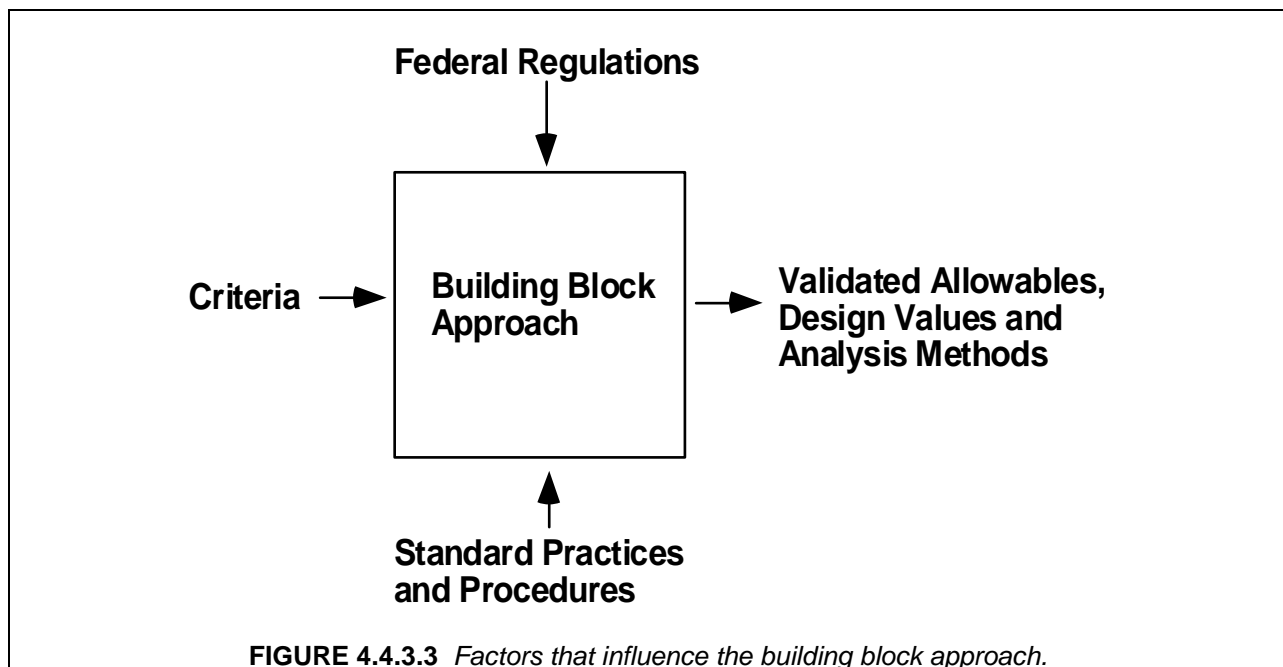
Both approaches have unique requirements and impact how the building block approach is implemented. When establishing an allowable/design-values program, the engineer needs to clearly understand what analysis approach is being used for the structure, the data requirements for the approach taken and the validation requirements for the selected analysis. In either case care must be taken to account for the variability introduced by the method of manufacturing as well as the base materials used to fabricate the structure.

4.4.3.2.4 Product development

A sufficient amount of work is needed to understand the requirements and limitations of materials being considered for a specific product, and to ensure that these are understood before initiating allowable and design-value development. In most cases, these factors are examined in independent research and development (IR&D), early product development, or some other such program that examines the potential use of a structure and identifies the critical material and geometric considerations. Only after these critical considerations are known can the appropriate screening, allowables, and design-value testing be defined.

4.4.3.3 Composite road map

The development and validation of allowables and design values is not an independent activity, but part of the larger product-development process. It is only through the use of common design and analysis practices that information can be generated that is applicable to more than one specific application. Even then, special care must be taken to ensure that the unique features of a specific structure are taken into account. The engineer must be aware that the building block approach is only one part of the overall system. Figure 4.4.3.3 illustrates those processes that influence allowables development.



4.4.3.3.1 *Criteria*

Before starting any allowables program the engineer must have an understanding of the criteria being applied. The criteria define program structural requirements, operational environment requirements, durability and damage tolerance requirements, and many other factors that must be accounted for in the design of a structure. It is through the criteria that manufacturer, customer, and regulatory agency requirements are defined for the engineer.

4.4.3.3.1.1 *Generic criteria*

Generic criteria are needed to have commonality between programs and to promote standard processes within groups. For this application, “generic criteria” refers to criteria that apply to more than one program. It is vital to allow information generated on one program to be applicable to the next.

While it is true that details may vary between groups, there is a set of basic issues that must be addressed by any criteria.

- a. Design Philosophy - The general concept of how the structure will be analyzed and certified must be understood. This is especially important in those programs that involve teaming with other companies. There are a number of differing approaches in designing structure that require special and distinct allowables.
- b. Method of Certification - The method by which the structure will be certified affects the test requirements. The method of compliance is often directed by the certifying agency and usually reflects the current rules and regulations. Method of certification may also define the regulatory agency's and/or customer's involvement in the development and implementing of test plans.
- c. Design Requirements and Objectives - The criteria being applied must clearly define the operational requirements and objectives of the product. They must reflect the customer's intended use and operational environment.

4.4.3.3.1.2 *Program criteria issues*

While generic criteria allow common processes and procedures to be used for a family of structures, there is always a requirement to have program-specific criteria. It is through the program criteria that specific details of the structures performance requirements are passed to design engineers. The program criteria also provides a method for the incorporation of newly developed items that may not have made it into the generic criteria at the start of a program or, because of the uniqueness of the structure, cannot be put into the general criteria. Whenever possible, the program criteria should not be developed to supersede the generic criteria, but to supplement them. The more dependent on specific criteria a program becomes, the more difficult it is to incorporate lessons learned on one project into the next. For this reason, those criteria developed at the program level need to be continually evaluated for possible inclusion into the generic criteria documentation.

4.4.3.3.2 *Regulations*

Depending on the ultimate use of the structure, a host of regulations define how and when allowables and design values are used in design. In a majority of the cases, regulations are covered within the criteria.

Commercial airplane structure must be designed in compliance with Federal Aviation Administration (FAA) and other agencies regulations outside the USA. While these are generally covered by the criteria, often the engineer must directly use these regulations.

FAA regulations are published in a series of books titled “Federal Aviation Regulations (FAR),” with additional guidance provided in Advisory Circulars. Official memos from the FAA may further clarify regulations on specific topics. In addition to the FAA, other regulatory agencies (such as the European JAA and the Russian airworthiness agencies) may be involved. The engineer establishing allowables and design values must be aware of all of the regulations that may pertain to the structure.

4.4.3.4 Commercial building block approach

The commercial building blocks may be divided into three groups, as illustrated in Figure 4.4.3.2.

The strength estimation of complex structural details and their certification requirements found in commercial programs necessitates an integrated test plan. That plan will progress from small specimens, through the various degrees of specimen complexity, to full-scale structure. Each level in the test plan uniquely interrogates the structural response of the composite design. However, accurate interpretation of data from any level is normally dependent upon results from other levels.

Once the data for any given material are obtained, any change in material systems or processes may require a repeat of tests at different levels in the building block plan to maintain certification.

In this building block approach to composite materials, seven blocks are identified. For the purposes of this section, the seven blocks have been combined into three major groups: material property evaluation (Group A), design-value development (Group B), and analysis verification (Group C).

Each building block must be addressed regardless of the approach taken. It is the degree of risk each program is willing to assume that determines which blocks are to be used and which will be scaled back. For currently existing materials and methods, entire blocks may already be completed, while new materials need to be evaluated in every block.

4.4.3.5 Group A, material property development

This group deals with those blocks that have the main purpose of defining the general behavior of the material, illustrated in Figure 4.4.3.5. Because of the numerous tests generally involved, testing is often performed using smaller, less complex specimens. Program requirements may dictate that limited numbers of larger, more complex tests be conducted to determine the critical properties that need to be investigated during material screening. This will ensure that the correct decisions are made in terms of material selection.

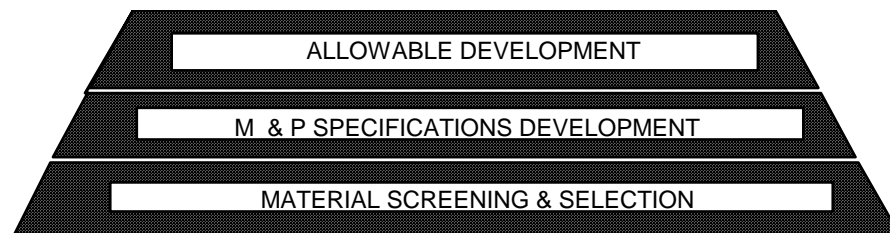


FIGURE 4.4.3.5 *Blocks in material property evaluation.*

4.4.3.5.1 Block 1 - material screening and selection

The first block's objective is to gather data on candidate materials and to make a decision on which material(s) will be selected for a given project. At this stage, the materials and the processes may not be well defined or controlled by specifications. This early testing has typically been confined to basic specimens because of the large number of candidate materials involved. Also, a program may require more complex tests if the final material selection must be based on configuration-specific tests. Since there are only limited controls (no specifications) placed on the materials at this point, it is impossible to establish firm allowables from this data alone. Estimates of basic material allowables may be provided to aid in trade studies and preliminary design. It is highly probable that the values will be adjusted as the understanding of the material system matures.

4.4.3.5.2 Block 2 - material and process specification development

The second block assumes that the preliminary material and processing specifications have been prepared for the material system that is selected. The objective of testing at this stage is to validate the specifications, thereby gaining an understanding of how the material behavior is affected by the process variables. This permits qualification of the material. It is important that the key mechanical properties needed to support design be identified by this stage so that these properties may be economically examined for a number of production batches. This will enhance understanding of the material behavior. Preliminary allowables may be derived from this level of testing because preliminary specifications are in place. However, not all material variables have been investigated, so firm allowables cannot be derived. Data obtained may be usable in the database needed to compute firm allowables, but the material and process specifications may not be modified. Specification changes after the fabrication of the test specimens may invalidate the test results and any allowables derived from them.

4.4.3.5.3 Block 3 - allowables development

In block 3 the material is fully controlled by both a material specification and a process specification. The objective is to provide "firm" material allowables suitable for design. Usually, the majority of the testing to be conducted on a new material is conducted at this stage of development. If the material specification has not been altered since the qualification tests, qualification data generated may be used as part of the allowables database. Only data from material purchased and fabricated under existing specifications are acceptable to certifying agencies for allowable development.

The main characteristics and objectives of these tests are summarized as follows:

- a. Development of statistically significant data - The database developed should be sufficient to develop "A" or "B" -basis allowables. Obtaining the required dataset involves information from several raw material production runs (batches) and from parts representing several fabrication runs.
- b. Determining the effects of environment - Test data should cover the complete environmental range necessary to design the structure. This includes the testing of moisture-conditioned specimens. This database will then provide environmental "compensation" factors relative to the room-temperature-ambient (RTA) condition. This facilitates interpretation of RTA tests on specimens of subcomponent-type complexity and greater.
- c. Determination of notch effects - Notch sensitivity is included in the allowables by testing specimens with both filled and open holes. The influence of fastener torque must also be examined.
- d. Defining changes in properties due to lamination effects - The data should be derived from specimens covering the complete range of laminate configurations used in the structure. This includes ply orientations percentages, stacking sequences, laminate thicknesses, tape/fabric hybrids, etc.

- e. Understanding the effects of manufacturing induced anomalies ("effects of defects") on the structure - Evaluation of permitted defects needs to be understood at the structural element level in order to establish process specifications and to provide data for MRB actions on rejectable defects.
- f. Understanding how sensitive the structure is to the fabrication process. Testing of structural elements are needed to evaluate the effects of any change in processing to the structural response.

The properties required for in-plane, tension, and compression allowables should be developed from uniaxially loaded specimens. The test matrix should include laminates encompassing the complete range of structural configurations in the design. Allowables should be generated for both unnotched and notched configurations. Notched testing may involve open and/or filled hole test coupons, depending on specific program design criteria. Use of a typical fastener and/or type used in the actual structure is recommended. While not classically considered material properties, allowables derived for geometry-dependent features (open- and filled-hole specimens) are frequently required for design.

Since allowables specimens are small coupons, it is economical to obtain enough tests to have statistical significance. Basic material properties are being obtained at this level. In fact, the engineer needs to be aware that values being obtained are configuration dependent. Values such as open-hole compression, filled-hole tension, and bearing, as well as some out-of-plane tests (short-beam shear and other interlaminar tests) are often used directly in the analysis methods used to design structure. These tests are strongly influenced by their configurations. Standard specimen configurations are designed to provide information that is directly applicable in Boeing analysis procedures.

4.4.3.6 Group B, design-value development

As illustrated in Figure 4.4.3.6, the objectives of Group B are to develop design values that reflect the actual structure. This testing may overlap those tests conducted to determine material allowables, as described in Section 4.4.3.5.3. Unlike those tests, testing for design values requires a preliminary configuration with general sizing. Design-value tests may become very specific and not applicable for use on other programs unless similar structures are being designed. The engineer must exercise caution when using design values developed for other programs.

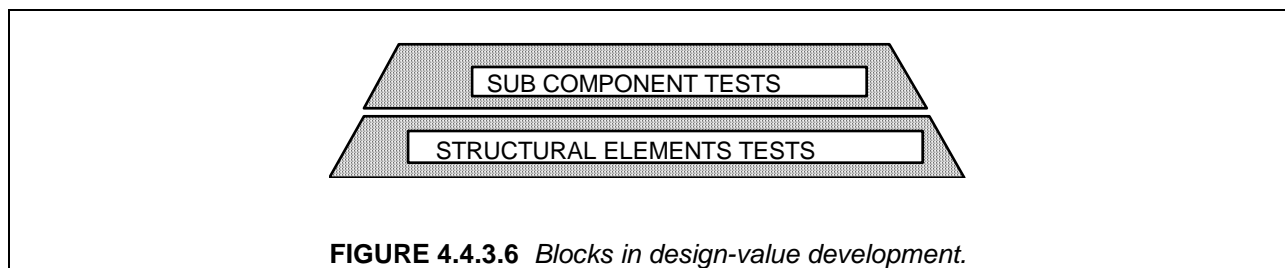


FIGURE 4.4.3.6 *Blocks in design-value development.*

4.4.3.6.1 Block 4 - structural element tests

Block 4 comprises local structural details that are repeated within the structure. The intent is to develop design values that are related more to structure than to basic material allowables developed per Section 4.4.3.5.3. For example, bearing is considered to be a structural, rather than a material, property. Typical structural elements are joints, frame sections (e.g., radius parts), and standard stiffener sections.

The main characteristics and objectives of these tests are summarized as follows:

- a. Development of design values that are structural configuration related. This contrasts with the basic material allowables developed in block 3 which are generic to most configurations.

- b. Understanding the effects of manufacturing induced anomalies ("effects of defects") on the structure. Evaluation of permitted defects needs to be understood at the structural element level in order to establish process specifications and to provide data for MRB action on rejected defects.
- c. Understanding how sensitive the structure is to the fabrication process. Testing of structural elements are needed to evaluate the effects of any change in processing to the structural response.

Generally, these factors are very dependent upon repetitive local structural details, and are developed from tests of these details referred to as "elements" in the building block plan. The data developed, which may be generic in nature, is frequently used to support analytical techniques. These techniques are used for developing margins of safety in composite structure and they normally have a strong semi-empirical basis. The following subsections illustrate typical examples.

4.4.3.6.1.1 *Bolted joints*

The properties required for the strength determinations of bolted joints are:

- a. Bearing - This property is a combination of a number of potential failure modes (compression bearing, shearout, cleavage, net section, fastener pull-through, etc.) which are strongly influenced by joint geometry and configuration, ply percentages, stacking sequence, fastener type and other variables. All of these effects must be accounted for in the bearing design values. Present analytical capability cannot account for fastener rotation (tilting) in bolted joints. Bearing design data must be obtained from tests on realistic joint configurations (typically stabilized, single-shear joints).
- b. Bypass - The material-related allowables database includes basic open- and filled-hole strengths. These are derived by using fasteners and hole sizes typical of those in the actual structure. These can be used to represent pure bypass strength. However, it is frequently necessary to generate data for other fasteners and also to evaluate fastener pattern effects. Special attention should be paid to fastener clamp-up. Filled-hole tension details are generally tested with full clamp-up, while filled-hole compression is conservatively tested at a value less than full clamp-up.
- c. Bearing-bypass - The interaction strength is a predictable property. However, the present analytical techniques rely upon the development of empirical interaction curves from tests of realistic joint configurations.
- d. Fastener pull-through - For reliable verification of structural integrity, tests must be conducted on realistic structural details.
- e. Fastener strength—While not a composite property in itself, the strength of the fastener will influence the behavior of the composite material being joined, and must be considered in bolted joint analysis and design value development. The strength of the fastener itself is influenced by the joint configuration and strap materials. The lower interlaminar stiffnesses and strengths typical of composite laminates, compared to metallic materials, result in a much greater occurrence of fastener failure modes in composite joints. Analytical methods using empirical fastener factors have been developed to predict fastener failure mode strengths in joints with composite straps.

4.4.3.6.1.2 *Stiffener sections*

Data is required to support the analysis of stiffener strengths, many of which are standard parts repeated throughout the structure. Typical failure modes requiring data are as follows:

- a. Crippling properties - Most structure, with any form of compression and/or shear loading, requires the development of a crippling strength database. This database can be used to support post-buckling strength methodology.

- b. Stiffener pull-off - This failure mode is relevant when a design employs any form of a cobonded or cocured stiffener. Present analytical capability cannot reliably predict this failure mode, and the development of detail test data is essential.

4.4.3.6.1.3 *Beam and clip flanges*

Data is required to analyze out-of-plane failures in curved beams. Properties are predictable on a linear basis from the material allowables database. Strength prediction in the out-of-plane direction requires failure data from tests on representative parts. Data is typically developed from bending tests of a curved laminate section. The resulting design values should be grouped along with interlaminar shear data under the heading of out-of-plane properties. These properties are particularly sensitive to processing, and can be used in evaluation of process sensitivity.

4.4.3.6.1.4 *Sandwich structure*

Test data is normally required to analyze the strength of sandwich structure. This data accounts for effects such as cocure, core and facesheet thickness', bagside waviness, and impact damage not found in laminate test articles.

4.4.3.6.2 *Block 5 - subcomponent tests*

In block 5, configurations are more complex than those in block 4. They are typically sections of a component. These tests permit assessment of load redistribution due to local damage. Specimen boundary and load introduction conditions are more representative of the actual structure than in the element tests. Biaxial loading can be applied. The level of specimen complexity allows incorporation of representative structural details. Typical examples of subcomponent configurations include picture-frame shear, deep-beam shear, and uniaxial tension and compression panels. The level of specimen complexity allows for the testing of multistiffened panels, panels with large cutouts, and damaged panels. Subcomponents must be of sufficient size to allow proper load redistribution around flaws and damage.

Secondary loading effects should be seen in this level of specimen complexity. The resulting load distributions and local bending effects become observable, and out-of-plane failure modes become more representative of full-scale structure.

Environmental testing may still be meaningful in these tests. Significant multiaxial loading and potentially different failure modes, when present, complicate interpretation of test results. The differing environmental sensitivity of the various failure modes contributes to this. For example, the elevated-temperature-wet (ETW) condition, while increasing sensitivity to compression-dominated failure, may reduce sensitivity to tension-dominated failure when compared to the RTA condition. The results from RTA tests should be adjusted to account for environmental sensitivity in the resulting failure mode. The characteristics and objectives can be summarized as follows:

- a. Applicability of design values and analysis - Evaluation of the effect of structural complexity and scale-up upon basic allowables data and data analysis methods.
- b. Effect of damage, static - Accounting for damage by development of configuration specific design values.
- c. Effect of damage, fatigue - Demonstration of "no detrimental damage growth" under operational fatigue loading.

4.4.3.7 *Group C, analysis verification*

These tests represent the final stage in the certification process for static and fatigue loading, illustrated in Figure 4.4.3.7. Success is very sensitive to program/customer criteria. At this level, it is desir-

able to perform extensive verification of analysis and computer modeling. This requirement is necessary due to the static-notch sensitivity of typical composite structure. Load redistribution capability does not exist to the same extent as that found in typical metal structure. Major objectives of these tests are:

- a. Verification of internal loads model and resulting stress, strain and deflection predictions.
- b. Large-scale verification of design and analysis methodology.

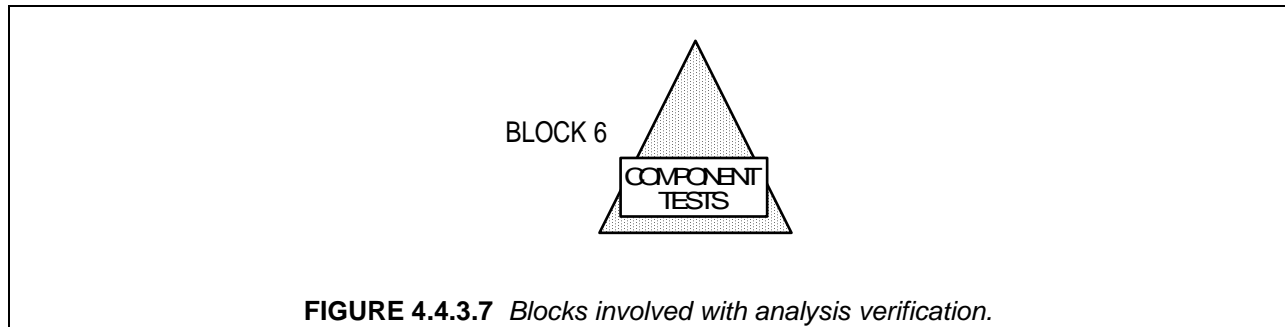


FIGURE 4.4.3.7 *Blocks involved with analysis verification.*

4.4.3.7.1 Block 6 - component test

Block 6 testing involves large and complex specimen configurations that are representative of the actual structure. In many cases these tests are performed only to design limit load to verify analytical strain and deflection predictions.

In some cases, the customer or regulatory agency may require that the test be performed to failure. In these cases, careful choice of the loading condition is essential because failure tests produce data relevant only to the particular failure mode, which may not be critical over the full environmental range. For example, tension-dominated failures are frequently not as environmentally critical as compression failures, (i.e., the tension-environmental compensation factor is normally less than the compression factor). Consequently, factoring of a tension-dominated failure load may not yield the minimum or maximum load capability of the structure over the full environmental range.

For successful verification of analytical predictions of the component's structural behavior, the component must be thoroughly instrumented with strain gages and deflection indicators. Choosing the gage types, instrumentation, and gage locations must be given careful consideration. The data collected must be correlated with the analysis methods predictions and discrepancies rationalized.

4.4.3.8 Boeing 777 aircraft composite primary structure building block approach

4.4.3.8.1 Introduction

This section outlines the building block approach for a large primary structure component for a commercial aircraft. The approach presented here is a summary of the approach used to support design and certification of the Boeing 777-200 CFRP empennage (Reference 4.4.3.8.1). The empennage has carbon fiber reinforced plastic (CFRP) main torque box structure in the horizontal and vertical stabilizers. The torque boxes are of two spar and multi-rib construction and use mechanical fasteners for major attachments. The structural design environment for the 777-200 empennage encompasses the range of temperatures from -65°F to +160°F.

Certification, in this case, was accomplished through structural analysis supported by test evidence obtained over a range of test article sizes. As described in Section 4.4.3.4 the "building block" approach involves tests at the coupon, element, subcomponent, and component levels. While much smaller in

quantity, the subcomponent and component test results comprise an important portion of the test evidence required to validate analytical methods and demonstrate the required levels of static strength and damage tolerance.

Certification requires the demonstration of required levels of static strength, durability and damage tolerance as well as the ability to predict stiffness properties. Demonstration of compliance for composite structure includes sustaining design ultimate loads with damage at the threshold of visual detectability (barely visible impact damage, BVID) and sustaining design limit loads with clearly visible damage. In addition, it must be demonstrated that levels of damage smaller than those that reduce the residual strength to Design Limit Load capability will not experience detrimental growth under operational loading conditions.

The regulatory requirements applicable to commercial transport aircraft are defined in FAR Part 25 and JAR Part 25. In addition to the regulations, the FAA and JAA have identified acceptable means of compliance for certification of composite structure: FAA Advisory Circular AC 20-107 and JAA ACJ 25.603, "Composite Aircraft Structure". The advisory circulars include acceptable means of compliance in the following areas: 1) effects of environment (including design allowables and impact damage); 2) static strength (including repeated loads, test environment, process control, material variability and impact damage); 3) fatigue and damage tolerance evaluation; 4) other items - such as flutter, flammability, lightning protection, maintenance and repair.

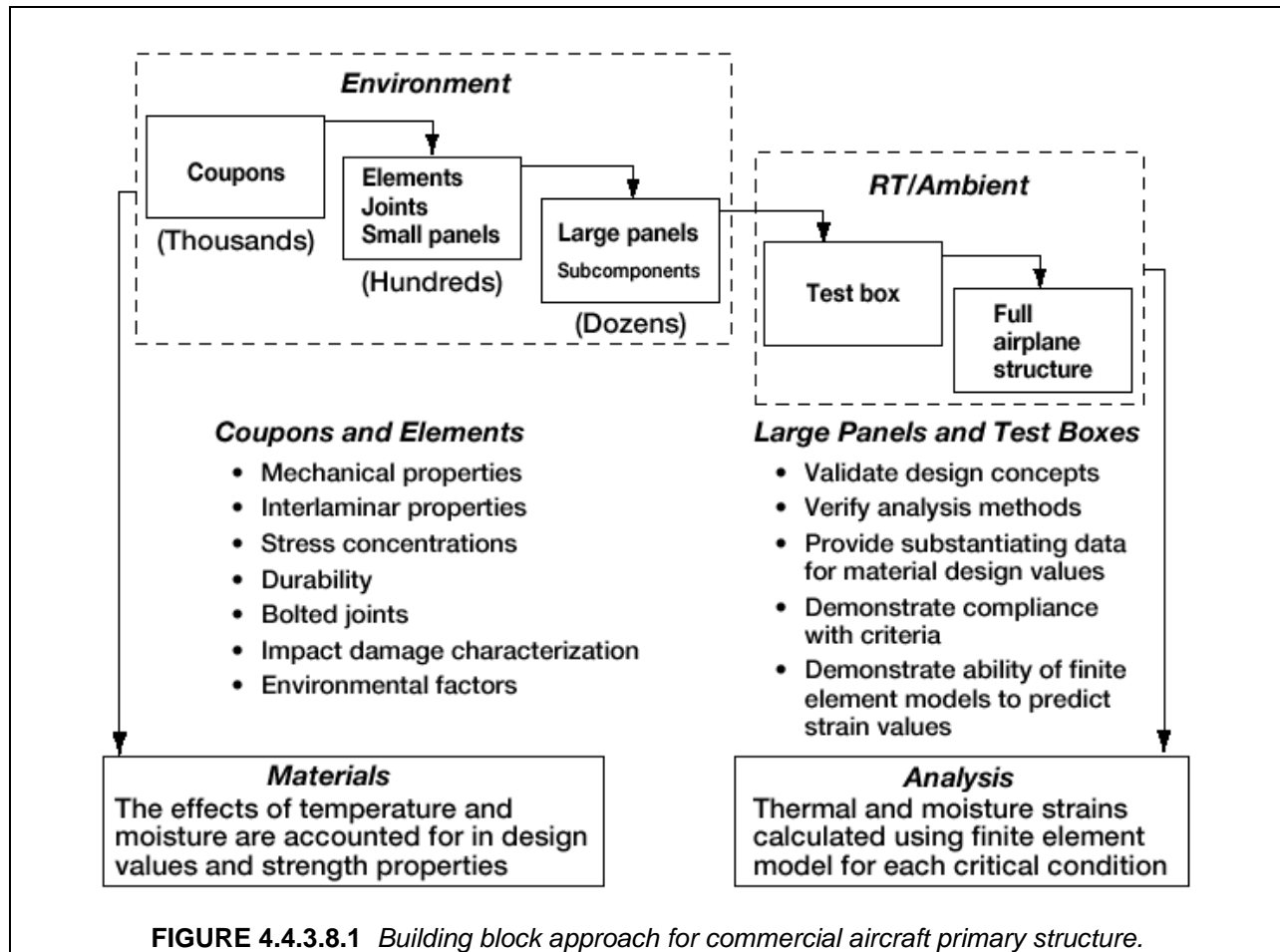
The typical composite structure certification approach is primarily analytical, supported by test evidence at the coupon, element, subcomponent and component level, and full-scale limit load test at ambient environment. The environmental effects on the composite structure are characterized at the coupon, element and subcomponent levels and are accounted for in the structural analysis. Supporting evidence includes testing through a "building block" approach where material characterization, allowables and analysis methods development, design concept verification, and final proof of structure are obtained. The approach is illustrated in Figure 4.4.3.8.1

Experience with similar structure was important in developing the 777 certification program. The 7J7 horizontal stabilizer and the 777 pre-production horizontal stabilizer programs validated analytical methods, design allowables, fabrication and assembly processes applied to the 777 empennage structure. Significant additional knowledge and experience was accumulated in characterizing the behavior of composite aircraft structure. This experience database has been augmented by the 737 composite stabilizer fleet experience and numerous other production applications in control surfaces, fixed secondary structure, fairings and doors.

4.4.3.8.2 Coupons and elements

Laminate level allowable design strain values covering each failure mode and environmental condition are obtained from coupon and element level tests using a range of lay-ups covering the design space. These are corrected for material variability following MIL-HDBK-17, Volume 1, Section 8 statistical analysis procedures. Detail design values are verified by representative subcomponent tests accounting for the effects of environment.

Coupon level tests are conducted in unnotched, open-hole and filled-hole configurations for in-plane laminate allowables. Statistical allowables curves are derived using regression analyses and room temperature test data. Factors to account for environmental effects are determined using smaller quantities of data. Additional coupon level tests are used to determine interlaminar properties, and to assess durability, manufacturing anomalies, bonded repair and environmental effects. Element level tests, such as bolted joints, radius details and crippling specimens, are used to derive specific design values for the range of tested configurations. These values, along with the statistical allowables, are used in analytical predictions of structural capability.



An extensive coupon and element level test program was conducted in support of new 777 composite structure applications. These tests were conducted to establish material stiffness properties, statistical allowables and strength design values, and to validate analytical methods. Laminate level statistical allowables were established for unnotched and notched conditions following Mil-HDBK-17 recommended procedures. Up to 16 separate batches of material were included in the statistical allowables. These batches included prepreg material from two carbon fiber lines and three prepreg facilities. Approximately 25 different laminate lay-ups were included in the allowables database, with 0° fiber percentages ranging from 10% to 70%, and +/-45° fiber percentages ranging from 20% to 80%.

Testing covered laminate, joint and structural configurations typical of the 777 empennage, temperatures from -65°F to 160°F, moisture conditioned laminates, and the effects of manufacturing variations and defects allowed within the process specifications. A limited amount of impact damage testing was performed at the element level. Test article configurations ranged from simple rectangular coupons to bolted joint, angle-section, I-section and shear panel element tests.

4.4.3.8.3 Subcomponents

Subcomponent tests are conducted to establish point design values and to validate methods of analysis for such design details as a skin panel, spar, rib, horizontal stabilizer centerline splice joint or vertical stabilizer root joint structure. These design values account for the effects of environment, the presence of barely visible impact damage, and for large damages. Design values accounting for the effects of impact damage are primarily derived from subcomponent testing. This is due to the fact that the critical impact damage locations are typically not at simple acreage locations, but at a stress concentration (such

as at the edge of an access hole) or over a substructure element (such as on the skin over the centerline of a stiffener). The subcomponent test results comprise a significant portion of the test evidence required to validate analytical methods and demonstrate the required levels of static strength and damage tolerance for the 777 empennage.

TABLE 4.4.3.8.3 *Summary of subcomponent tests for 777 empennage.*

Test Type	Number of Tests
Bolted Joints (Major Splices)	110
Rib Details	90
Spar Chord Crippling	50
Skin/Stringer Compression Panels	26
Skin/Stringer Tension Panels	4
Skin/Stringer Shear/Compression	6
Skin/Stringer Repair Panels	6
Skin Splice Panels	2
Stringer Runouts	4
Spar Shear Beams	6
Total	305

A number of the subcomponent test articles were moisture conditioned prior to test. Moisture conditioning was conducted in an environmental chamber at 140°F and 85% relative humidity. Test articles were left in the chamber until at least 90% of the equilibrium moisture content was reached.

The following critical design values and methods of analysis were validated by the subcomponent test results:

- a. Compression ultimate strength design value curve for stiffened skin panels.
- b. Shear-compression ultimate strength interaction curve for stiffened skin panels.
- c. Compression and tension damage tolerance analysis for stiffened skin panels.
- d. Strength of bolted and bonded repair designs for stiffened skin panels.
- e. Bolted joint analysis and design values for the skin panel-to-trailing edge rib joints.
- f. Static compression and tension strength, and tension fatigue performance of the horizontal stabilizer centerline splice joint.
- g. Analytical methods for spar strain distributions, web and chord stability, and peak strains at cutouts.
- h. Analytical methods for rib shear tie and chord strength and stiffness.
- i. Peak strain design values for rib shear tie cutouts.

Several test types were used to demonstrate no-growth of small damages under operational repeated loading. These tests complemented the results from the full-scale component fatigue testing, and involved:

- a. Axially loaded flat panels
- b. Shear loaded flat panels with cutouts
- c. Stiffened panel with a bonded repair
- d. Spar shear beams with web cutouts
- e. Centerline splice joint stiffened panel

4.4.3.8.4 Components

There are two primary damage tolerance requirements described in FAR and JAR 25.571 and the advisory circulars: damage growth characterization, and residual strength capability. As in the case of static strength, damage tolerance certification is based on analysis supported by tests at the element and subcomponent levels. Considering the applied strains, materials and design concepts, a no-growth approach for damage tolerance was selected for the 777 empennage, similar to that used for previous composite structure. This approach is based on demonstrating that any damage that is visually undetectable will not grow under operational loads. Structures with undetectable damage must be capable of carrying ultimate load for the operational life of the airplane.

The no-growth behavior of CFRP structure was demonstrated in numerous subcomponent tests and two full-scale cyclic load tests: the 7J7 horizontal stabilizer and the pre-production 777 horizontal stabilizer. In each case, visible damage was inflicted on the test article that underwent spectrum type repeated loading. Damage sites were inspected for growth during the test sequence. In addition, the full-scale tests demonstrated the following characteristics required for damage tolerance compliance:

- a. Manufacturing anomalies allowed per the process specifications will not grow for the equivalent of more than two design service lives.
- b. Visible damage due to foreign-object impact will not grow for the duration of two major inspection intervals (considered to be two "C" checks, 4000 flights per "C" check for the 777).
- c. The structure can sustain specified residual strength loads with damage that can reasonably be expected in service.
- d. The structure can sustain specified static loads ("continued safe flight loads") after incurring in-flight discrete-source damage.

4.4.3.8.5 777 pre-production horizontal stabilizer test

The 777 CFRP pre-production horizontal stabilizer test program was initiated to provide early test evidence supporting the 777 empennage structural configuration. The test article was a partial span box, nearly identical to the production component. The minimum gage outboard sections were eliminated for cost considerations and replaced with load application fixtures. The test article included typical, specification-allowed process anomalies, as well as low-velocity impact damage up to and beyond the visual threshold. The purpose of the test program was to:

- a. Demonstrate the 'no detrimental damage growth' design philosophy.
- b. Verify the strength, durability, and damage tolerance capability of the structure.
- c. Substantiate the methods of analysis and material properties used to design and analyze a CFRP stabilizer.

- d. Evaluate the combined load effects of shear, bending, and torsion that empennage structure would experience during flight.
- e. Verify the capability for predicting strain distributions.
- f. Substantiate mechanical repairs.
- e. Provide cost verification data on the fabrication of this type of structure.

The pre-production horizontal stabilizer test program consisted of 12 test sequences, as shown in Table 4.4.3.8.5.

TABLE 4.4.3.8.5 *Pre-production test box load and damage sequence.*

Test Sequence	Damage Types and Test Loadings
1.	Perform all small (BVID) damages
2.	Design limit load static strain survey.
3.	One lifetime fatigue spectrum, 50000 flights, including 1.15 LEF. (Load Enhancement Factor)
4.	Design limit load static strain survey.
5.	One lifetime fatigue spectrum, 50000 flights, including 1.15 LEF.
6.	Design limit load static strain survey.
7.	Design ultimate (select cases) load static strain survey.
8.	Two 'C' check fatigue spectrum (8000 flights) with small and visible damages, including 1.15 LEF.
9.	"Fail-safe" test; 100% design limit load static strain survey with small and visible damage.
10.	"Continued safe flight" loads test; 70% design limit load static strain survey with small, visible, and element damages.
11.	Visible and element damages repaired. Design ultimate load static strain survey.
12.	Destruction test. Strain survey up to destruction.

One of the test objectives was to validate the "no-growth" design philosophy for damage. To do this, impact damages were inflicted on the test box at the barely-visible level. Fatigue testing was conducted for load cycles representative of two design service lifetimes. Periodic ultrasonic inspection revealed an absence of detrimental damage growth. This test included a 15% L.E.F (load enhancement factor) to account for possible fatigue scatter associated with the flat S-N curves typical of composite materials.

Limit load strain surveys and initial ultimate load testing results demonstrated the predictive capability of the FEA internal loads model.

To demonstrate residual strength capability, the test box was further damaged with visible impacts. Visible damages are those that are easily detected by scheduled maintenance inspections. Fatigue testing representative of two inspection intervals again verified the no-growth approach. Limit load testing verified the structure was capable of carrying the required loads (FAR 25.571b) with these damages existing in the structure. The test box was then inflicted with major damage in the form of saw cuts to the front and rear spar chords and a completely severed stringer/skin segment. Capability to sustain continued

safe-flight load (approximately 70% of limit load for stabilizer structure) was demonstrated (FAR 25.571e). Again, the deliberately inflicted damages were ultrasonically inspected and showed no detrimental growth. Residual strength testing substantiated the analytical predictions and empirical results based on subcomponent test characterization.

Upon completion of the damage tolerance testing, the cut element damages and the major through-penetration impact damages were repaired using bolted, titanium sheet metal repairs. The configurations chosen were representative of the mechanical repairs planned for the 777-200 Structural Repair Manual. All repairs were designed to restore the structure to design ultimate load capability. Repairs were performed with external access only simulating in-service repair conditions. The test article was subjected to design ultimate loads (DUL) with the repairs in place.

The test article was loaded to destruction using a symmetric down bending load case. Final failure occurred above the required load level. The skin panel failure was predicted using the analytical methods and design values derived from five-stringer compressive panel subcomponent tests.

4.4.3.8.6 *Fin root attachment test*

Two large subcomponent tests were conducted to evaluate the primary joint of the 777 vertical stabilizer root attachment to the fuselage. The objectives of the tests were to:

- a. Verify the capability of the vertical stabilizer CFRP skin panel and titanium fittings to transmit design ultimate tensile and compressive loads.
- b. Verify the durability of the joint and determine the fatigue sensitive details.
- c. Validate the analytical methods used to design the structure.

The two test articles consisted of a four bay section of CFRP skin panel with two titanium root fittings. The first article was subjected to static testing in a series of limit and ultimate load conditions in tension and compression, culminating in a destruction test under tensile loads.

The objective of the fatigue test was to find potential fatigue critical areas, and investigate crack growth behavior. The second test article was tested with cyclic loads at a constant amplitude followed by a tensile residual strength test. The fatigue loading was conducted at four times the maximum 777-200 vertical stabilizer fatigue loads. The fatigue test was followed by residual strength tests in compression to limit load and in tension to failure.

4.4.3.8.7 *777 horizontal stabilizer tests*

The 777 horizontal stabilizer and elevators were tested to demonstrate limit load capability and verify accuracy of analytically calculated strains and deflections. The tests were conducted separately from the airplane since the attachment to the body is determinate. The test specimen was a structurally complete production article; omitted were non-structural components and systems not essential to the structural performance or induced loading of the stabilizer. Three critical static load conditions were included in the test: up, down and unsymmetric bending. The loading sequence was similar to the pre-production box. Limit load strain survey results were used to demonstrate the predictive capability of the FEA model.

Additional testing was performed which was not required for certification. This included fatigue, ultimate load and destruct testing. The horizontal stabilizer was subjected to 120,000 flights of spectrum fatigue loading, without any load enhancement factors, to satisfy the program objectives. This test was primarily intended to verify the fatigue characteristics of the metallic portion of the stabilizer. The composite structure was verified by the pre-production test box described earlier. Ultimate load and destruct testing was meant to supplement the data that was acquired as part of the certification program and to verify future growth capability. Three load cases were run representative of up, down and unsymmetric bend-

ing. The critical down bending load case was used for the destruct run. The test box was subjected to barely visible impact damage and loaded to failure.

4.4.3.8.8 777 vertical stabilizer test

The 777 vertical stabilizer including the rudder was tested as part of the airplane full-scale. Again, the purpose was to demonstrate limit load capability and verify accuracy of analytically calculated strains and deflections. Testing was conducted indoors at ambient conditions. Three critical conditions tested included maximum bending (engine-out), maximum torsion (hinge moment), and maximum shear (lateral gust).

A completely separate test using another production airframe was conducted to verify the fatigue behavior of the 777. As a part of this test, the vertical stabilizer and rudder were subjected to 120,000 flights (considered three design service objectives) of spectrum fatigue loading. No load enhancement factors were applied, as the primary purpose of the test was to validate the fatigue performance of the metallic parts of the structure.

4.4.3.8.9 Future programs

A building block approach used on a future program will take into account lessons learned on the Boeing 777. A pre-production test box will not be used on the next program unless significant changes in materials and configuration warrant such a test article. The “no damage growth” philosophy will be satisfied at the subcomponent level and include a L.E.F. Full scale testing will not use a L.E.F as the metallic fittings and joints are the critical articles to be concerned with. This assumes that future designs will still be a hybrid of composites and metallic structure. Testing a structural box to failure may or may not be required depending on the level of change when compared to past testing. If a program has future derivatives planned, testing to failure may be done to understand future airframe growth potential.

4.4.4 Business and private aircraft

4.4.4.1 High performance

This section is reserved for future use.

4.4.4.1.1 Introduction

This section is reserved for future use.

4.4.4.1.1.1 Background

The general aviation market ranges from 4 seater personal or trainer airplanes costing less than \$200,000 to intercontinental jets selling for close to \$40 million. Airplanes weighing over 12,500 lb take off weight or with more than 10 occupants must be certificated under FAR 25 regulations, in other words, to the same rules as the wide body airliners. The smaller commuter airliners may be still certificated under FAR 23 commuter category for take off weight less than 19,000 lb and less than 19 passengers. Although most general aviation airplanes will not see heavy hours per year usage there are commuter airliners in service which have seen over 50,000 flights. Another sub-set of the GA market is trainers, general transportation, and special mission aircraft for military customers, these include surveillance and air ambulance operations. Often these are certificated under FAA rules in order to give the customer a non-developmental airplane. Military trainers typically experience usage of about 1,000 hours per year.

4.4.4.1.1.2 Building Block Rationale

Element and sub component testing has been historically used in metallic airplanes to identify fatigue and crack growth characteristics of critical joints and details, especially since the introduction of damage tolerance requirements in FAR 25 in the late seventies. Also in the late seventies, carbon fiber reinforced

epoxy (CFRE) parts were first introduced into commercial airplane service. These parts tend to be anisotropic, statically notch sensitive (as opposed to the fatigue notch sensitivity of aluminum alloys), heavily process dependent, and tooling intensive. These characteristics add to the program risk. Full scale test articles will not be available until late in the development cycle, by which time the program risk of test revealed inadequacy or unacceptable materials or process is huge.

Risk reduction is the major justification for a building block approach. Cost reduction is also a factor: Material tests allow alternate materials to be specified; element tests can identify allowable intrinsic manufacturing defects; MRB and acceptable rework activity can also be substantiated during element tests; finally, the scope of full scale static and fatigue testing can be reduced with a program of analysis supported by smaller tests.

4.4.4.1.2 *Typical building block program*

4.4.4.1.2.1 *Material lamina tests*

These tests are conducted to qualify a new material and/or supplier, establish receiving inspection criteria, and to provide raw data from which lamina allowables may be defined. These tests are typically conducted at the material supplier with witnessing from and approval by the using company.

Typical Matrix—Material Lamina Tests

PROPERTY	NUMBER OF BATCHES (6 TESTS EA BATCH)		
	CTD	RTD	ETW
TENSION 0 Strength, modulus, and Poisson's	1	3	3
COMPRESSION 0 Strength and modulus	1	3	3
TENSION 90 Strength and modulus	1	3	3
COMPRESSION 90 Strength and modulus	1	3	3
IN-PLANE SHEAR Strength and modulus	1	3	3

4.4.4.1.2.2 *Material laminate tests*

These tests are conducted to compare the performance of new material to the baseline materials and to provide design guidelines for properties not readily calculated from the laminar properties. These tests are also typically conducted at the material supplier with witnessing from and approval of the using company.

Typical Matrix—Material Laminate Tests

PROPERTY	NUMBER OF BATCHES (6 TESTS EA BATCH)		
	CTD	RTD	ETW
Bearing strength	1	1	1
Compression after impact	1	1	1
Open hole tension strength	1	1	1
Open hole compression strength	1	1	1
Fluid Exposure			
Fuel		1	
Deice fluid		1	
Hydraulic fluid		1	
Cleaning solvent		1	

4.4.4.1.2.3 Element tests - critical laminates

The most simple of these tests are conducted to demonstrate that a classical laminated plate analysis will predict the strength and stiffness of critical laminates with input of lamina properties from the material test program.

Tests are also conducted to provide certification data for failure modes not readily predicted by currently accepted analysis methods. For example: strength after barely detectable impact damage, called threshold of detectability (TOD) impact damage in FAA advisory material; flaw growth from TOD impact damage; strength after detectable damage; flaw growth rates from detectable damage; lightning strike resistance; flame resistance.

In fabrication of specimens for the above tests, it will benefit a manufacturer to consider a range of defects intrinsic to the manufacturing process, but which may not significantly degrade the structural properties. Therefore, laminates may be deliberately fabricated with porosity, voids, and minor delaminations from which shop inspection and NDI criteria may be validated.

There may also be customer economic/maintenance issues which require tests of typical but not necessarily critical elements. These could include doorstep and floorboard damage resistance, runway debris potential damage, hail storm damage, baggage impact resistance, and step or no step criteria for external surfaces.

Typical Element Test Matrix—Critical Laminates

PROPERTY	NUMBER OF TESTS		
	CTD	RTD	ETW
Tension strength			
Virgin	3	3	3
Impact damage	3	3	3
Detectable	3	3	3
Compression strength			
Virgin	3	3	3
Impact damage	3	3	3
Detectable damage	3	3	3
Shear strength			
Virgin	3	3	3
Impact damage	3	3	3
Detectable damage	3	3	3
Tension flaw growth			
From impact damage		3	
From detectable damage		3	
Compression flaw growth			
From impact damage		3	
From detectable damage		3	
Shear flaw growth			
From impact damage		3	
From detectable damage		3	

4.4.4.1.2.4 Element tests - critical joints and details

Throughout a composite there may be joints and splices which must be shown to be capable of carrying ultimate loads under applicable environmental conditions and the required residual strength loads after damage or partial failure. Such critical details may also be subject to variability due to the manufacturing processes. For example: bolt torque loads, bond pressure, bond line max and min thickness, shop ambient conditions, cure cycle variations, misalignment during assembly, and so on. These joints and details are also likely to be exposed to in-service loads and damage cases; these could include: cyclic loading due to gust, maneuver, and landings, impact damage, direct lightning strike or internal current transfer due a strike elsewhere.

Critical details other than joints and splices might include such items as: reinforcing frames around doors, windows, and windshield openings, ply build-ups and drop offs, and reinforcements and attachments for systems and equipment.

The type of loading applied to validate joints and critical details will depend on the internal load applied in the loaded structure; typically derived from finite element analysis. The example in the typical matrix below assumes a bolted and bonded joint subjected to tension and bending in the full scale structure, and where the bolts alone must carry a required residual strength load.

Typical Test Matrix - Joints and Critical Details

PROPERTY	NUMBER OF TESTS		
	CTD	RTD	ETW
Tension strength			
Virgin	3	3	3
Max bond line	3	3	3
Bond voids	3	3	3
Lightning damage		1	
Bending strength			
Virgin	3	3	3
Max Bond line	3	3	3
Bond voids	3	3	3
Lightning damage		1	
Bolts alone strength			
Virgin	3	3	3
Max gap	3	3	3
Min e/d	3	3	3
Miss-aligned	3	3	3
Tension flaw growth			
Max bond line		3	
Bond voids		3	
Bending flaw growth			
Max bond line		3	
Bond voids		3	

4.4.4.1.2.5 Sub-component tests

Sub-component tests are tests of critical portions of a component, a component being a wing, fuselage, or empennage. The sub-components are themselves full scale and typically three dimensional, but a section of the component and not the whole component. Often small compromises will be made in order to fabricate the test articles early in the development program. Examples of the type of compromises applied are: wing box sections without airfoil contour or taper, fuselage sections made cylindrical and without taper, and window frames or access panel frames fabricated and tested as flat panels, neglecting exterior curvature.

Sub-component tests are conducted when new materials, new manufacturing methods, or new structural configurations are introduced; examples may include: RTM resin and process, co-cured parts, filament winding or automated fiber placement, and metal reinforcements or fittings.

Typical Sub Component Tests

Sub Component	Test type	Loading	Environment
Wing or stabilizer Box	Static	Bending/torsion	RTD and ETW
	D&DT	2 lifetimes	RTD
	Res Strength	Bending /torsion	RTD
Wing or stabilizer Box	Static	Bending/torsion	RTD
Pressure Bulkhd Installation	Static	Operating and ult	RTD
	D&DT	Pressure	
	Res strength	2 Lifetimes	RTD
		Oper and ult	RTD
		pressure	

4.4.4.1.2.6 Full scale tests - static

One of the benefits of a building block approach is that the extent of full scale testing can be reduced based on the test results from lower levels of testing and validation of analytical methods by comparison to those results. Based on this methodology, a limited number full scale test load cases will be tested, and tested under ambient temperature/moisture only. The other temperature/moisture conditions can be cleared by analysis or by direct comparisons of strain data to element test results. Similarly, other load cases can be cleared by analysis.

They may be interest from the customer or the certificating agency in a full scale test to failure. This would be conducted after all other uses for the test article had been exhausted and such a test would provide confirmation of the critical structure, failure mode, and margin of safety.

4.4.4.1.2.7 Full scale tests - durability and damage tolerance tests

Full scale testing of composite structure to demonstrate tolerance of in-service repeated loads both in the as-manufactured condition and after inflicted damage is the industry norm in aero structures. Usually a load enhancement factor of 1.15 is applied to enable two test lifetimes to represent one service lifetime with a B-basis relationship based on variability in flaw growth.

4.4.4.2 Lightweight and kit

This section reserved for future use.

4.4.5 Rotorcraft

As with the previous application examples, the BBA for rotorcraft is divided into Design Allowables, Design Development, and Full Scale Substantiation testing. Unlike the previous examples, both military and civilian substantiation methods are discussed interchangeably in this section. This combined treatment is due to the fact that, unlike fixed-wing aircraft, military and civilian rotorcraft are similar in size, cost, mission-profile, etc. (for utility, not attack helicopters).

Customer or regulatory substantiation requirements pertain only to assurance of structural integrity, not economic/programmatic risk. Nonetheless, since reducing programmatic risk is a major motivation for much of the building block test/analysis process, these types of tests are also addressed. Finally, relevant general references are listed at the end of this section (References 4.4.5(a) through (i)).

By far the most significant difference in design and substantiation of rotary- versus fixed-wing aircraft is the existence of a complex system of dynamic components in rotorcraft, which typically have more in common with gas turbine engine systems (blades, shafts, gearboxes, high cycle fatigue loads, etc.) than fixed-wing airframe structures. Common rotor system composite materials include glass/epoxy as well as carbon/epoxy, since flexibility and high inertia are preferred design attributes of certain rotor system components, such as blades and yokes. The high stiffness and low weight of carbon/epoxy is appropriate for other components, such as cuffs, grips, and certain large blade spars. Hybrid carbon-glass structures are also common. Note also that there are few, if any, secondary or nonstructural components (e.g., fairings or access covers) in the rotor system (and very few multiple load paths). The drive system is designed and analyzed separately from the main and tail rotors (typically by a different group of engineers), and consists of transmission, gear boxes, and drive shafts. Unlike the rotor and airframe, the drive system has few critical composite material applications, which are restricted mainly to carbon/epoxy shafts, although research has been done on continuous-fiber gearbox and transmission cases, and short-fiber bearing cages and races. An overview of structural criticality issues, or informal classifications, is given in Table 4.4.5.

TABLE 4.4.5 *Rotorcraft (composite) structural criticality.*

Type of Structure	Type of Component		
	Airframe	Rotor System	Drive System
non-redundant, primary	fully-monocoque tailboom, pylon support	single-lug joints, blades, cuffs, yokes, grips	drive shafts
multiple load path, primary	frames, longerons, ribs, spars, skins	multiple-lug joints, certain yokes and grips	none
flight-critical, secondary ^{1,2}	certain external doors and fairings	none	none
non-flight-critical, secondary (e.g., "nonstructural" in previous tables) ¹	all other doors, fairings, etc.	none	none

Notes:

1. FAR 29.613 does not distinguish between primary and secondary structures, only single vs. multiple load paths.
 2. Secondary structure is flight-critical when its failure causes system (rather than structural) failures, e.g., a door departing the airframe in flight critically damages the rotors or control system.
-

Unlike the dynamic systems, the rotorcraft airframe structure does share much in common with fixed-wing airframe structures, e.g., carbon/epoxy semi-monocoque shells, and is treated as such. In fact, rotorcraft companies often have separate design and stress analysis groups for airframe, rotor, and drive systems, all served by common aerodynamics, structural dynamics, external and internal loads, and fatigue groups. Thus, each of the following subsections is divided into separate airframe, rotor, and drive system discussions.

For airframe, rotor, and drive systems, the maximum physical defect size requirements for primary, secondary, and nonstructural classifications are similar to those noted in previous sections for DoD and transport category civilian fixed wing aircraft (see Tables 4.4.2.1(a) and 4.4.2.1(b)). The main difference being that since defect sizes should "be consistent with the inspection techniques employed during manufacture and service" (Reference 4.4.5(a), para. 7.a.(2)), the limited NDI capability of the typical civil rotor-

craft operator may result in larger allowable defect sizes (and may vary from one civil program to another). Thus, although discussion of these requirements will be minimized in this section, the manufacturing-level QA standards for rotorcraft, from coupons through full scale test articles, are of the same level as for large/complex fixed wing aircraft noted in Tables 4.4.2.xx and 4.4.3.xx, even though allowable defect sizes may be larger.

Within each subsection, static, fatigue, and damage tolerance substantiation requirements are addressed separately, if relevant. While these requirements are discussed at all levels of airframe substantiation, damage tolerance requirements for the rotor and drive systems are addressed exclusively at the full scale component testing level of the building block process, since that is the only level of the building block process at which they typically take place.

4.4.5.1 Design allowables testing

In general, design allowables testing is the most basic step in the building block process. Data from this level provide analytical input for strength, stiffness, and environmental/processing effect knockdown factors. Generally using small uniaxially loaded coupons, a great deal of statistical assurance is gained, but little or no analysis verification or structural substantiation is done. In this regard, rotorcraft do not differ significantly from the large/complex fixed-wing aircraft discussed in three of the building block examples considered previously.

4.4.5.1.1 Airframe

There are no significant differences between composite airframe design allowables testing for military EMD/production and FAR Part 25 fixed wing aircraft, and the subject military and civilian rotorcraft. In all cases, the airframes are separated into primary, secondary, and nonstructural components (or in terms of FAR 29.613, "single load path" or "multiple load path" instead of "primary" and "secondary"), each with differing levels of statistical assurance required for mechanical strength and differing levels of acceptable material quality. Suggested design allowables data guidelines for rotorcraft airframes may thus be found in Tables 2.3.1.1, 2.3.2.3, and 2.3.5.2.2 of Volume 1 and Tables 4.4.2.1(a) and 4.4.2.1(b) of this chapter. These guidelines should encompass all necessary data for point design analysis of laminates (strength and stiffness) and simple joints (e.g., bearing/by-pass for mechanical fastening), accounting for generic stress concentration (open holes), statistical (basis values), and environmental effects (temperature, humidity, and fluid soak), on all applicable material types and forms.

For airframes, fatigue life requirements are generally met through the use of conservative static design allowables, as in fixed-wing aircraft. However, when certain components (particularly the tailboom and roof beams/pylon supports) are deemed fatigue-critical, durability requirements are met via design development and full scale substantiation testing as described in later sections.

For airframes, damage resistance/tolerance requirements are met via development of B-basis design allowables using open hole (OHT and OHC) laminate-level, and sub-component-level static strength-after-impact testing (generally in compression, i.e., compression after impact (CAI)). A detailed description of damage resistance/tolerance requirements and approaches is given in Volume 3, Chapter 7. Further validation of damage resistance/tolerance is performed at the full scale test article level, as discussed below and in Volume 3, Chapter 7.

4.4.5.1.2 Rotor system

Design allowables testing for the rotor system is less extensive than for the airframe, since the components are generally substantiated via full scale fatigue testing, rather than by a combination of testing and analysis, as is the airframe. Stress analysis of rotor components is used for static sizing and also plays a critical role in programmatic risk mitigation (e.g., engineering and management confidence that there will be no surprises in full-scale testing) prior to full scale component fatigue testing. Thus B-basis ply strengths (developed per the Volume 1, Section 2.3.2.3 guidelines) are necessary (but not the extensive notched strength allowables used on airframes).

S-N curve shapes for environmental and stress ratio effects are developed in the design allowables phase of testing via a statistically significant number of coupon fatigue tests, using specimen geometries such as short beam strength (SBS) or unnotched tension, to later be applied to component-level mean S-N data. A preliminary check of fatigue endurance limit is also sometimes made using this coupon-level data. However, unless a component is well below its material endurance limit, more detailed life predictions must be made using component-level fatigue testing. Unlike metals, composite component fatigue life below the endurance limit is not typically predicted using coupon-level S-N curves, since delaminations and local geometric effects not found in coupons dominate composite structural fatigue failures.

Unlike fatigue-critical metallic structures, the lack of a validated damage-tolerance-based analytical fatigue life prediction methodology for composites precludes the use of coupon-level fracture toughness or strain energy release rate allowables (equivalent to metallic da/dN vs. ΔK testing) to predict life on a damage tolerance basis.

Suggested design allowables requirements for rotor system components, in addition to those of Table 2.3.2.3(b) in Volume 1, are shown in Table 4.4.5.1.2.

Table 4.4.5.1.2 *Example of additional rotor system design allowables testing guidelines beyond Volume 1, Table 2.3.2.3(b).*

Test Type	Static				Fatigue			
	CTD	RTA	ETW	Purpose	CTD	RTA	ETW	Purpose
Unnotched tension ^{1,2}	(2)	(2)	(2)		--	12	9	env. & statistical K
OHT ¹	6	6	--	point dsn allow.	9	12	--	env. & statistical K
OHC	--	6	6	point dsn allow.	--	--	--	
SBS ^{2,3}	(2)	(2)	(2)		--	12	9	env. & statistical K
core shear	--	12	9	generic allow.	--	--	--	
core crush	--	12	9	generic allow.	--	--	--	

Notes:

These tests are typically repeated for each significant variation in material form, process, and/or lay-up.

1. Either $R = 0.1$ or $R = -1$ for fatigue testing (depending on intended component).
2. Static data included in Table 2.3.2.3(b).
3. $R = 0.4$ for fatigue testing.

4.4.5.1.3 Drive system

Design allowables testing for the drive system is less extensive than either the airframe or the rotor system, since (a) the components are completely substantiated via full scale fatigue testing, rather than by a combination of testing and analysis, as in the airframe; and (b) the geometry and loading, at least for drive shafts, is more straightforward than either rotor system or airframe components. Requirements for B-basis ply strengths, and coupon-derived environmental and stress ratio knockdown factors are similar to those for the rotor system. Suggested design allowables requirements for drive system components, in addition to those of Table 2.3.2.3(b) in Volume 1, are shown in Table 4.4.5.1.3.

TABLE 4.4.5.1.3 *Example of additional drive system design allowables testing guidelines beyond Volume 1, Table 2.3.2.3(b).*

Test Type	Static				Fatigue			
	CTD	RTA	ETW	Purpose	CTD	RTA	ETW	Purpose
±45 Tension ^{1,2}	(2)	(2)	(2)		9	12	9	env. & statistical K
SBS ^{2,3}	(2)	(2)	(2)		--	12	9	env. & statistical K
bolt bearing	--	12	9	generic allow.	--	12	9	env. & statistical K

Notes:

1. R = 0.1 for fatigue testing.
2. Static data included in Table 2.3.2.3(b).
3. R = 0.4 for fatigue testing.

4.4.5.2 Design development testing

Design development testing may be separated into three general categories:

- Element - single load path,
- Subcomponent - multiple load path but subscale or partial component, and
- Component - multiple load path/full scale component (but not for structural substantiation purposes).

The purposes for these tests vary, and include specialized strength allowables (e.g., damage tolerance), design trade studies, analysis development and validation, and cost/schedule-based risk mitigation. Rotorcraft-specific details of these categories and purposes are discussed in the three following sub-sections.

4.4.5.2.1 Airframe

Similar to fixed-wing aircraft, rotorcraft airframe development testing mainly consists of critical joint and free-edge (e.g., tabouts, access holes, etc.) risk mitigation and analysis validation. In rotorcraft airframes, these tests are more likely to be performed in fatigue as well as statically, in order to validate fatigue life predictions and to reduce risk prior to (or in lieu of) full scale airframe fatigue substantiation testing. Unlike fixed-wing aircraft, lightly loaded rotorcraft airframe shells are more likely to be of sandwich panel design (even for primary structure) since they are often bending stiffness rather than strength critical. Facesheets can be as thin as one ply of fabric. Thus, panel buckling tests are also often performed at the element and subcomponent levels.

Fatigue testing is limited to the aforementioned joint and/or access hole fatigue issues. Damage tolerance testing is often done at the design development stage, and takes the form of specialized element-level allowables generation typically using impact-damaged structural elements (e.g., 3-stringer panels, curved honeycomb panels, etc.). Table 4.4.5.2.1 presents possible design development testing requirements for rotorcraft airframes.

TABLE 4.4.5.2.1 *Example of airframe design development testing guidelines.*

Test Type	Static			Fatigue ³		
	RTA	ETW	Purpose	RTA	ETW	Purpose
stiffener pull-off	12	5	special allowable ¹	3	--	design risk reduc.
stiffened CAI panel	12	5	special allowable ¹	--	--	
sandwich CAI panel	12	5	special allowable ¹	--	--	
bolted splice joint	6	3	trade study, analysis validation	3	--	design risk reduc.
shear panel w/cut-out	3	--	design risk reduc., analysis validation	3	--	design risk reduc.
stiffened shear panel	3	--	analysis validation	--	--	
sandwich shear panel	3	--	analysis validation	--	--	
stiffened compr. panel	3	--	analysis validation	--	--	
sandwich compr. panel	3	--	analysis validation	--	--	
complex subcomponent	5	3	design risk reduc.	3	--	design risk reduc.
tailboom component	3 ²	--	trade study	1	--	design risk reduc.

Notes:

1. Specimen quantities are highly variable for special allowables, reflecting case-specific trade-offs between testing cost and severity of statistical reduction.
2. Typically loaded to DUL*LEF rather than failure. Test article subsequently available for fatigue and/or damage tolerance testing. Impact damage sometimes included on early static article.
3. Typically constant amplitude unless a simple combination of load cases is available early in design process.

4.4.5.2.2 Rotor system

Rotor system design development testing mainly takes the form of single load path lug element static and fatigue testing to mitigate risk, generic subcomponent testing to screen rotor hub materials under multiaxial fatigue conditions, and design-specific subcomponent testing to mitigate design risk. Table 4.4.5.2.2 presents possible design development testing requirements for rotor systems.

4.4.5.2.3 Drive system

Drive system design development testing mainly takes the form of design-specific end-fitting element static and fatigue testing to mitigate risk. Table 4.4.5.2.3 presents possible design development testing requirements for drive systems.

TABLE 4.4.5.2.2 *Example of rotor system design development testing guidelines.*

Test Type	Static			Fatigue ¹		
	RTA	ETW	Purpose	RTA	ETW	Purpose
[0/45] laminate flexure	12	5	special allowable	12	12	allowable S-N curve
[0/45] laminate torsion	12	5	special allowable	12	12	allowable S-N curve
generic tension-bending flexbeam element	--	--		12	--	matl screening, effects of defects
M/R blade lug element	3	--	design risk reduc.	6	--	design risk reduc.
generic tension-torsion flexure element	3	--	design risk reduc.	6	--	design risk reduc.
M/R cuff subcomponent	3	--	design risk reduc., analysis validation	6	--	design risk reduc.
M/R grip component	3	--	design risk reduc., analysis validation	6	--	design risk reduc.
M/R flexure or yoke component	3	--	design risk reduc., analysis validation	6	--	design risk reduc.

Notes:

- Typically constant amplitude unless a simple combination of load cases is available early in design process.

TABLE 4.4.5.2.3 *Example of drive system design development testing guidelines.*

Test Type	Static			Fatigue ¹		
	RTA	ETW	Purpose	RTA	ETW	Purpose
[0/45] laminate torsion	12	5	special allowable	12	12	allowable S-N curve
generic multiple-bolt joint element	12	5	special allowable	12	12	allowable S-N curve
design-specific joint element	12	5	special allowable	12	12	allowable S-N curve
molded blower blisk spin test	--	--		3	--	design risk reduc.
driveshaft component	3	--	trade study	3	--	design risk reduc.

Notes:

- Typically constant amplitude unless a simple combination of load cases is available early in design process.

4.4.5.3 Full scale substantiation testing

Unlike the design development tests, full scale substantiation testing is performed on fully conforming (i.e., fabricated and inspected per production-level specifications) full scale components or systems, wit-

nessed by the procuring or regulating agency, in order to meet specific procurement/regulatory requirements.

4.4.5.3.1 Airframe

Static test articles of the complete airframe structure are always required of new designs unless significant commonality exists with prior production aircraft. A limited number of load cases (due to complexity and cost issues) are usually demonstrated under room temperature ambient conditions up to design ultimate load (DUL), which also includes factors for environmental effects and strength scatter developed from lower-level testing. Full scale airframe fatigue test articles (unlike static articles) are not always performed, but are becoming more prevalent as major components, such as cabins or tailbooms are switched from metal to composite for the first time. Table 4.4.5.3.1 presents possible full scale substantiation testing requirements for airframes.

TABLE 4.4.5.3.1 *Example of airframe full scale substantiation testing guidelines*

Test Type	Static			Fatigue		
	RTA	ETW	Purpose	RTA	ETW	Purpose
tiltrotor wing STA	1 ¹	--	cert./qual.	--	--	
tiltrotor fuselage STA	1 ¹	--	cert./qual.	--	--	
tiltrotor empennage STA/FTA	1 ¹	--	cert./qual.	1 ²	--	cert./qual.
tiltrotor wing/fuselage FTA	--	--		1 ²	--	cert./qual.
tailboom component	1 ¹	--	cert./qual.	1 ²	--	cert./qual.

Notes:

1. Loaded to DUL*LEF's, in some cases damaged (customer-dependent), then tested to failure.
2. Spectrum fatigue loaded for 2 lifetimes, damaged, spectrum fatigue loaded for 1 lifetime, then (sometimes) statically tested to failure. See Chapter 5 for more details.

Full-scale airframe fatigue test articles provide the ultimate substantiation of structural life when used, otherwise full-scale component-level testing suffices. Damage tolerance requirements are met via analysis (using CAI and OH allowables) and induced damage full-scale substantiation tests. Component and airframe system static test articles are typically damaged in several critical locations, via imbedded and/or impact-induced delaminations, and must survive up to DUL, including environmental and scatter factors (see Volume 3, Chapter 5 for further details). Certain regulatory requirements also include substantiation of damage tolerance for two inspection intervals or two fatigue lifetimes. Thus fatigue test articles are also tested in a damaged condition. If imbedded damage is not used, impact events are often induced after having already endured two component-lifetimes of undamaged testing, and the resulting spectrum-loading life, together with an appropriate scatter factor, defines the required inspection interval.

4.4.5.3.2 Rotor system

Full scale fatigue substantiation testing is performed on all new design rotor system components, either individually or as a system. Typically, the inboard and outboard ends of a main rotor blade are tested separately. Other composite parts, such as yokes/flexbeams, cuffs and grips are tested as complete components. Since rotor components are more amenable to environmental conditioning, it is often possible to test these components in a wet (e.g., 80% - 85% RH equilibrium) condition rather than applying

load factors to account for environment in an approximate sense. Typically, four to six components are tested at a variety of constant amplitude oscillatory load levels in order to generate a component-level S-N curve. A safe life/flaw tolerant method of life prediction is used under a variety of load spectra. Miner's rule is used to relate constant amplitude S-N data to spectral loading. Table 4.4.5.3.2 presents possible full scale substantiation testing requirements for rotor systems.

TABLE 4.4.5.3.2 *Example of rotor system full scale substantiation testing guidelines.*

Test Type	Static			Fatigue		
	RTA	ETW	Purpose	RTA	RTW	Purpose
M/R blade attachment & cuff component	1	1	cert./qual.	4 - 6 ¹ 2 ²	1 ¹ 1 ²	cert./qual. dam. tolerance
M/R grip component	1	1	cert./qual.	4 - 6 ¹ 2 ²	1 ¹ 1 ²	cert./qual. dam. tolerance
T/R blade attachment & cuff component	1	1	cert./qual.	4 - 6 ¹ 2 ²	1 ¹ 1 ²	cert./qual. dam. tolerance
M/R flexure or yoke component	1	1	cert./qual.	4 - 6 ¹ 2 ²	1 ¹ 1 ²	cert./qual. dam. tolerance
T/R flexure or yoke component	1	1	cert./qual.	4 - 6 ¹ 2 ²	1 ¹ 1 ²	cert./qual. dam. tolerance

Notes:

1. Constant amplitude (undamaged) certification testing.
2. Spectrum fatigue loaded for 2 lifetimes or inspection intervals, with imbedded manufacturing flaws (only); impact damage induced; then spectrum fatigue loaded for 1 lifetime or inspection interval. Combinations of constant amplitude and spectrum approaches are often used.

The full scale constant amplitude tests are performed to determine adequacy of the as-manufactured structure and to identify fatigue critical areas for implanting manufacturing flaws and inducing impact damage in subsequent damage tolerance substantiation full scale fatigue test articles. These flawed/damaged full scale components are tested under representative spectral loads in order to establish fatigue life and/or set inspection intervals. The sizes of initial damage/flaws are determined by analyzing their risk and detectability. Also, the recommended fatigue life and/or inspection intervals are reduced from the test results by factors based on the damage/flaw risk, its detectability, and criticality of failure modes induced by the damage/flaws. Further details of rotor system damage tolerance requirements are given in Volume 3, Chapter 7.

4.4.5.3.3 Drive system

Full scale fatigue substantiation testing is performed on all new design dynamic system components, either individually or as a system. Typically, composite drive shafts are tested separately, while gear-boxes are tested as complete mechanical systems. Since components such as drive shafts are more amenable to environmental conditioning, it is often possible to test these components in a wet (e.g., 80% - 85% RH equilibrium) condition rather than applying load factors to account for environment in an approximate sense. Typically, four to six components are tested at a variety of constant amplitude oscillatory load levels in order to generate a component-level S-N curve. A safe life/flaw tolerant method of life prediction is used under a variety of load spectra. Miner's rule is used to relate constant amplitude S-N

data to spectral loading. Table 4.4.5.3.3 presents possible full scale substantiation testing requirements for drive systems.

TABLE 4.4.5.3.3 *Example of drive system full scale substantiation testing guidelines.*

Test Type	Static			Fatigue		
	RTA	ETW	Purpose	RTA	RTW	Purpose
driveshaft component	1	--	cert./qual.	4 - 6 ¹ 2 ²	1 ¹ 1 ²	cert./qual. dam. tolerance
blower assembly	--	--		4 - 6 ¹	--	cert./qual.

Notes:

1. Constant amplitude (undamaged) certification testing.
2. Spectrum fatigue loaded for 2 lifetimes or inspection intervals, with imbedded manufacturing flaws (only); impact damage induced; then spectrum fatigue loaded for 1 lifetime or inspection interval. Combinations of constant amplitude and spectrum approaches are often used.

The full scale constant amplitude tests are preformed to determine adequacy of the as-manufactured structure and to identify fatigue critical areas for implanting manufacturing flaws and inducing impact damage in subsequent damage tolerance substantiation full scale fatigue test articles. These flawed/damaged full scale component flaw-size, damage tolerance and testing requirements are essentially the same as those described in Section 4.4.5.3.2 above for the rotor system.

4.4.6 Spacecraft

This section is reserved for future use.

4.5 SPECIAL CONSIDERATION AND VARIANCES FOR SPECIFIC PROCESSES AND MATERIAL FORMS

4.5.1 Room Temperature

This section is reserved for future use.

REFERENCES

- 4.1 Whitehead, R.S., Kan, H.P., Cordero, R., and Saether, E.S., "Certification Testing Methodology for Composite Structures," NADC-87042-60, Vol 2, Section 2, 1987.
- 4.4.1.1 Grimes, G.C., Dusablon, E.G., Malone, R.L., and Buban, J.P., "Tape Composite Materials Allowables Application in Airframe Design/Analysis," *Composites Engineering*, Vol 3, Nos. 7-8, Pergamon Press Ltd, 1993, pp. 777-804.
- 4.4.3.8.1 Fawcett, A., Trostle, J. and Ward, S., "777 Empennage Certification Approach", presented at the 11th International Conference for Composite Materials, Australia, 1997.
- 4.4.5(a) FAA Advisory Circular 20-107A, "Composite Aircraft Structure," 25 April 1984.
- 4.4.5(b) Adams, D.O. "Composites Qualification Criteria," *Proc., American Helicopter Society 51st Annual Forum*, Fort Worth, TX, 9 - 11 May, 1995.
- 4.4.5(c) Aeronautical Design Standard ADS-35, "Composite Materials for Helicopters," United States Army Aviation Systems Command, St. Louis, MO, Directorate for Engineering, February, 1990.
- 4.4.5(d) AIA Materials and Structures Committee Proposed Standard, "Standardization of Composite Damage Criteria for Military Rotary Wing Aircraft," Aerospace Industries Association, Washington, DC, 20 December, 1994.
- 4.4.5(e) JSGS-87221A(draft), "Air Force Guide Specification, General Specification for Aircraft Structures," 8 June 1990.
- 4.4.5(f) Kan, H.P., Cordero, R., and Whitehead, R.S., "Advanced Certification Testing Methodology for Composite Structure," DOT/FAA/CT-93/94, Northrup Corp. for FAA Tech Center and NADC, April, 1997.
- 4.4.5(g) Whitehead, R. S., Kan, H.P., Cordero, R., Saether, E.S., "Certification Testing Methodology for Composite Structure," NADC-87042-60, Northrup Corp. for NADC, Warminster, PA, 1986.
- 4.4.5(h) Sanger, K. B. "Certification Testing Methodology for Composite Structures," NADC-86132-60, McDonnell Douglas Corp. for NADC, Warminster, PA, 1986.
- 4.4.5(i) Shah, C., Kan, H.P., Mahler, M., "Certification Methodology for Stiffener Terminations," DOT/FAA/AR-95/10, Northrup Grumman Corp. for FAA Tech Center and NASA LaRC, April, 1996.

CHAPTER 5 DESIGN AND ANALYSIS

5.1 INTRODUCTION

The concept of designing a material to yield a desired set of properties has received impetus from the growing acceptance of composite materials. Inclusion of material design in the structural design process has had a significant effect on that process, particularly upon the preliminary design phase. In this preliminary design, a number of materials will be considered, including materials for which experimental materials property data are not available. Thus, preliminary material selection may be based on analytically-predicted properties. The analytical methods are the result of studies of micromechanics, the study of the relationship between effective properties of composites and the properties of the composite constituents. The inhomogeneous composite is represented by a homogeneous anisotropic material with the effective properties of the composite.

The purpose of this chapter is to provide an overview of techniques for analysis in the design of composite materials. Starting with the micromechanics of fiber and matrix in a lamina, analyses through simple geometric constructions in laminates are considered.

A summary is provided at the end of each section for the purpose of highlighting the most important concepts relative to the preceding subject matter. Their purpose is to reinforce the concepts, which can only fully be understood by reading the section.

The analysis in this chapter deals primarily with symmetric laminates. It begins with a description of the micromechanics of basic lamina properties and leads into classical laminate analysis theory in an arbitrary coordinate system. It defines and compares various failure theories and discusses the response of laminate structures to more complex loads. It highlights considerations of translating individual lamina results into predicted laminate behavior. Furthermore, it covers loading situations and structural responses such as buckling, creep, relaxation, fatigue, durability, and vibration.

5.2 BASIC LAMINA PROPERTIES AND MICROMECHANICS

The strength of any given laminate under a prescribed set of loads is probably best determined by conducting a test. However, when many candidate laminates and different loading conditions are being considered, as in a preliminary design study, analysis methods for estimation of laminate strength become desirable. Because the stress distribution throughout the fiber and matrix regions of all the plies of a laminate is quite complex, precise analysis methods are not available. However, reasonable methods do exist which can be used to guide the preliminary design process.

Strength analysis methods may be grouped into different classes, depending upon the degree of detail of the stresses utilized. The following classes are of practical interest:

1. Laminate level. Average values of the stress components in a laminate coordinate system are utilized.
2. Ply, or lamina, level. Average values of the stress components within each ply are utilized.
3. Constituent level. Average values of the stress components within each phase (fiber or matrix) of each ply are utilized.
4. Micro-level. Local stresses of each point within each phase are utilized.

Micro-level stresses could be used in appropriate failure criteria for each constituent to determine the external loads at which local failure would initiate. However, the uncertainties, due to departures from the

assumed regular local geometry and the statistical variability of local strength make such a process impractical.

At the other extreme, laminate level stresses can be useful for translating measured strengths under single stress component tests into anticipated strength estimates for combined stress cases. However this procedure does not help in the evaluation of alternate laminates for which test data do not exist.

Ply level stresses are the commonly used approach to laminate strength. The average stresses in a given ply are used to calculate first ply failure and then subsequent ply failure leading to laminate failure. The analysis of laminates by the use of a ply-by-ply model is presented in Section 5.3 and 5.4.

Constituent level, or phase average stresses, eliminate some of the complexity of the micro-level stresses. They represent a useful approach to the strength of a unidirectional composite or ply. Micromechanics provides a method of analysis, presented in Section 5.2, for constituent level stresses. Micromechanics is the study of the relations between the properties of the constituents of a composite and the effective properties of the composite. Starting with the basic constituent properties, Sections 5.2 through 6.4 develop the micromechanical analysis of a lamina and the associated ply-by-ply analysis of a laminate.

5.2.1 Assumptions

Several assumptions have been made for characterizing lamina properties.

5.2.1.1 *Material homogeneity*

Composites, by definition, are heterogeneous materials. Mechanical analysis proceeds on the assumption that the material is homogeneous. This apparent conflict is resolved by considering homogeneity on microscopic and macroscopic scales. Microscopically, composite materials are certainly heterogeneous. However, on the macroscopic scale, they appear homogeneous and respond homogeneously when tested. The analysis of composite materials uses effective properties which are based on the average stress and average strain.

5.2.1.2 *Material orthotropy*

Orthotropy is the condition expressed by variation of mechanical properties as a function of orientation. Lamina exhibit orthotropy as the large difference in properties between the 0° and 90° directions. If a material is orthotropic, it contains planes of symmetry and can be characterized by four independent elastic constants.

5.2.1.3 *Material linearity*

Some composite material properties are nonlinear. The amount of nonlinearity depends on the property, type of specimen, and test environment. The stress-strain curves for composite materials are frequently assumed to be linear to simplify the analysis.

5.2.1.4 *Residual stresses*

One consequence of the microscopic heterogeneity of a composite material is the thermal expansion mismatch between the fiber and the matrix. This mismatch causes residual strains in the lamina after curing. The corresponding residual stresses are often assumed not to affect the material's stiffness or its ability to strain uniformly.

5.2.2 Fiber composites: physical properties

A unidirectional fiber composite (UDC) consists of aligned continuous fibers which are embedded in a matrix. The UDC physical properties are functions of fiber and matrix physical properties, of their volume

fractions, and perhaps also of statistical parameters associated with fiber distribution. The fibers have, in general, circular cross-sections with little variability in diameter. A UDC is clearly anisotropic since properties in the fiber direction are very different from properties transverse to the fibers.

Properties of interest for evaluating stresses and strains are:

- Elastic properties
- Viscoelastic properties - static and dynamic
- Thermal expansion coefficients
- Moisture swelling coefficients
- Thermal conductivity
- Moisture diffusivity

A variety of analytical procedures may be used to determine the various properties of a UDC from volume fractions and fiber and matrix properties. The derivations of these procedures may be found in References 5.2.2(a) and (b).

5.2.2.1 Elastic properties

The elastic properties of a material are a measure of its stiffness. This information is necessary to determine the deformations which are produced by loads. In a UDC, the stiffness is provided by the fibers; the role of the matrix is to prevent lateral deflections of the fibers. For engineering purposes, it is necessary to determine such properties as Young's modulus in the fiber direction, Young's modulus transverse to the fibers, shear modulus along the fibers and shear modulus in the plane transverse to the fibers, as well as various Poisson's ratios. These properties can be determined in terms of simple analytical expressions.

The effective elastic stress-strain relations of a typical transverse section of a UDC, based on average stress and average strain, have the form:

$$\begin{aligned}\bar{\sigma}_{11} &= n^* \bar{\epsilon}_{11} + \ell^* \bar{\epsilon}_{22} + \ell^* \bar{\epsilon}_{33} \\ \bar{\sigma}_{22} &= \ell^* \bar{\epsilon}_{11} + (k^* + G_2^*) \bar{\epsilon}_{22} + (k^* - G_2^*) \bar{\epsilon}_{33}\end{aligned}\quad 5.2.2.1(a)$$

$$\begin{aligned}\bar{\sigma}_{33} &= \ell^* \bar{\epsilon}_{11} + (k^* - G_2^*) \bar{\epsilon}_{22} + (k^* + G_2^*) \bar{\epsilon}_{33} \\ \bar{\sigma}_{12} &= 2G_1^* \bar{\epsilon}_{12} \\ \bar{\sigma}_{23} &= 2G_2^* \bar{\epsilon}_{23} \\ \bar{\sigma}_{13} &= 2G_1^* \bar{\epsilon}_{13}\end{aligned}\quad 5.2.2.1(b)$$

with inverse

$$\begin{aligned}\bar{\epsilon}_{11} &= \frac{1}{E_1^*} \bar{\sigma}_{11} - \frac{\nu_{12}^*}{E_1^*} \bar{\sigma}_{22} - \frac{\nu_{12}^*}{E_1^*} \bar{\sigma}_{33} \\ \bar{\epsilon}_{22} &= -\frac{\nu_{12}^*}{E_1^*} \bar{\sigma}_{11} + \frac{1}{E_2^*} \bar{\sigma}_{22} - \frac{\nu_{23}^*}{E_2^*} \bar{\sigma}_{33} \\ \bar{\epsilon}_{33} &= -\frac{\nu_{12}^*}{E_1^*} \bar{\sigma}_{11} - \frac{\nu_{23}^*}{E_2^*} \bar{\sigma}_{22} + \frac{1}{E_2^*} \bar{\sigma}_{33}\end{aligned}\quad 5.2.2.1(c)$$

where an asterisk (*) denotes effective values. Figure 5.2.2.1 illustrates the loadings which are associated with these properties.

The effective modulus k^* is obtained by subjecting a specimen to the average state of stress $\bar{\epsilon}_{22} = \bar{\epsilon}_{33}$ with all other strains vanishing in which case it follows from Equations 5.2.2.1(a) that

$$(\bar{\sigma}_{22} + \bar{\sigma}_{33}) = 2k^*(\bar{\epsilon}_{22} + \bar{\epsilon}_{33}) \quad 5.2.2.1(d)$$

Unlike the other properties listed above, k^* is of little engineering significance but is of considerable analytical importance.

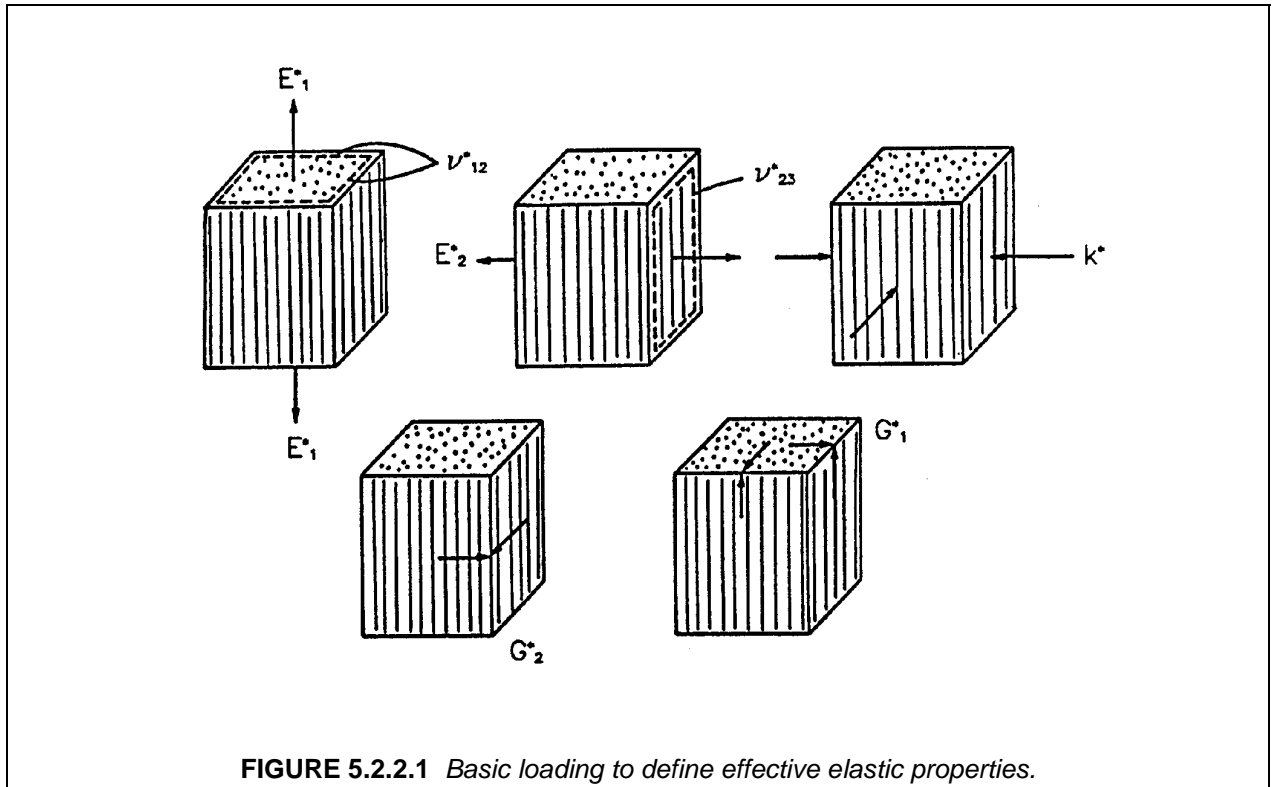


FIGURE 5.2.2.1 Basic loading to define effective elastic properties.

Only five of the properties in Equations 5.2.2.1(a-c) are independent. The most important interrelations of properties are:

$$n^* = E_1^* + 4k^* \nu_{12}^{*2} \quad 5.2.2.1(e)$$

$$\ell^* = 2k^* \nu_{12}^* \quad 5.2.2.1(f)$$

$$\frac{4}{E_2^*} = \frac{1}{G_2^*} + \frac{4\nu_{12}^{*2}}{E_1^*} \quad 5.2.2.1(g)$$

$$\frac{2}{1 - \nu_{23}^*} = 1 + \frac{k^*}{\left(1 + 4k^* \frac{\nu_{23}^{*2}}{E_1^*}\right) G_2^*} \quad 5.2.2.1(h)$$

$$G_2^* = \frac{E_2^*}{2(1 + \nu_{23}^*)} \quad 5.2.2.1(i)$$

Computation of effective elastic moduli is a very difficult problem in elasticity theory and only a few simple models permit exact analysis. One type of model consists of periodic arrays of identical circular fibers, e.g., square periodic arrays or hexagonal periodic arrays (References 5.2.2.1(a) - (c)). These models are analyzed by numerical finite difference or finite element procedures. Note that the square array is not a suitable model for the majority of UDCs since it is not transversely isotropic.

The composite cylinder assemblage (CCA) permits exact analytical determination of effective elastic moduli (Reference 5.2.2.1(d)). Consider a collection of composite cylinders, each with a circular fiber core and a concentric matrix shell. The size of the cylinders may vary but the ratio of core radius to shell radius is held constant. Therefore, the matrix and fiber volume fractions are the same in each composite

cylinder. One strength of this model is the randomness of the fiber placement, while an undesirable feature is the large variation of fiber sizes. It can be shown that the latter is not a serious concern.

The analysis of the CCA gives closed form results for the effective properties, k^* , E_1^* , ν_{12}^* , n^* , ℓ^* and G_1^* and closed bounds for the properties G_2^* , E_2^* , and ν_{23}^* . Such results will now be listed for isotropic fibers with the necessary modifications for transversely isotropic fibers (References 5.2.2(a) and 5.2.2.1(e)).

$$\begin{aligned} k^* &= \frac{k_m(k_f + G_m)v_m + k_f(k_m + G_m)v_f}{(k_f + G_m)v_m + (k_m + G_m)v_f} \\ &= k_m + \frac{v_f}{\frac{1}{(k_f - k_m)} + \frac{v_m}{(k_m + G_m)}} \end{aligned} \quad 5.2.2.1(j)$$

$$\begin{aligned} E_1^* &= E_m v_m + E_f v_f + \frac{4(\nu_f - \nu_m)^2 v_m v_f}{\frac{v_m}{k_f} + \frac{v_f}{k_m} + \frac{1}{G}} \\ &\approx E_m v_m + E_f v_f \end{aligned} \quad 5.2.2.1(k)$$

The last is an excellent approximation for all UDC.

$$\nu_{12}^* = \nu_m v_m + \nu_f v_f + \frac{(\nu_f - \nu_m) \left(\frac{1}{k_m} - \frac{1}{k_f} \right) v_m v_f}{\frac{v_m}{k_f} + \frac{v_f}{k_m} + \frac{1}{G_m}} \quad 5.2.2.1(l)$$

$$\begin{aligned} G_1^* &= G_m \frac{G_m v_m + G_f(1 + v_f)}{G_m(1 + v_f) + G_f v_m} \\ &= G_m + \frac{v_f}{\frac{1}{(G_f - G_m)} + \frac{v_m}{2G_m}} \end{aligned} \quad 5.2.2.1(m)$$

As indicated earlier in the CCA analysis for G_2^* does not yield a result but only a pair of bounds which are in general quite close (References 5.2.2(a), 5.2.2.1(d,e)). A preferred alternative is to use a method of approximation which has been called the Generalized Self Consistent Scheme (GSCS). According to this method, the stress and strain in any fiber is approximated by embedding a composite cylinder in the effective fiber composite material. The volume fractions of fiber and matrix in the composite cylinder are those of the entire composite. Such an analysis has been given in Reference 5.2.2(b) and results in a quadratic equation for G_2^* . Thus,

$$A \left(\frac{G_2^*}{G_m} \right)^2 + 2B \left(\frac{G_2^*}{G_m} \right) + C = 0 \quad 5.2.2.1(n)$$

where

$$\begin{aligned} A &= 3\nu_f \nu_m^2 (\gamma - 1)(\gamma + \eta_f) \\ &\quad + [\gamma \eta_m + \eta_f \eta_m - (\gamma \eta_m - \eta_f) \nu_f^3] [\nu_f \eta_m (\gamma - 1) - (\gamma \eta_m + 1)] \end{aligned} \quad 5.2.2.1(o)$$

$$\begin{aligned} B &= -3\nu_f \nu_m^2 (\gamma - 1)(\gamma + \eta_f) + \frac{1}{2} [\gamma \eta_m + (\gamma - 1) \nu_f + 1] [(\eta_m - 1)(\gamma + \eta_f) - 2(\gamma \eta_m - \eta_m) \nu_f^3] \\ &\quad + \frac{\nu_f}{2} (\eta_m + 1)(\gamma - 1) [\gamma + \eta_f + (\gamma \eta_m - \eta_f) \nu_f^3] \end{aligned} \quad 5.2.2.1(p)$$

$$C = 3\nu_f \nu_m^2 (\gamma - 1)(\gamma + \eta_f) + [\gamma \eta_m + (\gamma - 1) \nu_f + 1] [\gamma + \eta_f + (\gamma \eta_m - \eta_f) \nu_f^3] \quad 5.2.2.1(q)$$

$$\gamma = G_f / G_m \quad 5.2.2.1(r)$$

$$\eta_m = 3 - 4 \nu_m \quad 5.2.2.1(s)$$

$$\eta_f = 3 - 4 \nu_f \quad 5.2.2.1(t)$$

To compute the resulting E_2^* and ν_{23}^* , use Equations 5.2.2.1(g-h). It is of interest to note that when the GSCS approximation is applied to those properties for which CCA results are available (see above Equations 5.2.2.1(j-m)), the CCA results are retrieved.

For transversely isotropic fibers, the following modifications are necessary (References 5.2.2(a) and 5.2.2.1(e)):

For k^*	k_f is the fiber transverse bulk modulus
For E_1^*, ν_{12}^*	$E_f = E_{1f}$
	$\nu_f = \nu_{1f}$
	k_f as above
For G_1^*	$G_f = G_{1f}$
For G_2^*	$G_f = G_{2f}$
	$\eta_f = 1 + 2G_{2f}/k_f$

Numerical analysis of the effective elastic properties of the hexagonal array model reveals that the values are extremely close to those predicted by the CCA/GSCS models as given by the above equations. The results are generally in good to excellent agreement with experimental data.

The simple analytical results given here predict effective elastic properties with sufficient engineering accuracy. They are of considerable practical importance for two reasons. First, they permit easy determination of effective properties for a variety of matrix properties, fiber properties, volume fractions, and environmental conditions. Secondly, they provide the only approach known today for experimental determination of carbon fiber properties.

For purposes of laminate analysis, it is important to consider the plane stress version of the effective stress-strain relations. Let x_3 be the normal to the plane of a thin unidirectionally-reinforced lamina. The plane stress condition is defined by

$$\bar{\sigma}_{33} = \bar{\sigma}_{13} = \bar{\sigma}_{23} = 0 \quad 5.2.2.1(u)$$

Then from Equations 5.2.2.1(b-c)

$$\begin{aligned} \bar{\epsilon}_{11} &= \frac{1}{E_1^*} \bar{\sigma}_{11} - \frac{\nu_{12}^*}{E_2^*} \bar{\sigma}_{22} \\ \bar{\epsilon}_{22} &= \frac{\nu_{12}^*}{E_1^*} \bar{\sigma}_{11} + \frac{1}{E_2^*} \bar{\sigma}_{22} \\ 2\bar{\epsilon}_{12} &= \frac{\bar{\sigma}_{12}}{G_1^*} \end{aligned} \quad 5.2.2.1(v)$$

The inversion of Equation 5.2.2.1(v) gives

$$\begin{aligned} \bar{\sigma}_{11} &= C_{11}^* \bar{\epsilon}_{11} + C_{12}^* \bar{\epsilon}_{22} \\ \bar{\sigma}_{22} &= C_{12}^* \bar{\epsilon}_{11} + C_{22}^* \bar{\epsilon}_{22} \\ \bar{\sigma}_{12} &= 2G_2^* \bar{\epsilon}_{12} \end{aligned} \quad 5.2.2.1(w)$$

where

$$\begin{aligned}
C_{11}^* &= \frac{E_1^*}{1 - \nu_{12}^{*2} E_2^* / E_1^*} \\
C_{12}^* &= \frac{\nu_{12}^* E_2^*}{1 - \nu_{12}^{*2} E_2^* / E_1^*} \\
C_{22}^* &= \frac{E_2^*}{1 - \nu_{12}^{*2} E_2^* / E_1^*}
\end{aligned} \tag{5.2.2.1(x)}$$

For polymer matrix composites, at the usual 60% fiber volume fraction, the square of ν_{12}^* is close enough to zero to be neglected and the ratio of E_2^* / E_1^* is approximately 0.1 - 0.2. Consequently, the following approximations are often useful.

$$C_{11}^* \approx E_1^* \quad C_{12}^* \approx \nu_{12}^* E_2^* \quad C_{22}^* \approx E_2^* \tag{5.2.2.1(y)}$$

5.2.2.2 Viscoelastic properties

The simplest description of time-dependence is linear viscoelasticity. Viscoelastic behavior of polymers manifests itself primarily in shear and is negligible for isotropic stress and strain. This implies that the elastic stress-strain relation

$$\sigma_{11} + \sigma_{22} + \sigma_{33} = 3K(\epsilon_{11} + \epsilon_{22} + \epsilon_{33}) \tag{5.2.2.2(a)}$$

where K is the three-dimensional bulk modulus, remains valid for polymers. When a polymeric specimen is subjected to shear strain ϵ_{12}° which does not vary with time, the stress needed to maintain this shear strain is given by

$$\sigma_{12}(t) = 2G(t)\epsilon_{12}^\circ \tag{5.2.2.2(b)}$$

and $G(t)$ is defined as the shear relaxation modulus. When a specimen is subjected to shear stress, σ_{12}° , constant in time, the resulting shear strain is given by

$$\epsilon_{12}(t) = \frac{1}{2}g(t)\sigma_{12}^\circ \tag{5.2.2.2(c)}$$

and $g(t)$ is defined as the shear creep compliance.

Typical variations of relaxation modulus $G(t)$ and creep compliance $g(t)$ with time are shown in Figure 5.2.2.2. These material properties change significantly with temperature. The relaxation modulus decreases with increasing temperature and the creep compliance increases with increasing temperature, which implies that the stiffness decreases as the temperature increases. The initial value of these properties at "time-zero" are denoted G_0 and g_0 and are the elastic properties of the matrix. If the applied shear strain is an arbitrary function of time, commencing at time-zero, Equation 5.2.2.2(b) is replaced by

$$\sigma_{12}(t) = 2G(t)\epsilon_{12}(0) + 2 \int_0^t G(t-t') \frac{d\epsilon_{12}}{dt'} dt' \tag{5.2.2.2(d)}$$

Similarly, for an applied shear stress which is a function of time, Equation 5.2.2.2(c) is replaced by

$$\epsilon_{12}(t) = \frac{1}{2}g(t)\sigma_{12}(0) + \frac{1}{2} \int_0^t g(t-t') \frac{d\sigma_{12}}{dt'} dt' \tag{5.2.2.2(e)}$$

The viscoelastic counterpart of Young's modulus is obtained by subjecting a cylindrical specimen to axial strain ϵ_{11}° constant in space and time. Then

$$\sigma_{11}(t) = E(t)\epsilon_{11}^\circ \tag{5.2.2.2(f)}$$

and $E(t)$ is the Young's relaxation modulus. If the specimen is subjected to axial stress, σ_{11}° , constant in space and time, then

$$\epsilon_{11}(t) = e(t)\sigma_{11}^\circ \tag{5.2.2.2(g)}$$

and $e(t)$ is Young's creep compliance. Obviously $E(t)$ is related to K and $G(t)$, and $e(t)$ is related to k and $g(t)$. (See Reference 5.2.2.2(a).)

The basic problem is the evaluation of the effective viscoelastic properties of a UDC in terms of matrix viscoelastic properties and the elastic properties of the fibers. (It is assumed that the fibers themselves do not exhibit any time-dependent properties.) This problem has been resolved in general fashion in Ref-

erences 5.2.2.2(b) and (c). Detailed analysis shows that the viscoelastic effect in a UDC is significant only for axial shear, transverse shear, and transverse uniaxial stress.

For any of average strains $\bar{\epsilon}_{22}$, $\bar{\epsilon}_{23}$, and $\bar{\epsilon}_{12}$ constant in time, the time-dependent stress response will be

$$\begin{aligned}\bar{\sigma}_{22}(t) &= E_2^*(t) \bar{\epsilon}_{22} \\ \bar{\sigma}_{23}(t) &= 2 G_2^*(t) \bar{\epsilon}_{23} \\ \bar{\sigma}_{12}(t) &= 2 G_1^*(t) \bar{\epsilon}_{12}\end{aligned}\tag{5.2.2.2(h)}$$

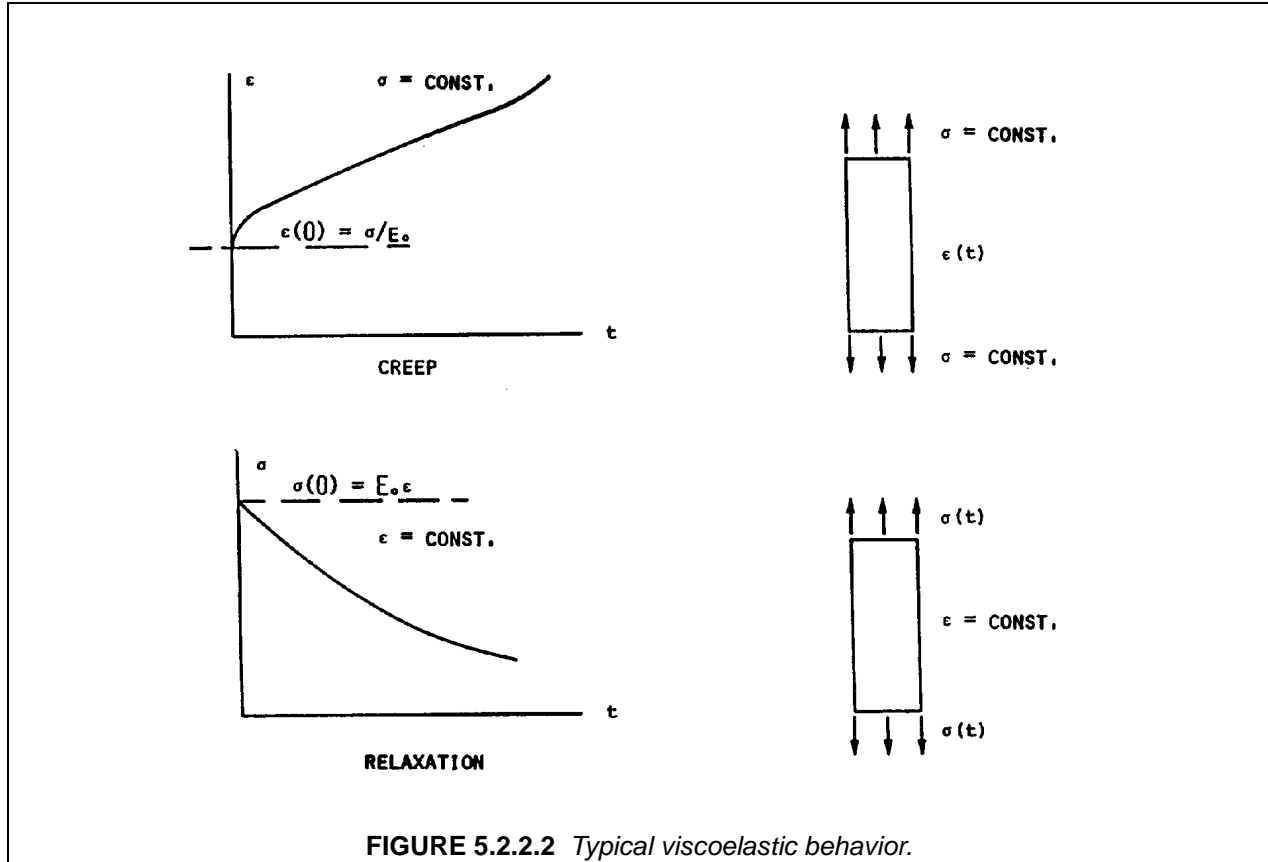


FIGURE 5.2.2.2 Typical viscoelastic behavior.

For any of stresses $\bar{\sigma}_{22}$, $\bar{\sigma}_{23}$, and $\bar{\sigma}_{12}$ constant in time, the time-dependent strain response will be

$$\begin{aligned}\bar{\epsilon}_{22}(t) &= e_2^*(t) \bar{\sigma}_{22} \\ \bar{\epsilon}_{23}(t) &= \frac{1}{2} g_2^*(t) \bar{\sigma}_{23} \\ \bar{\epsilon}_{12}(t) &= \frac{1}{2} g_1^*(t) \bar{\sigma}_{12}\end{aligned}\tag{5.2.2.2(i)}$$

where material properties in Equations 5.2.2.2(h) are effective relaxation moduli and the properties in Equations 5.2.2.2(i) are effective creep functions. All other effective properties may be considered elastic. This implies in particular that if a fiber composite is subjected to stress $\bar{\sigma}_{11}(t)$ in the fiber direction, then

$$\begin{aligned}\bar{\sigma}_{11}(t) &\approx E_1^* \bar{\epsilon}_{11}(t) \\ \bar{\epsilon}_{22}(t) &= \bar{\epsilon}_{33}(t) \approx \nu_{12}^* \bar{\epsilon}_{11}(t)\end{aligned}\tag{5.2.2.2(j)}$$

Volume 3, Chapter 5 Design and Analysis

where E_1^* and ν_{12}^* are the elastic results of Equations 5.2.2.2(k) with matrix properties taken as initial (elastic) matrix properties. Similar considerations apply to the relaxation modulus k^* .

The simplest case of the viscoelastic properties entering into Equations 5.2.2.2(h-i) is the relaxation modulus $G_1^*(t)$ and its associated creep compliance $g_1^*(t)$. A very simple result has been obtained for fibers which are infinitely more rigid than the matrix (Reference 5.2.2(a)). For a viscoelastic matrix, the results reduce to

$$\begin{aligned} G_1^*(t) &= G_m(t) \frac{1 + \nu_f}{1 - \nu_f} \\ g_1^*(t) &= g_m(t) \frac{1 - \nu_f}{1 + \nu_f} \end{aligned} \quad 5.2.2.2(k)$$

This results in an acceptable approximation for glass fibers in a polymeric matrix and an excellent approximation for boron fibers in a polymeric matrix. However, the result is not applicable to the case of carbon or graphite fibers in a polymeric matrix since the axial shear modulus of these fibers is not large enough relative to the matrix shear modulus. In this case, it is necessary to use the correspondence principle mentioned above (References 5.2.2(a) and 5.2.2.2(b)). The situation for transverse shear is more complicated and involves complex Laplace transform inversion. (Reference 5.2.2.2(c)).

All polymeric matrix viscoelastic properties such as creep and relaxation functions are significantly temperature dependent. If the temperature is known, all of the results from this section can be obtained for a constant temperature by using the matrix properties at that temperature. At elevated temperatures, the viscoelastic behavior of the matrix may become nonlinear. In this event, the UDC will also be nonlinearly viscoelastic and all of the results given here are not valid. The problem of analytical determination of nonlinear properties is, of course, much more difficult than the linear problem (See Reference 5.2.2.2(d)).

5.2.2.3 Thermal expansion and moisture swelling

The elastic behavior of composite materials discussed in Section 5.2.2.1 is concerned with externally applied loads and deformations. Deformations are also produced by temperature changes and by absorption of moisture in two similar phenomena. A change of temperature in a free body produces thermal strains while moisture absorption produces swelling strains. The relevant physical parameters to quantify these phenomena are thermal expansion coefficients and swelling coefficients.

Fibers have significantly smaller thermal expansion coefficients than do polymeric matrices. The expansion coefficient of glass fibers is 2.8×10^{-6} in/in/F° (5.0×10^{-6} m/m/C°) while a typical epoxy value is 30×10^{-6} in/in/F° (54×10^{-6} m/m/C°). Carbon and graphite fibers are anisotropic in thermal expansion. The expansion coefficients in the fiber direction are extremely small, either positive or negative of the order of 0.5×10^{-6} in/in/F° (0.9×10^{-6} m/m/C°). To compute these stresses, it is necessary to know the thermal expansion coefficients of the layers. Procedures to determine these coefficients in terms of the elastic properties and expansion coefficients of component fibers and matrix are discussed in this section.

When a laminate absorbs moisture, there occurs the same phenomenon as in the case of heating. Again, the swelling coefficient of the fibers is much smaller than that of the matrix. Free swelling of the layers cannot take place and consequently internal stresses develop. These stresses can be calculated if the UDC swelling coefficients are known.

Consider a free cylindrical specimen of UDC under uniform temperature change ΔT . Neglecting transient thermal effects, the stress-strain relations (Equation 5.2.2.1(c)) assume the form

$$\begin{aligned}
\bar{\varepsilon}_{11} &= \frac{1}{E_1^*} \bar{\sigma}_{11} - \frac{\nu_{12}^*}{E_1^*} \bar{\sigma}_{22} - \frac{\nu_{12}^*}{E_1^*} \bar{\sigma}_{33} + \alpha_1^* \Delta T \\
\bar{\varepsilon}_{22} &= -\frac{\nu_{12}^*}{E_1^*} \bar{\sigma}_{11} + \frac{1}{E_2^*} \bar{\sigma}_{22} - \frac{\nu_{23}^*}{E_2^*} \bar{\sigma}_{33} + \alpha_2^* \Delta T \\
\bar{\varepsilon}_{33} &= -\frac{\nu_{12}^*}{E_1^*} \bar{\sigma}_{11} - \frac{\nu_{23}^*}{E_2^*} \bar{\sigma}_{22} + \frac{1}{E_2^*} \bar{\sigma}_{33} + \alpha_2^* \Delta T
\end{aligned}
\tag{5.2.2.3(a)}$$

where

α_1^* - effective axial expansion coefficient

α_2^* - effective transverse expansion coefficient

It has been shown by Levin (Reference 5.2.2.3(a)) that there is a unique mathematical relationship between the effective thermal expansion coefficients and the effective elastic properties of a two-phase composite. When the matrix and fibers are isotropic

$$\begin{aligned}
\alpha_1^* &= \alpha_m + \frac{\alpha_f - \alpha_m}{\frac{1}{K_f} - \frac{1}{K_m}} \left[\frac{3(1 - 2\nu_{12}^*)}{E_1^*} - \frac{1}{K_m} \right] \\
\alpha_2^* &= \alpha_m + \frac{\alpha_f - \alpha_m}{\frac{1}{K_f} - \frac{1}{K_m}} \left[\frac{3}{2k^*} - \frac{3(1 - 2\nu_{12}^*)}{E_1^*} - \frac{1}{K_m} \right]
\end{aligned}
\tag{5.2.2.3(b)}$$

where

α_m, α_f - matrix, fiber isotropic expansion coefficients

K_m, K_f - matrix, fiber three-dimensional bulk modulus

E_1^*, ν_{12}^*, k^* - effective axial Young's modulus, axial Poisson's ratio, and transverse bulk modulus

These equations are suitable for glass/epoxy and boron/epoxy. They have also been derived in References 5.2.2.3(b) and (c). For carbon and graphite fibers, it is necessary to consider the case of transversely isotropic fibers. This complicates the results considerably as shown in Reference 5.2.2.1(c) and (e).

Frequently thermal expansion coefficients of the fibers and matrix are functions of temperature. It is not difficult to show that Equations 5.2.2.3(b) remain valid for temperature-dependent properties if the elastic properties are taken at the final temperature and the expansion coefficients are taken as secant at that temperature.

To evaluate the thermal expansion coefficients from Equation 5.2.2.3(b) or (c), the effective elastic properties, k^* , E_1^* , and ν_{12}^* must be known. These may be taken as the values predicted by Equations 5.2.2.1(j-l) with the appropriate modification when the fibers are transversely isotropic. Figures 5.2.2.3(a) and (b) shows typical plots of the effective thermal expansion coefficients of graphite/epoxy.

When a composite with polymeric matrix is placed in a wet environment, the matrix will begin to absorb moisture. The moisture absorption of most fibers used in practice is negligible; however, aramid fibers alone absorb significant amounts of moisture when exposed to high humidity. The total moisture absorbed by an aramid/epoxy composite, however, may not be substantially greater than other epoxy composites.

Volume 3, Chapter 5 Design and Analysis

When a composite has been exposed to moisture and sufficient time has elapsed, the moisture concentration throughout the matrix will be uniform and the same as the boundary concentration. It is customary to define the specific moisture concentration c by

$$c = C/\rho \quad 5.2.2.3(c)$$

where ρ is the density. The swelling strains due to moisture are functions of Δc and the swelling coefficients, β_{ij}

$$\varepsilon_{ij} = \beta_{ij} \Delta c \quad 5.2.2.3(d)$$

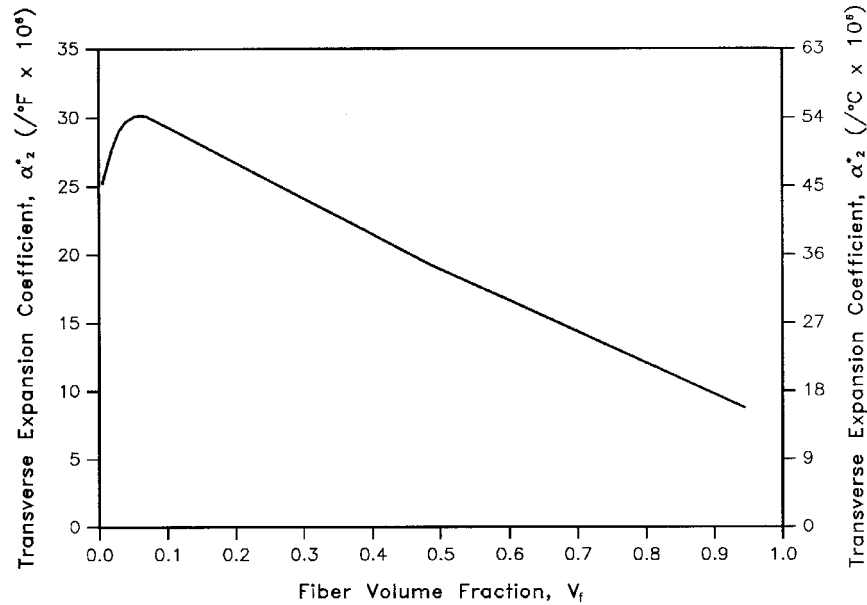


FIGURE 5.2.2.3(a) Effect of fiber volume on thermal expansion for representative carbon/epoxy composite. E_{if} 50 Msi (340 GPa).

If there are also mechanical stresses and strains, then the swelling strains are superposed on the latter. This is exactly analogous to the thermoelastic stress-strain relations of an isotropic material. The effective swelling coefficients β_{ij}^* are defined by the average strains produced in a free sample subjected to a uniform unit change of specific moisture concentration in the matrix. For discussions of other aspects of moisture absorption, both transient and steady state, see References 5.2.2.3(d) and (e).

Finally, simultaneous moisture swelling and thermal expansion, or hygrothermal behavior can be considered. The simplest approach is to assume that the thermal expansion strains and the moisture swelling strains can be superposed. For a free specimen,

$$\begin{aligned} \bar{\varepsilon}_{11} &= \alpha_1^* \Delta T + \beta_1^* \Delta c \\ \bar{\varepsilon}_{22} = \bar{\varepsilon}_{33} &= \alpha_2^* \Delta T + \beta_2^* \Delta c \end{aligned} \quad 5.2.2.3(e)$$

Volume 3, Chapter 5 Design and Analysis

In this event, the matrix elastic properties in Equations 5.2.2.3(a) and (b) may be functions of the final temperature and moisture concentration. This dependence must be known to evaluate α_1^* , α_2^* , β_1^* , and β_2^* in Equation 5.2.2.3(e).

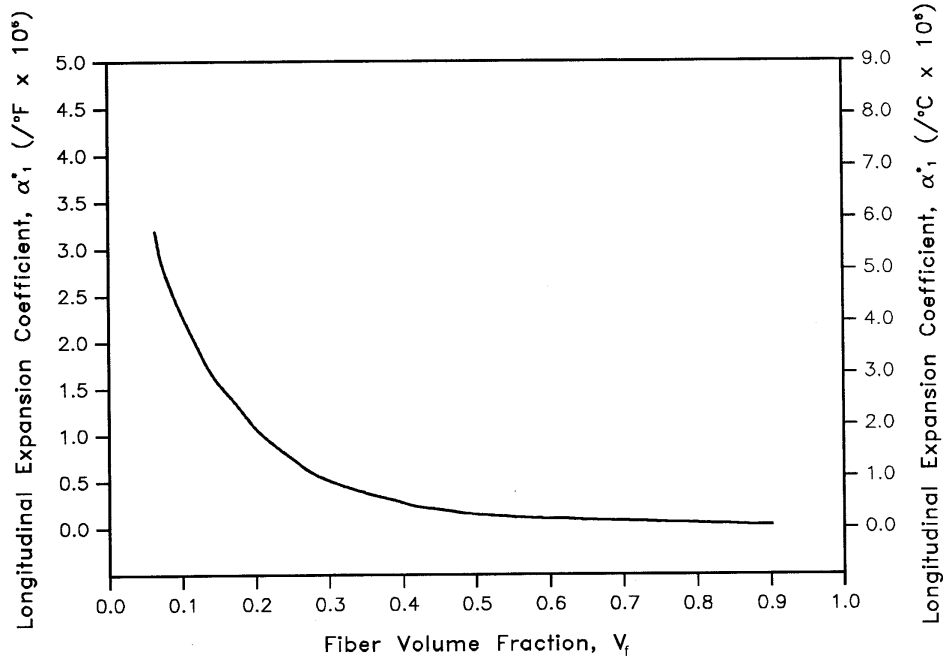


FIGURE 5.2.2.3(b) Effect of fiber volume on thermal expansion for representative carbon/epoxy composite. $E_{lf} = 50 \text{ Msi (340 GPa)}$.

5.2.2.4 Thermal conduction and moisture diffusion

The thermal conduction analysis has many similarities with the analyses for moisture diffusion, as well as electrical conduction, and dielectric and magnetic properties. Since these conductivity problems are governed by similar equations, the results can be applied to each of these areas.

Let $T(x)$ be a steady state temperature field in a homogeneous body. The temperature gradient is given by

$$H_i = \frac{\partial T}{\partial x_i} \quad 5.2.2.4(a)$$

and the heat flux vector by

$$D_i = \mu_{ij} H_j \quad 5.2.2.4(b)$$

where μ_{ij} is the conductivity tensor. It may be shown (Reference 5.2.2(a)) that for isotropic matrix and fibers, the axial conductivity μ_1^* is given by

$$\mu_1^* = \mu_m v_m + \mu_f v_f \quad 5.2.2.4(c)$$

and for transversely isotropic fibers

$$\mu_1^* = \mu_m v_m + \mu_{Lf} v_f \quad 5.2.2.4(d)$$

where μ_{Lf} is the longitudinal conductivity of the fibers. The results of Equations 5.2.2.4(c) and (d) are valid for any fiber distribution and any fiber cross-section.

The problem of transverse conductivity is mathematically analogous to the problem of longitudinal shearing (Reference 5.2.2(a)). All results for the effective longitudinal shear modulus G_1^* can be interpreted as results for transverse effective conductivity μ_2^* . In particular, for the composite cylinder assemblage model

$$\begin{aligned} \mu_2^* &= \mu_m \left[\frac{\mu_m v_m + \mu_f (1 + v_f)}{\mu_m (1 + v_f) + \mu_f v_m} \right] \\ &= \mu_m + \frac{v_f}{\frac{1}{(\mu_f - \mu_m)} + \frac{v_m}{2\mu_m}} \end{aligned} \quad 5.2.2.4(e)$$

These results are for isotropic fibers. For carbon and graphite fibers μ_f should be replaced by the transverse conductivity μ_{2f} of the fibers (Reference 5.2.2.1(e)). As in the elastic case, there is reason to believe that Equation 5.2.2.4(e) accurately represents all cases of circular fibers which are randomly distributed and not in contact. Again the hexagonal array numerical analysis results coincide with the number predicted by Equation 5.2.2.4(e).

To interpret the results for the case of moisture diffusivity, the quantity μ_m is interpreted as the diffusivity of the matrix. Since moisture absorption of fibers is negligible, μ_f is set equal to zero. The results are then

$$\begin{aligned} \mu_1^* &= \mu_m v_m \\ \mu_2^* &= \mu_m \frac{v_m}{1 + v_f} \end{aligned} \quad 5.2.2.4(f)$$

These equations describe the moisture diffusivity of a composite material.

5.2.3 Fiber composites: strength and failure

The mathematical treatment of the relationships between the strength of a composite and the properties of its constituents is considerably less developed than the analysis for the other physical property relationships discussed in Section 5.2.2. Failure is likely to initiate in a local region due to the influence of the local values of constituent properties and the geometry in that region. This dependence upon local characteristics of high variability makes the analysis of the composite failure mechanisms much more complex than the analyses of the physical properties previously discussed.

Because of the complexity of the failure process, it may be desirable to regard the strength of a unidirectional fiber composite subjected to a single principal stress component as a quantity to be measured experimentally, rather than deduced from constituent properties. Such an approach may well be the practical one for fatigue failure of these composites. Indeed, the issue of determining the degree to which heterogeneity should be considered in the analysis of composite strength and failure is a matter for which there exists a considerable degree of difference of opinion. At the level of unidirectional composites, it is well to examine the effects upon failure of the individual constituents to develop an understanding of the nature of the possible failure mechanisms. This subject is discussed in the following sections. The general issue of the approach to failure analysis is treated further in laminate strength and failure.

The strength of a fiber composite clearly depends upon the orientation of the applied load with respect to the direction in which the fibers are oriented as well as upon whether the applied load is tensile or compressive. The following sections present a discussion of failure mechanisms and composite-constituent property relations for each of the principal loading conditions.

5.2.3.1 Axial tensile strength

One of the most attractive properties of advanced fiber composites is high tensile strength. The simplest model for the tensile failure of a unidirectional fiber composite subjected to a tensile load in the fiber direction is based upon the elasticity solution of uniform axial strain throughout the composite. Generally, the fibers have a lower strain to failure than the matrix, and composite fracture occurs at the failure strain of the fibers alone. This results in a composite tensile strength, F_1^u , given by:

$$F_1^u = v_f F_f^u + v_m \sigma_m^f \quad 5.2.3.1$$

where F_f^u - the fiber tensile strength
 σ_m^f - the stress in the matrix at a strain equal to the fiber failure strain

The problem with this approach is the variability of the fiber strength. Non-uniform strength is characteristic of most current high-strength fibers. There are two important consequences of a wide distribution of individual fiber strengths. First, all fibers will not be stressed to their maximum value simultaneously. Secondly, those fibers which break earliest during the loading process will cause perturbations of the stress field near the break, resulting in localized high fiber-matrix interface shear stresses. These shear stresses transfer the load across the interface and also introduce stress concentrations into adjacent unbroken fibers.

The stress distribution at each local fiber break may cause several possible failure events to occur. The shear stresses may cause a crack to progress along the interface. If the interface is weak, such propagation can be extensive. In this case, the strength of the composite material may differ only slightly from that of a bundle of unbonded fibers. This undesirable mode of failure can be prevented by a strong fiber-matrix interface or by a soft ductile matrix which permits the redistribution of the high shear stresses. When the bond strength is high enough to prevent interface failure, the local stress concentrations may cause the fiber break to propagate through the matrix, to and through adjacent fibers. Alternatively, the stress concentration in adjacent fibers may cause one or more of such fibers to break before failure of the intermediate matrix. If such a crack or such fiber breaks continue to propagate, the strength of the composite may be no greater than that of the weakest fiber. This failure mode is defined as a weakest link failure. If the matrix and interface properties are of sufficient strength and toughness to prevent or arrest these failure mechanisms, then continued load increases will produce new fiber failures at other locations in the material. An accumulation of dispersed internal damage results.

It can be expected that all of these effects will occur before material failure. That is, local fractures will propagate for some distance along the fibers and normal to the fibers. These fractures will initiate and grow at various points within the composite. Increasing the load will produce a statistical accumulation of dispersed damage regions until a sufficient number of such regions interact to provide a weak surface, resulting in composite tensile failure.

5.2.3.1.1 Weakest link failure

The weakest link failure model assumes that a catastrophic mode of failure is produced with the occurrence of one, or a small number of, isolated fiber breaks. The lowest stress at which this type of failure can occur is the stress at which the first fiber will break. The expressions for the expected value of the weakest element in a statistical population (e.g., Reference 5.2.3.1.1(a)) have been applied by Zweben (Reference 5.2.3.1.1(b)) to determine the expected stress at which the first fiber will break. For practical materials in realistic structures, the calculated weakest link failure stress is quite small and, in general, failure cannot be expected in this mode.

5.2.3.1.2 Cumulative weakening failure

If the weakest link failure mode does not occur, it is possible to continue loading the composite. With increasing stress, fibers will continue to break randomly throughout the material. When a fiber breaks, there is a redistribution of stress near the fracture site. The treatment of a fiber as a chain of links is ap-

proprate to the hypothesis that fracture is due to local imperfections. The links may be considered to have a statistical strength distribution which is equivalent to the statistical flaw distribution along the fibers. Additional details for this model are given in References 5.2.3.1.1(a) and 5.2.3.1.2. The cumulative weakening model does not consider the overstress on adjacent fibers or the effect of adjacent laminae.

5.2.3.1.3 Fiber break propagation failure

The effects of stress perturbations on fibers adjacent to broken fibers are significant. The load concentration in the fibers adjacent to a broken fiber increases the probability that a second fiber will break. Such an event will increase the probability of additional fiber breaks, and so on. The fiber break propagation mode of failure was studied by Zweben (Reference 5.2.3.1.1(b)). The occurrence of the first fracture of an overstressed fiber was proposed as a measure of the tendency for fiber breaks to propagate, and, hence, as a failure criterion for this mode. Although the first multiple break criterion may provide good correlations with experimental data for small volumes of material, it gives very low failure stress predictions for large volumes of material. Additional work in this area can be found in References 5.2.3.1.3(a) and (b).

5.2.3.1.4 Cumulative group mode failure

As multiple broken fiber groups grow, the magnitude of the local axial shear stress increases and axial cracking can occur. The cumulative group mode failure model (Reference 5.2.3.1.4) includes the effects of the variability of fiber strength, load concentrations in fibers adjacent to broken fibers, and matrix shear failure or interfacial debonding which will serve to arrest the propagating cracks. As the stress level increases from that at which fiber breaks are initiated to that at which the composite fails, the material will have distributed groups of broken fibers. This situation may be considered as a generalization of the cumulative weakening model. In practical terms, the complexity of this model limits its use.

Each of these models has severe limitations for the quantitative prediction of tensile strength. However, the models show the importance of variability of fiber strength and matrix stress-strain characteristics upon composite tensile strength.

5.2.3.2 Axial compressive strength

Both strength and stability failures must be considered for compressive loads applied parallel to the fibers of a unidirectional composite. Microbuckling is one proposed failure mechanism for axial compression (Reference 5.2.3.2(a)). Small wave-length micro-instability of the fibers occurs in a manner analogous to the buckling of a beam on an elastic foundation. It can be demonstrated that this instability can occur even for a brittle material such as glass. Analyses of this instability were performed independently in References 5.2.3.2(b) and (c). The energy method for evaluation of the buckling stress has been used for these modes. This procedure considers the composite as stressed to the buckling load. The strain energy in this compressed but straight pattern (extension mode) is then compared to an assumed buckling deformation pattern (shear mode) under the same load. The change in strain energy in the fiber and the matrix can be compared to the change in potential energy associated with the shortening of the distance between the applied loads at the ends of the fiber. The condition for instability is given by equating the strain energy change to the work done by the external loads during buckling.

The results for the compressive strength, F_1^{cu} , for the extension mode is given by

$$F_1^{cu} = 2 v_f \sqrt{\frac{v_f E_m E_f}{3(1 - v_f)}} \quad 5.2.3.2(a)$$

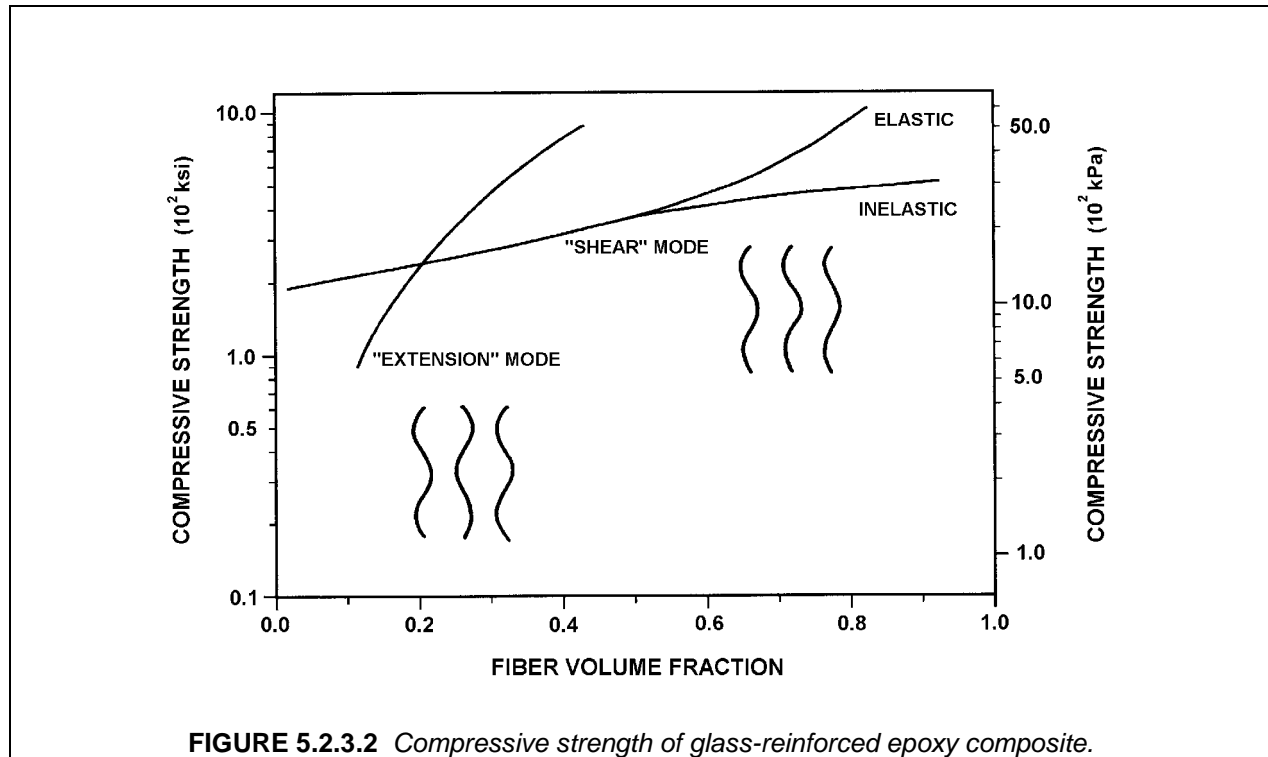
The result for the shear mode is

$$F_1^{cu} = \frac{G_m}{1 - v_f} \quad 5.2.3.2(b)$$

The compressive strength of the composite is plotted as a function of the fiber volume fraction, v_f , in Figure 5.2.3.2 for E-glass fibers embedded in an epoxy matrix. The compressive strength of glass-reinforced plastic, with a fiber volume fraction of 0.6 to 0.7, is on the order of 460 to 600 ksi (3100 to 4100 MPa). Values of this magnitude do not appear to have been measured for any realistic specimens. However, the achievement of a strength of half a million psi in a composite of this type would require an average shortening greater than 5%. For the epoxy materials used in this calculation, such a shortening would result in a decrease in the effective shear stiffness of the matrix material since the proportional limit of the matrix would be exceeded. Hence, it is necessary to modify the analysis to consider the inelastic deformation of the matrix. As a first approximation, the matrix modulus in Equations 5.2.3.2(a) and (b) can be replaced by a reduced modulus. A more general result can be obtained by modeling the matrix as an elastic, perfectly plastic material. For this matrix, the secant value at each axial strain value may be assumed to govern the instability. These assumptions (Reference 5.2.3.2(d)) yield the following result for the shear mode:

$$F_1^{cu} = \sqrt{\frac{v_f E_f F^{cpl}}{3(1 - v_f)}} \quad 5.2.3.2(c)$$

where F^{cpl} is the matrix yield stress level.



For the generally dominant shear mode, the elastic results of Equation 5.2.3.2(b) are independent of the fiber modulus, yet the compressive strength of boron/epoxy is much greater than that of glass/epoxy composites. One hypothesis to explain this discrepancy, is that use of the stiffer boron fibers yields lower matrix strains and less of a strength reduction due to inelastic effects. Thus, the results of Equation 5.2.3.2(c) show a ratio of $\sqrt{6}$ or 2.4 for the relative strengths of boron compared to glass fibers in the same matrix.

All of the analytical results above indicate that compressive strength is independent of fiber diameter. Yet different diameter fibers may yield different compressive strengths for composites because large di-

ameter fibers such as boron (0.005 inch, 0.13 mm D) are better collimated than small diameter fibers, such as glass (0.0004 in, 0.010 mm D). For small diameter fibers, such as aramid and carbon, local out-of-straightness can introduce matrix shear stresses, cause fiber debonding, and produce lower instability stress levels (References 5.2.3.2(e) and 5.2.2.1(d)). Carbon and aramid fibers are anisotropic and have extremely low axial shear moduli. As a result, the elastic buckling stress in the shear mode is reduced to:

$$F_{ccr} = \frac{G_m}{1 - \nu_f(1 - G_m / G_{lf})} \quad 5.2.3.2(d)$$

where G_{lf} is the fiber longitudinal shear modulus (Reference 5.2.3.2(e)). For high fiber shear moduli, this equation reduces to Equation 5.2.3.2(b).

Another failure mechanism for oriented polymeric fibers such as aramid fibers (Reference 5.2.3.2(e)) is a kink-band formation at a specific angle to the direction of compressive stress. The formation of kink-bands is attributed to the fibrillar structure of the highly anisotropic fiber and poor fiber shear strength. Breakup of the fiber into very small diameter fibrils results in degradation of shear stiffness and hence the compressive strength.

The results of the compressive strength analyses indicate that for the elastic case, the matrix Young's modulus is the dominant parameter. For the inelastic case, however, there are strength limitations which depend both upon the fiber modulus and upon the matrix strength. For some materials, performance is limited by a matrix yield strength at a given fiber modulus. For other materials, a gain in compressive strength can be achieved by improving the matrix modulus.

5.2.3.3 Matrix mode strength

The remaining failure modes of interest are transverse tension and compression and axial shear. For each of these loading conditions, material failure can occur without fracture of the fibers, hence the terminology "matrix-dominated" or "matrix modes of failure". Micromechanical analyses of these failure modes are complex because the critical stress states are in the matrix, are highly non-uniform, and are very dependent upon the local geometry. As a result, it appears that the most fruitful approaches will be those that consider average states of stress.

There are two types of shearing stresses which are of interest for these matrix-dominated failures: (1) in a plane which contains the filaments, and (2) in a plane normal to the filaments. In the first case, the filaments provide very little reinforcement to the composite and the shear strength depends on the shear strength of the matrix material. In the second case, some reinforcement may occur; at high volume fractions of filaments, the reinforcement may be substantial. It is important to recognize that filaments provide little resistance to shear in any surfaces parallel to them.

The approach to shear failure analysis is to consider that a uniaxial fibrous composite is comprised of elastic-brittle fibers embedded in an elastic-perfectly plastic matrix. For the composite, the theorems of limit analysis of plasticity (e.g., References 5.2.3.3(a) and (b)) may be used to obtain upper and lower bounds for a composite limit load (Reference 5.2.3.3(c)). The limit load is defined as the load at which the matrix yield stress permits composite deformation to increase with no increase in load. The failure strength of a ductile matrix may be approximated by this limit load.

5.2.4 Strength under combined stress

It is possible to apply the micro-mechanical models for failure described above, to combined stresses in the principal directions. Little work of this type has been done however. Generally the strengths in principal directions have been used in a failure surface for a homogeneous, anisotropic material for estimation of strength under combined loads. The understanding of failure mechanisms resulting from the above micro-mechanical models can be used to define the general form of failure surface to be utilized. This approach is outlined in the following sections.

Knowledge of the different failure mechanisms and quantitative experimental data for a UDC under single stress components can be used to formulate practical failure criteria for combined stresses. Plane

Volume 3, Chapter 5 Design and Analysis

stress failure criteria are discussed below with references also given for more complicated stress systems. The stresses considered are averaged over a representative volume element. The fundamental assumption is that there exists a failure criterion of the form:

$$F(\sigma_{11}, \sigma_{22}, \sigma_{12}) = 1 \quad 5.2.4(a)$$

which characterizes the failure of the UDC. The usual approach to construction of a failure criterion is to assume a quadratic form in terms of stress or strain since the quadratic form is the simplest form which can adequately describe the experimental data. The various failure criteria which have been proposed all use coefficients based on experimental information such as ultimate stresses under single load components (References 5.2.4(a) - (d)). For example, the general quadratic version of Equation 5.2.4(a) for plane stress would be:

$$\begin{aligned} C_{11}\sigma_{11}^2 + C_{22}\sigma_{22}^2 + C_{66}\sigma_{12}^2 + 2C_{12}\sigma_{11}\sigma_{22} + 2C_{16}\sigma_{11}\sigma_{12} \\ + 2C_{26}\sigma_{22}\sigma_{12} + C_1\sigma_{11} + C_2\sigma_{22} + C_6\sigma_{12} = 1 \end{aligned} \quad 5.2.4(b)$$

The material has different strengths in uniaxial, longitudinal, and transverse tension and compression. Evidently the shear strength is not affected by the sign of the shear stress. It follows that all powers of shear stress in the failure criterion must be even. Consequently, the criterion simplifies to

$$C_{11}\sigma_{11}^2 + C_{22}\sigma_{22}^2 + C_{66}\sigma_{12}^2 + 2C_{12}\sigma_{11}\sigma_{22} + C_1\sigma_{11} + C_2\sigma_{22} = 1 \quad 5.2.4(c)$$

The ultimate stresses under single component stress conditions for each of σ_{11} , σ_{22} , and σ_{12} determine the constants for the failure criterion.

$$\begin{aligned} C_{11} &= \frac{1}{F_1^{tu} F_1^{cu}} & C_{22} &= \frac{1}{F_2^{tu} F_2^{cu}} \\ C_1 &= \frac{1}{F_1^{tu}} - \frac{1}{F_1^{cu}} & C_2 &= \frac{1}{F_2^{tu}} - \frac{1}{F_2^{cu}} \\ C_{66} &= \frac{1}{(F_1^{su})^2} \end{aligned} \quad 5.2.4(d)$$

However, C_{12} cannot be determined from the single component ultimate stresses. Biaxial stress tests must be performed to determine this coefficient. Frequently, the coefficient is established by relating Equation 5.2.4(c) to the Mises-Henky yield criterion for isotropic materials, yielding

$$C_{12} = -\frac{1}{2}(C_{11}C_{22})^{1/2} \quad 5.2.4(e)$$

The above failure criterion is the two-dimensional version of the Tsai-Wu criterion (Reference 5.2.4(c)). Its implementation raises several problems; the most severe of these is that the failure criterion ignores the diversity of failure modes which are possible.

The identification of the different failure modes of a UDC can provide physically more realistic, and also simpler, failure criteria (Reference 5.2.4(e)). Testing a polymer matrix UDC reveals that tensile stress in the fiber direction produces a jagged, irregular failure surface. Tensile stress transverse to the surface produces a smooth, straight failure surface (See Figures 5.2.4(a) and (b)). Since the carrying capacity deterioration in the tensile fiber mode is due to transverse cracks and the transverse stress σ_{22} has no effect on such cracks, it is assumed that the plane tensile fiber mode is only dependent on the stresses σ_{11} and σ_{12} .

For compressive σ_{11} , failure is due to fiber buckling in the shear mode and the transverse stress σ_{22} has little effect on the compressive failure. In this *compressive fiber mode*, failure again depends primarily on σ_{11} . The dependence on σ_{12} is not known and arguments may be made for and against including it in the failure criterion.

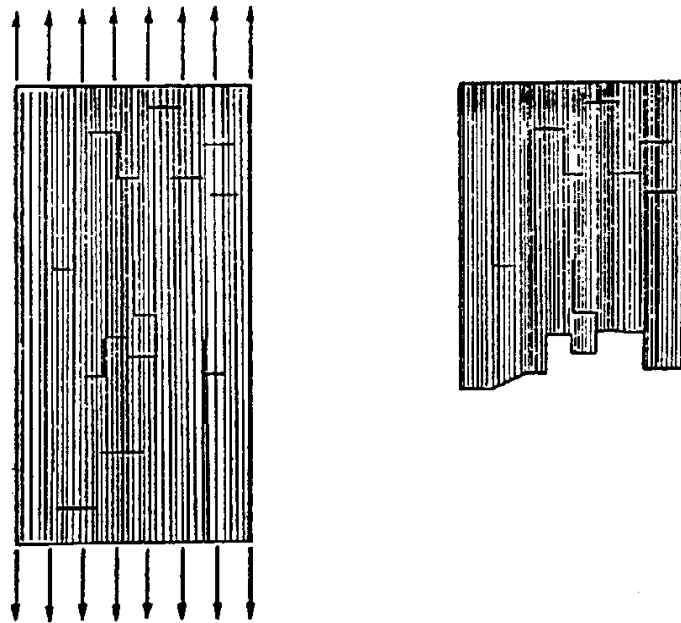


FIGURE 5.2.4(a) *Tensile fiber failure mode.*

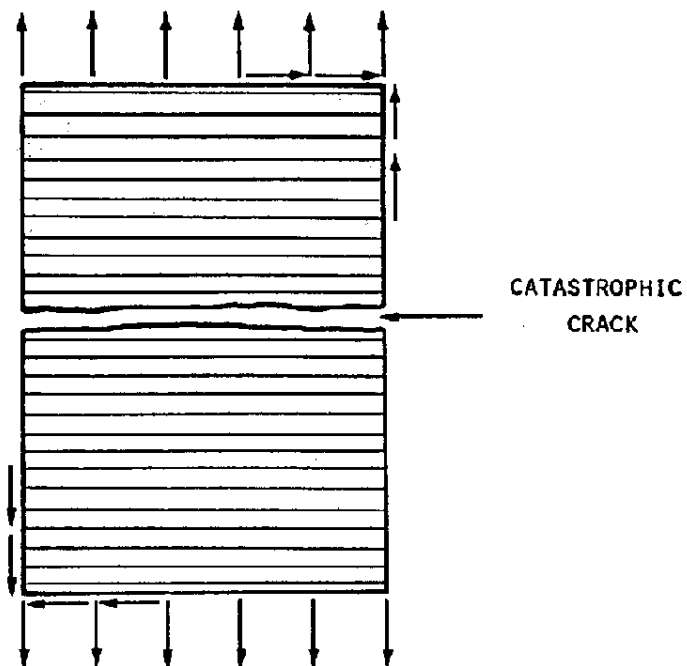


FIGURE 5.2.4(b) *Tensile matrix failure mode.*

Volume 3, Chapter 5 Design and Analysis

For tension transverse to the fibers, the *tensile matrix mode*, failure occurs by a sudden crack in the fiber direction as shown in Figure 5.2.4(b). Since stress in the fiber direction has no effect on a crack in the fiber direction, this failure mode is dependent only on σ_{22} and σ_{12} .

For compressive stress transverse to the fibers, failure occurs on some plane parallel to the fibers, but not necessarily normal to σ_{22} . This *compressive matrix mode* is produced by normal stress and shear stress on the failure plane. Again, the stress σ_{11} does not effect this failure.

Each of the failure modes described can be modeled separately by a quadratic polynomial (Reference 5.2.4(e)). This approach provides four individual failure criteria. Note the choice of stress components included in each of these criteria, and the particular mathematical form used, are subjects which are not yet fully resolved. The following criteria appear to a reasonable set with which the different modes of failure can be handled separately.

Fiber modes

Tensile

$$\left(\frac{\sigma_{11}}{F_1^{tu}}\right)^2 + \left(\frac{\sigma_{12}}{F_{12}^{su}}\right)^2 = 1 \quad 5.2.4(f)$$

Compressive

$$\left(\frac{\sigma_{11}}{F_1^{cu}}\right)^2 + \left(\frac{\sigma_{12}}{F_{12}^{su}}\right)^2 = 1 \quad 5.2.4(g)$$

Matrix modes

Tensile

$$\left(\frac{\sigma_{22}}{F_2^{tu}}\right)^2 + \left(\frac{\sigma_{12}}{F_{12}^{su}}\right)^2 = 1 \quad 5.2.4(h)$$

Compressive

$$\left(\frac{\sigma_{22}}{2 F_{23}^{su}}\right)^2 + \left[\left(\frac{F_2^{cu}}{2 F_{23}^{su}}\right)^2 - 1\right] \left(\frac{\sigma_{22}}{F_2^{cu}}\right) + \left(\frac{\sigma_{12}}{F_{12}^{su}}\right)^2 = 1 \quad 5.2.4(i)$$

Note that F_2^{cu} in Equation 5.2.4(i) should be taken as the absolute value. The ultimate transverse shear stress, $\sigma_{23} = F_{23}^{su}$, is very difficult to measure. A reasonable approximation for this quantity is the ultimate shear stress for the matrix. For any given state of stress, one each of Equations 5.2.4(f) and (g) and Equations 5.2.4(h) and (i) are chosen according to the signs of σ_{11} and σ_{22} . The stress components are introduced into the appropriate pair and whichever criterion is satisfied first is the operative criterion.

The advantages are Equations 5.2.4(f) - (i) are:

1. The failure criteria are expressed in terms of single component ultimate stresses. No biaxial test results are needed.
2. The failure mode is identified by the criterion which is satisfied first.

The last feature is of fundamental importance for analysis of fiber composite structural elements, since it permits identification of the nature of initial damage. Moreover, in conjunction with a finite element analysis, it is possible to identify the nature of failure in elements, modify their stiffnesses accordingly, and proceed with the analysis to predict new failures.

5.2.5 Summary

- Composite strength analysis is most commonly performed, by industry, on the macromechanics level given that the analysis of composite materials uses effective lamina properties based on average stress and strain.
- Ply level stresses are the commonly used approach to laminate strength analysis.
- Lamina stress/strain is influenced by many properties of interest, but is dominated by mechanical load and environmental sensitivity.
- Stress-strain elastic behavior, in its simplest form, may be described as a function of a composite materials constitutive properties (i.e., E , G , ν , α).
- Several practical failure criteria exist today that: 1) depend upon cross-ply laminate coupon data to determine lamina stress/strain allowables and 2) identify the failure mode based on the allowable that is first exceeded by its stress/strain counterpart.

5.3 ANALYSIS OF LAMINATES

5.3.1 Lamina stress-strain relations

A laminate is composed of unidirectionally-reinforced laminae oriented in various directions with respect to the axes of the laminate. The stress-strain relations developed in the Section 5.2 must be transformed into the coordinate system of the laminate to perform the laminate stress-strain analysis. A new system of notation for the lamina elastic properties is based on x_1 in the fiber direction, x_2 transverse to the fibers in the plane of the lamina, and x_3 normal to the plane of the lamina.

$$\begin{aligned} E_1 &= E_1^* & \nu_{12} &= \nu_{12}^* \\ E_2 &= E_3 = E_2^* & \nu_{23} &= \nu_{23}^* \\ G_{12} &= G_1^* & G_{23} &= G_2^* \end{aligned} \quad 5.3.1(a)$$

In addition, the laminae are now treated as effective homogeneous, transversely isotropic materials.

$$\begin{Bmatrix} \epsilon_{11} \\ \epsilon_{22} \\ \epsilon_{33} \\ 2\epsilon_{23} \\ 2\epsilon_{13} \\ 2\epsilon_{12} \end{Bmatrix} = \begin{bmatrix} \frac{1}{E_1} & \frac{-\nu_{12}}{E_1} & \frac{-\nu_{12}}{E_1} & 0 & 0 & 0 \\ \frac{-\nu_{12}}{E_1} & \frac{1}{E_2} & \frac{-\nu_{23}}{E_2} & 0 & 0 & 0 \\ \frac{-\nu_{12}}{E_1} & \frac{-\nu_{23}}{E_2} & \frac{1}{E_2} & 0 & 0 & 0 \\ 0 & 0 & 0 & \frac{1}{G_{23}} & 0 & 0 \\ 0 & 0 & 0 & 0 & \frac{1}{G_{12}} & 0 \\ 0 & 0 & 0 & 0 & 0 & \frac{1}{G_{12}} \end{bmatrix} \begin{Bmatrix} \sigma_{11} \\ \sigma_{22} \\ \sigma_{33} \\ \sigma_{23} \\ \sigma_{13} \\ \sigma_{12} \end{Bmatrix} \quad 5.3.1(b)$$

It has become common practice in the analysis of laminates to utilize engineering shear strains rather than tensor shear strains. Thus the factor of two has been introduced into the stress-strain relationship of Equation 5.3.1(b).

The most important state of stress in a lamina is plane stress, where

$$\sigma_{13} = \sigma_{23} = \sigma_{33} = 0 \quad 5.3.1(c)$$

Volume 3, Chapter 5 Design and Analysis

since it occurs from both in-plane loading and bending at sufficient distance from the laminate edges. The plane stress version of Equation 5.3.1(b) is

$$\begin{Bmatrix} \varepsilon_{11} \\ \varepsilon_{22} \\ \varepsilon_{12} \end{Bmatrix} = \begin{bmatrix} \frac{1}{E_1} & \frac{-\nu_{12}}{E_1} & 0 \\ \frac{-\nu_{12}}{E_1} & \frac{1}{E_2} & 0 \\ 0 & 0 & \frac{1}{G_{12}} \end{bmatrix} \begin{Bmatrix} \sigma_{11} \\ \sigma_{22} \\ \sigma_{12} \end{Bmatrix} \quad 5.3.1(d)$$

which may be written as

$$\{\varepsilon_\ell\} = [S]\{\sigma_\ell\} \quad 5.3.1(e)$$

Here [S], the compliance matrix, relates the stress and strain components in the principal material directions. These are called laminae coordinates and are denoted by the subscript ℓ .

Equation 5.3.1(d) relates the in-plane strain components to the three in-plane stress components. For the plane stress state, the three additional strains can be found to be

$$\begin{aligned} \varepsilon_{23} = \varepsilon_{13} &= 0 \\ \varepsilon_{33} &= -\sigma_{11} \frac{\nu_{13}}{E_1} - \sigma_{22} \frac{\nu_{23}}{E_2} \end{aligned} \quad 5.3.1(f)$$

and the complete state of stress and strain is determined.

The relations 5.3.1(d) can be inverted to yield

$$\{\sigma_\ell\} = [S]^{-1}\{\varepsilon_\ell\} \quad 5.3.1(g)$$

or

$$\{\sigma_\ell\} = [Q]\{\varepsilon_\ell\} \quad 5.3.1(h)$$

The matrix [Q] is defined as the inverse of the compliance matrix and is known as the reduced lamina stiffness matrix. Its terms can be shown to be

$$[Q] = \begin{bmatrix} Q_{11} & Q_{12} & 0 \\ Q_{12} & Q_{22} & 0 \\ 0 & 0 & Q_{66} \end{bmatrix} \quad 5.3.1(i)$$

$$\begin{aligned} Q_{11} &= \frac{E_1}{1 - \nu_{12}^2} \frac{E_2}{E_1} & Q_{12} &= \frac{\nu_{12} E_2}{1 - \nu_{12}^2} \frac{E_2}{E_1} \\ Q_{22} &= \frac{E_2}{1 - \nu_{12}^2} \frac{E_2}{E_1} & Q_{66} &= G_{12} \end{aligned} \quad 5.3.1(j)$$

In the notation for the [Q] matrix, each pair of subscripts of the stiffness components is replaced by a single subscript according to the following scheme.

$$\begin{array}{lll} 11 \rightarrow 1 & 22 \rightarrow 2 & 33 \rightarrow 3 \\ 23 \rightarrow 4 & 31 \rightarrow 5 & 12 \rightarrow 6 \end{array}$$

Volume 3, Chapter 5 Design and Analysis

The reduced stiffness and compliance matrices 5.3.1(i) and (d) relate stresses and strains in the principal material directions of the material. To define the material response in directions other than these coordinates, transformation relations for the material stiffnesses are needed.

In Figure 5.3.1(a), two sets of coordinate systems are depicted. The 1-2 coordinate system corresponds to the principal material directions for a lamina, while the x-y coordinates are arbitrary and related to the 1-2 coordinates through a rotation about the axis out of the plane of the figure. The angle θ is defined as the rotation from the arbitrary x-y system to the 1-2 material system.

The transformation of stresses from the 1-2 system to the x-y system follows the rules for transformation of tensor components.

$$\begin{Bmatrix} \sigma_{xx} \\ \sigma_{yy} \\ \sigma_{xy} \end{Bmatrix} = \begin{bmatrix} m^2 & n^2 & -2mn \\ n^2 & m^2 & 2mn \\ mn & -mn & m^2 - n^2 \end{bmatrix} \begin{Bmatrix} \sigma_{11} \\ \sigma_{22} \\ \sigma_{12} \end{Bmatrix} \quad 5.3.1(k)$$

or

$$\{\sigma_x\} = [\theta] \{\sigma_l\} \quad 5.3.1(l)$$

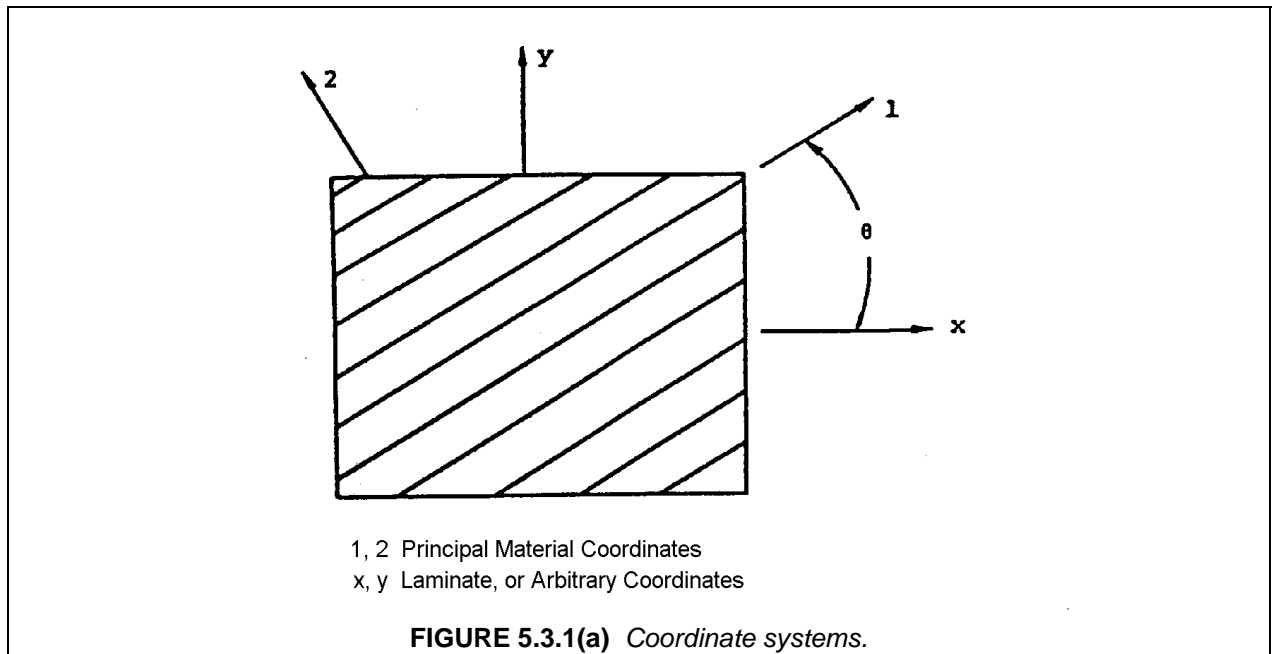
where $m = \cos \theta$, and $n = \sin \theta$. In these relations, the subscript x is used as shorthand for the laminate coordinate system.

The same transformation matrix $[\theta]$ can also be used for the tensor strain components. However, since the engineering shear strains have been utilized, a different transformation matrix is required.

$$\begin{Bmatrix} \epsilon_{xx} \\ \epsilon_{yy} \\ 2\epsilon_{xy} \end{Bmatrix} = \begin{bmatrix} m^2 & n^2 & -mn \\ n^2 & m^2 & mn \\ 2mn & -2mn & m^2 - n^2 \end{bmatrix} \begin{Bmatrix} \epsilon_{11} \\ \epsilon_{22} \\ 2\epsilon_{12} \end{Bmatrix} \quad 5.3.1(m)$$

or

$$\{\epsilon_x\} = [\psi] \{\epsilon_l\} \quad 5.3.1(n)$$



Given the transformations for stress and strain to the arbitrary coordinate system, the relations between stress and strain in the laminate system can be determined.

$$\{\sigma_x\} = [\bar{Q}]\{\epsilon_x\} \quad 5.3.1(o)$$

The reduced stiffness matrix $[\bar{Q}]$ relates the stress and strain components in the laminate coordinate system.

$$[\bar{Q}] = [\theta][Q][\psi]^{-1} \quad 5.3.1(p)$$

The terms within $[\bar{Q}]$ are defined to be

$$\begin{aligned} \bar{Q}_{11} &= Q_{11}m^4 + Q_{22}n^4 + 2m^2n^2(Q_{12} + 2Q_{66}) \\ \bar{Q}_{12} &= m^2n^2(Q_{11} + Q_{22} - 4Q_{66}) + (m^4 + n^4)Q_{12} \\ \bar{Q}_{16} &= [Q_{11}m^2 - Q_{22}n^2 - (Q_{12} + 2Q_{66})(m^2 - n^2)]mn \\ \bar{Q}_{22} &= Q_{11}n^4 + Q_{22}m^4 + 2m^2n^2(Q_{12} + 2Q_{66}) \\ \bar{Q}_{26} &= [Q_{11}n^2 - Q_{22}m^2 + (Q_{12} + 2Q_{66})(m^2 - n^2)]mn \\ \bar{Q}_{66} &= (Q_{11} + Q_{22} - 2Q_{12})m^2n^2 + Q_{66}(m^2 - n^2)^2 \\ \bar{Q}_{21} &= \bar{Q}_{12} \quad \bar{Q}_{61} = \bar{Q}_{16} \quad \bar{Q}_{62} = \bar{Q}_{26} \end{aligned} \quad 5.3.1(q)$$

where the subscript 6 has been retained in keeping with the discussion following Equation 5.3.1(j).

$$[\bar{Q}] = \begin{bmatrix} \bar{Q}_{11} & \bar{Q}_{12} & \bar{Q}_{16} \\ \bar{Q}_{21} & \bar{Q}_{22} & \bar{Q}_{26} \\ \bar{Q}_{16} & \bar{Q}_{26} & \bar{Q}_{66} \end{bmatrix} \quad 5.3.1(r)$$

A feature of $[\bar{Q}]$ matrix which is immediately noticeable is that $[\bar{Q}]$ is fully-populated. The additional terms which have appeared in $[\bar{Q}]$, \bar{Q}_{16} and \bar{Q}_{26} , relate shear strains to extensional loading and vice versa. This effect of a shear strain resulting from an extensional strain is depicted in Figure 5.3.1(b). From Equations 5.3.1(q), these terms are zero for θ equal to 0° or 90° . Physically, this means that the fibers are parallel or perpendicular to the loading direction. For this case, extensional-shear coupling does not occur for an orthotropic material since the loadings are in the principal directions. The procedure used to develop the transformed stiffness matrix can also be used to find a transformed compliance matrix.

$$\{\epsilon_\ell\} = [S]\{\sigma_\ell\} \quad 5.3.1(s)$$

$$\{\epsilon_x\} = [\psi][S][\theta]^{-1}\{\sigma_x\} \quad 5.3.1(t)$$

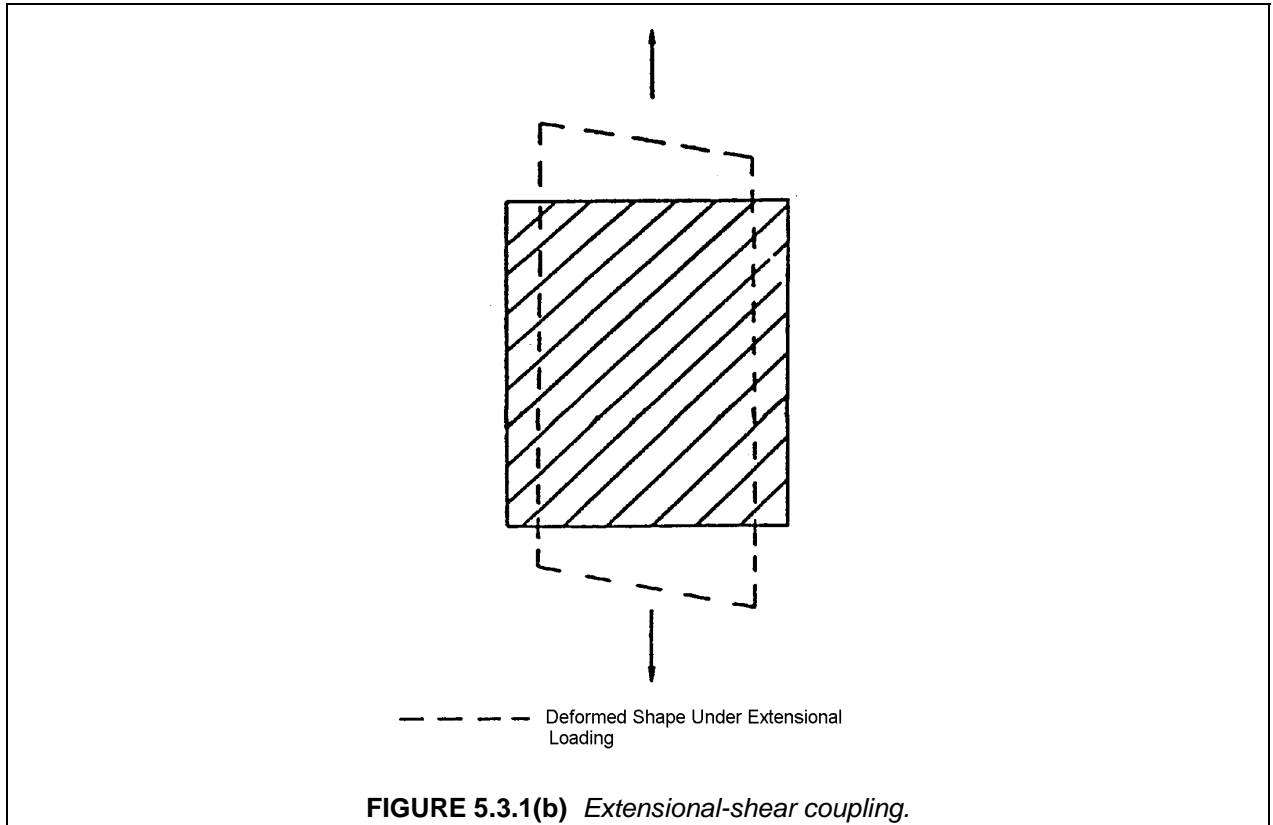
$$\{\epsilon_x\} = [\bar{S}]\{\sigma_x\} \quad 5.3.1(u)$$

Noting that the stress-strain relations are now defined in the laminate coordinate system, lamina stiffnesses can also be defined in this system. Thus, expanding the last of Equations 5.3.1(s) - (u):

$$\begin{Bmatrix} \epsilon_{xx} \\ \epsilon_{yy} \\ 2\epsilon_{xy} \end{Bmatrix} = \begin{bmatrix} \bar{S}_{11} & \bar{S}_{12} & \bar{S}_{16} \\ \bar{S}_{21} & \bar{S}_{22} & \bar{S}_{26} \\ \bar{S}_{16} & \bar{S}_{26} & \bar{S}_{66} \end{bmatrix} \begin{Bmatrix} \sigma_{xx} \\ \sigma_{yy} \\ \sigma_{xy} \end{Bmatrix} \quad 5.3.1(v)$$

The engineering constants for the material can be defined by specifying the conditions for an experiment. For $\sigma_{yy} = \sigma_{xy} = 0$, the ratio $\sigma_{xx} / \epsilon_{xx}$ is Young's modulus in the x direction. For this same stress state, $-\epsilon_{yy} / \epsilon_{xx}$ is Poisson's ratio. In this fashion, the lamina stiffnesses in the coordinate system of Equations 5.3.1(s) - (u) are found to be:

$$\begin{aligned} E_x &= \frac{1}{\bar{S}_{11}} & E_y &= \frac{1}{\bar{S}_{22}} \\ G_{xy} &= \frac{1}{\bar{S}_{66}} & \nu_{xy} &= \frac{-\bar{S}_{21}}{\bar{S}_{11}} = \frac{-\bar{S}_{12}}{\bar{S}_{11}} \end{aligned} \quad 5.3.1(w)$$



It is sometimes desirable to obtain elastic constants directly from the reduced stiffnesses, $[\bar{Q}]$, by using Equations 5.3.1(o). In the general case where the \bar{Q}_{ij} matrix is fully populated, this can be accomplished by using Equations 5.3.1(w) and the solution for \bar{S}_{ij} as functions of \bar{Q}_{ij} obtained from the inverse relationship of the two matrices. An alternative approach is to evaluate extensional properties for the case of zero shear strain. For single stress states and zero shear strain, the elastic constants in terms of the transformed stiffness matrix terms are:

$$E_x = \bar{Q}_{11} - \frac{\bar{Q}_{12}^2}{\bar{Q}_{22}}$$

$$E_y = \bar{Q}_{22} - \frac{\bar{Q}_{12}^2}{\bar{Q}_{11}}$$

$$\nu_{xy} = \frac{\bar{Q}_{12}}{\bar{Q}_{22}} = \frac{\bar{Q}_{21}}{\bar{Q}_{11}}$$
5.3.1(x)

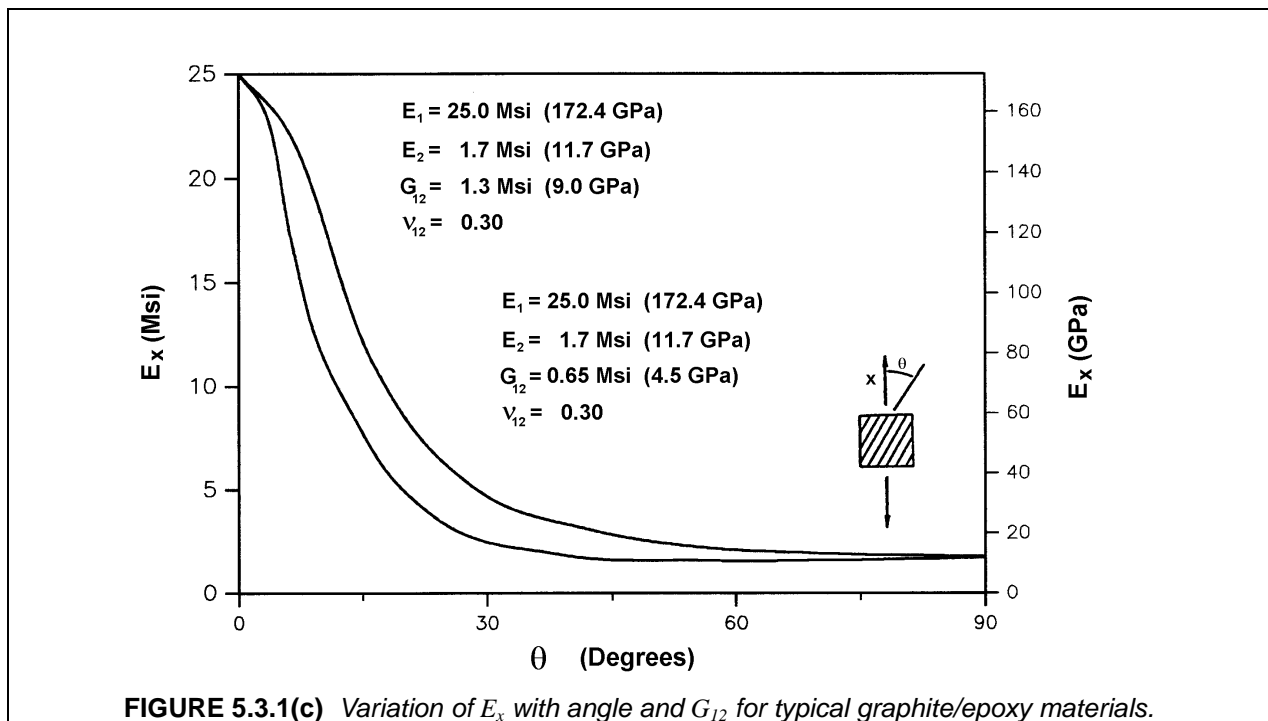
Also,

$$G_{xy} = \bar{Q}_{66}$$

From the terms in the $[\bar{Q}]$ matrix (Equation 5.3.1(q)) and the stiffness relations (Equation 5.3.1(x)), the elastic constants in an arbitrary coordinate system are functions of all the elastic constants in the principal material directions as well as the angle of rotation.

The variation of elastic modulus E_x with angle of rotation is depicted in Figure 5.3.1(c) for a typical graphite/epoxy material. For demonstration purposes, two different shear moduli have been used in generating the figure. The differences between the two curves demonstrate the effect of the principal material shear modulus on the transformed extensional stiffness. The two curves are identical at 0° and 90° , as expected since E_x is simply E_1 or E_2 . Between these two endpoints, substantial differences are present. For the smaller shear modulus, the extensional stiffness is less than the E_2 value from approximately 50° to just less than 90° . For these angles, the material stiffness is more strongly governed by the principal material shear modulus than by the transverse extensional modulus. The curves of Figure 5.3.1(c) can also be used to determine the modulus E_y by simply reversing the angle scale.

With the transformed stress-strain relations, it is now possible to develop an analysis for an assemblage of plies, i.e., a laminate.



5.3.2 Lamination theory

The development of procedures to evaluate stresses and deformations of laminates is crucially dependent on the fact that the thickness of laminates is much smaller than the in-plane dimensions. Typical thickness values for individual plies range between 0.005 and 0.010 inch (0.13 and 0.25 mm). Consequently, laminates using from 8 to 50 plies are still generally thin plates and, therefore, can be analyzed on the basis of the usual simplifications of thin plate theory.

In the analysis of isotropic thin plates it has become customary to analyze the cases of in-plane loading and bending separately. The former case is described by plane stress elastic theory and the latter by classical plate bending theory. This separation is possible since the two loadings are uncoupled for symmetric laminates; when both occur, the results are superposed.

The classical assumptions of thin plate theory are:

1. The thickness of the plate is much smaller than the in-plane dimensions;
2. The shapes of the deformed plate surface are small compared to unity;
3. Normals to the undeformed plate surface remain normal to the deformed plate surface;
4. Vertical deflection does not vary through the thickness; and
5. Stress normal to the plate surface is negligible.

On the basis of assumptions (2) - (4), the displacement field can be expressed as:

$$\begin{aligned} u_z &= u_z^{\circ}(x, y) \\ u_x &= u_x^{\circ}(x, y) - z \frac{\partial u_z}{\partial x} \\ u_y &= u_y^{\circ}(x, y) - z \frac{\partial u_z}{\partial y} \end{aligned} \quad 5.3.2(a)$$

with the x - y - z coordinate system defined in Figure 5.3.2(a). These relations (Equation 5.3.2(a)) indicate that the in-plane displacements consist of a mid-plane displacement, designated by the superscript ($^{\circ}$), plus a linear variation through the thickness. The two partial derivatives are bending rotations of the mid-surface. The use of assumption (4) prescribes that u_z does not vary through the thickness.

The linear strain displacement relations are

$$\begin{aligned} \epsilon_{xx} &= \frac{\partial u_x}{\partial x} & \epsilon_{yy} &= \frac{\partial u_y}{\partial y} \\ \epsilon_{xy} &= \frac{1}{2} \left(\frac{\partial u_x}{\partial y} + \frac{\partial u_y}{\partial x} \right) \end{aligned} \quad 5.3.2(b)$$

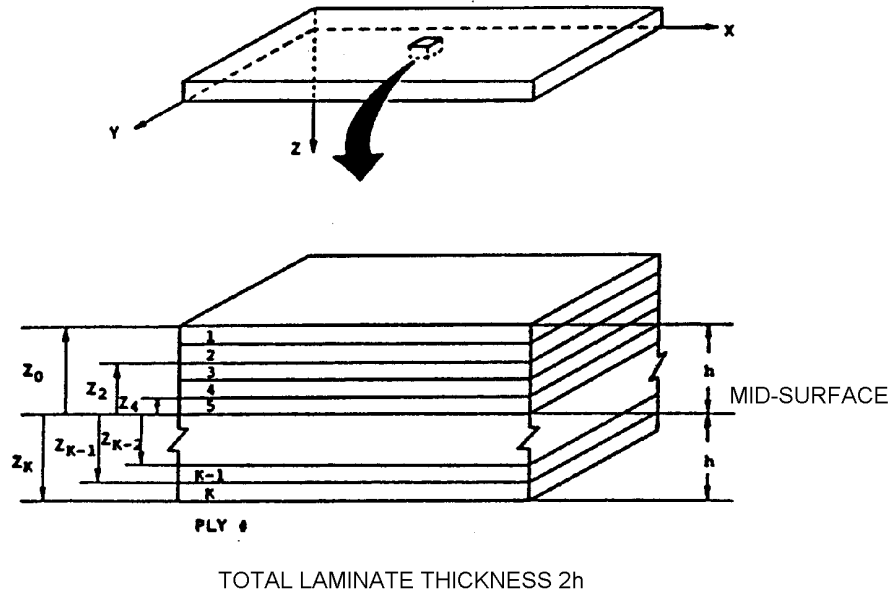
and performing the required differentiations yields

$$\begin{aligned} \epsilon_{xx} &= \epsilon_{xx}^{\circ} + z \kappa_{xx} \\ \epsilon_{yy} &= \epsilon_{yy}^{\circ} + z \kappa_{yy} \\ 2 \epsilon_{xy} &= 2 \epsilon_{xy}^{\circ} + 2 z \kappa_{xy} \end{aligned} \quad 5.3.2(c)$$

or

$$\{\epsilon_x\} = \{\epsilon^{\circ}\} + z \{\kappa\} \quad 5.3.2(d)$$

where

**FIGURE 5.3.2(a)** *Laminate construction.*

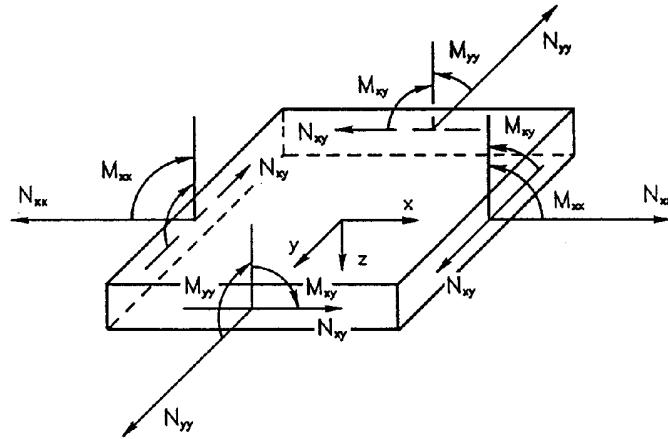
$$\{\varepsilon^{\circ}\} = \begin{Bmatrix} \frac{\partial u_x^{\circ}}{\partial x} \\ \frac{\partial u_y^{\circ}}{\partial y} \\ \left[\frac{\partial u_x^{\circ}}{\partial y} + \frac{\partial u_y^{\circ}}{\partial x} \right] \end{Bmatrix} \quad 5.3.2(e)$$

and

$$\{\kappa\} = \begin{pmatrix} \kappa_{xx} \\ \kappa_{yy} \\ \kappa_{xy} \end{pmatrix} = \begin{pmatrix} -\frac{\partial^2 u_z}{\partial x^2} \\ -\frac{\partial^2 u_z}{\partial y^2} \\ -2\frac{\partial^2 u_x}{\partial x \partial y} \end{pmatrix} \quad 5.3.2(f)$$

The strain at any point in the plate is defined as the sum of a mid-surface strain $\{\varepsilon^{\circ}\}$, and a curvature $\{\kappa\}$ multiplied by the distance from the mid-surface.

For convenience, stress and moment resultants will be used in place of stresses for the remainder of the development of lamination theory (see Figure 5.3.2(b)). The stress resultants are defined as



$$\{N\} = \int_{-h}^h \{\sigma_x\} dz$$

$$\{M\} = \int_{-h}^h \{\sigma_x\} z dz$$

FIGURE 5.3.2(b) Stress and moment resultants.

$$\{N\} = \begin{pmatrix} N_{xx} \\ N_{yy} \\ N_{xy} \end{pmatrix} = \int_{-h}^h \{\sigma_x\} dz \quad 5.3.2(g)$$

and the moment resultants are defined as

$$\{M\} = \begin{pmatrix} M_{xx} \\ M_{yy} \\ M_{xy} \end{pmatrix} = \int_{-h}^h \{\sigma_x\} z dz \quad 5.3.2(h)$$

where the integrations are carried out over the plate thickness.

Noting Equations 5.3.1(o) and 5.3.2(c), relations between the stress and moment resultants and the mid-plane strains and curvatures can be written as

$$\{N\} = \int_{-h}^h \{\sigma_x\} dz = \int_{-h}^h [\bar{Q}] (\{\epsilon^0\} + z\{\kappa\}) dz \quad 5.3.2(i)$$

$$\{M\} = \int_{-h}^h \{\sigma_x\} z dz = \int_{-h}^h [\bar{Q}] (\{\epsilon^0\} + z\{\kappa\}) z dz \quad 5.3.2(j)$$

Since the transformed lamina stiffness matrices are constant within each lamina and the mid-plane strains and curvatures are constant with respect to the z-coordinate, the integrals in Equations 5.3.2(i) and (j) can be replaced by summations.

Introducing three matrices equivalent to the necessary summations, the relations can be written as

$$\{N\} = [A]\{\epsilon^0\} + [B]\{\kappa\} \quad 5.3.2(k)$$

$$\{M\} = [B]\{\varepsilon^o\} + [D]\{\kappa\} \quad 5.3.2(l)$$

where the stiffness matrix is composed of the following 3x3 matrices:

$$\begin{aligned} [A] &= \sum_{i=1}^N [\bar{Q}]^i (z_i - z_{i-1}) \\ [B] &= \frac{1}{2} \sum_{i=1}^N [\bar{Q}]^i (z_i^2 - z_{i-1}^2) \\ [D] &= \frac{1}{3} \sum_{i=1}^N [\bar{Q}]^i (z_i^3 - z_{i-1}^3) \end{aligned} \quad 5.3.2(m)$$

where N is the total number of plies, z_i is defined in Figure 5.3.2(a) and subscript i denotes a property of the i th ply. Note that $z_i - z_{i-1}$ equals the ply thickness. Here the reduced lamina stiffnesses for the i th ply are found from Equations 5.3.2(k) and (l) using the principal properties and orientation angle for each ply in turn. Thus, the constitutive relations for a laminate have been developed in terms of stress and moment resultants.

Classical lamination theory has been used to predict the internal stress state, stiffness and dimensional stability of laminated composites (e.g., References 5.3.2(a) - (e)). The constitutive law for CLT couples extensional, shear, bending and torsional loads with strains and curvatures. Residual strains or warpage due to differential shrinkage or swelling of plies in a laminate have also been incorporated in lamination theory using an environmental load analogy (See Sections 5.3.3.3 and 5.3.3.4.). The combined influence of various types of loads and moments on laminated plate response can be described using the ABD matrix from Equations 5.3.2(k) and (l). In combined form:

$$\begin{bmatrix} N_x \\ N_y \\ N_{xy} \\ M_x \\ M_y \\ M_{xy} \end{bmatrix} = \begin{bmatrix} A_{11} & A_{12} & A_{16} & B_{11} & B_{12} & B_{16} \\ A_{12} & A_{22} & A_{26} & B_{12} & B_{22} & B_{26} \\ A_{16} & A_{26} & A_{66} & B_{16} & B_{26} & B_{66} \\ B_{11} & B_{12} & B_{16} & D_{11} & D_{12} & D_{16} \\ B_{12} & B_{22} & B_{26} & D_{12} & D_{22} & D_{26} \\ B_{16} & B_{26} & B_{66} & D_{16} & D_{26} & D_{66} \end{bmatrix} \begin{bmatrix} \varepsilon_x \\ \varepsilon_y \\ \varepsilon_{xy} \\ \kappa_x \\ \kappa_y \\ \kappa_{xy} \end{bmatrix} \quad 5.3.2(n)$$

where N are loads, M are moments, ε are strains, κ are curvatures and

A_{ij} = extensional and shear stiffnesses
 B_{ij} = extension-bending coupling stiffnesses
 D_{ij} = bending and torsional stiffnesses

Several observations regarding lay-up and laminate stacking sequence (LSS) can be made with the help of Equation 5.3.2(n). These include:

- (1) The stiffness matrix A_{ij} in Equation 5.3.2(n) is independent of LSS. Inversion of the stiffness matrix $[ABD]$ yields the compliance matrix $[A'B'D']$. This inversion is necessary in order to calculate strains and curvatures in terms of loads and moments. The inversion results in a relationship between LSS and extension/shear compliances. However, this relationship is eliminated if the laminate is symmetric.
- (2) Nonzero values of A_{16} and A_{26} indicates that there is extension/shear coupling (e.g., longitudinal loads will result in both extensional and shear strains). If a laminate is balanced A_{16} and A_{26} become zero, eliminating extension/shear coupling.

- (3) Nonzero values of B_{ij} indicates that there is coupling between bending/twisting curvatures and extension/shear loads. Traditionally, these couplings have been suppressed for most applications by choosing an LSS that minimizes the values of B_{ij} . All values of B_{ij} become zero for symmetric laminates. Reasons for designing with symmetric laminates include structural dimensional stability requirements (e.g., buckling, environmental warping), compatibility of structural components at joints and the inability to test for strength allowables of specimens that have significant values of B_{ij} .
- (4) In general, the values of D_{ij} are nonzero and strongly dependent on LSS. The average plate bending stiffnesses, torsional rigidity and flexural Poisson's ratio can be calculated per unit width using components of the compliance matrix $[A'B'D']$, i.e.,

$$\begin{aligned} 1/D'_{11} &= \text{bending stiffness about y-axis} \\ 1/D'_{22} &= \text{bending stiffness about x-axis} \\ 1/D'_{66} &= \text{torsional rigidity about x- or y-axis} \\ -D'_{12}/D'_{11} &= \text{flexural Poisson's ratio.} \end{aligned}$$

The D'_{16} and D'_{26} terms should also be included in calculations relating midplane curvatures to moments except when considering a special class of balanced, unsymmetric laminates.

- (5) Nonzero values of D_{16} and D_{26} indicates that there is bending/twisting coupling. These terms will vanish only if a laminate is balanced and if, for each ply oriented at $+\theta$ above the laminate midplane, there is an identical ply (in material and thickness) oriented at $-\theta$ at an equal distance below the midplane. Such a laminate cannot be symmetric, unless it contains only 0° and 90° plies. Bending/twisting coupling can be minimized by alternating the location of $+\theta$ and $-\theta$ plies through the LSS (Section 5.6.5.2.2, Recommendation 5).

Additional information on laminate stacking sequence effects is found in Section 5.6.5.

5.3.3 Laminate properties

The relations between the mid-surface strains and curvatures and the membrane stress and moment resultants are used to calculate plate bending and extensional stiffnesses for structural analysis. The effects of orientation variables upon plate properties are also considered. In addition to the mechanical loading conditions treated thus far, the effects of temperature changes upon laminate behavior must be understood. Further, for polymeric matrix composites, high moisture content causes dimensional changes which can be described by effective swelling coefficients.

5.3.3.1 Membrane stresses

Recalling Equations 5.3.2(k) and (l) and noting that for symmetric laminates the $[B]$ matrix is zero, the relations can be rewritten as

$$\begin{pmatrix} N_{xx} \\ N_{yy} \\ N_{xy} \end{pmatrix} = \begin{bmatrix} A_{11} & A_{12} & A_{16} \\ A_{12} & A_{22} & A_{26} \\ A_{16} & A_{26} & A_{66} \end{bmatrix} \begin{pmatrix} \epsilon_{xx}^o \\ \epsilon_{yy}^o \\ 2\epsilon_{xy}^o \end{pmatrix} \quad 5.3.3.1(a)$$

and

$$\begin{pmatrix} M_{xx} \\ M_{yy} \\ M_{xy} \end{pmatrix} = \begin{bmatrix} D_{11} & D_{12} & D_{16} \\ D_{12} & D_{22} & D_{26} \\ D_{16} & D_{26} & D_{66} \end{bmatrix} \begin{pmatrix} \kappa_{xx} \\ \kappa_{yy} \\ 2\kappa_{xy} \end{pmatrix} \quad 5.3.3.1(b)$$

Since the extensional and bending behavior are uncoupled, effective laminate elastic constants can be readily determined. Inverting the stress resultant mid-plane strain relations yields

$$\{\varepsilon^o\} = [A]^{-1}\{N\} = [a]\{N\} \quad 5.3.3.1(c)$$

from which the elastic constants are seen to be

$$\begin{aligned} E_x &= \frac{1}{2ha_{11}} & G_{xy} &= \frac{1}{2ha_{66}} \\ E_y &= \frac{1}{2ha_{22}} & \nu_{xy} &= -\frac{a_{12}}{a_{11}} \end{aligned} \quad 5.3.3.1(d)$$

where the divisor $2h$ corresponds to the laminate thickness.

Note that the $[A]$ matrix is comprised of $[Q]$ matrices from each layer in the laminate. It is obvious that the laminate elastic properties are functions of the angular orientation of the plies. This angular influence is illustrated in Figure 5.3.3.1 for a typical high modulus carbon/epoxy system which has the lamina properties listed in Table 5.3.3.1(a). The laminae are oriented in $\pm\theta$ pairs in a symmetric, balanced construction, creating what is called an angle-ply laminate.

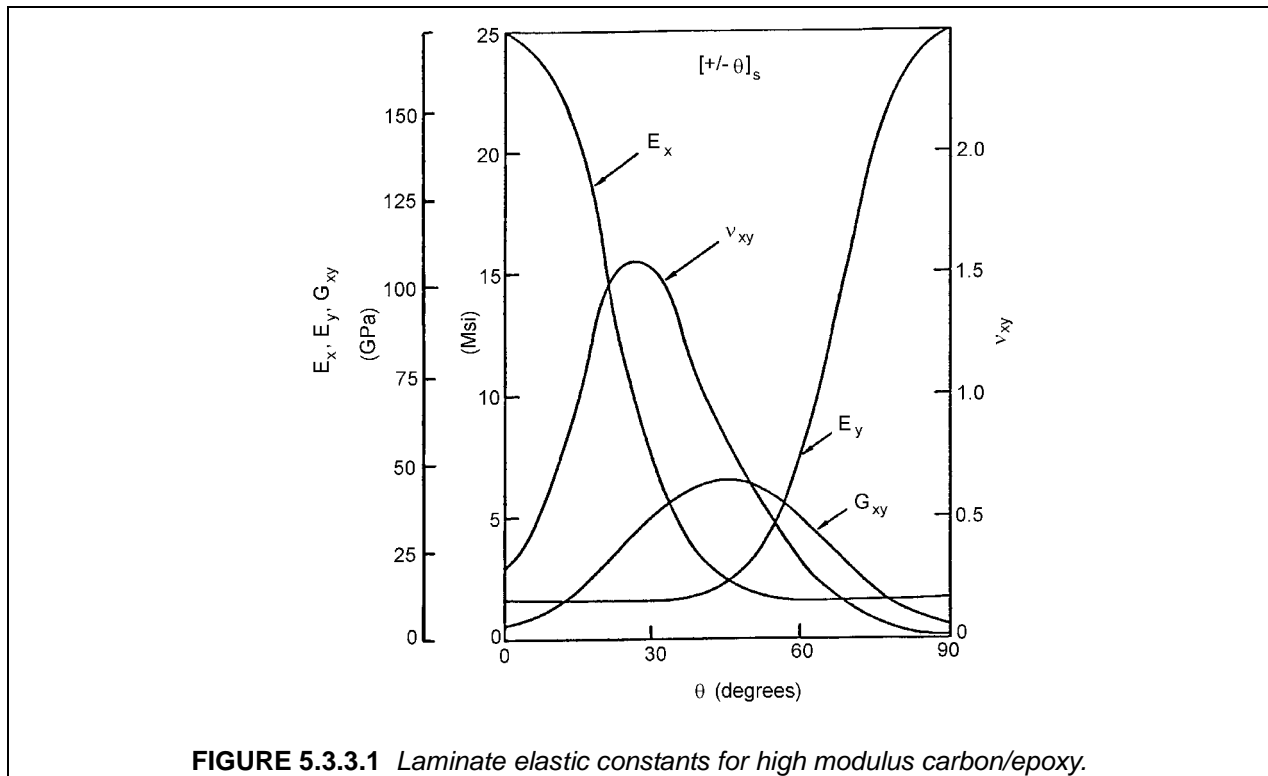


FIGURE 5.3.3.1 *Laminate elastic constants for high modulus carbon/epoxy.*

The variation of shear modulus and Poisson's ratio are noteworthy in Figure 5.3.3.1. The shear modulus is equal to the unidirectional value for 0° and 90° and rises sharply to a maximum at 45° . The peak at 45° can be explained by noting that shear is equivalent to a combined state of tensile and compressive loads oriented at 45° . Thus, the shear loading on a $[\pm 45]_s$ laminate is equivalent to tensile and compressive loading on a $[0/90]_s$ laminate. Effectively, the fibers are aligned with the loading and, hence, with the large shear stiffness.

An even more interesting effect is seen in the variation of Poisson's ratio. The peak value in this example is greater than 1.5. In an isotropic material, this would be impossible. In an orthotropic material, the isotropic restriction does not hold and a Poisson's ratio greater than one is valid and realistic. In fact,

large Poisson's ratios are typical for laminates constructed from unidirectional materials with the plies oriented at approximately 30°.

TABLE 5.3.3.1(a) *Properties of a high-modulus carbon/epoxy lamina.*

$E_1 = 25.0 \text{ Msi} = 172 \text{ GPa}$	$\alpha_1 = 0.30 \times 10^{-6} \text{ in/in/F}^\circ = 0.54 \times 10^{-6} \text{ mm/mm/C}^\circ$
$E_2 = 1.7 \text{ Msi} = 12 \text{ GPa}$	$\alpha_2 = 19.5 \times 10^{-6} \text{ in/in/F}^\circ = 35.1 \times 10^{-6} \text{ mm/mm/C}^\circ$
$G_{12} = 0.65 \text{ Msi} = 4.5 \text{ GPa}$	
$\nu_{12} = 0.30$	
$\rho = 0.056 \text{ lb/in}^3 = 1.55 \text{ g/cm}^3$	
$F_1^{\text{tu}} = 110 \text{ ksi} = 760 \text{ MPa}$	$F_1^{\text{cu}} = 110 \text{ ksi} = 760 \text{ MPa}$
$F_2^{\text{tu}} = 4.0 \text{ ksi} = 28 \text{ MPa}$	$F_2^{\text{cu}} = 20.0 \text{ ksi} = 138 \text{ MPa}$
$F_{12}^{\text{su}} = 9.0 \text{ ksi} = 62 \text{ MPa}$	
$\nu_f = 0.6$	$t_R = 0.0052 \text{ in} = 0.13 \text{ mm}$

Because of the infinite variability of the angular orientation of the individual laminae, one would assume that a laminate having a stiffness which behaves isotropically in the plane of the laminate could be constructed by using many plies having small, equal differences in their orientation. It can be shown that a symmetric, quasi-isotropic laminate can be constructed with as few as six plies as a $[0/\pm 60]_s$ laminate. A general rule for describing a quasi-isotropic laminate states that the angles between the plies are equal to π/N , where N is an integer greater than or equal to 3, and there is an identical number of plies at each orientation in a symmetric laminate. For plies of a given material, all such quasi-isotropic laminates will have the same elastic properties, regardless of the value of N .

A quasi-isotropic laminate has in-plane stiffnesses which follow isotropic relationships

$$E_x = E_y = E_\theta \quad 5.3.3.1(e)$$

where the subscript θ indicates any arbitrary angle. Additionally,

$$G_{xy} = \frac{E_x}{2(1 + \nu_{xy})} \quad 5.3.3.1(f)$$

There are two items which must be remembered about quasi-isotropic laminates. First and foremost, only the elastic in-plane properties are isotropic; the strength properties, in general, will vary with directions. The second item is that two equal moduli $E_x = E_y$ do not necessarily indicate quasi-isotropy, as demonstrated in Table 5.3.3.1(b). The first two laminates in Table 5.3.3.1(b) are actually the same (a $[0/90]_s$ laminate rotated 45° is a $[\pm 45]_s$ laminate). Note that the extensional moduli of these laminates are not the same and that the shear modulus of each laminate is not related to the extensional modulus and Poisson's ratio. For these laminates, the π/N relation has not been satisfied and they are not quasi-isotropic. The third laminate has plies oriented at 45° to each other but there are not equal numbers of plies at each angle. This laminate is also not quasi-isotropic.

This discussion of symmetric laminates has centered on membrane behavior. Symmetric laminates can be constructed which are very well behaved in the membrane sense. The bending behavior of symmetric laminates is considerably more complex, primarily due to the arrangement of plies through the thickness of the laminate.

TABLE 5.3.3.1(b) *Elastic properties of laminates.*

	$E_x = E_y$	ν_{xy}	G_{xy}
	Msi (GPa)		Msi (GPa)
$[0^\circ/90^\circ]_s$	13.4 (92.5)	0.038	0.65 (4.5)
$[\pm 45^\circ]_s$	2.38 (16.4)	0.829	6.46 (44.5)
$[0^\circ/90^\circ/\pm 45^\circ/-45^\circ/90^\circ/0^\circ]_s$	11.0 (75.6)	0.213	2.59 (17.9)

5.3.3.2 Bending

The equations for bending analysis of symmetric laminates has been developed with the extensional analysis. The first complication that arises in the treatment of laminate bending deals with relationships between the extensional (A) and bending (D) elastic properties. In composite laminates, there is no direct relationship between extensional and bending stiffnesses, unlike the case of a homogeneous material where

$$D = \frac{A(2h)^2}{12} \quad 5.3.3.2(a)$$

In determining the membrane stiffnesses (A), the position of the ply through the thickness of the laminate does not matter (Equation 5.3.2(m)). The relations for the bending stiffnesses are a function of the third power of the distance of the ply from the mid-surface. Therefore, the position of the plies with respect to the mid-surface is critical. The effects of ply position in a unit thickness laminate are shown in Table 5.3.3.2(a).

The three laminates shown in Table 5.3.3.2(a) are all quasi-isotropic. The membrane properties are isotropic and identical for each of the laminates. The bending stiffnesses can be seen to be a strong function of the thickness position of the plies. Additionally, bending stiffness calculations based on homogeneity (Equation 5.3.3.2) do not correspond to lamination theory calculations. Thus, the simple relations between extensional and bending stiffnesses are lost and lamination theory must be used for bending properties. Table 5.3.3.2(a) also demonstrates that quasi-isotropy holds only for extensional stiffnesses.

Another complication apparent in Table 5.3.3.2(a) involves the presence of the bending-twisting coupling terms, D_{16} and D_{26} . The corresponding extensional-shear coupling terms are zero because of the presence of pairs of layers at $\pm 60^\circ$ orientations. Noting that the bending-twisting terms can be of the same order of magnitude as the principal bending terms, D_{11} , D_{22} , and D_{66} , the bending-twisting effect can be severe. This effect can be reduced by the proper selection of stacking sequence.

TABLE 5.3.3.2(a) *Extensional and bending stiffnesses.*

	$[0/\pm 60]_s$	$[\pm 60/0]_s$	$[60/0/-60]_s$	Homogeneous Laminate
A_{11}	1.05×10^7 (7.30×10^{10})	1.05×10^7 (7.30×10^{10})	1.05×10^7 (7.30×10^{10})	1.05×10^7 (7.30×10^{10})
A_{12}	3.42×10^6 (2.38×10^{10})	3.42×10^6 (2.38×10^{10})	3.42×10^6 (2.38×10^{10})	3.42×10^6 (2.38×10^{10})
A_{22}	1.05×10^7 (7.30×10^{10})	1.05×10^7 (7.30×10^{10})	1.05×10^7 (7.30×10^{10})	1.05×10^7 (7.30×10^{10})
A_{66}	3.55×10^6 (2.47×10^{10})	3.55×10^6 (2.47×10^{10})	3.55×10^6 (2.47×10^{10})	3.55×10^6 (2.47×10^{10})
D_{11}	1.55×10^6 (1.08×10^{10})	3.36×10^5 (2.34×10^9)	7.42×10^5 (5.16×10^9)	8.75×10^5 (6.09×10^9)
D_{12}	1.50×10^5 (1.04×10^9)	3.92×10^5 (2.73×10^9)	3.12×10^5 (2.17×10^9)	2.85×10^5 (1.98×10^9)
D_{16}	4.74×10^4 (3.30×10^8)	9.50×10^4 (6.61×10^8)	1.42×10^5 (9.88×10^8)	0.0 (0.0)
D_{22}	4.69×10^5 (3.26×10^9)	1.20×10^6 (8.35×10^9)	9.59×10^5 (6.67×10^9)	8.75×10^5 (6.09×10^9)
D_{26}	1.42×10^5 (9.88×10^8)	2.81×10^5 (1.95×10^9)	4.22×10^5 (2.94×10^9)	0.0 (0.0)
D_{66}	1.63×10^5 (1.13×10^9)	4.04×10^5 (2.81×10^9)	3.23×10^5 (2.25×10^9)	2.96×10^5 (2.06×10^9)

Lamina properties are from Table 5.3.3.1(a); unit thickness laminate.

[A] lb/in (N/m) [D] in-lb (N/m)

Another example that shows how the laminate stacking sequence (LSS) can significantly affect composite behavior is the bending stiffness of a laminated beam with rectangular cross-section ($h \equiv$ laminate thickness). For the purpose of this example, define effective in-plane and bending moduli along the beam axis as

$$E_x = \frac{1}{A'_{11} h} \quad 5.3.3.2(b)$$

$$E_x^b = \frac{12}{D'_{11} h^3} \quad 5.3.3.2(c)$$

respectively. The relationship,

$$\Delta = \frac{E_x^b - E_x}{E_x} \times 100 \quad 5.3.3.2(d)$$

provides a relative measure of the effect of LSS on beam bending stiffness. Bending moduli of laminated beams approach those of homogeneous beams as the number of plies increase provided that there is no preferential stacking of ply orientations through the thickness.

Table 5.3.3.2(b) shows lamination theory predictions of in-plane and effective bending moduli for beams with seven different LSS variations of a 16-ply, carbon/epoxy, quasi-isotropic lay-up.¹ Note that the in-plane moduli are independent of LSS because all lay-ups are symmetric. Bending moduli are

¹The LSS used in Table 5.3.3.2(b) were chosen for illustrative purposes only and do not represent optimal LSS for a given application.

shown to vary significantly above or below the in-plane moduli depending on preferential stacking of 0° plies towards the surface or center of the laminate, respectively.

TABLE 5.3.3.2(b) *Stiffness predictions for seven different LSS for 16-ply, quasi-isotropic, carbon/epoxy, laminated beams.*

Stacking Sequence	In-plane Modulus E_x		Bending Modulus E_x^b		Percent Difference Δ
	Msi	GPa	Msi	GPa	%
$[0_2/(\pm 45)_2/90_2]_s$	7.67	52.9	12.8	88.2	67
$[0/\pm 45/90]_{2s}$	7.67	52.9	10.1	69.6	32
$[\pm 45/0_2/\pm 45/90_2]_s$	7.67	52.9	7.80	53.8	1.7
$[\pm 45/0/90]_{2s}$	7.67	52.9	6.51	44.9	-15
$[(\pm 45)_2/0_2/90_2]_s$	7.67	52.9	4.45	30.7	-42
$[(\pm 45)_2/90_2/0_2]_s$	7.67	52.9	3.42	23.6	-55
$[90_2/(\pm 45)_2/0_2]_s$	7.67	52.9	3.25	22.4	-58

Properties for T300/934 ($V_f = 0.63$): $E_{11} = 20.0$ Msi (138 GPa), $E_{22} = 1.4$ Msi (9.7 GPa), $G_{12} = 0.65$ Msi (4.5 GPa), $\nu_{12} = 0.31$, Ply Thickness = 0.0056 in. (0.14 mm)

In general, the relationship between effective bending moduli and stacking sequence can be more complex than that shown in Table 5.3.3.2(b). Predictions in the table assumed that the basic lamina moduli were constant (i.e., linear elastic behavior). Depending on material type and the degree of accuracy desired, this assumption may lead to poor predictions. Lamina moduli for graphite/epoxy have been shown to depend on environment and strain level. Since flexure results in a distribution of tension and compression strains through the laminate thickness, nonlinear elastic lamination theory predictions may be more appropriate.

The example from Table 5.3.3.2(b) shows a significant effect of LSS on bending moduli of laminated beams. Similarly, calculations with Equation 5.3.2(n) can be used to indicate that LSS has a strong influence on the bending behavior of laminated plates. However, the bending response of common structures may depend more on the resulting moment of inertia, I , for a given geometry than on LSS. This is particularly true for stringer geometries typically used to stiffen composite plates in aerospace structures.

Figure 5.3.3.2 illustrates how structural geometry of a beam section can overshadow the effects of LSS on bending. Web and flange members of each I-beam have LSS indicated in the legend of Figure 5.3.3.2¹ These LSS are the same as those used in Table 5.3.3.2(b). The ordinate axis of the figure indicates a percent difference between laminated and homogeneous beam calculations. As shown in Figure 5.3.3.2, the effect of LSS on the EI of an I-beam diminishes rapidly with increasing web height.

¹The LSS used in Figure 5.3.3.2 were chosen for illustrative purposes only and do not represent optimal LSS for a given application.

Additional information on laminate stacking sequence effects is found in Section 5.6.5.

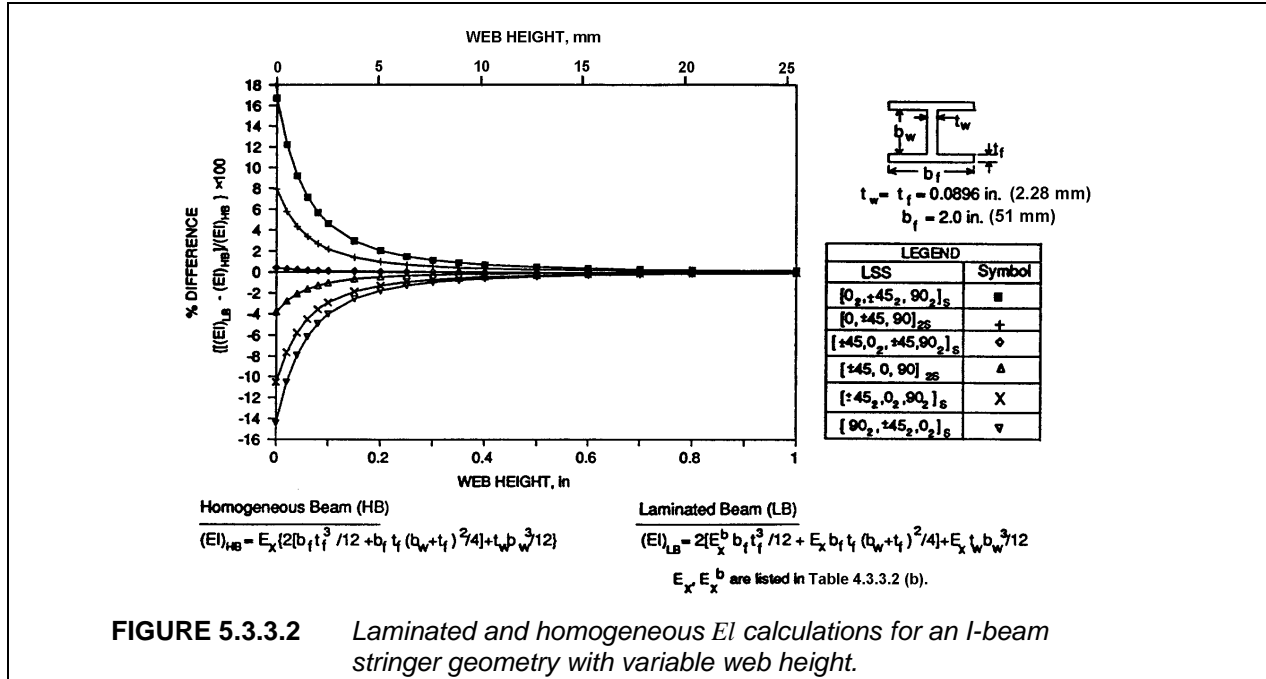


FIGURE 5.3.3.2 Laminated and homogeneous EI calculations for an I-beam stringer geometry with variable web height.

5.3.3.3 Thermal expansion

As the use of composite materials becomes more commonplace, they are subjected to increasingly severe mechanical and environmental loading conditions. With the advent of high temperatures in systems, the range of temperatures over which composite systems can be used has increased. The response of laminates to temperature and moisture, as well as to applied loads, must be understood. Previously, laminate extensional and bending stiffnesses were determined; in this section laminate conductivities and expansion coefficients will be defined.

To determine the laminate thermal expansion coefficients and thermally-induced stresses quantitatively, begin at the ply level. The thermoelastic relations for strain in the principal material directions are

$$\{\epsilon_\ell\} = \{\epsilon_\ell^M\} + \{\alpha_\ell\} \Delta T \quad 5.3.3.3(a)$$

or

$$\{\epsilon_\ell\} = \{\epsilon_\ell^M\} + \{\epsilon_\ell^T\} \quad 5.3.3.3(b)$$

where

$$\{\epsilon_\ell^M\} = \text{strain induced by stress}$$

The change in temperature is represented by ΔT and the vector $\{\alpha_\ell\}$ represents the free thermal expansion coefficients of a ply. The individual components are

$$\{\alpha_\ell\} = \begin{pmatrix} \alpha_1 \\ \alpha_2 \\ 0 \end{pmatrix} \quad 5.3.3.3(c)$$

The thermal strains, $\{\alpha_\ell\} \Delta T$, are the lamina free thermal expansions, which produce no stress in an unconstrained lamina. The thermal expansion coefficients α_1 and α_2 are the effective thermal expansion coefficients α_1^* and α_2^* of the unidirectional composite.

Substituting for the mechanical strain terms in Equation 5.3.3.3(a) and inverting yields

$$\{\sigma_\ell\} = [Q]\{\varepsilon_\ell\} - \{\Gamma_\ell\}\Delta T \quad 5.3.3.3(d)$$

where

$$\{\Gamma_\ell\} = [Q]\{\alpha_\ell\}$$

The components in the thermal stress coefficient vector $\{\Gamma_\ell\}$ are

$$\{\Gamma_\ell\} = \begin{Bmatrix} \frac{E_1 \alpha_1 + \nu_{12} E_2 \alpha_2}{\Delta} \\ \frac{E_2 \alpha_2 + \nu_{12} E_1 \alpha_1}{\Delta} \\ 0 \end{Bmatrix} \quad 5.3.3.3(e)$$

where

$$\Delta = 1 - \frac{E_2}{E_1} \nu_{12}^2$$

The vector $\{\Gamma_\ell\}\Delta T$ physically represents a correction to the stress vector which results from the full constraint of the free thermal strains in a lamina. Both the thermal expansion vector, $\{\alpha_\ell\}\Delta T$, and the thermal stress vector, $\{\Gamma_\ell\}\Delta T$, can be transformed to arbitrary coordinates using the relations developed for stress and strain transformations, Equations 5.3.1(k) - (n).

With the transformed thermal expansion and stress vectors, the thermal elastic laminate relations can be developed. Following directly from the development of Equations 5.3.2(g) - (l), the membrane relations are:

$$\{N\} = [A]\{\varepsilon^\circ\} + [B]\{\kappa\} + \{N^T\} \quad 5.3.3.3(f)$$

where

$$\{N^T\} = - \int_{-h}^h \{\Gamma_x\} \Delta T dz \quad 5.3.3.3(g)$$

Similarly, the bending relations are

$$\{M\} = [B]\{\varepsilon^\circ\} + [D]\{\kappa\} + \{M^T\} \quad 5.3.3.3(h)$$

where

$$\{M^T\} = - \int_{-h}^h \{\Gamma_x\} \Delta T z dz \quad 5.3.3.3(i)$$

The integral relations for the thermal stress resultant vector $\{N^T\}$ and thermal moment resultant vector $\{M^T\}$ can be evaluated only when the change in temperature through the thickness is known. For the case of uniform temperature change through the thickness of a laminate, the term ΔT is constant and can be factored out of the integral, yielding:

$$\{N^T\} = -\Delta T \sum_{i=1}^N \{\Gamma_x\}^i (z_i - z_{i-1}) \quad 5.3.3.3(j)$$

$$\{M^T\} = -\frac{1}{2} \Delta T \sum_{i=1}^N \{\Gamma_x\}^i (z_i^2 - z_{i-1}^2) \quad 5.3.3.3(k)$$

With Equations 5.3.3.3(f) - (i), it is possible to determine effective laminate coefficients of thermal expansion and thermal curvature. These quantities are the extension and curvature changes resulting from a uniform temperature distribution.

Noting that for free thermal effects $\{N\} = \{M\} = 0$, and defining a free thermal expansion vector as

$$\{\alpha_x\} = \{\varepsilon^\circ\} \frac{1}{\Delta T} \quad 5.3.3.3(l)$$

and a free curvature vector as

$$\{\delta_x\} = \{\kappa\} \frac{1}{\Delta T} \quad 5.3.3.3(m)$$

Equations 5.3.3(f) - (i) can be solved. After suitable matrix manipulations, the following expressions for thermal expansion and thermal curvature for symmetric laminates are found:

$$\{\alpha_x\} = -\frac{1}{\Delta T}[A]^{-1}\{N^T\} \quad 5.3.3.3(n)$$

$$\{\delta_x\} = -\frac{1}{\Delta T}[D]^{-1}\{N^T\} \quad 5.3.3.3(o)$$

If the relation for $\{M^T\}$ in Equation 5.3.3.3(i) is examined, symmetry eliminates the $\{M^T\}$ vector. Therefore $\{\delta_x\} = 0$ and no curvatures occur due to uniform temperature changes in symmetric laminates.

The variation of the longitudinal thermal expansion coefficient for a symmetric angle-ply laminate is shown in Figure 5.3.3.3 to illustrate the effect of lamina orientation. At 0° the term α_x is simply the axial lamina coefficient of thermal expansion, and at 90° , α_x equals the lamina transverse thermal expansion coefficient. An interesting feature of the curve is the large negative value of α_x in the region of 30° . Referring to Figure 5.3.3.1, the value of Poisson's ratio also behaves peculiarly in the region of 30° . The odd variation of both the coefficient and Poisson's ratio stems from the magnitude and sign of the shear-extensional coupling present in the individual laminae.

Previously, classes of laminates were shown to have isotropic stiffnesses in the plane of the laminate. Similarly, laminates can be specified which are isotropic in thermal expansion within the plane of the laminate. The requirements for thermal expansion isotropy are considerably less restrictive than those for elastic constants. In fact, any laminate which has two identical, orthogonal thermal expansion coefficients and a zero shear thermal expansion coefficient is isotropic in thermal expansion. Therefore, $[0/90]_s$ and $[\pm 45]_s$ laminates are isotropic in thermal expansion even though they are not quasi-isotropic for elastic stiffnesses.

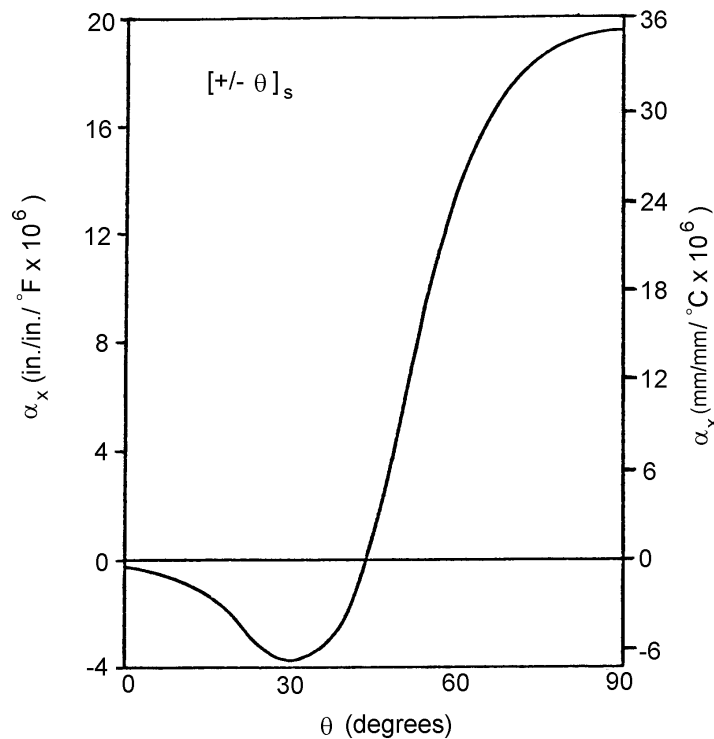


FIGURE 5.3.3.3 Thermal expansion coefficients for high modulus carbon/epoxy.

Laminates which are isotropic in thermal expansion have thermal expansions of the form:

$$\alpha_x = \begin{Bmatrix} \alpha_x \\ \alpha_y \\ \alpha_{xy} \end{Bmatrix} = \begin{Bmatrix} \alpha^* \\ \alpha^* \\ 0 \end{Bmatrix} \quad 5.3.3.3(p)$$

where the term α^* can be shown to be a function of lamina properties only, as follows:

$$\alpha^* = \alpha_1 + \frac{(\alpha_2 - \alpha_1)(1 + \nu_{12})}{1 + 2\nu_{12} + \frac{E_1}{E_2}} \quad 5.3.3.3(q)$$

Thus, all laminates of a given ply material, which are isotropic in thermal expansion, have identical thermal expansion coefficients.

5.3.3.4 Moisture expansion

The term hygroelastic refers to the phenomenon in resin matrix composites when the matrix absorbs and desorbs moisture from and to the environment. The primary effect of moisture is a volumetric change in the laminae. When a lamina absorbs moisture, it expands, and when moisture is lost, the lamina contracts. Thus, the effect is very similar to thermal expansion.

In a lamina, a free moisture expansion vector can be defined as

$$\{\epsilon_\ell\} = \{\beta_\ell\} \Delta c \quad 5.3.3.4(a)$$

where

$$\{\beta_\ell\} = \begin{Bmatrix} \beta_1 \\ \beta_2 \\ 0 \end{Bmatrix} \quad 5.3.3.4(b)$$

and Δc is the change in specific moisture. Noting that the relations 5.3.3.4(a) and (b) are identical to thermal expansion with $\{\beta_\ell\}$ substituted for $\{\alpha_\ell\}$ and Δc for ΔT , it can easily be seen that all the relations developed for thermal effects can be used for moisture effects.

5.3.3.5 Conductivity

The conductivity (thermal or moisture) of a laminate in the direction normal to the surface is equal to the transverse conductivity of a unidirectional fiber composite. This follows from the fact that normal conductivity for all plies is identical and unaffected by ply orientation.

In-plane conductivities will be required for certain problems involving spatial variations of temperature and moisture. For a given uniform state of moisture in a laminate, the effective thermal conductivities in the x and y directions can be obtained by methods entirely analogous to those used for stiffnesses in Section 5.3.2:

$$\mu_x = \frac{1}{2h} \sum_{i=1}^N (\mu_1 m^2 + \mu_2 n^2) t_\ell^i \quad 5.3.3.5$$

where

μ_1	= conductivity in the fiber direction
μ_2	= conductivity transverse to the fibers
m	= $\cos \theta^i$
n	= $\sin \theta^i$
θ^i	= orientation of ply i
t_ℓ^i	= thickness of ply i
N	= the number of plies
$2h$	= laminate thickness

The results apply to both symmetric and unsymmetric laminates. The results for moisture conductivity are identical.

5.3.4 Thermal and hygroscopic analysis

The distribution of temperature and moisture through the thickness of a laminate influences the behavior of that laminate. The mathematical descriptions of these two phenomena are identical and the physical effects are similar. Some of these aspects have already been discussed in Sections 5.2.2.3 - 5.2.2.4 and 5.3.3.3 - 5.3.3.5.

A free lamina undergoes stress-free deformation due to temperature change or moisture swelling. In a laminate, stress-free deformation is constrained by adjacent layers producing internal stresses. In addition to these stresses, temperature and moisture content also affect the properties of the material. These effects are primarily related to matrix-dominated strength properties.

The principal strength-degrading effect is related to a change in the glass transition temperature of the matrix material. As moisture is absorbed, the temperature at which the matrix changes from a glassy state to a viscous state decreases. Thus, the elevated-temperature strength properties decrease with increasing moisture content. Limited data suggest that this process is reversible. When the moisture content of the composite is decreased, the glass transition temperature increases and the original strength properties return.

The same considerations also apply for a temperature rise. The matrix, and therefore the lamina, lose strength and stiffness when the temperature rises. Again, this effect is primarily important for the matrix-dominated properties such as $E_2, G_{12}, F_2^{tu}, F_2^{cu}$, and F_{12}^{su} .

The differential equation governing time-dependent moisture sorption of an orthotropic homogeneous material is given by

$$D_1 \frac{\partial^2 c}{\partial x_1^2} + D_2 \frac{\partial^2 c}{\partial x_2^2} + D_3 \frac{\partial^2 c}{\partial x_3^2} = \frac{\partial c}{\partial t} \quad 5.3.4(a)$$

where

- t = time
- x_1, x_2, x_3 = coordinates in principal material directions
- c = specific moisture concentration
- D_1, D_2, D_3 = moisture diffusivity coefficients

Equation 5.3.4(a) is based on Fick's law of moisture diffusion. The equation is analogous to the equation governing time dependent heat conduction with temperature ϕ replacing concentration c and thermal conductivities μ_1, μ_2 , and μ_3 replacing the moisture diffusivities. For a transversely isotropic lamina with x_1 in the fiber direction, x_2 in the transverse direction, and $x_3 = z$ in the direction normal to the lamina,

$$D_2 = D_3 \quad 5.3.4(b)$$

These quantities are analogous to the thermal conductivities of a unidirectional fiber composite and have been discussed in Section 5.2.2.4.

An important special case is one-dimensional diffusion or conduction through the thickness of a lamina. In this case, Equation 5.3.4(a) reduces to

$$D_3 \frac{\partial^2 c}{\partial z^2} = \frac{\partial c}{\partial t} \quad 5.3.4(c)$$

This equation also applies to moisture diffusion or thermal conduction through a laminate, in the direction normal to its laminae planes, since all laminae are homogeneous in the z direction with equal diffusion coefficients, $D_3 = D_z$.

Equation 5.3.4(c) is applicable to the important problem of time-dependent moisture diffusion through a laminate where the two faces are in different moisture environments. After a sufficiently long time has

elapsed, the concentration reaches a time-independent state. In this state, since c is no longer time-dependent, Equation 5.3.4(c) simplifies to

$$\frac{d^2c}{dz^2} = 0 \quad 5.3.4(d)$$

The specific moisture concentration is a linear function of z and, if the laminate faces are in environments with constant saturation concentrations, c_1 and c_2 , then

$$c = \frac{1}{2}[(c_2 - c_1)z/h + c_2 + c_1] \quad 5.3.4(e)$$

where the laminate thickness is $2h$ and z originates at the mid-surface. In the case where $c_1 = c_2$, Equation 5.3.4(e) reduces to $c = c_1 = \text{constant}$ as would be expected.

The above discussion of moisture conduction also applies to heat conduction.

Solutions to the time-dependent problem are readily available and considerable work has been performed in the area of moisture sorption (Reference 5.3.4). The most interesting feature of the solutions relates to the magnitude of the coefficient D_z . This coefficient is a measure of how fast moisture diffusion can occur. In typical epoxy matrix systems, D_z is of the order of 10^{-8} (in²/s, cm²/s) to 10^{-10} (in²/s, cm²/s). The diffusion coefficient is sufficiently small that full saturation of a resin matrix composite may require months or years even when subjected to 100% relative humidity.

The approach typically taken for design purposes is to assume a worst case. If the material is assumed to be fully saturated, it is possible to compute reduced allowable strengths. This is a conservative approach, since typical service environments do not generate full saturation. This approach is used since it allows for inclusion of moisture effects in a relatively simple fashion. It is to be expected that as the design data base and analytical methodologies mature, more physically realistic methods will be developed.

For heat conduction, the time required to achieve the stationary, or time-independent, state is extremely small. Therefore, the transient time-dependent state is generally of little practical importance for laminates.

5.3.4.1 Symmetric laminates

The laminate stacking sequence (LSS) can be chosen to control the effects of environment on stiffness and dimensional stability. When considering the special case of constant temperature and moisture content distributions in symmetric laminates, the effect of environment on in-plane stiffness relates to the relative percentages of chosen ply orientations. For example, LSS dominated by 0° plies will have longitudinal moduli that are nearly independent of environment. Note that increasing the environmental resistance of one laminate in-plane modulus may decrease another.

Bending and torsional stiffnesses depend on both LSS and environment. Preferential stacking of outer ply groups having relatively high extensional or shear moduli will also promote high bending or torsional stiffness, respectively. As with in-plane moduli, the higher the bending or torsional stiffness the better the corresponding environmental resistance. When optimizing environmental resistance, compromises between longitudinal bending, transverse bending and torsion need to be made due to competing relationships with LSS.

Unsymmetric temperature and moisture content distributions will affect the components of the stiffness matrix [ABD] differently, depending on LSS. In general, coupling components which were zero for symmetric laminates having symmetric temperature and moisture content distributions become nonzero for an unsymmetric environmental state. This effect can be minor or significant depending on LSS, material type, panel thickness and the severity of temperature/moisture content gradients.

Environmentally-induced panel warpage will occur in symmetric laminates when conditions yield an unsymmetric residual stress distribution about the laminate midplane. This may occur during the cure process due to uneven heating or crystallization through the laminate thickness. Unsymmetric tempera-

ture and moisture content distributions can also lead to panel warpage in symmetric laminates. This is due to the unsymmetric shrinkage or swelling through the laminate thickness.

5.3.4.2 Unsymmetric laminates

The in-plane thermal and moisture expansion of unsymmetric laminated plates subjected to any environmental condition (i.e., constant, symmetric and unsymmetric temperature and moisture content distributions) is dependent on LSS (e.g., Reference 5.3.4.2(a)). In general, environmentally induced panel warpage occurs with unsymmetric laminates.

Panel warpage in unsymmetric laminates depends on LSS and changes as a function of temperature and moisture content. Zero warpage will occur in unsymmetric laminates only when temperature and moisture content distributions result in either zero or symmetric residual stress distributions. Equilibrium environmental states that result in zero residual stresses are referred to as stress-free conditions (see Reference 5.3.2(e)).

Since unsymmetric LSS warp as a function of temperature and moisture content, their use in engineering structures has generally been avoided. The warped shape of a given unsymmetric laminate has been found to depend on LSS and ratios of thickness to in-plane dimensions (e.g., References 5.3.4.2(b) and (c)). Relatively thin laminates tend to take a cylindrical shape rather than the saddle shape predicted by classical lamination theory. This effect has been accurately modeled using a geometrically nonlinear theory.

Additional information on laminate stacking sequence effects is found in Section 5.6.5.

5.3.5 Laminate stress analysis

The physical properties defined in Section 5.3.3 enable any laminate to be represented by an equivalent homogeneous anisotropic plate or shell element for structural analysis. The results of such analyses will be the definition of stress resultants, bending moments, temperature, and moisture content at any point on the surface which defines the plate. With this definition of the local values of state variables, a laminate analysis can be performed to determine the state of stress in each lamina to assess margins for each critical design condition.

5.3.5.1 Stresses due to mechanical loads

To determine stresses in the individual plies, the laminate mid-plane strain and curvature vectors are used. Writing the laminate constitutive relations

$$\begin{Bmatrix} N \\ \vdots \\ M \end{Bmatrix} = \begin{bmatrix} A & B \\ \vdots & \vdots \\ B & D \end{bmatrix} \begin{Bmatrix} \epsilon^o \\ \vdots \\ \kappa \end{Bmatrix} \quad 5.3.5.1(a)$$

a simple inversion will yield the required relations for $\{\epsilon^o\}$ and $\{\kappa\}$. Thus

$$\begin{Bmatrix} \epsilon^o \\ \vdots \\ \kappa \end{Bmatrix} = \begin{bmatrix} A & B \\ \vdots & \vdots \\ B & D \end{bmatrix}^{-1} \begin{Bmatrix} N \\ \vdots \\ M \end{Bmatrix} \quad 5.3.5.1(b)$$

Given the strain and curvature vectors, the total strain in the laminate can be written as

$$\{\epsilon_x\} = \{\epsilon^o\} + z\{\kappa\} \quad 5.3.2(d)$$

The strains at any point through the laminate thickness are now given as the superposition of the mid-plane strains and the curvatures multiplied by the distance from the mid-plane. The strain field at the center of ply i in a laminate is

$$\{\epsilon_x\}^i = \{\epsilon^o\} + \frac{1}{2}\{\kappa\}(z^i + z^{i-1}) \quad 5.3.5.1(c)$$

where the term

$$\frac{1}{2}(z^i + z^{i-1})$$

corresponds to the distance from the mid-plane to the center of ply i . It is possible to define curvature induced strains at a point through the laminate thickness simply by specifying the distance from the mid-plane to the point in question.

The strains defined in Equation 5.3.5.1(c) correspond to the arbitrary laminate coordinate system. These strains can be transformed into the principal material coordinates for this ply using the transformations developed previously (Equation 5.3.1(m)). Thus

$$\{\varepsilon_\ell\}^i = [\theta^i]^{-1} \{\varepsilon_x\}^i \quad 5.3.5.1(d)$$

where the superscript i indicates which layer and, therefore, which angle of orientation to use.

With the strains in the principal material coordinates defined, stresses in the same coordinates are written by using the lamina reduced stiffness matrix (Equation 5.3.1(h)).

$$\{\sigma_\ell\}^i = [Q^i] \{\varepsilon_\ell\}^i \quad 5.3.5.1(e)$$

Again, the stiffness matrix used must correspond to the correct ply, as each ply may be a different material.

The stresses in the principal material coordinates can be determined without the use of principal material strains. Using the strains defined in the laminate coordinates (Equation 5.3.5.1(c)) and the transformed lamina stiffness matrix (Equations 5.3.1(o,q,r)), stresses in the laminate coordinate system can be written as

$$\{\sigma_x\}^i = [\bar{Q}^i] \{\varepsilon_x\}^i \quad 5.3.5.1(f)$$

and these stresses are then transformed to the principal material coordinates using the relations 5.3.1(m). Thus

$$\{\sigma_\ell\}^i = [\theta^i]^{-1} \{\sigma_x\}^i \quad 5.3.5.1(g)$$

By reviewing these relations, it can be seen that, for the case of symmetric laminates and membrane loading, the curvature vector is zero. This implies that the laminate coordinate strains are identical in each ply and equal to the mid-plane strains. The differing angular orientation of the various plies will promote different stress and strain fields in the principal material coordinates of each ply.

5.3.5.2 Stresses due to temperature and moisture

In Section 5.3.3.3, equations for the thermoelastic response of composite laminates were developed. It was indicated that thermal loading in laminates can cause stresses even when the laminate is allowed to expand freely. The stresses are induced because of a mismatch in thermal expansion coefficients between plies oriented in different directions. Either the mechanical stresses of the preceding section or the thermomechanical stresses can be used to evaluate laminate strength.

To determine the magnitude of thermally induced stresses, the thermoelastic constitutive relations (Equations 5.3.3.3(f) - (i)) are required. Noting that free thermal stress effects require that $\{N\} = \{M\} = 0$, these relations are written as

$$\begin{Bmatrix} 0 \\ \vdots \\ 0 \end{Bmatrix} = \begin{bmatrix} A & B \\ B & D \end{bmatrix} \begin{Bmatrix} \varepsilon^0 \\ \kappa \end{Bmatrix} + \begin{Bmatrix} N^T \\ M^T \end{Bmatrix} \quad 5.3.5.2(a)$$

Inverting these relations yields the free thermal strain and curvature vectors for the laminate. Proceeding as before, the strain field in any ply is written as

$$\{\varepsilon_x\}^i = \{\varepsilon^0\} + \frac{1}{2}(z^+ - z^{i-1})\{\kappa\} \quad 5.3.5.2(b)$$

Stresses in the laminate coordinates are

$$\{\sigma_x\}^i = [\bar{Q}]^i \{\varepsilon_x\}^i - \{\Gamma_x\}^i \Delta T^i \quad 5.3.5.2(c)$$

which can then be transformed to the principal material coordinates. Thus

$$\{\sigma_\ell\} = [\theta^i]^{-1} \{\sigma_x\}^i \quad 5.3.5.2(d)$$

The stresses can also be found by transforming the strains directly to principal material coordinates and then finding the principal material coordinate stresses.

For uniform temperature fields in symmetric laminates, the coupling matrix, $[B]$, and the thermal moment resultant vector, $\{M^T\}$, vanish and:

$$\{\varepsilon^\circ\} = \{\alpha_x\} \Delta T \quad 5.3.5.2(e)$$

and

$$\{\kappa\} = 0 \quad 5.3.5.2(f)$$

In this case, the strains in the laminate coordinates are identical in each ply with the value

$$\{\varepsilon_x\}^i = \{\varepsilon^\circ\} = \{\alpha_x\} \Delta T \quad 5.3.5.2(g)$$

and the stresses in the principal material coordinates are

$$\{\sigma_x\}^i = [\bar{Q}]^i (\{\alpha\} - \{\alpha_x\})^i \Delta T \quad 5.3.5.2(h)$$

These relations indicate that the stresses induced by the free thermal expansion of a laminate are related to the differences between the laminate and ply thermal expansion vectors. Therefore, the stresses are proportional to the difference between the amount the ply would freely expand and the amount the laminate will allow it to expand.

A further simplification can be found if the laminate under investigation is isotropic in thermal expansion. It can be shown that, for this class of laminates subjected to a uniform temperature change, the stresses in the principal material coordinates are identical in every ply. The stress vector is

$$\{\sigma_\ell\} = \frac{E_{11}(\alpha_{22} - \alpha_{11})\Delta T}{1 + 2\nu_{12} + \frac{E_{11}}{E_{22}}} \begin{Bmatrix} 1 \\ -1 \\ 0 \end{Bmatrix} \quad 5.3.5.2(i)$$

where it can be seen that the transverse direction stress is equal and opposite to the fiber direction stress.

Similar developments can be generated for moisture-induced stresses. All of the results of this section apply when moisture swelling coefficients, $\{\beta_\ell\}$, are substituted for thermal expansion coefficients, $\{\alpha_\ell\}$.

5.3.5.3 Netting analysis

Another approach to the calculation of ply stresses is sometimes used for membrane loading of laminates. This procedure is netting analysis and, as the name implies, treats the laminate as a net. All loads are carried in the fibers while the matrix material serves only to hold the geometric position of the fibers.

Since only fibers are assumed to load in this model, stress-strain relations in the principal material directions can be written as

$$\sigma_{11} = E_1 \varepsilon_{11} \quad 5.3.5.3(a)$$

or

$$\epsilon_{11} = \frac{1}{E_1} \sigma_{11} \quad 5.3.5.3(b)$$

and

$$E_2 = G_{12} = \sigma_{22} = \sigma_{12} = 0 \quad 5.3.5.3(c)$$

The laminate stiffnesses predicted with a netting analysis will be smaller than those predicted using lamination theory, due to the exclusion of the transverse and shear stiffnesses. This effect is demonstrated in Table 5.3.5.3 for a quasi-isotropic laminate comprised of high-modulus graphite/epoxy. The stiffness properties predicted using a netting analysis are approximately 10% smaller than lamination theory predictions. Experimental work has consistently shown that lamination theory predictions are more realistic than netting analysis predictions.

Although the stiffness predictions using netting analysis are of limited value, the analysis can be used as an approximation of the response of a composite with matrix damage. It may be considered as a worst case analysis and is frequently used to predict ultimate strengths of composite laminates

TABLE 5.3.5.3 *Laminate elastic constants.*

Analysis	E_x Msi (GPa)	E_y Msi (GPa)	G_{xy} Msi (GPa)	γ_{xy}
Lamination Theory	9.42 (64.9)	9.42 (64.9)	3.55 (24.5)	0.325
Netting Analysis	8.33 (57.4)	8.33 (57.4)	3.13 (21.6)	0.333

5.3.5.3.1 *Netting analysis for design of filament wound pressure vessels*

Netting analysis is a simple tool for approximating hoop and axial stresses in filament wound pressure vessels. The technique assumes that the stresses induced to the structure are carried entirely by the reinforcing fiber, and that all fibers are uniformly stressed in tension. The load carrying contribution of the matrix is neglected, and its only function is to hold the geometric position of the fibers. Netting analysis cannot be used to determine bending, shear or discontinuity stresses or resistance to buckling.

To illustrate the netting analysis principles, consider a filament wound pressure vessel of radius R with an internal pressure P . Assume the vessel is wound with only helical fibers at a wrap angle of $\pm\alpha$, an allowable fiber stress of σ_f , and thickness t_f . Figure 5.3.5.3.1(a) illustrates the forces acting on the $\pm\alpha$ helical layer in the axial direction. The running load, N_x , is the force per unit length in the axial direction.

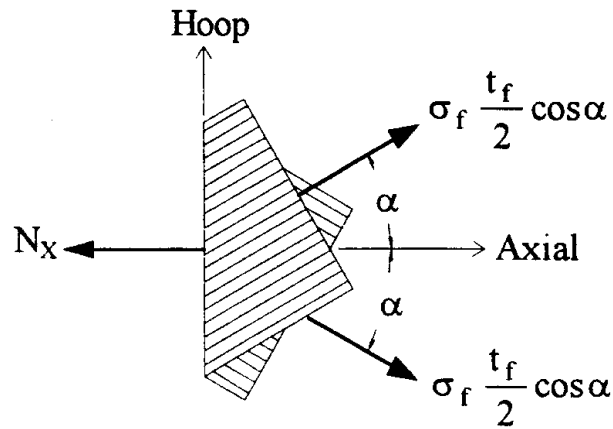


FIGURE 5.3.5.3.1(a) *Helical layer element - axial direction.*

Summing forces in the axial direction:

$$N_x = \frac{PR}{2} = \sigma_f t_f \cos^2 \alpha \quad 5.3.5.3.1(a)$$

Solving for t_f provides the helical fiber thickness required to carry the internal pressure:

$$t_f = \frac{PR}{2\sigma_f \cos^2 \alpha} \quad 5.3.5.3.1(b)$$

Figure 5.3.5.3.1(b) shows the forces acting in the $\pm\alpha$ helical layer in the hoop direction. The running load, N_H , is the force per unit length in the hoop direction.

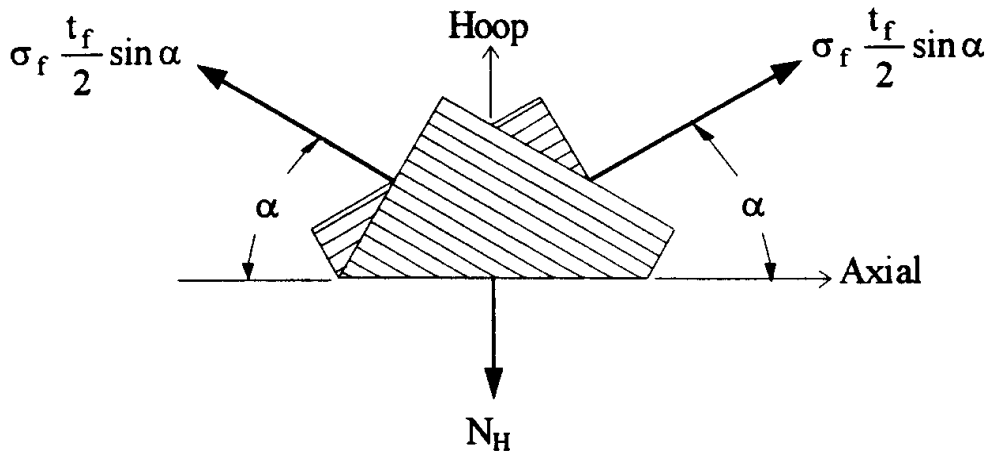


FIGURE 5.3.5.3.1(b) *Helical layer element - hoop direction.*

Summing forces in the hoop direction:

$$N_h = PR = \sigma_f t_f \sin^2 \alpha \quad 5.3.5.3.1(c)$$

Solving for t_f ,

$$t_f = \frac{PR}{\sigma_f \sin^2 \alpha} \quad 5.3.5.3.1(d)$$

Substituting t_f for Equation 5.3.5.3.1(b) in Equation 5.3.5.3.1(c), yields $\tan^2 \alpha = 2$, solving for wrap angle, $\alpha = \pm 54.7$ degrees. This is the wrap angle required for a pressure vessel utilizing only helical layers.

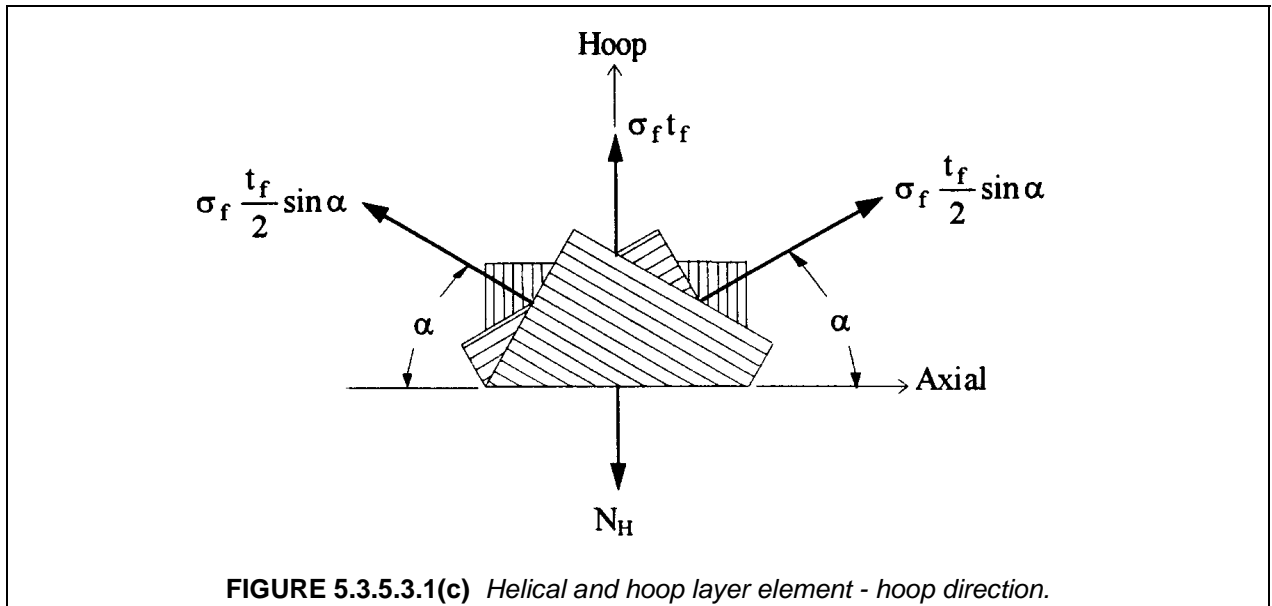
Now consider a filament wound pressure vessel with both helical and hoop layers. Where the helical layers have a wrap angle of $\pm \alpha$ and the hoop layers have a wrap angle of 90 degrees. Again, Figure 5.3.5.3.1(a) illustrates the forces acting on the $\pm \alpha$ helical layer in the axial direction. Summing forces in the axial direction and solving for t_f , yields Equation 5.3.5.3.1(b), which is the helical fiber thickness required to carry the internal pressure. Figure 5.3.5.3.1(c) shows the forces acting on the $\pm \alpha$ helical layer and the hoop layer in the hoop direction. Summing forces in the hoop direction and substituting t_f from Equation 5.3.5.3.1(b) yields:

$$t_f = \frac{PR}{2\sigma_f} (2 - \tan^2 \alpha) \quad 5.3.5.3.1(e)$$

where t_f is the hoop layer thickness required to carry the internal pressure.

The fiber thickness (t_f) and allowable fiber stress (σ_f) can also be expressed in the following standard filament winding terms. Band density (A), which is the quantity of fiber reinforcement per inch of band width, where the band width (W) is the width of fiber reinforcement as it is applied to the mandrel. Tow tensile capacity (f), which is the load carrying capability of one tow of reinforcement fiber, and layers (L), which is the number of layers required to carry the internal pressure. Substituting these terms into Equation 5.3.5.3.1(b) and solving for L:

$$L = \frac{PR}{2Af_{\text{HELIX}} \cos^2 \alpha} \quad 5.3.5.3.1(f)$$



Where L is the number of helical layers required to carry the internal pressure. Substituting these terms into Equation 5.3.5.3.1(e) and solving for L:

$$L = \frac{PR}{2Af_{\text{HOOP}} (2 - \tan^2 \alpha)} \quad 5.3.5.3.1(g)$$

Where L is the number of hoop layers required to carry the internal pressure.

The tow tensile capacities (f_{HELIX} and f_{HOOP}) can be determined experimentally. Standard practice is to design and fabricate pressure vessels that will fail in either helix or hoop during hydroburst testing. Sub-

stituting the design parameters and hydroburst results into Equations 5.3.5.3.1(f) and 5.3.5.3.1(g), and solving for f provides the tow tensile capacity for the given fiber in both the helix and hoop directions.

Netting analysis is a useful tool for approximating hoop and axial stresses in filament wound pressure vessels. It is a conservative analysis technique that considers only the strength of the reinforcing fiber. However, when utilizing experimentally determined tow tensile capacities, netting analysis is an excellent preliminary design tool that is still used throughout the filament winding industry.

5.3.5.4 Interlaminar stresses

The analytical procedures which have been developed can be used to predict stresses within each lamina of a laminate. The stresses predicted are planar due to the assumed state of plane stress. There are cases where the assumption of plane stress is not valid and a three-dimensional stress analysis is required.

An example of such a case exists at certain free edges in laminates where stress free boundary conditions must be imposed.

5.3.5.5 Nonlinear stress analysis

All the preceding material in this chapter has related to laminae which behave in a linear elastic fashion. Composites can behave in a nonlinear manner due to internal damage or nonlinear behavior of the matrix material. Matrix nonlinearity or micro-cracking can result in laminae which have nonlinear stress-strain curves for transverse stress or axial shear stress. When this situation exists, the elastic laminate stress analysis of Section 5.3.5.1 must be replaced by a nonlinear analysis. A convenient procedure for the nonlinear analysis is presented in Reference 5.3.5.5.

5.3.6 Summary

- When laminae are at an angle to the laminate reference axes, the lamina stiffness relations described in Section 5.2 must be transformed into the laminate coordinate system to perform laminate stress-strain analysis.
- Stresses and strains are related in the principal lamina material directions by 6 x 6 symmetric compliance $[S]$ and stiffness $[Q]$ matrices.
- The transformation of stresses and strains from the principal lamina material direction to the laminate coordinate system is accomplished by following the rules for transformation of tensor components (Equations 5.3.1(k) and 5.3.1(m)).
- Lamination theory makes the same simplifications as classical thin plate theory for isotropic materials. Therefore, the procedures used to calculate stresses and deformations are dependent on the fact that laminate thickness is considerably smaller than the laminate's in-plane dimensions.
- The strain at a y point in a laminate is defined as the sum of the mid-surface strain (ϵ), and the product of the curvature (κ) and the distance from the mid surface (z).
- Laminate load (N) and moment (M) resultants are related to mid-plane strains and curvatures as described by the $[A]$, $[B]$, and $[D]$ 3 x 3 stiffness matrices (Equations 5.3.2 (k) - (m)).
- Two-dimensional lamination theory can generally be used to predict stresses within each lamina of a laminate. The planar stresses are predicted based on an assumption of plane stress. In cases where interlaminar stresses exist, three-dimensional stress analysis is required.

- In symmetric laminates, bending-extensional coupling is eliminated by a symmetric stacking sequence whereby $[B] = 0$.
- Since they are susceptible to warping as a result of processing and usage conditions, use of unsymmetric laminates in composite structures should generally be avoided for both design and manufacture.

5.4 LAMINATE STRENGTH AND FAILURE

Methods of stress analysis of laminates subjected to mechanical loads, temperature changes, and moisture absorption were presented in Section 5.3.5. The results of such a stress analysis can be used to assess the strength of a laminate. As a result of the complexity of the structure of a composite laminate, several modes of failure are possible, and it is desirable for the failure mode as well as the failure stress or strain to be predicted. The analytical problem is to define the failure surface for the laminate in either stress or strain space.

Laminate failure may be calculated by applying stress or strain limits at the laminate level or, alternatively, at the ply level. Ply level stresses or strains are the more frequently used approach to laminate strength. The average stresses in a given ply may be used to calculate either an onset of damage, which is frequently called "first ply failure", or a critical failure which is regarded as ultimate strength. In the former case, subsequent damages leading to laminate failure are then calculated. This calculation of subsequent damage is sometimes performed using the "sequential ply failure" methodology, and sometimes performed using "netting" analysis. These approaches are discussed subsequently. Four factors should be considered in assessing the validity of using ply level stresses for failure calculation. The first is the question of which tests (or analyses) should be used to define the ply strength values. In particular, it must be recognized that a crack parallel to the fibers may result in failure of a transverse tensile test specimen of a unidirectional composite, while the same crack may have an insignificant effect in a laminate test. The second factor is the assumption that local failures within a ply are contained within the ply and are determined solely by the stress/strain state in that ply. There is evidence that the former assumption is not valid under fatigue loading, during which a crack within one ply may well propagate into adjacent plies. In this case, the ply-by-ply model may not be the best analytical approach. Furthermore, matrix cracking within one ply is not determined uniquely by the stresses and strains within that ply but is influenced by the orientation of adjacent layers as well as by the ply thickness (Reference 5.4). The third factor is the existence of residual thermal stresses, usually of unknown magnitude, resulting from the fabrication process. The fourth factor is that it does not cover the possibility of delaminations which can occur, particularly at free edges. Thus, the analysis is limited to in-plane failures.

5.4.1 Sequential ply failure approach

5.4.1.1 Initial ply

To predict the onset of damage, consider stresses remote from the edges in a laminate which is loaded by in-plane forces and/or bending moments. If there is no external bending, if the membrane forces are constant along the edges, and if the laminate is balanced and symmetric, the stresses in the i th layers are constant and planar. With reference to the material axes of the laminae, fiber direction x_1 and transverse direction x_2 , the stresses in the i th ply are written σ_{11}^i , σ_{22}^i , and σ_{12}^i . Failure is assumed to occur when the selected semi-empirical failure criteria involving these calculated stresses or the associated strains are satisfied. Numerous criteria have been proposed for calculation of onset of damage. These may be grouped into two broad categories - mode-based and purely empirical. Mode based criteria treat each identifiable physical failure mode, such as fiber-direction tensile failure and matrix-dominated transverse failure, separately. A purely empirical criterion generally consists of a polynomial combination of the three stress or strain components in a ply. Such criteria attempt to combine the effects of several different failure mechanisms into one function and may, therefore, be less representative than physically

based criteria. All criteria rely on test data at the ply level to set parameters and are therefore at least partially empirical in nature.

The selection of appropriate criteria can be a controversial issue and the validity of any criterion is best determined by comparison with test data. As a consequence, different criteria may be best for different materials. Two mode-based failure criteria are presented here as examples: the maximum strain criteria and the failure criteria proposed by Hashin. It is important, however, for the engineer to consider the material, the application, and the test data in choosing and utilizing a failure criterion.

The maximum strain criteria may be written as

$$\begin{aligned}\epsilon_{11}^{cu} &\leq \epsilon_{11}^i \leq \epsilon_{11}^{tu} \\ \epsilon_{22}^{cu} &\leq \epsilon_{22}^i \leq \epsilon_{22}^{tu} \\ |\epsilon_{12}^i| &\leq \epsilon_{12}^{su}\end{aligned}\tag{5.4.1.1(a)}$$

For given loading conditions, the strains in each ply are compared to these criteria. Whichever strain reaches its limiting value first indicates the failure mode and first ply to fail for those loading conditions. The limiting strains, ϵ_{11}^{tu} , ϵ_{11}^{cu} , etc., are the specified maximum strains to be permitted in any ply. Generally, these quantities are specified as some statistical measure of experimental data obtained by uniaxial loading of a unidirectional laminate. For example, in the case of axial strain, ϵ_{11} , a B-basis strain allowable from unidirectional tests can be used. Other limits may also be imposed. For example, in the case of shear strain, something equivalent to a "yield" strain may be used in place of the ultimate shear strain.

The failure criteria proposed by Hashin (Reference 5.4.1.1(a)) may be written as:

Fiber modes

Tensile

$$\left(\frac{\sigma_{11}}{F_1^{tu}}\right)^2 + \left(\frac{\sigma_{12}}{F_{12}^{su}}\right)^2 = 1\tag{5.2.4(f)}$$

Compressive

$$\left(\frac{\sigma_{11}}{F_1^{cu}}\right)^2 = 1\tag{5.2.4(g)}$$

Matrix modes

Tensile

$$\left(\frac{\sigma_{22}}{F_2^{tu}}\right)^2 + \left(\frac{\sigma_{12}}{F_{12}^{su}}\right)^2 = 1\tag{5.2.4(h)}$$

Compressive

$$\left(\frac{\sigma_{22}}{2 F_{23}^{su}}\right)^2 + \left[\left(\frac{F_2^{cu}}{2 F_{23}^{su}}\right)^2 - 1\right] \left(\frac{\sigma_{22}}{F_2^{cu}}\right)^2 + \left(\frac{\sigma_{12}}{F_{12}^{su}}\right)^2 = 1\tag{5.2.4(i)}$$

It should be noted that some users of these criteria add a shear term to equation 5.2.4(g) to reflect the case in which shear mode instability contributes to the compressive failure mechanism (Reference 5.4.1.1(b)). In that case, equation 5.2.4(g) is replaced by:

$$\left(\frac{\sigma_{11}}{F_1^{cu}}\right)^2 + \left(\frac{\sigma_{12}}{F_{12}^{su}}\right)^2 = 1\tag{5.4.1.1(b)}$$

The limiting stresses in the criteria, F_1^{cu} , F_{12}^{su} , etc., are the specified maximum stresses to be permitted in any ply. As with the case of strains, statistical data from unidirectional tests are generally used to define these quantities. However, as an example of the care required, it should be noted that the stress which produces failure of a 90° specimen in tension is not necessarily a critical stress level for a ply in a multi-directional laminate. One may wish to use, instead, the stress level at which crack density in a ply reduces the effective stiffness by a specified amount. Such a stress level could be determined by either a fracture mechanics analysis or testing of a crossply laminate (Reference 5.4).

In an onset of damage approach, the selected failure criteria are used for each layer of the laminate. The layer for which the criteria are satisfied for the lowest external load set will define the loading which produces the initial laminate damage. The layer which fails and the nature of the failure (i.e., fiber failure or cracking along the fibers) are identified. This is generally called first-ply failure. When the first ply failure is the result of fiber breakage, the resulting ply crack will introduce stress concentrations into the adjacent plies. In this case, it is reasonable to consider that first ply failure is equivalent to laminate failure. A different criterion exists when the first ply failure results from matrix cracking and/or fiber/matrix interface separations. Here it is reasonable to consider that the load-carrying capacity of the ply will be changed significantly when there is a substantial amount of matrix mode damage. Treatment of this case is discussed in the following section.

Additional concerns to be addressed in considering the initial failure or onset of damage include bending, edge stresses, and residual thermal stresses. Bending occurs when there are external bending and/or twisting moments or when the laminate is not symmetric. In these cases the stresses σ_{11}^i , σ_{22}^i , and σ_{12}^i in a layer are symmetric in x_3 . Consequently, the stresses assume their maximum and minimum values at the layer interfaces. The failure criteria must be examined at these locations for each layer. Different approaches utilize the maximum value or the average value in such cases.

The evaluation of onset of failure as a result of the edge stresses is much more complicated as a result of the sharp gradients (indicated by analytical singularities) in these stresses. Numerical methods cannot uncover the nature of such stress singularity, but there are analytical treatments (e.g. Reference 5.4.1.1(a)) which can. The implication of such edge stress fields for failure of the laminate is difficult to assess. This situation is reminiscent of fracture mechanics in the sense that stresses at a crack tip are theoretically infinite. Fracture mechanics copes with this difficulty with a criterion for crack propagation based on the amount of energy required to open a crack, or equivalently, the value of the stress intensity factor. Similar considerations may apply for laminate edge singularities. This situation in composite materials is more complicated since a crack initiating at the edge will propagate between anisotropic layers. It appears, therefore, that at the present time the problem of edge failure must be relegated to experimentation, or approximate analysis.

In the calculation of first-ply failure, consideration must also be given to residual thermal stresses. The rationale for including residual thermal stresses in the analysis is obvious. The stresses exist after processing. Therefore, they can be expected to influence the occurrence of first-ply failure. However, matrix materials exhibit viscoelastic, or time-dependent, effects, and it may be that the magnitude of the residual stresses will be reduced through a process of stress relaxation. Additionally, the processing stresses may be reduced through the formation of transverse matrix microcracks. The question of whether to include residual stresses in the analysis is complicated by difficulties in measuring these stresses in a laminate and by difficulties in observing first-ply failure during a laminate test. It is common practice to neglect the residual thermal stresses in the calculation of ply failure. Data to support this approach do not appear to be available. However, at the present time, damage tolerance requirements limit allowable strain levels in polymeric matrix laminates to 3000 to 4000 $\mu\epsilon$. This criterion becomes the dominant design restriction and obviates, temporarily, the need to resolve the effects of residual thermal stresses.

5.4.1.2 Subsequent failures

Often laminates have substantial strength remaining after the first ply has experienced a failure, particularly if that first failure is a matrix-dominated failure. A conservative approach for analyzing subsequent failure is to assume that the contribution of that first failed ply is reduced to zero. If failure occurs in the fiber-dominated mode, this may be regarded, as discussed earlier, as ultimate laminate failure. If not, then the stiffness in the fiber direction E_L is reduced to zero. If failure occurs in the matrix-dominated mode, the elastic properties E_T and G_L are reduced to zero. The analysis is then repeated until all plies have failed. Generally, the progressive failures of interest are initial and subsequent failures in the matrix mode. In that case, the basic assumptions for netting analysis result where the ultimate load is defined by E_T and G_L vanishing in all laminae. The basic issues involved in modeling post-first-ply behavior are described in Reference 5.4.2. For some materials and/or for some properties, matrix mode failures may not have an important effect. However, for some properties, such as thermal expansion coefficients, ply cracking may have a significant effect.

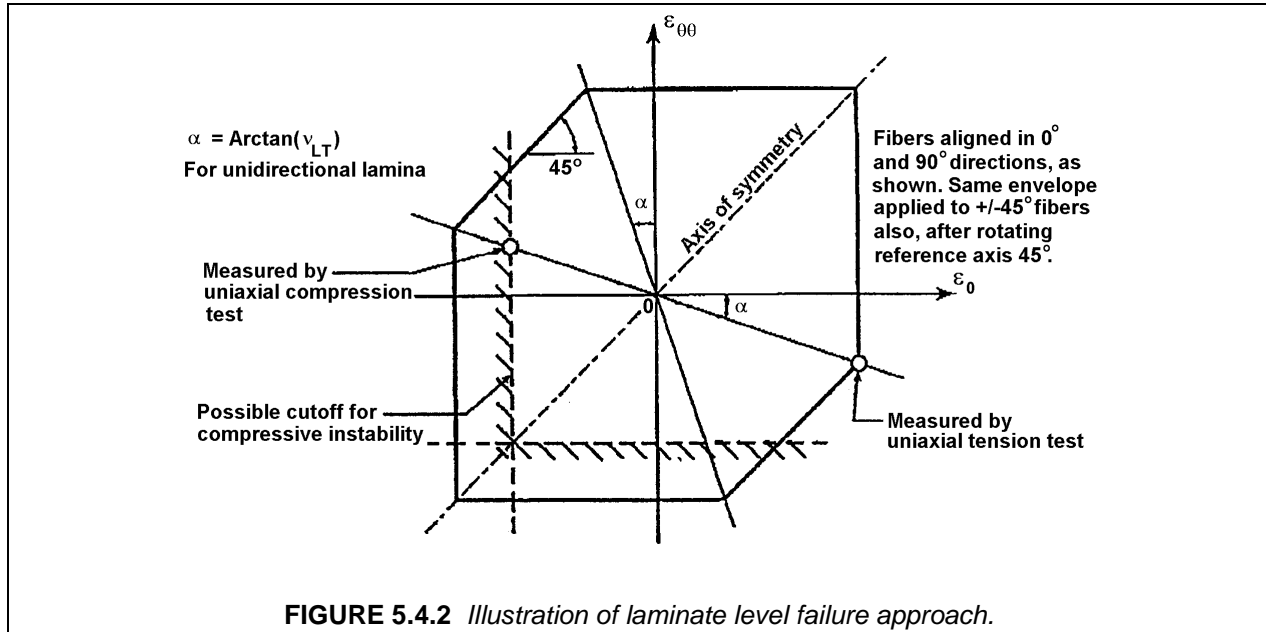
5.4.2 Fiber failure approach (laminate level failure)

In composites laminates, there are two characteristic stress or strain levels which can be considered in the evaluation of strength. One is the stress or strain state at which a non-catastrophic first-ply failure can occur and the other is the maximum static stress or strain state which the laminate can carry. In those cases where the material exhibits minimal micro-cracking, or where the application is such that effects of micro-cracking need not be considered, a failure criterion based only upon fiber failure may be used. A common practice in the aerospace industry is to use a failure criterion based only upon fiber strain allowables, for which fiber failure in any lamina is considered laminate ultimate failure. Hence, failure is a single event rather than the result of a process.

Perhaps the most common example of this laminate level failure criterion is a modification of the maximum strain criterion. The same assumptions of no external bending, membrane forces constant along the edges, and a balanced and symmetric laminate, are initially used. The basic lamina failure envelope is the same as the conventional maximum-strain envelope for tension- and compression-dominated loads, but introduces truncations in the tension-compression (shear) quadrants as shown in Figure 5.4.2. A critical assumption in this criterion is that the laminate behavior is fiber-dominated meaning that there are fibers in sufficient multiple directions such that strains are limited by the presence of the fibers to inhibit matrix cracking. In many practical applications, this typically translates into having fibers in (at least) each of four directions relative to the primary loads: 0° , 90° , and $\pm 45^\circ$. Furthermore, plies are not "clustered" (that is, several plies of the same orientation are not laid together) in order to inhibit matrix macrocracking. With these assumptions, the first translation of the maximum strain criterion to the laminate level is a limiting of the strain in the transverse direction, θ_{90} , to the fiber direction limiting strain to reflect the fact that such "well-designed" laminates with fibers in multiple directions restrict strains in any in-plane direction. Alternatively, if there is reason to believe that matrix cracking will be structurally significant, the 90° strain cutoff based on fiber direction strain could be replaced by an empirically established tensile limit reflecting a matrix-dominated mode. This limit was originally expressed as a constant strain limit. However, if such a limit is based upon the case of a constant 90° stress in a ply, this would result in a sloped line in the strain plane with the slope related to the Poisson's ratio of the unidirectional lamina:

$$\alpha = \tan^{-1} (\nu_{LT}^{\text{lamina}}) \quad 5.4.2(a)$$

Such a cutoff is parallel to the uniaxial load line shown in Figure 5.4.2. It should be further noted that possible limitations due to lamina level shear strains are inoperative due to the assumption that the fibers in multiple directions restrict such strains to values below their failure values.



Many users recognize a need to truncate the maximum strain predictions in the tension-compression quadrants. While the particular truncations vary, perhaps the most widely used version is that shown in Figure 5.4.2. These truncations were originally based on data obtained for shear loading of such fiber-dominated laminates. These data lie in the second and fourth quadrants. The 45° cutoffs represent the locus of constant shear strain. These two symmetric truncations are located by finding the intersections of the limiting uniaxial strain lines with the lines representing pure uniaxial stress conditions in fiber directions in 0° and 90° unidirectional plies. At this point, the axial strain now becomes more critical than the shear. The endpoints of the truncations are therefore found by drawing lines through the origin with angles from the relative axes of a which account for the unidirectional ply Poisson's ratio:

$$\alpha = \tan^{-1} (v_{LT}^{\text{lamina}}) \quad 5.4.2(b)$$

thereby yielding the desired pure uniaxial state of stress in the fiber direction. The intersection of these two lines with the greater of the two pure uniaxial stress conditions in the unidirectional plies locates the endpoint of each cutoff. It is always necessary that the cutoff be located by the higher of the uniaxial strengths since, otherwise, the cutoff would undercut the measured uniaxial strain to failure at the other end. This procedure results in the same failure diagram for all fiber-dominated laminates. It should be emphasized that this procedure requires the use of the Poisson's ratio of the unidirectional ply even when the laminate contains fabric plies.

This failure model, as represented in Figure 5.4.2, has been developed from experience with fiber-reinforced polymer matrix composites used on subsonic aircraft, particularly with carbon/epoxy materials, for which the lamina ν_{TL} is approximately zero. It should not be applied to other composites, such as whisker-reinforced metal-matrix materials. Figure 5.4.2 addresses only fiber-dominated failures because, for the fiber polymer composites used on subsonic aircraft, the microcracking in the matrix has not been found to cause reductions in the static strength of laminates, particularly if the operating strain level has been restricted by the presence of bolt holes or provision for damage tolerance and repairs. However, with the advent of new composite materials, cured at much higher temperature to withstand operation at supersonic speeds, this approach may no longer be appropriate. The residual stresses developed during cool-down after cure will be far higher, because of the greater difference between the cure temperature and the minimum operating temperature.

This set of truncations together at the laminate level with the original maximum strain criterion results in the following operative set of equations applied *at the laminate level* with respect to axes oriented along and normal to each fiber direction in the laminate

$$\begin{aligned}\epsilon_{11}^{cu} &\leq \epsilon_{11}^i \leq \epsilon_{11}^{tu} \\ \epsilon_{11}^{cu} &\leq \epsilon_{22}^i \leq \epsilon_{11}^{tu} \\ |\epsilon_{11}^i - \epsilon_{22}^i| &\leq (1 + \nu_{LT}^{lamina}) |\epsilon_{11}^{tu} \text{ or } \epsilon_{11}^{cu}|^*\end{aligned}\tag{5.4.2(c)}$$

* whichever is greater

However, it is important to note that these equations can only be applied in the context of a fiber-dominated laminate as previously described. It should further be noted that the limits on the transverse strain in each ply, ϵ_{22}^i , are set by the fibers in plies transverse to the ply under consideration and thus cannot characterize matrix cracking. This must be carefully taken into account if hybrid laminates are utilized. Furthermore, as previously discussed, if matrix cracking is considered to be structurally significant, a stress or strain cutoff must be added based on empirical observation. In this case, an assessment of the effects of the matrix cracks on subsequent properties of the laminate must be made.

As noted in Section 5.4.1, bending occurs when there are external bending and/or twisting moments or when the laminate is not symmetric. In these cases, as with other failure criteria, it is necessary to take into account the fact that the laminate level strains vary through the thickness.

5.4.3 Laminate design

Design charts in the form of "carpet plots" are valuable for selection of the appropriate laminate. Figure 5.4.3 presents a representative carpet plot for the axial tensile strength of laminates having various proportions of plies oriented at 0°, ±45°, and 90°.

The development of laminate stacking sequence (LSS) optimization routines for strength-critical designs is a difficult task. Such a scheme must account for competing failure mechanisms that depend on material, load type (e.g., tension versus compression), environment (e.g., temperature and moisture content) and history (e.g., fatigue and creep). In addition, the load transfer must be adequately modeled to account for component geometry and edge effects. Even for a simple uniaxial load condition, the relationship between LSS and strength can be complex. Some qualitative rules currently exist for optimizing LSS for strength but they have been developed for a limited number of materials and load cases.

Relationships between LSS and laminate strength depend on several considerations. The initiation and growth of local matrix failures are known to depend on LSS. As these failures occur, internal stress distributions also depend on LSS strength through local stiffness and dimensional stability considerations. For example, delamination divides a base laminate into sublaminates having LSS that are generally unsymmetric. Reduced stiffness due to edge delaminations, causes load redistribution and can decrease the effective tensile strength of laminates. Likewise, local instability of sublaminates also causes load redistribution which can lower the effective compressive strength of laminates. As a result, both laminate and sublaminate LSS affect laminate strength.

Shear stress distributions play a significant role in determining the mechanical behavior and response of multi-directional laminates. As was the case for ply transverse tensile strength, ply shear strength depends on LSS. Laminates with homogeneous LSS have been found to yield higher in-situ ply shear strengths than those with ply orientations clumped in groups (Reference 5.4.3(b)). An inherent flaw density and interlaminar stresses appear to be major factors affecting the distribution of ply shear strengths in a LSS.

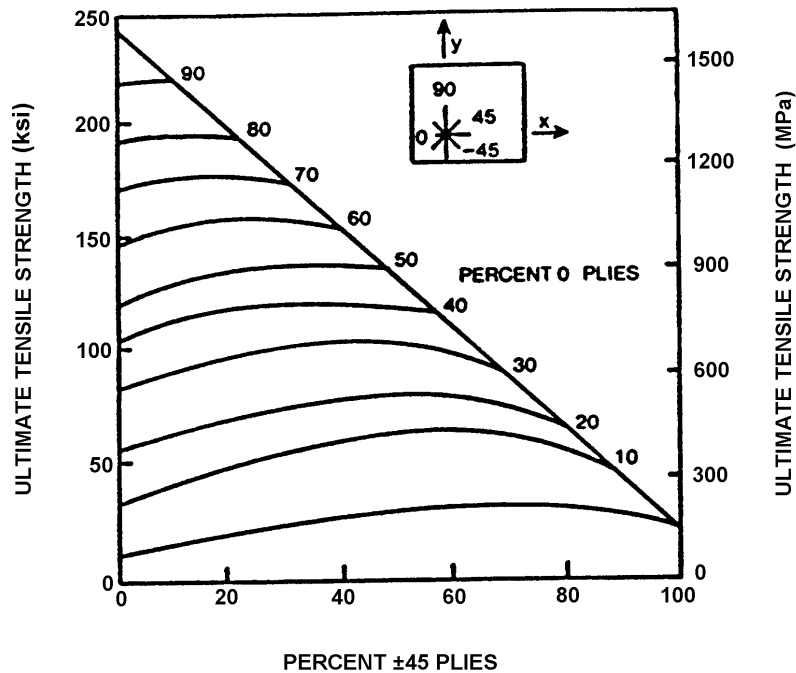


FIGURE 5.4.3 Tensile strength of $[0_i/\pm 45_j/90_k]_s$ family of high strength carbon/epoxy laminates (Reference 5.4.3).

As was the case for bending stiffness, bending strength in composite laminates is strongly dependent on LSS. Failure mechanisms characteristic of tension, shear, and compression load conditions may all combine to affect bending strength. Table 5.3.3.2(b) showed that preferential stacking of plies in outer layers of the LSS increased bending stiffness. The bending strength performance of undamaged laminates may show similar trends; however, surface damage due to impact or other in-service phenomena would cause severe degradation to such laminates.

Additional information on laminate stacking sequence effects is found in Section 5.6.5.

5.4.4 Stress concentrations

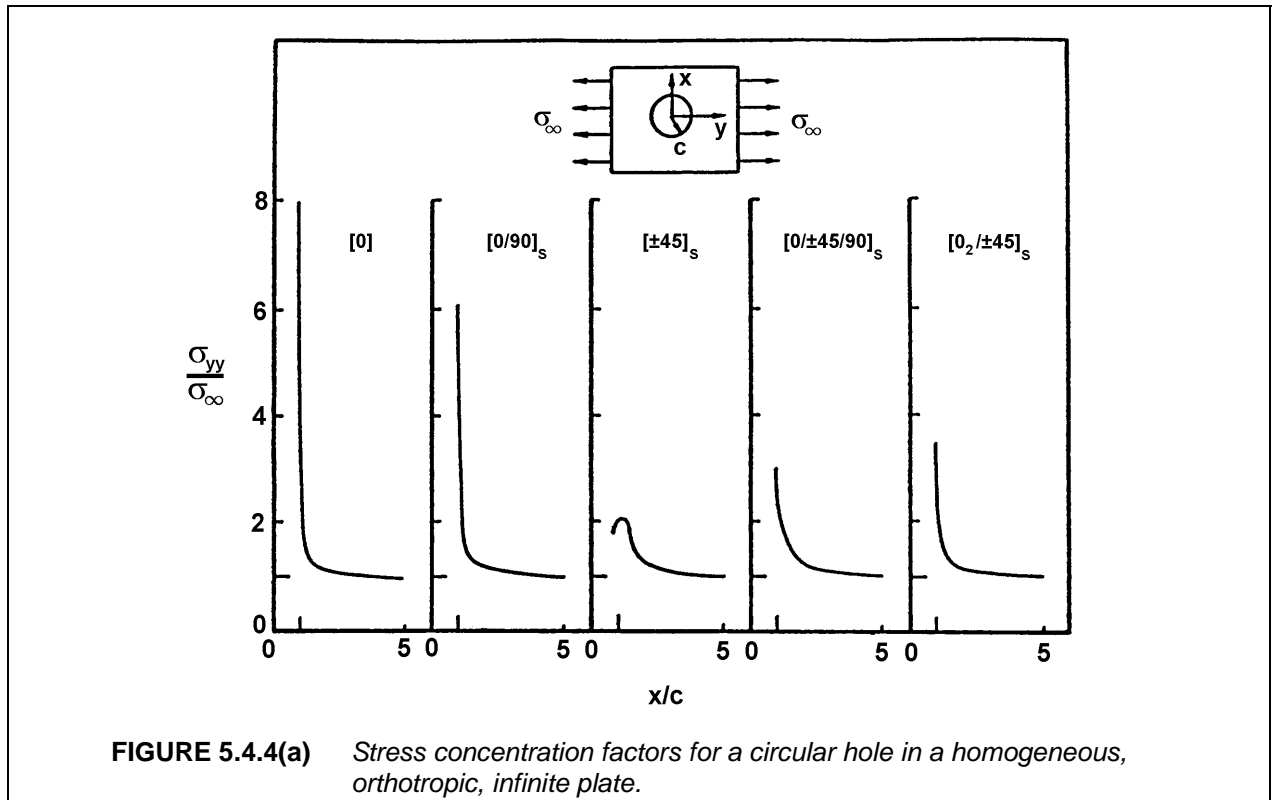
The presence of a hole or other discontinuity in a structure introduces local stress concentrations. These high local stresses can result in initial localized failure. The analysis of failure due to cracking, or fracture, which can result in this situation is complicated for composite materials because of material heterogeneity at the microscale and in a layer-to-layer basis. Effective in-plane laminate stiffnesses, E_x , E_y , and G_{xy} , may be calculated for any laminate by using the methods presented in Section 5.3.3. With these properties specified, a balanced symmetric laminate may be regarded as a homogeneous orthotropic plate, for structural analysis. Orthotropic elasticity theory may be used for the evaluation of stresses around a hole in such a plate (Reference 5.4.4(a)). Examples of the resulting stress concentrations are shown in Figure 5.4.4(a) for carbon/epoxy laminates. The laminae orientation combinations influence both the magnitude and the shape of the stress variation near the hole. The high stresses at the edge of the hole may initiate fracture.

If the laminate fails as a brittle material, fracture will be initiated when the maximum tensile stress at the edge of the hole equals the strength of the unnotched material. In a tensile coupon with a hole, as

shown in Figure 5.4.4(a), failure will occur at the minimum cross-section. The failure will initiate at the edge of the hole, where the stress concentration is a maximum.

Consider the stress concentration factor in a finite width isotropic plate with a central circular hole. Stress distribution for this configuration are shown in Figure 5.4.4(b) for various ratios of hole diameter, a , to plate width, W . The basic stress concentration factor for this problem is the ratio of the axial stress at the edge of the hole ($x = a/2$, $y = 0$) to the applied axial stress, σ_∞ . For small holes in an isotropic plate, this factor is three. The average stress at the minimum section, σ_n , is higher than the applied stress, σ_∞ , and is given by the following relationship:

$$\sigma_n = \frac{\sigma_\infty}{(1 - \frac{a}{W})} \quad 5.4.4(a)$$



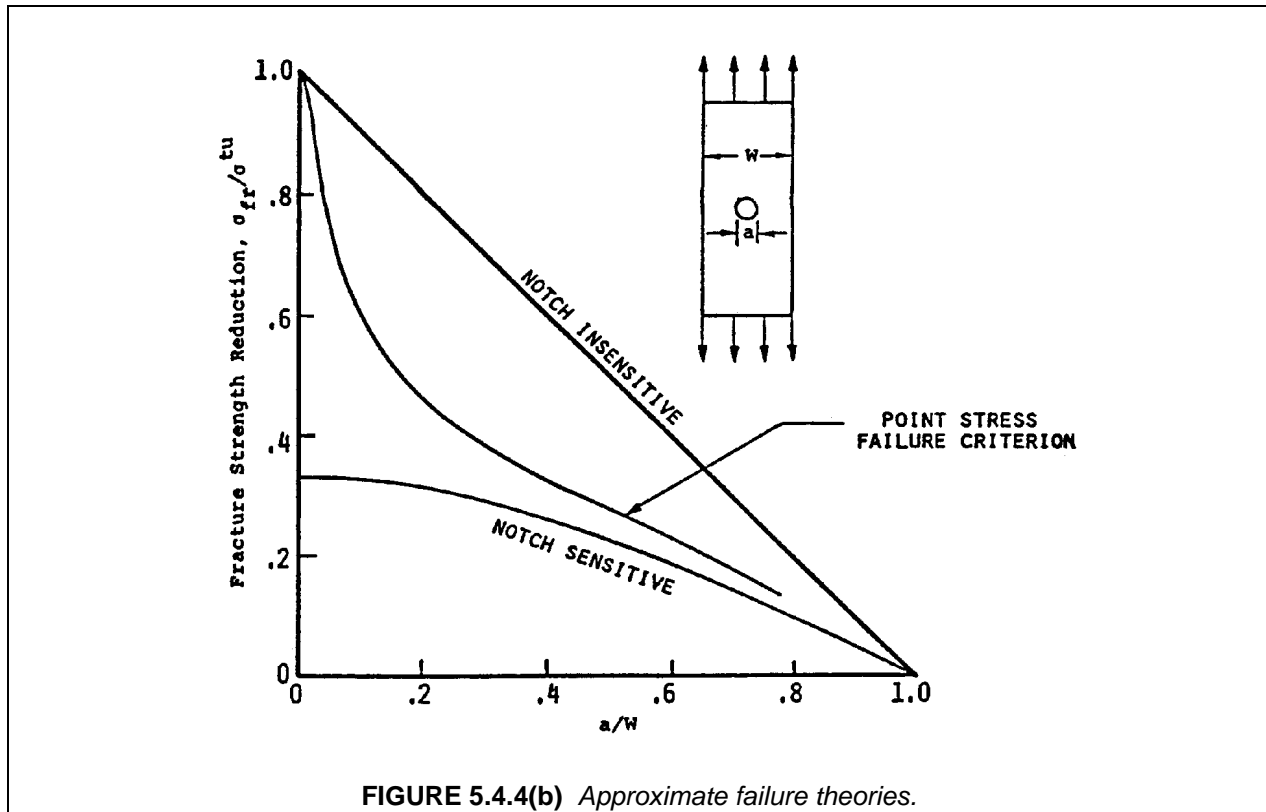
The net section stress concentration factor, k_n , is the ratio of the maximum stress to this average stress.

$$k_n = \frac{\sigma(\frac{a}{2}, 0)}{\frac{\sigma_\infty}{(1 - \frac{a}{W})}} \quad 5.4.4(b)$$

Laminate fracture for the elastic-brittle case will occur at stress σ_{fr} :

$$\sigma_{fr} = F^{tu} / k_n \quad 5.4.4(c)$$

A material which fails in this fashion is denoted a notch-sensitive material. In contrast, a ductile, or notch-insensitive, material will yield locally to alleviate the stress concentration effect.



Various matrix damage effects are expected to occur at the maximum stress locations. This localized damage reduces the material stiffness and diminishes and spreads the stress concentration effects. Semi-empirical methods have been proposed to account for this reduction in the stress concentration.

The "point stress theory" (Reference 5.4.4(b)) proposes that the elastic stress distribution curve, e.g., Figure 5.4.4(a), be used, but that the stress concentration be evaluated at a distance, d_o , from the edge of the hole. The numerator of Equation 5.4.4(b) is evaluated at $x = a/2 + d_o$. The characteristic length, d_o , must be evaluated experimentally. The "average stress theory" (Reference 5.4.4(b)) takes a similar approach by proposing that the elastic stress distribution be averaged over a distance, a_o , to obtain the stress concentration.

$$k_n = \frac{\int_{a/2}^{(a/2)+a_o} \sigma_y dx}{\int_{a/2}^{W/2} \sigma_y dx} \quad 5.4.4(d)$$

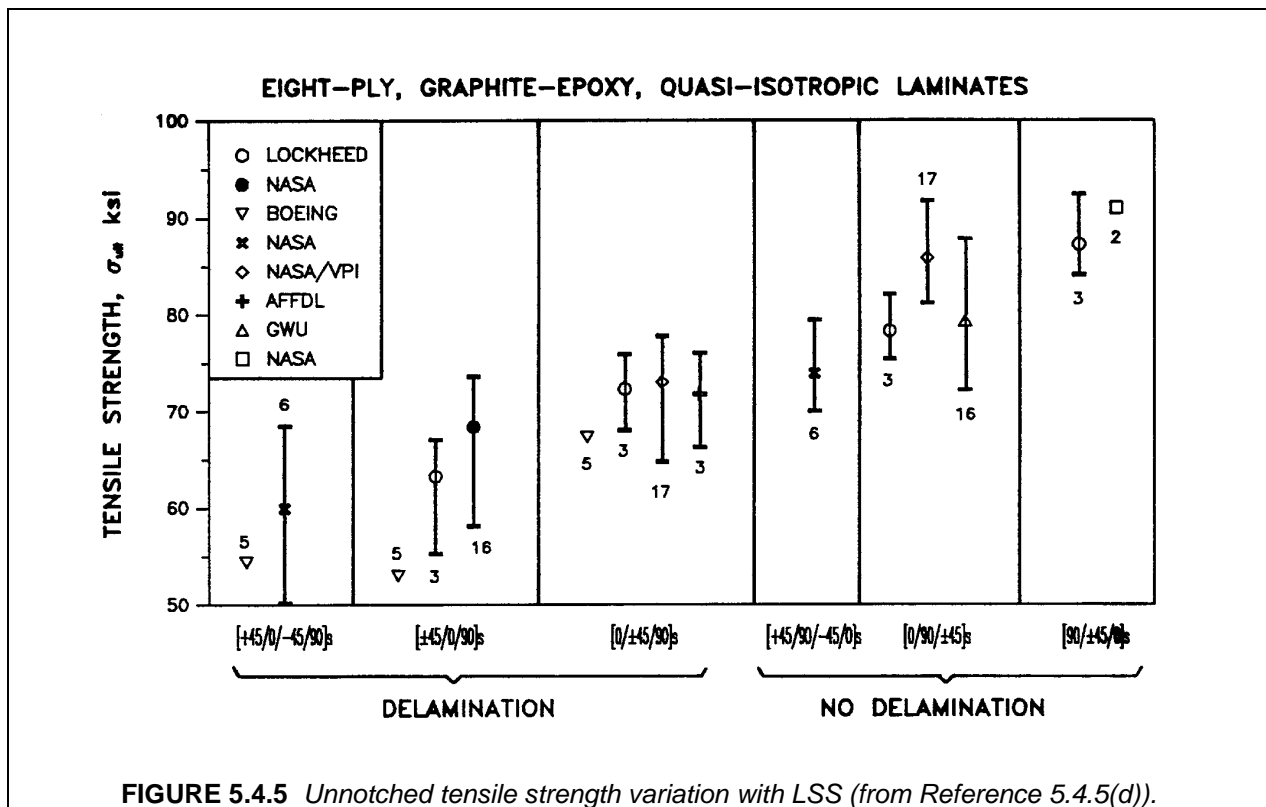
Again, the characteristic dimension, a , must be found experimentally. For both methods, the resulting stress concentration is used in Equation 5.4.4(c) to define the fracture stress. Representative results are plotted in Figure 5.4.4(b) to illustrate the differences associated with different types of material behavior.

The relationship between tensile strength and laminate stacking sequence (LSS) for laminates with holes, cutouts, and through-penetrations (i.e., a damage tolerance consideration) is complex (see References 5.4.4(c) - (g)). Certain combinations of ply splitting and delamination that occur at the tip of a notch can enhance residual strength by effectively reducing the stress concentration. Delaminations which uncouple plies, allowing individual plies to fail without fiber breaks, reduce the residual strength. Most existing analysis methods for predicting notched tensile strength are based on parameters determined by some notched laminate tests (e.g., characteristic dimension, fracture energy parameter). The effects of LSS on failure is included in the test parameter. Future analysis development that simulates progressive damage accumulation will provide a more efficient approach for studying the effects of LSS. Additional information on laminate stacking sequence effects is found in Section 5.5.5.

5.4.5 Delamination

The formation and growth of delaminations is generally related to LSS. Delaminations can have varying effects on tensile strength performance, depending on delamination location and the specific property of interest. Most studies performed to date have considered specimens with significant free edge surface area where interlaminar stresses are known to concentrate. Although all structures have some free edges, it is important to realize the limits of analysis and tests performed with specimen geometries. For example, the magnitude of interlaminar tensile stresses, which are crucial to edge delamination, approach zero for plate width to thickness ratios of 30 and greater (Reference 5.4.5(a)).

As shown in Figure 5.4.5, laminated specimens prone to edge delamination have been shown to exhibit generally lower strength (ultimate stress level) when loaded in uniaxial tension (e.g., References 5.5.5.1.1(b), 5.4.5(b) - (f)). The reduction in strength has been directly tied to a drop in stiffness with increased edge delamination area for laminates exhibiting stable delamination growth (References 5.5.5.1(b), 5.4.5(b) - (e)). The onset of edge delamination has been shown to relate to tensile strength for laminates exhibiting unstable delamination growth coupled with matrix cracks (Reference 5.4.5(f)).



The reduced laminate stiffness due to edge delamination can affect the measured tensile strength in two distinct ways (e.g., Reference 5.4.5(e)). If all plies remain loaded after delamination, the ultimate laminate strain has been found to equal the critical strain of primary load bearing plies. In these cases laminate strength drops in proportion to the apparent axial modulus. However, if off-axis plies cease to carry loads because they have been isolated by an interconnected network of matrix cracks and delamination, a local strain concentration can form. When this occurs, the global laminate strain for failure can be less than the critical strain of primary load bearing plies.

Free edge delaminations split a laminate into sublaminates, each of which continue to carry tensile loads. The apparent modulus of this laminate depends on delamination length and the sublaminate

moduli which may be calculated using lamination theory. These moduli will depend on LSS if unsymmetric sublaminates with strong extension/bending couplings are involved (References 5.4.5(g) and (h)). A simple rule-of-mixtures approach has been used to accurately calculate apparent moduli for edge delamination (References 5.4.5(e), (g) and (h)).

Local coupling between intralaminar matrix cracks and delaminations can cause complete or partial ply isolation. Note that complete ply isolation cannot occur unless associated damage extends the full laminate width. When this occurs, the apparent laminate stiffness and strain concentration can be calculated in a modified rule-of-mixtures approach which discounts isolated ply groups (References 5.5.5.1.1(c) and 5.4.5(e)). A local area of reduced stiffness also causes strain concentration (Reference 5.4.5(i)). The strain concentration depends on both the local reduced stiffness and global laminate stiffness. For example, hard laminates with strong anisotropy, such as lay-ups dominated by 0° plies and loaded uniaxially, will have large strain concentration factors. Consequently, hard laminates will be less tolerant of local damage than relatively soft laminates (e.g., quasi-isotropic).

When high interlaminar shear stresses are present, coupled edge delamination and matrix crack growth are possible and may lead to catastrophic failure. Edge delamination behavior of laminates commonly used in design (e.g., quasi-isotropic laminates) become dominated by interlaminar shear stresses when subjected to off-axis loading. Note that for this problem the laminate lay-up is generally unbalanced relative to the loading axis. The measured tensile strength coincides with the onset of edge delamination for such laminates (Reference 5.4.5(f)). As a result, failure criteria that account for interlaminar stresses are needed to predict the tensile strength.

The use of a suitable analysis method is recommended to evaluate edge effects in composite materials (e.g., References 5.4.5.1.1(f), 5.4.5(d), (g), (h), (j) - (l)). Applied mechanical loads and environmental effects should be included in the free edge analysis. Two approaches have been successfully applied to quantify free edge stresses and predict edge delamination: (1) a fracture mechanics based method using strain energy release rates (References 5.5.5.1.1(f), 5.4.5(d), (g), (h), (j)), and (2) a strength of materials based approach using an average stress failure criterion (References 5.4.5(k) and (l)).

The combined use of resin interlayers between the plies in a laminate and specimen edge polishing have been found to be effective methods for suppressing edge delamination (Reference 5.4.5(f)). Materials with high interlaminar toughness have an inherent resistance to delamination. Other methods that have been used to suppress edge delamination include resin interlayer strips at critical interfaces along the edge of laminates (Reference 5.4.5(m)), termination of critical plies offset from the edge (Reference 5.4.5(n)), hybridization (References 5.4.5(o) and (p)), and serrated edges (Reference 5.4.5(p)).

Most of the above discussion on the effects of delamination suggest a decrease in tensile properties. This is generally true for unnotched specimen geometries prone to edge delamination. Isolated delaminations that occur away from the edge of a laminate (e.g., manufacturing defects) and are not coupled with matrix cracks have been shown to have little effects on tensile strength (Reference 5.4.5(r)). Theoretically, such delaminations do not result in local reduced laminate stiffness when loaded in tension due to compatibility considerations. Multiple delaminations located away from the edge of a laminate have been shown to cause a small reduction in tensile strength (Reference 5.4.5(r)). This was explained by coupling between delaminations and other matrix damage (e.g., ply splits) that occurred during loading, resulting in partial ply isolation and local reduced stiffness. Most of the discussion in this section is related to free edge effects (Section 5.5.3) and laminate stacking sequence effects (Section 5.5.5).

5.4.5.1 Compression

Delaminations generally have a stronger affect on compressive strength than on tensile strength. As a result, the potential for delamination should always be considered when selecting a suitable LSS. The effect of delamination occurring due to manufacturing defects and/or in-service events such as impact needs to be included in this evaluation. For example, the best LSS for avoiding edge delamination in specimen geometries may not be best for suppressing the effects of delaminations occurring in structures due to impact.

Delamination breaks the laminate into sublaminates, each having associated stiffness, stability, and strength characteristics. Sublaminates are usually unsymmetric and, therefore, all of the sublaminate stiffnesses will depend on LSS. As shown in Figure 5.4.5.2, stability and local compressive performance of sublaminate ply groups ultimately determines catastrophic failure.

Compressive failure in composite laminates having delaminations is strongly tied to the stability of sublaminate plates. Since delaminations may occur at many different interfaces in a laminate, sublaminates LSS will generally not be balanced and symmetric. As discussed earlier, the bending/extension couplings characteristic of such LSS reduce buckling loads. The sublaminate boundary conditions and shape are also crucial to the relationship between LSS and stability.

Several methods exist for predicting sublaminate stability in composite laminates (e.g., References 5.4.5.1(a) - (e)). These models differ in assumed bending stiffness, boundary conditions, and sublaminate shape. Experimental data bases are needed to determine which assumption is appropriate for a given problem. The in-plane and out-of-plane stress redistribution due to a buckled sublaminate is crucial to compressive strength.

Environment can play a significant role in delamination growth and load redistribution if the environmental resistance of combined sublaminate stiffnesses are significantly different than those of the base laminate. The combined effects of environment and LSS on laminate dimensional stability were covered in earlier sections. The stability of unsymmetric sublaminates is expected to relate to warpage. The warp depends on both LSS and environmental conditions. Warp may be treated as an imperfection in stability analysis.

The initiation of free edge delamination in compressively loaded laminates can be predicted using methods similar to those used for tension (e.g., Reference 5.4.5.1(a)). Once initiated, delamination growth depends on sublaminate stability. An adequate sublaminate stability analysis model must, therefore, be coupled with the growth model (e.g., References 5.4.5.1(b) and (c)). Delamination growth can be stable or unstable, depending on sublaminate LSS, delamination geometry, structural geometry, and boundary conditions. Growth of multiple delaminations, characteristic of impact damage, is currently not well understood.

5.4.6 Damage and failure modes

5.4.6.1 Tension

Tensile rupture of laminates with multidirectional plies normally involves a series of pre-catastrophic failure events, including both matrix damage and localized fiber breaks. Catastrophic failure is expected whenever the longitudinal tensile strength of any ply in a laminate is exceeded; however, laminates can separate without fiber failure by coupling various forms of matrix damage. Example laminates that can fail due to matrix damage include those with less than three distinct ply orientations (angle-ply laminates loaded in the 0° direction). Recommendation 2 in Section 5.6.5.2.1 is intended to avoid the low strengths associated with catastrophic failures occurring without fiber breaks.

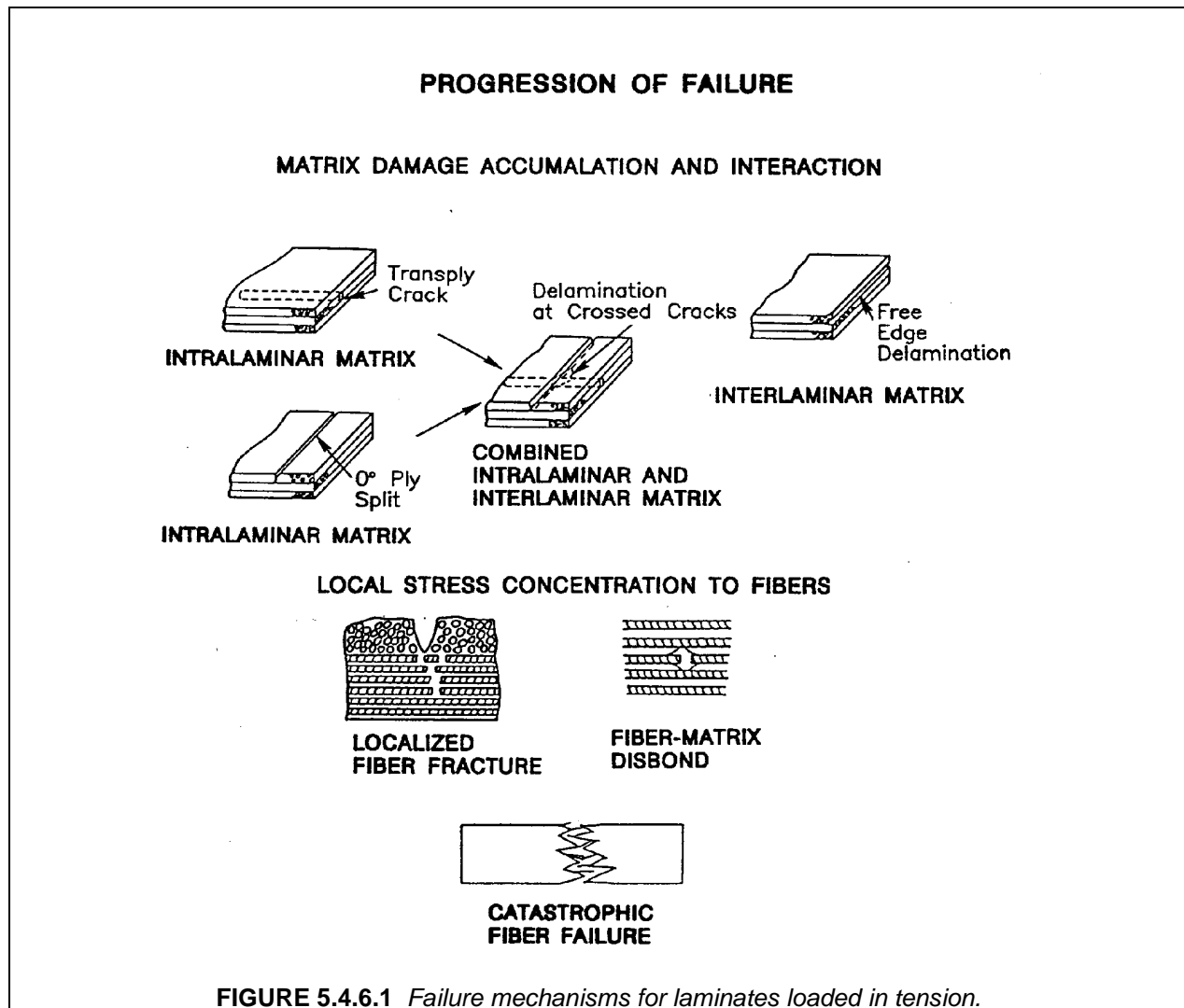
Figure 5.4.6.1 shows the various failure mechanisms that can occur at micro and lamina dimensional scales for a multidirectional laminate loaded in tension. Depending on load conditions and material properties, matrix failure (e.g., transverse matrix cracks, delamination) or isolated fiber breaks occur at stress levels less than the static strength. Load redistributes around local failures until a critical level of damage is reached, upon which catastrophic fiber failure occurs. Resin is of secondary importance through its effect on resistance to matrix damage accumulation and local load transfer (i.e., near matrix damage and isolated fiber breaks). The LSS also plays a secondary role by affecting damage accumulation and load transfer.

Critical micro failure mechanisms shown in Figure 5.4.6.1 include localized fiber failure and fiber/matrix interfacial cracking. These mechanisms occur mostly in plies aligned with a major axis of ten-

sile stress. The laminate stress levels at which these failures occur depend on load redistribution due to the characteristic damage state in adjacent plies. A limited number of fiber breaks are tolerated within a lamina before the entire ply fails, which can trigger catastrophic laminate failure.

Matrix failure mechanisms at the lamina scale for laminates with multidirectional plies are also shown in Figure 5.4.6.1. Intralaminar matrix cracks align parallel to the fiber direction and span the thickness of a ply or group of plies stacked with the same orientation. These have also been referred to as transply cracks or ply splits depending on whether a crack orients at an angle or parallel to the tensile load axis, respectively.

Interlaminar matrix failure, often referred to as delamination, can form near free edges or at intersections between intralaminar cracks. Delaminations form due to excessive interlaminar normal and shear stresses. The accumulation of intralaminar and interlaminar matrix failures depends strongly on LSS.



5.4.6.1.1 Matrix cracks

Matrix cracks occur in plies of laminated composites due to combined mechanical and environmental stresses. These transverse cracks align with fibers and, when fully formed, span the thickness of individ-

ual plies or ply groups stacked together in the same orientation. Matrix cracks redistribute local stress in multidirectional laminates, allowing a crack density to develop in the ply of ply group as a function of load and environmental history. These cracks can also form prior to service exposure due to processing.

Studies with specimens loaded in uniaxial tension have shown that initial fiber failures found in 0° plies occur near intralaminar matrix cracks in neighboring off-axis plies (Reference 5.4.6.1.1(a)). When matrix cracks span a single off-axis ply, the stress concentration in a neighboring 0° ply is generally small and localized over a small portion of the neighboring ply thickness. This has been found to influence the location of laminate failure, but has little effect on tensile strength (References 5.4.6.1.1(b) and (c)).

Intralaminar matrix cracks normally span the full thickness of multiple off-axis plies that have been stacked together. The associated stress concentration in a neighboring ply increases with the thickness of a cracked group of stacked plies. The stress concentration in a 0° ply due to matrix cracks in a large group of stacked 90° plies was found to significantly decrease laminate tensile strength (References 5.4.6.1.1(c) and (d)). This is one of the reasons for Recommendation 3, Section 5.5.5.2.1.

Even when strength is not altered by the presence of matrix cracks, it is important to understand the mechanics of matrix cracking for composite materials used in aerospace applications. For example, matrix cracks can play a fundamental role in the generation of delaminations. The increased surface area due to a network of matrix cracks can also alter physical properties such as composite thermal expansion, liquid permeability, and oxidative stability.

Residual stresses, that develop due to differences in thermal and moisture expansion properties of constituents, affect the formation of matrix cracks. In general, tensile residual stress develops in the transverse-fiber directions of lamina when multidirectional polymer matrix composites are exposed to temperatures below the residual stress free temperature. This occurs during a temperature drop because unconstrained shrinkage of tape lamina is much greater in transverse-fiber directions than in fiber directions. As moisture is absorbed into a laminate, matrix swelling counteracts thermal shrinkage, decreasing the transverse-fiber tensile stress.

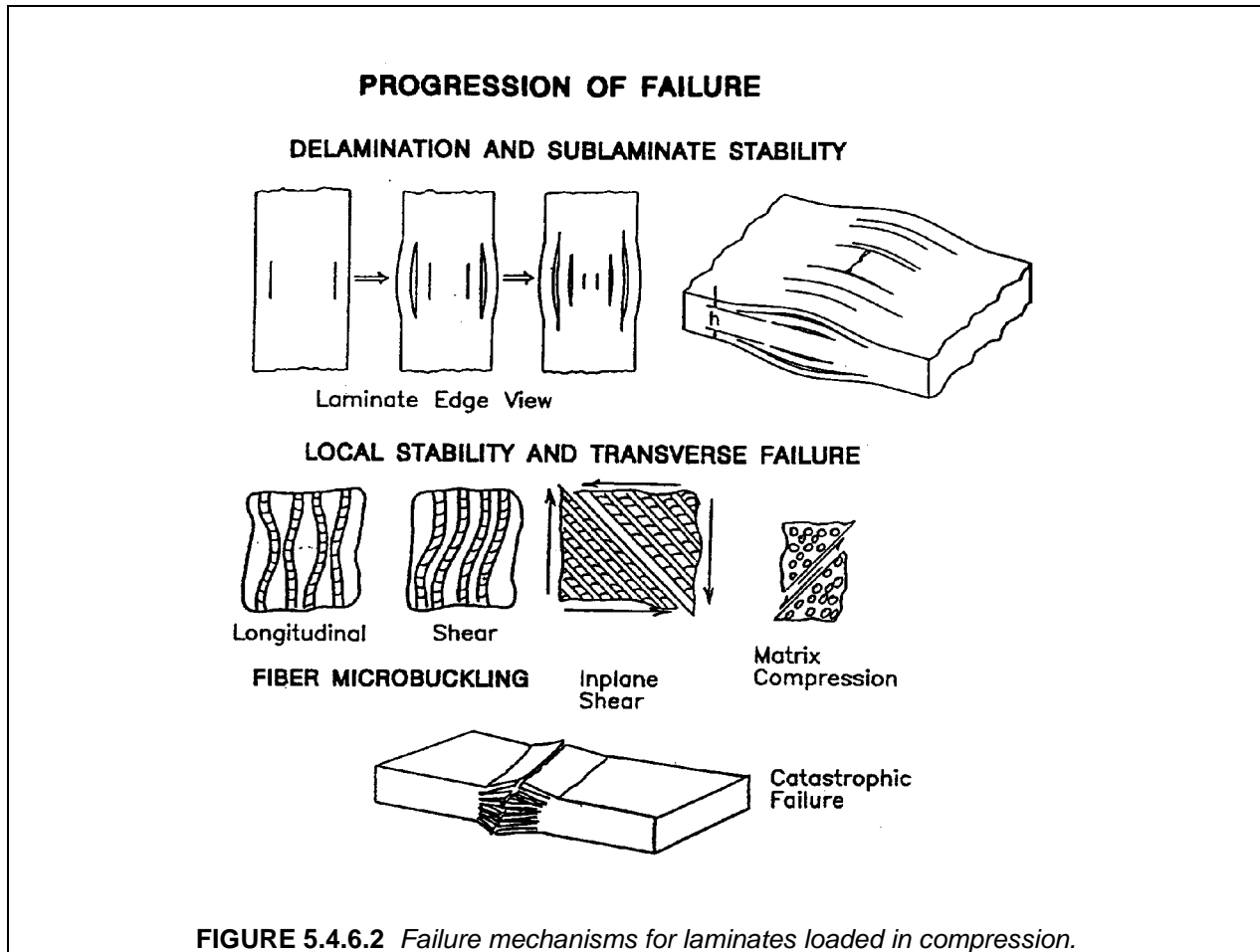
The critical stress or strain causing the onset of matrix cracking in plies of a laminate has been referred to as in situ transverse lamina strength. This strength is not a material constant since it depends on LSS. Experiments and analysis have shown that in situ strength increases as the thickness of plies grouped together with the same orientation decreases (e.g., References 5.4.6.1.1(e) - (i)). These studies have also shown that neighboring plies can impose differing constraints on matrix crack formation, depending on fiber orientation. Many materials currently used in the aerospace industry have resin-rich interlaminar layers (RIL). The magnitude of the in situ strengthening effect decreases if a RIL with significant thickness exists between plies (Reference 5.4.6.1.1(j)). Relatively soft RIL eliminate some of the constraint imposed by neighboring plies.

5.4.6.2 Compression

Compressive strength is ultimately related to the local response of individual ply groups. Assuming no matrix damage exists due to impact or previous load history, the local stability and strength of plies aligned with the axis of loading will determine final failure. The location of load-carrying plies relative to the laminate surface can play a role in this instance. The short wavelength buckling load is reduced when critical plies are located in outer layers of the laminate stacking sequence. When matrix damage does exist, the combined local response of individual ply groups affects the compression strength. The stability and load redistribution within individual ply groups or sublaminates is crucial to the local response.

Figure 5.4.6.2 shows three different types of local compressive failure mechanisms. These mechanisms were observed to occur as a function of θ for $(\pm\theta)_s$ type laminates (References 5.4.6.2(a) and (b)). When delamination occurs, all three of the local failure modes may combine to determine the compressive strength of a laminate stacking sequence. (Additional information on the effects of the laminate stacking sequence is found in Section 5.6.5.) In-plane matrix shearing and matrix compression failures

were observed for $(\pm\theta)_s$ type laminates with $15^\circ \leq \theta \leq 90^\circ$ and $60^\circ \leq \theta \leq 90^\circ$, respectively. The shear mode of fiber microbuckling is most commonly observed for composites. This mode was shown to initiate compressive failure for $(\pm\theta)_s$ type laminates with $0^\circ \leq \theta \leq 10^\circ$. Depending on matrix and fiber combination, final local failures for such laminates involved some combination of fiber failure (shear, kinking, or bending) and matrix splitting or yielding (References 5.4.6.2(c) and (d)).



5.4.7 Summary

- Ply level stresses are commonly used to predict first ply and subsequent ply failures leading up to laminate failure. Once a ply has failed, its contribution to laminate strength and stress is conservatively reduced. Typically, in-plane failure criteria are applied only to lamina fiber loading conditions; in-plane matrix-dominated static failure criteria should not be used since it will generally lead to overly conservative failure predictions.
- Under static loading conditions, composites are particularly notch-sensitive as a function of lay-up and more specifically stacking sequence.

5.5 COMPLEX LOADS

5.5.1 Biaxial in-plane loads

This section is reserved for future use.

5.5.2 Out-of-plane loads

This section is reserved for future use.

5.6 LAMINA TO LAMINATE CONSIDERATIONS

5.6.1 Residual stresses and strains

Residual curing stresses and strains have virtually no effect on fiber-dominated laminate properties. However, residual stresses in the resin can be greater than the mechanical stresses needed to cause failure. Neglecting these residual stresses therefore may be nonconservative. The residual stresses may be high enough that resin microcracking may occur before any mechanical load is applied. Consequently, the principle of superposition may not be applicable as the mechanical loading may result in nonlinear behavior. As an example, typical epoxy matrix residual strains at the microlevel, resulting from cool down after curing at 350°F (180°C), may be approximately 25 to 100% of the laminate failure strain.

5.6.2 Thickness effects

Much of the difference in properties found when comparing laminates with different thicknesses can be explained by the residual stresses developed during processing. Internal stresses developed during processing may produce voids, delaminations, and microcracks or cause residual stresses in the laminate that may affect material properties. Excessive porosity, generally caused by poor processing, or environmental effects due to temperature and moisture conditions may also degrade the material and affect its behavior.

Variations in material properties between thick laminate test data from different sources, for laminates having the same thickness, can generally be attributed to differences in processing. Such variations can be minimized by optimizing the cure cycle and by proper process control.

The residual stresses may be caused by non-isothermal conditions present during the solidification phase. Different layers of the laminate will undergo different degrees of volume contraction at any given time during the process cycle. This gives rise to a self-equilibrating force system producing tension stresses in the center and compression stresses in the surface layers of the laminate as reported by Manson and Seferis (Reference 5.6.2(a)). Thickness effects observed in composite laminates are primarily due to this phenomena.

In thermosetting materials, these through-the-thickness stress gradients can be virtually eliminated by modeling the total process, including cool-down, so isothermal conditions are present near the resin gelation point and are maintained for a sufficient period of time. In some high-temperature processing materials where rapid cooling is required, significant thermal stresses may build up in the laminate.

In their work, the authors in Reference 5.6.2(a) present a method to experimentally determine and analyze the internal stresses developed during processing of a composite laminate. This method consists of laying up a certain number of plies, separated by a release ply that can be removed after processing. The internal stresses in the laminate can then be analyzed by considering the deformations of the individual sublaminates.

In summary, variations in material properties in laminated composites are mostly the result of thermally induced residual stresses, although environmental effects and process parameters other than tem-

perature may affect test data. True thickness effects are caused by temperature gradients across the thickness of the laminate. These effects may be minimized by mathematical modeling of the total process and can be virtually eliminated in thermosetting materials. Advance process models such as ROAST, described in Reference 5.6.2(b), may be used to optimize the process parameters.

5.6.3 Edge effects

Consideration of edge effects in laminated composites is necessary due to behavior not observed in homogeneous solids. A complex stress state exists between the layers of different orientation at the free edge of a laminate, such as along a straight edge or around the perimeter of a hole. Where a fiber in a laminate has been subjected to thermal or mechanical strain, the end of the cut fibers must transfer the load to adjacent fibers. If these adjacent fibers have a different orientation, they will present a locally stiffer path and accept the load. The matrix is the only mechanism for this load transfer. The stresses due to this load, namely interlaminar stresses, can be sufficient to cause local microcracking and edge delamination. These interlaminar stresses, in general, include normal (peel stress σ_z) and shear components (τ_{yz} , τ_{xz}) and are only present in a small region near the free edge. A typical interlaminar stress distribution is shown in Figure 5.6.3. The high gradients of these stresses depend on differences in Poisson's ratio and in-plane shear stiffness that exist between the laminae groups in a laminate. The same kinds of stresses are induced by residual thermal stresses due to cool-down after cure at elevated temperatures.

Failure often occurs as a result of delamination at the locations of high interlaminar stresses because of low interlaminar strength. The effects of free edge stress are sufficient to reduce the strength of certain specimens in both static and fatigue tests significantly. This premature failure makes coupon data difficult to apply to large components because of the local effects of the free edge failure mode. Classical laminate theory which assumes a state of plane stress is incapable of predicting the edge stresses. However, determination of such stresses by higher order plate theory or finite element analysis is practical. Therefore, consideration of edge interlaminar stresses in a laminate design is feasible. The gradients of this stress can be reduced by such measures as 1) changing the laminate stacking order, 2) minimizing the mismatch of the Poisson's ratio, the coefficient of mutual influence, and coefficients of thermal and moisture expansion between adjacent laminae, and 3) by inserting an inner layer which has a lower shear modulus and a finite thickness between laminae, thus allowing greater local strain to occur (Reference 5.6.3(a)).

Edge effects may be analyzed by fracture mechanics, strength of materials, or other methods (References 5.6.3(a) - (d)). These methods can be used to provide a guideline for designers to select the laminate configuration and material system best suited for a particular application.

Very little work has been performed to date on free edge effects for load conditions other than uniaxial tension or compression. Some analysis results indicate that in-plane shear, out-of-plane shear/bending, in-plane bending, twisting moments, and combined loading yield a higher magnitude of interlaminar stress relative to those associated with axial load conditions (Reference 5.6.3(f)). For example, out-of-plane shear due to bending causes free edge interlaminar stresses that are an order of magnitude higher than that caused by axial tension. For more information on delaminations and free edge effects, see Section 5.4.5. Information on the laminate stacking sequence effects is found in Section 5.6.5.

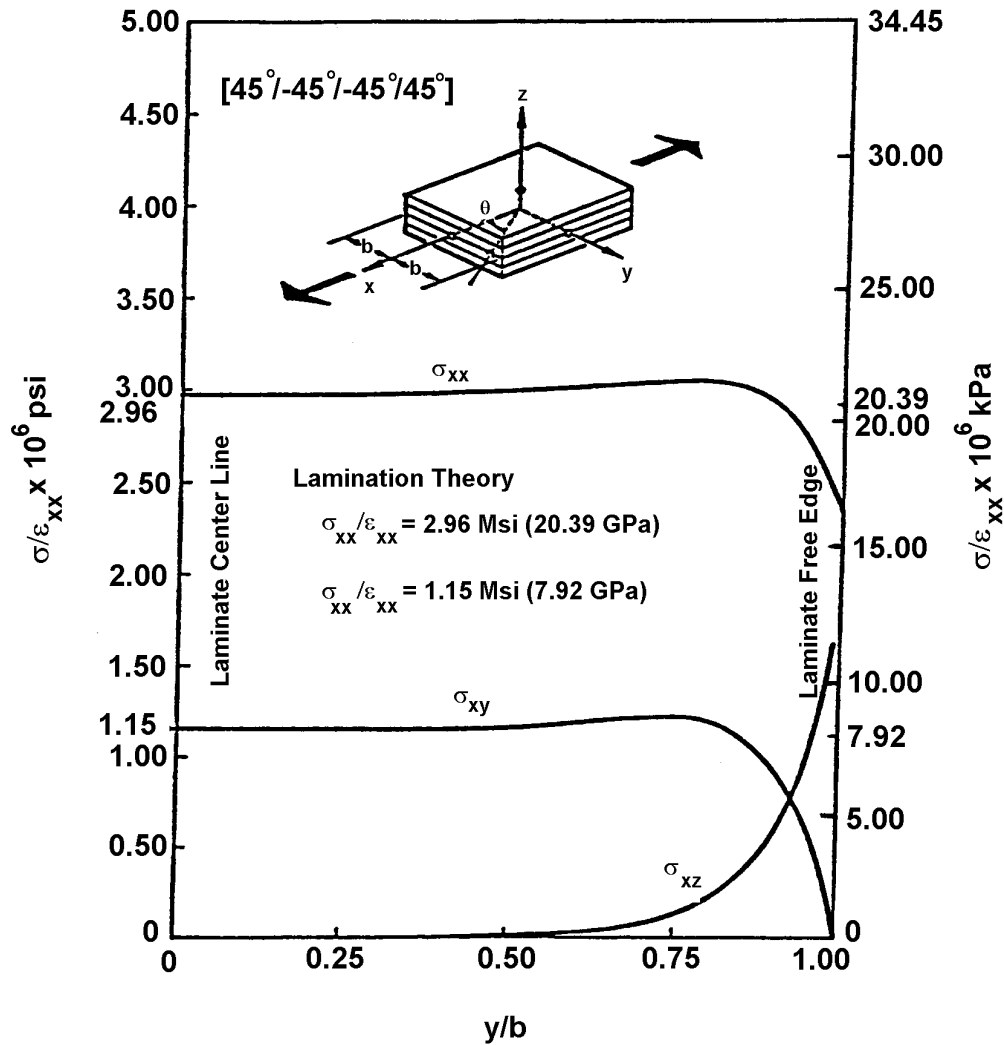


FIGURE 5.6.3 Interlaminar stresses normalized with respect to the applied strain (reproduced by permission from Reference 5.6.3(e)).

5.6.4 Effects of transverse tensile properties in unidirectional tape

The transverse strength properties play only a minor role in establishing cross-ply laminate strengths. It is, however, well-known that the effective "in-situ" transverse strength of transverse plies is much greater than the strength measured on the lamina. This effect has been handled by post-first ply failure analysis methods.

In-plane shear tests on laminae exhibit relatively high strains to failure (4 -5%). The much lower transverse tensile strains to failure (1/2%) indicate a marked notch sensitivity that is suppressed in cross-ply laminates. The initial cracks that fail laminae are arrested by fibers in other directions; thus laminae with microcracks are still effective. Most laminae develop cracks due to residual thermal stresses and continue to function.

5.6.5 Laminate stacking sequence effects

5.6.5.1 Introduction

Stacking sequence describes the distribution of ply orientations through the laminate thickness. As the number of plies with chosen orientations increase, more stacking sequences are possible. For example, a symmetric 8-ply laminate with four different ply orientations has 24 different stacking sequences. This presents a predicament when attempting to optimize composite performance as a function of stacking sequence.

Laminated composite structural properties such as stiffness, dimensional stability, and strength have all been found to depend on laminate stacking sequence (LSS). Generally, each property has a different relationship with LSS. Therefore, the choice of LSS for a particular design application may involve a compromise. Design optimization requires verified analysis methods and an existing materials database. The development of verified analysis methods for predicting stiffness and stability of laminated composites is more mature than that for predicting strength.

Some simplified design guidelines for LSS are provided in Section 5.6.5.2. These guidelines are generally conservative; however, they limit design optimization, and may even be misleading for some special cases. As a result, a comment on the reason for each guideline is included in the discussion. Verified analysis methods should be used to help judge the effects of LSS whenever possible.

Additional discussion of stacking sequence effects on particular topics are provided in the sections noted in Table 5.6.5.1.

TABLE 5.6.5.1 *Additional discussions on stacking sequence effects.*

Topic	Section	Page
Bending	4.3.3.2, 4.4.3	4-42, 4-62
Buckling	4.7.1.8	4-88
Compression after impact	4.11.1.4	4-107
Delamination	4.4.5	4-69
Free edge effects	4.5.3	4-77
Hygroscopic analysis	4.3.4	4-50
Lamination theory	4.3.2	4-33
Notched strength	4.4.4	4-63
Ply shear strength	4.4.3	4-62
Thermal analysis	4.3.4	4-50
Vibration	4.12.2	4-118

5.6.5.2 Design guidelines

Laminate design starts by selecting the number of plies and ply angles required for a given application. Once the number of plies and ply angles are selected, a LSS is chosen. A LSS is considered het-

erogeneous when there is preferential stacking of specific ply orientations in different locations through the thickness of the laminate. Thick laminates with heterogeneous LSS are created by clumping plies of similar orientation. A LSS is said to be homogeneous if ply angles are evenly distributed through the laminate thickness. The ability to generate homogeneous LSS depends on the number of plies and ply angles. For example, it is impossible to create a homogeneous LSS for a four-ply laminate consisting of four different ply angles.

The following LSS guidelines are based on past experience from test and analysis. Guidelines are lumped under two categories; (1) strong recommendation, and (2) recommendation. Despite this classification, exceptions to the guidelines should be considered based on an engineering evaluation of the specific application.

5.6.5.2.1 Strong recommendations

1. Homogeneous LSS are recommended for strength controlled designs (In other words, thoroughly intersperse ply orientations throughout the LSS).

Comment: *Heterogeneous laminates should be avoided for strength-critical designs unless analysis and test data is available that indicates a clear advantage. In cases where heterogeneous laminates cannot be avoided (e.g., minimum gage laminates), it is generally best to stack primary load-carrying plies toward the laminate core. The best way to view possible strength problems with heterogeneous LSS is to consider the behavior of individual sublaminates (i.e., groups of plies separated by delaminations) that may be created during manufacturing or service exposure. This will be discussed later in greater detail.*

Heterogeneous LSS can yield optimum stiffness or stability performance; however, the effects on all other aspects of the design (e.g., strength, damage tolerance, and durability) should be considered before ignoring Recommendation 1. For example, interlaminar stress distributions are affected by variations in the in-plane stress field around the periphery of holes and cutouts and the "effective" LSS (i.e., ply orientations relative to a tangent to the edge). Since it is difficult to optimize for a single lay-up in this case, the best solution is to make the LSS as homogeneous as possible.

2. A LSS should have at least four distinct ply angles (e.g., 0° , $\pm\theta^\circ$, 90°) with a minimum of 10% of the plies oriented at each angle. Ply angles should be selected such that fibers are oriented with principal load axes.

Comment: *This rule is intended to avoid the matrix-dominated behavior (e.g., nonlinear effects and creep) of laminates not having fibers aligned with principal load axes. Such behavior can lead to low strengths and dimensional stability problems.*

3. Minimize groupings of plies with the same orientation. For tape plies, stack no more than four plies of the same orientation together (i.e., limit stacked ply group thicknesses ≤ 0.03 in. (0.8 mm)). In addition, stacked ply group thicknesses with orientations perpendicular to a free edge should be limited to ≤ 0.015 in. (0.38 mm).

Comment: *This guideline is used for laminate strength-critical designs. For example, it will help avoid the shear-out failure mode in bolted joints. It also considers relationships between stacked ply group thickness, matrix cracking (i.e., transverse tension and shear ply failures) and delamination.*

In general, ply group thickness should be limited based on details of the design problem (e.g., loads, free edges, etc.) and material properties (e.g., interlaminar toughness). Note that the absolute level of ply group thickness identified in this guideline is based on past experience. It should be confirmed with tests for specific materials and design considerations.

4. If possible, LSS should be balanced and symmetric about the midplane. If this is not possible due to other requirements, locate the asymmetry or imbalance as near to the laminate midplane as possible. A LSS is considered symmetric if plies positioned at an equal distance above and below the midplane are identical (i.e., material, thickness, and orientation). Balanced is defined as having equal numbers of $+\theta$ and $-\theta$ plies, where θ is measured from the primary load direction.

Comment: *This guideline is used to avoid shear/extension couplings and dimensional stability problems (e.g., warpage which affects component manufacturing tolerances). The extension/bending coupling of unsymmetric laminates can reduce buckling loads. Note that some coupling may be desired for certain applications (e.g., shear/extension coupling has been used for aeroelastic tailoring).*

5.6.5.2.2 Recommendations

5. Alternate $+\theta$ and $-\theta$ plies through the LSS except for the closest ply either side of the symmetry plane. A $+\theta/-\theta$ pair of plies should be located as closely as possible while still meeting the other guidelines.

Comment: *This guideline minimizes the effect of bending/twisting coupling, which is strongest when angle plies are separated near the surface of a laminate. Modifications to this rule may promote more efficient stiffness and stability controlled designs.*

6. Shield primary load carrying plies from exposed surfaces.

Comment: *The LSS for laminates primarily loaded in tension or compression in the 0° direction should start with angle and transverse plies. Tensile strength, microbuckling resistance, impact damage tolerance and crippling strength can all increase by shielding the main load bearing plies from the laminate surface. With primary load fibers buried, exterior scratches or surface ply delamination will not have a critical effect on strength. For laminates loaded primarily in shear, consideration should be given to locating $+45^\circ$ and -45° plies away from the surface. For cases in which an element is shielded by other structures (e.g., shear webs), it may not be necessary to stack primary load carrying plies away from the surface.*

7. Avoid LSS that create high interlaminar tension stresses (σ_z) at free edges. Analyses to predict free edge stresses and delamination strain levels are recommended to help select LSS.

Comment: *Composite materials tend to have a relatively low resistance to mode I delamination growth. Edge delamination, followed by sublaminar buckling can cause premature failure under compressive loads. Edge delamination occurring under tensile loads can also effectively reduce stiffness and lower the load carrying capability. Since delaminations occurring at the core of the laminate can have the strongest effect on strength, avoid locating tape plies with fibers oriented perpendicular to a free edge at the laminate midplane.*

8. Minimize the Poisson's ratio mismatch between adjacent laminates that are cocured or bonded.

Comment: *Excessive property mismatches between cobonded elements (e.g., skin and stringer flange) can result in delamination problems. In the absence of more sophisticated analysis tools, a general rule of thumb is*

$$\left| \nu_{xy}(\text{laminates 1}) - \nu_{xy}(\text{laminates 2}) \right| < 0.1 \quad 5.6.5.2.2$$

As opposed to static strength, composites are not particularly notch-sensitive in fatigue; hole wear is often used as the governing criterion constituting fatigue failure of composites loaded in bearing.

5.6.6 Lamina-to-laminate statistics

This section is reserved for future use.

5.6.7 Summary

- Laminate properties such as strength, stiffness, stability, and damage resistance and damage tolerance have been found to have some dependency upon laminate stacking sequence (LSS). Each property can have a different relationship with LSS. Thus, each given design application may involve a compromise relative to LSS determination.
- Homogeneous LSS are recommended for strength controlled designs (in other words, thoroughly intersperse ply orientations throughout the LSS).
- A LSS should have at least four distinct ply angles (e.g., 0° , $\pm\theta^\circ$, 90°) with a minimum of 10% of the plies oriented at each angle. Ply angles should be selected such that fibers are oriented with principal load axes.
- Minimize groupings of plies with the same orientation. For tape plies, stack no more than four plies of the same orientation together (i.e., limit stacked ply group thicknesses <0.03 in. (0.8 mm)). In addition, stacked ply group thicknesses with orientations perpendicular to a free edge should be limited to ≤ 0.015 in. (0.38 mm).
- If possible, LSS should be balanced and symmetric about the midplane. If this is not possible due to other requirements, locate the asymmetry or imbalance as near to the laminate midplane as possible. A LSS is considered symmetric if plies positioned at an equal distance above and below the midplane are identical (i.e., material, thickness, and orientation). Balanced is defined as having equal numbers of $+\theta$ and $-\theta$ plies, where θ is measured from the primary load direction.

5.7 COMPRESSIVE BUCKLING AND CRIPPLING

5.7.1 Plate buckling and crippling

5.7.1.1 Introduction

Rectangular flat plates are readily found in numerous aerospace structures in the form of unstiffened panels and panels between stiffeners of a stiffened panel, and as elements of a stiffener. Closed form classical buckling solutions available in the literature are limited to orthotropic plates with certain assumed boundary conditions. These boundary conditions may be fixed, simply supported, or free. For expediency, the engineer may wish to assume the most appropriate boundary conditions and obtain a quick solution rather than resort to using a buckling computer program such as Reference 5.7.1.1(a). However, the closed form solutions of laminated orthotropic plates are appropriate only when the lay-ups are symmetrical and balanced. Symmetrical implies identical corresponding plies about the plate mid-surface. Balanced refers to having a minus θ ply for every plus θ ply on each side of the mid-surface. Symmetrical and balanced laminated plates have B_{ij} terms vanish and the D_{16} and D_{26} terms virtually vanish. However, the balanced plies ($\pm\theta$) should be adjacent; otherwise the D_{16} and D_{26} terms could become significant and invalidate the use of the orthotropic analysis. The buckling solutions could be significantly nonconservative for thin unbalanced or unsymmetric plates (see Reference 5.7.1.1(b)). Note that not all closed form solutions give direct answers; sometimes the equations must be minimized with respect to certain parameters as will be shown later.

The behavior of flat plates in compression involves initial buckling, postbuckling out-of-plane displacements, and crippling (ultimate postbuckling failure). Only at crippling does permanent damage occur, usually some form of delamination due to interlaminar tensile or shear stresses.

Nomenclature used to describe the buckling behavior of composite plates in Section 5.7.1 is given in Table 5.7.1.1.

TABLE 5.7.1.1 *Buckling and crippling symbols.*

SYMBOL	DEFINITION
a	length
b	width
B_{ij}	stiffness coupling terms of laminated plate
D_{ij}	flexural/twisting stiffness terms of laminated plate
$F_{x,cl}^{cr}$	classical orthotropic longitudinal compressive buckling stress
$F_{x,i}^{cr}$	initial longitudinal compressive buckling stress from test
F_x^{cc}	longitudinal crippling stress from test
F_x^{cu}	longitudinal ultimate compressive stress of laminate
$N_{x,cl}^{cr}, N_{y,cl}^{cr}$	classical orthotropic longitudinal and transverse compressive uniform buckling loads, respectively
$N_{x,i}^{cr}$	initial longitudinal uniform buckling load from test
$N_{x,w}^{cr}$	longitudinal compressive uniform buckling load based on anisotropic theory, including transverse shear effects
N_x, N_y	longitudinal and transverse applied uniform loads, respectively, on a plate
$P_{x,i}^{cr}$	total longitudinal initial buckling load from test
$P_{x,i}^{cc}$	total longitudinal crippling load from test
t	thickness

5.7.1.2 Initial buckling

Initial buckling is defined to occur at a load that results in incipient out-of-plane displacements. The classical equations are elastic, and finite transverse shear stiffness effects are neglected. (Reference 5.7.1.2). The buckling of certain plate geometries, however, can be influenced by the finite shear stiffness effects as shown in Section 5.7.1.8.

5.7.1.3 Uniaxial loading - long plate with all sides simply supported

The case of a long plate ($a/b > 4$) with all sides simply supported (SS) and loaded uniaxially is shown in Figure 5.7.1.3(a) and described by Equation 5.7.1.3.

$$N_{x,cl}^{cr} = \frac{2\Pi^2}{b^2} \left[(D_{11}D_{22})^{1/2} + D_{12} + 2D_{66} \right] \quad 5.7.1.3$$

Equation 5.7.1.3 is the most frequently used plate buckling equation. It can be shown by the use of the STAGS computer program (Reference 5.7.1.1(a)) that this equation is also valid for fixed boundary conditions (FF) on the loaded edges, which is important since all testing is performed with fixed boundary conditions on the loaded edges to prevent local brooming. Comprehensive testing has shown these equation to be valid except for very narrow plates. Figure 5.7.1.3(b) shows the comparisons between experiment and classical theory from References 5.7.1.3(a) and (b), where the test results are plotted as $N_{x,i}^{cr} / N_{x,cl}^{cr}$ versus the b/t ratios. Notice the discrepancy becomes worse at the low b/t ratios (narrow plates). Thus

the equation should be used with caution at b/t ratios less than 35. In Figure 5.7.1.3(c) the same experimental data has been normalized by the buckling load prediction which includes the effects of transverse shear ($N_{x,w}^{cr}$) from References 5.7.1.3(c) and (d)). Note that most available computer buckling programs will not account for this transverse shear effect.

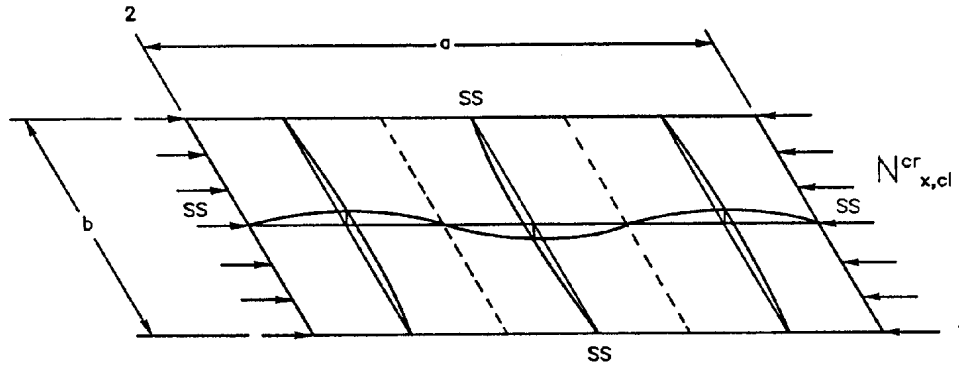


FIGURE 5.7.1.3(a) Uniaxial loading - long plate ($a/b > 4$) with all sides simply supported (SS).

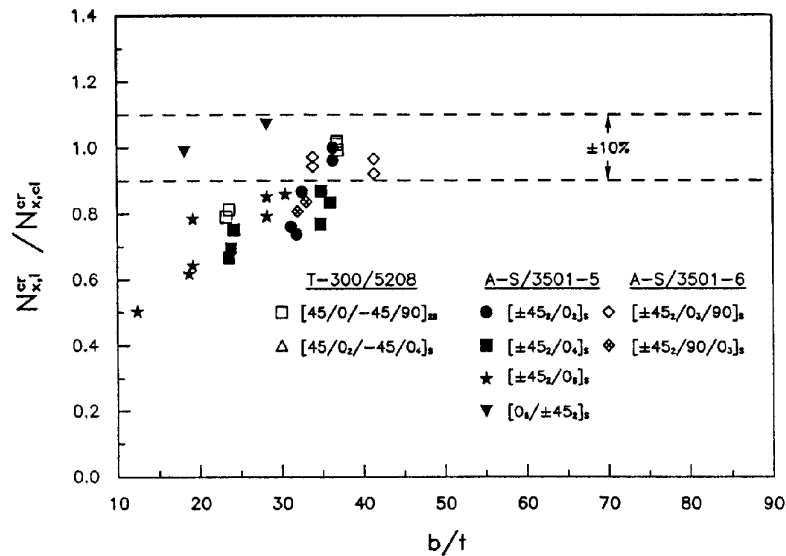


FIGURE 5.7.1.3(b) Predicted classical buckling loads compared to experimental data (Reference 5.7.1.3(b)).

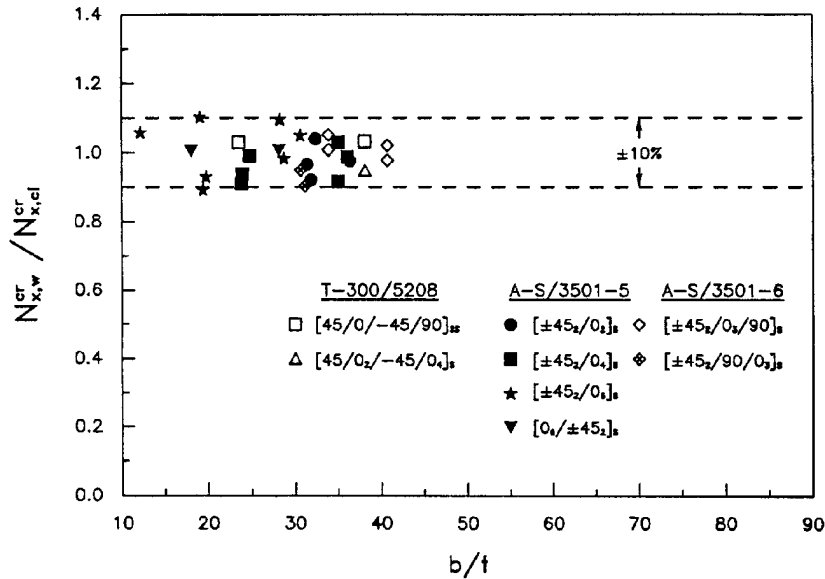


FIGURE 5.7.1.3(c) Predicted buckling loads of the current theory compared to experimental data (Reference 5.7.1.3(b)).

5.7.1.4 Uniaxial loading - long plate with all sides fixed

The case of a long plate ($a/b > 4$) with all sides fixed (FF) and loaded uniaxially is shown in Figure 5.7.1.4 and described by Equation 5.7.1.4.

$$N_{x,cl}^{cr} = \frac{\Pi^2}{b^2} \left[4.6(D_{11}D_{22})^{1/2} + 2.67D_{12} + 5.33D_{66} \right] \quad 5.7.1.4$$

This equation has not had the comprehensive experimental study as has Equation 5.7.1.3. However, by conjecture the effect of transverse shear for narrow plates would be quite similar to that found for plates with all edges simply supported.

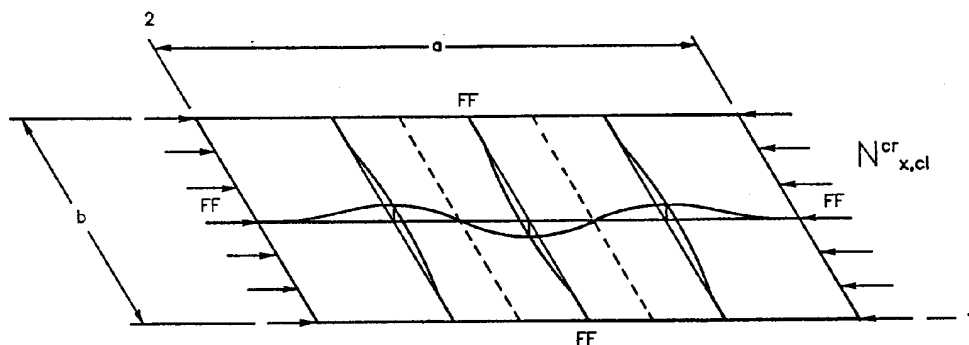


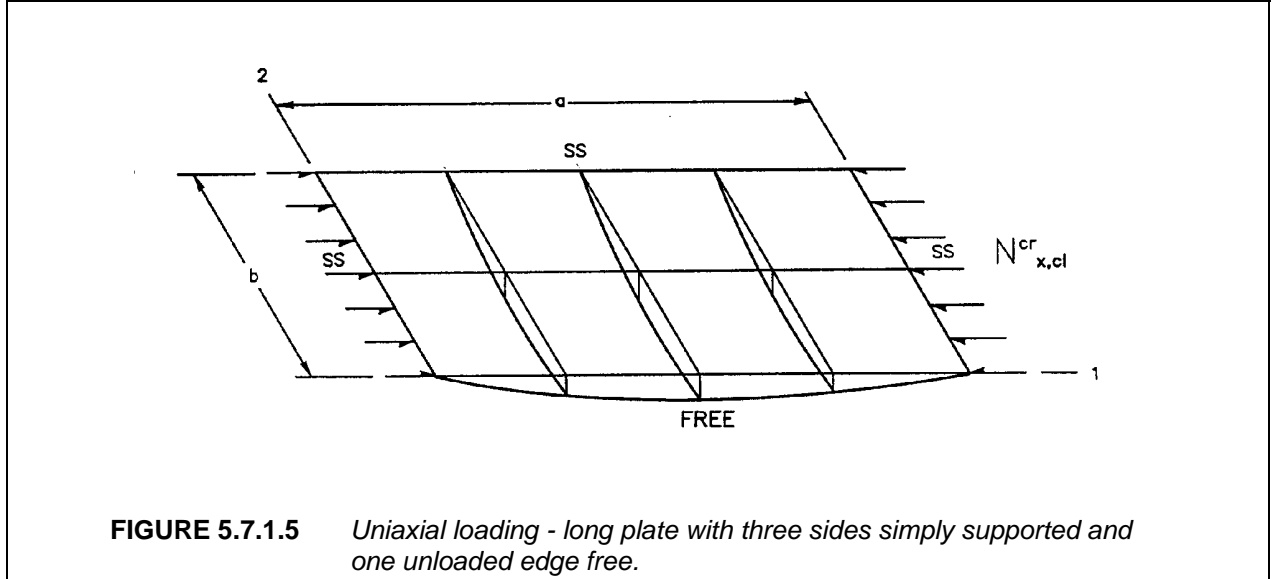
FIGURE 5.7.1.4 Uniaxial loading - long plate ($a/b > 4$) with all sides fixed.

5.7.1.5 Uniaxial loading - long plate with three sides simply supported and one unloaded edge free

Figure 5.7.1.5 shows the case of a long plate ($a/b > 4$) with three sides simply supported and the remaining unloaded edge free. This plate is uniaxially loaded. This loading situation is described by Equation 5.7.1.5.

$$N_{x,cl}^{cr} = \frac{12 D_{66}}{b^2} + \frac{\Pi^2 D_{11}}{a^2} \quad 5.7.1.5$$

where b/t must be greater than 20 because of transverse shear effects in narrow plates as discussed in Section 5.7.1.3.



5.7.1.6 Uniaxial and biaxial loading - plate with all sides simply supported

Biaxial and uniaxial loading of a simply supported plate is shown in Figure 5.7.1.6, where $1 < a/b < \infty$. The following classical orthotropic buckling equation must be minimized with respect to the longitudinal and transverse half-waves numbers, m and n :

$$N_{x,cl}^{cr} = \frac{\Pi^2}{b^2} \frac{D_{11} m^4 (b/a)^4 + 2(D_{12} + 2 D_{66}) m^2 n^2 (b/a)^4 + D_{22} n^4}{m^2 (b/a)^2 + \phi n^2}, \min \quad 5.7.1.6(a)$$

where

$$\phi = N_y / N_x \quad 5.7.1.6(b)$$

which is the ratio of applied transverse to longitudinal loading. Accordingly, the corresponding transverse buckling load is

$$N_{y,cl}^{cr} = \phi N_{x,cl}^{cr} \quad 5.7.1.6(c)$$

For uniaxial loading, let $\phi = 0$.

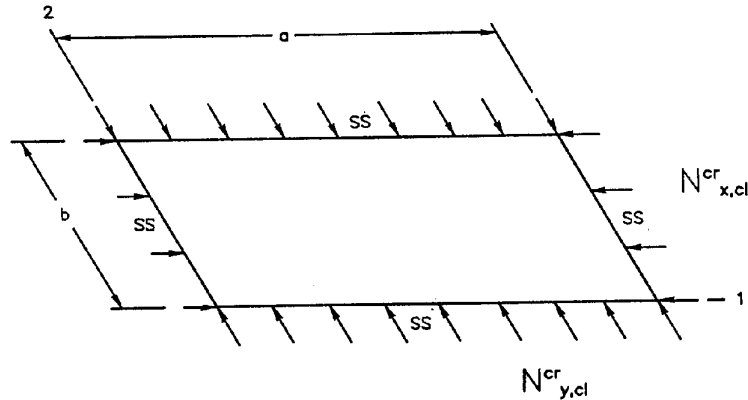


FIGURE 5.7.1.6 Uniaxial and biaxial loading - plate with all sides simply supported.

5.7.1.7 Uniaxial loading - plate with loaded edges simply supported and unloaded edges fixed

The case of a uniaxially loaded plate ($1 < a/b < \infty$) with the loaded sides simply supported (SS) and the unloaded sides fixed (FF) can also be considered. For this case, the following classical orthotropic buckling equation must be minimized with respect to the longitudinal half-wave number, m :

$$N_{x,cl}^{cr} = \frac{\Pi^2}{b^2} \left\{ D_{11} m^2 (b/a)^2 + 2.67 D_{12} + 5.33 \left[D_{22} (a/b)^2 + (1/m)^2 + D_{66} \right] \right\} \quad 5.7.1.7$$

5.7.1.8 Stacking sequence effects in buckling

Methods to accurately predict the stability of laminated plates have been documented (e.g., References 5.7.1.8(a)-(c)). Laminated plate stability can be strongly affected by LSS. However, factors such as plate geometry, boundary conditions and load type each contribute to the relationship between LSS and plate stability. As a result, general rules that define the best LSS for plate stability do not exist. Instead, such relationships must be established for specific structure and loading types. Three examples that illustrate this point will be shown in this section. Two different analysis methods were used in these examples. The first, utilized design equations from Reference 5.7.1.8(c) and bending stiffnesses as calculated using lamination theory. This method assumed the plate bending behavior to be "specially orthotropic" (D_{16} and D_{26} terms were set equal to zero). The second method was a Boeing computer program called LEOTHA (an enhanced version of OTHA, Reference 5.7.1.8(a) which uses the Galerkin method to solve equations for buckling. This method allowed nonzero D_{16} and D_{26} terms.

Figures 5.7.1.8(a), (b), and (c) show plate buckling predictions for the seven LSS used in an earlier example (see Table 5.3.3.2(b)).¹ All plates were assumed to have simply-supported boundary conditions on the four edges. Figures 5.7.1.8(a) and (b) are rectangular plates loaded by uniaxial compression in long and short directions, respectively. Figure 5.7.1.8(c) shows shear buckling predictions for a square plate. Horizontal dashed lines on Figures 5.7.1.8(a) - (c) represent the results obtained when using the DOD/NASA design equations and assuming no LSS effect (i.e., a homogeneous orthotropic plate). The homogeneous plate assumption results in a buckling load that is roughly an average of the predictions for all LSS shown in the figures.

¹The LSS used in Figures 5.7.1.9(a), (b), and (c) were chosen for illustrative purposes only and do not represent optimal LSS for a given application.

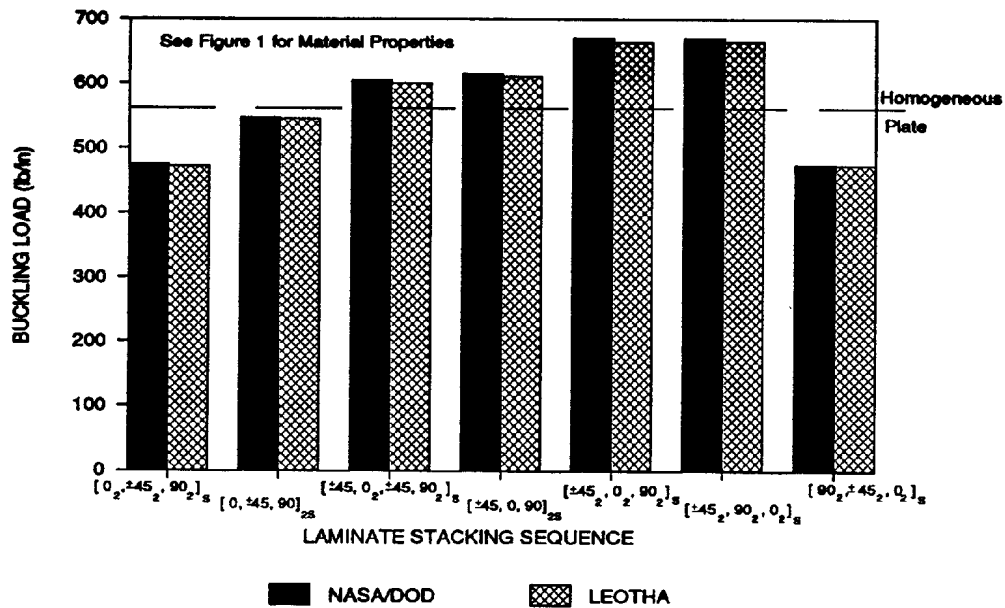


FIGURE 5.7.1.8(a) Buckling analysis of 4 sides simply-supported, 24 in. by 6 in., laminated plates loaded in the long direction.

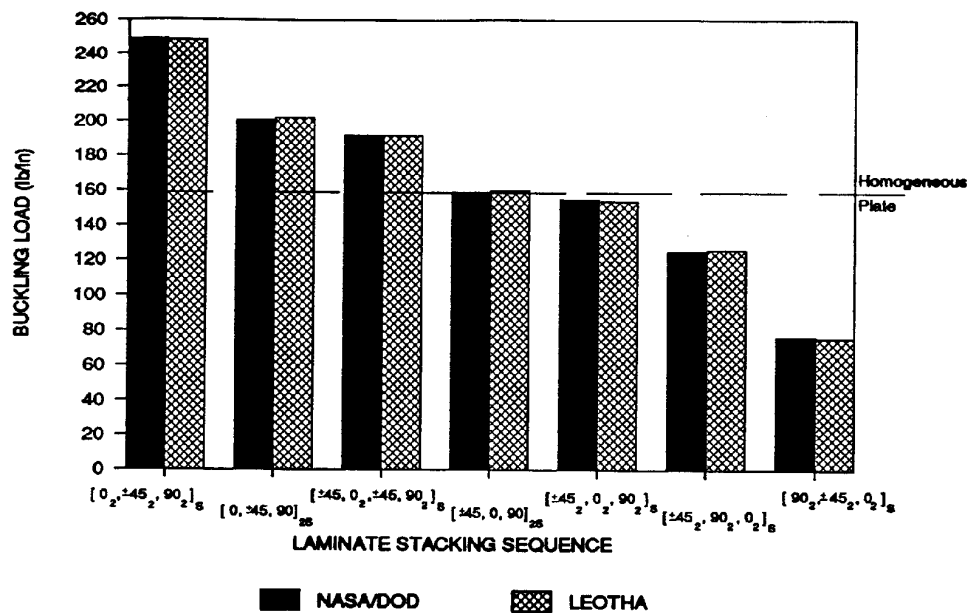


FIGURE 5.7.1.8(b) Buckling analysis of 4 sides simply-supported, 6 in. by 24 in., laminated plates loaded in the short direction.

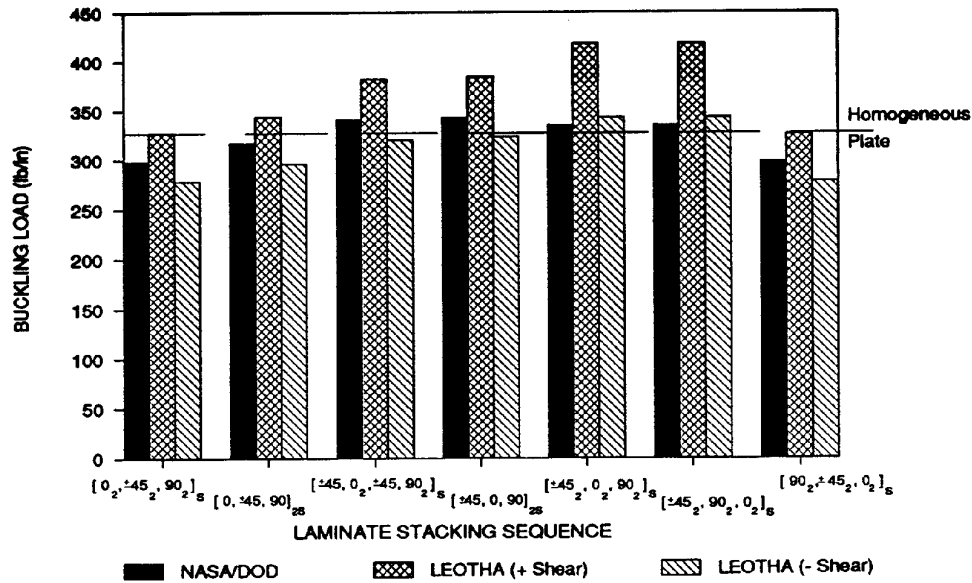


FIGURE 5.7.1.8(c) Buckling analysis of 4 sides simply-supported, 12 in. by 12 in., laminated plates loaded in shear.

The highest buckling loads for rectangular plates loaded in the long direction occur with preferential clumping of $\pm 45^\circ$ plies toward the surface layers (Figure 5.7.1.8(a)). Such is not the case for rectangular plates loaded in the short direction, where preferential stacking of 0° plies yield the highest buckling loads (Reference 5.7.1.8(b)). Note that predictions using the homogeneous plate assumption can be conservative or nonconservative depending on LSS. The DOD/NASA equations compare well with LEOTHA for conditions shown in Figures 5.7.1.8(a) and (b).

The highest buckling loads for square plates loaded in shear occur with preferential clumping of $\pm 45^\circ$ plies toward the surface layers (Reference 5.7.1.8(d)). Predictions using LEOTHA are different for positive and negative shear due to the relative positions of $+45^\circ$ and -45° plies. Predictions from DOD/NASA equations were generally lower than those of LEOTHA for positive shear loads. The opposite was true for negative shear loads. Differences may be attributed to the influence of D_{16} and D_{26} terms which were not included in the DOD/NASA design equations.

As with bending, structural geometry can overshadow the effects of LSS on stability (see the discussion pertaining to Figure 5.3.3.2). For example, the Euler buckling load of a laminated I-section used as a column is more strongly dependent on geometrical dimensions than on LSS of web and flanges. In fact, the effects of LSS on Euler buckling load diminishes sharply with increasing web height.

Design for local buckling and crippling of composite plates has typically relied on empirical data (e.g., Reference 5.7.1.8(e)). Local buckling and crippling have been found to relate to LSS. The lowest values for local buckling and crippling under uniaxial compression occurred with preferential stacking of 0° plies towards the outside surface of a laminate. Hence, when considering an I-section, Euler buckling loads may be independent of LSS while local buckling and crippling can relate to LSS.

The effects of LSS on the stability of a stiffened panel is more complex. Assuming no local buckling and crippling, stiffener stability will not depend directly on LSS. However, post-buckling behavior of the skin and load redistribution to the stringer is strongly affected by the skin's LSS. As a result, overall stiffened panel stability can be influenced by the skin's LSS.

Basic information on laminate stacking sequence effects is found in Section 5.6.5.

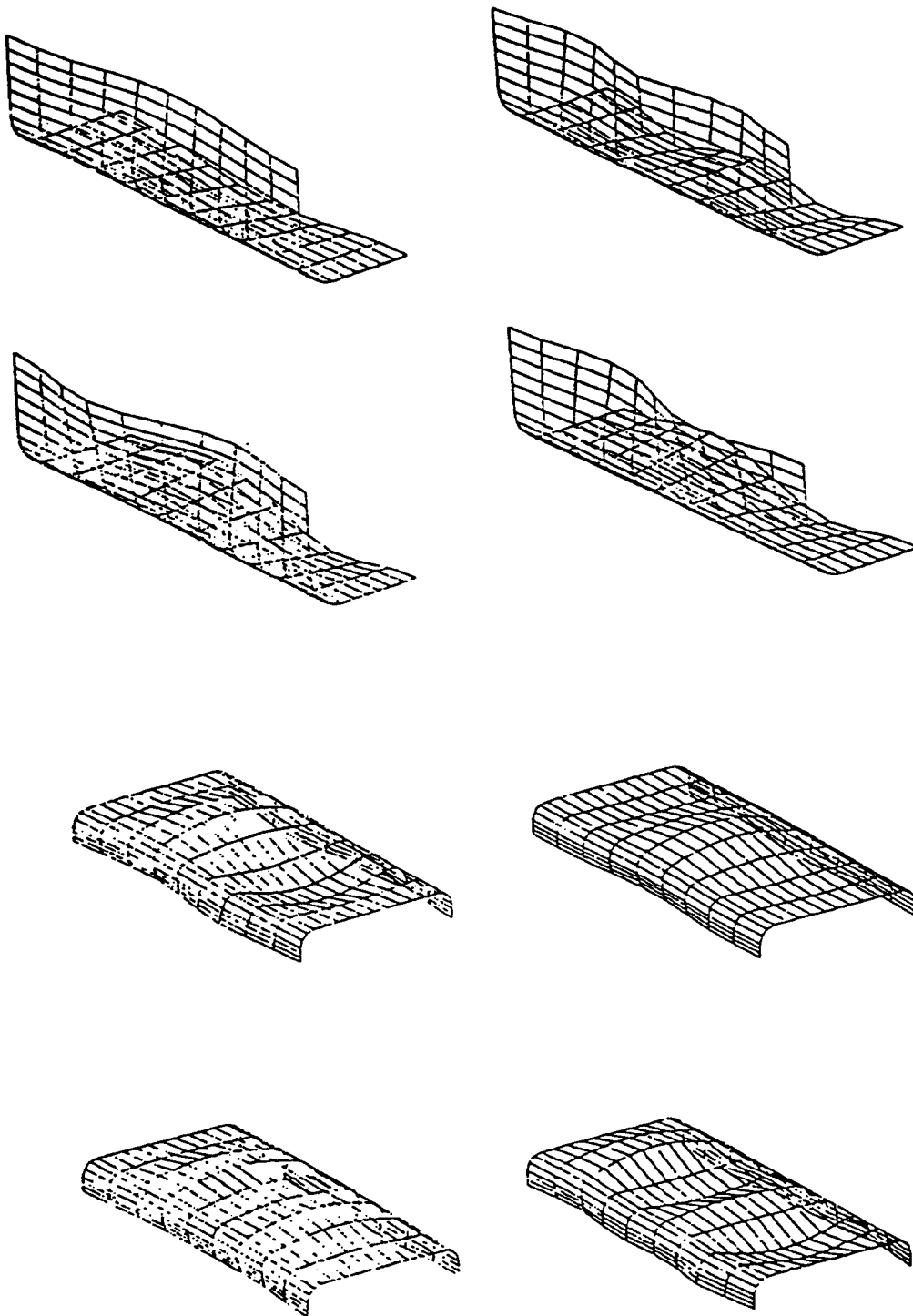
5.7.2 Compressive postbuckling and crippling

Wide exploitation of advanced composites in stability critical structural designs depends to a large degree on the ability of composites to support loads well beyond the initial buckling level. Unquestionably, the high stiffness-to-weight ratio of composites renders them potentially attractive up to initial buckling. However, since postbuckling design has been established over several decades for certain types of conventional metallic alloy construction, it should be anticipated that composites demonstrate a similar capability. Hence, this section addresses this vitally important issue as it pertains to the design of structural compressive members.

Postbuckling. Postbuckling is the ability of a compressive member or stiffened panel to carry loads well in excess of the initial buckling load. The "postbuckling range" may be considered to exist between the initial buckling load and some higher load representing failure, e.g., delamination at the free edge of a compressive member or the disbonding of a stiffener from the panel in a stiffened panel. When stiffened panels are loaded in compression, load is shared between skin and stiffeners in proportion to their respective stiffnesses. At initial buckling, the tangent stiffness of the skin is reduced sharply and as a result, a greater portion of the total load will be carried by the stiffeners. For an isotropic material with linear elastic behavior prior to initial buckling, the tangent stiffness at buckling is reduced to one half of its initial value. For composite panels, tangent stiffnesses are a function of material properties and lay-up. Local buckling of one or more of the plate elements comprising a stiffener will similarly reduce the in-plane stiffnesses of the affected elements and will cause the load to shift to the unbuckled portions of the stiffener. The upper limit of the postbuckling range is sometimes referred to as "local crippling" or simply "crippling".

Crippling. Compressive crippling is a failure in which the cross section of a stiffener is loaded in compression and becomes distorted in its own plane without translation or rotation of the entire column taking place. Typical deflected shapes seen in crippling tests of angles and channel section stiffeners are shown in Figure 5.7.2(a). Angles or cruciforms loaded in compression are commonly used as crippling specimens for the "one-edge-free" case. Channels or simply supported compressive panels are normally used for the "no-edge-free" case, in which the center channel segment is approximately simply supported with "no-edge-free".

The postbuckling behavior of composite plates presented here is derived from the empirical graphite tape data obtained from References 5.7.2(a) through (h). Relatively narrow plates, with simply supported unloaded edges or one-edge-free and fixed loading edges were tested and analyzed. The simply supported unloaded edges were simulated by the use of steel V-blocks mounted on the compression test fixture. Specifically, the plates with both unloaded edges simply supported are defined as "no-edge-free". Plates with one unloaded edge simply supported and the other free are defined as "one-edge-free". A typical no-edge-free test in progress with the specimen in the postbuckling range is shown in Figure 5.7.2(b). In addition, a typical one-edge-free test where crippling of the specimen has occurred is shown in Figure 5.7.2(c). Typical load-displacement curves of no-edge-free and one-edge-free tests are shown in Figures 5.7.2(d) and 5.7.2(e), respectively. Figure 5.7.2(d) clearly shows the reduction in stiffness at initial buckling as indicated by the change in slope of the load deflection curve at that point. A convenient plot that exemplifies the postbuckling strength of the no-edge-free composite plates is shown in Figure 5.7.2(f). The value for F_{11}^{cu} is the ultimate compressive strength of the particular laminate. A typical failed test specimen is shown in Figure 5.7.2(g). Figure 5.7.2(h) illustrates the postbuckling strengths of one-edge-free plates. Note that all the empirical data presented involved the testing of high strength carbon/epoxy tape. Other material systems or other forms of carbon/epoxy composites may yield different results.

**FIGURE 5.7.2(a)** *Typical crippling shapes.*

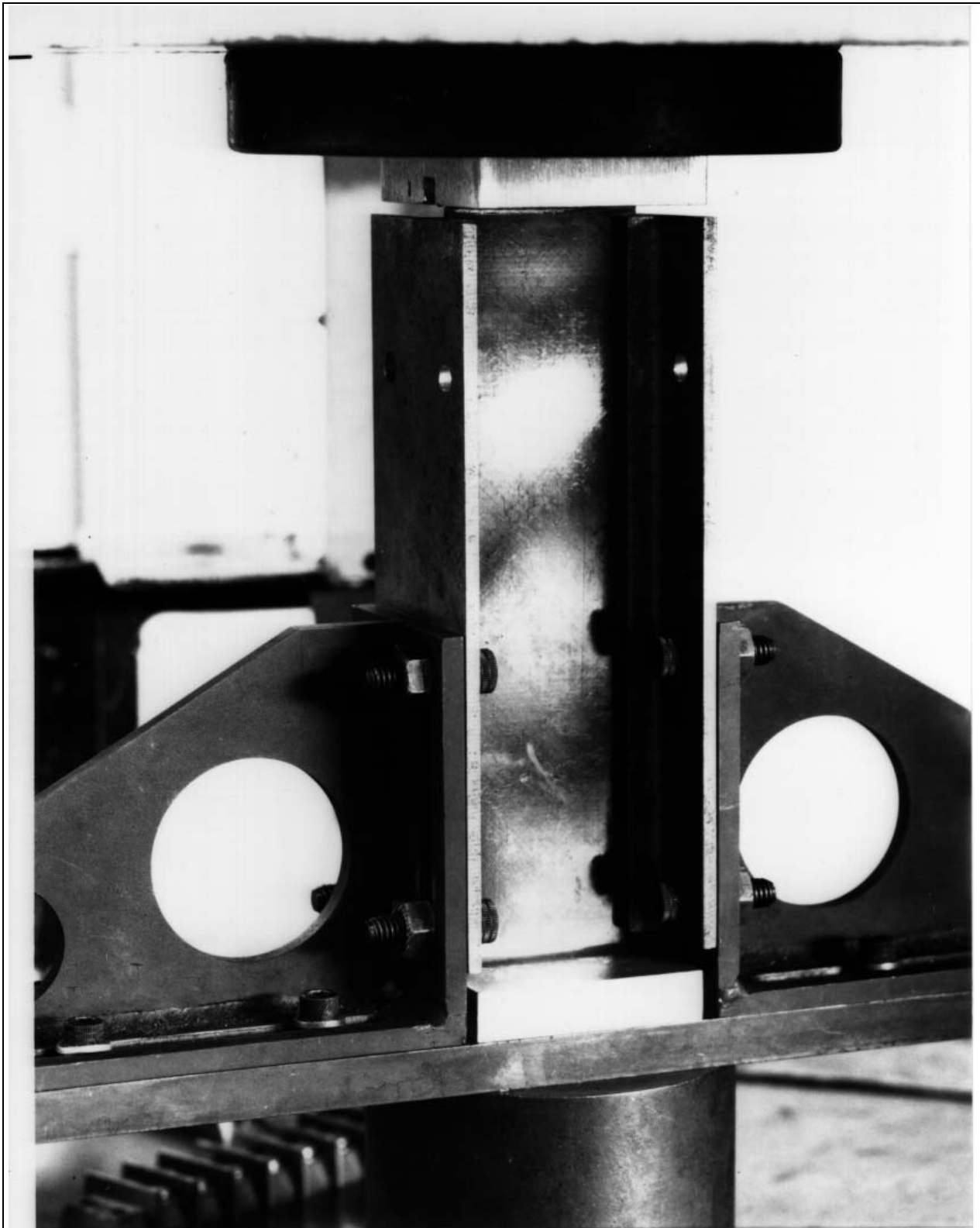


FIGURE 5.7.2(b) *No-edge-free carbon/epoxy test.*

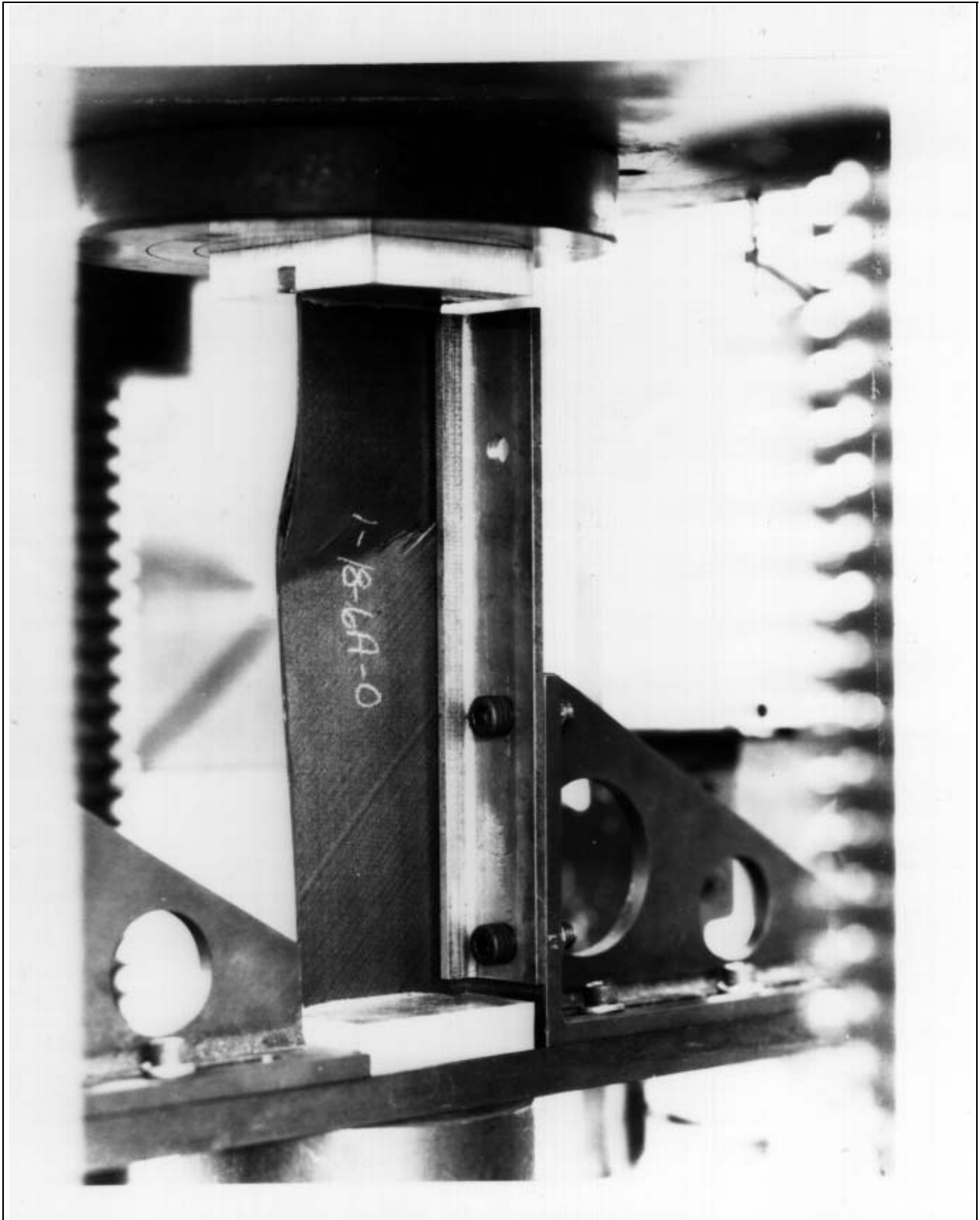


FIGURE 5.7.2(c) *One-edge-free carbon/epoxy postbuckling test at crippling.*

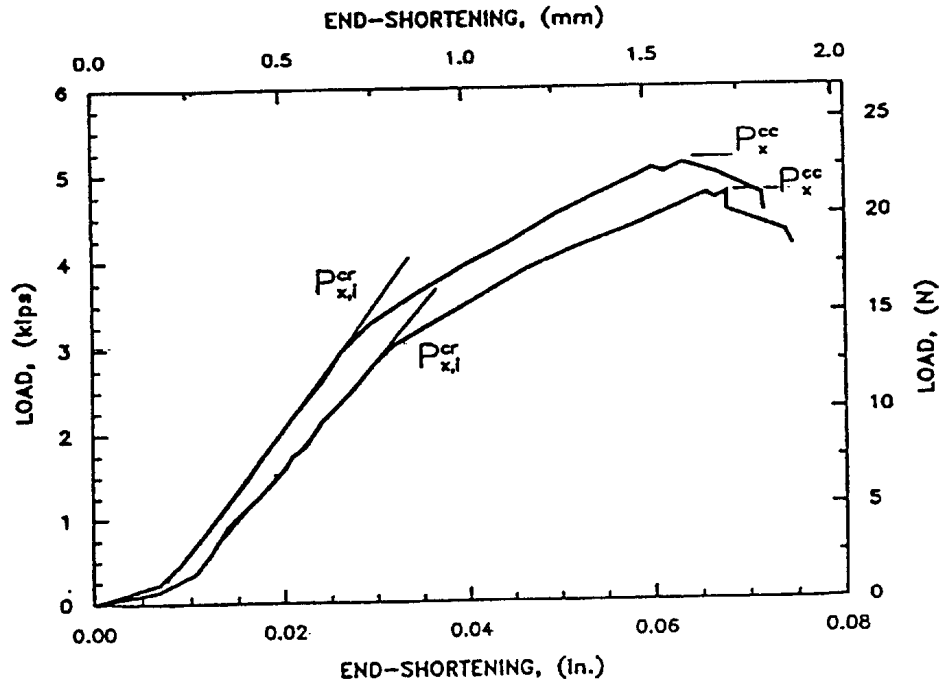


FIGURE 5.7.2(d) No-edge-free plate. Crippling tests - AS/3501-6 [$\pm 45/90/0_3$]_s - $b/t \approx 32$.

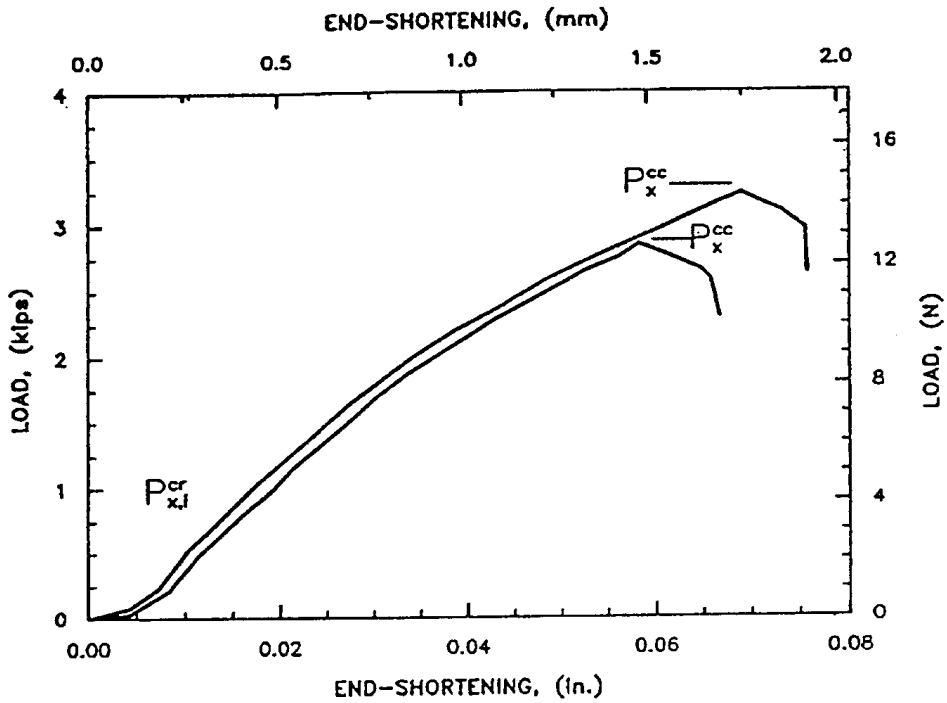


FIGURE 5.7.2(e) One-edge-free plate. Crippling tests - AS/3501-6 [$\pm 45/90/0_3$]_s - $b/t \approx 30$.

Normalized Crippling Data – No Edge Free

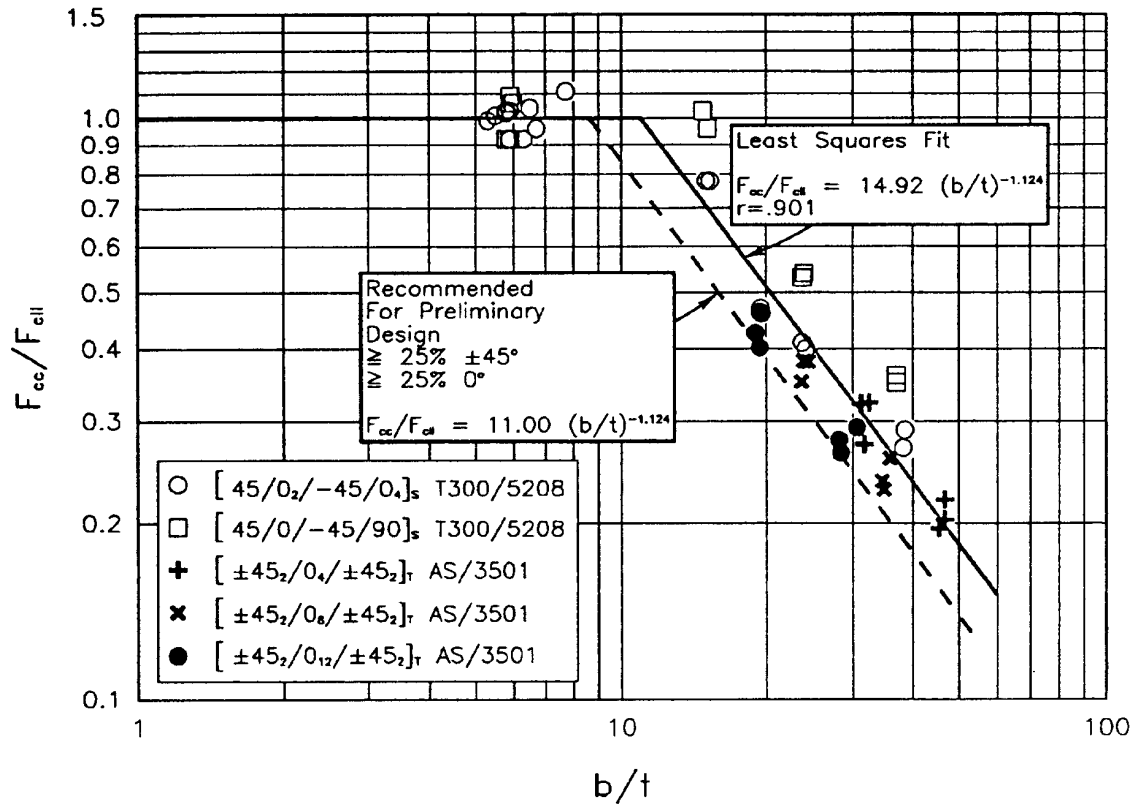


FIGURE 5.7.2(f) Normalized crippling data - no-edge-free.

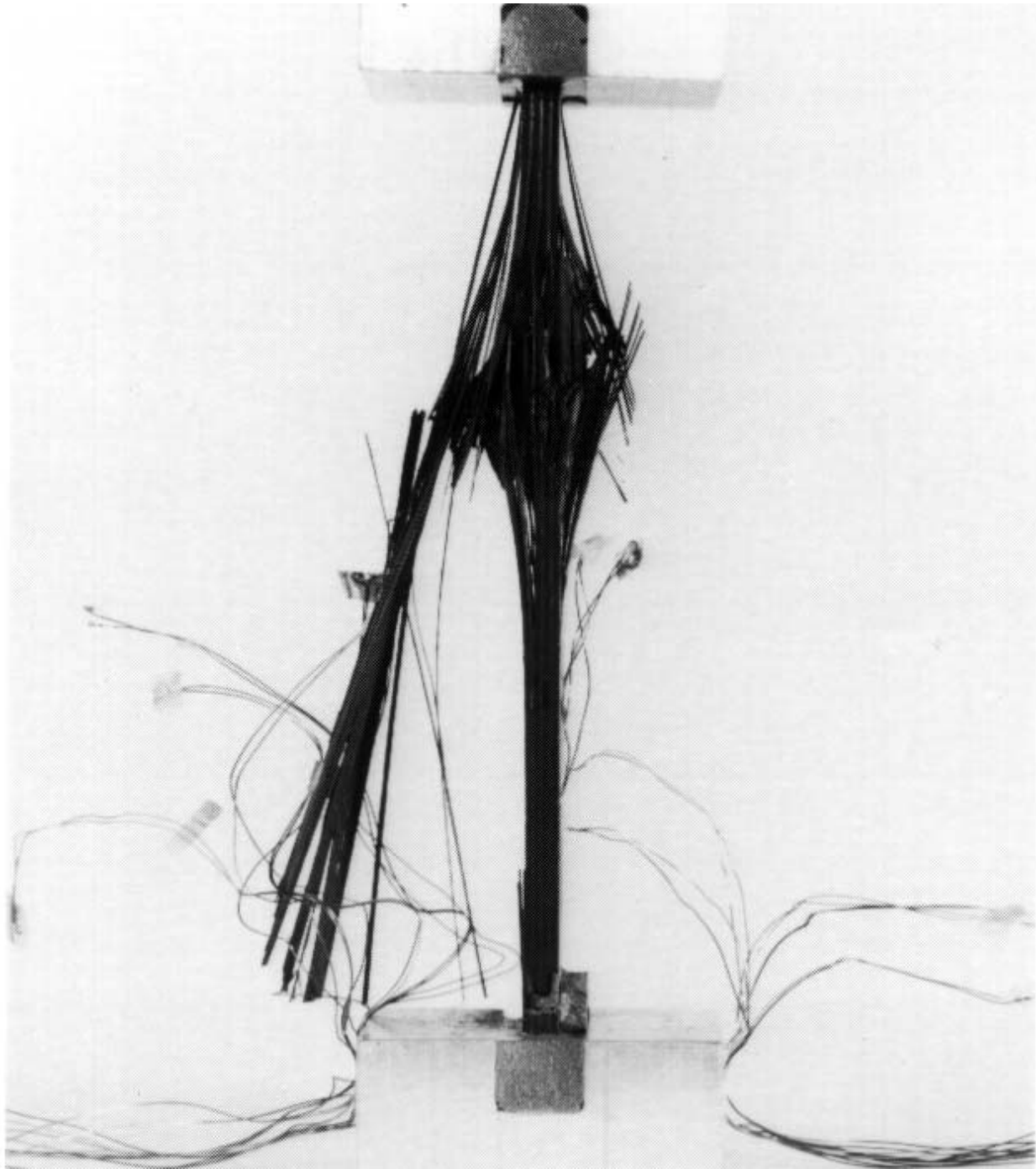


FIGURE 5.7.2(g) *Typical carbon/epoxy failed ultimate compression specimen.*

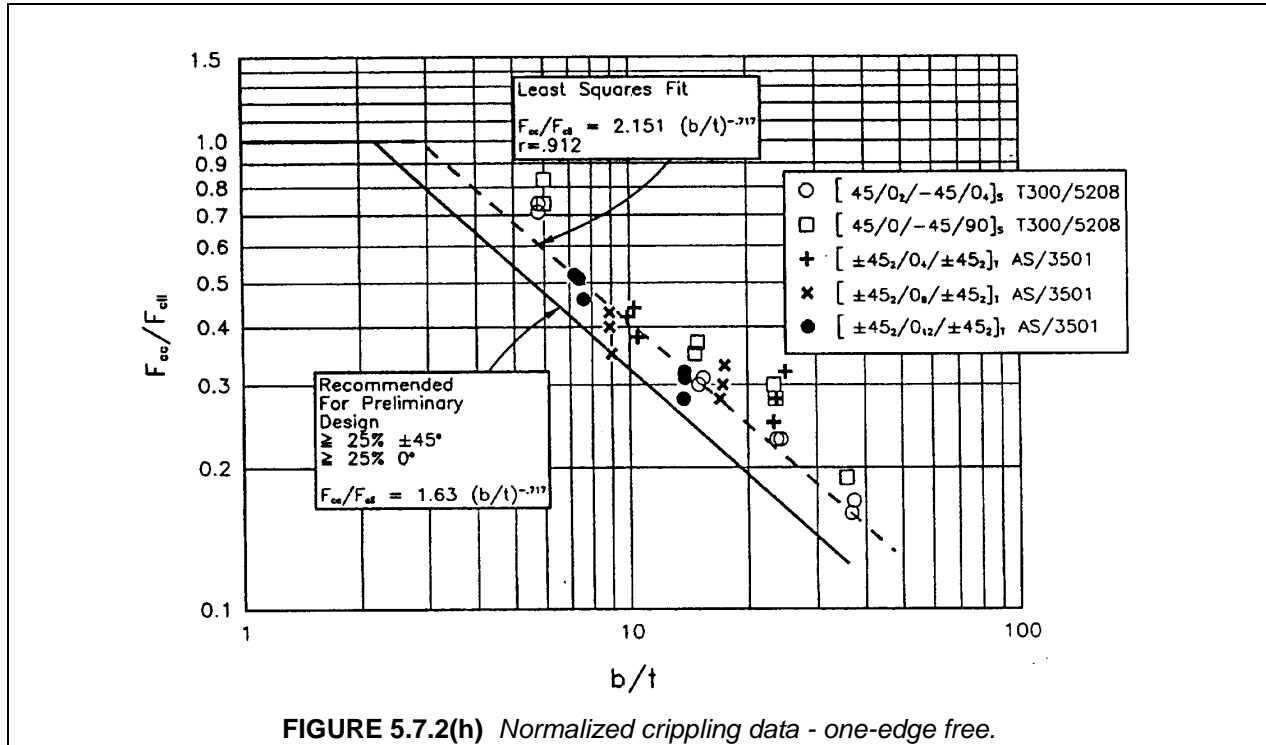


FIGURE 5.7.2(h) Normalized crippling data - one-edge free.

5.7.2.1 Analytical models

As stated in Section 5.7.1.2, initial buckling is more accurately determined by including the effects of transverse shear and material nonlinearity as is done in References 5.7.1.3(c) and (d). Transverse shear effects become especially important for thick laminates ($b/t < 20$). Stress-strain curves for laminates with a high percentage of $\pm 45^\circ$ plies may show significant material nonlinearity prior to initial buckling. These effects are equally important, of course, for plates loaded in the postbuckling range. Some examples of test results vs. the theory of these references are shown in Figures 5.7.2.1(a) and (b). Unfortunately, most of the computer programs available today are based on linear elastic theory and do not include transverse shear effects. Consequently, experimental data must be obtained to correct for these and other deficiencies in the analytical models.

The theoretical buckling loads for orthotropic one-edge-free and no-edge-free plates are given by:

$$N_X^{cr} (\text{OEF}) = \frac{12D_{66}}{b^2} + \frac{\pi^2 D_{11}}{L^2} \quad 5.7.2.1(a)$$

$$N_X^{cr} (\text{NEF}) = \frac{2\pi^2}{b^2} \left[\sqrt{D_{11}D_{22}} + D_{12} + 2D_{66} \right]$$

These expressions do not include the bending-twisting terms D_{16} and D_{25} . These terms are present in all laminates that contain angle plies but, except in laminates having very few plies, their effect on the initial buckling load is generally not significant. Hence, the above equations are accurate for most practical laminates that are balanced and symmetrical about their mid-surface. The reader is referred to studies performed by Nemeth (Reference 5.7.2.1(a)) for additional information on the buckling of anisotropic plates and the effect of the various parameters on the buckling loads.

The Euler term in the first of the above equations is generally found to be negligible and, therefore, initial buckling of a one-edge-free plate is largely resisted by the torsional stiffness (D_{66}) of the laminate. This explains why higher initial buckling loads may be obtained for a given lay-up when the $\pm 45^\circ$ plies are on the outside surfaces of the plate.

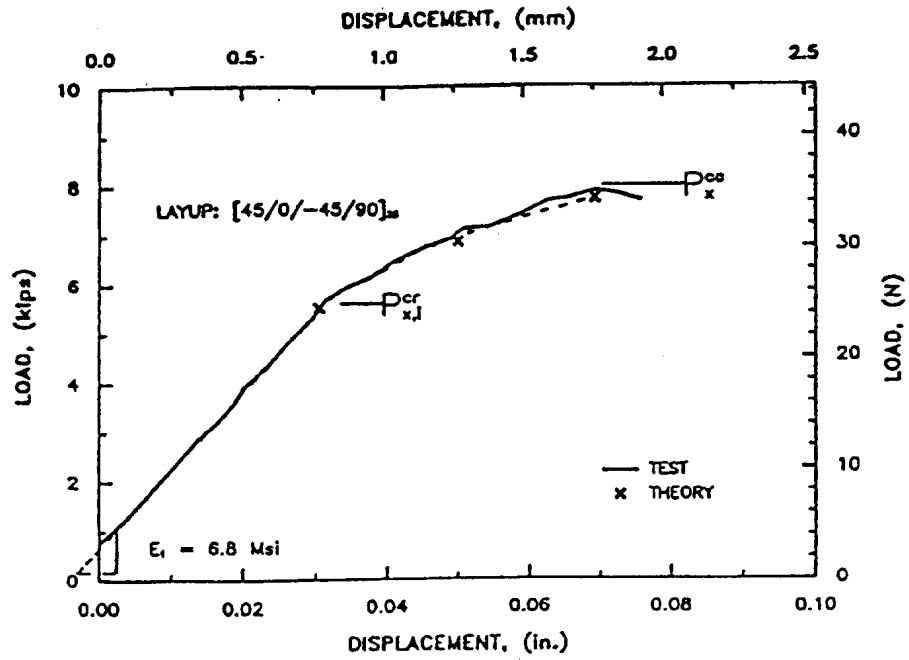


FIGURE 5.7.2.1(a) Comparison of theory in References 5.7.1.3(b) and (c) with experiments for postbuckling curves and crippling strengths.

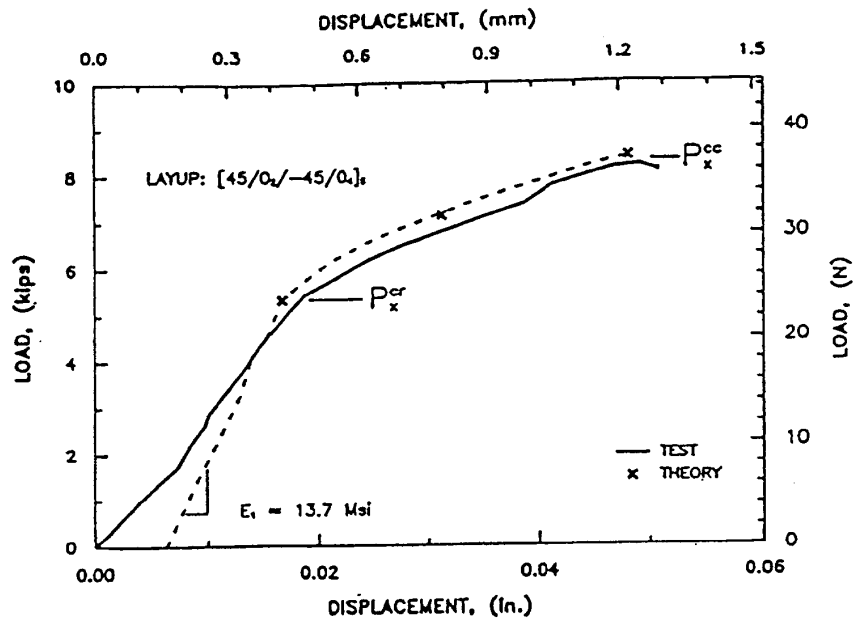


FIGURE 5.7.2.1(b) Comparison of theory in References 5.7.1.3(b) and (c) with experiments for postbuckling curves and crippling strengths.

Volume 3, Chapter 5 Design and Analysis

For laminates that are only slightly unbalanced or unsymmetrical, approximate values for the initial buckling load may be obtained by substituting "equivalent" bending stiffnesses \bar{D}_{ij} in place of D_{ij} in the buckling equations, where

$$[\bar{D}] = [D] - [B][A]^{-1}[B] \quad 5.7.2.1(b)$$

The analysis of panels loaded in the postbuckling range becomes a geometrically nonlinear problem and, therefore, "conventional" plate buckling programs or other linear analysis codes cannot be used to accurately predict the crippling strength of composite plates. One example is shown in Figure 5.7.2.1(c), which shows experimental crippling curves and theoretical buckling curves for a quasi-isotropic T300/5208 laminate. (The AS/3501 and T300/5208 carbon/epoxy crippling data was taken from References 5.7.2(b) - (e)). The theoretical buckling curves shown in Figure 5.7.2.1(c) are very conservative at high b/t values and very unconservative at low b/t values. This may be explained by the fact that thin plates buckle at low strain levels and may thus be loaded well into the postbuckling range. On the other hand, neglecting transverse shear effects will cause strength predictions at low b/t ratios to be unconservative. The analysis of laminated plates is further complicated by the fact that high interlaminar stresses in the corners or at the free edge of the plate may trigger a premature failure.

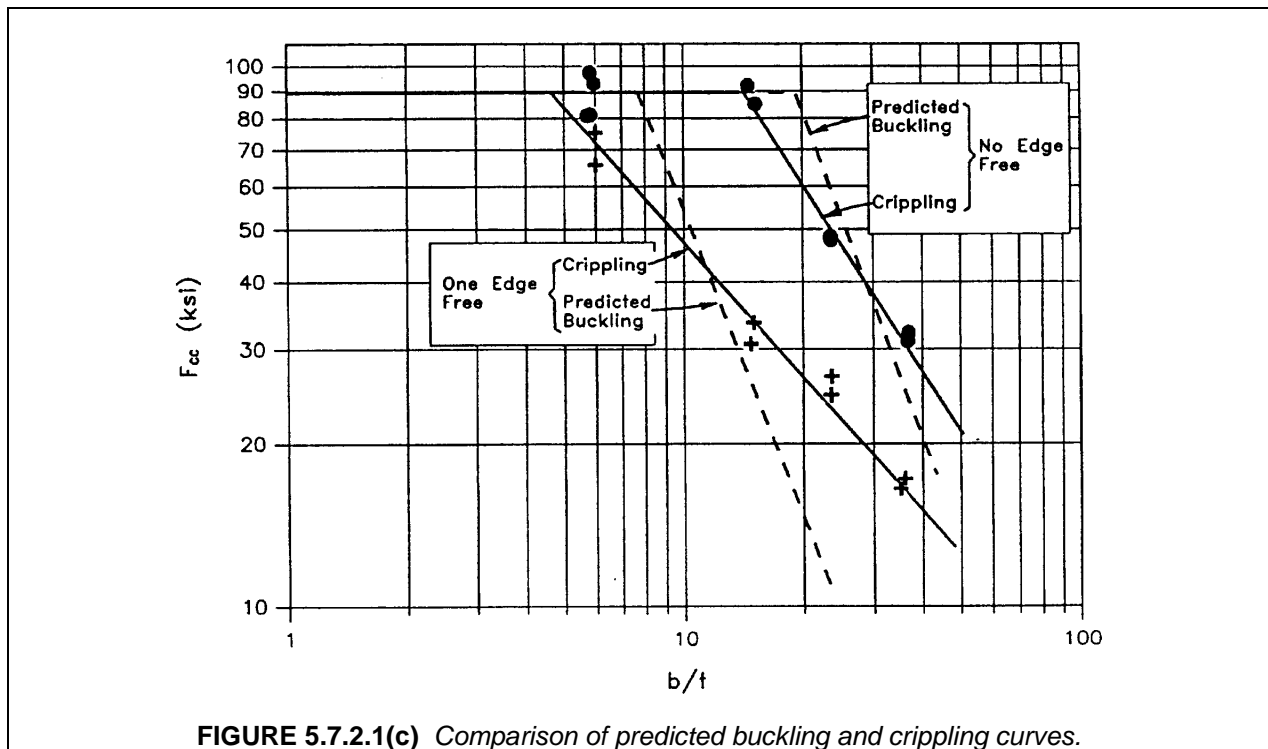


FIGURE 5.7.2.1(c) Comparison of predicted buckling and crippling curves.

As it would not be practical during preliminary design to conduct nonlinear analyses for a large number of lay-ups and b/t ratios, a better approach may be to use semi-empirical data to correct initial buckling predictions.

5.7.2.2 Fatigue effects

Postbuckling fatigue may be permitted under certain circumstances without jeopardizing the structural integrity of the plate (References 5.7.2(b), 5.7.2(g), and 5.7.2(h)). Significant conclusions identified in Reference 5.7.2(h) stated: "Composite panels demonstrated a high fatigue threshold relative to the initial skin buckling loads. Composite panels showed a greater sensitivity to shear dominated fatigue loading as compared with compression dominated fatigue loading. The fatigue failure mode in composite panels was separation between the cocured stiffener and skin."

5.7.2.3 Crippling curve determination

Non-dimensional crippling curves are used to determine the crippling strength of the one-edge and no-edge-free composite elements. Different normalization techniques have been suggested for composites, most of which are modifications of those currently used in the aircraft industry for metallic structures. Perhaps, the most obvious change in the analysis and presentation of crippling data is the proposed use of the ultimate compression strength, F^{cu} to normalize the crippling strength, F^{cc} , for composites, instead of the material yield stress, F^{cy} commonly used for metallic elements.

Crippling curves for carbon/epoxy one- and no-edge-free plates are presented in Reference 5.7.2(e) in terms of the non-dimensional parameters F^{cc}/F^{cu} and $(b/t) \cdot [F^{cu} / (E_x \cdot E_y)^{1/2}]^{1/2}$. The latter parameter was chosen to reflect the orthotropic nature of composites. Test data for the one-edge-free plate elements were found to be in excellent agreement with the expected behavior, when the data were presented in terms of these non-dimensional parameters, but test results for the no-edge-free elements fell below the expected values.

A shortcoming in the methodology presented in Reference 5.7.2(e) is that the curves are non-dimensionalized on the basis of laminate extensional modulus only. The plate bending stiffnesses play an important role in determining the initial buckling and crippling loads of the element. Unlike in metallic plates, however, there exists no direct relationship between the extensional and bending stiffnesses of a composite plate and, therefore, laminates with equal in-plane stiffnesses may buckle at different load levels if their stacking sequences are not identical. Tests conducted by Lockheed and McDonnell Douglas under their respective Independent Research and Development (IRAD) programs have confirmed that more accurate buckling and crippling predictions may be obtained when the curves are defined in terms of the non-dimensional parameters

$$\frac{F^{cc}}{F^{cu}} \frac{E_x}{\bar{E}} \quad \text{and} \quad \frac{b}{t} \frac{\bar{E}}{E_x} \sqrt{\frac{F_{cu}}{E_x E_y}} \quad 5.7.2.3(a)$$

in which

$$\bar{E} = \frac{12D_{11}}{t^3} (1 - \nu_{xy} \nu_{yx}) \quad 5.7.2.3(b)$$

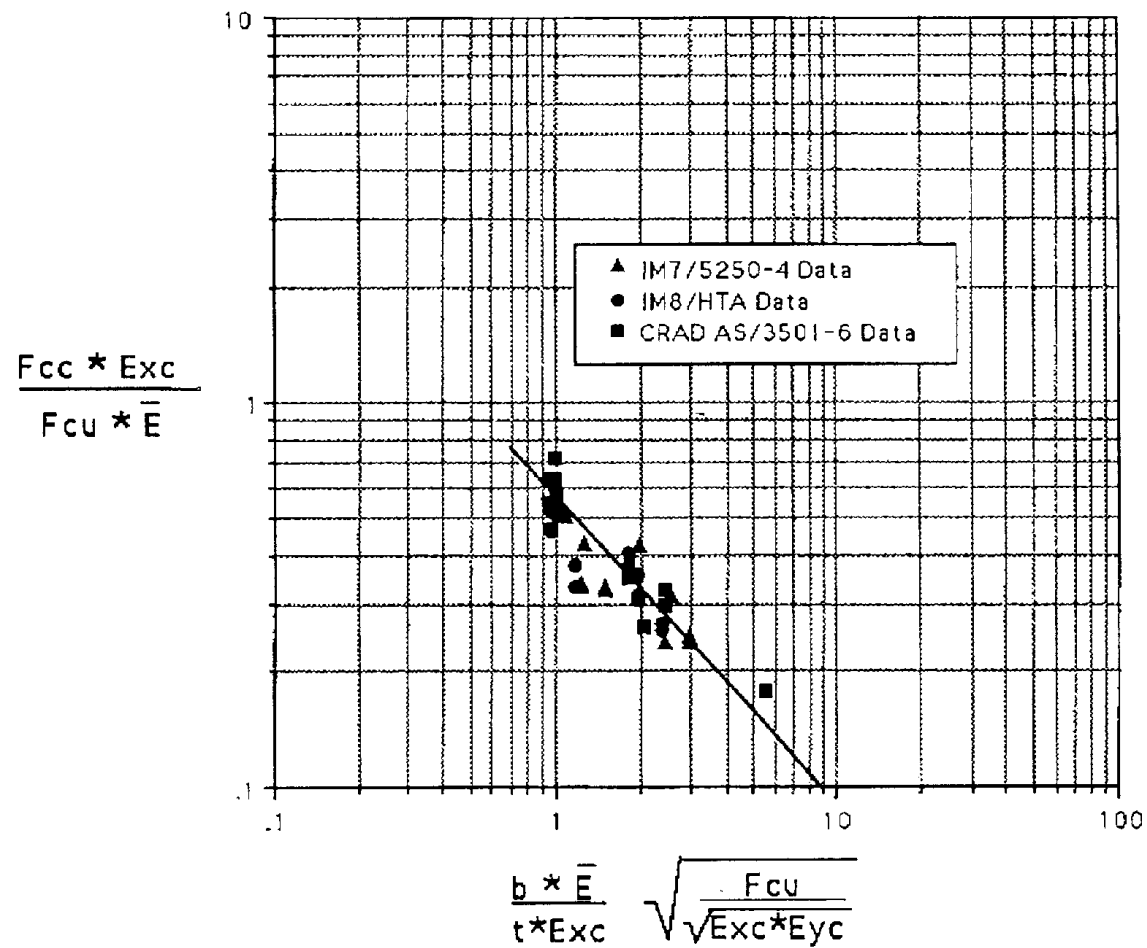
is an effective modulus accounting for stacking sequence effects through the bending stiffness term D_{11} .

5.7.2.4 Stiffener crippling strength determination

The commonly used procedure for predicting the crippling strength of a metallic stiffener, composed of several one-edge and no-edge-free elements, is to compute the weighted sum of the crippling strengths of the individual elements:

$$F_{ST}^{cc} = \frac{\sum_{i=1}^N F_i^{cc} \cdot b_i \cdot t_i}{\sum_{i=1}^N b_i \cdot t_i} \quad 5.7.2.4$$

Test results appear to indicate that the same procedure can be successfully applied to composite stiffeners of uniform thickness if the element crippling strengths are determined with the aid of the non-dimensional parameters in Equation 5.7.2.3(a). Lockheed tests involved crippling of angles and channels made from thermoplastic (IM8/HTA) and thermoset (IM7/5250-4) materials. Tests results for one- and no-edge-free plates are presented in Figures 5.7.2.4(a) and 5.7.2.4(b). McDonnell Douglas also reported that, using this approach, predictions for carbon/epoxy stiffeners and AV-8B forward fuselage longerons have shown excellent correlation with test results.



A diagram of a one-edge-free L-shaped cross-section. The vertical leg has a height of $t/2$ and the horizontal leg has a width of b . The thickness of the material is t . The diagram is used to illustrate the geometry for the calculation of the effective modulus \bar{E} .

$$\bar{E} = \frac{12(1 - \nu_{xy} * \nu_{yx}) D_{11}}{t^3}$$

FIGURE 5.7.2.4(a) One-edge-free crippling test results.

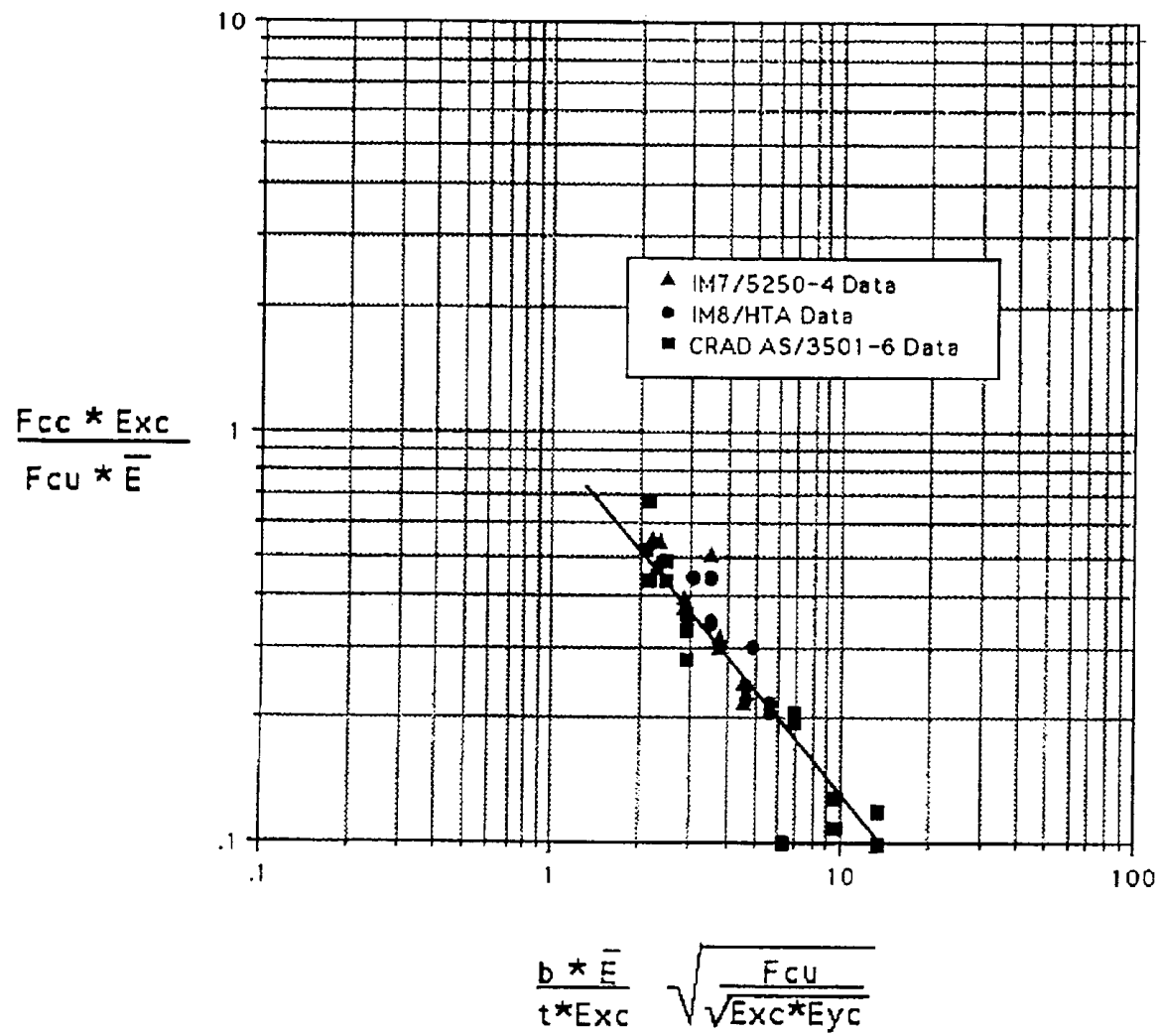
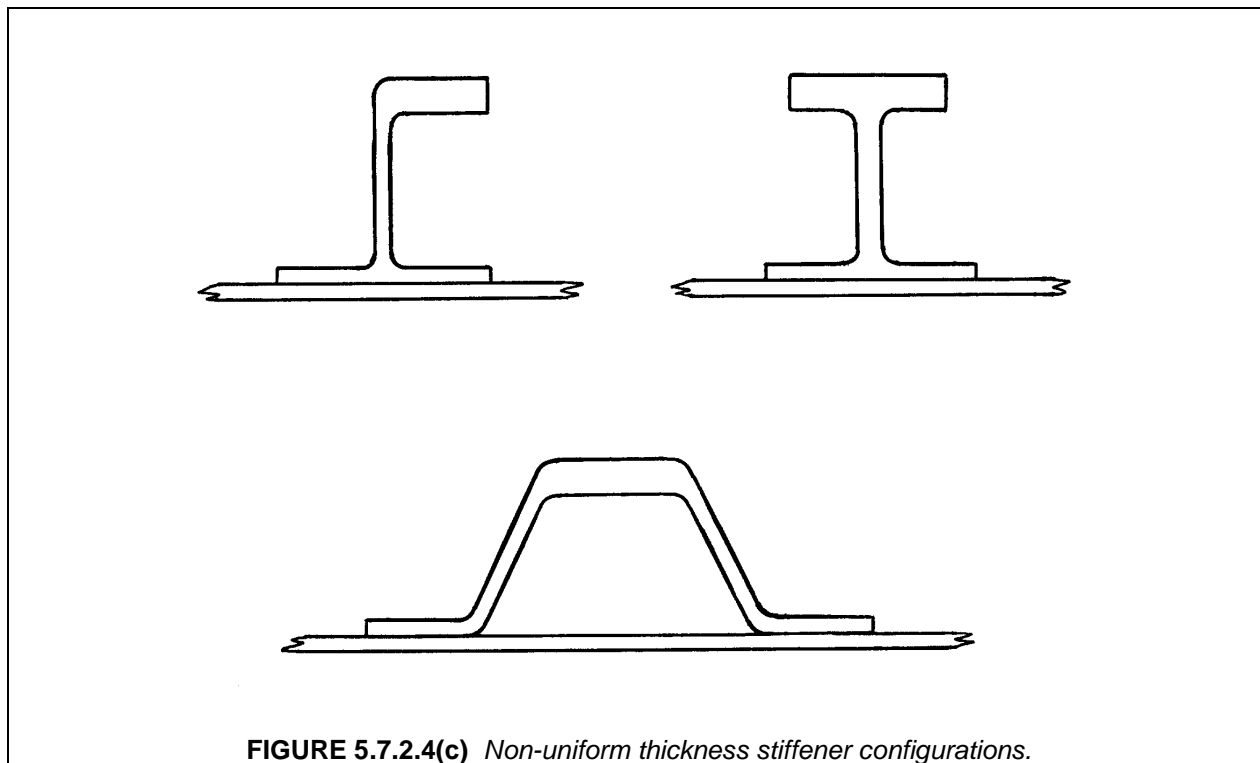


Diagram of a rectangular cross-section with width b and thickness t . The top edge is labeled $t/2$. The formula for the effective modulus \bar{E} is given as:

$$\bar{E} = \frac{12(1 - \nu_{xy} * \nu_{yx}) D_{11}}{t^3}$$

FIGURE 5.7.2.4(b) No-edge-free crippling test results.

Optimum design of stiffened panels made of composite materials may require the use of stiffeners of non-uniform thickness. Typical examples of frequently used stiffener configurations are shown in Figure 5.7.2.4(c). Insufficient experimental data currently exist to accurately predict the crippling strength of such stiffeners. At the juncture of two plate elements of different thickness, the thicker element will provide additional restraint to the thinner element. As a result, both the buckling and crippling strength of the thinner element will be increased while that of the thicker one will be decreased. The net effect could be an increase or decrease of the allowable stiffener stress depending on which of these two elements is more critical and thus is driving the buckling process. Equation 5.7.2.4 may be used to predict stiffener crippling but appropriate adjustments should be made to the crippling strength of the affected elements if that strength was based on data obtained from uniform thickness test specimens.

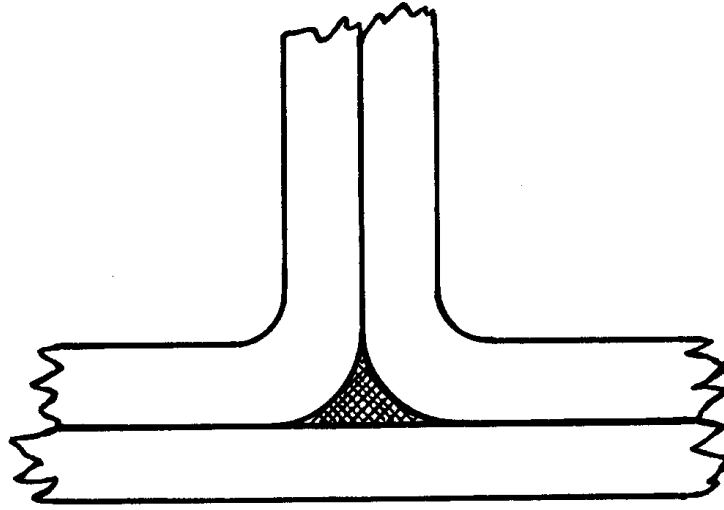


5.7.2.5 Effects of corner radii and fillets

In channel, zee, or angle section stiffeners where crippling rather than delamination is the primary mode of failure, the corner radii do not appear to have an appreciable effect on the ultimate strength of the section. The opposite is true, however, for I or J stiffeners, where the corner radii do play an important role. It has been common practice to use unidirectional tape material to fill the corners of these stiffeners, as shown in Figure 5.7.2.5. The addition of this very stiff corner material increases the crippling strength of the stiffener. Since the cross-sectional area of the fillet, and thus the amount of 0° material, is proportional to the square of the radius, the increase in crippling strength may be significant for stiffeners with large corner radii. A conservative estimate for the increase in crippling strength may be obtained from the following expression:

$$\bar{F}^{cc} = F^{cc} \frac{1 + \frac{E_f A_f}{\sum E_i b_i t_i}}{1 + \frac{A_f}{\sum b_i t_i}} \quad 5.7.2.5$$

which is based on the assumption that the critical strain in the corner region is no greater than that for a stiffener without the additional filler material.

**FIGURE 5.7.2.5** *Corner fillet.*

5.7.2.6 Slenderness correction

As the unsupported length increases, the stiffener may fail in a global buckling mode rather than by local crippling. The usual procedure to account for this is to apply a correction factor to the crippling strength, F_{cc} , based on the slenderness ratio (L'/ρ) of the column. The critical stress for the stiffener now becomes

$$F^{cr} \propto F^{cc} \left[1 - \frac{F^{cc}}{4\pi^2 E_x^c} \left(\frac{L'}{\rho} \right)^2 \right] \quad 5.7.2.6(a)$$

The radius of gyration for the cross-section of a composite column is defined as

$$\rho = \sqrt{\frac{(EI)_{st}}{(EA)_{st}}} \quad 5.7.2.6(b)$$

where $(EA)_{st}$ and $(EI)_{st}$ are the extensional and bending stiffnesses of the stiffener.

5.7.3 Summary

- The buckling strength, or stability, of flat and curved composite skin panels is strongly affected by geometry, stacking sequence, boundary conditions, and loading conditions. In many cases, it may be estimated using existing closed form solutions for orthotropic plates ($r/t > 100$), such as Equations 5.7.1.3 - 5.7.1.7.

5.8 CARPET PLOTS

This section is reserved for future use.

5.9 CREEP AND RELAXATION

This section is reserved for future use.

5.10 FATIGUE

This section is reserved for future use.

5.11 VIBRATION

5.11.1 Introduction

5.11.2 Stacking sequence effects

Vibration characteristics of laminated plates are also sensitive to laminate stacking sequence (LSS). As was the case with bending and buckling of laminated plates, complex interactions between LSS, plate geometry and boundary conditions will not allow simple rules relating LSS to vibrations. Instead, such rules must be established for specific structure and boundary conditions. This indicates a need to use proven analysis methods as design tools for predicting dimensional stability of composite structure subjected to dynamic load conditions.

Figure 5.11.2 is one example of the complex interactions between LSS, plate geometry, and the natural frequency in the first vibrational mode.¹ A design equation from Reference 5.7.1.8(c) which was based on analysis from Reference 5.11.2 was used to make the predictions shown in the figure. Note that the relative difference in fundamental frequencies for various LSS changes with plate geometry. Higher frequencies occur for square plates with preferential stacking of $\pm 45^\circ$ plies in outer layers. The strongest effect of LSS occurs for rectangular plates in which preferential stacking of outer plies oriented perpendicular to the longest plate dimension have the highest fundamental frequencies. Basic information on laminate stacking sequence effects is found in Section 5.5.5.

5.12 OTHER STRUCTURAL PROPERTIES

This section is reserved for future use. It is intended to include methods of analysis for properties and loading conditions not included in the preceding subsections.

5.13 COMPUTER PROGRAMS

Numerous programs for finite element analysis and prediction of composite material properties are available. Information on many of these programs can be found in Reference 5.13. In addition, there are programs available from NASA through COSMIC, Computer Software Management Information Center, 112 Barrow Hall, The University of Georgia, Athens, Georgia, 30602, (404) 542-3265. It should be noted that the use of and the results from these computer codes rely on the model developed, the material properties selected, and the experience of the user.

5.14 CERTIFICATION REQUIREMENTS

This section is reserved for future use.

¹The LSS used in Figure 5.12.2 were chosen for illustrative purposes only and do not represent optimal LSS for a given application.

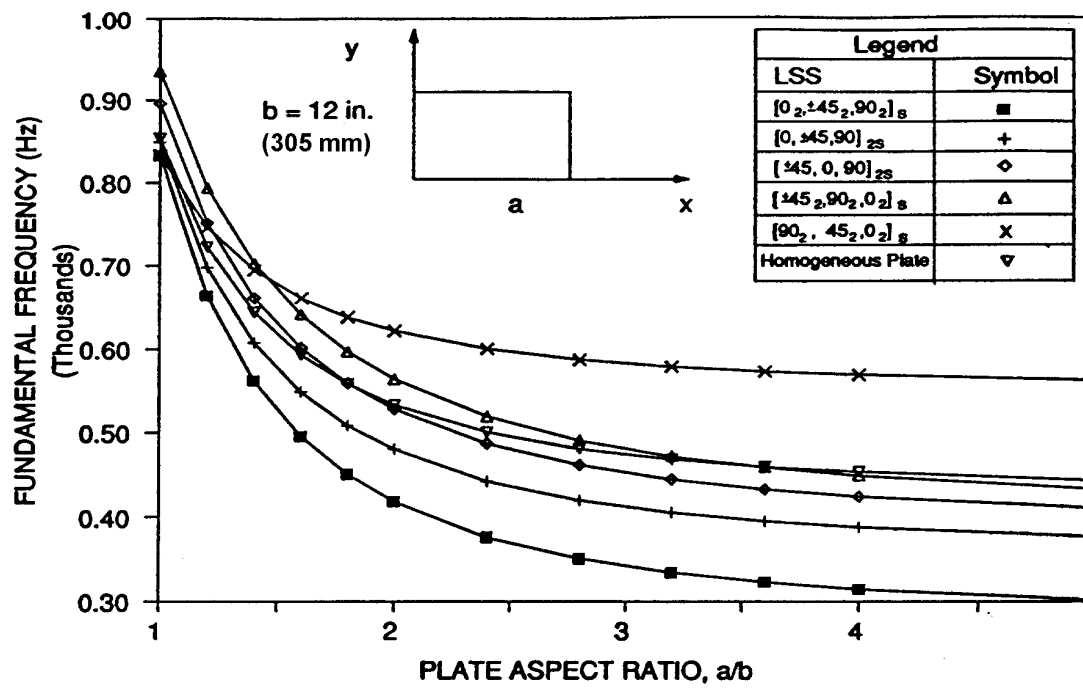


FIGURE 5.11.2 *Vibration analysis results for four sides simply-supported plates with variable aspect ratio.*

REFERENCES

- 5.2.2(a) Hashin, Z., "Theory of Fiber Reinforced Materials," NASA CR-1974, 1972.
- 5.2.2(b) Christensen, R.M., *Mechanics of Composite Materials*, Wiley-Interscience, 1979.
- 5.2.2.1(a) Pickett, G., AFML TR-65-220, 1965.
- 5.2.2.1(b) Adams, D.F., Doner, D.R., and Thomas, R.L., *J. Composite Materials*, Vol 1, 1967, pp. 4, 152.
- 5.2.2.1(c) Sendeckyj, G.P., "Elastic Behavior of Composites," *Mechanics of Composite Materials*, Vol. II, ed. Sendeckyj, G.P., Academic Press, 1974.
- 5.2.2.1(d) Hashin, Z. and Rosen, B.W., "The Elastic Moduli of Fiber-Reinforced Materials," *J. Appl. Mech.*, Vol 31, 1964, p. 223.
- 5.2.2.1(e) Hashin, Z., "Analysis of Properties of Fiber Composites with Anisotropic Constituents," *J. Appl. Mech.*, Vol 46, 1979, p. 543.
- 5.2.2.2(a) Christensen, R.M., *Theory of Viscoelasticity*, Academic Press, 1971.
- 5.2.2.2(b) Hashin, Z., "Viscoelastic Behavior of Heterogeneous Media," *J. Appl. Mech.*, Vol 32, 1965, p. 630.
- 5.2.2.2(c) Hashin, Z., "Viscoelastic Fiber Reinforced Materials," *AIAA Journal*, Vol 4, 1966, p. 1411.
- 5.2.2.2(d) Schapery, R.A., "Viscoelastic Behavior of Composites," in *Mechanics of Composite Materials*, Vol. II, ed. Sendeckyj, G.P., Academic Press, 1974.
- 5.2.2.3(a) Levin, V.M., "On the Coefficients of Thermal Expansion of Heterogeneous Materials," *Mekh. Tverd. Tela*, Vol 1, 1967, p. 88. English translation: *Mechanics of Solids*, Vol 2, 1967, p. 58.
- 5.2.2.3(b) Schapery, R.A., "Thermal Expansion Coefficients of Composite Materials Based on Energy Principles," *J. Composite Materials*, Vol 2, 1968, p. 380ff.
- 5.2.2.3(c) Rosen, B.W., "Thermal Expansion Coefficients of Composite Materials," Ph.D. Dissertation, Univ. of Pennsylvania, 1968.
- 5.2.2.3(d) Springer, G.S., "Environmental Effects on Epoxy Matrix Composites," ASTM STP 674, ed. Tsai, S.W., 1979, p. 291.
- 5.2.2.3(e) Tsai, S.W. and Hahn, H.T., *Introduction to Composite Materials*, Technomic, 1980.
- 5.2.3.1.1(a) Gucer, D.E. and Gurland, J., "Comparison of the Statistics of Two Fracture Modes," *J. Mech. Phys. Solids*, 1962, p. 363.
- 5.2.3.1.1(b) Zweben, C., "Tensile Failure Analysis of Composites," *AIAA Journal*, Vol 2, 1968, p. 2325.
- 5.2.3.1.2 Rosen, B.W., "Tensile Failure Analysis of Fibrous Composites," *AIAA Journal*, Vol 2, 1964, p. 1982.
- 5.2.3.1.3(a) Zweben, C., "A Bounding Approach to the Strength of Composite Materials," *Eng. Frac. Mech.*, Vol 4, 1970, p. 1.

Volume 3, Chapter 5 Design and Analysis

- 5.2.3.1.3(b) Harlow, D.G. and Phoenix, S.L., "The Chain-of-Bundles Probability Model for the Strength of Fibrous Materials. I. Analysis and Conjectures, II. A Numerical Study of Convergence," *J. Composite Materials*, Vol 12, 1978, pp. 195, 300.
- 5.2.3.1.4 Rosen, B.W. and Zweben, C.H., "Tensile Failure Criteria for Fiber Composite Materials," NASA CR-2057, August 1972.
- 5.2.3.2(a) Dow, N.F. and Grundfest, I.J., "Determination of Most Needed Potentially Possible Improvements in Materials for Ballistic and Space Vehicles," GE-TIS 60SD389, June 1960.
- 5.2.3.2(b) Rosen, B.W., "Mechanics of Composite Strengthening," *Fiber Composite Materials*, Am. Soc. for Metals, Metals Park, Ohio, 1965.
- 5.2.3.2(c) Schuerch, H., "Prediction of Compressive Strength in Uniaxial Boron Fiber-Metal Matrix Composite Materials," *AIAA Journal*, Vol 4, 1965.
- 5.2.3.2(d) Rosen, B.W., "Strength of Uniaxial Fibrous Composites," in *Mechanics of Composite Materials*, Pergamon Press, 1970.
- 5.2.3.2(e) Chen, C.H. and Cheng, S., "Mechanical Properties of Fiber Reinforced Composites," *J. Composite Materials*, Vol 1, 1967, p. 30.
- 5.2.3.3(a) Drucker, D.C., Greenberg, H.J., and Prager, W., "The Safety Factor of an Elastic-Plastic Body in Plane Strain," *J. Appl. Mech.*, Vol 18, 1951, p. 371.
- 5.2.3.3(b) Koiter, W.T., "General Theorems for Elastic-Plastic Solids," *Progress in Solid Mechanics*, Sneddon and Hill, ed., North Holland, 1960.
- 5.2.3.3(c) Shu, L.S. and Rosen, B.W., "Strength of Fiber Reinforced Composites by Limit Analysis Method," *J. Composite Materials*, Vol 1, 1967, p. 365.
- 5.2.4(a) Tsai, S.W., "Strength Characteristics of Composite Materials," NASA CR-224, 1965.
- 5.2.4(b) Ashkenazi, E.K., *Zavod. Lab.*, Vol 30, 1964, p. 285; *Mezh. Polim*, Vol 1, 1965, p. 60.
- 5.2.4(c) Tsai, S.W. and Wu, E.M., "A General Theory of Strength for Anisotropic Materials," *J. Composite Materials*, Vol 5, 1971, p. 58.
- 5.2.4(d) Wu, E.M., "Phenomenological Anisotropic Failure Criterion," *Mechanics of Composite Materials*, ed. Sendeckyj, G.P., Academic Press, 1974.
- 5.2.4(e) Hashin, Z., "Failure Criteria for Unidirectional Fiber Composites," *J. Appl. Mech.*, Vol 47, 1980, p. 329.
- 5.3.2(a) Agarwal, B.D. and Broutman, L.J., *Analysis and Performance of Fiber Composites*, John Wiley & Sons, New York, NY, 1980.
- 5.3.2(b) Ashton, J.E. and Whitney, J.M., *Theory of Laminated Plates*, Technomic Publishing Co., Inc., Westport, CT, 1970.
- 5.3.2(c) Hussein, R.M., *Composite Panels/Plates: Analysis and Design*, Technomic Publishing Co., Inc., Westport, CT, 1985.
- 5.3.2(d) Jones, R.M., *Mechanics of Composite Materials*, Scripta Book Co., Washington, DC, 1975.

Volume 3, Chapter 5 Design and Analysis

- 5.3.2(e) Tsai, S.W. and Hahn, H.T., *Introduction to Composite Materials*, Technomic Publishing Co., Inc., Westport, CT, 1980.
- 5.3.4 Shen, C. and Springer, G.S., "Moisture Absorption and Desorption of Composite Materials," *J. Composite Materials*, Vol 10, 1976, p. 1.
- 5.3.4.2(a) Chamis, C.C., "A Theory for Predicting Composite Laminate Warpage Resulting From Fabrication," 30th Anniversary Technical Conf., Reinforced Plastics/Composites Institute, The Society of Plastics Industry, Inc., Sec 18-C, 1975, pp. 1-9.
- 5.3.4.2(b) Hyer, M.W., "Some Observations on the Cured Shape of Thin Unsymmetric Laminates," *J. Composite Materials*, Vol. 15, 1981, pp. 175-194.
- 5.3.4.2(c) Hyer, M.W., "Calculations of Room Temperature Shapes of Unsymmetric Laminates," *J. Composite Materials*, Vol. 15, 1981, pp. 296-310.
- 5.3.5.5 Hashin, Z., Bagchi, D., and Rosen, B.W., "Nonlinear Behavior of Fiber Composite Laminates," NASA CR-2313, April 1974.
- 5.4 Flaggs, D.L. and Kural, M.H., "Experimental Determination of the In Situ Transverse Lamina Strength in Graphite/Epoxy Laminates," *Journal of Composite Materials*, Vol. 16, March, 1982, pp. 103-115.
- 5.4.1.1(a) Hashin, Z., "Failure Criteria for Unidirectional Fiber Composites," *Journal of Applied Mechanics*, Vol. 47, June, 1980, pp. 329-334.
- 5.4.1.1(b) Fiber Composite Analysis and Design, Federal Aviation Administration, DOT/FAA/CT-85/6)
- 5.4.4(a) Savin, G.N., "Stress Distribution Around Holes," NASA TT-F-607, November, 1970.
- 5.4.4(b) Whitney, J.M. and Nuismer, R.J., "Stress Fracture Criteria for Laminated Composites Containing Stress Concentrations," *J. Composite Materials*, Vol 8, 1974, p. 253.
- 5.4.4(c) Daniel, I.M., Rowlands, R.E., and Whiteside, J.B., "Effects of Material and Stacking Sequence on Behavior of Composite Plates With Holes," *Experimental Mechanics*, Vol. 14, 1974, pp. 1-9.
- 5.4.4(d) Walter, R.W. Johnson, R.W. June, R.R., and McCarty, J.E., "Designing for Integrity in Long-Life Composite Aircraft Structures," *Fatigue of Filamentary Composite Materials*, ASTM STP 636, pp. 228-247, 1977.
- 5.4.4(e) Aronsson, C.G., "Stacking Sequence Effects on Fracture of Notched Carbon Fibre/Epoxy Composites," *Composites Science and Technology*, Vol. 24, pp. 179-198, 1985.
- 5.4.4(f) Lagace, P.A., "Notch Sensitivity and Stacking Sequence of Laminated Composites," ASTM STP 893, pp. 161-176, 1985.
- 5.4.4(g) Harris C.E. and Morris, D.H., "A Fractographic Investigation of the Influence of Stacking Sequence on the Strength of Notched Laminated Composites," ASTM STP 948, 1987, pp. 131-153.
- 5.4.5(a) Murthy P.L.N, and Chamis, C.C., "Free-Edge Delamination: Laminate Width and Loading Conditions Effects," *J. of Composites Technology and Research*, JCTRER, Vol. 11, No. 1, 1989, pp. 15-22.

Volume 3, Chapter 5 Design and Analysis

- 5.4.5(b) O'Brien, T.K., "The Effect of Delamination on the Tensile Strength of Unnotched, Quasi-isotropic, Graphite/Epoxy Laminates," *Proc. of the SESA/JSME International Conf. on Experimental Mechanics*, Honolulu, Hawaii, May, 1982.
- 5.4.5(c) Bjeletich, J.G., Crossman F.W., and Warren, W.J., "The Influence of Stacking Sequence on Failure Modes in Quasi-isotropic Graphite-Epoxy Laminates," *Failure Modes in Composites IV*, AIME, 1977, pp. 118.
- 5.4.5(d) Crossman, F.W., "Analysis of Delamination," *Proc. of a Workshop on Failure Analysis and Mechanisms of Failure of Fibrous Composite Structures*, NASA Conf. Publ. 2278, 1982, pp. 191-240.
- 5.4.5(e) O'Brien, T.K., "Analysis of Local Delaminations and Their Influence on Composite Laminate Behavior," *Delamination and Debonding of Materials*, ASTM STP 876, 1985, pp. 282-297.
- 5.4.5(f) Sun C.T. and Zhou, S.G., "Failure of Quasi-Isotropic Composite Laminates with Free Edges," *J. Reinforced Plastics and Composites*, Vol. 7, 1988, pp. 515-557.
- 5.4.5(g) O'Brien, T.K., "Characterization of Delamination Onset and Growth in a Composite Laminate," *Damage in Composite Materials*, ASTM STP 775, 1982, pp. 140-167.
- 5.4.5(h) Whitcomb J.D. and Raju, I.S., "Analysis of Free-Edge Stresses in Thick Composite Laminates," *Delamination and Debonding of Materials*, ASTM STP 876, 1985, pp. 69-94.
- 5.4.5(i) Lekhnitskii, S.G., *Anisotropic Plates*, Gordon and Breach Science Publ., 1968.
- 5.4.5(j) Garg, A.C., "Delamination-A Damage Mode In Composite Structures," *Eng. Fracture Mech.*, Vol. 29, No. 5, 1988, pp. 557-584.
- 5.4.5(k) Lagace, P.A., "Delamination in Composites: Is Toughness the Key?" *SAMPE J.*, Nov/Dec, 1986, pp. 53-60.
- 5.4.5(l) Soni S. R. and Kim, R.Y., "Delamination of Composite Laminates Stimulated by Interlaminar Shear," *Composite Materials: Testing and Design (Seventh Conf.)*, ASTM STP 893, 1986, pp. 286-307.
- 5.4.5(m) Chan, W.S., Rogers, C., and Aker, S., "Improvement of Edge Delamination Strength of Composite Laminates Using Adhesive Layers," *Composite Materials: Testing and Design (Seventh Conf.)*, ASTM STP 893, 1986, pp. 266-285.
- 5.4.5(n) Chan W.S. and Ochoa, O.O., "Suppression of Edge Delamination in Composite Laminates by Terminating a Critical Ply near the Edges," Presented at the AIAA/ASMR/ASCE/AHS 29th Structures, Structural Dynamics and Materials Conf., AIAA Paper #88-2257, 1988, pp. 359-364.
- 5.4.5(o) Vizzini, A.J., "Prevention of Free-Edge Delamination via Edge Alteration," Presented at the AIAA/ASME/ASCE/AHS 29th Structures, Structural Dynamics and Materials Conference, AIAA Paper #88-2258, 1988, pp. 365-370.
- 5.4.5(p) Sun, C.T., "Intelligent Tailoring of Composite Laminates," *Carbon*, Vol. 27, No. 5, 1989, pp. 679-687.
- 5.4.5(r) Lagace P.A. and Cairns, D.S., "Tensile Response of Laminates to Implanted Delaminations," *Proc. of 32nd Int. SAMPE Sym.*, April 6-9, 1987, pp. 720-729.

Volume 3, Chapter 5 Design and Analysis

- 5.4.5.1(a) Shivakumar K.N. and Whitcomb, J.D., "Buckling of a Sublaminates in a Quasi-Isotropic Composite Laminates," NASA TM-85755, Feb, 1984.
- 5.4.5.1(b) Chai H. and Babcock, C.D., "Two-Dimensional Modelling of Compressive Failure in Delaminated Laminates," *J. of Composite Materials*, 19, 1985, pp. 67-98.
- 5.4.5.1(c) Vizzini A.J. and Lagace, P.A., "The Buckling of a Delaminated Sublaminates on an Elastic Foundation," *J. of Composite Materials*, 21, 1987, pp. 1106-1117.
- 5.4.5.1(d) Kassapoglou, C., "Buckling, Post-Buckling and Failure of Elliptical Delaminations in Laminates Under Compression," *Composite Structures*, 9, 1988, pp. 139-159.
- 5.4.5.1(e) Yin, W.L., "Cylindrical Buckling of Laminated and Delaminated Plates," Presented at the AIAA/ASMR/ASCE/AHS 27th Structures, Structural Dynamics and Materials Conference, AIAA Paper #86-0883, 1986, pp. 165-179.
- 5.4.6.1.1(a) Jamison, R.D., "On the Interrelationship Between Fiber Fracture and Ply Cracking in Graphite/Epoxy Laminates," *Composite Materials: Fatigue and Fracture*, ASTM STP 907, 1986, pp. 252-273.
- 5.4.6.1.1(b) Kim, R.Y., "In-plane Tensile strength of Multidirectional Composite Laminates," UDRI-TR-81-84, University of Dayton Research Institute, Aug, 1981.
- 5.4.6.1.1(c) Ryder J.T. and Crossman, F.W., "A Study of Stiffness, Residual Strength and Fatigue Life Relationships for Composite Laminates," NASA CR-172211, Oct, 1983.
- 5.4.6.1.1(d) Sun C.T. and Jen, K.C., "On the Effect of Matrix Cracks on Laminates Strength," *J. Reinforced Plastics and Composites*, Vol. 6, 1987, pp. 208-222.
- 5.4.6.1.1(e) Bailey, J.E., Curtis, P.T., and Parvizi, A., "On the Transverse Cracking and Longitudinal Splitting Behavior of Glass and Carbon Fibre Reinforced Epoxy Cross Ply Laminates and the Effect of Poisson and Thermally Generated Strain," *Proc. R. Soc. London*, series A, 366, 1979, pp. 599-623.
- 5.4.6.1.1(f) Crossman, F.W. and Wang, A.S.D., "The Dependence of Transverse Cracking and Delamination on Ply Thickness in Graphite/Epoxy Laminates," *Damage in Composite Materials*, ASTM STP 775, American Society for Testing and Materials, 1982, pp. 118-139.
- 5.4.6.1.1(g) Flaggs, D.L. and Kural, M.H., "Experimental Determination of the In situ Transverse Laminates Strength in Graphite/Epoxy Laminates," *J. of Composite Materials*, Vol. 16, Mar. 1982, pp. 103-115.
- 5.4.6.1.1(h) Narin, J.A., "The Initiation of Microcracking in Cross-Ply Laminates: A Variational Mechanics Analysis," *Proc. Am Soc for Composites: 3rd Tech. Conf.*, 1988, pp. 472-481.
- 5.4.6.1.1(i) Flaggs, D.L., "Prediction of Tensile Matrix Failure in Composite Laminates," *J. Composite Materials*, 19, 1985, pp. 29-50.
- 5.4.6.1.1(j) Ilcewicz, L.B., Dost, E.F., McCool, J.W., and Grande, D.H., "Matrix Cracking in Composite Laminates With Resin-Rich Interlaminar Layers," Presented at 3rd Symposium on Composite Materials: Fatigue and Fracture, Nov. 6-7, Buena Vista, Fla., ASTM, 1989.
- 5.4.6.2(a) Shuart, M.J., "Short-Wavelength Buckling and Shear Failures for Compression-Loaded Composite Laminates," NASA TM-87640, Nov, 1985.

Volume 3, Chapter 5 Design and Analysis

- 5.4.6.2(b) Shuart, M.J., "Failure of Compression-Loaded Multi-Directional Composite Laminates," Presented at the AIAA/ASME/ASCE/AHS 19th Structures, Structural Dynamics and Materials Conf, AIAA Paper No. 88-2293, 1988.
- 5.4.6.2(c) Hahn, H.T. and Williams, J.G., "Compression Failure Mechanisms in Unidirectional Composites," *Composite Materials: Testing and Design (Seventh Conf.)*, ASTM STP 893, 1986, pp. 115-139.
- 5.4.6.2(d) Hahn H.T. and Sohi, M.M., "Buckling of a Fiber Bundle Embedded in Epoxy," *Composites Science and Technology*, Vol 27, 1986, pp. 25-41.
- 5.6.2(a) Manson, J. A. and Seferis, J. C., "Internal Stress Determination by Process Simulated Laminates," *ANTEC '87 Conference Proceedings*, SPE, May 1987.
- 5.6.2(b) Kays, A.O., "Exploratory Development on Processing Science of Thick-Section Composites," AFWAL-TR-85-4090, October 1985.
- 5.6.3(a) Chan, W.S., Rogers, C. and Aker, S., "Improvement of Edge Delamination Strength of Composite Laminates Using Adhesive Layers," *Composite Materials: Testing and Design*, ASTM STP 893, J.M. Whitney, ed., American Society for Testing and Materials, 1985.
- 5.6.3(b) Chan, W.S. and Ochoa, O.O., "An Integrated Finite Element Model of Edge-Delamination Analysis for Laminates due to Tension, Bending, and Torsion Loads," *Proceedings of the 28th Structures, Dynamics, and Materials Conference*, AIAA-87-0704, 1987.
- 5.6.3(c) O'Brien, T.K. and Raju, I.S., "Strain Energy Release Rate Analysis of Delaminations Around an Open Hole in Composite Laminates," *Proceedings of the 25th Structures, Structural Dynamics, and Materials Conference*, 1984, pp. 526-536.
- 5.6.3(d) Pagano, N.J. and Soni, S.R., "Global - Local Laminate Variational Method," *International Journal of Solids and Structures*, Vol 19, 1983, pp. 207-228.
- 5.6.3(e) Pipes, R.B. and Pagano, N.J., "Interlaminar Stresses in Composites Under Uniform Axial Extension," *J. Composite Materials*, Vol 4, 1970, p. 538.
- 5.7.1.1(a) Almroth, B. O., Brogan, F. W., and Stanley, G. W., "User's Manual for STAGS," NASA Contractor Report 165670, Volumes 1 and 2, March 1978.
- 5.7.1.1(b) Ashton, J. E. and Whitney, J. M., *Theory of Laminated Plates*, Technomic Publishers, 1970, pp. 125-128.
- 5.7.1.2 *Advanced Composites Design Guide, Volume II - Analysis*, Air Force Materials Laboratory, Advanced Development Division, Dayton, Ohio, January 1973, Table 2.2.2-1, pp. 2.2.2-12.
- 5.7.1.3(a) Spier, E. E., "On Experimental Versus Theoretical Incipient Buckling of Narrow Graphite/Epoxy Plates in Compression," AIAA-80-0686-Paper, published in *Proceedings of AIAA/ASME/ASCE/AHS 21st Structures, Structural Dynamics, & Materials Conference*, May 12-14, 1980, pp. 187-193.
- 5.7.1.3(b) Spier, E. E., "Local Buckling, Postbuckling, and Crippling Behavior of Graphite-Epoxy Short Thin Walled Compression Members," Naval Air Systems Command Report NASC-N00019-80-C-0174, June 1981, p. 22.
- 5.7.1.3(c) Arnold, R. R., "Buckling, Postbuckling, and Crippling of Materially Nonlinear Laminated Composite Plates," Ph.D. Dissertation, Stanford University, March 1983, p. 65.

Volume 3, Chapter 5 Design and Analysis

- 5.7.1.3(d) Arnold, R. R. and Mayers, J., "Buckling, Postbuckling, and Crippling of Materially Nonlinear Laminated Composite Plates," *Internal Journal of Solids and Structures*, Vol 20, pp. 863-880. 82-0779-CP, AIAA/ASME/ASCE/AHS, published in the *Proceedings of the 23rd Structures, Structural Dynamics, and Materials Conference*, New Orleans, Louisiana, May 1982, pp. 511-527.
- 5.7.1.8(a) Chamis, C.C., "Buckling of Anisotropic Composites," *Journal of the Structural Division*, Am. Soc. of Civil Engineers, Vol. 95, No. 10, 1969, pp. 2119-2139.
- 5.7.1.8(b) Whitney, J.M., *Structural Analysis of Laminated Anisotropic Plates*, Technomic Publishing Co., Inc., Westport, CT, 1987.
- 5.7.1.8(c) "DOD/NASA Advanced Composites Design Guide, Volume II Analysis," Structures/Dynamics Division, Flight Dynamics Laboratory, Air Force Wright Aeronautical Laboratories, Wright-Patterson Air Force Base, OH, 1983.
- 5.7.1.8(d) Davenport, O.B., and Bert, C.W., "Buckling of Orthotropic, Curved, Sandwich Panels Subjected to Edge Shear Loads," *Journal of Aircraft*, Vol. 9, No. 7, 1972, pp. 477-480.
- 5.7.1.8(e) Spier, E.E., "Stability of Graphite/Epoxy Structures With Arbitrary Symmetrical Laminates," *Experimental Mechanics*, Vol. 18, No. 11, 1978, pp. 401-408.
- 5.7.2(a) Spier, E.E., "On Experimental Versus Theoretical Incipient Buckling of Narrow Graphite/Epoxy Plates in Compression," AIAA-80-0686-Paper, published in Proceedings of AIAA/ASME/ASCE/AHS 21st Structures, Structural Dynamics, & Materials Conference, May 12-14, 1980, pp. 187-193.
- 5.7.2(b) Spier, E.E., "Local Buckling, Postbuckling, and Crippling Behavior of Graphite-Epoxy Short Thin Walled Compression Members," Naval Air Systems Command Report NASC-N00019-80-C-0174, June 1981.
- 5.7.2(c) Spier, E.E., "On Crippling and Short Column Buckling of Graphite/Epoxy Structure with Arbitrary Symmetrical Laminates," Presented at SESA 1977 Spring Meeting, Dallas, TX, May 1977.
- 5.7.2(d) Spier, E.E. and Klouman, F.K., "Post Buckling Behavior of Graphite/Epoxy Laminated plates and Channels," Presented at Army Symposium on Solid Mechanics, AMMRC MS 76-2, Sept. 1975.
- 5.7.2(e) Renieri, M.P. and Garrett, R.A., "Investigation of the Local Buckling, Postbuckling and Crippling Behavior of Graphite/Epoxy Short Thin-Walled Compression Members," McDonnell Aircraft Report MDC A7091, NASC, July 1981.
- 5.7.2(f) Bonanni, D.L., Johnson, E.R., and Starnes, J.H., "Local Crippling of Thin-Walled Graphite-Epoxy Stiffeners," AIAA Paper 88-2251.
- 5.7.2(g) Spier, E.E., "Postbuckling Fatigue Behavior of Graphite-Epoxy Stiffeners," AIAA Paper 82-0779-CP, AIAA/ASME/ASCE/AHS, published in the Proceedings of the 23rd Structures, Structural Dynamics, & Materials Conference, New Orleans, LA, May 1982, pp. 511-527.
- 5.7.2(h) Deo, R.B., et al, "Design Development and Durability Validation of Postbuckled Composite and Metal Panels," Air Force Flight Dynamics Laboratory Report, WRDC-TR-89-3030, 4 Volumes, November 1989.

Volume 3, Chapter 5 Design and Analysis

- 5.11.2 Lackman, L.M., Lin, T.H., Konishi, D.Y., and Davidson, J.W., "Advanced Composites Data for Aircraft Structural Design - Volume III," AFML-TR-70-58, Vol. III, Los Angeles Div/Rockwell, Dec, 1970.
- 5.13 Brown, R. T., "Computer Programs for Structural Analysis," *Engineered Materials Handbook, Volume 1 Composites*, ASM International, Metals Park, Ohio, 1987, pp. 268 - 274.

This page intentionally left blank

CHAPTER 6 STRUCTURAL BEHAVIOR OF JOINTS

6.1 INTRODUCTION

It would be difficult to conceive of a structure that did not involve some type of joint. Joints often occur in transitions between major composite parts and a metal feature or fitting. In aircraft, such a situation is represented by articulated fittings on control surfaces as well as on wing and tail components which require the ability to pivot the element during various stages of operation. Tubular elements such as power shafting often use metal end fittings for connections to power sources or for articulation where changes in direction are needed. In addition, assembly of the structure from its constituent parts will involve either bonded or mechanically fastened joints or both.

Joints represent one of the greatest challenges in the design of structures in general and in composite structures in particular. The reason for this is that joints entail interruptions of the geometry of the structure and often, material discontinuities, which almost always produce local highly stressed areas, except for certain idealized types of adhesive joint such as scarf joints between similar materials. Stress concentrations in mechanically fastened joints are particularly severe because the load transfer between elements of the joint have to take place over a fraction of the available area. For mechanically fastened joints in metal structures, local yielding, which has the effect of eliminating stress peaks as the load increases, can usually be depended on; such joints can be designed to some extent by the "P over A" approach, i.e., by assuming that the load is evenly distributed over load bearing sections so that the total load (the "P") divided by the available area (the "A") represents the stress that controls the strength of the joint. In organic matrix composites, such a stress reduction effect is realized only to a minor extent, and stress peaks predicted to occur by elastic stress analysis have to be accounted for, especially for one-time monotonic loading. In the case of composite adherends, the intensity of the stress peaks varies with the orthotropy of the adherend in addition to various other material and dimensional parameters which affect the behavior of the joint for isotropic adherends.

In principle, adhesive joints are structurally more efficient than mechanically fastened joints because they provide better opportunities for eliminating stress concentrations; for example, advantage can be taken of ductile response of the adhesive to reduce stress peaks. Mechanically fastened joints tend to use the available material inefficiently. Sizeable regions exist where the material near the fastener is nearly unloaded, which must be compensated for by regions of high stress to achieve a particular required average load. As mentioned above, certain types of adhesive joints, namely scarf joints between components of similar stiffness, can achieve a nearly uniform stress state throughout the region of the joint.

In many cases, however, mechanically fastened joints can not be avoided because of requirements for disassembly of the joint for replacement of damaged structure or to achieve access to underlying structure. In addition, adhesive joints tend to lack structural redundancy, and are highly sensitive to manufacturing deficiencies, including poor bonding technique, poor fit of mating parts and sensitivity of the adhesive to temperature and environmental effects such as moisture. Assurance of bond quality has been a continuing problem in adhesive joints; while ultrasonic and X-ray inspection may reveal gaps in the bond, there is no present technique which can guarantee that a bond which appears to be intact does, in fact, have adequate load transfer capability. Surface preparation and bonding techniques have been well developed, but the possibility that lack of attention to detail in the bonding operation may lead to such deficiencies needs constant alertness on the part of fabricators. Thus mechanical fastening tends to be preferred over bonded construction in highly critical and safety rated applications such as primary aircraft structural components, especially in large commercial transports, since assurance of the required level of structural integrity is easier to guarantee in mechanically fastened assemblies. Bonded construction tends to be more prevalent in smaller aircraft. For non-aircraft applications as well as in non-flight critical aircraft components, bonding is likewise frequently used.

This chapter describes design procedures and analytical methods for determining stresses and deformations in structural joints for composite structures. Section 6.2 which follows deals with adhesive joints. (Mechanically fastened joints will be the subject of a future revision of the Handbook.)

In the case of adhesive joints, design considerations which are discussed include: effects of adherend thickness as a means of ensuring adherend failure rather than bond failure; the use of adherend tapering to minimize peel stresses; effects of adhesive ductility; special considerations regarding composite adherends; effects of bond layer defects, including surface preparations defects, porosity and thickness variations; and, considerations relating to long term durability of adhesive joints. In addition to design considerations, aspects of joint behavior which control stresses and deformations in the bond layer are described, including both shear stresses and transverse normal stresses which are customarily referred to as "peel" stresses when they are tensile. Finally, some principles for finite element analysis of bonded joints are described.

Related information on joints in composite structures which is described elsewhere in this handbook includes Volume 1, Chapter 7, Section 7.5 (Mechanically Fastened Joints) and 6.3 (Bonded Joints) together with Volume 3, Chapter 2, Section 2.7.8 on Adhesive Bonding.

6.2 ADHESIVE JOINTS

6.2.1 Introduction

Adhesive joints are capable of high structural efficiency and constitute a resource for structural weight saving because of the potential for elimination of stress concentrations which cannot be achieved with mechanically fastened joints. Unfortunately, because of a lack of reliable inspection methods and a requirement for close dimensional tolerances in fabrication, aircraft designers have generally avoided bonded construction in primary structure. Some notable exceptions include: bonded step lap joints used in attachments for the F-14 and F-15 horizontal stabilizers as well as the F-18 wing root fitting, and a majority of the airframe components of the Lear Fan and the Beech Starship.

While a number of issues related to adhesive joint design were considered in the earlier literature cited in References 6.2.1(a)- 6.2.1(h), much of the methodology currently used in the design and analysis of adhesive joints in composite structures is based on the approaches evolved by L.J. Hart-Smith in a series of NASA/Langley-sponsored contracts of the early 70's (References 6.2.1(i) - 6.2.1(n)) as well as from the Air Force's Primary Adhesively Bonded Structures Technology (PABST) program (References 6.2.1(o) - 6.2.1(r)) of the mid-70's. The most recent such work developed three computer codes for bonded and bolted joints, designated A4EG, A4EI and A4EK (References 6.2.1(s) - 6.2.1(u)), under Air Force contract. The results of these efforts have also appeared in a number of open literature publications (Reference 6.2.1(v) - (z)). In addition, such approaches found application in some of the efforts taking place under the NASA Advanced Composite Energy Efficient Aircraft (ACEE) program of the early to mid 80's (Reference 6.2.1(x) and 6.2.1(y)).

Some of the key principles on which these efforts were based include: (1) the use of simple 1-dimensional stress analyses of generic composite joints wherever possible; (2) the need to select the joint design so as to ensure failure in the adherend rather than the adhesive, so that the adhesive is never the weak link; (3) recognition that the ductility of aerospace adhesives is beneficial in reducing stress peaks in the adhesive; (4) careful use of such factors as adherend tapering to reduce or eliminate peel stresses from the joint; and (5) recognition of slow cyclic loading, corresponding to such phenomena as cabin pressurization in aircraft, as a major factor controlling durability of adhesive joints, and the need to avoid the worst effects of this type of loading by providing sufficient overlap length to ensure that some of the adhesive is so lightly loaded that creep cannot occur there, under the most severe extremes of humidity and temperature for which the component is to be used.

Much of the discussion to follow will retain the analysis philosophy of Hart-Smith, since it is considered to represent a major contribution to practical bonded joint design in both composite and metallic

structures. On the other hand, some modifications are introduced here. For example, the revisions of the Goland-Reissner single lap joint analysis presented in Reference 6.2.1(k) have again been revised according to the approach presented in References 6.2.1(z) and 6.2.1(aa).

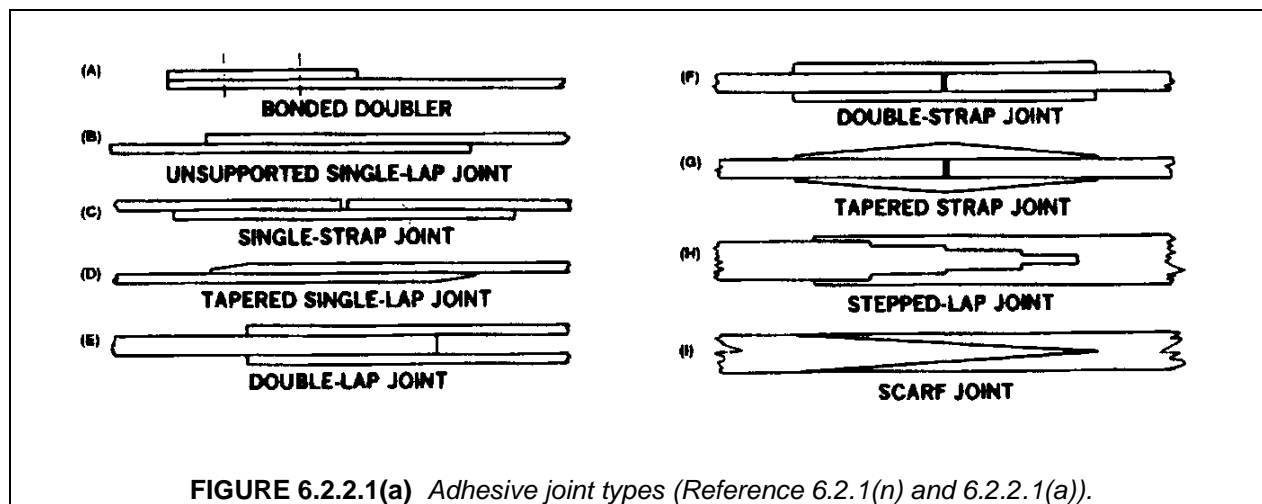
Certain issues which are specific to composite adherends but were not dealt with in the Hart-Smith efforts will be addressed. The most important of these is the effect of transverse shear deformations in organic composite adherends.

Although the main emphasis of the discussion is on simplified stress analysis concepts allowed by shear lag models for shear stress prediction and beam-on-elastic foundation concepts for peel stress prediction, a brief discussion will be provided on requirements for finite element modeling of adhesive joints. Similarly, although joint failure will be considered primarily from the standpoint of stress and strain energy considerations, some discussion of fracture mechanics considerations for adhesive joints will also be included.

6.2.2 Joint design considerations

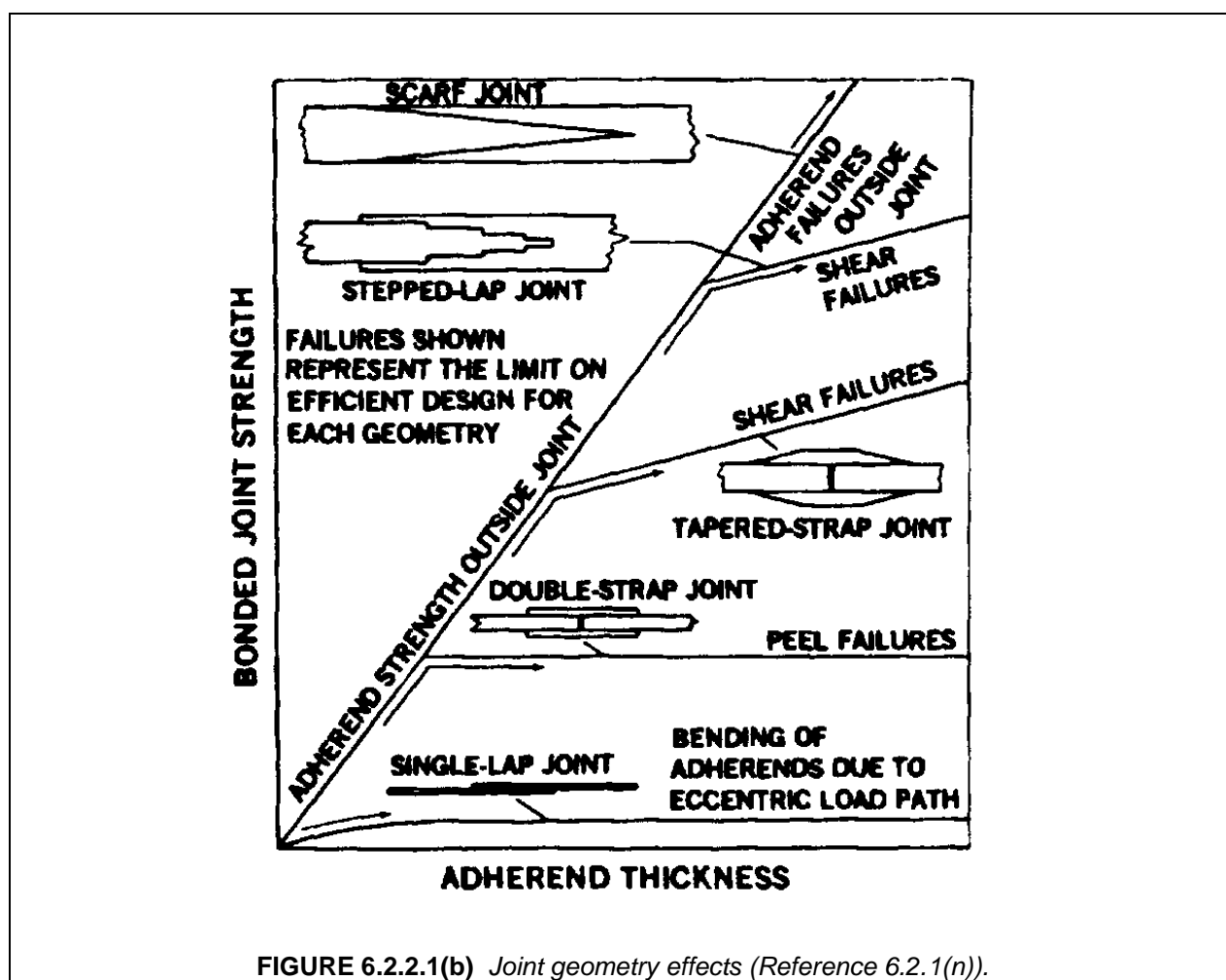
6.2.2.1 Effects of adherend thickness: adherend failures vs. bond failures

Figure 6.2.2.1(a) shows a series of typical bonded joint configurations. Adhesive joints in general are characterized by high stress concentrations in the adhesive layer. These originate, in the case of shear stresses, because of unequal axial straining of the adherends, and in the case of peel stresses, because of eccentricity in the load path. Considerable ductility is associated with shear response of typical adhesives, which is beneficial in minimizing the effect of shear stress joint strength. Response to peel stresses tends to be much more brittle than that to shear stresses, and reduction of peel stresses is desirable for achieving good joint performance.



From the standpoint of joint reliability, it is vital to avoid letting the adhesive layer be the weak link in the joint; this means that, whenever possible, the joint should be designed to ensure that the adherends fail before the bond layer. This is because failure in the adherends is fiber controlled, while failure in the adhesive is resin dominated, and thus subject to effects of voids and other defects, thickness variations, environmental effects, processing variations, deficiencies in surface preparation and other factors that are not always adequately controlled. This is a significant challenge, since adhesives are inherently much weaker than the composite or metallic elements being joined. However, the objective can be accomplished by recognizing the limitations of the joint geometry being considered and placing appropriate restrictions on the thickness dimensions of the joint for each geometry. Figure 6.2.2.1(b), which has frequently been used by Hart-Smith (References 6.2.1(n), 6.2.2.1(a)) to illustrate this point, shows a pro-

gression of joint types which represent increasing strength capability from the lowest to the highest in the figure. In each type of joint, the adherend thickness may be increased as an approach to achieving higher load capacity. When the adherends are relatively thin, results of stress analyses show that for all of the joint types in Figure 6.2.2.1(b), the stresses in the bond will be small enough to guarantee that the adherends will reach their load capacity before failure can occur in the bond. As the adherend thicknesses increase, the bond stresses become relatively larger until a point is reached at which bond failure occurs at a lower load than that for which the adherends fail. This leads to the general principle that for a given joint type, the adherend thicknesses should be restricted to an appropriate range relative to the bond layer thickness. Because of processing considerations and defect sensitivity of the bond material, bond layer thicknesses are generally limited to a range of 0.005-0.015 in. (0.125-0.39 mm). As a result, each of the joint types in Figures 6.2.2.1(a) and 6.2.2.1(b) corresponds to a specific range of adherend thicknesses and therefore of load capacity, and as the need for greater load capacity arises, it is preferable to change the joint configuration to one of higher efficiency rather than to increasing the adherend thickness indefinitely.



6.2.2.2 Joint geometry effects

Single and double lap joints with uniformly thick adherends (Figure 6.2.2.1(a) - Joints (B), (E) and (F)) are the least efficient joint type and are suitable primarily for thin structures with low running loads (load per unit width, i.e., stress times element thickness). Of these, single lap joints are the least capable be-

cause the eccentricity of this type of geometry generates significant bending of the adherends that magnifies the peel stresses. Peel stresses are also present in the case of symmetric double lap and double strap joints, and become a limiting factor on joint performance when the adherends are relatively thick.

Tapering of the adherends (Figure 6.2.2.1(a) - Joints (D) and (G)) can be used to eliminate peel stresses in areas of the joint where the peel stresses are tensile, which is the case of primary concern. No tapering is needed at ends of the overlap where the adherends butt together because the transverse normal stress at that location is compressive and rather small. Likewise, for double strap joints under compressive loading, there is no concern with peel stresses at either location since the transverse extensional stresses that do develop in the adhesive are compressive in nature rather than tensile; indeed, where the gap occurs, the inner adherends bear directly on each other and no stress concentrations are present there for the compression loading case.

For joints between adherends of identical stiffness, scarf joints (Figure 6.2.2.1(a) - Joint (I)) are theoretically the most efficient, having the potential for complete elimination of stress concentrations. (In practice, some minimum thickness corresponding to one or two ply thicknesses must be incorporated at the thin end of the scarfed adherend leading to the occurrence of stress concentrations in these areas.) In theory, any desirable load capability can be achieved in the scarf joint by making the joint long enough and thick enough. However, practical scarf joints may be less durable because of a tendency toward creep failure associated with a uniform distribution of shear stress along the length of the joint unless care is taken to avoid letting the adhesive be stressed into the nonlinear range. As a result, scarf joints tend to be used only for repairs of very thin structures. Scarf joints with unbalanced stiffnesses between the adherends do not achieve the uniform shear stress condition of those with balanced adherends, and are somewhat less structurally efficient because of rapid buildup of load near the thin end of the thicker adherend.

Step lap joints (Figure 6.2.2.1(a) - Joint (H)) represent a practical solution to the challenge of bonding thick members. These types of joint provide manufacturing convenience by taking advantage of the layered structure of composite laminates. In addition, high loads can be transferred if sufficiently many short steps of sufficiently small "rise" (i.e., thickness increment) in each step are used, while maintaining sufficient overall length of the joint.

6.2.2.3 Effects of adherend stiffness unbalance

All types of joint geometry are adversely affected by unequal adherend stiffnesses, where stiffness is defined as axial or in-plane shear modulus times adherend thickness. Where possible, the stiffnesses should be kept approximately equal. For example, for step lap and scarf joints between quasi-isotropic carbon/epoxy (Young's modulus = 8 Msi (55 GPa)) and titanium (Young's modulus = 16 Msi (110 GPa)) ideally, the ratio of the maximum thickness (the thickness just beyond the end of the joint) of the composite adherend to that of the titanium should be $16/8=2.0$.

6.2.2.4 Effects of ductile adhesive response

Adhesive ductility is an important factor in minimizing the adverse effects of shear and peel stress peaks in the bond layer. Figure 6.2.2.4(a) reconstructed from Reference 6.2.2.4(a) shows the shear stress-strain response characteristics of typical adhesives used in the aerospace industry as obtained from thick adherend tests (Volume 1, Section 7.3). Figure 6.2.2.4(a), part (A) represents a relatively ductile film adhesive, FM73, under various environmental conditions, while Figure 6.2.2.4(a), part (B) represents a more brittle adhesive (FM400) under the same conditions. Similar curves can be found in other sources such as Reference 6.2.2.4(b). Even for the less ductile material such as that represented in Figure 6.2.2.4(a), part (B), ductility has a pronounced influence on mechanical response of bonded joints, and restricting the design to elastic response deprives the application of a significant amount of additional structural capability. In addition to temperature and moisture, effects of porosity in the bond layer can have an influence on ductile response. Porosity effects are illustrated in Figure 6.2.2.4(b) (Reference 6.2.1(s)) which compares the response of FM73 for porous (x symbols) and non-porous (diamond symbols) bond layers for various environmental conditions. This will be further discussed in Section 6.2.2.6.

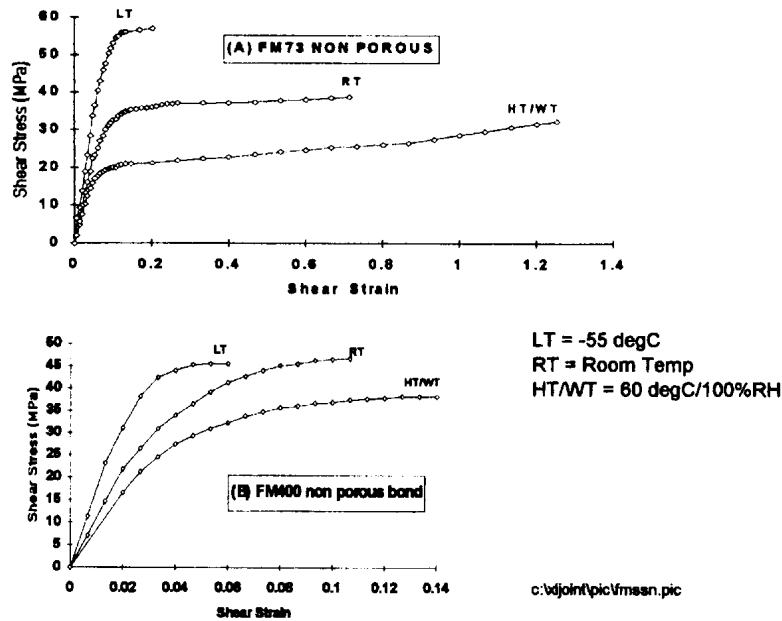


FIGURE 6.2.2.4(a) Typical characteristics of aerospace adhesives (Reference 6.2.2.4(a)).

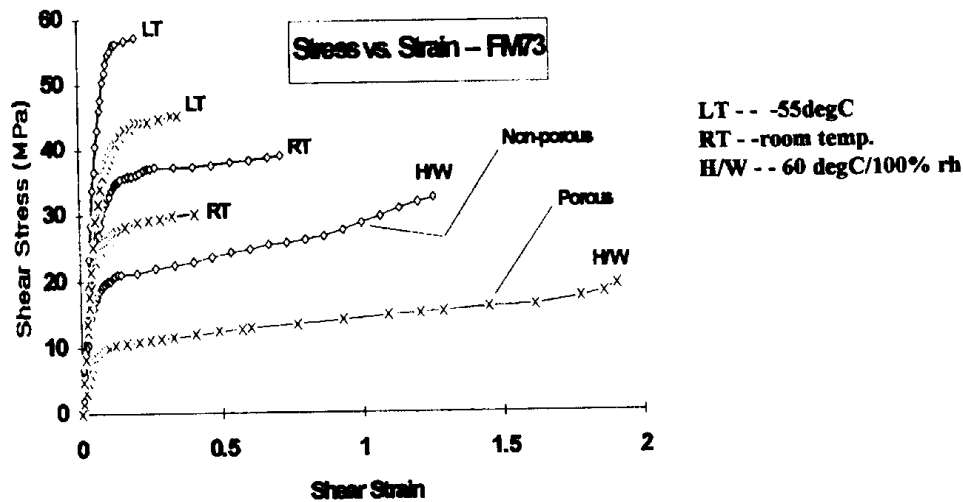


FIGURE 6.2.2.4(b) Effect of porosity on adhesive stress-strain characteristics (Reference 6.2.1(s)).

If peel stresses can be eliminated from consideration by such approaches as adherend tapering, strain energy to failure of the adhesive in shear has been shown by Hart-Smith (Reference 6.2.1(i)) to be the key parameter controlling joint strength; thus the square root of the adhesive strain energy density to failure determines the maximum static load that can be applied to the joint. The work of Hart-Smith has also shown that for predicting mechanical response of the joint, the detailed stress-strain curve of the adhesive can be replaced by an equivalent curve consisting of a linear rise followed by a constant stress

plateau (i.e. elastic-perfectly plastic response) if the latter is adjusted to provide a strain energy density to failure equal to that of the actual stress-strain curve gives. Test methods for adhesives (see Volume 1, Section 7.6) should be aimed at providing data on this parameter. Once the equivalent elastic-perfectly plastic stress strain curve has been identified for the selected adhesive in the range of the most severe environmental conditions (temperature and humidity) of interest, the joint design can proceed through the use of relatively simple one-dimensional stress analysis, thus avoiding the need for elaborate finite element calculations. Even the most complicated of joints, the step lap joints designed for root-end wing and tail connections for the F-18 and other aircraft, have been successfully designed (Reference 6.2.1(t)) and experimentally demonstrated using such approaches. Design procedures for such analyses which were developed under Government contract have been incorporated into the public domain in the form of the "A4EG", "A4EI" and "A4EK" computer codes mentioned previously in Section 6.2.1 and are currently available from the Air Force's Aerospace Structures Information and Analysis Center (ASIAC). Note that the A4EK code permits analysis of bonded joints in which local disbonds are repaired by mechanical fasteners.

6.2.2.5 Behavior of composite adherends

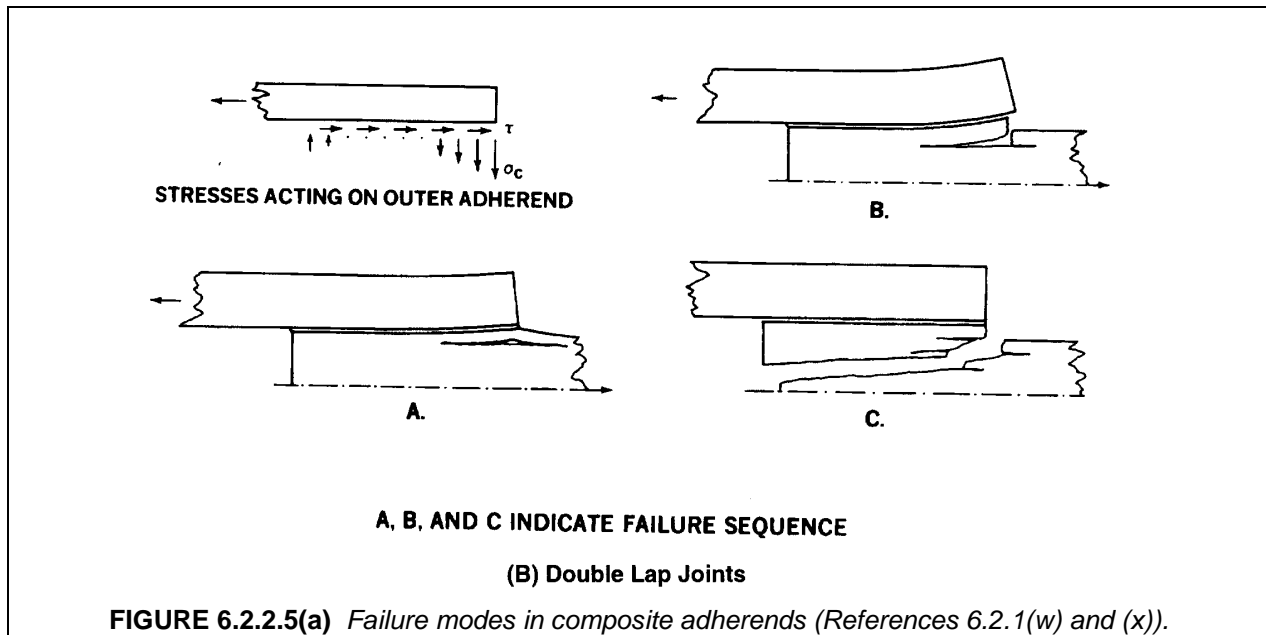
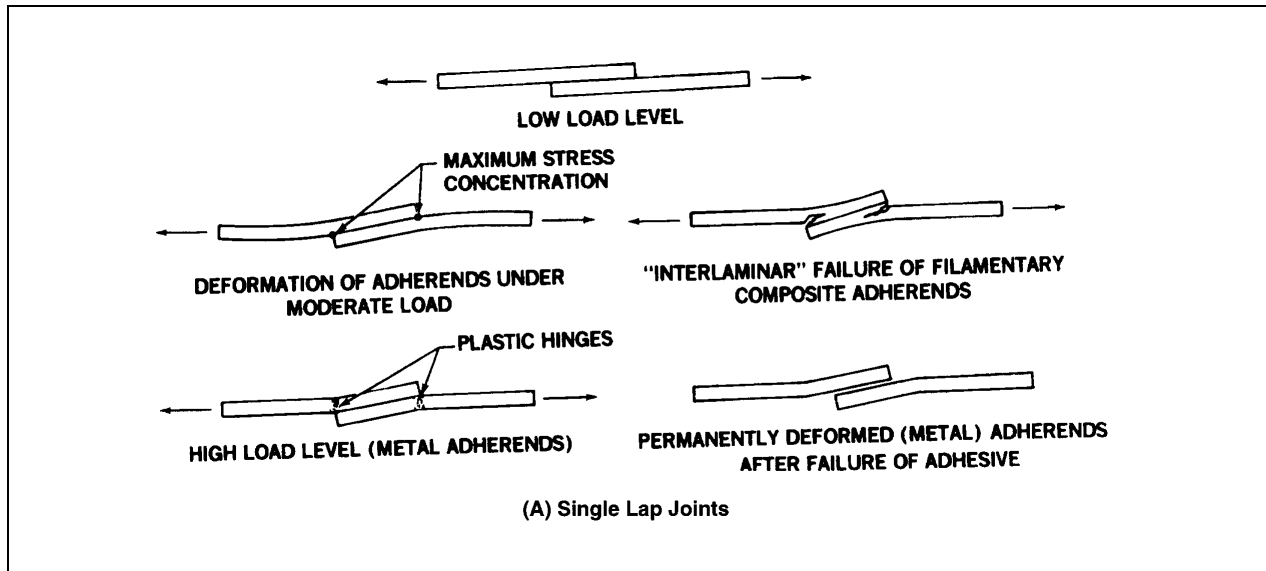
Polymer matrix composite adherends are considerably more affected by interlaminar shear stresses than metals, so that there is a significant need to account for such effects in stress analyses of adhesively bonded composites. Transverse shear deformations of the adherends have an effect analogous to thickening of the bond layer and result in a lowering of both shear and peel stress peaks. (See Section 6.2.3.4.4).

In addition, because the resins used for adherend matrices tend to be less ductile than typical adhesives, and are weakened by stress concentrations due to the presence of the fibers, the limiting element in the joint may be the interlaminar shear and transverse tensile strengths of the adherends rather than the bond strength (Figure 6.2.2.5(a)). In the case of single lap joints (Figure 6.2.2.5(a), part (A)) bending failures of the adherends may occur because of high moments at the ends of the overlap. For metal adherends, bending failures take the form of plastic bending and hinge formation, while for composite adherends the bending failures are brittle in nature. In the case of double lap joints, peel stress build up in thicker adherends can cause the types of interlaminar failures in the adherends illustrated in Figure 6.2.2.5(a), part (B).

The effect of the stacking sequence of the laminates making up the adherends in composite joints is significant. For example, 90-degree layers placed adjacent to the bond layer theoretically act largely as additional thicknesses of bond material, leading to lower peak stresses, while 0-degree layers next to the bond layer give stiffer adherend response with higher stress peaks. In practice it has been observed that 90-degree layers next to the bond layer tend to seriously weaken the joint because of transverse cracking which develops in those layers, and advantage cannot be taken of the reduced peak stresses.

Large differences in thermal expansion characteristics between metal and composite adherends can cause severe problems. (See Section 6.2.3.4.2) Adhesives with high curing temperatures may be unsuitable for some low temperature applications because of large thermal stresses which develop as the joint cools down from the curing temperature.

In contrast with metal adherends, composite adherends are subject to moisture diffusion effects. As a result, moisture is more likely to be found over wide regions of the adhesive layer, as opposed to confinement near the exposed edges of the joint in the case of metal adherends, and response of the adhesive to moisture may be an even more significant issue for composite joints than for joints between metallic adherends.



6.2.2.6 Effects of bond defects

Defects in adhesive joints which are of concern include surface preparation deficiencies, voids and porosity, and thickness variations in the bond layer.

Of the various defects which are of interest, surface preparation deficiencies are probably the greatest concern. These are particularly troublesome because there are no current nondestructive evaluation techniques which can detect low interfacial strength between the bond and the adherends. Most joint design principles are academic if good adhesion between the adherends and bond layer is poor. The principles for achieving this (Reference 6.2.2.6(a) - 6.2.2.6(c)) are well established for adherend and adhesive combinations of interest. Hart-Smith, Brown and Wong (Reference 6.2.2.6.(a)) give an account of the most crucial features of the surface preparation process. Results shown in Reference 6.2.2.6.(a) suggest that surface preparation which is limited to removal of the peel ply from the adherends may be

suspect, since some peel plies leave a residue on the bonding surfaces that makes adhesion poor. (However, some manufacturers have obtained satisfactory results from surface preparation consisting only of peel ply removal.) Low pressure grit blasting (Reference 6.2.2.6(b)) is preferable over hand sanding as a means of eliminating such residues and mechanically conditioning the bonding surfaces.

For joints which are designed to ensure that the adherends rather than the bond layer are the critical elements, tolerance to the presence of porosity and other types of defect is considerable (Reference 6.2.1(t)). Porosity (Reference 6.2.1(z)) is usually associated with over-thickened areas of the bond, which tend to occur away from the edges of the joint where most of the load transfer takes place, and thus is a relatively benign effect, especially if peel stresses are minimized by adherend tapering. Reference 6.2.1(z) indicates that in such cases, porosity can be represented by a modification of the assumed stress-strain properties of the adhesive as determined from thick-adherend tests, allowing a straightforward analysis of the effect of such porosity on joint strength as in the A4EI computer code. If peel stresses are significant, as in the case of over-thick adherends, porosity may grow catastrophically and lead to non-damage-tolerant joint performance.

In the case of bond thickness variations (Reference 6.2.1(aa)), these usually take place in the form of thinning due to excess resin bleed at the joint edges, leading to overstressing of the adhesive in the vicinity of the edges. Inside tapering of the adherends at the joint edges can be used to compensate for this condition; other compensating techniques are also discussed in Reference 6.2.1(aa). Bond thicknesses per se should be limited to ranges of 0.005-0.01 in. (0.12-0.24 mm) to prevent significant porosity from developing, although greater thicknesses may be acceptable if full periphery damming or high minimum viscosity paste adhesives are used. Common practice involves the use of film adhesives containing scrim cloth, some forms of which help to maintain bond thicknesses. It is also common practice to use mat carriers of chopped fibers to prevent a direct path for access by moisture to the interior of the bond.

6.2.2.7 Durability of adhesive joints

Two major considerations in the joint design philosophy of Hart-Smith are: (1) either limiting the adherend thickness or making use of more sophisticated joint configurations such as scarf and step lap joints, to insure that adherend failure takes precedence over bond failure; (2) designing to minimize peel stresses, either by keeping the adherends excessively thin or, for intermediate adherend thicknesses, by tapering the adherends (see discussion of effects of adherend tapering, Section 6.2.2.2 and 6.2.3.5.). In addition, it is essential that good surface treatment practices (Section 6.2.2.6) be maintained to insure that the bond between the adhesive and adherends does not fail. When these conditions are met, reliable performance of the joint can be expected for the most part, except for environmental extremes, i.e., hot-wet conditions. The Hart-Smith approach focuses primarily on creep failure associated with slow cyclic loading (i.e., 1 cycle in several minutes to an hour) under hot wet conditions; this corresponds, for example, to cyclic pressurization of aircraft fuselages. In the PABST program, References 6.2.1(n)-(q) (see also Reference 6.2.1(v)), 18 thick adherend specimens, when tested at high cycling rates (30 Hz) were able to sustain more than 10 million loading cycles without damage, while tests conducted at the same loads at one cycle per hour produced failures within a few hundred cycles. Similar conclusions regarding the effects of cycling rate were presented in Reference 6.2.2.7(a). On the other hand, specimens representative of structural joints, which have a nonuniform shear stress distribution that peaks at the ends of the joint and is essentially zero in the middle (see Section 6.2.3.4.3 on ductile response of joints and Figure 6.2.3.4.3(b), part (B) in particular) are able to sustain hot-wet conditions even at low cycling rates if ℓ_e , the length of the region of elastic response in the bond layer, is sufficient. Based on experience of the PABST program, the Hart-Smith criterion for avoidance of creep failure requires that $\tau_b|_{\min}$, the minimum shear stress along the bond length, be no greater than one tenth the yield stress of the adhesive. But the stress analysis for the elastic-plastic case (Section 6.2.3.4.3) using a bilinear adhesive response model leads to an expression for the minimum shear stress in double lap joints with identical adherends given by

$$\tau_b|_{\min} = \frac{\tau_p}{\sinh \beta_{bd} \ell_e / 2 t_o} \quad 6.2.2.7(a)$$

where τ_p is the adhesive yield stress and β_{bd} is given by

$$\beta_{bd} = [2 G_{b0} t_o / E_o t_b]^{1/2}$$

where G_{b0} is the initial shear modulus, t_b the bond thickness and E_o and t_o the adherend axial modulus and thickness. Because $\sinh(3) \approx 10$, this amounts to a requirement that $\beta_{bd} \ell_e / 2 t_o$ be at least 3, i.e., that the elastic zone length be greater than $6 t_o / \beta_{bd}$. Since ℓ_e is equivalent to the total overlap length, ℓ , minus twice the plastic zone length ℓ_p , then making use of the expression given in Section 6.2.3.4.3 for ℓ_p :

$$\ell_p = (\bar{\sigma}_x / 2 \tau_p - 1 / \beta_{bd}) t_o$$

where $\bar{\sigma}_x$ is the nominal adherend loading stress, the criterion for elastic zone length reduces to a criterion for total overlap length corresponding to a lower bound on ℓ which can be stated as

$$\ell \geq \left(\frac{\bar{\sigma}_x}{\tau_p} + \frac{4}{\beta_{bd}} \right) t_o \quad 6.2.2.7(b)$$

Equation 6.2.2.7(b) for the joint overlap length is the heart of the Hart-Smith approach to durability of bonded joints for cases where adherend failure is enforced over bond failure for static loading, and in which peel stresses are eliminated from the joint design. This type of requirement has been used in several contexts. In Reference 6.2.1(s) for example, it becomes part of the requirement for acceptable void volume, since in this case the voids, acting essentially as gaps in the bond layer, reduce the effective length of the overlap. The criterion has to be modified numerically for joints other than symmetric double lap joints with equal stiffness adherends and uniform thickness. For more sophisticated joint configurations such as step lap joints, the A4EI computer code provides for a step length requirement equivalent to that of Equation 6.2.2.7(b) for simple double lap joints.

In addition to creep failures under hot-wet conditions, the joint may fail due to cracking in the bond layer. Johnson and Mall (Reference 6.2.2.7(b)) presented the data in Figure 6.2.2.7(a) which shows the effect of adherend taper angle on development of cracks at ends of test specimens consisting of composite plates with bonded composite doublers, at 10^6 cycles of fatigue loading; here the open symbols represent the highest load levels that could be identified at which cracks failed to appear, while the solid symbols are for the lowest loads at which cracks just begin to appear. The predicted lines consist of calculated values of applied cyclic stress required to create a total strain energy release rate threshold value, G_{th} , at the debond tip for a given taper angle. The values of G_{th} for the two adhesives were experimentally determined on untapered specimens. The angle of taper at the end of the doubler was used to control the amount of peel stress present in the specimen for static loading. It is noted that even for taper angles as low as 5° (left-most experimental points in Figure 6.2.2.7(a)) for which peel stresses are essentially non-existent for static loading, crack initiation was observed when the alternating load was raised to a sufficient level. A number of factors need to be clarified before the implications of these results are clear. In particular, it is of interest to establish the occurrence of bond cracking at shorter cycling times, say less than 3×10^5 cycles corresponding to expected lifetimes of typical aircraft. Effects of cycling rate and environmental exposure are also of interest. Nevertheless, the data presented in Reference 6.2.2.7(b) suggests the need for consideration of crack growth phenomena in bonded composite joints. Indeed, a major part of the technical effort that has been conducted on the subject of durability of adhesive joints (see Reference 6.2.2.7(c)-(i) for example) has been based on the application of fracture mechanics based concepts. The issue of whether or not a fracture mechanics approach is valid needs further examination. Apparently, no crack-like failures occurred in the PABST program, which was a metal bonding program, even when brittle adhesives were examined at low temperatures. The amount of effort which has been expended by a number of respected workers on development of energy release rate calculations for bonded joints certainly suggests that there is some justification for that approach, and the results obtained by Johnson and Mall appear to substantiate their need for composite joints in particular.

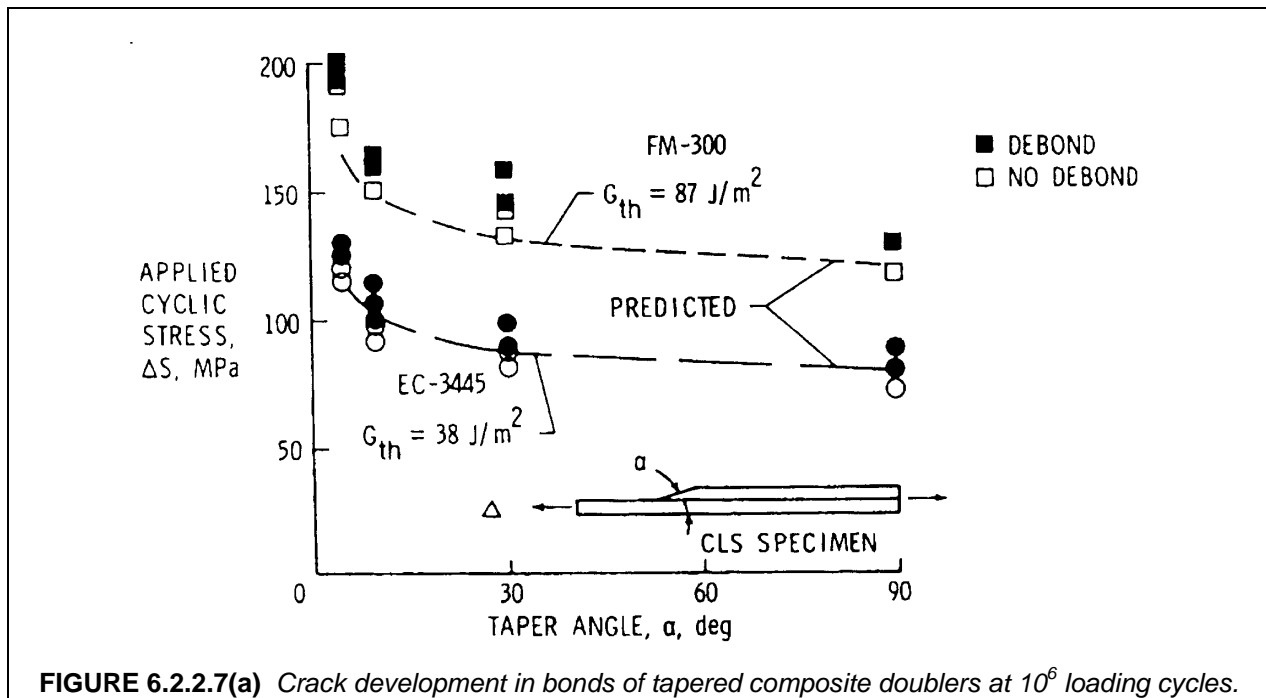


FIGURE 6.2.2.7(a) Crack development in bonds of tapered composite doublers at 10^6 loading cycles.

6.2.3 Stresses and structural behavior of adhesive joints

6.2.3.1 General

Stress analyses of adhesive joints have ranged from very simplistic "P over A" formulations in which only average shear stresses in the bond layer are considered, to extremely elegant elasticity approaches that consider fine details, e.g., the calculation of stress singularities for application of fracture mechanics concepts. A compromise between these two extremes is desirable, since the adequacy of structural joints does not usually depend on a knowledge of details at the micromechanics level, but rather only at the scale of the bond thickness. Since practical considerations force bonded joints to incorporate adherends which are thin relative to their dimensions in the load direction, stress variations through the thickness of the adherend and the adhesive layer tend to be moderate. Such variations do tend to be more significant for polymer matrix composite adherends because of their relative softness with respect to transverse shear and thickness normal stresses. However, a considerable body of design procedure has been developed based on ignoring thickness-wise adherend stress variations. Such approaches involve using one-dimensional models in which only variations in the axial direction are accounted for. Accordingly, the bulk of the material to be covered in this chapter is based on simplified one-dimensional approaches characterized by the work of Hart-Smith, and emphasizes the principles which have been obtained from that type of effort, since it represents most of what has been successfully applied to actual joint design, especially in aircraft components. The Hart-Smith approach makes extensive use of closed form and classical series solutions since these are ideally suited for making parametric studies of joint designs. The most prominent of these have involved modification of Volkersen (Reference 6.2.1(a)) and Goland-Reissner (Reference 6.2.1(b)) solutions to deal with ductile response of adhesives in joints with uniform adherend thicknesses along their lengths, together with classical series expressions to deal with variable adherend thicknesses encountered with tapered adherends, and scarf joints. Simple lap joint solutions described below calculate shear stresses in the adhesive for various adherend stiffnesses and applied loadings. For the more practical step lap joints, the described expressions can be adapted to treat the joint as a series of separate joints each having uniform adherend thickness.

6.2.3.2 Adhesive shear stresses

Figure 6.2.3.2(a) shows a joint with ideally rigid adherends, in which neighboring points on the upper and lower adherends align vertically before sliding horizontally with respect to each other when the joint is loaded. This causes a displacement difference $\delta = u_U - u_L$ related to the bond layer shear strain by $\gamma_b = \delta / t_b$. The corresponding shear stress, τ_b , is given by $\tau_b = G_b \gamma_b$. The rigid adherend assumption implies that δ , γ_b and τ_b are uniform along the joint. Furthermore, the equilibrium relationship indicated in Figure 6.2.3.2(a) (C), which requires that the shear stress be related to the resultant distribution in the upper adherend by

$$dT_U / dx = \tau_b \quad 6.2.3.2(a)$$

leads to a linear distribution of T_U and T_L (upper and lower adherend resultants) as well as the adherend axial stresses σ_{xU} and σ_{xL} , as indicated in Figure 6.2.3.2(b). These distributions are described by the following expressions:

$$T_U = \bar{T} \frac{x}{\ell} ; \quad T_L = \bar{T} \left(1 - \frac{x}{\ell} \right) \quad \text{i.e.,} \quad \sigma_{xU} = \bar{\sigma}_x \frac{x}{\ell} ; \quad \sigma_{xL} = \bar{\sigma}_x \left(1 - \frac{x}{\ell} \right) \quad 6.2.3.2(b)$$

where $\bar{\sigma}_x = \bar{T} / t$. In actual joints, adherend deformations will cause shear strain variations in the bond layer which are illustrated in Figure 6.2.3.2(c). For the case of a deformable upper adherend in combination with a rigid lower adherend shown in Figure 6.2.3.2(c) (A) (in practice, one for which $E_L t_L \gg E_U t_U$), stretching elongations in the upper adherend lead to a shear strain increase at the right end of the bond layer. In the case shown in Figure 6.2.3.2(c) (B) in which the adherends are equally deformable, the bond shear strain increases at *both* ends of the joint. This is due to the increase in axial strain in whichever adherend is stressed (noting that only one adherend is under load) at a particular end of the joint. For both cases, the variation of shear strain in the bond results in an corresponding variation in shear stress which, when inserted into the equilibrium equation (Equation 6.2.3.2(a)) leads to a nonlinear variation of the bond and adherend stresses. The Volkersen shear lag analysis (Reference 6.2.1(a)) provides for calculations of these stresses for cases of deformable adherends.

Introducing the notation (see Figure 6.2.3.2(d))

E_U, E_L, t_U , and t_L = Young's moduli and thicknesses of upper and lower adherends
 G_b and t_b = shear modulus and thickness of bond layer

with

$$B_U = E_U t_U, \quad B_L = E_L t_L$$

while, denoting \bar{T} as the applied axial resultant with

$$\bar{\sigma}_{xU} = \bar{T} / t_U \quad \text{and} \quad \bar{\sigma}_{xL} = \bar{T} / t_L$$

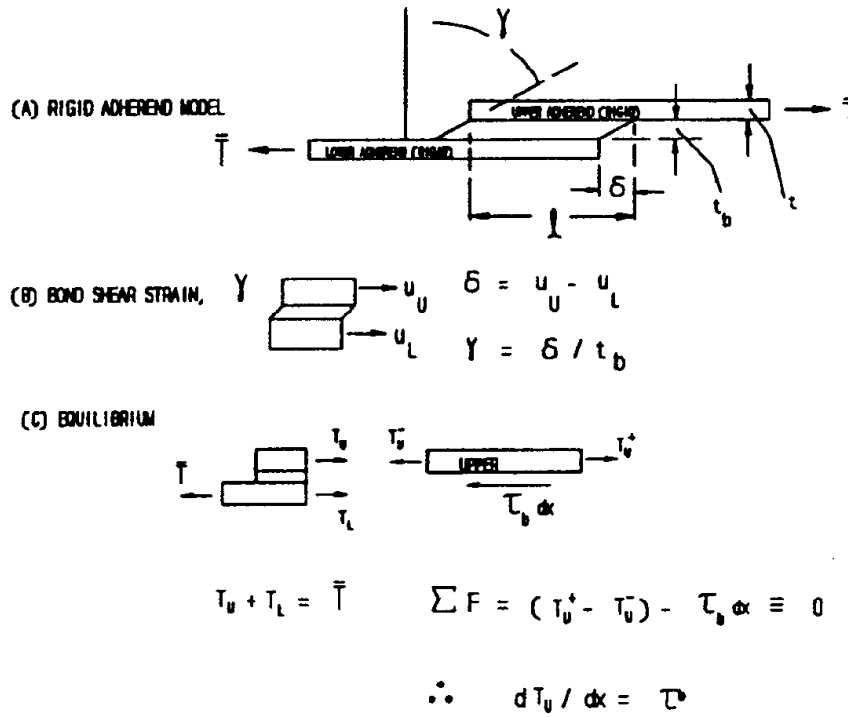
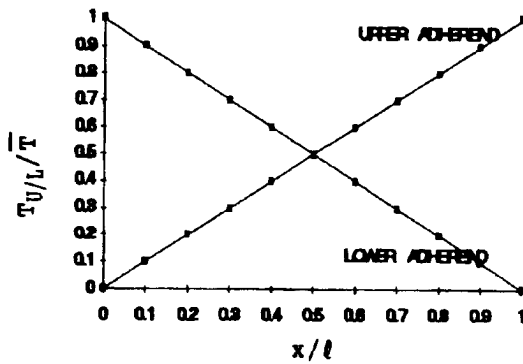


FIGURE 6.2.3.2(a) Elementary joint analysis (Rigid adherend model).

(A) AXIAL RESULTANT DISTRIBUTION



(B) AXIAL STRESS DISTRIBUTION

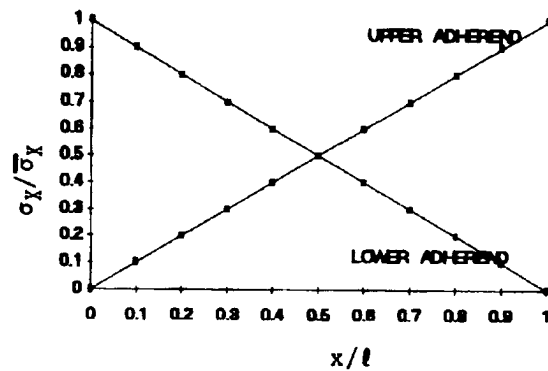


FIGURE 6.2.3.2(b) Axial stresses in joint with rigid adherends.

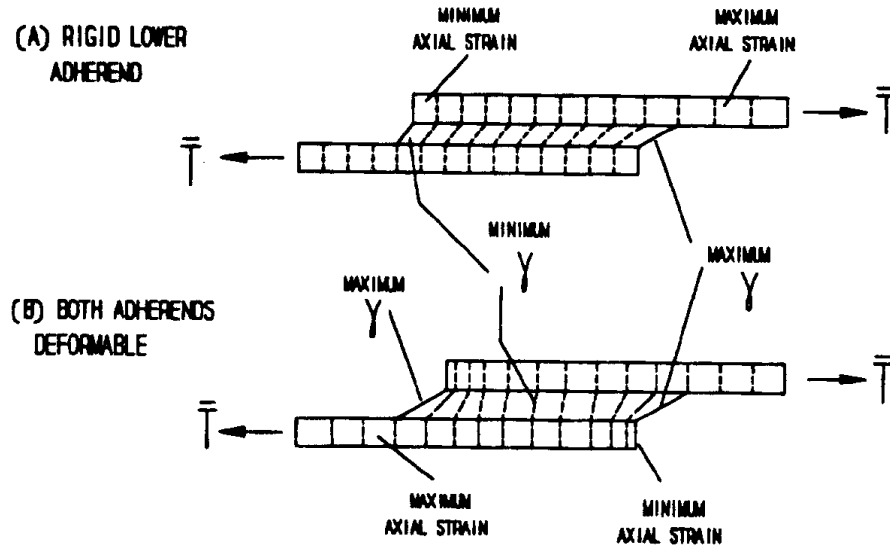


FIGURE 6.2.3.2(c) Adherend deformations in idealized joints.

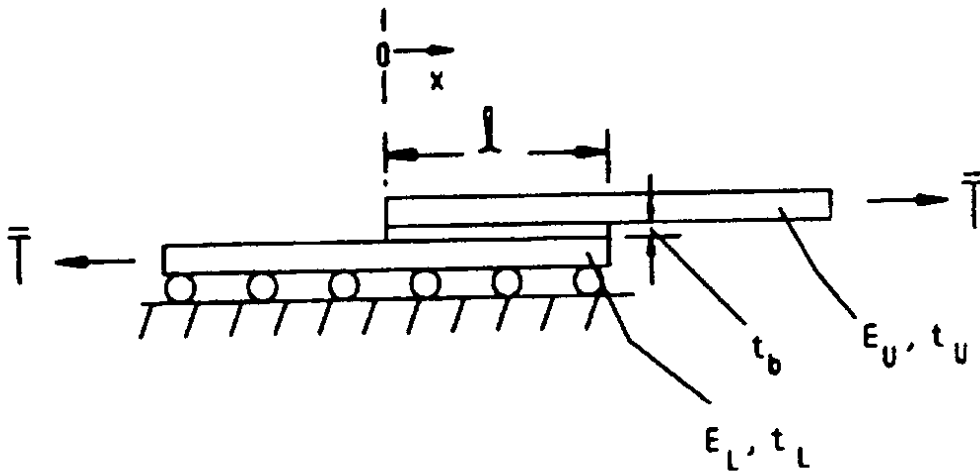


FIGURE 6.2.3.2(d) Geometry for Volkersen solution.

denoting the stresses in the two adherends at their loaded ends, together with

$$\beta = \left[G_b \frac{\bar{t}^2}{t_b} \left(\frac{1}{B_U} + \frac{1}{B_L} \right) \right]^{1/2} ; \quad \bar{t} = \frac{t_U + t_L}{2} ; \quad \rho_B = B_L / B_{LU} \quad 6.2.3.2(c)$$

then the distribution for the axial stress in the upper adherend, $\sigma_{xU}(x)$, obtained from the Volkersen analysis is given by

$$\sigma_{xU} = \bar{\sigma}_{xU} \left\{ \frac{B_U}{B_U + B_L} \left[1 + \frac{\sinh \beta(x - \ell) / \bar{t}}{\sinh \beta \ell / \bar{t}} \right] + \frac{B_U}{B_U + B_L} \frac{\sinh \beta x / \bar{t}}{\sinh \beta \ell / \bar{t}} \right\} \quad 6.2.3.2(d)$$

A comparison of the distribution of axial stresses together with the bond shear stresses for the case of equal thicknesses in the adherends but a relatively rigid lower adherend ($E_L = 10E_U$) vs. that of two equally deformable adherends ($E_L = E_U$) is given in Figure 6.2.3.2(e) below. The results in Figure 6.2.3.2(e) are for $t_U = t_L$ (so that the loading stresses at the adherend ends are equal) and for a bond shear modulus and thickness chosen so that $\beta = 0.387$ and $\ell / t = 20$ for both cases (giving $\beta \ell / t = 7.74$) and a nominal adherend stress $\sigma_{xU} = \sigma_{xL} = 10$ (in unspecified units). The maximum shear stresses are to a good approximation given by

$$\begin{aligned} x = 0 \quad \tau_b|_{\max} &\approx \bar{T} \frac{\beta}{t} \frac{B_U}{B_U + B_L} \\ x = \ell \quad \tau_b|_{\max} &\approx \bar{T} \frac{\beta}{t} \frac{B_L}{B_U + B_L} \end{aligned} \quad 6.2.3.2(e)$$

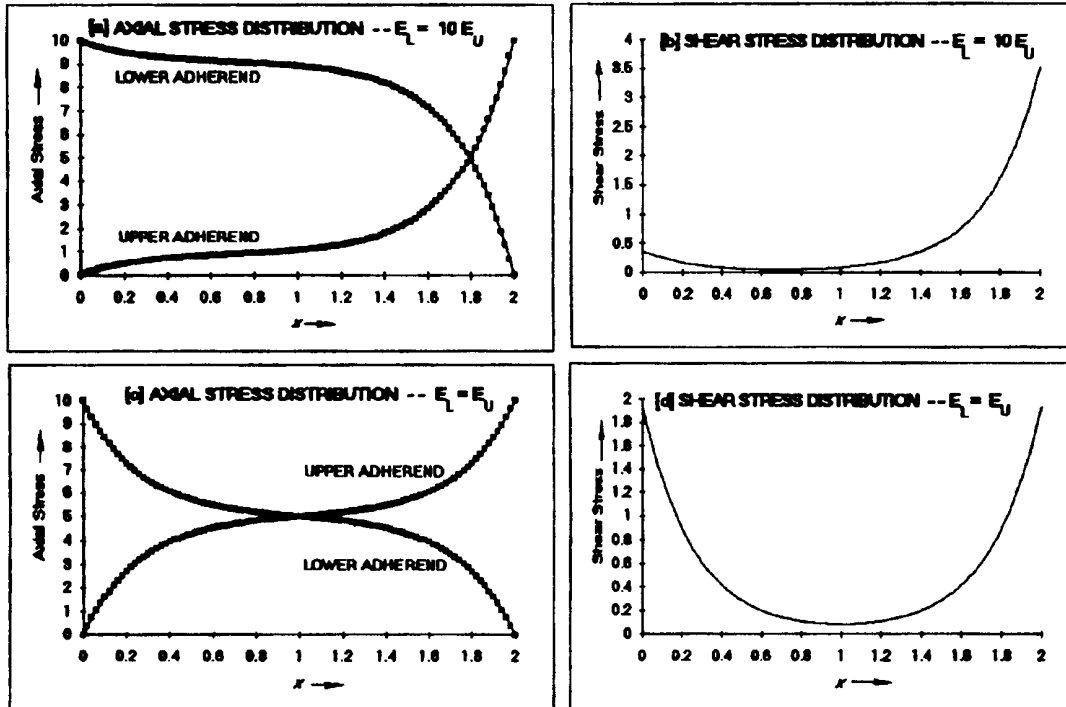


FIGURE 6.2.3.2(e) Comparison of adherend stresses and bond shear stresses for $E_L = E_U$ vs. $E_L = 10E_U$, β and adherend thicknesses equal for both cases.

Typical characteristics of the shear stress distributions are seen at the rights (parts (B) and (D)) in Figure 6.2.3.2(e) in the form of peaks at both ends for equally deformable adherends ($B_L = B_U$); for dissimilar adherends with the lower adherend more rigid ($B_L > B_U$), the higher peak stress obtained from Equation 6.2.3.2(e) occurs at the right end of the joint where $x = \ell$. Because of the shear strain characteristics which are illustrated in Figure 6.2.3.2(c) part (A), the higher peak generally occurs at the loaded end of the more flexible adherend.

As a practical consideration, we will be interested primarily in long joints for which $\beta\ell/t \gg 1$. For these cases Equation 6.2.3.2(e) reduces to

$$\beta\ell/t \gg 1 \quad 6.2.3.2(f)$$

$$B_L \gg B_U; \quad \tau_{b|_{\max}} \approx \beta\bar{\sigma}_x; \quad B_L = B_U; \quad \tau_{b|_{\max}} \approx \frac{1}{2}\beta\bar{\sigma}_x$$

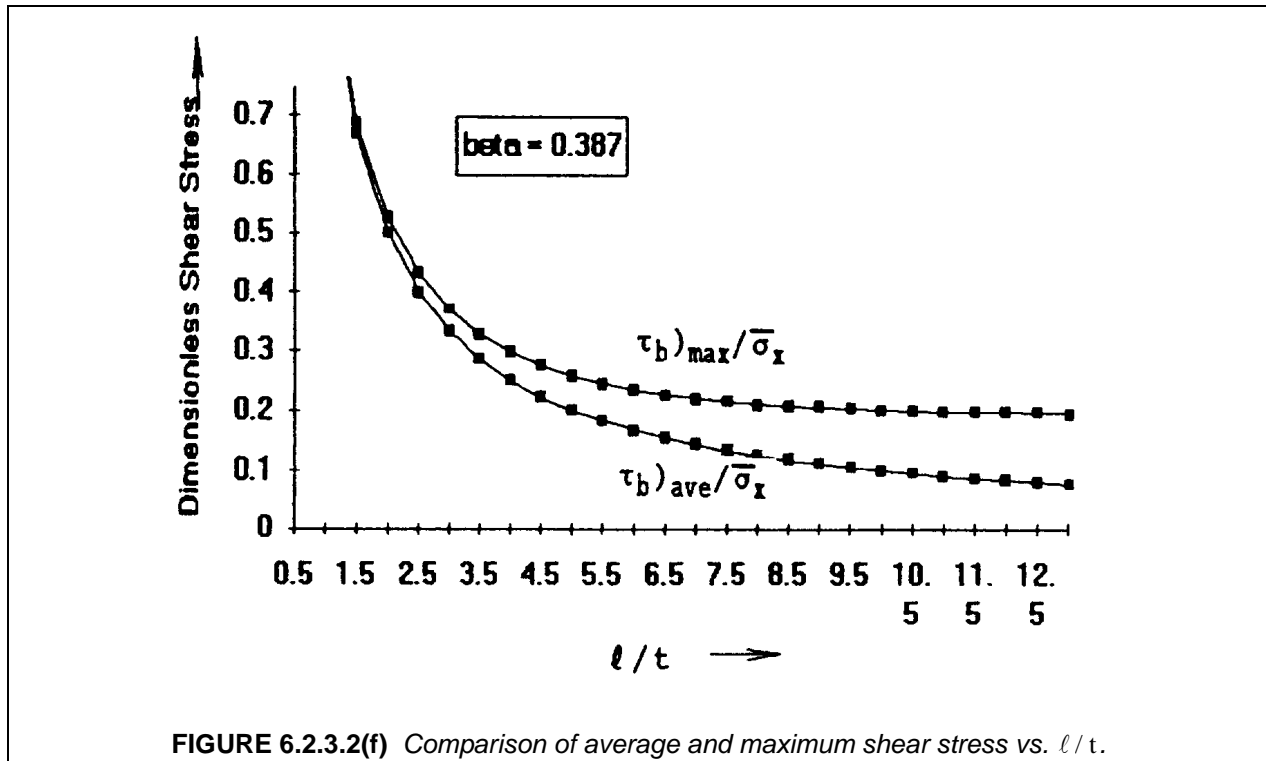
i.e., for long overlaps, the maximum shear stress for the rigid adherend case tends to be twice as great as that for the case of equally deformable adherends, again illustrating the adverse effect of adherend unbalance on shear stress peaks.

An additional point of interest is a typical feature of bonded joints illustrated in Figure 6.2.3.2(e) Part (d) which gives the shear stress distribution for equal adherend stiffness; namely, the fact that high adhesive shear stresses are concentrated near the ends of the joint. Much of the joint length is subjected to relatively low levels of shear stress, which implies in a sense that region of the joint is structurally inefficient since it doesn't provide much load transfer; however, the region of low stress helps to improve damage tolerance of the joint since defects such as voids, and weak bond strength may be tolerated in regions where the shear stresses are low, and in joints with long overlaps this may include most of the joint. As discussed in Section 6.2.2.7, Hart-Smith has suggested that when ductility and creep are taken into account, it is a good idea to have a minimum shear stress level no more than 10% of the yield strength of the adhesive, which requires the minimum value of overlap length given in Equation 6.2.2.7(a).

One other point of interest here is illustrated in Figure 6.2.3.2(f), which compares the behavior of the maximum shear stress in the bond with the average shear stress as a function of the dimensionless joint length, ℓ/t (for the particular case of equal adherend stiffnesses). The average shear stress in the bond line is always the same as the uniform shear stress in the hypothetical joint with rigid adherends discussed earlier, and from equilibrium is given by

$$\tau_{b|_{ave}} = \frac{t}{\ell}\bar{\sigma}_x \quad (t_U = t_L \equiv t; \quad \bar{\sigma}_{xU} = \bar{\sigma}_{xL} \equiv \bar{\sigma}_x)$$

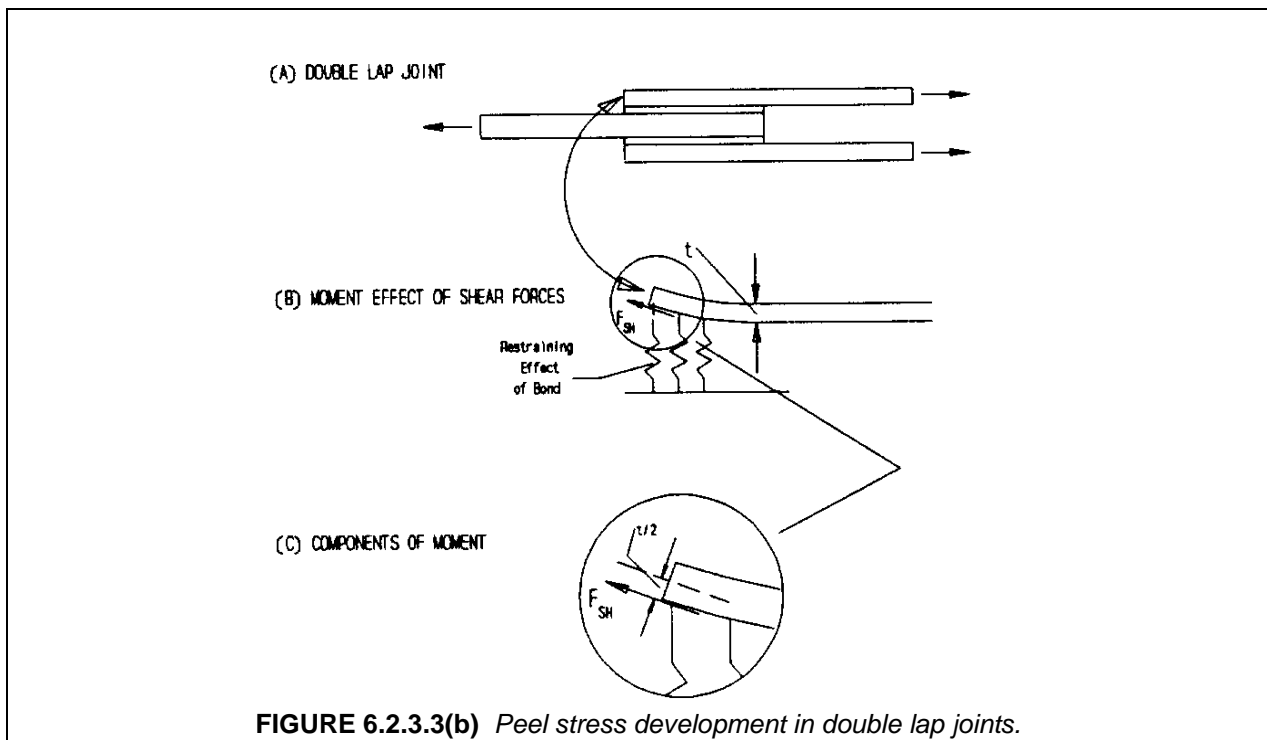
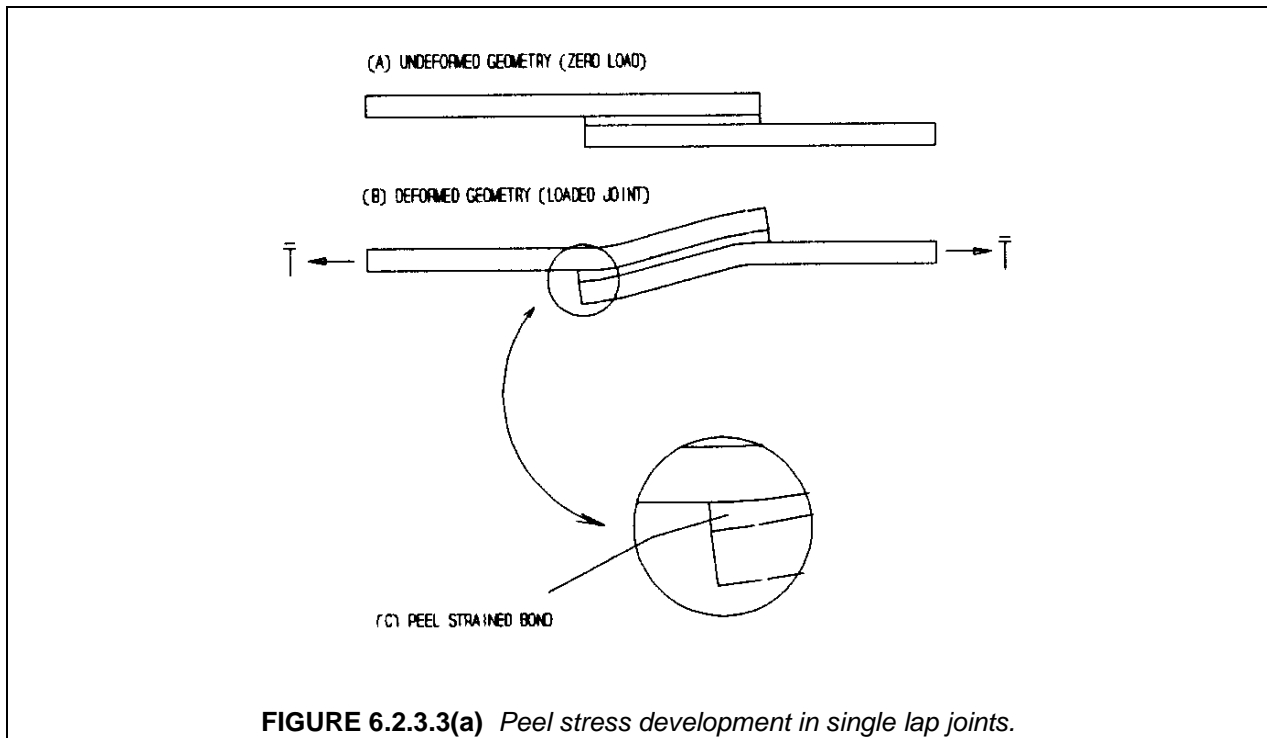
The point illustrated here is the fact that although the *average* shear stress continuously decreases as the joint length increases, for the *maximum* shear stress which controls the load that can be applied without failure of the adhesive, there is a diminishing effect of the increased joint length when $\beta\ell/t$ gets much greater than about 2. Joint design has sometimes been considered only a matter of choosing the joint length ℓ long enough to reduce the average shear stress given in Equation 6.2.3.2(f) to a value less than the allowable shear stress in the bond layer. Obviously if the adhesive responds elastically to failure and if the joint is long enough, the peak stresses at the joint ends will be much larger than the average stress, and joint failure will occur much below the load for which the average is equal to the allowable. On the other hand, ductility tends to dominate the behavior of structural adhesives, and design based on setting the peak stress equal to the allowable is too conservative. The effect of ductility which has already been discussed in Section 6.2.2.4 will be considered in the subsequent discussion.

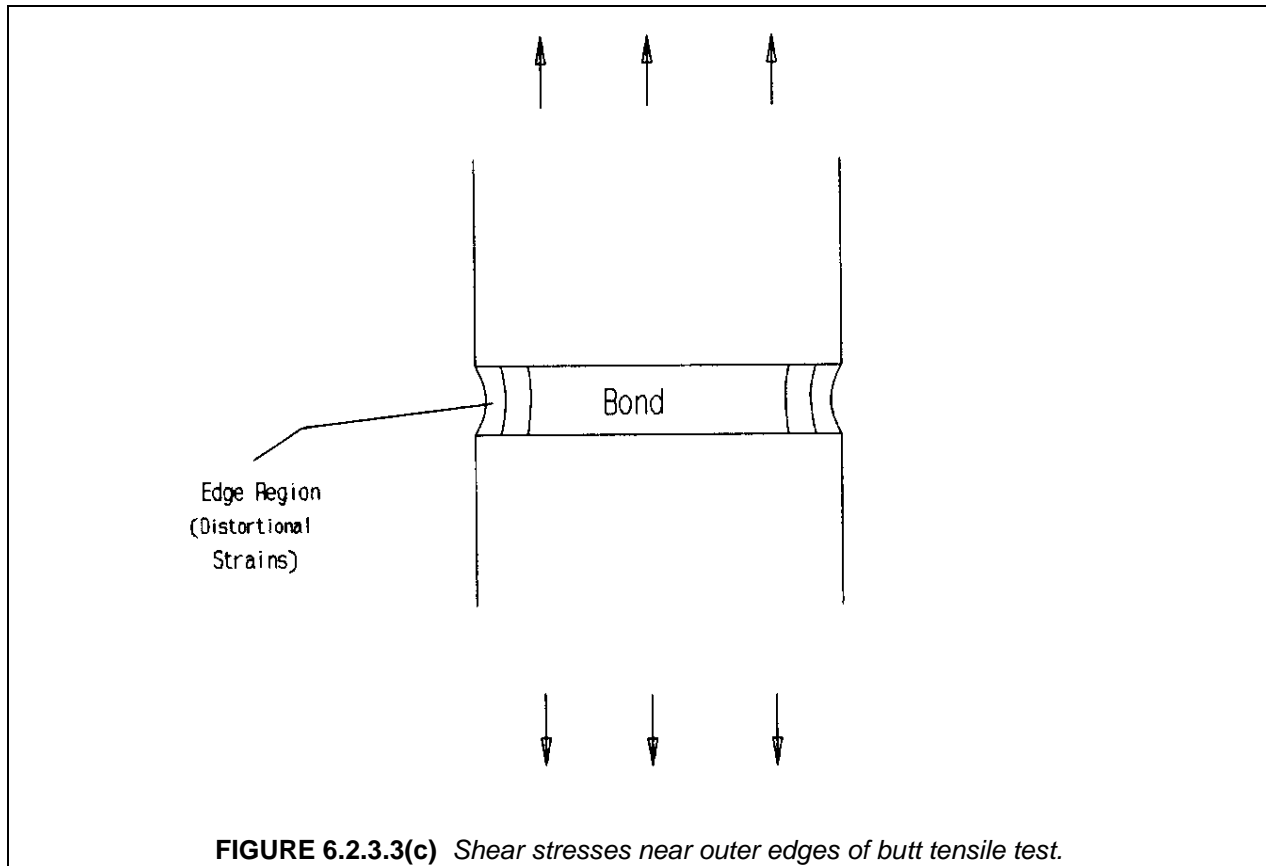


6.2.3.3 Peel stresses

Peel stresses, i.e., through the thickness extensional stresses in the bond, are present because the load path in most adhesive joint geometries is eccentric. It is useful to compare the effect of peel stresses in single and double lap joints with uniform adherend thickness, since peel stresses are most severe for joints with uniform adherend thickness. The load path eccentricity in the single lap joint (Figure 6.2.3.3(a)) is relatively obvious due to the offset of the two adherends which leads to bending deflection as in Figure 6.2.3.3(a) (B). In the case of double lap joints, as exemplified by the configuration shown in Figure 6.2.3.3(b), the load path eccentricity is not as obvious, and there may be a tendency to assume that peel stresses are not present for this type of joint because, as a result of the lateral symmetry of such configurations, there is no overall bending deflection. However, a little reflection brings to mind the fact that while the load in the symmetric lap joint flows axially through the central adherend prior to reaching the overlap region, there it splits in two directions, flowing laterally through the action of bond shear stresses to the two outer adherends. Thus eccentricity of the load path is also present in this type of joint. As seen in Figure 6.2.3.3(b) (C), the shear force, designated as F_{SH} , which represents the accumulated effect of τ_b for one end of the joint, produces a component of the total moment about the neutral axis of the upper adherend equal to $F_{SH}t/2$. (Note that F_{SH} is equivalent to $\bar{T}/2$, since the shear stresses react this amount of load at each end.) The peel stresses, which are equivalent to the forces in the restraining springs shown in Figure 6.2.3.3(b) (B) and (C) have to be present to react the moment produced by the offset of F_{SH} about the neutral axis of the outer adherend. Peel stresses are highly objectionable. Later discussion will indicate that effects of ductility significantly reduce the tendency for failure associated with shear stresses in the adhesive. On the other hand, the adherends tend to prevent lateral contraction in the in-plane direction when the bond is strained in the thickness direction, which minimizes the availability of ductility effects that could provide the same reduction of adverse effects for the peel stresses. This is illustrated by what happens in the butt-tensile test shown in Figure 6.2.3.3(c) in which the two adherend surfaces adjacent to the bond are pulled away from each other uniformly. Here the shear stresses associated with yielding are restricted to a small region whose width is about equal to the thickness of the bond layer, near the outer edges of the system; in most of the bond, relatively little yielding can take

place. For polymer matrix composite adherends, the adherends may fail at a lower peel stress level than that at which the bond fails, which makes the peel stresses even more undesirable.





It is important to understand that peel stresses are unavoidable in most bonded joint configurations. However, it will be seen that they can often be reduced to acceptable levels by selecting the adherend geometry appropriately.

6.2.3.4 Single and double lap joints with uniform adherend thickness

In this section, joints with uniform adherend thickness are considered, since most important features of structural behavior of adhesive joints are illustrated by this case. Section 6.2.3.4.1 below deals with joint behavior under elastic response of the bond layer for structural loading alone. The effect of thermal stresses is treated in Section 6.2.3.4.2, while effects of adhesive ductility in the bond layer and transverse shear deformations in composite adherends are discussed in Sections 6.2.3.4.3 and 6.2.3.4.4, respectively.

6.2.3.4.1 Joint behavior with elastic response of the bond layer

Double lap joints will be considered first since they are somewhat simpler to discuss than single lap joints because of lateral deflection effects which occur in the latter. The following notation (see Figure 6.2.3.4.1(a)) is introduced for reference in the discussion:

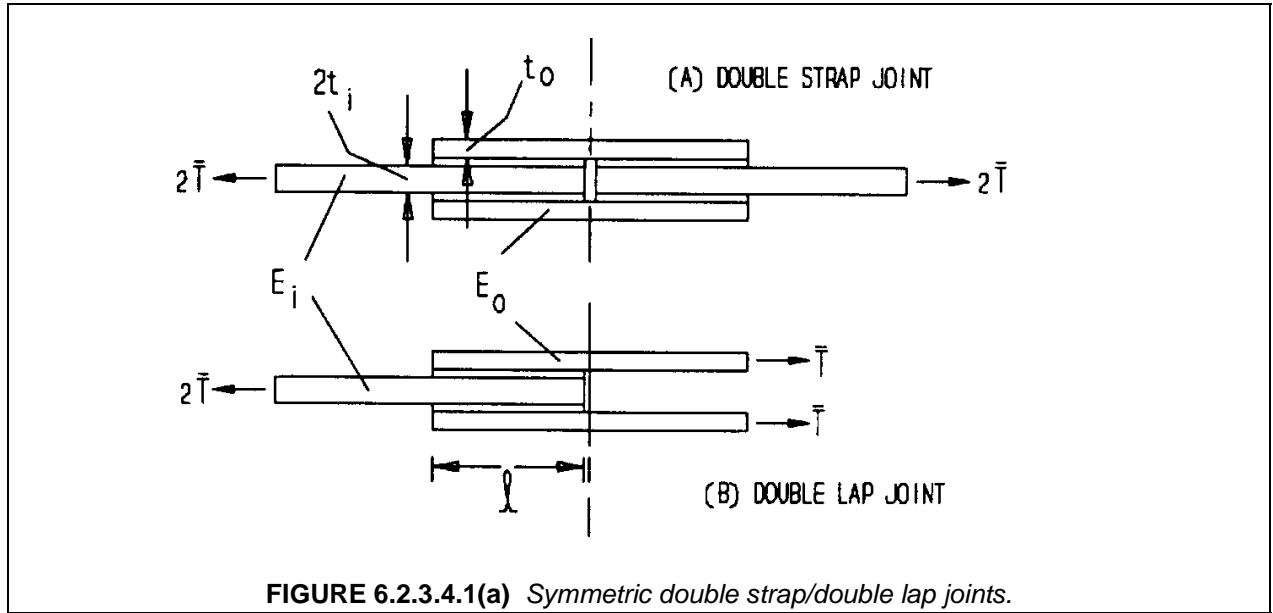


FIGURE 6.2.3.4.1(a) Symmetric double strap/double lap joints.

$E_i, t_i, E_o, t_o \equiv$ axial moduli and thickness of inner and outer adherends

$G_b, E_b, t_b \equiv$ bond shear and peel modulus and thickness

$\sigma_{x0}, \sigma_{xi} =$ axial adherend stresses ; $T_o \equiv \sigma_{x0} t_o, T \equiv \sigma_{xi} t_i$ - - axial resultants

τ_b, σ_b - - bond shear and peel stress

6.2.3.4.1(a)

$$B_0 = t_o E_o ; B_i = t_i E_i ; \beta = \left[G_b \frac{\bar{t}^2}{t_b} \left(\frac{1}{B_0} + \frac{1}{B_i} \right) \right]^{1/2} ; \bar{t} = \frac{t_o + t_i}{2} ; \rho_B = B_i / B_0$$

$$\hat{T}_{th} = \frac{B_0 B_i}{B_0 + B_i} (\alpha_0 - \alpha_i) \Delta T ; \bar{\sigma}_x = \bar{T} / \bar{t} ; \hat{\sigma}_{th} = \hat{T}_{th} / \bar{t}$$

(thermal expansion coeffs α_0, α_i ; temperature change ΔT)

Shear and peel stresses in double lap joints with uniform adherend thickness, including thermal mismatch effects have been treated in a number of places, in particular by Hart-Smith in Reference 6.2.1(i). Using the notation of Equation 6.2.3.4.1(a), the structural response of the joint accounting for both shear and peel stresses in the bond layer can be modeled using a combination of the Volkersen shear lag analysis (Reference 6.2.1(a)) which gives

$$\frac{d^2 T_o}{dx^2} = \frac{G_b}{t_b} \left[\left(\frac{1}{B_0} + \frac{1}{B_i} \right) T_o - \frac{1}{B_i} \bar{T} + \Delta T (\alpha_o \alpha_i) \right] \quad 6.2.3.4.1(b)$$

together with a beam-on-elastic foundation equation modified for the effect of tangential shear loading on the beam:

$$\frac{d^4 \sigma_b}{dx^4} + 4 \frac{\gamma_d^4}{t^4} \sigma_b = \frac{1}{2} t_o \frac{d \tau_b}{dx} \quad 6.2.3.4.1(c)$$

$$\gamma_d = \left(3 \frac{E_b t_o}{E_o t_b} \right)^{1/4} \quad 6.2.3.4.1(d)$$

Results from these equations will first be obtained in the absence of thermal stress effects. Modifying Equation 6.2.3.2a for the current notation gives

$$dT_o/dx = \tau_b \quad 6.2.3.4.1(e)$$

so that solving Equation 6.2.3.4.1(b) under the end conditions $T_o|_{x=0} = 0$; $T_o|_{x=\ell} = \bar{T}$ and differentiating T_o with respect to x gives an expression for t_b .

$$\tau_b = \beta \bar{\sigma}_x \left[\frac{1}{1 + \rho_B} \frac{\cosh \beta(x - \ell) / \bar{t}}{\sinh \beta \ell / \bar{t}} + \frac{\rho_B}{1 + \rho_B} \frac{\cosh \beta x / \bar{t}}{\sinh \beta \ell / \bar{t}} \right] + \beta \hat{\sigma}_{th} \left[\frac{\cosh \beta x / \bar{t}}{\sinh \beta \ell / \bar{t}} - \frac{\cosh \beta(\ell - x) / \bar{t}}{\sinh \beta \ell / \bar{t}} \right] \quad 6.2.3.4.1(f)$$

For the usual situation in which the overlap is long enough so that $\beta \ell / \bar{t}$ is greater than about 3, the peak shear stresses at the ends of the joint are given to a good approximation by

$$x = 0; \tau_{b0} = \beta \left(\frac{1}{1 + \rho_B} \bar{\sigma}_x - \hat{\sigma}_{th} \right); x = \ell; \tau_{b\ell} = \beta \left(\frac{\rho_B}{1 + \rho_B} \bar{\sigma}_x + \hat{\sigma}_{th} \right) \quad 6.2.3.4.1(g)$$

and for the special case of equal adherend stiffnesses ($B_i = B_o$) we have

$$B_i = B_o \quad (\rho_B = 1); \quad \tau_{b|_{\max}} = \frac{1}{2} \beta \bar{\sigma}_x \pm \hat{\sigma}_{th} \quad 6.2.3.4.1(h)$$

In the absence of thermal effects ($\bar{T}_{th} = 0$) and assuming that $B_i \geq B_o$, the maximum value of the shear stresses occurs at the ends of the joint as noted earlier (Figure 6.2.3.2(e)).

Once the shear stress distribution is determined, the peel stresses in the double lap joint are obtained from Equation 6.2.3.4.1(c). The solution to this equation depends (see Figure 6.2.3.4.1(a)) on whether a strap joint (outer adherend rotation restrained at $x = \ell$) or a lap joint (zero outer adherend moment at $x = \ell$) is considered. The exact form of the solution contains products of hyperbolic and trigonometric functions but for the practical situation of joints longer than one-or-two adherend thicknesses and $\beta \ll \gamma_d$, are given by

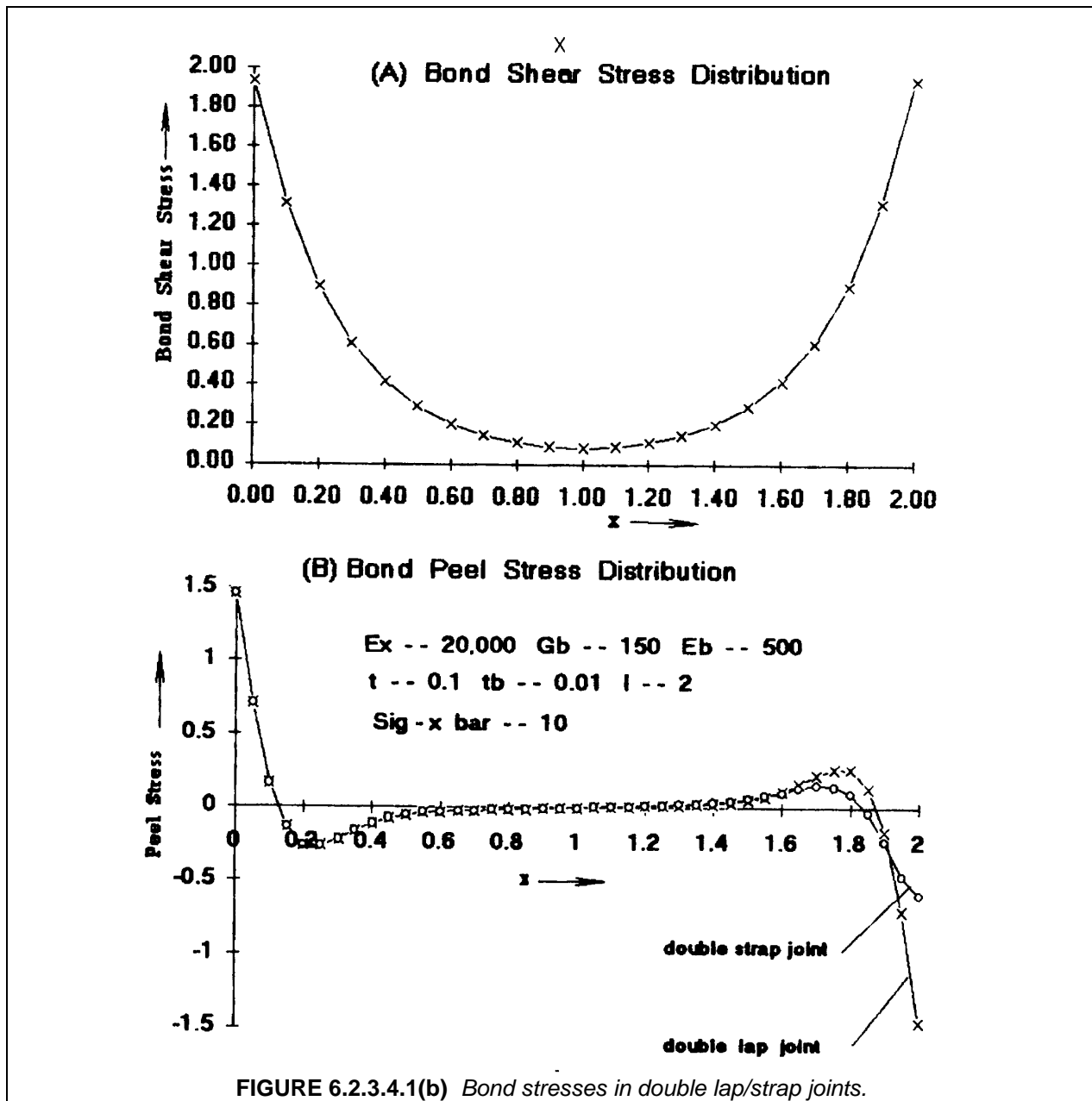
$$\begin{aligned} \text{Double lap joint } \sigma_b &\approx \sigma_{b|_{\max}} \left(\cos \gamma_d \frac{x}{t} e^{-\gamma_d x/t} - \cos \gamma_d \frac{x - \ell}{t} e^{\gamma_d(x - \ell)/t} \right) \\ \text{Double strap joint } \sigma_b &\approx \sigma_{b|_{\max}} \left(\cos \gamma_d \frac{x}{t} e^{-\gamma_d x/t} - \frac{1}{2} \cos \gamma_d \frac{x - \ell}{t} e^{\gamma_d(x - \ell)/t} \right) \end{aligned} \quad 6.2.3.4.1(i)$$

For the case of identical adherends, the maximum peel stresses, which occur at $x=0$, are given by

$$\begin{aligned} \sigma_{b|_{\max}} &= t_b)_{\max} \gamma_d \\ \tau_{b|_{\max}} &= \beta \bar{\sigma}_x / 2 \quad (\text{identical adherends}). \end{aligned} \quad 6.2.3.4.1(j)$$

Here $t_b)_{\max}$ is taken to be the peak stress at *left* end of the joint. Note that the out-of-plane normal stresses are compressive at $x = \ell$ for $\bar{T} > 0$ (tensile load). For $\bar{T} < 0$ (compressive load), the situation would reverse for the double *lap* joint (Figure 6.2.3.4.1(a) part(B)), with the positive out-of-plane stresses occurring at the right end of the joint ($x = \ell$); in the case of the double *strap* joint (Figure 6.2.3.4.1(a) part(A)), the peak out-of-plane stresses would be compressive at the left end of the joint and would be zero at $x = \ell$ (i.e., where the gap between the inner adherends occurs), since the inner adherends would then butt against each other there and act as a continuous element.

Figure 6.2.3.4.1(b) compares the peel and shear stress distributions for $\hat{\sigma}_{th} = 0$, in a typical joint having balanced adherend stiffnesses (the sum of the outer adherend stiffnesses equal to the inner adherend stiffness) whose parameters are listed in Figure 6.2.3.4.1(b) part(B). The diagram at the top indicates the origin of x at the left end of the overlap. Note that the distribution of peel stresses is somewhat more concentrated near the ends than that of the shear stresses. Moreover, the peel stresses at the right end of the joint are negative. In addition, note that the compressive peak at the right end is half as great for the strap joint as for the lap joint, which is the result of the restraint of bending rotations in the strap joint for a gap which is essentially zero. If the loading were compressive rather than tensile, the inner adherends would bear directly on each other and no shear or peel stress peak would occur at the gap, whereas in the lap joint the right end of the overlap would experience the same peak stresses for compressive loading as the left end does for tensile loading.



The situation for the single lap joint (Figure 6.2.3.4.1(c)) is complicated by the effects of lateral deflection which are indicated in Figure 6.2.3.4.1(d). (The literature on the single lap joint is extensive. In addition to Reference 6.2.1(b), pertinent literature for the following discussion on the single lap joint is given in Reference 6.2.1(j), (ab) and (ac). See 6.2.1(ab) and (ac) for other sources.) The deflection effect is dependent on the joint load, given in terms of the quantity $U\ell/2(8)^{1/2}t_U$ where

$$U = t_U \sqrt{\frac{\bar{T}}{D_U}} \equiv \sqrt{12 \frac{\bar{\sigma}_x}{E_U}} \quad ; \quad D_U = \frac{1}{12} E_U t_U^3 \quad 6.2.3.4.1(k)$$

The effects of lateral deflections on the bond stresses were first evaluated by Goland and Reissner (GR) in Reference 6.2.1(b). The GR analysis was restricted to the case of equal adherend thicknesses, so that t_U and t_L , which are equal, are denoted by t in the following. The lateral deflections can then be stated in terms of a dimensionless ratio, k , with respect to the adherend thickness, and are of the following form:

$$t_U = t_L \equiv t$$

$$x \leq \ell_0 \quad ; \quad w = k \frac{t \sinh Ux/t}{2 \sinh U\ell_0/t} - \frac{1}{2} \frac{t + t_b}{L} x \quad 6.2.3.4.1(l)$$

$$\ell_0 \leq x \leq \ell + \ell_0 \quad ; \quad w = W_2 \frac{\sinh[U/\sqrt{8}(x-L)/t]}{\sinh[U\ell/\sqrt{8}t]} + \frac{t_U}{2} - \frac{1}{2} \frac{t + t_b}{L} x \quad ; \quad W_2 = \frac{t}{2}(1-k)$$

The GR expression given in Reference 6.2.1(b) for the parameter k has been reexamined by Hart-Smith (Reference 6.2.1(k)) and more recently by Oplinger (Reference 6.2.1(ab), (ac)); based on the discussion in Reference 6.2.1(ac), the GR expression appears to provide adequate accuracy unless the adherends are excessively thin, i.e., not much more than about twice the bond layer thickness, in which case the expressions given in Reference 6.2.1(ab) and (ac) provide corrections for the adherend thickness effects. A reasonable approximation to the expression for k given in Reference 6.2.1(ab) and (ac) is

$$k = \frac{\tanh U \lambda_0}{\tanh U \lambda_0 + \sqrt{8} C_p \tanh(U \lambda / 2 C_p)} \quad 6.2.3.4.1(m)$$

$$\text{where } C_p = \left(1 + \frac{3}{2} \rho_t + \frac{3}{4} \rho_t^2\right)^{1/2} \quad ; \quad \rho_t = \frac{t_b}{t} \quad ; \quad \lambda = \ell/t \quad ; \quad \lambda_0 = \ell_0/t \quad 6.2.3.4.1(n)$$

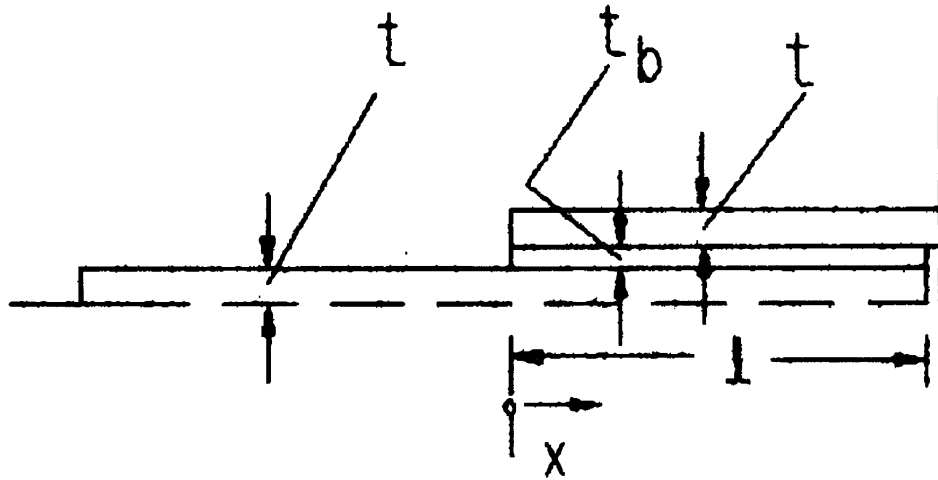
The original GR expression for k is recovered if C_p is set equal to 1 corresponding to $t \gg t_b$ (i.e., relatively thick adherends) and $\tanh U \lambda_0$ is likewise set to 1 corresponding to very long outer adherend lengths. A plot of k vs. the adherend loading stress $\bar{\sigma}_x$ is given in Figure 6.2.3.4.1(e) for two different values of adherend thickness corresponding to bond thickness-to-adherend thickness ratios (ρ_t in Equation 6.2.3.4.1(m)) of 0.5 and 0.1. This plot suggests that k is fairly constant at a value of about 0.25 for a wide range of applied stress values once the initial drop has occurred. The effect of bond-to-adherend thickness ratio is not particularly great and can perhaps be ignored in many situations.

The lateral deflections of the joint have a significant influence on the stresses in the bond layer, which show this through the presence of the k parameter in expressions for them. The shear stress is given by

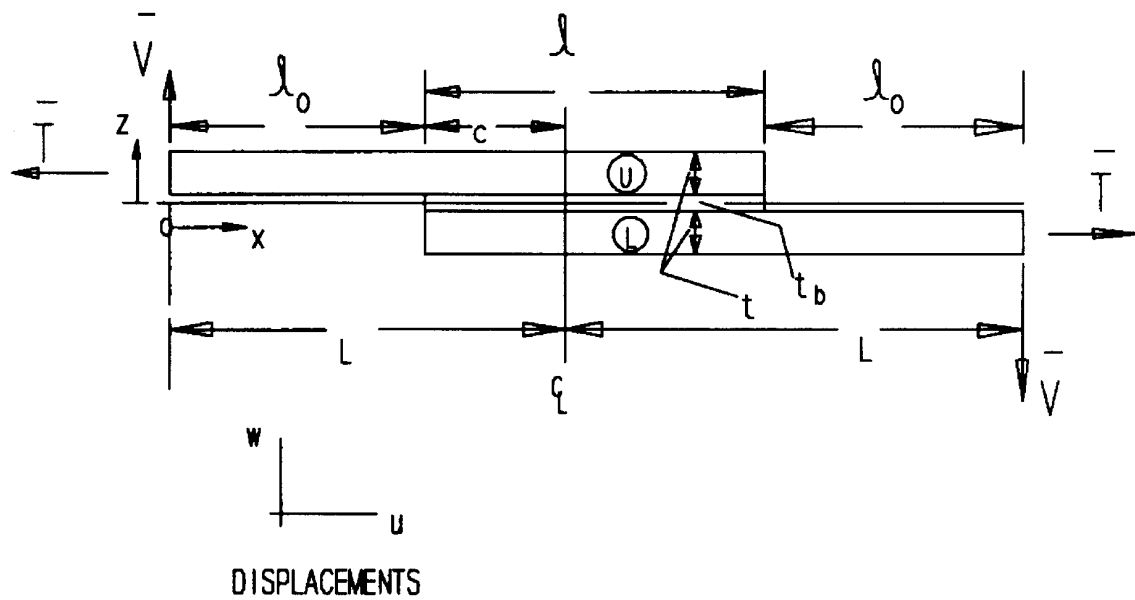
$$\tau_b = \bar{\sigma}_x \left\{ \frac{\beta_s}{4} (1 + 3k) \frac{\cosh[2\beta_s(x-L)/t]}{\sinh(\beta_s \gamma/t)} + \frac{3}{8\sqrt{8}} U(1+k) \frac{\cosh[U(x-L)/\sqrt{8}t]}{\sinh(u\gamma/2\sqrt{8})} \right\} \quad 6.2.3.4.1(o)$$

where $\beta_s \equiv (G_b t / E_x t_b)^{1/2}$, $E_x \equiv$ adherend axial modulus and U is given by Equation 6.2.3.4.1(k). Equation 6.2.3.4.1(o), which represents a slight modification of the GR expression, reduces to the latter for small values of $U\ell/t$. In addition, the peel stresses, for joints in which the overlap length is more than one or two adherend thicknesses (essentially the only case of practical interest) are given by

Quarter Plane Symmetry

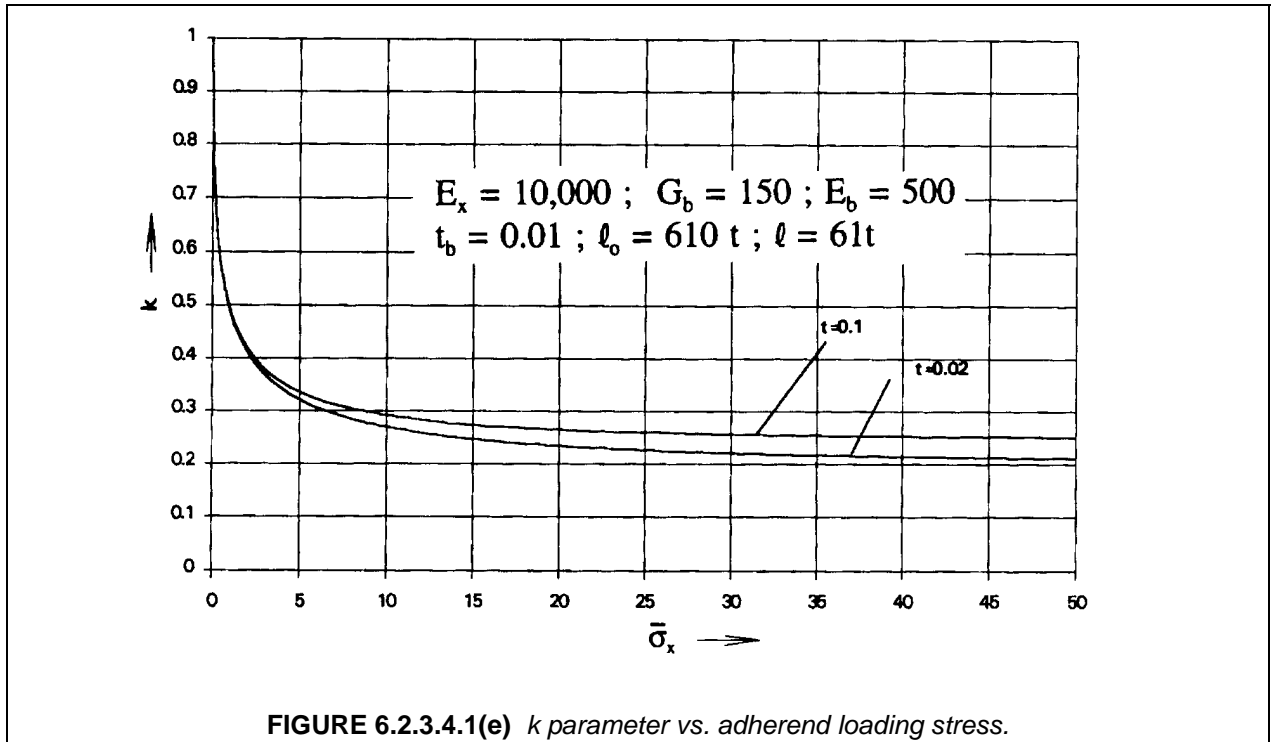
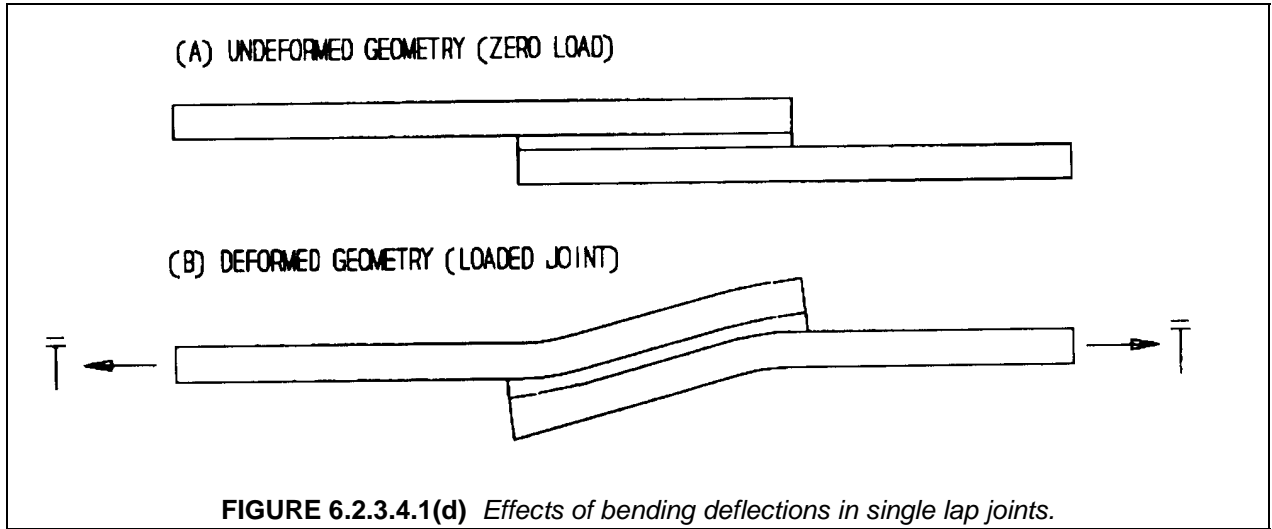


A) Model



B) Dimension

FIGURE 6.2.3.4.1(c) Single lap joint geometry.



$$\sigma_b = \frac{\sigma_x}{2} \frac{k \gamma_s}{2}$$

$$\left\{ \left[\gamma_s \left(\cos \gamma_s \frac{\ell_0 + \ell - x}{t} + \sin \gamma_s \frac{\ell_0 + \ell - x}{t} \right) + U \cos \gamma_s \frac{\ell_0 + \ell - x}{t} \right] \exp \gamma_s \frac{x - \ell_0 - \ell}{t} \right. \quad 6.2.3.4.1(p)$$

$$\left. + \left[\gamma_s \left(\cos \gamma_s \frac{x - \ell_0}{t} - \sin \gamma_s \frac{x - \ell_0}{t} \right) + U \cos \gamma_s \frac{x - \ell_0}{t} \right] \exp \gamma_s \frac{\ell_0 - x}{t} \right\}$$

where

$$\gamma_s = (6E_b t / E_x t_b)^{1/4} \quad 6.2.3.4.1(q)$$

The maximum stresses in the bond layer are given by

$$\tau_{b|_{\max}} = \bar{\sigma}_x \left[\frac{\beta_s}{4} (1+3k) 1 / \tanh \beta_s \lambda + \frac{3}{8\sqrt{8}} U(1-k) / \tanh \left(\frac{U\lambda}{2\sqrt{8}} \right) \right] \quad 6.2.3.4.1(r)$$

Maximum Bond Shear Stress Maximum bond peel stress:

$$\sigma_{b|_{\max}} = \bar{\sigma}_x \frac{k\gamma_s}{2} (\gamma_s + U) \quad 6.2.3.4.1(s)$$

Figure 6.2.3.4.1(f) gives a comparison of the maximum bond stresses as functions of the loading stress $\bar{\sigma}_x$ for two different adherend thicknesses in a joint with a bond layer thickness of 0.01. It is interesting to note that the peel and shear stresses take on quite similar values. Since the maximum peel stress varies approximately as γ_s^2 according to Equation 6.2.3.4.1(s) (the contribution of U being relatively minor), the relationship for γ_s given in Equation 6.2.3.4.1(q) suggests that the peel stresses should be expected to vary as $(t/t_b)^{1/2}$, while the same variation is seen from Equation 6.2.3.4.1(r) for the maximum shear stresses since β_s also contains $(t/t_b)^{1/2}$ as a factor. Thus both stresses should vary with the thickness ratio by the same factor. The fact that they are numerically close together for all stresses is partly due to the effect of other parameters that enter into Equations 6.2.3.4.1(r) and 6.2.3.4.1(s) and partly due to the fact that k does not vary much with load for $\bar{\sigma}_x$ greater than 5. A slight nonlinearity can be observed in the curves of Figure 6.2.3.4.1(f) for the lower loading stresses.

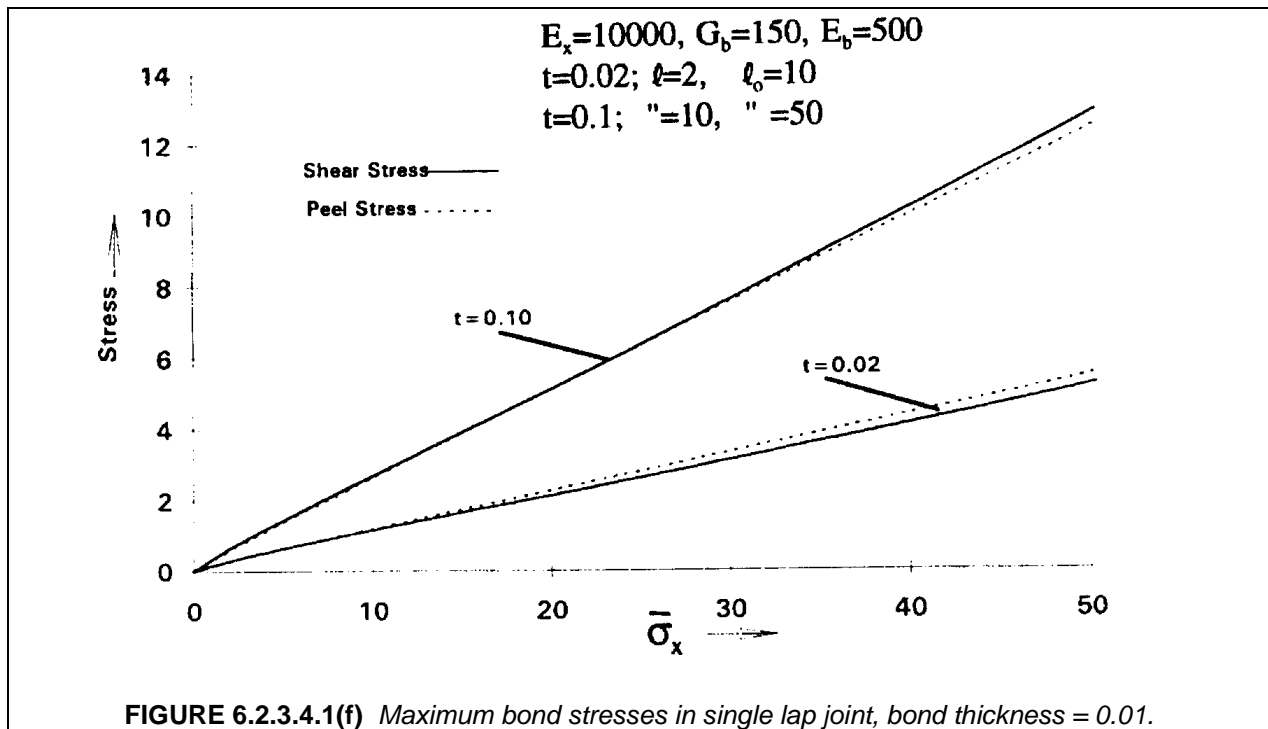


Figure 6.2.3.4.1(g) gives a comparison of maximum bond stresses in single and double lap joints for a fixed value of the loading stress $\bar{\sigma}_x$. For loading stresses above this value the bond stresses vary essentially in proportion to the load even in the single lap joint, as just discussed. The stresses are plotted in

this figure as a function of adherend thickness with the adherend axial modulus as a parameter. The trend discussed in Section 6.2.2 toward higher bond stresses and therefore a greater tendency toward bond failure with increasing adherend thickness is clearly born out in these curves. Note also that reduction of the adherend modulus tends to aggravate the bond stresses. In addition, it is apparent that there is considerable separation between the peel and shear stresses in the case of the double lap joint, the peel stresses for this case being smaller. This reflects the fact that the peel stresses vary linearly as γ_d defined in Equation 6.2.3.4.1(d) and therefore vary as $(t/t_b)^{1/4}$ rather than as $(t/t_b)^{1/2}$ as in the single lap case. Thus peel stresses for double lap joints are not as much of a factor in joint failure as they are in single lap joints, although they are still large enough relative to the shear stresses that they can not be ignored.

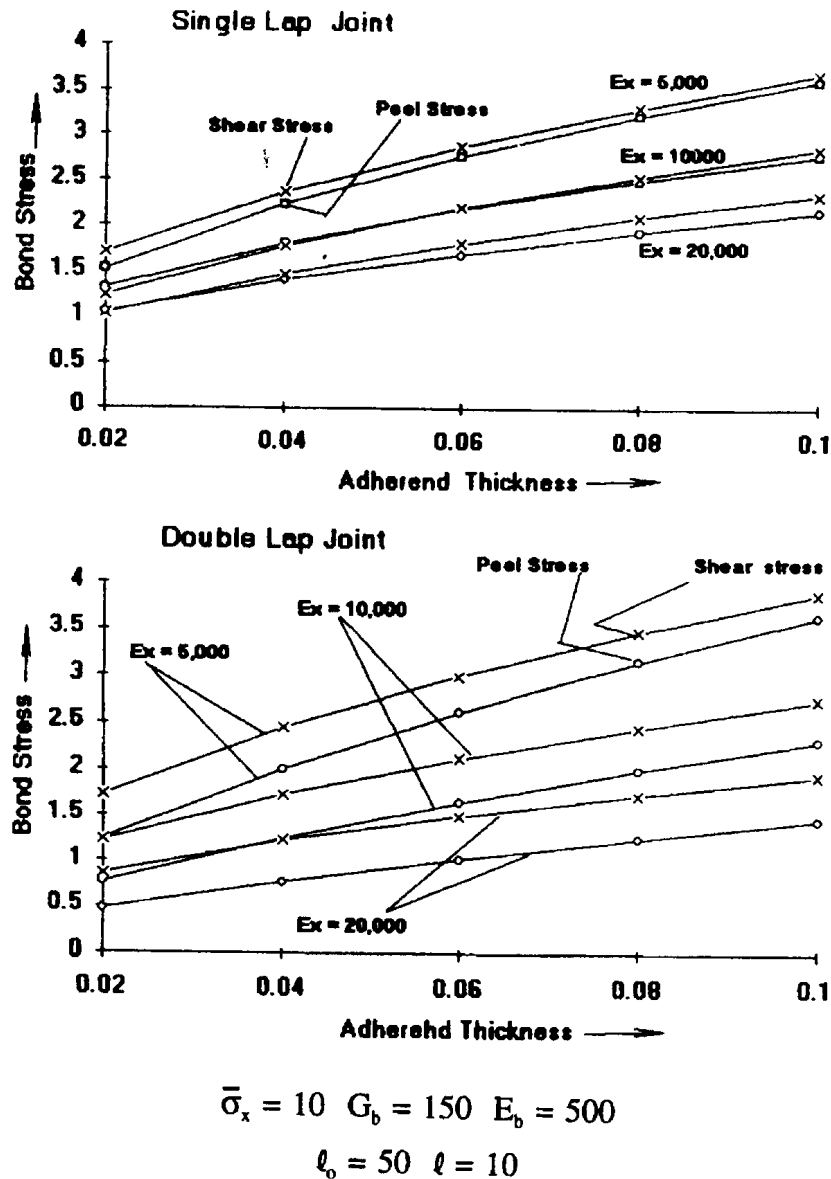
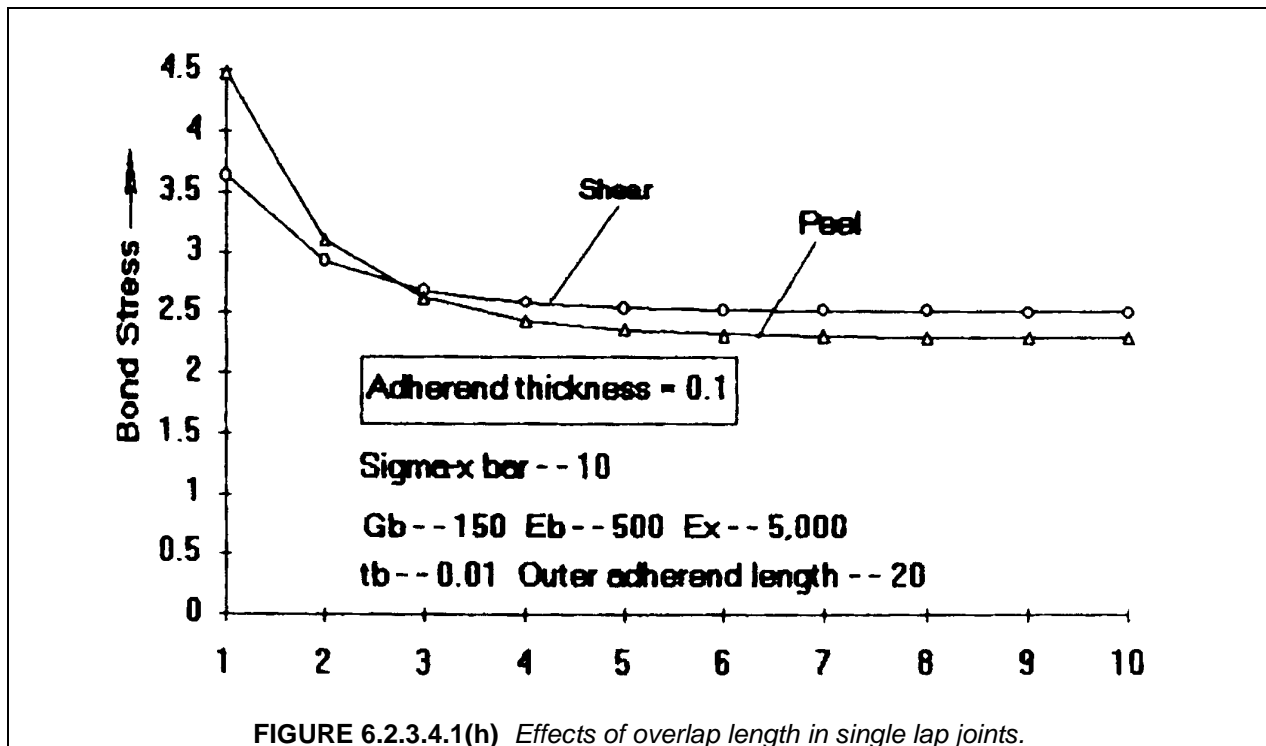


FIGURE 6.2.3.4.1(g) Maximum bond stresses in single and double lap joints, fixed $\bar{\sigma}_x = 10$.

Failure characteristics of single and double lap joints were discussed in Section 6.2.2.5. If the adherends are thin enough, failure in double lap joints should be in the form of adherend axial (tensile or compressive) failure. For single lap joints, adherend bending stresses are significant at the ends of the overlap because of the deflections indicated in Figure 6.2.3.4.1(d) part(D); using standard beam formulas, the maximum axial stress for combined bending and stretching (the latter stress corresponding to the single lap joint in tension loading) for the bending deflection given in Equation 6.2.3.4.1(l) can be expressed as

$$\sigma_x|_{\max} = \bar{\sigma}_x (1 + 3(1 + t_b / t)k) \quad 6.2.3.4.1(t)$$

The maximum adherend axial stress is largest for adherends which are particularly thin with respect to the bond thickness; these will be prone to brittle bending failures for composite adherends or to yielding associated with bending for metal adherends. Hart-Smith discusses difficulties with the use of standard single lap shear test specimens in Reference 6.2.1(v). The problem is that adherend bending failures rather than bond failures are likely to occur with such specimens and the test results obtained in these cases tend to be irrelevant and misleading. One additional characteristic difference between single and double lap joints should be discussed. The effect of lateral deflections on single lap joint performance are felt for a long distance along the joint compared with those of the shear and peel stresses. Figure 6.2.3.4.1(h) shows that for a joint with an adherend thickness of 0.1 inch (2.54 mm) and a loading stress of 10 ksi (70 MPa), the bond stresses do not reduce to their minimum values until the overlap length reaches about 40-50 adherend thicknesses, i.e., 4-5 inch (100-120 mm). Double lap joints also require some minimum length before stresses settle out as a function of overlap length, but in this case the stresses reach minimum values in much shorter lengths, on the order of 5 to 10 adherend thicknesses, in the present case amounting to 0.5 to 1 inch (13 to 25 mm).



6.2.3.4.2 Thermal stress effects

Thermal stresses are a concern in joints with adherends having dissimilar thermal expansion coefficients. Thermal stresses in bond layers of double lap joints can be determined from the expressions given in Equations 6.2.3.4.1(a)-(e). (These calculations are all based and assumed elastic response of the adhesive. References 6.2.1(i)-(l) provides corrections for ductile response in the presence of thermal effects. Thermal effects for one specific combination of composite and metal adherends are considered in Figure 6.2.3.4.2(a) while peak peel and shear stresses for various combinations of metal and composite adherends (see Tables 6.2.3.4.2(a) and (b) for mechanical properties) are shown in Table 6.2.3.4.2(c).

Figure 6.2.3.4.2(a) illustrates the effect of thermal stresses in an aluminum - 0/90° carbon/epoxy joint. The stresses due to thermal mismatch between the aluminum and composite arise if the cure temperature of the bond is substantially different from the temperature at which the joint is used. The case considered here represents a 250°F (121°C) cure temperature for the adhesive and a room temperature application, a temperature difference of -175°F (-79°C), which (see Tables 6.2.3.4.2(a) and (b)) would result in a strain difference of 0.002 between the aluminum and composite if no bond were present. (The material combination considered here, aluminum and carbon/epoxy, represents the greatest extreme in terms of thermal mismatch between materials normally encountered in joints in composite structures.)

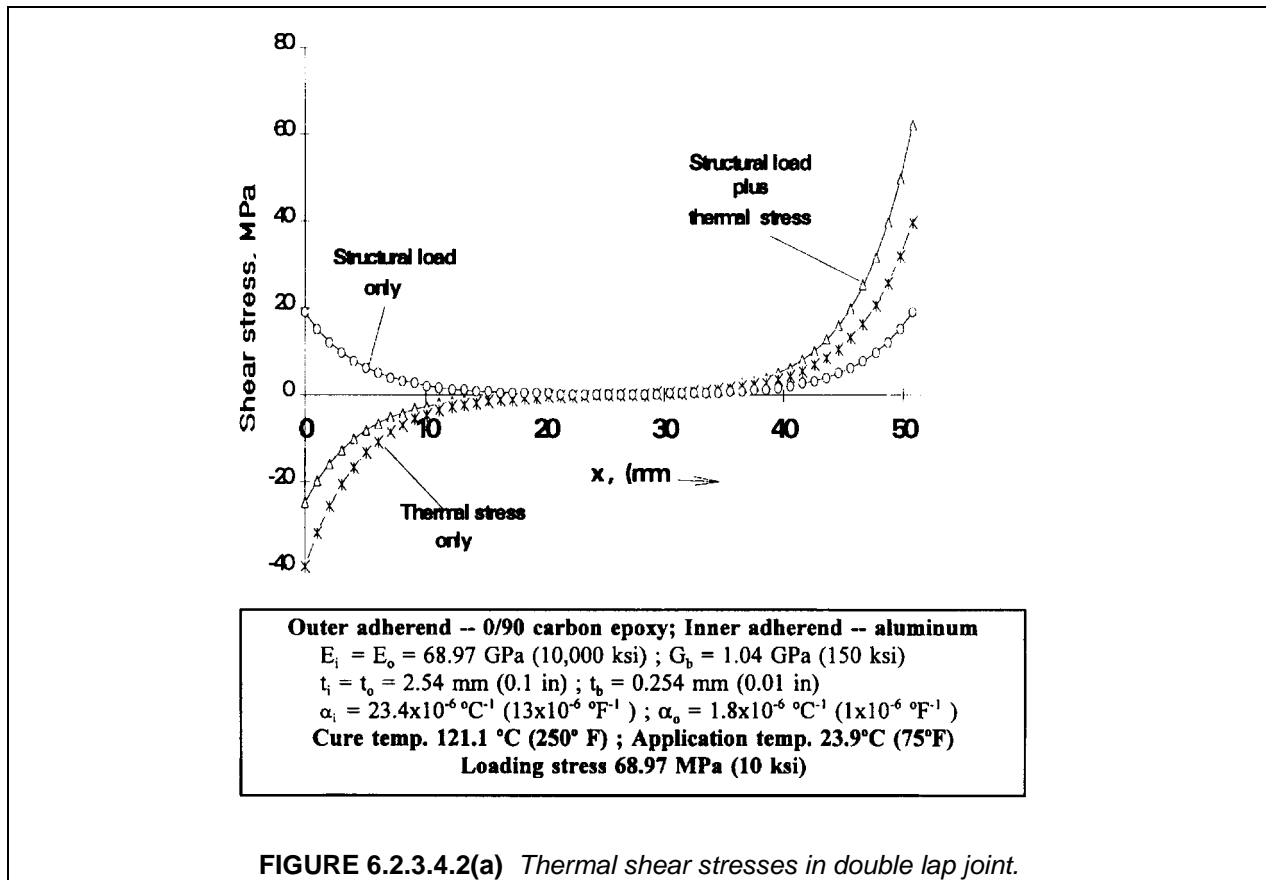


TABLE 6.2.3.4.2(a) *Generic mechanical properties of composites (Reference 6.2.3.4.2(a)).*

Composite	Unidirectional Lamina					0/90 Laminate	
	E_L , Msi (GPa)	E_T , Msi (GPa)	ν_{LT}	α_L 10-6/F° (10 ⁻⁶ /C°)	α_T 10-6/F° (10 ⁻⁶ /C°)	E_x Msi (GPa)	α_x 10-6/F° (10 ⁻⁶ /C°)
Boron/ epoxy	29.1 (201)	2.91 (20.1)	0.17	6.50 (11.7)	16.9 (30.4)	16.5 (114)	4.8 (8.6)
S-glass/ epoxy	8.80 (60.7)	3.60 (24.8)	0.23	2.10 (3.78)	4.28 (16.7)	6.34 (43.7)	4.40 (7.92)
Carbon/ epoxy	20.0 (138)	1.00 (6.90)	0.25	0.40 (0.72)	16.4 (29.5)	10.5 (72.6)	1.30 (2.34)

TABLE 6.2.3.4.2(b) *Generic metal properties (Reference 6.2.3.4.2(b)).*

	Ti-6-Al-4-V	1025 Steel	2014 Aluminum
Young's Modulus, Msi (GPa)	16.0 (110.3)	30.0 (206.9)	10.0 (69.0)
Poisson Ratio	0.3	0.3	0.3
α , 10-6/F° (10 ⁻⁶ /C°)	4.90 (8.82)	5.70 (10.3)	13.0 (23.4)

TABLE 6.2.3.4.2(c) *Bond layer thermal stress in double lap joints (0/90 composite outer adherend, metal inner adherend)*

	Boron/epoxy	Glass/epoxy	Carbon/epoxy
TITANIUM			
shear stress – ksi	0.061	0.338	2.27
MPa	0.419	2.33	15.64
peel stress – ksi	-0.067	-0.541	-2.817
MPa	-0.465	-3.73	-19.43
STEEL			
shear stress – ksi	0.789	1.16	3.80
MPa	5.44	7.99	26.22
peel stress – ksi	-0.914	-2.17	-5.52
MPa	-6.30	-15.0	-38.1
peel stress – ksi	-3.54	-5.82	-6.47
MPa	-24.4	-40.1	-44.6
ALUMINUM			
shear stress – ksi	4.02	4.08	5.86
MPa	27.7	28.2	40.47
t_i -- 0.2 inch (5.08 mm); t_o adjusted for equal adherend stiffnesses; t_b = .01 inch (0.253 mm) Adhesive properties: shear modulus -- 150 ksi (1.03 GPa) peel modulus -- 500 ksi (3.49 GPa) Cure temperature 250°F (121°C); Application temperature 75°F (24°C)			

Figure 6.2.3.4.2(a) demonstrates how the thermal stresses combine with the stresses due to structural load to determine the actual stress distribution in the adhesive. The thermal stresses in themselves develop an appreciable fraction of the ultimate stress in the adhesive, and although they oppose the stresses due to structural loading at the left end of the joint, they add at the right end and give a total shear stress that is somewhat beyond the yield stress of typical adhesives, even with as small a structural loading stress as 10 ksi (69 MPa). Similar effects occur with the peel stresses, although the peel stresses due to thermal mismatch alone have the same sign at both ends of the joint; with a composite outer adherend, the thermally induced peel stresses are negative, which is beneficial to joint performance. For joints with an aluminum inner adherend, the difference in thermal expansion between the adherends is relatively large, giving considerably higher thermal stresses for the most part. In addition, carbon/epoxy has a particularly low thermal expansion, so that carbon/epoxy adherends in combination with metals tend to produce higher thermal stresses with than other material combinations do. Note, for example, that boron/epoxy in combination with titanium gives particularly small thermal stresses because of similarity of the thermal expansion coefficients shown in Tables 6.2.3.4.2(a) and 6.2.3.4.2(b) for these materials. As discussed earlier, the "peel" stresses shown in Table 6.2.3.4.2(c) are all negative (i.e. compressive) because of the location of the composite on the outside of the joint, although the shear stresses are unaffected by this aspect of the joint. Composite repair patches on aluminum aircraft structure benefit from this type of behavior, in that peel stresses are not a problem for temperatures below the cure temperature. Placing the metal rather than the composite on the outside of a double lap joint would reverse the signs of the peel stresses, making them tensile and aggravating the effects of differential thermal expansion of the adherends.

6.2.3.4.3 Effect of ductility on joint stresses

Ductility of typical structural adhesives was discussed in Section 6.2.2.4 and illustrated in Figures 6.2.2.4(a) and 6.2.2.4(b) taken from Reference 6.2.2.4(a). Similar curves can be found in other sources such as Reference 6.2.2.4(b). Temperature and strain rate dependence of the stress-strain characteristics are important considerations; these are also addressed in Reference 6.2.2.7(a). Even for the less ductile materials such as FM400 (Figure 6.2.2.4(a) part(B)), ductility has a pronounced influence on mechanical response of bonded joints, and restricting the design to elastic response deprives the application of a significant amount of additional structural capability. In general, the maximum elastic strain of the adhesive provides to the limit load capability of the joint, while the maximum strain in the ductile part of the stress-strain curve provides the margin of ultimate load over limit load.

The work of Hart-Smith (Reference 6.2.1(i)-(q)) emphasized the importance of ductile adhesive response and introduced the relationship between the strain energy to failure of the adhesive and the load capacity of the joint. As a means of simplifying the stress analysis of the joint in the presence of ductile adhesive response, Hart-Smith showed that any bilinear stress-strain curve which has the same ultimate shear strain and maximum strain energy as that of the actual stress-strain curve will produce the same total load in the joint. Figure 6.2.3.4.3(a) (Reference 6.2.2.4(a)) gives an example of the method for fitting a bilinear curve to the actual stress-strain curve of the adhesive in shear. With the strain energy of the adhesive given by

$$SE = \tau_p \gamma_{\max} - \tau_p^2 / 2G_{b0} \quad 6.2.3.4.3(a)$$

where G_{b0} , γ_{\max} and SE are the initial modulus of the stress-strain curve, the maximum strain and the strain energy of the adhesive at γ_{\max} , respectively, then the equivalent bilinear curve consists of an initial straight line of slope G_{b0} together with a horizontal part at an abscissa which can be obtained by solving for τ_p from Equation (6.2.3.4.3a), using the expression

$$\tau_p = G_{b0} \gamma_{\max} - \sqrt{(G_{b0} \gamma_{\max})^2 - 2G_{b0} SE} \quad 6.2.3.4.3(b)$$

Hart-Smith has also used an equivalent bilinear representation in which the horizontal part of the curve is set equal to τ_{\max} , the maximum shear stress of the actual stress strain curve, and the initial modulus G_{b0} adjusted to give the strain energy match, using the expression

$$G_{bo} = \tau_{\max}^2 / 2(\tau_{\max} \gamma_{\max} - SE)$$

6.2.3.4.3(c)

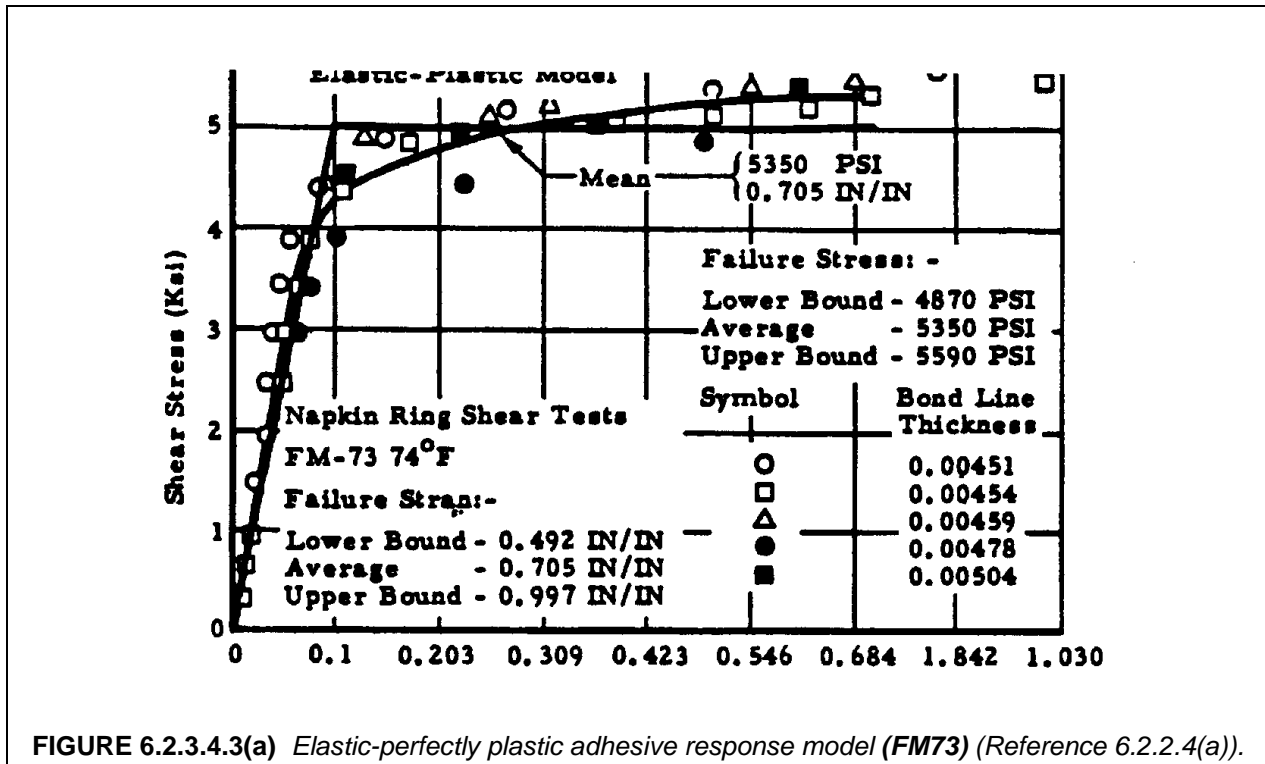
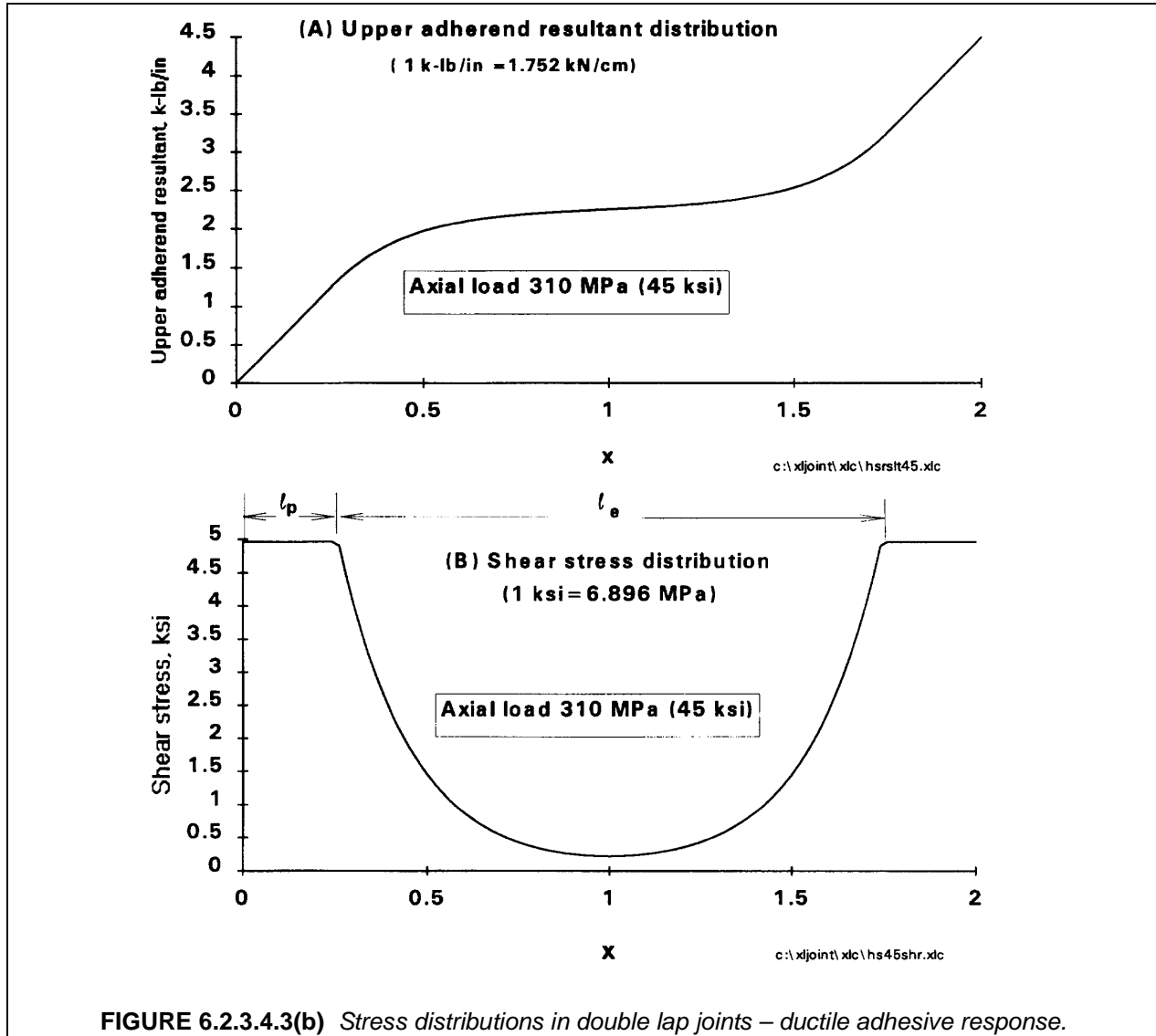


FIGURE 6.2.3.4.3(a) Elastic-perfectly plastic adhesive response model (FM73) (Reference 6.2.2.4(a)).

which is also obtained from Equation (6.2.3.4.3a) when τ_{\max} is substituted for τ_p . In either case the use of a bilinear representation of the stress-strain curve for the response of the adhesive in shear makes it straightforward to obtain one dimensional stress distributions in various types of joint geometry with adhesive ductility accounted for; References 6.2.1(i)-(l) gave solutions for single and double lap joints with uniform and tapered adherends, as well as more sophisticated joint designs such as scarf and step lap geometries. These have been subsequently incorporated in the "A4Ex" series of computer programs (Reference 6.2.1(s)) mentioned previously in Section 6.2.2.4. Figure 6.2.3.4.3(b) shows the application of the bilinear stress-strain curve approximation to a symmetric double lap joint with equal adherend stiffnesses. Part (A) of Figure 6.2.3.4.3(b) gives the distribution of upper adherend axial stress resultant while part (B) gives the shear stress distribution in the bond layer. The linear portion at the ends of the resultant distribution in part (A) corresponds to the ends of the shear stress distribution in part (B) where the shear stress is a constant because of the plateau in the bilinear representation of the stress-strain curve. Following the analysis developed by Hart-Smith, the lengths of the plastic zones designated in Figure 6.2.3.4.3(b) part (B) as ℓ_p are given by

$$\ell_p = (\bar{\sigma}_x / 2 \tau_p - 1 / \beta_{bd}) t_o ; \quad \beta_{bd} = [2 G_{bo} t_o / E_o t_b]^{1/2} \quad 6.2.3.4.3(d)$$



Here β_{bd} (subscript "bd" denoting balanced double lap) is equivalent to β given in Equation (6.2.3.4.1a) when the latter is specialized for the case of equal-stiffness adherends, while $\bar{\sigma}_x$ is the nominal loading stress at either end of the overlap. The expression for l_p given in Equation (6.2.3.4.3d) is valid only if greater than 0, of course, negative values of plastic zone length not having any meaning. As a result, if $\beta_{bd} \bar{\sigma}_x / 2 < \tau_p$, no plastic zone is present and the behavior of the joint can be considered to be purely elastic. The maximum value of $\bar{\sigma}_x$ for this case can be expressed by inverting the shear stress expression in Equation 6.2.3.4.1(f), for the case of equal adherend stiffnesses, and setting $\tau_{b|_{\max}}$ to τ_p . For the case of $\beta_{bd} \bar{\sigma}_x / 2 \geq \tau_p$ which corresponds to ductile response of the adhesive, the Hart-Smith analysis given in Reference 6.2.1(i) provides the required expression for $\bar{\sigma}_x$. The two cases are summarized as follows:

$\beta_{bd} \bar{\sigma}_x / 2 < \tau_p$ (elastic response):

$$\bar{\sigma}_{x|_{\max}} = 2\tau_p / \beta_{bd} = \sigma_e \quad 6.2.3.4.3(e)$$

$\beta_{bd} \bar{\sigma}_x / 2 \geq \tau_p$ (ductile response):

$$\bar{\sigma}_x|_{\max} = \frac{2}{\beta_{bd}} \tau_p \sqrt{2 \frac{G_{b0} \gamma_{\max}}{\tau_p} - 1} \equiv \sigma_e \sqrt{2 \frac{G_{b0} \gamma_{\max}}{\tau_p} - 1} \quad 6.2.3.4.3(f)$$

Note that if $\gamma_{\max} = \tau_p / G_{b0}$ which is the maximum strain in the elastic part of the bilinear representation, then Equations 6.2.3.4.3(e) and 6.2.3.4.3(f) give the same value. The factor $(2G_{b0}\gamma_{\max} / \tau_p - 1)^{1/2}$ in Equation 6.2.3.4.3(f) acts as a load enhancement factor and represents the increase of joint load capacity due to ductile adhesive response over the maximum load allowed by elastic response of the adhesive. Note that Equation 6.2.3.4.3(f) can be rearranged to express $\bar{\sigma}_x|_{\max}$ in terms of the maximum strain energy of the adhesive:

$$SE = \tau_p^2 / G_{b0} + \tau_p (\gamma_{\max} - \gamma_e) \quad \text{where} \quad \gamma_e = \tau_p / G_{b0} \quad 6.2.3.4.3(g)$$

Equation 6.2.3.4.3(f) can then be written

$$\bar{\sigma}_x|_{\max} = \frac{2}{\beta} \sqrt{2G_{b0}SE} \quad 6.2.3.4.3(h)$$

The Hart-Smith analysis based on the equivalent bilinear stress-strain law was shown in Reference 6.2.1(j) to give the same joint load capacity as the solution for the problem using the actual stress-strain curve of the adhesive. The convenience of the bilinear stress-strain description is in the simplicity of the solutions it allows; once the length of the plastic zone at each end is determined, the same types of solution apply for the elastic zone as were given in Equation 6.2.3.4.1(f) for the shear stress distributions, together with linear resultant and constant shear stress distributions in the plastic zones.

The most obvious effect of ductility in the adhesive behavior is the reduction of peak shear stresses. In addition, there is a beneficial effect on reduction of peel stresses. For the double lap joint considered in Figure 6.2.3.4.3(b), the maximum peel stresses denoted by $\bar{\sigma}_x|_{\max}$, which occur at the ends of the joint, are given (Reference 6.2.1(l)) by

$$\sigma_b|_{\max} = \gamma \tau_b|_{\max} : \gamma = \left(3 \frac{E_b t_o}{E_o t_b} \right)^{1/4} ; E_b = \text{peel modulus of adhesive} \quad 6.2.3.4.3(i)$$

where $\bar{\tau}_b|_{\max}$ is the maximum shear stress, either $\beta \bar{\sigma}_x / 2$ for the elastic case or τ_p for the case of ductile response. The maximum peel stresses are thus reduced by the same ratio as the maximum shear stresses in the case of ductile response of the adhesive.

As stated earlier, the ductile response of the adhesive provides additional structural capability of the joint over its limit load capacity. Under normal operation, it is advisable to keep the applied load in the joint low enough to insure purely elastic response for most practical situations where time-varying loading is encountered. Some damage to the adhesive probably occurs in the ductile regime which would degrade the long term response. The main benefit of ductile behavior is to provide increased capacity for peak loads and damage tolerance with regard to flaws -- voids, porosity and the like -- in the adhesive layer.

6.2.3.4.4 Transverse shear and stacking sequence effects in composite adherends

Classical analyses such as the Volkersen shear lag model for shear stresses in the bond layer (Sections 6.2.3.2 and 6.2.3.4.1) are based on the assumption that the only significant deformations in the adherends are axial, and that they are uniformly distributed through the adherend thicknesses. This is a good assumption for metal adherends which are relatively stiff with respect to transverse shear deformation, but for polymer matrix composite adherends which have low transverse shear moduli, transverse shear deformations are more significant and can have an important influence on bond layer shear

stresses. Finite element analysis will take such effects into account in a routine manner, but for the closed form type of solutions on which most of the results of this chapter are based, allowance for transverse shear and thickness normal deformations is absent. A useful correction to the classical Volkersen solution which allows for transverse shear deformations in the adherends can be obtained by initially assuming that the axial stresses are constant through the adherend thickness and that as a result, (because of equilibrium with the axial stresses), the transverse shear stresses and strains are distributed linearly. (For a non-unidirectional laminate the shear stresses and strains will be **piecewise** linear, corresponding to the jumps in axial moduli of the laminate plies.) Integrating the shear strain distribution through the thickness then leads to a quadratic correction term to the distribution of axial displacements and stresses, which can be absorbed as a simple modification (Reference 6.2.3.4.4) of the Volkersen shear lag analysis. Modifying the shear modulus of the adhesive from its actual value, G_b , to an effective value, $G_{b|eff}$, given by

$$G_{b|eff} = G_b / K_{sh} \quad \text{where} \quad K_{sh} = 1 + \frac{1}{3} \left(\frac{G_b}{G_{xzo}} \frac{t_o}{t_b} + \frac{G_b}{G_{xzi}} \frac{t_i}{2t_b} \right) \quad 6.2.3.4.4(a)$$

then the resulting $G_{b|eff}$ can be substituted for G_b to obtain the parameter β in Equation 6.2.3.4.1(a) and the resulting β can be used to obtain the shear stress distribution using Equation 6.2.3.4.1(f). Note that G_{xzo} and G_{xzi} in Equation 6.2.3.4.4(a) are the transverse shear moduli of the adherends. A similar modification is also given in Reference 6.2.3.4.4 for the single lap joint analysis. The correction given here amounts to treating 1/3 the thickness of each adherend as an extension of the bond layer, and assigning the shear stiffness of the adherend for that part of the effective bond layer. The factor 1/3 corresponds to a linear distribution of shear stress through the adherend thicknesses, which as noted above, is consistent with the assumption that the axial deformations are approximately uniform through the adherend thickness.

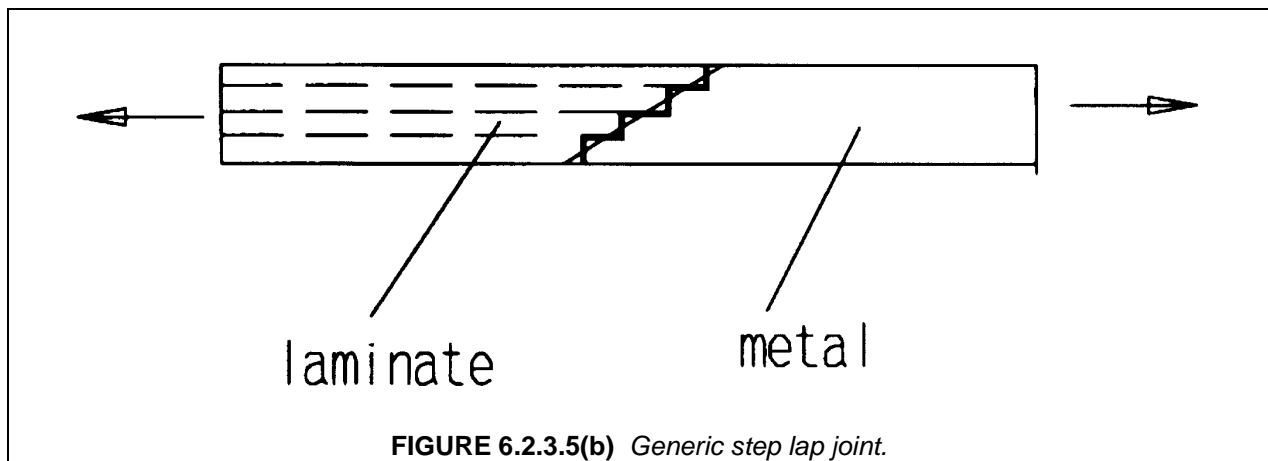
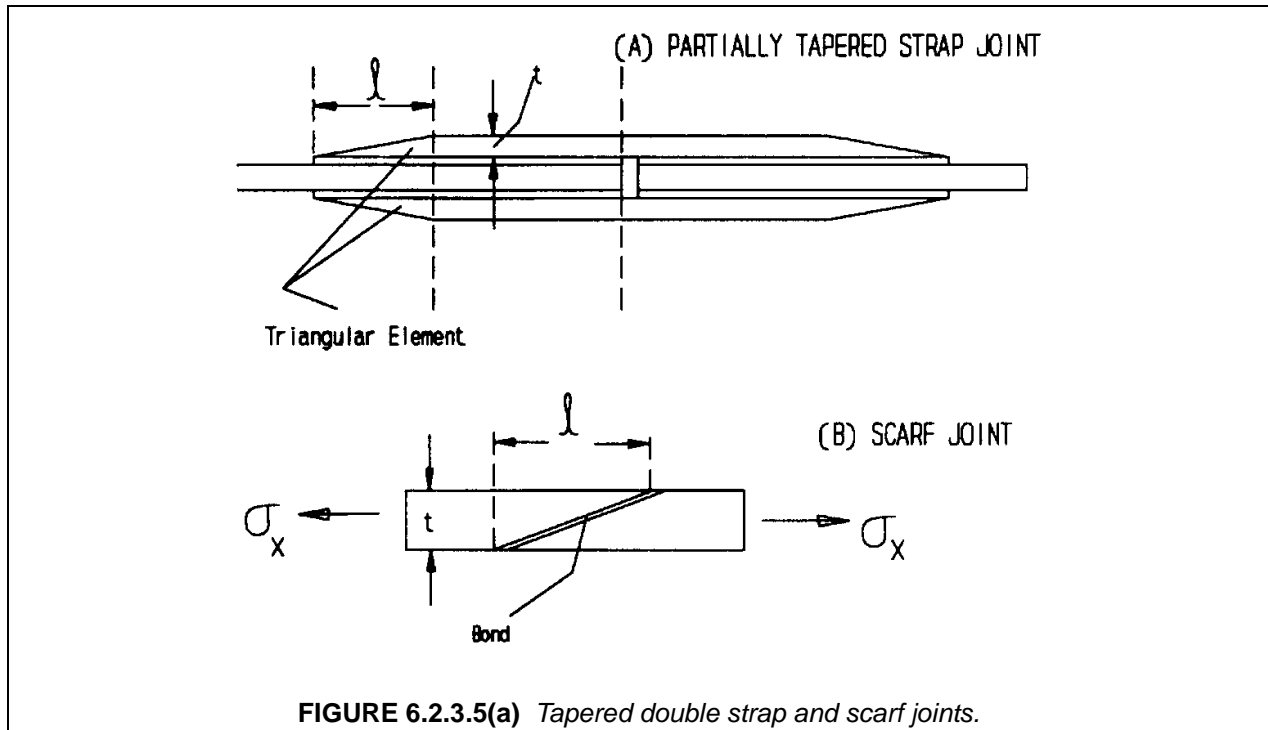
As an example, consider a double lap joint with unidirectional carbon/epoxy inner and outer adherends, with adherend thicknesses of 0.1 in (2.53 mm) and 0.2 in (5.06 mm), respectively, and a 0.01 in (0.253 mm) bond thickness. Assume a shear modulus of the bond layer of 150 ksi (1.06 GPa) and transverse shear moduli of 700 ksi (4.82 GPa) for the adherends. A value of 2.48 is then obtained for K_{sh} in Equation 6.2.3.4.4(a), and the value of β and the maximum shear and peel stresses which depend on it are reduced by a factor of $(K_{sh})^{1/2}$ or 1.56 for this case. The shear and peel stresses are therefore approximately 36% lower than the values predicted in Equations 6.2.3.4.1(f) and 6.2.3.4.1(h) with the unmodified bond shear modulus. This type of correction appears to give relatively good predictions of the adhesive stresses in comparison with finite element analyses. An example will be presented in Section 6.2.3.6 (see Figure 6.2.3.6 (b)). The distribution of shear stress in the bond is shown there to be predicted with impressive accuracy by the Volkersen shear lag analysis with the modification of the effective bond shear modulus just discussed.

The modification presented above applies only to unidirectional reinforcement of the adherends. However, the same type of approach can be applied to adherends with general stacking sequences, although in this case, while the axial **strain** distribution is again initially assumed to be uniform through the thickness, the axial **stress** distribution will be piecewise uniform, varying from layer to layer with the axial moduli of the adherend plies. The resulting transverse shear stress- and therefore the shear-strain distribution will be piece-wise linear rather than continuously linear, and can be integrated through the thickness to get a correction to the conventional shear lag analysis which is similar to that described above, with a suitable modification of the formula for K_{sh} given in Equation 6.2.3.4.4(a). Similar modifications of the Hart-Smith analysis for ductile adhesive response are possible.

The approach presented here is a simplified version of a more elaborate method for correcting the classical closed form solutions developed in the early 1970's (References 6.2.1(d), (f) and (g)). The latter approach allowed for both bending and stretching deformations in the adherends. The present correction appears to be adequate for most practical purposes, however.

6.2.3.5 Tapered and multi-step adherends

In this section we will consider joints with adherend thicknesses that vary along the joint length. These include double strap joints with tapered outer adherends shown in Figure 6.2.3.5(a) part (A), scarf joints, Figure 6.2.3.4(a) part(B), and step lap joints, Figure 6.2.3.5(b) .



As discussed in Section 6.2.2.2, tapering the outer adherends of strap joints as in Figure 6.2.3.5(a) part (A) is beneficial mainly for reducing peel stresses, while scarf and step lap joints (Figures 6.2.3.5(a) part(B) and 6.2.3.5(b)) can reduce both shear- and peel-stress peaks. With both tapered-adherend lap joints and scarf joints it can be shown from equilibrium considerations that the bond stresses can be related to the ratio of thickness t to taper length l by

$$\tau_b \approx \sigma_x t / l ; \quad \sigma_b \approx \sigma_x t^2 / l^2 \quad 6.2.3.5(a)$$

For a scarf joint, standard stress transformation relationships give this approximation, for small scarf angles, for the relation between axial stress in the adherend and resolved stresses in the inclined plane corresponding to the bond line. For the strap joint of Figure 6.2.3.5(a) part (A) it corresponds to the relation between the stresses in the triangular element at the left end of the joint for a traction free condition at the inclined upper surface of the element. Equation 6.2.3.5(a) is quite accurate for scarf joints having the same maximum stiffness (axial modulus times maximum thickness) in each adherend, although for unequal stiffnesses the stresses will vary along the joint and exhibit peaks at the ends of the joint (although not as severe as those for untapered joints) which causes a deviation from Equation 6.2.3.4.1(a). For tapered strap joints the equation holds approximately along the tapered part of the joint if the length of the taper is short enough to avoid stretching effects that cause the shear strain in the bond to vary, as discussed in Section 6.2.3.4.1 for the case of uniform adherend thickness. Note that Equation 6.2.3.5(a) implies that the bond stresses are constant along the length of the joint and can be reduced to any arbitrary level by making t/ℓ small enough, i.e., making the joint long enough with respect to the maximum adherend thickness. Note also that the effect of t/ℓ on the peel stresses is especially strong, being governed by the *square* of the thickness-to-length ratio. This is particularly important when outer adherend tapering is used as a means of reducing peel stresses in strap and lap joints.

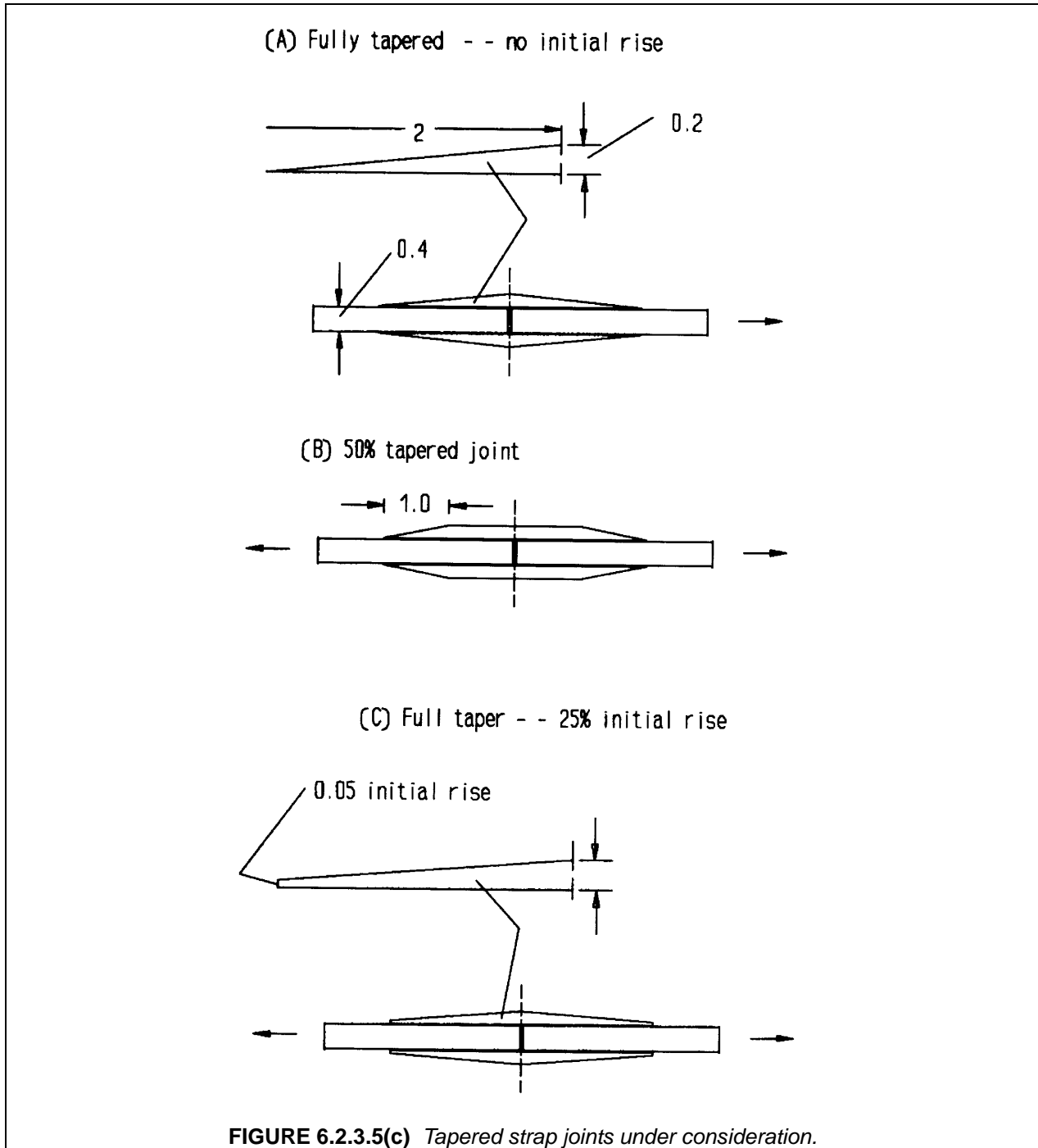
Aside from the finite element approach, various stress analysis methods are available for joints with tapered adherends. Hart-Smith, in Reference 6.2.1(k), presented power series solutions for stresses for such joints. In addition, Reference 6.2.3.5(a) discusses a finite difference approach leading to a PC-based computer code, `TJOINTNL`, that allows for ductile response of the bond layer along with tapered adherends. This code forms the basis for the results presented below on scarf joints and lap and strap joints with tapered outer adherends.

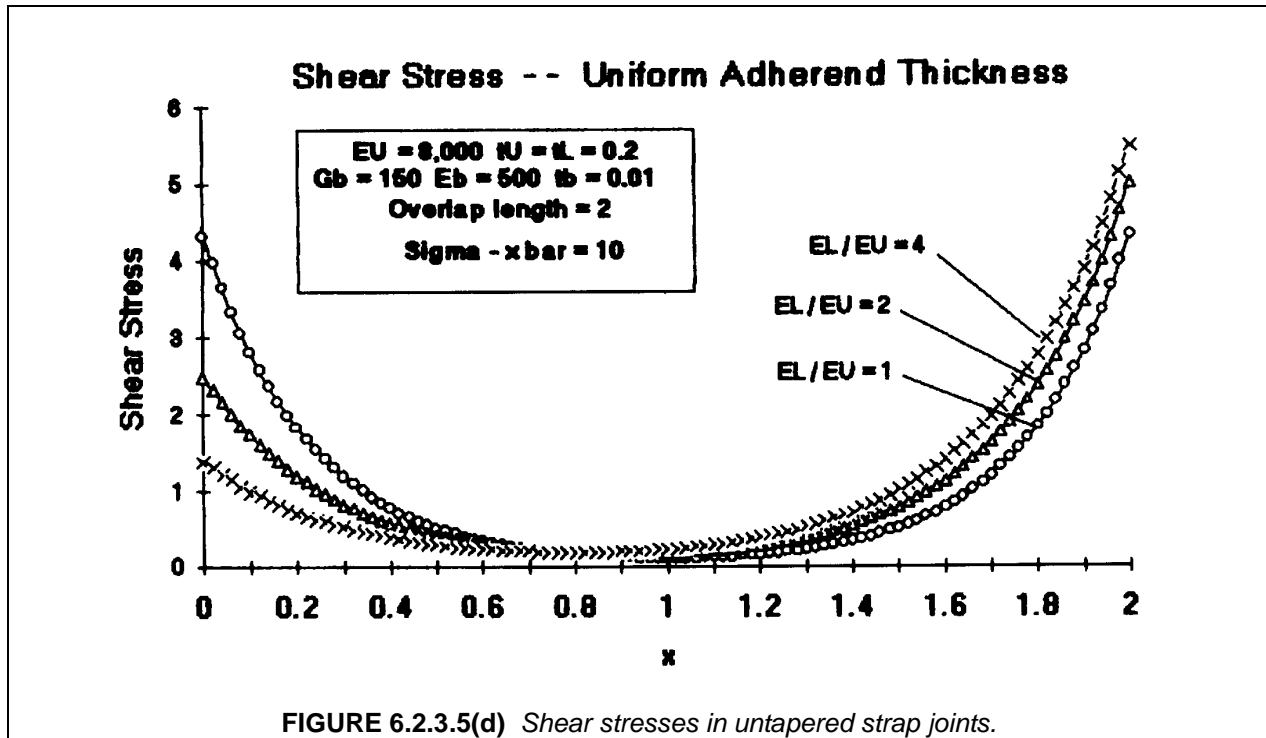
The following discussion will address the specific benefits of adherend tapering in adhesive joints. The objective is to achieve high joint efficiency by reducing effects of shear and peel stress concentrations at the ends of the joint. Ideally, we would like to achieve the joint strength provided by the "P over A" concept obtained with the case discussed in Section 6.2.3.2 for perfectly rigid adherends (Figure 6.2.3.2(a)), in which increasing the joint length indefinitely brings the shear stress in the bond down to any required level regardless of the magnitude of load being supported by the joint. For scarf and step lap joints this objective is achievable, although in tapered double lap and strap joints it is not. While tapering does reduce the peel stresses markedly in these types of joint as will be seen below, shear stress peaks can not be avoided completely, and the law of diminishing returns illustrated previously for uniform thickness adherends by Figure 6.2.3.2(f) continues to prevail with regard to the ultimate lack of effectiveness of increasing the joint length to obtain greater load capacity, although adhesive ductility will still enhance the strength beyond what elastic analysis predicts.

Various features of strap joints with tapered outer adherends are illustrated in Figure 6.2.3.5(c). Figure 6.2.3.5(d) gives shear stress predictions for joints with uniform adherend thickness to provide a basis for comparison with the tapered cases.) The "initial rise" feature of Figure 6.2.3.5(c) part (C) has been included in the joints considered here since bringing the tapered end of the joint to a knife edge may weaken the adherend and cause premature failure.

Figure 6.2.3.5(e) shows the bond stresses in various double strap joints with tapered outer adherends. Pertinent dimensions for the joint configurations on which these results are based are shown in Figure 6.2.3.5(c). The notation used in Figure 6.2.3.5(e), i.e., fully tapered outer adherends, partially tapered adherends (with the taper expressed as a percentage of joint length), and adherends with an initial rise (expressed in Figure 6.2.3.5(e) as a percentage of maximum adherend thickness) is also given in Figure 6.2.3.5(c). For the situation of no initial rise, two cases are considered in Figure 6.2.3.5(e), the case of 50% taper and that of full taper. There is an appreciable difference in the shear stress distribution at the left end of the joint for these two cases, the peak values agreeing reasonably well with the approximate predictions of Equation (6.2.3.5a). In the case of the peel stresses, these are too small to be distinguished in the plots, but the peak values at the left end of the joint, while appreciably less than the predictions of Equation 6.2.3.5(a), are found to be related to each other approximately as the square of the taper ratio which is 0.2 for the fully tapered case and 0.1 for the 50% taper. (The actual values for the

peel stresses at the left end amount to 0.045 for the fully tapered case and 0.16 for the 50% taper) For both the full taper and 50% taper cases, a tensile secondary peel stress peak is present at the right end of the Figure 6.2.3.5(e) in the vicinity of the midpoint of the joint.





In the case of a 25% initial rise, much greater peel stresses, about 80% of the level occurring for the case of no tapering (the case of uniform adherend thickness considered in Section 6.2.3.4.1), arise at the left end of the joint than for the fully feathered cases. The initial rise also causes a greater increase in shear stress at the left end of the joint than the case of 50% taper with no initial rise does.

Thus, tapering is advantageous mainly as a way of eliminating the effects of peel stresses in double strap joints. Once this is accomplished, the effects of shear stress peaks can be controlled to a significant extent by taking advantage of adhesive ductility. Tapered strap joints can not achieve the ideal behavior which is possible with scarf joints, but they do provide a simpler solution to good joint performance if the adherends are sufficiently thin.

Shear stress distributions in scarf joints (Figure 6.2.3.5(f)) are given in Figure 6.2.3.5(g). Note that as in Figure 6.2.3.5(f), practical scarf joints can be arranged in a symmetric double lap configuration which avoids bending effects as well as providing a balanced stiffness design for dissimilar materials. In Figure 6.2.3.5(f) this is achieved by a continuous change of total (inner adherend + outer adherend) thickness over the length of the joint. The most important parameter for the scarf joint is the effect of adherend stiffness unbalance ($E_o \neq E_i$; "o" and "i" refer to the outer and inner adherends as in Figure 6.2.3.4.1(a)). The results given in Figure 6.2.3.5(g) which were obtained from the finite difference analysis discussed in Reference 6.2.3.5(a) represent the effect of varying degrees of stiffness unbalance and may be compared with the results for uniform thickness adherends given in Figure 6.2.3.5(d). The ratio of peak-to-average shear stresses in Figure 6.2.3.5(g) compare well with the values given by Hart-Smith in References 6.2.1(l) and 6.2.3.5(b), although the Hart-Smith analysis did not give the distribution of stresses along the length of the joint because of limitations of the power series solution approach which Hart-Smith used. Note that for fairly sizeable stiffness unbalances, up to 4:1, the maximum shear stress peak is not as great as that observed in Figure 6.2.3.5(d) for the uniform adherend case. However, it is clear that a stiffness unbalance *will* increase the maximum shear stress and weaken the joint in comparison with the performance in joints with balanced stiffnesses. It is emphasized that for the equal stiffness case the shear stress in the bond is constant and equal to the average stress at all points.

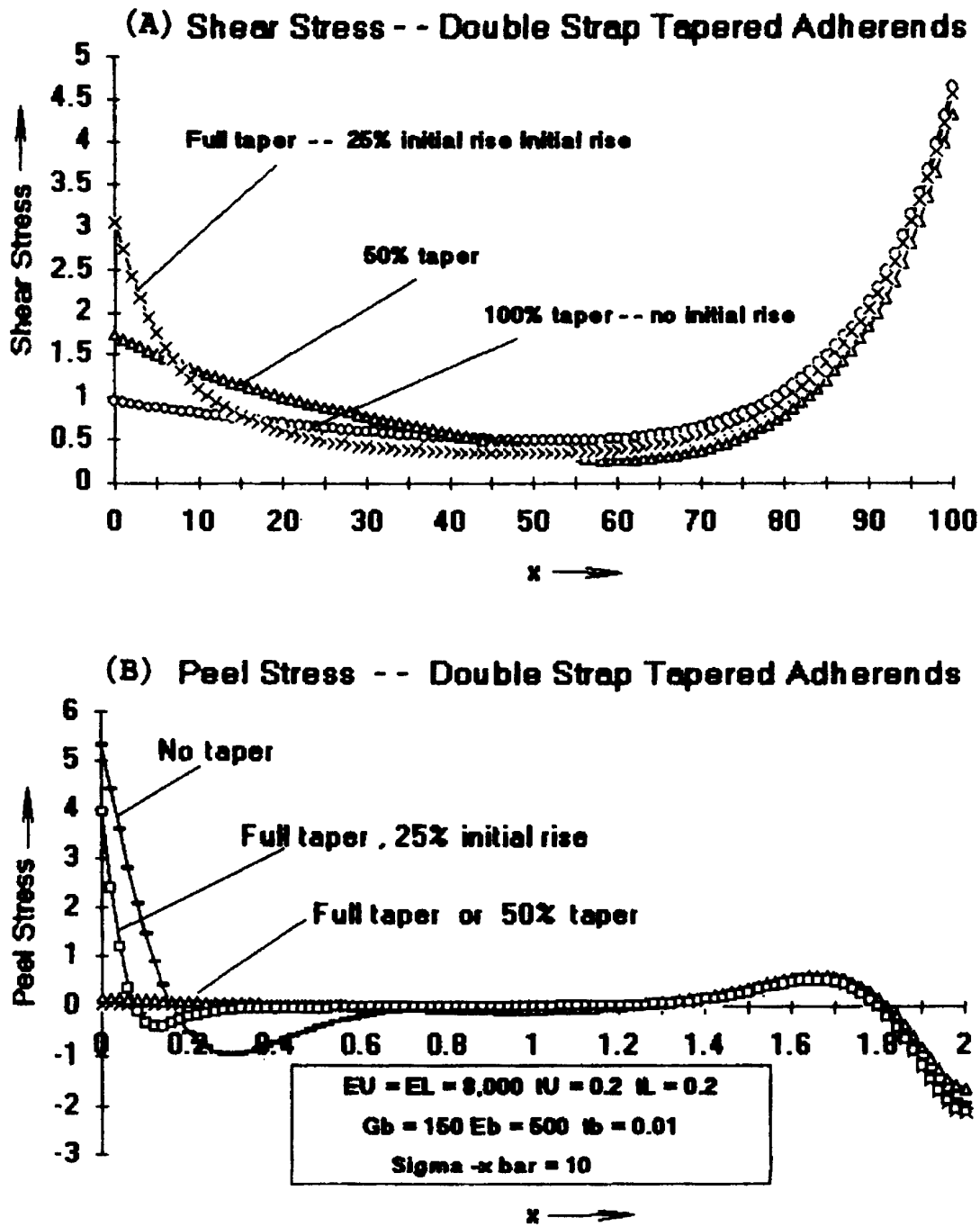
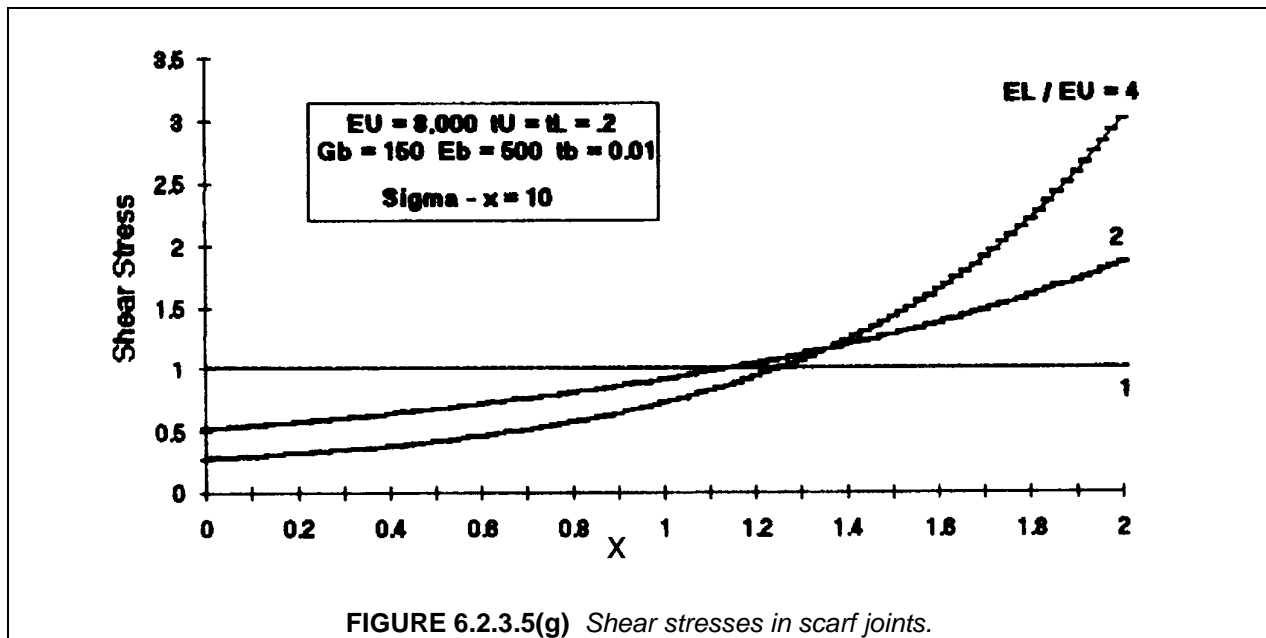
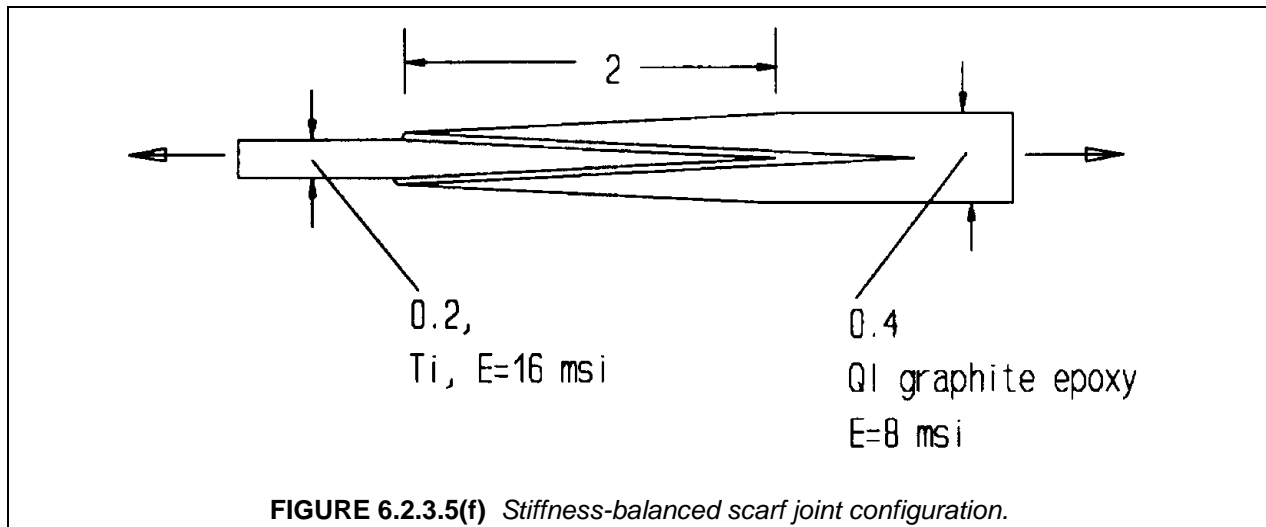


FIGURE 6.2.3.5(e) Stresses in tapered double strap joints.

It appears that most practical scarf joints can be configured for dissimilar materials as in Figure 6.2.3.5(f) to provide for balanced stiffnesses. In principle, the scarf joint then provides a near ideal solution to achieving as much load capacity as is required in any situation without overstressing the bond layer. However, the dimensions of the joint may grow too large to be practical for high joint load. In addition, an extremely good fit, for example, to tolerances on the order of the bond thickness over large lengths, has to be maintained to insure that the joint can provide uniform load transfer over its entire

length. Even with balanced stiffness configurations, thermal stresses which arise when the adherend materials are dissimilar will prevent the ideal form of behavior from being achieved.



Step lap joints (Figure 6.2.3.5(b)) represent an approximation to the scarf joint which can take advantage of the layered structure of the composite adherend. The average slope of the region represented by the line through the steps in Figure 6.2.3.5(b) tends to control the average shear stresses developed in the bond. Within each horizontal section, equivalent to the tread of a staircase, the behavior is analogous to a joint with constant adherend thickness, and the differential equation given earlier as Equation 6.2.3.4.1(b) applies locally when t_U and t_L are adjusted to match the situation in each step. An expression similar to Equation 6.2.3.4.1(f):

$$\tau_{bj}|_{\max} = \beta_j \bar{T} \left(\frac{1}{1 + \rho_{Bj} \sinh \beta_j \ell_j / \bar{t}} + \frac{\rho_{Bj}}{1 + \rho_{Bj} \tanh \beta_j \ell_j / \bar{t}} \right)$$

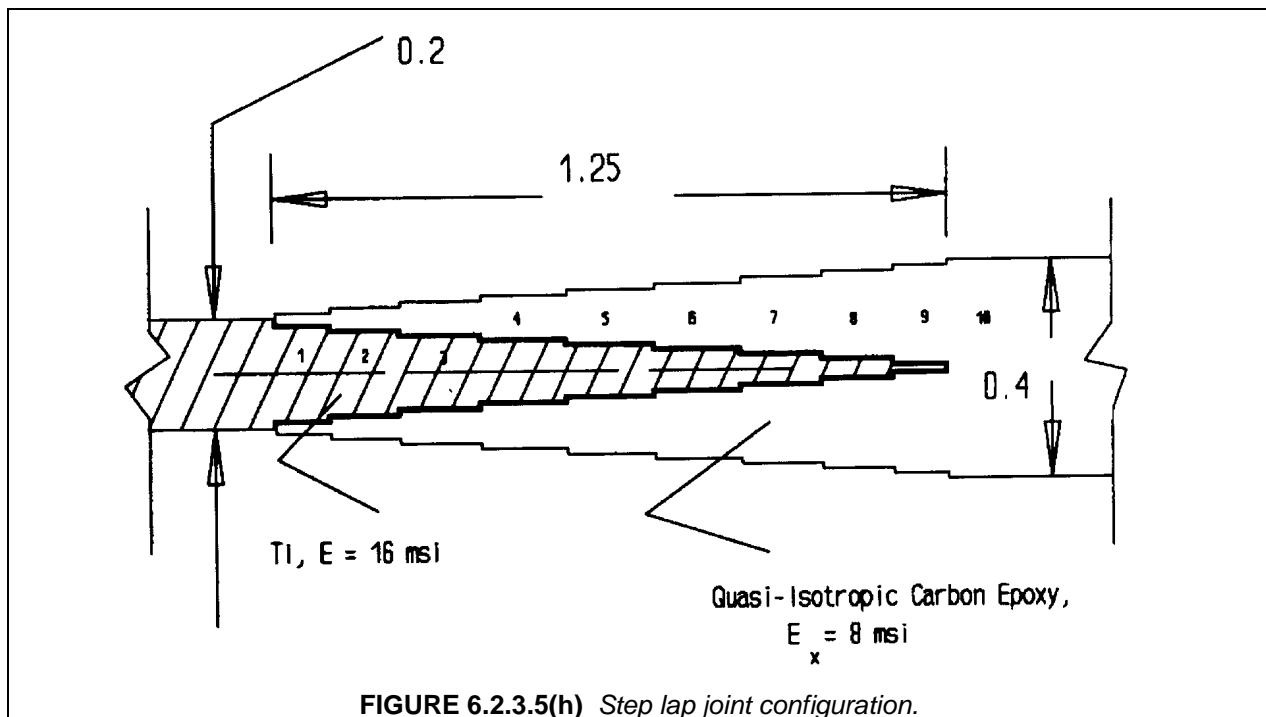
where

6.2.3.5(b)

$$\beta_j = \left[G_b \bar{t}^2 \left(\frac{1}{B_{Uj}} + \frac{1}{B_{Lj}} \right) \right]^{1/2} ; \quad \bar{t} = \frac{t_{Uj} + t_{Lj}}{2} ; \quad \rho_{Bj} = B_{Lj} / B_{Uj}$$

gives the maximum shear stresses for the j th step, and the overall solution is a chain of such expressions with allowance for continuity of the shear strain and resultants, T_{Uj} and T_{Lj} at the points where neighboring steps join. In each step of the joint the shear stresses will have a distribution similar to that of Figure 6.2.3.4.1(b) part(A), the size of the peaks being governed primarily by the length of the step through the parameter $\eta_{sl} = \beta_j \ell_j / \bar{t}$. The aspect ratio for the step, ℓ_j / \bar{t} , can in principle be kept small enough to almost completely avoid any peaking by using a large number of steps and keeping the length of each one small. In practice, the number of steps is governed by the number of plies in the laminate. In addition, if the joint is used to connect a composite adherend to a metal component, machining cost and tolerance requirements for the metal part enter into the selection of the number of steps.

Figure 6.2.3.5(h) shows a generic step lap joint configuration that illustrates some of the effects of design parameters on stresses in the joint. The results presented in Figures 6.2.3.5(i) and 6.2.3.5(j) were generated for this discussion using a linear elastic response model for the adhesive; in practice, considerable strength capability of the adhesive is unused if elastic response of the adhesive is assumed; Figure 6.2.3.5(k) taken from the discussion by Hart-Smith in Reference 6.2.3.5(b) is an example of joint design using elastic-plastic response for the adhesive. However, the elastic adhesive model used to generate Figure 6.2.3.5(i) and 6.2.3.5(j) is adequate for illustrating some of the parameters controlling the joint design. The results given in these figures are based on the classical Volkersen-type analysis which forms the basis of Equation 6.2.3.5(b).



The five-step design in Figure 6.2.3.5(i) and the ten-step design in Figure 6.2.3.5(j) were chosen with the following characteristics:

- Except for the first and last steps, the adherend thickness was incremented equally for each step
- For the first and last steps, the thickness increments were half those of the generic steps
- The lengths of each step were chosen with a fixed value of the parameter $\eta_{sl} = \beta_j \ell_j / \bar{t}_j$, where ℓ_j is the length of step j

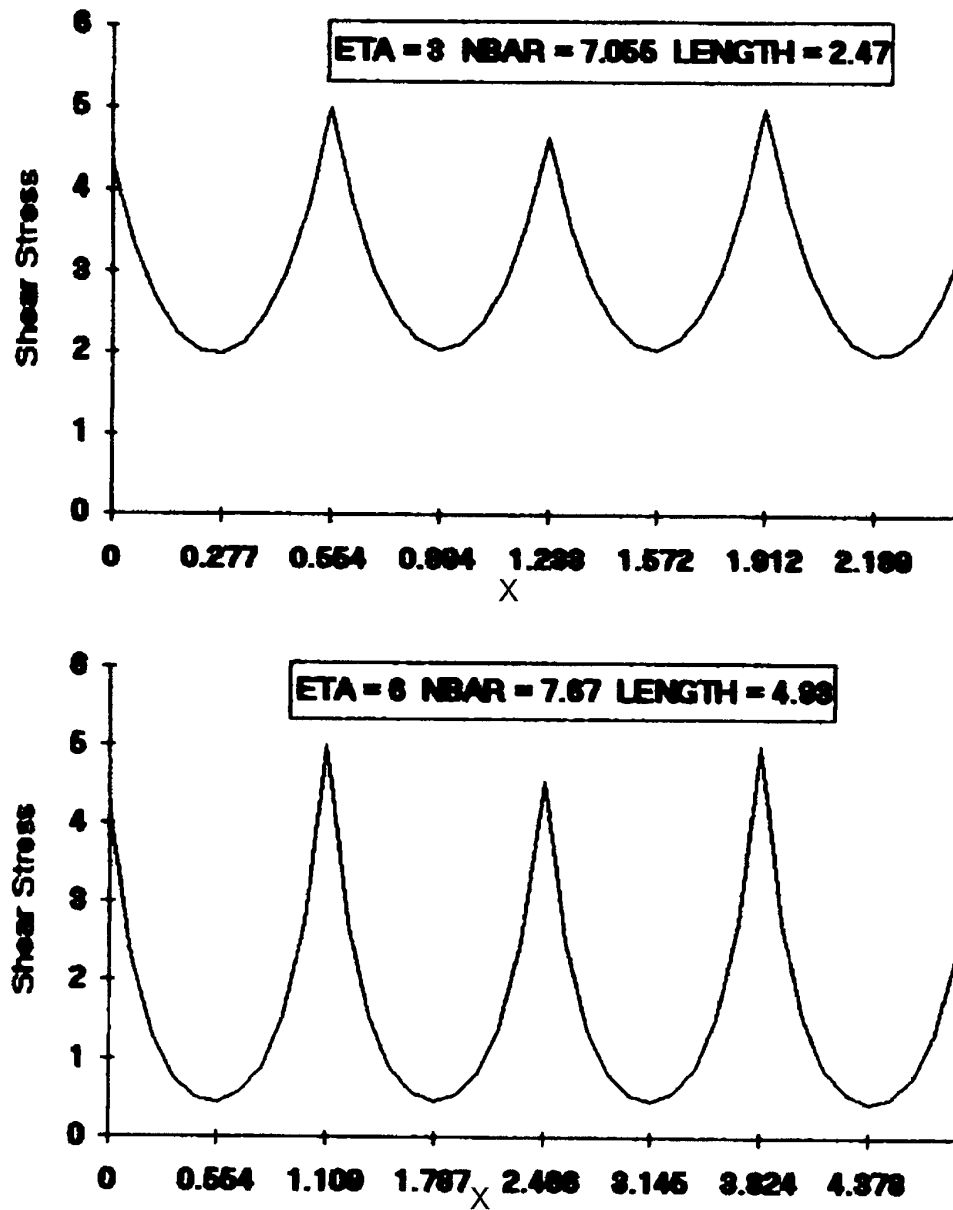
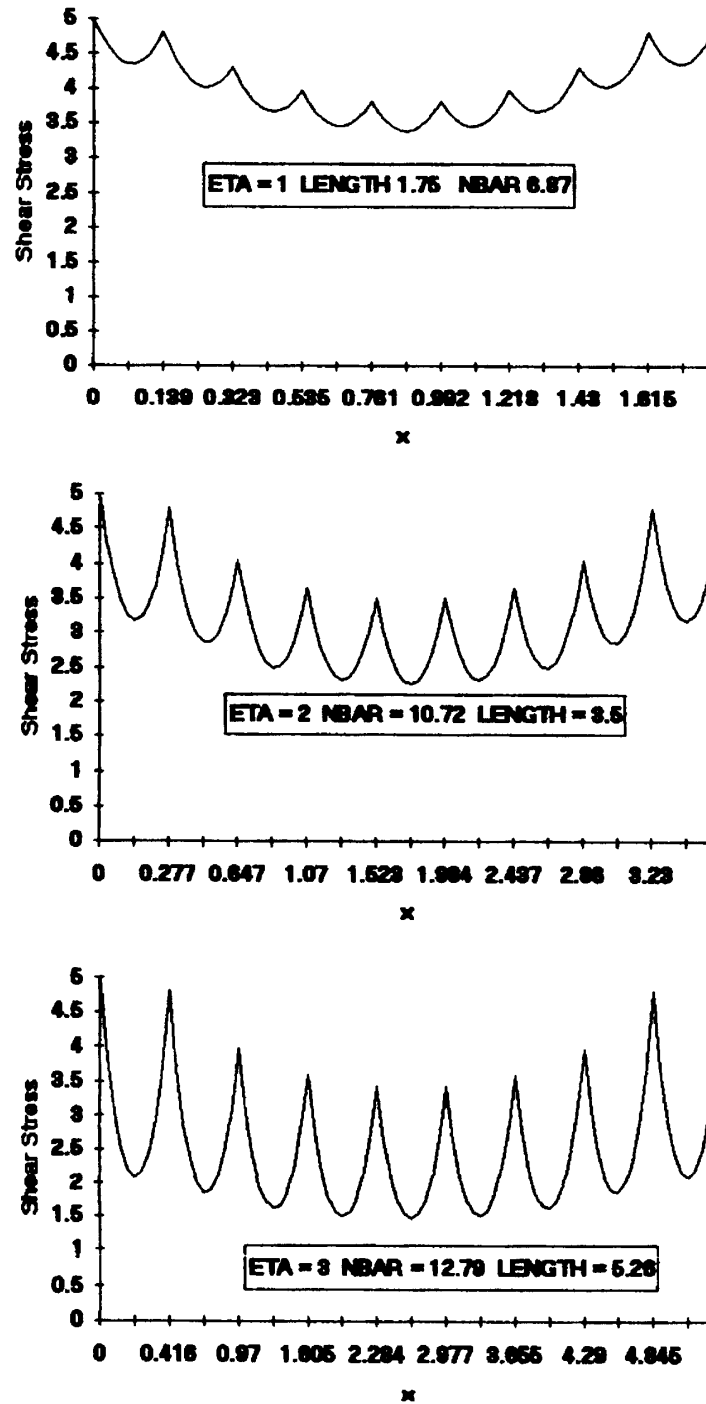
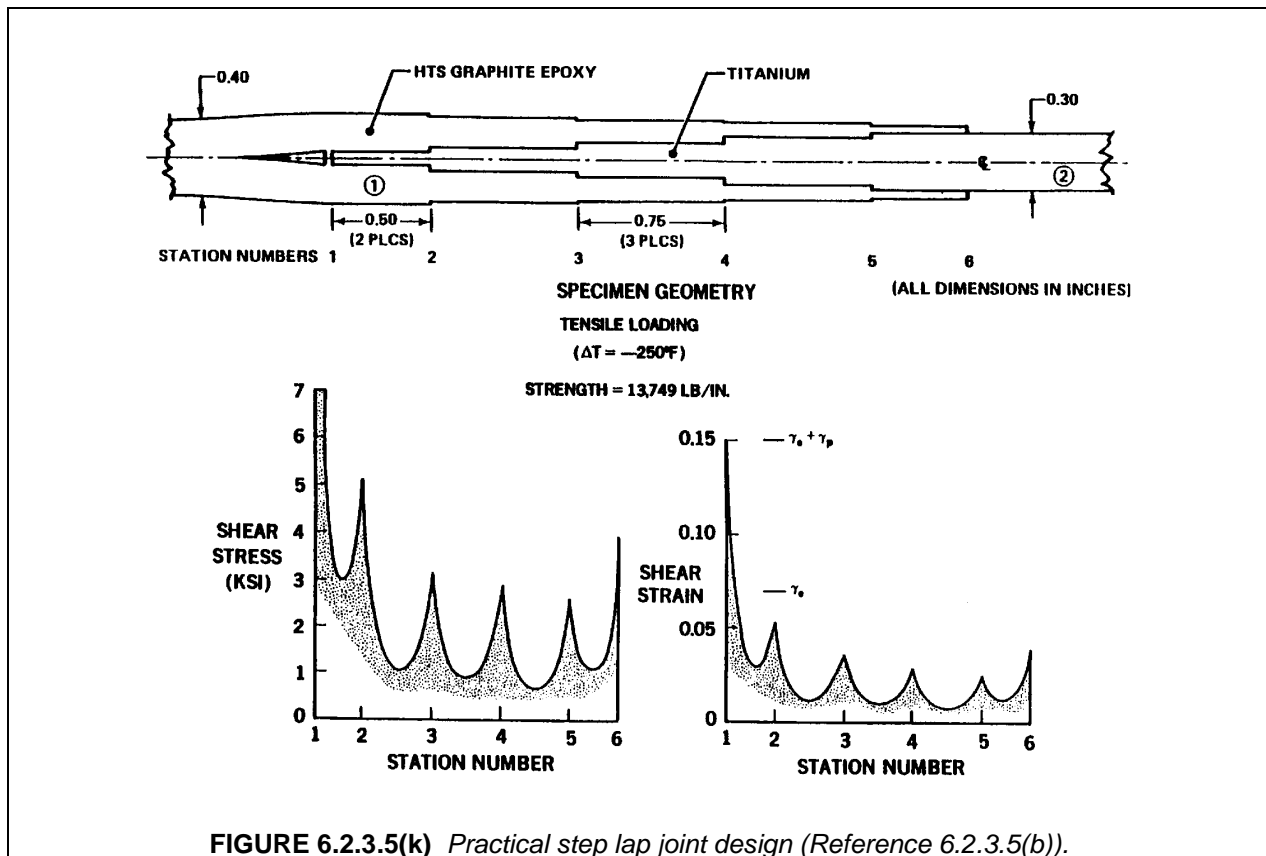


FIGURE 6.2.3.5(i) Shear stresses in five-step joint.

FIGURE 6.2.3.5(j) *Shear stresses in ten-step joint.*

The half-thickness increments of the end steps gave a more uniform shear stress distribution than maintaining the same thickness increment for all steps. Note that for the symmetric joint configurations shown in Figures 6.2.3.5(h) and 6.2.3.5(k), the thickness increment for the outer adherend (composite) was greater than that for the inner adherend by the inverse of the modulus ratio, to achieve a stiffness balance for the dissimilar adherends. Note also that the parameter "ETA" listed in Figures 6.2.3.5(i) and

6.2.3.5(j) refers to η_{sl} defined above. This parameter essentially controls the length of the joint. Both Figures 6.2.3.5(i) and 6.2.3.5(j) show an increase in joint length with η_{sl} ("ETA" in the two figures). Note further that the load capacity of the joint in terms of the allowed resultant listed as "NBAR" in the Figures 6.2.3.5(i) and 6.2.3.5(j), corresponds to an assumed bond shear stress limitation of 5 ksi (34 MPa); this allowable load shows a general increase with joint length, but with diminishing increase when η_{sl} gets much beyond 3. Table 6.2.3.5 gives a summary of the results shown in the two figures. As discussed above, the joint design shown in Figure 6.2.3.5(k) taken from References 6.2.1(l) and 6.2.3.5(b) represents a practical joint approach which accounts for several considerations that the simplified elastic analysis approach used for Figures 6.2.3.5(i) and 6.2.3.5(j) neglects. The neglect of ductility effects has already been mentioned. In addition, the use of as large a number of steps as 10 in Figure 6.2.3.5(j) may not be practical.



The joint design shown in Figure 6.2.3.5(k) represents the evolution of step-lap joint design over many years. Early analytical work was presented by Corvelli and Saleme (Reference 6.2.3.5(c)); this was later enhanced by Hart-Smith (Reference 6.2.1(l)), under NASA funding, to provide for elastic-plastic response, culminating in the A4EG and A4EI programs (Reference 6.2.1 (s)) discussed in Section 6.2.1, to allow for variations in thickness, porosity, flaw content, and moisture content in the bond layer. Hart-Smith (Reference 6.2.3.5(b)), notes that in mathematical treatments of step joints, all properties have to be constant within each step; however, in an actual joint such as that shown in Figure 6.2.3.5(k), artificial breaks may be inserted to permit changes in porosity or bond thickness.

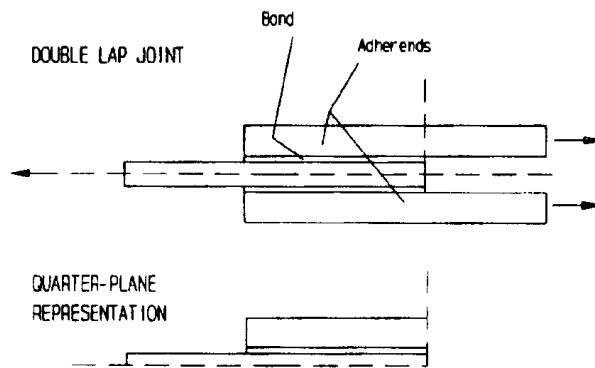
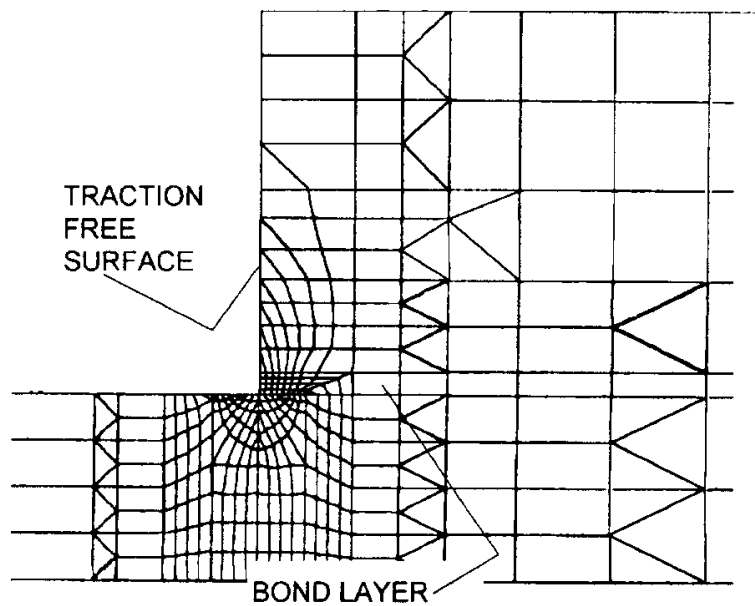
TABLE 6.2.3.5 *Summary of step lap joint results (Figure 6.2.3.5(i), 6.2.3.5(j)).*

No. of Steps	10	10	10	5	5
η_{sl}	1	2	3	3	6
Joint length, in (cm)	1.75 (4.44)	3.5 (8.89)	5.25 (13.33)	2.47 (6.05)	4.93 (12.5)
Allowed resultant, kN/cm (10 ³ lb/in)	6.87 (12.03)	10.72 (12.03)	12.59 (22.05)	7.05(12.35)	7.67 (13.43)

6.2.3.6 Finite element modeling

Finite element methods have often been used for investigating various features of bonded joint behavior, but there are serious pitfalls which the analyst must be aware of to avoid problems in such analyses, mainly because of the tendency of the bond layer thinness to unbalance the finite element model. To achieve adequate accuracy, it is especially important to provide a high degree of mesh refinement around the ends of the overlap (see Figure 6.2.3.6(a)) and yet transition the mesh to a coarser representation away from the ends of the overlap to avoid unneeded computational costs. Without such approaches, the need for limiting the aspect ratios of elements will force either a crude representation of the bond layer or an excessively over-refined mesh for the adherends. The mesh shown in Figure 6.2.3.6(a) was generated with a custom designed automated mesh generator developed by C. E. Freese of the Army Research Laboratory Materials Directorate, Watertown, MA (Reference 6.2.3.6). The elements shown consist of 8-point isoparametric quadrilaterals and 6-point isoparametric triangles, providing a quadratic distribution of displacements within each element. A number of commercially available finite element codes are presently available for developing such refined meshes. The commonly used displacement-based finite element methods are not capable of satisfying exact boundary conditions such as the traction free condition shown at the left end of the upper adherend in Figure 6.2.3.6(a) (C). In addition, a mathematical stress infinity occurs at the corner formed by the left end of the bond layer and the lower adherend.

These characteristics cannot be represented exactly, but a measure of the adequacy of the mesh refinement is provided by the degree to which the solution achieves the traction free condition shown in Figure 6.2.3.6(a) (C). Pertinent results are shown in Figure 6.2.3.6(b) which gives a solution for a double lap joint with unidirectional carbon/epoxy adherends. The finite element results represented by the "x" and "Δ" symbols are relevant to the issue under consideration. These represent the distribution of shear stresses along the interface between the upper adherend and the bond layer as indicated in the insert at the top of Figure 6.2.3.6(b). Since this line intersects the left end at a point fairly near the corner where the singularity occurs, it is reasonable to expect some difficulty in satisfying traction free conditions at the left end. The computer results did not go to zero at the end (where $x = 1.1953$) but did show signs of heading in that direction since the end stress is slightly below the peaks for the two curves. Note that the Δ symbols represent a condition in which the bond is replaced by a continuation of the upper adherend, a considerably more difficult situation to deal with than that of the x's which allow for an actual bond layer. The third curve shown in Figure 6.2.3.6(b) indicated by open circles represents a modification of Volkersen's one-dimensional shear lag analysis which allows for transverse shear deformations in the adherends; the latter agrees surprisingly well with the prediction for the finite element analysis with the bond layer present (x's) for most of the joint length, although the peak stress predicted by the approximation is somewhat less than that of the FE analysis.

**(A) Joint configuration****(B) Overall mesh****(C) Detailed Mesh****FIGURE 6.2.3.6(a)** Mesh details for finite element analysis of double lap joint.

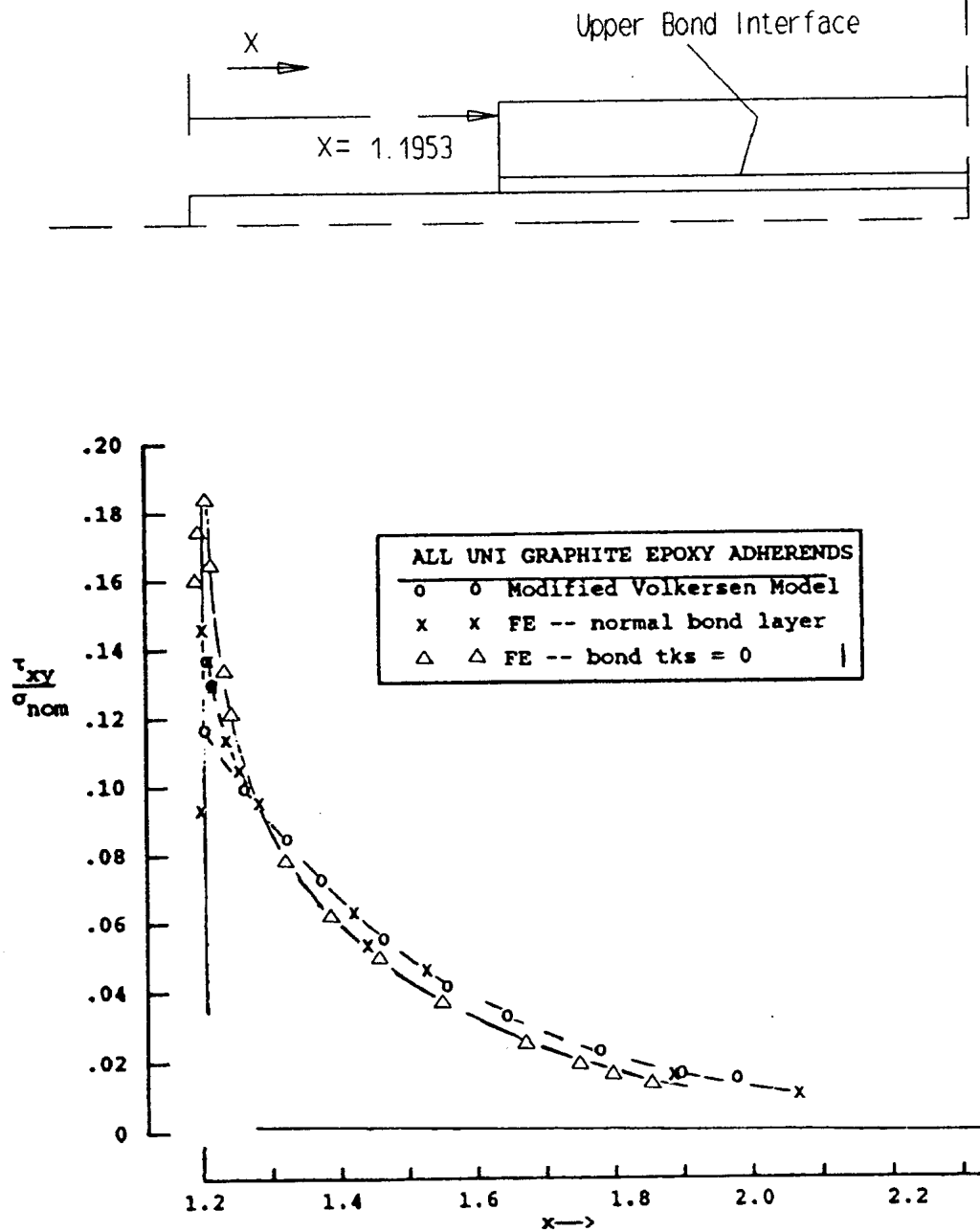


FIGURE 6.2.3.6(b) Finite element predictions of shear stress distribution along bond-upper adherend interface, double lap joint shown in Figure 6.2.3.6(a).

6.2.4 Mechanical response of adhesives

This section is reserved for future use.

6.2.5 Mechanical response of composite adherends

This section is reserved for future use.

6.2.6 Adhesive joint conclusions

This section is reserved for future use.

6.3 MECHANICALLY FASTENED JOINTS

6.3.1 Introduction

Mechanically-fastened joints for composite structures have been studied since the mid-1960's when high modulus, high strength composites first came into use. It was found early in this period that the behavior of composites in bolted joints differs considerably from what occurs with metals. The brittle nature of composites necessitates more detailed analysis to quantify the level of various stress peaks as stress concentrations dictate part static strength to a larger extent than in metals (no local yielding). As a result, composite joint design is more sensitive to edge distances and hole spacings than metal joint designs. Low through-the-thickness composite laminate strength has led to specialized fasteners for composites and eliminated the use of rivets. The special fasteners feature larger tail footprint areas which improve pull-through and bearing strengths. Galvanic corrosion susceptibility between carbon and aluminum has all but eliminated the use of aluminum fasteners.

Mechanically-fastened joints can be divided into two groups - single row and multi-row designs. Typical lightly loaded non-critical joints require a single row of fasteners. The root joint of a wing, or a control surface, is an example of a highly loaded joint, where all the load accumulated on the aerodynamic surface is off-loaded into another structure. The bolt pattern design, consisting of several rows, distributes the load for more efficient transfer.

There have been numerous government and privately funded programs for the purpose of developing composite mechanically-fastened joint analysis methods. A majority of these efforts has been concentrated on developing two-dimensional analyses to predict stresses and strength at a single fastener within the joint. This is because existing analysis techniques for determining multi-fastener joint load apportionment (in metals) have proven adequate. Additional analysis methods (Section 6.3.2) have been developed to address composite-related stress variations in stepped and scarf (i.e., tapered thickness) joints.

The material presented here reflects the state of the art as practiced primarily in the aircraft industry. The objective is to give the reader some insight into the key factors that control the behavior of mechanically-fastened joints in composite structures. The discussion that follows is arranged primarily to achieve that objective.

6.3.2 Structural analysis

6.3.2.1 Load sharing in a joint

Most of the mechanical joints encountered in aircraft structures have multiple fasteners. The number and type of fasteners needed to transfer the given loads are usually established by airframe designers by considerations of available space, producibility, and assembly. Although the resulting joint design is usually sufficient for finite element (FE) modeling purposes, further structural analyses are required before joint design drawings are released for fabrication. These analyses should consist of two distinct calculations: (1) computation of individual loads and orientation at each fastener with possible optimization to obtain near equal loading of each equal diameter fastener, and (2) stress analysis of load transfer for each critical fastener using fastener loads from previous analysis.

An example of a joint is shown in Figure 6.3.2.1(a). In order to obtain individual fastener loads for this or any other joint configuration (including single in-line row of fasteners), overall loading, geometry, plate stiffnesses, and individual fastener flexibilities must be known. Two structural analysis approaches have evolved in the aircraft industry. One performs the analysis in two steps, the first step being a calculation of individual bolt flexibilities followed by FE analysis with the fastener flexibilities as input. The second type includes the computation of the joint flexibility as a special FE in the overall FE analysis. An example of the latter is the SAMCJ code developed for the Air Force, Reference 6.3.2.1(a). Both approaches approximate a nonlinear joint load-displacement response, Figure 6.3.2.1(b), by a bilinear representation. This simplification permits the overall finite element problem to be linear. Recently a closed form analytical model has been developed and programmed for the personal computer to deal with the multiple hole joint strength problem (Reference 6.3.2.1(b)).

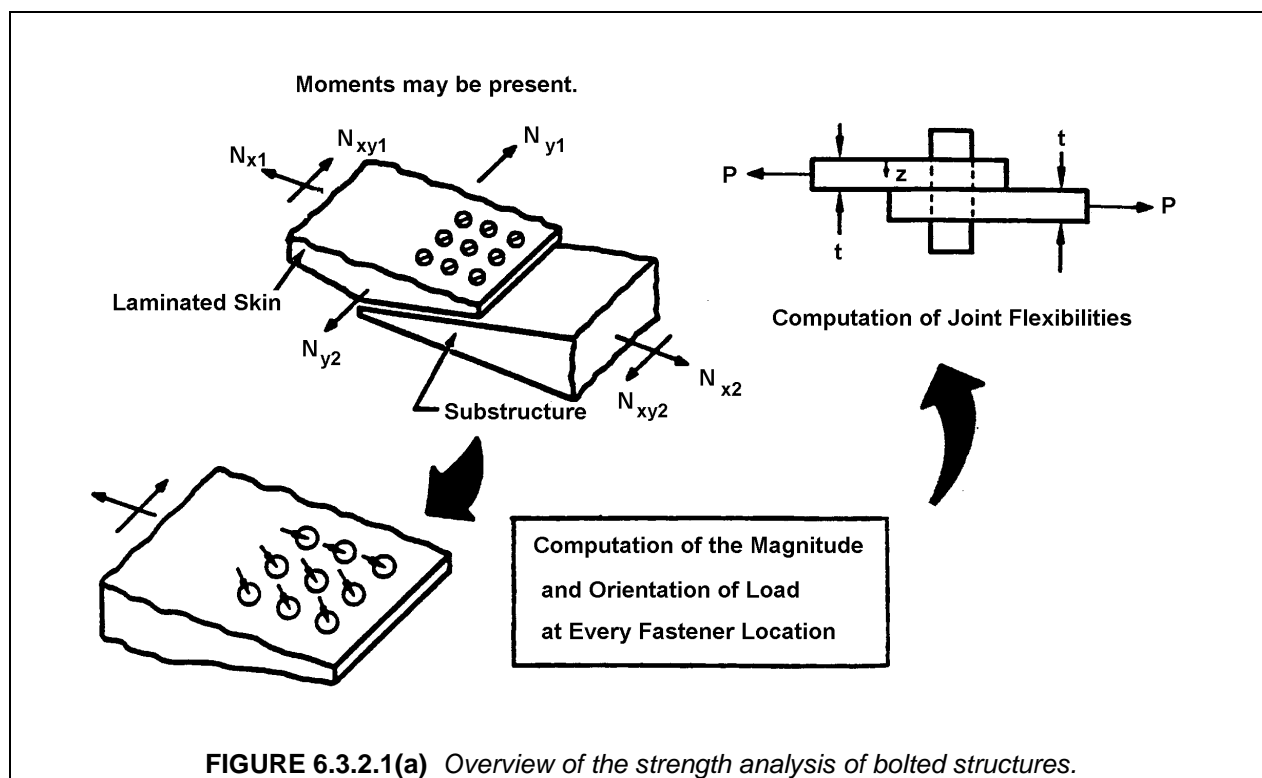
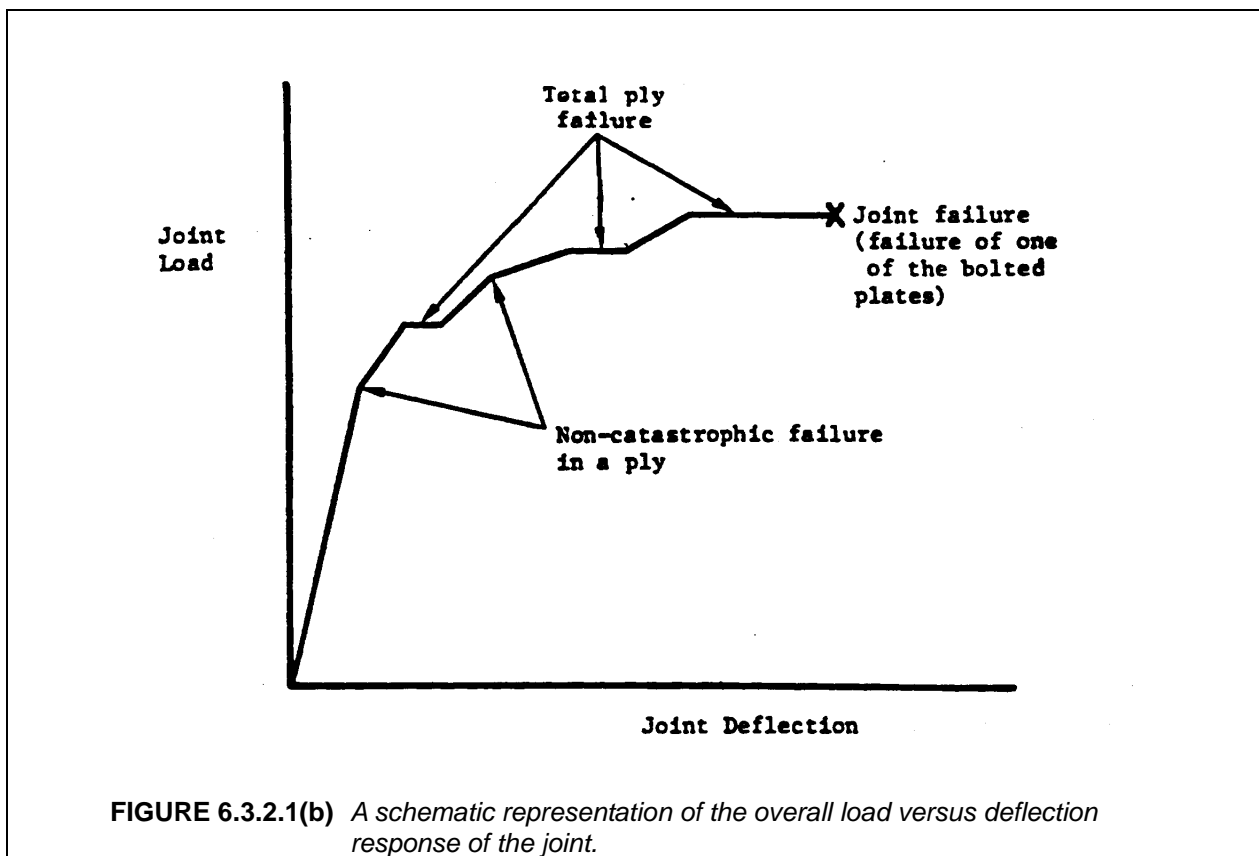


FIGURE 6.3.2.1(a) Overview of the strength analysis of bolted structures.

Fastener flexibility is based on joint displacement not only due to the axial extension of the joining plates but to other effects not easily modeled. These are fastener deflection in shear and bending, joint motion attributable to localized bearing distortions, and fastener rigid body rotation in single shear joints. Additionally, for composite laminates the value of joint flexibility should reflect the material orientation, ply fractions, and the stacking sequence of the laminates being joined. Other variables to be considered are the fit of the pin in the hole, presence of a free edge close to the hole, and head/tail restraint. Because of the many variables, test data for joint flexibility is the best type of input for the overall FE model of the multi-fastener joint. However, the data is not always available for all the different design situations. Hence, various modeling schemes have evolved to obtain flexibility values. Calculation of joint flexibility can be quite complex if the joint contains multiple stack-ups of plates with gaps. Analytical models to solve for the joint flexibility range from representing plates as springs to those where the fastener is idealized as a flexible beam on an elastic foundation provided by the plate or laminate.



For thick plates fasteners, flexibility may not be as important a parameter as for thin plates. Reference 6.3.2.1(c) has shown that good correlation between test and analysis for bolt load distribution using rigid inclusions to represent bolts. Reference 6.3.2.1(c) also included effects of the contact problem with and without gaps to calculate bearing stress distributions.

Load sharing in mechanically fastened joints is strongly dependent on the number and the diameter and material of the bolts, and the stiffness of joining members. For a single in-line row of bolts the first and the last bolt will be more highly loaded, if the plates are of uniform stiffness. This is illustrated in Figure 6.3.2.1(c) in which, in addition to the equal stiffness members (configuration 2), other combinations of fastener diameters/plate configurations are shown, which can alter the bolt distributions appreciably.

6.3.2.2 Analysis of local failure in bolted joints

Once the load sharing analysis has been performed, bolted joint analysis reduces to modeling a single bolt in a composite plate as shown in a free body diagram in Figure 6.3.2.2.(a). A number of analysis codes have been developed that perform the stress analysis and provide useful failure predictions for problem of Figure 6.3.2.2.(a). One cannot depend on analysis alone, and the design of a bolted composite joint will entail an extensive test program involving various joint configurations, laminates, and bearing/bypass ratios. However, because of the variety of laminates and load conditions present in a complex structure, testing frequently cannot cover all conditions of interest. Therefore, analytical methods are needed to extend the applicability of the test data to a wider range of cases.

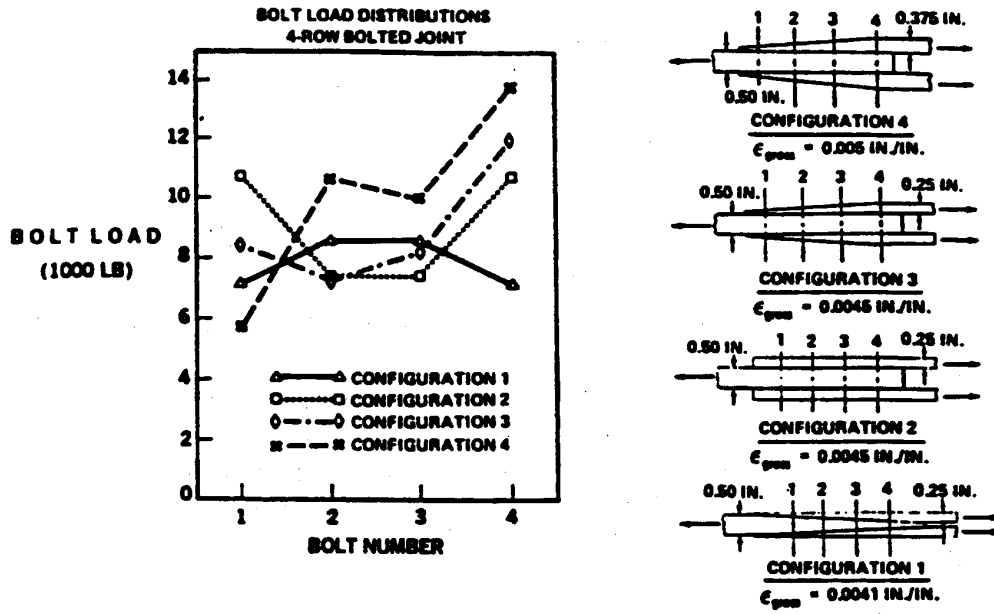


FIGURE 6.3.2.1(c) Effect of joint configuration on fastener load distribution (Reference 6.3.2.1(d)).

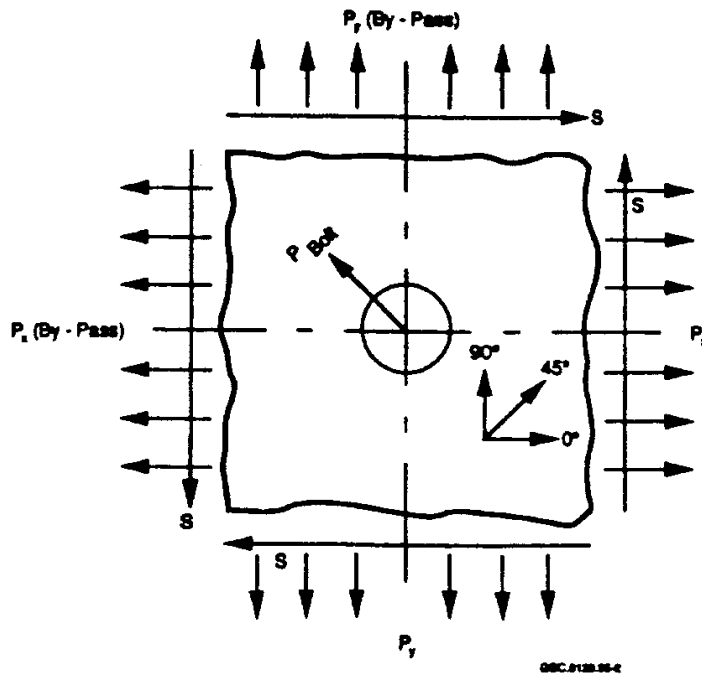


FIGURE 6.3.2.2(a) Bolted joint under generalized loading.

There are multiple failure modes that must be considered. The first is net section failure of the composite. Alternatively, the laminate may fail immediately ahead of the bolt due to bearing pressure or the specimen will fail by pull-through. Depending on hole spacing, edge distances, or lay-up, shear-out may occur before bearing failure is reached. Delaminations may also be present but these are not the primary cause of failure. Finally, failure of the fastener must be considered. A more comprehensive description of possible failure modes is discussed in the next section.

The analysis of fiber dominated in-plane failure modes, such as net-section failure, has typically been accomplished using variations of the approach by Whitney and Nuismer (Reference 6.3.2.2(a)), or the semi-empirical model of Hart-Smith (Reference 6.3.2.2(b)). The basis of the approach is to evaluate a ply-level failure criterion at a characteristic distance, d_0 away from the edge of the hole. The characteristic distance accounts for two experimentally observed effects. First, the strength of laminates containing a hole is greater than would be implied by dividing the unnotched strength by the theoretical stress concentration for the open hole. Second, the strength is observed to be a function of hole diameters, with strength decreasing as hole diameter increases. The use of a fixed d_0 simulates these effects, Figure 6.3.2.2(b).

The characteristic distance is treated as it was a laminate material property, and is determined by correlating the analysis to the ratio between the unnotched and open-hole strengths of laminates. More extensive correlations may reveal that d_0 is a function of the laminate ply fractions. The value of d_0 will also depend on the ply-level failure criterion used.

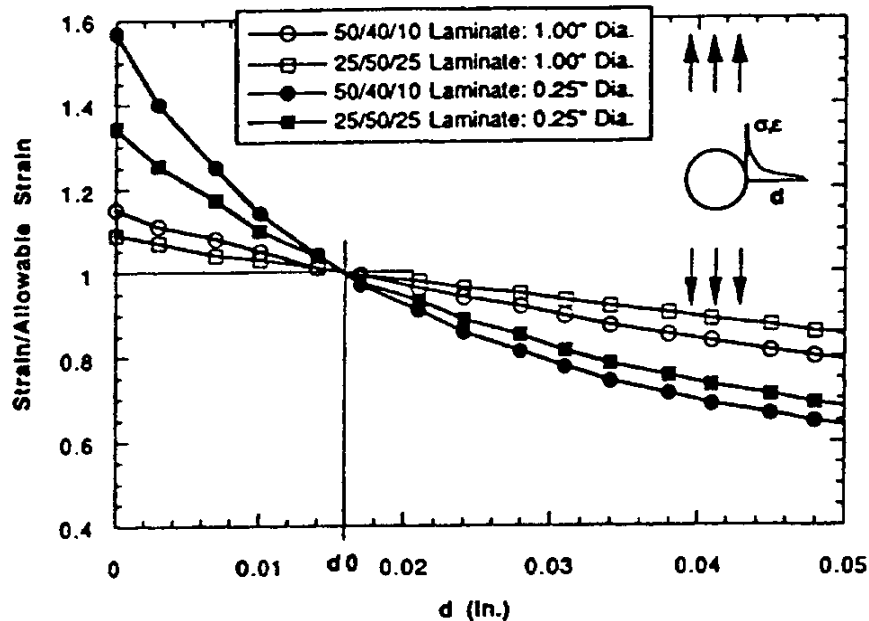


FIGURE 6.3.2.2(b) Strain distributions near an open hole for different hole diameters and tape laminates. Applied far field load is equivalent to the expected failure load. Laminates are given as percentages of $0^\circ/\pm 45^\circ/90^\circ$. Crossing point of curves defines characteristic distance, d_0 .

The establishment of laminate material allowables for the failure prediction must include a consideration of the material variability, and the inherent inability of current failure theories to completely account for changes in laminate stacking sequence, joint geometry, and hole size. One approach is to establish

B-basis allowables for the ply-level failure criterion based on unnotched ply data. The d_0 is then selected such that the predicted values of failure are equivalent to the B-basis value of the notched laminate tests. The B-basis d_0 can also be obtained directly from notched laminate tests if sufficient number of different laminates with various hole sizes are tested.

Although the Whitney-Nuismer method was originally conceived for failure under uniaxial tension, the method has been applied to compression, and biaxial loading. The compression d_0 will be different than the tension value and the edgewise shear d_0 different from either. Reference 6.3.2.2(c) suggests a smooth characteristic curve for connecting the tension and compression values. When biaxial loads are introduced, one must search for the most critical location around the hole. A search algorithm is needed even for the case of uniaxial loading as it can be shown that the maximum circumferential stress may not occur at a point tangential to the load direction when the percentage of $\pm 45^\circ$ plies is large, or when an off-axis laminate is considered.

Use of this failure criterion for predicting failure implies that an accurate stress solution for the vicinity of the hole is available. A solution for a hole in an infinite, anisotropic sheet was given by Lekhnitskii (Reference 6.3.2.2(d)). This solution can be extended to the case of an assumed pressure distribution for a loaded bolt, and can be combined with boundary integral techniques to include the effects of nearby boundaries and multiple holes. General boundary element methods and finite element methods have also been applied. Care should be exercised in the use of finite-element techniques due to the high stress gradients present at the hole. The finite element model should be compared against the theoretical stress concentration at the edge of the hole to ensure sufficient mesh refinement.

The behavior of joints with bearing-loaded bolts has often been simulated by assuming a pressure distribution around the perimeter of the hole, although the actual behavior is governed by the displacement condition corresponding to the circular cross section of the bolt bearing into the surrounding plate. A typical assumption in the modeling of the joint is that the radial pressure due to the bolt follows a cosine function distribution over a 180° contact zone (Figure 6.3.2.2(c)) and zero pressure elsewhere (with zero tangential stresses around the whole circumference). In many cases this gives satisfactory results for predicting the critical stress peaks, e.g., the peak net-section stress at the 90° degree points around the fastener. Figure 6.3.2.2(c) in Reference 6.3.2.2(e) shows a comparison of the predicted stress concentration factors for an assumed "half-cosine" radial *pressure* distribution vs. the more accurate solution which assumes a radial *displacement* condition along the edge of the hole. The "K" values tabulated at the left side of the figure represent peak stresses normalized with respect to the gross stress, P/Wt (thus the subscript "G"), including the peak net section stress (K_G^{nt}) at $=90^\circ$, peak bearing stress (K_G^b) at $=0^\circ$ and peak shear stress (K_G^s) at $=45^\circ$. These results were predicted for $W/D=2$, $e/W=1$ and a neat fitting fastener. For these conditions, the stress concentration factors obtained from the two approaches are not substantially different, suggesting that the "half cosine" radial pressure distribution is an adequate approximation for the more accurate analysis which solves for the radial displacement distribution.

There are some important situations for which the "half cosine" pressure distribution will give poor results, however. Figure 6.3.2.2(d), which compares a variety of situations, includes one case in which the edge distance is relatively small (square symbols, $e/W=0.375$, $W/D=2$); the radial pressure distribution is characterized by a dip in the pressure near $\theta=0$. This corresponds to the tendency for the part of the plate in front of the fastener to deform as if in beam bending (Figure 6.3.2.2(e)) in the case of short edge distances, relieving the pressure in front of the fastener so as to account for the drop in radial pressure near $\theta=0^\circ$ which is seen in Figure 6.3.2.2(d).

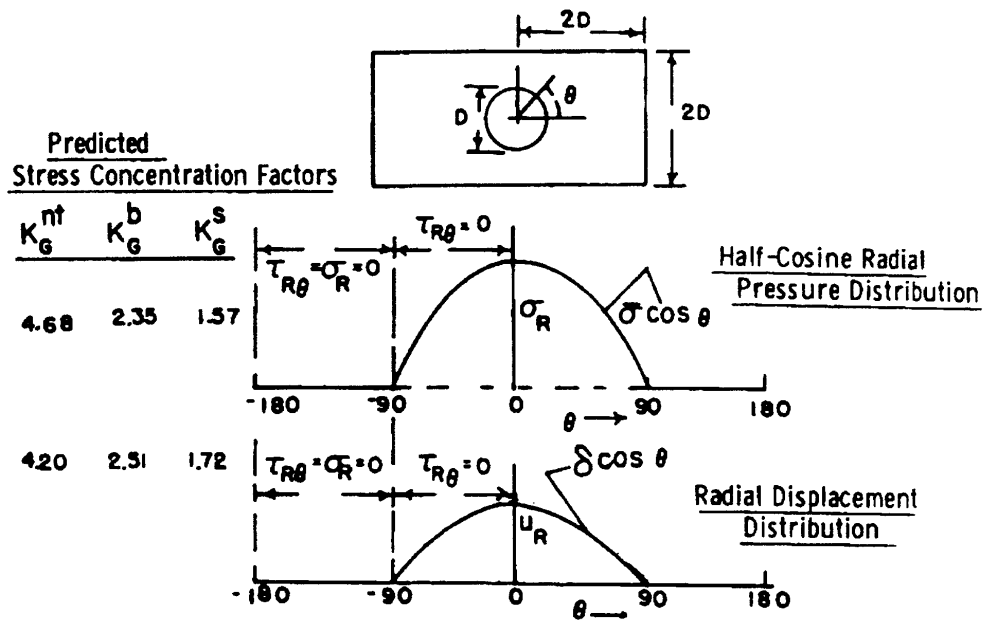


FIGURE 6.3.2(c) Comparison of predicted stress concentrations for assumed radial pressure distribution vs. radial displacement distribution (Reference 6.3.2.2(e)).

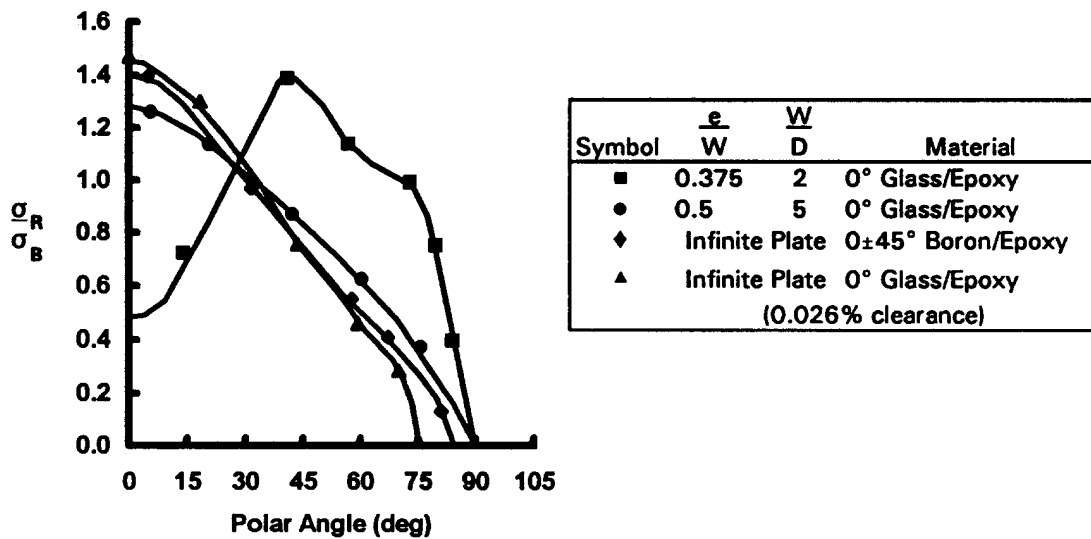
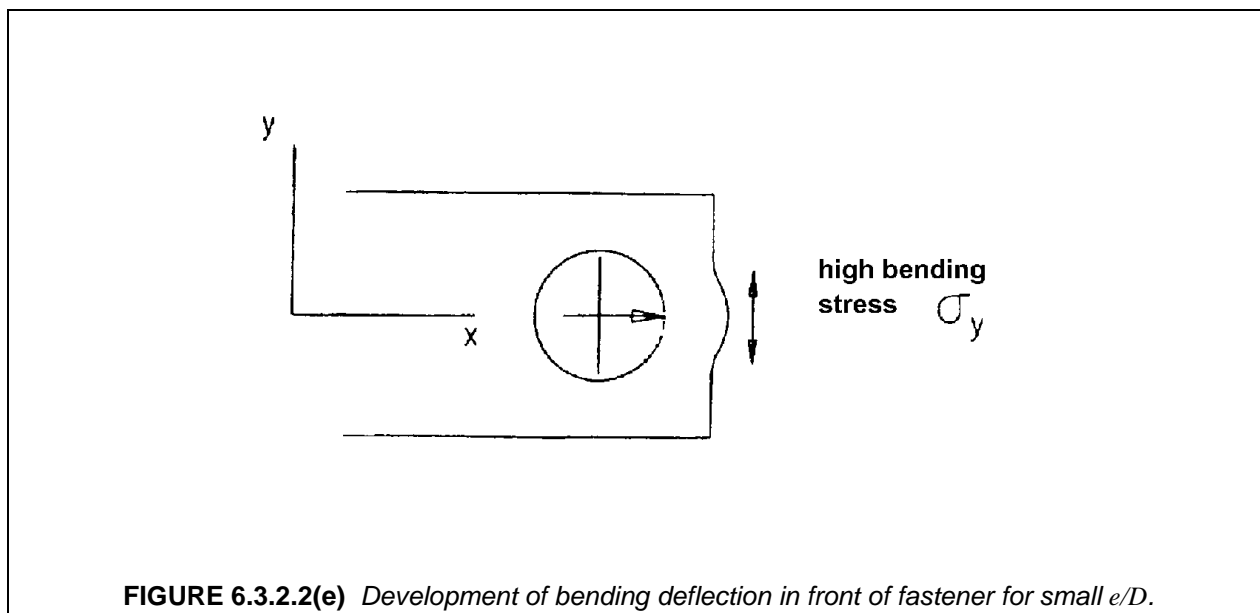


FIGURE 6.3.2(d) Radial pressure distributions for various joint configurations (Reference 6.3.2.2(e)).



In addition to the case of small edge distances, combined bearing and bypass loads can result in radial pressure distributions which deviate excessively from the "half-cosine" distribution. This can be understood in terms of the displacement behavior illustrated in Figure 6.3.2.2(f), for pure bypass loading in which there are two gaps between the plate and fastener centered about 0° and 180° , vs, the case of pure bearing load in which a single gap located between $q=90^\circ$ and 270° occurs. For low bypass loads one would, therefore, expect a single region of contact centered about $q=0^\circ$, while for large bypass loads a split contact region would be expected. In terms of the notation defined in Figure 6.3.2.2(g), this type of behavior is predicted by stress analyses which correctly model the contact situation between the fastener and plate as illustrated in Figure 6.3.2.2(h). Note in Figure 6.3.2.2(g) that P_{TOT} is the total load at the left of end of the joint, which is the sum of P_F , the fastener load, and P_{BP} , the bypass load.

Figure 6.3.2.2(i) illustrates how taking into account the effect of the radial displacements at the edge of the hole can influence predictions of the net section stress peaks. In this figure, predictions of K_G^{nt} (peak net section stress divided by gross stress) for the conventional superposition approach obtained by a linear combination of K_G^{nt} values for pure bearing load and pure bypass load (denoted "linear approximations" in Figure 6.3.2.2(i)), are compared with the corresponding results obtained when the contact problem is taken into account (open circles and squares). For the latter case, the curves are fairly flat over most of the range of load ratios, dropping rapidly near the high bypass end to a little above 3, the classical open hole value for isotropic plates having boundaries at infinity. Strength values for joints under combined bearing and bypass loading should follow similar trends with respect to the load ratio.

The above results apply to cases of exact fastener fits. Additional complications occur with clearance fits corresponding to tolerances which are representative of available machining practice. Clearance fit cases have been analyzed extensively by Crews and Naik (Reference 6.3.2.2(f)) for clearances on the order of 0.0025 in. (0.04 mm) with fastener diameters of 0.25 in. (6.3 mm), i.e., clearances about 1% of the fastener diameter¹. Significant changes in the radial pressure distribution occur with respect to the exact fit case. The angle subtended by the contact region becomes a function of load for this case, starting at zero for incipient loads and growing to only about 60° on either side of the axial direction for typical peak loads. The reduction of the angle of contact by the effects of clearance results in significant increases in the peak bearing stress. Again, the "half-cosine" load distribution can not be used to predict this type of behavior.

¹Note that the SI equivalent dimensions provided throughout Section 6.3 are "soft" conversions, that is SI dimensions for fastener sizes are provided but sizes are not converted to SI standard sizes.

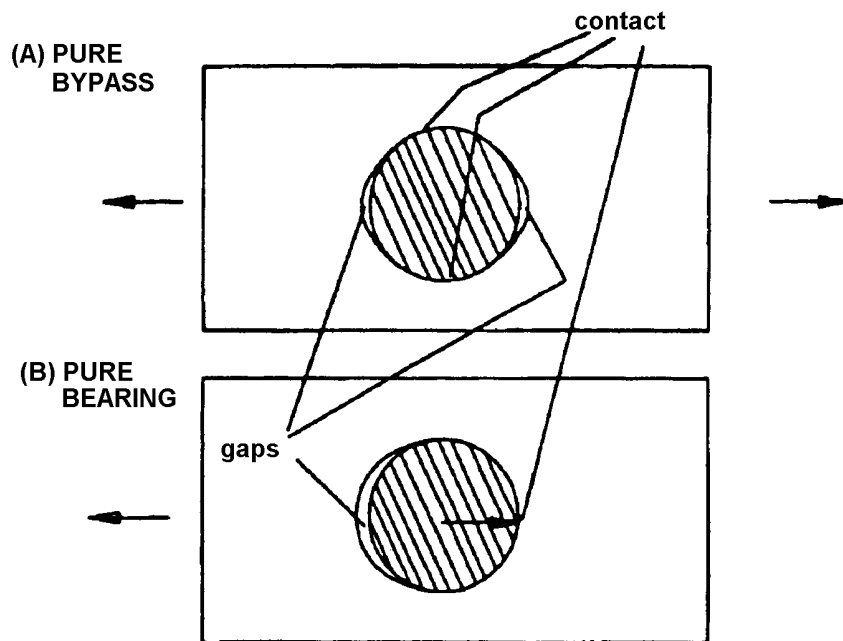


FIGURE 6.3.2.2(f) Bolt shank/hole contact regions for pure bypass vs. pure bearing loads.

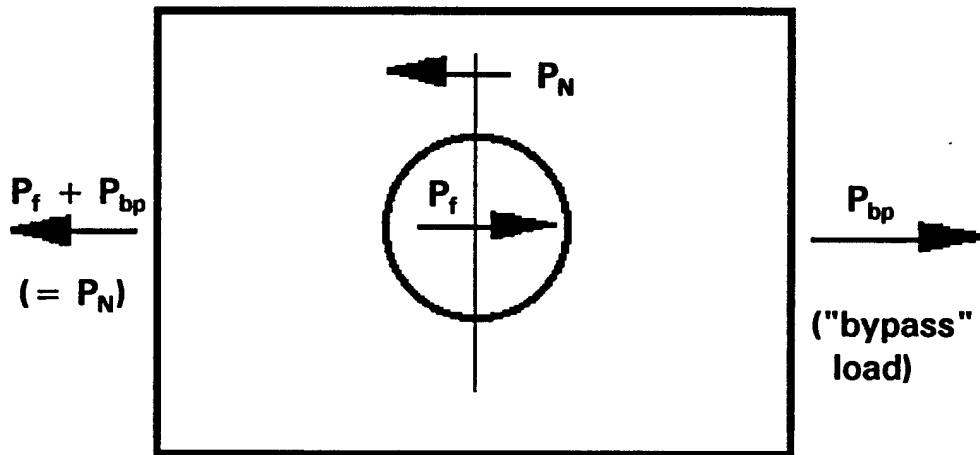


FIGURE 6.3.2.2(g) Load definitions for combined bearing and bypass loads.

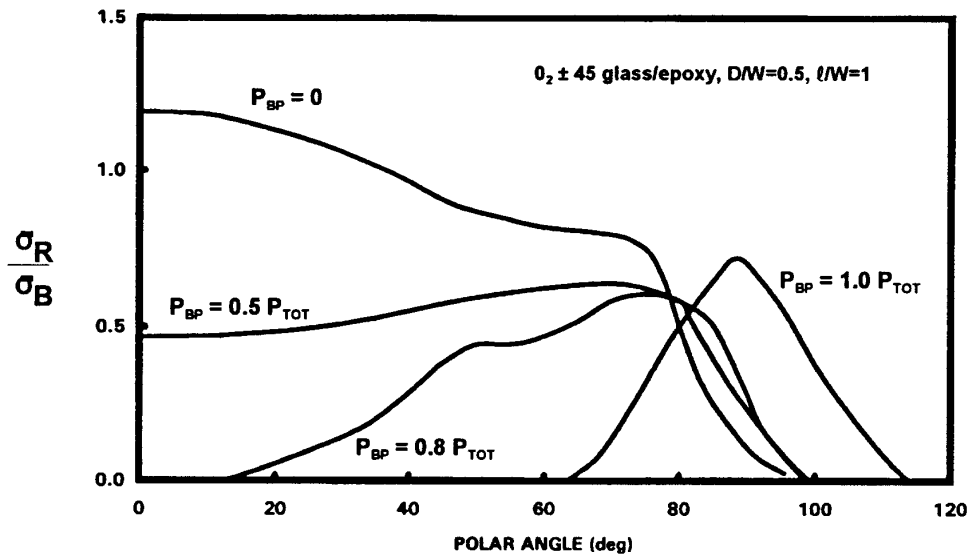


FIGURE 6.3.2.2(h) Effect of bearing/bypass load ratio on radial pressure distribution (Reference 6.3.2.2(e)).

Crews and Naik also addressed the applicability of the superposition method for predicting failure under combined bearing and bypass loading, on the basis of their analytical results with the Nuismer Whitney correction taken into account. They observed that the superposition approach gives adequate accuracy for predictions of the net-section tensile failures, although the predictions of radial pressure distributions are quite bad so that bearing failures cannot be treated by superposition.

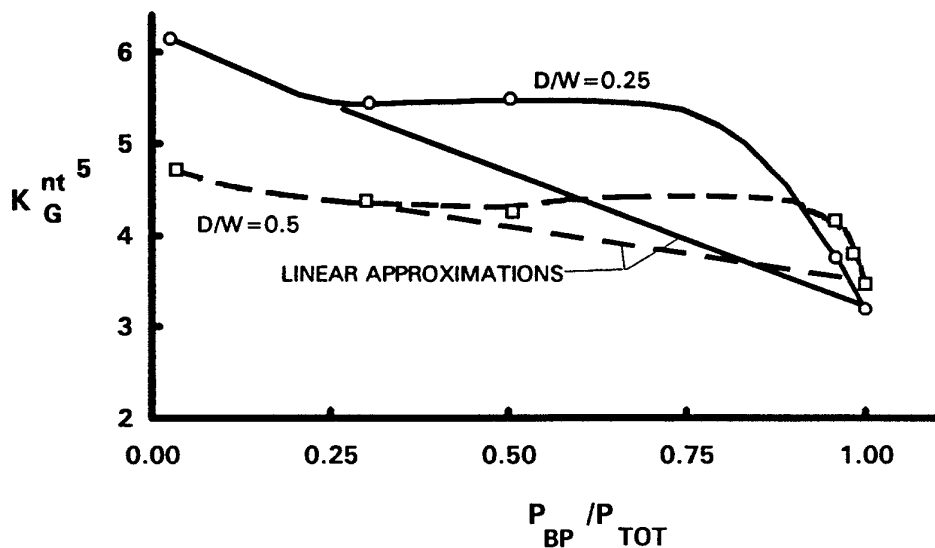


FIGURE 6.3.2.2(i) Effect of bearing/bypass load ratio on peak net section stresses-neat fit fastener (Reference 6.3.2.2(e)).

The basic analytical steps described above have been implemented in several computer codes. Codes developed under government sponsorship include *BJSFM* (Reference 6.3.2.2(g)), *SAMCJ* (Reference 6.3.2.2(h)), *BOLT* (References 6.3.2.2(c) and 6.3.2.2(i)), *SCAN* (Reference 6.3.2.2(j)), and *BREPAIR* (Reference 6.3.2.2(k)). *BREPAIR* has been specialized for the case of bolted repairs for composites, and also computes the bolt loads from the fastener and plate flexibilities.

In principle, the analysis methods described should be able to account for the shear-out failure mode if the stress analysis method used includes the effects of multiple holes and plate edges. However, because of the variety of ply-level failure criteria used, and the details of the analysis implementation, it is recommended that additional test correlation be performed before applying these methods to cases involving small edge distances, or close hole spacing.

Furthermore, current analysis methods should not be relied upon to predict matrix dominated modes such as bearing failure. Generally, the analysis codes can be used to predict net-section failures, while bearing failure is checked by direct comparison of the average bearing stress (P/dt) to test data.

The actual bearing pressure due to a bolt varies considerably through the thickness of the laminate. For this reason, the test configuration must closely match the actual joint geometry in terms of laminate thickness, gaps and shims, and configuration (double versus single shear) and type of fastener. The bearing strength will depend on factors such as the countersink depth and angle, joint rotation under load, and the type of fastener head. The through-thickness distribution of bearing stresses can be estimated by treating the bolt as a beam, and the laminate as an elastic foundation (Reference 6.3.2.2(l)). These methods are suitable for estimating the changes in the bearing stress due to changes in gap distances or laminate thickness. They may also be useful for determining the moment and shear distribution in the bolt to predict fastener failure.

Clamp-up forces have been shown to have a significant effect on laminate failure, particularly under fatigue loading. Clamp-up can suppress delamination failure modes, and changes the fastener head restraint. This effect cannot be included in the two-dimensional analysis methods described above. Before taking advantage of the beneficial effects of clamp-up, long-term relaxation of the laminate stresses should be considered. Because of this effect, minimum clamp-up (if possible) should be used when conducting bolt bearing tests, i.e., finger tight or 10-20 in.-lb (1-2 N-m) torque up on a 1/4 in. (6.4 mm) diameter bolt. This may not be the normal torque installation of the fastener.

6.3.2.3 Failure criteria

The design of a mechanically fastened joint must assure against all possible failures of the joint. These are illustrated in Figure 6.3.2.3. Accepted design practice is to select edge distances, plate thicknesses, and fastener diameters so that of all the possible failure modes probable failures would be net section and bearing. There is no consensus whether the joint should fail in net section tension/compression or bearing. Reference 6.3.2.3(a) recommends that highly loaded structural joints be designed to fail in a bearing mode to avoid the catastrophic failures associated with net section failures. Although this is a commendable goal, particularly for single bolt joints, it is impractical in most cases as the increase in edge distances adds weight to the structure. For usual width to bolt diameter ratios of 6 both, net and bearing failures are possible, and the stress engineer is satisfied if he can show a positive margin against both failure modes. He does not try to get a higher margin for net failure than for bearing failure. Steering the joint design to have bearing failures by having large bearing allowables may result in in-service problems of bolt hole wear, fuel leakage, and fastener fatigue failures. Furthermore, net tension failure is unavoidable for multi-row joints.

In contrast to metals, load redistribution in a multi-fastened joint cannot be counted on and hence a single fastener failure in bearing constitutes failure of the joint. Failure criteria in bearing should be either bearing yield, defined either as the $0.02D$ or $0.04D$ based on actual bearing load displacement curves, or B-basis ultimate load, whichever is lower. The beneficial effects of clamp-up on bearing failure has to be evaluated in light of relaxation during service.

Failure criteria for single fastener joint were discussed in Section 6.3.2.2. For complex loading or proximity to other fasteners, the failure location or mode identification may not be as shown in Figure 6.3.2.3 for unidirectional loading. For thick composites, recent work (Reference 6.3.2.3(b)) has shown that net section failures do not necessarily occur at 90° to the load direction but at some other locations around the hole.

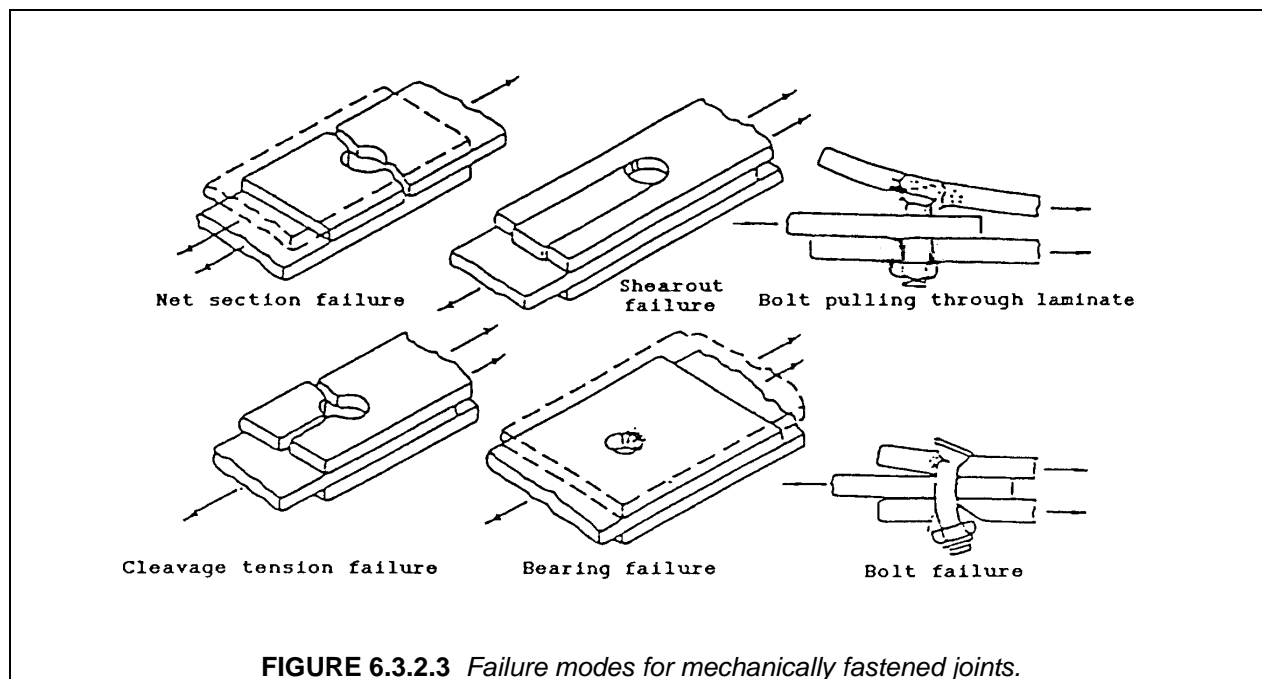


FIGURE 6.3.2.3 Failure modes for mechanically fastened joints.

6.3.3 Design considerations

6.3.3.1 Geometry

This section is reserved for future use.

6.3.3.2 Lay-up and stacking sequence

This section is reserved for future use.

6.3.3.3 Fastener selection

The use of mechanical fasteners to join non-metallic composite structures is bound by certain constraints which do not exist in the design of metallic joints. In other words, special care must be taken to select fasteners that are appropriate with polymer composite structures. Because of these special requirements fastener manufacturers have developed fasteners especially for use with composites. These fasteners develop the full bearing capability of the composite (which, at least for carbon/epoxy, is equal or better than aluminum) without encountering local failure modes and are not susceptible to corrosion. Therefore, these fasteners or those having such properties, should be used. Nondiscriminant use of off-the-shelf fasteners will lead to premature joint failures.

Design of mechanically fastened joints has always been guided by the principle that the material being joined should fail before the fastener, and this is the practice with composites. Although composites have high strength/stiffness to weight ratios with good fatigue resistance, it is a fact that today's composites must be treated very carefully when designing joints. The major structural limitation in this area is the

insufficient through-thickness strength of the laminates. This has given rise to the term "pull-thru strength". It has become necessary to increase the bearing area of fastener heads (or tails) in order to reduce the axial stresses against the laminate when the fastener is loaded in tension.

Another area of concern is the bearing stress which a fastener applies to the edge of the hole in a composite laminate as its axis rotates due to secondary bending of the joint. This condition can impose a severe limitation on a joint with limited stiffness. Another problem is the composite's inability to support installation stresses of formed fasteners, such as solid rivets or blind fasteners with bulbed tails. In addition to surface damage, such as digging-in into composite, subsurface damage to the laminate may occur. For this reason, these fastener types are avoided in favor of two piece fasteners and blind fasteners which do not generate this type of loading during installation.

For the above reasons, tension head 100° countersunk fasteners rather than shear heads should be selected as the projected area of the tension head fastener is larger than that of a shear head fastener. The larger area improves pull-through and delamination resistance in composites, while reducing overturning forces from bolt bending. These fasteners are also recommended for double shear joints. Caution should be observed in the use of 130° countersunk head fasteners. Although this type of fastener increases the bearing area of the fastener and permits it to be used in thin laminates, pull-through strength and resistance to prying moments can be adversely affected.

The full bearing capability of composites can only be attained using fasteners with high fixity (good clamp-up). Fixity is a function of fastener stiffness, fastener fit, installation forces, torque and rotational resistance of the fastener head and collar or formed backside. However, because of relaxation with service usage, normal design/analysis practice uses data based on tests where the fasteners were installed finger tight or with light torque. As part of the allowables program, testing should also be done with fasteners installed per fastener supplier's recommended procedures.

Although close tolerance fit fasteners are desirable for use with composites, interference fit fasteners cannot be used due to potential delamination of plies at the fastener hole. There are exceptions to this rule. Some automatic high impact driving equipment which was used in production has been shown not to cause composite damage.

Presence of galvanic corrosion between metallic fasteners and non-metallic composite laminates has eliminated several commonly used alloys from consideration. Conventional plating materials are also not being used because of compatibility problems. The choice of fastener materials for composite joints has been limited to those alloys which do not produce galvanic reactions. The materials currently used in design include unplated alloys of titanium and certain corrosion resistant stainless steels (cres) with aluminum being eliminated. The choice is obviously governed by the makeup of the composite materials being joined, weight, cost, and operational environment. Aircraft practice has been to coat fasteners with anti-corrosion agent to further alleviate galvanic corrosion.

6.3.4 Fatigue

Fatigue performance of bolted composite joints is generally very good as compared to metal joints. Under maximum cyclic load level as high as 70% of the static strength, composite bolted joints have been observed to endure extremely long fatigue life and with minimal reduction in residual strength. The predominant damage mechanism under cyclic loads is usually bearing failure in form of hole elongation with net section failure for static residual test.

Even though the general trends of fatigue behavior of bolted composites has been well established, the influence of individual parameters on the fatigue performance needs to be investigated. For bolted composite joints, the parameters include material system, geometry, attachment details, loading mode and environment. Several government funded programs have been conducted to evaluate the influence of specific design on composite bolted joints. Typical examples are given in References 6.3.4(a) - 6.3.4(e). However, the large number of design variables makes it very difficult to develop an overall understanding of the specific influence of each of the primary design parameters. Based on the results of

References 6.3.4(a) - 6.3.4(e), the following paragraphs summarize the significant effects of key design parameters on the fatigue performance of bolted composite joints. Because the parameters used in each reference are significantly different, direct comparison of the results is difficult. Only the trends of the data, based on coupon tests, are discussed.

6.3.4.1 Influence of loading mode

Under a constant amplitude fatigue situation, the most severe loading condition is fully reversed loading ($R = -1$). The results in Reference 6.3.4(a) indicate that fatigue failures will occur within 10^6 cycles if the maximum cyclic bearing stress is above 35% of the static bearing strength. However, the results of Reference 6.3.4(d) show that a 10^6 cycles fatigue threshold exceeds 67% of the static strength. Failure observed in the specimens exposed to fully reversed fatigue loads were induced by local bearing and excessive hole elongation. The hole elongation increases slowly for the major portion of the specimen's fatigue life, but increases rapidly near the end of the fatigue life. That is, once the bearing mode of failure is precipitated, hole elongation increases from a low value (1 to 2% of the original hole diameter) to a prohibitive value (>10%) within a few cycles. The fatigue threshold increases with decreasing R-ratio for tension-compression loading, and tension-tension loading is the least severe constant amplitude fatigue load.

Typical aircraft spectra loading were used in References 6.3.4(a), 6.3.4(c) and 6.3.4(d) to investigate the effects of variable amplitude cyclic loading on the fatigue performance of composite bolted joints. The results in Reference 6.3.4(a) show that the specimens survived two lifetimes of a typical vertical stabilizer spectrum loading without fatigue failure. The maximum spectrum load used in these tests ranges from 0.66 to 1.25 times of the static strength. Four loading spectra were tested in Reference 6.3.4(d) to investigate the influence of spectrum profile and load truncation levels. The results of these tests showed no fatigue failure and no distinguishable difference in the fatigue life for the spectrum loading investigated. The maximum spectrum stress was 78% of the static strength and the minimum stress at -49% of the static strength.

An extensive spectrum sensitivity database for bolted composite joints was generated in Reference 6.3.4(c). In this reference, the spectrum parameters investigated included load frequency, spectrum truncation, stress level, extended life, temperature and moisture, and specimen size. With approximately 600 specimens tested in the reference, there were no fatigue failures observed within the composite portion of the bolted joint specimens. This absence of composite fatigue failures confirmed that composite bolted joints are fairly insensitive to fatigue in tension loading at normal operating loads. These results also showed that composite bolted joints are insensitive to fatigue even in severe environments, such as real flight time loads and temperature, and 15 lifetimes of accelerated fatigue at 70% of the static strength in a 250°F (120°C) hot-wet condition. This does not mean that fastener failures have not occurred, sometimes precipitated by composite stiffness or fitup.

6.3.4.2 Influence of joint geometry

The influence of fastener diameter and fastener spacing on the fatigue performance of bolted composite joints is investigated in Reference 6.3.4(d). Three fastener diameters (0.25, 0.375 and 0.5 in. (6.4, 9.5, and 13 mm)) and three fastener spacing-to-diameter ratios (3.0, 4.0 and 6.0) are considered in the investigation. The results indicate that larger spacing to diameter ratio specimens have lower fatigue performance than specimens with lower ratios. The limited amount of data in the reference is not sufficient to draw a general conclusion. However, the results in Reference 6.3.4(d) are presented in terms of gross area stress, the lower fatigue performance of the wider specimens may be caused by the higher loads in the fastener and result in fastener or joint failure.

The fatigue performances of single lap joint and double lap joint are compared in Reference 6.3.4(a). Test results in the reference indicate that the threshold bearing stress value is relatively unaffected by the differences in the two joint configurations.

The effects of bolt bearing/by-pass stress interaction on the fatigue performance is also investigated in Reference 6.3.4(a). Joints with bolt-to-total load ratios of 0.0, 0.2, 0.33 and 1.0 are considered in the reference. The results of these tests show change in failure mode with bolt bearing/by-pass stress ratio. Net section failures were observed for specimens tested with a bolt bearing/by-pass ratio of 0.0 (or open hole). When 20% of the total load was introduced directly as a bearing load, half the specimens suffered a net section failure, and the other half suffered local bearing failures. For the test case where 33% of the total load was presented as the fastener bearing load, the observed failures were local bearing induced excessive hole elongation, similar to the results of full-bearing.

6.3.4.3 Influence of attachment details

The effects of attachment details on the fatigue performance of bolted composite joints are investigated in References 6.3.4(a) and 6.3.4(d). The influence of fastener fit is studied in Reference 6.3.4(d) by considering four levels of hole diameter for controlled over and under size, including slight interference. At applied cyclic load levels greater than 50% of static strength, no significant difference in fatigue performance for the different fastener fits was observed. The specimens were tested at a stress ratio of $R=-1.0$.

The effects of fastener torque on fatigue performance is studied in Reference 6.3.4(a). The results of these tests showed that there was no change in the failure mode and the fatigue performance improved with increased torque. The results also indicated that at low torque levels, hole elongation increased gradually with fatigue cycling and at high torque levels, the cyclic hole elongation rate was very abrupt.

The effect of countersink on joint performance was investigated in Reference 6.3.4(a). When countersunk (100° tension head) steel fasteners were used, approximately half of the tests resulted in fastener failure. The fasteners failed in a tensile mode near the head/shank boundary. Comparing these results with those with protruding head steel fasteners, the effect of the countersink is seen to be earlier elongation at a constant cyclic bearing stress amplitude. It is also seen that the fatigue threshold is lower when countersunk fasteners are used. When countersunk titanium fasteners were used instead of the steel fasteners, fastener failures occurred in every specimen.

6.3.4.4 Influence of laminate lay-up

The effect of laminate lay-up on the joint performance was investigated in Reference 6.3.4(a) by considering three laminate lay-ups--(50/40/10), (70/20/10) and (30/60/10). The results of this investigation indicated that despite the difference in static bearing strength of these laminates, the 10^6 cycle fatigue threshold is approximately equal.

6.3.4.5 Influence of environment

The effects of temperature and moisture are experimentally evaluated in References 6.3.4(a) and 6.3.4(c). The results of these studies indicate that the fatigue threshold may be lower under the hot/wet (218°F/wet (103°C/wet)) condition.

6.3.4.6 Influence of specimen thickness

The effect of laminate thickness on fatigue performance is examined in Reference 6.3.4(d) and the effect of specimen size is evaluated in Reference 6.3.4(c). The results of Reference 4 show that within the thickness of 0.25 to 0.50 inch (6.4 to 13 mm) the fatigue threshold is not significantly affected. In comparing the fatigue performance of small and large scale joints, Reference 6.3.4(c) showed that there is no significant scale up effect.

6.3.4.7 Residual strength

The extensive amount of residual strength data generated in Reference 6.3.4(c) suggested that bolted composite joints have an excellent capability of retaining static strength. This trend is also sup-

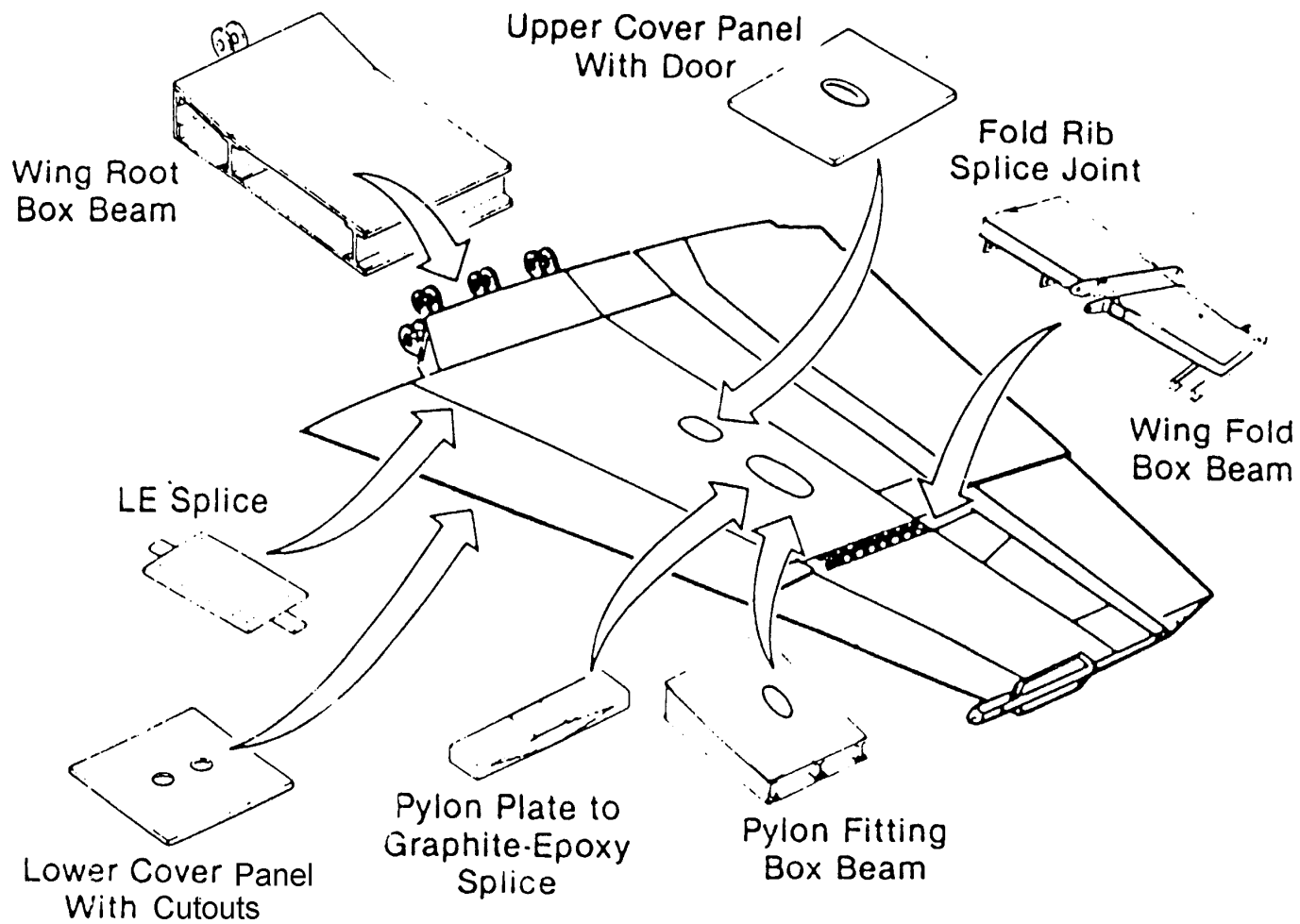
ported by the results of other investigations. The largest percentage of fatigue strength reduction observed in Reference 6.3.4(c), when compared with static strength, was 8%. There were no real time or environmental effects on residual strength reduction that were greater than this. Therefore, a design static tension strength reduction factor is appropriate to account for tension fatigue effects on bolted composite joints under practical service environments.

6.3.5 Test verification

In addition to joint coupon testing which is performed to obtain baseline data, element testing should be performed to verify joint analysis, failure mode, and location. This is particularly important for primary connections and where the load transfer is complex. The purpose of testing is to obtain assurance that the joint behaves in the predicted manner or where analysis is inadequate.

The structural joints to be tested are usually identified early in the design process and are part of the certification process, if the building block approach is used, see Section 2.1.1, Volume 1. The test specimens are classified by levels of complexity as elements, subcomponents, or components. Some examples of types of joints that are tested are shown for a fighter wing structure in Figures 6.3.5(a) and 6.3.5(b).

The bolted joint element or subcomponent tests are usually performed at ambient conditions with sufficient instrumentation to fully characterize load transfer details: direction and amplitude of bolt and by-pass loads. Tests at other than ambient conditions are necessary in cases when the low or elevated temperatures with associated moisture contents substantially change the load distributions.

**FIGURE 6.3.5(a)** *Wing subcomponent tests.*

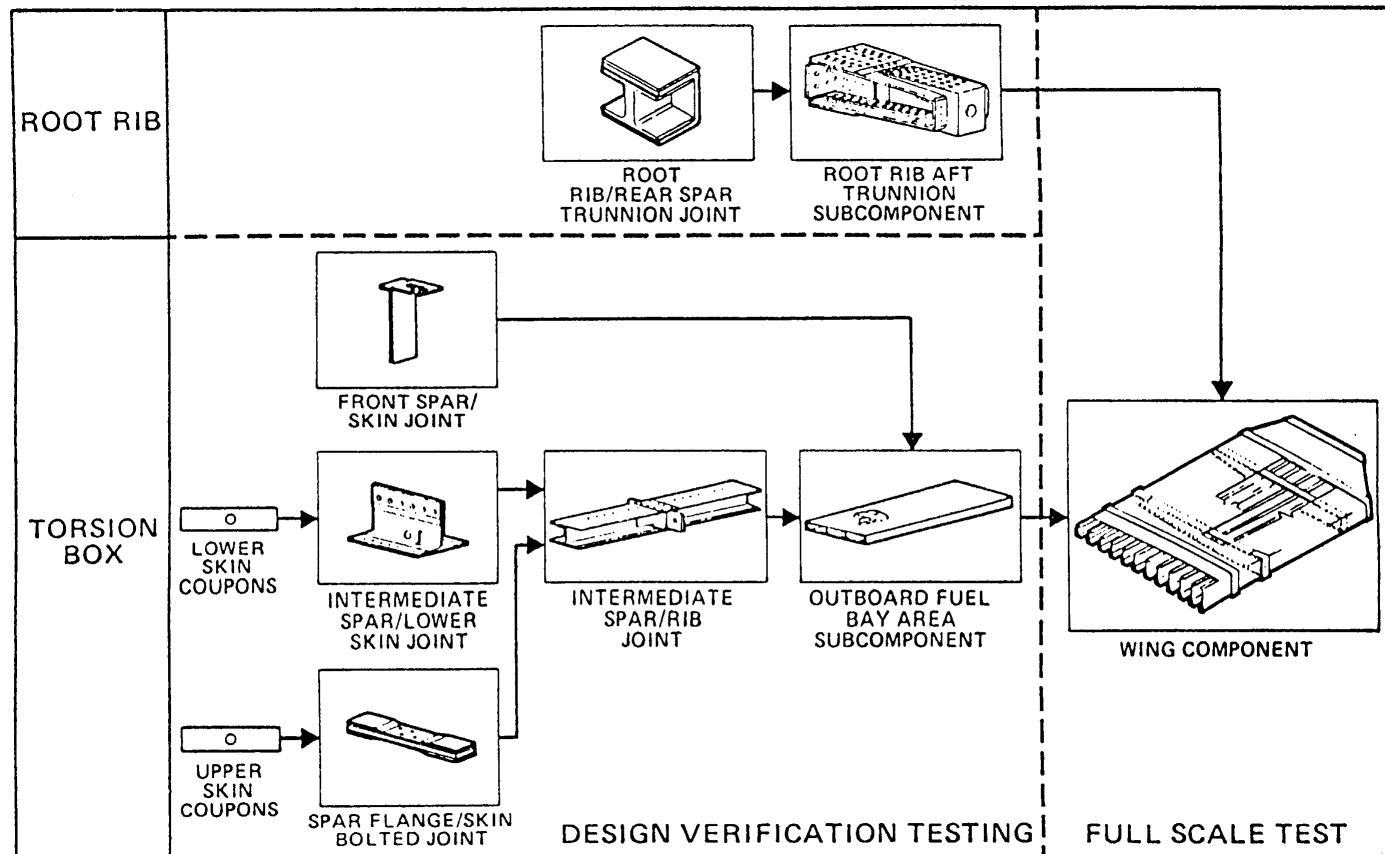


FIGURE 6.3.5(b) Building block approach for the wing structure in the composite wing/fuselage program (Reference 6.3.5).

REFERENCES

- 6.2.1(a) Volkersen, O., "Die Nietkraftverteilung in Zugbeanspruchten Nietverbindungen mit Konstanten Laschenquerschnitten," *Luftfahrtforschung*, Vol 15, 1938, pp. 4-47.
- 6.2.1(b) Goland, M. and Reissner, E., "Stresses In Cemented Joints," *Journal of Applied Mechanics*, Vol 11, 1944, pp. A17-A27.
- 6.2.1(c) Kutscha, D. and Hofer, K., "Feasibility of Joining Advanced Composite Flight Vehicle Structures," Air Force Materials Laboratory Report AFML-TR-68-391, 1968.
- 6.2.1(d) Dickson, J.N., Hsu, T.N., and McSkinney, J.N., "Development of an Understanding of the Fatigue Phenomena of Bonded and Bolted Joints In Advanced Filamentary Composite Materials, Volume I, Analysis Methods," Lockheed Georgia Aircraft Company, USAF Contract Report AFFDL-TR 72-64, Volume I, June 1972.
- 6.2.1(e) Grimes, G.C., Wah, T., et al, "The Development of Non-Linear Analysis Methods for Bonded Joints in Advanced Filamentary Composite Structures," Southwest Research Institute, USAF Contract Report AFML-TR-72-97, September 1972.
- 6.2.1(f) Renton, W.J., "The Analysis and Design of Composite Materials Bonded Joints Under Static and Fatigue Loadings," PhD Thesis, University of Delaware, 1973.
- 6.2.1(g) Renton, W.J. and Vinson, J.R., "The Analysis and Design of Composite Materials Bonded Joints under Static and Fatigue Loadings," Air Force Office of Scientific Research Report TR-73-1627, 1973
- 6.2.1(h) Oplinger, D.W., "Stress Analysis of Composite Joints," *Proceedings of 4th Army Materials Technology Conference*, Brook Hill Publishing Co., Newton MA, 1975, pp 405-51.
- 6.2.1(i) Hart-Smith, L.J., AFFDL-TR-72-130, pp 813-856.
- 6.2.1(j) Hart-Smith, L.J., "Adhesive Bonded Double Lap Joints," NASA Langley Contractor Report NASA CR-112235 1973.
- 6.2.1(k) Hart-Smith, L.J., "Adhesive Bonded Single Lap Joints," NASA Langley Contractor Report NASA CR-112236, 1973.
- 6.2.1(l) Hart-Smith, L.J., "Adhesive Bonded Scarf and Stepped-Lap Joints," NASA Langley Contractor Report NASA CR-112237, 1973.
- 6.2.1(m) Hart-Smith, L.J., "Analysis and Design of Advanced Composite Bonded Joints," NASA Langley Contractor Report NASA CR-2218, 1973.
- 6.2.1(n) Hart-Smith, L.J., "Advances in the Analysis and Design of Adhesive-Bonded Joints in Composite Aerospace Structures," *SAMPE Process Engineering Series*, Vol 19, SAMPE, Azusa, 1974, pp 722-737.
- 6.2.1(o) *Primary Adhesively Bonded Structure (PABST) Technology*, Air Force Contract F33615-75-C-3016, 1975.
- 6.2.1(p) Thrall, E.W., "Primary Adhesively Bonded Structure Technology (PABST) Phase 1b: Preliminary Design," Air Force Flight Dynamics Laboratory Report AFFDL-TR-76-141, 1976.

Volume 3, Chapter 6 Structural Behavior of Joints

- 6.2.1(q) Shannon, R.W., et al, "Primary Adhesively Bonded Structure Technology (PABST) General Material Property Data," Air Force Flight Dynamics Laboratory Report AFFDL-TR-77-101 1977.
- 6.2.1(r) Land, K.L., Lennert, F.B., et al, "Primary Adhesively Bonded Structure Technology (PABST): Tooling, Fabrication and Quality Assurance Report," USAF Technical Report AFFDL-TR-79-3154, October 1979.
- 6.2.1(s) Hart-Smith, L.J., "Adhesive Bond Stresses and Strains at discontinuities and Cracks in Bonded Structures," *Transactions of the ASME, Journal of Engineering Materials and Technology*, Vol 100, January 1978, pp. 15-24.
- 6.2.1(t) Hart-Smith, L.J., "Differences Between Adhesive Behavior in Test coupons and Structural Joints," Douglas Aircraft Company paper 7066, Presented to ASTM Adhesives Committee D-14 Meeting, Phoenix, Arizona, 1981.
- 6.2.1(u) Hart-Smith, L.J., "Design Methodology for Bonded-Bolted Composite Joints," Douglas Aircraft Company, USAF Contract Report AFWAL-TR-81-3154, Vol I and II, February 1982.
- 6.2.1(v) Thrall, E.W., Jr., "Failures in Adhesively Bonded Structures," AGARD-NATO Lecture Series No. 102, "Bonded Joints and Preparation for Bonding," Oslo, Norway, and The Hague, Netherlands, April 1979 and Dayton, Ohio, October 1979.
- 6.2.1(w) Hart-Smith, L.J., "Further Developments in the Design and Analysis of Adhesive-Bonded Structural Joints," Douglas Aircraft Co. Paper No. 6922, presented at the ASTM Symposium on Joining of Composite Materials, Minneapolis MN April 1980
- 6.2.1(x) Hart-Smith, L.J., "Adhesive Bonding of Aircraft Primary Structures," Douglas Aircraft Company Paper 6979, Presented to SAE Aerospace Congress and Exposition, Los Angeles, California, October 1980.
- 6.2.1(y) Hart-Smith, L.J., "Stress Analysis: A Continuum Analysis Approach" in *Developments in Adhesives - 2*, ed. A. J. Kinloch, Applied Science Publishers, England, 1981, pp. 1-44.
- 6.2.1(z) Hart-Smith, L.J., "Effects of Adhesive Layer Edge Thickness on Strength of Adhesive-Bonded Joints" Quarterly Progress Report No. 3, Air Force Contract F33615-80-C-5092, 1981.
- 6.2.1(aa) Hart-Smith, L.J., "Effects of Flaws and Porosity on Strength of Adhesive-Bonded Joints" Quarterly Progress Report No. 5, Air Force Contract F33615-80-C-5092, 1981.
- 6.2.1(ab) Hart-Smith, L.J. and Bunin, B.L., "Selection of Taper Angles for Doublers, Splices and Thickness Transition in Fibrous Composite Structures," *Proceedings of 6th Conference On Fibrous Composites in Structural Design*, Army Materials and Mechanics Research Center Manuscript Report AMMRC MS 83-8, 1983.
- 6.2.1(ac) Nelson, W.D., Bunin, B.L., and Hart-Smith, L.J., "Critical Joints in Large Composite Aircraft Structure," *Proceedings of 6th Conference On Fibrous Composites in Structural Design*, Army Materials and Mechanics Research Center Manuscript Report AMMRC MS 83-8, 1983.
- 6.2.1(ad) Oplinger, D.W., "A Layered Beam Theory for Single Lap Joints," U.S. Army Materials Technology Laboratory Report MTL TR 91-23, 1991.
- 6.2.1(ae) Oplinger, D.W., "Effects of Adherend Deflections on Single Lap Joints," *Int. J. Solids Structures*, Vol 31, No. 18, 1994, pp. 2565-2587.

- 6.2.2.1(a) Hart-Smith, L.J., "Adhesively Bonded Joints in Fibrous Composite Structures," Douglas Aircraft Paper 7740; presented to the International Symposium on Joining and Repair of Fibre-Reinforced Plastics, Imperial College, London, 1986.
- 6.2.2.1(b) Hart-Smith, L.J., "Induced Peel Stresses in Adhesive-Bonded Joints," Douglas Aircraft Company, Technical Report MDC-J9422A, August 1982.
- 6.2.2.6(a) Hart-Smith, L.J., Brown, D. and Wong, S., "Surface Preparations for Ensuring that the Glue will Stick in Bonded Composite Structures," *10th DoD/NASA/FAA Conference on Fibrous Composites in Structural Design*, Hilton Head Is, SC, 1993.
- 6.2.2.6(b) Hart-Smith, L.J., Ochsner, W., and Radecky, R.L., "Surface Preparation of Fibrous Composites for Adhesive Bonding or Painting," *Douglas Service Magazine*, First quarter 1984, pp 12-22.
- 6.2.2.6(c) Hart-Smith, L.J., Ochsner, W., and Radecky, R.L., "Surface Preparation of Fibrous Composites for Adhesive Bonding or Painting," *Canadair Service News*, Summer 1985, 1985, pp. 2-8.
- 6.2.2.7(a) Frazier, T.B. and Lajoie, A.D., "Durability of Adhesive Joints," Air Force Materials Laboratory Report AFML TR-74-26, Bell Helicopter Company, 1974.
- 6.2.2.7(b) Becker, E.B., et al, "Viscoelastic Stress Analysis Including Moisture Diffusion for Adhesively Bonded Joints," Air Force Materials Laboratory Report AFWAL-TR-84-4057, 1984.
- 6.2.2.7(c) Jurf, R. and Vinson, J., "Effects of Moisture on the Static and Viscoelastic Shear Properties of Adhesive Joints," Dept. of Mechanical and Aerospace Engineering Report MAE TR 257, University of Delaware, 1984.
- 6.2.2.7(d) Mostovoy, S., Ripling, E.J., and Bersch, C.F., "Fracture Toughness of Adhesive Joints," *J. Adhesion*, Vol 3, 1971, pp. 125-44.
- 6.2.2.7(e) DeVries, K.L., Williams, M.L., and Chang, M.D., "Adhesive Fracture of a Lap Shear Joint," *Experimental Mechanics*, Vol 14, 1966, pp 89-97.
- 6.2.2.7(f) Trantina, G.G. "Fracture Mechanics Approach to Adhesive Joints," University of Illinois Dept. of Theoretical and Applied Mechanics Report T&AM 350, Contract N00019-71-0323, 1971.
- 6.2.2.7(g) Trantina, G.G., "Combined Mode Crack Extension in Adhesive Joints," University of Illinois Dept. of Theoretical and Applied Mechanics Report T&AM 350, Contract N00019-71-C-0323, 1971.
- 6.2.2.7(h) Keer, L.M., "Stress Analysis of Bond Layers," *Trans. ASME J. Appl. Mech.*, Vol 41, 1974, pp 679-83.
- 6.2.2.7(i) Knauss, J.F., "Fatigue Life Prediction of Bonded Primary Joints," NASA Contractor Report NASA-CR-159049, 1979.
- 6.2.2.7(j) Wang, S.S. and Yau, J.F., "Analysis of Interface Cracks in Adhesively Bonded Lap Shear Joints," NASA Contractor Report NASA-CR-165438, 1981.
- 6.2.2.7(k) Johnson, W.S. and Mall, S., "A Fracture Mechanics Approach for Designing Adhesively Bonded Joints".

Volume 3, Chapter 6 Structural Behavior of Joints

- 6.2.3.6 Oplinger, D.W. "Effects of Mesh Refinement on Finite Element Analysis of Bonded Joints," U.S. Army Research Laboratory Study (Unpublished), 1983.
- 6.3.1 Whitman, B., Shyprikevich, P., and Whiteside, J.B., "Design of the B-1 Composite Horizontal Stabilizer Root Joint," *Third NASA/USAF Conference on Fibrous Composites in Flight Vehicles Design*, Williamsburg, VA, November 4-6, 1976.
- 6.3.2.1(a) Ramkumar, R.L., Saether, E.S., Appa, K., "Strength Analysis of Laminated and Metallic Plates Bolted Together by Many Fasteners," AFWAL-TR-86-3034, July, 1986.
- 6.3.2.1(b) Xiong, Y. and Poon, C., "A Design Model for Composite Joints with Multiple Fasteners," National Research Council, Canada, IAR-AN-80, August 1994.
- 6.3.2.1(c) Griffin, O.H., et. al., "Analysis of Multifastener Composite Joints," *Journal of Spacecraft and Rockets*, Vol 31, No. 2, March-April 1994.
- 6.3.2.1(d) ACEE Composite Structures Technology, *Papers by Douglas Aircraft Company*, ed. M. Klotzsche, NASA-CR-172359, August 1984.
- 6.3.2.2(a) Whitney, J.M. and Nuismer, R.J., "Stress Fracture Criteria for Laminated Composites Containing Stress Concentrations," *J. Composite Materials*, Vol 8, July, 1974, pp. 235-265.
- 6.3.2.2(b) Hart-Smith, J., "Mechanically-Fastened Joints for Advanced Composites Phenomenological Considerations and Simple Analysis," *Fibrous Composites in Structural Design*, ed. Edward M. Lenoe, Donald W. Oplinger, John J. Burke, Plenum Press, 1980.
- 6.3.2.2(c) Chang, F., Scott, R.A., Springer, G.S., "Strength of Mechanically Fastened Composite Joints," Air Force Wright Aeronautical Laboratories Technical Report AFWAL-TR-82-4095.
- 6.3.2.2(d) Lekhnitskii, S.G., *Anisotropic Plates*, Gordon and Breach Science Publishers, New York, 1968.
- 6.3.2.2(e) Oplinger, D.W., "On the Structural Behavior of Mechanically Fastened Joints" in *Fibrous Composites in Structural Design*, ed. Edward M. Lenoe, Donald W. Oplinger, John J. Burke, Plenum Press, 1980.
- 6.3.2.2(f) Crews, J.H., and Naik, R.A., "Combined Bearing and Bypass Loading on a Graphite/Epoxy Laminate," *Composite Structures*, Vol 6, 1968, pp. 21-40.
- 6.3.2.2(g) Garbo, S.P. and Ogonowski, J.M., "Effect of Variances and Manufacturing Tolerances on the Design Strength and Life of Mechanically Fastened Composite Joints, Volume 3 - Bolted Joint Stress Field Model (BJSFM) Computer Program User's Manual," Air Force Wright Aeronautical Laboratories Technical Report AFWAL-TR-81-3041, April 1981.
- 6.3.2.2(h) Ramkumar, R.L., Saether, E.S., and Appa, K., "Strength Analysis of Laminated and Metallic Plates Bolted Together by Many Fasteners," Air Force Wright Aeronautical Laboratories Technical Report AFWAL-TR-86-3034, July 1986.
- 6.3.2.2(i) Chang, F., Scott, R.A., and Springer, G.S., "Strength of Bolted Joints in Laminated Composites," Air Force Wright Aeronautical Laboratories Technical Report AFWAL-TR-84-4029.
- 6.3.2.2(j) Hoehn, G., "Enhanced Analysis/Design Methodology Development for High Load Joints and Attachments for Composite Structures," Naval Air Development Center Technical Report.

Volume 3, Chapter 6 Structural Behavior of Joints

- 6.3.2.2(k) Bohlmann, R.E., Renieri, G.D., Horton, D.K., "Bolted Repair Analysis Methodology," Naval Air Development Center Technical Report NADC-81063-60, Dec. 1982.
- 6.3.2.2(l) Harris, H.G., Ojalvo, I. U., and Hooson, R.E., "Stress and Deflection Analysis of Mechanically Fastened Joints," Air Force Flight Dynamics Laboratory Technical Report AFFDL-TR-70-49, May 1970.
- 6.3.2.3(a) Ramkumar, R.L., Saether, E.S., Cheng, D., "Design Guide for Bolted Joints in Composite Structures," Air Force Wright Aeronautical Report AFWAL-TR-86-3035, March 1986.
- 6.3.2.3(b) Cohen, D., Hyer, M. W., Shuart, M. J., Griffin, O. H., Prasad, C., Yalamanchili, S. R., "Failure Criterion for Thick Multifastener Graphite-Epoxy Composite Joints," *Journal of Composites Technology & Research*, JCTRER, Vol . 17, No. 3, July 1995, pp. 237-248.
- 6.3.4(a) Ramkumar, R.L., and Tossavainen, E.W., "Bolted Joints in Composite Structures: Design, Analysis and Verification, Task I Test Results--Single Fastener Joints," AFWAL-TR-84-3047, August 1984.
- 6.3.4(b) Garbo, S.P., and Ogonowski, J.M., "Effects of Variances and Manufacturing Tolerances on the Design Strength and Life of Mechanically Fastened Composite Joints," Vol 1, 2 and 3, AFWAL-TR-81-3041, April 1981.
- 6.3.4(c) Jeans, L.L., Grimes, G.C., and Kan, H.P., "Fatigue Spectrum Sensitivity Study for Advanced Composite Materials, Volume I - Technical Summary," AFWAL-TR-80-3130, Vol I, December 1980.
- 6.3.4(d) Walter, R.W., and Tuttle, M.M., "Investigation of Static and Cyclic Failure Mechanisms for GR/EP Laminates," *Proceedings of the Ninth DoD/NASA/FAA Conference on Fibrous Composites in Structural Design*, DOT/FAA/CT-92-25, September 1992, p. I-167.
- 6.3.4(e) Walter, R.W., and Porter, T.R., "Impact of Design Parameters on Static, Fatigue and Residual Strength of GR/EP Bolted Joints," *Proceedings of the Tenth DoD/NASA/FAA Conference on Fibrous Composites in Structural Design*, NAWCADWAR-94096-60, p. III-75, April 1994.
- 6.3.5 Whitehead, R.S., et al., "Composite Wing/Fuselage Program," AFWAL-TR-883098, Vol 1-4., February, 1989.

This page intentionally left blank

CHAPTER 7 DAMAGE RESISTANCE, DURABILITY, AND DAMAGE TOLERANCE

7.1 OVERVIEW AND GENERAL GUIDELINES

7.1.1 Principles

Engineered structures must be capable of performing their function throughout a specified lifetime while meeting safety and economic objectives. These structures are exposed to a series of events that include loading, environment, and damage threats. These events, either individually or cumulatively, can cause structural degradation, which, in turn, can affect the ability of the structure to perform its function.

In many instances, uncertainties associated with existing damage as well as economic considerations necessitate a reliance on inspection and repair programs to ensure the required structural capability is maintained. The location and/or severity of manufacturing flaws and in-service damage can be difficult to anticipate for a variety of reasons. Complex loading and/or structural configurations result in secondary load paths that are not accurately predicted during the design process. Some manufacturing flaws may not be detectable until the structure is exposed to the service environment. For example, joints with contaminated surfaces during bonding may not be detectable until the weak bond further deteriorates in service. The numerous variables associated with damage threats (e.g., severity, frequency, and geometry) are rarely well defined until service data is collected. Moreover, established engineering tools for predicting damage caused by well-defined damage events often do not exist. Economic issues can include both non-recurring and recurring cost components. The large number of external events, combined with the interdependence of structural state, structural response, and external event history, can result in prohibitive non-recurring engineering or test costs associated with explicitly validating structural capability under all anticipated conditions. Moreover, large weight-related recurring costs associated with many applications rule out the use of overly conservative, but simpler approaches.

The goal in developing an inspection plan is to detect, with an acceptable level of reliability, any damage before it can reduce structural capability below the required level. To accomplish this, inspection techniques and intervals for each location in the structure must be selected with a good understanding of damage threats, how quickly damage will grow, the likelihood of detection, and the damage sizes that will threaten structural safety. To avoid costs associated with excessive repairs, inspection methods should also quantify structural degradation to support accurate residual strength assessments.

This concept of combining an inspection plan with knowledge of damage threats, damage growth rates and residual strength is referred to as “damage tolerance”. Specifically, *damage tolerance is the ability of a structure to sustain design loads in the presence of damage caused by fatigue, corrosion, environment, accidental events, and other sources until such damage is detected, through inspections or malfunctions, and repaired.*

Durability considerations are typically combined with damage tolerance to meet economic and functionality objectives. Specifically, *durability is the ability of a structural application to retain adequate properties (strength, stiffness, and environmental resistance) throughout its life to the extent that any deterioration can be controlled and repaired, if there is a need, by economically acceptable maintenance practices.* As implied by the two definitions, durability addresses largely economic issues, while damage tolerance has a focus on safety concerns. For example, durability often addresses the onset of damage from the operational environment. Under the principles of damage tolerance design, the small damages associated with initiation may be difficult to detect, but do not threaten structural integrity.

7.1.2 Composite-related issues

All structural applications should be designed to be damage tolerant and durable. In using composite materials, a typical design objective is to meet or exceed the design service and reliability objectives of the same structure made of other materials, without increasing the maintenance burden. The generally good fatigue resistance and corrosion suppression of composites, help meet such objectives. However,

the unique characteristics of composite materials also provide some significant challenges in developing safe, durable structure.

The brittle nature of some polymer resins causes concern about their ability to resist damage and, if damaged, their ability to carry the required loads until the damage is detected. While the primary concerns in metal structure relate to tension crack growth and corrosion, other damages, such as delamination and fiber breakage resulting from impact events and environmental degradation are more of a concern in polymer matrix composites. In addition, composites have unique damage sensitivities for compression and shear loading, as well as tension.

In composite structure, the damage caused by an impact event is typically more severe and can be less visible than in metals. As a result of the increased threat of an immediate degradation in properties, another property, damage resistance, has been used for composite structures and material evaluation. *Damage resistance is a measure of the relationship between parameters which define an event, or envelope of events (e.g., impacts using a specified impactor and range of impact energies or forces), and the resulting damage size and type.*

Damage resistance and damage tolerance differ in that the former quantifies the damage caused by a specific damage event, while the latter addresses the ability of the structure to tolerate a specific damage condition. Damage resistance, like durability, largely addresses economic issues (e.g., how often a particular component needs repair), while damage tolerance addresses safe operation of a component.

Optimally balancing damage resistance and damage tolerance for a specific composite application involves considering a number of technical and economic issues early in the design process. Damage resistance often competes with damage tolerance during the design process, both at the material and structural level. In addition, material and fabrication costs, as well as operational costs associated with inspection, repair, and structural weight, are strongly influenced by the selected material and structural configuration. For example, toughened-resin material systems typically improve damage resistance relative to untoughened systems, which results in reduced maintenance costs associated with damage from low-severity impact events. However, these cost savings compete with the higher per-pound material costs for the toughened systems. In addition, these materials can also result in lower tensile capability of the structure with large damages or notches, which might require the addition of material to satisfy structural capability requirements at Limit Load. This extra material and associated weight results in higher material and fuel costs, respectively.

7.1.3 General guidelines

There are a large number of factors that influence damage resistance, durability and damage tolerance of composite structures. In addition, there are complex interactions between these factors which can lead to non-intuitive results, and often a change in a factor can improve one of the areas of damage resistance, durability, or damage tolerance, while degrading the other two. It is important for a developer of a composite structure to understand these factors and their interactions as appropriate to the structure's application in order to produce a balanced design that economically meets all of the design criteria. For these reasons, this chapter contains detailed discussions of influencing factors and design guidelines in each of the areas of damage resistance, durability, and damage tolerance (Sections 7.5 through 7.8). The following paragraphs outline some of the areas where significant and important interactions occur. The intent is to highlight these items that involve areas of several of the following detailed information sections.

- An important part of a structural development program is to determine the damages that the structure is capable of carrying at the various required load levels (ultimate, limit, etc.). This information can be used to develop appropriate maintenance, inspection and real-time monitoring techniques to ensure safety. The focus of damage tolerance evaluations should be on ensuring safety in the event of "rogue" and "unanticipated" events, not solely on likely scenarios of damage.

- The damage tolerance approach involves the use of inspection procedures and structural design concepts to protect safety, rather than the traditional factors of safety used for Ultimate Loads. The overall damage tolerance database for a structure should include information on residual strength characteristics, sensitivities to damage growth and environmental degradation, maintenance practices, and in-service usage parameters and damage experiences.
- Fiber and matrix materials, material forms, and fabrication processes are constantly changing. This requires a strong understanding of the durability and damage tolerance principles, the multitude of parameter interactions, and an intelligent, creative adaptation of them to achieve durability and safety goals. Also, new materials and material forms may have significantly different responses than exhibited by previous materials and structures (i.e., "surprises" will occur). Therefore, the information and guidelines based on previous developments should not be blindly followed.
- Focusing strictly on meeting regulatory requirements will not ensure economical maintenance practices are established. For example, the Ultimate Load requirements for barely visible impact damage, BVID, in critical locations (see FAR 23.573, AC 20-107A, etc.) result in insufficient data to define allowable damage limits (ADLs) in higher-margin areas. Similarly, demonstrating compliance for discrete source damage requirements typically involves showing adequate structural capability with large notches at critical locations. Neither of these requirements ensure safe maintenance inspection practices are established to find the least detectable, yet most severe defect (i.e., those reducing structural capability to Limit Loads). As a result the supporting databases should not be limited to these conditions. An extensive residual strength database addressing the full range of damage variables and structural locations is needed to provide insights on ADLs for use in Structural Repair Manuals. For example, clearly visible damage may be acceptable (i.e., below the ADLs) away from stiffening elements and in more lightly loaded portions of the structure. A more extensive characterization of the residual strength curves for each characteristic damage type (impact, holes, etc.) will also help define damage capable of reducing strength to Limit Load.
- Well-defined inspection procedures that (a) quantify damage sufficiently to assess compliance with Allowable Damage Limits (ADLs) and (b) reliably find damage at the Critical Damage Threshold (CDT), discussed in Section 7.2.1, will help provide maintenance practices which are as good or better than those used for metal structure. Clearly defined damage metrics facilitate quantitative inspection procedures, which can be used to define the structural response of the detected damage.
- Currently, most initial inspections of composite structure have involved visual methods. Therefore, dent depth has evolved as a common damage metric. Development efforts should define the dent depths that correspond to the threshold of detectability for both general visual (surveillance in Boeing terminology) and detailed visual levels. The influence of dent-depth decay, which can come from viscoelastic and other material or structural behaviors, must be considered for maintenance inspection procedures and the selection of damage that will be used to demonstrate compliance.
- Another factor motivating a more complete characterization of damage and structural variables is that the internal damage state for a specific structural detail is not a unique function of the dent depth. It is a complex function of the impact variables (i.e., impactor geometry, energy level, angle of incidence, etc.). A range of these variables should be evaluated to understand the relationship between them and to determine the combinations that result in the largest residual strength degradation.
- Structure certified with an approach that allows for damage growth must have associated in-service inspection techniques, which are capable of adequately detecting damage before it becomes critical. These inspection methods should be demonstrated to be economical before committing to such a certification approach. In addition, the damage growth must be predictable such that inspection intervals can be reliably defined.

7.1.4 Section organization

This chapter of the handbook addresses the multitude of issues associated with the damage resistance, durability, and damage tolerance of composite materials. Discussions are heavily reliant on experience gained in the aircraft industry, since it represents the area where composites and damage tolerant philosophy have been most used. As the associated composite technologies continue to evolve, additional applications and service history should lead to future updates with a more complete understanding of: (1) potential damage threats, (2) methods to achieve the desired reliability in a composite design, and (3) improved design and maintenance practices for damage tolerance.

Section 7.2 focuses on the requirements for military and civilian aviation applications, as well as methods of compliance. Discussion of the characteristics of various types of composite damage and a list of possible sources of the damage are given in Section 7.3. Composite damage inspection methods and their limitations are discussed in Section 7.4. Sections 7.1 through 7.4 are relatively mature in their content.

Sections 7.5 through 7.8, which comprise the bulk of this section, address the major material and structural responses: damage resistance, durability, damage growth under cyclic loading, and residual strength, respectively. Each section includes detailed discussions of: (a) the major factors that affect response; (b) design-related issues and guidelines for meeting objectives and requirements; (c) testing methods and issues; and (d) analytical predictive methods, their use, and their success at predicting observed responses.

At this point in time, not all parts of Sections 7.5 through 7.8 are complete. Section 7.5, Damage Resistance, currently contains information on influencing factors and guidelines; sections on test and analysis methods will be added in the future. Section 7.6, Durability, currently contains only limited information. Future updates will complete this section. Section 7.7, Damage Growth Under Cyclic Loading, contains some limited information on the growth of impact damages. Additional parts of this section will be added in the future. Section 7.8, Residual Strength, contains extensive information on influencing factors, guidelines and analysis methods; the section on test methods will be added in the future.

Section 7.9 includes several examples of successful damage-tolerant designs from a number of composite aircraft applications. These examples illustrate how different aspects of damage tolerance come to the forefront as a function of application.

7.2 AIRCRAFT DAMAGE TOLERANCE

Damage tolerance provides a measure of the structure's ability to sustain design loads with a level of damage or defect and be able to perform its operating functions. Consequently, the concern with damage tolerance is ultimately with the damaged structure having adequate residual strength and stiffness to continue in service safely until the damage can be detected by scheduled maintenance inspection (or malfunction) and be repaired or until the life limit is reached. The extent of damage and detectability determines the required load level to be sustained. Thus, safety is the primary goal of damage tolerance.

Damage tolerance methodologies are most mature in the military and civil aircraft industry. They were initially developed and used for metallic materials, but have more recently been extended and applied to composite structure. The damage tolerance philosophy has been included in regulations since the 1970's. It evolved out of the "Safe Life" and "Fail Safe" approaches (Reference 7.2).

The safe-life approach ensures adequate fatigue life of a structural member by limiting its allowed operational life. During its application to commercial aircraft in the 1950's, this approach was found to be uneconomical in achieving acceptable safety, since a combination of material scatter and inadequate fatigue analyses resulted in the premature retirement of healthy components. The approach is still used today in such structures as high-strength steel landing gear. Due to the damage sensitivities and relatively flat fatigue curves of composite materials, a safe-life approach is not considered appropriate.

The fail-safe approach assumes members will fail, but forces the structure to contain multiple load paths by requiring specific load-carrying capability with assumed failures of one or more structural elements. This approach achieved acceptable safety levels more economically, and, due to the relative severity of the assumed failures, was generally effective at providing sufficient opportunity for timely detection of structural damage. Its redundant-load-path approach also effectively addressed accidental damage and corrosion. However, the method does not allow for explicit limits on the maximum risk of structural failure, and it does not demonstrate that all partial failures with insufficient residual strength are obvious. Moreover, structural redundancy is not always efficient in addressing fatigue damage, where similar elements under similar loading would be expected to have similar fatigue-induced damage.

7.2.1 Evolving military and civil aviation requirements

The “duration of damage or defect” factor based on degree of detectability has been the basis for establishing minimum Air Force damage tolerance residual strengths for composite structures in requirements proposed for inclusion in AFGS-87221, “General Specification for Aircraft Structures”. These strength requirements are identical to those for metal structure having critical defects or damage with a comparable degree of detectability. Requirements for cyclic loading prior to residual strength testing of test components are also identical. The non-detectable damage to be assumed includes a surface scratch, a delamination and impact damage. The impact damage includes both a definition of dent depth, i.e., detectability, and a maximum energy cutoff. Specifically, the impact damage to be assumed is that “caused by the impact of a 1.0 inch (25 mm) diameter hemispherical impactor with a 100 ft-lb (136 N-m) of kinetic energy, or that kinetic energy required to cause a dent 0.10 inch (2.54 mm) deep, whichever is least.” For relatively thin structure, the detectability, i.e., the 0.1 inch (2.5 mm) depth, requirement prevails. For thicker structure, the maximum assumed impact energy becomes the critical requirement. This will be illustrated in Section 7.5. The associated load to be assumed is the maximum load expected to occur in an extrapolated 20 lifetimes. This is a one-time static load requirement. These requirements are coupled with assumptions that the damage occurs in the most critical location and that the assumed load is coincident with the worst probable environment.

In developing the requirements, the probability of undetected or undetectable impact damage occurring above the 100 ft-lb (136 N-m) energy level was considered sufficiently remote that when coupled with other requirements a high level of safety was provided. For the detectability requirement, it is assumed that having damage greater than 0.10 inch (2.5 mm) in depth will be detected and repaired. Consequently, the load requirement is consistent with those for metal structure with damage of equivalent levels of detectability. Provisions for multiple impact damage, analogous to the continuing damage considerations for metal structure, and for the lesser susceptibility of interior structure to damage are also included.

In metal structure, a major damage tolerance concern is the growth of damage prior to the time of detection. Consequently, much development testing for metals has been focused on evaluating crack growth rates associated with defects and damage, and the time for the defect/damage size to reach residual strength criticality. Typically, the critical loading mode has been in tension. Crack growth, even at comparatively low stress amplitudes, may be significant. In general, damage growth rates for metals are consistent and, after test data has been obtained, can be predicted satisfactorily for many different aircraft structural configurations. Thus, knowing the expected stress history for the aircraft, inspection intervals have been defined that confidently ensure crack detection before failure.

By contrast, composites have unique damage sensitivities for both tension and compression loads. However, the fibers in composite laminates act to inhibit tensile crack growth, which only occurs at relatively high stress levels. Consequently, through the thickness damage growth, which progressively breaks the fibers in a composite, has generally not been a problem. In studying the effects of debonds, delaminations or impact damage, the concern becomes compression and shear loads where local instabilities may stimulate growth. Unlike cracks in metal, growth of delaminations or impact damage in composites may not be detected using economical maintenance inspection practices. In many cases, the degraded performance of composites with impact damage also cannot be predicted satisfactorily. Hence, there is a greater dependence on testing to evaluate composite residual strength and damage growth

under cyclic loads. In the absence of predictive tools for growth, design values are typically established with sufficient margins to ensure that damage growth due to repeated loads will not occur. This method for avoiding the potential growth of damage in design and certification is known as the "no-growth" approach. It has been practical for most composite designs, which have proved to be fatigue insensitive at typical design stress levels.

The damage tolerance design procedures for civil/commercial aircraft are expressed more generally but with equal effectiveness. Civil aviation requirements are addressed in Federal Aviation Regulations (FAR) 23.573, 25.571, 27.571, 29.571 and Joint Airworthiness Requirements (JAR) 25.571. Advisory Circular 20-107A and ACJ 25.603 provide means of compliance with the regulations concerning composite material structure. Advisory Circular AC25.571-1 (rev. B was issued 2/18/97) provides means of compliance with provision of FAR Part 25 dealing with damage tolerance and fatigue life (25.571). Unlike military requirements, civil/commercial ones do not recommend any energy level or detectability thresholds. In fact, they do not assume the inspections will be visual. Relative to impact damage, it is stated in the FAA guidelines in AC20-107A, Paragraph 6.g. "It should be shown that impact damage that can be realistically expected from manufacturing and service, but not more than the established threshold of detectability for the selected inspection procedure, will not reduce the structural strength below Ultimate Load capability. This can be shown by analysis supported by test evidence, or by tests at the coupon, element, or subcomponent level." This guidance is to ensure that structure with barely detectable impact damage will still meet ultimate strength requirements. A similar wording to the above has been added to FAR 23.573. In practice, visual inspections are most often used for initial detection. It is important to consider lighting conditions when determining visibility. Dent depth thresholds are typically used to quantify visibility, with typical values being 0.01 to 0.02 inches (0.25 to 0.50 mm) for tool-side impacts and 0.05 inches (1.3 mm) for bag-side impacts.

It is also stated in 7.a(2) of AC 20-107A "The extent of initially detectable damage should be established and be consistent with the inspection techniques employed during manufacture and in service. Flaw/damage growth data should be obtained by repeated load cycling of intrinsic flaws or mechanically introduced damage." And, in 7.a.(3) of AC 20-107A, it is stated "The evaluation should demonstrate that the residual strength of the structure is equal to or greater than the strength required for the specified design loads (considered as ultimate)." This guidance is to ensure that visible impact damage (VID) will be detected in a timely manner and will be repaired before strength is reduced below Limit Load capability. Damage such as runway debris, which may not be immediately obvious, would likely be considered as VID. The difference in the Air Force specification and the FAA guideline is primarily in the residual strength value. Also, while the Air Force specification assumes visual inspection, the FAA guideline leaves the inspection method to be selected. Consequently, since specifications and guidelines differ with the type of aircraft, the manufacturer must be aware of the differences and apply those guidelines and specifications appropriate to the situation.

The FAA guidelines for discrete source damage are stated in 8.b of AC 25.571-1A. They state that "The maximum extent of immediately obvious damage from discrete sources (§ 25.571(e)) should be determined and the remaining structure shown, with an acceptable level of confidence, to have static strength for the maximum load (considered as Ultimate Load) expected during completion of the flight." It is stated in 8.c.(2) of AC 25.571-1A "(2) Following the incident: Seventy percent (70%) limit flight maneuver loads and, separately, 40 percent of the limit gust velocity (vertical or lateral) at the specified speeds, each combined with the maximum appropriate cabin differential pressure (including the expected external aerodynamic pressure)." The discrete sources listed in 25.571(e) are as follows: (1) Impact with a 4-pound bird; (2) Uncontained fan blade impact; (3) Uncontained engine failure; or (4) Uncontained high energy rotating machinery failure. These high-energy sources are likely to penetrate structures. Damage from a discrete source that is not immediately obvious must be considered as VID with Limit Load. MIL-A-83444 has similar requirements for "in-flight" and "ground evident damage". The design loads for these two conditions are the maximum loads expected in 100 flights.

The following summarize current aeronautical requirements for composite aircraft structures with damage:

1. Structure containing likely damage or defects that are not detectable during manufacturing inspections and service inspections must withstand Ultimate Load and not impair operation of the aircraft for its lifetime (with appropriate factor).
2. Structure containing damage that is detectable during maintenance inspections must withstand a once per lifetime load, which is applied following repeated service loads occurring during an inspection interval (with appropriate factor).
3. All damage that lowers strength below Ultimate Load must be repaired when found.
4. Structure damaged from an in-flight, discrete source that is evident to the crew must withstand loads that are consistent with continued safe flight.
5. Any damage that is repaired must withstand Ultimate Load.

Static and fatigue tests are usually conducted during design development and validation to show that composite structures satisfy certification requirements (Reference 7.2.1(a)).

The [inverse] relationship between design load levels and damage severity is shown in Figure 7.2.1(a). As is the case with metal commercial aircraft components, ultimate strength and damage tolerance design philosophies are used to help maintain the reliable and safe operation of composite structure. The load and damage requirements are balanced such that there is an extremely low probability of failure. Residual strength design requirements for relatively small damage, which are likely to occur in service, are matched with very high (unlikely) load scenarios (ultimate). The design requirement for more severe damage states, such as those caused by impact events that have a very low probability of occurrence, are evaluated for the upper end of realistic load conditions (limit). The most severe damage states considered in design are those occurring in flight (e.g., engine burst). The flight crew generally has knowledge of such events and they limit maneuvers for continued safe flight. Depending on the specific structure and an associated load case, continued safe flight load requirements may be as high as limit (e.g., pressure loads for fuselage).

Maintenance technology for composite aircraft structure benefits from a complete assessment of service damage threats on structural performance. Unfortunately, the necessary links between composite design practices and maintenance technology has not received the attention required to gain acceptance by commercial airlines and other customers. In the past, damages selected to size structure for the design load conditions shown in Figure 7.2.1(a) have not met all the needs of maintenance. A more complete database is needed to determine the effects of a full range of composite damages on residual strength. A complete characterization of the residual strength curve (i.e., residual strength versus a measurable damage metric) can help establish the Allowable Damage Limits (ADL) and Critical Damage Threshold (CDT) as a function of structural location. Well-defined ADLs can help airlines accurately determine the need for repair. Generous ADLs in areas prone to damage may help minimize maintenance costs by allowing cosmetic repairs instead of structural repairs that require more equipment and time.

The amount of damage that reduces the residual strength to the regulatory requirements of FAR 25.571 are referred to as the Critical Damage Threshold (CDT). It is desirable to design structure such that service damage falling between the ADL and CDT limits can be found and characterized using practical inspection procedures. This goal provides aircraft safety and maintenance benefits. By definition, all damage of this extent must be repaired when found. Damage approaching the CDT must be found with extremely high probability using the selected inspection scheme (i.e., it should be reliably detectable with the specified inspection scheme). A complete description of the critical damage characteristics, as related to the inspection scheme, is valuable information for maintenance planning activities. As with metals, damage tolerant design to relatively large CDTs provides the confidence for safe aircraft operations with economical inspection intervals and procedures.

The ADL and CDT definitions in Figure 7.2.1(a) both imply zero margins of safety for respective load cases. These parameters will vary over the surface of the structure as a function of the loads and other factors driving the design. As such, they have meaning to maintenance and should not be thought of as the design requirement for ultimate and Limit Loads. Design requirements and objectives are established for a given application, within general guidelines set by industry experience and the FAA. The design cri-

teria used to meet these requirements become even more program-specific, depending on available databases for the selected structural concept.

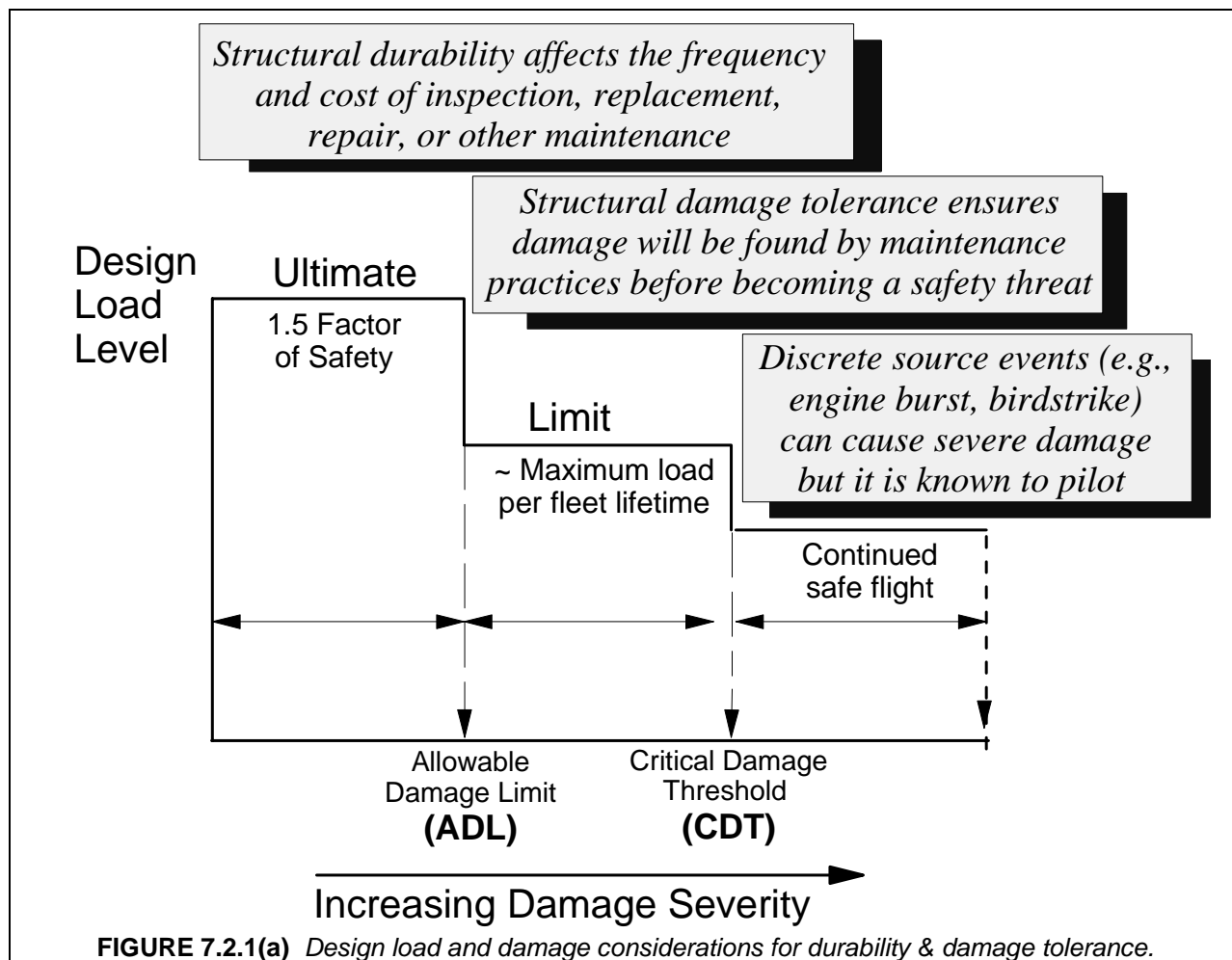


Figure 7.2.1(b) helps illustrate the requirements for damage subjected to time in service (i.e., repeated loads and environmental cycling). For relatively small damages, which likely exist in the structure and may be undetected by either quality control at the time of manufacturing or service inspection, the structure should retain static strength for Ultimate Loads over the aircraft's life. When detailed visual inspection techniques are used for service, barely visible impact damage (BVID) is usually classified as a threshold for undetectable damage. If damage is of a size and characteristic that can be detected by selected service inspections (e.g., visible impact damage, VID), then the load requirement drops to Limit Load. Structure with such damage is only expected to sustain the service environment for a period of time related to the inspection interval. In the cases of both undetectable and detectable damages, factors are typically applied in fatigue testing, damage tolerant design and maintenance to account for the variability in material behavior under repeated loading and the reliability of inspection techniques. In certification practice for composite materials, a load enhancement factor is often used to reduce the additional test cycles needed to account for material variability (References 7.2.1(b) to 7.2.1(d)).

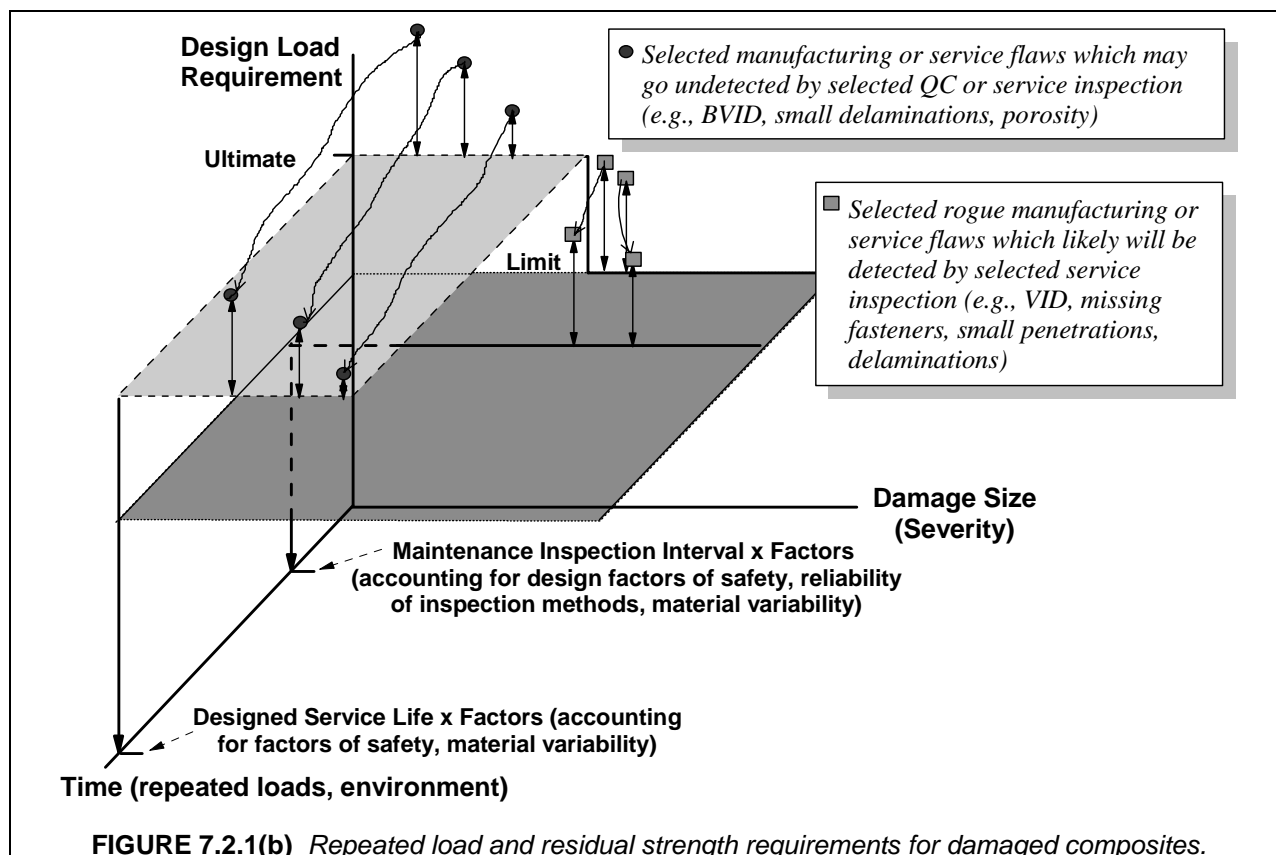
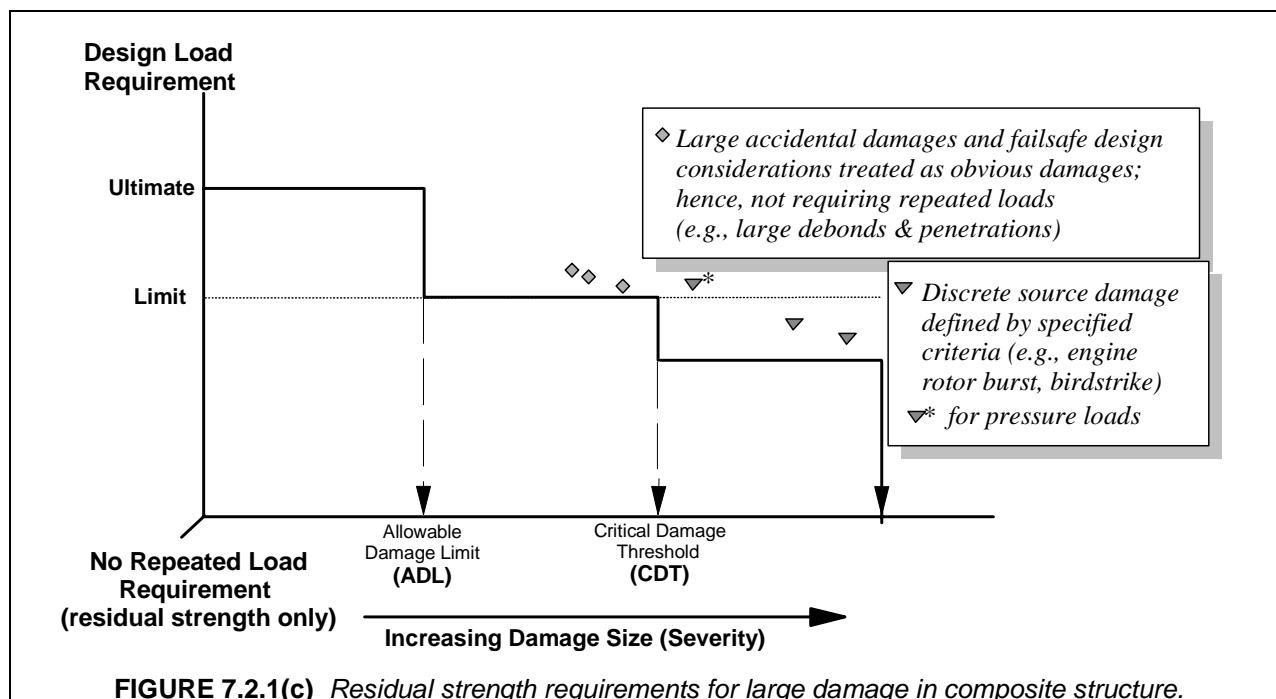


Figure 7.2.1(c) illustrates another important aspect of damage tolerance, which is related to rare accidental damage and discrete source impact events that yield relatively large damages. Such damages are typically treated as obvious or assumed to exist when a discrete source event occurs in service that is known to the crew. In both cases, there is no repeated load requirement. The requirements for discrete source damage are defined in aeronautical regulations. There is generally no specific damage size requirements for obvious damage, but to be classified as such, it must be detectable without directed inspection (e.g., large penetrations or part malfunction). Service databases have shown that such damage does occur and may go undiscovered for a short period of time. As a result, it is good fail-safe design practice to ensure structure is capable of sustaining Limit Load with obvious damage. The analyses and test databases used to meet discrete source damage requirements typically characterize the residual strength curve, which can also be used to meet design criteria for obvious damage. For bonded structure, there are other requirements to ensure fail safety in the case of large debonds (e.g., FAR 23.573). Such requirements relate to the unreliability of secondary bonding.

The range of damages shown in Figures 7.2.1(b) and 7.2.1(c) have traditionally provided a basis for durability and damage tolerance assessments of composite structure. However, complex design details and secondary load paths can also result in damage initiation and significant growth in composites structures. Since these details and load paths are difficult to analyze, the resulting damage initiation and growth are often not identified until large-scale tests of configured structure are conducted. Alternatively, damage growth must either be arrested by design features or be predictable and stable (e.g., analogous to metal crack growth). In this case, safety is achieved through damage tolerant design and maintenance practices similar to those for metal structures.



7.2.2 Methods of compliance to aviation regulations

There is a notable difference between military and civil aviation methods of compliance. For military aircraft, the government defines the requirements (Military Specifications) and works with the manufacturer to establish the method of compliance. The government is also the customer in this instance. In civil aviation, the government defines the requirements through regulations (FAR's, JAR's) and accepted means of compliance through guidance material (Advisory Circulars). Compliance must be demonstrated to the agency (FAA, JAA). In this instance the government is a neutral, third party.

This difference in ultimate ownership also influences the attitude the different agencies adopt regarding durability. To the extent that durability is an economic issue, it is not generally of concern to civil aviation authorities. It is a concern to military agencies because maintainability expenses affect their cost of ownership.

The reason why visual inspection methods, rather than a special one (requiring some special techniques like ultrasonic pulse echo for instance), is preferred by the aircraft manufacturers and operators for impact damage detection is purely economic. Unlike fatigue cracks in metallic structure that can only be initiated at restricted and easily identifiable areas (where stress raisers and/or corrosion exist) impact damage may occur anywhere on large exposed surfaces, raising the cost of an inspection plan covering the entire surface of the structure.

The use of visual methods for initial damage detection results in a more conservative (i.e., heavier) design than would the use of more stringent inspection methods, since the damage level required for visibility is more severe. However, the visual approach results in improved damage tolerance capability, since the structural strength is typically less sensitive to changes in damage severity as damage severity increases. A majority of the compression strength reduction occurs for energy levels below the detectability threshold that will govern static strength requirements. Then, limited extra strength reductions should be expected for higher energies to be considered for damage tolerance evaluation.

7.2.2.1 Compliance with static strength requirements (civil aviation)

As far as impact damage is concerned, the AC 20-107A (§ 6g) proposes the following means for complying with the regulations: *It should be shown that impact damage that can be realistically expected from manufacturing and service, but no more than the established threshold of detectability for the selected inspection procedure, will not reduce the structural strength below Ultimate Load capability.*

This sentence explicitly defines energy cut-offs and detection thresholds, which are illustrated in Figure 7.2.2.1. The first cut-off threshold is the established threshold of detectability for the inspection method used. The second cut-off threshold is the maximum impact energy that the structure can be expected to tolerate during manufacturing and in service. These two thresholds are assumed to describe accidental damage for new structure representative of the minimum quality. Minimum values of these cut-offs and thresholds need to be established so that there is consistency between the detectable size and the selected NDT procedure plus consideration of realistic energy levels.

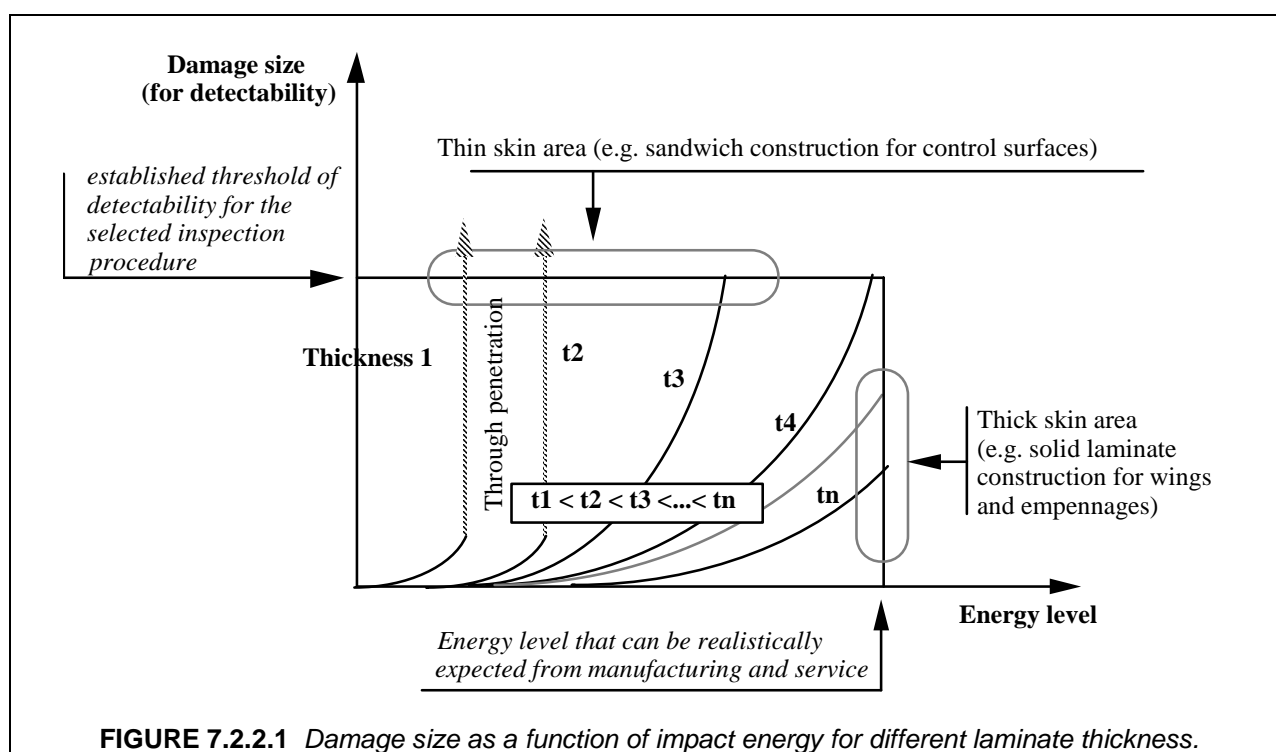


FIGURE 7.2.2.1 Damage size as a function of impact energy for different laminate thickness.

Establishing the energy cut-off values requires defining the energy level associated with the word *realistic*. The rectangle in Figure 7.2.2.1 represents the domain in which structure is capable of withstanding Ultimate Loads, without necessary repairs. This applies to the start of service life, when the aircraft rolls out of the manufacturer's plant, as well as at the end of lifetime when composite parts are likely to have accumulated some accidental damage below the detectability thresholds. Damages that are above the rectangle in Figure 7.2.2.1, are assumed to be detected and repaired with cosmetic or structural solutions so that the structure's residual capability to withstand Ultimate Loads is preserved or restored, respectively.

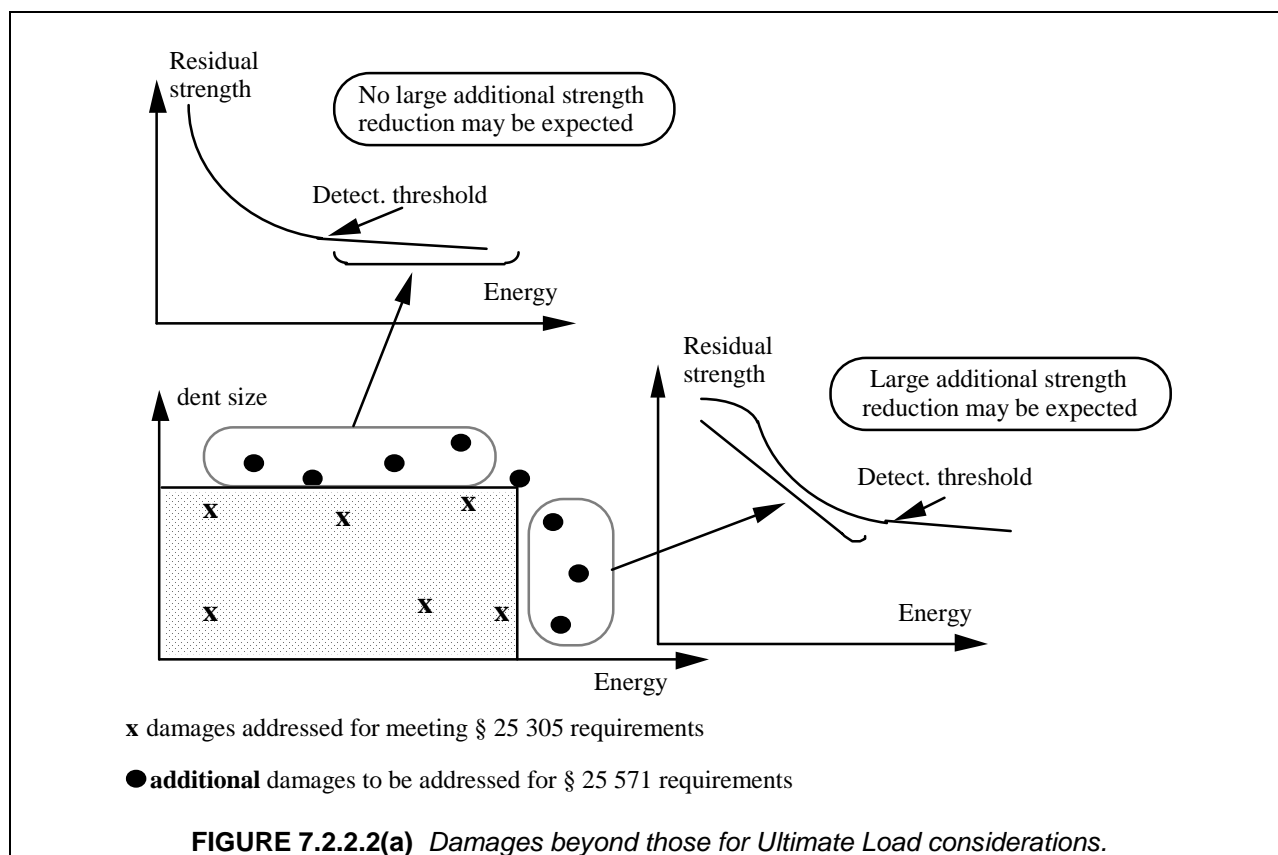
The purpose of "damage tolerance" is to address situations with only a limited occurrence; therefore, a large majority of the aircraft structure should retain Ultimate Load capability during the service life. A discussion of one method of estimating these realistic energy levels is given in Section 7.3.3.

7.2.2.2 Compliance with damage tolerance requirements (civil aviation)

Damage tolerance has to address the situation where, due to fatigue, corrosion or accidental occurrence, Ultimate Load strength capability may not exist and will have to be restored before the damage becomes critical. As far as accidental impact is concerned, two situations have to be addressed. The first case involves those damages that meet static strength requirements (as per 25.305) and that might evolve during fatigue loading, while still remaining undetectable with the selected inspection procedure. The second case involves those damages that are outside the coverage illustrated by Figure 7.2.2.1, due to higher energy levels that will produce:

- More easily detectable damages associated with additional strength reduction for thin gage laminates (detectability threshold situation),
- Additional strength reduction without visual detection capability, in case of energy cut-off ($E > E_{co}$).

Obviously, there will be an intermediate situation where damages that were not previously detectable will become detectable. The damages that have to be addressed in a damage tolerance substantiation are illustrated in Figure 7.2.2.2(a).



Depending on their detectability, different § 25.571 sub-paragraphs will apply:

- For those accidental impacts that will never be detected by the selected (visual) inspection procedure, meaning those already accounted for in the scope of static strength requirements plus those with an increased energy, damage tolerance as per 25.571 (b) is impractical. Then, demonstration will have to be made according to sub paragraph 25.571 (c), fatigue (safe-life) evaluation. In fact, due to the presence of initial damage in that fatigue demonstration, the latter is usually called "safe-life flaw tolerant" or "enhanced safe-life" demonstration.
- For those visually detectable accidental impacts, damage tolerance as per § 25.571 (b) applies.

As for § 25 305 requirements, new cut-offs and thresholds have to be defined:

- A new energy cut-off level limited to the maximum value that is to be assumed in a risk analysis and that should correspond to extremely improbable events (less than 10^{-9} per hour according to ACJ 25 1309),
- A new detectability threshold above which damage will become “obvious” (detectable within a very small number of flights by walk-around inspection).

Between the damage size detectable at detailed scheduled inspections and this new threshold, residual static strength requirements are laid down in the regulatory documents § 25 571(b). There is no residual strength requirement associated with “obvious” damage. However, aircraft take off is not allowed in such situations before assessment and restoration of Ultimate Load capability

There is a third detectability threshold which corresponds to the situation where the flight crew is at once aware of the event; then, lower loads (per § 25 571(e)) are required. This situation is referred to as “discrete source” damage. All these new thresholds are illustrated in Figure 7.2.2.2(b).

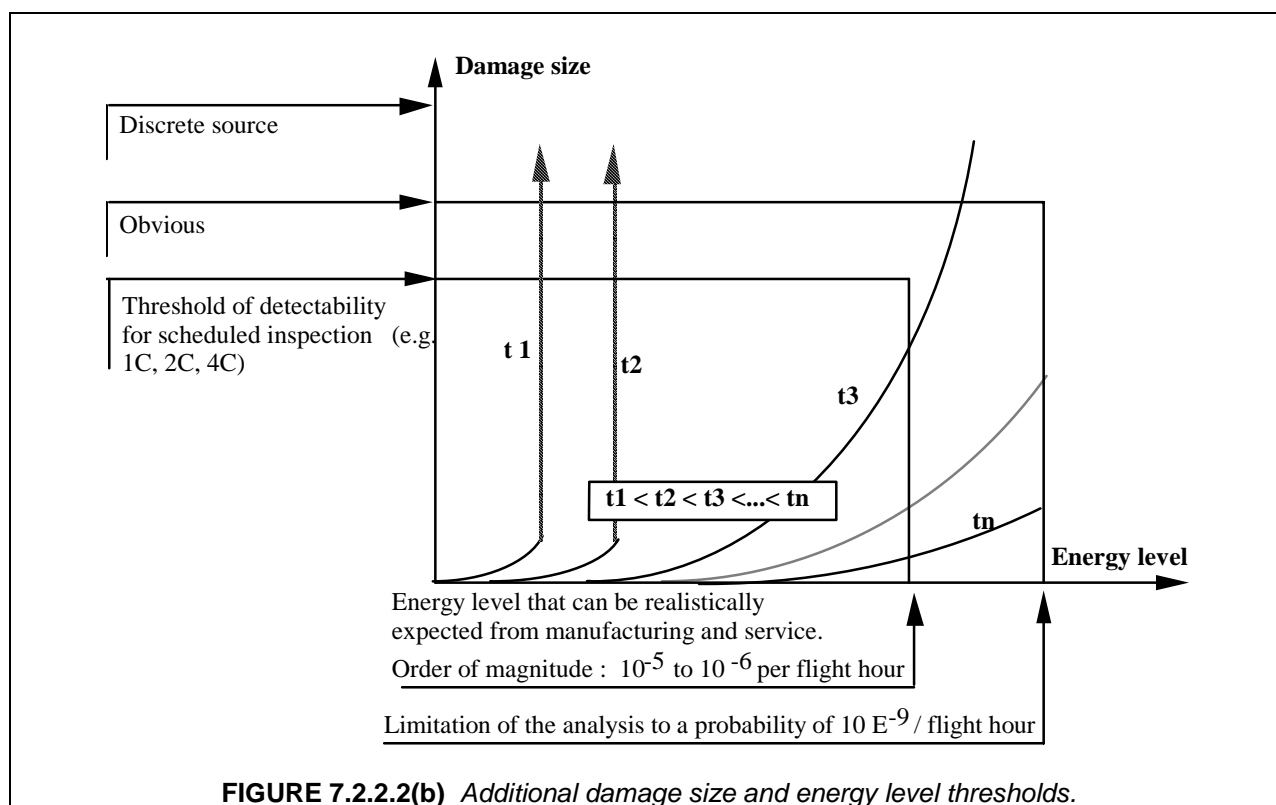
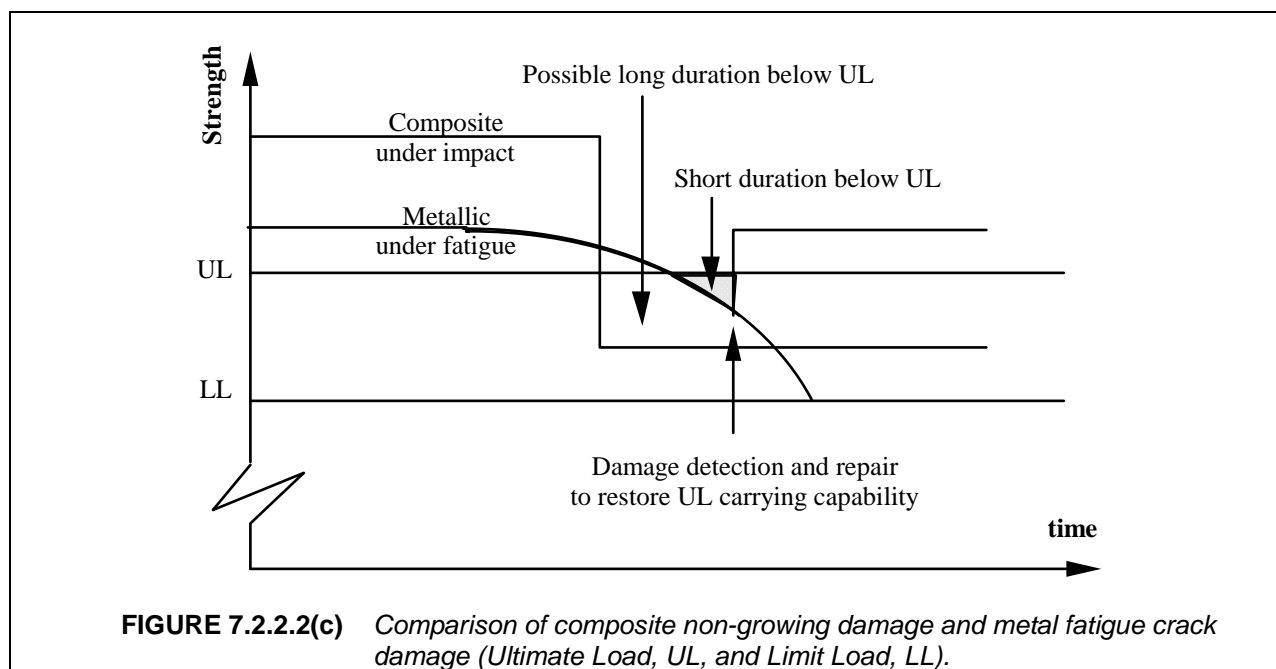


FIGURE 7.2.2.2(b) Additional damage size and energy level thresholds.

As discussed previously, impact damage can cause an immediate drop in composite residual strength. In most cases, such damage does not grow due to the generally good fatigue resistance of composites. The fact that an accidental impact damage in a composite structure is generally not expected to propagate in fatigue raises a specific issue for interpreting § 25 571 (b), as illustrated in Figure 7.2.2.2(c). This sketch shows the difference that can be found between non-growing impact damage in a composite structure and a, prone to grow, fatigue crack in a metallic one. Whatever the damage source is, damage tolerance per § 25 571(b) requires the following: "The residual strength evaluation must show that the remaining structure is able to withstand loads (considered as Ultimate Loads) corresponding to the following conditions...". As shown with the metal curve in Figure 7.2.2.2(c), an inspection interval can

be rationally derived such that fatigue damage in metallic structure is safely detected and repaired before the strength drops below Limit Loads. Metal crack growth analyses and tests have matured to support such an assessment.



For the case of the no-growth, composite concept, a structure with impact damage could sustain a long duration below Ultimate Load without a threat of the residual strength further dropping to the critical threshold defined by § 25.571(b) (i.e., Limit Load). This interpretation could lead to the situation of a composite structure allowed to fly a long time with residual strength just above Limit Loads, as illustrated in Figure 7.2.2.2(c). Regardless of the damage growth resistance of composite structure, damage that lowers the residual strength below Ultimate Load must be detected and repaired when found. Hence, the issue becomes one of defining a rationale inspection interval to attain equivalent or higher levels of safety than metal practice.

The advisory circular AC 20.107A, addresses the issue illustrated in Figure 7.2.2.2(c) in the paragraph 7a (4), which is related to the selection of inspection intervals: *"For the case of the no-growth concept, inspection intervals should be established as part of the maintenance program. In selecting such intervals, the residual strength associated with the assumed damages should be considered"*. In other words, the larger the strength reduction is, the sooner the damage should be detected. Also, the probability of damage occurrence plays a major role in deriving inspection intervals. For instance, more frequent inspections should normally be required for a flap, which is subjected to more damage threats, than for a vertical fin. In other words, both the capability of the composite structure and service history should be considered in defining the inspection intervals. Although metal structure has similar considerations for accidental damage, an inherent resistance to foreign object impact makes fatigue damage growth a dominant factor in defining inspection intervals for metal parts.

In considering the issues of damage severity and probability of occurrence for a composite structure, damage reducing residual strength to Limit Load should be extremely unlikely. The residual strength curve, damage growth resistance, service databases and user maintenance practices should all be considered in establishing the inspection intervals. In addition, the design criteria and certification approach used to substantiate the composite structure for damage tolerance should be coupled with subsequent maintenance practices. In the end, the composite structure should be sufficiently tolerant to damage such

that economical maintenance practices can be safely implemented (e.g., detailed damage inspections and repair at scheduled maintenance intervals).

7.2.2.3 *Deterministic compliance method (civil aviation example)*

This section describes an analysis and testing methodology to support certification and maintenance of composite structures based on: (a) establishing residual-strength-versus-damage-size relationships; (b) establishing methods of damage detection and minimum detectable damage sizes; and (c) determining damage sizes that reduce capability to both to Ultimate Load and Limit Load. Flow charts outlining an approach for achieving damage tolerant and fail-safe designs are presented.

Several composite primary structures, such as the Boeing 777 empennage and NASA-ACEE/Boeing 737 horizontal stabilizers, have been certified per FAR 25 and JAR 25. The 737 stabilizers have demonstrated excellent service performance (Reference 7.2.2.3(a)). This service experience, as well as component testing (References 7.2.2.3(b) through 7.2.2.3(e)), has shown that current composite primary aircraft structure has excellent resistance to environmental deterioration and fatigue damage. This leaves accidental damage as the primary consideration for damage tolerance design and maintenance planning for the relatively thicker-gage composites associated with primary structure.

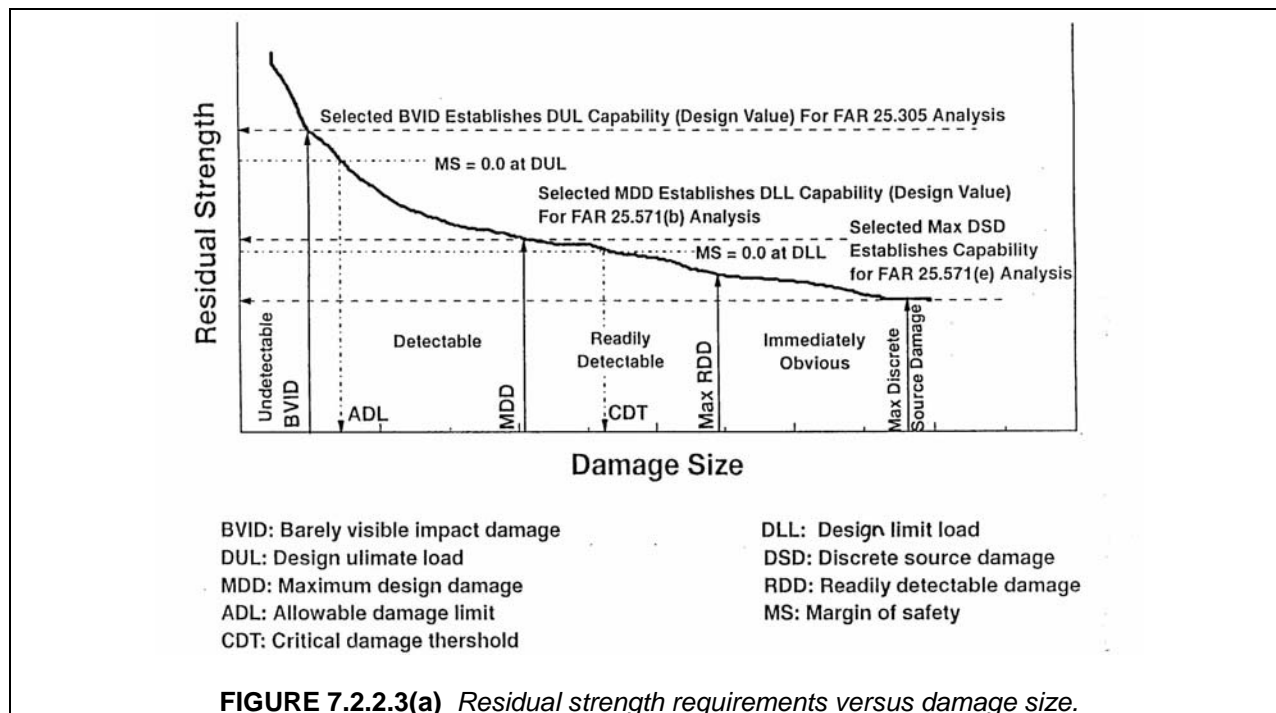
In-service damage resistance and repair of thin gage composite structure has become a major issue for the commercial airlines. In order to make composites cost effective for the airlines, allowable damage limits (ADLs) must be as large as possible while still meeting regulatory Ultimate Load requirements. To achieve this goal, test data and analytical methods encompassing the complete range of potential damage sizes and types are required.

This discussion presents a design approach to ensure that composite structures have low in-service maintenance costs as well as adequate damage tolerance. Several damage sizes based on detectability levels are described, and requirements for each damage size relative to FAA and JAA regulations are discussed. Suggestions are made for developing appropriate databases to satisfy regulatory damage tolerance requirements and achieve low maintenance costs.

Several methods for improving the performance of impacted composite panels and components have been proposed (References 7.2.2.3(f) and (g)). One approach is to increase the inherent toughness of the composite by using tougher resin matrices; this is only appropriate for medium to thick gage laminates as increased toughness has little benefit for thin laminates or sandwich facesheets. Although this method improves damage resistance and reduces maintenance costs, increased material costs, reductions in matrix stiffness at elevated temperatures, and potential reductions in large notch residual strengths must be considered in the final selection.

In metallic structures, damage tolerance has been demonstrated using fracture mechanics to characterize crack growth under cyclic loading, predict the rate of crack growth in the structure under anticipated service loads, and establish inspection intervals based on realistic damage detection reliability considerations (Reference 7.2.2.3(h)). Since typical CFRP composites have relatively flat S-N curves, and because these damages do not propagate under aircraft wing/empennage operational loading spectra, the above method normally cannot be used to establish inspection plans. Instead, a *no-growth approach* has been used to demonstrate compliance with damage tolerance requirements for composite primary structures on commercial aircraft for current composite structures.

The types and sizes of damages that are barely detectable or larger are classified into several groups based on the likelihood of damage detection, as shown in Figure 7.2.2.3(a). The selection of damage sizes must be consistent with the established inspection program and with the corresponding reduction in static strength. The following paragraphs describe the different damage types and sizes:



1. Barely visible impact damage (BVID) establishes the strength design values to be used in analyses demonstrating compliance with the regulatory Ultimate Load requirements of FAR 25.305. For small aircraft and different classes of rotorcraft the corresponding requirements are 23.305, 27.305 and 29.305. In the case of small aircraft, the BVID static strength requirement has been added to the regulation for composite damage tolerance, FAR 23.573. The extent of such damage needs to be established as part of criteria defined prior to the design phase. The term visible is used since the primary inspection method in current use involves visual observation. An upper limit of 100 ft-lb (140 Joules) on the BVID impact energy level is applied based on this value being at the upper limit of what could be realistically expected.
2. Allowable damage limits (ADL), defined as damage that reduces the residual strength to the regulatory Ultimate Load requirements of FAR 25.305, are determined to support maintenance documents. Given that the structure's strength with BVID damage will result in positive margins at design Ultimate Load (DUL), the corresponding ADL will generally be larger than the BVID (see Figure 7.2.2.3(a)). Characteristics describing the detectability of the ADL as well as the type and extent of the damage are documented to support maintenance programs.
3. Maximum design damage (MDD) establishes the strength design values to be used in analyses demonstrating compliance with the regulatory damage tolerance requirements of FAR 25.571(b). In the case of small aircraft, the regulation for composite damage tolerance, FAR 23.573, while analogous rotorcraft rules can be found in 27.571 and 29.571. Current efforts are underway to develop a unique composite damage tolerance rule for rotorcraft, which will be given the numbers 27.573 and 29.573, depending on the class of rotorcraft. The extent of such damage needs to be established as part of criteria defined prior to the design phase.
4. Critical damage thresholds (CDT) are defined as damages that reduce the residual strength to the regulatory requirements of FAR 25.571(b) (or the equivalent for other types of aircraft). Given that the structure's strength with MDD-sized damage will result in positive margins at design Limit Load (DLL), the corresponding CDT will be larger than the MDD. Characteristics describing the detectability of the CDT as well as the type and extent of the damage are documented to support the establishment of required inspection methods and intervals. Using the selected inspection

technique, realistic damages smaller than the corresponding CDT are shown to be detectable with high probability before any growth causes it to exceed the CDT.

5. Readily detectable damage (RDD) can be detected within a small number of flights during routine aircraft servicing. For damage that is not readily detectable, the structure should be evaluated for all possible damage growth mechanisms. The maximum extent of damage that is considered readily detectable, but which is not immediately obvious, should be established. The advisory circular for damage tolerance, ACJ 25.571(a), allows the residual strength of RDD to be confirmed at load levels less than the regulatory loads specified in FAR/JAR 25.571(b) (Reference 7.2.2.3(i)).
6. Damages larger than the maximum RDD are considered to be immediately obvious. Except for damage resulting from in-flight discrete sources (rotor burst, bird strike, etc.), no residual strength analysis is required for obvious damage.

The residual strength curve shown in Figure 7.2.2.3(a) starts near ultimate strength and spans the range to discrete source damage sizes. This range encompasses damage conditions critical to meeting all requirements such as:

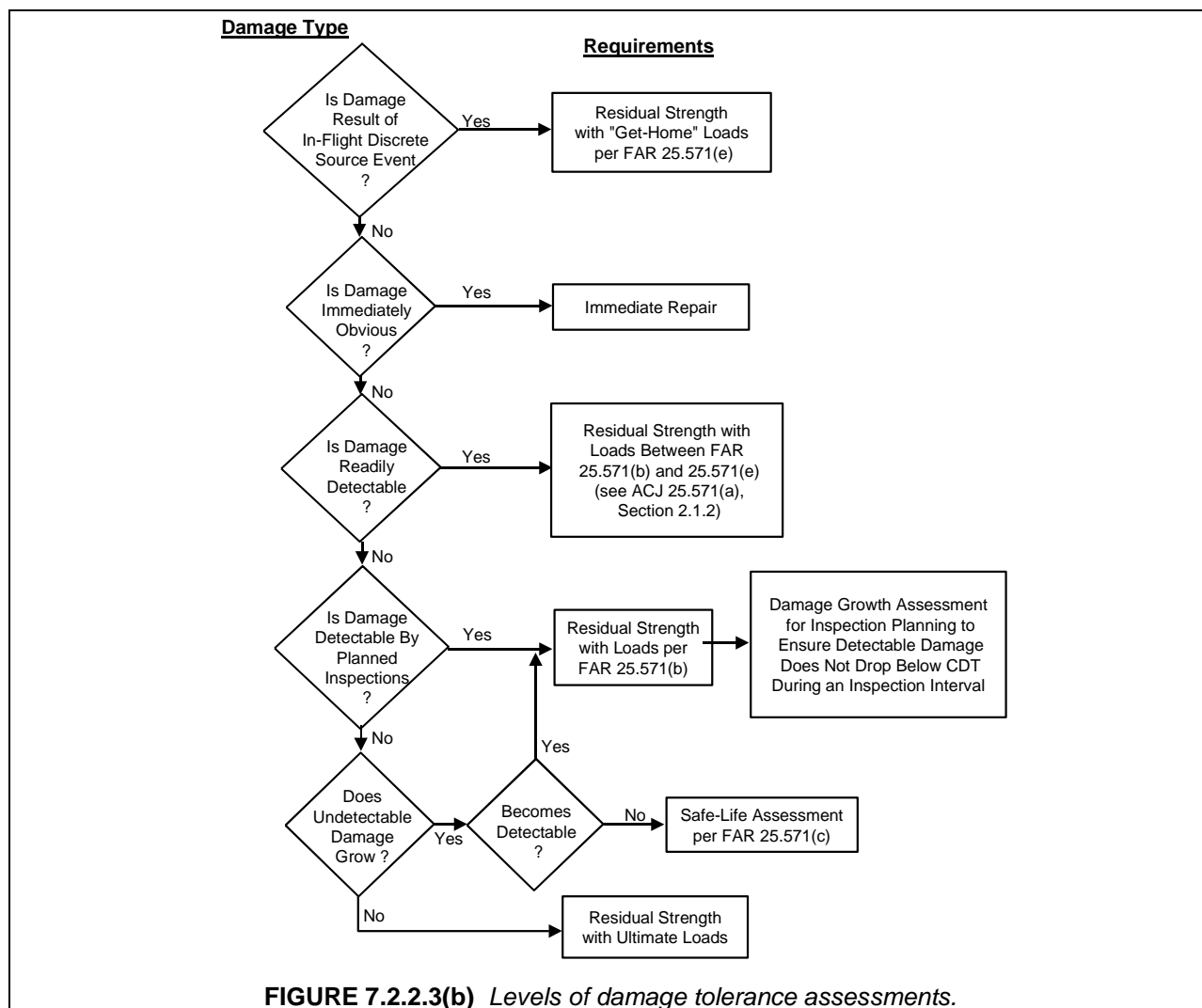
1. Damage sizes and states which support the ADL (Ultimate Load levels) and repairable damage sizes to be placed into the Structural Repair Manual;
2. CDT damages for Limit Load design values;
3. RDD for less than Limit Load but greater than continued safe flight load design values; and
4. "Discrete source" damage for continued safe flight load design values.

Test data and analysis methods developed by the Boeing-NASA/ACT program (References 7.2.2.3(j) through 7.2.2.3(l)) show that the inspection methodologies and damage growth mechanisms should be established to ensure accidental damage occurring in service can be found and repaired before compromising limit strength capabilities. Visual inspection is the preferred damage detection method, and the no-growth approach for damages less than Limit Load size has been the basis for certification. For new composite primary structure application, these approaches will require revalidation.

Figures 7.2.2.3(b) and 7.2.2.3(c) identify the inspection decision points, requirements, development tasks, analyses and actions required to meet the damage tolerance requirements of a principal structural element (PSE). Figure 7.2.2.3(b) outlines the levels of damage tolerance requirements and can be used for test, analysis and maintenance planning. Figure 7.2.2.3(c) defines the flow of events and actions to be used to develop the data required for damage tolerance certification.

The deterministic compliance method is based on a minimum of two sets of testing and analysis. The first set is designed to show positive margins of safety at design Ultimate Load with BVID size damages. This testing includes mostly coupons and subcomponents containing BVID. The second set of testing is designed to show positive margins of safety with large damage at design Limit Load. This testing includes subcomponent (e.g., five-stringer panels) and component structures with through the thickness damage, skin-stiffener debonds, large impact damages, etc. These types of damage are considered to be maximum design damage (MDD). Tests are used to show MDD-sized damage is easily detectable. Tests are also used to show MDD-sized damage and smaller will not grow under operational loads.

Although this method meets FAA requirements for damage tolerance, it may not provide enough data to support the definition of accurate ADLs in structural repair manuals. Consequently, allowable damage sizes are conservatively set to smaller values. This has had the effect of increasing in-service repair costs of thin composite honeycomb sandwich panels in commercial aircraft.

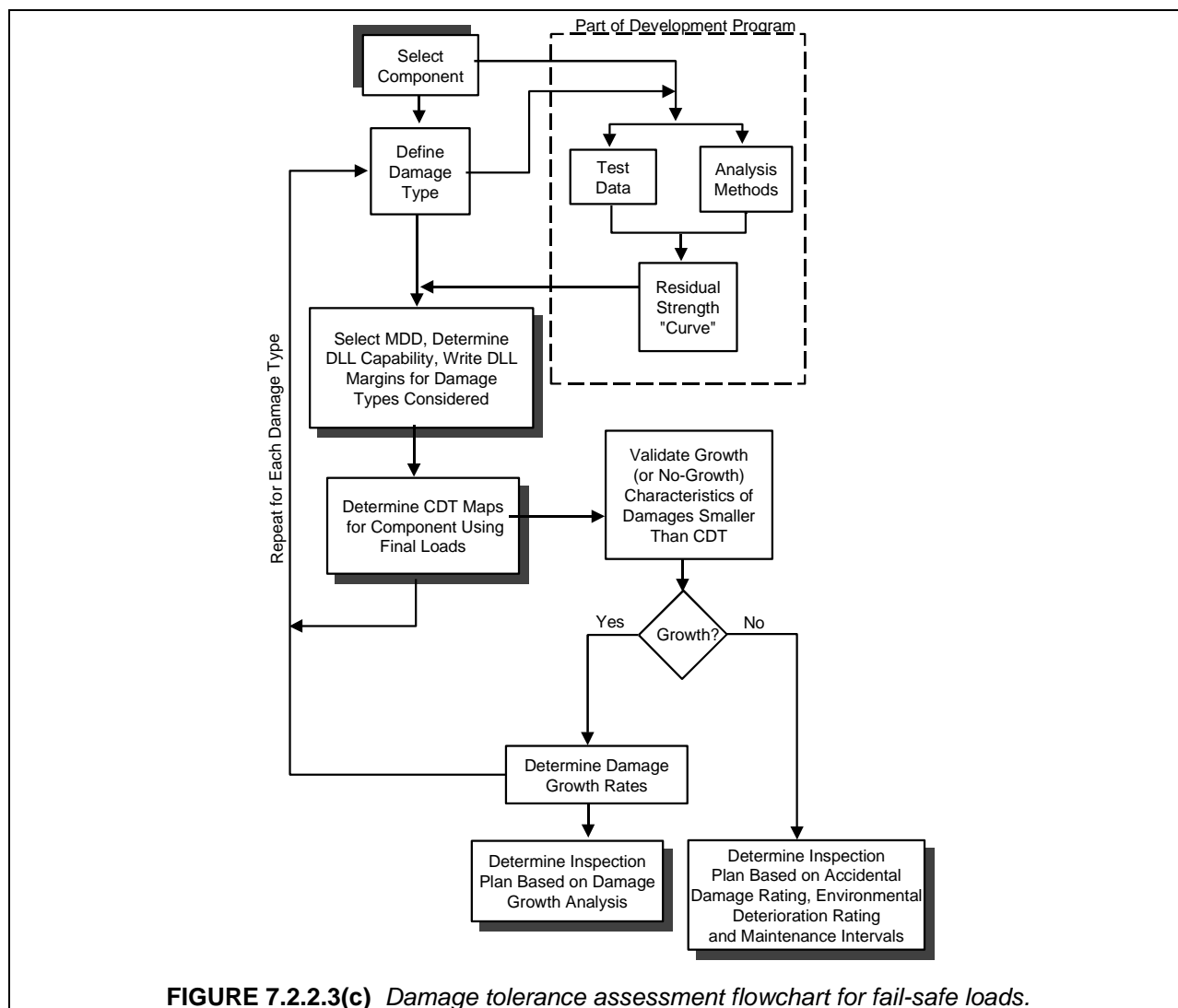


The following are recommended approaches for developing data to support certification and to allow for reduced maintenance costs of composite aircraft structures:

1. The residual strength curve for each significant type of potential damage on each principal structural element should be determined by analysis and/or test.
2. Characteristics describing the inspectability of the CDT as well as the type and extent of the damage should be documented to support maintenance planning activities.
3. For readily detectable damage, the magnitude of the threats that should be considered, similar to those in FAR 25.571(e), should include impact damage by ground vehicles and ground handling equipment, impact with jet gates, runway debris and thrown tire treads. Service experience has shown that damage associated with such events may persist for a few flights before the damage is detected and the structure repaired. The extent of damage that should be considered must be established by taking into account susceptibility to each type of accident.

Structural damage design should be coupled with development of the aircraft maintenance plan in order to reduce in-service damage occurrences and repair costs. Test validation and analyses should address design ultimate strength, damage growth, residual strength, and maintenance issues for composite structures. Independent studies of design Ultimate Load or Limit Load strength without data and analyses at intermediate load levels will not provide a balanced design that supports cost-effective main-

tenance. For example, damage considered for ultimate strength analyses is more likely to occur in-service while the associated loads are very unlikely. The reverse is true for limit strength analyses. A database that covers a range of damage scenarios increasing in severity will allow for more cost-effective use of composite structures in commercial aircraft service.

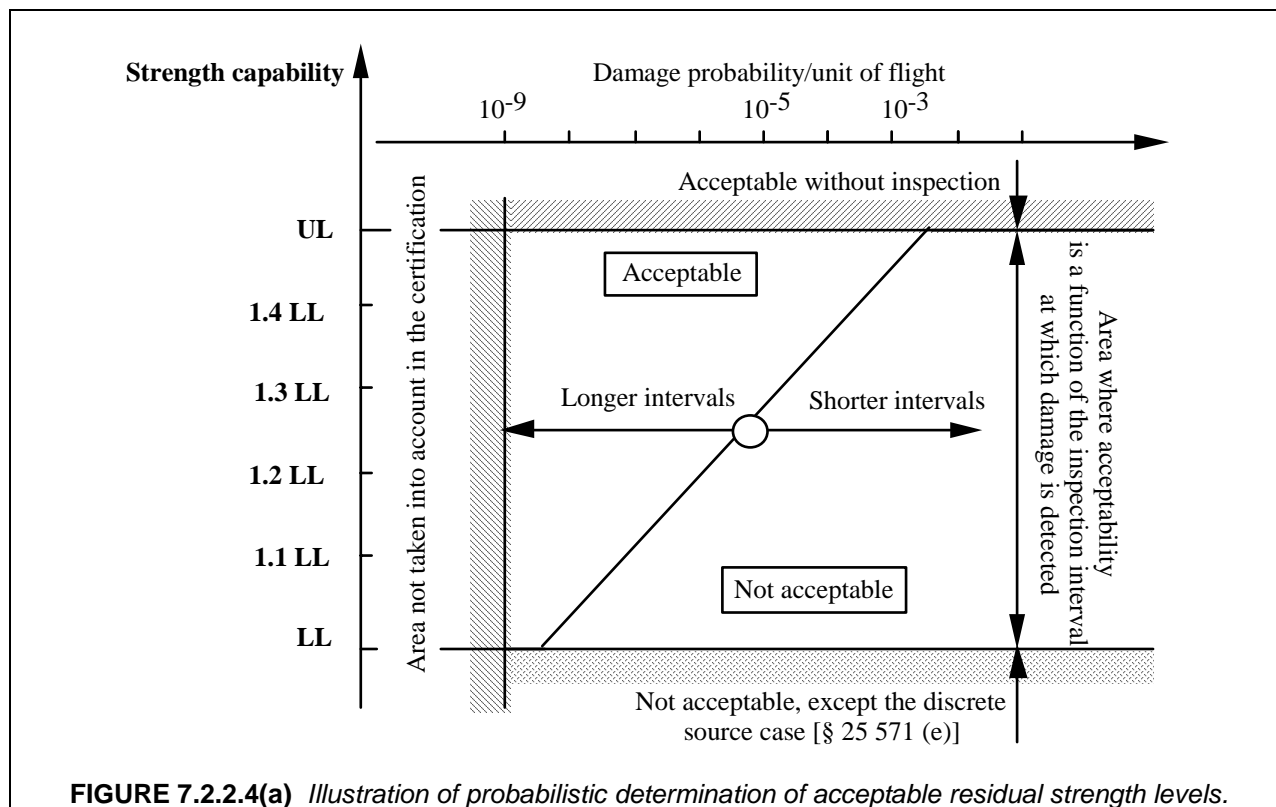


7.2.2.4 Probabilistic or semi-probabilistic compliance methods (civil aviation)

Probabilistic or semi-probabilistic methods consider first that the scheduled inspection program must account for damage severity. The use of these methods are acceptable for civil aviation as they comply with paragraph 7a (4) of the FAA Advisory Circular AC20 107A: *“For the case of the no-growth concept, inspection intervals should be established as part of the maintenance program. In selecting such intervals, the residual strength associated with the assumed damages should be considered.”*

In other words the larger the strength reduction is, the sooner the damage should be detected. Furthermore, these methods also consider that the need for inspection cannot disregard the likelihood of damage occurrence. The more likely the damage is, the sooner it should be detected. As a result, these

methods depend on service data. Figure 7.2.2.4(a) illustrates how this “residual strength associated with the assumed damage” is governed by both the inspection interval and the damage probability.



Since these methods require some probabilistic input data, they are referred to as probabilistic or semi-probabilistic approaches. They were initially developed by Aerospatiale for certification of the ATR 72 outer wing, and later for the A330/340 ailerons. Subsequently a probabilistic approach was implemented by ALENIA for the ATR carbon tail.

The basis of a probabilistic approach is to demonstrate that the inspection program will ensure that the combination of an occurrence of a load having “ $k \times LL$ ” intensity, with the presence of a “missed” accidental impact damage reducing the structure strength to “ $k \times LL$ ” load level, remains acceptable. The term “ $k \times LL$ ” refers to a factor times Limit Load. For primary structure catastrophic failure, this combination must be extremely remote (probability $\leq 10^{-9}$ per flight hour according to ACJ 25 1309). Higher probabilities can be accepted for less critical parts.

Except for the case of hailstone impacts, load and damage occurrences can be considered as independent phenomena. Then it should be demonstrated that:

$$\text{Probability}_{\text{load}}(k.LL) * \text{Probability}_{\text{missed damage}}(k.LL) \leq 10^{-9} \quad 7.2.2.4(a)$$

The following elements are contained in all probabilistic methodologies:

1. Perform a building block approach for deriving strength versus energy curves for all critical parts of the structure.
2. Investigate impact damage scenarios in order to derive the impact threat probability laws.
3. Demonstrate the no-growth concept of all damages up to VID threshold, in general through a full-scale fatigue test.

4. Perform residual static tests for checking the assumed strength of the damaged structures.

General Method

The first step of a probabilistic damage tolerance evaluation is the identification of each critical part of the structure with respect to low-velocity, impact damage tolerance. External skins of the aircraft, subjected to high compression stresses, which are exposed to in-service accidental impacts, are of prime concern. The following steps are applied to each critical zone:

1. Derive the entire residual static strength versus impact energy curve from analysis supported by test.
2. Determine accidental impact threats in terms of energy versus probability curves.
3. Calculate, within each scheduled inspection interval, the probability to have such accidental damages on the structure.
4. Determine load (or stress, or strain) occurrences versus probability curves.
5. Check that the scheduled inspection program will make damage detection highly probable before the probability target is exceeded.

Such probabilistic or more exactly semi-probabilistic approaches are detailed in References 7.2.2.3(e), 7.2.2.4(a) and (b). Since not all of the input parameters used in these referenced methods are expressed through a probability law, for instance the residual static strength versus impact energy, the methods are semi-probabilistic.

The input parameters for the method are defined as follows (Reference 7.2.2.3(e)):

The Impact Threat. The method takes into account a complex threat consisting of miscellaneous damage sources, including occasional sources that may occur only during maintenance operations between two scheduled detailed inspections, and continuous sources for which damage may occur at each flight. Each source of damage is described by a probability function to model the impact energies involved (log-normal law).

The typical impact sources, which are taken into account in the analysis, are:

- Continuous impact sources: Tool drop, foot traffic, collision with service vehicles, projection of runway debris.
- Occasional impact sources: Fall of a removable component during a maintenance operation.

The Inspection Program. The method takes into account a complex maintenance program composed of several types of inspections (see Section 7.4) with a different periodicity. The efficiency of each type of inspection is described by a probability distribution to model the detection probability as a function of the damage dent depth. This means that damages that have to be taken into consideration are not only those naturally omitted by the inspection level (damages up to "visible" impact damage (VID) are to be assumed between two detailed inspections), but also those existing and not noticed by the inspector during the procedure. The latter still have to be accounted for during the next inspection intervals.

For commercial aircraft composite structures, complex non-destructive methods are typically not used to find damage. Once the damage is found, other methods (e.g., ultrasonic) may be used to better characterize its extent. The three methods of inspection considered to initially find damage include general visual inspection, external detailed visual inspection and internal detailed visual inspection. The mathematical modeling of the detection probability is based on statistical studies, which allow for each type of inspection to derive a probability distribution (log-normal law).

The Occurrence of Static Loads. The probability of occurrence of static loads (between limit and ultimate Load) is described by a log-linear probability distribution. The probability of occurrence of static loads varies uniformly (on a log-linear basis) from the range of 10^{-5} per flight hour for a static load equal to Limit Load up to 10^{-9} per flight hour for a static load equal to Ultimate Load.

The Residual Strength of the Impacted Structure. A B-basis curve is assumed for the residual static strength versus impact energy. The effects of environment are taken into account by the use of residual strength values obtained under worst environmental conditions.

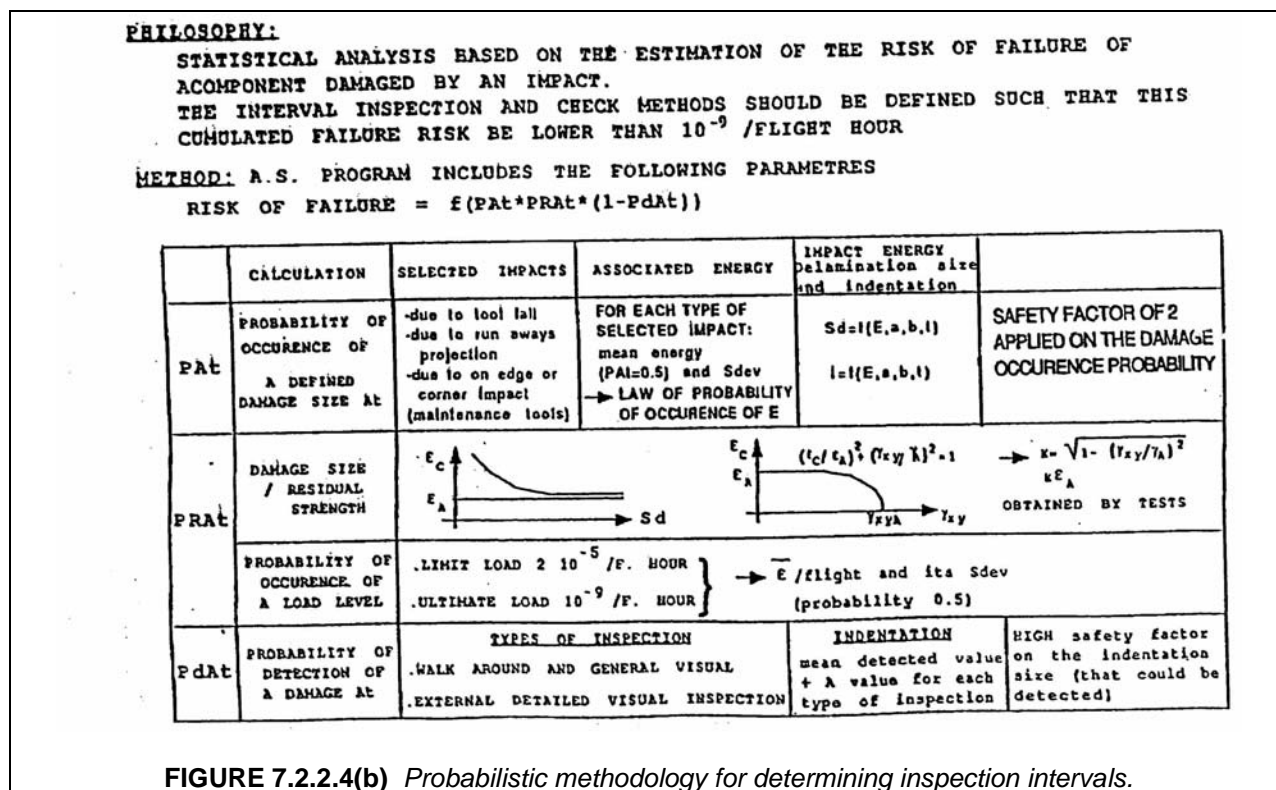
The Relationships Between Energy, Damage Size, and Indentation. Two empirical deterministic relationships are taken into account in the analysis. The first one links impact energy to the associated damage size (delaminated area), and the second one relates the damage size (and thus the impact energy) to an associated indentation parameter (this latter being the relevant parameter for the visual detectability of the damage).

The analysis enabling the assessment of the probability of failure (calculated at its maximum, i.e., during the last flight hour of the aircraft's life) is then based on a partition of the energy range involved in the description of the impact sources.

The two main steps of the method are:

1. The calculation of the probability of existence of a damage of a given size at the beginning of the last hour of the aircraft life. This calculation takes into account the different damage sources (continuous and occasional in-service sources) as well as the complex maintenance program (date and type of each inspection).
2. The calculation of the probability of failure during the last flight hour, which must be less than 10^{-9} per flight hour (see Figure 7.2.2.4(b)).

A special use of this probabilistic method also enables the determination of the load level $k \times LL$ to be sustained by a structure damaged by a VID, in such a way that the static test at $k \times LL$ implies an acceptable in-service risk level for the structure with its inspection program.



Simplified Method

In References 7.2.2.4(a) and (b) there is, first, no differentiation between discrete and continuous damage sources. Therefore, all damage threats are equally shared throughout the inspection interval. Secondly, this method does not include any probability law for detecting the dent - the BVID energy or dent depth must be selected high enough to prevent any oversight.

Both assumptions allow calculations to be simplified in the following way:

Let p_a = probability of accidental damage at the end of unit aircraft utilization (e.g., one flight hour, one flight).

n = inspection interval expressed in terms of unit aircraft utilization (n flights, n hours)

Pr = probability of occurrence of the flight load (e.g., gust), the intensity of which combined with the accidental damage of probability p_a would lead to a catastrophic failure.

The probability to have at least one accidental damage at the last flight preceding the inspection (where the likelihood of a damaged structure is higher) is then equal to:

$$1-(1-p_a)^n \cong (n)(p_a) \quad 7.2.2.4(b)$$

The relationship 7.2.2.4(a) then takes the following simple formulation:

$$(Pr)(n)(p_a) < 10^{-9} \quad 7.2.2.4(c)$$

The following steps of the damage tolerance evaluation are illustrated in Figure 7.2.2.4(c) taken from Reference 7.2.2.4(b):

1. The residual static strength versus energy curve is evident as the first quadrant of the diagram. A "B" basis value curve is recommended.
2. The damaged state of the structure after n flights is represented in the fourth quadrant. This is a probability law assumed here to be log-linear in order to simplify the sketch. Actually this law is close to log-linear. From equation 7.2.2.4(b) this curve can be easily obtained through a simple translation of the damage threat per flight. For this illustration, " n " has been assumed to be a thousand flights.
3. The probability law for load (or stresses, or strain) occurrences is represented in the second quadrant. This law is assumed to be log-linear in the interval between limit and Ultimate Loads. Figures reported on the horizontal axis are typical of a commercial aircraft.
4. Each point on the strength versus energy curve (quadrant 1) corresponds to:
 - a. One energy level with its associated probability to have at least one damage of such severity (or higher) on the structure at the last flight before inspection.
 - b. One residual static strength with the associated probability to encounter a load of the same magnitude per flight.
5. The product of these two probabilities is plotted in the third quadrant where a picture of the whole first quadrant curve can be drawn. In the same quadrant, a line representative of equation 7.2.2.4(c) splits the diagram into two domains:

- Acceptable values (probabilities lower than 10^{-9}), top right
- Not acceptable values (probabilities higher than 10^{-9}), bottom left

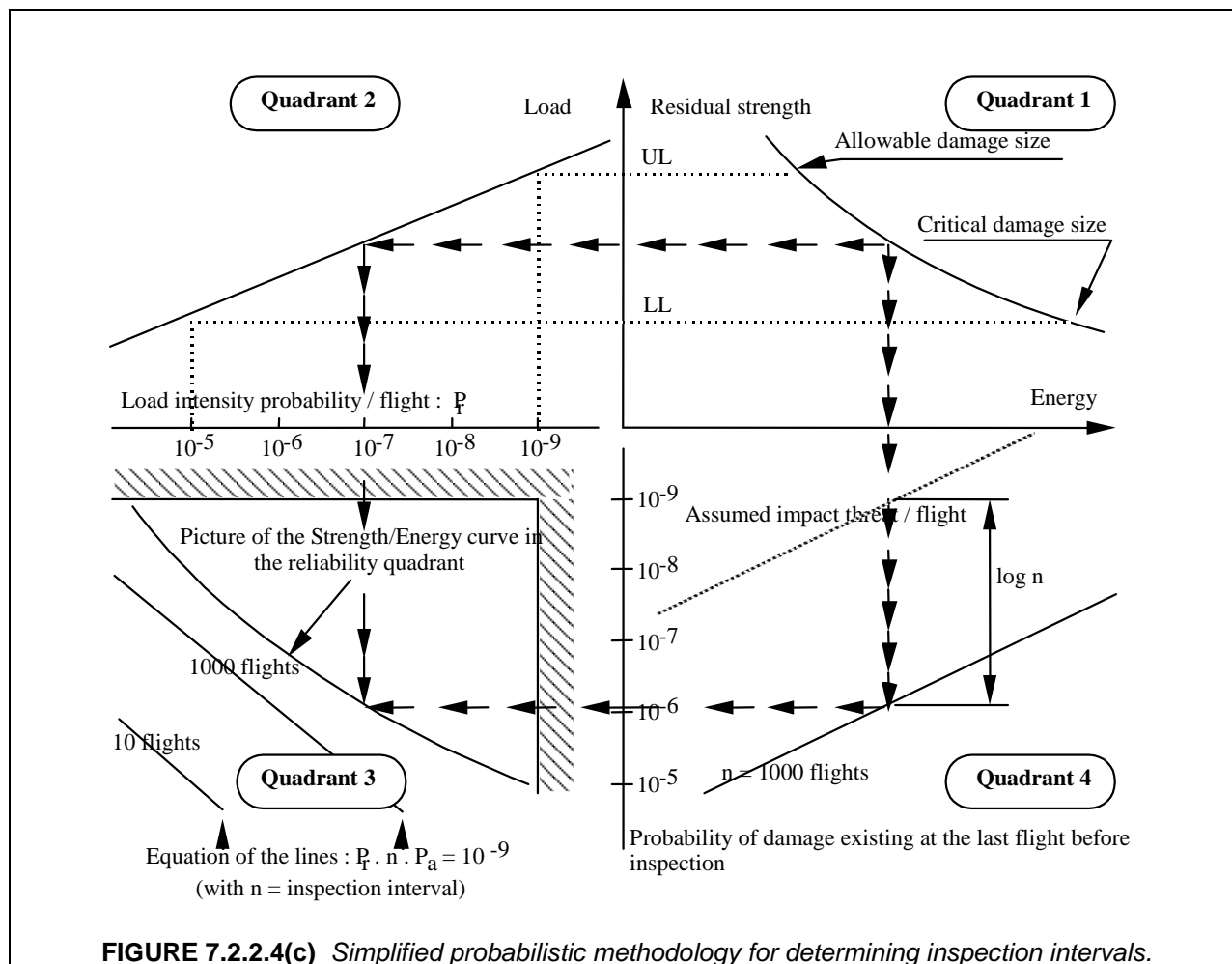


FIGURE 7.2.2.4(c) Simplified probabilistic methodology for determining inspection intervals.

Acceptable damage tolerance is demonstrated for an inspection interval equal to n if the whole curve is located above the border line. This illustration shows that when the inspection interval (n) increases, the strength-energy picture curve moves downward while the straight line delimiting the 10^{-9} probability target moves upward. Acceptable damage tolerance is not achieved when both curves cross.

For very thick laminates where VID is extremely improbable, the calculation is performed with n equal to the whole aircraft lifetime. For thinner laminates where VID can be expected, the maximum acceptable inspection interval is the highest one, among those of the scheduled inspection program, containing the whole strength-energy picture curve above it.

7.2.2.5 Comparison of deterministic and probabilistic methods

The following paragraphs briefly summarize the major differences between the deterministic compliance method and the semi-probabilistic method given in the previous two sections. Both of these methods have been used to successfully certify composite primary structure on commercial transport aircraft. Other probabilistic approaches, covering various aspects of composite design and certification, are reviewed (Reference 7.2.2.5). In the same reference, Northrop Grumman Commercial Aircraft Division (NGCAD) proposes a quite comprehensive method covering both static and damage tolerance require-

ments, with an application exercise to the Lear Fan. Nevertheless, none of these methods have so far been implemented in an aircraft certification program.

In the deterministic method, an upper limit of 100 ft-lb (140 Joules) is used for ultimate strength impact damage, whereas in the probabilistic method, lower levels have been used based on the assessments discussed in Section 7.3.3.

In the deterministic method there is no upper limit on the energy level for impact damages to be considered for Limit Load analyses; damage is considered up to the point of being readily detectable. In the probabilistic method, the upper limit on impact energy for Limit Load analyses is set at a probability of 10^{-9} .

In the deterministic method, inspection intervals have been set based on a qualitative rating system, which is derived based on structural capability and aircraft service experience for the effects of accidental damage and environmental degradation. In the probabilistic method, the maximum inspection intervals are derived using the probabilities of damage and load occurrence, with a reliability of at least 10^{-9} .

7.2.2.6 Full-scale tests for proof of structure (civil aviation)

Compliance with the requirements is built, step by step, through what is usually called a “building block approach” (see Volume 3, Chapter 4). Tests carried out to support the analysis are arranged like a pyramid, where a full-scale test culminates at the top, the bottom referring to generic tests dedicated to the derivation of a statistical basis for allowable values. Low velocity impacts, with their relevant thresholds, should be addressed throughout this pyramid of tests, from the “allowable” level to the full-scale demonstration.

When introducing a low velocity impact damage in a test article, it is important that the selected detectability threshold captures the worst possible situation in terms of internal damage, hence the need to use blunt impactors. Hemispherical impactor geometry, with the smallest size at least 0.5 inch (12.5 mm) diameter, are recommended.

Due to the absence of interaction between high static stresses and fatigue behavior, it is current practice of transport aircraft manufacturers to conduct tests on only one full-scale test article, for both static and fatigue/damage tolerance demonstration. A typical arrangement of tests for this purpose (from various Airbus applications), is illustrated Figure 7.2.2.6.

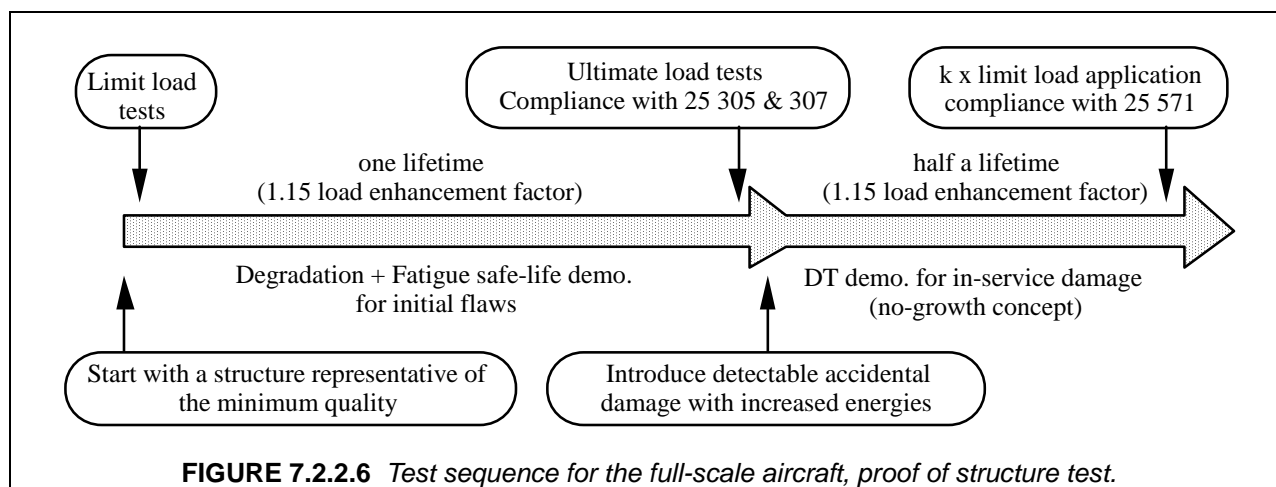


FIGURE 7.2.2.6 Test sequence for the full-scale aircraft, proof of structure test.

Proof of structure, full-scale static test. The test program starts with an article provided with simulated low velocity impact damages, limited by the selected energy cut-off levels and deliberately inflicted at the most stressed areas of the structure. The Ultimate Load capability is demonstrated after fatigue, allowing for environmental adverse conditions. This is in line with the means of compliance provided by the AC 20 107A § 6 Proof of structure-static, sub § (a) : *The effects of repeated loading and environmental exposure which may result in material property degradation should be addressed in the static evaluation.*

Proof of structure, full-scale fatigue/damage tolerance test. When considering the effects of material variability on the repeated load behavior of composite structures, a factor on loads is preferred to a factor on life. The rationale of such approach and the recommended load enhancement factors can be found in References 7.2.1(a) to 7.2.1(d). The demonstration has two parts.

First, an enhanced safe life (flaw tolerant) demonstration, to show that no damage will initiate and grow in a structure representative of the minimum quality allowed by the quality control specification (considering not only impact damage but also various manufacturing flaws). This phase is in line with AC 20 107A § 7 Proof of structure - Fatigue/Damage tolerance, (b) fatigue (safe life) evaluation: *Fatigue substantiation should be accomplished by component fatigue tests or by analysis supported by test evidence, accounting for the effects of the appropriate environment. The test articles should be fabricated and assembled in accordance with production specifications and processes so that the test articles are representative of production structure, etc.*

Second, a no-growth demonstration for more severe impact damages, some of which may become detectable at the scheduled inspection intervals. This phase is in line with AC 20 107A § 7 Proof of structure - Fatigue/Damage tolerance, sub § (a): *Structural details, elements, and subcomponents of critical structural areas should be tested under repeated loads to define the sensitivity of the structure to damage growth. This testing can form the basis for validating a no growth approach to damage tolerance requirements.*

A demonstration of the regulatory static load capability is needed to complete this second phase. A “k” value higher than 1.0 can be required depending on the result of a probabilistic approach, if used for certification. It is the second phase of the full-scale test that brings most to the demonstration of the structural safety. At this stage, a precise definition of damage growth is required. For instance, there may be a possibility where an impact damage will grow under the first service loads following the occurrence and, then reach a definite size after a certain time. This is still to be assumed as a “no-growth” situation, since the “growth” is not detrimental to the structural capability. On another hand, a damage can be definitely arrested by a design precaution (a bolt row for instance). Provided regulatory load capability exists after this size extension, the result is comparable to a no-growth situation.

7.3 TYPES, CHARACTERISTICS, AND SOURCES OF DAMAGE

Damages are generally discussed in two frames of reference - by stage of occurrence and by physical anomaly. Stage of occurrence is separated into manufacturing and in-service categories. Damages occurring during manufacturing are more accurately classified as “flaws” rather than “damages”. They are not distinguished as such in this write-up.

Composite aircraft parts can be damaged during manufacturing, shipping, and service. A primary focus in composites is low velocity impacts that can cause significant damage that may not be clearly visible. Sources of such impact damage include falling tools and equipment, runway debris, hail, birds, and collision with other airplanes or ground vehicles. Airplanes can also be damaged by high velocity impacts from discrete source events (e.g., parts of rotating machinery that fail in turbofan engines and penetrate the engine containment system, the aircraft skin, and supporting structure). All of the above damages can occur to either military or commercial aircraft. Military aircraft may also suffer ballistic damage, as may occur in battle.

Concerns about the effects of impact damage can be quite different, depending on the specific design and application. Compressive residual strength of laminated composite material forms is known to depend on the extent of delaminations and fiber failure caused by transverse impacts. Tensile residual strength is affected by fiber failure. Impact damage can also affect the environmental resistance of a composite structural component or the integrity of associated aircraft systems. For example, impact damage may allow moisture to penetrate into the sandwich core in light-gauge fairing panels or provide a path for fuel leaks in stiffened wing panels. These effects must be understood for safe and economic composite applications.

7.3.1 Damages characterized by stage of occurrence

7.3.1.1 Manufacturing

Manufacturing damage includes anomalies such as porosity, microcracking, and delaminations resulting from processing discrepancies and also such items as inadvertent edge cuts, surface gouges and scratches, damaged fastener holes, and impact damage. The inadvertent (non-process) damage can occur in detail parts or components during assembly or transport or during operation. A list of sources of manufacturing defects is given below:

- Improper cure or processing
- Improper machining
- Mishandling
- Improper drilling
- Tool drops
- Contamination
- Improper sanding
- Substandard material
- Inadequate tooling
- Mislocation of holes or details

Most manufacturing damage, if beyond acceptance limits, will be detected by routine quality inspection. For every composite part, there should be acceptance/rejection criteria to be used during inspection of the part. Damage that is acceptable will be incorporated in the substantiation analysis and test program to demonstrate ultimate strength in the presence of this damage. Some "rogue" defects or damage beyond specification limits may go undetected and consequently, their existence must be assumed as part of damage tolerant design. Establishing the size of the "rogue" or missed flaw is part of the design criteria development process.

Examples of rogue flaws occurring in manufacturing include a contaminated bondline surface, or inclusions such as prepreg backing paper or separation film that is inadvertently left between plies during lay-up. Current inspection methods may not detect these types of defects. As a result, current design practices include the effect of large debonds in damage tolerance criteria which may impose severe weight penalties. In the future, advanced inspection techniques and in-process quality control may lead to less severe criteria. Without adequate inspection techniques, in-process quality controls must be sufficiently rigid to preclude this type of defect.

7.3.1.2 Service

The main characteristic of in-service damage is that it occurs during service in a random manner. Damage characteristics, location, size, and frequency of occurrence can only be predicted statistically, which involves a large amount of data accumulation. In-service damage is typically classified as non-detectable and detectable (often referred to as non-visible and visible). A part has to be designed in such a way that likely, non-detectable damage (per the selected inspection method) can be tolerated under Ultimate Loads and for the life of the structure. The most common in-service damage is due to an impact event. A list of sources of in-service damage threats is given below:

Hailstones
Runway debris
Ground vehicles, equipment, and structures
Lightning strike
Tool drops
Birdstrike
Turbine blade separation
Fire
Wear
Ballistic damage (Military)
Rain erosion
Ultraviolet exposure
Hygrothermal cycling
Oxidative degradation
Repeated loads
Chemical exposure

7.3.2 Damages characterized by physical imperfection

Damage can occur at several scales within the composite material and structural configuration. This ranges from damage in the matrix and fiber to broken elements and failure of bonded or bolted attachments. The extent of damage controls repeated load life and residual strength, and is, therefore, critical to damage tolerance.

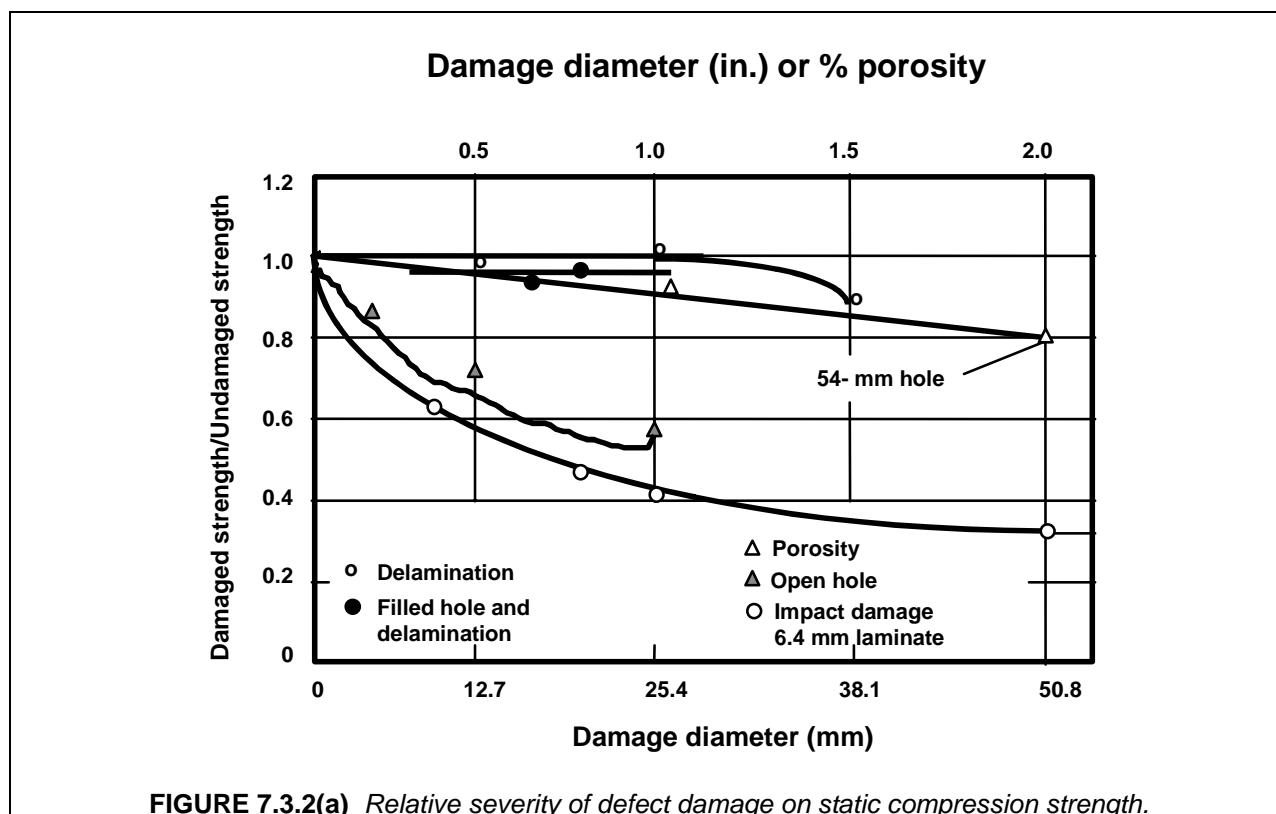
Fiber Breakage. This defect can be critical because structures are typically designed to be fiber dominant (i.e., fibers carry most of the loads). Fortunately, fiber failure is typically limited to a zone near the point of impact, and is constrained by the impact object size and energy. Only a few of the service related events listed in the previous section could lead to large areas of fiber damage.

Matrix Imperfections. (Cracks, porosity, blisters, etc.) These usually occur on the matrix-fiber interface, or in the matrix parallel to the fibers. These imperfections can slightly reduce some of the material properties but will seldom be critical to the structure, unless the matrix degradation is widespread. Accumulation of matrix cracks can cause the degradation of matrix-dominated properties. For laminates designed to transmit loads with their fibers (fiber dominant), only a slight reduction of properties is observed when the matrix is severely damaged. Matrix cracks, a.k.a. micro-cracks, can significantly reduce properties dependent on the resin or the fiber/resin interface, such as interlaminar shear and compression strength. For high temperature resins, micro-cracking can have a very negative effect on properties. A discussion of the effects of matrix damage on the tensile strength can be found in Reference 7.3.2(a). Matrix imperfections may develop into delaminations, which are a more critical type of damage.

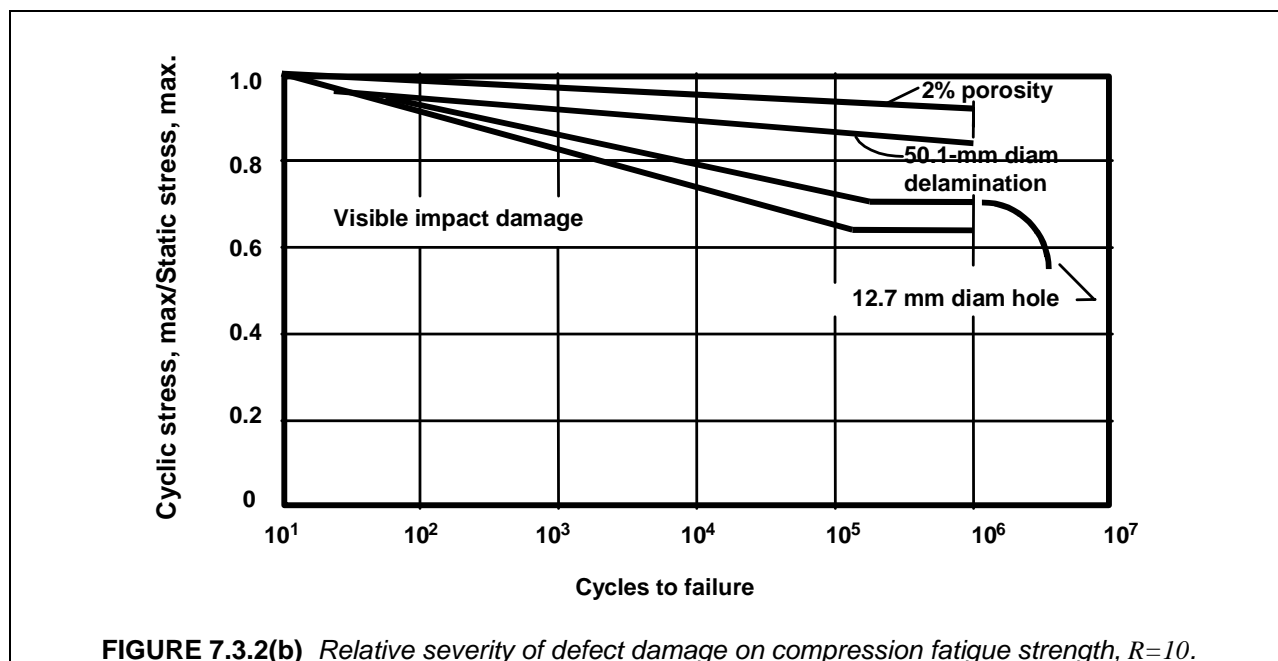
Delamination and debonds. Delaminations form on the interface between the layers in the laminate. Delaminations may form from matrix cracks that grow into the interlaminar layer or from low energy impact. Debonds can also form from production non-adhesion along the bondline between two elements and initiate delamination in adjacent laminate layers. Under certain conditions, delaminations or debonds can grow when subjected to repeated loading and can cause catastrophic failure when the laminate is loaded in compression. The criticality of delaminations or debonds depend on:

- Dimensions
- Number of delaminations at a given location.
- Location - in the thickness of laminate, in the structure, proximity to free edges, stress concentration region, geometrical discontinuities, etc.
- Loads - behavior of delaminations and debonds depend on loading type. They have little affect on the response of laminates loaded in tension. Under compression or shear loading, however, the sublaminates adjacent to the delaminations or debonded elements may buckle and cause a load redistribution mechanism, which leads to structural failure. Methods to estimate the criticality of delamination and debonds are presented in Section 7.8.4.2.

Combinations of Damages. In general, impact events cause combinations of damages. High-energy impacts by large objects (i.e., turbine blades) may lead to broken elements and failed attachments. The resulting damage may include significant fiber failure, matrix cracking, delamination, broken fasteners, and debonded elements. Damage caused by low-energy impact is more contained, but may also include a combination of broken fibers, matrix cracks and multiple delaminations. There is some experimental evidence that, for relatively small damage sizes, impact damage is more critical than other defects (see Figures 7.3.2(a) and (b), References 7.3.2(b) and (c)). Note that all of the data shown in these figures are for damage sizes less than 2 inches (50 mm). Some results for damages greater than 2 inches (50 mm) suggest large holes or penetrations are at least as severe as equivalent sizes of impact damage.



Flawed Fastener Holes. Improper hole drilling, poor fastener installation, and missing fasteners may occur in manufacturing. Hole elongation can occur due to repeated load cycling in service. Such issues can effectively extend the size of the hole and lead to assumptions that the hole is open (or filled, depending on which leads to the greater notch sensitivity). The notch sensitivity of a composite has generally been dealt with by using semi-empirical analyses.



7.3.3 Realistic impact energy threats to aircraft

As discussed in Section 7.2.2, certification of aircraft composite structure requires the establishment of realistic impact energy level cut-offs for Ultimate Load considerations. A conservative assumption is to set the energy level at a 90% probability, analogous with the concept of a B-basis strength value. This then means that the *realistic* energy cut-off has been selected in such a way that, at the end of lifetime of the aircraft, no more than 10% of them will have been impacted with an energy value equal to this cut-off level or higher. For these 10% corresponding to a more damaged situation, and then possibly not being able to comply with the Ultimate Load requirements, damage tolerance considerations will demonstrate the regulatory safety level.

Letting E_{co} = energy cut-off value, and with P_a the probability, per flight, to encounter one impact with an energy $E \geq E_{co}$, then, $(1-P_a)$ is the probability for an aircraft to have encountered either no impact or impacts of a lower energy on that flight. In fact the risk of low velocity impact damage is not likely to occur during the actual flight, but during the various operations associated with this flight, e.g., aircraft servicing and a shared part of the risk associated with the scheduled inspections.

Then it follows that:

$(1-P_a)^n$ is the probability to have never encountered any impact with an energy of $E \geq E_{co}$ after n flights, and then the probability to have encountered at least one damage created by an impact with an energy of $E \geq E_{co}$ after n flights is given by:

$$P = 1 - (1-P_a)^n$$

Assuming that:

$n = 50,000$ flights for a short/medium range commercial aircraft,
 $P = 0.1$

Then $P_a = 2.1 \times 10^{-6}$

In this case, the realistic energy level to be allowed for is the one corresponding to a probability of occurrence of $2 \cdot 10^{-6}$ per flight. Should the target of P be 0.01, P_a would then be equal to $2.1 \cdot 10^{-7}$, which obviously corresponds to a higher energy level, though not very far from it since the probability versus energy relationship is assumed to be log-linear.

In the case of FAR 25 fixed wing structures, both values for P_a are lower than the probability commonly associated with Limit Loads occurrences, which can be assumed in the range of 10^{-5} per flight hour. It may be unreasonable to state that such so-called "realistic" energy level occurrence is more "realistic" than a limit Loads event. Then, clipping this probability figure at the 10^{-5} per flight value should also be acceptable where the average duration of one flight is around one hour.

At this stage, one must unfortunately admit that there is very little data for quantifying energy levels in relation to these probability values. Just for the purpose of an exercise to illustrate this approach, some figures drawn from the literature are given hereafter.

In reality, P_a is the product of two probabilities since associated events are assumed as independent:

$$P_a = \text{Probability (impact damage occurrence)} \times \text{Probability (damage energy} \geq E_{co})$$

As far as the second term is concerned, the only results known from a field survey are reported in Reference 7.3.3(a). With the analysis of 1644 impacts, this survey can be considered as quite comprehensive. Although, these records are representative of military aircraft from the US Navy Forces (F-4, F-111, A-10 and F-18), they can be extended to transport category aircraft investigations since maintenance tools and operations should not be very different. In this study, all the 1644 impact dents observed on the metallic structures have been converted into energy levels through a calibration curve obtained on a F-15 wing, shown in Figure 7.3.3(a). According to this reference, the upper limit impact energy for the aircraft surveyed is approximately 35 ft-lb (48 joules).

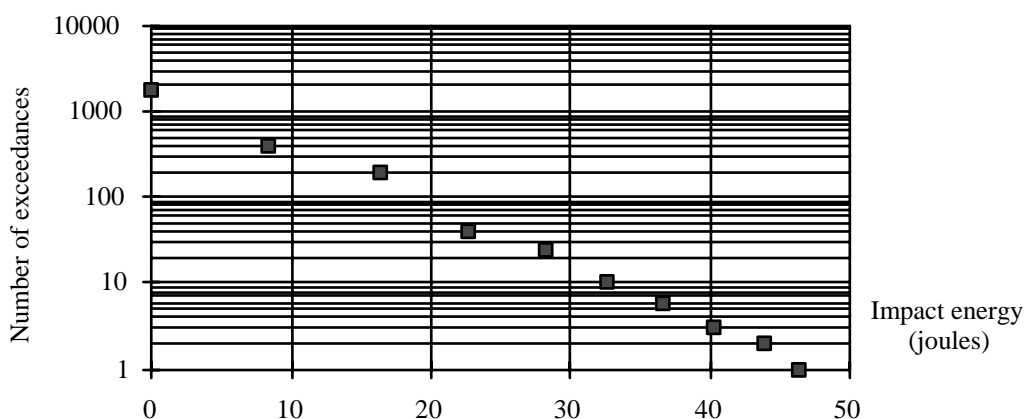


FIGURE 7.3.3(a) Number of exceedances versus impact energy level for an aircraft lifetime.

Since this report does not mention the aircraft lifetime in relation to each identified damage and the impact location, it is impossible to derive an impact hazard per flight hour. Nevertheless, this survey provides: 1) the order of magnitude of the expected energy, should an impact occur, and 2) the shape of the curve of exceedance (N_e) versus energy. The latter can be assumed as log-linear in this range of energy, with a slope of about -11 ft-lb/Log N_e (-15 joules/Log N_e).

The probability (P_e) of exceeding a given level of energy, should an accidental impact occur, can be then easily drawn from this curve through the relationship:

$$\text{Log } P_e = -x(j) / 15$$

More rigorously, a two-parameter, Weibull distribution has been established from this field survey (Reference 7.3.3(a)), with shape and scale parameters equal to 1.147 and 8.2 (5.98 for ft-lb energy units), respectively.

In regards to the probability of damage occurrence, useful data are published in Reference 7.3.3(b). Data collected from visits to American Airlines, Delta Airlines, United Airlines, the North Island Naval Aviation Depot and from communications with De Havilland Aircraft Inc. are summarized in this report. Records concerning 2100 aircraft shared by 19 operators have been analyzed. For a total number of 3,814,805 flight hours, 1484 maintenance induced damages - which correspond to low velocity impact damages - have been noticed. Statistics on hail storms, lightning strikes and bird strikes are also reported in this reference. Unfortunately, the energy level associated with these maintenance-induced and service damages have not been investigated.

From these data, the low velocity impact damage probability of occurrence can be estimated at 3.9×10^{-4} per Flight Hour. This figure obviously concerns the whole aircraft and the probability associated to a dedicated part - e.g. a rudder skin - should be lower. Given that "Murphy's law" should not be ignored, impact damage probabilities of the same order of magnitude should be assumed. With a figure ranging between 10^{-3} and 10^{-5} per hour, the event should be assumed as reasonably probable, according to the definitions provided by the ACJ 25 1309.

Now combining all these field survey data, Figure 7.3.3(b) shows the value of P_a versus impact energy for various damage occurrence probabilities (per hour) in the reasonably probable domain. With the objective that the "realistic" energy level encompasses 90% of the aircraft population at the end of lifetime ($P_a = 2.1 \times 10^{-6}$), assuming a damage occurrence probability at the upper bound of the reasonably probable domain and one flight times one hour, the result of this application exercise is:

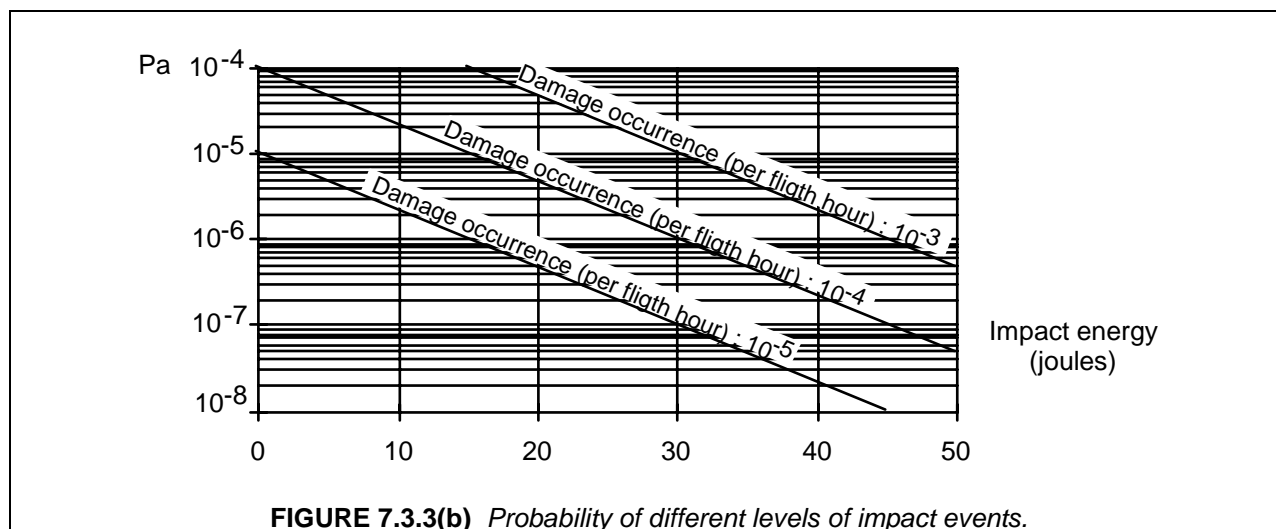


FIGURE 7.3.3(b) Probability of different levels of impact events.

Eco should not be below 30 ft-lbs (40 joules). Assuming now $P_a = 10^{-5}$, the associated energy level is 22 ft-lbs (30 joules).

The energy cut-off threshold selected for Airbus programs (since the A320 type certification and after) is 37 ft-lb (50 joules), except for the inboard part of the horizontal tailplane, where the cut-off is 103 ft-lb (140 joules). Reflecting USAF requirements and company design criteria, Boeing has used an impact energy cut-off threshold of 100 ft-lb (136 joules) for commercial aircraft certification programs.

With the view to implement a probabilistic approach in the damage tolerance demonstration of the ATR 72 CFRP outer wing, Aerospatiale investigated accidental impact scenarios for deriving the figures needed by their method (Reference 7.3.3(c)). After these investigations, a 27 ft-lb (36 joules) cut-off threshold for structural substantiations was used.

7.4 INSPECTION FOR DAMAGE

The ability to detect damage is the cornerstone of any maintenance program employed to ensure the damage tolerance of a specific structure. Such a program must combine one or more inspection methods with an appropriate schedule to reliably detect damage prior to unacceptable performance degradation. Inspection methods are also relied upon to quantify such damage in support of residual strength assessments. Accessibility for inspection must be accounted for in the design and in maintenance plans.

To achieve economic goals, in-service inspection programs often rely on combinations of frequent, relatively simple inspections (usually of broad areas) and less frequent, but more intense, examinations (typically of more localized areas). The capabilities of each inspection method (i.e., detectability threshold, detection reliability) must be well understood as a function of damage state for each structural location. Since the impact variables (i.e., impactor geometry, velocity, angle of incidence, etc.) strongly influence the damage state at a specific location, the detectability thresholds and reliabilities should be quantified considering the ranges of these variables expected in service.

Inspection procedures can be divided into two main classes. The first, which is most general, includes both destructive and nondestructive methods used for concept development, detailed design, production, and maintenance. The second class includes only those nondestructive evaluation (NDE) methods that can be practically used in service to locate and quantify the effects of impact damage. The second class is a subset of the first and depends on a technology database suitable for relating key damage characteristics to structural integrity.

7.4.1 Aircraft inspection programs

In aircraft applications, scheduled inspections are the basis for initially detecting damage that does not result in an obvious malfunction. Aircraft structures have historically relied heavily on visual methods in this process. Typical scheduled inspections for these applications are:

- Walk around – long distance visual inspection to detect punctures and large areas of indentation or fiber breakage, i.e., readily detectable damage.
- General visual inspection – careful visual examination of relatively large areas of internal and/or external structure for indications of impact damage (e.g., dents, fiber breakout) or other structural anomaly. Adequate lighting and appropriate access to gain proximity (e.g., removal of fairings and access doors, use of ladders and work stands) are required. Inspection aids (e.g., mirrors) and surface cleaning may also be necessary.
- Detailed visual inspection – close-proximity, intense visual examination of relatively localized areas of internal and/or external structure for indications of impact damage or other structural anomaly. Like general visual inspections, adequate lighting and appropriate access to gain proximity are required. Inspection aids and techniques may be more sophisticated (e.g., lenses, grazing light on a clean element) and surface cleaning may also be necessary.

- Special detailed inspection – inspections of specific locations for non-visible damage using non-destructive procedures (e.g., ultrasonics, x-ray, and shearography).

The use of visual inspection methods for initial damage detection is likely to continue due to the cost and time associated with applying other NDE procedures over the full surface of a structure. Advances in optical techniques, for example, allow large areas of a structure to be quickly inspected for local defects; however, the high cost of equipment needed for such procedures remains as a barrier to implementation of the technology by aircraft operators.

The widespread use of visual inspection procedures for finding service damage in composite structure has led to the use of barely visible impact damage (BVID) thresholds in design sizing (Reference 7.4.1(a)). The FAA has recommended such design practice for composite structure to account for damage that may never be found in service. Past interpretations of the threshold for visibility have been somewhat subjective, with different commercial and military applications defining minimum visible dent depths between 0.01 in. (0.25 mm) and 0.10 in. (2.5 mm).

When damage is initially detected, more detailed visual measurements and various types of ultrasound are used in directed inspections to quantify its extent. Surface damage measurements (e.g., location, dent depth, or crack length) can be quantified with gages and scales commonly used in maintenance. "Coin tapping," which is based on principles similar to lamb wave propagation, provide a rough measure of the extent of sub-surface damage. Pulse-echo ultrasound, which requires equipment and some training, has also been applied in service to get a more accurate measurement of the extent of sub-surface damage with single-side access. These procedures are simple to apply without having to disassemble the structure, but tend to yield very subjective results. More repeatable measurements are conceivable when the structural repair manual (SRM) provides instructions on how they should be applied to specific structure.

Aerospatiale (Reference 7.4.1(b)) has shown that a dent depth between 0.01 and 0.02 in. (0.3 and 0.5 mm) is detectable, through a detailed visual inspection, with a probability better than 0.90. However, the use of dent depth as a damage metric has several shortcomings. First, dent depths depend on a number of impact variables, including the impactor geometry, and may not be a good indication of the extent of underlying damage. Also, in Reference 7.4.1(c) it was shown that the impact dent could decay with time under the combination of fatigue and aging due to viscoelastic phenomena. In some cases, the initial impact indentation dent depth (δ_i) may be as much as 3 times that of the decayed dent depth. This was also confirmed by Canadian investigations reported in Reference 7.4.1(d). Dent decay versus time is probably material dependent. When using maintenance damage detection schemes based on visibility, it is thus necessary that damages used to demonstrate tolerance to BVID have decayed dent depths greater than or equal to the detectability thresholds (δ_d). Therefore, in the absence of data, an initial dent depth of at least .04 in. (1 mm) should be selected to remain detectable at the end of the longest scheduled inspection interval.

7.4.2 Recommendations for damage inspection data development

Aircraft manufacturers apply a range of inspection procedures to help meet development and application goals. These goals include identifying: (a) critical damage types and design criteria for specific structural details, (b) process and quality controls for production parts, and (c) reliable procedures for maintenance in the field. Impact surveys, which involve applying a range of impact damage to representative structure, are recommended to support the development of enabling inspection technologies. They should result in definition of visual damage characteristics for routine inspections, and more rigorous, but reliable, NDE procedures that may be used to quantify residual strength. These efforts should include quantification of the impact event, and application of both nondestructive (e.g., through-transmission ultrasound) and destructive (e.g., microscopic cross-sections) measurements of the resulting damage. Note that, as discussed in Section 7.5 (Damage Resistance), impact surveys provide the most meaningful results when applied to specific structural configurations and design details.

7.4.2.1 Goals

The most obvious goal of the impact survey inspection results is the definition of detectability limits and detection probabilities for the recommended in-service inspection methods. Comparison of results from the in-service techniques with more sophisticated laboratory methods provides a strong basis for quantifying both parameters. The range of impact variables and structural configurations included in the impact survey allow variations in the detectability limits and detection probabilities with these variables to be addressed.

A less apparent, but equally important goal of the impact survey inspection results is the development of techniques for quantifying structural degradation. Reductions in structural performance parameters (i.e., stiffness, strength) must be defined to avoid overly conservative assumptions in residual strength assessments, which lead to excessive repair requirements. The impact survey results provide the opportunity to accomplish this through the development of relationships between field-measurable damage parameters and the actual degradation determined from destructive evaluation. Note that there is little relevance to relationships between impact *event* metrics and the resulting structural degradation since, generally, little or nothing is known about the event that caused the damage (e.g., impactor geometry, energy levels, time since occurrence).

7.4.2.2 Inspection techniques

Both destructive and NDE methods should be applied to maximize the information gained from impact surveys. All of the NDE methods recommended for field maintenance should be included in the survey. Correlation between field NDE techniques and more rigorous laboratory evaluations, including destructive mechanical tests (to be discussed in Section 7.8.3) and microscopy of cross-sections, should help establish key characteristics of impact damage.

Inspection methods which are generally only suitable for impact surveys conducted in the laboratory include through transmission ultrasound (TTU), microscopy, thermal deply, local reduced stiffness measurements, and residual strength tests. The last one will be presented in Section 7.8.3. The use of TTU requires access to both sides of a structure, special equipment (e.g., ultrasonic signal generators and transducers capable of frequencies between 1 and 10 MHz) and a grease or fluid media to couple probes with the damaged structure. Microscopic cross-sections are best used to see matrix cracks and delamination. A polished cylindrical-section highlighted by dye penetrant may help define how such matrix damage combines to form sublaminates (which will be discussed further in Sections 7.8.2 and 7.8.3). Destructive methods which burn away resin (referred to as thermal deply for laminates) are the most efficient laboratory procedures for characterizing the extent of fiber damage. Although such methods were first applied to laminates made from unidirectional tape, they also work for other material forms, such as textiles.

Pulse-echo ultrasound (PEU) and X-ray, which both require special equipment, can be used in either laboratory or field applications. Only one-side access is needed for PEU. It has been used to provide some measure of the extent of delamination at different levels. As was the case with TTU, some fluid media is normally required to couple the PEU transducer with a damaged structure's surface. More advanced ultrasonic methods using laser pulses and optical data reduction (one-sided, no contact access) are expected to emerge as NDE technology progresses. X-ray typically requires the penetration of special fluids to highlight the damaged substructure.

The reduced stiffness resulting from damage may be quantified in a test laboratory, without generating further damage, by applying an out-of-plane load at the impact site and measuring the local deflection. This technique, which applies load in a manner similar to quasi-static impact tests, provides a measure of local load carrying capability. Local reduced stiffness measurements help to quantify effective mechanical properties rather than discrete damage characteristics and, therefore, can result in simpler residual strength analyses. An ultrasonic method, which (with more development) may be suitable for field applications, uses lamb wave dispersion measurements to quantify axial and flexural stiffness (Reference 7.2.2.3(j) and 7.4.2.2). Lamb waves propagate in a flexural mode at wavelengths on the order of struc-

tural thickness. Relatively low frequencies (less than 1 MHz) are required to generate such waves. Changes in velocity as a function of frequency (i.e., wave dispersion) relate to structural bending and extensional stiffness through analysis. This method has been successfully applied to quantify the reduced stiffness of impact damage created by a wide range of sources. Figure 7.4.2.2 shows a plot correlating a mechanical measurement of local reduced bending stiffness with that obtained from flexural wave propagation. Note that neither dent depth nor ultrasonic C-scan area had as good a correlation with mechanical measurements of reduced stiffness.

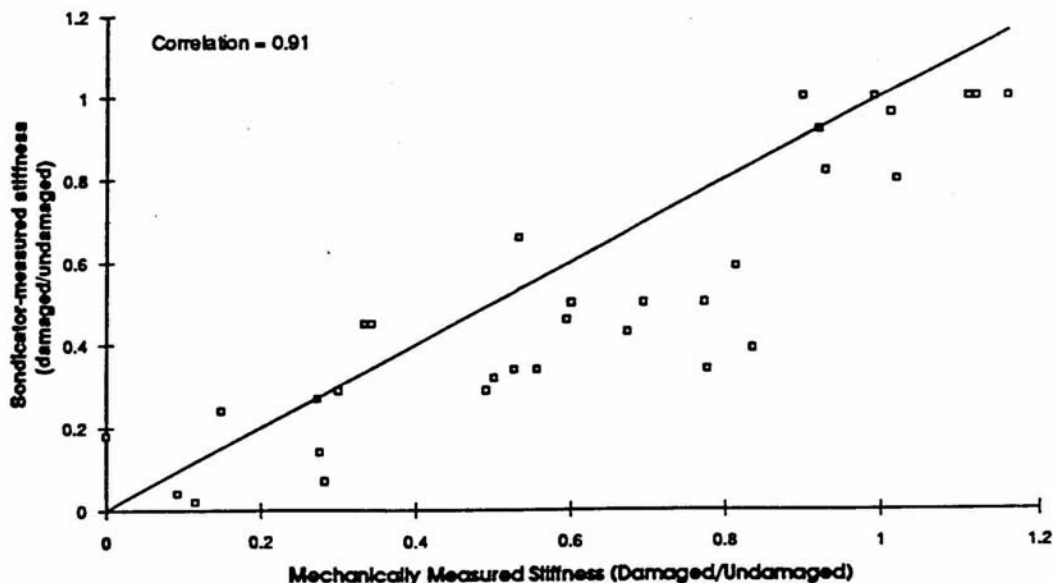


FIGURE 7.4.2.2 Mechanical and ultrasonic experimental measures of local reduced stiffness at impact damage (References 7.2.2.3(j) and 7.4.2.2).

7.5 DAMAGE RESISTANCE

Damage resistance, as used in the context of this discussion, relates to a structure's resistance to various forms of damage occurring from specific events. It is generally an issue of structural weight for the designer, and of economics for the operator. Considering potential threats for commercial and military aircraft, this covers a large range of damage states. Based on the specific structural configuration and design details, some damage types pose a more serious threat to structural performance than others. The ensuing discussion will highlight known damage resistance mechanisms and the trade in properties one can expect in selecting a particular material type or design configuration for different applications.

7.5.1 Influencing factors

The composite impact damage characteristic that has been given the most attention to date is delamination and/or element disbond resistance. Numerous attempts at improving this property through material developments were pursued during the 1980s and into the 1990s. These included toughened resin systems, stitching, z-pinning, and textile material forms (with varying degrees of through the thickness reinforcement). Fiber stress versus strain properties were also found to be important to the resistance of impact damage dominated by fiber failure. The high tensile strain-to-failure of fiberglass and

aramid fibers make them significantly more resistant to failure under impact loads than carbon. Finally, impact damage resistance has been found to depend on both the structural configuration and local design detail. Examples of the former have been noted in differing impact damage characteristics for composite structures stiffened by sandwich core materials and discrete elements. Laminate stacking sequence, local thickness buildups at bonded elements, adhesive layer inserts, proximity of discrete structural elements, and redundant mechanical fasteners are some typical examples of structural details crucial to impact damage resistance.

7.5.1.1 Summary of results from previous impact studies

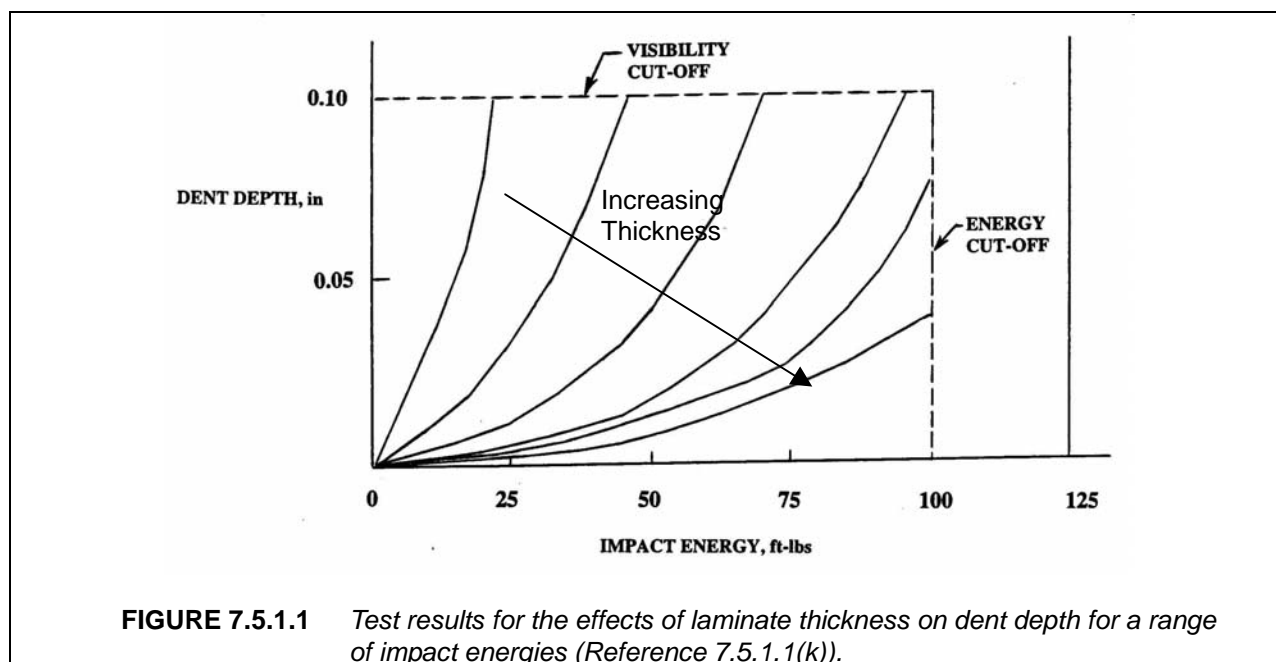
The majority of composite damage studies performed to date have pursued the fundamentals of composite material response. Reviews of studies addressing the fundamentals of composite material response, as related to damage resistance, can be found in References 7.5.1.1(a) through 7.5.1.1(d).

Many impact studies performed in the past concentrated on relatively thick wing-type structures (References 7.5.1.1(e) through 7.5.1.1(i)). Impact testing was performed on both coupons and subcomponents using simulated impact threats, usually with a hemispherical impactor tip (typically referred to as a “tup”). These tests correlated well with industry studies involving various shop tools dropped onto test articles. Documented studies for tests performed at the structural level generally evaluated damage by visibility and residual strength, although planar ultrasonic C-scans have also been used in some cases. More detailed evaluations of impact usually occurred only at the coupon level. For example, results shown in Figure 7.5.1.3 are characteristic of those obtained with standard test coupons developed by NASA (impact specimen size = 7 in. X 12 in. (180 mm x 300 mm) and machined CAI specimen size = 5 in. X 10 in. (130 mm x 250 mm)) and Boeing (impact and CAI specimen size = 4 in. X 6 in. (100 mm x 150 mm)).

The damage states and resulting residual strengths observed in these early tests were found to be a strong function of impact energy and relatively independent of the impactor shape. Transverse cracks and delaminations were found to be the primary failure mechanism for the “brittle” epoxy laminates under study at that time, with the areal extent of damage being a strong function of the impact energy. Local fiber failures were suppressed, until penetration was achieved, by the formation of large delaminations which reduced contact forces by locally softening the laminate. Matrix damage was primarily responsible for reduced CAI strength, while fiber failure, which would be influenced by impactor geometry, was not found to be a strong contributor to the observed compression strength degradation. These findings, along with ease of analytical modeling, led to the use of spherical shaped impactors with diameters between 0.5 in. (13 mm) and 1.0 in. (25 mm) for the majority of impact studies on fibrous composites to date.

Towards the end of the 1980s, an extensive evaluation of impact in wing-gage structure was performed by Northrop and Boeing under contract with the U.S. Air Force (Reference 7.5.1.1(j)). The focus of this study was on the impact damage resistance of material, laminate, and structural geometry. A building-block test approach was used, including coupons, 3- and 5-stringer stiffened panels, and wing boxes (multi-spar and multi-rib). Those variables that were found to have a significant effect on the test results included laminate thickness, laminate lay-up, material toughness (as quantified by interlaminar G_{Ic}), stiffener type, impact location, and panel boundary conditions. Tests and analyses were documented on the impact structural response, characteristics of the resulting damage, and CAI strength. Figure 7.5.1.1 shows typical results from this extensive study. Note the effects of laminate thickness and impact energy on the resulting damage, as measured by visible dent depth. As shown in Figure 7.5.1.1, an energy cut-off, rather than visibility limits, has been used to bound Ultimate Load design requirements for thick structure. Also worthy of note for stiffened structure is the importance of local fiber failure in the flange and webs of stiffeners subjected to impact. This effect is not shown in Figure 7.5.1.1 although the high levels of impact energy required to create such damage may also lead to an energy cut-off for ultimate design considerations. Realistic impact threat levels should also be considered when establishing Limit Load requirements; however, an energy cut-off is not appropriate since aircraft safety is dependent on detecting any damage occurring in a multitude of real-world scenarios.

More recently, the impact damage resistance of relatively thin-gage stiffened fuselage and sandwich structures were studied by Boeing under contract with NASA (References 7.5.1.1(l) through 7.5.1.1(n)). Several material, laminate and structural variables were evaluated in a designed experiment which also included a wide range of extrinsic variables related to the impact event. The extent and type of impact damage to the matrix and fibers was measured using several different destructive and nondestructive methods. Some of the thicker-gage fuselage panels included in this study were on the order of outboard wing or empennage panels (skin gages ≈ 0.18 in. (4.6 mm)).



As was the case with previous studies, impact energy and laminate thickness were found to have a strong effect on the resulting damage in fuselage gage structure (Reference 7.5.1.1(l)). Of the extrinsic variables found to be important, impactor diameter and shape had the most important implications to damage resistance, inspectability and post-impact residual strength. At high impact energies, impactors with relatively large diameter created more extensive damage and less surface indication (i.e., dent depth) than smaller impactors which typically penetrated the laminate. Unlike the relatively thick laminates (0.2 to 0.5 in. (5.1 mm to 13 mm)) considered for wing structures, matrix toughness had little effect on the damage area of minimum gage fuselage structure (i.e., 0.09 in. (2.3 mm) thick). Other design variables affecting impact damage resistance included stiffener geometry, addition of adhesive layers at skin/stiffener interfaces, carbon fiber type, and matrix toughness for the thicker laminates. Several interactions between these variables were found to be as strong as the individual variable main effects. Test correlation with analytical simulations showed that the fixture used to support the stiffened panel had a significant effect on the structure's dynamic response during impact. This shows the need to test panels with boundary conditions as close to those of the configured structure as feasible or use static indentation tests.

7.5.1.2 Through-penetration impacts

Few investigations have addressed resistance to high-energy impact events that penetrate the entire laminate. Reference 7.5.1.2 performed limited through-penetration impacts of all-CFRP and GFRP/CFRP hybrid laminates using a blade-like impactor, shown in Figure 7.5.1.2(a). Impact energies were selected to be at least sufficient to result in penetration. Comparison of the instrumented force-displacement results for through-penetration impacts revealed significant differences between material types.

Curves for several CFRP materials are shown in Figure 7.5.1.2(b). The AS4/938 tow has a higher load than the AS4/938 tape, resulting in an approximately 60% higher event energy. This difference may be attributed to the larger damage formed adjacent to the penetration in the tow-placed laminate, as observed in ultrasonic scans.

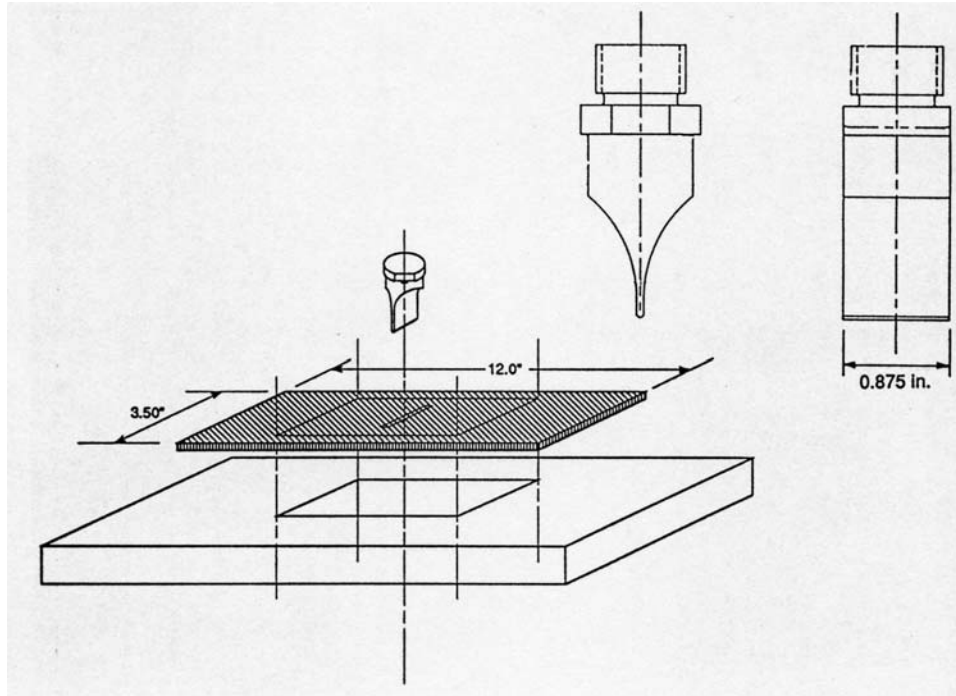


FIGURE 7.5.1.2(a) Penetrating impact support fixture.

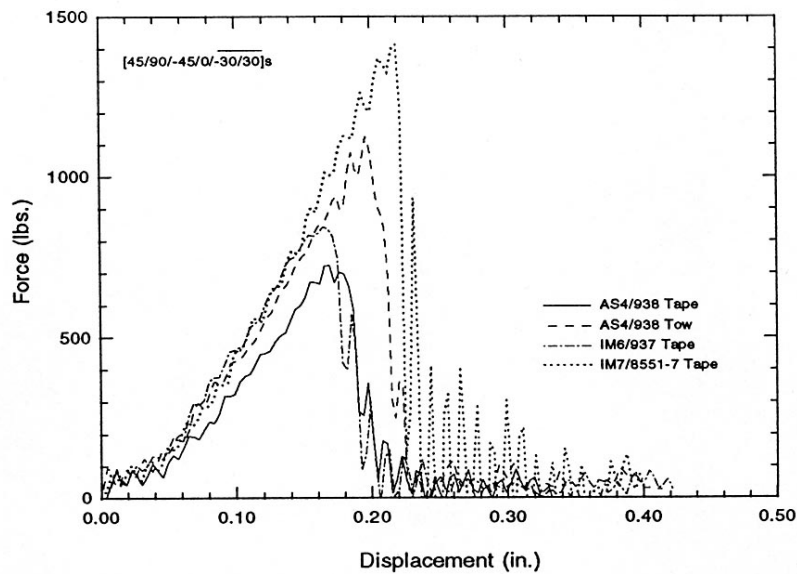


FIGURE 7.5.1.2(b) Instrumented impact results for through-penetration of AS4/938 tow and tape, IM6/3501-6, and IM7/8551-7.

The IM6/937A tape results showed a peak load and total event energy that were 20-25% above that of the AS4/938 tape. The amount of damage area created was similar for the two materials, as might be expected for equivalent resin systems. The energy differences, therefore, might be due to the slightly higher laminate bending stiffness and fiber strengths, both a result of the higher stiffness of the IM6 fiber.

Penetration of IM7/8551-7 tape resulted in a 40% higher maximum load and a 65% higher total event energy than IM6/937A tape. Ultrasonic scans indicated that damage created adjacent to the penetration was significantly smaller in IM7/8551-7 than in any of the other materials. Possible causes for the energy difference include: (a) the slightly higher bending stiffness and fiber strength with the IM7 fiber, and (b) the increased energy absorbed per unit damage due to the higher toughness of 8551-7. Neither of these, though, appear likely to account for a majority of the energy increase. Extension of the crack beyond the net impactor length, however, would require additional fiber failure and associated energy. This scenario is plausible since 8551-7 resin is resistant to matrix damage that would reduce the stress concentration near the corners of the penetrator. Note that the ultrasonic methods used for the current study are unable to distinguish fiber failure zones.

Force-displacement curves are presented in Figure 7.5.1.2(c) for tow-placed laminates of 100% AS4/938, 100% S2/938, and an intraply hybrid consisting of 50% AS4 / 50% S2 / 938 with a 12 tow repeat unit width. As expected from the fiber stiffness difference, the slope of the 100% S2/938 curve is less than that of the 100% AS4/938, and that of the intraply hybrid falls midway between. The total event energy of the S2/938 was over twice as large as that of the AS4/938, and the intraply hybrid energy was midway between. Another conspicuous feature of the intraply hybrid curve is the relative ductility of the failure, as compared to either the AS4/938 or S2/938.

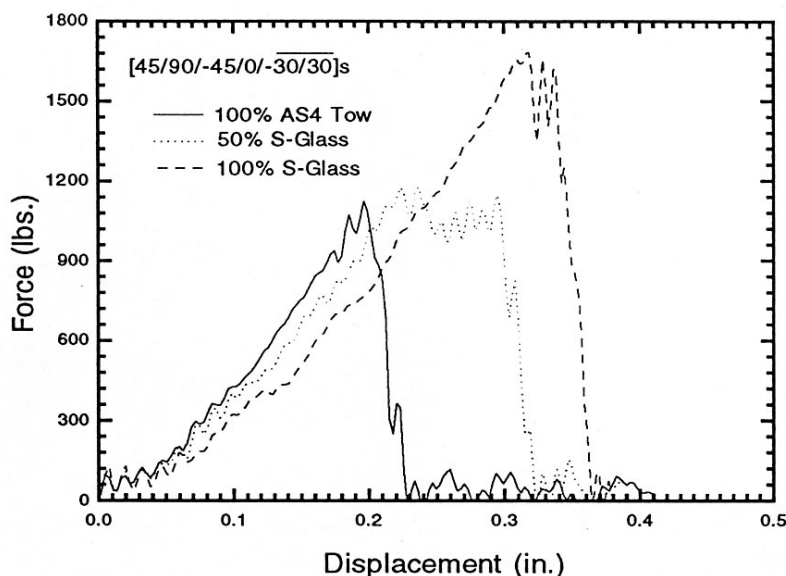
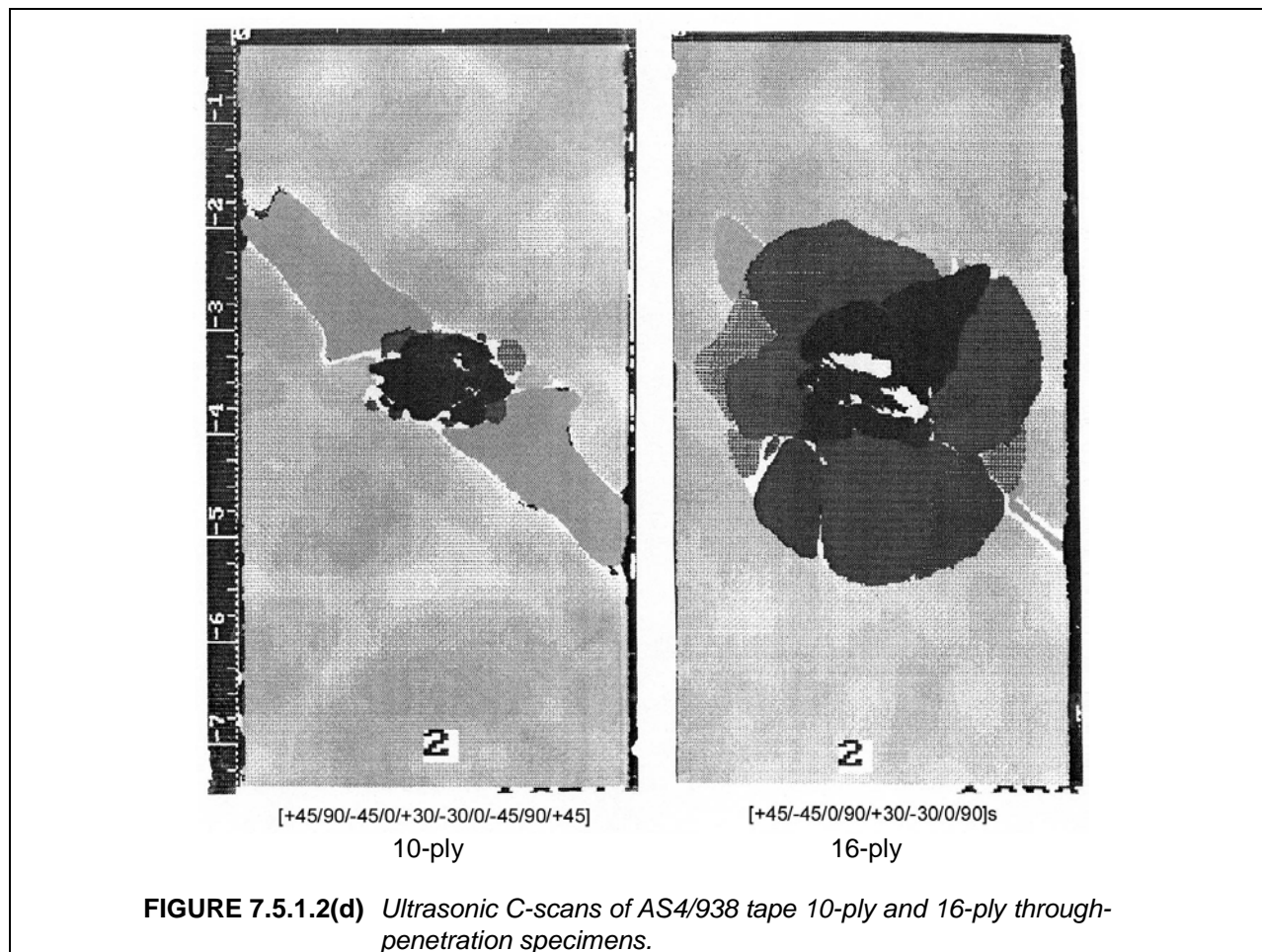


FIGURE 7.5.1.2(c) Instrumented impact results for through-penetration of tow-placed laminates consisting of various percentages of AS4 and S2.

Lay-up and/or thickness effects were also observed to significantly affect the resulting damage state. Figure 7.5.1.2(d) compares the delamination extent for the 10-ply laminate with that of the 16-ply laminate. The relatively high bending stiffness of the 16-ply laminate may result in the formation of larger matrix splits and delaminations near the crack tip.



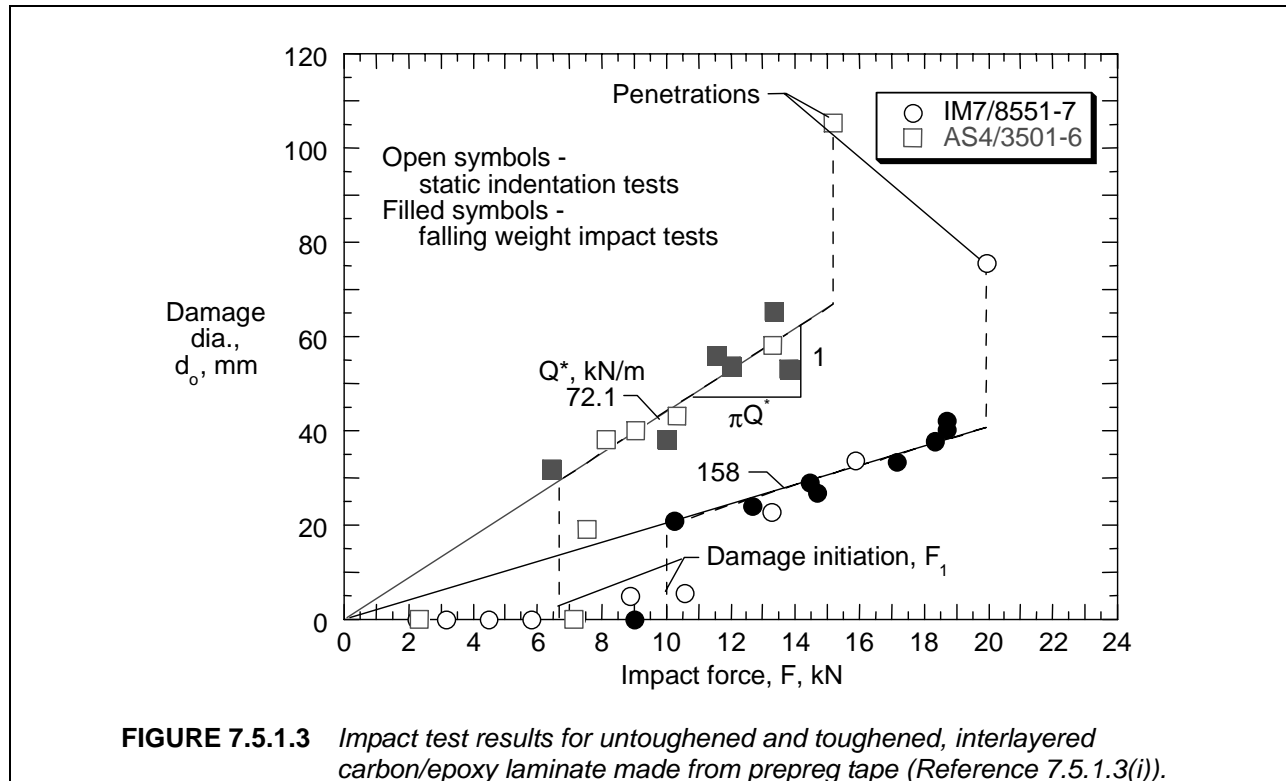
7.5.1.3 Material type and form effects

The ability of composite structures to resist or tolerate damage is strongly dependent on the constituent resin and fiber material properties and the material form. The properties of the resin matrix are most significant and include its ability to elongate and to deform plastically. The area under a resin's stress-strain curve indicates the material's energy absorption capability. Damage resistance or tolerance is also related to the material's interlaminar fracture toughness, G , as indicated by energy release rate properties. Depending on the application G_I , G_{II} , or G_{III} may dominate the total G calculation. These parameters represent the ability of the resin to resist delamination, and hence damage, in the three modes of fracture. The beneficial influence of resin toughness on impact damage resistance has been demonstrated by tests on newer toughened thermoset laminates and with the tougher thermoplastic material systems.

Investigations have been conducted on the effect of fiber properties on impact resistance. In general, laminates made with fabric reinforcement have better resistance to damage than laminates with unidirectional tape construction. Differences among the carbon fiber tape laminates, however, are small. Some studies have been made of composites with hybrid fiber construction, that is, composites in which two or more types of fibers are mixed in the lay-up. For example, a percentage of the carbon fibers are replaced with fibers with higher elongation capability, such as fiberglass or aramid. Results (References 7.5.1.3(a) through 7.5.1.3(d)) in both cases have shown improvement in damage resistance and residual compression strength after impact. Basic undamaged properties, however, were usually reduced.

Figure 7.5.1.3 shows typical standard flat specimen test results which distinguish the impact damage resistance of a toughened composite (IM7/8551-7) and an untoughened material system (AS4/3501-6).

The toughened material resists delamination growth under transverse loading, resulting in smaller damage diameter per given level of impact force. Studies have shown that mode II interlaminar fracture toughness (G_{IIc}) is the critical property for resisting delamination growth under transverse load conditions (References 7.5.1.3(e) and (f)). The G_{IIc} of a laminate can be enhanced by toughening the matrix. The value of G_{IIc} has also been found to be a strong function of the thickness of toughened resin interlayers existing between plies in the laminate. Composite laminates with this microstructure have improved delamination resistance. However, systems that use toughened resins throughout the laminate may have a significant loss of hot/wet compressive strength, reduced large notched tensile strength, and other drawbacks.



It should be noted that the test results in Figure 7.5.1.3 are a strong function of the laminate thickness, stacking sequence, and specimen geometry. All of these structural variables were held constant for both materials in the figure. Although the relationship between damage size and impact force may differ somewhat, test trends shown in Figure 7.5.1.3 are similar to those obtained from impacts occurring mid-bay (centered between longitudinal and transverse stiffening elements) in stiffened skin panels which have similar laminate thickness. Figure 7.5.1.3 also shows static indentation tests produced similar damage sizes to those obtained in falling-weight impact events.

Some textile material forms offset the effects of matrix damage through delamination growth resistance and/or other mechanisms (Reference 7.5.1.3(g)). Stitching, which can be achieved by a number of different fabrication processes, does not completely suppress the formation and growth of matrix damage when a structure is subjected to impact. However, stitching improves sublaminar buckling resistance; and hence, helps to minimize reductions in compression-after-impact (CAI) strength related to matrix damage (Reference 7.5.1.3(h)).

7.5.1.4 Depth of damage

Impacts to thin composites cause damage throughout the thickness even for relatively small impact forces and energies. In the contact region, the damage consists of fiber and matrix damage; beyond the contact region, the damage consists only of matrix damage. The diameter of the contact region is only a small fraction of the impactor radius and of the same order of magnitude as the thickness. For example, the contact diameters for the impact tests in Figure 7.5.1.3 are only a few millimeters compared to damage diameters from 0.4 to 2.8 in. (10 to 70 mm). (The impacts were conducted using 0.5 in. (12.7 mm) diameter tups.) Because the damage extends far beyond the contact region, the shape of the impactor has little effect on the extent of the damage. Impacts to thick composites, on the other hand, will not cause damage throughout the thickness except for very large impact forces and energies.

Damage depth measured in radiographs is plotted against impact force in Figure 7.5.1.4 for a 1.4 in. (36-mm) thick, AS4/epoxy composite (Reference 7.5.1.4). (The radiographs were made from the sides of the specimens, which were only 1.5 in. (38 mm) wide.) This material represented the Filament Wound Case (FWC) made for the solid motors of the Space Shuttle. The FWC was composed of 0° (hoop) and $\pm 56.5^\circ$ (helical) layers. The impacts were made with the following indenters: a 0.25 in. (6.35 mm) diameter rod, a 90° corner, and 0.5 and 1 in. (12.7 and 25.4 mm) diameter hemispheres. The mass of the impactor was 11 lb (5.0 kg) and each symbol is the mean value for several specimens. The diameters of the contact region were much smaller than the thickness. The rod made the deepest damage, followed by the corner, the small hemisphere, and large hemisphere. The rod acted like a punch and, after a critical force was exceeded, plunged through the composite with only a small increase in force. The data for the corner and hemispheres had similar slopes, and impact force to cause damage of a given depth was greater for the more blunt indenter. The filled and open symbols indicate visible and non-visible damage, respectively, as viewed on the impacted surface. All the damage for the rod, corner, and most of that for the small hemisphere was visible. But damage as deep as 0.2 in. (4 mm) was not visible for the 1.0 in. (25.4 mm) hemisphere. Thus, impactor shape has a significant effect on the depth and visibility of damage for thick composites. Also, notice that the impact forces in Figure 7.5.1.4 are much greater than those in Figure 7.5.1.3.

7.5.1.5 Laminate thickness effects

Low velocity impact damage is potentially more of a problem for thin laminates than for thick laminates, see Figures 7.5.1.5(a) and (b). Figure 7.5.1.5(a) contains a graph of kinetic energy versus thickness for two different dent depths for the tests. For the range of thicknesses shown, kinetic energy required to produce a given level of damage (as characterized by indentation depth) increases with increasing thickness to approximately the $3/2$ power. Figure 7.5.1.5(b) contains a graph of damage diameter versus force for static indentation tests of the same composites in Figure 7.8.1.2.7(a). The force to initiate damage also increases with increasing thickness to approximately the $3/2$ power. The 16-ply composite was penetrated with a force of 700 lb_f. Composites of 24, 32, and 48 plies were not penetrated with even larger forces. Thus, the force to penetrate likewise increases with increasing thickness.

For very thick composites, damage does not develop throughout the thickness, as shown in Figure 7.5.1.4, and the damaged layers may fail under in-plane tension loading and disbond from the remaining layers. Residual tension strengths for the 1.4 in. (36 mm) thick specimens in Figure 7.5.1.4 are plotted against damage depth in Figure 7.5.1.5(c). The strengths were normalized by the undamaged strength, and each symbol is the mean value for several specimens. The filled symbols indicate the stress when the damaged layers failed, and the open symbols indicate the stress when the remaining layers failed (maximum load). (All stresses were calculated using the total area.) The damaged layers debonded from the remaining layers when they failed. For very shallow damage, the initial failure was catastrophic; but for deeper damage additional load was required to fail the remaining layers. The decrease in strength with increasing damage depth was greater for the damaged layers than the remaining layers. The damaged layers were shown to fail according to a surface crack analysis (Reference 7.5.1.4), that is strength varies inversely with square root of damage depth. The remaining layers were shown to fail approximately as an unnotched laminate.

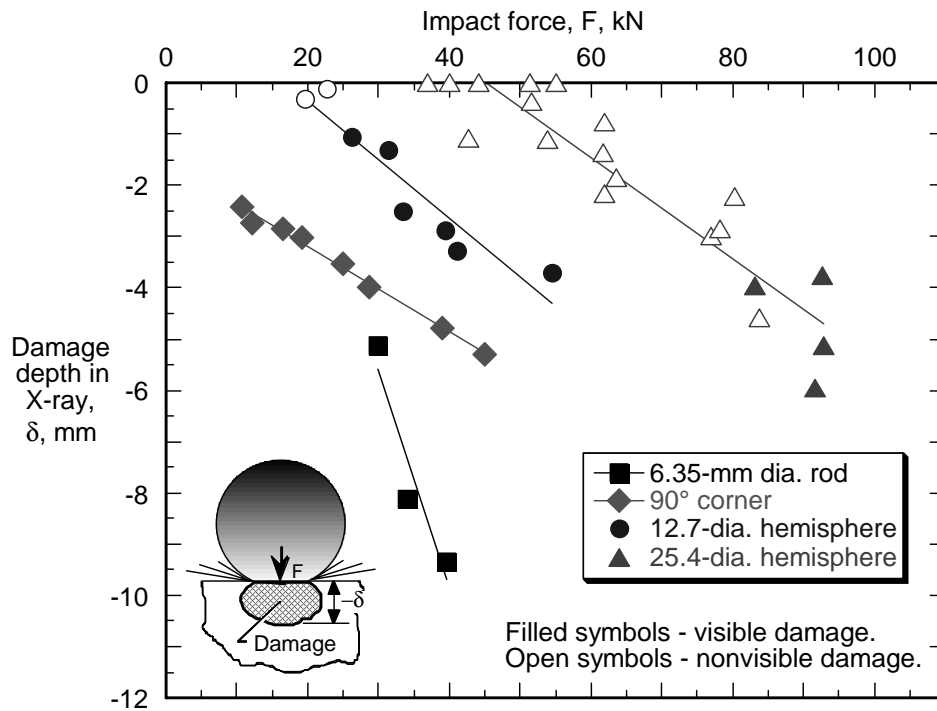


FIGURE 7.5.1.4 Impact damage for 1.4 in. (36 mm) thick AS4/epoxy filament wound case (FWC) with impactors of various shapes (Reference 7.5.1.4).

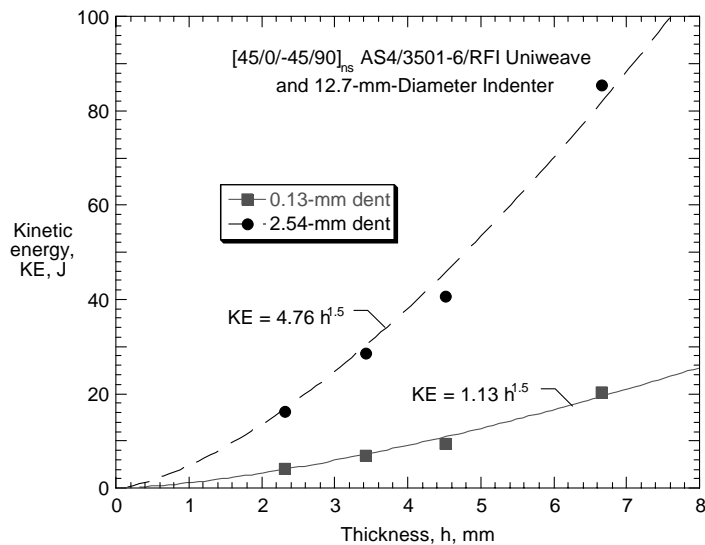


FIGURE 7.5.1.5(a) Impact response for a given dent depth.

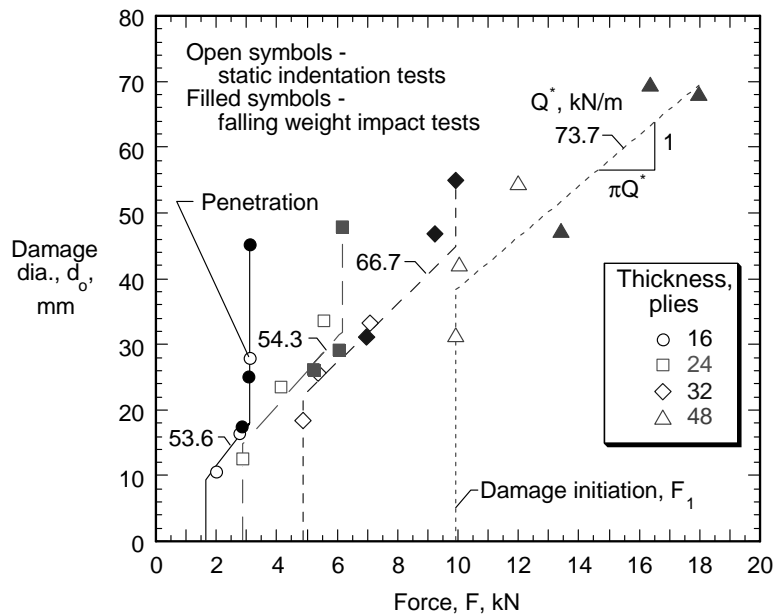


FIGURE 7.5.1.5(b) Damage resistance of $[45/0/-45/90]_{ns}$ AS4/3501-6/RFI uniweave using 0.5 in. (12.7 mm) diameter indenter.

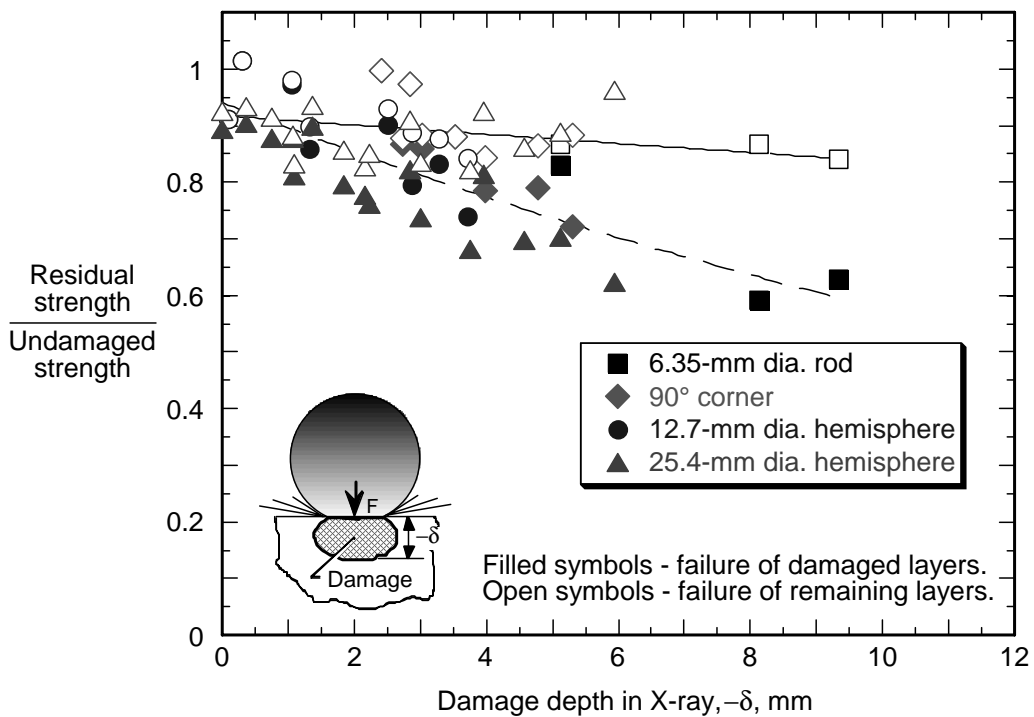


FIGURE 7.5.1.5(c) Residual tensile strengths for 1.4 in. (36 mm) thick AS4/epoxy filament wound case (FWC) with impactors of various shapes.

7.5.1.6 Structural size effects

Impact response for coupons and structures can be quite different. Consider a plate with transverse force and flexural stiffness k and natural frequency ω impacted by a mass m_i . When the ratio of $\omega^2/(k/m_i)$ is greater than 100, the impact response is essentially quasi-static (Reference 7.5.1.3(i)). That is, the force displacement relationships for an impact and for quasi-static loading are the same. Moreover, from energy balance considerations, the impact force F_{\max} is given by:

$$\frac{1}{2} m_i v_i^2 = \frac{1}{2} \frac{F_{\max}^2}{k} + \frac{2}{5} \frac{F_{\max}^{5/3}}{n^{2/3}} \quad 7.5.1.6(a)$$

where

$$n = \frac{4}{3} E_2 \sqrt{R_i} \quad 7.5.1.6(b)$$

V_i is the velocity of the impactor, R_i is the radius of the spherical impactor, and E_2 is the modulus in the thickness direction. The second term on the right hand side of equation 7.5.1.6(a) accounts for local indentation. Thus, when k is small compared to n , the impact force increases in proportion to the square root of the product of kinetic energy and flexural stiffness. Thus, impact force increases with decreasing size, increasing thickness, and the addition of stiffeners. Also, damage resistance increases with increasing thickness, and stiffeners can increase strength by arresting a fracture.

It should also be noted that when the ratio of $\omega^2/(k/m_i)$ is less than 100, the impact response is transient (Reference 7.5.1.3(i)). That is, the plate behaves as though it were smaller, resulting in larger impact forces than those given by Equation 7.5.1.6(a). On the other hand, the development of damage has the effect of reducing impact force. In Equation 7.5.1.6(a), both k and n decrease with increasing damage, thereby reducing F_{\max} . The maximum value of impact force is limited by the resistance of the plate to penetration. Thus, the effect of plate size can be counteracted by damage.

The effects of size are illustrated in Figures 7.5.1.6(a) through 7.5.1.6(c). Figure 7.5.1.6(a) contains a bar graph of minimum kinetic energy to reduce burst pressure for two filament-wound cylinders with the same membrane material and lay-up but with different sizes (Reference 7.5.1.6(a)). The minimum kinetic energy to reduce burst pressure for the 18.0 in. (45.7 cm) diameter was almost ten times that for the 5.7 in. (14.6 cm) diameter.

Figures 7.5.1.6(b) and (c) contain graphs of impact force and resulting damage diameter, respectively, versus kinetic energy for .25 in. (6.3 mm) - thick, quasi-isotropic plates of various sizes (Reference 7.5.1.6(b)). For a given kinetic energy, the impact force and accompanying damage size decrease with increasing plate size - no damage at all was discernible in the 8.2 in.-square (53 cm-square) plates for energies less than 30 ft-lb (41 J). Thus, the energy threshold for causing damage increases with increasing size in a manner consistent with the energy threshold for burst strength in Figure 7.5.16(a). It should be noted that damage reduces impact force by reducing the flexural stiffness, more so for a small plate than a large plate. Thus, the impact forces for the two smallest plates in Figure 7.5.1.6(b) were similar in magnitude due to damage.

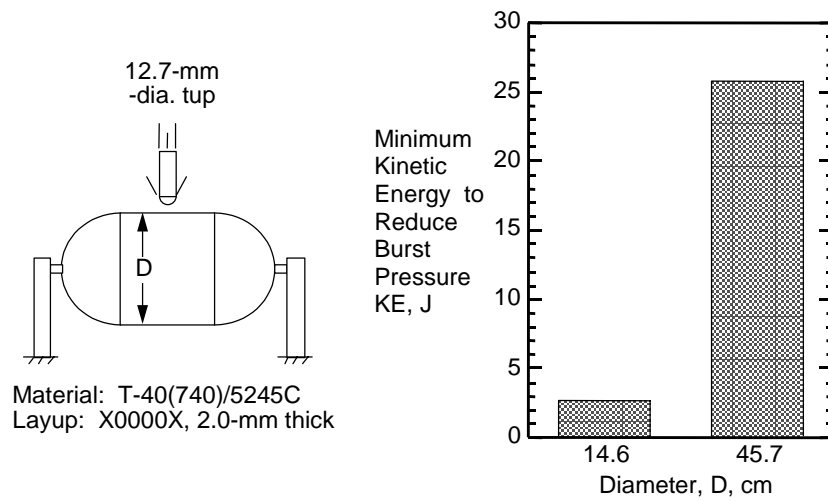


FIGURE 7.5.1.6(a) Impact response of small and large pressure vessels (Reference 7.5.1.6(a)).

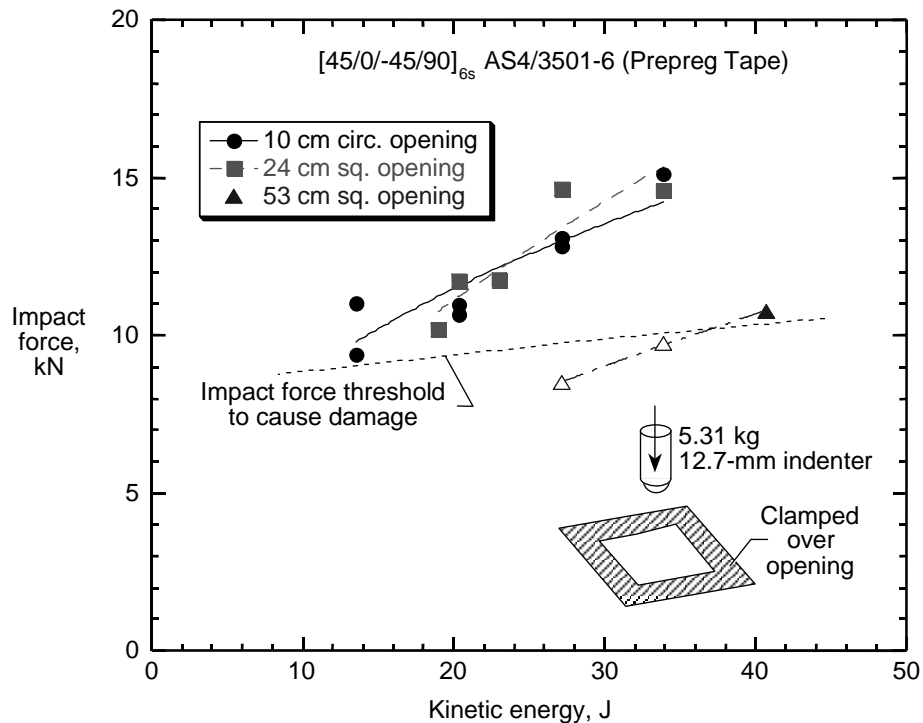


FIGURE 7.5.1.6(b) Impact force for plates of various sizes (Reference 7.5.1.6(b)).

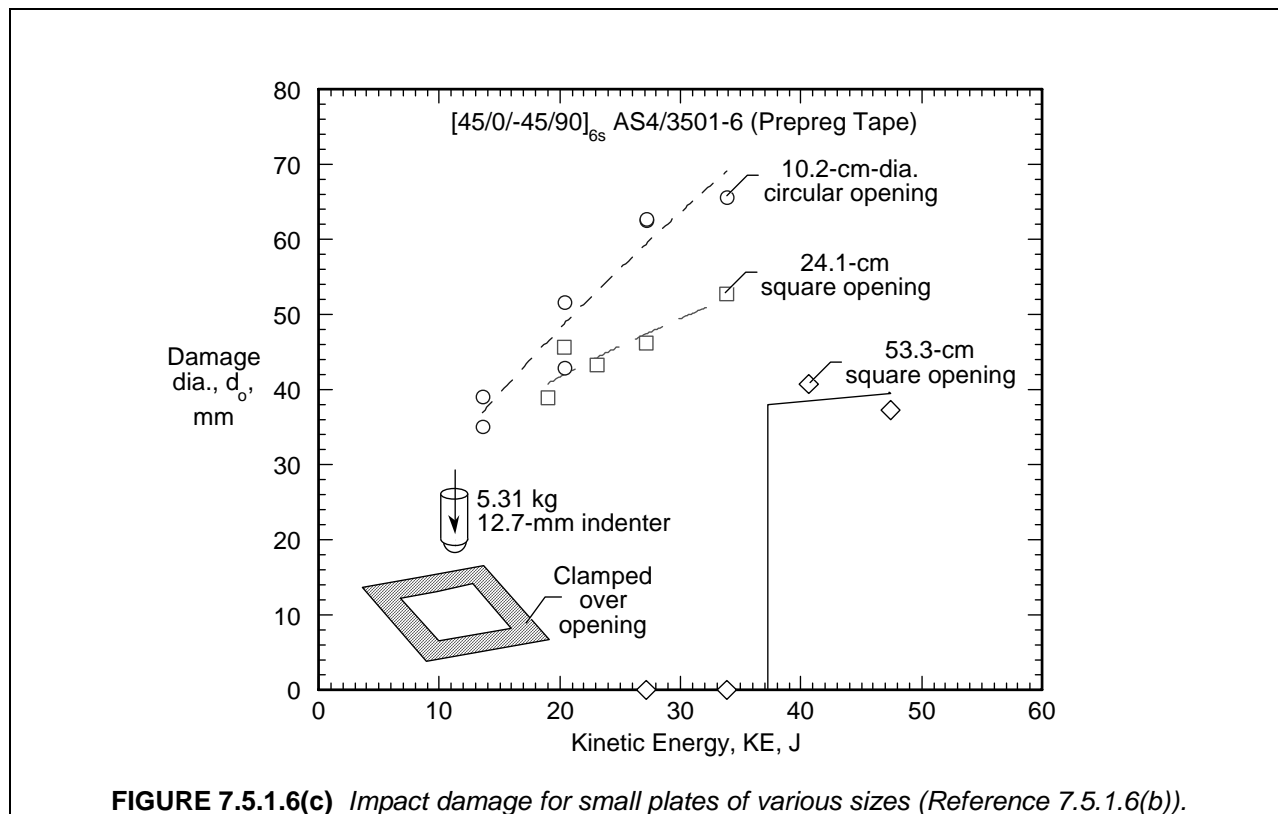


FIGURE 7.5.1.6(c) Impact damage for small plates of various sizes (Reference 7.5.1.6(b)).

7.5.1.7 Sandwich structure

The core and facesheet thickness in sandwich stiffened designs play an important role in impact damage resistance. Critical core variables include density, fiber type, matrix type, cell geometry, and fiber orientation. Most of the impact test and analysis evaluations performed to date were with sandwich panels having a facesheet thickness between 0.03 in. and 0.15 in. (0.8 mm and 3.8 mm). The extent of damage in the core and outer impacted facesheet has been found to approach an asymptote. For example, the database collected by Boeing in the early 1990's under contract with NASA found this asymptote to be somewhat larger than the impactor diameter and dependent on the specific combination of composite core and laminate materials for panels with facesheets on the order of 0.08 in. (2.0 mm) thick (Reference 7.5.1.1(n)). Such inherent resistance to the development of large impact damage areas can have significant benefits in minimizing the effects on residual strength.

Thin-gauge honeycomb panels (facesheets less than 0.02 in. (0.5 mm) thick) have been found to damage at very low levels of impact and allow environmental degradation of the core (e.g., moisture ingress), leading to significant durability problems. Also, limited testing suggests that, for thick-facesheet sandwich panels (i.e., $t > 0.20$ in. (5.1 mm)), that a damage diameter much larger than the impactor diameter is possible with less surface visibility; however, residual strength tests suggest that this damage was asymmetric because the CAI strength was large and not commensurate with extensive through-thickness damage of the size noted.

Some sandwich core materials have failure mechanisms which are not limited to the local area of the impact event. Instead, core damage propagates, allowing the composite facesheet to absorb energy in deflection without failure. Damage created for such combinations of material become a threat to sandwich panel integrity when significant compression or shear loads exist because the failed core does not stabilize the facesheet over a large area. In addition, an undamaged facesheet springs back after impact, reducing visible indications of massive core failure. This phenomenon was observed in previous NASA-funded contract work performed at Boeing in the mid-1980s (Reference 7.5.1.7). The honeycomb core

material used in these studies (a bias weave glass fabric impregnated with a heat resistant resin) propagated a failure that was much larger than the local "core crush region," which typically occurs below the impactor. Figure 7.5.1.7 shows measurements of the extent of this damage. The compressive residual strength with such damage was found to be very low. As a result, the particular honeycomb core material used in these studies would not be a good candidate for primary structure applications.

For sandwich materials with thin faces, impact can result in visible core damage which has been shown to reduce the compressive and shear strengths. Impact damage which causes a break in the facesheet of the sandwich (as well as porosity, a manufacturing defect) also presents a long term durability problem in that it can allow water intrusion into the core.

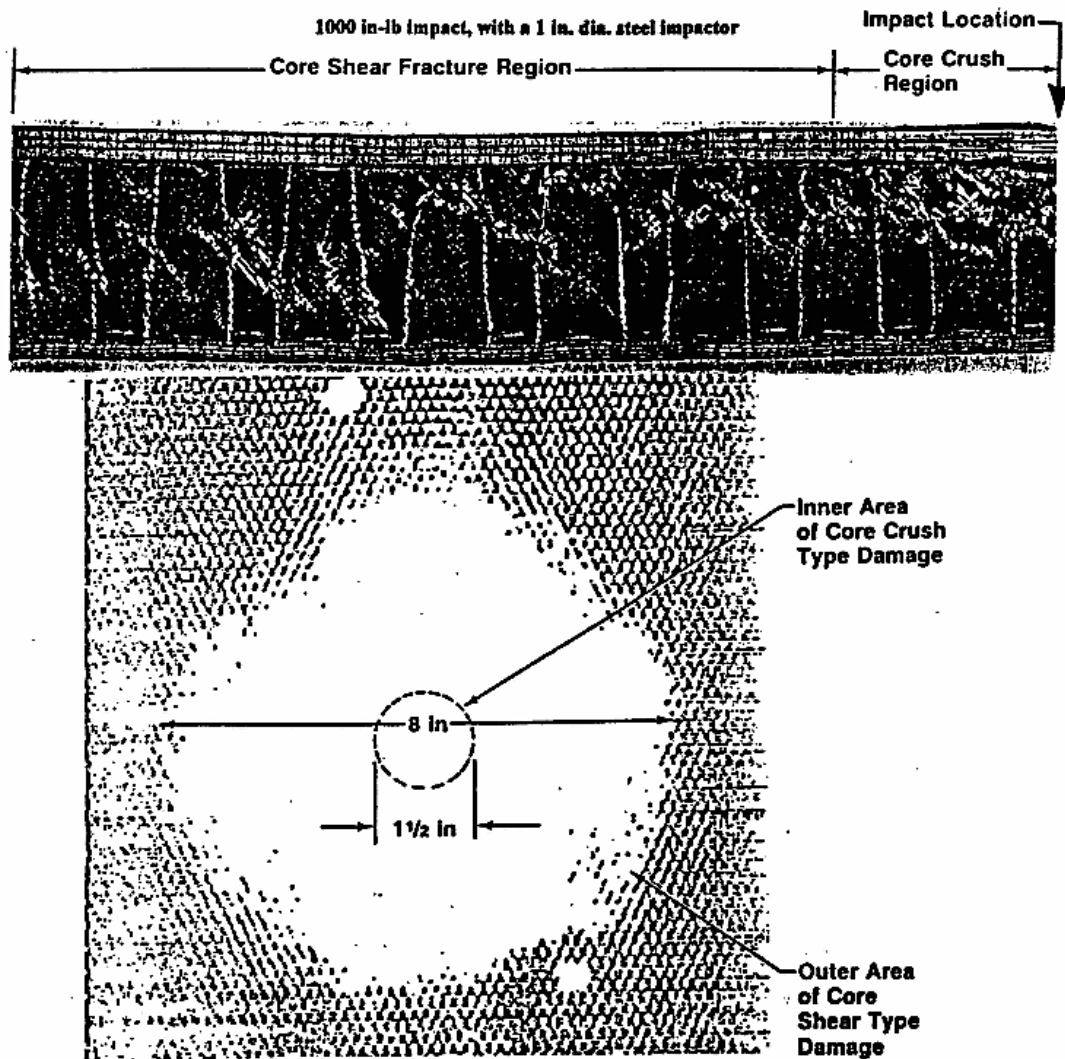


FIGURE 7.5.1.7 Micrograph and through-transmission ultrasound data for an undesirable core impact failure mode (Reference 7.5.1.7).

7.5.2 Design issues and guidelines

In normal operation, aircraft are subjected to potential damage from a variety of sources, including maintenance personnel and tools, runway debris, service equipment, hail, and lightning. Even during initial manufacturing and assembly, parts are subject to dropped tools, bumps during transportation to assembly locations, etc. The aircraft structure must be able to endure a reasonable level of such incidents without requiring costly rework or downtime. Providing this necessary damage resistance is an important design function. Unfortunately for the designer, providing adequate damage resistance may not always be the most popular task. Resistance to damage requires robustness, and commonly necessitates the addition of extra material above that necessary to carry the structural loads. It also influences the choice of materials, lay-up, design details, etc. As a result, there are many pressures to compromise because of competing goals for minimum weight and cost.

In order to establish minimum levels of damage resistance, various requirements for aircraft structure have been identified in the past. For example, the Air Force requirements are defined in their General Specification for Aircraft Structures, AFGS-87221A (Reference 7.5.2). In general, the Specification defines the type and level of low energy impact that must be sustained without structural impairment, moisture ingestion or a requirement for repair. It provides provision for such incidents as dropped tools, hail, and impact from runway debris. The aircraft may be zoned depending on whether the region has high or low susceptibility to damage. In some cases, commercial airline operators have requested specific levels of damage resistance, or particular material selections for components in high impact threat areas.

7.5.2.1 Use of impact surveys for establishing critical damages

Impact surveys with configured structure are required to establish critical damage scenarios for particular design and inspection procedures suitable for field maintenance. These surveys can help establish design features crucial to structural integrity. A range of impact scenarios and structural locations are included in an impact survey. Critical damage can be identified based on post-impact evaluations of: (1) damage visibility, (2) extent of delamination and fiber failure, (3) reduced local stiffness (i.e., loss of load path) and (4) residual strength. Due to the large number of material, structural, and extrinsic variables affecting damage, impact surveys have been found to provide the most meaningful results when applied to specific built-up structure. As a result, surveys using large structural configurations with representative design detail and boundary conditions are recommended. Such studies are practical because numerous impacts can be applied to a single test article. Smaller "building block" panels (e.g., 3- and 5-stringer panels) with representative impact damage are also generally required to quantify residual strength.

7.5.2.2 Structural arrangement and design details

An impact survey consists of a series of impacts applied at varying impact energies and locations to a structure. The goal of an impact survey is usually to define the relationships between impact energy, damage detectability and damage characteristics. The results of the survey are often used to establish the impact variables (energy, location, etc.) to be applied to structural test articles used to determine post-impact residual strength.

Impact at design details. The damage resistance of composite structure is strongly dependent on design detail (e.g., material form, constituents, lay-up, thicknesses, and structural configuration). It is crucial to get early design development data from structural element and subcomponent tests in order to meet goals for damage resistance. For example, impact damage in bonded or bolted structure accumulates differently than it does in flat plates. Design development data should consider a range of damage scenarios, from those known to cause durability or maintenance problems in service to those having a significant effect on residual strength requirements for ultimate and Limit Loads.

In defining the requirements for damage resistance, the type of structure is pertinent. For example, the level of impact energy which typically must be sustained by honeycomb sandwich control surfaces without requiring repair or allowing moisture ingestion is quite low, e.g., 4 to 6 in-lb (0.5 to 0.7 J). One reason these parts have been kept very light is to minimize weight and mass balancing, consequently,

damage resistance is minimal. Repair is facilitated somewhat because these parts can usually be readily replaced with spares while repairs are being accomplished in the shop. Because of their light construction, however, they must be handled carefully to prevent further damage during processing or transport. By contrast, the damage resistance requirement for primary laminate structure, which is not normally readily removable from the aircraft, is typically much higher, e.g., 48 in-lb (5.4 J).

Damage-susceptible regions and details. There are certain damage-susceptible regions of the airplane that require special attention. Examples of these are the lower fuselage and adjacent fairings, lower surfaces of the inboard flaps and areas around doors. These need to be reinforced with heavier structure and perhaps glass fiber reinforcement, instead of carbon. In addition to the above, structure in the wheel well area needs special attention because of damage susceptibility from tire disintegration. Similarly, structure in the vicinity of the thrust reversers is damage prone due to ice or other debris thrown up from the runway.

Minimum weight structure, such as that used for fairings, can cause excess maintenance problems if designed too light. Sandwich structure with low density honeycomb core is an example. Also, face sheets must have a minimum thickness to prevent moisture entrance to the core. The design should not rely on the paint to provide the moisture barrier. Experience has shown that the paint often erodes or is abraded and then moisture enters.

Honeycomb sandwich areas with thin skins adjacent to supporting fittings are particularly vulnerable to damage during component installation and removal. Consequently, solid laminate construction is commonly used within a reasonable working distance of fittings.

Trailing edges of control panels are highly vulnerable to damage. The aft 4 inches (102 mm) are especially subject to ground collision and handling, as well as to lightning strike. Repairs in this region can be difficult because both the skins and the trailing edge reinforcement may be involved. A desirable approach for the design is to provide a load carrying member to react loads forward of the trailing edge, and material for the trailing edge, itself, that will be easily repairable and whose damage will not compromise the structural integrity of the component. Close out details should avoid the use of potting compounds due to the tendency to crack and cause sealing problems.

7.5.2.3 Ground hail

It may also be desirable to design composite aircraft structure to be resistant to typical hail strike energies to minimize the amount of repair required after a hailstorm. Such damage typically only occurs when the aircraft is on the ground, except for leading edges, which can experience in-flight hail damage.

7.5.2.4 Lightning

High-energy lightning strikes can cause substantial damage to composite surface structure. For civil aircraft and rotorcraft, the FAA regulations for lightning protection are FAR 25.581, 23.867, 27.601, and 29.610. Fuel system lightning protection requirements are in 25.954 and 23.954. System lightning protection requirements are in 25.1316. Advisory circulars AC20-53 and AC20-136 provide means of compliance with the regulations. Military requirements are defined in Mil-STD-1795 - Lightning Protection of Aerospace Vehicles and Hardware, Mil-Std-1757 - Qualification Test Techniques for Lightning Protection and Mil-B-5087 - Bonding, Grounding and Lightning Protection for Aerospace Systems.

There are zones on the airplane with high probability of lightning strike occurrence. These zones are called lightning strike zones. Protection of composite structure by conductive materials is required on lightning strike zones and beyond them to enable conductivity of induced currents away from attachment zones. An all-composite wing may have to be completely covered by a conductive layer, even if the attachment zone is located near the wing tip.

At fasteners and connections, electrical resistance to current flow generated by lightning produces heat that causes burning and delaminations. Minor lightning attachment also can cause significant dam-

age, particularly to the tips and trailing edges. The following are guidelines to reduce the repair requirement:

- Provide easily replaceable conductive material with adequate conductive properties.
- Provide protection at tips and along trailing edge spans.
- Make all conductive path attachments easily accessible.

7.5.2.5 Handling and step loads

In addition to impact induced loads, there also needs to be requirements of resistance to damage from normal handling and step loads that might be encountered in manufacturing and operational environments. The following are suggested considerations:

Handling loads:

Difficult access - interpreted as finger tips only.

Overhead easy access - the ability to grip and hang by one hand.

Step loads:

Difficult access - interpreted as allowing, with difficulty, a foothold on a structure.

Easy access from above - interpreted as allowing a 2g step or "hop" onto the structure.

Note that contact areas, locations, and weights associated with each of these conditions must be defined.

7.5.2.6 Exposed edges

Laminate edges should not be positioned so they are directly exposed to the air stream since they are then subject to delamination. Options include:

1. Provide non-erosive edge protection such as a co-cured metal edge member.
2. Provide an easily replaceable sacrificial material to wrap the edges.
3. Locate the forward edge below the level of the aft edge of the next panel forward.

7.5.3 Test issues

This section is reserved for future use.

7.5.4 Analysis methods - description and assessment

This section is reserved for future use.

7.6 DURABILITY (DAMAGE INITIATION)

7.6.1 Introduction

In general, composite materials exhibit superior fatigue properties relative to that of metals. Their corrosion resistance also provides better durability for aircraft structures. Composite structural designers can usually utilize the high fatigue threshold that has been observed for commonly applied materials to simplify the fatigue design processes.

However, special considerations must be applied in fatigue/durability design of composites due to increased scatter in both strength and fatigue life due to the presence of multiple constituents. The fatigue life scatter in composites and metals are compared in Figure 7.6.1 (Reference 7.6.1) in terms of Weibull shape parameters (α). As it may be noted, a higher value of Weibull shape parameter signifies

lower data variation. As shown in the figure, the modal Weibull shape parameter for commonly used composites is approximately 1.25, compared with approximately 7.0 for metals.

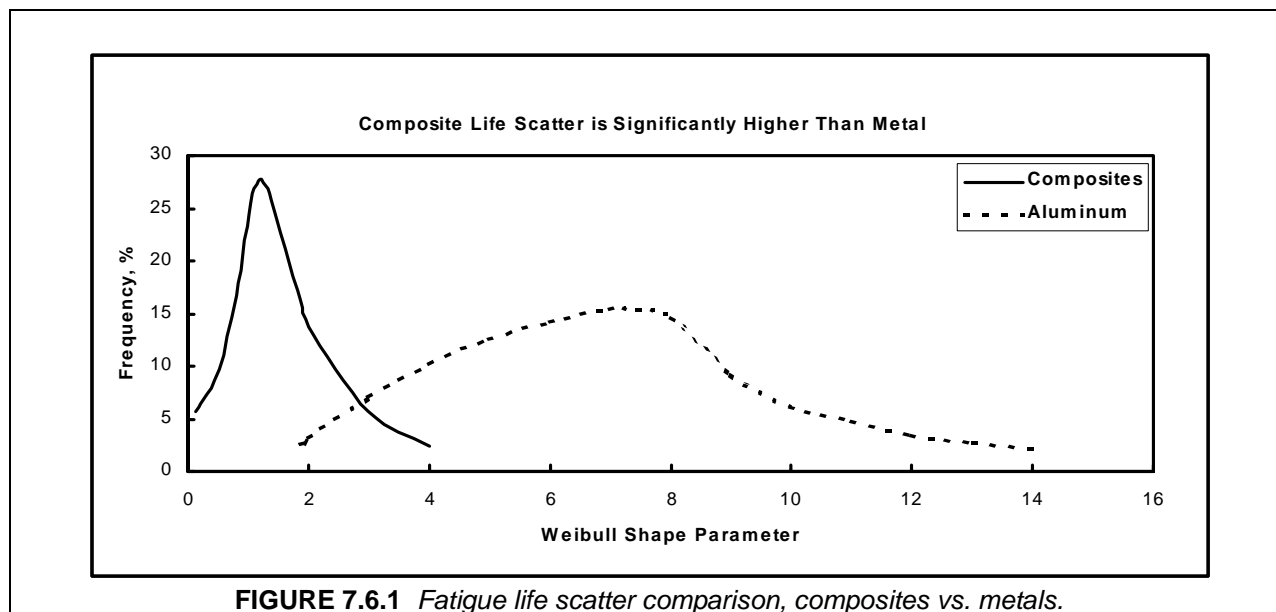


FIGURE 7.6.1 Fatigue life scatter comparison, composites vs. metals.

In addition to the higher scatter, two other factors significantly affect damage initiation and damage progression of composites: (1) multiple damage modes, and (2) no dominant strain energy release mechanisms.

Because composites consist of more than one constituent material, fatigue damage can initiate and propagate in any one material and/or along any material interface. Possible damage modes include fiber breakage, matrix cracking, fiber pull-out, and multi-mode delamination. Depending on the type of structural loading and the laminate construction, different modes of fatigue damage can occur at rather random locations in the composite during the process of damage initiation. Once a damage is initiated, its progression is driven by strain energy release to create new surfaces. However, because of the many modes of damage and because there is no dominate energy release mechanism, there is no clear path for damage progression. It has been observed that damage in composites often advances as a progressive damage zone that includes multiple damage types.

Unlike metallic structure, where single mode damage is propagated in a self-similar manner, the complex damage initiation and progression in composite makes analytical modeling extremely difficult. Therefore, durability of composite structures is mostly assured by performing adequate fatigue tests. Several fatigue test schemes have been proposed to overcome the scatter issue and to take advantage of the superior fatigue behavior of composites. These test schemes are discussed below.

7.6.2 Life factor approach

The life factor test approach has been successfully used for metal to assure structural durability. In this approach, the structure is tested for additional fatigue life to achieve the desired level of reliability. The test duration is determined based on the material fatigue life scatter, the number of test specimens, and the required reliability. For example, for B-basis reliability (i.e., 90% probability that the structural life exceeds the design lifetime, with 95% confidence), the required test life for typical composites and aluminum alloys are shown in Figure 7.6.2(a). As shown, the conventional two-lifetime test for aluminum structure is sufficient to assure B-basis life reliability. However, 14 lifetimes would be required for composites

to assure equal reliability. The required test lives for the typical range of Weibull shape parameters for composites is tabulated in Figure 7.6.2(b) and plotted in Figure 7.6.2(c).

	n = 1	n = 5	n = 15
Composites Alpha = 1.25	13.558	9.143	7.625
Metals Alpha = 4.0	2.093	1.851	1.749

FIGURE 7.6.2(a) Comparison of B-basis life factors, composites vs. metals.

ALPHA	Mean/B-basis		
	n = 15	n = 5	n=1
0.50	383.569	603.823	1616.895
0.75	39.596	53.584	103.327
1.00	13.849	17.376	28.433
1.25	7.625	9.143	13.558
1.50	5.206	6.056	8.410
1.75	3.999	4.552	6.032
2.00	3.298	3.694	4.726
2.25	2.848	3.151	3.921
2.50	2.539	2.780	3.385
2.75	2.314	2.513	3.006
3.00	2.144	2.313	2.726
3.50	1.906	2.034	2.342
4.00	1.749	1.851	2.093
5.00	1.553	1.625	1.793

FIGURE 7.6.2(b) Values of B-basis life factor as a function of Weibull shape parameter.

The Weibull shape parameter for fatigue life distribution of commonly used composites has a modal value of 1.25, as observed in Reference 7.6.1. That is, the fatigue life variability has a coefficient of approximately 0.805. The required test life for a sample size of between 5 to 15 is from 9.2 to 7.6. For a single test article, such as a full-scale component test, the required life factor is 13.6. Such a test would cause significant cost and schedule impact in an engineering program. In addition, a prolonged fatigue test would cause fatigue failure in the metal parts of a mixed metal-composite structure, precluding the verification of the composite's reliability.

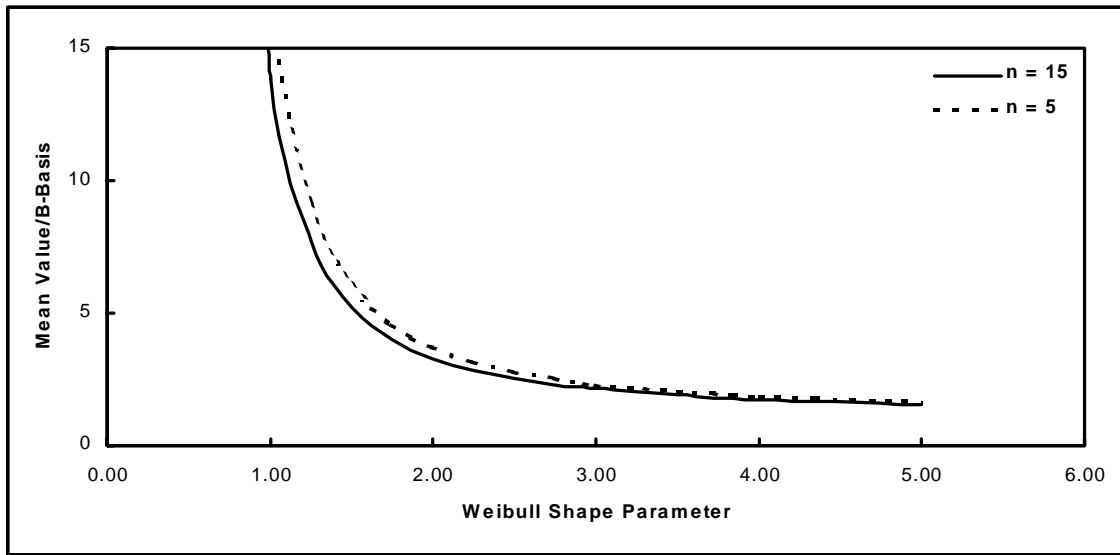


FIGURE 7.6.2(c) Life factor for commonly used composites.

7.6.3 Load enhancement factor approach

In order to relieve the cost and schedule impacts of composite structural fatigue tests, a combined load factor and life factor approach is developed in References 7.6.1 and 7.6.3. The objective of this approach is to increase the applied loads in the fatigue tests so that the same level of reliability can be achieved with a shorter-duration test. The required load enhancement and test life depend on the statistical distributions of both the baseline fatigue life and the residual strength.

Assuming that both the fatigue life and residual strength distributions can be described by two-parameter Weibull distribution, then the Load Enhancement Factor (LEF) in terms of test duration, N , can be written as (Reference 7.6.1):

$$LEF = \frac{\left[\Gamma\left(1 + \frac{1}{\alpha_L}\right) \right]^{\alpha_L / \alpha_R}}{\left[\frac{-\ln(l) \cdot N^{\alpha_L}}{\chi^2_{\gamma}(2n) / 2n} \right]^{1 / \alpha_R}} \quad 7.6.3$$

where α_R is the Weibull shape parameter of the residual strength distribution,

α_L is the Weibull shape parameter of the fatigue life distribution,

l is the reliability, 0.9 for B-basis, 0.99 for A-basis,

γ is the level of confidence,

N is the test duration,

n is the sample size,

Γ is the Gamma function,

χ^2 is the Chi-square value.

Equation (7.6.3) indicates that the LEF also depends on the sample size and the required reliability. For $\alpha_L = 1.25$ and $\alpha_R = 20.0$, the A-basis and B-basis LEF in terms of test duration, N , are plotted in Fig-

ure 7.6.3(a). Required LEF for one-lifetime and two-lifetime tests are shown in Figure 7.6.3(b). Depending upon the number of specimens tested, Figure 7.6.3(b) shows that for B-basis reliability, the required load enhancement is less than 18%.

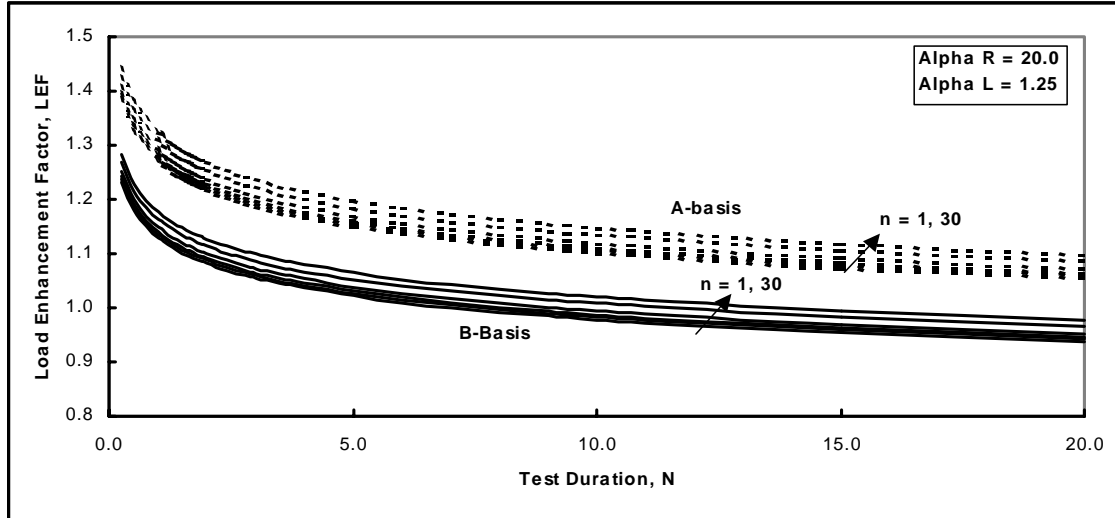


FIGURE 7.6.3(a) LEF for commonly used composites.

The LEF approach provides an efficient way to assure the structural life reliability. However, other effects may also require a load enhancement and resulted in an undesirably high load factor. For example, an environmental compensation factor is usually applied in order to account for service environment effects, and a spectrum severity factor is usually applied for military aircraft. Thus, an LEF of 1.18, an environmental compensation factor of 1.06, and a spectrum severity factor of 1.20 would result in an overall fatigue test factor of 1.50. This would either change the fatigue failure mode or reach the static strength of the structure. Therefore, in the application of the LEF approach, it is very important to ensure that the fatigue failure mode is preserved.

Sample Size	One Lifetime Test		Two Lifetime Test	
	A-Basis	B-Basis	A-Basis	B-Basis
1	1.324	1.177	1.268	1.127
2	1.308	1.163	1.253	1.114
5	1.291	1.148	1.237	1.100
10	1.282	1.140	1.227	1.091
15	1.277	1.135	1.223	1.087
30	1.270	1.130	1.217	1.082

FIGURE 7.6.3(b) Typical LEF for one-lifetime and two-lifetime tests.

7.6.4 Ultimate strength approach

The Ultimate Strength Approach uses an increased static strength margin in conjunction with the fatigue threshold to demonstrate adequate fatigue life. This approach is discussed in detail in References

7.6.1 and 7.6.4. This is a conservative approach, but, if it is satisfied, no structural fatigue test is necessary. This approach assumes that a fatigue threshold exists at a relatively high proportion of the static strength. In order to apply the ultimate static strength approach, it is necessary to design structures such that the maximum spectrum design load is no greater than the B-basis fatigue threshold.

The ultimate strength approach has seen limited application in rotorcraft design since the number of fatigue load cycles in rotorcraft fatigue spectra are approximately two orders of magnitude higher than for fixed-wing aircraft. Fatigue thresholds are not fully established at such high load cycles. Further research is needed to develop a database in order to apply this approach.

7.6.5 Spectrum truncation

In addition to the Load Enhancement Approach and Ultimate Strength Approach, spectrum truncation also utilizes the high fatigue threshold behavior to reduce composite fatigue test time. This is because the composite fatigue process, unlike that of metals, is relatively insensitive to the low stress (strain) cycles and fatigue life is dominated by the high stress (strain) cycles. It has also been observed that composite behavior is not affected by fatigue load sequence, possibly due to the brittleness of the material. In fact, the results of References 7.6.5(a) and (b) indicated that under certain types of fatigue load spectra, most of the fatigue failures were “quasi-static failure”. That is, damage initiation and progression only take place under a limited number of high stress (strain) load cycles. Removing the low stress (strain) cycles will not affect the fatigue life nor the damage evolution processes. An extensive database was developed in Reference 7.6.5(c) to demonstrate the validity of the spectrum truncation technique. References 7.6.5(d) and (e) also successfully applied this technique to modify the fatigue load spectrum.

Although there are no general guidelines for spectrum truncation for composite fatigue tests, the fatigue threshold of the material is usually used to determine the cycles to be truncated. Stress (strain) levels below the fatigue threshold are considered to cause no fatigue damage (initiation or progression) and theoretically can be removed from the spectrum without changing the test results. However, in practice, the truncation level is usually a certain percentage of the A- or B-basis fatigue threshold (e.g. 60% to 70%).

7.6.6 Durability certification

Because of the unique fatigue behavior of composites (high threshold, high data scatter and multiple fatigue damage mechanisms) durability certification of composite structures should be addressed differently from that of metallic structures. Also because of their particular fatigue behavior, durability of composite structures is assured mostly by testing instead of analysis. The building block approach is recommended for durability certification testing of composite structures. The emphasis in planning the building block test plan should be in the design development testing, which include coupons, elements, element combinations, and subcomponents. Durability and fatigue life should be verified at these lower levels of testing. The environmental effects on structural durability should also be considered in the test planning. At the full-scale level, fatigue tests should be used to verify the life of the metallic parts only. The time and cost of the durability testing can be significantly reduced by proper combination of the load enhancement factor approach and the spectrum truncation techniques. The ultimate strength approach is conservative, in general, and an extended database must be developed for application to high cycle fatigue structures, such as rotorcraft components.

7.6.7 Influencing factors

This section is reserved for future use.

7.6.8 Design issues and guidelines

This section is reserved for future use.

7.6.9 Test issues

This section is reserved for future use.

7.6.10 Analysis methods - description and assessment

This section is reserved for future use.

7.7 DAMAGE GROWTH UNDER CYCLIC LOADING

7.7.1 Influencing factors

Just after compression strength reduction due to low velocity impact was recognized in the late 1970's, many composite research teams then took up investigating the fatigue behavior of impacted CFRP specimens. Among all available results, those shown in this section are drawn from a French-German collaborative program (Reference 7.7.1(a)) involving CEAT, Aerospatiale, DASA Munich and the WIM (in Erding).

In this program, specimens representative of real world stacking sequences were impacted with various energy levels but not higher than those corresponding to the creation of visible impact damages. Usually impact damages that are to be assumed for fatigue (safe-life) investigations are those not sufficiently visible for being readily detectable. Those more severe, easily detectable, should not have to prove their capability to sustain a large number of fatigue cycles in service.

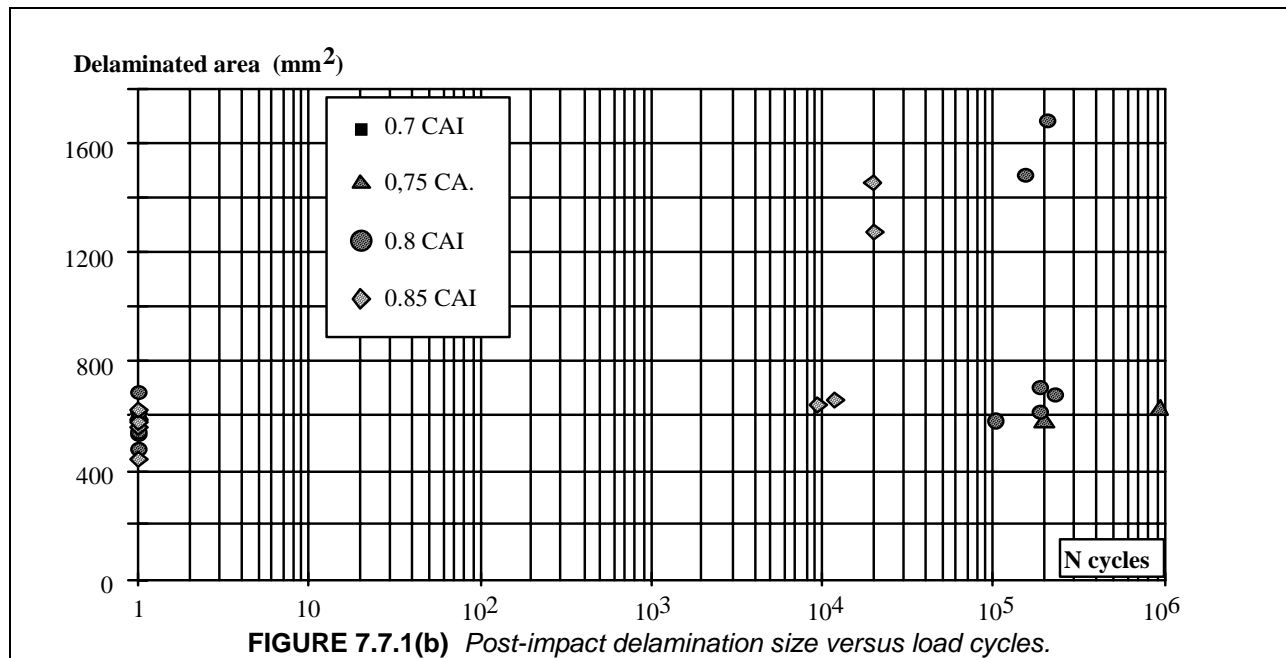
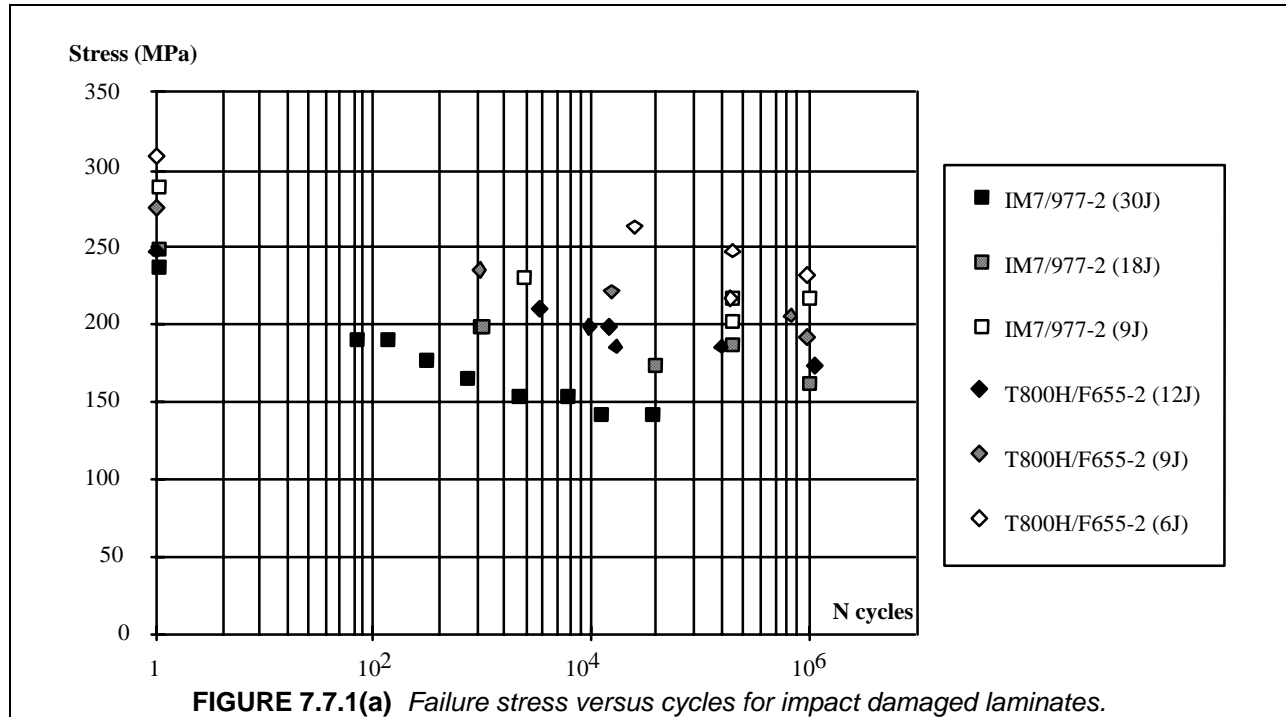
These specimens were then tested in compression-compression fatigue ($R = 10$) in order to :

- Plot Wöhler curves for several energy levels,
- Monitor damage growth and residual static strength versus time.

Wöhler curves for the IM7/977-2 and the T800H/F-655-2 material references are reported in Figure 7.7.1(a) for various energy levels. The ratio between the endurance limit at 10^6 cycles and the initial static strength turned out to be between 0.50 and 0.75. This means that sizing a structure (with these materials) using Ultimate Loads should push fatigue loads down to a level likely to limit fatigue problems with low energy impact damages.

Figure 7.7.1(b) illustrates damage growth, measured by C-SCAN, versus fatigue cycles for the T800H/F655-2 material. Unrealistic fatigue stresses (above 75% of the static strength) were needed to allow such measurement. This illustration shows that, despite the log axis, damage growth starts very close to the end of the specimen lifetime (between 85% and 95% for all cases investigated in this program), with a very high slope.

From these results it is apparent that, as far as low velocity impact damages are concerned, assuming the possibility of a stable (or slow) growth approach for certification purposes may not be possible. This conclusion is also supported by other laboratory results such as, for example, those presented in Reference 7.7.1(b) where very high slopes have also been shown for da/dN versus ΔG curves. These data were obtained on Double Cantilever Beam specimens made of two composite materials - the IM7/8552 and the HTA/6376 - and are representative of a mode I delamination growth phenomenon.



Aside from this intrinsic material behavior, another reason for avoiding the use of a slow growth concept in certification is that the composite community is still short of analytical tools for predicting impact damage growth in fatigue. Single delaminations for which tools have been developed are not representative of the complex damage state induced by an impact.

In summary, impact damage growth under fatigue should not be used as an aircraft certification approach except in the cases of:

- Readily detectable damage
- Situations where the structural design provides a damage arrest capability

The use of a no-growth approach is then recommended for aircraft certification purposes. Due to the low fatigue sensitivity of impacted composites, this no-growth approach should be able to cover most situations.

7.7.2 Design issues and guidelines

This section is reserved for future use.

7.7.3 Test issues

This section is reserved for future use.

7.7.4 Analysis methods - description and assessment

7.7.4.1 Large through-penetration damage

This section is reserved for future use.

7.7.4.2 Single delaminations and disbonds

This section is reserved for future use.

7.7.4.2.1 Delamination growth

Under certain conditions delaminations subject to out-of-plane displacements or loading can grow and reach critical dimensions. The growth of delaminations can be treated according to the principles of fracture mechanics, using the Fracture Energy Criterion. The general procedure is as developed in Reference 7.7.4.2.1.

1. Stress field around the delaminated area is calculated (in most cases numerically).
2. A growth direction is assumed. This requires experience, otherwise several directions have to be checked.
3. The crack is expanded by a_d , as small as possible.
4. The energy dissipated between the two stages, G , is calculated and compared to the experimentally obtained G_c . If $G > G_c$ the delamination grows.

It should be noted that delamination growth is a competing failure mechanism with the in-plane stress concentration described in Section 7.8.3.2.1. As a result, some stable delamination growth may occur prior to an increase in stress concentration and fiber kink failure.

7.7.4.3 Impact damages

This section is reserved for future use.

7.7.4.4 Cuts and gouges

This section is reserved for future use.

7.8 RESIDUAL STRENGTH

One of the key aspects of the damage tolerance design approach involves ensuring that damaged structure has adequate residual strength and stiffness to continue safely in service until the damage can be detected by scheduled maintenance inspection and be repaired, or until the life limit is reached. The potential damage threats, the extent of damage to be considered, the structural configuration and the detectability of the damage using the selected inspection methods determine the required damage sizes to be evaluated for the regulatory load levels to be sustained. This section discusses influencing factors on the residual strength characteristics of damaged composite structure, guidelines for testing of damaged structure, and analytical methods for predicting residual strength.

7.8.1 Influencing Factors

This section discusses the varied factors that influence the residual strength of a damaged composite structure. These factors include material properties, structural configuration, loading conditions and characteristics of the damage state within the structure. Analysis methods and test programs must be configured to account for the range of these variables appropriate for the design in order to establish a set of residual strength versus damage curves.

7.8.1.1 *Relationships between damage resistance and residual strength*

The characteristics of the response of a material/structure to an impact event (damage resistance) and the strength of a structure with a given damage state (residual strength) are often confused. While these two items are somewhat interrelated, the following should be understood. The damage tolerance design approach uses the capabilities of a selected inspection method to establish the damage sizes to be considered for residual strength analysis. This means that the required damage sizes are functions of the detectability of the damage for the selected inspection method, and are not typically functions of a specific energy level. Practically, this means that a "tougher" structure that is more resistant to a given damage threat (impact energy level) may require more impact energy to achieve the same level of damage detectability as a "brittle" structure. Given the same level of damage detectability, the residual strength of the tougher structure may or may not be greater than the brittle structure.

Some of the material and structural characteristics that improve damage resistance tend to degrade residual strength, especially for large damage sizes, while other characteristics have a beneficial effect on both damage resistance and residual strength. The effects of these characteristics on damage resistance are discussed in Section 7.5, while the effects on residual strength are discussed in the following subsections. As is the case in other material and structural property tradeoffs, several technical and economic issues must be considered in balancing the damage resistance and residual strength of a given composite design. It should be kept in mind that a highly-damage-resistant structure may not be very damage tolerant and vice versa.

7.8.1.2 *Structure with impact damage*

7.8.1.2.1 *Material effects*

Material parameters, including matrix toughness, form (tape or fabric), and stacking sequence, mostly influence the damage pattern, thus the damage resistance. Material properties may, however, influence both damage propagation under repeated loads and residual strength. The response of a given damage will be influenced by a combination of structural parameters, like strength and stiffness of sublaminae, or fiber fracture and matrix cracking at notch tips.

Some studies have been made of composites with hybrid fiber construction, that is, composites in which two or more types of fibers are mixed in the lay-up. For example, a percentage of the carbon fibers are replaced with fibers with higher elongation capability, such as fiberglass or aramid. Results (References 7.8.1.2.1(a) through 7.8.1.2.1(d)) in both cases have shown improvement in damage resistance

and residual compression strength after impact. Basic undamaged properties, however, were usually reduced.

In thin gage structures, such as a two-or three-ply fabric facesheet sandwich construction, materials can have a significant effect on damage resistance and residual strength. Investigations have generally shown that compression strength (both before and after impact) increases with the fiber-strain-to-failure capability within a particular class of materials. Higher strain capability aramid or glass fiber structures tend to be more impact resistant than high-strength carbon fiber structure. However, the compressive strengths of the undamaged and damaged aramid and glass structures are lower than that of carbon. Structure incorporating high-modulus, intermediate-strength carbon fibers, with higher strain-to-failures offer significant impact resistance while retaining higher strength.

7.8.1.2.2 Interlaminar toughness effects

In thermoset material systems, the nominal matrix toughness variations influence the impact resistance of thin gage structures but generally to a lesser extent than in thicker structures. For thermoplastic material systems, however, the generally much larger increase in the fracture toughness (G_{IC} , G_{IIC} , etc.) of the resins do translate into significant impact resistance and residual strength improvements.

Although interlaminar toughness is crucial to the extent of damage created in a given impact event, the CAI of laminates with equivalent damage states (size and type) was found to be independent of material toughness (References 7.8.1.2.2(a) through 7.8.1.2.2(c)). The model from Reference 7.8.1.2.2(b) (see also Section 7.8.4.3.1), which accounts for the in-plane stress redistribution due to sublaminar buckling, has worked equally well for tough and brittle resin systems studied. Since delamination growth may be possible with some materials and laminate stacking sequences (LSS), a more general model would also account for out-of-plane stresses.

A comparison of results from Figures 7.5.1.3 and 7.8.1.2.2 show that the toughened material has greater impact damage resistance, but essentially the same CAI strength for damages greater than 0.8 in. (20 mm) in diameter. Although the curves shown in Figure 7.8.1.2.2 are best-fit to the data, similar accuracy has been achieved for these materials and stacking sequences using the engineering analysis described in Section 7.8.4.3.1 (References 7.8.1.2.2(a) through 7.8.1.2.2(d)).

7.8.1.2.3 Stacking sequence effects

The laminate stacking sequence (LSS) can affect compression after impact strength (CAI) in several ways. First, the bending stiffness of a laminate, and failure mechanisms that occur during an impact event, are strongly dependent on the LSS. Load redistribution near the impact site is dependent on the distribution of damage through the laminate thickness (e.g., the LSS of sublaminae affects their stability). Finally, damage propagation leading to final failure also depends on the LSS. Additional discussion of LSS effects is contained in Section 7.8.4.3.1.

Many of the impact damage states studied in the past have been dominated by matrix failures. The creation of matrix cracks and delaminations which combine to form sublaminae depends strongly on LSS (References 7.8.1.2.2(a) and 7.8.1.2.2(d)). Homogeneous stacking sequences have been found to lead to characteristic damage states which repeat through the laminate thickness. Alternatively, plies can be stacked in a sequence which concentrates damage in specific zones on the laminate. Figure 7.8.1.2.3 shows experimental data indicating that LSS has a strong effect on CAI strength.

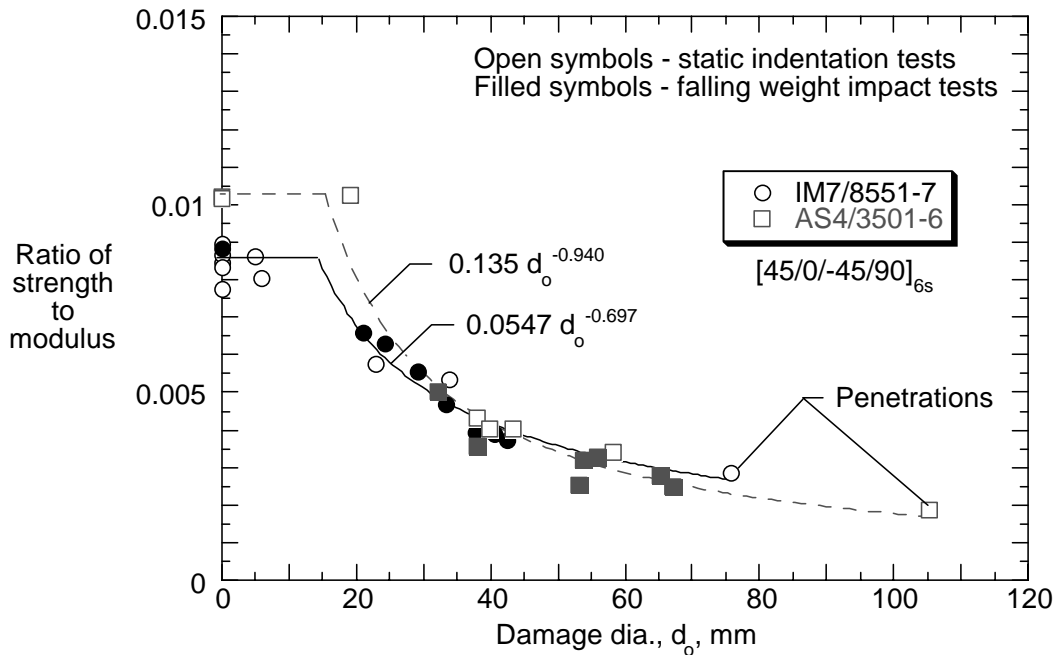


FIGURE 7.8.1.2.2 CAI test results for untoughened and toughened, interlayered carbon/epoxy laminates made from prepreg tape (lines were fit to the data).

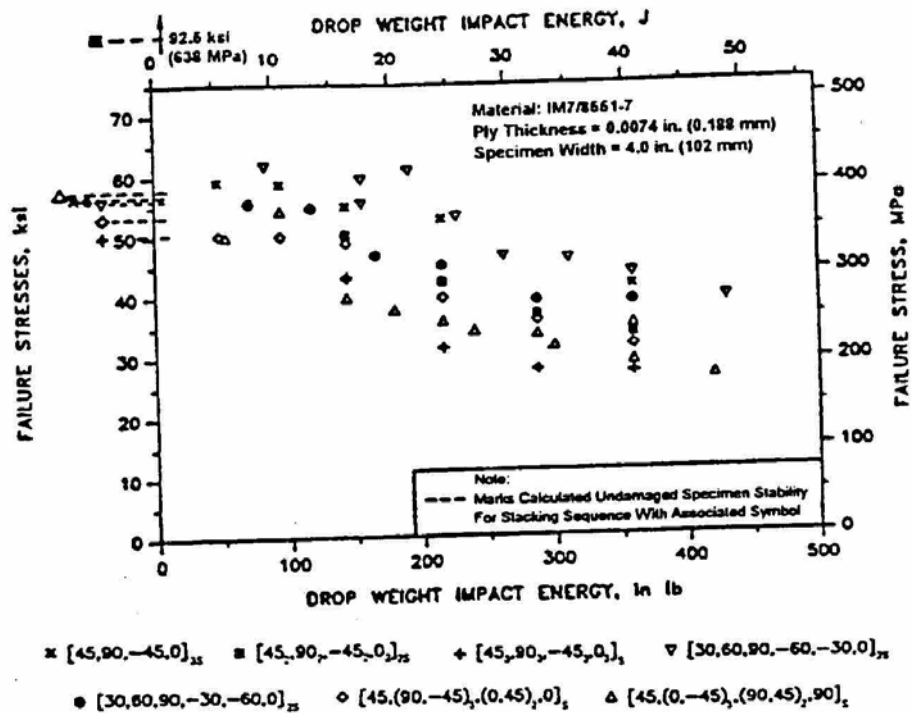


FIGURE 7.8.1.2.3 Test data for CAI performance as a function of LSS (from Reference 7.8.1.2.3).

7.8.1.2.4 *Laminate thickness effects*

Some data exists which indicates thicker laminates have higher compressive residual strength for a given damage size. This has been observed for both laminated plates and sandwich panels (Reference 7.8.1.2.4(a) and (b)). Most of this strength data was collected for open holes and notch-like large penetrations. However, based on failure due to the local compressive stress concentration next to buckled sublaminae, such an understanding of this behavior would also be crucial to accurately predicting CAI.

7.8.1.2.5 *Through-thickness stitching*

Methods such as through-thickness stitching have also been used to improve damage resistance and residual strength. The effect of stitching has been to reduce the size of internal delaminations due to impact and arrest damage growth. Tests involving conventional carbon/epoxies have shown increases in the residual strength of up to 15% for comparative impact energy levels (however, when comparing on a equivalent damage "detectability" criteria, the increase in residual strength may be lower). The stitching process is quite expensive, however, and probably should be considered for applications in selected critical areas only. Additionally, the stitches tend to cause stress concentrations and the tensile strength, transverse to the stitching row, is usually reduced.

7.8.1.2.6 *Sandwich structure*

Core density and material type has been found to have a significant influence on the damage resistance of sandwich panels. Lightweight, weak core materials allow for through-penetration damage of the facesheet under the impacting object. Damage in this case is typically localized to the rough size of the impactor. Also, lightweight core materials have a tendency to fracture under even small impact energies; if the energy is low then the facesheet may be undamaged and may spring back leaving non-visible damage to the core material. Conversely, dense, high-strength cores are less likely to fracture under the impact load, and the resulting damage is typically a dented area somewhat larger than the impacting object.

The residual strength of an impact damaged sandwich facesheet is not significantly dependent on core density if the failure mode is predominately controlled by the resulting in-plane stress concentration. However, core density can have a significant effect on the residual strength of the sandwich if the failure mode is an instability type (e.g., face wrinkling).

Although the inherent bending stiffness of a sandwich design will minimize the effect of impact location, the characteristic damage state (CDS) will have some relationship with internal stiffening elements (e.g., frames, ribs, edge closeouts, and bulkheads). For impact occurring away from stiffening elements, the CDS is expected to be similar to that observed when impacting sandwich test panels. As discussed in Section 7.4, the extent of planar impact damage in the core and impacted facesheet were found to be nearly the same for many combinations of materials and a facesheet thickness on the order of 0.08 in. (2.03 mm) (Reference 7.8.1.2.4(a)). Figure 7.8.1.2.6 shows a correlation between the extent of measured core and facesheet damage. The relationship shown in the figure may relate to mechanisms whereby the core first fails under the impactor, and then facesheet damage develops directly above the planar area where core damage has greatly reduced the local shear stiffness of the sandwich panel.

7.8.1.2.7 *Impact characteristic damage states*

Low velocity impacts, e.g., impacts from dropped tools as opposed to ballistic impacts, present a special problem. Impacts on the laminate surface, especially those made by a blunt object, may cause considerable internal damage without producing visible indications on the surface. Damage to the resin may be particularly severe as evidenced by transverse shear cracks and delaminations. Consequently, the resin loses its ability to stabilize the fibers in compression and the local failure may initiate total structural collapse. Similarly, the impact may damage fibers and cause local stress concentrations, which could result in significant loss of tensile, shear, or compressive strength. With conventional graphite/epoxy systems, which are quite brittle, losses in tensile and compressive strength for non-detectable impact may

approach 50% and 60%, respectively. Post-impact failing strains from Reference 7.8.1.2.7 are plotted against dent depth in Figure 7.8.1.2.7(a). The AS4/3501-6 plates, which were made by resin film infusion of uniweave fabric, were 16, 24, 32, and 48 plies thick. The post-impact failing strains were lower for compression than tension. The failing strains for tension were larger than those for compression because the size of the region with damaged fibers was much smaller than that with damaged matrix.

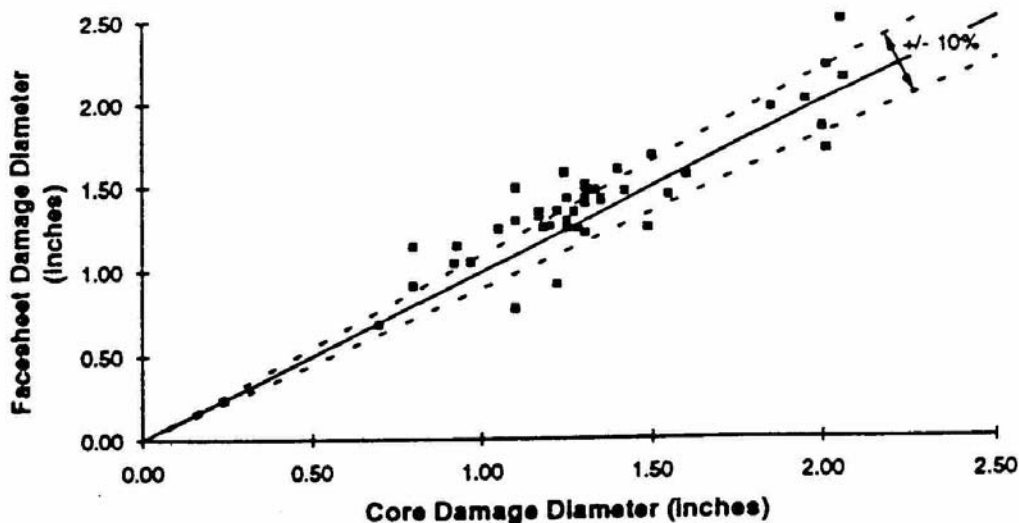


FIGURE 7.8.1.2.6 Comparison of the planar extent of impact damage in sandwich facesheet and core materials (Reference 7.8.1.2.4).

Much of the work documented to date on specific characteristics of impact damage has focused on impact normal to the surface of a flat plate. Figure 7.8.1.2.7(b) shows a schematic diagram classifying planar and cross-sectional views of damage observed in flat laminates following low-velocity impact by spherical objects. Three main classes of damage are shown. These include fiber failure, matrix damage, and combined fiber and matrix damage. As shown at the bottom of Figure 7.8.1.2.7(b), symmetric or unsymmetric cross-sections further distinguish each class of damage. As discussed in Section 7.4, numerous material, structural, and extrinsic variables affect damage size and type.

The most general classification of impact damage involves both fiber and matrix failures. The importance of each type of damage to structural integrity depends on the loads, part function, and further service exposure. Fiber damage, when present, tends to concentrate at an impact site. Typical matrix damage includes both matrix cracking and delamination. Matrix damage is also centered at the impact site but tends to radiate away from this point to a size dependent on the impact event and delamination resistance. Impacted laminates tend to develop a characteristic damage state (CDS) or pattern of through the thickness fiber and matrix failures. This CDS has been found to depend on the laminate stacking sequence (References 7.8.1.2.2(a), 7.8.1.2.2(b), and 7.8.1.2.2(d)).

Many factors can affect the symmetry of a CDS. Test observations indicate that thin laminates, particularly those with heterogeneous stacking sequences, tend to have asymmetric CDS, with damage initiated towards the side opposite the impacted surface (such as that shown in the bottom of Figure 7.8.1.2.7(b)). Very thick laminates also have asymmetric damage, but with the damage initiating close to the impacted surface. Work with laminates consisting of materials that have high delamination resistance, also have a greater tendency for asymmetric CDS than brittle materials tested with the same impact variables. This probably relates to the specific damage initiation and growth mechanisms.

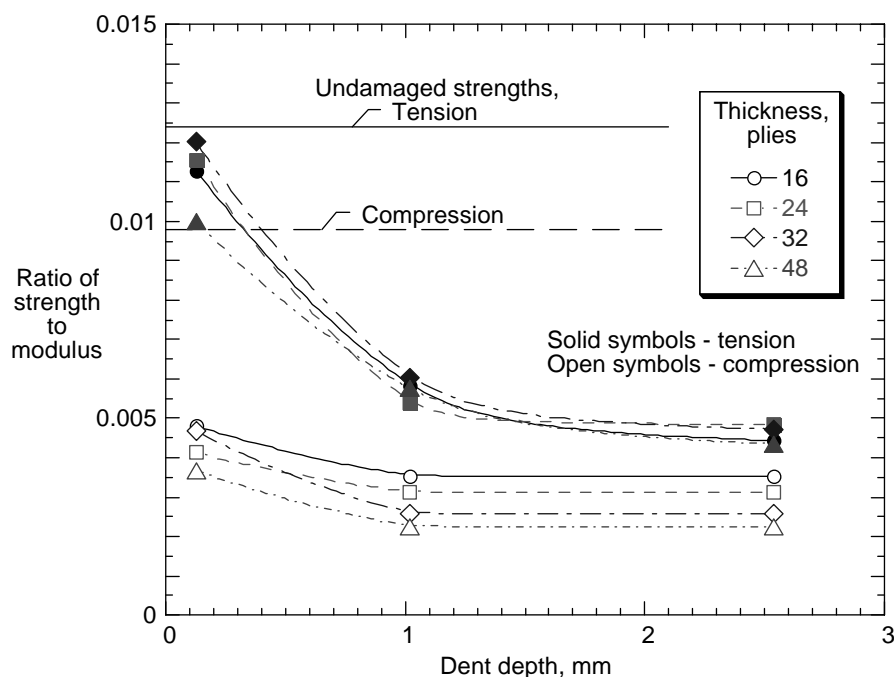


FIGURE 7.8.1.2.7(a) Post-impact tension and compression strengths for $[45/0/-45/90]_{ns}$ AS4/3501-6/RFI uniweave (0.5 in. (12.7 mm-diameter tup)) (Reference 7.8.1.2.7).

The tendency for CDS to develop in a composite material subjected to an impact event is very important to subsequent inspection and residual strength assessments. The extent of impact damage grows with the magnitude of a given impact event but the basic CDS tends to remain the same. The CDS of a specific configuration can be defined, prior to service exposure, during impact surveys that support detailed design. During such studies, the correlation between destructive laboratory measurements of the CDS and those obtained using NDE methods that are suitable for service can help establish a link to the residual strength prediction. For example, microscopy and TTU may be used to define the full extent of matrix and fiber failure in a CDS, while dent depth and coin tapping may be used to define the damage periphery. The combination of this information can then be used to predict residual strength. In practice, NDE data from service will yield a metric on the size of damage, while existing databases that define the CDS provide a link to residual strength prediction.

Compression and shear loaded structure are sensitive to both fiber and matrix damage that exist in the CDS. Matrix cracks and delaminations can link to locally break the base laminate into multiple “sub-laminates” that can become unstable under compression or shear loads. Figure 7.8.1.2.7(c) shows a schematic diagram of one CDS which was defined for a quasi-isotropic laminate lay-up with repeating stacking sequence (References 7.8.1.2.2(a), 7.8.1.2.2(b), and 7.8.1.2.2(d)). This is the same laminate stacking sequence that is commonly used for impact material screening tests with standard specimens (Reference 7.8.1.2.2(c)).

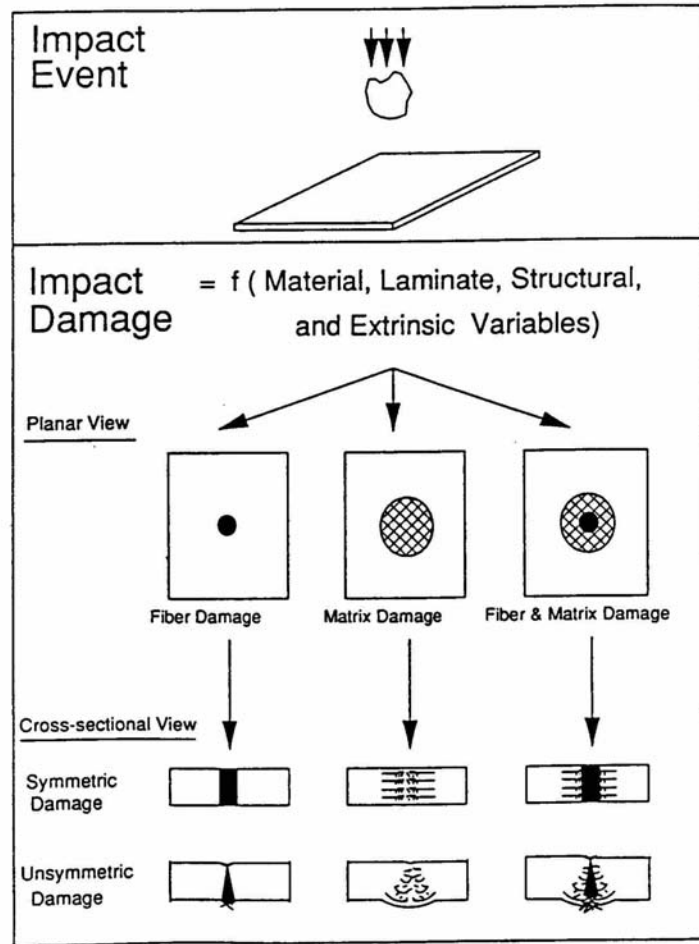


FIGURE 7.8.1.2.7(b) Potential impact damage states for laminated composites (Reference 7.8.1.2.2(a)).

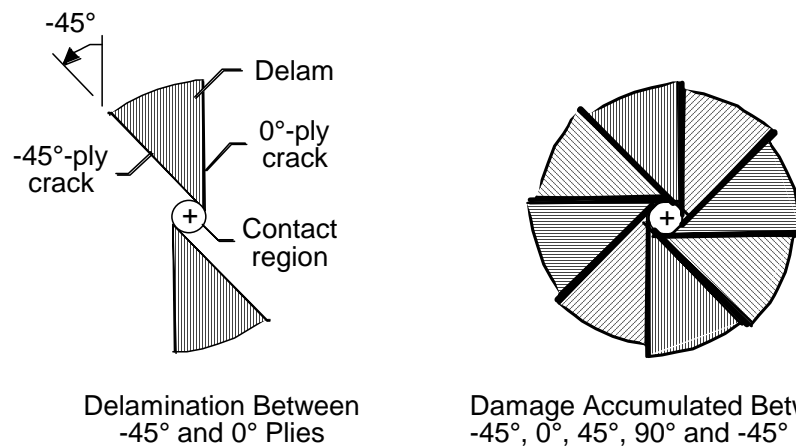


FIGURE 7.8.1.2.7(c) Matrix cracks and delaminations for a quasi-isotropic stacking sequence combine to form distinct sublaminates (References 7.8.1.2.2(a), 7.8.1.2.2(b), and 7.8.1.2.2(d)).

Transverse cracks bridge wedge shaped delaminations between adjacent plies in the CDS shown in Figure 7.8.1.2.7(c). This pattern continues through the laminate thickness, with interconnected delaminations spiraling toward the center, reversing direction, and proceeding out toward the back side. Depending on the specific stacking sequence, the sublaminates in a particular CDS are likely to change. Procedures that provide a circular cross-section for microscopic evaluation may be best for identifying the internal structure of sublaminates (See Reference 7.5.1.1(l)). Application of dye penetrant to the circular section's edge help to highlight the sublaminate structure.

7.8.1.2.8 *Residual strength - compressive/shear loads*

Experimental data using 1.0 in. (25.4 mm) diameter impactors with rounded tups show that compressive strength is reduced with damage size, see Figure 7.3.2(a), but levels off at the so-called "damage tolerance strain" (3000 to 3500 microstrain for brittle carbon epoxy systems (Reference 7.3.2(a))). This is a conservative but powerful and frequently used preliminary design strength value for Ultimate Load considerations.

Compressive failure prediction depends on the observed failure characteristics of a laminate with buckled sublaminates. Results obtained to date for a limited number of material types and laminate stacking sequences have shown that the dominant failure mode is associated with local in-plane compressive stress concentration. As a result, similar compressive residual strength curves are observed for laminates having either a toughened or untoughened matrix. Figure 7.8.1.2.2 shows normalized CAI curves for the interlayer-toughened (IM7/8551-7) and untoughened (AS4/3501-6) materials used as examples in Section 7.3.1 (note that Figure 7.5.1.3 shows transverse impact test results for the same specimens).

Delamination growth may be a critical failure mechanism for compression after impact (CAI) strength, depending on the specific damage size, laminate lay-up, and delamination growth resistance of a material (References 7.8.1.2.8(a) and (b)). Analysis of such failure modes show that damage growth tends to be stable, requiring larger compressive strains to grow larger damage. As a result, the local compressive failure due to in-plane stress redistribution remains the dominant mode, particularly for larger damage sizes. This can be explained physically by considering how much load is carried by large diameter sublaminates, which buckle at very low compressive strains. When little load is required to buckle the sublaminate, its effect on the adjacent structure is like that of a large open hole. In a sufficiently large structure, the material adjacent to the buckled impact damage may fail in compression before enough out-of-plane displacement occurs in the buckled sublaminates for significant growth. This occurs because large buckling displacements require sufficient compressive strain in adjacent undamaged material. Nevertheless, the delamination growth of buckled sublaminates should be evaluated as a potential failure mode since it has been observed in some very brittle matrix materials. Note the future development of materials with higher in-plane compression strength (i.e., greater fiber microbuckling strength) may also lead to the potential for competing failure modes.

When the CDS is dominated by fiber failure, both tension and compression residual strength will be affected. Although sublaminate buckling is not an issue, prediction of the residual strength of composites with local fiber failure still requires an estimate of the effective reduced stiffness. Once a measure of the effective reduced stiffness is known, methods which predict the stress concentration for a soft inclusion (References 7.8.1.2.8(c) and (d), 7.8.1.2.2(b)) and notched strength failure criteria can be applied (References 7.8.1.2.8(e) through 7.8.1.2.8(g) and 7.8.1.2.2(b)). Recent efforts have shown that a strain softening analysis provides an alternative to semi-empirical criteria traditionally used for the latter (References 7.8.1.2.8(h) and (i), 7.8.1.2.4(a)).

When the CDS includes both fiber failure and matrix damage (e.g., sublaminates), it is likely that a combination of methods will be needed to predict compressive strength. Fiber damage at the center of the damage may only affect the strength for relatively small damage sizes in which sublaminates buckle at relatively high strains. When the damage is larger, sublaminates buckle at much lower strains, effectively masking the effects of local fiber failure in the center of the CDS. Note that CAI results with small

damage for the toughened material in Figure 7.8.1.2.2 are affected by local fiber failure (Reference 7.8.1.2.2(a)).

Figure 7.8.1.2.2 shows post-impact compressive strength results that are similar to those observed for holes or penetrations. Such behavior is recognized by the shape of the residual strength curve that initially drops steeply as a function of increasing damage size, and then flattens out for large damage. Based on the sublaminar residual strength analysis described above, impact damage larger than 2 in. (50 mm) diameter would tend to collapse onto the compressive residual strength curve for open holes. Whether this trend can be expected for all laminates and other composite material forms loaded in compression or shear remains to be demonstrated.

The compressive residual strength behavior of a given material form and laminate should be determined in support of detailed design. As mentioned earlier, the thickness of laminated composites has been shown to effectively increase the compressive residual strength. Some stitched and textile composites have been found to have very flat residual strength curves, implying reduced notch sensitivity. These examples highlight the importance of studying specific design detail (laminate, thickness, lay-up, and material form). There are currently no theories to reliably predict the compressive residual strength of composite materials without some notched strength data. A limited amount of test data indicates some dependence of compressive residual strength on notch geometry with ellipse-shaped damage having a high aspect ratio resulting in the lowest strength.

7.8.1.2.9 Residual strength - tensile loads

Degradation in the residual strength of tensile-loaded structure is most sensitive to fiber failure. As discussed earlier, fiber failure localizes within a zone that is roughly the size of the impactor. As a result, the size and shape of an impactor are crucial to the extent of fiber failure. Although impact by large diameter objects pose the most severe threats, rare impact events of significant magnitude (e.g., service vehicle collision) would be required to cause extensive fiber damage over a large area of an aircraft structure's surface. Delamination and matrix cracks do not generally decrease the integrity of tensile-loaded structure. However, the combined effect of matrix damage surrounding fiber failure should not be ignored because the former may actually increase tensile residual strength by softening the stress concentration.

In the case of tensile-loaded structure, delamination growth is generally not an alternate failure mode (Reference 7.8.1.2.9(a)). It seems reasonable to expect that the tensile residual strength of a structure with through-penetrations will be lower than one with similar sized impact damage (i.e., a softened impact damage zone carries some load). Penetrations caused by impact events may be more or less severe than those obtained by machining the same sized notch. In some materials, the penetration may include an extended zone of fiber failure beyond visible penetration. This tends to further reduce residual strength. Other materials have a large zone of matrix failure surrounding the penetration, helping to soften the stress concentration and provide higher residual strength. Many factors have been found to affect the tensile residual strength of composite materials, including fiber, matrix, manufacturing process, hybridization, and lay-up (References 7.8.1.2.9(b), 7.8.1.2.8(e) through 7.8.1.2.8(g), and 7.8.1.2.8(i)). As is the case for compression, some notched strength testing is required to establish reliable failure criteria.

7.8.1.2.10 Stiffened panels

Characteristics of impact damage in structural configurations are strongly dependent on the impact location. The CDS of panels stiffened by discrete elements will also depend on whether the element is bonded or mechanically fastened. Skin impacts spaced sufficiently far from the stiffening elements will have a CDS similar to those obtained in tests with plates. Impacts occurring near an element will experience a much stiffer structural response, with potential failures occurring within the element and its attachment with the skin. Bondline and/or delamination failures are common between bonded elements and skin. The extent of such failure will depend on the impact event and design variables (e.g., the use of adhesive layers, doubler plies, and material delamination resistance). Delaminations may originate at the interface between skin and stiffener, and then penetrate to grow delaminations between base laminate plies having lower toughness than the adhesive. Fiber failures typically occur in blade, I- or J-stiffeners

when impacts occur on the outer skin's surface, directly over the stiffener's web. Figure 7.8.1.2.10(a) shows an example of this type of local failure. The distribution of fiber failure for this type of damage is an important component of the CDS since it affects the section bending properties (see Reference 7.5.1.1(l)).

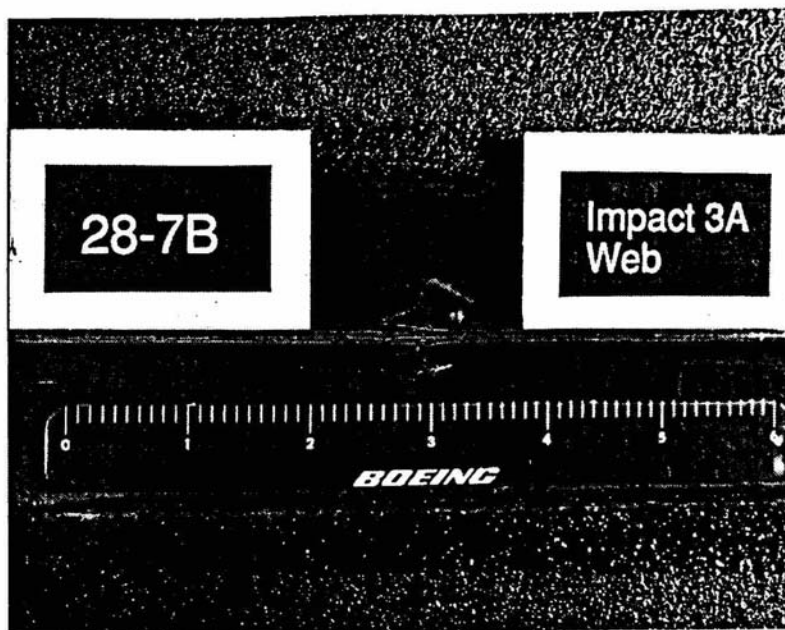


FIGURE 7.8.1.2.10(a) Stiffener web damage in blade-stiffened skin panels (Reference 7.5.1.1(l)).

The difference between impact responses of coupons and three-spar stiffened panels is illustrated in Figure 7.8.1.2.10(b). Post-impact compressive failing strains are plotted against kinetic energy for "hard" wing skins. The skins were nominally $\frac{1}{4}$ inch (6.35 mm) thick and were made with [38/50/12] and [42/50/8] lay-ups for coupons and panels, respectively. (The notation [38/50/12] indicates the percentage of 0° plies, $\pm 45^\circ$ plies, and 90° plies, respectively.) The spacing of the bolted titanium stiffeners was 5.5 inches (139.7 mm). A $\frac{1}{2}$ inch (12.7 mm) diameter tup and 10-lbm (5 kg) impactor was used for the coupons, and, a 1 inch (25.4 mm) diameter tup and 25 lbm (11 kg) impactor was used for the panels. The two panels impacted with 40 and 60 ft-lbf (54 and 81 N-m) energies were impacted two times on the transverse centerline (over skin only), once midbay of the center spar and left-most spar and once midbay of the center spar and right-most spar. The panel impacted with 20 ft-lbf (27 N-m) energy was impacted at only one midbay location. The three panels impacted with 100 ft-lbf (135 N-m) energy were impacted three times each: once midbay (between stiffeners - over skin only), once over the skin only but near the edge of a stiffener, and once over a stiffener. A curve was fit to the coupon results. Failures were catastrophic for coupons and for panels with mid-bay impacts and failing strains were essentially equal. Failures of the panels with multiple 100 ft-lbf (135 N-m) impacts were not catastrophic. After fracture arrest by the stiffeners, the loads were increased 36% and 61% to cause complete failure. The initial failing strains for the panels with multiple 100 ft-lbf (135 N-m) impacts agreed with an extrapolation of the coupon data. Thus, the stiffeners reduced the effective size of the panel by increasing flexural stiffness and increased strength by arresting fractures.

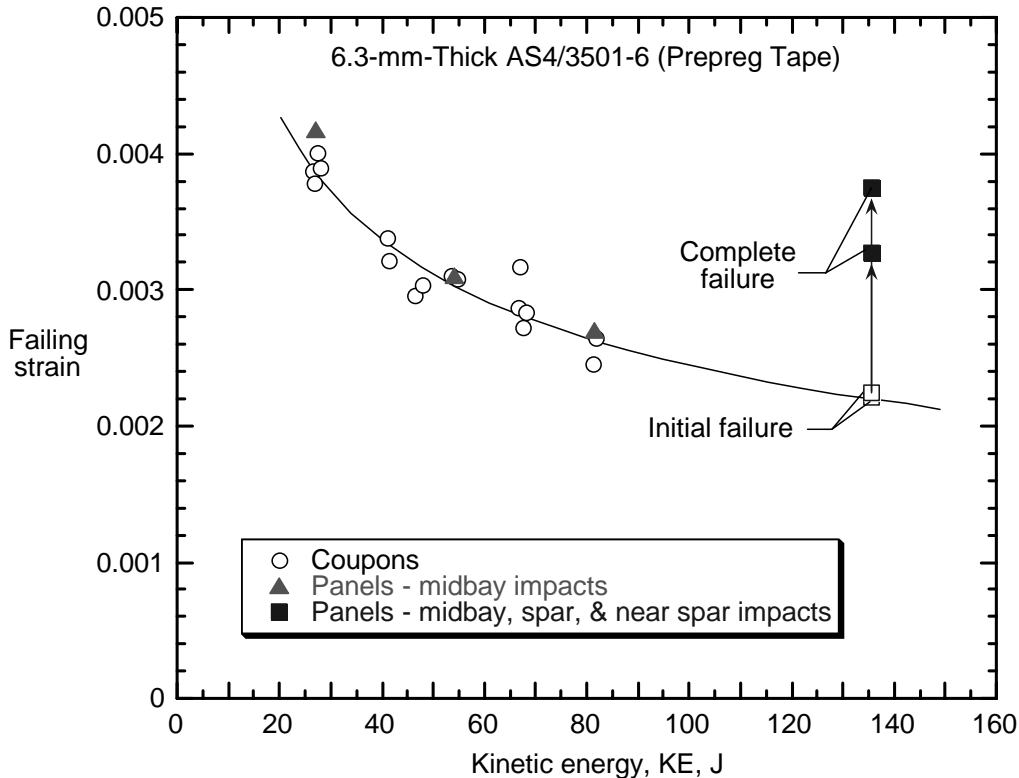


FIGURE 7.8.1.2.10(b) *Impact response of coupons and panels with three bolted spars (Reference 7.8.1.2.3)*

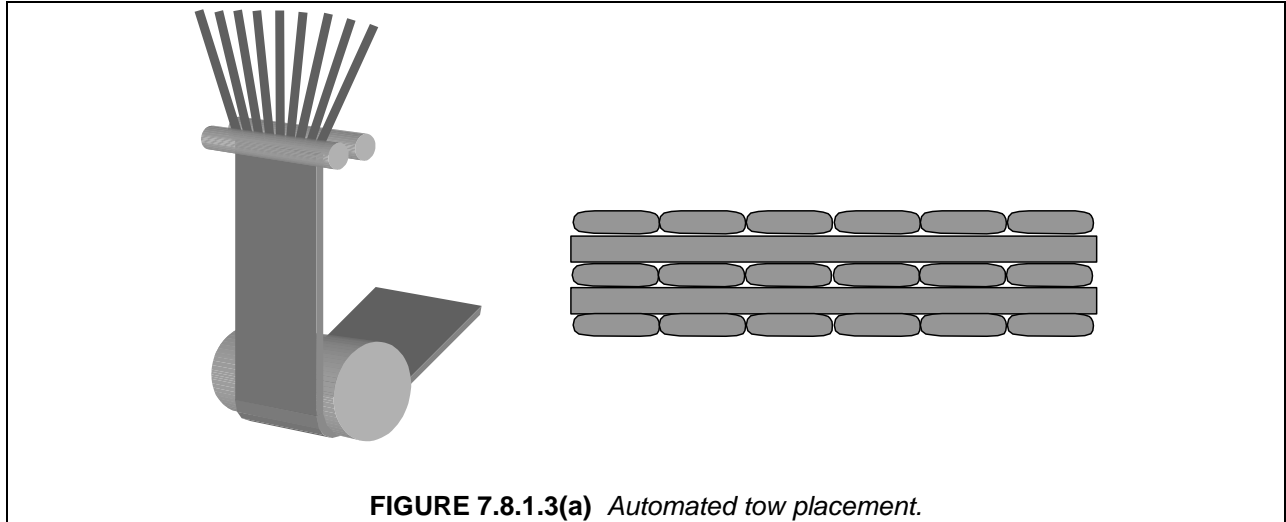
Structural panel level residual strength prediction involves more analysis steps than that for flat composite plates. As a result, additional structural building block tests are required. The analysis still starts with a quantitative metric which provides effective properties of the CDS for loads of interest. This measure is used to estimate the local stress or strain concentration. The effects of a given structural configuration on this stress concentration must be analyzed to predict the onset of damage growth. In redundant structural configurations, growth and load redistribution simulations may be needed for final failure prediction. Damage growth has often not been observed in composite structure because relatively small damage has typically been tested. For example, severe impact damage localized at a stiffener will require significant panel loads before gross damage propagation initiates (e.g., panel strains on the order of 0.004 in/in). Since the damage was small to start, a dynamic growth phenomena is observed, whereby the adjacent stiffening elements are unable to arrest damage growth. When the initial damage is significantly larger (e.g., a penetration which completely severs the stiffener and adjacent skin material), growth to the adjacent stiffening elements is more stable and arrest has been observed. (Reference 7.8.1.2.10).

7.8.1.3 Structure with through-penetration damage

A significant database addressing through-thickness notches was generated on a NASA/Boeing contract during the early 1990's. This activity addressed the response for a range of materials, notch sizes and structural complexity. The following discussion, except where noted, is based on those findings (References 7.8.1.3(a) through 7.8.1.3(e), 7.8.1.2.4(a), 7.8.1.2.8(g), 7.8.1.2.8(i), and 7.8.1.2.10).

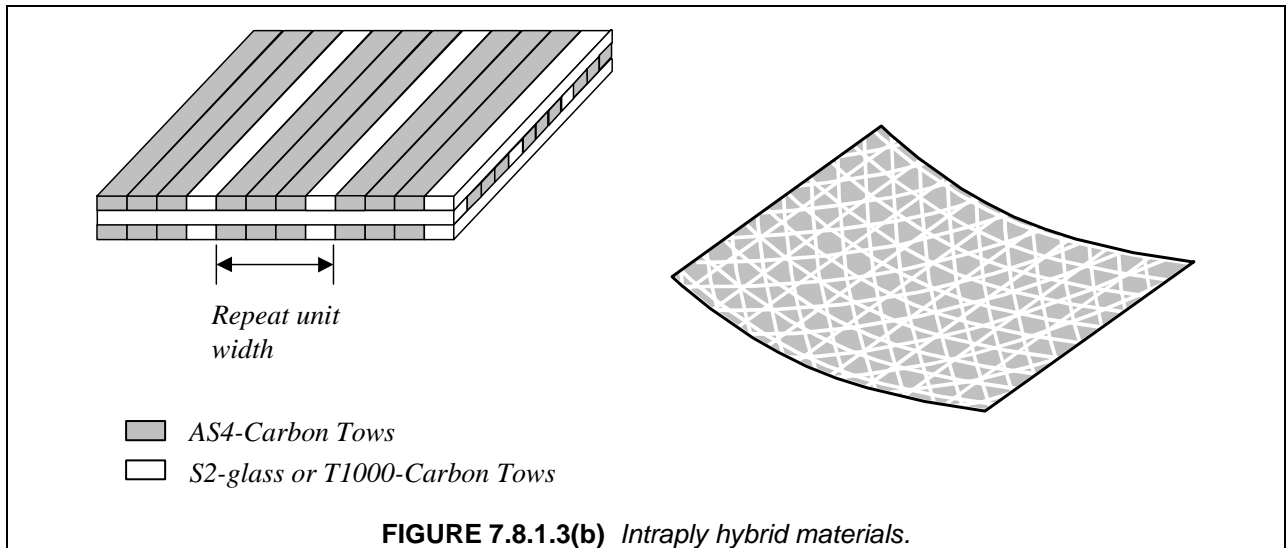
A major component of that activity was the use of tow placement (a.k.a. fiber placement) for lay-up of the skin materials. The tow placement process uses prepregged tow as the raw material form, and

lays down multiple tows in a single pass of the tow-placement head, as illustrated in Figure 7.8.1.3(a). This technique allows the cost-effective use of intraply hybrid materials, which are materials with tows of more than one fiber type combined in a repeating pattern within each individual ply (e.g., S2-glass), as shown in Figure 7.8.1.3(b). In this program, such intraply hybrids were explored, primarily with the hybridization occurring in all plies.



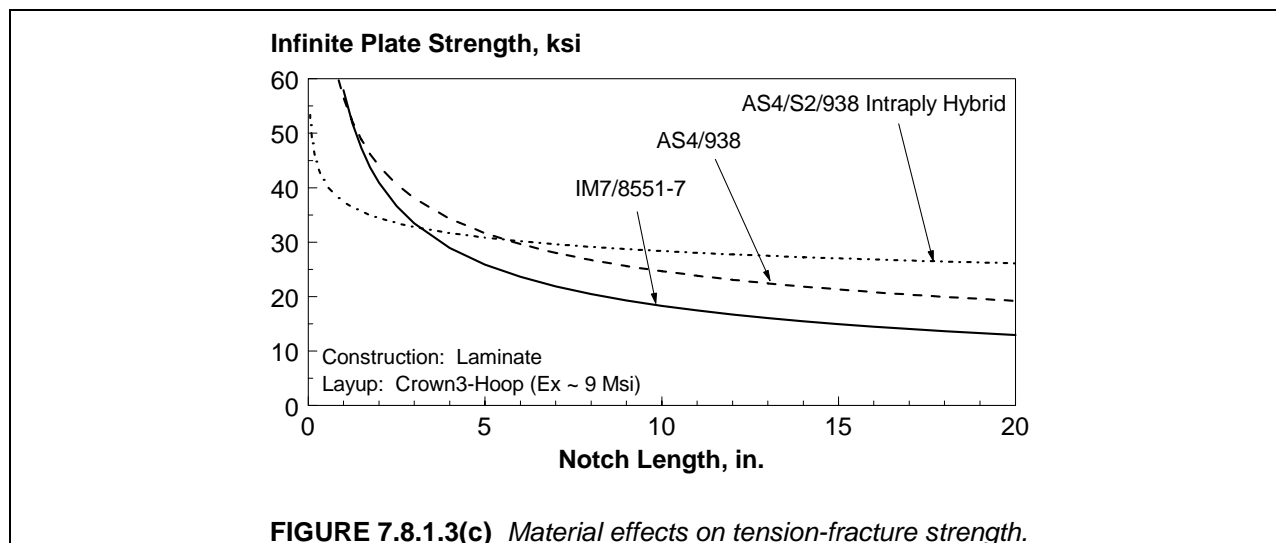
Tension.

A number of variables strongly affect tensile residual strength response in the presence of through-thickness notches. In general, there is a trade-off between small-notch strength (i.e., "strength") and large-notch strength (i.e., "toughness"); high strengths are typically accompanied by low toughnesses, and visa versa. Low-strength, high-toughness behavior is characterized by lower sensitivity to changes in notch length, resulting in flatter residual strength curves.



The effect of material for a single laminate is illustrated in Figure 7.8.1.3(c). The toughened-matrix materials (IM7/8551-7) demonstrate high strength and low toughnesses, while brittle-matrix materials

(AS4/938) exhibit lower strengths but higher toughness. An intraply hybrid of 75% AS4/938 and 25% S2/938 demonstrated the highest toughness through a very low sensitivity to changes in notch length. Note that this increased strength occurs despite a lower stiffness (i.e., higher stiffness carbon fibers were replaced with lower-stiffness glass fibers), indicating that the increase in failure strain was even higher. As shown in the figure, strengths of different materials can vary 30 to 50% for large notch lengths of interest to damage tolerance assessments (e.g., greater than 10 in. (250 mm)).



The effects of hybridizing variables on tensile fracture strength for notch lengths of 2.5 in. (63 mm) and less were reported in Reference 7.8.1.3(c). High-strain glass (S2) and carbon (T1000) fibers were used to hybridize the baseline carbon fiber (AS4) laminate. Results for 2.5 in. (63 mm) notches are shown in Figure 7.8.1.3(d). The hybrids exhibited reduced notch sensitivities and large amounts of matrix splitting and delamination prior to failure, as shown in Figure 7.8.1.3(e). The AS4/S2-glass hybrids also had significant post-failure load carrying capability.

Lay-up was found to have a similar effect on tensile fracture strengths as does material, with higher-modulus laminates exhibiting higher strengths and lower toughnesses relative to lower-modulus laminates. High-modulus laminates of toughened-resin materials tend to have notch-length sensitivities similar to those predicted by linear elastic fracture mechanics (LEFM), while the sensitivities of other material/laminate combinations are lower. Figure 7.8.1.3(f) illustrates a representative magnitude of this effect.

A ply of plain-weave fabric included on each surface of each facesheet for manufacturing reasons resulted in significant tensile fracture improvements over tow-only laminates for most lay-ups, as shown in Figure 7.8.1.3(g). While a direct comparison of identical laminates was not available in the test results, the trend is convincing. The improvement is likely due to the added energy absorption of the fabric plies during the failure process and/or to a decreased stress concentration resulting from an increased repeatable inhomogeneity created by the fabric.

A comparison of AS4/8552 sandwich panel test results with those of AS4/938, AS4/S2/938 hybrid, and IM7/8551-7, all of which include notch sizes of 8 to 12 in. (200 to 300 mm), are shown in Figure 7.8.1.3(h). Lay-up differences are present within and between materials, confounding comparisons. The AS4/8552 results appear closest to a less-stiff AS4/938 laminate. This indicates that the impact-damage-resistance advantages of toughened-resin materials may be attainable without the loss of the tension-fracture advantages of the brittle-resin materials by incorporating fabric surface plies.

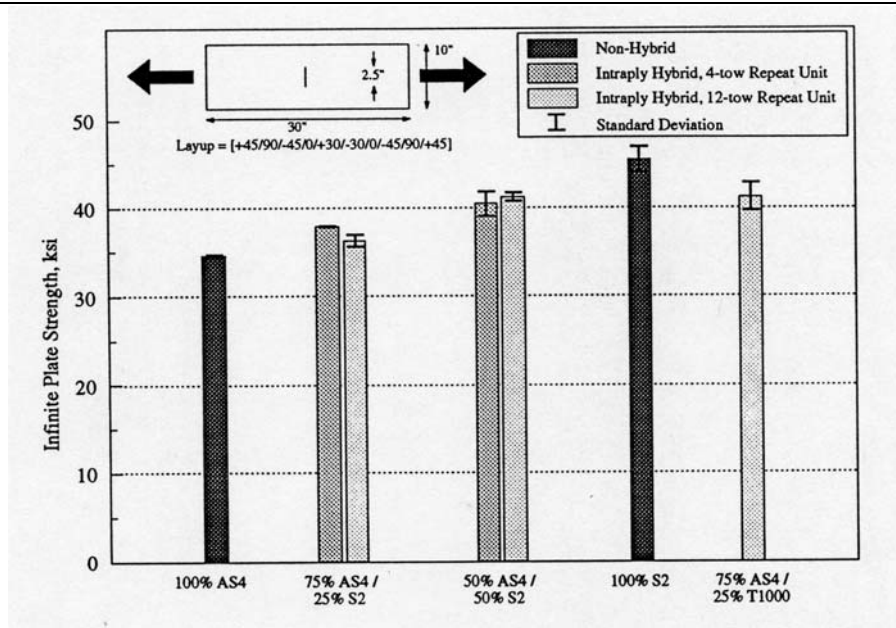
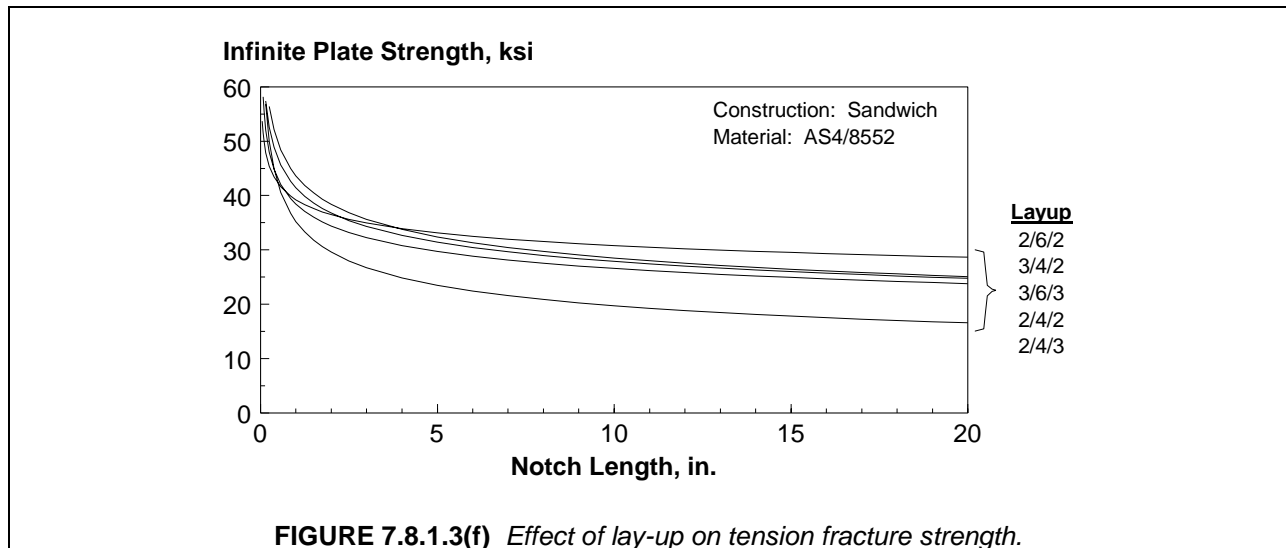
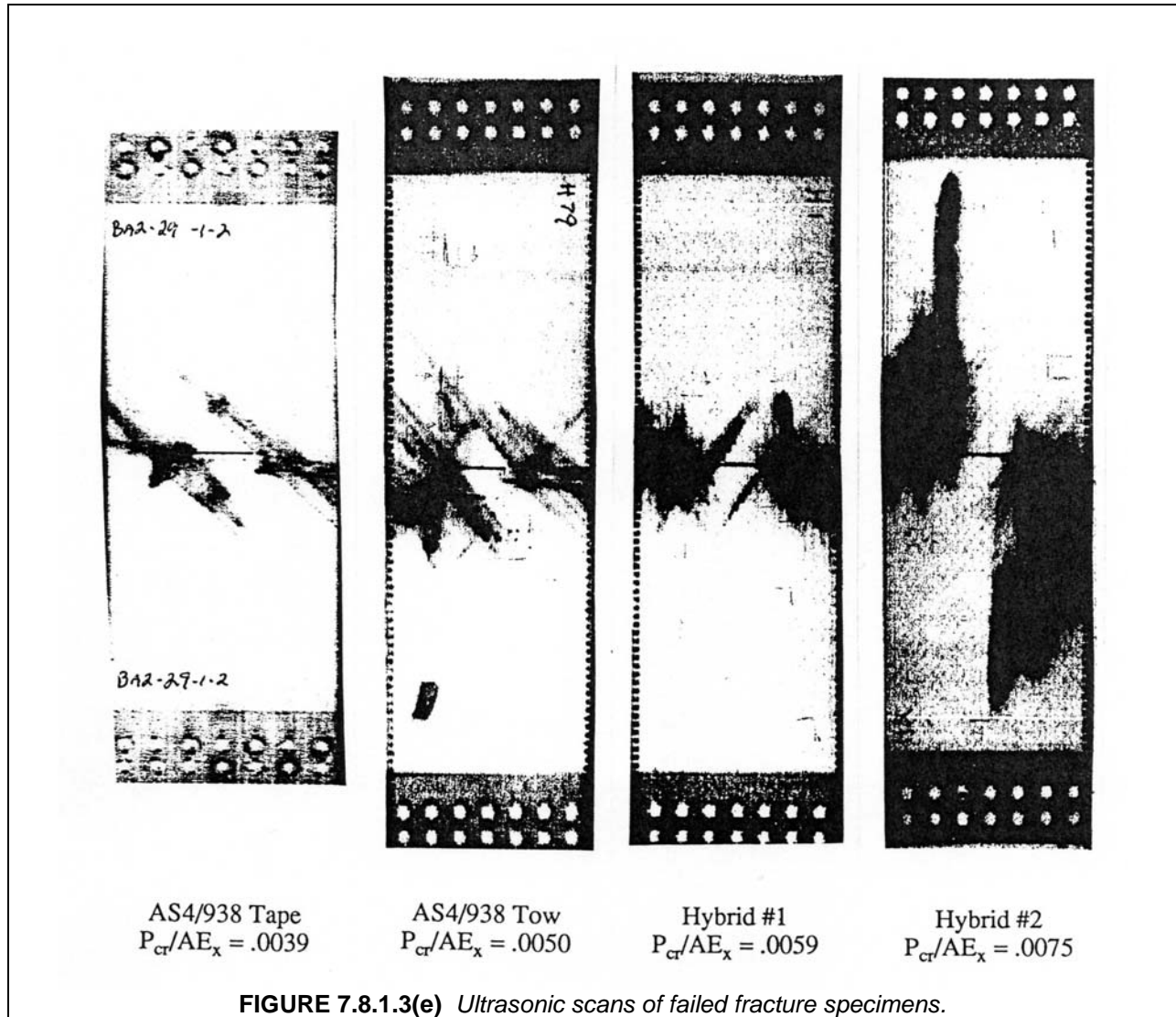


FIGURE 7.8.1.3(d) Tension fracture strength of intraply hybrids for 2.5 inch (63 mm) crack.

Material form and processing variables also were found to have a significant influence on tensile fracture performance. Tests from the AS4/3501-6 tape laminate are compared with results for AS4/938 tow and AS4/938 tape in Figure 7.8.1.3(i). These data indicate significantly reduced tensile fracture performance of tape when compared to tow (i.e., approximately 44% for a 9 in. (230 mm) notch). It was hypothesized that the most significant contributor to this difference was the larger scale of repeatable inhomogeneity in the fiber-placed laminates, resulting from geometrical nonuniformities in the band cross-section. This characteristic can be observed in ultrasonic scans, as shown in Figure 7.8.1.3(j). In tape, a more uniform thickness, and offset of the course-to-course splices for similarly oriented plies results in much smaller, and non-repeatable, inhomogeneities. It should be noted that the AS4/3501-6 tape panel had a resin content significantly below the process specification.

The improved tow performance, however, did not appear to be robust relative to processing parameters. Results from a series of panels are compared in Figure 7.8.1.3(k). The two 32-tow band panels both demonstrated lower tensile fracture strengths than the 12-tow band panels throughout the full range of notch sizes tested, eliminating a large portion of the tow's performance advantage over tape. The slightly reduced sensitivity to notch size of the 32-tow band panels, however, may result in superior performance for notches above 30 to 40 in. (760 to 1000 mm). Their lower strengths for notch sizes below that range are likely due to a combination of

- Differing tow-placement heads and the resulting band cross-sectional geometry changes,
- Reduced panel thickness and the associated reductions in resin content and/or fiber areal weight (likely caused by different bagging procedures), and
- Reduced prepreg tow unidirectional strength.



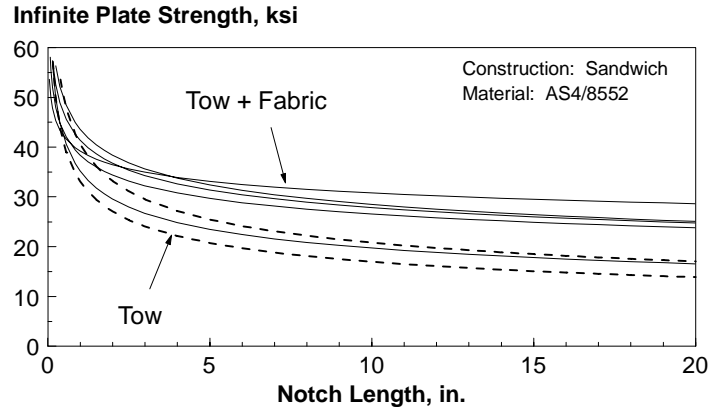


FIGURE 7.8.1.3(g) Effect of fabric surface plies on tensile fracture strength of AS4/8552.

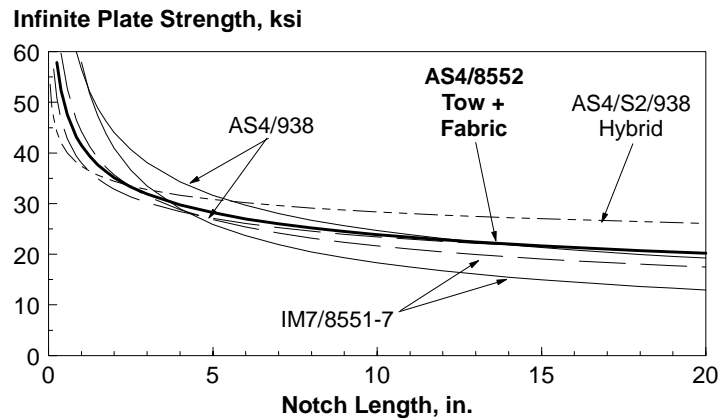


FIGURE 7.8.1.3(h) Comparison of AS4/8552 (tow/fabric) sandwich tensile fracture results with those of AS4/938 (tow), AS4/S2/938 intraply hybrid (tow) and IM7-8551-7 (tape) laminates.

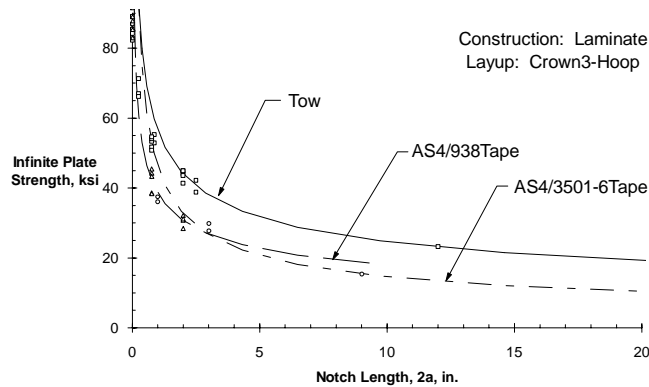
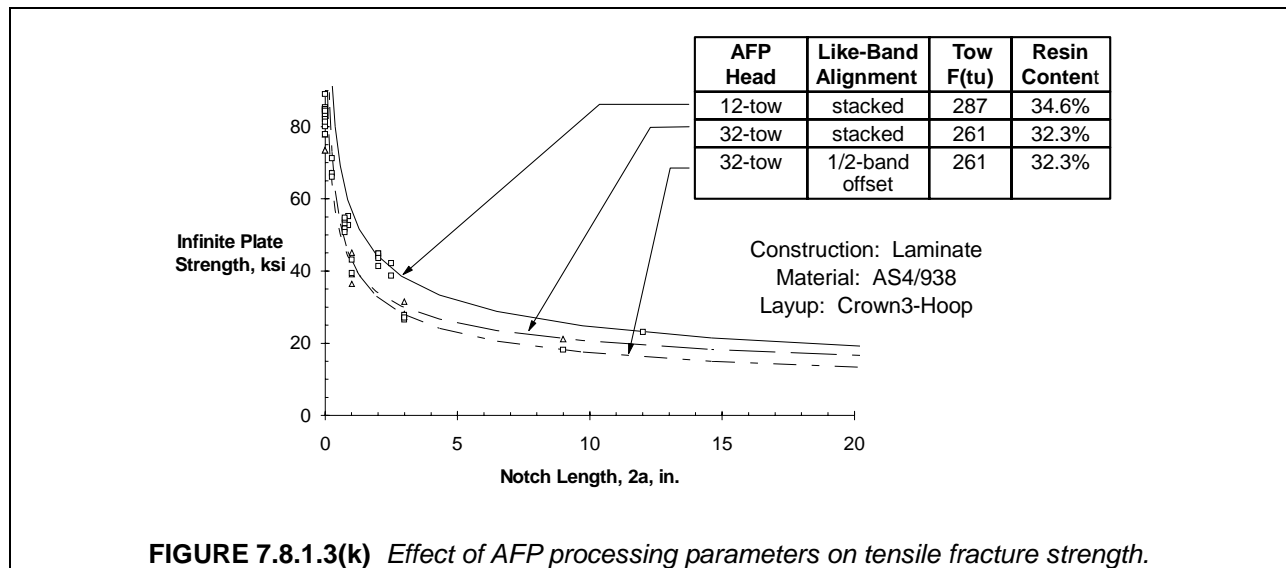
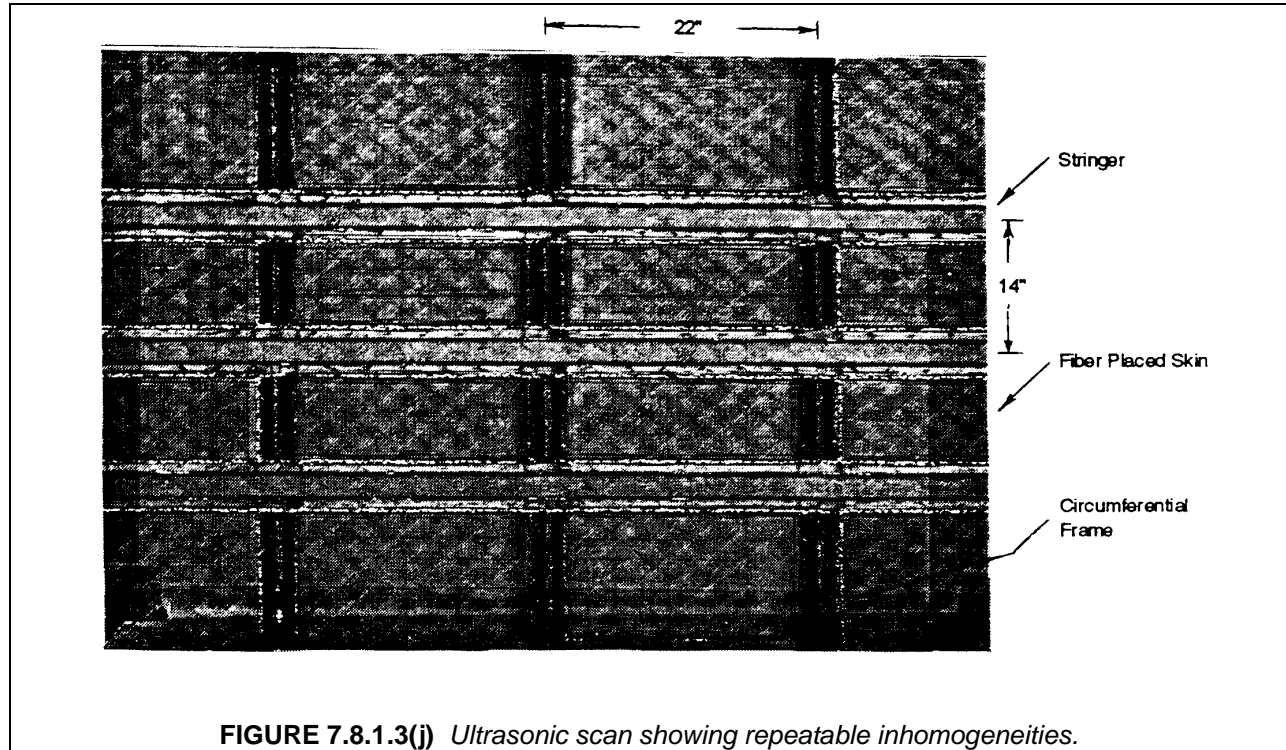


FIGURE 7.8.1.3(i) Comparison of tow and tape tensile fracture strengths.



An additional contributor may have been the age of the material for the 32-tow band panels (approximately 2 years), which could have affected the AFP processing characteristics.

This strength-toughness trade is not unlike that observed in metallic structure. Figure 7.8.1.3(l) compares the response of a brittle-resin (AS4/938) and a toughened-resin (IM7/8551-7) composite material with that of a brittle (7075-T651) and a ductile (2024-T3) aluminum.

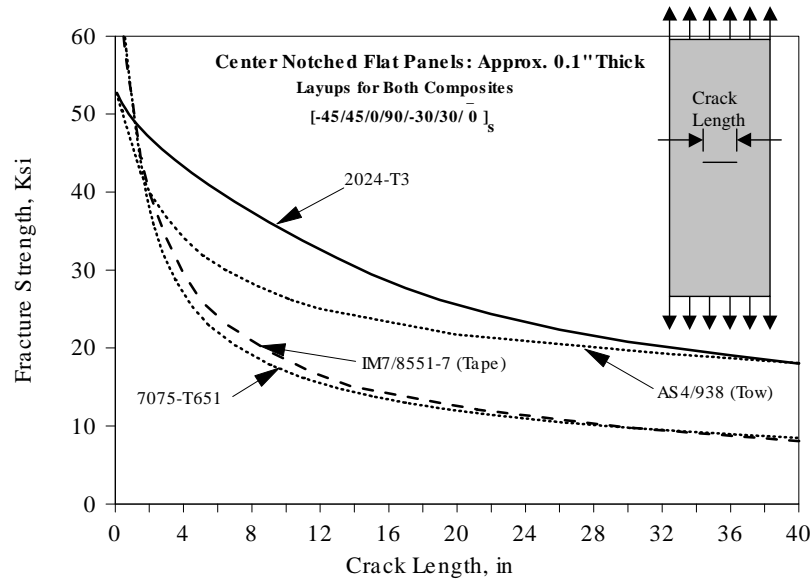


FIGURE 7.8.1.3(I) Comparison of composite and metallic tensile response.

Figure 7.8.1.3(m) summarizes the influencing factors on the strength-toughness trade in composite tension fracture. Higher strength but lower toughness resulted from toughened-resin materials and hard (0°-dominated) laminates. Lower strength and higher toughness resulted from brittle-resin materials, soft laminates and intraply hybridization with S2-Glass. Larger scales of repeatable material inhomogeneity appeared to result in improved toughness with little effect on strength. Matrix toughness appeared to have a larger influence on the behavior than laminate type.

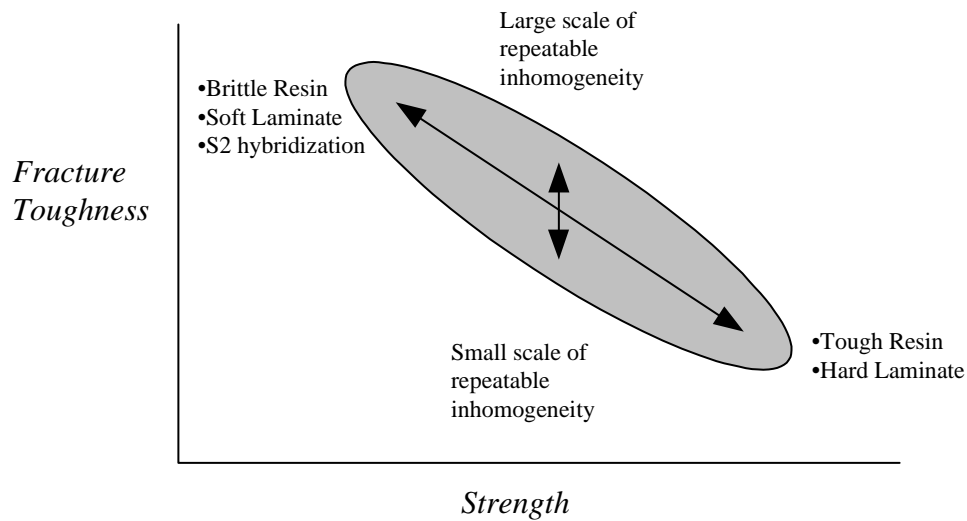


FIGURE 7.8.1.3(m) Strength-toughness trade-off in tension.

In addition to the strong strength-toughness trade-offs, non-classical material responses were observed. Notch-tip strain distributions prior to any damage formation were seen to be less severe, and more gradual, than classical theoretical predictions, as shown in Figure 7.8.1.3(n). Similar distributions

are predicted by non-local material models, suggesting that such behavior may be active. Large specimen finite-width effects were also found to occur, particularly with those laminate/material combinations that exhibited reduced notch-length sensitivity. As shown in Figure 7.8.1.3(o), isotropic finite-width correction factors, which have been found to differ only slightly from similar orthotropic factors, were unable to account for the differences in the two notch-to-specimen-width data sets. This has been attributed to the significant damage zones created prior to failure, and the resulting interaction with the specimen boundaries.

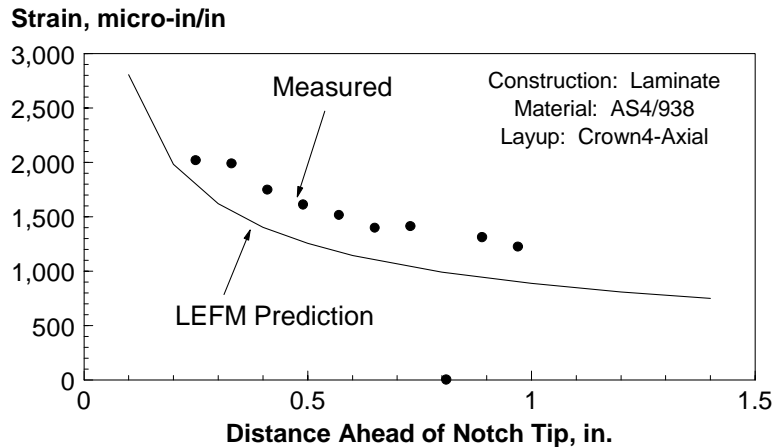


FIGURE 7.8.1.3(n) *Non-classical notch tip strains observed in large-notch tensile fracture tests.*

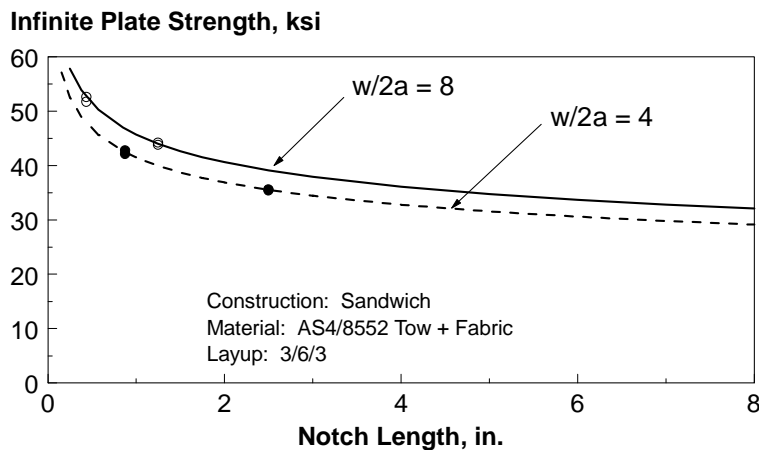


FIGURE 7.8.1.3(o) *Specimen finite width effects for quasi-isotropic AS4/8552 sandwich.*

Most efforts addressing through-penetration damage have used machined notches to represent the damage state created by a penetrating event. Reference 7.8.1.3(c) conducted limited tensile fracture comparisons of 0.875 in. (22.2 mm) through-penetrations and machined cracks. Creation of the penetrations and the resulting damage are discussed in Section 7.5.1.2. The strength results are shown in Figure 7.8.1.3(p). For the thinner specimens ($t = .059 - .074$ in. (1.50 - 1.80 mm)), penetration strengths were within 10% of the machined-crack strengths. One notable exception was for a toughed resin material (IM7/8551-7), which had post-impact tensile fracture strengths that were 20% lower than those for

specimens with machined cracks. Evidence suggests that impact penetration of these laminates may result in effective crack extension via fiber breakage. In the case of the thickest laminates tested ($t = 0.118$ in. (3.00 mm)), the tensile fracture strengths of specimens with impact penetrations were up to 20% higher than those for specimens with machined cracks. This difference in response from the thinner laminates was attributed to the formation of larger delaminations near the crack tip, which reduced the stress concentration.

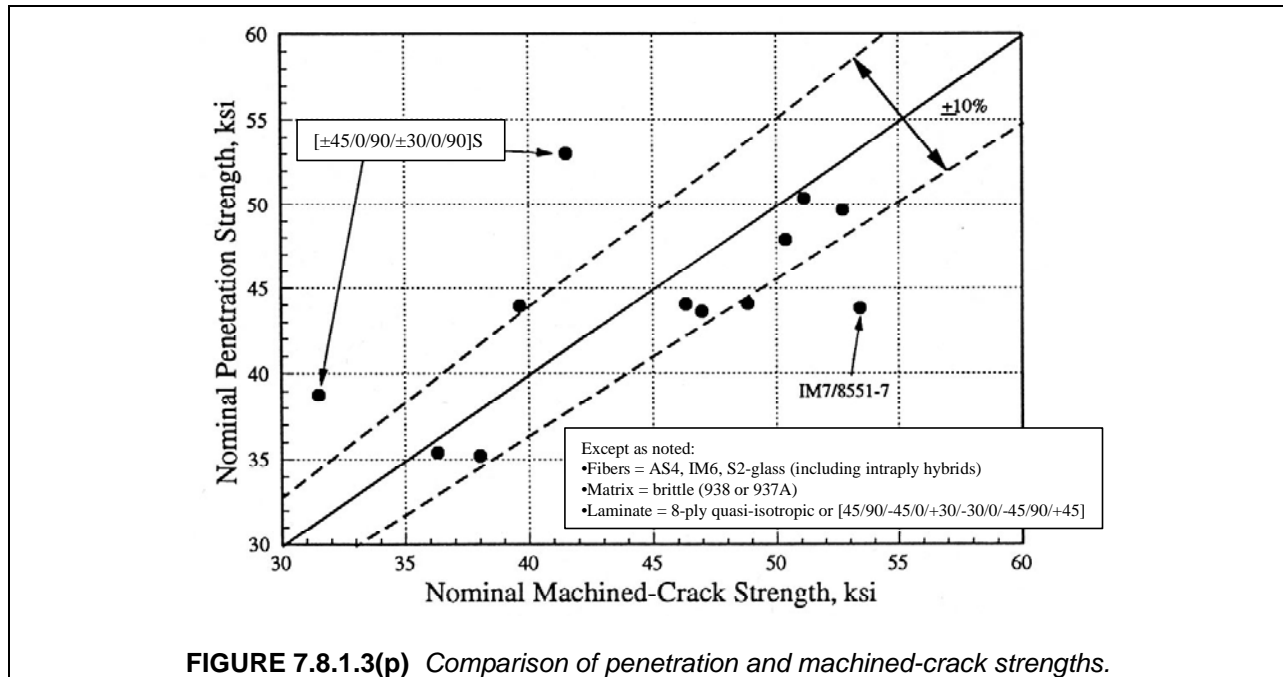


FIGURE 7.8.1.3(p) Comparison of penetration and machined-crack strengths.

Compression. The compressive fracture results showed significantly lower strengths than for tension, as illustrated in Figure 7.8.1.3(q). The effect of lay-up appears somewhat smaller than that for tension. The compression results also exhibit a reduced notch-length sensitivity relative to LEFM.

Unlike the tensile fracture case, where strong specimen finite-width effects accompanied reduced notch-length sensitivities, the finite-width effects in compressive fracture did not differ significantly from those predicted by isotropic correction factors, as shown in Figure 7.8.1.3(r). This suggests that large damage zones are not present prior to specimen failure, which is consistent with experimental observations.

The strongest effect observed in the compression testing was that of thickness. As shown in Figure 7.8.1.3(s), notched strengths of a wide range of materials, lay-ups, cores, and construction all with total laminate/facesheet thicknesses between 0.11 and 0.20 in. (2.80 and 5.1 mm) are within approximately $\pm 10\%$ of an average curve. The several tests of sandwich laminates with total facesheet thicknesses of 0.44 in. (11 mm) resulted in strengths approximately 25% higher than those of the thinner laminates. This behavior was also seen in a subsequent study; the results are shown in Figure 7.8.1.3(t) (Reference 7.8.1.2.4(b)). This insensitivity to material and lay-up variables and the strong sensitivity to thickness suggest that local instability may be controlling failure.

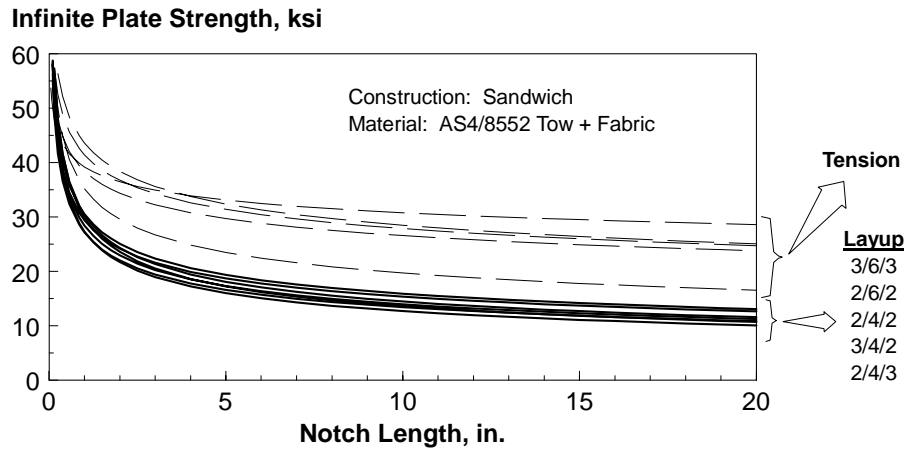


FIGURE 7.8.1.3(q) Comparison of compressive and tensile fracture results.

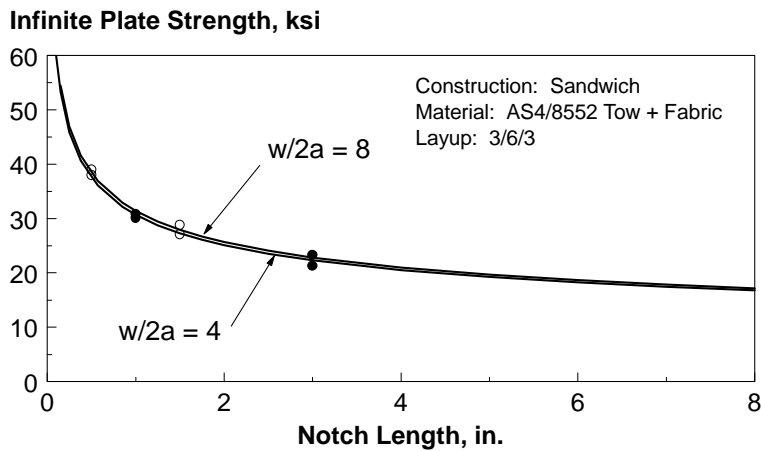


FIGURE 7.8.1.3(r) Specimen finite width effects in compression.

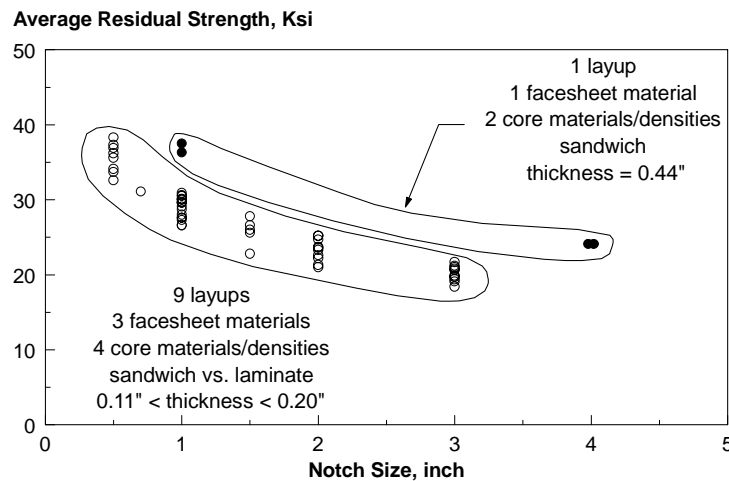


FIGURE 7.8.1.3(s) Thickness effects on compressive fracture strength.

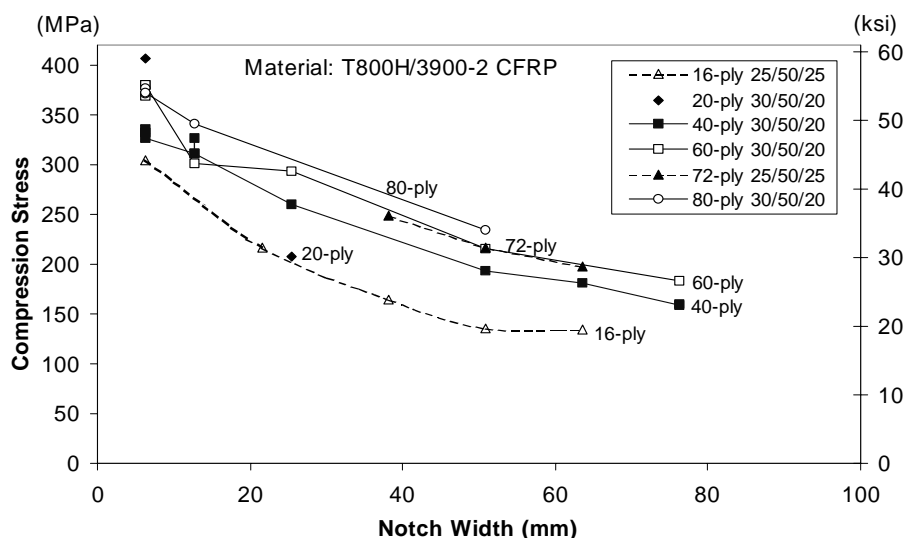


FIGURE 7.8.1.3(t) Thickness effects on compression-fracture strength.

7.8.1.3.1 Stitched skin/stiffener panels

A large flat wing panel with blade stiffeners containing an 8.0 in. (20.3 cm) long cut that also severed the central stiffener was tested in tension (References 7.8.1.3.1(a) and (b)). The skin material was made from 54 layers of dry uniweave fabric that were stitched together using Kevlar 29 thread. The lay-up of the skin was $[0/45/0/-45/90/-45/0/45/0]_{3S}$. The stiffener material was made from 36 layers of the dry uniweave fabric with a lay-up $[0/45/0/-45/90/-45/0/45/0]_{2S}$. The T-section stiffeners were made by stitching together dry angle-section stiffeners that were formed from the dry skin fabric. The flanges of the T-section stiffeners were stitched to the skin, and the panel was then infiltrated with 3501-6 resin. The skin fractured at a strain of 0.0023 in/in, the fracture propagated to the edge of the stiffener and was arrested. With increasing load, the fracture turned and grew parallel to the stiffener. At a strain of 0.0034 in/in, failure occurred at the loading grips. Thus, the stitched stiffeners resulted in considerable increase in failure strain.

7.8.2 Design issues and guidelines

7.8.2.1 Stacking sequences

When impact damage is dominated by fiber failure (e.g., Reference 7.8.1.2.8(c)), it is desirable to stack primary load carrying plies in locations that minimize fiber failure. Since fiber failure typically occurs first near outer surfaces, primary load carrying plies should be concentrated towards the center of the LSS. Experience to date suggests that a homogeneous LSS might be best for overall CAI performance dominated by matrix damage (Reference 7.8.2.1).

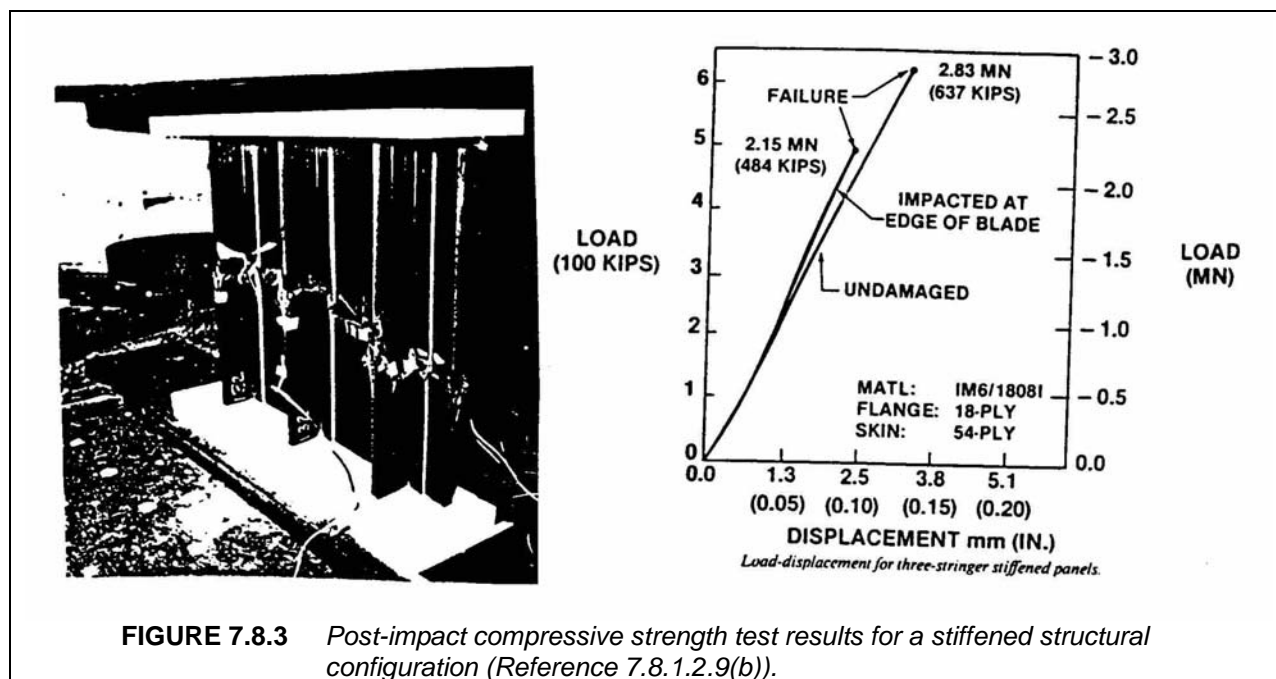
7.8.2.2 Sandwich structure

Caution should be applied when using sandwich material combinations where significant impact damage can occur within the core, without visible surface indications in the facesheet. (This type of impact critical damage state (CDS) has been identified for certain types of honeycomb (Reference 7.8.1.2.2(d)) and foam cores.) This is particularly true for compressive or shear loaded structures in

which such damage may grow undetected to critical sizes. Simple impact screening tests can be used to identify this failure mechanism and the related drops in residual strength.

7.8.3 Test issues

Structural residual strength tests are typically performed to support impact surveys, detailed design development and provide structural substantiation data. Figure 7.8.3 shows the results from such a test performed with a stiffened skin panel design. Multiple impacts, spaced far enough to avoid interactions, may be used in such studies to identify the critical impact location. A range of impact damage sizes in smaller test panels and elements can help to establish the shape of the residual strength curve. This should provide the necessary building blocks to analytically determine ADL and CDT as a function of structural load paths. Tests supporting the analysis of structural configurations should be large enough to allow load redistribution and the associated damage accumulation/arrest. As a further word of caution, residual strength tests with very wide but short panels should be avoided because the effects of damage may be masked by an insufficient length for proper load introduction. The results from such tests may be unconservative. Also, the skin buckling pattern of the test panel should match that of the full-scale structure, otherwise the local stresses in the vicinity of the impact damages may not be representative and thereby produce an invalid failure result.



7.8.3.1 Impact tests on coupons

This section is reserved for future use.

7.8.3.2 Impact tests on stiffened panels

This section is reserved for future use.

7.8.3.3 Impact tests on sandwich panels

This section is reserved for future use.

7.8.3.4 Tests for large through-penetration damage to stiffened panels

This section is reserved for future use.

7.8.3.5 Tests for large through-penetration damage to sandwich panels

This section is reserved for future use.

7.8.4 Analysis methods - description and assessment

7.8.4.1 Large through-penetration damage

In many instances, damage tolerance assessments require the consideration of residual strength in the presence of large notches (i.e., greater than 6 inches (150 mm)). Analysis methods that can extrapolate from small notch strengths, determined from relatively small tests, to large notch sizes are highly desirable.

This section focuses on analytical methods for large through-penetration type damage in unstiffened and stiffened panels resulting from severe accidental or "discrete source" damage. For metal skins of commercial transport structures, discrete source damage is usually represented by a cut. The length of cut has traditionally been two bays of skin including one severed stiffener or frame (see Figure 7.8.4.1(a)). Similar configurations are cited in MIL-A-83444 for "fail safe crack arrest structure." For composite laminates, cuts also give a lower bound to tension strengths. See the results in Figure 7.8.4.1(b) for cuts, impact damage, and holes (References 7.8.4.1(a), 7.8.1.2.8(c), and 7.8.2.1).

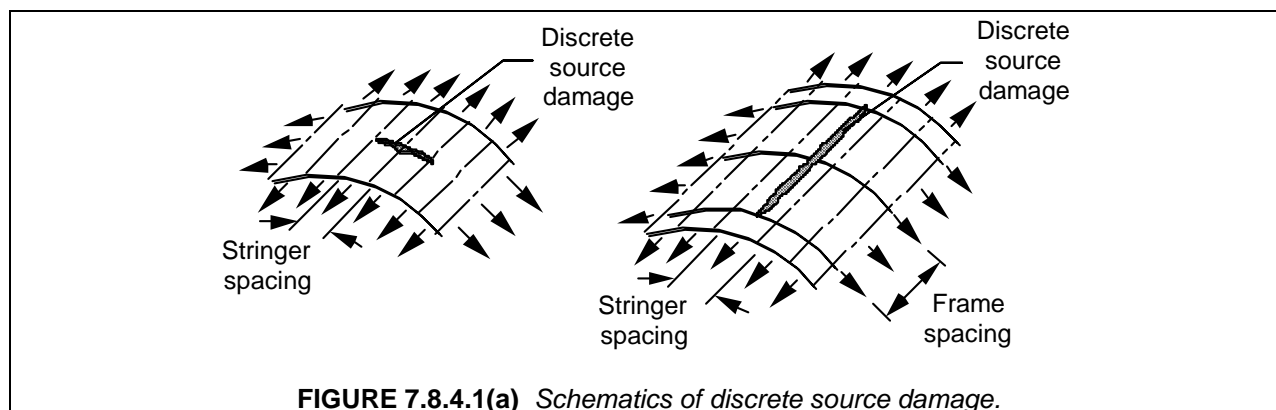


FIGURE 7.8.4.1(a) *Schematics of discrete source damage.*

Numerous models and methods have been developed for fracture of composites with crack-like cuts and tension loads. The following is a list of the methods discussed in the following sections. All of these methods represent a composite structure as an anisotropic continuum amenable to classical lamination theory.

1. Mar-Lin model.
2. Strain softening method.
3. Linear elastic fracture mechanics (LEFM)
4. R-curve method.

The primary purpose of fracture analysis methods is to provide failure predictions beyond the notch sizes and structural geometries tested during material characterization. To ensure this extrapolation capability, suitable models must revolve around theories with a basis in the physics of the problem. It is also desirable to minimize the number of degrees-of-freedom in a model to reduce material testing require-

ments. The following is a discussion of various analysis methods, and a brief evaluation of how well they predict the test data.

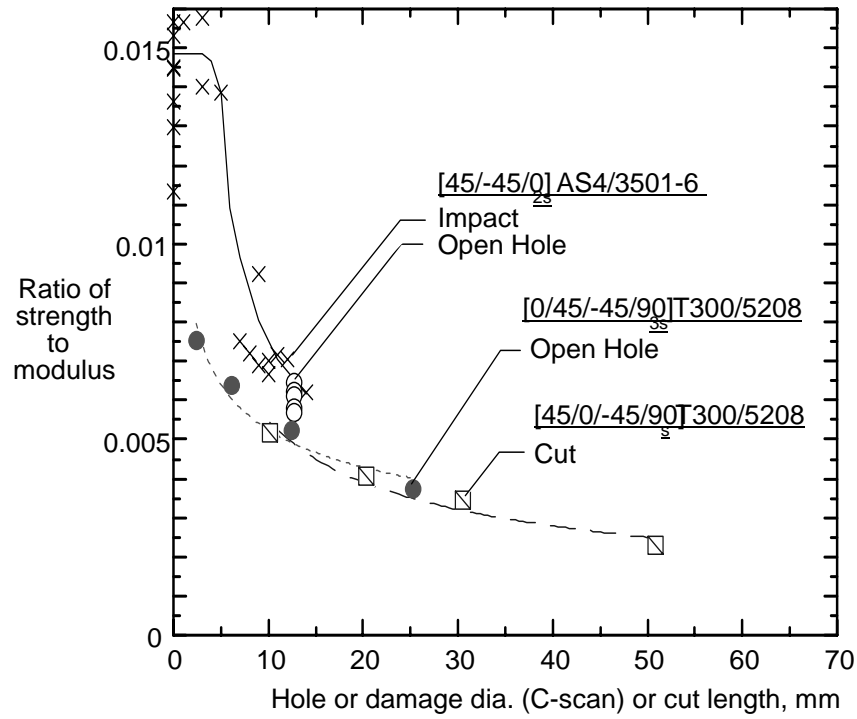


FIGURE 7.8.4.1(b) Tension strengths of laminates (prepreg tape) with impact damage, open holes, and cuts. (References 7.8.4.1(a), 7.8.1.2.8(c), and 7.8.2.1).

Summary of Tensile Failure Criteria. Several failure criteria have been proposed for tensile fracture. In the following discussion of the criteria, σ_n^∞ and σ_0 are the notched and unnotched strengths of an infinite plate, respectively, and a is the half-crack length (Reference 7.8.1.2.8(e)).

The stress distribution at a crack tip is singular for classical continuum theories. In linear elastic fracture mechanics (LEFM) for homogeneous materials, a square-root singularity exists, and failure is predicted by

$$\sigma_n^\infty = \frac{K_{IC}}{\sqrt{\pi a}} \quad 7.8.4.1(a)$$

where K_{IC} is the critical stress intensity factor. This approach suffers from the physically unacceptable situation of infinite stresses at the crack tip. As a consequence, σ_n^∞ increases rapidly with decreasing a and σ_0 becomes infinite, in the limit, as a approaches 0.

In composites, this has been addressed by several theories through the use of a characteristic dimension, inherent flaw size or critical damage zone length. The Whitney-Nuismer (WN) point-stress criteria (References 7.8.4.1(b) and (c)), for example, predicts failure when the stress at a characteristic dimension, d_1 , ahead of the crack tip equals or exceeds σ_0 . The notched strength, then, is given by

$$\sigma_n^\infty = \sigma_0 \sqrt{1 - \left(\frac{a}{a + d_1} \right)^2} \quad 7.8.4.1(b)$$

The two parameters in this model that must be determined are σ_0 and d_1 .

The Pipes-Wetherhold-Gillespie (PWG) model (References 7.8.4.1(d) and (e)) extends the WN point-stress model to include an exponential variation of d_1 with crack length. This provides added flexibility in predicting small crack data, but requires an additional parameter to be determined.

Another multi-parameter model, proposed by Tan (Reference 7.8.4.1(f)), uses a characteristic dimension to predict failure of a plate with an elliptical opening subjected to uniaxial loading. In this model, a high-aspect-ratio ellipse is used to simulate a crack. Notched strengths are predicted by factoring the actual unnotched laminate strength by the ratio of predicted notched to predicted unnotched strengths. Both of these predicted strengths are obtained using a quadratic failure criterion in conjunction with the first-ply-failure technique. The predicted notch strength is determined by applying the failure criterion at a characteristic dimension away from the crack. The coefficients in this criterion are the additional parameters that must be determined.

The Poe-Sova (PS) model (References 7.8.4.1(g) and (h)) may also be formulated with a characteristic dimension, d_2 , but predicts failure when the strain at that distance ahead of the crack tip equals or exceeds the fiber failure strain. The notched failure stress is given by

$$\sigma_n^\infty = \frac{\sigma_0}{\sqrt{1 + \frac{a\xi^2}{2d_2}}} \quad 7.8.4.1(c)$$

where ξ is a functional that depends on elastic constants and the orientation of the principal load carrying plies. The characteristic dimension relates to a material toughness parameter, which was found to be relatively independent of lay-up. The two parameters that must be determined for this model are the fiber failure strain and d_2 .

Two other frequently-used models, Waddoups-Eisenmann-Kaminski (WEK) and WN average stress, each have undamaged strength as the first parameter. The second parameters for WEK and WN average stress models are referred to as critical damage size and average stress characteristic dimension, respectively. The WEK model (Reference 7.8.4.1(i)) applies LEFM to an effective crack that extends beyond the actual crack by the inherent flaw size. The WN average stress model (References 7.8.4.1(b) and (c)) assumes failure when the average stress across the characteristic dimension equals or exceeds σ_0 . Both the WEK and WN average stress models were found to be functionally equivalent to the PS model if a linear strain-to-failure is assumed.

The approaches described above which use a length parameter (e.g., characteristic dimension) were formulated to account for observed experimental trends for composites. In practice, these length parameters are determined from notched strength data and given limited physical meaning in relationship to any micro-structural dimension of the material. They are often thought of as classical analysis correction factors, which enable the user to account for apparent changes in the stress distribution or fracture toughness with increasing crack size. It should be noted that the length parameter calculated for the WN point stress, WN average stress, PS, WEK, and Tan models will generally take on different values for the same set of data.

A more physically acceptable approach to predicting composite fracture may involve changes in the crack tip stress distribution as a function of material length parameters that define levels of inhomogeneity. Simplified analysis performed to evaluate the effect of inhomogeneities at the fiber/matrix scale indicated that the crack size should be at least three orders of magnitude larger than the fiber diameter to

vindicate the classical continuum homogeneity assumption (Reference 7.8.4.1(j)). The results of Reference 7.8.4.1(j) show that inhomogeneity tends to reduce stress intensity factors for a range of crack lengths that is related to the level of inhomogeneity. Considering the fiber/matrix dimensional scale, the crack length range affected by inhomogeneity is smaller than that for which characteristic lengths are needed to correct classical fracture analyses for graphite/epoxy composites. However, higher levels of inhomogeneity exist in tape and tow-placed laminates due to manufacturing processes. These characteristics of composite materials may be responsible for the reduced stress concentrations traditionally found for small cracks.

Solutions to fracture problems using generalized continuum theories have also yielded results consistent with experimental trends in composites, without a semi-empirical formulation. Generalized continuum theories are formulated to have additional degrees of freedom which characterize micro-structural influence. The stress concentrations for such theories change as a function of relationships between notch geometry and material characteristic lengths (e.g., References 7.8.4.1(k) through 7.8.4.1(m)). Note that the characteristic lengths of generalized continuum models are different than those in models described earlier because they are fundamentally based on moduli from the theory. As a result, the moduli have relationships with other material behavior (e.g., wave propagation) and their values can be confirmed from a number of independent experimental measurements. Ultrasonic wave dispersion measurements have been used to predict the moduli and notched stress concentration for wood composite materials (Reference 7.8.4.1(l)). Unfortunately, considerably more work is needed to develop generalized continuum theories for applications with laminated composite plates.

For inhomogeneous materials, the stress distribution at the crack tip is also not limited to a square-root singularity. The Mar-Lin (ML) model (References 7.8.4.1(e) and 7.8.4.1(n)) allows the singularity, n , to be other than square-root. The notched failure stress is given by

$$\sigma_n^\infty = \frac{H_c}{(2a)^n} \quad 7.8.4.1(d)$$

where H_c is the composite fracture toughness. In general, H_c and the exponent n are the two parameters that must be determined. In the Reference 7.8.4.1(e) and 7.8.4.1(n) studies, the exponent, n , was related to the theoretical singularity of a crack in the matrix, with the tip at the fiber/matrix interface. For this case, the singularity is a function of the ratio of fiber and matrix shear moduli and Poisson's ratios. Using this method, the singularities for a range of typical fiber/matrix combinations were determined to be between 0.25 and 0.35.

The Tsai-Arocho (TA) model (Reference 7.8.4.1(o)) combines the non-square-root singularity of the ML model with the inherent flaw concept of the WEK method. At the expense of another parameter, additional flexibility in predicting small-crack strengths is gained, although this effect lessens as the order of the singularity is reduced.

Other theoretical approaches which have been applied to predict tension fracture in composites include damage zone models, DZM (e.g., References 7.8.4.1(p) and (q)), and progressive damage analysis, PDA (e.g., References 7.8.4.1(r) and (s)). Both methods use finite elements to account for notch tip stress redistribution as damage progresses. The DZM utilized a Dugdale/Barenblatt type analysis for cohesive stresses acting on the surface of an effective crack extension over the damage zone length. As was the case for characteristic-length-based failure criteria described above, a Barenblatt analysis (Reference 7.8.4.1(t)) resolves the stress singularity associated with cracks. The PDA methods account for the reduced stress concentration associated with mechanisms of damage growth at a notch tip by reducing local laminate stiffness. From a practical viewpoint, both DZM and PDA methods may be more suitable in determining finite width effects and for predicting the performance of final design concepts.

Failure Criteria Functionality. This subsection reviews the degrees of freedom in curves from two parameter models which have been used extensively to predict tensile fracture for composite laminates (Reference 7.8.1.3(c)). This background will help to interpret discussions that compare theory with ex-

perimental databases. Predictions for both small crack ($2a \sim 1.2$ in. (30.5 mm)) and large crack ($2a$ up to 20 in. (510 mm)) sizes will be compared. The former crack sizes are characteristic of much of the data collected for composites to date. Four theories are covered in detail; classical LEFM, WN (point stress), PS (point strain), and Mar-Lin. As a baseline for comparing changes in crack length predicted by the four theories, curves will be generated based on average experimental results (finite width corrected) for the IM6/937A tape material with $W/2a = 4$ and a lay-up of $[+45/90/-45/0/+30/-30/0/-45/90/+45]$. This will ensure that all theories agree for at least one crack length.

Figure 7.8.4.1(c) shows a comparison of the four theories for small crack sizes. Only a small difference is seen between PS and WN criteria. A close examination of the LEFM and ML curves indicates that the singularity has a significant effect on curve shape. For crack lengths less than the baseline point, ML predictions are less than those of LEFM. For crack lengths greater than the baseline point, the opposite is true, and theories tend to segregate based on singularity (i.e., WN, PS, and LEFM yield nearly the same predictions).

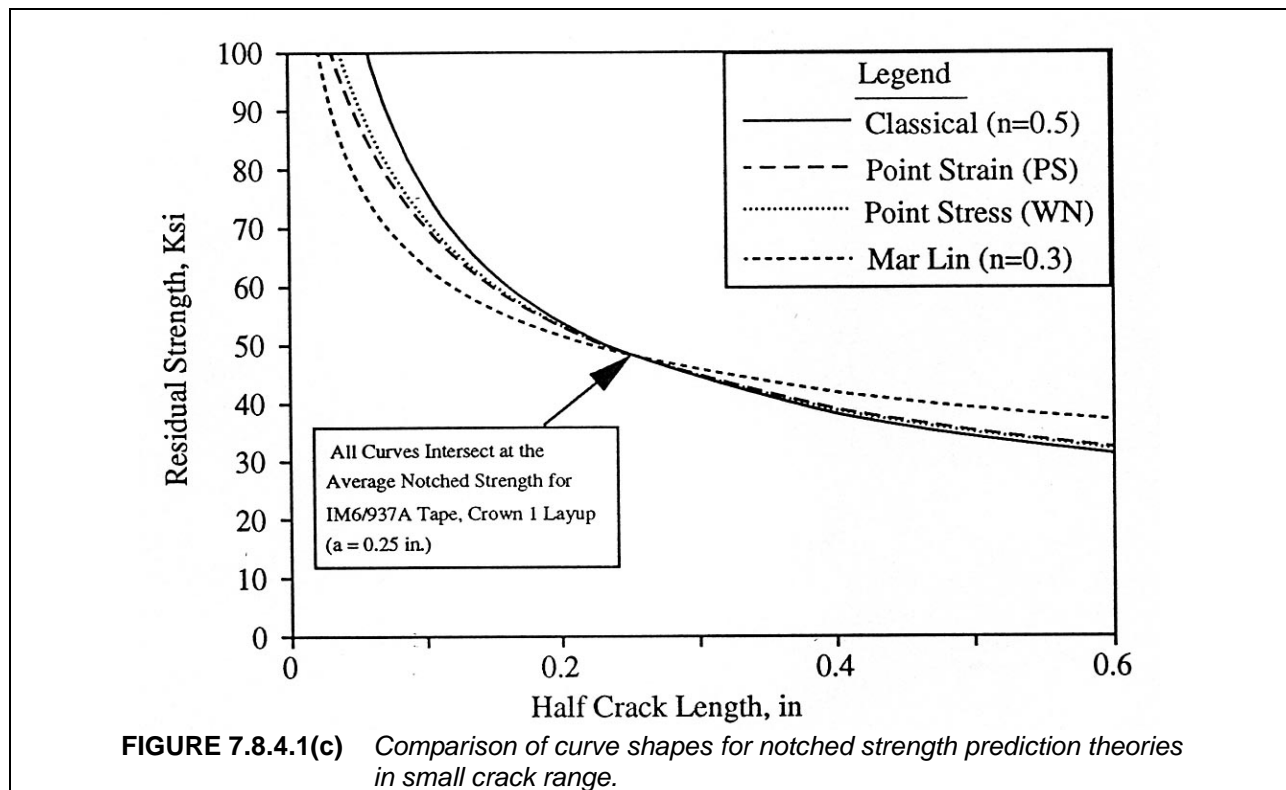
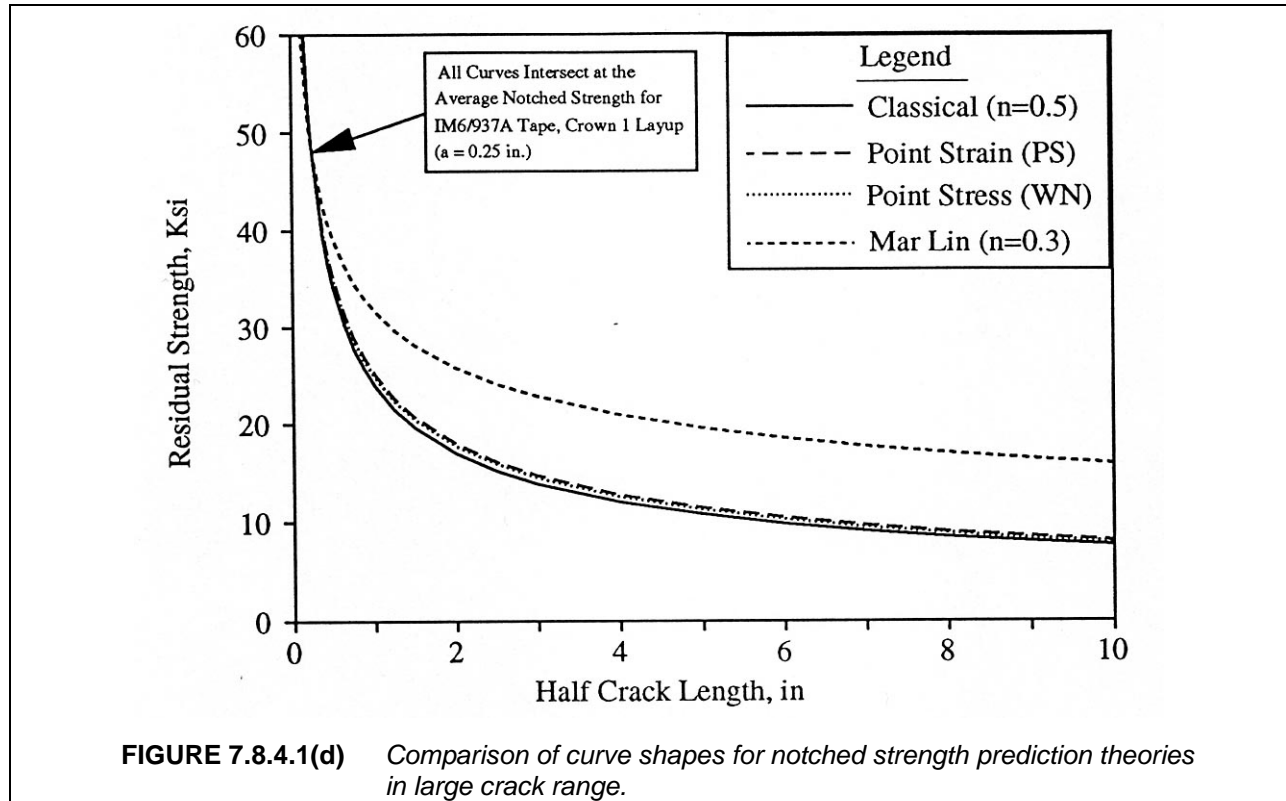


Figure 7.8.4.1(d) shows that singularity dramatically affects differences between predictions in the large crack length range. The ratio of notched strength predictions for theories with the same order of singularity becomes a constant. For example, WN and LEFM become functionally equivalent and the relationship

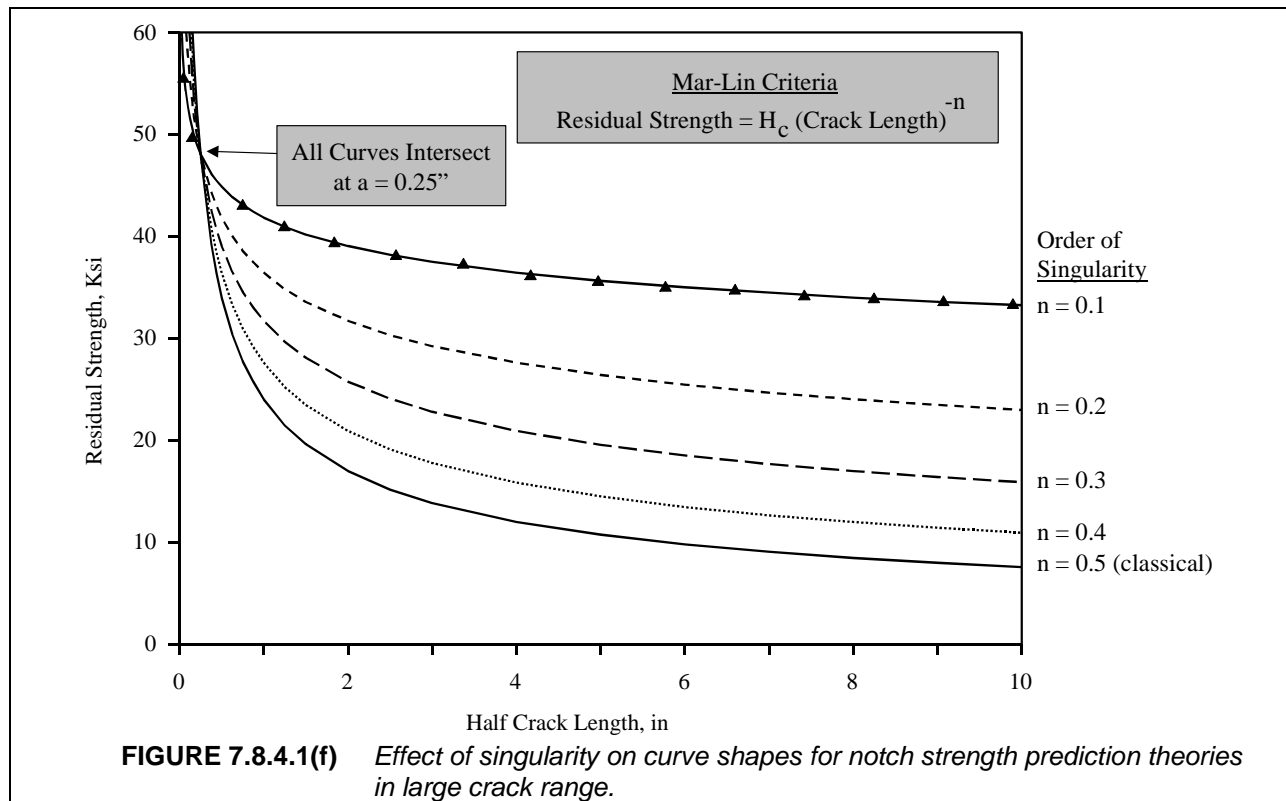
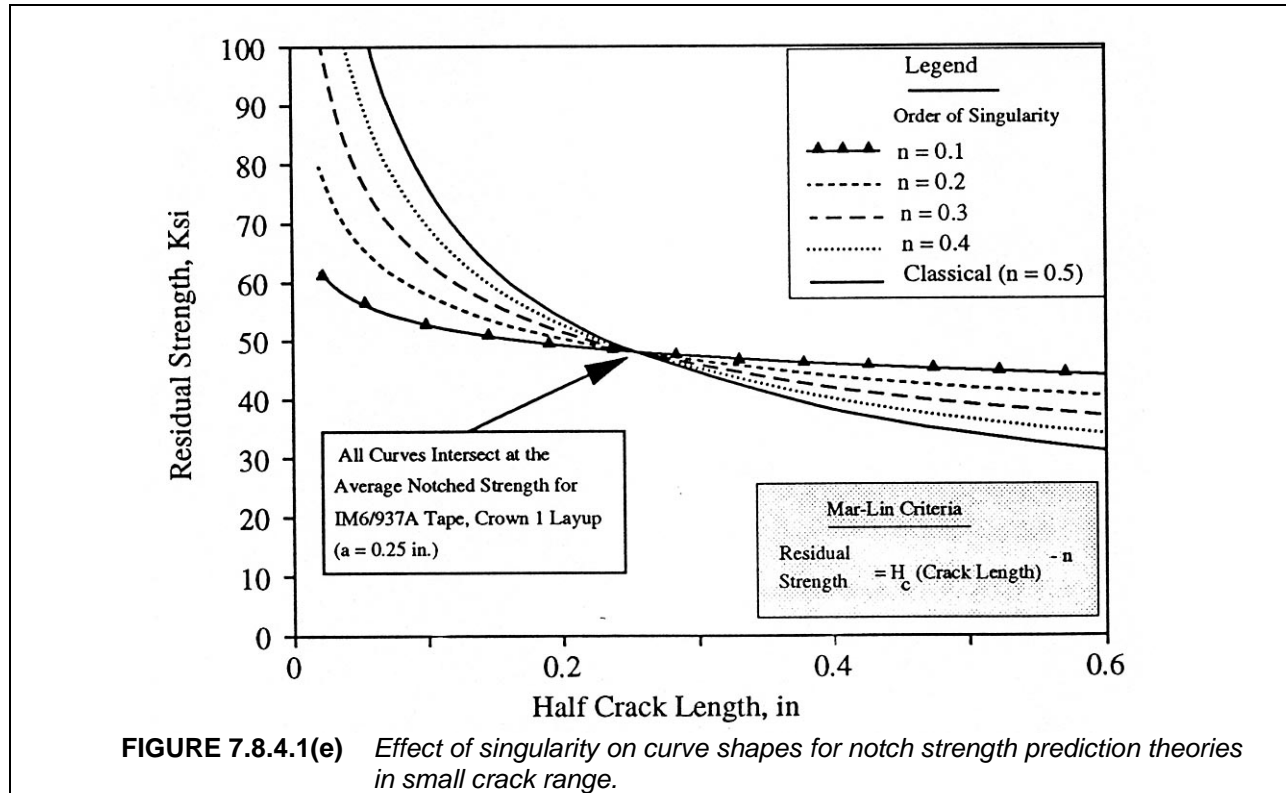
$$K_{IC} = \sigma_0 \sqrt{2\pi d_1} \quad 7.8.4.1(e)$$

will yield a value for K_{IC} such that the two theories compare exactly for large cracks.



In order to compare the effect of a range of singularities on notched strength predictions, curves in Figures 7.8.4.1(e) and (f) vary the value of n from 0.1 to 0.5. All curves in Figure 7.8.4.1(e) cross at the baseline point used to determine the corresponding fracture toughness values. By allowing both variations in fracture toughness and order of singularity, the ML criterion could statistically fit a wide range of notched strength data trends for small crack sizes. Extreme caution should be used in implementing such an approach however, since, as shown in Figure 7.8.4.1(f), projections to large crack sizes are strongly dependent on the assumed singularity.

Figures 7.8.4.1(g) and (h) show how the two parameters in the WN point stress criteria, σ_o and d_1 , affect both the shape and relative positions of notched strength curves. Again comparisons are made with classical LEFM equations passing through common points. The lower set of curves corresponds to the baseline data point. Unlike the LEFM curves which rise sharply with decreasing crack length, the point stress theory has a finite strength, σ_o , at $a = 0$. For a given value of σ_o , increasing d_1 tends to increase the predicted notched strength and, hence, has an effect similar to increasing K_{Ic} in LEFM (see upper curves in Figures 7.8.4.1(g) and (h)).



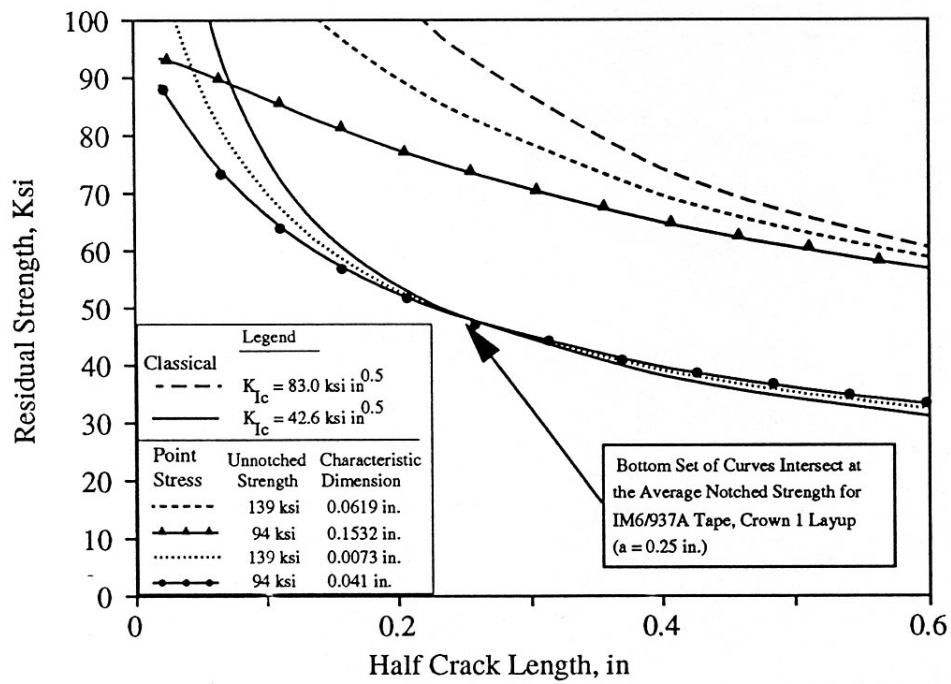


FIGURE 7.8.4.1(g) Effects of characteristic dimension and unnotched strength on curve shapes for notch strength prediction theories in small crack range.

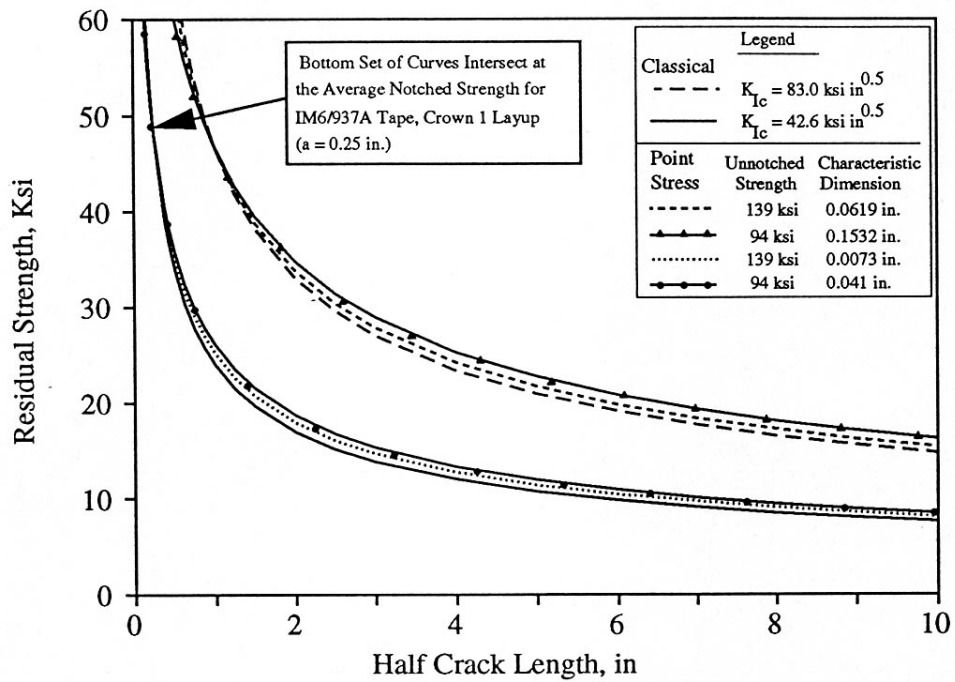


FIGURE 7.8.4.1(h) Effects of characteristic dimension and unnotched strength on curve shapes for notch strength prediction theories in large crack range.

In the small crack length range, a reduced value of σ_o can have the appearance of reducing the singularity. The curve shapes for lower curves in Figure 7.8.4.1(g) indicate that various combinations of σ_o and d_1 could be selected to represent data trends that follow any of the singularities shown in Figure 7.8.4.1(e) (particularly for $a \leq 0.25$). For small crack sizes characteristic of past databases, the curve-fits for WN and ML theories are nearly indistinguishable (Reference 7.8.1.2.8(e)). This inability to distinguish lower orders of singularity in past composite data may relate to measured values of σ_o that were low due to edge delamination phenomena in finite width specimens. For large crack lengths, Figure 7.8.4.1(h) shows that the magnitude of σ_o and d_1 determine residual strength, but curve shape is dominated by the order of singularity. As discussed in reference to Figure 7.8.4.1(f), the proper order of singularity is best judged at large crack lengths.

Modified analysis methods that include "characteristic dimensions" are better at predicting small crack experimental trends than LEFM with the classical singularity of 0.5. This suggests the classical crack stress intensity is inaccurate for composites and that the actual distribution has characteristics that have an effect similar to the point stress and point strain formulations (i.e., stress intensity that is generally lower and a function of notch size). A hypothesis was posed based on evidence from analysis and experiments that suggest small crack stress distribution is strongly influenced by material inhomogeneity. Reductions in stress concentration occur for cracks having a length within several orders of magnitude of the material inhomogeneity scale. For a given crack size, therefore, notched strength increases with increasing scale of inhomogeneity. Possible scales of inhomogeneity include fiber diameter, tow width, and hybrid repeat unit width.

Each fracture theory converges to a curve dominated by the order of singularity at large crack sizes. Larger crack data (i.e., up to 2.5 in. (63 mm) long) for several materials and laminate lay-ups tended to converge with failure criteria having a singularity of 0.3. One notable exception was a toughened material, IM7/8551-7, that tended to converge to the classical curve for singularity of 0.5. This and other evidence suggested that the effective singularity was dependent on matrix splitting. The ability to split and relieve the notch stress concentration relates to characteristics of the material and laminate lay-up.

The finite element method provides the flexibility and accuracy for the multitude of configurations encountered in aircraft structure. Two methods exist to account for the effects of damage progression on load redistribution in finite element models. Progressive damage methods that degrade various stiffness properties of individual elements as specified failure criteria are met (e.g., Reference 7.8.4.1(s)) have shown some successes in modeling damage growth in specimen configurations. The magnitude of the calculations, however, provides a significant obstacle to incorporating them into the complex models required for stiffened structure.

Strain-softening models (e.g., References 7.8.4.1(d) and 7.8.4.1(u)), however, appear to have the required simplicity. Such models have been successfully used in the reinforced concrete industry, and provide the ability to capture the global load redistribution that occurs as the crack-tip region is softened by damage formation, without the computational concerns of detailed progressive damage models. These strain-softening models use a nonlinear stress-strain law that allows for a decreasing load-carrying capability of the material as strains increase beyond a critical value. A range of softening laws has been proposed. In finite element models, nonlinear springs can be used to simulate this behavior. The models can be calibrated using small-notch test results, then extended to large-notch configurations. Issues associated with modeling and calibrating bending stiffness reductions are being evaluated. These reductions are of concern for most structural configurations, where out-of-plane loading, load eccentricities, and bending loads are common. A more detailed discussion of strain-softening methods is given in Section 7.8.4.1.2

7.8.4.1.1 Reduced singularity (Mar-Lin) model

References 7.8.1.3(c) and (d) demonstrated that many material/laminate combinations have significantly lower sensitivities to large changes in notch size than predicted by classical fracture mechanics. The Mar-Lin model (References 7.8.4.1(e) and 7.8.4.1(n)) allows for non-square-root singularities that

capture these reduced sensitivities by having a variable exponent, n . Specifically, the notched failure stress is given by

$$\sigma_N^\infty = \frac{H_c}{(2a)^n} \quad 7.8.4.1.1(a)$$

where σ_N^∞ is the infinite plate notched strength, and H_c is the composite fracture toughness. In the Reference 7.8.4.1(e) and 7.8.4.1(n) studies, the exponent, n , was related to the theoretical singularity of a crack in the matrix, with the tip at the fiber/matrix interface. For this case, the singularity is a function of the ratio of fiber and matrix shear moduli and Poisson's ratios. Using this method, the singularities for a range of typical fiber/matrix combinations were determined to be between 0.25 and 0.35.

However, this idealization is overly simplistic for a notch through a multi-directional composite laminate. Alternatively, the functional form can be used, but both H_c and the exponent, n , can be considered simply as two degrees-of-freedom in the model. This approach maintains the advantages of the functional form, without requiring the exponent to depend on the simplistic idealization. Figure 7.8.4.1(f) illustrates the effect of the exponent, n , on residual strength, as n varies from 0.5 (classical) to 0.1. Each curve in the figure goes through the same point for a 0.25 in. (6.3 mm) notch. Decreases in the exponent, n , result in large increases in large-notch strength.

This functional form was successfully used (e.g., References 7.8.1.2.4(a) and 7.8.1.3(d)) to predict unconfigured large notch strength (i.e., 8 to 12 in. (200 to 300 mm)) from smaller notch data (i.e., ≤ 2.5 in. (63 mm)). The following procedure was used to determine the values for H_c and n .

1. The infinite-width strength was determined for each test data point using the isotropic finite-width correction factor (FWCF).

$$\sigma_N^\infty = \text{FWCF} * \sigma_N \quad 7.8.4.1.1(b)$$

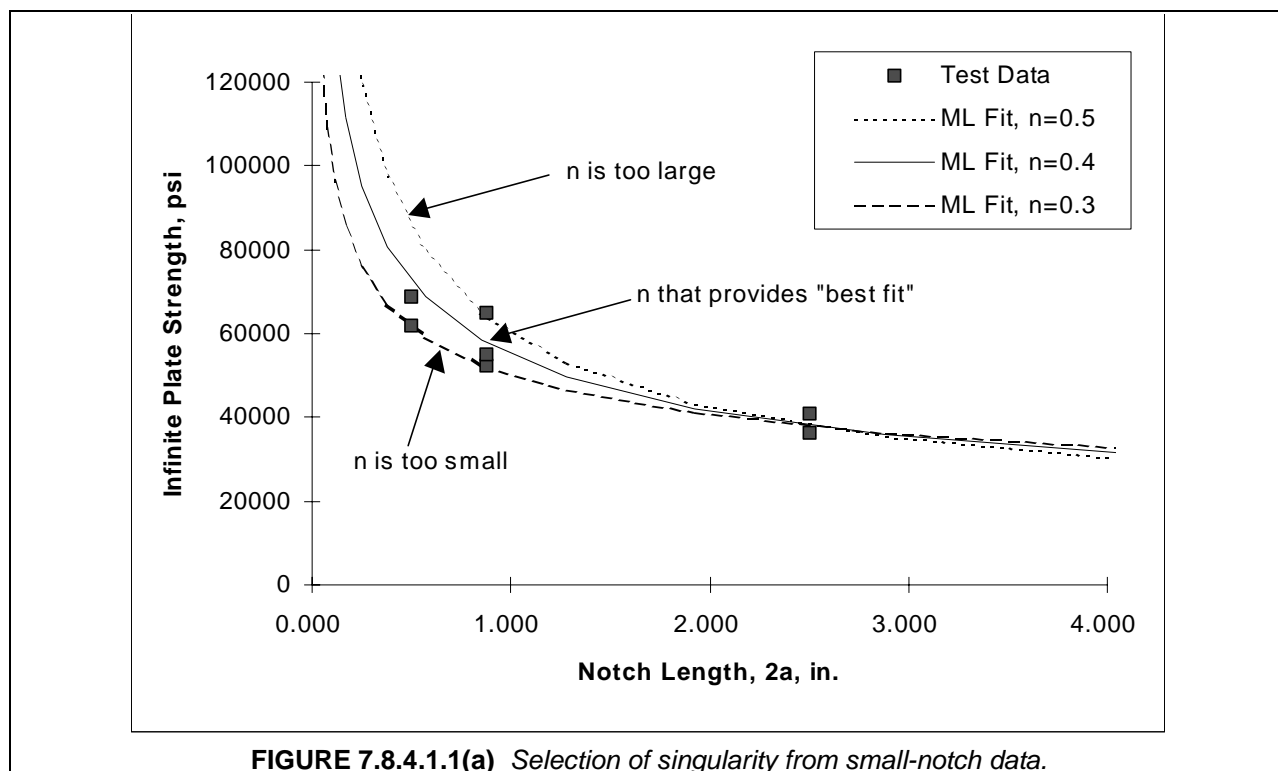
where

$$\text{FWCF} = \sqrt{\sec\left(\frac{\pi a}{W}\right)}, \quad a = \text{half notch length}, \quad W = \text{specimen width}$$

Note that all data was tested using the same width-to-notch-length ($W/2a$) ratio, avoiding problems associated with having data obtained by varying this ratio (see Reference 7.8.1.3(c)).

2. The curve was required to go through the average strength of the largest of the small-notch data (typically 2.5 in. (63 mm)). This requirement determines H_c for any selected value of n .
3. A precise, verified method for determining the appropriate order of singularity, in the absence of large notch data, has not been developed. In the method developed and applied during the Reference 7.8.1.2.4(a) and 7.8.1.3(e) studies, the value of n was generally selected as the smallest value that resulted in (a) the actual small-notch data being less than or equal to the resulting Mar-Lin curve, and (b) an increasingly larger difference between the two as notch size decreases. This approach, which is illustrated in Figure 7.8.4.1.1(a), is justified since the small-notch response is typically characterized by increasing fracture toughness with notch size until the "parent" fracture toughness curve is reached.

Caution should be exercised in selecting exponents for extrapolation, since it is possible to select values that over-predict large-notch capability (i.e., are unconservative). In general, verification tests should be conducted with notch lengths of sufficient size to minimize the extent of extrapolation. In the absence of related large-notch data, a somewhat conservative selection of the exponent is prudent to avoid potential design deficiencies.



This reduced-singularity method described in this section has been successfully used in assessing residual strength of configured structure, as well (References 7.8.1.2.10 and 7.8.1.3(e)). The approach mimicked that often used in metallic analysis, which involves applying empirical or semi-empirical elastic/plastic factors that account for configurational effects to the unconfigured notch strength (e.g., Reference 7.8.4.1.1). Factors developed for metallic configurations were used after modification for directional and part-to-part modulus differences.

Semi-Empirical Mar-Lin Examples

Strength prediction models, including square-root and reduced-singularity approaches, were discussed and compared in Reference 7.8.1.3(c). The four primary models included in the functionality assessment were: linear elastic fracture mechanics (LEFM), Whitney-Nuismer point stress (WN, References 7.8.4.1(b) and (c)), Poe-Sova (PS, References 7.8.4.1(g) and (h)), and Mar-Lin (ML, References 7.8.4.1(e) and 7.8.4.1(n)). When calibrated through a single notch-length/failure-strength point, the WN and PS methods were found to be functionally equivalent. The effect of the characteristic dimensions used in these methods is to reduce the small notch strength predictions from the parent LEFM curve. As crack lengths increase, differences between these characteristic-dimension methods and LEFM converge to a constant value that is small in comparison with the prediction.

The ability of the LEFM, PS, and ML methods to predict residual tensile strength over a wide range of notch sizes were assessed in Reference 7.8.1.3(d). These findings will be summarized here. Additional work on tension and compression of sandwich configurations were reported in References 7.8.1.2.4(a) and 7.8.1.3(e), with similar results.

Three material systems and three lay-ups were included in the evaluation, as described in Figures 7.8.4.1.1(b) and (c), respectively. In each case, the LEFM, PS, and ML methods were calibrated through the average strength with a 2.5 inch (63 mm) notch. The ML exponent, n , was varied to determine the singularity providing the best prediction of the largest-notch strength.

Material	Description
IM7/8551-7	Intermediate modulus carbon fiber in a particulate-toughened resin
AS4/938	Standard modulus carbon fiber in an untoughened resin
S2/AS4/938	Intraply hybrid, with each ply consisting of alternating bands of 1 tow of S-glass fiber and 3 tows of standard modulus carbon fiber, both in an untoughened resin

FIGURE 7.8.4.1.1(b) *Material description for tension tests.*

Laminate	Ply Orientations	Relative Stiffness in Load Direction
Crown3-Axial	[45/-45/90/0/60/-60/90/-60/60/0/90/-45/45]	soft
Crown3-Hoop	[-45/45/0/90/-30/30/0/30/-30/90/0/45/-45]	hard
Crown4-Axial	[45/-45/90/0/60/-60/15/90/-15/-60/60/0/90/-45/45]	hard

FIGURE 7.8.4.1.1(c) *Lay-up definition for tension tests.*

Figure 7.8.4.1.1(d) contains the five material/lay-up combinations that were evaluated, as well as the singularity that best fits the 2.5 in. (63 mm) and large-notch (8-12 in. (200-300 mm)) data for each case. Figures 7.8.4.1.1(e) through 7.8.4.1.1(i) compare LEFM, PS, and ML curves with all test data for each configuration. In all but the first case, the square-root-singularity methods provide conservative estimates of the measured large-notch capability. While this conservatism may appear small in absolute magnitude, it can be large as a percentage of the actual capability. This latter relationship defines the required material, assuming that large-notch strength is controlling the design. Note that the Mar-Lin functionality allows excessive conservatisms to be avoided.

Material	Lay-up	Relative Stiffness	"Best" Singularity
IM7/8551-7	Crown3-Hoop	Hard	0.5
	Crown3-Axial	Soft	0.3
AS4/938	Crown3-Hoop	Hard	0.3
	Crown4-Axial	Soft	0.2
S2/AS4/938	Crown4-Axial	Soft	0.1

FIGURE 7.8.4.1.1(d) *Reduced singularity comparisons of material/lay-up combinations in tension.*

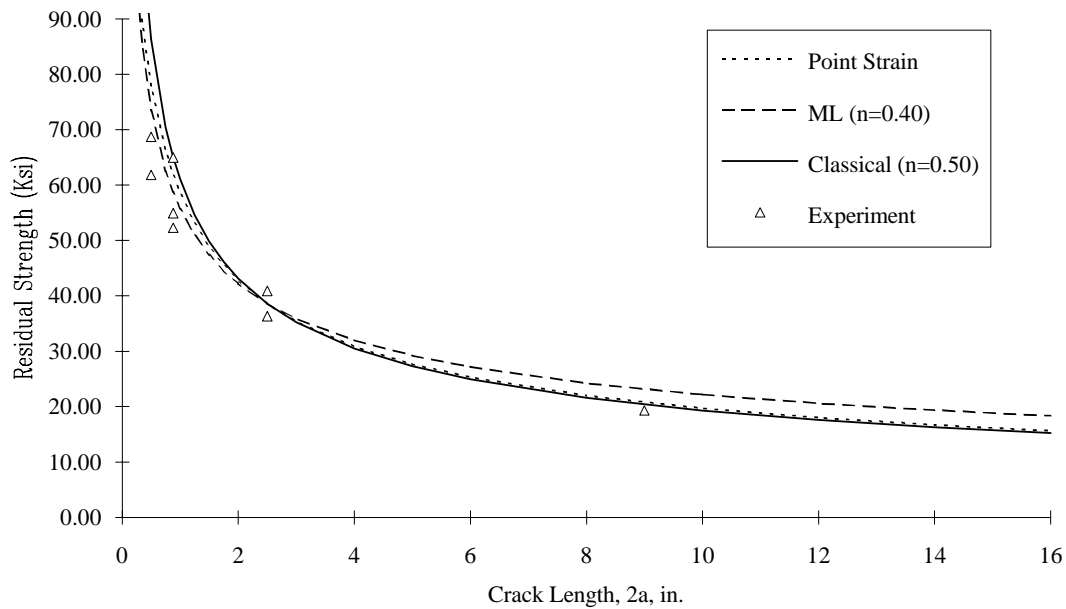


FIGURE 7.8.4.1.1(e) Comparison of IM7/8551-7, Crown3-Hoop experimental tension results with different failure criteria.

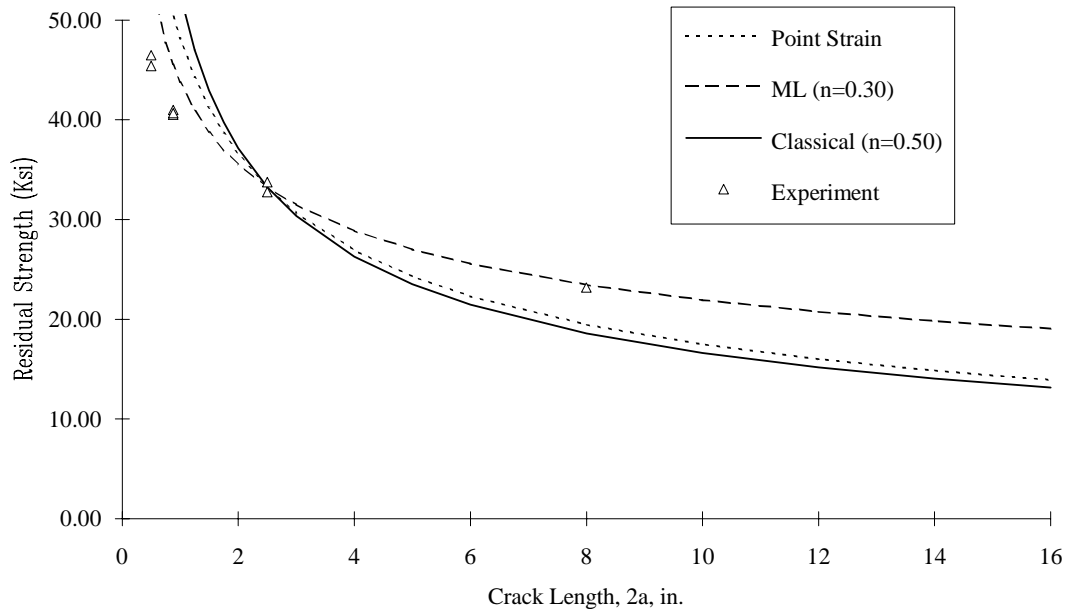


FIGURE 7.8.4.1.1(f) Comparison of IM7/8551-7, Crown3-Axial experimental tension results with different failure criteria.

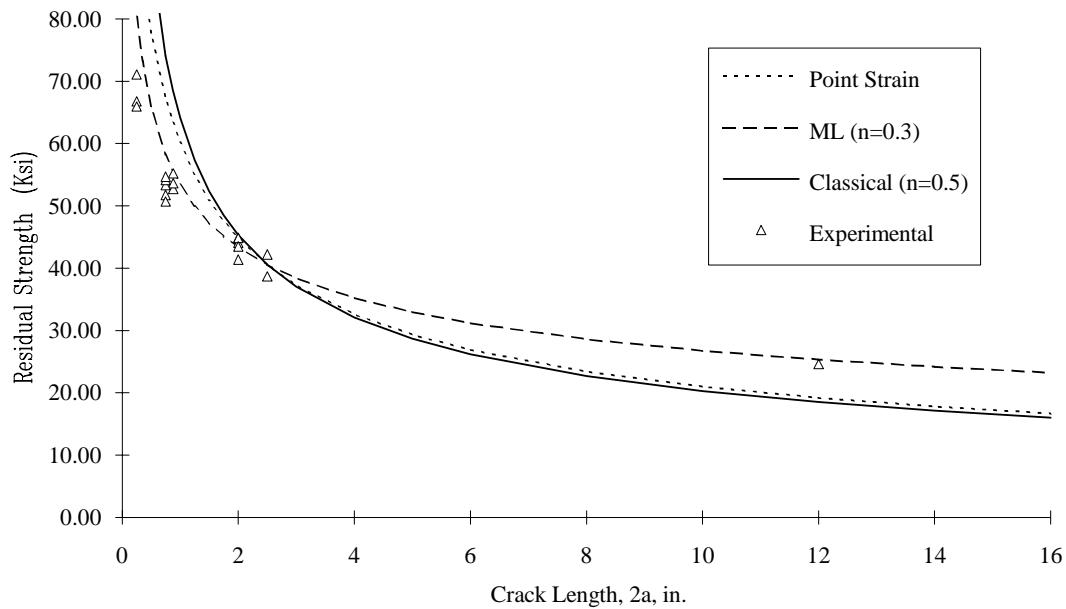


FIGURE 7.8.4.1.1(g) Comparison of AS4/938, Crown3-Hoop experimental tension results with different failure criteria.

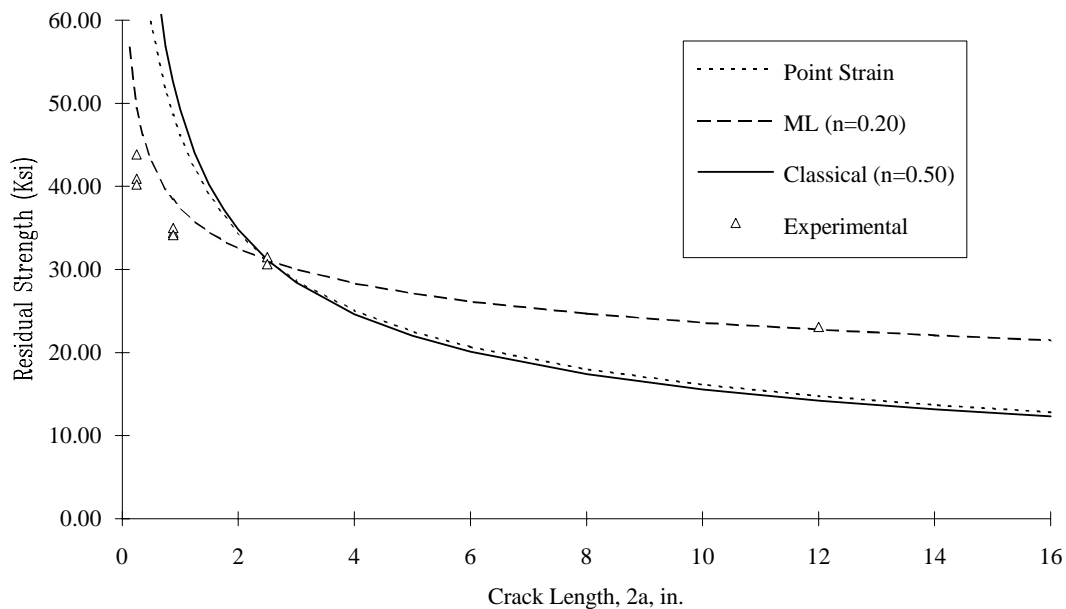


FIGURE 7.8.4.1.1(h) Comparison of AS4/938, Crown4-Axial experimental tension results with different failure criteria.

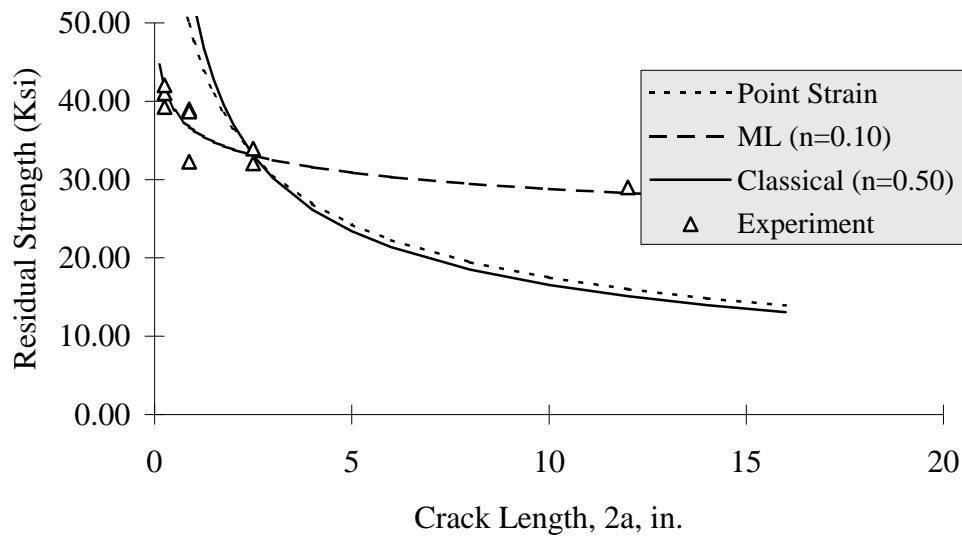


FIGURE 7.8.4.1.1(i) Comparison of 25%-Glass Hybrid, Crown4-Axial experimental tension results with different failure criteria.

This approach was also applied to sandwich configurations with facesheets using higher-toughness resins (AS4/8552). Several small-notch (0.875 and 2.5 in. (22.2 and 63.5 mm)) specimens and a single large-notch (9 in. (230 mm)) panel were tested. As shown in Figure 7.8.4.1.1(j), the Mar-Lin extrapolation of the 0.875 and 2.5 in. (22.2 and 63 mm) notch data was significantly more accurate than the LEFM prediction, but it over-predicted the large-notch strength by approximately 10%. The “best” Mar-Lin curve reflects the fit between the two largest notch sizes. This example illustrates the benefit of conservatively selecting the exponent when related large-notch data does not exist.

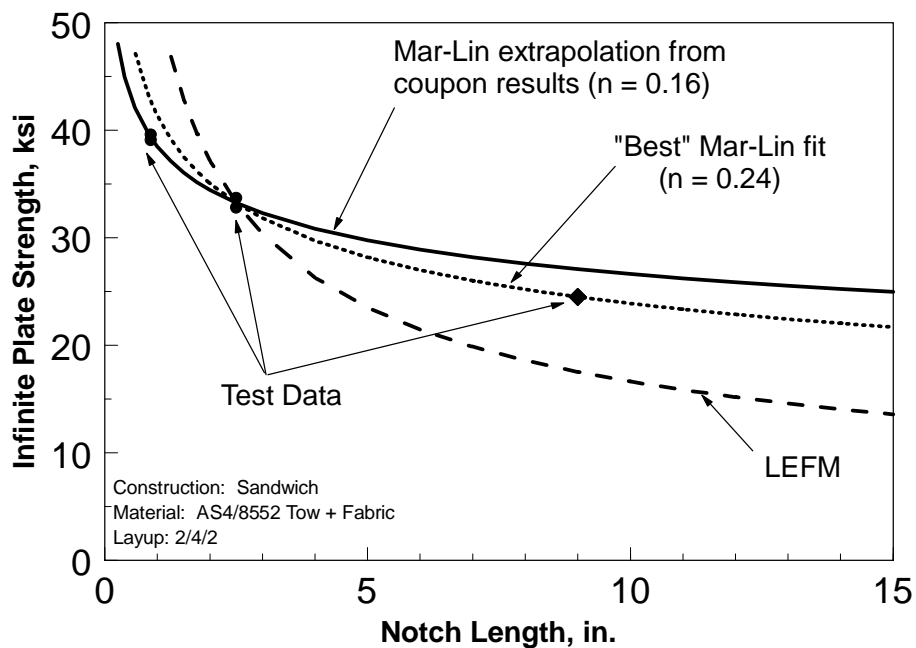
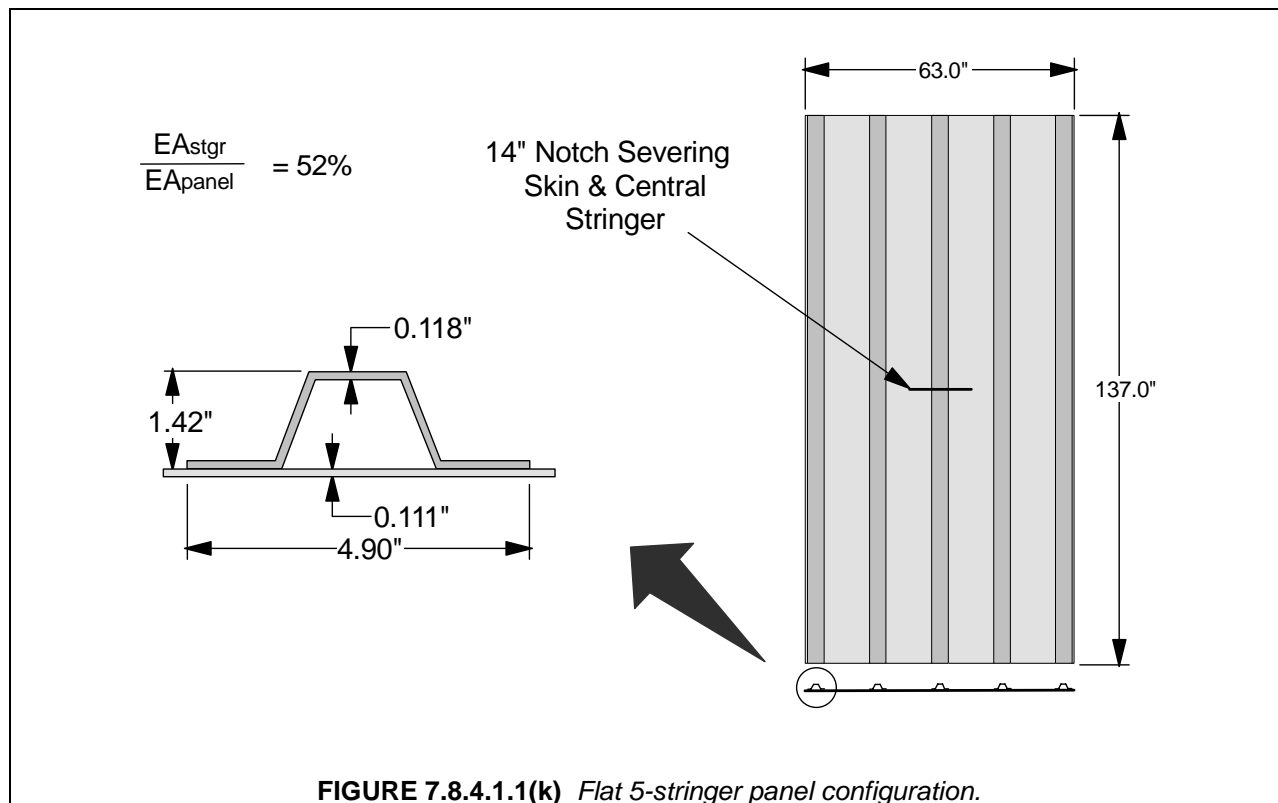


FIGURE 7.8.4.1.1(j) Extrapolation of small-notch results to large-notch sizes for AS4/8552 sandwich.

In Reference 7.8.1.2.10, unconfigured notched-strength predictions based on the reduced-singularity method were extended to structural configurations using configuration factors. The response of a 5-stringer panel, shown in Figure 7.8.4.1.1(k), was predicted and compared to experimental measurements. The panel was tow placed from AS4/938, and contained a 14 in. (360 mm) notch that severed a full skin bay and the central stringer.



In the test panel, damage grew asymmetrically from the notch tips in a stable manner within the skin to the adjacent stringers, where it arrested. The final failure sequence was caused by extension of the fiber failure beyond the adjacent stringer. Reduction of the skin-to-stringer load transfer, caused by delamination growth that accompanied extension of fiber failure beyond the stringer, provided additional driving force during the failure sequence.

X-rays taken at pre-failure load levels allowed construction of a residual strength curve, shown in Figure 7.8.4.1.1(l). The elastic prediction curve significantly overpredicts the effectivity of the adjacent, unsevered stiffening element in reducing the skin notch tip stresses. A prediction based on elastic/plastic analysis and tests of metallic configurations, similar to those shown in Reference 7.8.4.1.1, provided very good correlation with the observed behavior. This may be coincidental, however, since the metallic configuration included inverted, mechanically-fastened hats while the tested configuration had non-inverted, co-cured hats. The important factor, however, is that consideration of inelastic behavior reduces the effectivity of the unsevered stiffening element, decreasing skin-strength predictions.

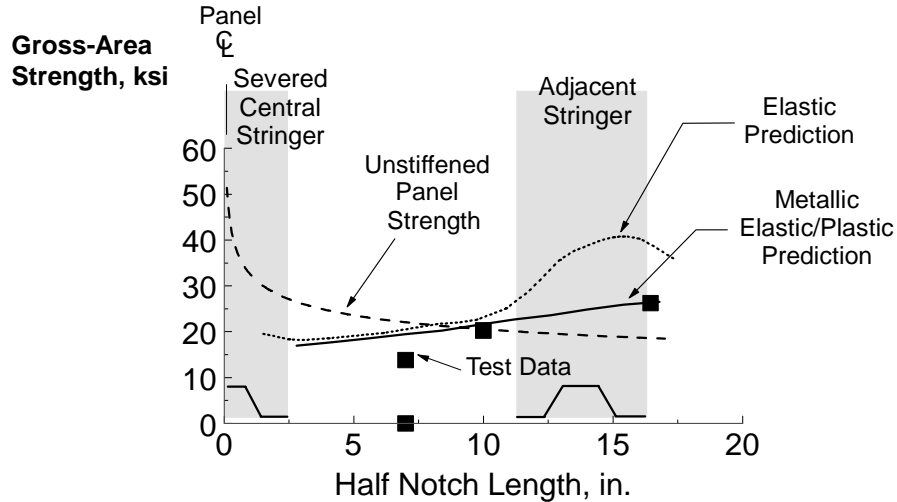


FIGURE 7.8.4.1.1(i) Comparison of crown 5-stringer tension damage tolerance results with predictions.

A similar approach was applied to two curved panels tested under biaxial loading in a pressure-box test fixture. The general arrangement of the panels is shown in Figure 7.8.4.1.1(m). These panels, designated Panel 11b and TCAPS-5, each contained a 22 in. (560 mm) longitudinal notch severing skin and the central frame. Differences in design detail are highlighted in Figures 7.8.4.1.1(n) and (o). Panel 11b included all-graphite skins with a relatively high hoop modulus, and bolted frames with mouseholes that extend beyond the full width of the stringers. TCAPS-5 featured a graphite-glass intraply hybrid skin with a relatively low hoop modulus and higher-stiffness bolted frames. Glass-fabric pads beneath the frame allowed a direct bolted attachment between the frame and the stringer flange and the mousehole configuration to be significantly narrower.

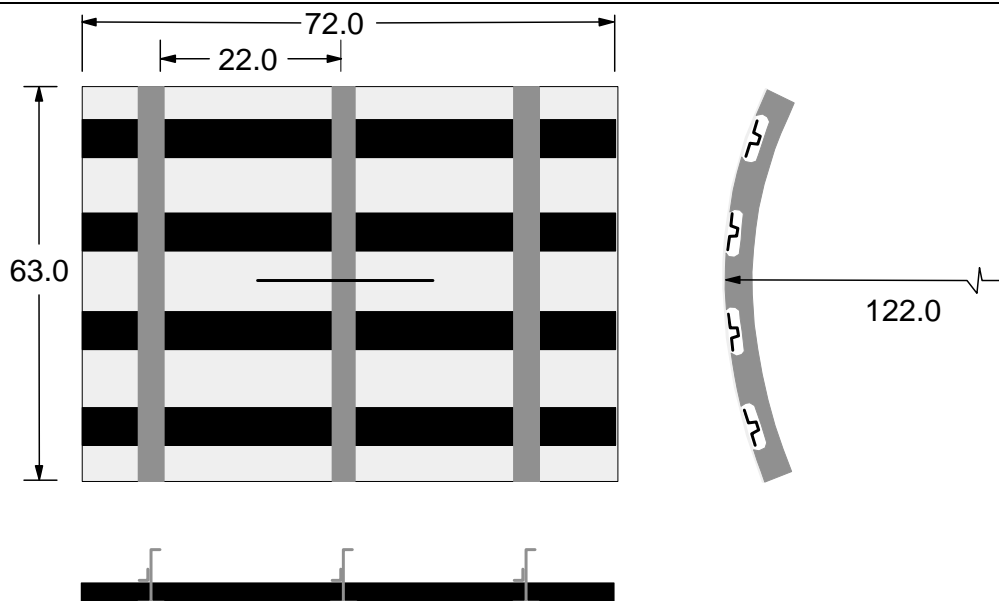
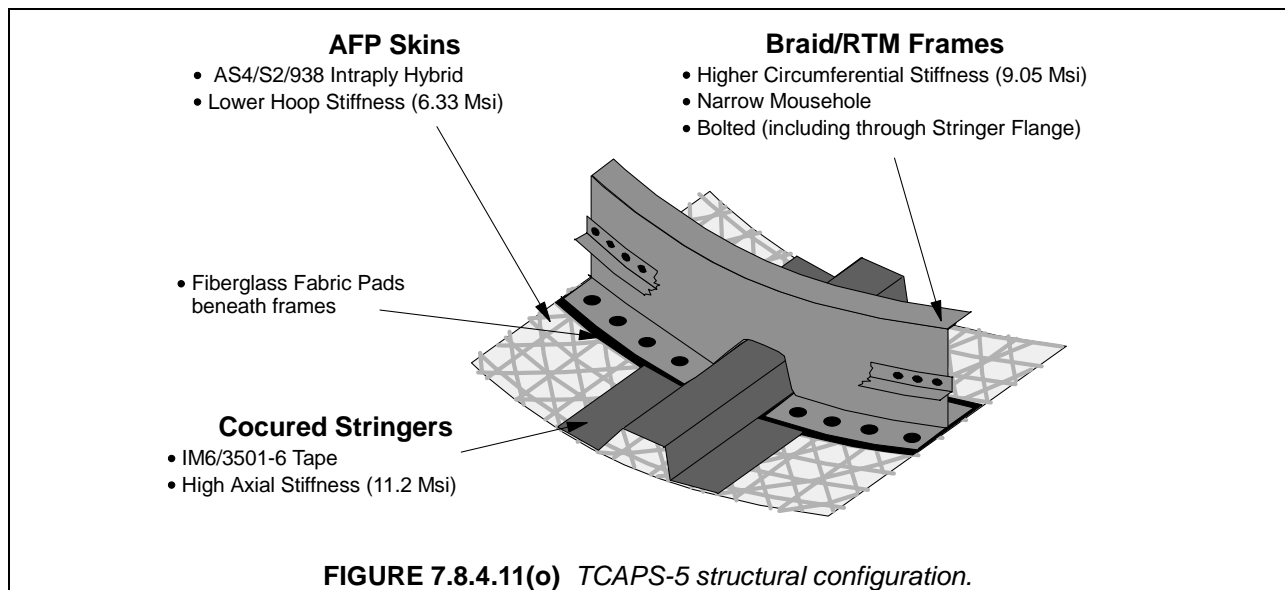
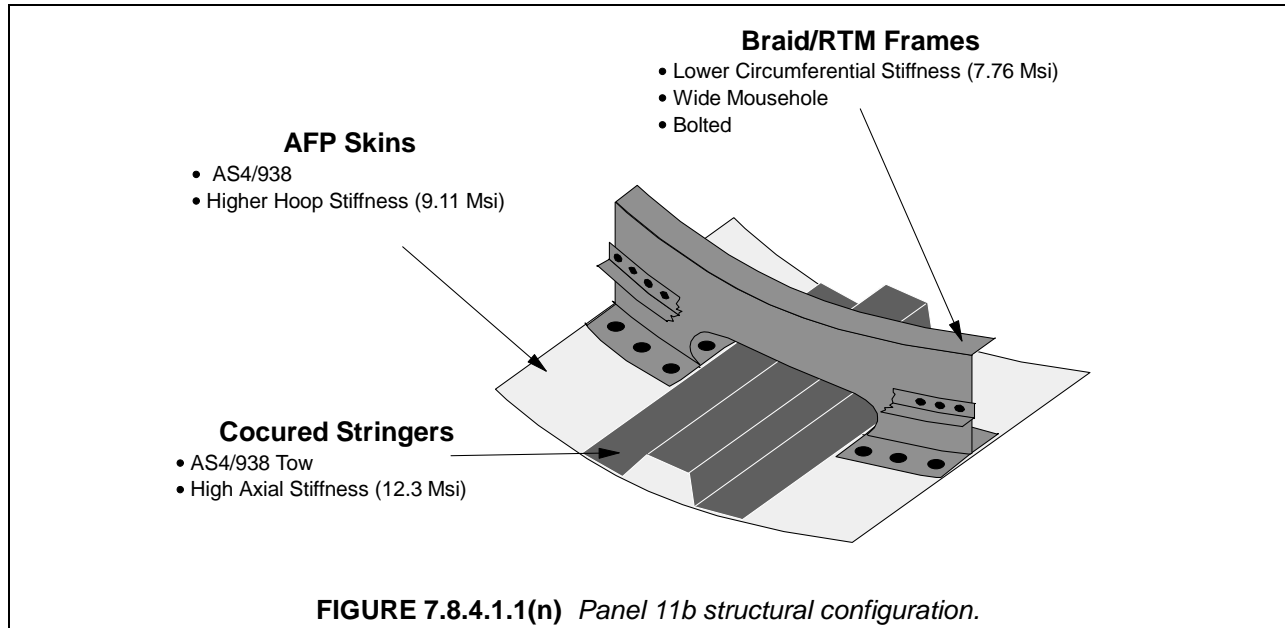
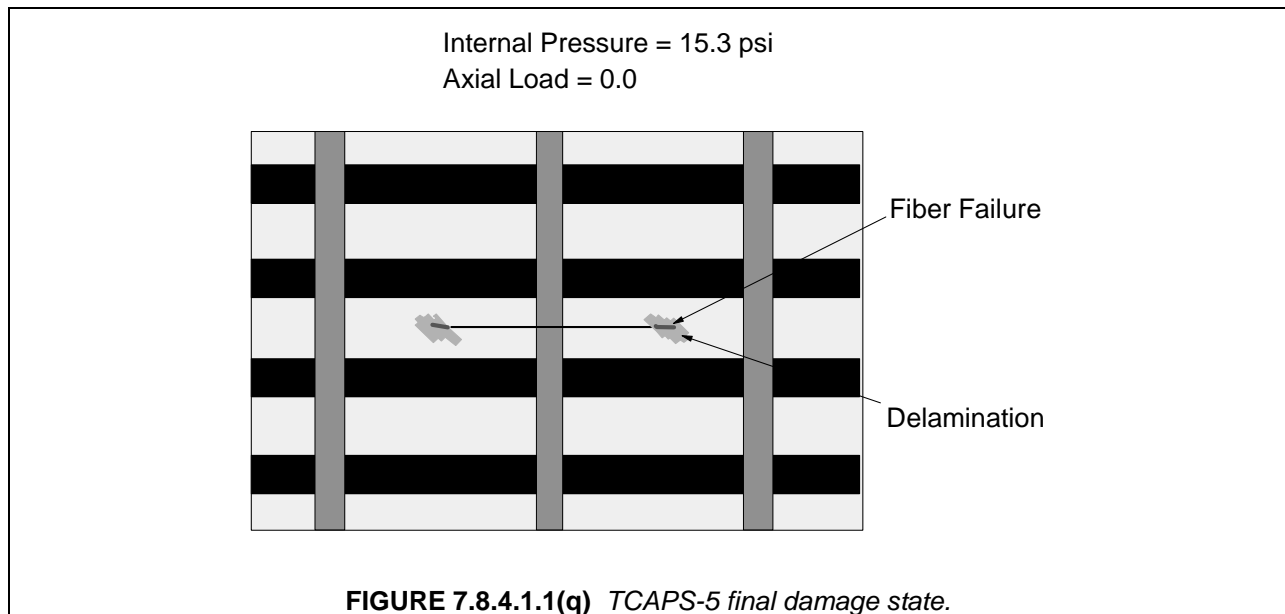
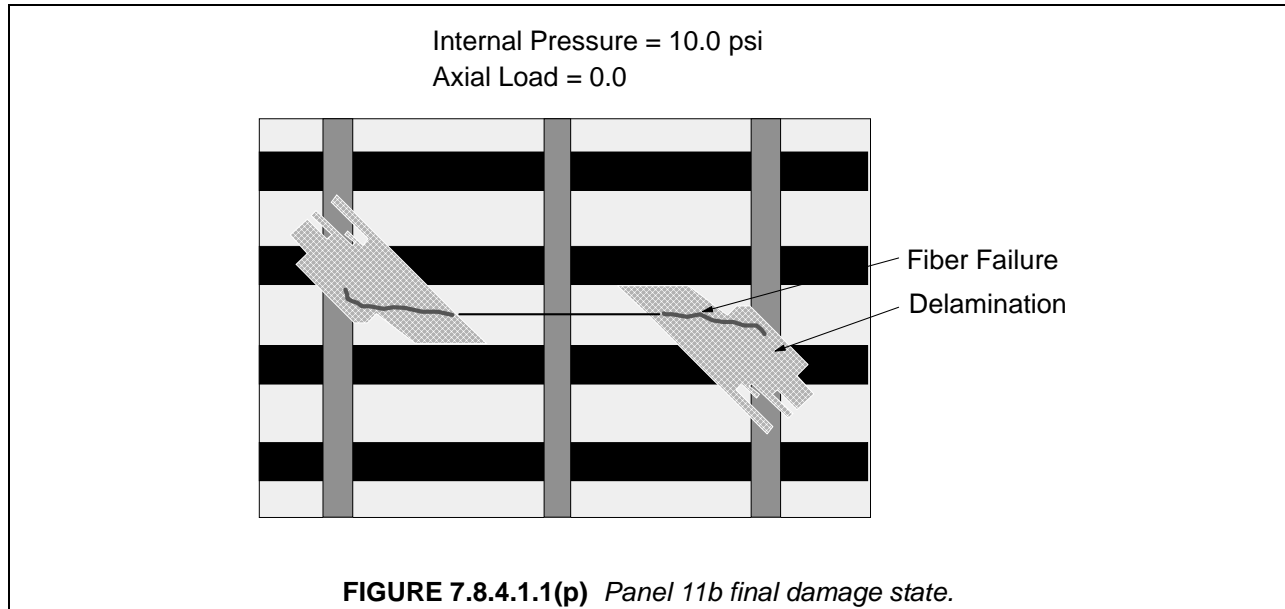


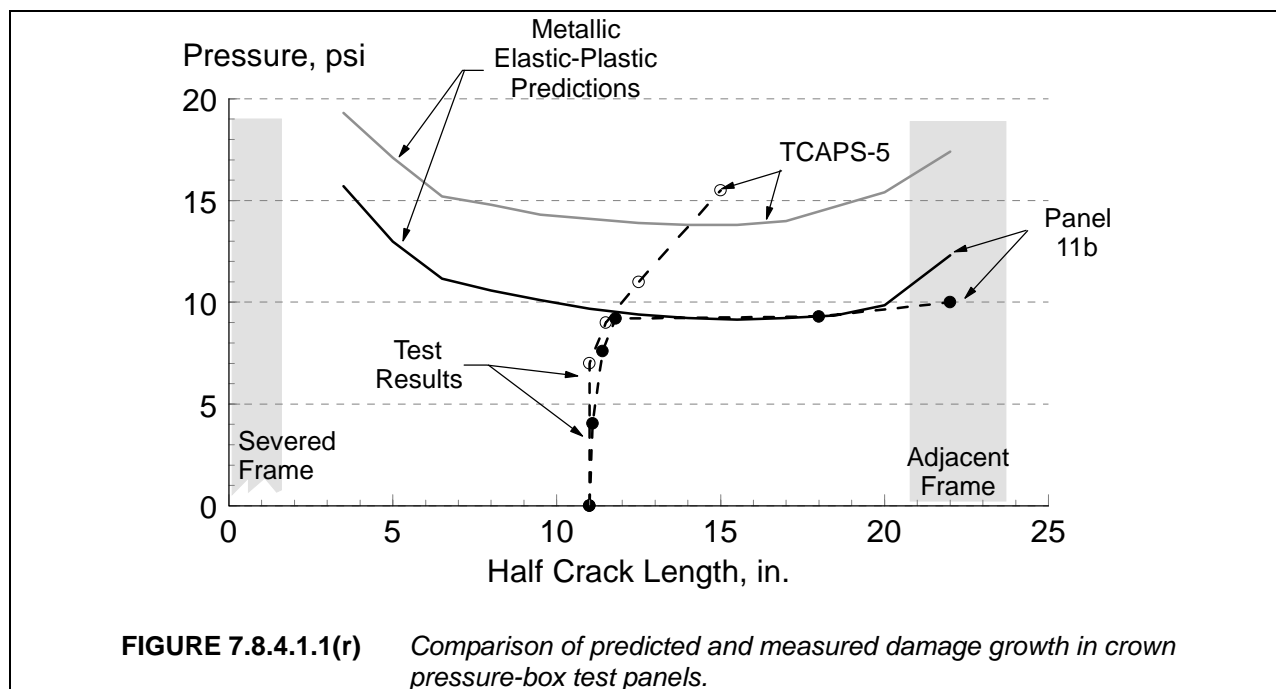
FIGURE 7.8.4.1.1(m) Pressure-box test panel geometry.



Both panels were subjected to internal pressure only. Figures 7.8.4.1.1(p) and (q) illustrated the damage state in each panel after completion of the tests. The maximum pressure for Panel 11b was 10.0 psi, at which time an explosive decompression occurred. The damage was characterized by extensive delamination and an intense region of fiber failure extending approximately 11 in. (280 mm) from the notch tips to the adjacent frames. TCAPS-5 reached a maximum pressure of 15.5 psi, when air supply limitations precluded further loading. Its final damage state was characterized by delaminations and fiber failure regions on the order of only 3-4 in. (80-100 mm), despite sustaining 55% higher pressure.

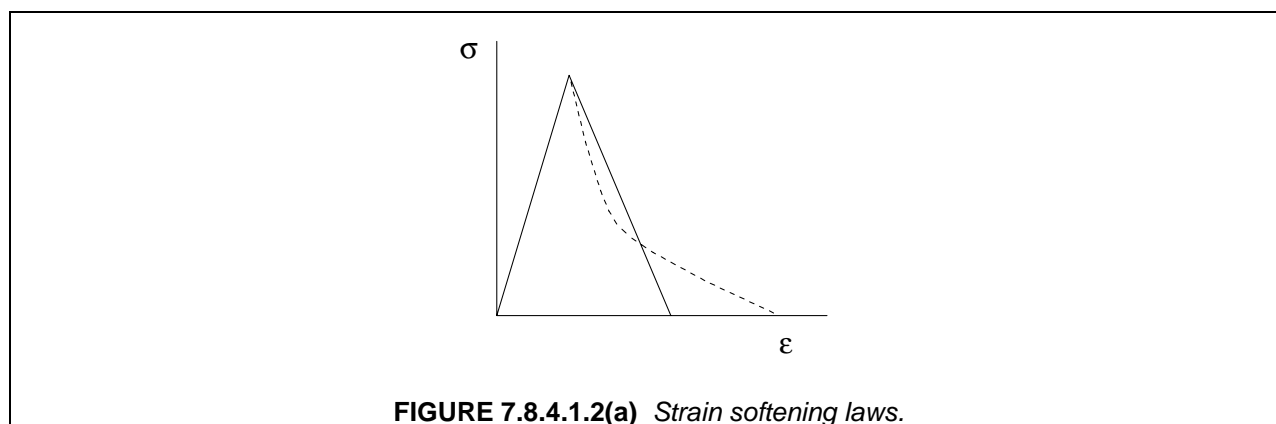


Residual strength response was predicted for these panels using Mar-Lin extrapolations of notched strength data from flat unstiffened laminates in combination with metallic elastic-plastic configurational correction factors that were modified to account for modulus differences. These predictions are compared with the actual damage growth in Figure 7.8.4.1.1(r). The prediction for Panel 11b was quite accurate for damage growth in the skin, but overpredicted the load transfer to, and hence the beneficial effect of, the undamaged adjacent frames. This reduced load transfer observed in the test is again related to skin delaminations effectively decoupling the frame from the skin. Predictions of TCAPS-5 response were not as accurate. The response, however, exceeded its much higher predicted capability.



7.8.4.1.2 Strain softening laws

Experimental evidence has demonstrated that composite materials exhibit significant strain capability beyond that associated with the maximum load-carrying capability (Reference 7.8.1.2.8(i)). This strain-softening characteristic, shown in Figure 7.8.4.1.2(a), is not readily apparent in unnotched or small-specimen testing, where failures can appear brittle due to limited load redistribution after localized failures. In notched specimens or in structures capable of load redistribution, however, the strain-softening response is more easily observed.

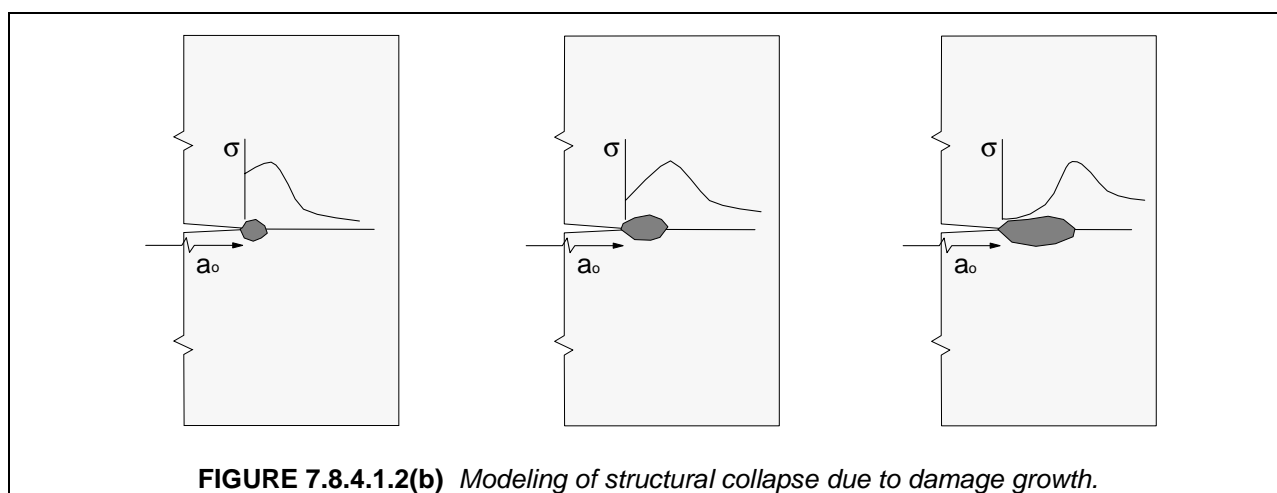


To date, most engineering applications using strain-softening approaches have occurred in analyzing inhomogeneous materials used in the building industry (e.g., concrete). References 7.8.4.1.2(a) and (b) extensively document the use of strain-softening methods for analyzing the fracture and collapse of engineering structures. Strain-softening methods have been applied to some laminated composite problems (e.g., References 7.8.4.1.2(c), 7.8.4.1(d) and 7.8.4.1(p)). The most significant application of these methods to large-notch residual strength of composite structure was performed in a series of NASA/Boeing

contracts reported in References 7.8.4.2.1(d) and (e), 7.8.1.2(g), 7.8.1.2.4(a), 7.8.1.2.8(h) and (i), and 7.8.1.3(e). The following discussion is based on the findings from that work.

The use of strain softening laws to simulate damage progression has several attractive features. First, it is a generalized continuum approach and is, therefore, more compatible with the complex finite element models required to properly approximate structural configurations than are rigorous progressive damage models (i.e., those with ply-by-ply assessment and tracking of multiple failure mechanisms). The approach also captures the load redistribution caused by local damage formation and growth, and the resulting influence on deformations and other potential failure modes.

Strain-softening laws are typically incorporated into geometrically nonlinear finite element analyses as non-linear, non-monotonic material stress-strain curves. The global analysis becomes a structural collapse problem, as shown in Figure 7.8.4.1.2(b); the damage growth forces load redistribution toward the specimen edges until insufficient material exists to sustain the applied load.



Strain-softening laws are strongly dependent on a numerous variables, including material, lay-up, stacking sequence, manufacturing process, environment, and loading. As illustrated in Figure 7.8.4.1.2(c), the shape of the strain-softening curve has a strong influence on the predicted notch-strength response. Material laws with relatively high maximum stresses but low total fracture energy are required to predict high strength, low toughness response. These laws also capture the relatively small notch-tip damage zones and small specimen size effects observed in tests. Conversely, laws with low maximum stresses but high total fracture energies are necessary to capture low strength, high toughness behavior. They also predict the large notch-tip damage zones and the significant specimen size effects observed in tests.

Efficient methods for determining the strain-softening law for a specific combination of these variables are not fully developed for composites. They can be found either by indirectly by matching analysis with small coupon test data (e.g., Reference 7.8.4.1.2(e)) or directly from test measurements (e.g., Reference 7.8.4.1.2(f)). Once determined, these laws are used in finite element models to predict the response of other geometries.

A number of significant difficulties arise in attempting to implement this method, and not all have well-established solutions. The following subsections attempt to summarize the current state-of-the-art for the significant implementation issues.

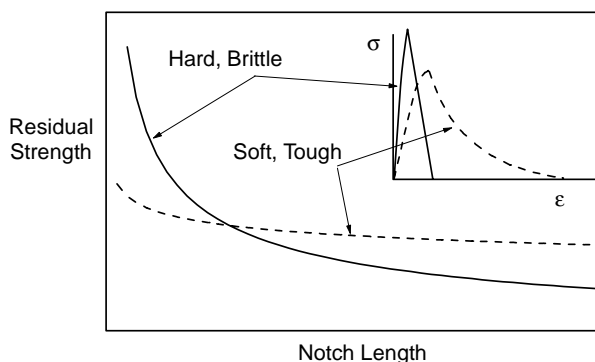


FIGURE 7.8.4.1.2(c) Effect of strain softening material law on notch-length sensitivity.

Complexity of Strain-Softening Modeling. Application of the strain-softening law can be accomplished in a variety of ways. The method chosen for a specific problem depends on the loading and damage growth assumptions. For uniaxial in-plane loading, where the assumption of self-similar crack growth is reasonable, a uniaxial implementation can be used. In this case, uniaxial springs, with nonlinear stiffnesses directly related to the strain-softening material law, can be placed between the surfaces of the crack plane, as shown in Figure 7.8.4.1.2(d).

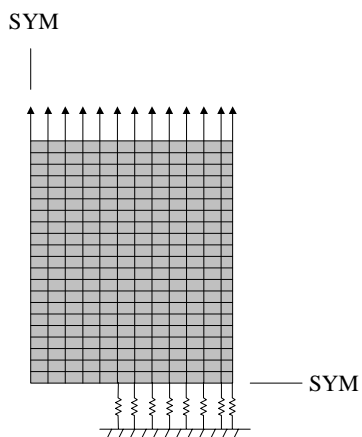


FIGURE 7.8.4.1.2(d) Spring implementation of strain softening.

For multi-directional in-plane loading, a multi-directional strain-softening law must be defined, since the direction of damage propagation cannot be assumed. In References 7.8.4.1.2(d) and (e), 7.8.1.2.4(a), 7.8.1.2.8(g) through 7.8.1.2.8(i), and 7.8.1.3(e), the strain-softening laws were defined for the two orthotropic directions of the laminate, and a Hill yield function used for the interaction.

For situations with significant variations of load, geometry, or damage through the thickness of the part, (e.g., bending moments, post-buckled structure, out-of-plane loading, unsymmetrical damage), the modeling approach must also allow variable softening through the thickness. In Reference 7.8.4.1.2(d), this was accomplished by defining several integration points in the thickness direction of the finite element representing the laminate, and applying the strain-softening relationship independently to each of these points. However, it was also noted that a more general formulation is required if the laminate properties

vary significantly through the thickness, since the stress-strain relationship is generally developed for the whole laminate assuming homogeneous ply stacking sequences.

Numerical Solution Issues. Finite element solutions of problems involving a strain-softening material laws involve a number of complexities not often associated with static structural analysis. Specifically, singular stiffness matrices are encountered when material failure is occurring in a sufficiently large area and/or when the structure is buckling. In the Reference 7.8.4.1.2(d) studies, ABAQUS® was selected because it has a variety of robust, nonlinear solution algorithms and is capable of modeling strain-softening response for orthotropic materials. Arc length methods, such as Riks (Reference 7.8.4.1.2(g)), have proven useful in dealing with snap-through stability problems, and were useful in initial efforts to model tension loaded strain-softening problems. However, numerical stability problems and very long solution times were frequently encountered, particularly when the unloading portion of the strain-softening curve was very abrupt or steep.

Solving the problem dynamically minimizes a number of numerical difficulties. Similar to real structures, damping and inertial forces smooth out system response and greatly reduce numerical noise in the solution process. As the maximum load is reached, local failure occurs thus accelerating parts of the system. The numerical integration in time can be stopped when a minimum acceleration related to system failure has been achieved. This has proven to be very accurate failure criterion for compression-loaded structural systems (Reference 7.8.4.1.2(d)).

Element Size and Formulation. Strain-softening laws and the finite element size are interrelated, due to the effect of element size on notch-tip strain distribution. Larger elements result in less-severe, but broader, stress concentrations. This is similar to the response of non-classical material models (i.e., Cosserat, non-local) in the presence of a stress concentration (e.g., References 7.8.4.1.2(h) and 7.8.4.1(m)), and also similar to deviations observed in actual strain distributions from classical predictions. Larger element sizes result in strain-softening curves with steeper unloading segments (Reference 7.8.4.1.2(d)).

Element size, therefore, is another degree-of-freedom in the strain-softening approach that must be determined. Fortunately, damage in composite materials typically localizes on a relatively large scale (e.g., relative to plastic yielding at a crack tip in metal). Relatively large elements (i.e., ≥ 0.20 inches (5.0 mm)) are, therefore, found to provide good results. Element sizes required to accurately predict notch-length and finite-width effects in compression are typically larger than those required for tension.

Finite element analyses based on non-local formulations (i.e., the stress at a point is dependent on the strain at that point and the strain in the vicinity of that point) can overcome this element-size dependency. The need to combine strain-softening laws with non-local material models has also been seen in work related to civil engineering structures (e.g., References 7.8.4.1.2(a), 7.8.4.1.2(i), and 7.8.4.1(u)). Several methods (other than element size) have been used to account for non-local responses. The most widely used method to incorporate non-local analysis is based on an integral approach, where a weighted average strain is determined as a material property and is referred to as the characteristic size of the material. Another approach is based on a second order differential method, where the strain used for the stress calculation is based on both the value and second derivative of the point strain. In fact, these two methods are related, and, with selected weighting functions, there is a one-to-one correspondence. A third proposed method involves an imbricated element formulation (Reference 7.8.4.1.2(i)). An approximation of this technique (i.e., overlaid and offset 8-noded elements), shown in Figure 7.8.4.1.2(e), was attempted, but was abandoned due to difficulties associated with modeling at specimen and crack boundaries.

Element formulation and strain softening laws are also interrelated. Limited studies of 4-, 8-, and 9-noded shell elements found that higher order elements lead to higher fracture strengths and large damage zones (Reference 7.8.1.2.8(h)).

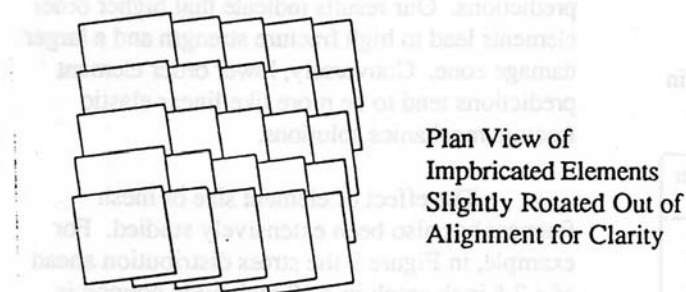


FIGURE 7.8.4.1.2(e) *Staggered layering of 8-node shell elements used to model nonlocal effects of a stress concentration.*

Determination of Strain-Softening Law. Using the indirect method to determine a strain-softening law requires an understanding of the key characteristics of strain-softening curves, and their influence on the structural response. The law is iterated until small-notch data is matched. Test results to support this approach are not well established, but the goal is to have sufficient data to capture notch-size effects and specimen finite-width effects. In the NASA/Boeing research studies, for example, typical test data for determining the tension law consisted of three or four specimen configurations, as shown in Figure 7.8.4.1.2(f). Laws obtained in this manner were typically used to predict the response of configurations with notches in the range of 8 to 20 inches (200 to 500 mm).

Notch Size, in. (mm)	Specimen Width, in. (mm)	Width-to-Notch- Size Ratio
0.88 (22.4)	3.5 (89)	4
1.75 (44.5)	3.5 (89)	2
2.50 (63.5)	10.0 (254)	4
5.00 (127)	10.0 (254)	2

FIGURE 7.8.4.1.2(f) *Typical test for determining strain-softening law in the NASA/Boeing research programs.*

Determination of the strain-softening material laws for both tension and compression through trial and error requires a relatively large number of tests, and is computationally intensive. Approaches have been presented to determine these laws from relatively few tests via energy methods (e.g., Reference 7.8.4.1.2(f)). These require measurement of crack opening displacements (COD) for two specimens of identical geometry and differing notch lengths. Attempts to accomplish this with center-notch specimen configurations were unsuccessful. Two specimens of each of two notch lengths were tested. The resulting strain softening laws for the four specimen combinations are shown in Figure 7.8.4.1.2(g) along with an average response. The scatter was unacceptably large, and is likely a result of the small differences in response of specimens with differing notch lengths relative to experimental error.

Development of improved specimen geometries has also been pursued (e.g., University of British Columbia). In particular the over-height compact tension specimen, shown in Figure 7.8.4.1.2(h), is being evaluated. The greater dependence of specimen compliance on notch length should resolve the problems associated with the center-notch specimens. Test measurements and destructive evaluations are being conducted to provide further insights into the damage growth mechanisms. One unresolved issue with this specimen configuration is the effect of the bending stress distribution on the strain-softening law.

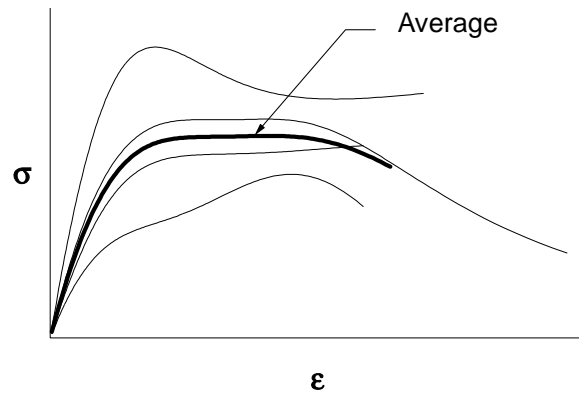


FIGURE 7.8.4.1.2(g) *Strain-softening laws determined from center-notch specimens using energy methods.*

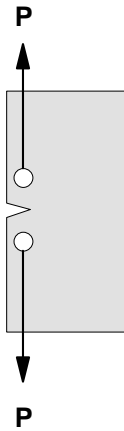


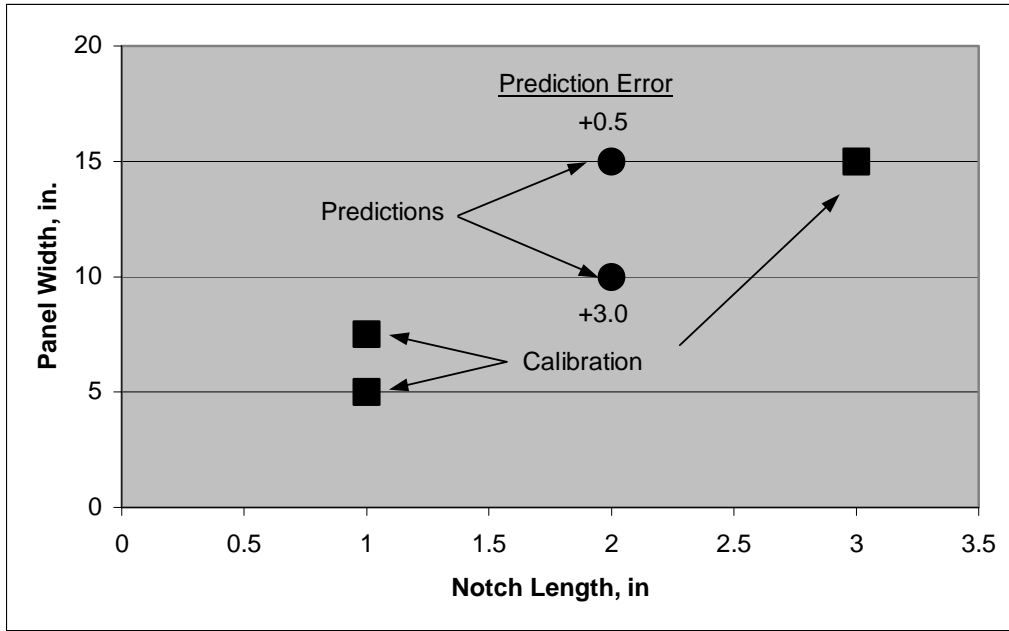
FIGURE 7.8.4.1.2(h) *Over-height compact tension specimen for strain-softening law determination.*

Any approach to determine the material laws directly from test measurements must use tests of sufficient size to capture process-induced performance characteristics.

Load Transfer to Stiffening Elements. In structural configurations with stiffening elements, the ability to model the degradation of the load-transfer capability between the skin and the stiffener is crucial to predict final failure. Physically, this degradation occurs as the damage approaches the stiffener, and can be caused by delamination damage in the skin, or yielding of either the bonded or mechanical attachment. Strain-softening models do not discretely address delamination damage in laminates, and the model fidelity required to predict either yielding for bonded or bolted joints is not compatible with structural-scale models. A practical method to address these issues has not been identified.

Strain-Softening Examples

The described approaches were used to predict unconfigured and configured notched compression strength. The unconfigured results are summarized in Figure 7.8.4.1.2(i). Three test points were used to calibrate the material law, while the other two tests were predicted. The predictions were within 3% of the test results.



Lay-up: [45/0/-45/90/0/-45/45/0/90/-45/0/45]
 Material: AS4/8552
 Core: 3/4" (19.0 mm) 8 pcf (128 kg/m³) HRP

Panel Sizes: 1" notch – 5 x 10, 7.5 x 10
 (25 mm – 127 x 254 mm), (191 x 254 mm)
 2" notch – 10 x 20, 15 x 20
 (51 mm – 254 x 508 mm), (381 x 508 mm)
 3" notch – 15 x 30
 (76 mm – 381 x 762 mm),

FIGURE 7.8.4.1.2(i) Strain softening prediction on unconfigured notched compression strength.

Predictions were also made of 30 x 44 in. (80 x 1100 mm) curved panels (122 in. (310 mm) radius) with 4 in. (100 mm) notches and a 66 x 88 in. (1.7 x 2.2 m) curved panel with and 8.8 in. (223.5 mm) notch. The predictions are compared with the experimental results in Figure 7.8.4.1.2(j). Predictions were within 7% of the measured values.

7.8.4.1.3 LEFM - based methods

Using classical linear fracture mechanics, the strain in a fiber direction at a distance r directly ahead of a crack tip can be written in the following infinite series (Reference 7.8.4.1(h)).

$$\varepsilon_1 = Q(2\pi r)^{-1/2} + O(r^0) \quad 7.8.4.1.3(a)$$

where

$$Q = K\xi/E_x \quad 7.8.4.1.3(b)$$

$$\xi = \left[1 - (v_{xy}v_{yx})^{1/2} \right] \left[(E_x/E_y)^{1/2} \sin^2 \alpha + \cos^2 \alpha \right] \quad 7.8.4.1.3(c)$$

r is the distance from the crack tip, K is the usual stress intensity factor, x and y are Cartesian coordinates with x perpendicular to the crack, E is a modulus of elasticity, ν is a Poisson's ratio, α is the angle that the fiber makes to the x axis (perpendicular to the crack), and $O(r^0)$ indicates terms of order r^0 and greater. For small r , the terms $O(r^0)$ are negligible.

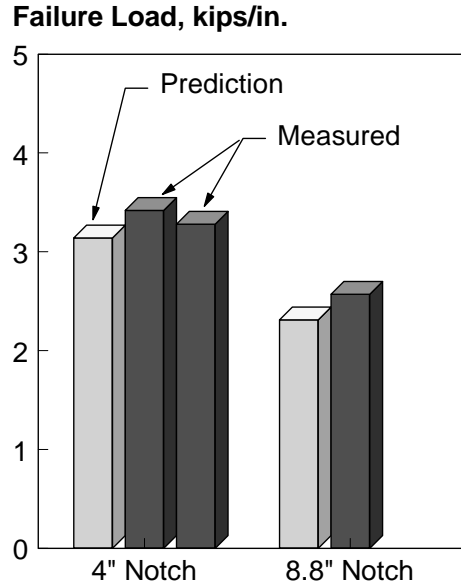


FIGURE 7.8.4.1.2(j) Comparison of measured notched compression failure loads with strain softening predictions.

For the point strain failure criterion, $\epsilon_1 = \epsilon_{tuf}$ at $r = d_o$, where ϵ_{tuf} is the ultimate tensile failure strain of the fibers. Thus, rearranging equation 7.8.4.1.3(a),

$$(2\pi d_o)^{1/2} = Q_c / \epsilon_{tuf} \quad 7.8.4.1.3(d)$$

and

$$K_Q = Q_c E_x / \xi = (2\pi d_o)^{1/2} \epsilon_{tuf} E_x / \xi \quad 7.8.4.1.3(e)$$

where the subscript c indicates critical value and K_Q is the laminate fracture toughness.

Equation 7.8.4.1.3(e) can be used to predict fracture toughness without conducting fracture tests. The elastic constants and the failing strain of the fibers can usually be obtained using data from the material supplier and classical lamination theory. Residual strengths can be calculated by equating the fracture toughness and stress intensity factors determined by theory of elasticity or finite element analyses. Approximate stress intensity factors for panels with bonded stiffeners are given in Reference 7.8.1.3.1(a).

7.8.4.1.4 R-curves

For many composites, the value of the normalized characteristic dimension, $(2\pi d_o)^{1/2}$, is not a constant but increases with crack length, especially for thin laminates made with brittle resins. Values of $(2\pi d_o)^{1/2}$ are plotted against damage growth in Figure 7.8.4.1.4(a) for a 13-ply fuselage crown laminate

made of prepreg tape using a tow-placement process (Reference 7.8.1.3.1(a)). The damage growth measured in radiographs and calculated from measurements of crack-opening displacements (COD) are in good agreement. (The crack length including damage growth is proportional to the COD, which was measured by a "displacement gage" located midway between the ends of the cut).

The maximum value of $(2\pi d_o)^{1/2}$ in Figure 7.8.4.1.4(a) is about 63% greater than the LEFM value, and the maximum damage growth was one third of the cut length. The values of $(2\pi d_o)^{1/2}$ were calculated using the length of cut plus growth. The curve in Figure 7.8.4.1.4(a) can be used as a crack-growth resistance curve (R-Curve) with failure defined by the tangency of the R-Curve and the crack-driving-force curve (F-Curve) calculated using Equation 7.8.4.1.3(d) and stress intensity factors determined by theory of elasticity or finite element analyses. In the ASTM E561-86 standard (Reference 7.8.4.1.4(a)), the R- and F-Curves are expressed in terms of stress intensity factor. However, for composites, it is convenient to use $(2\pi d_o)^{1/2}$ instead of stress intensity factor to normalize for lay-up and material.

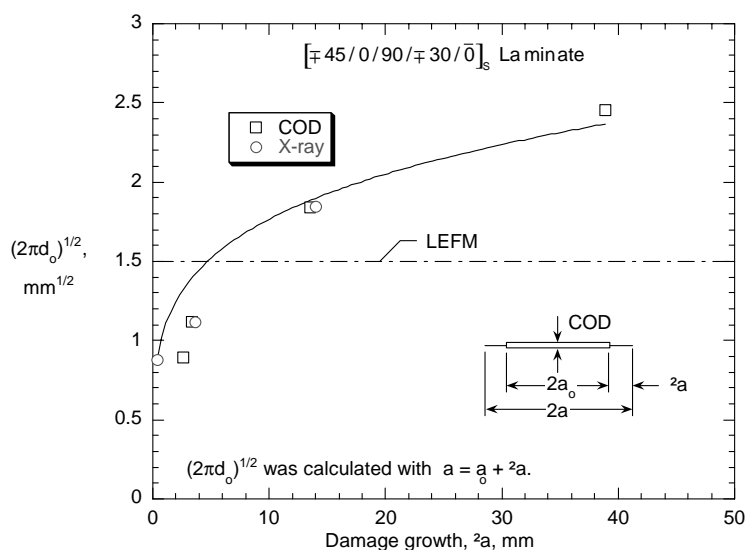


FIGURE 7.8.4.1.4(a) *R-curve for tow-placed AS4/938 fuselage crown laminate (cut length = 9 in. (23 cm) and width = 36 in. (91 cm)) (Reference 7.8.1.3.1(a)).*

R-Curve Examples

Tensile failing strains for large flat fuselage panels with straps and hat-section stiffeners are plotted against cut length in Figures 7.8.4.1.4(b) and (c) (Reference 7.8.1.3.1(a)). The panel with straps contained a 10.0 in. (25.4 cm) cut and that with hat-section stiffeners contained a 14.0 in. (35.6 cm) cut. The central stiffener in both panels was severed, and the skins were [-45/45/0/90/-30/30/0/30/-30/90/0/45/-45] AS4/938 tow placed fuselage crown laminates. The stiffness of the straps was 56% of that of the hat-section stiffeners. The amount of crack growth observed in the test is indicated by the arrow drawn to the right of the "test failure" symbol. The panel with straps in Figure 7.8.4.1.4(b) failed catastrophically at an applied strain of 0.00275 with about 1.0 in. (2.5 cm) of stable tearing at each end of the cut. The cut in the panel with hat-section stiffeners grew stably into the stiffener (about 7 in. (18 cm) at each end of the cut) before catastrophic failure at an applied strain of 0.00274.

Tensile failing strains calculated using LEFM and R-Curve are also plotted against cut length in Figures 7.8.4.1.4(b) and (c). Approximate, closed-form equations in Reference 7.8.1.3.1(a) were used to calculate F-Curves for the various cut lengths. An envelope of F-Curves in Reference 7.8.1.3.1(a) similar to the one in Figure 7.8.4.1.4(a) was used for the R-Curve. The jumps in failing strains occur when the end of the cut (LEFM) or the end of the cut plus stable growth (R-Curve) coincide with the edge of the stiffener. The horizontal dashed lines indicate the region of cut lengths for fracture arrest and give the failing strains with subsequent loading. For cut lengths to the left of the dashed line, failures are catastrophic. The LEFM predictions were 45 and 58% below the test values for the straps and hat-section stiffeners, respectively, and the R-Curve predictions were 14% below and 16% above the test values for the straps and hat-section stiffeners, respectively. The nature of failure, that is catastrophic versus fracture arrest, were predicted correctly by both LEFM and R-Curve.

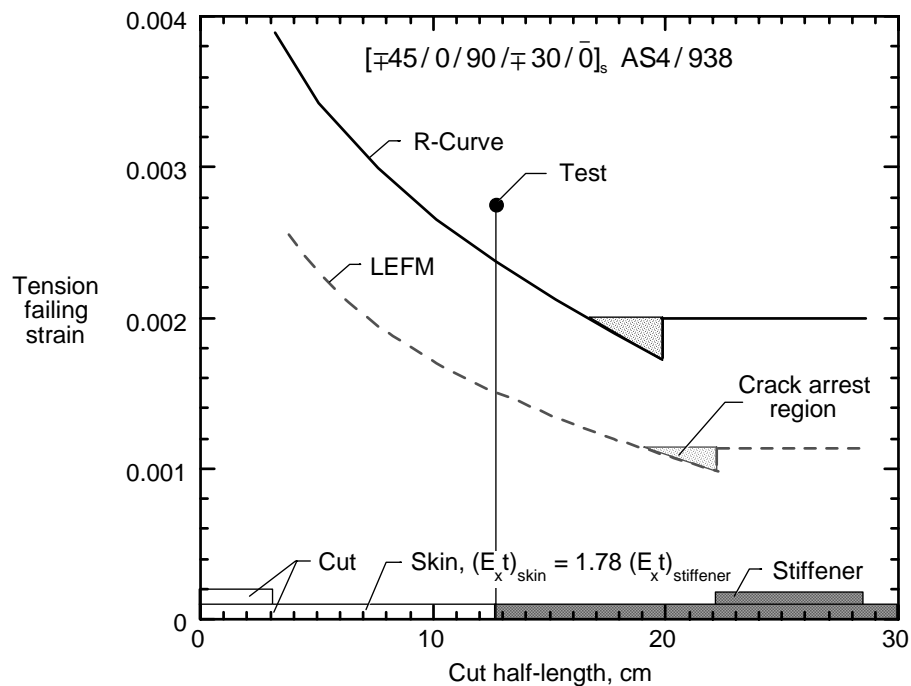


FIGURE 7.8.4.1.4(b) Measured and predicted failing strains for three-stringer tow-placed fuselage crown panel 30 x 83.9 in. (76 by 213 cm) (Reference 7.8.1.3.1(a)).

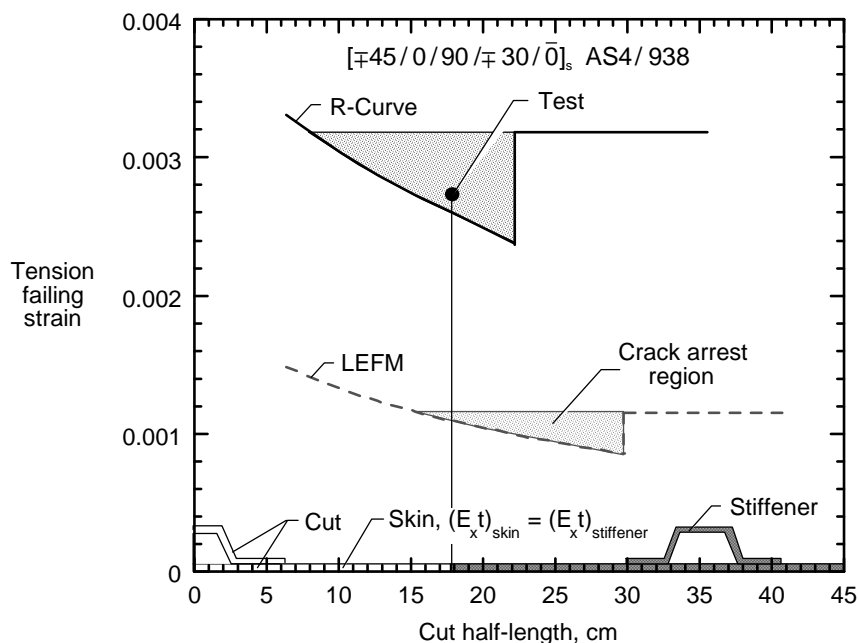


FIGURE 7.8.4.1.4(c) Measured and predicted failing strains for five-stringer tow-placed AS4/938 fuselage crown panel 63 by 137 in. (160 by 348 cm) (Reference 7.8.1.3.1(a)).

It should be noted that flat panel results can not be applied directly to shells with longitudinal cracks and internal pressure because stress intensity factors for pressurized shells can be much greater than those for flat plates. (Strengths and burst pressures vary inversely with stress intensity factor.) See Figure 7.8.4.1.4(d), where stress intensity correction factors from Reference 7.8.4.1.4(b) are plotted against a/\sqrt{Rt} for isotropic pressurized cylinders and spheres. For a wide body fuselage with a cut equal to two times the frame spacing, a/\sqrt{Rt} can be as large as five. In that case, the stress intensity factor for an unstiffened cylinder would be more than five times that for a flat unstiffened plate. Analytical results for specially orthotropic cylinders are given in References 7.8.4.1.4(c) and (d). These results were experimentally verified for 12 inch (30 mm) diameter pressurized composite cylinders with longitudinal cuts in Reference 7.8.4.1.4(e). Frames and tear straps can not only reduce the stress intensity factor (Reference 7.8.4.1.4(f)), they can also turn a fracture and limit a failure (see Reference 7.8.4.1.4(g)).

An R-Curve was also successfully used to predict residual strength of a curved panel with stiffeners, pressure loading, and discrete source damage in Reference 7.8.4.1.4(h). The F-Curve was calculated by a nonlinear finite element analysis taking into account out-of-plane displacements.

7.8.4.2 Single delaminations and disbonds

The previous section discussed severe accidental and discrete source damage only, represented by crack-like, penetrating cuts. Analysis of laminates containing single plane delaminations or disbonds can also be performed. As discussed earlier, delaminations have little effect on tension strength but delaminations can be critical for compression or shear loading. Analysis methods for damage (including delaminations) resulting from impact damage is contained in Section 7.8.4.3.

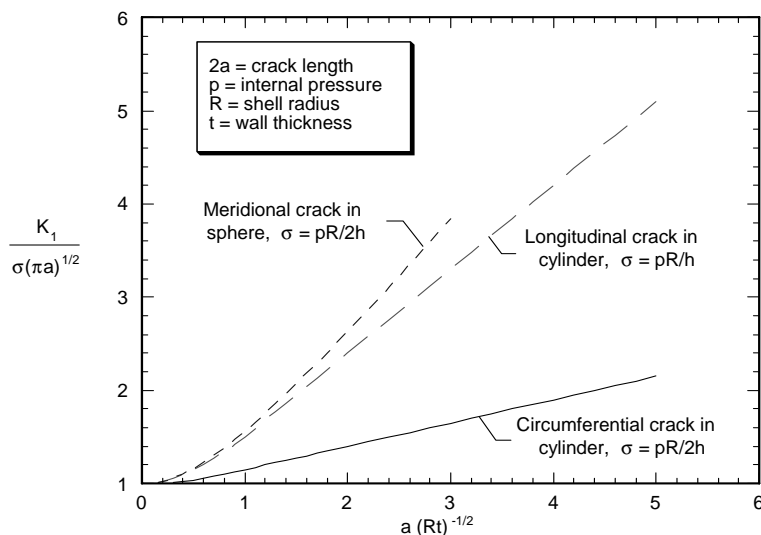


FIGURE 7.8.4.1.4(d) Stress intensity correction factors for pressurized shells with cuts (Reference 7.8.4.1.4(b)).

7.8.4.2.1 Fracture mechanics approaches

This section is reserved for future use.

7.8.4.2.2 Sublaminates buckling methods

Method A: Successive Sublaminates Buckling

This method is applicable to solid laminates or facings of sandwich structures. When loaded in compression or shear, the sublaminates adjacent to the delamination may buckle (Reference 7.8.4.2.2(a)). In sandwich structures only the surface sublaminates, not the one bonded to the core, can buckle. In solid laminates both sides can buckle. When the sublaminates buckle, out-of-plane loads develop at the edge of the sublaminates causing a growth of the delamination. A larger delamination will buckle at a lower load. Once a sublaminates buckles it is assumed that it is unable to sustain further loads. This is the basic conservative assumption of the analysis method. The analysis method (References 7.8.4.2.2(b) and (c)) is a step by step application of lamination theory together with first fiber mode failure criteria and buckling analysis of anisotropic plates. The following steps are performed:

1. The laminate is divided into sublaminates according to the through the thickness location of the delamination as obtained from NDE.
2. The external load is distributed between the sublaminates according to their stiffness.
3. The sublaminates are checked for static compression, shear or combined load according to lamination theory.
4. The sublaminates are checked for buckling. Simply supported boundary conditions are assumed for outer sublaminates. Clamped boundary conditions are assumed for inner sublaminates in a case of multiple delaminations.
5. A buckled sublaminates is conservatively assumed to be unable to sustain the buckling load. Additional load is transmitted to the unbuckled sublaminates.

For a single delamination, the strength of the delaminated laminate will equal the strength of the sublaminates with the larger resistance to buckling. For multiple delaminations, as in the case of impact damage (see Section 7.8.1), steps 2-5 are repeated until failure.

This simplified model gives conservative results for sandwich facings, and good results for solid laminates containing delaminations and impact damage.

Method B: In-Plane Stress Concentration Adjacent to Buckled Sublaminates

In Method B, the buckled sublaminates have reduced stiffness, carrying their buckling loads until laminate failure due to an in-plane stress concentration.

7.8.4.3 Impact damages

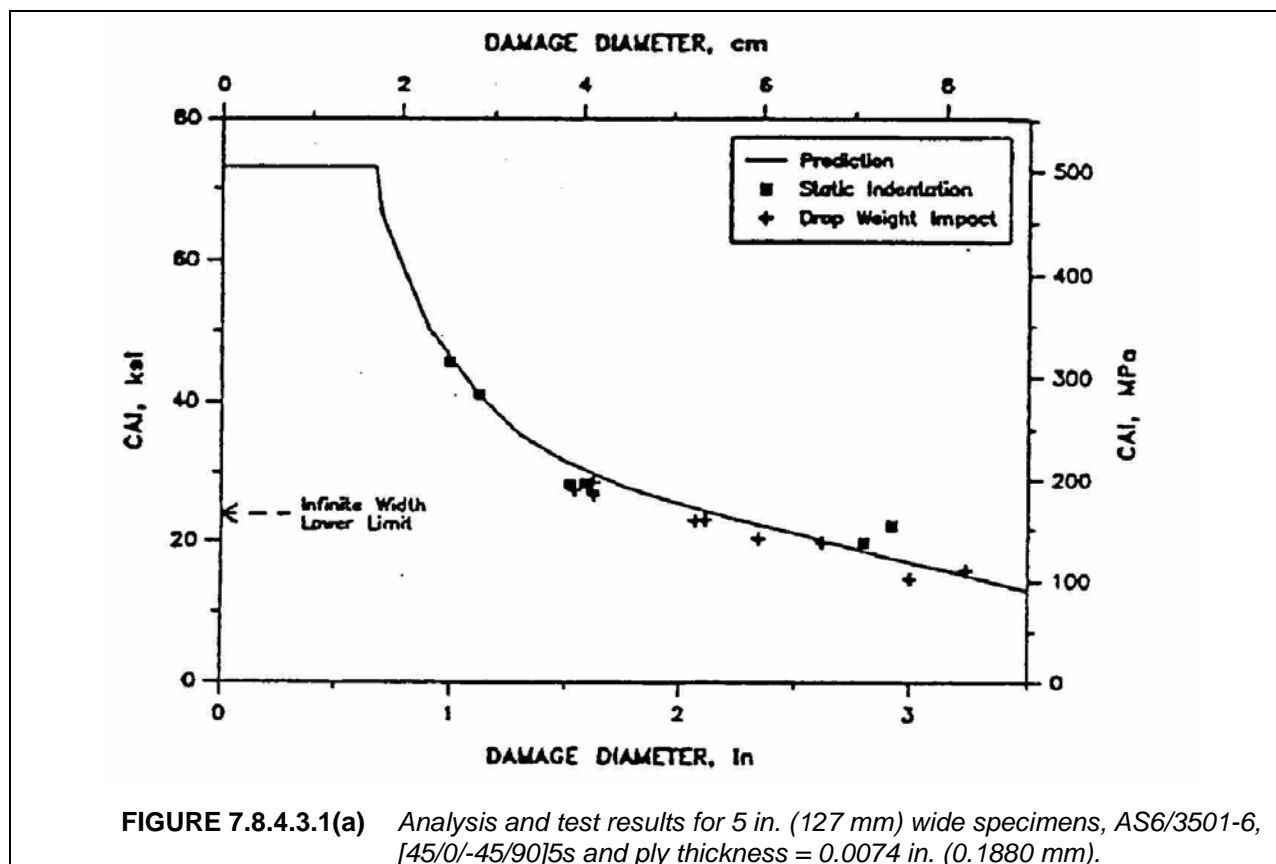
Impact damage has been shown to reduce structural residual strength under tension, compression, shear, and combined load cases. Post-impact residual strength is an important consideration for damage tolerant design and maintenance. Several different approaches to predicting post-impact residual strength have been documented in the literature. A semi-empirical analysis was developed from the large database collected during the U.S. Air Force contract (Reference 7.5.1.1(j)) for stiffened wing structure. This analysis predicted residual strength as a function of key design variables and impact energy. Although such an approach supports design, it has limited benefit to service problems in which little or no data is available on the impact event. Residual strength predictions based on a quantitative measure of the CDS have subsequently emerged.

7.8.4.3.1 Sublamine buckling methods

When impact damage is dominated by matrix cracks and delaminations, sublamine stability is crucial to compression or shear stress redistribution and reduction in residual strength (References 7.8.1.2.2(a) through 7.8.1.2.2(d)). The CDS must be known in order to predict sublamine stability. For example, the CDS shown in Figure 7.8.1.2.7(c) is dominated by 4-ply thick, unsymmetric sublaminates that repeat through the laminate thickness, depending on the number of repeating ply groups in the stacking sequence.

Once buckled, sublaminates may be assumed to carry a constant load and a stress concentration develops in the adjacent undamaged material. The stress concentration is related to the effective reduced stiffness of the buckled sublaminates, which changes as a function of the initial buckling stress and increasing loads. The reduced stiffness at failure can be estimated by matching the buckling stress with the material's local compressive strain at failure. Test measurements of local strains show that these analysis assumptions provide reasonable accuracy in estimating the stress concentration at the edge of buckled damage (Reference 7.5.1.1(m)). Prediction of CAI has also been confirmed by residual strength tests (References 7.8.1.2.2(a) through 7.8.1.2.2(d)). This engineering approach to predicting CAI has been successfully applied to sandwich panels (Reference 7.8.4.3.1(a)). More involved methods, including finite element simulation of the sublamine buckling and adjacent stress concentration, have also been used to predict failure of laminated composites (Reference 7.8.4.3.1(b)). Such an approach may be required for built-up structure, in which load redistribution occurs.

The basic sublamine stability analysis (Reference 7.8.4.1(a)) involves four steps. First, the damage state is characterized with the help of NDI and the damage is simulated as a series of sublaminates. Second, sublamine stability is predicted with a model that includes the effects of unsymmetric LSS. Third, the in-plane load redistribution is calculated with a model that accounts for structural geometry (e.g., finite width effects). Finally, a maximum strain failure criterion is applied to calculate CAI strength. Figure 7.8.4.3.1(a) shows typical results from this analysis procedure.



A similar model with slightly different assumptions has been developed in References 7.8.4.3.1(c) through 7.8.4.3.1(e). The residual strength of an impacted laminate loaded in compression and shear can be estimated by considering the successive buckling of sublaminates and load redistribution among non-buckled sublaminates, until fiber mode failure of the remaining laminate. This model requires input data from NDE to define position, number, and dimensions of the delaminations that divide the laminate into sublaminates. The Damage Model is built from the NDE data and conservative assumptions. The impacted region is simplified to a sequence of sublaminates bonded at the delamination boundaries, Figure 7.8.4.3.1(b). The failure analysis is described schematically in Figure 7.8.4.3.1(c). The applied load is distributed between the various sublaminates according to their relative stiffness. Failure of each sublaminate is checked for compressive strength and buckling. As one sublaminate buckles, it is assumed that it cannot carry additional load, and all the load is redistributed between the remaining sublaminates, until fiber mode failure of the remaining laminate. In spite of the many assumptions made in the interpretation of the NDE results as well as in the construction of the damage and failure model, the results are in very good agreement with compression after impact experimental data for various materials and impact energies (Figures 7.8.4.3.1(d) and (e)). This agreement exists because of the sequential nature of the model. Since the layers are failed one after another, the exact value of a sub-laminate failure is not important, as long as the failure sequence is correct. The overall precision of the calculation is the precision of the fiber mode failure of the last failed sublaminate.

Similar analysis can be applied to compression facings of sandwich structures (Reference 7.8.4.3.1(f)). Sublaminates can only buckle away from the core and the core has a stabilizing effect, so the predictions are more conservative than for thick laminates.

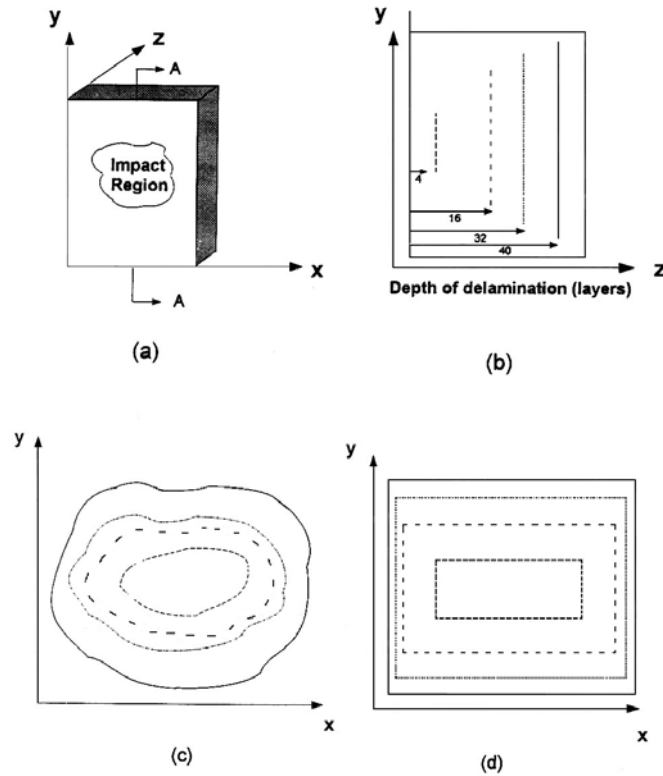


FIGURE 7.8.4.3.1(b) Construction of damage model (AS4/3502, impact energy of 67.8 ft-lbs (91.9 N-m)) (a) damaged specimen; (b) cross-section through damage region (aa); (c) shape of major delaminations; (d) rectangular delaminations used in the model (References 7.8.4.3.1(c) through 7.8.4.3.1(e)).

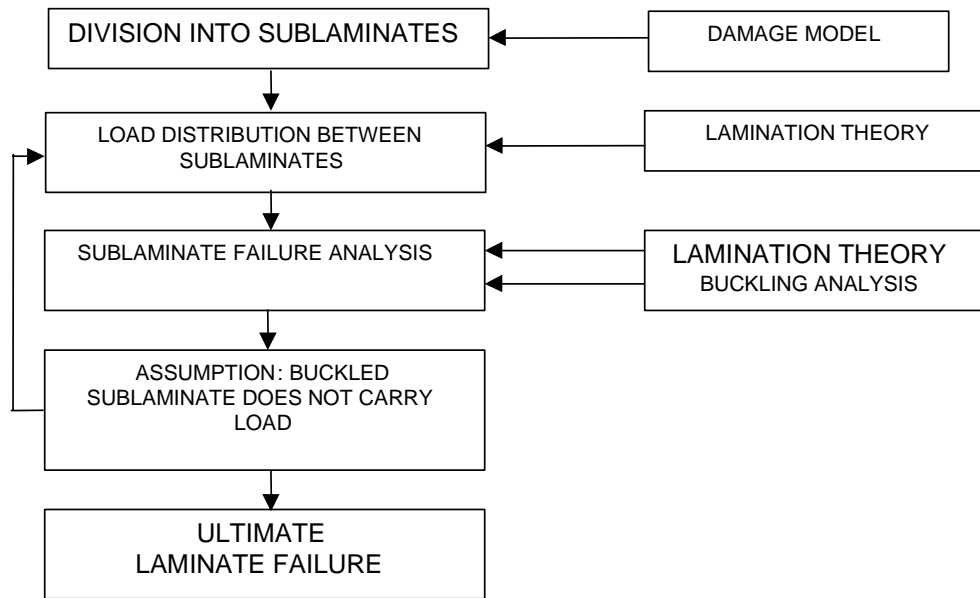


FIGURE 7.8.4.3.1(c) Schematic description of failure model (References 7.8.4.3.1(c) through 7.8.4.3.1(e)).

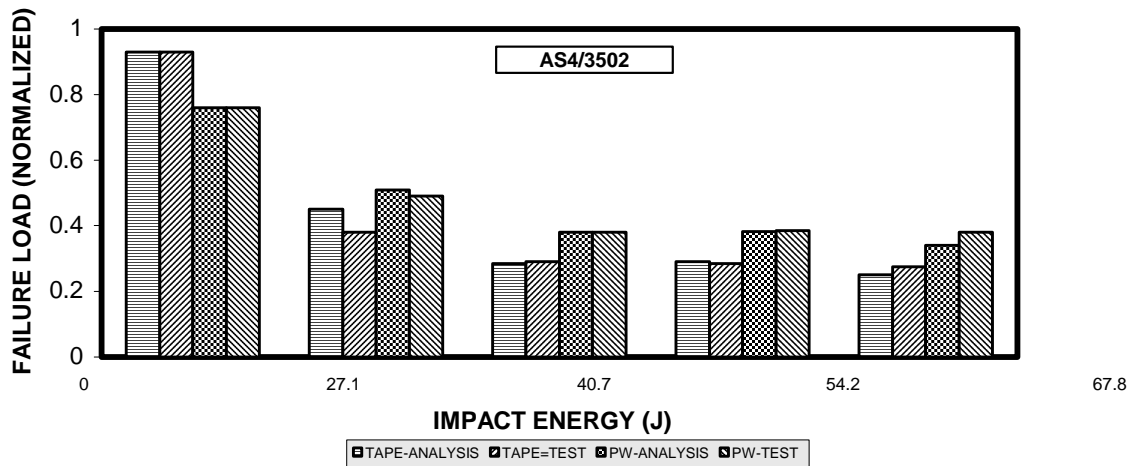


FIGURE 7.8.4.3.1(d) Failure Load as a function of impact energy (References 7.8.4.3.1(c) through 7.8.4.3.1(e)).

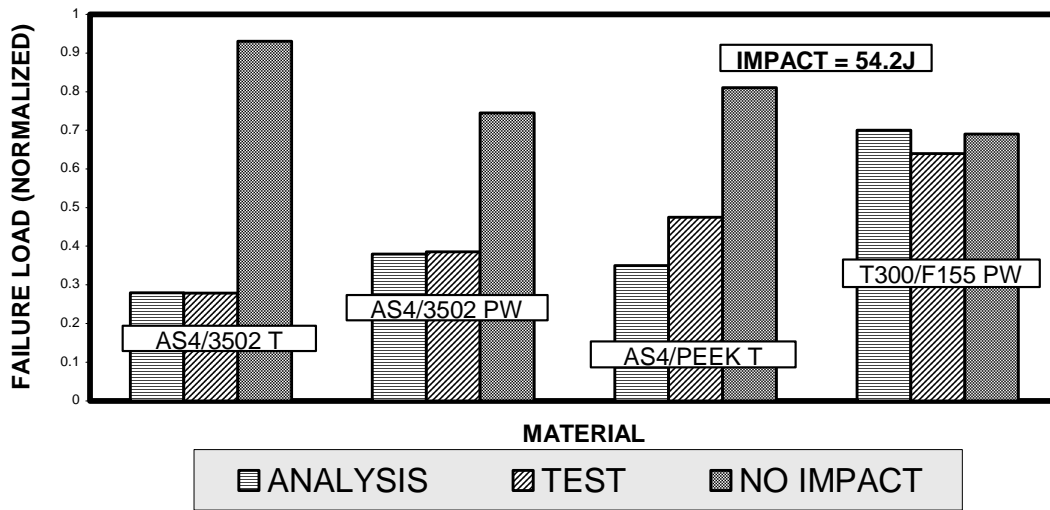


FIGURE 7.8.4.3.1(e) Failure load as a function of material (References 7.8.4.3.1(c) through 7.8.4.3.1(e)).

7.8.4.3.2 Strain softening methods

The strain-softening approaches discussed for large through-penetration damage in Section 7.8.4.1.2 can be adapted to address impact damage scenarios. In studies reported in References 7.8.1.2.8(g) and 7.8.1.3(e), material laws for the damaged facesheet material within the impact zone was scaled from the undamaged material law, as shown in Figure 7.8.4.3.2(a). The scaling factors were determined from tests conducted on relatively small specimens containing representative impacts. The indentation resulting from the impact was approximated by reducing the core height at nodes to best represent that measured in the impact trials. Note that the approximations of the perimeter were significantly limited by the fixed mesh size necessary to complement the strain-softening law.

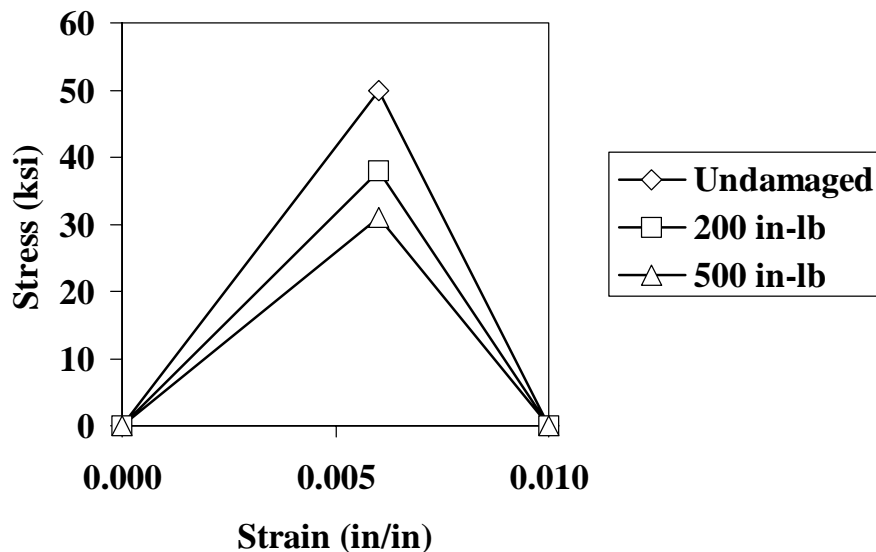
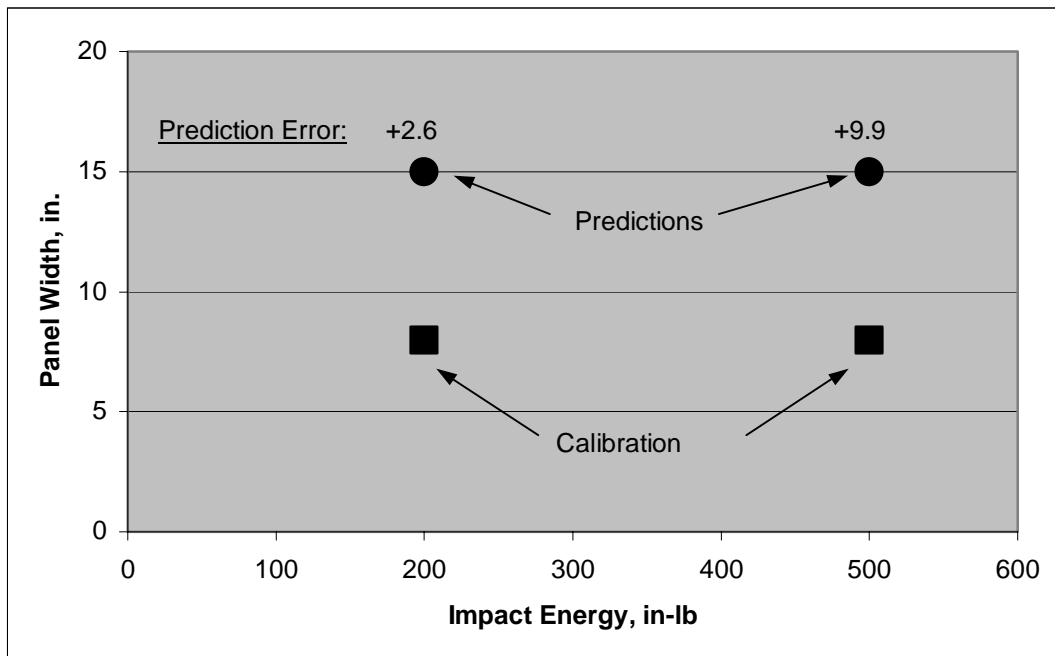


FIGURE 7.8.4.3.2(a) Strain-softening laws for impact damaged material.

The described approaches were used to predict unconfigured and configured impacted compressive strength. The unconfigured results are summarized in Figure 7.8.4.3.2(b). Two test points were used to calibrate the material law, while the other two tests were predicted. The predictions were within 10% of the test results.

Predictions were also made of two 30 x 44 in. (762 x 1118 mm) curved panels (122 in. (3.1 m) radius) with two circumferential frames. Both panels were impacted at 200 in-lb (22.6 N-m) impact damage, with one of the panels impacted on the inner (IML) facesheet, while the other was impacted on the outer (OML) facesheet. The predictions are compared with the experimental results in Figure 7.8.4.3.2(c). Predictions were within 7% of the measured values.



Lay-up: [45/0/-45/90/0/-45/45/0/90/-45/0/45] Panel Sizes: 8 x 15, 15 x 30
 Material: AS4/8552
 Core: $\frac{3}{4}$ " 8 pcf HRP

FIGURE 7.8.4.3.2(b) Strain softening predictions of unconfigured impacted compression strength.

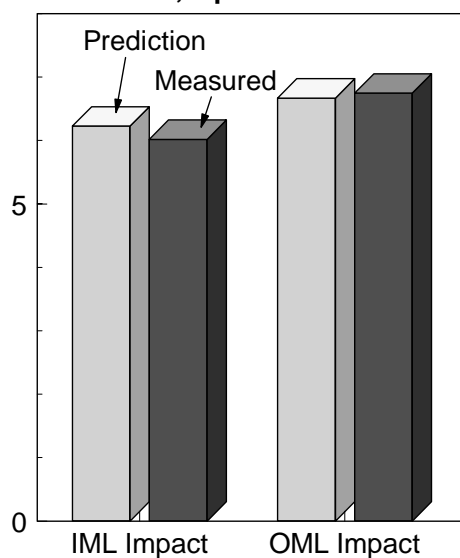
Failure Load, kips/in.

FIGURE 7.8.4.3.2(c) Comparison of measured impacted compression failure loads with strain softening predictions.

7.8.4.4 Cuts and gouges

Fortunately, most of the damage that is critical to tensile loading such as cuts and gouges is, to some degree, visible. Tests have shown that for tensile loading, the residual strength of a laminate with a cutout is primarily dependent on the width of the cutout and essentially independent of the cutout shape. Thus ultimate design values reduced to account for the presence of a 0.25 inch (6.4 mm) diameter hole also account for an equivalent length edge cut. Cuts of this type that might be produced during manufacturing are a special problem since they may be filled with paint, and consequently, not detected. Sufficient testing should be done as part of design verification programs to ensure that cuts and gouges that are on the threshold of visibility will not degrade the structural strength below Ultimate Load requirements.

Small cuts and gouges (≤ 0.25 inch (6.4 mm)) can also affect the residual strength for load cases dominated by compression and shear. Such damage has not been a design driver for compression and shear Ultimate Load requirements of composites with first-generation, brittle epoxy matrices because BVID is more critical for such materials. However, small cuts and gouges can be critical for such load requirements when using toughened matrix, textile, or stitched composite materials.

Larger cuts or gouges, which are clearly visible, lower compression, shear, and tensile strengths below Ultimate Load requirements. Methods discussed in Section 7.8.4.1 can be used to evaluate panels with this level of damage.

7.9 APPLICATIONS/EXAMPLES

Composite structure application in the aerospace industry has progressed to the extent that a number of vehicles containing primary composite components have been certified/qualified for use. This section presents a discussion of some representative applications in various categories and types of aircraft. The examples are intended to provide the reader with some insight to how vehicle prime contractors have approached durability and damage tolerance issues and successfully satisfied appropriate requirements.

Requirements are evolving and specific structural applications on various vehicles often contain unique features, hence the examples are not to be construed as the only way to accomplish damage tolerance and durability. Instead, they illustrate the thinking, focus, and scope of the task. It is hoped this will be of help in future programs.

7.9.1 Rotorcraft (Sikorsky)

The damage tolerance approach for composite rotorcraft under cyclic loading combines analysis and building block testing (from coupon to full scale level) to demonstrate the required level of reliability (A or B-basis) of composite parts in the presence of damage. The approach demonstrates no growth of damage under spectrum loading for the required number of cycles at the representative environment(s) and with the appropriate load enhancement factors for statistical reliability. At the end of the lifetime fatigue test, residual strength is demonstrated.

7.9.1.1 Damage

The damage should be representative of the type of damage expected during manufacturing and service. The size of damage is determined as a combination of the maximum damage size allowed by the inspection means selected and a statistical treatment of the expected threats (tool drops, hail, runway debris, etc.). The location of damage is based on statistical analysis of the damage scenarios and the threats to which the most highly loaded areas of the structure may be exposed. Since routine inspections during service are visual inspections, no damage growth of non-visible damage must be demonstrated for the full service life of the aircraft. For visible damage, no growth must be demonstrated for at least three inspection intervals.

7.9.1.2 Environment

The structure should be tested at the worst environment expected in service. For most composite materials used in rotorcraft, this means elevated temperature wet conditions for static and residual strength testing, and room temperature wet conditions for fatigue testing. To avoid increased costs associated with setting up and maintaining environmental chambers, tests can be conducted at room temperature ambient conditions provided the applied loads are adjusted for environment with the use of an appropriate load acceleration factor. This factor is defined by analysis, coupon, and element testing that determine the environmental knockdown factor from room temperature ambient to the service condition for the type of loading and particular failure mode.

7.9.1.3 Test loading conditions related to critical failure modes

The loads applied during testing at the element and component levels should simulate the internal loads in the vicinity of inflicted damage. This is critical in the case of open hole compression and compression after impact tests. Many rotorcraft components such as flexbeams are designed to interlaminar shear or peel loads. Therefore, open hole compression or compression after impact tests are not directly applicable without prior demonstration of equivalence through adjustment of loading and hole size.

7.9.1.4 Test loads - load enhancement factor (LEF)

In addition to the load acceleration factor to account for environmental effects, a load enhancement factor is used to account for material variability. The full scale specimen is tested at a combination of lifetimes (typically one for rotorcraft due to the large number of cycles per lifetime) and applied loads such that at the end of a successful test, the required reliability (A or B-basis) is demonstrated. The LEF depends on the static and fatigue scatter exhibited by the material(s) used. Sufficient tests at the coupon, element, and component level are necessary to quantify the scatter. Weibull statistics and the approach given in Reference 7.9.1.4 are used for the determination of the LEF.

7.9.1.5 Spectrum - truncation

Helicopter dynamic components such as rotor and transmission components as well as airframe or empennage components exposed to rotor wake loading experience a very large number of cycles per lifetime. Typically, a 30000 hour lifetime may include more than a billion cycles. For this reason, a truncation level is established to eliminate loads from the test spectrum which will not propagate damage in the aircraft lifetime.

The truncation level is determined as a ratio of the stress (or strain) corresponding to 10^8 cycles on the S-N curve to the static room temperature wet A basis (or B-basis) strength with damage. This is done for each of the R ratios, loading, and failure modes expected in service. It should be pointed out that the room temperature wet A basis strength value may be significantly higher than the corresponding Limit Load. The truncation level determination is depicted graphically in Figure 7.9.1.5.

The truncation ratio can be shown to depend on R ratio ($\sigma_{\min} / \sigma_{\max}$) and damage type (hole versus impact or delamination for example). It will also depend on the materials used. For this reason, coupon and element test data covering materials, lay-ups, and representative R-ratios are necessary to establish a conservative truncation level that covers all cases.

As an alternative approach for the determination of the truncation level, the wearout equation proposed by Sendekyj (Reference 7.9.1.5) and discussed in Reference 7.9.1.4 can be used. This requires sufficient data for each R ratio, material, and damage type which can be an exhaustive series of tests. The wearout equation in Reference 7.9.1.5 can be used to determine the truncation level as the A (or B) basis residual strength at a given number of cycles.

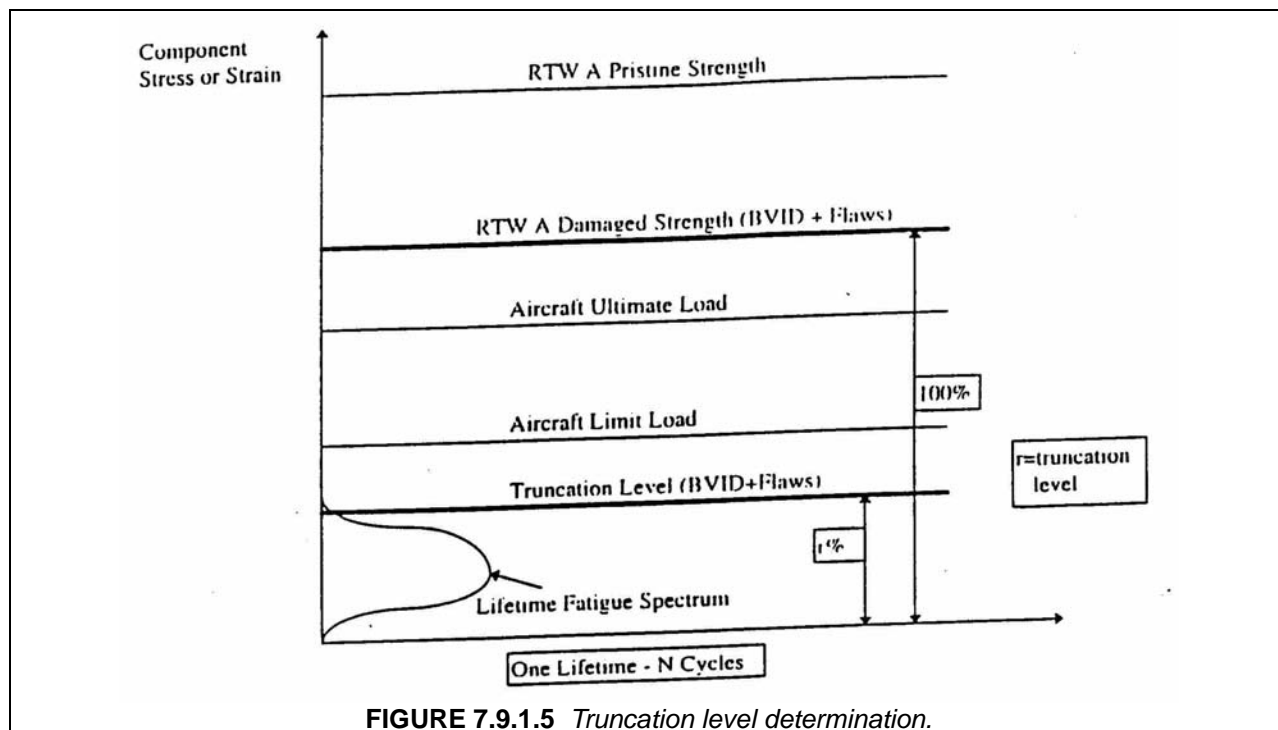


FIGURE 7.9.1.5 Truncation level determination.

7.9.1.6 Residual strength test

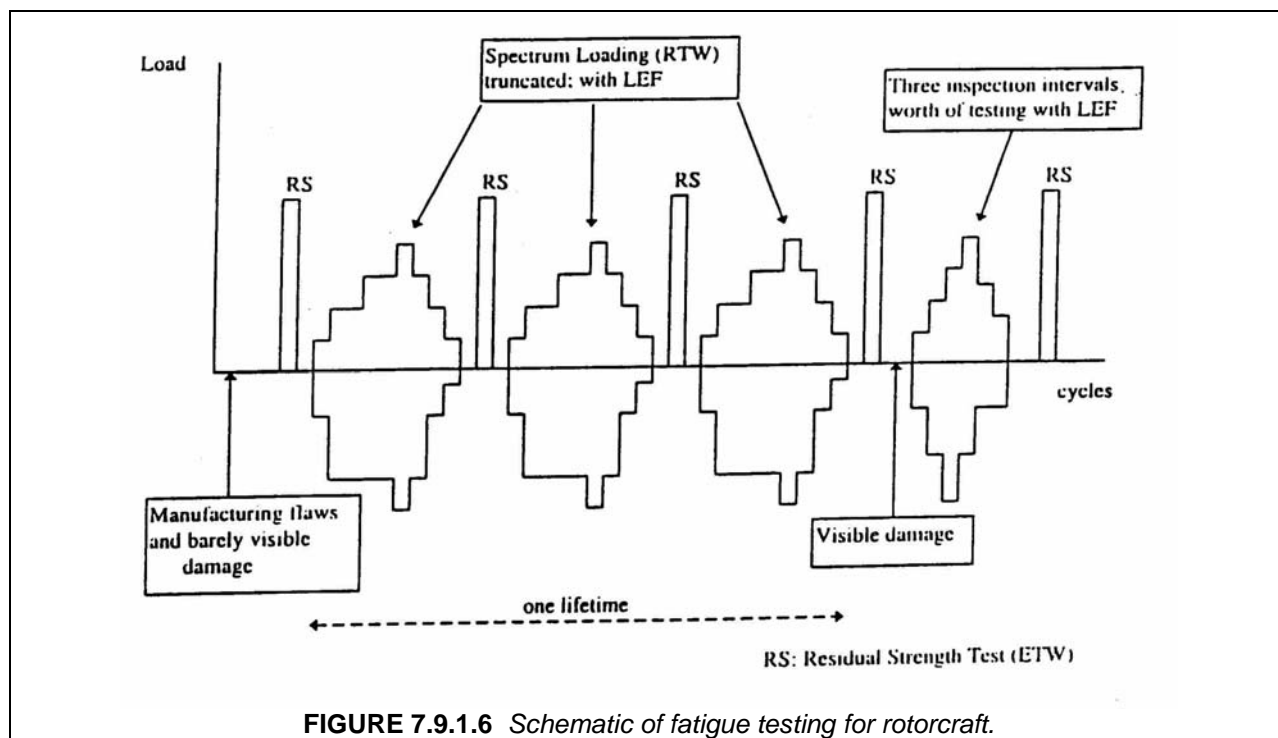
At the end of a successful fatigue test, residual strength must be demonstrated. Limit Load or Ultimate Load capability must be demonstrated depending on whether the damage present is visible or non-visible, respectively. The environment should be the worst environment for static loading (elevated temperature wet for most materials). Periodic residual strength tests can be incorporated during the fatigue test to protect against early failure or damage growth. In such a case, the last successful residual strength test marks the number of cycles for which the current design is certified.

The damage tolerance certification procedure for rotorcraft composites under fatigue loading is shown in Figure 7.9.1.6.

7.9.2 Commercial aircraft (Boeing 777 empennage torque boxes)

The damage tolerance approach for certification of commercial aircraft composite principal structural elements involves analysis and building block testing from the coupon to the full-scale levels (Reference 7.9.2). The approach demonstrates no growth of damage at the threshold of detectability (BVID) under repeated loading for a minimum of two airframe design service objectives ("lifetimes"). Residual strength for several damage scenarios is demonstrated after application of the repeated loading. The structural inspection plan is developed based on the maintenance program and on environmental deterioration and accidental damage ratings developed in accordance with FAR 25.571.

This section outlines the tests and analyses used to validate the damage tolerance of the Boeing 777 empennage main torque box structure.



7.9.2.1 Durability - environmental

Environmental durability of the materials and structure was validated by:

Volume 3, Chapter 7 - Damage Resistance, Durability, and Damage Tolerance

- Long term exposure of panels attached to racks in several locations. Periodically the panels are retrieved, specimens machined and tested, and the data compared to baseline data.
- Temperature-moisture cycling of a three (3) stringer skin panel section, bolted joints with moldable plastic shims (MPS), and laminates with resin rich areas.

7.9.2.2 Durability - mechanical loads

A series of coupons, element and sub-component level tests were used to validate that damage from repeated loading does not occur at operational load and strain levels. The following coupon tests were conducted to at least 106 load cycles:

- Unnotched laminates (edge delamination test).
- Laminates with an open hole.
- Laminates with pad-ups.
- Bolted joints (composite-composite, composite-titanium).
- Radius details.

The following sub-component tests were conducted without experiencing damage initiation in the composite structure:

- Five stringer panel with a bonded repair and "barely visible impact damage" (BVID) impacts; tested to 2 lifetimes of repeated loads.
- Horizontal stabilizer skin splice joint panel with BVID impacts; tested to 2 lifetimes of repeated loads + 1 lifetime with enhanced loads.
- Vertical fin-to-body root joint panel; tested to 38 equivalent lifetimes repeated loads.

In addition, a pre-production horizontal stabilizer test box and the 777 horizontal stabilizer and vertical fin were tested to at least two lifetimes of repeated loads without experiencing damage initiation in the composite structure.

7.9.2.3 Damage

The 777 empennage composite structure is designed to be resistant to corrosion, and strain levels are such that damage initiation or growth (of visible and non-visible damages) does not occur with repeated operating loads. Therefore, accidental events are the only realistic damage source for damage tolerance evaluation of the composite structure.

The damages for evaluation are representative of the type and severity expected during manufacturing and service. The size of damage is determined based on the capability of the selected inspection method(s). Structure with damage at the threshold of detectability (BVID) must be capable of Ultimate Loads and demonstrate "no damage growth" under operating loads for the expected service life of the airplane. If detrimental damage growth is indicated, then damage must be shown to be detectable before it reduces the structural strength below Limit Load capability. Damages are generally applied to the most critically loaded areas of the structure.

The main source of discrete source damage for the empennage main torque boxes is from impacting objects. The main torque boxes are located in lightning strike zone 3 (no direct attachment or swept lightning strikes) and, therefore, are not affected by direct lightning. The leading edge structures are of metal construction, and are designed to prevent bird strike damage to the main box.

7.9.2.4 Damage tolerance - "no growth" tests

Since routine inspections of the 777 composite structures during service are visual inspections, and since the characteristic growth of typical damage to composite structure is not visual, the "no growth" approach for damage tolerance certification is used. The "no growth" of damages at the threshold of detect-

ability must be demonstrated for the service life of the aircraft. For visible damages which are readily detectable by scheduled inspections, "no-growth" must be demonstrated for at least two inspection intervals. This is to insure that the damages will not progress beyond the critical damage threshold (CDT) for which the structure must maintain Limit Load capability.

The "no-growth" of small damages was demonstrated with element, sub-component and component level tests tested to a minimum of 2 lifetimes of repeated loads. The following element and sub-component repeated load tests demonstrated no damage growth:

- Laminates with BVID impacts.
- Shear panels with BVID impacts at the edge of cutouts.
- Five stringer panel with a bonded repair and BVID impacts.
- Horizontal stabilizer skin splice joint panel with BVID impacts.
- Spar shear beams with BVID impacts at the edge of web cutouts.

A pre-production horizontal stabilizer test box was subjected to a series of static and repeated spectrum loads to verify the materials, design concepts, manufacturing processes, analysis methods, "no-growth" of damages, and ultimate and residual strength capabilities. Compression has been shown to be the critical mode of loading for impact damaged composite structures. The damage emphasis in the test program was on the highest loaded compression areas.

The specific locations of the individual damages were chosen on the basis of strain patterns developed by FE modeling and previous test results of sub-component panels which indicated critical areas. Various levels of damages were introduced into the test article on three separate locations in the test sequence (see Figure 7.9.2.4).

Apply BVID (small) damages 60% Design Limit Load (DLL) Conditions - Strain Survey Repeated Loads (Fatigue Spectrum) - 1 Lifetime 60% DLL Conditions - Strain Survey Repeated Loads (Fatigue Spectrum) - 1 Lifetime
Apply visible damages Repeated Loads (Fatigue Spectrum) - 2 Inspection Intervals 100% DLL Conditions
Apply element damages 70% DLL Conditions - "Continued Safe Flight" Load Levels
Repair visible and element damages Design Ultimate Loads (DUL) Conditions Load to Destruction

FIGURE 7.9.2.4 *Testing sequence for pre-production horizontal stabilizer test box.*

The first damages applied were BVID or "small" damages. These were introduced before the start of testing. Small damages are defined as those which are visible at a distance of less than 5 feet (1.5 m) (threshold of detectability or BVID) or are the result of impacts at an energy level less than 1200 in-lb. (135 J), which is the energy level cutoff used for BVID. The small damages were inflicted at critical locations on the skin panels and spars to verify that the structure was capable of sustaining design Ultimate Loads with BVID present. All BVID were assumed to be undetectable and were not repaired during the test program. After application of BVID, the test box was subjected to two lifetimes of repeated loads that included a 1.15 load enhancement factor to account for potential data scatter in CFRP S-N curves. The second damages applied were "visible" damages. These damages were introduced after the end of the two lifetimes of repeated loads. Visible damages were defined as damages readily detectable during the

scheduled inspection plan, and included dents and small cuts to the skin panels and spars. The visible damages were then subjected to repeated load testing equivalent to two inspection intervals and then to design Limit Loads.

No significant damage growth was detected at any of the BVID or visible damage locations on the test box. Minor amounts of "rounding" of the damage shape and separation of delaminated surfaces were detected early in the load cycling (delaminations where the ply surfaces are in contact are sometimes not detected by NDI). No damage growth occurred thereafter.

7.9.2.5 Damage tolerance - residual strength

Residual strength tests were conducted on sub-components and the pre-production test box to verify required load levels and validate analytical methods. The following sub-component test types were used to demonstrate limit and discrete source level damage capability.

- Five stringer skin panels with disbonded stringer (Limit Load).
- Five stringer skin panels with visible impact damage (Limit Load).
- Five stringer skin panels with a cut skin bay (Limit Load).
- Five stringer skin panels with a cut center stringer and skin bay (continued safe flight load).

The third set of damages applied to the pre-production test box were "element" damages. These damages were introduced after the completion of the repeated loads testing and Limit Load testing of the visible damages discussed above. Element damages were defined as complete or partial failure of one or more structural units. Three damages were applied: a cut stringer and skin bay, a cut front spar chord and adjacent skin, and a cut rear spar chord and adjacent skin. The test box was then subjected to series of "continued safe flight" static load conditions (approximately 70% of the empennage design Limit Loads). No significant damage growth was detected after application of the load conditions.

Analytical methods were used to demonstrate residual strength capability of the 777 empennage structure for the following damage types. The methods were validated by the sub-component and test box results. Environmental effects were accounted for in the damage tolerance analyses by applying factors derived from coupon tests to material property inputs for the analyses.

- Disbonded stringer - load redistribution and crippling analysis.
- Visible impact damage on skin panel - notch fracture analysis.
- Cut skin - notch fracture analysis.
- Cut skin and stringer - notch fracture analysis.
- Cut spar chord and skin - FE load redistribution analysis.

7.9.2.6 Inspection plan

The inspection plan for the 777 empennage is based on visual inspections. Since the "no-growth" approach was adopted and validated, the inspection intervals are based on environmental deterioration and accidental damage ratings (EDRs/ADRs), rather than on damage growth characteristics. A C-check (a comprehensive inspection of installations with maximum access to components and systems) for the 777 is typically performed at 4000 flight cycles or two years, whichever comes first. Typically, external surveillance inspections for the composite structure are scheduled at 2C intervals. Internal surveillance inspections for the composite structure are scheduled at 4C intervals.

7.9.3 General aviation (Raytheon Starship)

7.9.3.1 Introduction

The first airplanes were built of wood, fabric, and resin. In a way, today's composite airplanes are re-turning to those basics, except now, the fibers are carbon and Kevlar and these are set in high tempera-

ture curing epoxy resins. The benefits of modern composite construction are obvious: low weight, high bending stiffness, and the ability to fabricate very large structures with compound curvature. These may be cured in a single piece, eliminating parts, joints, sub-assemblies, and associated inspection costs. The civil airplane certification of composite structures involves all the strength, stiffness, and damage tolerance evaluations normally applied to metallic structures; however, in damage tolerance evaluation of composite structures, although the same *principles* apply as those for metallic structures, the application of these principles must take into account the particular properties of composite structures.

7.9.3.2 *Damage tolerance evaluation*

7.9.3.2.1 *Regulatory basis*

Damage tolerance evaluation has been the norm for Transport Category Airplane structures (metal or composite) certified under Part 25 of the Federal Aviation Regulations since the late 1970's. The Starship was the first airplane to be certified to damage tolerance requirements under Part 23 Small Airplane regulations. Raytheon engineers worked in cooperation with FAA specialists to establish Special Conditions for Fatigue and Damage Tolerance Evaluation which were first published for application specifically to the Starship in 1986. These conditions have since been codified into the main body of Part 23, Federal Aviation Regulations.

The intent of damage tolerance evaluation is the same regardless of the size of the airplane, even though the regulations may contain different wording. In general terms, the intent is to ensure long term safety based on published inspection procedures considering manufacturing quality intrinsic to the processes used and recognizing that certain damage may occur during service.

7.9.3.2.2 *Typical damage scenarios and related requirements*

Three different damage scenarios will normally be considered:

Scenario 1, Initial Quality. This covers items intrinsic to the manufacturing process and the inspection standards. Scenario number 1 represents the as-delivered state and, therefore, the structure must be capable of meeting all requirements in terms of strength, stiffness, safety, and longevity.

Scenario 2, Damage During Assembly or Service. Damage from scenario number 2 must exhibit predictable growth, or no growth, during a period of in-service loading (usually expressed in number of inspection intervals) and must be detectable by the specified in-service inspection methods. Also, the residual strength of the structure with such damage must always be at least equal to the applicable residual strength requirements.

Scenario 3, Damage from Discrete Sources. Damage resulting from scenario number 3 will be obvious to the crew during a flight (or be detected during a preflight inspection) and, therefore, a specific set of residual strength criteria apply which are concerned with safely completing a single flight.

7.9.3.2.3 *Damage source and modes*

Up to this point no details of damage mode, damage magnitude, or structural response have been discussed. It simplifies the evaluation to first recognize the generic scenarios and potential damage sources. Then, from those, identify the possible damage modes and the desired structural response. From the above definitions it is not too difficult to build a matrix such as the one shown in Table 7.9.3.2.3.

The damage modes from scenario 1 are typically not a significant problem from the load capability point of view. However, the potential damage modes from intrinsic manufacturing quality must be identified and controlled by the manufacturing specifications and acceptance criteria. Given this, it is usually easy to demonstrate that these small imperfections will not grow under cyclic loads typical of commercial airplane service.

Scenario 3 imparted damage is at the opposite end of the scale: these modes of damage are easily detectable and will need attention before further flight (except maybe for an authorized ferry flight to a repair facility). Therefore, inspection and longevity are not concerns.

The scenario which creates the most need for investigation is scenario 2, and a typical test program is described in the following section.

7.9.3.2.4 Element testing

To evaluate composite honeycomb structural performance under the various damage modes, element testing is usually performed. It is *possible* to conduct these evaluations on the full scale test articles, but this is a risky approach and the results will be too late to guide the design to a minimum weight and cost configuration.

TABLE 7.9.3.2.3 *Example matrix: damage source and potential modes.*

SCENARIO 1		SCENARIO 2		SCENARIO 3	
Source	Damage Modes	Source	Damage Modes	Source	Damage Modes
Manufacturing process	Small imperfections within the inspection sensitivity and acceptance criteria:	Tools	Resin cracking	Severe lightning	Plies burned
		Baggage	Delamination		Puncture
		Hail	Core crush	Bird strike	Delamination
		Gravel	Puncture		Core crush
	- Porosity - Voids - Disbonds	Lightning	Resin burn	Rotor burst	Puncture
			Delamination		Severed elements
			Loose rivets		
		Water intrusion	Core cell damage	Engine fire	Resin burn
		Cyclic loading	Delamination growth	Ground equipment	Delamination
			Disbond growth	Hangar doors	Puncture
		Bleed air	Resin burn		

Static Tests. Testing to validate tolerance to the damage modes in scenario 2 will include impact tests without puncture, puncture tests of detectable size and larger, water ingress tests with freeze/thaw cycles, and lightning strike tests. Strength testing will be performed for the failure modes shown to be critical based on the internal loads analysis, typically a finite element analysis.

The static strength portion of the element test matrix is shown in Table 7.9.3.2.4(a).

A larger number of undamaged specimens may be tested at a selected loading in order to validate the laminate analyses by comparison of mean and B-basis test results to analytical predictions. This may also be desirable in order to establish that undue variability is not introduced by a particular manufacturing process.

Cyclic Tests. The test matrix for cyclic loading follows the same pattern, except now loading at multiple stress levels is desirable to establish the sensitivity of flaw growth to cyclic stress level. Again an in-

creased number of specimens may be tested at a selected condition to identify variability, in this case as it affects flaw growth. Generally, cyclic testing of undamaged composite panels is not of great interest. Also, composite panels are less sensitive to flaw growth under tensile loading. This insensitivity can be demonstrated by testing at a constant amplitude of 67 percent of the maximum stress test result from similar specimens under static tensile loading, see Table 7.9.3.2.4(b). In addition to constant amplitude stress level testing, spectrum loads representing lifetime varying amplitude loads should be tested as there is, today, no industry-wide acceptance of analytical methods predicting flaw growth rates under lifetime variable amplitude loading.

Pressure Cabin Shell Residual Strength. Honeycomb construction has a particular advantage in maintaining residual strength after incurring large size damage from sources such as those described scenario 3. This is due to the honeycomb shell stiffness imparting great resistance to crack bulging which in thin skin structures is a source of high crack extension forces. Tests to validate residual strength in the presence of large puncture damage are usually conducted on cylinder wall samples loaded to simulate internal pressure or a combination of pressure and shear.

TABLE 7.9.3.2.4(a) *Element test matrix--static loading.*

TEST TYPE/ DAMAGE MODE	TENSION (Fuselage Top)		COMPRESSION (Fuselage Bottom)	SHEAR (Fuselage Side)
	Hoop	Longitudinal		
Undamaged	3	3	12	3
Impact	3	3	3	3
Detectable Puncture	3	3	3	3
Large Puncture	3	3	3	3

NOTE: Numbers in cells indicate number of replicates.

TABLE 7.9.3.2.4(b) *Element test matrix - cyclic loading.*

STRESS LEVEL	TENSION			COMPRESSION				SHEAR		
	1	2	3	1	2	3	Spectrum Loading	1	2	3
Impact	3			3	3	3	3	3	3	3
Detectable Puncture	3			3	12	3	3	3	3	3

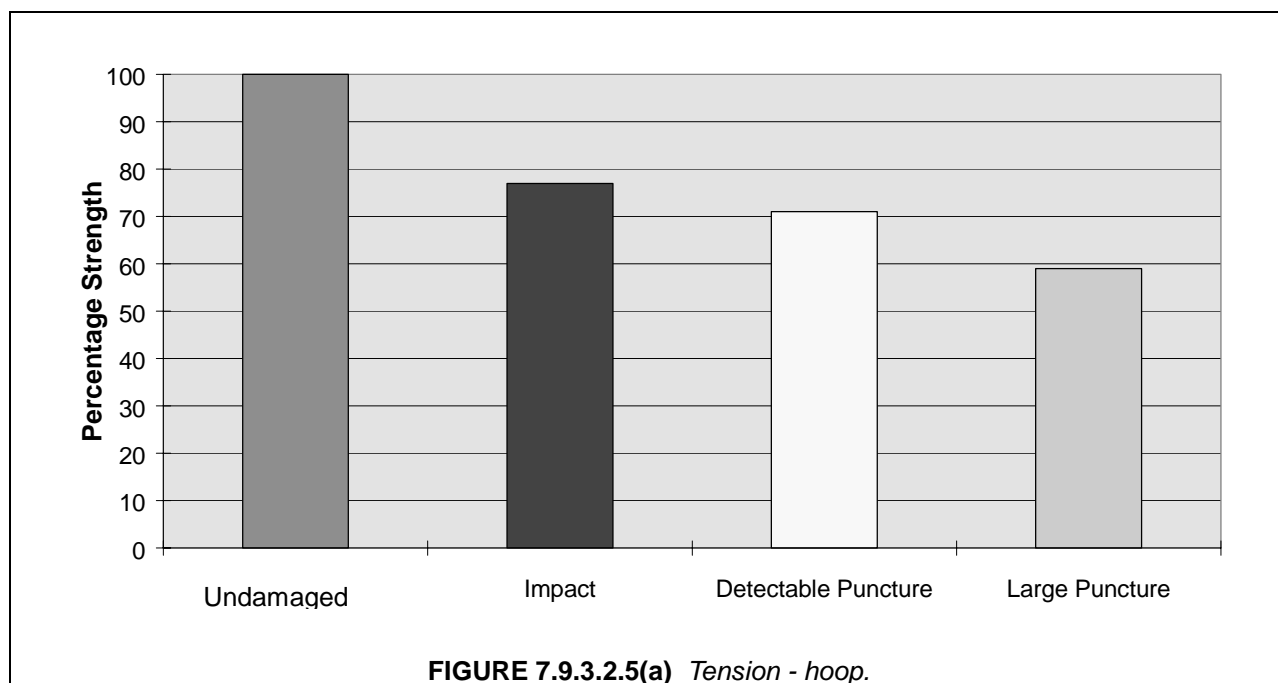
NOTE: Numbers in cells indicate number of replicates.

7.9.3.2.5 Test results

Selected examples of element test results in typical presentation formats are shown in the following figures. The results shown were obtained from samples representing fuselage shell construction on a business jet. However, scale matters, and different results might be obtained from tests on samples rep-

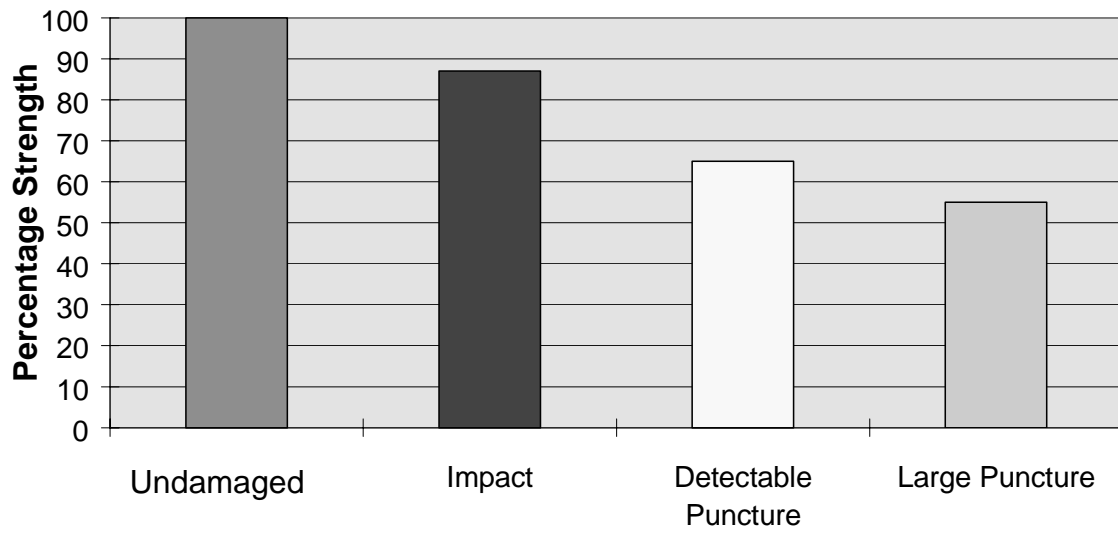
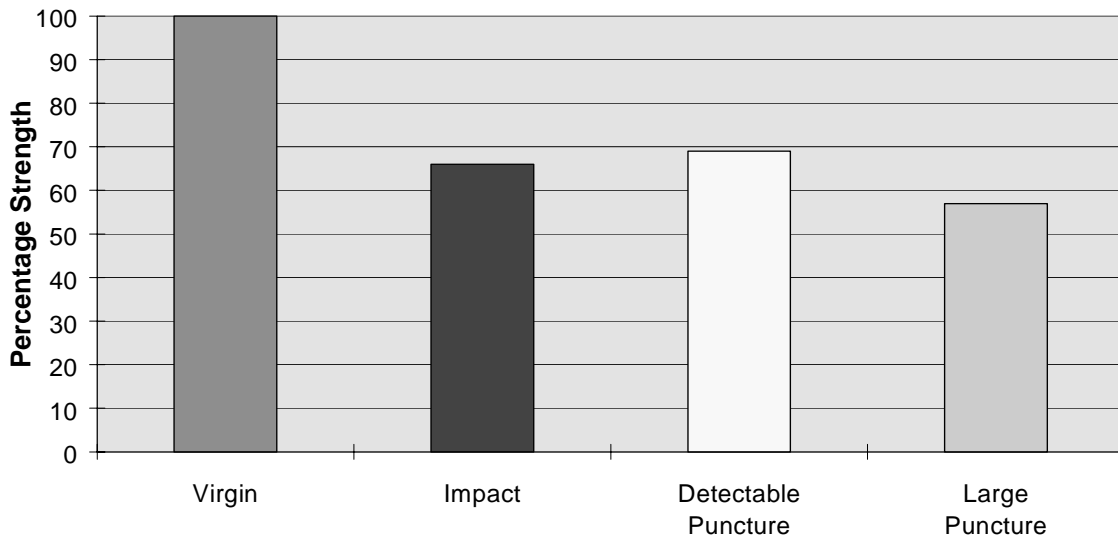
resenting large transport airplanes because of different face sheet thicknesses and core densities required to carry the basic pressure and bending loads.

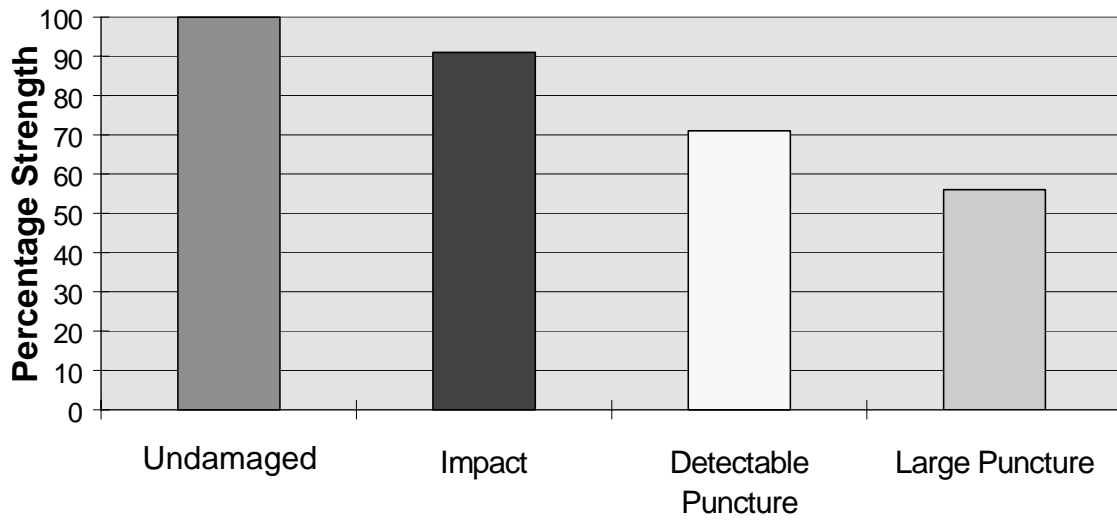
Tension. From Figure 7.9.3.2.5(a), hoop tensile loading from internal pressure, it's clear that designing for damage tolerance need not impose a serious weight penalty. Ultimate design pressure must be carried with the undamaged panel and this means that just a little additional material will enable the panel to meet the required residual strength load with large puncture damage. This is because residual strength required for the pressure case is about 60 percent of the ultimate pressure. In the case of longitudinal tensile loading from fuselage bending, Figure 7.9.3.2.5(b), the residual strength requirement is Limit Load, i.e., about 67 percent of the ultimate pressure, and again to carry that load with a large puncture a small amount of material must be added. In both cases a more robust structure would result if Ultimate Loads were to be carried with impact damaged panels. And this may be required by the regulations unless impact damage is readily detectable.



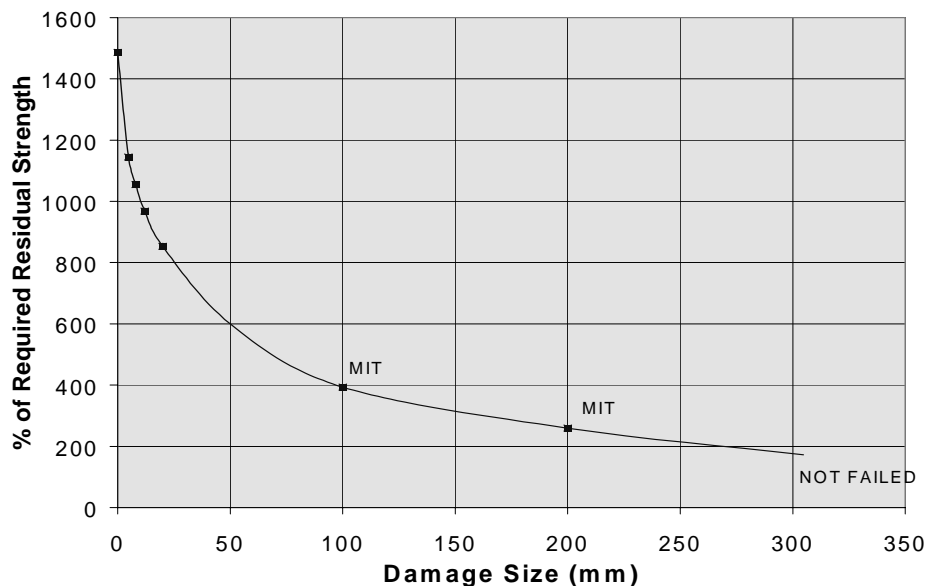
Compression. As shown in Figure 7.9.3.2.5(c), a similar situation exists in the case of compressive loading from fuselage bending. Designing to the residual strength requirement with large puncture damage would imply using approximately 85 percent of the allowable undamaged strength; but if impact damage is to be good for Ultimate Load then only 65 percent of the undamaged strength will be used. This may not be a serious penalty as the maximum compressive loads occur in the fuselage bottom from down-bending load cases and the lower fuselage is usually reinforced by cargo or passenger floor structure.

Shear. Maximum shear loading occurs along the side of the fuselage. Again, designing to carry Limit Load (67 percent of Ultimate Load) with large puncture damage is a slight weight penalty, approximately 82 percent of the maximum undamaged strength can be used. But in this case, 82 percent of undamaged strength will accommodate impact damage at Ultimate Load. This is illustrated in Figure 7.9.3.2.5(d).

**FIGURE 7.9.3.2.5(b)** *Tension - longitudinal.***FIGURE 7.9.3.2.5(c)** *Compression.*

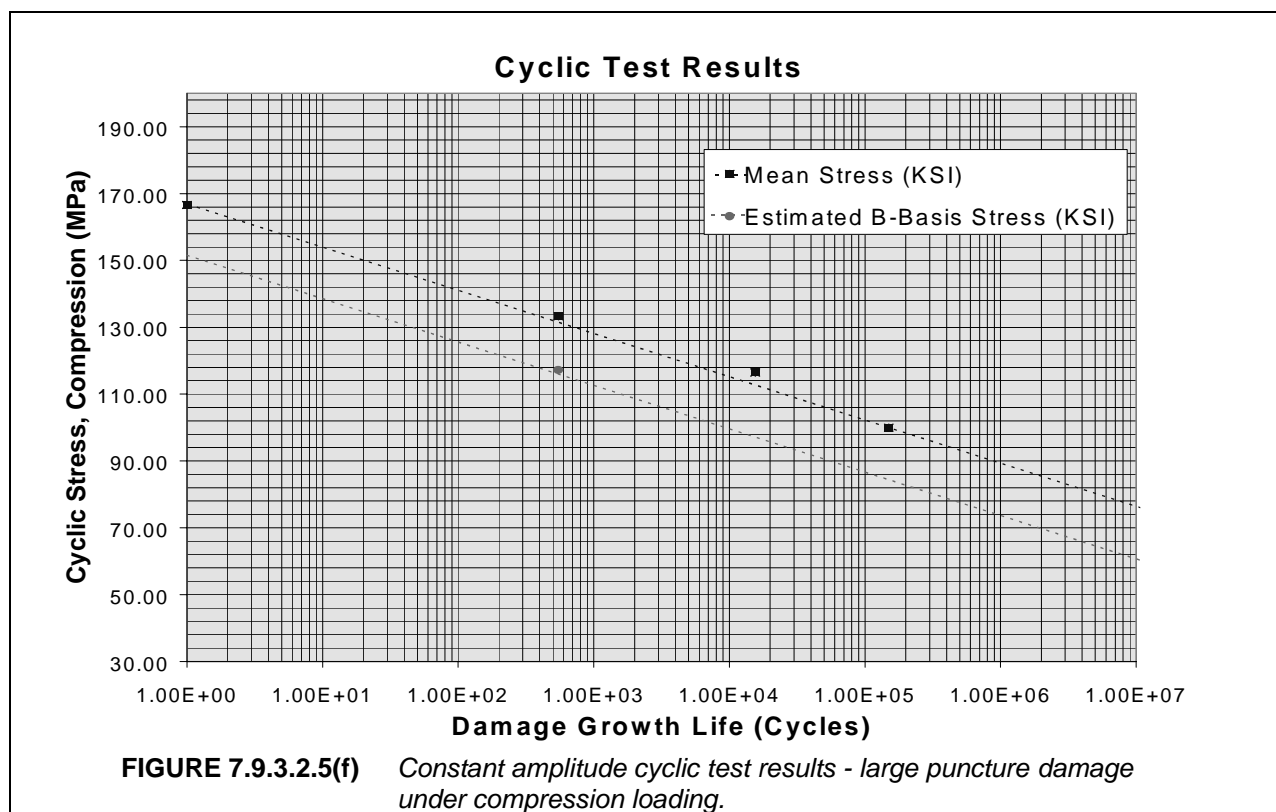
FIGURE 7.9.3.2.5(d) *Shear.*

Pressure Cylinder Results. Figure 7.9.3.2.5(e) presents an assemblage of test results illustrating the trend from no damage to massive damage. Massive damage being the type of wall puncture that could only occur from a serious collision with ground support equipment such as steps, generator carts, refueling equipment, baggage handling equipment, and so on. As mentioned previously, this type of damage should be obvious and should be detected before flight, but, just in case... tests are conducted to determine cylinder wall residual strength with large and obvious damage. The test points indicated as MIT in Figure 7.9.3.2.5(e) are from honeycomb wall cylinders tested at MIT, see Reference 7.9.3.2.5. The trend revealed is typical of test results from big and small airplane pressure containment structure in that with larger and larger damage a residual strength threshold becomes apparent.

FIGURE 7.9.3.2.5(e) *Cylinder wall test results (internal pressure).*

Cyclic Test Results. An example is presented in Figure 7.9.3.2.5(f) of typical constant amplitude test results for large puncture damage under constant amplitude compressive loading. The most useful presentation for these data is as shown, i.e., a best-fit straight line. This type of plot can be used to assess important damage tolerance characteristics of the materials tested. The significance of scatter in flaw growth life can be assessed by plotting a B-basis stress-life line assumed to be parallel to the mean life plot. The flaw growth threshold may then be determined by extrapolation of the B-basis life line to ten million cycles (100 million in the case of rotating equipment with high cycle loading).

A prime use of these data is to structure the full scale cyclic test to run in an economical, yet rational, manner. All stress cycles below the flaw growth threshold may be eliminated from the full scale test spectrum. Also, scatter in flaw growth life may be accounted for by a factor increasing the applied loads and, therefore, reducing the number of test lifetimes.



7.9.3.2.6 Full scale tests

Full Scale Cyclic Tests. Certification of major load carrying structure requires that components such as wings, fuselages, and tail structures are tested through a sequence of loads representing at least two lifetimes of expected missions. Each lifetime consists of thousands of load cycles, including wing lift, fuselage reactions, tail loads, pressure cycles, and landing loads. During these tests damage will be mechanically inflicted in the structure to simulate in-service damage. These situations include lightning strike, hail damage, runway damage, and tool impacts. These damage modes will be tested through as much as one lifetime of fatigue testing to prove that the structure is, in fact, damage tolerant in the full size articles, i.e., that damage will not grow in an unpredictable manner and will always be detected by the inspections specified.

Larger damage may be inflicted later in the full scale cyclic testing to simulate impacts with ground service equipment, impacts with hangar doors and other aircraft (hangar rash) and poor maintenance practices; all bad things that occasionally happen in the loading, handling, and maintenance of commercial airplanes. The larger damage modes should be detected before the next flight and so the demonstration for these modes may consist of a relatively few flights of cyclic loading and inclusion in the residual strength tests.

Full Scale Residual Strength Tests. After completion of the lifetimes of cyclic testing, the major components of wing, fuselage and tail will be subjected to load tests to verify that, in spite of all the load cycles and inflicted damage, the remaining structure will still carry the required residual strength loads (flight loads and/or pressure loads expected to be encountered during the service life of the aircraft, except for the larger damage modes which are associated with specific residual strength criteria).

7.9.3.2.7 Continued airworthiness inspections

Based on interpretation of the test results obtained, inspection procedures, threshold time, and frequency of inspections will be established and published in the airplane manuals. A factor is usually applied so that allowance is made for the damage to exist over several inspection intervals, depending on the criticality of the structure. A further factor may be needed to account for scatter revealed in the flaw growth test results.

7.9.3.3 Service experience

The service experience with primary composite structures in civil aviation has been excellent. Beech Starships have been flying since the late 80's and no problems with major structure have been encountered. Composite stabilizer structures have been in use on Beech 1900 commuters flying typically 2500 hours per year since the mid 80's; again no problems related to the composites have been reported.

Safety in the event of an emergency landing has also proven to be outstanding. A nose landing gear collapsed during a landing of one of the Starship test airplanes; the airplane was flown home and was back in service in 10 days. The repairs were made by procuring blank parts from the factory, cutting out the needed replacement sections, and splicing these into place by bonding and fastening.

An even more spectacular event occurred in Denmark in February, 1994. Starship number 35 ran off the runway into a snow bank at approximately 130 mph (210 km/hr) after an aborted take off. Crew and passengers were shaken but otherwise unhurt. No fuel was spilled, no seats came loose, no windshield or window glass was broken, or even cracked, and the cabin was undistorted enabling the cabin door to open normally. The crew and passengers unbuckled their seat belts and walked away. The right hand main gear collapsed, the other main gear and the nose gear were sheared off (not torn out, but the aluminum forgings severed) from the force of hitting the snow bank at high speed. The right hand wing tip was dragged along the ground and as a result suffered damage to the flaps, tip sail, and rudder. The nose section was damaged by the nose gear being severed and forced upward into the structure. The cabin underbelly was crushed through skidding along without the landing gear but the damage was localized to the area between the seats.

A team was sent to survey the damage and list the replacement parts needed. Later the airplane was repaired on-site by a crew of five technicians plus one engineer, one inspector, and one service manager. Some parts with localized damage were repaired using techniques published in the Starship Structural Repair Manual which allows damage to be repaired on-site by trained service staff. For more extensive damage, blank parts were delivered from the factory and were used as stock from which to cut replacement panels which were then bonded and/or fastened into place. Of course, aircraft systems such as landing gear, hydraulics, antennae, etc., were simply replaced with factory spare parts. The repairs were finished and the airplane rolled out for flight test in July of 1994. This was ahead of schedule and under budget, much to the surprise of the insurance company and the Danish aviation authorities who were both convinced that a metal airplane would have suffered much greater damage and would have been totaled by such an incident.

7.9.3.4 *Conclusions*

Modern manufacturing methods enable the fabrication of composite primary load carrying structures for commercial aircraft use which are low cost as well as low weight. These structures require a damage tolerance evaluation for certification to Part 23 or Part 25 of the FAA regulations. A rational damage scenario and a supporting element test program will considerably assist the damage tolerance evaluation.

Composite structures can be designed to tolerate large damage with a small weight penalty. It may not be required to design to carry Ultimate Loads after impact damage (it depends on the inspections specified). However, a more robust product will result when composite structures are designed to carry Ultimate Load with impact damage. In fact, the FAR 23 regulations are quite specific in this area and require Ultimate Load capability with impact damage at the level of detectability based on the inspection methods.

Composite structures are relatively insensitive to cyclic loading, and a flaw growth threshold may be defined from the test results. Scatter in flaw growth life should be examined in order to establish a relationship between test lifetimes and service lifetimes for full scale cyclic testing. This will also enable the full scale tests to be conducted more economically than on equivalent metal structures.

With the combination of careful analysis, rational testing, and advanced manufacturing techniques, further civil airplane applications of composite primary structures can be expected.

7.9.4 Military aircraft

Reserved for future use.

REFERENCES

- 7.2 Goranson, U.G., "Damage Tolerance Facts and Fiction," 14th Plantema Memorial Lecture presented at the 17th Symposium of the International Committee on Aeronautical Fatigue, Stockholm, June, 1993.
- 7.2.1(a) FAA Advisory Circular 20-107A, "Composite Aircraft Structure," April 25, 1984.
- 7.2.1(b) Whitehead, R.S., Kan, H.P., Cordero, R., and Seather, E.S., "Certification Methodology for Composite Structures," Volumes I and II, Report No. NADC-87042-60, October 1986.
- 7.2.1(c) Whitehead, R. S., "Certification of Primary Composite Aircraft Structures," ICAF Conference, Ottawa, Canada, 1987.
- 7.2.1(d) "Advanced Certification Methodology for Composite Structures," Report No. DOT/FAA/AR-96/111 or NAWCADPAX-96-262-TR, April 1997.
- 7.2.2.3(a) Quinlivan, J.T., Kent, J.A., and Wilson, D.R., "NASA-ACEE/Boeing 737 Graphite/Epoxy Horizontal Stabilizer Service," 9th DoD/NASA Conference on Fibrous Composite in Structural Design, 1991.
- 7.2.2.3(b) McCarty, J.E., Johnson, R.W., and Wilson, D.R. "737 Graphite/Epoxy Horizontal Stabilizer Certification," AIAA Paper 82-0745.
- 7.2.2.3(c) Schreiber, K.H., and Quinlivan, J.T., "The Boeing 777 Empennage," Presented at ICCM-9 Madrid 1993.
- 7.2.2.3(d) Takai, J., et.al., "CFRP Horizontal Stabilizer Development Test Program," Presented at ICCM-9, Madrid 1993.
- 7.2.2.3(e) Tropis, A., Thomas, M., Bounie, J.L., Lafon, P., "Certification of the Composite Outer Wing of the ATR 72," I Mech E, 1993.
- 7.2.2.3(f) Williams, J.G., O'Brien, T.K., and Chapman, A.C., "Comparison of Toughened Composite Laminates Using NASA Standard Damage Tolerance Tests," NASA CP 2321, Proceedings of the ACEE Composite Structures Technology Conference, Seattle, WA, August, 1984.
- 7.2.2.3(g) Carlile, D.R., and Leach, D.C., "Damage and Notch Sensitivity of Graphite/PEEK Composite," Proceedings of the 15th National SAMPE Technical Conference, October, 1983, pp. 82-93.
- 7.2.2.3(h) Hall, J., and Goranson, U.G., "Principles of Achieving Damage Tolerance With Flexible Maintenance Programs for New and Aging Aircraft," presented at 13th Congress of the International Council of the Aeronautical Sciences/AIAA Aircraft Systems, Seattle, WA, August 26, 1982.
- 7.2.2.3(i) ACJ25.571 (a) "Damage Tolerance and Fatigue Evaluation of Structure (Acceptable Means of Compliance)," Dec. 18, 1985.
- 7.2.2.3(j) Dost, E., Avery, W., Finn, S., Grande, D., Huiskens, A., Ilcewicz, L., Murphy, D., Scholz, D., Coxon, B., and Wishart, R., "Impact Damage Resistance of Composite Fuselage Structure," NASA CR-4658, 1996.
- 7.2.2.3(k) Walker, T., Scholz, D., Flynn, B., Dopker, B., Bodine, J., Ilcewicz, L., Rouse, M., McGowan, D., and Poe, C., Jr., "Damage Tolerance of Composite Fuselage Structure," Sixth NASA/DOD/ARPA Advanced Composite Technology Conference, NASA CP-3326, 1996.

- 7.2.2.3(l) Ilcewicz, L., Smith, P., Olson, J., Backman, B., Walker, T., and Metschan, S., "Advanced Technology Composite Fuselage," Sixth NASA/DOD/ARPA Advanced Composite Technology Conference, NASA CP-3326, 1996.
- 7.2.2.4(a) Rouchon, J., "Certification of Large Airplane Composite Structures, Recent Progress and New Trends in Compliance Philosophy," 17 ICAS Congress, Stockholm 1990.
- 7.2.2.4(b) Rouchon, J., "How to Address the Situation of the No-Growth Concept in Fatigue, with a Probabilistic Approach - Application to Low Velocity Impact Damage with Composites," ICAF 97, Edinburgh, Composite Workshop on Certification Issues.
- 7.2.2.5 "Development of Probabilistic Design Methodology for Composite Structures," Report DOT/FAA/AR-95/17, August 1997.
- 7.3.2(a) Gottesman, T. and Mickulinski, M., "Influence of Matrix Degradation on Composite Properties in Fiber Direction," Engineering Fracture Mechanics, Vol 20, No. 4, 1984, pp. 667- 674.
- 7.3.2(b) Horton, R. E. and McCarty, J. E. "Damage Tolerance of Composites," Engineering Materials Handbook, Vol 1, Composites, ASM International, ISBN 0-87170-279-7, 1987.
- 7.3.2(c) Whitehead, R. S., "Certification of Primary Composite Aircraft Structures," ICAF Conference, Ottawa, Canada, 1987.
- 7.3.3(a) "Advanced Certification Methodology for Composite Structures," Report No. DOT/FAA/AR-96/111 or NAWCADPAX-96-262-TR, April 1997.
- 7.3.3(b) "Development of Probabilistic Design Methodology for Composite Structures" Report DOT/FAA/AR-95/17, August 1997.
- 7.3.3(c) Tropis A., Thomas M., Bounie J.L., Lafon P., "Certification of the Composite Outer Wing of the ATR 72," I Mech E, 1993.
- 7.4.1(a) FAA Advisory Circular 20-107A, "Composite Aircraft Structure," April 25, 1984
- 7.4.1(b) "Substantiation of Composite Parts - Impact Detectability Criteria," Aerospatiale Report No. 440 225/91.
- 7.4.1(d) Thomas, M. "Study of the Evolution of the Dent Depth Due to Impact on Carbon/Epoxy Laminates, Consequences on Impact Damage Visibility and on in Service Inspection Requirements for Civil Aircraft Composite Structures," presented at MIL-HDBK 17 meeting, March 1994, Monterey, CA.
- 7.4.1(d) Komorowski, J.P., Gould, R.W., Simpson, D.L., "Synergy Between Advanced Composites and New NDI Methods," a paper from the Structures, Materials and Propulsion Laboratory, Institute for Aerospace Research, National Research Council of Canada.
- 7.4.2.2 Dost, E.F., Finn, S.R., Stevens, J.J., Lin, K.Y., and Fitch, C. E., "Experimental Investigations into Composite Fuselage Impact Damage Resistance and Post-Impact Compression Behavior," Proc. of 37th International SAMPE Symposium and Exhibition, Soc. for Adv. of Material and Process Eng., 1992.
- 7.5.1.1(a) Richardson, M.D.W., Wisheart, M.J., "Review of Low Velocity Impact Properties of Composite Material," Composites, Part A, 27A, 1996, pp. 1123-1131.

Volume 3, Chapter 7 - Damage Resistance, Durability, and Damage Tolerance

- 7.5.1.1(b) Abrate, S., "Impact on Laminated Composite Materials," *Composites*, Vol 24, No. 3, 1991, pp. 77-99.
- 7.5.1.1(c) Abrate, S., "Impact on Laminated Composites: Recent Advances," *Applied Mechanics Review*, Vol 47, No. 11, 1994, pp. 517-544.
- 7.5.1.1(d) Cantwell, W.J., and Morton, J., "The Impact Resistance of Composite Materials," *Composites*, Vol 22, No. 5, 1991, pp. 55-97.
- 7.5.1.1(e) Rhoades, M.D., Williams, J.G., and Starnes, J.H., Jr., "Effect of Impact Damage on the Compression Strength of Filamentary - Composite Hat -Stiffened Panels," *Society for the Advancement of Material and Process Engineering*, Vol 23, May, 1978.
- 7.5.1.1(f) Rhoades, M.D., Williams, J.G., and Starnes, J. H., Jr., "Low Velocity Impact Damage in Graphite-Fiber Reinforced Epoxy Laminates," *Proceedings of the 34th Annual Technical Conference of the Reinforced Plastics/Composites Institute, The Society of the Plastics Industry, Inc.* 1979.
- 7.5.1.1(g) Byers, B.A., "Behavior of Damaged Graphite/Epoxy Laminates Under Compression Loading," *NASA Contractor Report 159293*, 1980.
- 7.5.1.1(h) Smith, P.J., and Wilson, R.D., "Damage Tolerant Composite Wing Panels for Transport Aircraft," *NASA Contractor Report 3951*, 1985.
- 7.5.1.1(i) Madan, R.C., "Composite Transport Wing Technology Development," *NASA Contractor Report 178409*, 1988.
- 7.5.1.1(j) Horton, R., Whitehead, R., et al, "Damage Tolerance of Composites - Final Report," *AF-WAL-TR-87-3030*, 1988.
- 7.5.1.1(k) Horton, R.E., "Damage Tolerance of Composites: Criteria and Evaluation," *NASA Workshop on Impact Damage to Composites*, NASA CP 10075, 1991, pp. 421-472.
- 7.5.1.1(l) Dost, E. F., Avery, W.B., Finn, S.R., Grande, D.H., Huisken, A.B., Ilcewicz, L.B., Murphy, D.P., Scholz, D.B., Coxon, R., and Wishart, R.E., "Impact Damage Resistance of Composite Fuselage Structure," *NASA Contractor Report 4658*, 1997.
- 7.5.1.1(m) Dost, E.F., Finn, S.R., Stevens, J.J., Lin, K.Y., and Fitch, C. E., "Experimental Investigations into Composite Fuselage Impact Damage Resistance and Post-Impact Compression Behavior," *Proc. of 37th International SAMPE Symposium and Exhibition, Soc. for Adv. Of Material and Process Eng.*, 1992.
- 7.5.1.1(n) Scholz, D.B., Dost, E.F., Flynn, B.W., Ilcewicz, L.B., Lakes, R.S., Nelson, K.M., Sawicki, A.J., and Walker, T.W., "Advanced Technology Composite Fuselage-Materials and Processes," *NASA Contractor Report 4731*, 1997.
- 7.5.1.2 Walker, T. H., Avery, W. B., Ilcewicz, L. I., Poe, C. C., Jr., and Harris, C. E., "Tension Fracture of Laminates for Transport Fuselage - Part I: Material Screening," *Second NASA Advanced Technology Conference*, NASA CP 3154, pp. 197-238, 1991.
- 7.5.1.3(a) Dorey, G., Sidey, G.R., and Hutchings, J., "Impact Properties of Carbon Fibre/Kevlar49 Fibre Hybrid Composites," *Composites*, January 1978, pp. 25-32. old 5.8.1-a
- 7.5.1.3(b) Noyes, J.V., et al, "Wing/Fuselage Critical Component Development Program," Phase I Preliminary Structural Design, Interim Report for the Period 1 Nov. 1977 - 31 Jan. 1978. old 5.8.1-b

- 7.5.1.3(c) Rhodes, Marvin D., and Williams, Jerry G., "Concepts for Improving the Damage Tolerance of Composite Compression Panels," *5th DOD/NASA Conference on Fibrous Composites in Structural Design*, January 27-29, 1981. old 5.8.1-c
- 7.5.1.3(d) Nishimura, A., Ueda, N., and Matsuda, H.S., "New Fabric Structures of Carbon Fiber," Proceedings of the 28th National SAMPE Symposium, April 1983, pp. 71-88. old 5.8.1-d
- 7.5.1.3(e) Masters, J. E., "Characterization of Impact Damage Development in Graphite/Epoxy Laminates," Fractography of Modern Engineering Materials: Composites and Metals, ASTM STP 948, ASTM, Philadelphia, Pa., 1987.
- 7.5.1.3(f) Evans, R.E., and Masters, J.E., "A New Generation of Epoxy Composites for Primary Structural Applications: Materials and Mechanics," Toughened Composites, ASTM STP 937, ASTM, Philadelphia, Pa., 1987.
- 7.5.1.3(g) Poe, C.C., Jr., Dexter, H.B., and Raju, I.S., "A Review of the NASA Textile Composites Research," Presented at 38th Structures, Structural Dynamics, and Materials Conference, AIAA paper No. 97-1321, April 7-10, 1997.
- 7.5.1.3(h) Sharma, Suresh K., and Sankar, Bhavani, V., "Effects of Through-the-Thickness Stitching on Impact and Interlaminar Fracture Properties of Textile Graphite/Epoxy Laminates," NASA Contractor Report 195042, University of Florida, Gainesville, Florida, February, 1995.
- 7.5.1.3(i) Jackson, W.C., and Poe, C.C., Jr., "The Use of Impact Force as a Scale Parameter for the Impact Response of Composite Laminates," *Journal of Composites Technology & Research*, Vol 15, No. 4, Winter 1993, pp. 282-289.
- 7.5.1.4 Poe, C.C., Jr., "Impact Damage and Residual Tension Strength of a Thick Graphite/Epoxy Rocket Motor Case," *Journal of Spacecraft and Rockets*, Vol 29., No. 3, May-June 1992, pp. 394-404.
- 7.5.1.6(a) Lloyd, B.A., and Knight, G.K., "Impact Damage Sensitivity of Filament - Wound Composite Pressure Vessels," 1986 JANNAF Propulsion Meeting, CPIA Publication 455, Vol 1, Aug. 1986, pp. 7-15.
- 7.5.1.6(b) Jackson, Wade C., Portanova, Marc A., and Poe, C. C., Jr., "Effect of Plate Size on Impact Damage," Presented at Fifth ASTM Symposium on Composite Materials in Atlanta, GA., May 4-6, 1993.
- 7.5.1.7 Smith, P.J., Thomson, L.W., and Wilson, R. D., "Development of Pressure Containment and Damage Tolerance Technology for Composite Fuselage Structures in Large Transport Aircraft," NASA Contractor Report 3996, 1986.
- 7.5.2 AFGS-87221A (Previously MIL-A-87221) General Specification for Aircraft Structures.
- 7.6.1 Whitehead, R.S., Kan, H. P., Cordero, R., and Saether, E. S., "Certification Testing Methodology for Composite Structures," Volumes I and II, Report No. NADC-87042-60 (DOT/FAA/CT-86-39), October 1986.
- 7.6.3 Sendekyj, G. P., "Fitting Models to Composite Materials Fatigue Data," ASTM STP 734, 1981, pp 245-260.
- 7.6.4 Sanger, K. B., "Certification Testing Methodology for Composite Structures," Report No. NADC-86132-60, January 1986.

- 7.6.5(a) Ratwani, M.M. and Kan H.P., "Compression Fatigue Analysis of Fiber Composites," NADC-78049-60, September 1979.
- 7.6.5(b) Ratwani, M.M. and Kan H.P., "Development of Analytical Techniques for Predicting Compression Fatigue Life and Residual Strength of Composites," NADC-82104-60, March 1982.
- 7.6.5(c) Jeans, L.L., Grimes, G.C., and Kan, H.P. "Fatigue Spectrum Sensitivity Study for Advanced Composite Materials," AFWAL-TR-80-3130, Volume I-III, November 1980.
- 7.6.5(d) Whitehead, R. S., et al., "Composite Wing/Fuselage Program," Volume I-IV, AFWAL-TR-88-3098, August 1989.
- 7.6.5(e) Horton, R. E., Whitehead, R. S., et al., "Damage Tolerance of Composites," Volumes I – III, AFWAL-TR-87-3030, July 1988.
- 7.7.1(a) Lorient G. Ansart Th., "Fatigue damage behaviour and post-failure analysis in new generation of composite materials" Test Report No. S-93/5676000.
- 7.7.1(b) Ireman T., Thesken J.C., Greenhalgh E., Sharp R., Gädke M., Maison S., Ousset Y., Roudolff F., La Barbera A., "Damage Propagation in Composite Structural Element-Coupon Experiment and Analyses" - Garteur collaborative programme (1996), *Composite Structures*, v. 36, pp. 209-220, Elsevier Science Ltd.
- 7.7.4.2.1 Wilkens, D.J., Eisenmann, J.R., Camin, R.A., Margolis, W.S., and Benson, W.A., "Characterizing Delamination Growth in Graphite Epoxy," *Damage in Composite Materials*, ASTM STP 775, Edited by K.L. Reifsnider, American Society for Testing and Materials, 1982, pp. 168-183.
- 7.8.1.2.1(a) Dorey, G., Sidey, G.R., and Hutchings, J., "Impact Properties of Carbon Fibre/Kevlar49 Fibre Hybrid Composites," *Composites*, January 1978, pp. 25-32.
- 7.8.1.2.1(b) Nishimura, A., Ueda, N., and Matsuda, H.S., "New Fabric Structures of Carbon Fiber," *Proceedings of the 28th National SAMPE Symposium*, April 1983, pp. 71-88.
- 7.8.1.2.1(c) Noyes, J.V., et al, "Wing/Fuselage Critical Component Development Program," Phase I Preliminary Structural Design, Interim Report for the Period 1 Nov. 1977 - 31 Jan. 1978.
- 7.8.1.2.1(d) Rhodes, Marvin D., and Williams, Jerry G., "Concepts for Improving the Damage Tolerance of Composite Compression Panels," 5th DOD/NASA Conference on Fibrous Composites in Structural Design, January 27-29, 1981.
- 7.8.1.2.2(a) Dost, E.F., Ilcewicz, L.B., Avery, W.B., and Coxon, B.R., "Effects of Stacking Sequence on Impact Damage Resistance and Residual Strength for Quasi-Isotropic Laminates," *Composite Materials: Fatigue and Fracture (Third Volume)*, ASTM STP 1110, T.K. O'Brien, Ed., American Society for Testing and Materials, Phil., 1991, pp. 476-500.
- 7.8.1.2.2(b) Dost, E.F., Ilcewicz, L.B., and Gosse, J.H., "Sublaminar Stability Based Modeling of Impact Damaged Composite Laminates," in *Proc. of 3rd Tech. Conf. of American Society for Composites*, Technomic Publ. Co., 1988, pp. 354-363.
- 7.8.1.2.2(c) Ilcewicz, L.B., Dost, E.F., and Coggeshall, R.L., "A Model for Compression After Impact Strength Evaluation," in *Proc. of 21st International SAMPE Tech. Conf., Soc. for Adv. of Material and Process Eng.*, 1989, pp. 130-140.

Volume 3, Chapter 7 - Damage Resistance, Durability, and Damage Tolerance

- 7.8.1.2.2(d) Gosse, J.H., and Mori, P.B.Y., "Impact Damage Characterization of Graphite/Epoxy Laminates," in Proc. of 3rd Tech. Conf. of American Society for Composites, Technomic Publ. Co., 1988, pp. 344-353.
- 7.8.1.2.3 Horton, R.E., and Whitehead, R.S., "Damage Tolerance of Composites," Vol I. Development of Requirements and Compliance Demonstration," AFWAL-TR-87-3030, July 1988.
- 7.8.1.2.4(a) Scholz, D., et al., "Advanced Technology Composite Fuselage - Materials and Processes," NASA CR-4731, 1997.
- 7.8.1.2.4(b) Ward, S. H., and H. Razi, "Effect of Thickness on Compression Residual Strength of Notched Carbon Fiber/Epoxy Composites," 28th International SAMPE Technical Conference, Seattle, WA. November 4-7, 1996.
- 7.8.1.2.7 Portanova, Marc, "Impact Testing of Textile Composite Materials," Proceedings of Textile Mechanics Conference, NASA Langley Research Center, Hampton, VA., NASA CP-3311, Dec. 6-8, 1984.
- 7.8.1.2.8(a) Chai, H., and Babcock, C.D., "Two-Dimensional Modeling of Compressive Failure in Delaminated Laminates," J. Composite Materials, 19, 1985, pp. 67-98.
- 7.8.1.2.8(b) Whitcomb, J.D., "Predicted and Observed Effects of Stacking Sequence and Delamination Size on Instability Related Delamination Growth," J. Composite Technology and Research, 11, 1989, pp. 94-98.
- 7.8.1.2.8(c) Cairns, Douglas S. "Impact and Post-Impact Response of Graphite/Epoxy and Kevlar/Epoxy Structures," Technology Laboratory for Advanced Composites (TELAC), Dept. Of Aeronautics and Astronautics, Massachusetts Institute of Technology, Cambridge, MA, TELAC Report 87-15, August 1987.
- 7.8.1.2.8(d) Lekhnitskii, S.G., "Anisotropic Plates," Gordon and Breach Science Publishers, New York, N.Y., 1968, Chapter VI-43.
- 7.8.1.2.8(e) Awerbuch, J., and Madhukar, M.S., "Notched Strength of Composite Laminates : Predictions and Experiments - A Review," J. of Reinforced Plastics and Composites, 4, 1985, pp. 1-159.
- 7.8.1.2.8(f) Poe, C.C., Jr., "A Parametric Study of Fracture Toughness of Fibrous Composite Materials," J. of Offshore Mechanics and Arctic Eng., Vol III, 1989, pp. 161-169.
- 7.8.1.2.8(g) Walker, T.H., Minguet, P.J., Flynn, B.W., Carbery, D.J., Swanson, G.D., and Ilcewicz, L.B., "Advanced Technology Composite Fuselage - Structural Performance," NASA Contractor Report 4732, 1997.
- 7.8.1.2.8(h) Dopker, B., Murphy, D., Ilcewicz, L.B., and Walker, T., "Damage Tolerance Analysis of Composite Transport Fuselage Structure," 35th AIAA/ASME/ASCE/AHS/ASC Structures, Structural Dynamics, & Materials Conference, AIAA Paper 94-1406, 1994.
- 7.8.1.2.8(i) Ilcewicz, L.B., Walker, T.H., Murphy, D.P., Dopker, B., Scholz, D.B., and Cairns, D.S., and Poe, C.C., Jr., "Tension Fracture of Laminates for Transport Fuselage - Part 4: Damage Tolerance Analysis," Fourth NASA/DoD Advanced Composite Technology Conference, NASA CP-3229, 1993, pp. 265-298.
- 7.8.1.2.9(a) Lagace, P.A., and Cairns, D.S., "Tensile Response of Laminates to Implanted Delaminations," Advanced Materials Technology "87, SAMPE, April 1987, pp. 720-729.

- 7.8.1.2.9(b) Madan, R.C., "The Influence of Low-Velocity Impact on Composite Structures," *Composite Materials: Fatigue and Fracture (Third Volume)*, ASTM STP 1110, T.K. O'Brien, Ed., American Society for Testing and Materials, Phil., pp. 457-475.
- 7.8.1.2.10 Walker, T., et al., "Tension Fracture of Laminates for Transport Fuselage - Part III: Structural Configurations," *Fourth NASA Advanced Technology Conference*, NASA CP-3229, pp. 243-264, 1994.
- 7.8.1.3(a) Ilcewicz, L., et al., "Advanced Technology Composite Fuselage - Program Overview," NASA CR-4734, 1996.
- 7.8.1.3(b) Walker, T.H.; Ilcewicz, L.B.; Bodine, J.B.; Murphy, D.P.; and Dost, E.F., "Benchmark Panels," NASA CP-194969, August 1994.
- 7.8.1.3(c) Walker, T., et al., "Tension Fracture of Laminates for Transport Fuselage - Part I: Material Screening," *Second NASA Advanced Technology Conference*, NASA CP-3154, pp. 197-238, 1992.
- 7.8.1.3(d) Walker, T., et al., "Tension Fracture of Laminates for Transport Fuselage - Part II: Large Notches," *Third NASA Advanced Technology Conference*, NASA CP-3178, pp. 727-758, 1993.
- 7.8.1.3(e) Walker, T., et al., "Damage Tolerance of Composite Fuselage Structure," *Sixth NASA/DOD/ARPA Advanced Composite Technology Conference*, NASA CP-3326, 1996.
- 7.8.1.3.1(a) Poe, C.C., Jr., Harris, Charles E., Coats, Timothy W., and Walker, T.H., "Tension Strength with Discrete Source Damage," *Fifth NASA/DoD Advanced Composites Technology Conference*, Vol I, Part 1, NASA CP-3294, pp. 369-437.
- 7.8.1.3.1(b) Sutton, J., Kropp, Y., Jegley, D., and Banister-Hendsbee, D., "Design, Analysis, and Tests of Composite Primary Wing Structure Repairs," *Fifth NASA/DoD Advanced Composites Technology Conference*, Vol I, Part 2, NASA CP-3294, pp. 913-934.
- 7.8.2.1 Rhodes, Marvin D., Mikulus, Jr., Martin M., and McGowan, Paul E., "Effects of Orthotropy and Width on the Compression Strength of Graphite-Epoxy Panels with Holes," *AIAA Journal*, Vol 22, No. 9, September 1984, pp. 1283-1292.
- 7.8.4.1(a) Poe, C. C., Jr., "Fracture Toughness of Fibrous Composite Materials," NASA TP 2370, November 1984.
- 7.8.4.1(b) Nuismer, R. J. and Whitney, J. M., "Uniaxial Failure of Composite Laminates Containing Stress Concentrations," in *Fracture Mechanics of Composites*, ASTM STP 593, American Society of Testing and Materials, pp. 117-142 (1975).
- 7.8.4.1(c) Whitney, J. M. and Nuismer, R. J., "Stress Fracture Criteria for Laminated Composites Containing Stress Concentrations," *J. Composite Materials*, Vol 8, pp. 253-265, 1974.
- 7.8.4.1(d) Llorca, J., and Elices, M., "A Cohesive Crack Model to Study the Fracture Behavior of Fiber-Reinforced Brittle-Matrix Composites," *Int. J. of Fracture*, Vol 54, pp. 251-267, 1992.
- 7.8.4.1(e) Lin, K. Y. and Mar, J. W., "Finite Element Analysis of Stress Intensity Factors for Cracks at a Bi-Material Interface," *Int. J. of Fracture*, Vol 12, No. 2, pp. 521-531, 1977.
- 7.8.4.1(f) Tan, S. C., "Notched Strength Prediction and Design of Laminated Composites Under In-Plane Loadings," *J. of Composite Materials*, Vol 21, pp. 750-780, 1987.

- 7.8.4.1(g) Poe, C. C., Jr. and Sova, J. A., "Fracture Toughness of Boron/Aluminum Laminates with Various Proportions of 0° and ±45° Plies," NASA Technical Paper 1707, 1980.
- 7.8.4.1(h) Poe, C. C., Jr., "A Unifying Strain Criterion for Fracture of Fibrous Composite Laminates," Engineering Fracture Mechanics, Vol 17, No. 2, pp. 153-171, 1983.
- 7.8.4.1(i) Waddoups, M. E., Eisenmann, J. R., and Kaminski, B. E., "Macroscopic Fracture Mechanics of Advanced Composite Materials," J. Composite Materials, Vol 5, pp. 446-454, 1971.
- 7.8.4.1(j) Chiang, C. R., "Inhomogeneity Effect on the Stress Intensity Factor," J. Composite Materials, Vol 21, pp. 610-618, 1987.
- 7.8.4.1(k) Eringen, A. C., Speziale, C. G., and Kim, B. S., "Crack-Tip Problem in Nonlocal Elasticity," J. Mech. Phys. Solids, Vol 25, pp. 339-355, 1977.
- 7.8.4.1(l) Ilcewicz, L. B., Shaar, C., Kennedy, T. C., and Wilson, J. B., "Experimental Evidence of a Relationship Between Ultrasonic Wave Dispersion and Fracture," Engineering Fracture Mechanics, Vol 26, pp. 895-908, 1986.
- 7.8.4.1(m) Nakamura, S., and Lakes, R. S., "Finite Element Analysis of Stress Concentration Around a Blunt Crack in a Cosserat Elastic Solid," Computer Methods in Applied Mechanics and Engineering, Vol 66, pp. 257-266, 1988.
- 7.8.4.1(n) Mar, J. W. and Lin, K. Y., "Fracture Mechanics Correlation for Tensile Failure of Filamentary Composites with Holes," Journal of Aircraft, Vol 14, No. 7, pp. 703-704, 1977.
- 7.8.4.1(o) Tsai, H. C., and Arocho, A. M., "A New Approximate Fracture Mechanics Analysis Methodology for Composites with a Crack or Hole," Report NADC-88118-60, 1990.
- 7.8.4.1(p) Aronsson, D. B., and Backlund, J., "Tension Fracture of Laminates With Cracks," J. Composite Materials, Vol 20, pp. 287-307, 1986.
- 7.8.4.1(q) Aronsson, C. G., and Backlund, J., "Damage Mechanics Analysis of Matrix Effects in Notched Laminates," in Composite Materials: Fatigue and Fracture, ASTM STP 907, pp. 134-157, 1986.
- 7.8.4.1(r) Chamis, C. C., "Computational Simulation of Progressive Fracture in Fiber Composites," NASA TM-87341, 1986.
- 7.8.4.1(s) Chang, F. K., and Chang, K. Y., "A Progressive Damage Model for Laminated Composites Containing Stress Concentrations," J. of Composite Materials, Vol 32, pp. 834-855, 1987.
- 7.8.4.1(t) Barenblatt, G. I., "The Mathematical Theory of Equilibrium Cracks in Brittle Fracture," Advances in Applied Mechanics (Edited by Dryden, H.L. and von Karman, T.), Vol 7, pp. 55-129, 1962.
- 7.8.4.1(u) Mazars, J., and Bazant, Z. P., Eds. "Strain Localization and Size Effects due to Cracking and Damage," Proceedings of France-U. S. Workshop held at E. N. S de Cachan, University Paris, Sept. 1988, Elsevier, London, U. K.
- 7.8.4.1.1 Swift, T., "Fracture Analysis of Stiffened Structure," Damage Tolerance of Metallic Structures: Analysis Methods and Application, ASTM STP 842, J. Chang and J. Rudd, eds., ASTM, pp. 69-107, 1984.
- 7.8.4.1.2(a) Bazant, Z. P., and Cedolin, L., "Stability of Structures: Elastic, Inelastic, Fracture, and Damage Theories," Oxford University Press, Inc., New York, 1991.

- 7.8.4.1.2(b) Bazant, Z. P., and Planas, J., *Fracture and Size Effect in Concrete and Other Quasibrittle Materials*, CRC Press, Boca Raton, 1998.
- 7.8.4.1.2(c) Sutcliffe, M. P. F., and Fleck, N. A., "Effect of Geometry On Compressive Failure of Notched Composites," *Int. J. of Fracture*, Vol 59, pp. 115-132, 1993.
- 7.8.4.1.2(d) Dopker, B., et al., "Composite Structural Analysis Supporting Affordable Manufacturing and Maintenance," *Sixth NASA Advanced Technology Conference*, NASA CP-3326, 1995.
- 7.8.4.1.2(e) Walker, T., et al, "Nonlinear and Progressive Failure Aspects of Transport Composite Fuselage Damage Tolerance," *Computational Methods for Failure Analysis and Life Prediction*, NASA-CP-3230, pp. 11-35, 1993.
- 7.8.4.1.2(f) Basham, K. D., Chong, K. P., and Boresi, A. P., "A New Method to Compute Size Independent Fracture Toughness Values for Brittle Materials," *Engineering Fracture Mechanics*, Vol 46, No. 3, pp. 357-363, 1993.
- 7.8.4.1.2(g) Riks, E., "An Incremental Approach to the Solution of Snapping and Buckling Problems," *International Journal of Solid Structures*, Vol 15, pp. 529-551, 1979.
- 7.8.4.1.2(h) Cairns, D.S., Ilcewicz, L.B., Walker, T.H., and Minguet, P.J., "The Consequence of Material Inhomogeneity on Fracture of Automated Tow Placed Structures With Stress Concentrations," *Fourth NASA/DoD Advanced Technology Conference*, NASA CP-3229, 1993.
- 7.8.4.1.2(i) Bazant, Z. P., and Chang, T. P., "Nonlocal Finite Element Analysis of Strain-Softening Solids," *Journal of Engineering Mechanics*, Vol 113, pp. 89-105, No. 1, 1987.
- 7.8.4.1.4(a) "Standard Practice for R-Curve Determination," ASTM designation: E 561-86, Volume 03.01 of 1988 Annual Book of ASTM Standards, c. 1988, pp. 563-574.
- 7.8.4.1.4(b) Tada, H., Paris, P.C., and Irwin, G., *The Stress Analysis of Crack Handbook*, 2nd Edition, Paris Production Incorporated (and Del Research corp.), 226 Woodbourne Dr., St. Louis, Mi. 63105, 1985.
- 7.8.4.1.4(c) Erdogan, F., Ratwani, M., and Yuceoglu, U., "On the Effect of Orthotropy in a Cracked Cylindrical Shell," *International Journal of Fracture*, Vol 10, 1974, pp. 117-60.
- 7.8.4.1.4(d) Erdogan, F., "Crack Problems in Cylindrical and Spherical Shells," *Mechanics of Fracture*, Vol 3, Noordhoff International, 1977, pp. 161-99.
- 7.8.4.1.4(e) Graves, Michael J., and Lagace, Paul A., "Damage Tolerance of Composite Cylinders," *Composite Structures*, Vol 4, 1985, pp. 75-91.
- 7.8.4.1.4(f) Yahsi, O. Selcuk, and Erdogan, F., "The Crack Problem in a Reinforced Cylindrical Shell," NASA CP-178140, June 1986.
- 7.8.4.1.4(g) Ranniger, C.U., Lagace, Paul A., and Graves, Michael J., "Damage Tolerance and Arrest Characteristics of Pressurized Graphite/Epoxy Tape Cylinders," *Fifth Symposium on Composite Materials*, ASTM STP 1230, 1995.
- 7.8.4.1.4(h) Wang, J.T., Xue, D.Y., Sleight, D.W., and Housner, J.M., "Computation of Energy Release Rates for Cracked Composite Panels with Nonlinear Deformation," AIAA Paper No. 95-1463, in *Proceedings of the 36th AIAA/ASME/ASCE/AHS Structures, Structural Dynamics, and Materials Conference*, April 10-14, 1995.

Volume 3, Chapter 7 - Damage Resistance, Durability, and Damage Tolerance

- 7.8.4.2.2(a) Chai, H., Knauss, W.G., and Babcock, C.D., "Observation of Damage Growth in Compressively Loaded Laminates," Mechanics of Composite Materials, the Winter Annual Meeting of the American Society of Mechanical Engineers, Boston, 1983, pp. 329-337.
- 7.8.4.2.2(b) Bass, M., Gottesman, T., and Fingerhut, U., "Criticality of Delaminations in Composite Material Structures," Proceedings, 28th Israel Conference on Aviation and Astronautics, 1986, pp. 186-190.
- 7.8.4.2.2(c) Gottesman, T. and Green, A.K., "Effect of Delaminations on Inplane Shear Mechanical Behaviour of Composites," Proceedings of Mechanics and Mechanisms of Damage in Composites and Multi-Materials, MECAMAT, November 1989, pp. 119-132.
- 7.8.4.3.1(a) Kassapoglou, C., "Compression Strength of Composite Sandwich Structures After Barely Visible Impact Damage," J. Composite Technology and Research, 18, 1996, pp. 274-284.
- 7.8.4.3.1(b) Pavier, M.J., and Clarke, M.P., "Finite Element Prediction of the Post-Impact Compressive Strength of Fibre Composites," Composite Structures, 36, 1996, pp. 141-153.
- 7.8.4.3.1(c) Gerhartz, J.J., Idelberger, H. and Huth, H., "Impact Damage in Fatigue Loaded Composite Structures," 15th ICAF Conference, 1989.
- 7.8.4.3.1(d) Girshovich, S., Gottesman, T., Rosenthal, H., et al., "Impact Damage Assessment of Composites," Damage Detection in Composite Materials, ASTM STP 1128, J.E. Masters, Ed., American Society for Testing and Materials, Philadelphia, 1992, pp. 183-199.
- 7.8.4.3.1(e) Gottesman, T., Girshovich, S., Drukker, E., Sela, N. and Loy, J., "Residual Strength of Impacted Composites: Analysis and Tests," Journal of Composites Technology and Research, JCTRER, Vol 16, No. 3, July 1994, pp. 244-255.
- 7.8.4.3.1(f) Gottesman, T., Bass, M., and Samuel, A., "Criticality of Impact Damage in Composite Sandwich Structures," Proceedings, ICCM6 & ECCM2, Vol 3, Matthews et al., Eds., Elsevier Applied Science, 1987, pp. 3.27 - 3.35.
- 7.9.1.4 Whitehead, R.S., Kan, H.P., Cordero, R., and Saether, E.S., "Certification Testing Methodology for Composite Structures," Volumes I and II, Report No. NADC-87042-60 (DOT/FAA/CT - 86/39), October, 1986.
- 7.9.1.5 Sendekyj, G.P., "Fitting Models to Composite Materials Fatigue Data," ASTM STP 734, 1981, pp 245-260.
- 7.9.2 A. Fawcett, J. Trostle and S. Ward, "777 Empennage Certification Approach," 11th International Conference on Composite Materials (ICCM-11), Gold Coast, Australia. July 14-18, 1997.
- 7.9.3.2.5 Trop, David W., "Damage Tolerance of Internally Pressurized Sandwich Walled Graphite/Epoxy Cylinders," MS Thesis, MIT, 1985.

CHAPTER 8 SUPPORTABILITY

8.1 INTRODUCTION

Supportability is an integral part of the design process that ensures support requirements are incorporated in the design and logistics resources are defined to support the system during its operating or useful life. Support resource requirements include the skills, tools, equipment, facilities, spares, techniques, documentation, data, materials, and analysis required to ensure that a composite component maintains structural integrity over its intended lifetime. When the load carrying capability of an aircraft, or product is compromised, (i.e., loss of design function), the damaged structure must be restored quickly and at low cost. Customer requirements can dictate maintenance philosophy, materials availability, and repair capabilities that a design team must incorporate throughout the design process. As the contributors to this chapter were primarily from the aircraft industry, the text is slanted towards its particular needs. However, the guiding principles can be beneficial in other composite applications.

Since the operating and support cost of a vehicle continues to escalate throughout its life, it becomes imperative to select and optimize those designs that maximize supportability. Life cycle cost, being comprised of research and development, acquisition, operational and support, and disposal costs, is often a crucial customer requirement for any new weapon system or commercial transport. Often, design changes that enhance producibility, improve vehicle availability, and reduce operational and support costs, far outweigh the short-term increases in acquisition costs. Lost airline profits and reduced wartime readiness are a direct result of designs that did not incorporate supportability early in the design process. Telltale indicators of non-supportable designs include expensive spares, excessive repair times, and unneeded inspections.

Aircraft users are often constrained to perform maintenance during aircraft turnaround, after each day's usage, and during scheduled maintenance. Repair time limitations can range from several minutes to several days. In each case users of aircraft containing composite components require durable structures that, when damaged, can be repaired within the available support infrastructure including skills, materials, equipment, and technical data.

Composite designs are usually tailored to maximize performance by defining application dependent materials, ply orientation, stiffening concepts, and attachment mechanisms. High performance designs are often less supportable due to increased strain levels, fewer redundant load paths, and a mix of highly tailored materials and geometries. Product design teams should focus on a variety of features that improve supportability including compatibility of available repair materials with those used on the parent structure, available equipment and skill, improving subsystem accessibility, and extended shelf-life composite repair materials. Structural elements and materials should be selected that are impervious to inherent and induced damage especially delaminations, low velocity impacts, and hail damage. Each supportability enhancement feature results from the designer having an explicit knowledge of the aircraft's operational and maintenance environment and associated requirements and characteristics. Other design considerations also have an impact on supportability including durability, reliability, damage tolerance, and survivability. A supportable design integrates all the requirements, criteria, and features necessary to provide highly valued products in terms of performance, affordability and availability.

This section is designed to assist integrated product teams in the development of supportable products through five basic sections: 1) Introduction - which provides an overview of the Supportability chapter; 2) Design for Supportability - which provides the designer with design criteria, guidelines and checklists to ensure a supportable design; 3) Support Implementation - which defines and demonstrates those key elements of supportability that must be performed to insure mission success; 4) Composite Repairs of Metal Structure - which provides an alternative means to standard metal repair options, and (5) Logistics Requirements - which establishes the support resources needed to maintain the backbone of the support structure. Each section provides the designer and aircraft user with the supportability data and lessons learned that will reduce cost of ownership and improve aircraft availability. Other sections throughout MIL-HDBK-17 discuss the details needed to design supportable components. Sections contained in Vol-

ume 1 include material and structural testing, material types and properties, and joint types; in Volume 3 include materials and processes, quality, design, joints, reliability, and lessons learned needed to supplement those decisions that influence supportability.

8.2 DESIGN FOR SUPPORTABILITY

8.2.1 In-service experience

The first step toward designing reliable and cost-effective design details is to understand the history of composite structure. Composite materials, as we know them today, were introduced into the commercial aircraft industry during the early 1960's and used mostly glass fiber. Development of more advanced fibers such as boron, aramid, and carbon offered the possibility of increased strength, reduced weight, improved corrosion resistance, and greater fatigue resistance than aluminum. These new material systems, commonly referred to as advanced composites, were introduced to the industry very gradually and cautiously to ensure their capabilities.

The early success of the first simple components, such as wing spoilers and fairings, led to the use of advanced composites in more complex components such as ailerons, flaps, nacelles, and rudders. The increased specific stiffness and strengths of composites over aluminum, coupled with weight-driven requirements caused by fuel shortages, led to the application of thin-skin sandwich structures. Long-term durability requirements of the original aluminum parts were not fully accounted for when these composite parts were originally designed. To compound the problem further, damage phenomena such as delamination and microcracking were new and complex in comparison to traditional aluminum structure.

The original composite parts, particularly thin-gage sandwich panels, experienced durability problems that could be grouped into three categories: low resistance to impact, liquid ingress, and erosion. These parts were either control panels or secondary structure, such as fixed trailing edge panels, and given the emphasis placed on weight and performance, the face sheets of honeycomb sandwich parts were often only three plies or less with a Tedlar™ film. This approach was adequate for stiffness and strength, but never considered the service environment where parts are crawled over, tools dropped, and where service personnel are often unaware of the fragility of thin-skinned sandwich parts. Damages to these components, such as core crush, impact damages and disbonds, are quite often easily detected with a visual inspection due to their thin face sheets. However, sometimes they are overlooked, or damaged by service personnel, who do not want to delay aircraft departure or bring attention to their accidents, which might reflect poorly on their performance record. Therefore, damages are sometimes allowed to go unchecked, often resulting in growth of the damage due to liquid ingress into the core. Non-durable design details (e.g., improper core edge close-outs) also led to liquid ingress.

The repair of parts due to liquid ingress can vary depending upon the liquid, of which water and Skydrol (hydraulic fluid) are the two most common. Water tends to create additional damage in repaired parts when cured unless all moisture is removed from the part. Most repair material systems cure at temperatures above the boiling point of water, which can cause a disbond at the skin-to-core interface wherever trapped water resides. For this reason, core drying cycles are typically included prior to performing any repair. Some operators will take the extra step of placing a damaged but unrepaired part in the autoclave to dry so as to preclude any additional damage from occurring during the cure of the repair. This is done to assure they will only need to repair the part once. Skydrol presents a different problem. Once the core of a sandwich part is saturated, complete removal of Skydrol is almost impossible. The part continues to weep the liquid even in cure such that bondlines can become contaminated and full bonding does not occur. Removal of contaminated core and adhesive as part of the repair is highly recommended.

Erosion capabilities of composite materials have been known to be less than that of aluminum and, as a result, their application in leading edge surfaces has been generally avoided. However, composites have been used in areas of highly complex geometry, but generally with an erosion coating. The durability and maintainability of some erosion coatings are less than ideal. Another problem, not as obvious as

the first, is that edges of doors or panels can erode if they are exposed to the air stream. This erosion can be attributed to improper design or installation/fit-up. On the other hand, metal structures in contact or in the vicinity of these composite parts may show corrosion damage due to:

- Inappropriate choice of aluminum alloy
- Damaged corrosion sealant of metal parts during assembly or at splices
- Insufficient sealant and/or lack of glass fabric isolation plies at the interfaces of spars, ribs and fittings

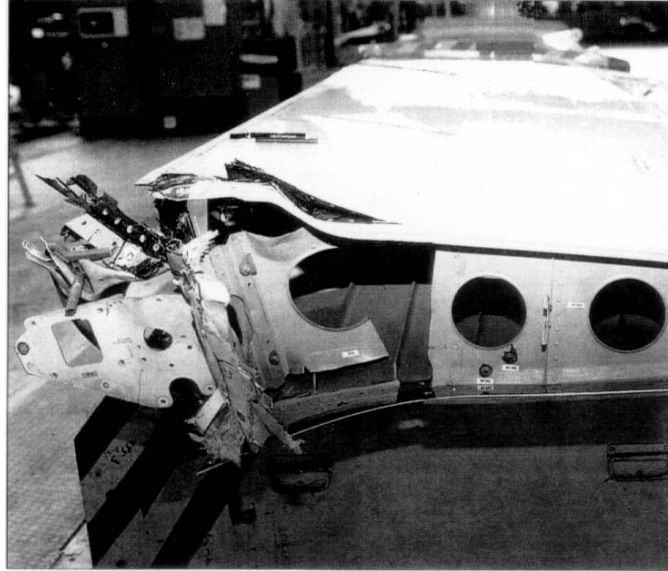
Assessing operator experience with composite structure is, taken as a whole, an extremely difficult task. A survey of operators provides responses depending on the composite application ranging from horror stories for thin skinned sandwich structures, to outstanding success for thick skinned sandwich or solid laminate primary structures. Some of the facts and data that are available are the detailed reports that were received from the operators on parts involved in the NASA-sponsored Advanced Composites Energy Efficiency (ACEE) program, which supported the design and fabrication of composite parts such as the B727-200 elevators and the B737 spoilers and horizontal stabilizers. Five shipsets of B727 elevators have accumulated more than 331,000 hrs. and 189,000 cycles; 108 B737 spoilers have accumulated more than 2,888,000 hrs. and 3,781,000 cycles. Five shipsets of B737 horizontal stabilizers, which incorporated laminate torque boxes and sandwich ribs, had amassed over 133,500 flight hours and 130,000 landings as of May, 1995. The service exposure data collected for these parts have not indicated any durability or corrosion problems. One B737-200 aircraft with the ACEE stabilizers was removed from service after 19,295 flight cycles and 17,302 flight hours, and one stabilizer was acquired by Boeing for a detailed tear-down inspection. The stabilizer was found to be in excellent condition with no fatigue damage, and the only corrosion discovered was some minor pitting found in some fastener holes of the aluminum trailing edge fittings. This was determined to be due to a fastener sealing practice which has since been obsoleted. Several repairs have been satisfactorily performed on the 727 elevators and remaining 737 horizontal stabilizers which are still in service.

The in-service success of these ACEE components is in part due to the integrated teams which developed them. The teams for both the B727 sandwich elevators and the B737 stiffened-skin configured horizontal stabilizers considered maintainability during the developmental programs. They devised repair and inspection schemes, and for each component, Maintenance Planning Manuals were compiled and released as part of the NASA contractual obligation. The airlines, United for the ten B727 elevators, and Delta and Mark Air for the five shipsets of B737 stabilizers, were in essence part of the teams who planned these documents. As mentioned above, both of these components have been damaged and repaired using the repair schemes designed for them. In all of the instances, the repairs were satisfactorily performed in-place on the aircraft.

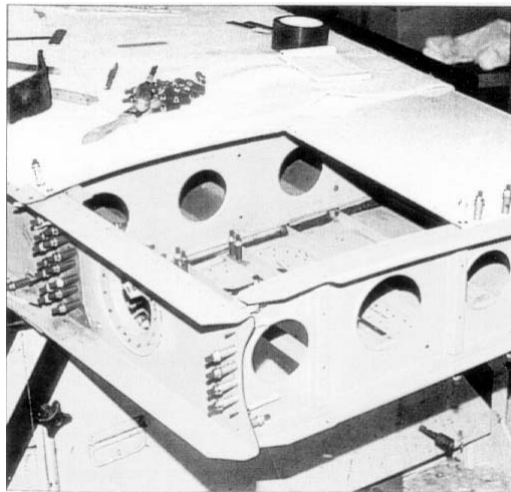
An in-service evaluation, launched in 1980, with twenty-two airbrakes/spoilers (14 fabricated with carbon-epoxy tape, and 8 fabricated from carbon-epoxy fabric) installed on Air France A300 aircraft, is still going on. Non-destructive inspections (visual and ultrasonic) are performed on aircraft and in the laboratory during the service life. Thirteen airbrakes are still on aircraft, and seven have been withdrawn from service for testing to assess stiffness and residual strength. As of November, 1995, these components had accumulated 405,698 flight hours and 236,588 flight cycles. The component with the most time in service had accumulated 32,069 flight hours and 16,802 flight cycles. Bolted repairs (metal patches for temporary, and composite precured patches for permanent repairs) were designed. Two components have been repaired with blind fasteners to arrest manufacturing produced disbonds between the skins and ribs. Some minor corrosion pitting was found on the aluminum (7075) spar at the central fitting splice due to the protect scheme having been damaged and not restored during assembly. A modification of the trailing edge was implemented early in the program; the rubber one being replaced by a solid carbon one.

As an example of successful thicker solid laminate structure, the ATR 72 outer wing box has accumulated 1,429,539 flight cycles and 1,163,333 flight hours since entering into service in 1989. The aircraft with the most time service has accumulated 23,343 flight cycles and 14,988 flight hours. Service experience has been very good with only one accidental damage being reported; an aircraft crashed into a hangar door at a speed of 15 miles/hr (25 km/hr). The composite outer wing box was repaired using bolted

carbon-epoxy and metal patches (see Figure 8.2.1(a)), while all the metal parts of the center box were replaced due to permanent deformations. One aircraft exhibited erosion of the outer ply at the leading edge of the upper skin, and a chamfer was introduced in the design, and no other problems have been reported.



a) Damaged ATR 72 carbon outer wingbox: carbon front spar and carbon wing skins



b) Repaired carbon spar before repair of wing skins

FIGURE 8.2.1(a) *Repairs to badly damaged ATR 72 wing.*

Production carbon-epoxy sandwich parts, such as trailing edge panels, cowls, landing gear doors, and fairings have demonstrated weight reduction, delamination resistance, fatigue improvement and corrosion prevention. The poor service records of some parts can be attributed to fragility, the inclusion of non-durable design details, poor processing quality, porous face sheets (insufficient thickness), and badly installed or poorly sealed fasteners. Many of the design problems were a result of insufficient technology

transfer from development programs such as NASA-ACEE. Many flight control and secondary structural panels were designed using composite materials without consideration of the applicability of composites and the service environment. As a result, many components were designed around weight-efficient sandwich configurations with face sheets of only two or three plies. Not only is the damage resistance of these components poor, but they are difficult to seal from fluids.

Fragility, so much an issue in these thin-gage sandwich structures, is much less an issue in thicker-gage primary structures (sandwich or solid laminate) such as main torque boxes of empennages and wings, and fuselages. The thicker skins of the Boeing B777 and the Airbus series of composite empennage main torque boxes, the US Air Force B-2 wings and fuselage, the ATR 72, US Air Force F-22, the US Navy/Marine F/A 18, and the RAF/Royal Navy/US Marines AV8B Harrier outboard wing boxes, to list a few examples, are much more damage resistant than the vast number of light gage sandwich flight control and secondary structural components that are currently in service, and are still being introduced to service. In addition to their highly damage resistant primary structural components, the latest Airbus aircraft and the B777 have incorporated improved light gage composite structural designs. However, they will still be more vulnerable to damage in service than the primary structural components, due to their minimum gage, mainly sandwich, construction.

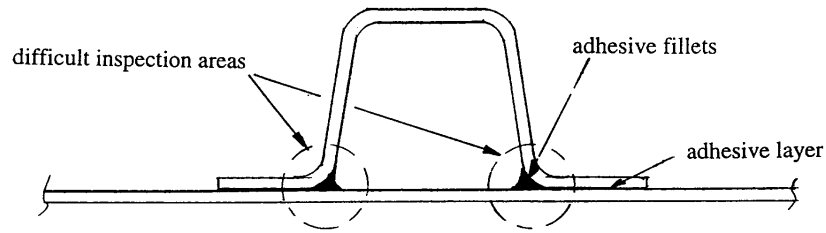
8.2.2 Inspectability

During the design of composite structural components consideration should be given to the inspection methods available to both the manufacturer and the customer. Typical composite in-process non-destructive inspection (NDI) methods available to the manufacturer are: visual, through-transmission ultrasonics (TTU), pulse-echo ultrasonics, x-ray, and other advanced NDI methods such as enhanced optical schemes and thermography. Most airlines and military operators use visual inspections supplemented with both mechanical (i.e., some form of tap test) and electronic (i.e., pulse echo and low-frequency bond testing) to locate damage. Because of the predominance of visual inspections, provisions should be made during the design phase for complete external and internal access for visual inspection of all components, regardless of whether they are critical primary structural components or secondary structures such as fairings. If a visual inspection indicates potential damage, then the more sophisticated inspection techniques can be used to provide more accurate damage assessments. Additional suggestions can be found in Section 8.3.1.

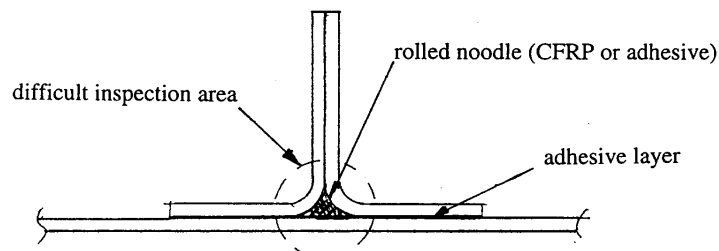
8.2.2.1 General design guidelines

Whether one chooses a laminate stiffened skin or a sandwich configuration for a specific component, there are inspectability issues within each configuration category. For example, the use of closed hat stiffeners to stiffen laminate skins, while extremely efficient from a structural point of view, create three areas in the skin and stiffener that are difficult to inspect by any method (Figure 8.2.2.1(a), section (a)). A blade stiffener, on the other hand, has only the one difficult inspection area (Figure 8.2.2.1(a), section (b)). The adhesive fillets of the closed-hat stiffener, and the rolled noodle of the blade stiffener, are contributors to these inspection difficulties. These areas are difficult to inspect during the manufacturing process, and are even more of a problem for the service operator with limited access to the internal surfaces.

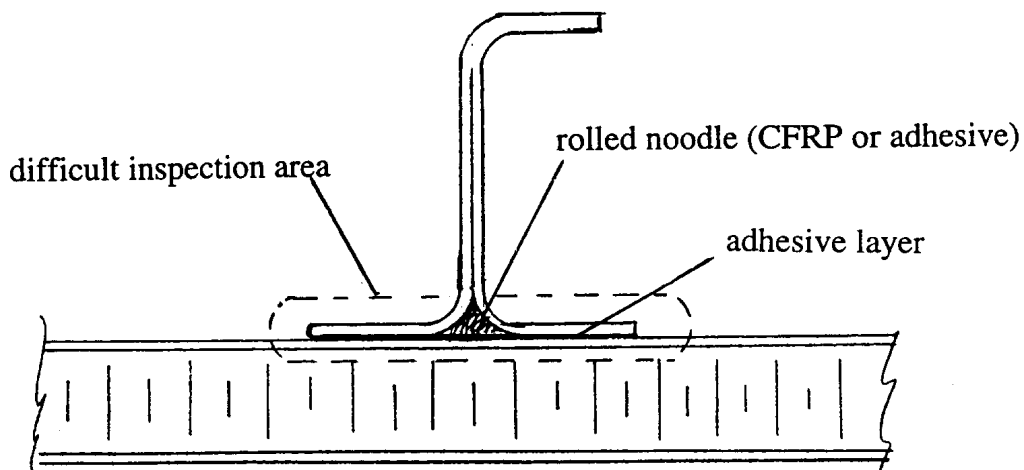
With a sandwich configuration there are inspection difficulties associated with potted areas, detection of fluids that have leached into the sandwich honeycomb core, disbonds of face sheets, foam core, and damages within the core. Also difficult for operators are inspections of bondlines of stiffeners or frames that are bonded to the internal face sheets of sandwich components (Figure 8.2.2.1(b)). When airplane operators are forced to use inspection methods that are subjective, i.e., the tap test, they are handicapped by lack of knowledge of damage sizes and criticality. This is a significant problem for operators, and while sandwich structural configurations can be very efficient from a performance point of view, they tend to be fragile, easily damaged, and difficult to inspect. Interestingly some airline operators prefer sandwich over laminate stiffened skins from a repair point of view, but virtually all express frustration with the durability and inspection of sandwich structures.



(a) Closed-hat stiffened configuration



(b) Blade stiffened configuration

FIGURE 8.2.2.1(a) *Difficult to inspect areas on laminate skin stiffened designs.***FIGURE 8.2.2.1(b)** *Difficult inspection area of sandwich structural configurations.*

Most composite structural components will include metal fittings or interfaces with metal parts. It is desirable to ensure that these metal parts can be visually inspected for corrosion and/or fatigue cracking. In addition, if the mating metal parts are aluminum, then it is important to be able to inspect them for po-

tential galvanic corrosion that may be caused by contact with the carbon fibers. This may require removal of fasteners at mating surfaces, so blind fasteners should not be used in these applications. The use of blind titanium fasteners should be kept to a minimum because, when installed, they are literally impossible to inspect to verify correct installation. They are also very difficult to remove when repairing or replacing a component.

8.2.2.2 Accessibility for inspection

Composite structural components should not be designed such that they must be removed in order for inspections to be made. Some disassembly may be unavoidable, but should be kept to a minimum. This will not only reduce the maintenance burden on the operators, but also reduce airplane out-of-service time.

All composite components should be designed to ensure visual accessibility of the external surfaces without detaching any parts, including access panels, from the airplane. In some instances, fairing panels may have to be removed, such as the horizontal stabilizer-to-fuselage fairing for access to the stabilizer skin joints-to-side-of-body rib, or spar-to-center-section attachments.

An internal inspection implies that there is visual accessibility that is achieved by removal of detachable parts, such as access plates or panels. For internal inspection of torque boxes with ribs, spars and stringers, there must be complete visual accessibility through access holes in spars and ribs. These access holes must be designed such that maintenance technicians can, through the use of flashlights and mirrors, visually inspect all of the internal structure. There must also be accessibility to critical joints or attachment fittings where pins can be removed so that they and the holes can be inspected.

8.2.3 Material selection

8.2.3.1 Introduction

Chapter 2 in Volume 3 offers an in-depth review of advanced composite materials. Each one of the composite materials described in Chapter 2 can offer benefits over metallic materials to the designer in terms of performance and costs. However, these benefits will be erased if, when designing a component, the design is focused only on the mechanical and thermal performance of the component and does not take into consideration where the part will be used and how it will be repaired if it is damaged. The goal of the designer must be to design a part that will be both damage tolerant and damage resistant as well as easy to maintain and repair. This section is offered as a guideline for the designer when selecting a material system.

8.2.3.2 Resins and fibers

When selecting a resin, it is important to look at where the resin system will be used, how the resin system has to be processed, what is its shelf life and storage requirements, and is it compatible with surrounding materials. Table 8.2.3.2 describes the common resin types, their process conditions and their advantages and disadvantages in terms of repairability. An in-depth review of these materials can be found in Section 2.2.

Refer to Section 2.3 for available fibers for composite structures.

In terms of supportability, the minimum number of resin systems and material specifications should be chosen. This will reduce the logistic problems of storage, shelf life limitations and inventory control.

TABLE 8.2.3.2 *Supportability concerns with resin types.*

Resin Type	Cure Temp. Ranges	Pressure Ranges	Processing Options	Supportability Advantages	Ease of Repair	Damage Resistance	Supportability Disadvantages
Epoxy Non-Toughened	RT to 350°F (180°C)	Vacuum to 100 psi (690 kPa)	Autoclave, press, vacuum bag, resin transfer molding	Low level of volatiles, low temp processing, vacuum bageable	Good	Poor	Time limited storage
Epoxy -Toughened	RT to 350°F (180°C)	Vacuum to 100 psi (690 kPa)	Autoclave, press, vacuum bag and resin transfer molding	Low level of volatiles, low temp processing, vacuum bageable	Good	Good	Time limited storage
Polyester	RT to 350°F (180°C)	Vacuum Bag to 100 psi (690 kPa)	Same as epoxies	Ease of processing, quick cure with elevated temp., low cost	Very good	Good	Poor elevated temp performance, health (Styrene)
Phenolic	250 to 350°F (120 to 180°C) with post cure	Vacuum Bag to 100 psi (690 kPa); lower pressure gives high void content	Autoclave, press molding		Poor	Poor	Water off gassing, high temp cure/post cure, high void content
Bismaleimides (BMI)	350F (180°C) with 400 to 500°F (200 to 260°C) post cure required	45 to 100 psi (310 to 690 kPa)	Autoclave, press molding, RTM	Lower pressure processing than polyimides	Poor	Poor	High temperature processing
Polyimides	350 to 700°F (180 to 370°C) post cure required	85 to 200+ psi (590 to 1400+ kPa)	Autoclave and press molding		Poor	Poor	Cost, availability of adhesives, high pressure
Structural Thermoplastic	500°F+ (260°C+)	Vacuum bag to 200 psi (1400 kPa)	Autoclave and press molding	Reformable	Poor	Very good	High temperature processing

8.2.3.3 Product forms

A detailed description of available composite product forms can be found in Section 2.5.

The goal when repairing a composite part is to return it to its original performance capability while incurring the least cost and weight gain. Therefore, the ease of repairing different product forms should be taken into consideration when selecting the material system. Figure 8.2.3.3 shows the relative ease of repairing various product forms.

8.2.3.4 Adhesives

Table 8.2.3.4 provides descriptions of issues for use of adhesives in repairs.

8.2.3.5 Supportability issues

Table 8.2.3.5 offers a list of Material Support issues for your consideration.

8.2.3.6 Environmental concerns

Health and safety: There are recognized hazards that go with advanced composite materials. Knowing about these hazards, one can protect oneself and others from exposure to them. It is important to read and understand the Material Safety Data Sheets (MSDS) and handle all chemicals, resins and fibers correctly. Refer to SACMA publication "Safe Handling of Advanced Composite Materials" for additional information (Reference 8.2.3.6).

Disposal of scrap and waste: When selecting materials, consideration must be given to the disposal of scrap and waste. Disposal of scrap and waste should be specified under federal, state and local laws. See Section 8.2.5.6 on how to dispose of uncured materials.

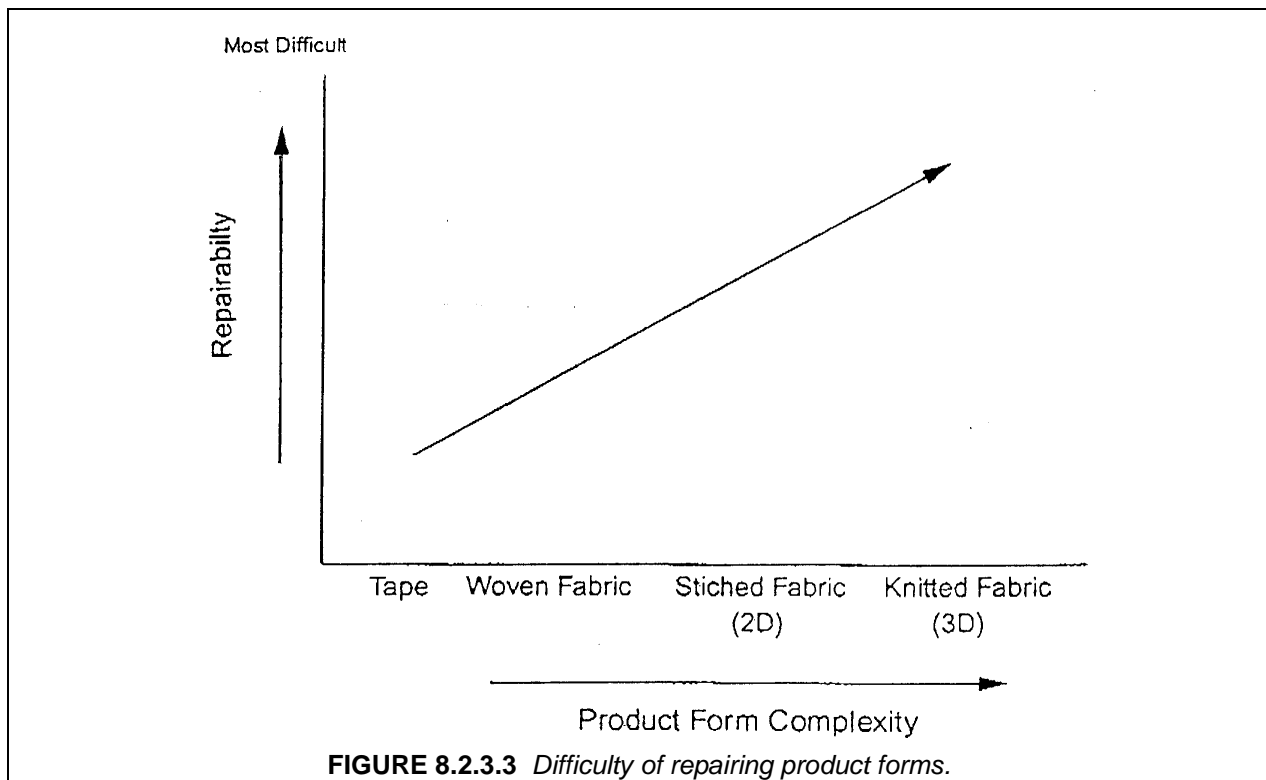


TABLE 8.2.3.4 *Repair adhesive considerations.*

Consideration	Response
Performance properties	The adhesive system must be capable of transferring structural, thermal, acoustic loads through a patch material and back into the parent structure. The adhesive system must also be capable of transferring those loads while operating within the vehicles environmental envelope (i.e., presence of hydraulic fluid, fuel, and dirt, and vibro-acoustic conditions).
Service temperature	The maximum surface temperature a structure will operate over the vehicle life. Exhaust sections and leading edges typically will operate at 50 - 500% higher temperatures than surrounding areas. The surface preparation method, adhesive primer, cure profile, heat sinks, and coatings and treatments can all influence the maximum temperature of the structure and associated repair.
Compatibility with surface preparation technique	Surface preparation can be anything from nothing to an electrochemically etched surface containing a commingled primer system. In addition the surface could be dirty, contain oxidation, hydrocarbons or moisture, or not lend itself well to chemically bonding with the adhesive.
Wetability	The ability of an adhesive to flow within all areas of the repair. Improvements in wetability reduce resin-starved areas and associated porosity, maintain bondline tolerances, and in general produce more reliable bonds.
Porosity of bondline	Curing without external pressure (i.e., vacuum bags) increases the potential of trapping volatiles created during the cure process. Application of heat and vacuum/pressure in the correct sequence will minimize porosity and, therefore, provide better bonds.
Tolerance of temperature deltas across repair area	All repair areas have varying thermal densities (substructure, patch ply drop-offs) which create a wide range of temperature deltas during adhesive cure. Adhesives that can cure well over a broad temperature range are more suited for repair applications. In addition, during repair only a small area of the structure is heated while the remaining structure is at ambient temperature which could be as low as -10°F or as high as 180°F.
Outtime at ambient temperature	Repairs can take a long time to assemble before the cure starts. Adhesives that are stable and fully thawed for several hours at ambient temperature will produce better and more reliable repairs.
Tolerance of bondline thickness	Uniform bondlines produce the best load transfer medium. Maintaining a uniform bondline thickness is difficult on structures that are wavy and have ply discontinuities. Adhesives that perform well with bondlines from 3-15 mils will produce the best repair performance.
Cure time	Ideally, cure time should be as short as possible to reduce vehicle downtime. Adhesives that can be heated at 5-7°F/min and dwelled at the cure temperature for less than 2 hrs. are optimum.
Cure pressure	In repair applications the only patch compaction force available is from atmospheric or mechanical pressure. Since autoclaves and associated tooling are not readily available and components are difficult to remove, vacuum bags or mechanical clamps will be the pressure devices of choice.
Cure temperature	A rule of thumb for repair applications is to use an adhesive with the lowest cure temperature that meets all the performance constraints. As temperatures increase, the tolerance of acceptable cure decreases. In addition, most hot bond control units manage the upper temperature limit, therefore, the cure temperature variance should be +0 and -40°F.
Storability at ambient temperature	Since many materials must be cold stored to minimize the effects of crosslinking, an adhesive that is tolerant of sustained outtime at ambient temperature is more suited for the repair environment. In addition, some repair facilities lack the cold storage equipment necessary and must rely on temporary cold storage methods such as iced coolers or just in time delivery of repair materials from distribution centers.

TABLE 8.2.3.5 *Material support issues.*

Issue	Support Impact
Autoclave only cure	1. Equipment not available in the field and at small repair facilities 2. Part has to be removed and disassembled for repair
Press curing	1. Equipment not available in the field and at small repair facilities. Part has to be removed and disassembled for repair
High temperature cure	1. Damage to surrounding structure in repair on aircraft 2. Protective equipment needed to handle high temperatures
Transit	1. Dry ice packing requirements may be problematic
Freezer storage required	1. Equipment not available not available in the field and at small repair facilities

8.2.4 Damage resistance, damage tolerance, and durability

In normal operating condition, components can be expected to be subject to potential damage from sources such as maintenance personnel, tools, runway debris, service equipment, hail, lightning, etc. During initial manufacturing and assembly, these components may be subject to the same or similar conditions. To alleviate the effects of the expected damage, most composite components are designed to specific damage resistance, damage tolerance, and durability criteria. How these design criteria affect supportability are discussed in this section. (Ideally, a supportable airframe structure must be able to sustain a reasonable level of damaging incidents without costly rework or downtime. Sustainability is being defined as showing no damage after such incidents and having the required residual strength and stiffness capability.)

8.2.4.1 Damage resistance

Damage resistance is a measure of the relationship between the force or energy associated with a damage event and the resulting damage size and type of damage. A material or structure with high damage resistance will incur less physical damage from a given event. For composite airframe structures repair actions are based on visibility, hence, if the damage is not visible, a repair activity is not needed. Therefore, to reduce repair activity, damage resistance levels should be such that at low impact energy levels (4 ft-lb) the damage is not visible and is negligible in high susceptibility areas. This can be accomplished by zoning the structure based on regions that have high or low susceptibility to damage and its residual strength and stiffness requirements. In defining the requirements, the type of structure (primary or secondary structures), construction method (sandwich or solid laminate), and whether its a removable or non-removable structure are pertinent. In practice, damage resistance is a critical design parameter for supportability, particularly for thin-skinned components. A more detailed discussion of damage resistance can be found in Section 7.5.

Damage resistance maybe improved by increasing laminate thicknesses and for sandwich applications by using denser core. However, the decrease in visibility may lead to the increase in nonvisible

damage that must be considered for aspects of damage tolerance. The selection of reinforcement fibers that have high strain capability can also have a positive effect. Additionally, the selection of toughened matrix material can greatly enhance damage resistance. The selection of integrally stiffened panels over a honeycomb sandwich construction usually results in a more damage resistant configuration as the skin thicknesses are usually thicker and the impact energy is absorbed by the bending action for the integrally stiffened panel as compared to sandwiches. Possible water ingress into the sandwich panel after impact damage is another supportability drawback of sandwich construction.

Other items to improve damage resistance include the use of a layer of fabric as the exterior ply over tape to resist scratches, abrasion, softening of impact, and reduction of fiber breakout during drilling of fastener holes. Laminate edges should not be exposed directly into the air stream that could possibly subject it to delaminations. Avoidance of delaminations is achieved by using non-erosive edge protection, replaceable sacrificial materials or locating the forward edge below the level of the aft edge of the next forward panel.

Areas prone to high energy lightning strike should utilize replaceable conductive materials, provide protection at tips and trailing edge surfaces, and make all conductive path attachments easily accessible.

8.2.4.2 Damage tolerance

Damage tolerance for structural parts is a measure of the ability of such a part to maintain functionality, sufficient residual strength and stiffness, with damage for required loadings. In aircraft design, damage tolerance is a safety issue but does affect supportability. A very damage tolerant structure will require large area repair capability, although it may be of low frequency. On the other hand, a structure that can tolerate only small damage sizes will require frequent repair actions.

Damage tolerance is achieved by reducing allowable strain levels in damage and strength/stiffness critical areas and/or providing multiple load paths. For civil-aircraft composite parts, it is a requirement that the structure can sustain ultimate load with any damage less or equal to the barely visible size. Therefore, the designer of a structure highly resistant to surface damage has to make sure that the structure is also damage tolerant to hidden damage. Larger damages have lesser load residual strength requirements. See Section 5.12.1 for a more detailed discussion.

Except in areas where the margin of safety is near zero, a composite structure can tolerate larger than visible damage while still able to sustain ultimate load. A reduction in the number of repair actions would be possible if the part manufacturer provides a map of permissible damage sizes. Such a map would have to include not only the effect of static loads but of durability and functional requirements.

8.2.4.3 Durability

Durability of the structure is its ability to maintain strength and stiffness throughout the service life of the structure. In general, structural durability is inversely related to maintenance cost. A durable structure is the one that does not incur excessive maintenance cost during its service life. A composite structure that was designed for damage resistance will have excellent durability as carbon composites have excellent corrosion resistance characteristics (assuming no galvanic corrosion) and fatigue characteristics when compared to metals.

In composites, fatigue damage due to repeated mechanical loads usually initiates as cracks in the matrix material at laminate edges, notches, and stress discontinuities and then may progress as interlaminar delaminations. For currently designed structures with low allowable strain levels, in part due to damage tolerance and repair requirements, the fatigue loads are generally below the levels that would cause extensive matrix cracking. One exception is in the vicinity of fastener holes, where, if the bearing stresses are high, hole elongation may cause bolt fatigue failures and other anomalies due to internal load redistribution. Thus, good supportability design should feature low bearing stresses (see Section 5.3.2.3). A general discussion on durability can be found in Section 5.12.2.

8.2.5 Environmental compliance

Many aspects of the design, repair and maintenance of polymer matrix composites are impacted by environmental rules and regulations. Many people associate environmental compliance with the correct disposal of hazardous wastes. This is certainly an important factor, but is by no means the only factor to consider. In fact, by the time we are concerned with the disposal of hazardous waste, we have missed a tremendous number of opportunities to reduce the generation of waste in the first place. The concept of reduction of hazardous waste before it is generated, known as pollution prevention, can begin as early as the initial design phase. It can greatly reduce labor, cost, and paperwork associated with the disposal of hazardous wastes generated by repair and maintenance of the component throughout its life cycle. This section will identify factors to consider during the design and repair design phase to facilitate true life cycle pollution prevention.

8.2.5.1 *Elimination/reduction of heavy metals*

The requirement for heavy-metal containing coatings and treatments not only presents environmental compliance difficulties during manufacture, but presents additional challenges every time the coating needs to be removed, repaired or replaced. Traditional requirements for chromic acid anodizing or alodine processes impact mostly metal components, however, we encounter similar issues with polymer matrix composites as well. Typical culprits include cadmium plated fasteners, and chromated sealants and primers. When designers consider environmental compliance along with cost and quality when specifying design materials, we may be able to eliminate the specification of these materials in the first place.

Non-chromated sealants and primers are currently available and research and development initiatives are underway to evaluate their suitability for long term use on military aircraft. The specification of a non-chromated primer or sealant in the design of a component will create benefits throughout its life cycle by reducing hazardous waste and personnel exposure to hazardous materials.

8.2.5.2 *Consideration of paint removal requirements*

During the design of polymer matrix composite components, consideration must be given to removal of coatings. Chemical paint removers are not acceptable for most polymer matrix composites because the active ingredients that attack the organic coating also attack the matrix. Abrasive paint removal techniques, such as plastic media blasting, have proven successful on polymer matrix composites but their use can be limited by substrate thickness and specialized surface treatments or coatings. The consideration of paint removal techniques during manufacture may highlight minor changes in design that can affect major savings in maintenance over the life cycle of the component.

8.2.5.3 *Shelf life and storage stability of repair materials*

A significant portion of a waste stream is made up of materials that cannot be used within their useful life. In its worst case, this involves materials that are purchased, sit on the shelf and are then disposed of as hazardous waste without ever making it to the work center. At best, it represents containers that have been opened but not finished before the shelf life expires. The following are some of the ways this waste stream can be minimized by design decisions.

- a) *Specify common materials.* Maintainers have difficulty “using up” materials if they are specific to a single aircraft or component. In many cases material manufacturers establish “minimum buys” of their product dictating the minimum purchase of several gallons when only a pint is required. The excess material often simply sits on the shelf until it is no longer useable and is then sent to disposal. This issue can be alleviated through the specification of materials that are already in the inventory, or that are used on a wide variety of components.
- b) *Specify long shelf life, and/or room temperature storable materials.* Obviously, the longer the shelf life of a product, and the less restrictive the storage, handling and transportation require-

ments, the better the chances that the material can be consumed before its shelf life expires. Designers should be aware that even though these materials may be slightly more expensive, or may not be the material of choice during the manufacture of the product - they may well be suitable for repair and/or maintenance.

8.2.5.4 Cleaning requirements

Cleaning is one of the primary maintenance processes that create hazardous waste. The construction of the component often dictates the cleaning options available for that part. Many of the cleaning processes that previously utilized ozone depleting solvents and other hazardous chemicals are being replaced with aqueous cleaning processes. If a component is constructed such that water intrusion is a concern, then aqueous cleaning of the part may also be a problem. The requirement for solvent cleaning places a heavy burden on the maintainer - which will continue to worsen as environmental restrictions tighten. Designing components so they can tolerate aqueous cleaning will facilitate maintenance requirements throughout the life cycle.

8.2.5.5 Non-destructive inspection requirements

The requirement to perform non-destructive inspection on a component often requires cleaning and paint removal (resulting in hazardous waste generation) that would not otherwise be necessary. Often, non-destructive inspection requirements set during the design phase are maintained throughout the life cycle regardless of whether defects are ever found during the inspection. Periodic reviews of inspection requirements will present the opportunity to eliminate non-value added requirements thereby saving money, time and hazardous waste generation.

8.2.5.6 End of life disposal considerations

Unlike the situation for metals, there is not a widespread market waiting to buy composite materials from scrap aircraft. There are several initiatives underway to find uses for these materials. Designers need to stay abreast of these initiatives so that if a market is identified for certain polymer composites, this can be given consideration when selecting design materials.

Machining of carbon fiber laminates during cutting and trimming operations produces particulates that are nominally considered a nuisance dust by bio-environmental engineers. TLV (Threshold Limit Values) limits were updated in 1997 by the American Conference of Government and Industrial Hygienists (ACGIH) to define loose composite fiber/dust exposure limits for composite workers. Excessive exposure may require the use of NIOSH-certified respirators with HEPA filters. Resins used in composite materials and adhesives may cause dermal sensitization in some workers, thus silicon-free/lint-free gloves should be mandated for use. This will also ensure a contaminant-free laminate.

Uncured prepreps and resins are treated as hazardous materials in waste stream analyses. Scrap materials should be cured prior to disposal to inert the resins and reduce the HazMat disposal costs. It is important to ensure that scrap materials containing carbon fibers are sent to non-burning landfills; pyrolyzed carbon fibers freed by resin burn-off can represent a respiratory and electrical hazard.

8.2.6 Reliability and maintainability

The maintainability of a structure is achieved by developing schemes for methods of inspection and maintenance during the design phase. The designer with the overall knowledge of the performance and operational characteristics of the structure should assess, based on the construction method, configuration, material selection, etc., whether the structure is maintainable. Such factors in assessment would include development of cradle-to-grave inspection methodology, techniques, protection schemes and defined inspection intervals for maintenance.

8.2.7 Interchangeability and replaceability

A composite structure can be maintained using a variety of methods, each dependent on the support plan and maintenance concept selected. One of the first design considerations that must be determined is the ease with which a damaged piece of structure can be repaired. Large integral structural elements, such as a wing skin panel, cannot be readily removed from the aircraft and, therefore, must be repaired in-place. Many panels, however, can be removed and the damaged panel replaced with a new panel.

Ease of maintenance can have a direct impact on the design and surrounding structure. By developing the maintenance concept early in the design process, tradeoffs can be made before the design is finalized that will provide the aircraft operator with more maintenance options and provide aircraft that are potentially more available to perform their design function.

The design of removable panels can have significant impact on the ease of maintenance and the associated maintenance and downtime cost. There are two commonly used types of panels used for structural maintenance - interchangeable and replaceable.

The **interchangeable panel** is one that can be installed onto the aircraft without any trimming, drilling, or other customizing. Interchangeable parts are designed through a selection of materials, tolerances, and fastening techniques to fit a production run of aircraft within the same model series.

Replaceable panels may or may not fit between different aircraft and usually require trimming and drilling on installation.

Figure 8.2.7 shows the differences between interchangeable and replaceable panels.

Interchangeability and replaceability (I&R) requirements for non-repairable, high-unit cost, frequently damaged, or highly loaded components need to be assessed early in the design process to ensure cost and operational effectiveness. Typically, I&R components are more costly to manufacture due to the close tolerances, materials and design attributes. Designers must be assured that form, fit, and function are fully realized with removable parts and realize that thermal and material mismatches, part number changes, and different manufacturing techniques, may alter a component's ability to be replaceable or interchangeable. In some cases, I&R are design requirements and can easily be met using loose tolerances and numerically controlled master tooling during the manufacturing process.

Components that must be removed frequently (<1000 flight hours) to facilitate other maintenance actions are typically good candidates for interchangeable panels. Components that are large and contain a variety of inner mold line geometries and fastener configurations (fuselage skins and components that have attachment fittings, i.e., landing gear doors) are good candidates for replaceable panels. Mil-I-8500, The Use of Interchangeable Components, provides requirements and guidance.

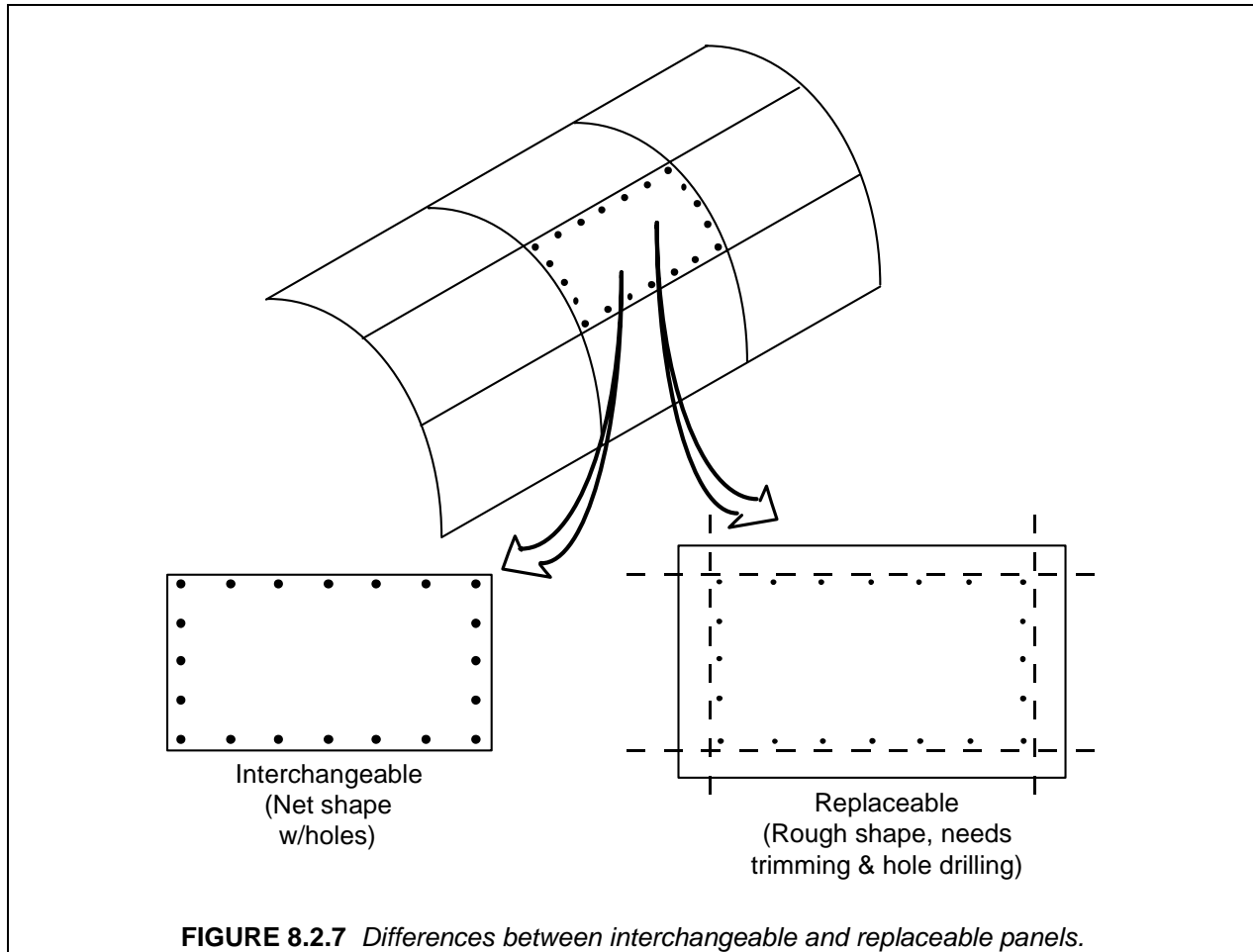
8.2.8 Accessibility

Accessibility is an important factor when designing structures for repair. Sufficient access should always be provided to properly inspect, prepare the damage structure, fit and install the repair parts and use repair tools and bonding equipment. Limited access may dictate the repair approach, i.e., use of pre-cured patches, use of mechanical fasteners in lieu of curing, etc. If feasible, two-sided access is preferred.

8.2.9 Repairability

Designing for repairability is an essential element in the effective use of composite materials in aircraft structures. Selecting a repair approach during the design phase will influence the choice of lay-up patterns and design strain levels. It is important that the repair philosophy be set during the conceptual design stage and that the repair designs be developed along with the component design. Candidate repair designs should be tested as part of the development test program. Repair concepts and materials should

be standardized to the maximum extent possible, and repair considerations are appropriate for concept development of any aircraft structural component. This section lists recommendations for design approaches that will improve the reparability of composite aircraft structural components.

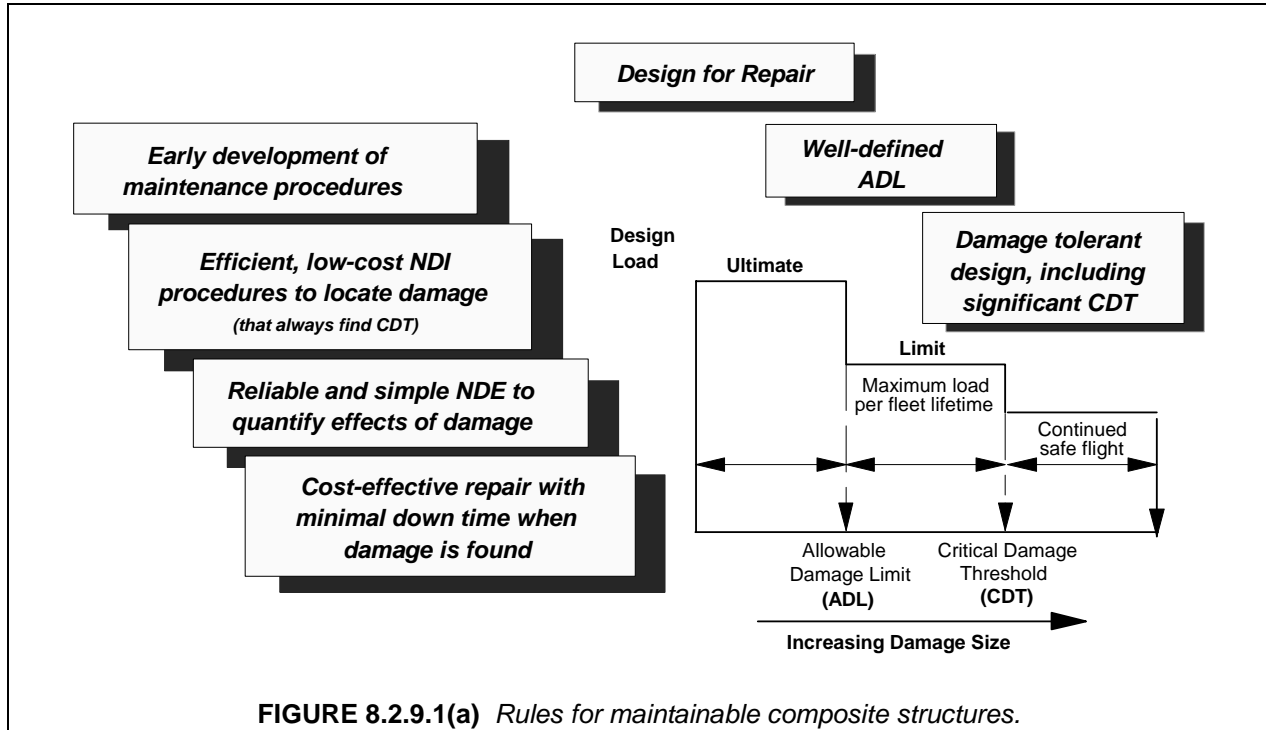


8.2.9.1 General design approach

The approach for the composite structures design team needs to be based upon input and knowledge gained from a working relationship established between the design team and airline maintenance personnel. This can be accomplished through repair workshops, or inquiries, involving airline and OEM customer support personnel, engineering personnel and involvement with the Commercial Aircraft Composite Repair Committee (CACRC). Reference 8.2.9.1 is a product of this committee and provides general guidance. The time spent within these efforts will provide a broader understanding of the overall environment in which operators operate. OEM involvement in the CACRC has contributed to addressing the problems that operators voice. The CACRC is pioneering standards and recommendations for the design and maintenance of future composite structure based on current and past experience.

Figure 8.2.9.1(a) shows the maintenance development philosophy established during Phase B of the Boeing/NASA Advanced Technology Composite Aircraft Structures (ATCAS) composite fuselage program. Maintenance procedures such as inspection and repair, which are applicable to a service environment, must be considered during design selection. Considerations should be made for bolted repairs, for example, there should be sufficient edge distances on stiffener and frame flanges, and sandwich edge bands to allow for repair bolts. Skin thicknesses should be sufficient to prevent knife-edges when using

countersunk repair fasteners. Fabric outer plies should be considered to help reduce breakout when drilling holes for repair bolts in laminates or face sheets. Any lightning strike protection systems that are needed on specific components should be designed to be repairable. It should be assumed that bolted and bonded repairs would follow general practice guidelines.



Some composite structural details, while weight and cost efficient, are difficult to repair. Closed hat-section stringers, for instance, are compatible with inexpensive manufacturing techniques and minimum weight, but pose difficulties relative to inspection and attachment in repair applications. The use of blind fasteners should also be kept to a minimum because of difficulties in removing them in order to make a repair or a replacement. Where fasteners are necessary, the removable types are preferable. Quite often, when removing fasteners performing a repair, the drilling out of blind fasteners the surrounding structure is damaged, thus incurring more cost and down-time. Material choices may also be affected. The designer should avoid the use of different material systems with different curing temperatures on one part. For instance, skins and stiffeners are sometimes precured at 350°F (177°C) and then, for manufacturing ease, secondarily bonded with 250°F (121°C) adhesive. This can present problems when the skins or stiffeners are repaired at 350°F (177°C); the integrity of the 250°F (121°C) adhesive at the bond interface may be compromised with no indication of degradation.

Design concept developments should include parallel efforts to establish maintenance procedures. Maintenance procedures established *after* design features for manufacturing scale-up are set will typically result in unnecessarily complex repair designs and processes.

Another important aspect of concept development critical to maintenance is damage tolerant design practices. The allowable damage limits (ADL) and critical damage thresholds (CDT) defined in Figure 8.2.9.1(a) must be established to support the structural repair manual and inspection procedures.

The former allows rapid determination of the need for repair during scheduled inspection, while the latter should be sufficiently large to allow safe aircraft operation between inspection intervals. Knowledge of residual strength and inspection capabilities should allow determination of both ADL and CDT as a

function of structural location. Damages smaller than the ADL limit may never be discovered, whereas the CDT damage level must always be found by visual inspection.

The design of some areas of the structure can be controlled by manufacturing and durability considerations. Specific examples of these considerations are minimum gage (to provide a minimum of impact damage resistance and avoid knife-edge at countersink fasteners), stiffener, rib and frame flange width, bolt spacing and edge distance requirements, and avoiding rapid ply drops and buildups. Areas of the structure designed to these considerations will, therefore, have higher margins for damage tolerance. Figure 8.2.8.1(b) shows the minimum margins of safety for a composite fuselage side panel, illustrating the "over-designed" regions. These regions have ADLs and CDTs larger than the rest of the fuselage section. Zoned ADL and CDT information should prove useful to operators desiring minimum maintenance costs. Structural Repair Manuals quite often point to critical zones on components for special directed inspections, so zoned ADL and CDT information could be included in these manuals.

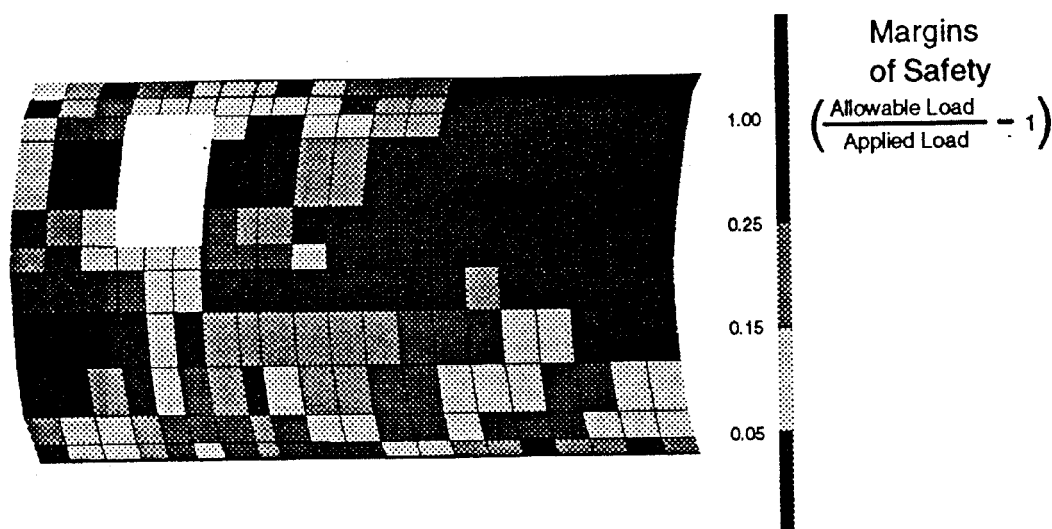


FIGURE 8.2.9.1(b) *Strength margin of safety distribution for a fuselage side panel subjected to ultimate loads.*

Returning to Figure 8.2.9.1(a), another requirement for maintainable composite structure is the establishment of non-destructive inspection (NDI) and evaluation (NDE) procedures for practical damage location and quantitative assessment, respectively, during scheduled maintenance. The latter, which may require ultrasonic methods, should only be required to assess the effects of damage found by more easily performed procedures (e.g., visual).

Damage Levels. When damage is found, efficient repair procedures are needed that the operators can accomplish with available resources (tooling, equipment, etc.) and with a minimum amount of airplane down time. In order to develop repair concepts for a broad range of damage scenarios, the repair design philosophy is focusing on more generic repairs that are not damage-specific. This approach will be beneficial because generic designs and corresponding repair procedures can be developed for various levels of damage which are, within certain limits, independent of specific damages. This is intended to greatly reduce the need to develop repairs for each damage event as it occurs, providing a higher level of maintainability. Initially, three damage levels have been defined and are shown in Table 8.2.9.1(a) as they apply to a skin/stringer configuration.

TABLE 8.2.9.1(a) *Example of skin/stringer damage level definitions.*

Designation	Damage Description	Repair
Level 0	Edge skin delamination or disbond from stiffening elements	Fastener restraint or injection resin repair
Level 1	Critical damage to a single structural element (skin or stiffener)	Mechanically fastened or bonded patch and/or splice
Level 2 (and higher)	Multiple occurrences of Level 1 damage	Same as Level 1

Designs should address repair in such a way that each bay is looked upon as a unit, or building block. Restoration of that unit (rib, frame, stringer, and/or skin) should be designed so that larger multiple-bay damages can be handled with less effort. Structural units are less easily defined for sandwich structure; however, the same general philosophy applies. The strategy behind this approach is to address the repair scenarios for a large range of damage at the beginning of the design process to ease the maintenance burden.

Multiple Options. Another aspect of the approach is to provide operators with multiple options for a given repair situation. Options might include, as examples, temporary vs. permanent repair, bonded composite patches versus bolted composite or metal patches, or wet lay-up or prepreg patches versus pre-cured bonded patches. An operator's choice might depend on the severity of the damage, the time available to perform the repair, the operator's facilities and capabilities, inspection/overhaul schedules, and/or current field environmental conditions.

Durability versus weight trades. The understanding derived from residual strength analyses and tests will also ultimately lead to cost and weight trades that affect all of the total direct operating costs (DOC). Small increases in manufacturing cost and structural weight may be traded against increased damage tolerance and durability to reduce maintenance costs. Decisions may be required to balance the ADL and CDT. For example, test results for laminate tensile notch sensitivity may show an inverse relationship between small and large notch strength. Under such circumstances it may be desirable to have some ADL capability to avoid having to repair small damages but not at the expense of CDTs that allow sufficiently long inspection intervals and satisfactory fail-safe behavior.

8.2.9.2 Repair design issues

Skin/stringer structure repair issues. Solid laminate skin/stringer designs are quite often repaired using mechanically fastened external skin patches and nested substructure splice angles. Mechanically fastened repairs require care and accuracy in the drilling of holes and the alignment of parts during assembly. Fastener hole breakout is a characteristic problem, commonly solved by using a layer of fabric as the outermost ply for all laminates. Typically, even though there may be other methods to avoid fastener hole breakout, there are numerous situations in the real world that challenge a good mechanic's ability to consistently drill high quality holes. Provisions to locate the position of the drilled holes in the structure include alignment marks and templates. Each skin/stringer component design should have laminates lay-ups that have sufficient thickness and numbers of plies in each of the 0°, 90°, and 45° directions so that they are repairable with mechanically fastened patches.

Sandwich structure repair issues. Sandwich structure is generally repaired with insitu processed bonded scarf or stepped patches. The typical scarf/step taper ratios employed when repairing thin face sheets of control panels and fixed secondary structure are quite shallow (e.g., 20:1). When repairing sandwich structures with thicker face sheets in more highly loaded areas, however, scarf repairs with these traditional shallow taper ratios result in the removal of a large amount of undamaged material, and

hence, very large patch sizes. In these situations, repairs may be combinations of scarfed and external patches, so that the repair sizes can be minimized. Flush repairs may be required for some components for aerodynamic reasons or to prevent chafing. Also, thick face sheets require thick patches, which may require special processing to achieve proper consolidation. Patch and bondline porosity are of particular concern with normal field processing, which is accomplished with vacuum pressure and heat blankets. Lower temperature cures are generally preferred due to concerns over causing additional damage via vaporization of water that has infiltrated the core. Also, the surrounding structure may act as a heat sink, making it difficult to achieve and control the higher temperatures with heat blankets, and may contribute to thermal gradients that can result in warpage or degradation of the surrounding structure. For thick sandwich, heat blankets on both sides of the structure may be required to control the through thickness temperature. Still, the shorter processing times generally associated with higher temperature cures are very attractive in terms of minimizing the out-of-service time for a damaged airplane.

Sandwich moisture ingress issues. Consideration must be given to moisture ingress when designing maintainable, repairable sandwich structures. Sandwich designs must address the effects of moisture in the core, both by minimizing the degree of moisture ingress, and by determining what its presence does to the performance of the structure. Moisture ingress can occur through face sheet damages, and part edge and end seals, so special care must be taken to design durable sandwich parts. Unfortunately, to make durable face skins, additional thickness is needed, and this may not be desirable from a performance point of view. Durable edge and end seals can be designed, see Ref. 8.2.1.1. When repairing damaged sandwich structures, a drying cycle is typically performed prior to the accomplishment of any bonded repair. This is performed so that any retained moisture does not interfere with the curing cycle. There have been numerous cases of face skins blowing off sandwich components during the vacuum bag heating cure cycle.

8.3 SUPPORT IMPLEMENTATION

A repair has the objective of restoring a damaged structure to an acceptable capability in terms of strength, durability, stiffness, functional performance, safety, cosmetic appearance or service life. Ideally, the repair will return the structure to original capability and appearance.

The design assessment of a repair for a given loading condition involves the selection of a repair concept, the choice of the appropriate repair materials and processes, then specifying the detailed configuration and size of the repair. Most repairs are basically designed as a joint to transfer load into and out of a patch. To ensure that the repair configuration will have adequate strength and stiffness, the repair joint must be analyzed to predict its strength.

The selection of the type of load-transfer joint to be used for a patch/strap is a tradeoff between simplicity, strength and stiffness. The easier configurations are generally not as strong as the more difficult ones. It is critical that the materials and process information is available prior to the system being put into place.

8.3.1 Part Inspection

Presence of damage in aircraft composite parts is usually found in the course of a routine on-line inspection, depot inspection, or, for large damages, noticed by the pilot. The predominant mode of inspection is visual with more sophisticated modes of inspection performed at the depot. Once damage is identified visually in-service, the damage should be characterized quantitatively by measuring dent depth, extent of surface damage, and length of scratches before proceeding to more complex NDI. This will generally consist of tap testing to define the boundary between damaged and undamaged portions of the structure and followed, for major repairs, with instrumented NDI techniques (ultrasonics, radiography, etc.) to locate the through the thickness characteristics of the damage. At a depot other NDI methods, such as shearography or thermography, may be available. A good general reference on inspection methods is SAE ARP 5089 "Composite Repair NDI and NDT Handbook" (Reference 8.3.1). A summary of common nondestructive test methods and their utilization is shown in Table 8.3.1.

TABLE 8.3.1 *Common non-destructive test methods.*

METHOD	STRUCTURE	DAMAGE DETECTED	RELIABILITY
Visual	All	Surface damage	Good
Tap test	Thin laminate Thin face sheet	Delaminations near surface	Good
		Lack of bond	Good
		Disbond near surface	Good
		Voids	Poor
		Blown core (core damage)	Poor
		Lack of tie-in at closure	Good
		Lack of tie-in at core splice	Poor
Ultrasonics	All	Delaminations	Good
		Lack of bond	Good
	Sandwich	Crushed core	Poor
		Blown core (core damage)	Poor
		Water in core	Poor
Radiography	All	Disbonds/delaminations	Poor
		Delaminations in corners	Good
	Sandwich	Node separation	Good
		Crushed core	Good
		Blown core (core damage)	Good
		Water in core	Good
Shearography	All	Disbonds/delaminations	Good
Thermography	All	Disbonds/delaminations	Good
	Sandwich	Water in core	Good

8.3.1.1 Visual

Nondestructive inspection by visual means is by far the oldest and most economical NDI method. Consequently, visual inspection is performed routinely as a means of quality control and damage assessment for both the manufacturer and the repair technician. Fortunately, most types of damage either scorch, stain, dent, penetrate, abrade, or chip the composite surface making the damage visually verifiable. Once detected, the affected area becomes a candidate for closer inspection. Flashlights, magnifying glasses, mirrors, and borescopes are employed as aids in the visual inspection of composites. They are used to magnify defects which otherwise might not be seen easily and to allow visual inspection of areas that are not readily accessible. Resin starvation, resin richness, wrinkles, ply bridging, discoloration (due to overheating, lightning strike, etc.), impact damage by any cause, foreign matter, blisters, and disbonding are some of the discrepancies readily discernable by a visual inspection. Visual inspection can not find internal flaws in the composite, such as delaminations, disbonds, and matrix crazing. More sophisticated NDI is needed to detect these, although an experienced (with the part and composites in general) technician can often surmise if there is any internal damage. Additionally, tight surface cracks and edge delaminations may not be detected visually.

Therefore, visual inspection techniques need to be supplemented by other methods of nondestructive testing. Because many of the defects associated with composites are hidden within the composite component's structure (i.e., within the ply lay-up or common to the honeycomb core), special techniques dealing with the analysis of sound attenuation are utilized to assure structural continuity within the composite.

8.3.1.2 Tap testing

Sometimes referred to as audio, sonic, or coin tap, this technique makes use of frequencies in the audible range (10Hz. to 20Hz.). A surprisingly accurate method in the hands of experienced personnel, tap testing is perhaps the most common technique used for the detection of delamination and/or disbond. The method is accomplished by tapping the inspection area with a solid round disk or lightweight hammer-like device, as shown in Figure 8.3.1.2 and listening to the response of the structure to the hammer. A clear, sharp, ringing sound is indicative of a well-bonded solid structure while a dull or thud like sound indicates a discrepant area. The tapping rate needs to be rapid enough to produce enough sound such that any difference in sound tone is discernable to the ear. Tap testing is effective on thin skin to stiffener bondlines, honeycomb sandwich with thin face sheets or even near the surface of thick laminates such as rotorcraft blade supports. Again, inherent in the method is the possibility that changes within the internal elements of the structure might produce pitch changes that might be interpreted as defects, when in fact they are present by design. This inspection should be accomplished in as quiet an area as possible and by experienced personnel familiar with the part's internal configuration.

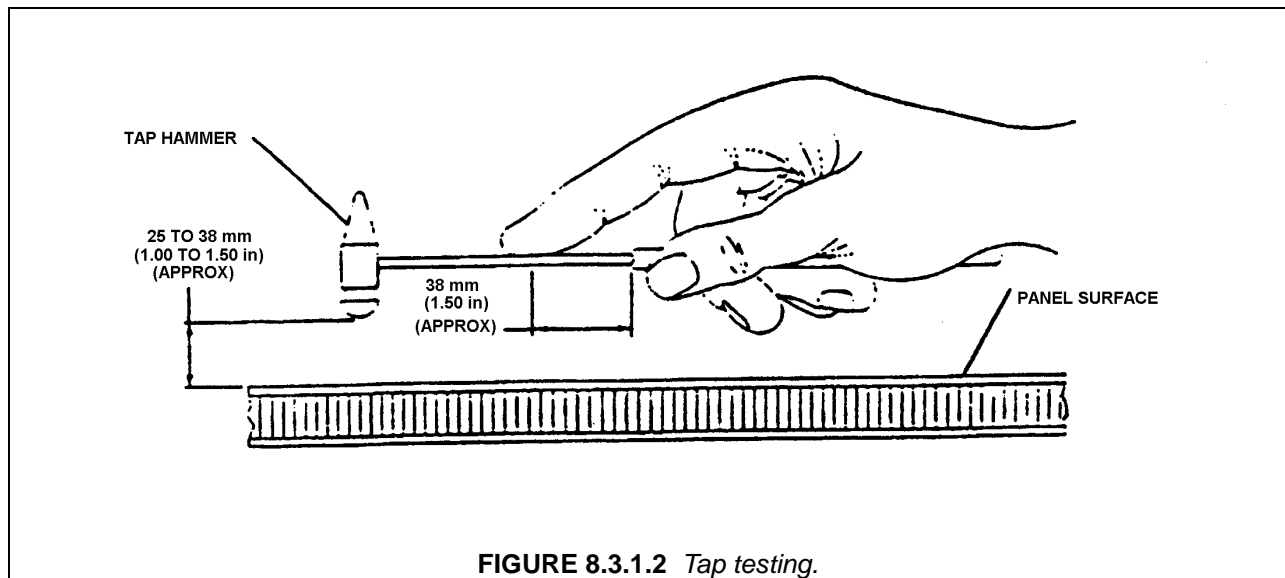


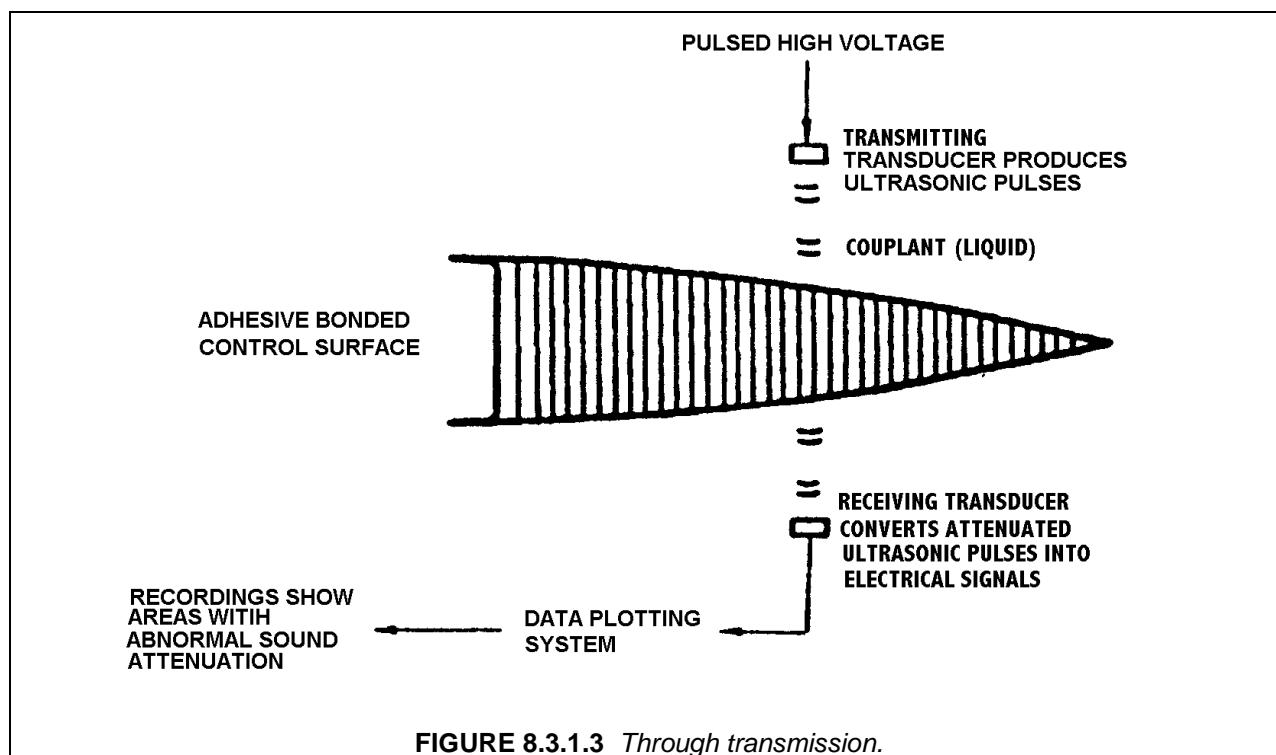
FIGURE 8.3.1.2 Tap testing.

8.3.1.3 Ultrasonics

Ultrasonic inspection has proven to be a very useful tool for the detection of internal delaminations, voids, or inconsistencies in composite components not otherwise discernable using visual or tap methodology. There are many ultrasonic techniques, however, each technique uses sound wave energy with a frequency above the audible range. A high frequency (usually several MHz) sound wave is introduced into the part and may be directed to travel normal to the part surface, or along the surface of the part, or at some predefined angle to the part surface. Different directions are used as the flow may not be visible only from one direction. The introduced sound is then monitored as it travels its assigned route through the part for any significant change. Ultrasonic sound waves have properties similar to light waves. When an ultrasonic wave strikes an interrupting object, the wave or energy is either absorbed or reflected back to the surface. The disrupted or diminished sonic energy is then picked up by a receiving transducer and converted into a display on an oscilloscope or a chart recorder. The display allows the operator to comparatively evaluate the discrepant indications against those areas known to be good. To facilitate the comparison, reference standards are established and utilized to calibrate the ultrasonic equipment.

The repair technician must realize that the concepts outlined here work fine in the repetitious manufacturing environment, but are likely to be more difficult to implement in a repair environment given the vast number of different composite components installed on the aircraft and the relative complexity of their construction. The reference standards would also have to take into account the transmutations that take place when a composite component is exposed to an in-service environment over a prolonged period, or has been the subject of repair activity or similar restorative action. The two most common ultrasonic techniques applicable to damage definition are discussed next.

Through Transmission. This technique may be utilized when both sides of the part to be inspected are accessible. The basic principle of through transmission ultrasonics is shown in Figure 8.3.1.3. Pulsed high voltage is applied to a piezoelectric crystal contained within the transducer. This crystal transforms the electrical energy to mechanical energy in the form of ultrasonic sound waves. The ultrasonic waves are propagated through the part to the receiving transducer where the mechanical energy is transformed back into electrical energy. A couplant other than air is needed for the method to work. In production environment the part is immersed in water or a squirted water system is utilized. Caution must be exercised when using couplant material other than water so as not to contaminate the laminate. Water soluble couplants work well. New techniques are being developed which do not need a couplant. The output may be plotted on a recording system or displayed by a meter or an oscilloscope. Defects within the test article will disrupt or absorb a portion of the energy and thereby change the amount of energy detected by the receiving transducer. The defects resultant diminished energy then becomes discernable on the display.

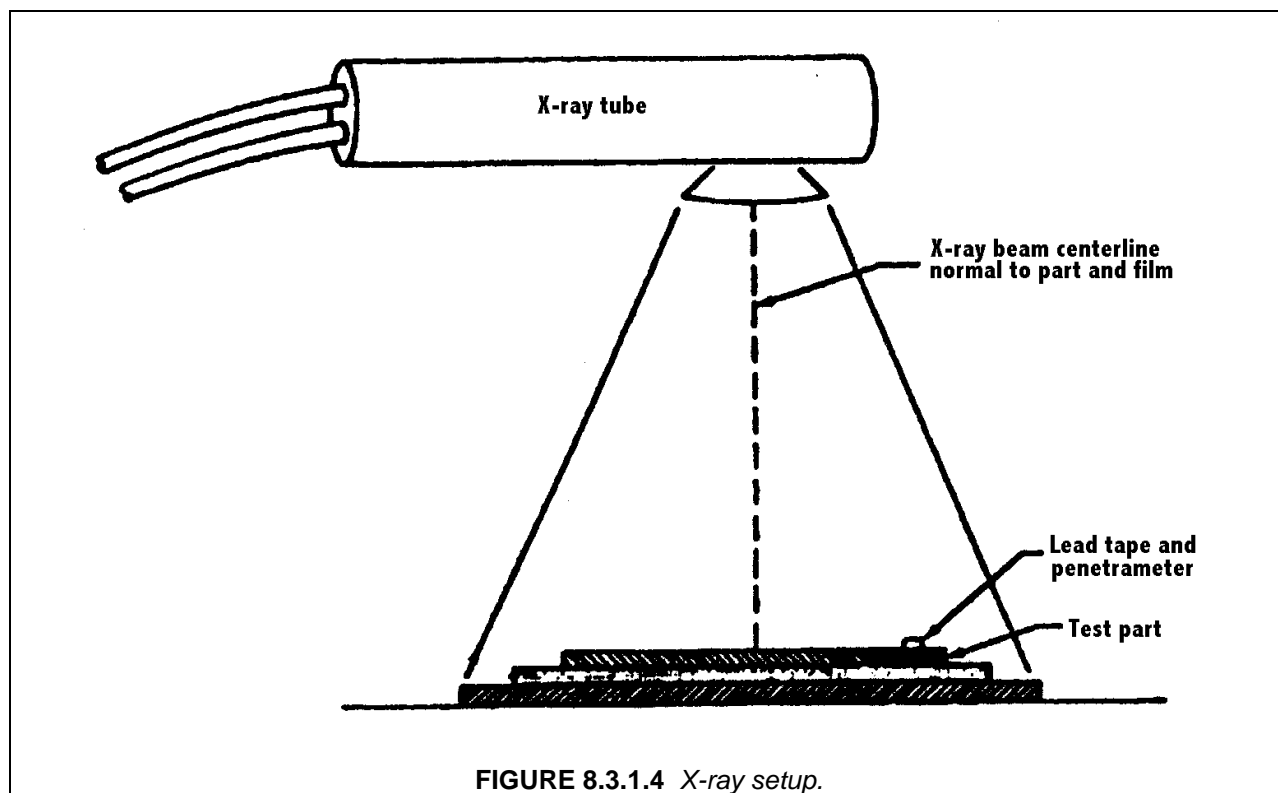


Pulse Echo. Single side ultrasonic inspection may be accomplished using pulse echo techniques. In this method a single search unit is working as a transmitting and a receiving transducer which is excited by high voltage pulses. Each electrical pulse activates the transducer element. This element converts the electrical energy into mechanical energy in the form of an ultrasonic sound wave. The sonic energy travels through a Teflon or a Methacrylate contact tip into the test part. A wave-form is generated in the test part and is picked up by the transducer element. Any change in amplitude of the received signal, or

time required for the echo to return to the transducer, indicates the presence of a defect. In pulse echo the couplant is directly applied to the part.

8.3.1.4 Radiography

Radiography, or X-ray, as it is often referred to, is a very useful NDI method in that it essentially allows a view into the interior of the part. This inspection method is accomplished by passing X-rays through the part or assembly being tested while recording the absorption of the rays onto a film sensitive to X-rays. A typical radiographic exposure setup is shown in Figure 8.3.1.4. The exposed film, when developed, allows the inspector to analyze variations in the opacity of the exposure recorded onto the film, in effect creating a visualization of the relationship of the component's internal details. Since the method records changes in total density through its thickness, it is not a preferred method for detecting defects such as delaminations that are in a plane that is normal to the ray direction. It is a most effective method, however, for detecting flaws parallel to the X-ray beam's centerline. Internal anomalies such as delaminations in the corners, crushed core, blown core, water in core cells, voids in foam adhesive joints, and relative position of internal details can readily be seen via radiography. Most composites are nearly transparent to X-rays so low energy rays must be used. Opaque penetrant can be used to enhance the visibility of surface breaking defects, however, it is generally not available for in-service inspections.



Because of the picture-like quality of the results, radiographic inspection lends itself to easy interpretation, although honeycomb X-ray radiographs are best analyzed by experienced technicians. However, because of safety concerns it is impractical to use around aircraft. Operators should always be protected by sufficient lead shields, as the possibility of exposure exists either from the X-ray tube or from scattered radiation. Maintaining a minimum safe distance from the X-ray source is always essential.

8.3.1.5 Shearography

Shearography is an optical NDI technique that detects defects by measuring the variations in reflected light (speckle pattern) from the surface of the object. Using a laser light source, an original image of the illuminated surface is recorded via a video image. The part is subsequently stressed by heating, changes in pressure, or acoustic vibrations during which a second video image is made. Changes in the surface contour caused by disbonding or delaminating become visible on the video display.

Shearography is being used in production environments for rapid inspection of bonded composite structure assemblies including carbon/epoxy skin and Nomex core sandwiches. This is accomplished by inducing stresses by partial vacuum. Partial vacuum stressing causes air content defects to expand, leading to slight surface deformations that are detected before and during stressing comparisons. Display of the computer processed video image comparisons reveals defects as bright and dark concentric circles of constructive and destructive reflected light wave interference. A schematic of an inspection system currently in use is shown in Figure 8.3.1.5.

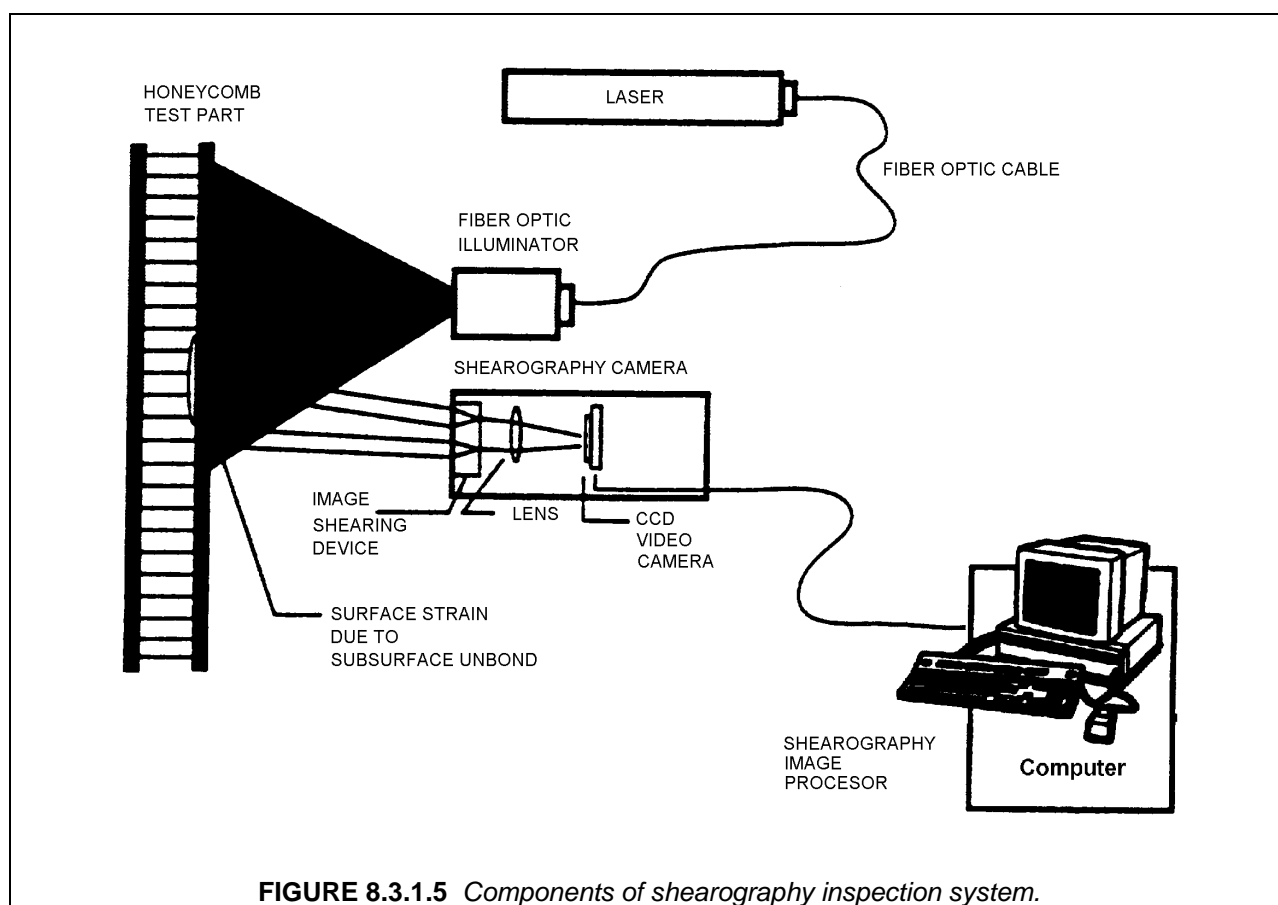


FIGURE 8.3.1.5 Components of shearography inspection system.

8.3.1.6 Thermography

Thermal inspection comprises all methods in which heat-sensing devices are used to measure temperature variations for parts under inspection. The basic principle of thermal inspection consists of measuring or mapping of surface temperatures when heat flows from, to, or through a test object. All thermographic techniques rely on differentials in thermal conductivity between normal, defect free areas and those having a defect. Normally, a heat source is used to elevate the temperature of the article being examined while observing the surface heating effects. Because defect free areas conduct heat more effi-

ciently than areas with defects, the amount of heat that is either absorbed and reflected indicates the quality of the bond. The type of defects that affect the thermal properties include debonds, cracks, impact damage, panel thinning, and water ingress into composite materials and honeycomb core. Thermal methods are most effective for thin laminates or for defects near the surface.

The most widely used thermographic inspection technique uses an infrared (IR) sensing system to measure temperature distribution. This type of inspection can provide rapid, one-sided non-contact scanning of surfaces, components, or assemblies. Figure 8.3.1.6 illustrates the components of such a system that would measure near-static heat patterns. The heat source can be as simple as a heat lamp so long as the appropriate heat energy is applied to the inspection surface. The induced temperature rise is a few degrees and dissipates quickly after the heat input is removed. The IR camera records the infrared patterns. The resulting temperature data are processed to provide more quantitative information. An operator analyzes the screen and determines whether a defect was found. Because infrared thermography is a radiometric measurement, it can be done without physical contact. Depending on the spatial resolution of the IR camera and the size of the expected damage, each image can be of relatively large area. Furthermore, as composite materials do not radiate heat nearly as much as aluminum and have higher emissivity, thermography can provide better definition of damage with smaller heat inputs. Understanding of structural arrangement is imperative to ensure that substructure is not mistaken for defects or damage.

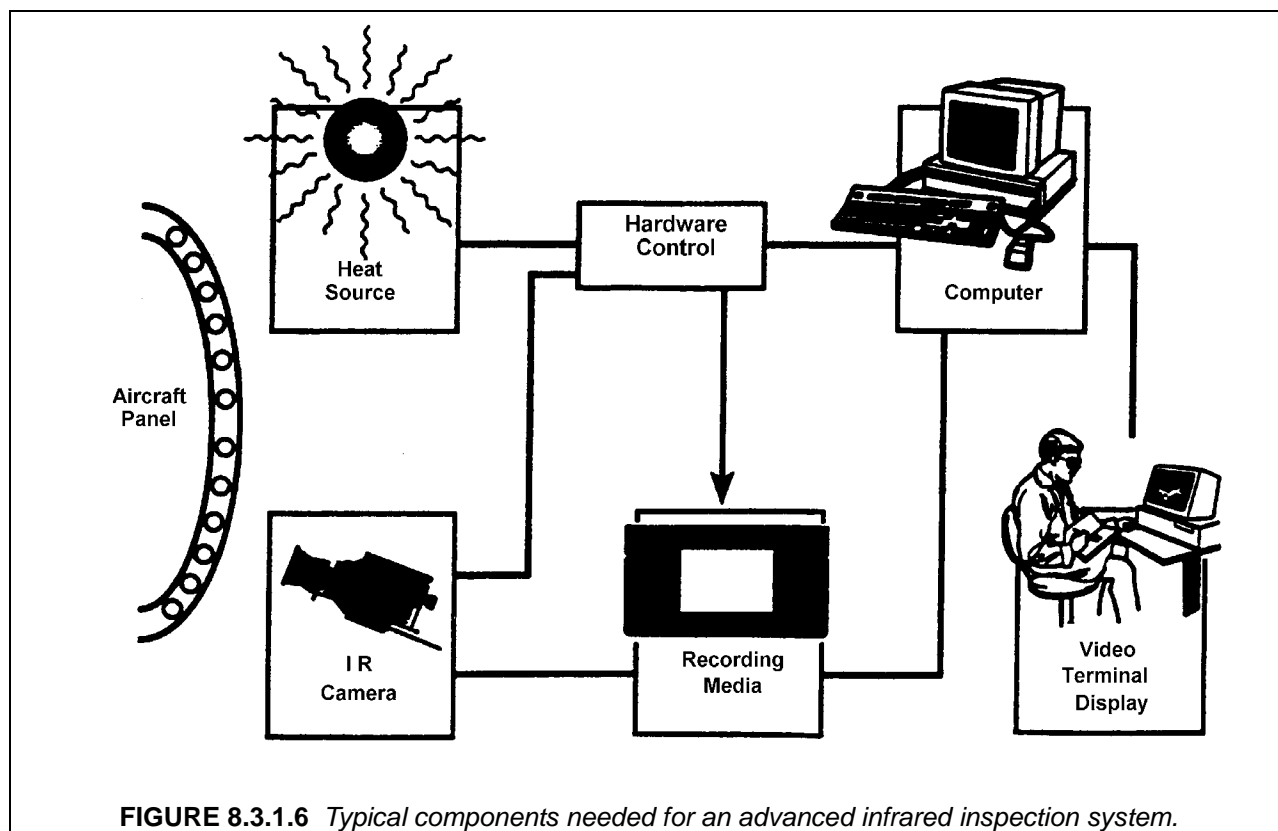


FIGURE 8.3.1.6 *Typical components needed for an advanced infrared inspection system.*

8.3.2 Damage assessment for composite repairs

8.3.2.1 General

The damage assessment is the intermediate stage between inspection and repair and includes taking a decision about if and how to repair a damaged structure, the nature of the repair (permanent or temporary), and the needed inspection after the repair and during the residual life of the repaired structure.

This decision depends upon where the damage is detected, the accuracy of damage characterization, the means available in determining the severity of the damage, and designing and performing an adequate repair.

8.3.2.2 Mandate of the assessor

The mandate of the assessor is the authority to interpret the inspection results and to decide about the needed repair and residual life of the structure. This is strongly dependent on the available information and expertise of the assessor. In the field, the mandate of the assessor is limited to following the manufacturer's instructions. In a repair station, and at the manufacturer's facilities, it can be extended, provided that engineering approvals and for civil aircraft authority approvals, are obtained. For larger damages, experimental substantiation may be required.

8.3.2.3 Qualification of the assessor

The assessment process is one of integration. The assessor should have the technical background to understand the inspection results, to understand the available design information, be familiar with the repair capabilities and have the necessary skills and experience. The demands on its technical expertise vary according to the repair location, for example, FAR Part 65, Certification: Airman other than crew members, prescribes the requirements for issuing Mechanics and Repairman certificates. The assessment of in field damage for civil aircraft are done by a certified mechanic, appropriately rated, with knowledge in composites and under the restrictions stated by the aircraft manufacturer in the Maintenance Manual and Structural Repair Manual. In other fields of activity, for example, in the military, similar criteria exist to define skill and experience requirements. In a Repair Station and at the Manufacturers Site, the assessment should involve a team, including engineering design and analysis.

8.3.2.4 Information for damage assessment

The following information is needed in the assessment process:

Damage Characterization

- Damage geometry, includes damage kind (delamination, cut, hole, etc.), dimension, form.
- Damage location, includes position on the part (in composite laminates in-plane location as well as depth should be considered), vicinity to other structural elements or systems, vicinity to other damages and repairs.

This information is a function of the inspection capability.

Degradation of the structure due to the damage

The assessor must consider the design requirements of the structure and the criteria to which it was designed before embarking on any repair actions.

Repair Capabilities

The repair methods recommended for composite structures are detailed in the next section. However, the repair capability and the availability of means to perform the repair have to be evaluated at this stage as part of the decision if and which repair to perform. For example, if bonding facilities are not available or if not enough time for the curing process is available, an equivalent bolted repair may be performed, or a temporary repair may be chosen, in order to arrive at a site where capabilities are available.

8.3.2.5 Dependence on repair location

The information for damage assessment depends on the location of damage detection and repair. Table 8.3.2.5 summarizes the information available at different locations.

TABLE 8.3.2.5 *Damage assessment per location.*

Location	Damage Information	Design Information	Repair Capability	Qualification of Assessor	Mandate of Assessor
In the field	Limited	Limited, manufacturer instructions	Limited, means and time, facility conditions	Mechanic or repairman*	Limited to manufacturer repair manual
Repair Station	Partial, varies according to station	Partial, manufacturer instructions and some functional and design information	Partial, varies according to station	Mechanic or repairman* and engineering support	Partial, requires manufacturer and civil authority approval or military depot engineering deposition
Manufacturer	Complete, equipment and know how available	Complete, design information, analytical capabilities, knowledge and mandate for certification	All facilities, from complicated repairs to rework	Engineering and manufacturing team	Ample, needs civil authority approval for changes to certified products

* Appropriately rated, with knowledge in composites (FAR part 65)

In the field: airport, airline, air force base, navy carrier, harbor (boat), road (car)

- Limited inspection equipment and, therefore, limited knowledge on the real extent of the damage (for example, due to impact damage, the upper skin and paint have visible damage, by tapping there is an indication that there is a delamination, but the exact dimensions of the delamination, their depth, number, etc., are not known).
- No knowledge how the damage affects the structural integrity of the part.
- Limited repair capabilities.
- Time limits.

In this case, it is the responsibility of the designer of the part to define maximal damage that can be repaired in field conditions and the repair method based on his knowledge of the structure and knowledge of the inspection and repair capabilities of the user. For civil airplanes, this is required by FAA regulations, Part 43, which state that repair methods and personnel should be FAA approved. Reference 8.3.2.5(a) contains a chapter relating to Repair of Laminated Structures, limited to fiberglass. A standard repair

manual should include the detection method, the maximum damage which can be left unrepaired, the maximum damage which can be repaired and the repair methods.

Repair Station

Repair stations may vary according to capability and rating.

A repair station may be part of an airline, manufacturer, military repair station, or facility specializing in repair. For civil aircraft, the repair station has to be FAA approved. AC No. 145-6 (Reference 8.3.2.5(b)) provides information and guidance concerning means of demonstrating compliance with the requirements of 14 CFP parts 21, 43, 121, 125, 127, 135, and 147 regarding procedures and facilities for repair and alterations of structure consisting of metal bonded and fiber reinforced materials.

A repair station may repair damage exceeding the limits posed by the manufacturer in the repair manual under an appropriate engineering disposition. For civil aircraft, such a repair has to be FAA (or other civil authorities) approved. In the U.S. military, components requiring a repair that exceeds the limits specified in the repair manual are referred to the weapon system (aircraft) program manager for engineering disposition. Depending on the damage to the part and field capabilities, the engineering disposition may specify a field repair, the assignment of a depot repair team or transfer of the part to the depot for repair.

The following information is available at the repair station:

- Inspection capabilities of a repair station are more ample than the field capabilities, but may differ according to the type or class of station.
- Design information: engineering support (drawings, special problematic areas, lightning protection, electromagnetic transmission, etc.) should be supplied by the manufacturer. Analytical means have to be available to evaluate the performance of the designed repair.
- Repair facilities must be rated for the type of repair performed (for example, to include clean room, appropriate storage and curing facilities for bonded repairs).

Manufacturer

When a part is being returned for repair to the manufacturer, all resources concerning inspection, structural definition, and repair methods are available, and major repairs or reworks can be performed. The manufacturer may send a repair team to perform the repair in field; this will also be a manufacturer repair. Military repair depots perform remanufacture in-house to original manufacturer's specifications.

Again, the repairs have to be substantiated, and for civil aircraft, approved by the civil authorities.

8.3.3 Repair design criteria

Repair design criteria fulfill a function of assuring that the structural integrity and functionality of the repaired part are the same as that of the undamaged part. The repair design criteria should be established by the original manufacturer or cognizant engineering authority and used to develop repairs in the Structures Repair Manual (SRM). They are implicitly followed by the operator or the repair station when the repairs are made within the scope of the SRM. When a repair is designed which exceeds the limits of the SRM, the repairs must be substantiated and approved based on the specified repair criteria.

SRM's for specific aircraft frequently "zone" the structure to show the amount of strength restoration needed or the kinds of standard repairs that are acceptable. Zoning permits the use of simpler repairs in areas where large strength margins exist. Zoning also restricts operator repairs in areas where repairs are too complex and should be only repaired with original equipment manufacturer's (OEM's) involvement.

Repair design criteria for permanent repairs are fundamentally those that designed the part that is to be repaired. These are: restore stiffness of the original structure, withstand static strength at the expected environments up to ultimate load including stability (except for postbuckled structure), assure durability for the remaining life of the component, satisfy original part damage tolerance requirements, and restore functionality of aircraft systems. Additionally there are other criteria applicable in repair situations. These are: minimize aerodynamic contour changes, minimize weight penalty, minimize load path changes, and be compatible with aircraft operations schedule.

8.3.3.1 *Part stiffness*

First consideration in any repair is to replace structural material that is damaged. This means that especially for large repairs the stiffness and placement of repair material should match the parent material as closely as possible. This avoids any recalculations of the overall dynamic behavior of the component, such as flutter or structural load redistribution. Furthermore, many lightweight flight vehicle structures are designed to meet stiffness requirements that are more critical than their strength requirements. A repair made to a structure of this type must, therefore, maintain the required stiffness so that deflections or stability requirements are met.

Fixed aerodynamic surfaces, such as wings and tails, are frequently designed to have bending and torsion stiffness that are adequate to prevent excessive deflections under aerodynamic loading. This is to prevent divergence and control surface (such as aileron) reversal. Moveable surfaces are frequently sensitive to aerodynamic flutter and their stiffness may have been carefully tailored to obtain natural frequencies for which flutter will not occur. Effects of added weight are discussed in Section 8.3.3.7.

Increasing the stiffness of a control surface, especially the bending stiffness, can reduce the flutter speed to unacceptable levels; a decrease in stiffness can be equally damaging. Any significant change in stiffness must be evaluated for its effect on the dynamic behavior of structure. Stiffness can also affect the deflections of actuated doors, such as landing gear doors. Reduction in stiffness can result in excessive deflections under aerodynamic loading. These reduction may increase drag or in extreme cases cause loss of the structure.

8.3.3.2 *Static strength and stability*

Any permanent repair must be designed to support applied loads at the ultimate design load level at the extremes of temperature excursions, moisture levels, and barely visible damage levels. If the loads are not available, specific SRAM repair recommendations must be strictly adhered to. In the SRAM repairs, there is an implicit assumption that the specific repairs meet all static strength and stability requirements.

Load path changes are a special concern when designing repairs. When strength restoration is necessary, attention must be given to the effect of the stiffness of the repair on the load distribution in the structure. If a patch has less stiffness than the original structure, the patch may not carry its share of the load, and this causes an overload in the surrounding material. This condition can be caused by a patch made from a less stiff material, or from fasteners that fail to transfer full load because of loose fits or fastener deformation. Conversely, an overly stiff patch may attract more than its share of load, causing adjacent areas to which it is attached to be overloaded. Stiffness mismatch between parent material and the patch may cause peel stresses that can initiate debonding of the patch.

Structures loaded in compression or in shear, such as some wing skins, webs of spars or ribs, and fuselage structure, including both external skins and internal bulkheads, may be stability and not strength critical at ultimate design load. Two types of stability failure are possible:

1. Panel Buckling - The panel, such as a section of wing skin, buckles between its major supports, for example, spars and ribs. The repair must account for the stiffness of the panel and the amount of support provided by the attachment to the substructure. Some portions of structure,

i.e., wing skins between spars, are permitted to buckle below ultimate design load. These types of structures develop specific post-buckling behavior which redistributes the load and allows the structure to carry ultimate load. Any repair of a stability critical structure, and especially a structure that is permitted to buckle, should be considerate in not affecting its buckling and post-buckling modes. Matching of stiffness of the parent material is of utmost importance here.

2. Local Crippling and Buckling - This is buckling of the cross section of a member or its component, such as a spar cap, by distortion of the cross section rather than the overall buckling along its length or width. Restoration of local crippling strength must be considered when making repairs to substructure.

Composite laminates under compressive load can fail when individual fibers or bundles of fibers buckle where delaminations or penetrations result in fibers with reduced support. Because of the danger of microbuckling or local ply buckling, resin injection repair that fills a delamination without adequately bonding the delaminated plies together could be unsatisfactory.

8.3.3.3 *Durability*

Durability is the ability of a structure to function effectively throughout the life of the vehicle. For commercial transport aircraft, the design life can be greater than 50,000 cycles; military fighter aircraft are designed for 4,000 to 6,000 flight hours. Included among the factors affecting durability are temperature and moisture environments (covered in Sections 8.3.3.8 and 8.3.3.9).

Although the parent composite structure may not be durability critical, structural repairs may be more susceptible to damage caused by repeated loads during their service lives. This is because the repair process is not as well controlled and the repairs themselves create solitary joints and discontinuities in areas that are exposed. For bolted repairs, high bearing stresses on fastener holes should be avoided as they may elongate under repeated loading and lead to fastener fatigue. Bonded repairs should be well sealed as they can develop disbonds after being weakened by environmental effects. All found delaminations exceeding the acceptance/rejection criteria of the SRM should be repaired as unrepaired delaminations may grow under compressive or shear loading. Bolted repairs of sandwich structure must be sealed.

8.3.3.4 *Damage tolerance*

Composite structures are designed to be damage tolerant to accidental damage. In practice, this is accomplished by lowering design strains so that the structure with impact caused damage can withstand ultimate load. Repairs must also be capable of tolerating a predetermined level of impact damage. The level of impact damage is usually established by OEM's with concurrence of certifying agency. When using metal for large damage repair, damage tolerance requirements for metallic structure must be followed. Metallic doublers and parts will also require protection against galvanic corrosion and lightning strike.

8.3.3.5 *Related aircraft systems*

In addition to satisfying structural criteria, compatibility with related aircraft systems may also be required of the repair. These systems include:

1. Fuel System - Structure is frequently used to contain fuel, as in the "wet" wings of many aircraft. A repair must seal adequately to prevent leakage of the fuel. The repair may also be subjected to fuel pressure loading. Repair material must be compatible with fuel.
2. Lightning Protection System- Some composite structure has provision for conducting lightning strikes by use of flame-sprayed coatings, bonded metallic strips, wire mesh, etc. A repair to the structure must restore the electrical continuity as well as the structural strength. Bolted repairs around fuel tanks must avoid creating an electrical path.
3. Mechanical System - Components that are mechanically actuated, such as landing gear doors or control surfaces, must function correctly after repair. Clearances and fit-up to adjacent fixed structure may be critical. Re-rigging or re-balancing may be required after repair.

8.3.3.6 *Aerodynamic smoothness*

High-performance flight vehicles depend on smooth external surfaces to minimize drag. During initial fabrication, smoothness requirements are specified, usually by defining zones where different levels of aerodynamic smoothness are required. Most SRM's specify smoothness requirements for repairs consistent with initial part fabrication.

The most critical zones typically include leading edges of wings and tails, forward nacelles and inlet areas, forward fuselage, and overwing areas of the fuselage. The least critical zones typically include trailing edges and aft fuselage areas. In addition, intermediate zones may be specified. For the most critical zones, forward-facing steps are usually limited to 0.005 to 0.020 in. (0.13 to 0.51 mm) at permanent butt joints. At removable panels, mechanical doors, and major joints, forward-facing steps from 0.010 to 0.030 in. (0.25 to 0.76 mm) are typically allowed. At installed equipment, such as antennas and navigation lights, steps up to 0.020 to 0.040 in. (0.51 to 1.02 mm) are permitted. All sharp edges as the result of patch ply termination should be smoothed and feathered.

Whatever the requirements, each exterior repair should restore aerodynamic contour accurately and smoothly as structurally and economically feasible. Trade-off exist between accepting a slight reduction in performance in order to accept a repair that is more structurally sound and that is easier and quicker to accomplish.

8.3.3.7 *Weight and balance*

Compared to the overall weight of the vehicle, the weight added by most repairs is insignificant. Exceptions may exist for very large repairs or for space vehicles.

The weight of repair becomes a major concern when the repair changes the mass balance of components sensitive to dynamic response, such as moveable control surfaces, rotor blades, and rotating shafts. In such cases, it may be possible to remove as much damaged material as will be added by the repair so that there is little change in weight and moments of inertia. If that is not possible, the part must be re-balanced after repair.

8.3.3.8 *Operating temperatures*

Most flight vehicles experience extremes of temperature during use. Repairs to such flight vehicles must be acceptable for the temperature extremes for which the vehicle was designed. Low temperatures result from high-altitude flight or from extremes of ground storage in cold climates. Many aircraft are designed for a minimum service temperature of -65°F (-54°C). Elevated-temperature requirements vary with the type of vehicle. The maximum temperature for commercial transport aircraft and most rotary wing vehicles is 160°F (71°C) and generally occurs during ground soak on a hot day. However, components experiencing significant loads during takeoff and initial climb may require validation of design ultimate loads at temperatures up to 200°F (93°C). Supersonic transport, fighter, and bomber aircraft typically experience aerodynamic heating of up to 220°F (104°C) or in special cases as high as 265°F (130°C), especially on the leading edges of lifting surfaces. Components exposed to engine heat, such as nacelles and thrust reversers, may be required to withstand even higher temperatures in local areas.

Operating temperature influences the selection of repair materials: resin systems for prepreg repairs, resins for wet lay-up repairs, and adhesives for bonded repairs. Materials that develop adequate strength at the required temperature must be selected. The combination of temperature extremes with environmental exposure (especially moisture) frequently is the critical condition for which the repair must be designed.

8.3.3.9 *Environment*

Repairs may be exposed to many environmental effects, including those listed below:

1. Fluids - salt water or salt spray, fuel or lubricants, hydraulic fluid, paint stripper, and humidity
2. Mechanical loading - shock, acoustic or aerodynamic vibration, and operating loads
3. Thermal cycling

Moisture is particularly critical to the polymeric matrix composites. At elevated temperature absorbed moisture reduces the ability of the matrix to support the fibers, thereby reducing the strength of the laminate for compressive or shear loading. This effect is considered in the original design, and allowable loads are frequently limited by "hot-wet" conditions. The same considerations pertain to bonded repairs.

Absorbed moisture can affect bonded repairs in three ways. These must be considered in the selection of a repair procedure.

1. Parent Laminate Blistering- As a "wet" laminate is heated to cure a bonded repair, the absorbed moisture may cause local delaminations or blisters. Pre-bond drying at lower temperatures, slow heat-up rates, and reduced cure temperatures all diminish the tendency to blister.
2. Blown Skins/Core of Sandwich Structure - Moisture in the cells of honeycomb sandwich structure expands when the part is heated to cure a bonded repair and develops sufficient pressure to separate the skin from the core, especially if the strength of the adhesive has been reduced by temperature and moisture. Similarly, this process may be sufficiently severe to rupture cell walls in the low density core. Pre-drying is normally used to prevent bondline failure of this type.
3. Porosity in Bondlines - As a repair is bonded to a "wet" laminate, the moisture tends to cause porosity in the bondline. This porosity can reduce the strength of the bondline. This problem can be minimized by pre-drying, reduced temperature cure, and selection of moisture-resistant adhesives.

8.3.3.10 Surrounding structure

In the course of the repair process it is imperative that the surrounding structure does not sustain any damage. The predominant sources of damage are dropped tools, scratches caused by prying of bagging material, and the application of high temperatures during the cure of the repair. If there is a potential for the latter damage, resins should be selected that cure at sufficiently low temperature while still capable of hot, wet performance.

8.3.3.11 Temporary repair

Repair design criteria for temporary or interim repairs can be less demanding, but may approach permanent repairs if the temporary repair is to be on the airplane for a considerable time. Most users of aircraft and OEM's prefer permanent repairs, if at all possible, as the temporary repairs may damage parent structure necessitating a more extensive permanent repair or part scrapping. All temporary repairs have to be approved before the aircraft can be restored to operational status.

Temporary repair will restore functionality of the aircraft and its systems but on the temporary basis. Static strength requirements may be reduced to limit load or maximum load in the spectrum. Stiffness requirements may be reduced to a level where they do not cause overall buckling or flutter. Damage tolerance and durability goals are often severely reduced or not considered but are compensated by shorter inspection intervals.

A special subset of temporary repairs are those associated with aircraft battle damage repair (ABDR) and other emergency repairs. In this situation repair design criteria will require sufficient strength, stiffness, and functionality restoration to permit the aircraft to fly to a repair facility or sustain 100 hr of limited flight envelope, or in the ABDR scenario fly one more mission. In the military, there exist ABDR manuals which suggest the types of repairs to be implemented. These repairs are usually required to be accomplished within 24 hours.

8.3.4 Repair of composite structures

8.3.4.1 Introduction

The task of repair begins only after the extent of the damage has been established by cognizant personnel using inspection methods described in Section 8.3.1 and damage assessment as described in Section 8.3.2. The repair has the objective of restoring the damaged structure to a required capability in terms of strength, stiffness, functional performance, safety, service life, and cosmetic appearance. Ideally, the repair will return the structure to original capability and appearance. To start the repair process the structural makeup of the component must be known and the appropriate design criteria should be selected from the considerations described in Section 8.3.3. The continuity in load transfer is re-established in a damaged part by attaching new material by bolting or bonding thus bridging the gap or reinforcing the weakened portion. Thus the repair is in reality a joint where a load is transferred from the parent material into and out of the patch.

Repair design criteria, part configuration, and the logistic requirements will dictate whether the repair should be bolted or bonded. Some of the main drivers that determine the type of repair being more suitable are listed below.

Condition	Bolting	Bonding
Lightly Loaded, Thin (<0.10 in. [2.5 mm])		X
Highly Loaded, Thick (>0.10 in.[2.5 mm])	X	X
High Peeling Stresses	X	
Honeycomb Structure		X
Dry and Clean Adherend Surfaces	X	X
Wet and/or Contaminated Adherend Surfaces	X	
Sealing Required	X	X
Disassembly Required	X	
Restore Unnotched Strength		X

In any case, the Structures Repair Manual (SRM) for the particular component will provide guidance as to the type of repair to be applied.

8.3.4.2 Damage removal and site preparation

Once the repair perimeter has been established around the damage, the task of damage removal begins. The first step is the removal of finish topcoat by hand sanding or other mechanical means. The use of chemical paint stripper is prohibited as it can attack the composite resin system and can also become entrapped in the honeycomb core. Once the topcoat and primer are removed and the damaged plies clearly defined, the damaged plies are then removed either by sanding or other mechanical means, if the damage is partial through the thickness, or by trimming, if the damage is through the laminate. In either case, a well-prepared site should have a well-defined geometric shape with smoothed out corners. Damaged core must be cut out, with special care taken not to damage the inner surface of the opposite (non-damaged) composite skin.

Once the damage has been removed, the repair area should be checked for evidence of moisture and/or contaminants. Contaminants, such as hydraulic fluids or engine oils, will saturate the composite materials making it extremely difficult to obtain a clean bond surface. They may also degrade the mechanical properties of the composite materials. Undetected moisture will turn into steam during elevated temperature cure. The steam will seek an escape path from within the panel causing blown core and laminate disbonding. It has also been shown that patches bonded to parent composite material containing more than a nominal (0.3% moisture content by weight) experience lower adhesive bond strengths. For honeycomb parts cured at room temperature, presence of moisture is undesirable, particularly if the core material is aluminum. SAE ARP 4916 (Reference 8.3.4.2(a)) and ARP 4977 (Reference 8.3.4.2(b)) give guidelines how the composite part should be cleaned and dried before proceeding with the repair.

For bonded repairs, site preparation for installation of repair usually involves taper sanding or step cutting of plies. This is done so that there is gradual introduction of load into and out of the repair material. For external patches, additional consideration for step patching is to minimize intrusion into the air stream. SRM's usually specify the taper angle, overlap and step lengths.

8.3.4.3 Bolted repairs

8.3.4.3.1 Repair concepts

Bolted repairs can comprise an external or an internal patch that results in a single shear joint, or two patches, one on each side that leads to a double shear joint, see Figure 8.3.4.3.1. In both cases the load is transferred through the fasteners and the patch by shear forces, but in the case of the two-patch repair, transfer load eccentricity is minimized. The main disadvantage of bolted repairs is that the new holes created in the parent structure weaken the structure by creating stress concentrations that become damage initiation sites.

The external bolted patch is the easiest repair to fabricate. The patch overlaps the parent skin with sufficient area to install the required amount of fasteners to transfer the load. For large repairs the patch may be stepped and different size fasteners may be used in different rows to ease the load transfer. The external patch thickness may be limited by aerodynamic considerations and by the induced load eccentricity due to neutral axis offset. However, this type of repair does not need backside access as the fasteners can be blind, i.e., being able to be installed from one side only. If the external patch is unfeasible, an internal patch can be applied. When backside access is not possible, the patch is split to allow insertion through an elliptical or circular cutout in the skin. In some cases the damage must be enlarged in the direction of the primary load to effect the repair. Because of hardware, internal bolted patches may have interference problems with substructure members. The two-patch repair using external and internal patches is a desirable repair from the load transfer point-of-view, however, the repair is more complicated and is heavier.

For complex repairs, multi-row fastener patterns will be required to gradually introduce the load from the part being repaired into the repair patch. It is virtually impossible to distribute the load evenly between all the fasteners in a multiple row pattern, but careful design of patch geometry, fastener diameter and spacing can alleviate the high loads at the first fasteners. Such complex repairs are not usually identified in the approved repair manuals or procedures (SRM, TO, or TM) and normally need engineering input for design.

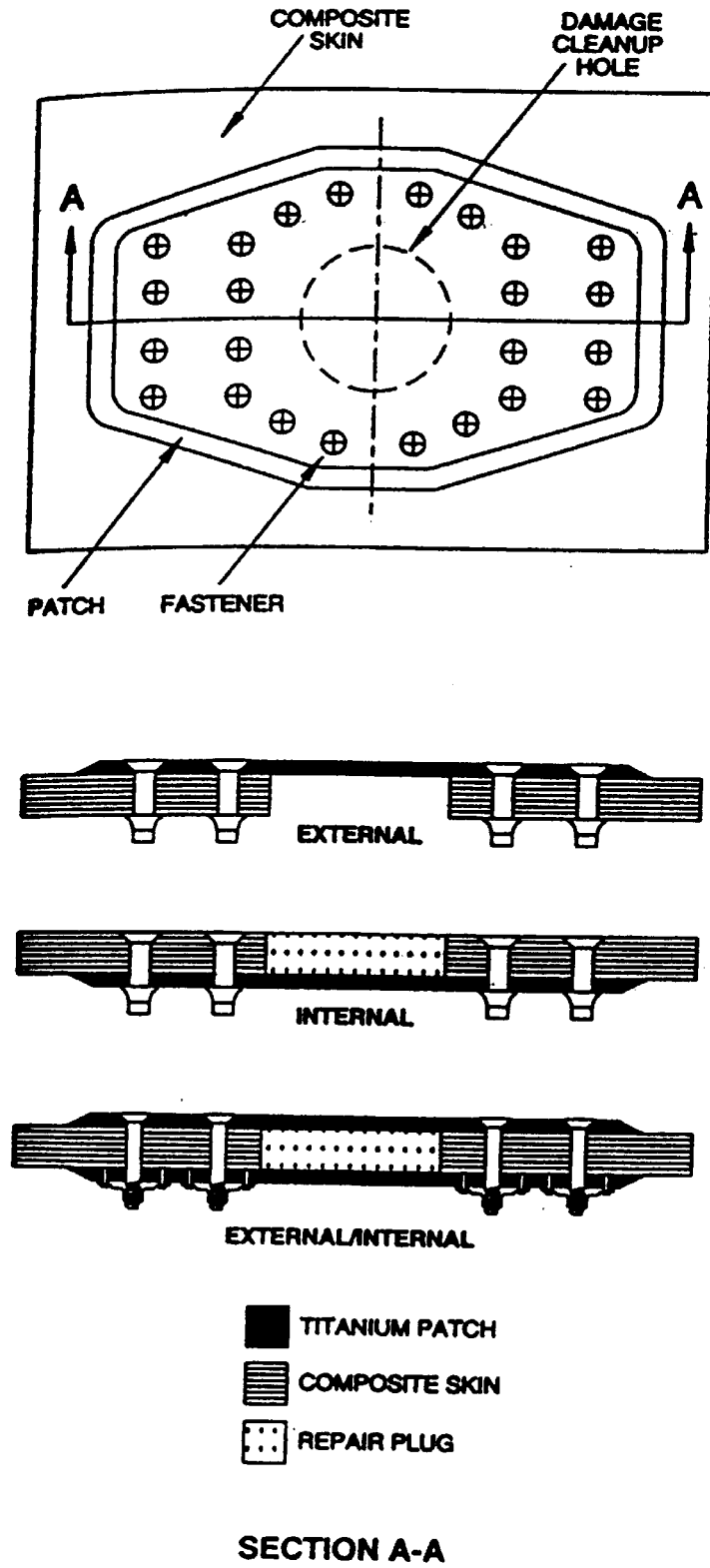


FIGURE 8.3.4.3.1 Basic repair joints (bolted).

8.3.4.3.2 *Repair materials*

For bolted repairs, there is only the need to select patch material and fasteners. Patches may be aluminum, titanium or steel, or pre-cured composite, carbon/epoxy or fiberglass epoxy. For aluminum patch repair on carbon parent material, a layer of fiberglass cloth is placed between them to prevent galvanic corrosion. For repair of highly loaded components, titanium or pre-cured carbon/epoxy patches are usually preferred. For repair of high strain structure coupled with severe fatigue load environment, carbon/epoxy patches can be more effective. Pre-cured carbon/epoxy patches will have the same strength and stiffness as the parent material as they are usually cured and inspected similarly. The major disadvantages of this type of patch are that they do not conform to curved or irregular surfaces and that warpage during pre-cure can result in poor fit requiring shimming.

For repair of composite parts the choice of fasteners is limited to titanium, Monel, or stainless steel. The choice of fastener type is strictly controlled by the SRM. A discussion on fasteners for composites can be found in Chapter 6 of this volume.

There is a general misconception that bolted repairs require very little logistics support in terms of materials. This is false, as many types of fasteners with different grip lengths need to be stored. As fasteners for composites are expensive, the inventory can be costly. If pre-cured carbon/epoxy patches are used, different patch sizes and thicknesses have to be available, as cutting to size requires specialized equipment.

8.3.4.3.3 *Repair analysis*

Analysis of a bolted repair follows the guidance lines of the analysis of a bolted joint, Volume 3, Chapter 6.3. In the following, the main steps will be presented, with emphasis on items specific for repairs.

a) Estimation of load transferred through the repair

As defined in the Introduction, the repair is a joint where load is transferred from the parent material into and out of the patch. The estimation of the transferred load through the repair is the first stage in the repair analysis.

The two situations where there is need for analyses of repair are during the writing of the SRM or when damage that exceeds the allowed SRM limits has to be repaired (Section 8.3.2 addresses the repair mandate and certification requirements). The SRM is written by the manufacturer, who has all the needed information from the analysis of the undamaged structure. In the second case, the load information has to be obtained from the manufacturer. In special occasions, especially for temporary repairs, loads can be approximated by reverse engineering, utilizing the known design of the parent structure. Care should be taken to use conservative approximations that are based on the maximum load that can be sustained by the geometry and lay-up of the parent structure.

b) Load sharing in the repair

After the load transferred through the repair is known, the distribution of this load between the various fasteners, and then, in the region of each fastener between the parent structure, the patch and the fasteners, has to be evaluated. The analysis is done according to Volume 3, Chapter 6.3.2.1.

c) Analysis of local failure

- *Parent structure:* The parent part of the joint may not be adequate to accommodate the mechanically fastened joint. It may not have the adequate thickness or the proper lay-up to provide the bearing resistance. As the lay-up cannot be changed, the only recourse is to bond additional plies. However, care must be taken so as not to end-up with a highly unsymmetrical lay-up. Care must also be taken to properly estimate the bearing/by pass ratio and to consider all possible

laminare failure modes (Volume 3, Figure 6.3.2.3(a)), in order to avoid increasing the damage by failing the periphery of the repair. Analysis techniques follow Volume 3, Chapters 6.2.2.2 and 6.3.2.3. For the case of repairs to be incorporated into the SRM, a test program is usually performed to verify the analysis and substantiate the repair.

- *Patch structure:* In the patch design there is freedom to select composite material, lay-up, and thickness according to the analytical results. Patches can be prepared to provide the accurate strength, stiffness, edge distance and bolt spacing. In cases where composite patches are being used the analysis can be performed according to Volume 3, Chapters 6.2.2.2 and 6.3.2.3.
- *Fasteners:* Fastener stiffness should be determined by test or analysis and subsequently used in the analysis of the overall repair. Fastener tensile and shear stresses should be determined as to their adequacy for static strength and for fatigue loading. Fastener selection is addressed in Volume 3, Chapter 6.3.3.3.

8.3.4.3.4 Repair procedures

This section will describe general procedures to complete a bolted repair. Specific repair procedures are given in SRM's, NAVAIR 01-1A-21 (Reference 8.3.4.3.4(a)), and Air Force TO 1-1-690 (Reference 8.3.4.3.4(b)). An example of typical bolted repair will be described at the end of this section. Bolted repair procedure consists of six distinct steps: (1) patch preparation and pilot drilling holes, (2) laying out hole pattern on the parent skin and pilot drilling skin holes, (3) the transfer of the holes in the skin to the patch if the patch covers some existing skin holes, (4) drilling/reaming of patch and skin, (5) patch and fastener installation, and (6) sealing of the repair.

The first step is to cut, form and shape the patch before attaching the patch to the damaged structure. In some cases the repair patches are stocked pre-shaped and pre-drilled. If cutting is to be performed, standard shop procedures should be used that are suitable for the patch material. Metal patches require filing to prevent crack initiation around the cut edges. When drilling pilot holes in the composite, the holes for repair fasteners must be a minimum of four diameters from existing fasteners and have a minimum edge distance of 2 1/2 fastener diameters. This is different than for metals where the edge distance of two is standard practice. Specific pilot hole sizes and drill types to be used should follow specific SRM.

To locate the patch on the damaged area, two perpendicular centerlines are drawn on the part that define the principal load or geometric directions. The hole pattern is then laid-out and the pilot holes in the skin are drilled. The principal directions of the patch are then aligned between the patch and the parent structure. The edges of the patch are marked so that it can be returned to the same location. After the patch is removed, it is advisable to check if there is sufficient edge distance between the patch perimeter and the outer holes. The pilot holes in the patch are then enlarged.

Composite skins should be backed-up to prevent splitting. The patch is then reattached through the interior fasteners so that the corner fastener holes can be enlarged. All holes are then reamed. A tolerance of (+0.0025/-0.000 in. [+0.06/-0.00 mm]) is usually recommended for aircraft parts. For composites this means interference fasteners are not used.

Once fastener holes are drilled full size and reamed, permanent fasteners are installed. Before installation the fastener grip length must be measured for each fastener using a grip length gage. As different fasteners are required for different repairs, SRM should be consulted for permissible fastener type and installation procedure. However, all fasteners should be installed wet with sealant and with proper torque for screws and bolts.

Sealants are applied to bolted repairs for prevention of water/moisture intrusion, chemical damage, galvanic corrosion and fuel leaks. They also provide contour smoothness. The sealant has to be applied to a clean surface. Masking tape is usually placed around the periphery of the patch parallel with the patch edges leaving a small gap between the edge of the patch and the masking tape. Sealing compound is applied into this gap.

8.3.4.3.5 *Example of a bolted repair*

External patch bolted repair of through penetration of the composite skin taken from NAVAIR 01-1A-21 (Reference 8.3.4.3.4(a)) is used here as an illustration example. The repair, shown schematically in Figure 8.3.4.3.5, is applicable to repair holes up to 4 in.(100 mm) in diameter of a thick monolithic skin. A single metallic plate is used to span the hole fastened to the skin by 40 blind fasteners. The repair assumes there is single side access. A scrim cloth is used to prevent galvanic corrosion. The applicability of this repair for specific application depends on loading conditions and laminate thickness.

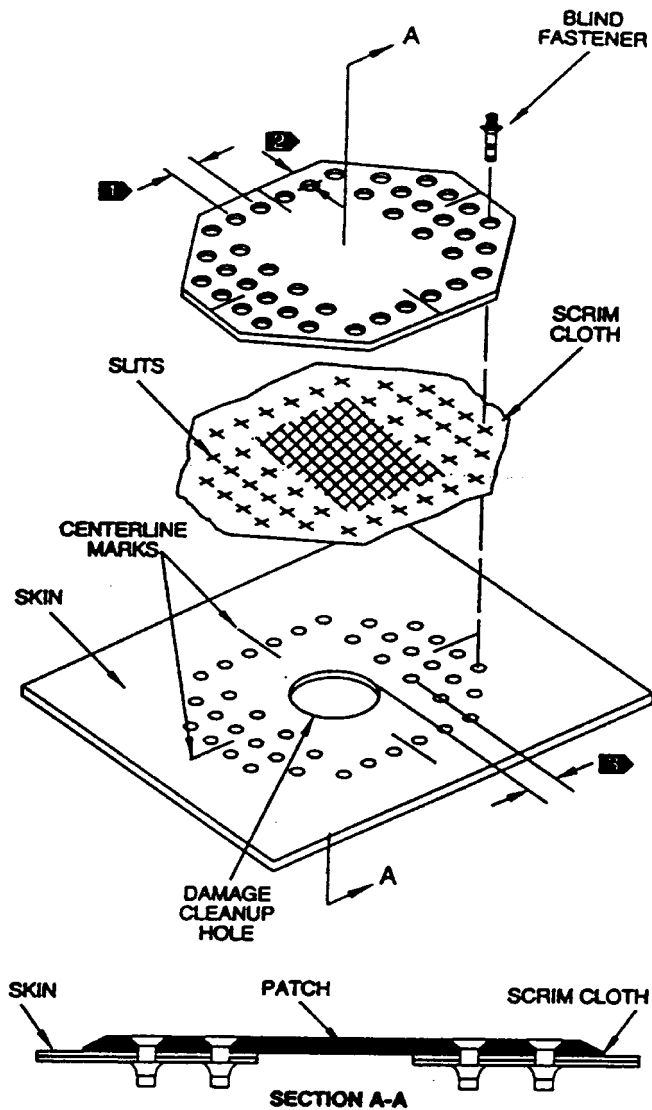
8.3.4.4 *Bonded repairs*

8.3.4.4.1 *Repair concepts*

The two most common bonded repairs use external patches or are internal patches that are made flush with the parent material, both shown in Figure 8.3.4.4.1. Combinations of both types of repairs are also common. Although the external patches are usually stepped, the internal repair can be stepped or more commonly scarfed. The scarf angles are usually small to ease the load into the joint and to prevent the adhesive from escaping. This translates into a thickness to length ratios between 1/10 to 1/40. The adhesive placed between the repair material and the parent material transfers the load from the parent material to the patch by shear. The external patch repair concept is the easier of the two to accomplish. Its drawbacks are eccentricity of the loading causing peel stresses and protrusion into the air stream. The stress concentration at the edge of the patch can be reduced by stepping or tapering the patch as shown in Figure 8.3.4.4.1. Because inspection of bonded repairs is difficult, bonded repairs, as contrasted with bolted repairs, require a higher commitment to quality control, better trained personnel, and cleanliness.

The scarf joint, Figure 8.3.4.4.1, is more efficient from the viewpoint of load transfer as it reduces load eccentricity by closely aligning the neutral axis of the parent and the patch. However, this configuration has many drawbacks in making the repair. First, to maintain a small taper angle, large quantity of sound material must be removed. Second, the replacement plies must be very accurately laid-up and placed in the repair joint. Third, curing of replacement plies can result in significantly reduced strength if not cured in the autoclave. Fourth, the adhesive can run to the bottom to the joint creating a non-uniform bond line. This can be alleviated by approximating the scarf with a series of small steps. For these reasons, unless the part is lightly loaded, this type of repair is usually performed at a repair facility, where if the part can be inserted into the autoclave, this type of repair can result in part strength as strong as the original part.

Although it may seem that there are only two common concepts, it is somewhat misleading as the two repair joints can be made by many different methods. The patch can be pre-cured and then secondarily bonded to the parent material. This procedure most closely approximates the bolted repair. The patch can be made from prepreg and then co-cured at the same time as the adhesive and lastly the patch can be made using dry cloth, paste resin, and co-cured. This latter repair is called "wet" lay-up repair. The curing cycle can also vary in length of time, cure temperature, and cure pressure, thus increasing the number of possible repair combinations.



LEGEND

- FASTENERS MUST HAVE MINIMUM SPACING OF 4D AND MAXIMUM OF 6D
- FASTENERS MUST HAVE MINIMUM EDGE DISTANCE OF 3D
- FASTENER TO EDGE OF DAMAGE CLEANUP HOLE MUST BE A MINIMUM OF 3D

NOTE:
DRILL PILOT HOLES (0.128 INCH DIAMETER)
IN PATCH FIRST. ENLARGE HOLES TO FINAL
SIZE AFTER TRANSFERRING PILOT HOLES
TO COMPOSITE SKIN.

FIGURE 8.3.4.3.5 Repair arrangement, bolted repair, external patch.

8.3.4.4.2 Repair materials

Bonded repairs require selection of both the repair material and adhesive. The selection cannot be independent as the curing parameters of the adhesive and the repair material must be compatible for co-cured repairs. Bonded repairs also require materials that are used in the processing of the repair but not remain with the repair. Many materials used in bonded repairs require special handling, are storage time and temperature sensitive, and may require controlled environment during the repair process.

A very good description of materials that are available and needed for bonded repair is provided in Air Force TO 1-1-690 (Reference 8.3.4.3.4(b)) and NAVAIR 01-1A-21 (Reference 8.3.4.3.4(a)). It should be noted that the mechanical properties of repair materials, other than metals, depend very strongly on the curing process used. As the repair curing process is usually different than the process used for fabricating the original part (lower curing temperature and/or pressure), material suppliers have developed unique materials that are optimized for the repair process. It should be noted that the repair materials are usually lower in strength and stiffness than the original part materials. Volume 2 contains a special section with repair material properties.

Metal patches for bonded repairs are constructed using sheet material that is bonded to each other to form a stepped patch. The same method is used for pre-cured composite patches where the sheets are made of two or more unidirectional plies of fabric or tape. Because the pre-cured patches can be cured in the autoclave, they are made from composite materials that were used in construction of the original part.

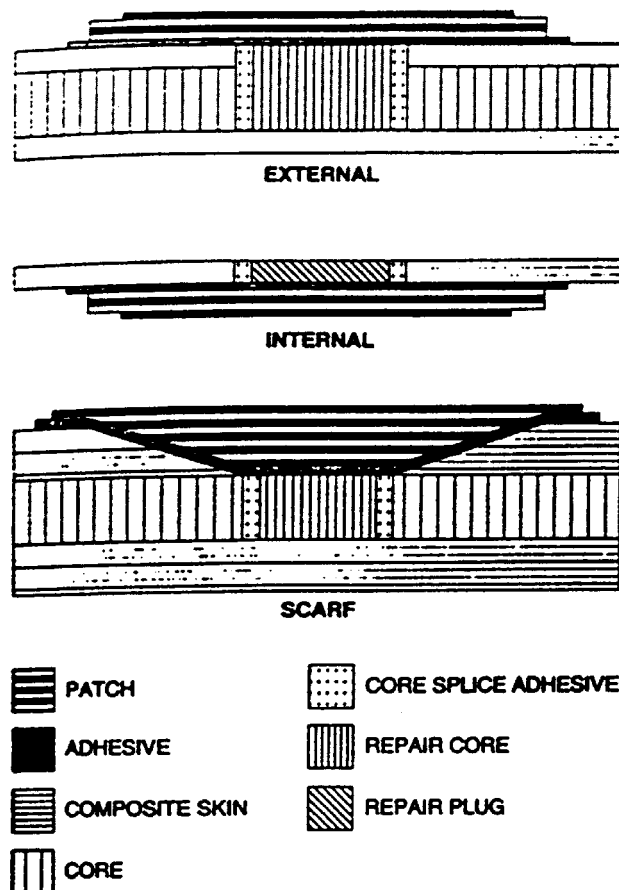


FIGURE 8.3.4.4.1 Basic repair joints (bonded).

Co-cured bonded repairs use parent material prepreg, if the repair can be cured in the autoclave, or repair material prepreg, or dry fabric with paste resin. The use of the latter materials defines 'wet' lay-up repair. The prepreg provides a uniform distribution of resin in the composite, but requires refrigeration for storage. The resin for the wet lay-up repair usually consists of two parts that do not require freezers. However, mixing of the two parts and spreading the mixed resin on the dry fabric requires strict adherence to written protocol and experienced personnel to effect consistent repairs. All composite repair materials require incoming material control or re-testing of key properties to assure the integrity of the material being used. AC 145-6 (Reference 8.3.2.5 (b)) has a discussion on incoming repair material requirements.

Adhesives for bonded repairs are discussed in Section 8.2.3 as to their desirable properties. Here the discussion will be limited to types of adhesive that are available and are being used. Two categories of adhesives are films and pastes. Films come with and without mesh carrier cloth with typical thickness between 0.0025 to 0.01 in. (0.064 to 0.25 mm). The carrier cloth provides improved handling, results in more uniform bondline, and helps reduce galvanic corrosion. Although films provide a more uniform bondline thickness than paste adhesives, repair part inaccessibility or a lack of refrigerated storage equipment sometimes necessitates use of paste adhesives. Wet lay-up repairs almost always use paste adhesives as they are more compatible with paste resins in terms of curing characteristics. As the paste resins, the paste adhesives consist of two separate parts that have a long shelf life. Conversely, film adhesives are more prevalent when prepreg is used to form repair patches as they usually require higher temperature and pressure for curing.

Bonding repairs require many ancillary materials. They do not become part of the repair and are removed and discarded after the repair is complete. They include items such as vacuum bag materials, scrim cloths, bleeder/breather materials, release films, tapes, wiping materials, and solvents. The specifications for these materials are usually given in the specific SRM.

8.3.4.4.3 Repair analysis

A bonded repair is from a structural point of view a bonded joint. As in a joint the load is transferred from the parent structure by the bond to a patch (single lap) bypassing the damaged portion of the parent structure. The geometry is usually two dimensional. If a sandwich structure is repaired, the core, repaired original or new replaced, forms a substrate which provides support for the out-of-plane loads. This is why bonded repairs are very efficient for sandwich structures. The repair analysis of a bonded repair follows the guidance lines of the analysis of a bonded joint, Volume 6, Chapter 6.2.3. The main steps as for bolted repairs (Section 8.3.4.3) are as followed:

a) *Estimation of load transferred through the repair*

As for bolted repairs, Section 8.3.4.3.3.

b) *Load sharing in the repair*

The load flow in a bonded repair is continuous. It depends on the elastic properties of the adherends and the adhesive and on joint geometry. In some cases, the geometry can be approximated by the use of models of lap or strap joint. A two dimensional finite element model can be used to calculate load distributions in the skin, patch, and adhesive layer. A nonlinear solution can be used to account for the nonlinear stress strain behavior of the adhesive (Volume 3, Chapter 6.2.3.6).

Several specially developed computer codes can be used for analyzing bonded repairs. In Reference 8.3.4.4.3(a) the codes PGLUE (Reference 8.3.4.4.3(b)), A4EI (Reference 8.3.4.4.3(c)) and ESDU8039 (Reference 8.3.4.4.3(d)) are discussed. The PGLUE program contains an automatic mesher which creates a three dimensional finite element model of a repaired panel containing three components - a plate with a cutout, a patch, and an adhesive connecting the patch and the plate. Plasticity of the adhesive is considered in the analysis. However, the version available through ASIAC does not consider peel

stresses, which can be critical. Traditional bonded joint codes, such as A4EI and ESDU8039, model only a slice through the repair and do not consider the two dimensional effects of stiffening of the sides of the panel. Both bonded joint codes allow the patch to be stepped. A4EI considers plasticity in the adhesive shear stress but does not predict peel stress, while ESDU8039 predicts peel stress in the joint but does not consider plasticity.

c) Analysis of local failure

- *Parent Structure:* As in the case of bolted repairs the parent structure is a given item in the repair design. The advantage of the bonded repair is that loads are introduced into the parent structure in a continuous way without inducing any stress concentrations in the parent structure and thus there is no need for increase in thickness in the joint region. After establishing the stress distribution in the parent structure, the stress and failure analyses are performed according to Volume 3, Chapters 5.3 and 5.4.
- *Patch Structure:* as for the parent structure.
- *Adhesive:* Volume 3, Chapter 6.2.3 deals extensively with stress analysis of adhesive joints, however, failure criteria are not covered presently. The following should be taken into consideration:
 - The joint should be designed in such a way that the adhesive layer is not the critical joint element.
 - Peel and transverse shear stresses should be minimized by design (tapered or stepped adherends, filleting, etc.).
 - Incorporation of nonlinear stress-strain behavior of the adhesive (usually approximated by elastic-plastic stress-strain curve).
 - Dependence of the measured elastic mechanical properties of adhesive on its thickness.
 - Change of adhesive properties as a function of the environment as well as long term degradation.

8.3.4.4.4 Repair procedures

This section will describe general procedures to complete secondarily bonded, co-cured with prepreg, and wet lay-up repairs. Specific repair procedures are given in SRM's, NAVAIR 01-1A-21 (Reference 8.3.4.3.4(a)), and Air Force TO 1-1-690 (Reference 8.3.4.3.4(b)). Bonded repairs require close control of the repair process and the repair environment. Structural integrity of the bonded joint is strongly dependent on the cleanliness of the work area and its ambient temperature and humidity. Other important factors are workmanship and geometrical fit of mating parts. An example of typical bonded repair will be described at the end of this section.

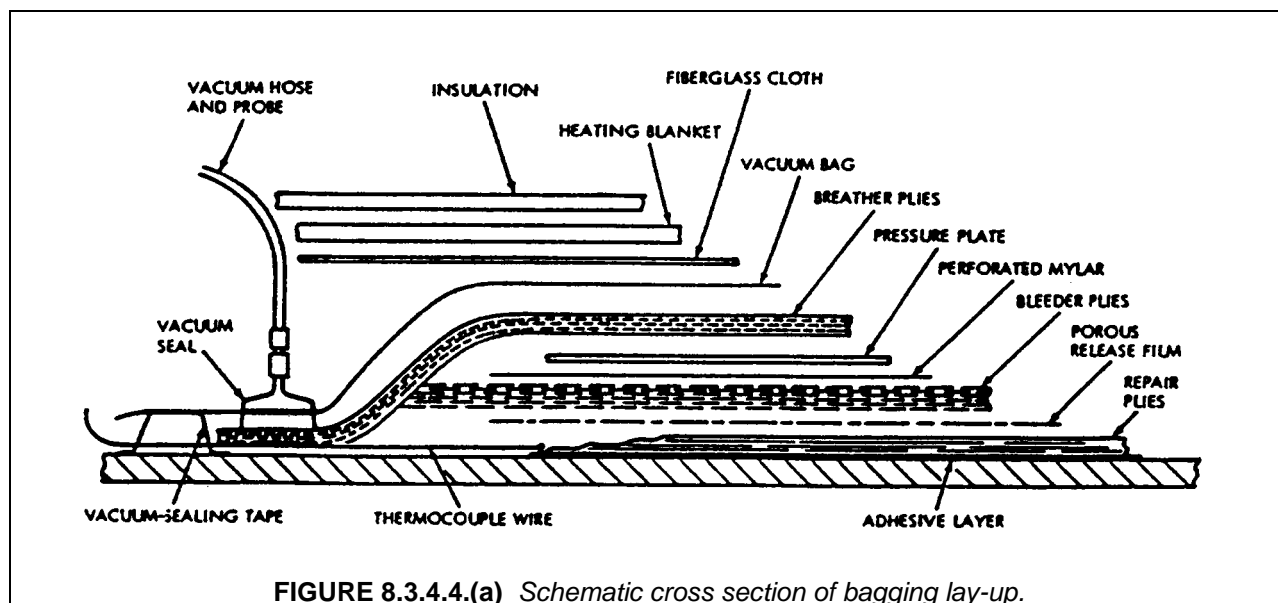
The four major activities to effect a bonded repair consist of patch and parent surface preparation, adhesive application, bagging, and curing. Each of these activities may be different for the type of bonded repair being attempted, materials used, and the part being repaired. Size of the repair may be limited by the allowable out-time of the adhesive. A drawing of the patch is used to lay-up the composite tape or fabric, sheet metal or dry fabric materials. Standard shop procedures are used to make the composite patch laminate from prepreg. Dry fabric plies for wet lay-up are cut first to size before impregnating with resin. This is done to minimize repair time. How to properly mix the resin is described in SAE document ARP 5256 - Resin Mixing (Reference 8.3.4.4.4(a)) and NAVAIR 01-1A-21 (Reference 8.3.4.3.4(a)). The impregnation of the dry fabric with the mixed resin is described in SAE document ARP 5319 - Impregnation of Dry Fabric Application of Repair Plies (Reference 8.3.4.4.4(b)).

Before adhesive application, the repair patch and the parent surfaces must be wiped clean with solvent and allowed to dry. At this point the composite surface should be abraded. A light grit blast gives a more uniform abrasion than hand sanding. The surface is then wiped dry with a clean, lint free cloth. Metal sheet patches have special surface preparation requirements depending on whether the patch is aluminum or titanium. They are specified in detail in the SRM and MIL-HDBK-337 (Reference

8.3.4.4(c)) and should be followed closely. Film adhesives are first attached to the patch, trimmed, and then applied to the damaged area.

Bagging is an operation wherein the repair is enclosed for the curing operation. As most of the repairs are done outside the autoclave, the process described here will address only vacuum bagging. This allows the repair to be cured under atmospheric pressure. When the repair can be cured in the autoclave, additional pressure and higher, more uniform heat can be applied. Figure 8.3.4.4(a) shows a typical bagging arrangement in which patch plies of prepreg are co-cured with a layer of adhesive and a heating blanket is used to supply heat. Starting from the top of the patch, the repair bagging assembly contains porous separator release film to prevent bleeder plies sticking to the repair plies, bleeder plies to absorb extra resin (it is assumed that the prepreg is not net resin type), Mylar separator ply perforated to allow venting, caul or pressure plate to help provide smooth finish to the repair, breather plies to provide for the air to be initially inside the bag to be drawn off by the vacuum source, and finally a rubberized vacuum bag. The vacuum bag is sealed on the periphery using tape. For a bonded repair with a metallic or pre-cured composite patch, bagging would still be needed to apply vacuum pressure to the adhesive but would be simpler.

An integral part of the bagging process is the placement of the thermocouples to monitor part and repair temperatures during cure. Thermocouples on the part are needed to make sure that the part is not overheated. Figure 8.3.4.4(a) shows only one thermocouple wire. (The more common practice is to place the heat blanket within the vacuum bag.) For larger repairs, more thermocouples are needed to map the temperature distribution for the complete repair area. Distributing the heat evenly on the repair is one of the goals of proper bagging technique. In some cases a thin aluminum or copper sheet is inserted inside the bag for that purpose. Care must than be taken not to puncture the bag. NAVAIR 01-1A-21 (Reference 8.3.4.3.4(a)) has a good description where the thermocouples should be placed. SAE ARP 5143 - Bagging (Reference 8.3.4.4.4(d)) gives guidance as to proper bagging techniques.



The process of curing structural adhesives and composite resins is achieved by a chemical cross-linking accelerated by heat. Therefore, cure temperatures should be sufficiently high to achieve this, but care must be taken not to reach temperatures that may damage the original structure. Keeping the cure temperature as low as possible to effect cure is the safest policy. The rate of heat-up is important as the resin and the adhesive undergo physical and chemical transformations. Therefore, the resin and the adhesive must have compatible cure cycles and follow prescribed time-temperature curve, i.e., rate of in-

crease in temperature, dwell temperature duration, and rate of decrease in temperature. If the repair is an autoclave cure, pressure must be applied according to cure specifications. The maximum thermocouple reading is usually used as a control on the maximum allowed temperature. Cure time is adjusted by monitoring the minimum thermocouple reading. After the cure is completed the repair assembly is cooled before relieving vacuum pressure. More details on this subject are contained in SAE ARP 5144 – Heat Application for Thermosetting Resin Cure (Reference 8.3.4.4.4(e)).

Heat blankets, individual or integral with repair kits, are most commonly used to cure bonded repairs. Autoclaves, ovens, and quartz lamps are other acceptable methods.

The double vacuum bag processing concept is one of several alternative approaches (Reference 8.3.4.4.4(f)) that has been investigated since the early 1980's (Reference 8.3.4.4.4(g)) in an effort to develop processes that would improve the overall quality of composite laminate repair patches for thicker laminates. In 1983, work performed by the Naval Air Warfare Center demonstrated that the double vacuum bag approach produced lower levels of porosity, improved resin distribution and improved resin dominated mechanical properties in prepreg repair patches (Reference 8.3.4.4.4(h)). This program also investigated the double vacuum bag process for use as an intermediate step to debulk, compact and stage ambient storable prepreg repair patch laminates for later use in co-bonded field repair patch applications with the intention of performing the final cure on-aircraft using a single vacuum bag process. This work was expanded in 1992 to address the use of the double vacuum bag process on wet lay-up as well as prepreg repair patches (Reference 8.3.4.4.4(i)). More recent work demonstrated that optimization of double vacuum bag processing parameters such as debulk and cure temperatures, heat up rates, debulk time, vacuum level, the number of bleeder plies, etc., for the specific resin system in use can further improve overall repair patch laminate quality (Reference 8.3.4.4.4(j)).

To fabricate wet lay-up repair laminates using the double vacuum bag process, an additional step is required wherein the impregnated fabric is placed within the de-bulking assembly shown in Figure 8.3.4.4.4(b).

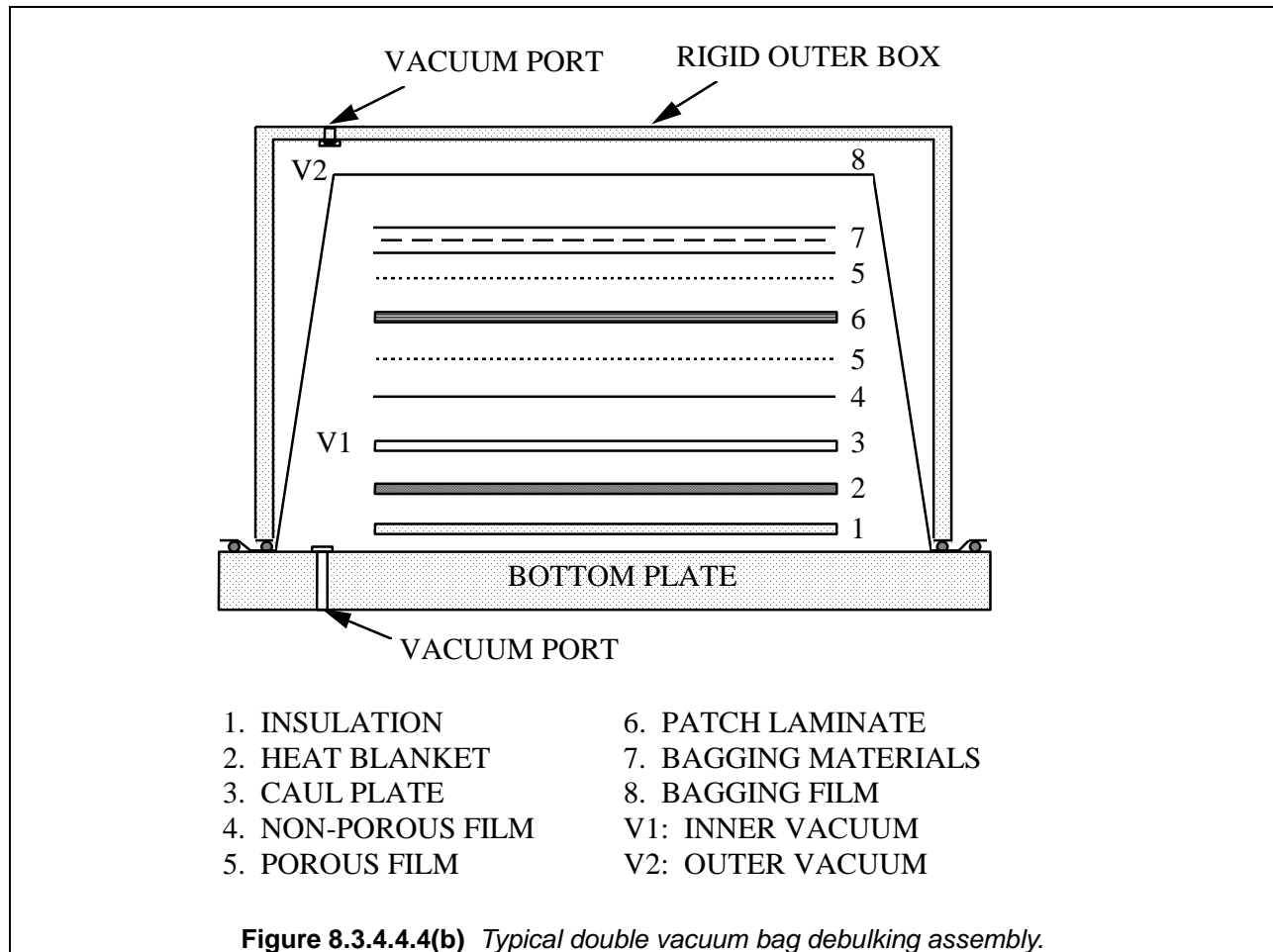
To begin the debulking process, air within the inner flexible vacuum bag is evacuated. The rigid outer box is then sealed onto the inner vacuum bag, and the volume of air between the rigid outer box and inner vacuum bag is evacuated. Since the outer box is rigid, the second evacuation prevents atmospheric pressure from pressing down on the inner vacuum bag over the patch. This subsequently prevents air bubbles from being "pinched-off" within the laminate and facilitates air removal by the inner vacuum. The laminate is then heated to a predetermined debulking temperature in order to reduce the resin viscosity and further improve the removal of air and volatiles from the laminate. The heat is applied through a heat blanket that is controlled using thermocouples placed directly on the heat blanket, in order to limit the amount of resin advancement during the debulk cycle.

Once the debulking cycle is completed, the laminate is then compacted to consolidate the plies by venting the vacuum source attached to the outer rigid box, thus allowing atmospheric pressure to reenter the box and provide positive pressure against the inner vacuum bag. Upon completion of the compaction cycle, the laminate is removed from the assembly and is prepared for cure.

In the case of prepreg repair patch laminates, the prepreg plies are cut, stacked, and placed within the double vacuum debulking assembly shown in Figure 8.3.4.4.4(b). In this process, the thermocouples are placed along the edges of the laminate, to ensure that all areas of the laminate reach the required debulk and compaction temperatures. No bleeder material is used in the prepreg staging process, in contrast to the wet lay-up staging process.

To begin the staging process, the inner vacuum bag and outer box are evacuated. The prepreg laminate is then heated to the debulking temperature. Once the debulking cycle is completed, the laminate is then compacted at temperature to consolidate the plies. Upon completion of the compaction cycle, the staged prepreg laminate is removed from the assembly and is either prepared for storage or immediately cured.

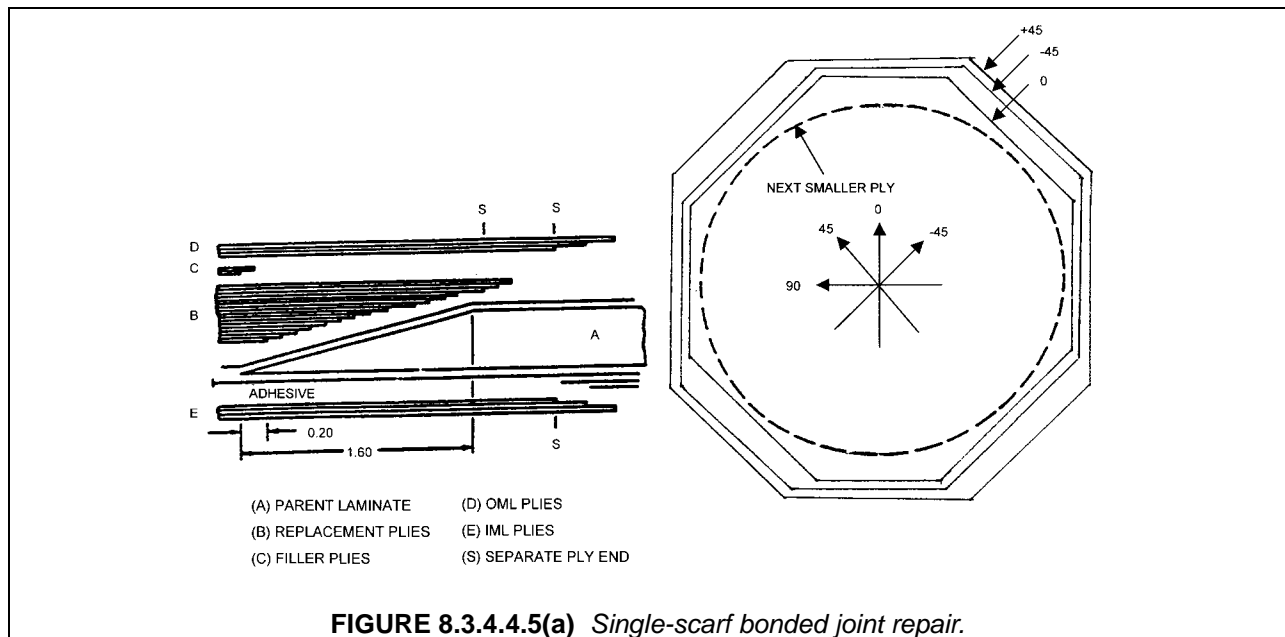
The double vacuum bag approach has been shown to produce repair laminates with low void content and good compaction approaching that of autoclave processed laminates. However, there are several limitations in application of the process due to the required use of a rigid outer vacuum box. In the case of co-bonded applications, the patch laminate must be debulked, compacted and staged off-aircraft. As the staged patch remains formable, the patch can then be transferred to the aircraft, formed to contour and co-bonded in place using a single vacuum bag process for the final cure. This two step process is necessary since using the rigid vacuum box assembly on-aircraft creates a peeling load that may be sufficient to further damage the parent structure. Likewise, the vacuum box assembly is difficult if not impossible to set up on a contoured surface. Overall patch dimensions are also limited by the maximum practical size of the rigid outer box (in practice, relatively portable vacuum boxes have been a maximum of approximately 24" wide by 24" in length).



8.3.4.4.5 Bonded repair examples

The first example of the bonded repair is a simple scarf repair of a penetration damage of a 16-ply laminate. The repair, shown in Figure 8.3.4.4.5(a), is from the Air Force TO 1-1-690 (Reference 8.3.4.3.4(b)). The scarf plies replace parent plies with the same orientation and thickness repair plies. The taper of the scarf is determined from the SRM. Additional plies on the outside and inside mold lines (OML and IML) are placed on top of the repair to compensate for the lower strength and stiffness of the replacement plies because of vacuum pressure cure and to protect the repair. The external plies are identical to each other to maintain symmetry. The 0° and the 45° plies are serrated to prevent peeling of the longer plies. From the ply directions that are serrated, one can assume that the primary axial load is

in the 0° direction with a shear component. The edges are cut with standard pinking shears producing 1/8-in. deep serrations.



An example of a more complex bonded repair is drawn in Figure 8.3.4.4.5(b). The repair is to a penetration damage to a skin and the underlying stiffener. This field repair was verified by test to restore original strength and stiffness. The skin is repaired using a circular external patch that is laid-up wet. The J-stiffener is reconstructed using Rohacell foam as the mold and the filler material over which a square composite patch is placed using wet lay-up method.

8.3.4.5 Sandwich (honeycomb) repairs

Most structural repairs that are performed due to service damage are on sandwich structure, metallic or composite. For composites, it is due to the fact that a large proportion of current components are light sandwich structures that are susceptible to damage and are also easily damaged. The repair experience gained on the repair of metallic sandwiches is applicable to composite sandwiches. Additional flexibility with composites is possible as flush scarf repairs can be accomplished.

8.3.4.5.1 Repair concepts

Because sandwich structure is a bonded construction and the face sheets are thin, damage to sandwich structure is usually repaired by bonding. Procedures to effect the repair are, therefore, similar to the bonded repairs discussed above with the additional task of restoring the damaged core. When repairing one face skin of the sandwich, one should remember that half of the in-plane load is transferred through that face sheet, and if the repair does not approximate in stiffness the undamaged face sheet extraneous bending moment could induce peel loads between the face sheets and core. Thus, external patch is usually applicable only for thin skin repairs while scarf concepts are used to repair thicker skins.

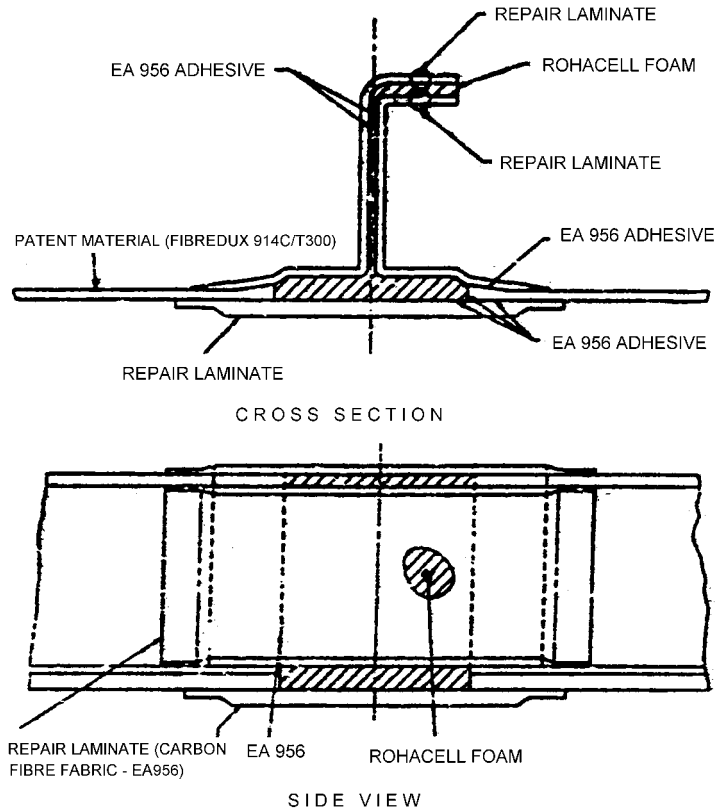


FIGURE 8.3.4.4.5(b) Field repair of the "J"-stiffened panel.

8.3.4.5.2 Core restoration

For full-depth core replacement there are three common methods, the core fill method, the paste adhesive method, and the film/foam method. The three methods are shown in Figure 8.3.4.5.2(a). The core fill method replaces the damaged honeycomb with glass floc filled paste adhesive and is limited to small damage sizes. The weight of the repairs must be calculated and compared with flight control weights and balance limits set out in the SRM. The other two methods can be used interchangeably depending on the available adhesives. However, the paste adhesive method results in a much heavier repair than the film/foam method, especially if the damage diameter is greater than 4 inches. The foaming adhesive required to utilize the film/foam method is a thin unsupported epoxy film containing a blowing agent which is liberated during cure causing a foaming action. The expansion process needs to be performed under positive pressure to become strong, highly structured foam. Like film adhesives, foaming adhesives require high temperature cure and refrigerator storage. Core replacement is usually accomplished with a separate curing cycle and not co-cured with the patch.

For partial-depth damage, different methods can be used to attach the replacement honeycomb to the parent honeycomb as shown in Figure 8.3.4.5.2(b). The two methods describe the prepreg/film adhesive bonding and the wet lay-up bonding. Both of these bonding methods were discussed in Section 8.3.4.4. A general description of how to perform core restorations for simple configuration is contained in SAE ARP 4991 - Core Restoration (Reference 8.3.4.5.2).

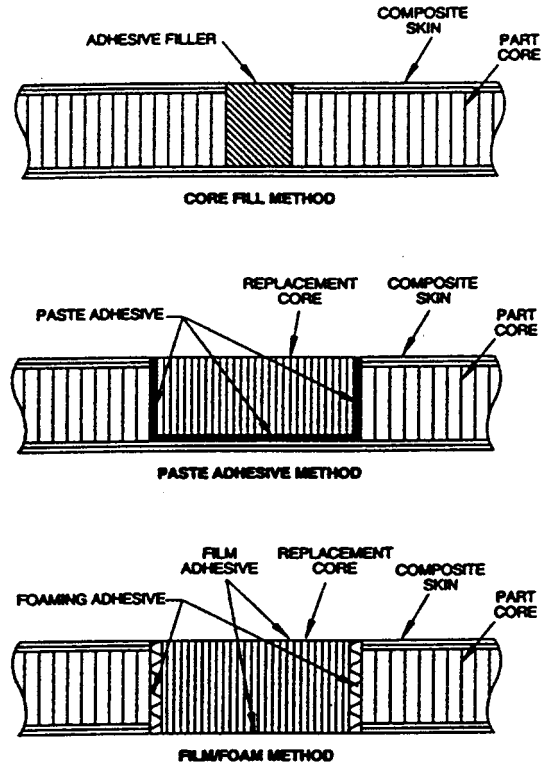


FIGURE 8.3.4.5.2(a) Core replacement methods – full depth.

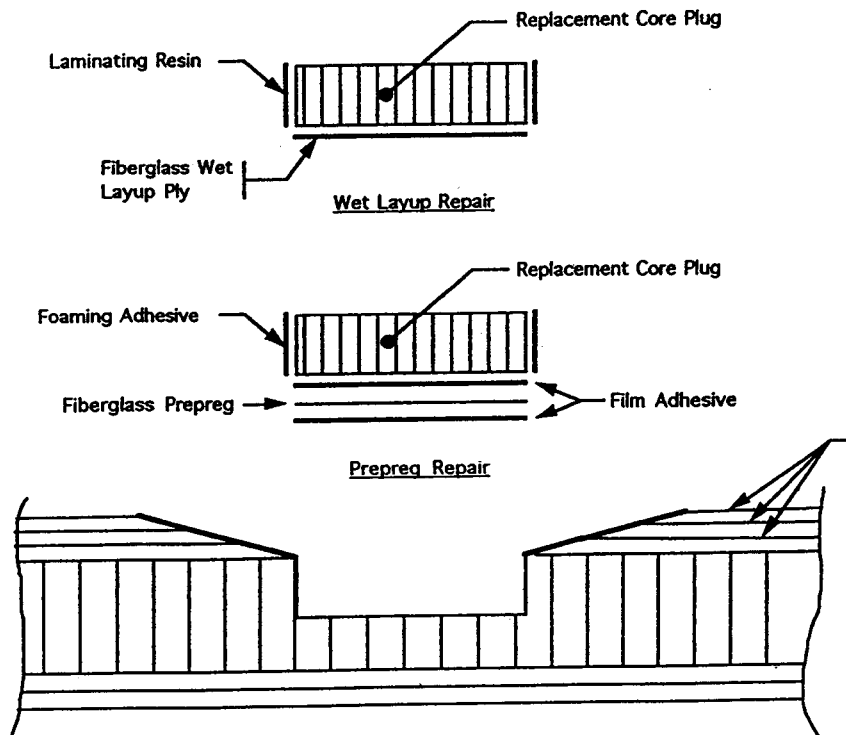


FIGURE 8.3.4.5.2(b) Core replacement – partial depth.

8.3.4.5.3 Repair procedures

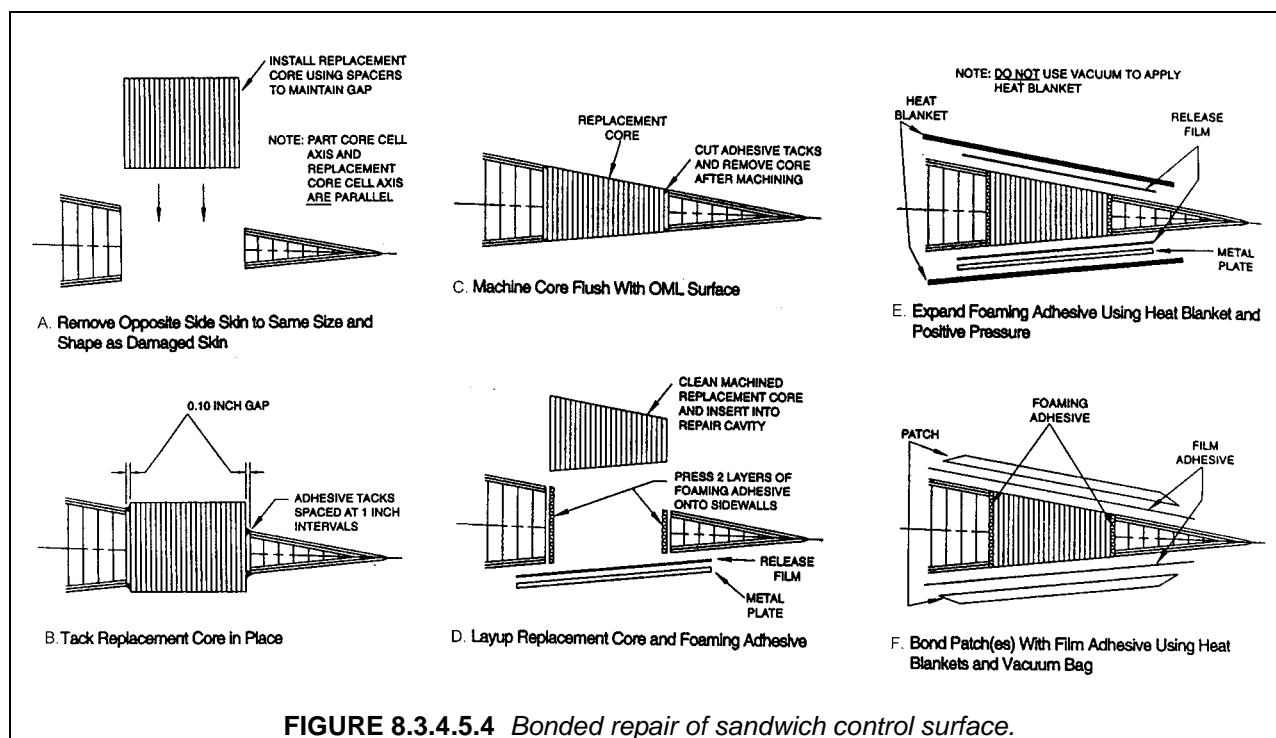
Following the core replacement, the sandwich repair proceeds as a bolted or bonded repair of the face sheets as was described in Sections 8.3.4.3 and 8.3.4.4, respectively. One more step has to be performed before proceeding with repair of the face sheets and that is to bond a pre-cured fiberglass plug on top of the exposed core. This preserves the continuity of the bond between the core and the face sheets.

Sandwich structures are usually repaired by bonding patches. For bonded repair of the sandwich structure, special considerations that have to be adhered to are: the honeycomb must be thoroughly dried to prevent face sheet disbond during curing, and the curing pressure must be low to prevent honeycomb crushing. If it is unfeasible to dry out the honeycomb, lower temperature (200°F (93°C)) curing and be used if this has been approved in the SRM.

Occasionally, sandwich structure is repaired using bolted external patches. In this case, the honeycomb where the bolts would pass through has to be strengthened by filling the core with the same filler as for core replacement. The diameter of this area should be at least three times the diameter of the bolt. Special bolts that have limited clamping force are used for such repairs.

8.3.4.5.4 Sandwich repair example

The sandwich repair example is taken from NAVAIR 01-1A-21 (Reference 8.3.4.3.4(a)). A repair of a full depth damage, of sufficient diameter to warrant core replacement, to a control surface is demonstrated. Actual steps in repair are shown in Figure 8.3.4.5.4. These consist of removing damaged material, drying the repair area, fitting replacement core, tacking the replacement core using filled paste adhesive with sufficient glass floc to make the adhesive into consistency of a putty, machining the core to match the contour of the part, installing core with the foaming adhesive using a heat blanket, and installing external patches using another cure cycle. The details of the final cure are simplified in this example. Unless the patch is pre-cured, the bagging details would be more complicated.



8.3.4.6 Repair inspection

8.3.4.6.1 In-process quality control

Bonded repairs require more in-process quality control to obtain structurally sound repairs than bolted repairs. Composite materials and adhesives require extensive record keeping to ensure they are within life, such as to storage time in the refrigerator, warm-up time, and out time on the shop floor. Lay-up operations need to be inspected as to the correct fiber orientation. Cure cycles must be monitored to assure they follow specifications. For large repairs, a small companion panel is cured with the repair. It is used for coupon testing to provide confidence in the quality of the repair, repair patch and adhesive bond.

Bolted repairs require inspection of holes for damage and size. Assembled repairs also require inspection of fastener installations.

8.3.4.6.2 Post-process inspection

Completed repairs should be inspected to determine their structural soundness. The NDI methods described previously in Section 8.3.1 are used to perform this function.

8.3.4.7 Repair validation

Successful inspection of a repair is not sufficient to guarantee that the repair will perform as designed and implemented. Repair designs need to be supported by an existing experimentally verified database and analysis. This helps to ensure the repair's capability to carry the intended loads or to replace the capability of the parent structure. The repair material allowables used in the design should be generated using approved testing and data reduction methods that reflect the amount of testing completed, material and process controls in place, and the criticality of the structure.

Both strength and stiffness must be taken into account when designing the repair as described in Sections 8.3.4.3.3 and 8.3.4.4.3. Analyses need to be done in each fiber direction with careful attention to limit the effects of hardpoints as described in Section 8.3.3.1. It must be understood that increases in stiffness do not correlate to increases in the repair factor of safety. Environments the parent material was designed to and details such as edgebands, cutouts, and fastener penetrations must also be considered.

Repair designs are based on using a specific material or a family of materials. Design properties are usually obtained by mechanical property testing specimens that mimic the particular repair process. Typically this testing is not as extensive as for the parent material and does not involve sufficient replication to obtain statistically based properties. Batch to batch variation of repair materials should be obtained which can be somewhat problematic for wet lay-up materials. Typically two practices are utilized for obtaining repair allowables. Allowables can be based on the parent material properties with knock down factors that reflect lower cure temperatures and pressures of the repair material relative to the parent material, or allowables and material properties are derived for the repair material to be used in the repair analysis. It is common to use large reductions from the mean value to the allowable design value as the process parameters such as fiber volume, pressure, and temperature of repair patches have more variability than the parent material.

For the repair material to have meaningful design allowables, rigid material purchasing and process specifications must be in place. This means that the material is purchased to a material specification with incoming material controls, that the material handling and storing is according to specification, and that the repair is performed to a process specification.

In addition to coupon testing, a variety of elements are tested to validate repair designs. These are usually performed to support repair designs included in the SRM and range from simple joint specimens, representing bolted or bonded load transfer, to tests of full-scale repairs. Simple joint specimens are used for development of repair designs. These are usually two-dimensional. Example of such elements would be single or double bolt specimens to obtain bearing, bearing/bypass and net tensile values, and lap

bonded specimens to obtain joint shear strengths. The more complex elements are used to validate the repair design and repair process. These are full-scale representations of the repair.

Final validation of bolted and bonded repairs as described in Section 8.3.4 rely on strict attention to all details, including: damage removal and site preparation, repair design, appropriate use of materials, repair analysis, material and fabrication processes, inspection, and appropriate design values supported by test evidence.

8.4 COMPOSITE REPAIR OF METAL STRUCTURE (CRMS)

Composite materials can be used to structurally repair, restore, or enhance aluminum, steel, and titanium components. Bonded composite doublers have the ability to slow or stop fatigue crack growth, replace lost structural area due to corrosion grindouts, and structurally enhance areas with small and negative margins. This technology has often been referred to as a combination of metal bonding and conventional on-aircraft composite bonded repair. The U.S. Air Force and the Royal Australian Air Force have been using the technology for over 25 years on aircraft ranging from F-5s to Boeing 747s to C-130s to C-141s to B1Bs. Commercial aircraft manufacturers and airlines are starting to adopt this technology to their needs.

Boron epoxy, GLARE[®] and graphite epoxy materials have been used as composite patches to restore damaged metallic wing skins, fuselage sections, floor beams, and bulkheads. As a crack growth inhibitor, the stiff bonded composite materials constrain the cracked area, reduce the gross stress in the metal, and provide an alternate load path around the crack. As a structural enhancement or blendout filler, the high-modulus fiber composites offer negligible aerodynamic resistance and tailorable properties.

An understanding of fracture mechanics, durability and damage tolerance and the structural and thermal load spectra are invaluable in deciding on a CRMS application. The repair techniques and design principles used for composite structures that are described in Section 8.3 are applicable to design bonded doubler for a metallic structure. To apply CRMS technology successfully one needs an understanding of laminate theory and behavior, failure modes in both the composite patch and the metallic structure, and structural and operational loads. Design decisions based on sound material allowables, confidence in the metallic surface preparation, and a full understanding of the structural behavior after repair will result in a fully restored structure. Finite element analysis and closed form analytic solutions have been used to design and analyze bonded composite and metallic doubler repairs. The U.S. Air Force (AFRL Materials Directorate) developed a comprehensive document that captures previously published data on the technology and uses "Guidelines for Composite Repair to Metallic Structures", AFRL –ML-TR-1998-4113, as a how-to manual for assessing, designing, analyzing and installing composite doublers. AFGROW and CalcuRep software programs in those guidelines can provide a basic understanding of a damage/repair situation and provide the initial doubler sizing.

Grit blast silane and phosphoric acid anodizing using the Phosphoric Acid Anodizing Containment System (PACS) have been the only surface preparation technologies authorized by the U.S. Air Force as suitable for durable and reliable bonded doubler installation on aluminum structures. Film adhesives using a 250°F (121°C) cure are used routinely to bond the doublers to the metallic structure. Critical areas of the installation process include a good thermal cure control, having and maintaining water break-free bond surfaces, chemically and physically prepared bond surfaces, technician training and certification, and managing a quality bonding site.

Secondarily bonded precured doublers and in-situ cured doublers have been used on a variety of structural geometries ranging from fuselage frames to door cutouts to blade stiffeners. Vacuum bags are used to apply the bonding and curing pressure between the doubler and metallic surface. Autoclaves and a tooling splash from the repair area are used to prepare precured doublers.

Inspection methods have been developed to monitor damage growth under the bonded doubler and to assess the bond quality. Procedures need to be developed for each group of repaired applications and

used to assess and manage the repairs while in-service. Eddy current inspection has been used to assess crack growth through bonded boron doublers. Since the boron doubler does not shield the bondline and parent structure, conventional eddy current techniques work quite well assessing crack growth. Pulse echo, through transmission ultrasonics and thermography have also been used to assess disbonds under metallic and composite doublers. These methods are described in Section 8.3.1.

In summary, to repair metallic structure with composite patches (doubblers), repair procedures described in Section 8.3 are applicable except special care in metallic surface preparation must be taken. However, Section 8.3 does not cover structural analysis techniques needed to assure life of the metallic component or parent structure. Such discussions on metallic fracture mechanics and durability and damage tolerance can be found in several textbooks and handbooks on aircraft structures. Materials and design allowable data for the composite doubler and metallic structure can be found in numerous DOD, OEM, and vendor literature. CMRS also requires not only initial inspection of the adhesive joint between the repair patch and the metallic structure, but also periodic inspections for crack growth emanating from the damage site of the metallic structure.

8.5 LOGISTICS REQUIREMENTS

8.5.1 Training

Specialized knowledge and skills are required to perform sound structural composite repairs. The orthotropic and process-dependent nature of the materials requires technicians who are attentive to detail and well-trained. Unlike conventional metal repair technicians, the composite technician must be counted on to not only assemble a damaged component, but create the material properties in the process. Also needed are engineering support members who are skilled in composite analysis and composite repair.

Repair technicians must be trained in a formal program for certification since they will be expected to perform bonded repairs on diverse structures with many different types of material. The general lack of means to non-destructively inspect the strength and stiffness of a complete component once it has been layed up and cured means the repair technician cannot be someone without training. This program should include a classroom lecture to provide in-depth information into the specifics of working with composite materials in addition to hands-on instruction so that proficiency can be demonstrated in practice. SAE document AIR 4938 (Reference 8.5.1) provides a curriculum for such training. This should be a prerequisite to on-the-job training (OJT) with actual components prior to achieving certification as a composite technician. A key to maintaining a core competency in composite repair is the availability of experienced and skilled mentors who will provide continuing guidance and instruction since this skill requires continual learning and practice to become proficient. The fundamental intent of such a program is to provide the knowledge, skills and abilities so that the technician can consistently make safe and effective repairs. The Office of Personnel Management is now considering a DoD-wide composite repair technician job series to formalize and standardize the skills required for this technology. The need for personnel qualification and training for repair personnel that work in approved repair stations for civil aircraft is defined in FAA Advisory Circular AC 145-6 (Reference 8.3.2.5 (b)).

Engineers supporting the design of composite structural repair will likely require a mechanical or aeronautical engineering background with a concentration in mechanics of materials. It is necessary to have a thorough understanding of structures designed using anisotropic and orthotropic materials. The engineer should have knowledge of composite laminate theory and joint analysis so that repairs can be analytically justified. Complicated repairs, such as those accomplished on three-dimensional laminates, may require FEA modeling in addition to the more traditional analysis techniques. Many undergraduate, graduate and continuing education programs offer selected courses on these topics and can be very useful in establishing and maintaining the skills necessary for composite repair design. A materials and process engineer to support materials testing and composite processing will be needed. These engineers must have a firm understanding of thermosetting material chemistry and rheology.

8.5.2 Spares

Field repair facilities have limited space, equipment, tooling, material, trained personnel, and time. Operational requirements dictate that the aircraft be returned to service as quickly as possible, and the cost of developing a depot-level capability at each field unit is prohibitive. Thus, damaged composite aircraft components must either be easily and quickly repaired on-aircraft or in a backshop, or removed and replaced (R&R) with a spare component. In the latter situation, the damaged component, if deemed repairable by the responsible depot, will be sent to the depot facility or original equipment manufacturer for repair. In some cases, a depot team may be dispatched to the field unit to perform the repair if it is not tooling- or equipment-intensive.

During aircraft design and acquisition, estimates must be made on the likelihood of significant damage to a structure during its life cycle. This damage may come as the result of unanticipated flight loads, insufficient design or incorrect manufacture (inherent damage), or as a result of induced damage such as mechanical impacts in flight or on the ground, lightning strikes, overheating, erosion, aging, fluid ingestion, chemical contamination, thermal or flight stresses. Mean Time Between Maintenance Actions (MTBMA) and Mean Time Between Failure (MTBF) estimates based on probabilistic analysis and comparison with a similar structure already in use are normally used to establish repair and replacement rates. This is then used to establish initial provisioning requirements by the aircraft procurement agency for spare/replacement components. As operational experience is gained with the parts, adjustments can be made to the on-going provisioning requirements.

Spares are normally stored at the designated aircraft depot in an enclosed storage facility. Accurate estimates when determining the number of spares to purchase are important. Too low a number may mean aircraft downtime or flight restrictions while awaiting part replacement. Too high a number of spares mean precious resources are tied up in storage and part costs.

From a logistics support perspective, components that are interchangeable are preferred. Pre-drilled panels can be taken from the supply depot or scavenged from another aircraft and easily installed on the affected aircraft. Trim-to-fit/match-drilled (replaceable) parts require additional labor for installation. Once trimmed, they may only be useable on the particular aircraft to which they were adjusted. The removed and repaired part must then either be stored for that aircraft, or the holes filled and edges rebuilt, which will probably then require depot tooling for contour matching. While interchangeable panels are usually more expensive to produce, the life-cycle cost differential between interchangeable and replaceable panels will often be minimal if these considerations are taken into account.

8.5.3 Materials

Repair materials present another logistics support issue. While most structural components on an aircraft are manufactured from prepreg composite materials, support considerations may make it desirable to use different repair materials. The materials required for repair are specified in the applicable repair manual. For the repair patch itself, the repair materials chosen may be prepreg or dry cloth with a laminating resin. Whichever material type is used, strength and/or stiffness should be matched with the parent laminate during design of the repair. Adhesives must also be available to accomplish any bonded repair. Film adhesives, while offering excellent structural properties, require cold storage. Cold storage is also required for foaming adhesives, which are used for splicing core in honeycomb assemblies, or for filling small gaps. Laminating resins and paste adhesives present a room-temperature storable alternative, but will have reduced performance at higher temperatures. If the damaged structure has a lightning-strike protection scheme, this must be restored. Thus, lightning-strike protection systems, such as copper, nickel, or aluminum mesh, must be available at the repair station. The materials and processes for the repair must be called out in the applicable structural repair manual.

The structural repair materials that are brought to the facility must be purchased and controlled by a materials specification. Some incoming material tests may be required to verify supplier material quality. AC-145-6 (Reference 8.3.2.5(b)) has a discussion on this topic.

Beyond the materials used in the actual repair, the repair station must also have additional consumable materials, which will be used during the repair process. These materials will likely consist of non-porous and porous fluorinated ethylene propylene (FEP) release films, peel ply, breather, bleeder cloth, bagging film, and tacky tape. Tooling materials are also a requirement if bondform tools (splash molds or constructed) are required for contoured repairs, as well as mold releases.

While the direct cost of materials used in a repair is normally a small part of the total cost, significant indirect costs can result from special handling requirements such as storage, safety, process control, procurement, and waste. These will become a consideration in the overall repair scheme selected by the repair design team. Shelf-life limited adhesives and prepregs will require an incoming certification as well as recertification once the manufacturer-specified shelf-life is exceeded. This certification must be accomplished by a laboratory with trained personnel and the proper equipment to measure resin advancement and material properties. Tensile and compressive test apparatus and fixtures are required for coupon testing of material strength and stiffness. Recertification typically looks at matrix dominated properties such as compression, flexure, and transverse shear, as well as resin physical properties such as flow, gel time and glass transition temperature. Normally, this facility will be placed at a depot because of material usage rates and the cost of this capability.

In the final analysis, it is often difficult to anticipate the proper kinds and amounts of repair materials, which should be on hand at a repair facility when commencing support of a new aircraft. As a result, availability often becomes a significant factor in material selection for repair.

8.5.4 Facilities

The basic requirements for a field or depot composite repair facility consist of a lay-up area, part preparation area, a part curing area, and a material storage area. An environmentally-controlled lay-up area is required to prevent contamination of the repair surface and materials from dust, dirt, oil, and moisture when a bonded repair is implemented. Ideally, the lay-up/bonding area will be enclosed, with a slight positive pressure to prevent dust from entering. Temperature and humidity in the area should be controlled to a maximum of 75°F (24°C) and 50% relative humidity. A chart recorder should be used to track conditions in this facility. General lay-up room requirements are defined in MIL-A-83377 (Reference 8.5.4), which can be superseded by specific requirements specified in weapon-system-specific technical manuals. Civil aircraft operators must demonstrate compliance with the requirements of Title 14 of the Code of Federal Regulation parts 21, 43, 121, 125, 127, 135, and 145 regarding procedures and facilities. AC-145-6 (Reference 8.3.2.5(b)) delineates facilities that may be required.

For on-aircraft repair, humidity and temperature control is unlikely. In the best case, a hangar will be available in which to perform the repair, giving some shielding from the environment and contaminants. In the worst case, the repair will have to be performed on the tarmac. Some form of shelter should then be devised around the repair area. Repair materials should be prepared and sealed in bags in the backshop, and the bags only opened immediately prior to installation.

Because a depot repair/rework facility must perform repairs which range from beyond the field support capability to out-right component remanufacture, these facilities must essentially replicate those existing at the original equipment manufacturer. Rework facilities must have all the equipment and tooling necessary to restore aircraft components to essentially original strength, stiffness, aerodynamic, and electrical requirements. Floor space is less at a premium at the depot than it would be in a field environment; thus separate lay-up, bonding, tool manufacture, part machining, and part and tool storage areas will be available.

During remanufacture, the components are off-aircraft and mobile. Therefore, large stationary industrial cold storage, curing, machining, and inspection equipment can be used to perform repair operations at the depot. A depot should also have a three- or five-axis core cutters and numerical control machines to accurately shape fittings, core, substructure, and tooling. Ample capability exists to store and use fixtures and tooling, or manufacture them. A phosphoric acid anodizing (PAA) line for surface preparation of

metal substructure in composite components must be accessible. Abrasive waterjet cutters for rapid and smooth trimming of composite panels may be a worthwhile consideration if workload warrants it.

8.5.5 Technical data

Personnel skill, facilities, and equipment make up only part of the logistics support requirement for structural repair of composites. Information, or technical data, in various forms is required to quickly and adequately support composite repair to aircraft structure. Technical data ranges from structural repair manuals/military technical manuals, to part drawings and CAD data, to loads books and finite element models for engineers. Hopefully, this data was acquired as part of the original aircraft acquisition process, and was available prior to initial operating capability (IOC), or provided soon thereafter. Airlines and repair stations may not have such data and may have to request it from the original equipment manufacturer (OEM).

Repairs for smaller damages (less than 4 inches) which are expected to commonly occur are found in Structural Repair Manuals (SRMs). A Non-Destructive Inspection Manual and NDI Standards panels should also be provided with the aircraft to allow accurate detection of damages to composite panels. The SRMs should define repair size limits for negligible (cosmetic), field-repairable, and non-repairable damage. Size and depth limits should be provided in the manual for scratches, gouges, dents, delaminations, disbonds, and partial- or full-through punctures. These limits are most useful when provided through "mapping/zoning" of the structure. A parts-breakdown graphic should be in the manual, with a listing of the materials contained within each sub component. Within the negligible and field-repairable limits, repairs should be defined which can be accomplished within the limited capabilities/conditions of the field but restore full strength and stiffness to the structure. This definition must specify repair materials, equipment, and well-written step-by-step instructions which can be understood by a structural repair technician.

For repairs not provided in the SRM or beyond field-repairable limits, cognizant engineers must be consulted. The engineers require access to design information, which define aircraft component loading conditions, and aircraft design manuals, which provide information on the design requirements and load distribution within the structure. With increasing use of finite element analyses (FEA) to design aircraft structure, the aircraft acquisition agency may find it useful to purchase the FEA models developed by the manufacturer. Otherwise, engineers will require FEA software and workstations to perform analyses for structurally-significant repairs. This means engineering will also require a fully dimensioned drawing package, to include material properties and process specifications for FEA model or table top analyses.

8.5.6 Support equipment

8.5.6.1 Curing equipment

Heat blankets, hot bonders, heat lamps, heat guns and convection ovens are examples of portable heating and curing equipment usually found in both the depot and field environments. These are usually used in conjunction with a vacuum bag, to expedite moisture removal prior to repair, and to provide some consolidation pressure to the repair. They can be used to manufacture pre-cured composite repair patches and to bond repairs to the component. Whatever the portable heat source, generous use of thermocouples must be made to closely monitor cure temperatures.

Heat blankets consist of heating elements sandwiched between temperature-tolerant and flexible materials, such as silicone. The heat blankets can be separately zoned to allow differential heating of the repair area. Blanket temperature is controlled by regulating power to the blanket, either manually through a rheostat or through a hot bonder. Heat blankets are inexpensive, and can be purchased in a variety of sizes and shapes. Blanket flexibility and element durability are limiting factors; highly contoured repair areas may make blanket use unfeasible.

Hot bonders are programmable heat and vacuum control units, which provide power to heat blankets automatically to an operator-specified cure cycle. The hot bonder monitors bondline temperatures through

thermocouples placed on or near the repair area, and varies power to the heat blanket according to cure requirements. This assures acceptable cure temperatures. Hot bonders often have a vacuum pump included. The electrical draw of a hot bonder is approximately 30 amps, and a suitable power source (110V) must be available. If they are to be used on-aircraft, some form of explosion-proofing of the hot bonder system is mandated. Fuel vapors, which seep into the hot bonder case, may present an explosion hazard.

Infrared heat lamps and heat guns are also used for elevated temperature cures of composite repairs. Some are available with thermostat controls. Heat lamps can quickly heat up surfaces; monitoring and control of the cure temperature is essential to avoid overheating and damaging the surrounding structure. However, they are useful when part contours and repair size makes a heat blanket unfeasible. Heat guns can be convenient sources of heated air for smaller repairs.

Industrial ovens are a necessity at depots, and worthwhile in the field support environment, as a means of drying and curing composite parts and repairs. They are stationary pieces of capital equipment, and most depots will have several ovens of various sizes to accommodate workload. Maximum convenience is gained from ovens that are automatically controlled, allowing the programming of multi-step heating and curing cycles. The temperature capability and size of the oven will usually be defined by weapon-system specific requirements. Multiple vacuum lines and thermocouple connections within the oven, and a vacuum pump, are required for vacuum-bag repairs. A large (10' x 7' x 12' [3 m x 2.1 m x 3.7 m]) 500°F (260°C)-capable oven will require 300 Amp, 480V power supply.

Autoclaves are pressurized ovens usually required at a depot facility for part repair and remanufacture. The typical 85 psi (586 kPa) pressures required to achieve maximum consolidation of a composite prepreg laminate make large structural repairs possible. Because components are off-aircraft, the autoclave should be sized to accommodate large parts and their associated tooling. Like the ovens, autoclaves should be automatically controlled, with multiple-step cure cycles accommodated, and numerous vacuum line and thermocouple connections. The autoclave should be capable of providing 100 psi (689 kPa) of pressure and 500°F (260°C) in temperature, to accommodate both epoxy and bismaleimide cure cycles. Nitrogen gas should be used to provide pressure and inerting to prevent a fire, or more importantly, an explosion. Because of the high pressure achieved during cure, tooling and bondforms are necessary to support the aircraft component to the correct contour. Because of the infrastructure involved in them, including but not limited to tooling and bondforms, experienced operators and technicians, and fairly high operating and acquisition costs, autoclaves are restricted to depot use.

For manufacture of smaller, non-contoured precured repair patches, a heated-platen press may be a useful piece of equipment in the depot, although multiple patches can be made in an autoclave and stored. Presses can also be used in the laboratory for the creation of coupons and specimens to accomplish receiving and shelf life certification testing.

8.5.6.2 Cold storage rooms

Non-frost free cold storage equipment that can maintain material at 0°F (-18°C) or lower is required to maintain shelf-life on the vast majority of preimpregnated materials and adhesives. Frost-free freezers remove frost by temporarily heating up above 32°F (0°C), which can reduce the shelf life of the cold-storage materials. Because of moderate usage rates on preimpregnated materials, and the number of different shelf-life-limited materials necessary for weapon-system support, as well as long procurement lead-times, depots will require walk-in freezers which have sufficient capacity to meet local, and potentially field, needs for six to twelve months. Procurement and manufacturer lead times for most specification materials can mean 8-week to 4-month wait before delivery. Walk-in freezers are relatively inexpensive; thus, a field unit may also opt to purchase one if space and weapon-system requirements dictate it. In many cases, a case freezer will be adequate for field use, however. In case of power or freezer failure, an alarm system tied to a 24-hour notification site may avoid an expensive loss of shelf-life and/or material. AC 145-6 (Reference 8.3.2.5(b)) has specific details on control and operation of freezers.

8.5.6.3 Sanding/grinding booths

For paint removal and machining of cured composite materials, facilities separate from the bonding and curing area are required. The facility should have the means to safely remove dust produced during machining operations. The use of a down- or side-draft booth to remove the dust from the part and the air is preferred. Grinding and sanding areas must be configured to allow the dust unobstructed transit into the filter system. Worker tables must not shadow each other, to prevent accidentally sending the dust from one grinding operation onto adjacent work areas and workers. At a minimum, a shop vacuum system should be provided to the technician to collect the composite dust.

8.5.6.4 NDI equipment

Both field and depot facilities require damage evaluation and verification equipment for non-destructive inspection of composite components. Radiography (X-ray), thermography (infra-red), ultrasonic and laser shearography inspection equipment may be required for pre-repair damage mapping, in-progress inspection, and post-repair inspection. Field equipment will likely be small and portable to allow its movement to the aircraft, and to reduce facility and equipment costs. Depots will usually require both portable and stationary NDI equipment. The use of robotics to scan an entire aircraft for damage is practicable at a depot if workload and timeliness warrant it. Some method of archiving NDI data, whether digitally or in hard copy/film, is usually necessary to track damage growth.

The above is equally valid for assessing the electrical properties of structures and coatings, as in the case of radomes and low-observable structures. Field and depot units with a regular radome repair workload may require a static radar test range to test repaired radomes. Improved hand-held equipment to measure infrared or electrical properties of repaired low-observable structures are being developed for field use. A depot may require a separate electrical test range for low observable (LO) structure. In addition, a fly-through test range for a particular LO weapon system may be required to verify the proper behavior of multiple repairs.

REFERENCES

- 8.2.3.6 "Safe Handling of Advanced Composite Materials," Suppliers of Advanced Composite Materials Association, Arlington, VA.
- 8. 2.9.1 "Guide for the Design of Durable, Repairable, and Maintainable Aircraft Composites" AE-27, SAE, 1997.
- 8.3.1 "Composite Repair NDI and NDT Handbook" ARP 5089, SAE, 1996
- 8.3.2.5(a) "Acceptable Methods, Techniques, and Practices – Aircraft Inspection and Repair, Volume II Airframe: Non-Metallic Structure, 1994
- 8.3.2.5(b) "Repair Stations for Composite and Bonded Aircraft Structure", Advisory Circular AC 145-6, 1996
- 8.3.4.2 (a) "Masking and Cleaning of Epoxy and Polyester Matrix Thermosetting Composite Materials", ARP 4916, SAE, 1997
- 8.3.4.2 (b) "Drying of Thermosetting Composite Materials", ARP 4977, SAE, 1996
- 8.3.4.3.4 (a) "General Composite Repair", Organizational and Intermediate Maintenance, Technical Manual, NAVAIR 01-1A-21, January 1994
- 8.3.4.3.4 (b) "General Advanced Composite Repair Manual", Technical Manual, TO 1-1-690, U.S. Air Force, July 1984
- 8.3.4.4.3(a) Francis, C.F., Rosenzweig, E., Dobyns, A., Brasie, S., "Development of Repair Methodology for the MH-53E Composite Sponson," in 1997 USAF Aircraft Structural Integrity Program Conference, San Antonio, TX, 2-4 December 1997.
- 8.3.4.4.3(b) Dodd, S., Petter, H., Smith, H., "Optimum Repair Design for Battle Damage Repair, Volume II: Software User's Manual," WL-TR-91-3100, McDonnell Douglas Corp., February, 1992.
- 8.3.4.4.3(c) Hart Smith, J., "Adhesive-Bonded Scarf and Stepped-Lap Joints," NASA CR 112237, Douglas Aircraft Co., January, 1973.
- 8.3.4.4.3(d) "Elastic Adhesive Stresses in Multistep Lap Joints loaded in Tension," ESDU 80039, Amendment B, Engineering Sciences Data Unit International plc, London, November 1995."
- 8.3.4.4.4(a) "Resin Mixing", ARP 5256, SAE, 1997
- 8.3.4.4.4(b) "Impregnation of Dry Fabric and Ply Lay-up", ARP 5319, SAE, 1998
- 8.3.4.4.4(c) MIL-HDBK-337
- 8.3.4.4.4(d) "Vacuum Bagging of Thermosetting Composite Repairs", ARP 5143, SAE, 1997
- 8.3.4.4.4(e) "Heat Application for Thermosetting Resin Curing", ARP 5144, SAE, 1997
- 8.3.4.4.4(f) Westerman, E.A., Keller, R.L., Rutherford, P. , "Improved Processing for Field Level Repair," The Boeing Company, Seattle, WA, Air Force Materials Directorate Wright Laboratory Report No. WL-TR-97-4119, December 1997.

Volume 3, Chapter 8 Supportability

- 8.3.4.4.4(g) Burroughs, B.A. and Hunziker, R.L., "Manufacturing Technology for Non-Autoclave Fabrication of Composite Structures," Air Force Contract F33615-80-C-5080, Final Report for period October 1980-April 1984, Report No. AFWAL-TR-85-4060.
- 8.3.4.4.4(h) Buckley, L.J., Trabocco, R.E., and Rosenzweig, E. L., "Non-Autoclave Processing for Composite Material Repair," Naval Air Warfare Center, Warminster, PA, Report No. NADC-83084-60, 1983.
- 8.3.4.4.4(i) Mehrkam, P.A., Cochran, R.C., and DiBerardino, M. F. , "Composite Repair Procedures for the Repair of Advanced Aircraft Structures," Naval Air Warfare Center, Warminster, PA, Report No. NAWCADWAR-92091-60, September 1992.
- 8.3.4.4.4(j) Bergerson, A., Marvin, M., Whitworth, D., "Fabrication of a Void Free Laminate by Optimizing a Non-Autoclave Cure," Society for the Advancement of Material and Process Engineering.
- 8.3.4.5.2 "Core Restoration of Thermosetting Composite Materials", ARP 4991, SAE, 1996
- 8.5.1 "Composite and Bonded Structure Technician/Specialist Training Document", AIR 4938, SAE, 1996
- 8.5.4 MIL-A-83377

This page intentionally left blank

CHAPTER 9 STRUCTURAL RELIABILITY

9.1 INTRODUCTION

Reliability is commonly defined (References 9.1(a) and (b)) as "the probability of a device performing its purpose adequately for the period of time intended under the operating conditions encountered". There are four elements to the definition that must be considered. First, *probability* refers to the *likelihood* that a device or structural component will work properly. These terms imply acceptance of some degree of uncertainty. The second element refers to adequate performance. In order to determine whether a component has performed adequately, a standard is needed to define what is meant by adequate performance. The third element is the intended period of time. This is the mission endurance or lifetime of the structure under consideration. The final element of the definition is the operating conditions. Environmental conditions play a large role in reliability of composite materials, particularly polymer matrix composites. Simply stated, structural reliability is a yardstick of the capability of a structure to operate without failure when put into service. In the broadest sense, structural reliability includes events that are safety and non-safety related.

Until recently, structural reliability was not routinely analyzed or quantified in the design process. Reliability was accounted for tacitly by the factor-of-safety approach to design. Also guidelines and lessons learned helped to improve reliability. The structural designer/analyst does not perform a formal risk analysis on newly designed structure. This task is performed by reliability specialists who employ methodologies that are empirically based. The reliability assessment is usually conducted after a drawing or concept is produced and bears little relationship to the structural margin-of-safety.

As implied in the definition, structural failure and, hence, reliability, is influenced by many factors. In its simplest form, the measure of reliability is made by comparing a component's stress to its strength. Failure occurs when the stress exceeds the strength. The larger this gap, the greater the reliability and the heavier the structure. Conversely, the smaller the gap, the lower the r , but the lighter the structure. The gap between stress and strength, enforced by the factor-of-safety, generally produces adequate although unmeasured reliability.

The complications that mask the ability to quantify reliability reside in the stochastic nature of design inputs. The calculations are relatively easy; statistical characterizations of the strength and stress distributions are compared mathematically and a probability of failure calculated. Definition of these distributions however, can be an imposing, if not impossible, task. Each is influenced by many considerations with relatively unknown effects.

The primary purpose for establishing a factor-of-safety for design is to ensure safety. Until recently, no objective analysis has gone into the choice for factor-of-safety. Consequently, no evaluations are performed on the factor-of-safety as new materials or technologies are developed. As suggested by methodologies developed in Reference 9.1(c), these evaluations can now be performed. This fact suggests that future design and design processes might benefit greatly by focusing on reliability targets rather than factors-of-safety. This may be particularly true for composite materials.

The following sections discuss some of the important factors that affect composite structure reliability.

9.2 FACTORS AFFECTING STRUCTURAL RELIABILITY

9.2.1 Static strength

An aircraft structure's capability to sustain operational flight loads is commonly assessed by comparing material performance parameters to limit or ultimate loads. Limit loads are generally defined as the maximum load expected during the life of the aircraft. Ultimate loads are obtained by multiplying limit

loads by the factor-of-safety. Limit loads are derived by considering the extremes of flight envelopes, gross weight, load factors, environments, and pilot inputs. In some cases, the likelihood of encountering limit load is very remote. The 1.5 factor-of-safety used to obtain ultimate design loads from applied loads has been widely accepted by generations of engineers, mostly without questioning the origin of the factor. Reference 9.2.1 provides an excellent historical review of the evolution of the 1.5 factor-of-safety in the United States.

From the beginning of flight, occupant safety has been a primary concern in designing manned vehicles and the "factor-of-safety" has been a prominent design criteria. Like many design requirements, the implementation of the 1.5 factor-of-safety evolved over a period of time and was influenced by many concerns.

Design criteria require structures to withstand ultimate loads without failure and limit loads with no permanent deformation. This has led to the impression that the 1.5 factor-of-safety was due to the performance of metals, 2024 in particular. At the time the 1.5 factor-of-safety was established, 2024 aluminum had a ratio of ultimate to yield stress of approximately 1.5. However, in the early 1930's when the 1.5 factor-of-safety was formally established by the Air Corps, material properties were not considered. Mr. A. Epstein, who worked for the United States Army Air Corps Material Center from 1929 to 1940, prepared the original Air Corps Structures Specification X-1803 in 1936. Mr. Epstein noted (Reference 9.2.1) that "the factor-of-safety of 1.5 has withstood many moves to alter it, but there was a period in 1939 when the Chief of the Structures Branch of Engineering Division at Wright Field thought seriously of reducing the value of the factor. Newer aluminum alloys were becoming available with higher ratios of yield to ultimate strength and he interpreted the factor as the ratio of ultimate to yield. However, no action was taken when the following explanation was offered: 'The factor-of-safety is not a ratio of ultimate to yield strength, but is tied in with the many uncertainties in airplane design, such as fatigue, inaccuracies in stress analysis, and variations of material gages from nominal values. It might also be considered to provide an additional margin of safety for an airplane subjected to shellfire.'" Thus, while the factor-of-safety does much to promote reliability, it was defined independently of any specific reliability goal.

Generally speaking, composite structures are sized by comparing ultimate internal stresses to statistically reduced material parameters (e.g., B-basis strengths). The internal stresses are a result of applied design ultimate loads ($1.5 \times \text{DLL}$). In general the deterministic approach produces adequate reliability, but not necessarily the same as metallic structure. This is because composite materials exhibit different statistical distribution and variation from metals (see Figure 9.2.1). The result is that even though materials may have equivalent B-basis strengths, their reliabilities may be quite different. Reliability-based design procedures may be necessary to account for this difference (see Reference 9.1(c)).

9.2.2 Environmental effects

Composite material components are subjected to a wide range of environments. The operating conditions in which the aircraft must perform are not well characterized. Environmental factors of major importance include a combination of humidity and temperature. Many studies have been conducted to investigate moisture absorption as well as the reduction of mechanical properties due to temperature and moisture exposure. The current approach used to account for environmental factors is to define exposures that are extremes and selectively evaluate by test the effects on material properties. These extremes are then considered to be invariant during the lifetime of the structure. Strength values are reduced to coincide with the environmental extremes.

9.2.3 Fatigue

Composite materials exhibit higher fatigue threshold stresses than metals. Once this threshold is exceeded, composites show more scatter in fatigue than metals and might tend toward lower reliability performance if the composite structures were stressed that highly. Because of this high threshold stress, fatigue is not the limiting factor in the design of composite structures. Design criteria such as damage tolerance limit the stress levels in composite structures to such low values that fatigue does not generally represent a design constraint. However, this is not necessarily true for high-cycle fatigue (e.g., $n > 10^7$)

dynamic system components in rotorcraft. (For more information on fatigue or durability of composite structures, see Volume 3, Sections 4.10 and 4.11.2).

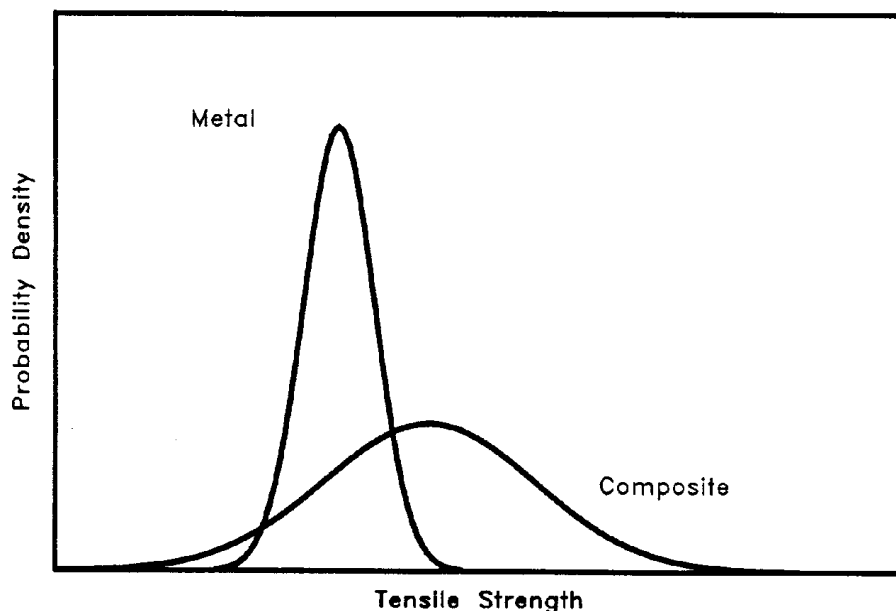


FIGURE 9.2.1 *Composites generally exhibit variation in material performance different from their metallic counterparts.*

9.2.4 Damage tolerance

As stated in Volume 3, Section 5.12.1, "damage tolerance is defined as a measure of a structure's ability to sustain a level of damage or presence of a defect and yet be able to safely perform its operating functions." Damage to composite structures can occur during manufacturing or operational usage. In order to design the structure to operate safely after sustaining such damage, a common practice is to limit the stress allowed in the composite structure. Typically, composite structures are designed to withstand the most severe of either of the following two conditions: a 0.25-inch open hole in any location at ultimate load or damage sustained when objects of specified size strike the surface (representative of barely visible impact damage threats). Both criteria assume the defect exists for the life of the part. These criteria reduce the allowable strength.

9.3 RELIABILITY ENGINEERING

Reliability is of such concern to the military that specific requirements are defined in contractual documents. Industry satisfies these requirements by employing engineers who specialize in reliability to guide the design. Currently, structural reliability is being increasingly emphasized. The reasons are twofold. First, advances in materials technology have resulted in higher performance materials that often possess detrimental side effects (e.g., high strength steels that exhibit low fracture toughness). Second, the need for higher vehicle performance has pushed operating stresses to higher levels in order to reduce structural weight.

Structural designs are documented via engineering drawings. Drawings are not "released" until they undergo scrutiny by several technical disciplines. Reliability is one of the concerns that is dealt with by the technical disciplines. Reliability specialists ensure that these concerns are incorporated into the design.

Customer reliability criteria typically specify three goals. These are: Mean Time Between Failure (MTBF), mission reliability, and Failure Modes Effects Criticality Analysis (FMECA). MTBF is measured in unscheduled maintenance events per million flight hours. Mission reliability is an indication of the probability of having to abort a flight. FMECA determines the impact of specific failures on mission performance, safety, and utilization.

In addition to supplying input to design, reliability engineering output is supplied to maintainability groups for maintenance man-hour predictions. Their results are used by logistics persons to establish provisioning requirements for spare parts.

9.4 RELIABILITY DESIGN CONSIDERATIONS

The following is a list of general composite structures considerations which provide insight on improved reliability and causes of poor reliability:

- Eliminate/minimize potential galvanic corrosion and/or thermal expansion problems by selecting compatible materials.
- Allow for the difference in thermal expansion when mating composites to metals. The coefficient of thermal expansion for composites is low.
- Assess carefully the use of honeycomb sandwich panels which utilize thin facesheets in areas where Foreign Object Damage (FOD) and bird strikes are likely to occur. Thin facesheets are susceptible to impact damage.
- Protect the structure for possible lightning strikes. Good electrical contact between all metallic and carbon/epoxy structural components must provide for the dissipation of static and lightning-induced electrical currents.
- Fasteners: Use titanium alloy or other materials that are compatible with carbon/epoxy to prevent galvanic corrosion.
- The current ability to detect flaws in composite structures, especially honeycomb, is evolving. Designs that enhance access for inspection tend to promote reliability.
- Improved reliability can be obtained by avoiding anomalies such as wrinkling and porosity in integral stiffeners. The ability to detect such flaws is limited.
- Extreme care should be taken during the repair of composite structures. Avoid damaging additional plies during patch or repair operations as it may result in a decline in reliability.
- Variations in manufacturing processes such as curing and machining can be responsible for a range of part strengths thus influencing reliability.
- The supplier's prepreg material should be closely monitored (i.e., acceptance testing) to assure incoming material consistency and conformance to design values.

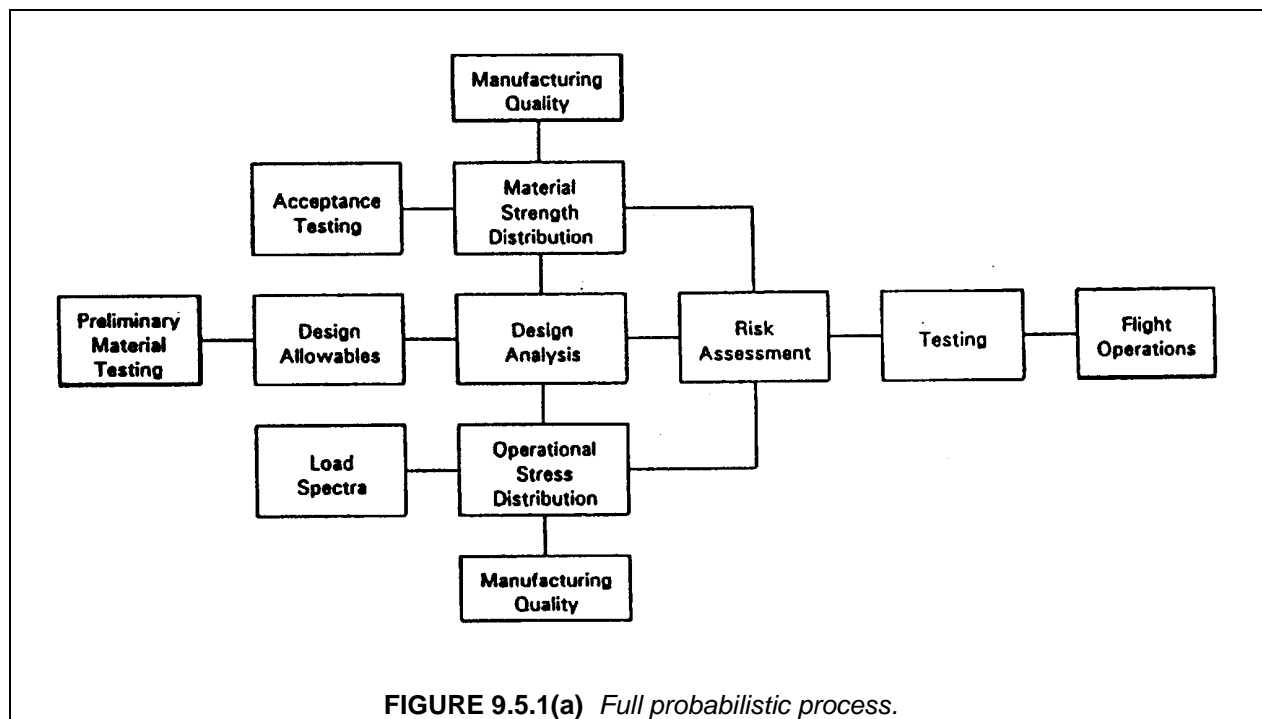
9.5 RELIABILITY ASSESSMENT AND DESIGN

9.5.1 Background

Advanced composite materials offer sizable improvements in weight savings, maintainability, durability, and reliability. There are a number of performance factors that have limited their success. Thus far, composite design and treatment of unique performance factors have been handled in a traditional metals approach in the aircraft industry. This approach is characteristically deterministic in nature. Probabilistic methods offer a different technology that can be used as a design tool, or, in a more conservative manner, as a risk analysis. The application of probabilistic methods opens up technical information not available in traditional approaches.

Probabilistic methods represent a technology that cannot be implemented without careful development. It is, however, a technology that is easily controllable. It may be used as an assessment of deterministic designs; it may be used to establish realistic criteria for deterministic designs; or it may be implemented as a preferred design approach. If used as the preferred design approach, probabilistic methods utilize a reliability target in lieu of factors-of-safety. Disclosure of risk characteristics alone should interest the designer in applying the technology.

Probabilistic design is an integrated process as shown schematically in Figure 9.5.1(a). The approach is to define/develop the functional relationships of the operations within the boxes, then build the relationships between them. This interconnects the entire process. In this way, when a factor in one operation changes, its effect can be determined on the others. The end result is the effect on failure probability.



A flowchart of a Probabilistic Design model is shown in Figure 9.5.1(b). This model consists of four major activities; namely, the design process, material production, manufacturing, and operations. Output from the design process is the expected operating stress distribution resulting from the flight spectra. The remaining three activities provide the material strength distribution, determined through Monte Carlo simulation of random variables representing random variation of incoming material strength, manufactur-

ing defects, and operational factors. Probability of failure occurs when the stress exceeds the strength. This is calculated by a double integral of the stress and the strength probability density functions to determine the probability that "stress exceeds strength".

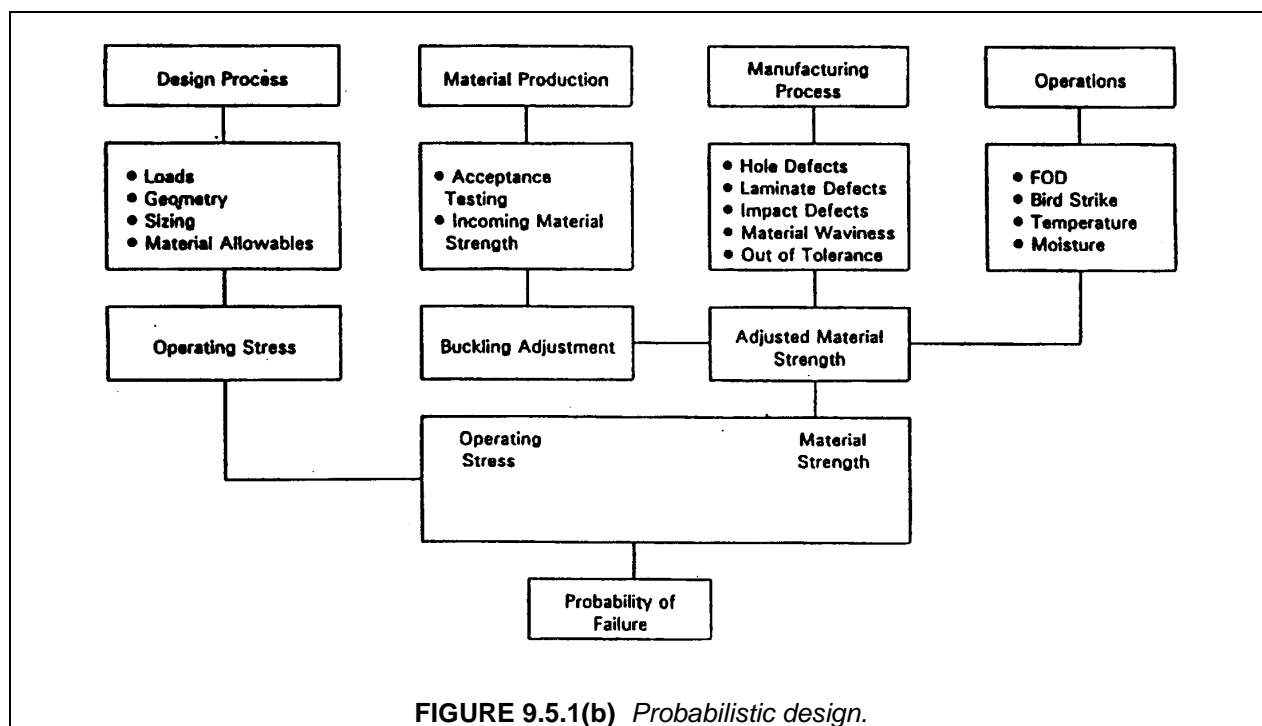


FIGURE 9.5.1(b) Probabilistic design.

9.5.2 Deterministic vs. Probabilistic Design Approach

Component dimensions, environmental factors, material properties, and external loads are design variables. They may be characterized with statistical modes. The deterministic approach seeks out and defines a worst case or an extreme value to meet in the design. The probabilistic approach utilizes the statistical characterization and attempts to provide a desired reliability in the design. The deterministic approach introduces conservatism by specifying a factor of safety to cover unknowns. The factor of safety is traditionally 1.5. The probabilistic approach depends on the statistical characterization of a variable to determine its magnitude and frequency. The amount of data (how well the variable is defined) influences its extreme values.

Application of a factor-of-safety to cover unknowns has a history of success. The danger in this approach is that the factor of safety may be too large, or in some cases, too small. Because it has worked in the past is no guarantee that it will suffice in the future. The whole approach of worst case extremes can lead to compounding and inefficiency. To select a factor-of-safety solely on the basis of "it worked in the past" should be examined.

Advanced composite materials were introduced in the early 1960's and since that time have undergone significant development. Some obstacles appeared insurmountable, including susceptibility of material strength degradation to elevated temperature, absorbed moisture, impact damage, and hidden flaws or damage. The approach to accommodate these material strength reduction factors has been to develop worst case manufacturing and operational scenarios and assume their existence for the life of the part. These factors, which are in reality variables, are thereby treated as constants.

Composite part design is governed by compounded conservatism illustrated by the following criteria:

- Worst case loading x safety factor (1.5)
- Worst case temperature
- Worst case moisture
- Worst case damage, undetected
- Material allowables derived from conservative statistical criteria

The effect of combining these conservative structural criteria is to produce inefficient products. Probabilistic methods offer an alternative to compound conservatism. They quantify the degree of safety and permit the designer to discover the risk drivers.

9.5.3 Probabilistic Design Methodology

The basic probabilistic design mathematical theory, shown below, accounts for the probability distributions of both material strength and operating stress. Because failure is a local phenomenon, division of a component into N numbers of nodes is done to represent all the locations at which failure is possible to occur. In general, the distributions are assumed to be identical at all the nodes. Step 6 assumes that material strengths at the nodes are independent from each other.

Step No.

1. Establish allowable failure rate.
2. Establish the number of nodes where failure is possible.
3. Determine probability distribution for loads.

$$P(X_x < x_s) = f(x_s)$$

4. Determine the operating stress probability density function $f_s(x)$.
5. Determine probability distribution for strength.

$$P(Y_M < y_m) = F(y_m)$$

6. Calculate failure probability P.

$$P_f = \int_x f_s(z) [1 - F_M(x)^N] dx$$

An alternative probabilistic design approach has been discussed in References 9.5.3(a) and 9.5.3(b). The fundamental elements of this approach are:

1. Identify all possible uncertain variables at all scales of composite structures. This includes variables at constituents scale, at all stages of fabrication process and assembly, and applied loads.
2. Assign a probabilistic distribution function for each variable.
3. Process all the random variables through an analyzer which consists of micro- and macro-composite mechanics and laminate theories, structural mechanics and probability theories.
4. Extract useful information from the output of the analyzer and check against defined probabilistic design criteria.

The IPACS (Integrated Probabilistic Assessment of Composite Structures) computer code developed at NASA Lewis integrated the above elements for probabilistic design of composite structures. A schematic of the computer code is shown in Figure 9.5.3.

9.5.4 Data Requirements

In order to conduct a probabilistic design exercise, the following parameters must be characterized as random variables:

1. Material mechanical properties
2. External loads anticipated during the life of the article
3. Manufacturing processes and their effect on material strength
4. Environmental effect on strength
5. Environmental history during operational usage
6. Flaw and/or damage locations, severity, probability of occurrence and effect on strength
7. Predictive Accuracy

Quality of incoming composite material is crucial to final product quality. To assure incoming material meets specifications, testing procedures and measurement value limits must be established to sufficiently discriminate between inferior and desired material. These criteria must be agreed upon by producer and consumer. Each wants to minimize their risk. The producer's risk is the probability of rejecting "good material" and the consumer's risk is the probability of accepting "inferior material".

9.5.5 Summary

Adopting specific structural criteria should not be done without a reason. The current criteria has its origins in metals technology. The goal of probabilistic design is to make reliability the foundation of composite structural criteria. It *will not* replace most structural mechanics functions.

Probabilistic Design is a powerful supplement/alternative to today's approach for composite design. It requires the development of sophisticated techniques in probability and characterization of statistical data for engineering variables. It is gaining momentum as more people become aware of its presence and benefits.

As the demand grows for more accurate, sophisticated designs, the requirement for probabilistic design methodology will become more and more accepted. The incorporation of Probabilistic Design, while quite challenging, offers significant payoffs not available with conventional technology.

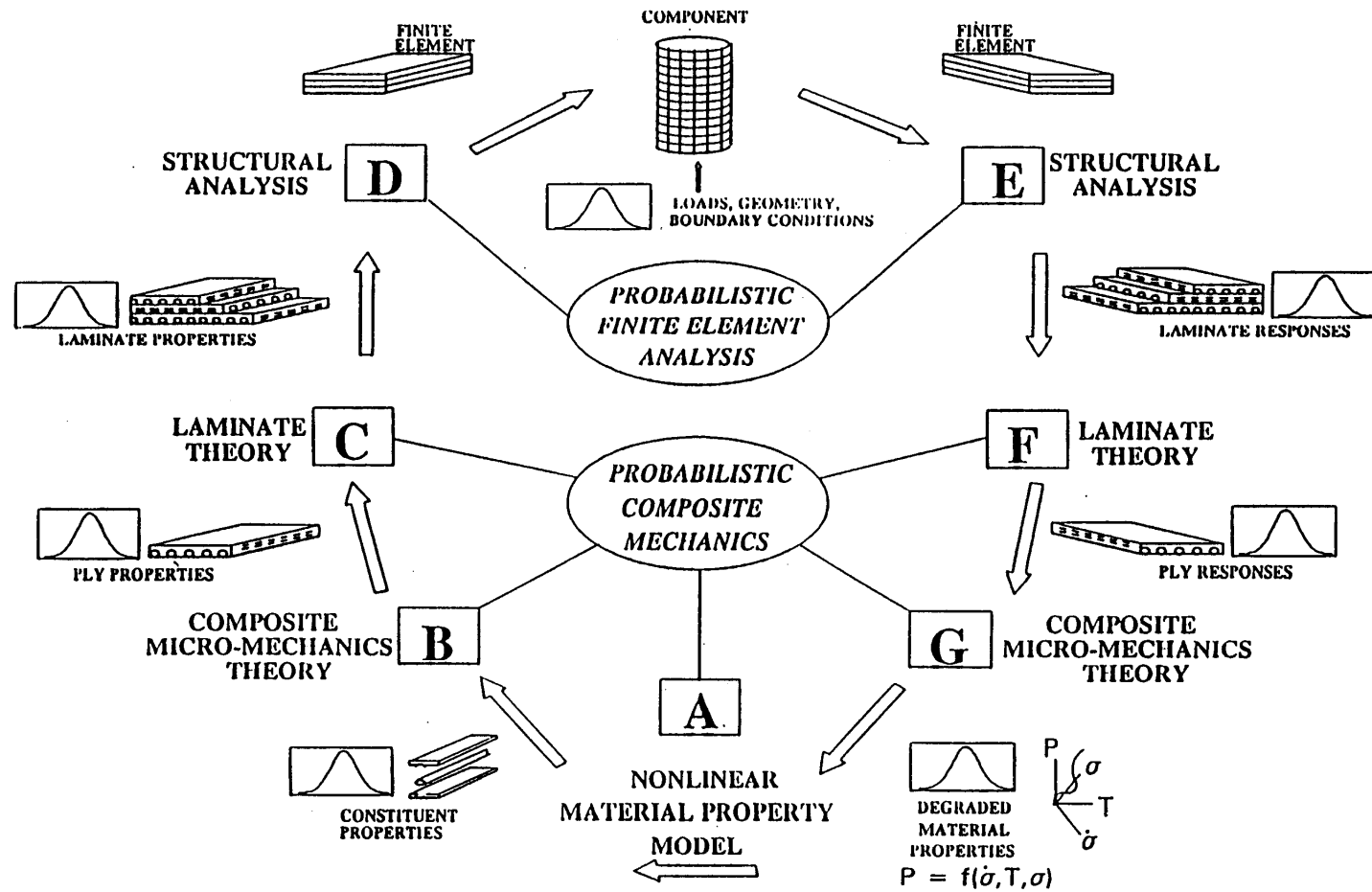


FIGURE 9.5.3 Schematic of the computer code IPACS.

9.6 RELIABILITY BASED STRUCTURAL QUALIFICATION

This section is reserved for future use.

9.6.1 Analysis

This section is reserved for future use.

9.6.2 Testing

This section is reserved for future use.

9.7 LIFE CYCLE REALIZATION

This section is reserved for future use.

9.7.1 Manufacturing

This section is reserved for future use.

9.7.2 Operational

This section is reserved for future use.

REFERENCES

- 9.1(a) Doty, L.A., "Reliability for the Technologies," Industrial Press, New York, New York, 1985, pp. 1-9.
- 9.1(b) Bazovsky, I., "Reliability Theory and Practice," Prentice-Hall, Inc., Englewood Cliffs, New Jersey, 1961, pp. 1-16.
- 9.1(c) Whitehead, R.S., Kan, H.P., Cordero, R., and Saether, E.S., "Certification Testing Methodology for Composite Structures," Vols. I and II, Final Report, Contract No. N62269-84-C-0243, October 1986.
- 9.2.1 Muller, G.E. and Schmid, C.J., "Factor of Safety - USAF Design Practice," Final Report, AFFDL-TR-78-8, April 1978.
- 9.5.3(a) Chamis, C.C. and Murthy, P.L.N., "Probabilistic Composite Analysis." First NASA Advanced Composites Technology Conference, Part 2, NASA CP3104-PT-2, 1991, pp. 891-900.
- 9.5.3(b) Chamis, C.C., Shiao, M.C., and Kan, H.P., "Probabilistic Design and Assessment of Aircraft Composite Structures." Fourth NASA/DoD Advanced Composites Technology Conference, June 7-11, 1993, Salt Lake City, Utah.

This page intentionally left blank

CHAPTER 10 THICK-SECTION COMPOSITES

10.1 INTRODUCTION AND DEFINITION OF THICK-SECTION

Thick-section composites are ones where the effect of geometry (thickness-to-span ratio), material constituents (matrix and fiber stiffness/strength properties), lamination scheme, processing, and service loading exhibit three-dimensional states of stress. For instance, all loadings induce multiaxial stresses into individual plies of composite materials that are made of multi-directional ply laminates (either woven or nonwoven), even though the overall loadings may only be uniaxial. When transverse (through-thickness) stresses and strains occur to a significant degree, they must be accounted for in analysis, design and testing. A significant degree is achieved when these effects contribute to failure (e.g., delamination), excessive deflection or vibration. Frequently, these stresses and strains induce failures that cannot be accurately predicted by conventional two-dimensional analyses for thin laminates. These two-dimensional analyses are usually based on material response data obtained from traditional shear and uniaxial tensile/compressive testing techniques. In thick section composites, where any one of six stress components may significantly contribute to failure, a failure criteria must distinguish between different types of failure modes by associating the contribution of each three-dimensional stress component to a unique mode of failure, be it fiber, matrix or interface dominated. An appropriate failure criteria for thick section composites must consider the following laminate failure modes:

<u>Fiber Dominated</u>	<u>Matrix Dominated</u>	<u>Interface Dominated</u>
. Fiber pull-out	. Transverse cracking	. Interface disbonding
. Fiber tensile failure	. Interlaminar cracking	. Interface delamination
. Fiber micro-buckling	. Intralaminar cracking	. Compressive delamination
. Fiber shear failure	. Edge delamination	

For example, thick-section composites made of high stiffness and strength fiber-reinforced plies often exhibit significant transverse shear and transverse normal deformations (the type of three-dimensional stress contributions that are negligibly small in thin laminates). The thickness effect can also be influenced by short wavelength loadings and, in dynamics, high frequency vibrations. These three-dimensional effects are considerably more pronounced in composites than in homogeneous isotropic materials due to their inherently high material compliances in the transverse direction relative to the axial fiber direction. Moreover, composite laminates exhibit much lower strength in the transverse direction, and at ply interfaces, making them particularly susceptible to matrix cracking and delamination.

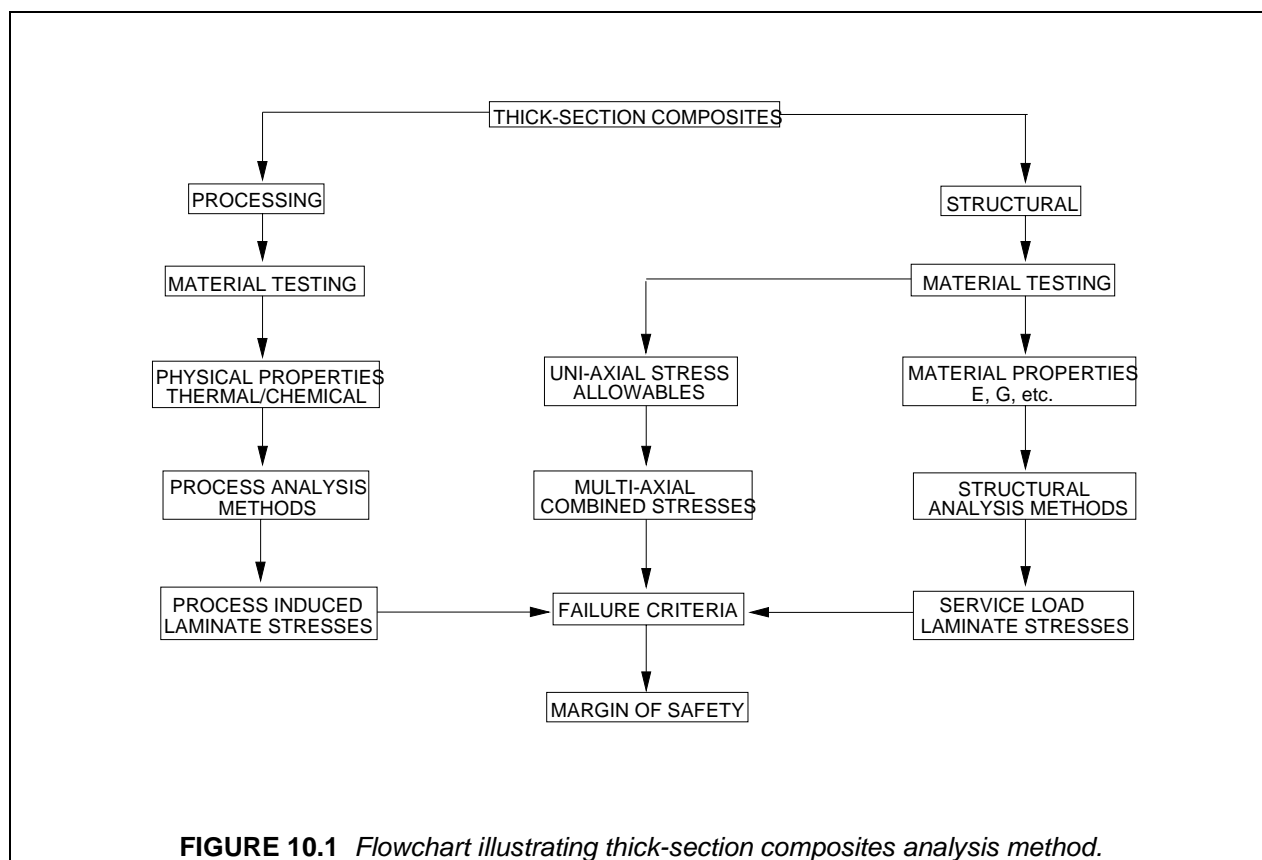
Thick section composites can also be defined from the standpoint of fabrication effects associated with a large number of plies. Process induced stresses can be significant and, therefore, warrant special attention. Fabrication effects of special concern include residual stresses, wrinkling, micro-cracking, exotherm, volatile removal, compaction, machining, and mechanical joining and/or adhesive bonding. To minimize these effects, special resins, processing, tooling, and cure cycles may be necessary.

In thick laminates, typically two competing objectives are desired, namely, minimization of process induced residual stresses and maximization of production rates (i.e., minimization of the processing time required to achieve complete cure). Fast cure cycle times, involving steep heating and cooling rates, will generally lead to high process induced residual stresses. On the other hand, slowly bringing all part thicknesses up to complete cure simultaneously will minimize, if not eliminate, all process induced residual stresses. This, however, is accomplished at the expense of extended cure cycle times. It is also important to note that process induced residual stresses may in fact be intentionally introduced to cancel, or otherwise mitigate, large superimposed in-service stresses.

In thick laminate design, cure simulation plays a very important role in developing a deeper understanding of the cure kinetics and the degree of cure at any point in the time domain. Such simulation is also able to predict processing stresses even during the cure cycle. This can be an important tool for prediction and preventing in-process part fabrication failures where both stresses and associated strengths are low.

The structural analyst needs to know the multiaxial strength and deformation characteristics for efficient thick composite material design. The full potential of thick composites cannot be realized until the material response under multiaxial service loadings can be established. Technical progress in the design, analysis and associated material testing of thick composites remain much less developed than the generally accepted methodology associated with thin composite material characterizations and applications.

The step-by-step method for analysis of thick section composites is illustrated by the flow chart in Figure 10.1.



10.2 MECHANICAL PROPERTIES REQUIRED FOR THICK-SECTION COMPOSITE THREE-DIMENSIONAL ANALYSIS

The purpose of this section is to define the three-dimensional (3-D) orthotropic stiffness properties necessary to conduct a 3-D point stress analysis, and the failure strength and strain allowables required to calculate a margin of safety. This section will:

- a) Define the stiffness properties currently used to conduct a conventional two-dimensional (2-D) analysis (Volume 1, Section 6.7).

- b) Define the additional stiffness properties needed to conduct a three-dimensional (3-D) stress analysis.
- c) Define the testing required to experimentally determine the 3-D stiffness properties and the failure strengths and strains for uniaxial loading (Section 10.2.3.1) and multiaxial loading (Section 10.2.3.2)
- d) Discuss the methodology for predicting laminate stiffness properties through the thickness using the 3-D lamina properties (Section 10.2.4).

The symbols and nomenclature used in the handbook (Volume 3, Section 1.3.1) apply to 2-D and 3-D composites and utilize 1, 2, 3 for lamina axes and x, y, z for an oriented laminate axis directions.

10.2.1 2-D composite analysis

The two-dimensional composite analysis procedures (Volume 3, Section 5.3.1) apply when the through the thickness stresses are not significant. For unidirectional laminates that have low stresses in the thickness or 3-direction ($\sigma_3 = \tau_{23} = \tau_{13}$), plane stress), the stress-strain relationship (Reference 10.2.1) is,

$$\{\epsilon_{ij}\} = [S]\{\sigma_{ij}\} \quad 10.2.1(a)$$

$$\begin{Bmatrix} \epsilon_1 \\ \epsilon_2 \\ \gamma_{12} \end{Bmatrix} = \begin{bmatrix} S_{11} & S_{12} & 0 \\ S_{12} & S_{22} & 0 \\ 0 & 0 & S_{66} \end{bmatrix} \begin{Bmatrix} \sigma_1 \\ \sigma_2 \\ \tau_{12} \end{Bmatrix} \quad 10.2.1(b)$$

In terms of the engineering elastic constants obtained by simple tests

$$\begin{Bmatrix} \epsilon_1 \\ \epsilon_2 \\ \gamma_{12} \end{Bmatrix} = \begin{bmatrix} \frac{1}{E_1} & -\frac{\nu_{12}}{E_1} & 0 \\ -\frac{\nu_{21}}{E_2} & \frac{1}{E_2} & 0 \\ 0 & 0 & \frac{1}{G_{12}} \end{bmatrix} \begin{Bmatrix} \sigma_1 \\ \sigma_2 \\ \tau_{12} \end{Bmatrix} \quad 10.2.1(c)$$

The reciprocity relationships for stiffness is

$$\frac{\nu_{12}}{E_1} = \frac{\nu_{21}}{E_2} \quad 10.2.1(d)$$

For the plane stress two-dimensional analysis, the four independent elastic material properties are:

$$E_1, E_2, G_{12}, \nu_{12}$$

In-plane failure stress and strain values can be obtained from the same test used for determining the stiffness as discussed in Section 10.2.3.1.

10.2.2 3-D composite analysis

When the stresses and strains in the thickness direction are significant, (applied values are approaching their allowables) the problem requires a three-dimensional orthotropic stress analysis. A 3-D analysis is frequently necessary as the section thickness of a composite increases or when thin sections have out-of-plane loading (bending moment, lateral pressures, etc.) which results in, for example, interlaminar tensile stresses in a corner radius or interlaminar shear stresses in a beam or plate.

10.2.2.1 Unidirectional lamina 3-D properties

For the orthotropic unidirectional lamina there are nine independent constants as shown by the following stress-strain relationship (Reference 10.2.1):

$$\begin{Bmatrix} \varepsilon_1 \\ \varepsilon_2 \\ \varepsilon_3 \\ \gamma_{23} \\ \gamma_{31} \\ \gamma_{12} \end{Bmatrix} = \begin{bmatrix} S_{11} & S_{12} & S_{13} & 0 & 0 & 0 \\ S_{12} & S_{22} & S_{23} & 0 & 0 & 0 \\ S_{13} & S_{23} & S_{33} & 0 & 0 & 0 \\ 0 & 0 & 0 & S_{44} & 0 & 0 \\ 0 & 0 & 0 & 0 & S_{55} & 0 \\ 0 & 0 & 0 & 0 & 0 & S_{66} \end{bmatrix} \begin{Bmatrix} \sigma_1 \\ \sigma_2 \\ \sigma_3 \\ \tau_{23} \\ \tau_{31} \\ \tau_{12} \end{Bmatrix} \quad 10.2.2.1(a)$$

or in terms of the engineering constants,

$$\begin{Bmatrix} \varepsilon_1 \\ \varepsilon_2 \\ \varepsilon_3 \\ \gamma_{23} \\ \gamma_{31} \\ \gamma_{12} \end{Bmatrix} = \begin{bmatrix} \frac{1}{E_1} & -\frac{\nu_{21}}{E_2} & -\frac{\nu_{31}}{E_3} & 0 & 0 & 0 \\ -\frac{\nu_{12}}{E_1} & \frac{1}{E_2} & -\frac{\nu_{32}}{E_3} & 0 & 0 & 0 \\ -\frac{\nu_{13}}{E_1} & -\frac{\nu_{23}}{E_2} & \frac{1}{E_3} & 0 & 0 & 0 \\ 0 & 0 & 0 & \frac{1}{G_{23}} & 0 & 0 \\ 0 & 0 & 0 & 0 & \frac{1}{G_{31}} & 0 \\ 0 & 0 & 0 & 0 & 0 & \frac{1}{G_{12}} \end{bmatrix} \begin{Bmatrix} \sigma_1 \\ \sigma_2 \\ \sigma_3 \\ \tau_{23} \\ \tau_{31} \\ \tau_{12} \end{Bmatrix} \quad 10.2.2.1(b)$$

There are three reciprocal relationships that must be satisfied for an orthotropic material. They are

$$\frac{\nu_{12}}{E_1} = \frac{\nu_{21}}{E_2}, \quad \frac{\nu_{13}}{E_1} = \frac{\nu_{31}}{E_3}, \quad \frac{\nu_{23}}{E_2} = \frac{\nu_{32}}{E_3} \quad 10.2.2.1(c)$$

There are nine independent elastic material properties required for an orthotropic lamina

$$E_1, E_2, E_3, G_{12}, G_{13}, G_{23}, \nu_{12}, \nu_{13}, \nu_{23}$$

When materials have a different stiffness in tension from in compression, it is common practice to use an average value when the difference is small. If the stiffness difference is significant, use the stiffness (tensile or compressive) that is representative of the application loading.

10.2.2.2 Oriented orthotropic laminate 3-D properties

The compliance matrix and associated nine elastic constants required to conduct a 3-D analysis are defined in this section and are for a oriented balanced and symmetric laminate loaded in the x, y, or z direction. Most practical composite laminate lay-ups generally are balanced and symmetric to prevent thermal warpage during processing. If the laminate is unbalanced and unsymmetric, or loaded "off-axis" to the principal orthogonal directions, then the matrix is fully populated with the Chentsov's coefficients ($\mu_{ij,kl}$) and coefficients of mutual influence ($\eta_{ij,i}, \eta_{i,ij}$) (see References 10.2.1, 10.2.2.2).

The compliance matrix for the balanced and symmetric laminate loaded in the x, y, or z direction is

$$\begin{Bmatrix} \epsilon_x \\ \epsilon_y \\ \epsilon_z \\ \gamma_{yz} \\ \gamma_{zx} \\ \gamma_{xy} \end{Bmatrix} = \begin{bmatrix} \bar{S}_{11} & \bar{S}_{12} & \bar{S}_{13} & 0 & 0 & 0 \\ \bar{S}_{12} & \bar{S}_{22} & \bar{S}_{23} & 0 & 0 & 0 \\ \bar{S}_{13} & \bar{S}_{23} & \bar{S}_{33} & 0 & 0 & 0 \\ 0 & 0 & 0 & \bar{S}_{44} & 0 & 0 \\ 0 & 0 & 0 & 0 & \bar{S}_{55} & 0 \\ 0 & 0 & 0 & 0 & 0 & \bar{S}_{66} \end{bmatrix} \begin{Bmatrix} \sigma_x \\ \sigma_y \\ \sigma_z \\ \tau_{yz} \\ \tau_{zx} \\ \tau_{xy} \end{Bmatrix} \quad 10.2.2.2(a)$$

In terms of the effective engineering elastic constants this relationship is,

$$\begin{Bmatrix} \epsilon_x \\ \epsilon_y \\ \epsilon_z \\ \gamma_{yz} \\ \gamma_{zx} \\ \gamma_{xy} \end{Bmatrix} = \begin{bmatrix} \frac{1}{E_x} & -\frac{\nu_{yz}}{E_y} & -\frac{\nu_{zx}}{E_z} & 0 & 0 & 0 \\ -\frac{\nu_{xy}}{E_x} & \frac{1}{E_y} & -\frac{\nu_{zy}}{E_z} & 0 & 0 & 0 \\ -\frac{\nu_{xz}}{E_x} & -\frac{\nu_{yz}}{E_y} & \frac{1}{E_z} & 0 & 0 & 0 \\ 0 & 0 & 0 & \frac{1}{G_{yz}} & 0 & 0 \\ 0 & 0 & 0 & 0 & \frac{1}{G_{zx}} & 0 \\ 0 & 0 & 0 & 0 & 0 & \frac{1}{G_{xy}} \end{bmatrix} \begin{Bmatrix} \sigma_x \\ \sigma_y \\ \sigma_z \\ \tau_{yz} \\ \tau_{zx} \\ \tau_{xy} \end{Bmatrix} \quad 10.2.2.2(b)$$

There are three reciprocal relationships that must be satisfied by the effective laminate stiffnesses. They are,

$$\frac{\nu_{xy}}{E_x} = \frac{\nu_{yx}}{E_y}, \quad \frac{\nu_{xz}}{E_x} = \frac{\nu_{zx}}{E_z}, \quad \frac{\nu_{yz}}{E_y} = \frac{\nu_{zy}}{E_z} \quad 10.2.2.2(c)$$

There are nine independent effective elastic material constants required for analysis of the oriented laminate,

$$E_x, E_y, E_z, G_{xy}, G_{xz}, G_{yz}, \nu_{xy}, \nu_{xz}, \nu_{yz}$$

10.2.3 Experimental property determination

The current and most commonly used approach for failure analysis of 2-D composites is to experimentally determine the strength and stiffness values for the unidirectional lamina from simple uniaxial tests and use a failure criterion to account for the various load direction interactions to calculate the margin of safety. These uniaxial tests are defined in Section 10.2.3.1 for 2-D and 3-D composites. Another approach is to conduct multiaxial tests that provide loading in the proper proportions to simulate the actual load applications. The multiaxial testing and methodology are discussed in Section 10.2.3.2.

There are considerable challenges associated with both uniaxial and multiaxial, mechanical testing of thick section composite materials. A partial list of experimental testing considerations is presented below:

- Test system and load introduction
- Gripping system and fixturing
- Computer control and interface
- Adequate displacement control over specimen centroid location
- Specimen design and optimization
- Unknown states of stress within thick composites
- Multiaxial extensometry and other measurement devices and techniques

Volume 3, Chapter 10 Thick-Section Composites

- Inclusion and treatment of environmental effects
- Data acquisition and analysis
- Multiaxial yield and failure criteria
- Size effect and scaling law
- Edge effects treatment
- Static and dynamic testing, including fatigue and impact loadings
- Sensitivity to stress concentrations
- NDE of damage

10.2.3.1 Uniaxial tests

The type of common tests conducted on the unidirectional laminate to obtain the conventional 2-D in-plane tensile, compressive, and shear stiffness, as well as failure strength and strains are summarized in Figures 10.2.3.1(a) through 10.2.3.1(c). These tests are also discussed in detail in Volume 1, Section 6.8. The additional unidirectional laminate design property tests needed when a 3-D (thick-section) analysis is required are summarized in Figure 10.2.3.1(d) and described in detail in Figures 10.2.3.1(e) and 10.2.3.1(f). Test methods available to obtain these properties are summarized in Table 10.2.3.1(a). Further test method development is needed for tension and compression testing in the 3 or through-thickness direction.

For oriented laminates, the additional design properties tests needed in addition to the 2-D tests for a 3-D analysis are summarized in Figure 10.2.3.1(g). The 3-D through the thickness stiffnesses can also be predicted from the unidirectional lamina stiffnesses by the methods discussed in Section 10.2.4 (Theoretical Property Determination). Table 10.2.3.1(b) summarizes the test methods available for determining 3-D properties for an oriented laminate. Furthermore, test method development is also needed for tension and compression testing in the z-thickness direction similar to the need for unidirectional laminate testing.

An example of representative thick-section composite properties for an intermediate modulus carbon/epoxy material system are presented in Tables 10.2.3.1(c) and (d) for the unidirectional lamina and [0/90] oriented laminate. The lamina properties were taken from Reference 10.2.3.1(a) and the [0/90] data were obtained by a Hercules test program from an 80-ply ($t=0.59$ in., 15mm) fiber-placed, autoclave-cured laminate (Reference 10.2.3.1(b)).

Tables 10.2.3.1(a) and (b) identify three uniaxial compressive test methods for testing composites greater than 0.250 inches (6.35 mm) in thickness. Both the David Taylor Research Center (DTRC) and the Alliant Techsystems testing fixtures, which are shown in Figures 10.2.3.1(h) and 10.2.3.1(i), respectively (see References 10.2.3.1(a) and 10.2.3.1(c), respectively), were developed for uniaxial compression testing of thick prismatic columnar shaped composite material specimens. The US Army Research Laboratory - Materials Directorate (ARL) (Reference 10.2.3.1(d)) test method utilizes a cubic specimen loaded directly between two steel platens with no associated fixturing. The development of compression data relative to the different material orientations identified in Tables 10.2.3.1(a) and (b) is accomplished through independent, successive uniaxial load applications. Successive uniaxial compression tests, that consist of one-directional load applications per material orientation, can be undertaken with conventional, medium-to-high capacity load frames. With proper care and specimen fixturing, these tests may also be used for determining unidirectional compressive material strengths and failure characteristics.

The primary feature that both the DTRC and the Alliant Techsystems test fixtures provide is that they have been developed for maintaining proper gripping and alignment of the test specimens as well as providing constraints to minimize any potential specimen end brooming (specimen splitting) under compressive load applications. Any potential onset of apparent, specimen end splitting and fixture-induced test specimen material cracking, may cause significant material strength reductions. Special tabbing as well as associated specimen-tabling connection detail may be required for some uniaxial compression testing of thick composites.

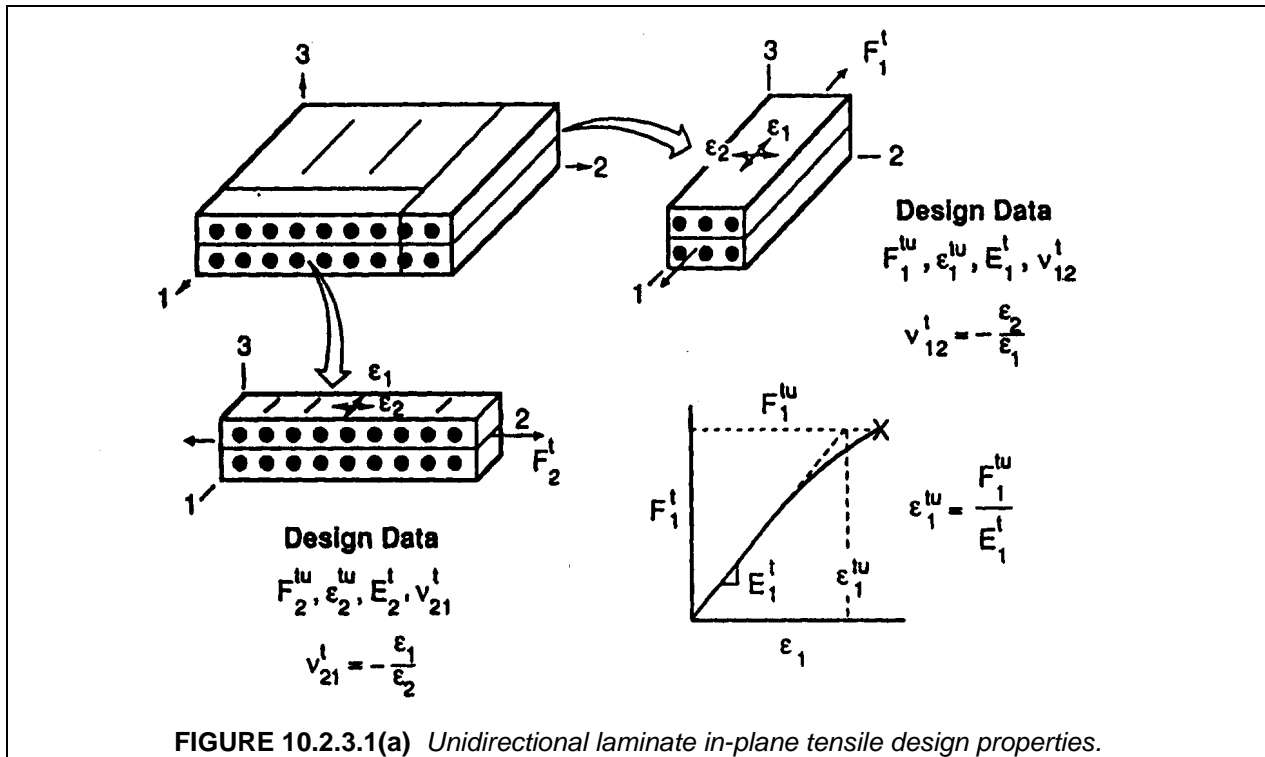


FIGURE 10.2.3.1(a) Unidirectional laminate in-plane tensile design properties.

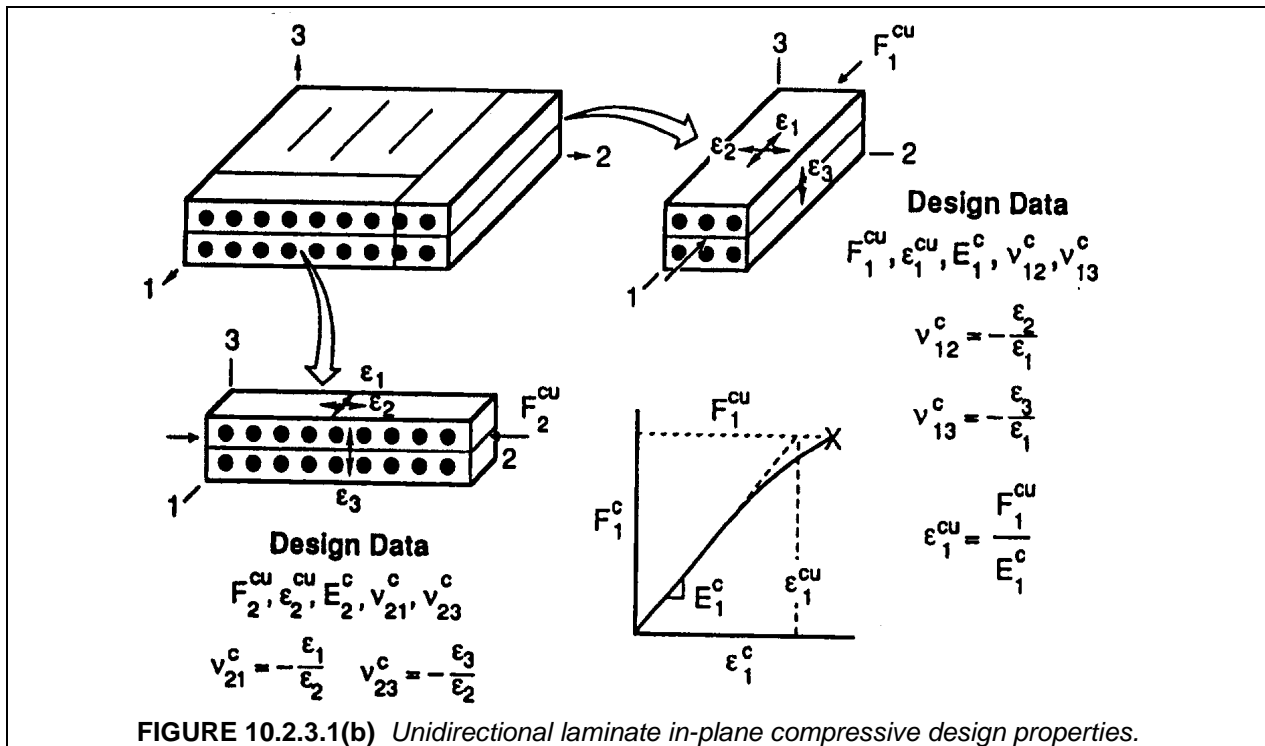


FIGURE 10.2.3.1(b) Unidirectional laminate in-plane compressive design properties.

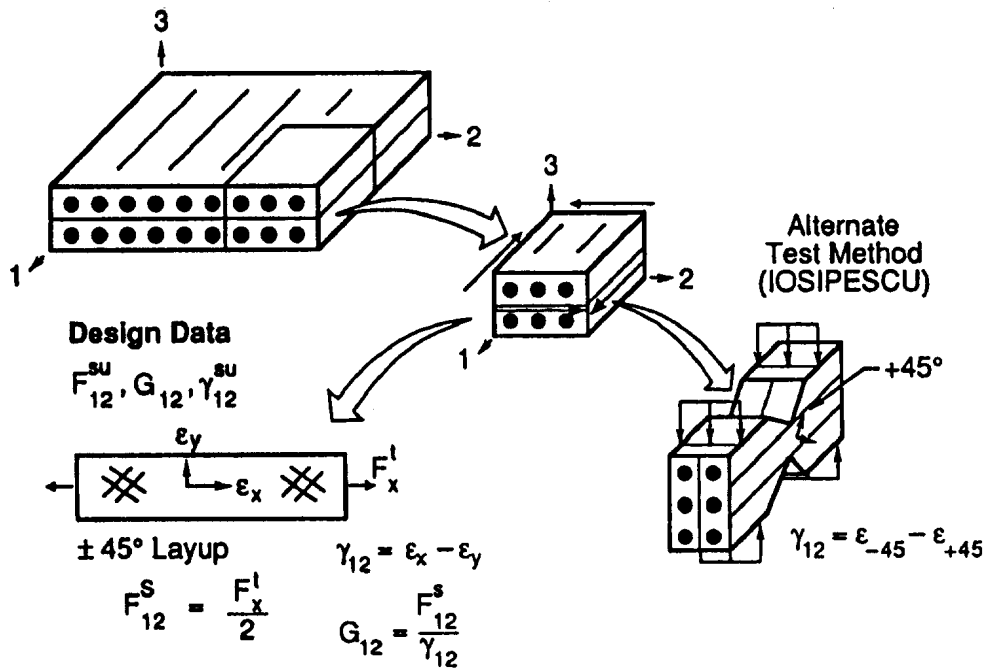


FIGURE 10.2.3.1(c) Unidirectional laminate in-plane shear design properties.

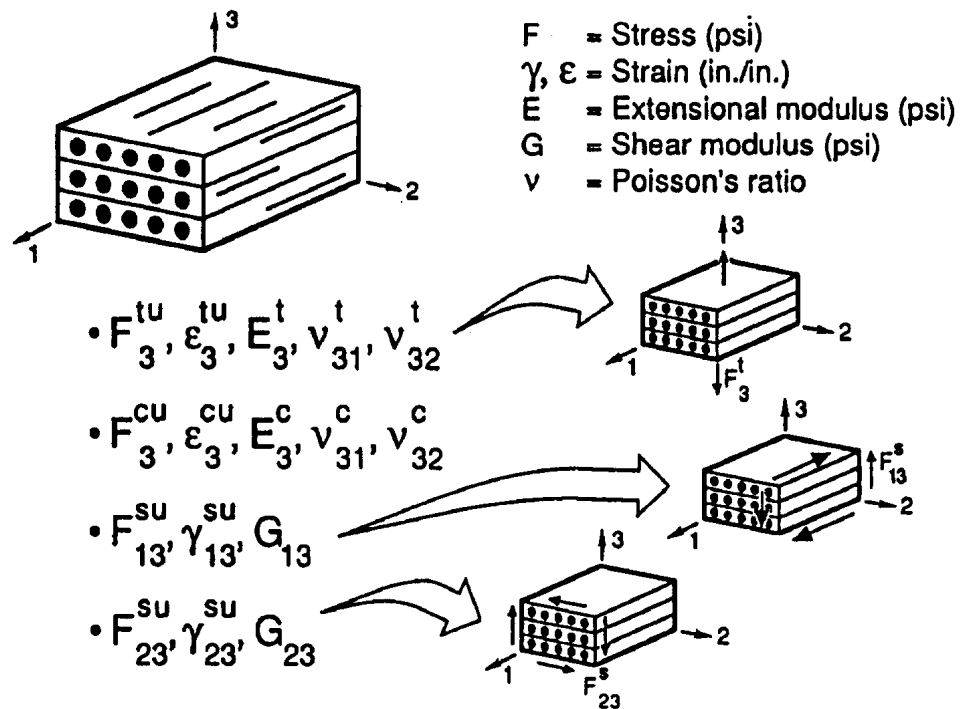


FIGURE 10.2.3.1(d) Unidirectional laminate thickness direction design properties.

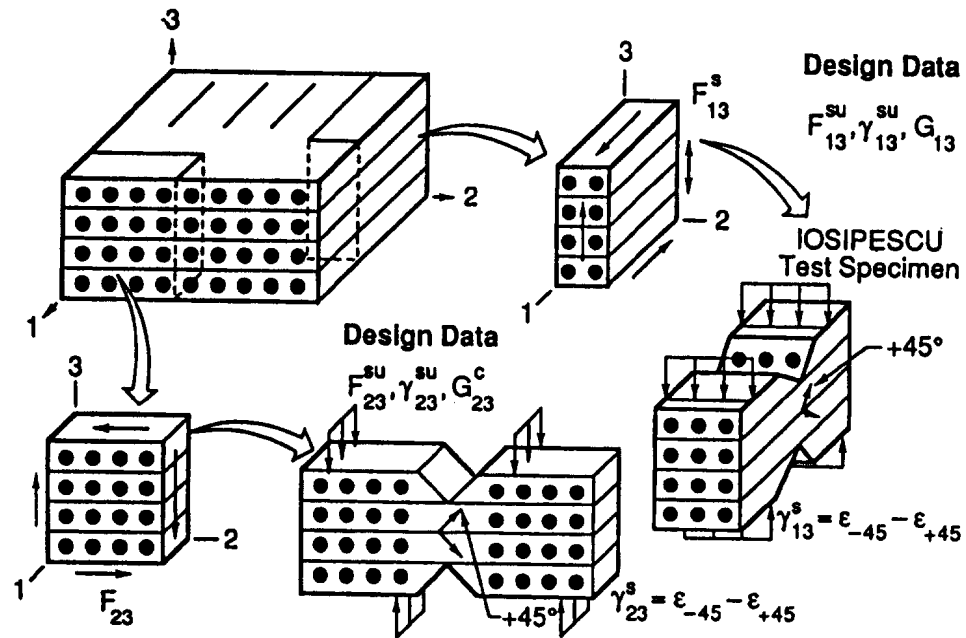


FIGURE 10.2.3.1(e) Unidirectional laminate design properties for shear thickness direction.

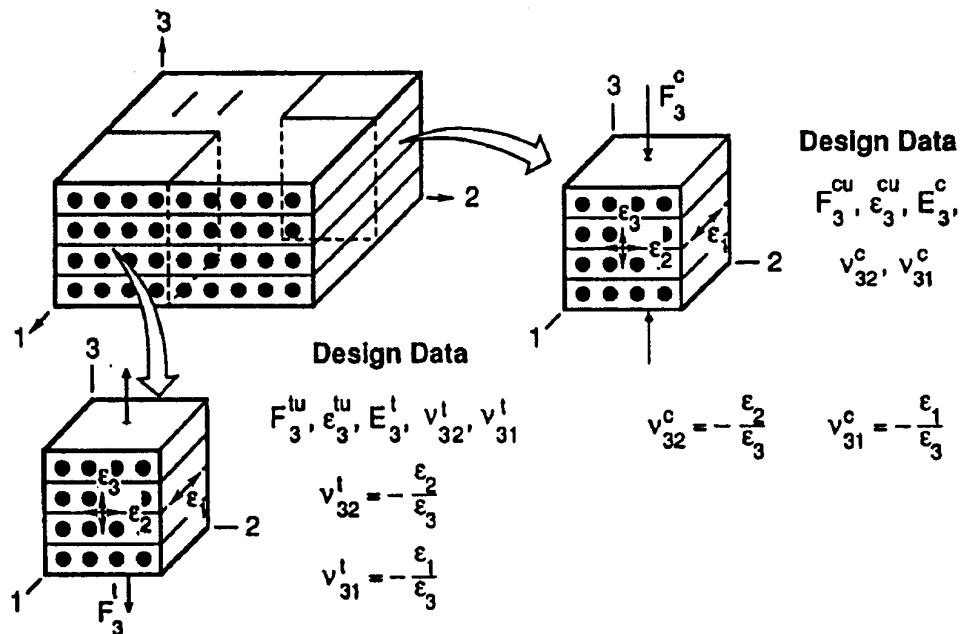
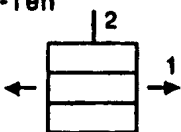
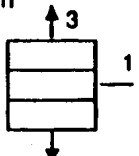
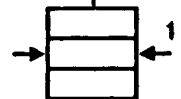
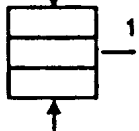
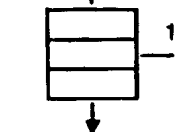
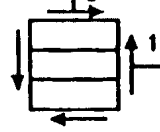
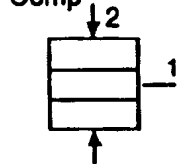
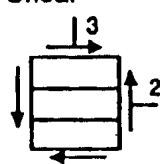
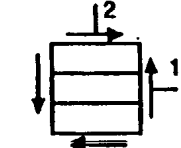


FIGURE 10.2.3.1(f) Unidirectional laminate tensile and compressive design properties in thickness direction.

TABLE 10.2.3.1(a) Test methods available for determining 3-D laminate properties.

Loading	Inplane Property	Test Method	Loading	Out-of-plane Property	Test Method
1-Ten 	F_1^{tu} E_1^{tu} ϵ_1^{tu} ν_{12}^{tu}	ASTM D3039 SACMA SRM-4	3-Ten 	F_3^{tu} E_3^{tu} ϵ_3^{tu} ν_{31}^{tu} ν_{32}^{tu}	To Be Developed
1-Comp 	F_1^{cu} E_1^{cu} ϵ_1^{cu} ν_{12}^{cu} ν_{13}^{cu}	ASTM D3410 SACMA SRM-1 ALLIANT TECHSYSTEMS DTRC ARL	3-Comp 	F_3^{cu} E_3^{cu} ϵ_3^{cu} ν_{31}^{cu} ν_{32}^{cu}	To Be Developed
2-Ten 	F_2^{tu} E_2^{tu} ϵ_2^{tu} ν_{21}^{tu}	ASTM D3039 SACMA SRM-4	13-Shear 	F_{13}^{su} G_{13}^{su} γ_{13}^{su}	ASTM D2344 SACMA SRM-8 IOSIPESCU
2-Comp 	F_2^{cu} E_2^{cu} ϵ_2^{cu} ν_{21}^{cu} ν_{23}^{cu}	ASTM D3410 SACMA SRM-1 ALLIANT TECHSYSTEMS DTRC ARL	23-Shear 	F_{23}^{su} G_{23}^{su} γ_{23}^{su}	IOSIPESCU
12-Shear 	F_{12}^{su} G_{12}^{su} γ_{12}^{su}	ASTM D3518 SACMA SRM-7	Notes:		

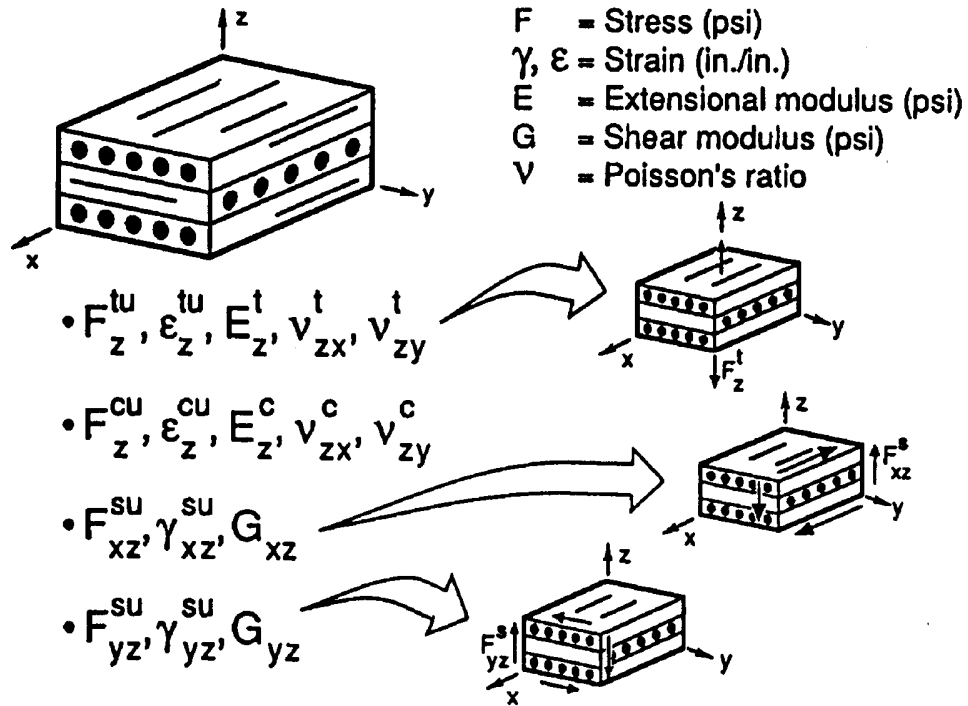


FIGURE 10.2.3.1(g) Oriented laminate thickness direction design properties.

TABLE 10.2.3.1(b) Test methods available for determining 3-D lamina properties.

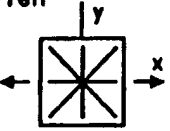
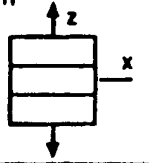
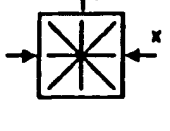
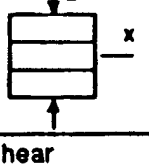
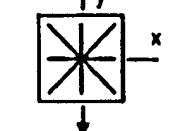
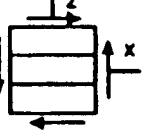
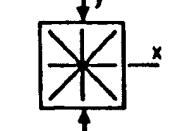
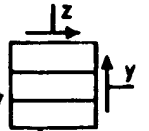
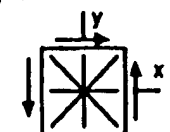
Loading	Inplane Property	Test Method	Loading	Out-of-Plane Property	Test Method
x-Ten 	F_x^{lu} ϵ_x^{lu} E_x^l ν_{xy}^l	ASTM D3039? SACMA SRM-4?	z-Ten 	F_z^{lu} ϵ_z^{lu} E_z^l ν_{zx}^l ν_{zy}^l	To Be Developed
x-Comp 	F_x^{cu} ϵ_x^{cu} E_x^c ν_{xy}^c ν_{xz}^c	ASTM D3410? SACMA SRM-1? ALLIANT TECHSYSTEMS DTRC ARL	z-Comp 	F_z^{cu} ϵ_z^{cu} E_z^c ν_{zx}^c ν_{zy}^c	To Be Developed
y-Ten 	F_y^{lu} ϵ_y^{lu} E_y^l ν_{yx}^l	ASTM D3039? SACMA SRM-1?	xz-Shear 	F_{xz}^{su} γ_{xz}^{su} G_{xz}	ASTM D2344? SACMA SRM-8? IOSIPESCU
y-Comp 	F_y^{cu} ϵ_y^{cu} E_y^c ν_{yx}^c ν_{yz}^c	ASTM D3410? SACMA SRM-1? ALLIANT TECHSYSTEMS DTRC ARL	yz-Shear 	F_{yz}^{su} γ_{yz}^{su} G_{yz}	IOSIPESCU
xy-Shear 	F_{xy}^{su} γ_{xy}^{su} G_{xy}	ASTM D4255? IOSIPESCU	Notes: ? - Applicability depends on laminate layup configuration.		

TABLE 10.2.3.1(c) Intermediate modulus carbon/epoxy lamina typical 3-D properties.

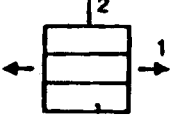
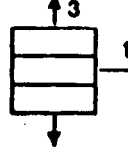
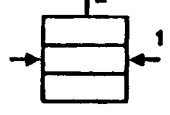
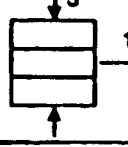
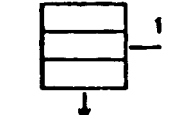
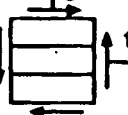
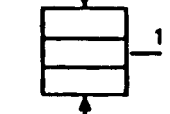
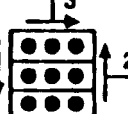
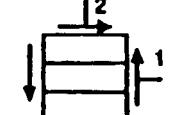
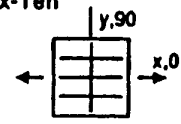
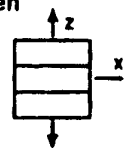
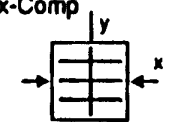
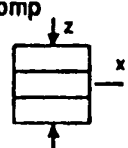
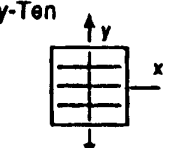
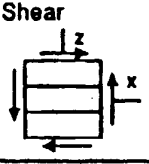
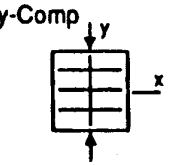
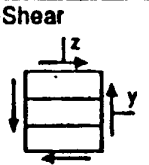
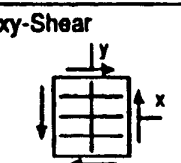
Loading	Inplane Property	RT/ Dry	Loading	Out-of-plane Property	RT/ Dry
1-Ten 	F_1^{lu} E_1^{lu} ϵ_1^{lu} ν_{12}^l	250. ksi (1720 MPa) 15200 $\mu\epsilon$ 16.5 Msi (114 GPa) 0.33	3-Ten 	F_3^{lu} E_3^{lu} ϵ_3^{lu} ν_{31}^l ν_{32}^l	8.00 ksi (55.2 MPa) 5700 $\mu\epsilon$ 1.40 Msi (9.65 GPa)
1-Comp 	F_1^{cu} E_1^{cu} ϵ_1^{cu} ν_{12}^c ν_{13}^c	170. ksi (1170 MPa) 10300 $\mu\epsilon$ 16.5 Msi (114 GPa)	3-Comp 	F_3^{cu} E_3^{cu} ϵ_3^{cu} ν_{31}^c ν_{32}^c	30.0 ksi (207 MPa) 21500 $\mu\epsilon$ 1.40 Msi (9.65 GPa)
2-Ten 	F_2^{lu} E_2^{lu} ϵ_2^{lu} ν_{21}^l	8.00 ksi (55.2 MPa) 5700 $\mu\epsilon$ 1.40 Msi (9.65 GPa)	13-Shear 	F_{13}^{su} G_{13}^l γ_{13}^{su}	12.0 ksi (82.7 MPa) 4000 $\mu\epsilon$ 0.87 Msi (6.0 GPa)
2-Comp 	F_2^{cu} E_2^{cu} ϵ_2^{cu} ν_{21}^c ν_{23}^c	30.0 ksi (207 MPa) 21500 $\mu\epsilon$ 1.40 Msi (9.65 GPa)	23-Shear 	F_{23}^{su} G_{23}^l γ_{23}^{su}	12.0 ksi (82.7 MPa) 22000 $\mu\epsilon$ 0.55 Msi (3.8 GPa)
12-Shear 	F_{12}^{su} G_{12}^l γ_{12}^{su}	15.0 ksi (103 MPa) 17000 $\mu\epsilon$ 0.87 Msi (6.0 GPa)	Notes: 1. Transverse isotropy assumed in 2-3 plane for stiffness, strength, strain. 2. Failure strain = strength/modulus. 3. 60% fiber volume.		

TABLE 10.2.3.1(d) Intermediate modulus carbon/epoxy $[0_3, 90]$ laminate typical 3-D properties.

Loading	Inplane Property	RT/ Dry	Loading	Out-of-Plane Property	RT/ Dry
x-Ten 	F_x^{lu} ϵ_x^{lu} E_x^{lu} ν_{xy}^{lu}	140. ksi (965 MPa) 9330 $\mu\epsilon$ 15.0 Msi (103 GPa) 0.10	z-Ten 	F_z^{lu} ϵ_z^{lu} E_z^{lu} ν_{zx}^{lu} ν_{zy}^{lu}	3.40 ksi (23.4 MPa) 3040 $\mu\epsilon$ 1.12 Msi (7.72 GPa)
x-Comp 	F_x^{cu} ϵ_x^{cu} E_x^{cu} ν_{xy}^{cu} ν_{xz}^{cu}	111 ksi (765 MPa) 8600 $\mu\epsilon$ 12.9 Msi (88.9 GPa) 0.12	z-Comp 	F_z^{cu} ϵ_z^{cu} E_z^{cu} ν_{zx}^{cu} ν_{zy}^{cu}	60.0 ksi (414 MPa) 3660 $\mu\epsilon$ 1.64 Msi (11.3 GPa)
y-Ten 	F_y^{lu} ϵ_y^{lu} E_y^{lu} ν_{yx}^{lu}	35.0 ksi (241 MPa) 6210 $\mu\epsilon$ 5.64 Msi (38.9 GPa) 0.03	xz-Shear 	F_{xz}^{su} γ_{xz}^{su} G_{xz}	4.06 ksi (28.0 MPa) 7700 $\mu\epsilon$ 0.53 Msi (3.7 GPa)
y-Comp 	F_y^{cu} ϵ_y^{cu} E_y^{cu} ν_{yx}^{cu} ν_{yz}^{cu}	72.9 ksi (503 MPa) 12900 $\mu\epsilon$ 5.66 Msi (39.0 GPa) 0.029	yz-Shear 	F_{yz}^{su} γ_{yz}^{su} G_{yz}	6.15 ksi (42.4 MPa) 9300 $\mu\epsilon$ 0.66 Msi (4.6 GPa)
xy-Shear 	F_{xy}^{su} γ_{xy}^{su} G_{xy}	15.3 ksi (105 MPa) 22000 $\mu\epsilon$ 0.70 Msi (4.8 GPa)	Notes: 1. $[0_3, 90]$ laminate (1 = .59 in.) average properties from reference 4, fiber volume = 61.4%, void = 0.04%. 2. Fiber placed, autoclave cured, flat panel data, 5-7 specimen average. 3. Failure strain = strength/modulus.		

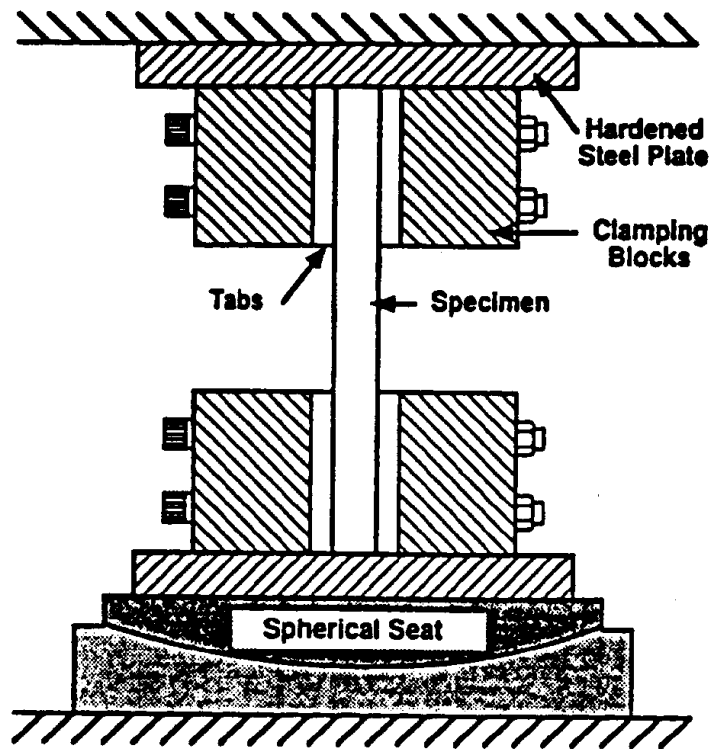


FIGURE 10.2.3.1(h) Uniaxial thick-section compression test fixture - David Taylor Research Center (DTRC).

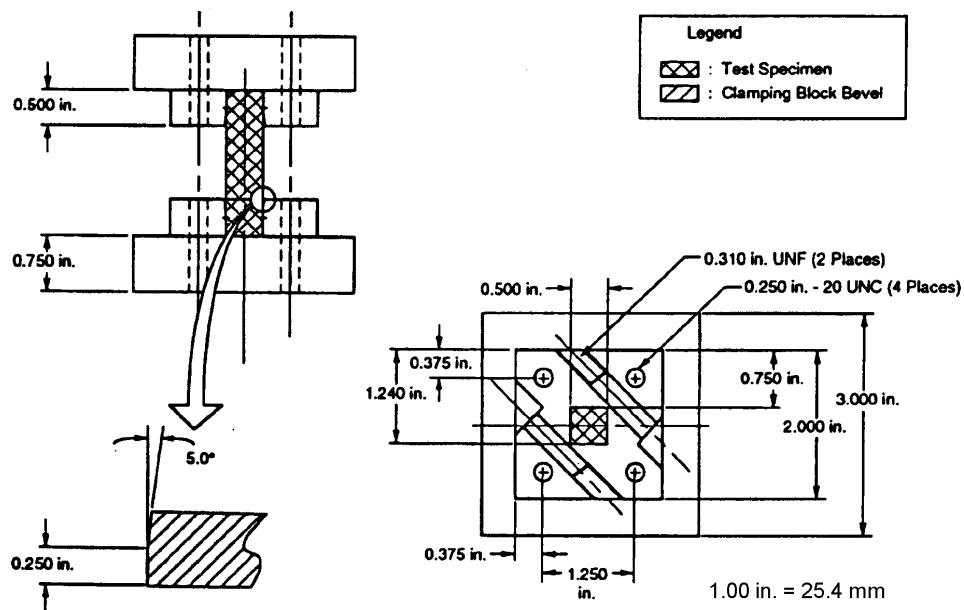


FIGURE 10.2.3.1(i) Uniaxial thick-section compression test fixture - Alliant Techsystems Inc.

10.2.3.2 Multiaxial tests

The purpose of this section is to provide information regarding multiaxial material testing methods. Some of these techniques, such as the two-dimensional methods (biaxial load applications), may be used for testing both thick and thin section composite materials. *However, the three-dimensional tests are primarily aimed at evaluating thick-section composite specimen material properties.* The importance of multiaxial testing becomes apparent when considering the need to evaluate the response of lamina and laminates to complex three-dimensional loads that result from service conditions. Multiaxial testing can help identify actual material strengths and failure mechanisms under properly proportioned loadings that simulate actual service conditions. Furthermore, multiaxial testing is recommended since the ability to predict the response of composites to multiaxial loadings has not been validated.

Currently, there is only limited experimental testing capability available to undertake all of the necessary work that is required to obtain a multidirectional material response data base. The testing procedures for thick composites are somewhat difficult to execute, have not yet been fully verified, and as such represent a major part of current and future research in themselves. However, the recently developed multiaxial testing techniques have been shown to be necessary in the determination of basic thick composite material parameters and actual material responses. These tests are also important in that the test results support the development of general and reliable three-dimensional numerical modeling, design, and analysis capabilities (i.e., finite element, boundary element, etc.) and failure theories for thick section composites in structural applications.

There are in current use two distinctively different multiaxial composite material testing techniques, associated mechanical testing load frames, and specimen fixturing arrangements. One method utilizes testing machines that apply loads/displacements along primary, mutually orthogonal coordinate axes to lineal test specimens. This broad class of machines consists of planar biaxial machines (Figure 10.2.3.2(a)), and true triaxial test frames (Figure 10.2.3.2(b)). The second method employs a class of machines that apply loads/displacements on tubular test specimens. The biaxial machines consist of a basic uniaxial - universal testing machine that has the additional capability to also apply a torque about the primary axis of the cylindrical specimen. The corresponding triaxial machine (Figure 10.2.3.2(c)) is similar to the biaxial test frame except that it has the added capacity to also apply either an internally or externally induced pressure differential across the wall of the cylindrical test specimen.



FIGURE 10.2.3.2(a) MTX biaxial tension/compression testing system.

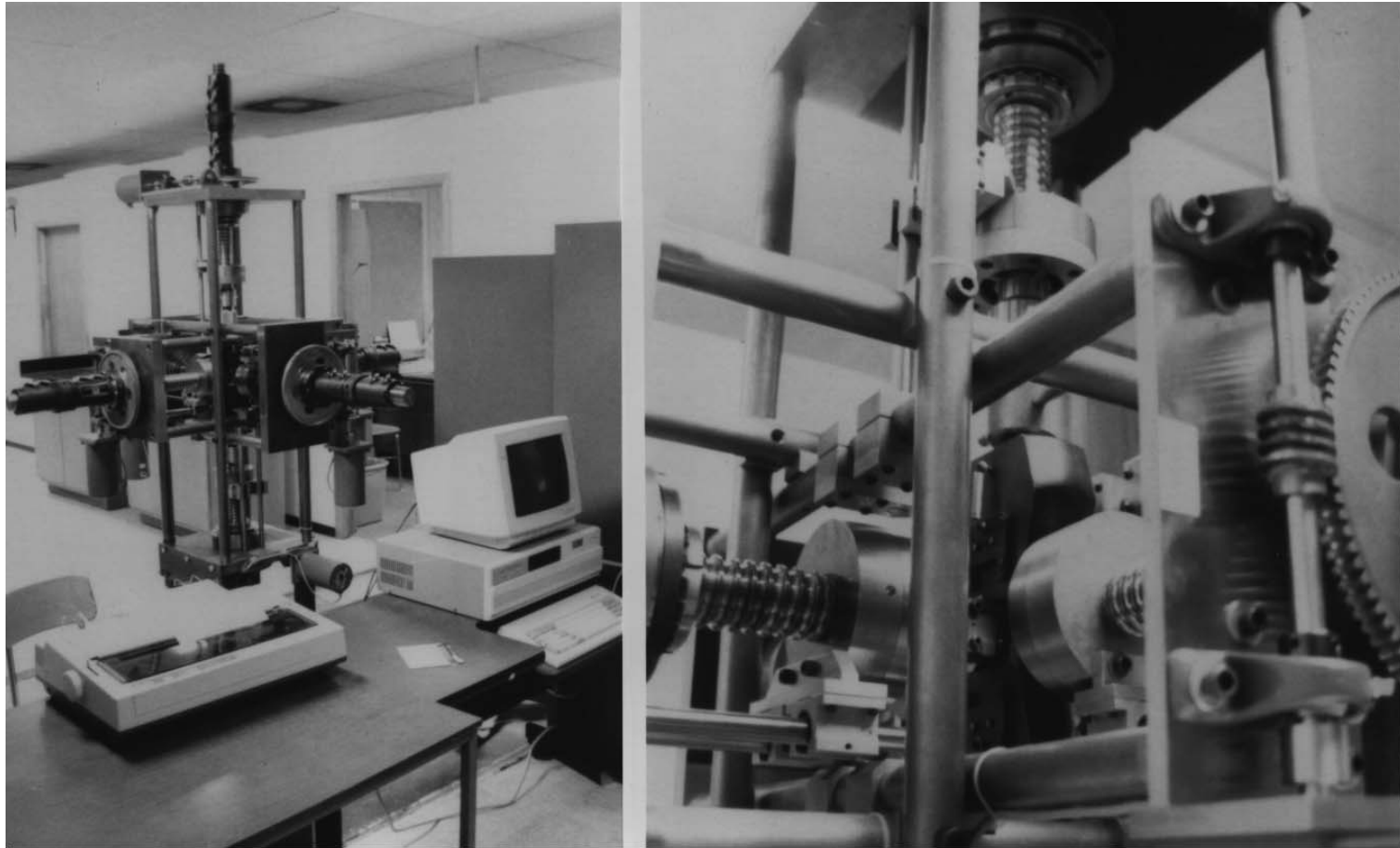


FIGURE 10.2.3.2(b) *Alliant Techsystems - University of Wyoming triaxial tension/compression testing system.*



FIGURE 10.2.3.2(c) *Three-dimensional axial/torsion pressure testing systems.*

10.2.3.2.1 Lineal test specimens/techniques

This material testing method utilizes the lineal test specimens, shown in Figure 10.2.3.2.1, such as cruciform or plate configured specimens for biaxial testing, and cubes or parallelopipeds for three-dimensional load applications.

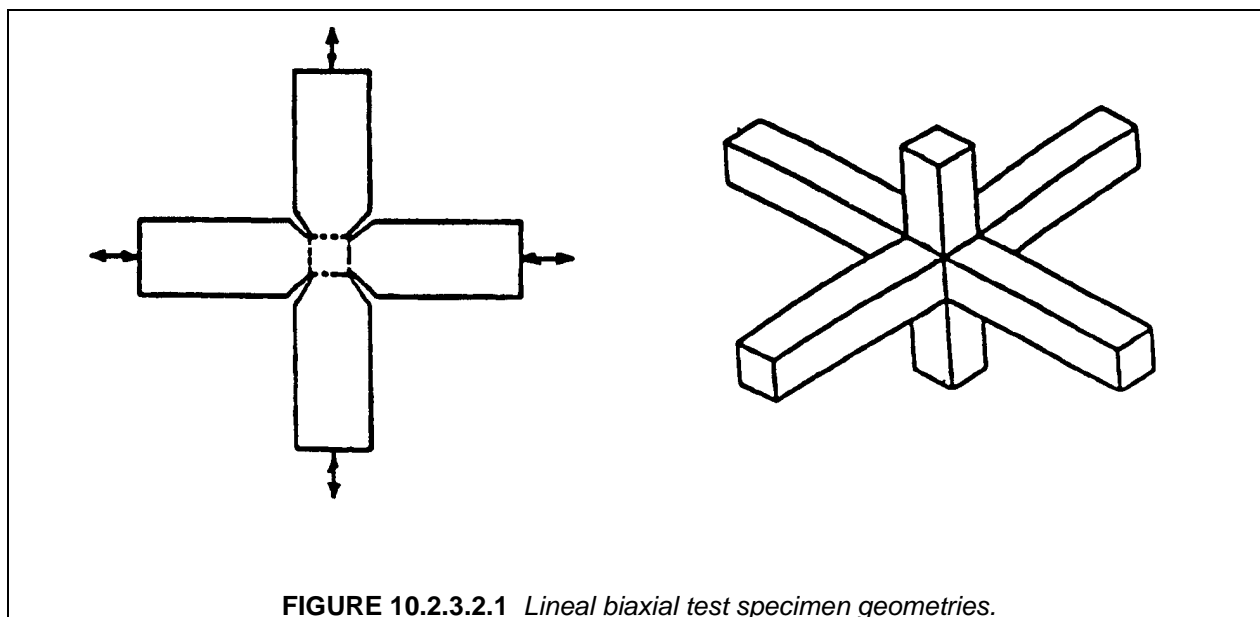


FIGURE 10.2.3.2.1 *Lineal biaxial test specimen geometries.*

Simultaneous, multiaxial tension/compression testing may be undertaken by applying loads along the principal, mutually orthogonal axes of the 2-D and 3-D specimens. Multiaxial testing is necessary for determining actual material strength/failure envelopes as well as for identifying failure mechanisms. This data is required in developing true multidirectional material constitutive equations and appropriate failure criteria.

There are available commercially fabricated, true biaxial machines for testing cruciform or plate configured material test specimens. These machines are typically of the servohydraulic-actuated type. There also exist special, non-commercially built, screw driven biaxial load frames. Both of these biaxial machine types are capable of simultaneously inducing tensile and/or compressive loads along two orthogonal axes. Thus, these load frames can be used to develop any general biaxial normal stress field within the test region of the material specimen. Special specimen fixturing, such as brush/comb flexible tabbing, has been developed and may be required to permit unrestricted in-plane movement and transverse constraints in order to minimize out-of-plane bending in biaxial tension/compression testing. This flexible specimen tabbing operates in a similar fashion as the brush/bearing platens typically used in compression testing of concrete.

True triaxial machines have also become available. These load frames have the capability of testing cubic anisotropic material specimens. These multidirectional, material testing machines may be either servo-hydraulically actuated or screw driven. Both of these types of three-dimensional machines may be used to apply any general combination of three-dimensional normal stress states to tabbed cubic test specimens. To the best of our knowledge, no comprehensive three-dimensional composite material testing has yet been undertaken with this equipment since special test specimen fixturing for these machines is currently under development and calibration of the load frames is in progress.

Both biaxial and triaxial machines require control systems that essentially maintain the test specimen centroid in a stationary position. This computer software - load frame control is a necessary feature in that

it is recommended that the specimen not be subjected to unwanted eccentric loading conditions. Lack of proper test frame displacement or load control may produce erroneous test measurements, inappropriate material failure mechanisms, as well as failures occurring outside the instrumented gage areas. In summary, the proper utilization of these one-, two-, and three-dimensional load frames requires special test specimen holding fixtures, well-designed specimen geometries, and effective tabbing and/or specimen end constraining methods. Extreme care has to be exercised in designing test specimens, fixtures, tabbing, and load application methods in order to avoid developing undesirable edge or end effects along with stress concentrations. The three-dimensional test method, described above, is often referred to as a true triaxial method since the cubical test specimen geometry permits complete freedom as to the fiber lay-up orientations in relation to the load application axes.

10.2.3.2.2 Cylindrical test specimens/techniques

To date, the most frequently used multiaxial, two- and three-dimensional, composite material testing method utilizes cylindrical test specimens shown in Figure 10.2.3.2.2. Predominantly, these test specimens are thin-walled tubes. There are well over a hundred commercially built biaxial machines which can apply an axial load (tension or compression) in conjunction with a torsional twisting loading about the longitudinal axis of cylindrical test specimens.

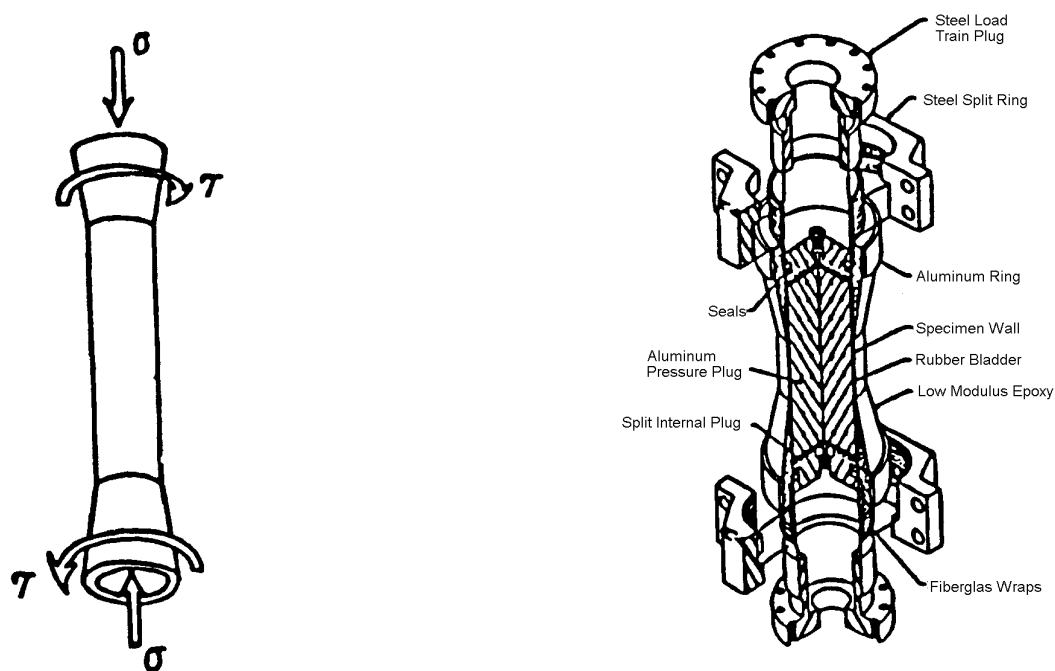


FIGURE 10.2.3.2.2 *Biaxial and triaxial thin tubular test specimen geometries, University of Utah triaxial specimen fixturing.*

The triaxial machines are similar to the 2-D test frames in their axial and torsional loads application utility. However, these load frames also have the additional capability of applying either an internal or external hydraulic pressurization across the wall thickness of hollow cylindrical specimens. By the very nature of hoop construction lay-ups of composite material cylinders, it would appear that this testing technique is very well suited for investigating material parameters and failure mechanisms of filament-wound test specimens. Typically, these cylindrical specimens do not exhibit edge effects in the gage section due to the geometric hoop continuity of cylindrical specimens. However, end effects such as brooming and

shearing may be a problem and require careful structural design and analyses of the connection detail and specimen configuration. The potential occurrence of structural instability such as buckling of the cylindrical test specimens, that are subjected to either an individual or a combination of axial, torsional, and pressurization loadings is a major consideration with this testing method. The development of any structural buckling of the test cylinders would mask material strength measurements. It should also be noted that this multiaxial testing technique has been used primarily for investigating only thin-walled tubular specimens.

10.2.4 Theoretical property determination

In considering the use of theoretical procedures to determine the mechanical properties of composite materials the most fundamental level that can be addressed is that of the individual constituents, or the micromechanics level. A theoretical development of composite micromechanics is summarized in Volume 3 Section 5.2.2.1 of this Handbook and in Section 4 of Reference 10.2.4. 3-D laminate properties can be determined from constituent data using micromechanical analyses and these references should be consulted for additional information and references on this topic.

Since properties at the lamina or laminate level are typically used for the analysis of a composite structure, only these properties will be discussed in this section and all analyses considered are linear elastic.

10.2.4.1 3-D lamina property determination

In Section 10.2, the nine independent elastic material properties required for a 3D lamina based analysis were listed as:

$$E_1, E_2, E_3, G_{12}, G_{13}, G_{23}, \nu_{12}, \nu_{13}, \nu_{23} \quad 10.2.4.1(a)$$

Of these properties E_1, E_2, G_{12} and ν_{12} can be readily generated by conventional experimental methods. Methods for determining out-of-plane properties are discussed in Section 10.2.3. In the absence of experimental data for these properties, the assumption of transverse isotropy in the 2-3 plane is often reasonable. The validity of this assumption has been demonstrated by the experimental data available in References 10.2.4.1(a) - (c). The assumption of transverse isotropy implies

$$E_3 = E_2, \quad G_{13} = G_{12}, \quad \nu_{13} = \nu_{12}, \quad \text{and} \quad G_{23} = \frac{E_2}{2(1 + \nu_{23})} \quad 10.2.4.1(b)$$

Even with this simplifying assumption ν_{23} must be measured or estimated for full knowledge of the nine independent elastic material properties.

Values for ν_{23} that have been experimentally determined have been reported in References 10.2.4.1(a) - (c). A value for ν_{23} determined in compression for T300/5208 is reported in Reference 10.2.4.1(a). A value for ν_{23} determined in tension and compression for T300/5208 is reported in Reference 10.2.4.1(b). Values for ν_{23} determined in compression for AS4/3501-6 and S2/3501-6 are reported in 10.2.4.1(c) and can be found in Table 10.2.4.1.

The need for all nine independent elastic constants does not imply that a 3-D analysis will be sensitive to the choice of the through-thickness material properties just discussed. For instance, a choice of ν_{23} of 0.50 versus 0.40 (a 20% difference) may only result in a 2% difference in the stress or strain results from a laminate or structural analysis. This sensitivity of a particular analysis to a particular material property should be evaluated through a parametric study if the value of the property is uncertain.

TABLE 10.2.4.1 3-D elastic constants for carbon and S2 glass reinforced epoxy (Reference 10.2.4.1(c)), E and G in Msi (GPa).

	AS4/3501-6 59.5% FVF	S2/3501-6 56.5% FVF
E_1 ¹	16.48 (113.6) (3.7) ²	7.15 (49.3) (4.0)
E_2 ¹	1.40 (9.65) (3.6)	2.13 (14.7) (2.2)
E_3 ¹	1.40 ³ (9.65)	2.13 ³ (14.7)
ν_{12} ¹	0.334 (3.0)	0.296 (4.1)
ν_{13} ¹	0.328 (1.2)	0.306 (2.8)
ν_{23} ¹	0.540 (1.6)	0.499 (1.4)
G_{12}	0.87 ⁴ (6.0)	0.98 ⁴ (6.8)
G_{13}	0.87 ⁵ (6.0)	0.98 ⁴ (6.8)
G_{23}	0.45 ⁶ (3.1)	0.71 ⁴ (4.9)

¹ E_1 , E_2 , ν_{12} , ν_{13} , and ν_{23} determined from thick, flat, compression test specimens
² coefficient of variation (%)

³ E_3 assumed equal to E_2

⁴ G_{12} determined from $[\pm 45]_{2s}$ tension test

⁵ G_{13} assumed equal to G_{12}

⁶ G_{23} from assumption of transverse isotropy

Likewise, the use of a linear analysis when certain material properties are extremely nonlinear (i.e., in-plane and through-thickness shear modulus) may not affect laminate or structural analysis and this too should be considered in 3-D analysis.

10.2.4.2 3-D laminate property determination

As for the case of a 3-D lamina properties, Section 10.2 lists the nine independent elastic material properties required for a 3-D laminate based analysis as:

$$E_x, E_y, E_z, G_{xy}, G_{xz}, G_{yz}, \nu_{xy}, \nu_{xz}, \nu_{yz} \quad 10.4.2.2(a)$$

E_x, E_y, G_{xy}, ν_y can be readily determined by conventional experimental or theoretical methods. Theoretically they can be determined using classical lamination theory as presented in Volume 3 Section 5.3.2 of this Handbook. The determination of the remaining out-of-plane laminate properties present a much greater challenge than for the in-plane properties. Little experimental data exists for out-of-plane laminate

properties and the test methodologies used to generate them can be described as very specific to the programs they have been used for, such as those in References 10.2.4.1(a) - (c).

A number of methods have been developed to theoretically predict the out-of-plane properties based on in-plane lamina properties (References 10.2.4.2(a) - (h)). These methods basically replace a layered inhomogeneous media of orthotropic layers with a homogeneous anisotropic media. This replacement is termed "smearing" and the resulting effective material properties are referred to as "smeared properties". These smeared anisotropic properties are commonly used in the analysis of composite structures. If average, global stress states or average displacements are sufficient for the analysis being conducted then an analysis with smeared properties is all that would be needed. If local stress states are needed then other analyses techniques must be employed such as a "global-local" technique. In this approach smeared anisotropic properties are used to determine global stress states, then this information is used to interrogate stress states in specific regions of concern on a ply-by-ply basis, therefore avoiding the costly use of a ply-by-ply analysis for an entire structure made of a thick-section composite material. The use of this global-local analysis technique is commonly referred to as the most rational way to approach the problem of design and analysis for thick composite materials.

The solution methods available to generate smeared anisotropic 3-D properties range from approximate formulations (Reference 10.2.4.2(a)) to exact formulations not including bending-extensional coupling (Reference 10.2.4.2(c)). The exact solutions by Pagano (Reference 10.2.4.2(c)) and Sun (Reference 10.2.4.2(b)) lend themselves to simple programming on personal computers. In fact Trethaway et al. (Reference 10.2.4.2(d)) and Peros (Reference 10.2.4.2(e)) have encoded the Pagano solution while Sun has encoded his own solution for a personal computer.

Tables 10.2.4.2(a) and (b) contain 3D laminate elastic constants for six laminate configurations and two materials as determined by laminate plate theory (LPT), and by the Pagano, Sun, and Roy solutions (Reference 10.2.4.2(g), (h)). Table 10.2.4.1 lists the lamina input properties used in each of the analyses. The three exact solutions (LPT, Pagano, Sun) yield identical results for both in-plane and through thickness properties for all of the cases presented. The results from the approximate solution by Roy differ from the others in the z-direction properties up to 12% in some cases.

Data verifying the results of these analyses are limited due to the difficulty in generating 3D experimental data. Data that does exist is documented in References 10.2.4.1(a) - (c), 10.2.4.2(h) and (i). Table 10.2.4.2(c) contains a comparison of theoretical predictions using the linear elastic theory by Pagano and experimental data from Reference 10.2.4.1(c) and Reference 10.2.4.2(i).

TABLE 10.2.4.2(a) 3-D effective properties of various AS4/3501-6 laminates, continued on next page.

Laminate Properties for AS4/3501-6, E and G in Msi												
	[0 ₂ /90] _s				[0/90] _{2s}				[0/90/±45] _s			
	LPT	Pagano	Sun	Roy	LPT	Pagano	Sun	Roy	LPT	Pagano	Sun	Roy
E _x	11.5	11.5	11.5	11.5	9.01	9.00	9.00	9.00	6.68	6.68	6.68	6.67
E _y	6.48	6.47	6.47	6.47	9.01	9.00	9.00	9.00	6.68	6.68	6.68	6.68
E _z	--	1.80	1.80	1.65	--	1.82	1.82	1.60	--	1.82	1.82	1.61
v _{xy}	0.073	0.073	0.074	0.072	0.052	0.052	0.053	0.052	0.297	0.297	0.298	0.296
v _{xz}	--	0.488	0.489	0.402	--	0.506	0.507	0.438	--	0.375	0.376	0.318
v _{yz}	--	0.519	0.520	0.465	--	0.506	0.508	0.427	--	0.375	0.376	0.317
G _{xy}	0.870	0.870	0.870	0.870	0.870	0.870	0.870	0.870	2.58	2.57	2.57	2.57
G _{xz}	--	0.664	0.664	0.780	--	0.593	0.593	0.612	--	0.593	0.593	0.627
G _{yz}	--	0.536	0.536	0.503	--	0.593	0.593	0.573	--	0.593	0.593	0.519

Laminate Properties for AS4/3501-6, E and G in Msi												
	[±30] _{2s}				[±45] _{2s}				[±60] _{2s}			
	LPT	Pagano	Sun	Roy	LPT	Pagano	Sun	Roy	LPT	Pagano	Sun	Roy
E _x	6.84	6.84	6.84	6.84	2.94	2.94	2.94	2.94	1.77	1.77	1.77	1.77
E _y	1.77	1.77	1.77	1.77	2.94	2.94	2.94	2.94	6.84	6.84	6.83	6.85
E _z	--	1.66	1.66	1.50	--	1.82	1.82	1.71	--	1.66	1.66	1.74
v _{xy}	1.14	1.41	1.41	1.13	0.691	0.691	0.691	0.689	0.295	0.295	0.295	0.294
v _{xz}	--	-0.095	-0.094	-0.197	--	0.165	0.165	0.211	--	0.390	0.390	0.434
v _{yz}	--	0.390	0.390	0.434	--	0.165	0.165	0.211	--	-0.095	-0.095	-0.197
G _{xy}	3.43	3.43	3.42	3.42	4.28	4.28	4.27	4.27	3.43	3.43	3.42	3.42
G _{xz}	--	0.705	0.705	0.708	--	0.593	0.593	0.596	--	0.512	0.512	0.515
G _{yz}	--	0.512	0.512	0.515	--	0.593	0.593	0.596	--	0.705	0.705	0.708

TABLE 10.2.4.2(a) 3-D effective properties of various AS4/3501-6 laminates, concluded.

Laminate Properties for AS4/3501-6, E and G in GPa												
	[0 ₂ /90] _s				[0/90] _{2s}				[0/90/±45] _s			
	LPT	Pagano	Sun	Roy	LPT	Pagano	Sun	Roy	LPT	Pagano	Sun	Roy
E _x	79.3	79.3	79.3	79.3	62.1	62.1	62.1	62.1	46.1	46.1	46.1	46.0
E _y	44.7	44.6	44.6	44.6	62.1	62.1	62.1	62.1	46.1	46.1	46.1	46.1
E _z	--	12.4	12.4	11.4	--	12.5	12.5	11.0	--	12.5	12.5	11.1
ν _{xy}	0.073	0.073	0.074	0.072	0.052	0.052	0.053	0.052	0.297	0.297	0.298	0.296
ν _{xz}	--	0.488	0.489	0.402	--	0.506	0.507	0.438	--	0.375	0.376	0.318
ν _{yz}	--	0.519	0.520	0.465	--	0.506	0.508	0.427	--	0.375	0.376	0.317
G _{xy}	6.00	6.00	6.00	6.00	6.00	6.00	6.00	6.00	17.8	17.7	17.7	17.7
G _{xz}	--	4.58	4.58	5.38	--	4.09	4.09	4.22	--	4.09	4.09	4.32
G _{yz}	--	3.70	3.70	3.47	--	4.09	4.09	3.95	--	4.09	4.09	3.58

Laminate Properties for AS4/3501-6, E and G in GPa												
	[±30] _{2s}				[±45] _{2s}				[±60] _{2s}			
	LPT	Pagano	Sun	Roy	LPT	Pagano	Sun	Roy	LPT	Pagano	Sun	Roy
E _x	47.2	47.2	47.2	47.2	20.3	20.3	20.3	20.3	12.2	12.2	12.2	12.2
E _y	12.2	12.2	12.2	12.2	20.3	20.3	20.3	20.3	47.2	47.2	47.1	47.2
E _z	--	11.4	11.4	10.3	--	12.5	12.5	11.8	--	11.4	11.4	12.0
ν _{xy}	1.14	1.41	1.41	1.13	0.691	0.691	0.691	0.689	0.295	0.295	0.295	0.294
ν _{xz}	--	-0.095	-0.094	-0.197	--	0.165	0.165	0.211	--	0.390	0.390	0.434
ν _{yz}	--	0.390	0.390	0.434	--	0.165	0.165	0.211	--	-0.095	-0.095	-0.197
G _{xy}	23.6	23.6	23.6	23.6	29.5	29.5	29.4	29.4	23.6	23.6	23.6	23.6
G _{xz}	--	4.86	4.86	4.88	--	4.09	4.09	4.11	--	3.53	3.53	3.55
G _{yz}	--	3.53	3.53	3.55	--	4.09	4.09	4.11	--	4.86	4.86	4.88

TABLE 10.2.4.2(b) 3-D effective properties of various S2/3501-6 laminates, continued on next page.

Laminate Properties for S2/3501-6, E and G in Msi												
	[0 ₂ /90] _s				[0/90] _{2s}				[0/90/±45] _s			
	LPT	Pagano	Sun	Roy	LPT	Pagano	Sun	Roy	LPT	Pagano	Sun	Roy
E _x	5.52	5.52	5.52	5.52	4.68	4.68	4.68	4.68	3.89	3.89	3.89	3.89
E _y	3.83	3.83	3.83	3.83	4.68	4.68	4.68	4.68	3.89	3.89	3.89	3.89
E _z	--	2.38	2.38	2.30	--	2.40	2.40	2.29	--	2.40	2.40	2.32
v _{xy}	0.166	0.166	0.166	0.165	0.136	0.136	0.136	0.135	0.281	0.281	0.281	0.280
v _{xz}	--	0.405	0.405	0.359	--	0.435	0.435	0.393	--	0.362	0.362	0.329
v _{yz}	--	0.459	0.459	0.427	--	0.435	0.435	0.392	--	0.362	0.362	0.329
G _{xy}	0.980	0.980	0.980	0.980	0.980	0.980	0.980	0.980	1.52	1.52	1.52	1.52
G _{xz}	--	0.870	0.870	0.918	--	0.823	0.823	0.830	--	0.823	0.823	0.838
G _{yz}	--	0.782	0.782	0.754	--	0.823	0.823	0.811	--	0.823	0.823	0.781

Laminate Properties for AS4/3501-6, E and G in Msi												
	[±30] _{2s}				[±45] _{2s}				[±60] _{2s}			
	LPT	Pagano	Sun	Roy	LPT	Pagano	Sun	Roy	LPT	Pagano	Sun	Roy
E _x	4.45	4.45	4.45	4.45	2.88	2.88	2.88	2.88	2.26	2.26	2.26	2.26
E _y	2.26	2.26	2.26	2.26	2.88	2.88	2.88	2.88	4.45	4.45	4.45	4.45
E _z	--	2.30	2.30	2.16	--	2.40	2.40	2.33	--	2.30	2.30	2.44
v _{xy}	0.546	0.546	0.546	0.545	0.468	0.468	0.468	0.467	0.278	0.278	0.278	0.277
v _{xz}	--	0.200	0.200	0.136	--	0.267	0.267	0.284	--	0.387	0.387	0.406
v _{yz}	--	0.387	0.387	0.406	--	0.267	0.267	0.284	--	0.200	0.200	0.136
G _{xy}	1.79	1.79	1.79	1.79	2.06	2.06	2.06	2.06	1.79	1.79	1.79	1.79
G _{xz}	--	0.895	0.895	0.895	--	0.823	0.823	0.823	--	0.762	0.762	0.763
G _{yz}	--	0.762	0.762	0.763	--	0.823	0.823	0.823	--	0.985	0.985	0.895

TABLE 10.2.4.2(b) 3-D effective properties of various S2/3501-6 laminates, concluded.

Laminate Properties for S2/3501-6, E and G in GPa												
	[0 ₂ /90] _s				[0/90] _{2s}				[0/90/±45] _s			
	LPT	Pagano	Sun	Roy	LPT	Pagano	Sun	Roy	LPT	Pagano	Sun	Roy
E _x	38.1	38.1	38.1	38.1	32.3	32.3	32.3	32.3	26.8	26.8	26.8	26.8
E _y	26.4	26.4	26.4	26.4	32.3	32.3	32.3	32.3	26.8	26.8	26.8	26.8
E _z	--	16.4	16.4	15.9	--	16.5	16.5	15.8	--	16.5	16.5	16.0
ν _{xy}	0.166	0.166	0.166	0.165	0.136	0.136	0.136	0.135	0.281	0.281	0.281	0.280
ν _{xz}	--	0.405	0.405	0.359	--	0.435	0.435	0.393	--	0.362	0.362	0.329
ν _{yz}	--	0.459	0.459	0.427	--	0.435	0.435	0.392	--	0.362	0.362	0.329
G _{xy}	6.76	6.76	6.76	6.76	6.76	6.76	6.76	6.76	10.5	10.5	10.5	10.5
G _{xz}	--	6.00	6.00	6.33	--	5.67	5.67	5.72	--	5.67	5.67	5.78
G _{yz}	--	5.39	5.39	5.20	--	5.67	5.67	5.59	--	5.67	5.67	5.04

Laminate Properties for AS4/3501-6, E and G in GPa												
	[±30] _{2s}				[±45] _{2s}				[±60] _{2s}			
	LPT	Pagano	Sun	Roy	LPT	Pagano	Sun	Roy	LPT	Pagano	Sun	Roy
E _x	30.7	30.7	30.7	30.7	19.9	19.9	19.9	19.9	15.6	15.6	15.6	15.6
E _y	15.6	15.6	15.6	15.6	19.9	19.9	19.9	19.9	30.7	30.7	30.7	30.7
E _z	--	15.9	15.9	14.9	--	16.5	16.5	16.1	--	15.9	15.9	16.8
ν _{xy}	0.546	0.546	0.546	0.545	0.468	0.468	0.468	0.467	0.278	0.278	0.278	0.277
ν _{xz}	--	0.200	0.200	0.136	--	0.267	0.267	0.284	--	0.387	0.387	0.406
ν _{yz}	--	0.387	0.387	0.406	--	0.267	0.267	0.284	--	0.200	0.200	0.136
G _{xy}	12.3	12.3	12.3	12.3	14.2	14.2	14.2	14.2	12.3	12.3	12.3	12.3
G _{xz}	--	6.17	6.17	6.17	--	5.67	5.67	5.67	--	5.25	5.25	5.26
G _{yz}	--	5.25	5.25	5.26	--	5.67	5.67	5.67	--	6.79	6.79	6.17

TABLE 10.2.4.2(c) Comparison of theoretical and experimental laminate results $[0_2/90]_{ns}$ from Reference 10.2.4.1(c), $[0_3/90]_{ns}$ from Reference 10.2.4.2(i), E and G in Msi (GPa).

	AS4/3501-6 $[0_2/90]_{ns}$		S2 glass/3501-6 $[0_2/90]_{ns}$		AS4/3501-6 $[0_3/90]_{ns}$	
	Theoretical	Experimental	Theoretical	Experimental	Theoretical	Experimental
E_x	11.53 (79.5)	11.63 ^A (80.2) [4.0] ^B [32]	5.52 (38.1)	5.82 (40.1) [6.9][32]	12.80 (88.3)	12.90 ^A (88.9)
E_y	6.47 (44.6)		3.83 (26.4)		5.27 (36.3)	5.66 ^A (39.0)
E_z	1.80 (12.4)		2.38 (16.4)		1.63 (11.2)	1.64 ^A (11.3)
ν_{xy}	0.073	0.069 ^A [6.7][7] ^C	0.166	0.166 [4.3][7]	0.090	0.120 ^A
ν_{xz}	0.488	0.469 ^A [3.0][14]	0.405	0.363 [2.7][14]	0.440	---
ν_{yz}	0.519		0.459		0.452	---
G_{xy}	0.87 (6.0)		0.98 (6.8)		0.87 (6.0)	0.70 ^D (4.8)
G_{xz}	0.73 (5.0)		0.78 (5.4)		0.72 (5.0)	0.53 ^D (3.7)
G_{yz}	0.63 (4.3)		0.64 (4.4)		0.54 (3.7)	0.66 ^D (4.6)

- ^A data from thick, flat, compression test specimens
^B coefficient of variation (%)
^C number of data points in average
^D data from Iosipescu shear test specimens

10.2.5 Test specimen design considerations

This section is reserved for future work.

10.3 STRUCTURAL ANALYSIS METHODS FOR THICK-SECTION COMPOSITES

This section is reserved for future work.

10.4 PHYSICAL PROPERTY ANALYSIS REQUIRED FOR THICK-SECTION COMPOSITE THREE-DIMENSIONAL ANALYSIS

This section is reserved for future work.

10.5 PROCESS ANALYSIS METHODS FOR THICK-SECTION COMPOSITES

This section is reserved for future work.

10.6 FAILURE CRITERIA

This section is reserved for future work.

10.7 FACTORS INFLUENCING THICK-SECTION ALLOWABLES (I.E., SAFETY MARGINS)

This section is reserved for future work.

10.8 THICK LAMINATE DEMONSTRATION PROBLEM

This section is reserved for future work.

REFERENCES

- 10.2.1 Jones, R.M., *Mechanics of Composite Materials*, 1975 Edition, Hemisphere Publishing Corporation.
- 10.2.2.2 Lekhnitskii, S.G., *Elasticity of an Anisotropic Body*, p. 30.
- 10.2.3.1(a) Camponeschi, E.T., Jr., *Compression Response of Thick-Section Composite Materials*, DTRC-SME-90/90, August 1990.
- 10.2.3.1(b) Abdallah, M.G., et al., *A New Test Method for External Hydrostatic Compressive Loading of Composites in Ring Specimens*, Fourth Annual Thick Composites in Compression Workshop, Knoxville, TN, June 27-28, 1990.
- 10.2.3.1(c) Bode, J.H., *A Uniaxial Compression Test Fixture for Testing Thick-Section Composites*, Fourth Annual Thick Composites in Compression Workshop, Knoxville, TN, June 27-28, 1990.
- 10.2.3.1(d) Goeke, E.C., "Comparison of Compression Test Methods for "Thick" Composites," *Composite Materials; Testing and Design (Eleventh Volume)*, ASTM STP 1206, ed. E.T. Camponeschi, American Society for Testing and Materials, 1993.
- 10.2.4. *Engineering Materials Handbook, Vol. 1, Composites*, ASM International, 1987.
- 10.2.4.1(a) Knight, M., "Three-Dimensional Elastic Moduli of Graphite/Epoxy Composites," *Journal of Composite Materials*, Vol. 16, 1982, pp. 153-159.
- 10.2.4.1(b) Sandorf, P.E., "Transverse Shear Stiffness of T300/5208 Graphite-Epoxy in Simple Bending," Lockheed-California Co. Report No. LR 29763, Burbank, CA, Nov. 30, 1981.
- 10.2.4.1(c) Camponeschi, E.T., Jr., "Compression Response of Thick-Section Composite Materials," David Taylor Research Center Report No. DTRC SME-90-60, Oct. 1990.
- 10.2.4.2(a) Christensen, R.M. and Zywickz, E., "A Three-Dimensional Constitutive Theory for Fiber Composite Laminated Media," *Journal of Applied Mechanics*, Jan. 1990.
- 10.2.4.2(b) Sun, C.T. and Li, S., "Three-Dimensional Effective Elastic Constants for Thick Laminates," *Journal of Composite Materials*, Vol. 22, No. 7, July, 1988.
- 10.2.4.2(c) Pagano, N.J., "Exact Moduli of Anisotropic Laminates," *Mechanics of Composite Materials*, ed. G. Sendeckyj, Academic Press, 1984, pp. 23-44.
- 10.2.4.2(d) Trethewey, B.R., Jr., Wilkins, D.J., and Gillespie, J.W., Jr., "Three-Dimensional Elastic Properties of Laminate Composites," CCM Report 89-04, University of Delaware Center for Composite Materials, 1989.
- 10.2.4.2(e) Peros, V., "Thick-Walled Composite Material Pressure Hulls: Three-Dimensional Laminate Analysis Considerations," University of Delaware Masters Thesis, Dec. 1987.
- 10.2.4.2(f) Herakovich, C.T., "Composite Laminates With Negative Through-The-Thickness Poisson's Ratios," *Journal of Composite Materials*, Vol. 18, Sept., 1984.
- 10.2.4.2(g) Roy, A.K. and Tsai, S.W., "Three-Dimensional Effective Moduli of Orthotropic and Symmetric Laminates," to appear in the *Journal of Applied Mechanics*, Trans. of ASME, 1991.

Volume 3, Chapter 10 Thick-Section Composites

- 10.2.4.2(h) Roy, A.K. and Kim, R.Y., "Effective Interlaminar Normal Stiffness and Strength of Orthotropic Laminates," Proceeding of the 45th Meeting of the Mechanical Failures Prevention Group, Vibration Institute, Willowbrook, IL, 1991, pp. 165-173.
- 10.2.4.2(i) Abdallah, M., Williams, T.O., and Muller, C.S., "Experimental Mechanics of Thick Laminates: Flat Laminate Mechanical Property Characterization," Hercules, Inc. IR&D Progress Report No. DDR 153253, Misc: 2/2-3249, June, 1990.

This page intentionally left blank

CHAPTER 11 ENVIRONMENTAL MANAGEMENT

11.1 INTRODUCTION

The objective of this chapter is to provide information for the environmental management of composite materials. Requirements for recycling of all classes of materials are increasing on a global basis and are not likely to be reduced. Many industries have found that taking a proactive approach to environmental management of their products can help to head off the enactment of complex regulations, which can be costly and less effective than market based solutions. Reuse and recycling of automobiles and components, for example, is performed by an efficient, nationwide network of used parts shops, automobile shredders, and resellers that extracts the maximum value out of recycled vehicles. This network is directed and motivated by interest in the value of the components and materials in end-of-use vehicles, rather than by an innate desire to comply with regulations.

The creation of a similar network for composite materials is an ongoing process at this time. It involves the development of size reduction and matrix digestion technologies, the organization of a collection system, identification of uses for recycled fibers and matrices, and perhaps most importantly, the education of the composites production and user community about recycling needs and opportunities.

Efforts to recycle composite materials are in an early stage of development compared with other aspects of composite's usage, and so much of the information in this chapter describes immature technologies. They are nevertheless included to provide an overview of the state-of-the-art and a resource for those interested in applying or developing composite reduction, reuse, and recycling technology.

11.1.1 Scope

The scope of this chapter is to provide guidance for the environmental management of composite materials as it pertains to the "reduce, reuse, and recycle" paradigm for controlling environmental impact. It does not address issues such as styrene emissions, handling of toxic materials, or disposal requirements for hazardous waste. Some aspects of composite manufacturing and use, such as lightweighting (defined later), prepreg usage, and the use of hybrid composites, are treated as they pertain to environmental management. These aspects will be discussed in this chapter only in the context of recycling, with other parts of the handbook referenced for broader discussions.

11.1.2 Glossary of recycling terms

Broad Categories -- General classifications of recyclable material, such as glass, plastic, metal, or paper.

Broker -- refers to an individual or group of individuals who act as an agent or intermediary between the sellers and buyers of recyclable materials.

Collector -- refers to public or private haulers that collect nonhazardous waste and recyclable materials from residential, commercial, institutional, and industrial sources.

Comingled recyclables -- refers to a mixture of several recyclable materials in one container.

Disposal Facilities -- refers to repositories for solid waste, including landfills and combustors, intended for permanent containment or destruction of waste materials.

Drop-Off Center -- refers to a method of collection whereby recyclable or compostable materials are taken by individuals to a collection site and placed in designated containers.

End-of-Service -- Components that have been used until failure or obsolescence.

Volume 3, Chapter 11 - Environmental Management

End User -- Facilities that purchase or secure recovered materials for the purpose of recycling. Examples include recycling plants and composting facilities. Excludes waste disposal facilities.

Exports -- Waste and recyclables that are transported outside the state or locality where they originated.

Generators -- Producers of solid waste.

Imports -- Solid waste and recyclables that have been transported to a state or locality for processing or final disposition, but that did not originate in that state or locality.

Incinerator -- A furnace for burning solid waste under controlled conditions.

Industrial Process Waste -- Residues produced during manufacturing operations.

Industrial Waste -- Nonhazardous wastes discarded at industrial sites from packaging and administrative sources. Examples include corrugated boxes, plastic film, wood pallets, and office paper. Excludes industrial process wastes from manufacturing operations.

Lightweighting -- Reduction of system weight by using lighter weight materials, careful design, avoidance of overdesign, and other engineering changes.

Large Generator -- Commercial businesses, institutions, or industries that generate sufficient quantities of solid waste and recyclables to warrant self-management of these materials.

Material Recovery Facility (MRF) -- A facility where recyclables are sorted into specific categories and processed or transported to processors for remanufacturing.

Mixed Plastic -- Recovered plastic that is not sorted into specific categories (HDPE, LDPE....)

Nonhazardous Industrial Process Waste -- Waste that is neither municipal solid waste nor considered a hazardous waste under Subtitle C of the Resource Recovery Act.

Other Plastic -- Plastic from appliances, furniture, trash bags, cups, eating utensils, sporting and recreational equipment, and other nonpackaging plastic products.

Other Solid Waste -- Nonhazardous solid wastes, other than municipal solid waste, covered under Subtitle D of the Resource Conservation and Recovery Act, such as municipal sludge, industrial nonhazardous waste, construction and demolition waste, agricultural waste, and mining waste.

Plastics Handler -- Companies that prepare recyclable plastics by sorting, baling, shredding, granulating, and/or storing plastics until a sufficient quantity is on hand.

Plastics Reclaimer -- Companies that further process plastics after the handling stage by performing at least one of the following functions: washing/cleaning, pelletizing, or producing a new product.

Postconsumer Materials/Waste -- Recovered materials that have been used as a consumer item and are diverted from municipal solid waste for the purpose of collection, recycling, and disposition. Excludes materials from industrial processes that have not reached the consumer, such as glass broken in the manufacturing process.

Preconsumer Materials/Waste -- Materials generated in manufacturing processes, such as manufacturing scrap and trimmings/cuttings. Also includes obsolete inventories.

Primary recycling -- Recycling clean materials and products to produce products that are similar to, or the same as, the original product.

Volume 3, Chapter 11 - Environmental Management

Processors -- Intermediate operators that handle recyclable materials from collectors and generators for the purpose of preparing materials for recycling (material recovery facilities, scrap metal yards, paper dealers....) Processors act as intermediaries between collectors and end users of recovered materials.

Quaternary Recycling -- Waste-to-energy conversion by incineration.

Recovery -- The diversion of materials from the solid waste stream for the purpose of recycling. Excludes reuse and source reduction activities.

Recyclables -- Materials recovered from the solid waste stream and transported to a processor or end user for recycling.

Recycling -- The series of activities by which discarded materials are collected, sorted, processed, and converted into raw materials and used in the production of new products. Excludes the use of these materials as a fuel substitute or for energy production.

Recycling Plant -- A facility where recovered materials are remanufactured into new products.

Residues -- The materials remaining after processing, incineration, composting, or recycling have been completed. Residues are usually disposed of in landfills.

Reuse -- The use, more than once, of a product or component of municipal solid waste in its original form.

Secondary recycling -- Recycling mixed materials or products to produce a product that is lower in quality than the original product.

Source Reduction -- The design, manufacture, purchase, or use of materials, such as products and packaging, to reduce the amount or toxicity of materials before they enter the solid waste management system. This may involve redesigning products or packaging; reusing products or packaging already manufactured; and lengthening the life of products to postpone disposal. Also referred to as "waste prevention."

Sortation -- The process of sorting comingled recyclables into separate types of materials for the purpose of recycling.

Tertiary Recycling -- Recycling that is accomplished by completely breaking down a material to its chemical constituents and restoring it to its original quality.

Transfer Station -- A facility where solid waste is transferred from collection vehicles to larger trucks or rail cars for longer distance transport.

Waste Characterization Studies -- The identification and measurement (by weight or volume) of specific categories of solid waste materials for the purpose of projecting landfill capacity, determining best management practices, and developing cost-effective recycling programs.

Waste Generation -- The amount (weight or volume) of materials and products that enter the waste stream before recycling, composting, landfilling, or combustion takes place.

Waste Stream -- The total flow of solid waste from homes, businesses, institutions, and manufacturing plants that must be recycled, incinerated, or disposed of in landfills; or any segment thereof, such as the "residential waste stream" or the "recyclable waste stream."

Waste-To-Energy Facility/Combustor -- A facility where recovered municipal solid waste is converted into a usable form of energy, usually through combustion.

11.2 RECYCLING INFRASTRUCTURE

The development of a viable infrastructure for recycling composite materials should ideally be pursued as a coordinated effort by composite suppliers, fabricators, and end users. Such an infrastructure will benefit the entire composites industry by improving the efficiency of composite manufacturing, changing the perception that composites are not recyclable and that metals are therefore preferable, and reducing the environmental impact of composites use. This section outlines some of the requirements for recycling infrastructure development.

11.2.1 Recycling infrastructure development models

The infrastructures for recycling many other materials have already been developed and can provide guidance for the establishment methods for composite materials recycling. Studying these examples can facilitate composites recycling development work and avoid costly mistakes that have been encountered in other industries.

One important lesson learned is that while the technology for actually recycling a material is important, the logistical, educational, and economic issues are equally important. Advanced recycling technologies cannot succeed unless they are integrated with consistent sources of consistent recycle sources, stable markets for the recycled materials, an efficient collection and transportation system, and a work force that has been educated in the requirements for proper handling of recyclable materials.

One of the most mature and efficient reuse/recycling infrastructures is in place for automobiles. A large, computer-integrated network of automobile recyclers procures end-of-service automobiles, removes fluids and toxic components such as batteries, catalogues reusable components, and either dismantles the vehicle or warehouses its parts in the vehicle. After all reusable components are removed, vehicles are shredded, ferrous metals are magnetically sorted, and lightweight "fluff" and other materials are separated. The result is that approximately 90% of the steel in automobiles is recycled, more than 12 million tons per year. Automotive manufacturers are increasingly paying attention to design for disassembly and recycling, and are giving consideration to the recyclability of the materials in their products.

A user-subsidized recycling model that may be instructive is that developed for nickel cadmium (NiCd) batteries in response to concerns about groundwater contamination from the cadmium content. Because of the widely dispersed nature of old NiCd batteries, a network of used battery collection centers was created by placing pre-paid, pre-addressed mailers at electronics retail outlets. When the mailers are filled with batteries, they are given to the parcel delivery service and transported to a single recycling facility for the entire North American continent. The recycler distills out the cadmium and processes the nickel content in an open hearth furnace along with other stainless steel waste. The high nickel content increases the value of the stainless steel recycle and helps to pay for the process.

In contrast, the vast majority of end-of-service composite materials and composite waste generated in manufacturing, are commonly thrown into landfills (References 11.2.1(a) - (b)). Although this adds only a small volume to the solid waste disposal problem, it returns no value. As regulations that mandate recycling of various products take effect, particularly in Europe, non-recyclable materials will be increasingly excluded from consideration. The desirable environmental influence that advanced composites can have, such as greater fuel efficiency from lightweighting, will be lost if recycling techniques are not implemented.

11.2.2 Infrastructure needs

Although technologies exist for digestion of composite matrices and recovery of fibers with high strength retention (References 11.2.1(b) and 11.2.2(a) - (d)), these technologies have only been demonstrated on laboratory prototype or pilot scale. Additional efforts to optimize and scale up these processes to complete implementation are underway.

A resource recovery network must be established, or "piggybacked" onto existing networks, to collect and channel post-consumer composites back to these material recovery facilities (MRFs). Because of the

relatively low volume of advanced composites in service, the most efficient transportation system may include a network of material transfer stations, which collect recyclables for consolidation into large shipments. A single transfer station may receive shipments of process waste and post-consumer composites from a state, or metropolitan area, and reship many small loads in a single truck or rail car load. Throughout this consolidation process, different types of composites must remain separate for the value of the recyclables to be maintained. It is almost always easier for materials to be kept separate in the first place than to go through sortation after the fact.

11.2.3 Recycling education

Although methods for reducing, reusing, and recycling thermoset matrix composites exist today, and services are available for exchanging unused fibers, prepreg, and other precursors, lack of awareness limits their application. Producers and users should familiarize themselves with opportunities for recycling as a first step in making it a routine part of their ways of doing business. An interest in recycling that is generated in both a top-down and bottom-up fashion can be the most effective in establishing programs, since programs that are mandated by management are likely to fail if not implemented on the shop floor, while individual efforts will not succeed without management support. Information from this chapter and its references can be used as a starting point for this education process.

11.3 ECONOMICS OF COMPOSITE RECYCLING

A complete discussion of the economics of recycling composite materials would need to address, in detail, numerous issues that are specific to the particular type of composite. Such a discussion is beyond the scope of this section. Some general considerations of composite recycling economics are helpful in designing and evaluating recycling programs and are discussed in this section.

The costs of recycling principally arise from collection, transportation, and processing. These costs should ideally be offset by the value of the products derived from the recycled material. There are also costs associated with disposing of waste, called "tipping fees," particularly if the material is a hazardous waste, as is the case for uncured resins. The reduction or elimination of disposal costs should be considered when evaluating the cost of a recycling operation.

In addition, there are significant costs associated with complying with existing environmental regulations and those that may be enacted if an industry fails to take action on its own initiative. Some recycling efforts have been initiated by industries to head off legislation that would place a greater burden on them, and result in a less efficient recycling structure. There are significant public relations benefits from making good faith efforts to recycle and strong negative effects when these efforts are not made. Large-scale implementation of composite materials in the infrastructure, transportation, offshore oil, and other industries will eventually require the further development of composite recycling programs.

Several considerations are involved in identifying the most favorable economics for recycling a material. Minimization of collection and transportation costs is a vital requirement for efficient recycling. For fiberglass materials, for instance, which are heavy, and which do not yield high value recycle, these costs could be prohibitive. For this reason it is most effective to situate recycling facilities close to the source of material.

Derivation of high value materials is another important requirement. Although carbon fiber composites can be completely incinerated for energy, in an open-hearth furnace, for example, their value would be reduced to that of the energy content. Some of the current technologies for fiberglass recycling grind the composite into a fine powder that is used as filler in new composite. This fill must compete with extremely inexpensive calcium carbonate fillers, and is therefore of low value. The primary benefits of these technologies are that the waste does not become a landfill, or disposal problem, and that the recycle fill is less dense than mineral fill, resulting in a lighter weight composite.

Technologies that recover fibers in usable condition can achieve higher value for the recyclate, and can pay for the entire recycling process. Technologies that recover glass fibers have this advantage compared to grinding, but the fiber extraction process must still be very inexpensive to justify on an economic basis, due to the low cost of glass fiber. The greater cost of carbon fibers can, therefore, be an advantage for recycling of this class of material. If carbon fibers can be extracted from the matrix in sufficiently good condition to compete with low-end fibers in the \$5/pound range, a substantial value can be obtained and the recycling process can be feasible on an economic basis.

Composite materials will always have to compete with monolithic metals, which can, in most cases, be recycled back to virtually their original quality, a process known as tertiary recycling. Finding high value secondary uses for composite recyclate is a necessary factor for successful competition.

Cyclical markets for recycled materials have been a problem for most types of materials (References 11.3(a) - (b)). Expensive plants have been built and commitments made when the value of recycled materials is high, and then market changes have left companies with unused capability or mandates to purchase materials at costs far greater than their value. The primary source of these market fluctuations has been a kind of teething pain, in which, at first, a great deal of material is recycled, but no buyers are available for a product that did not previously exist, and then when a market is created, demand exceeds supply. Paper and plastic materials have been particularly prone to these fluctuations.

These cyclical changes can leave manufacturers dependent on a flow of recycled material that cannot be reliably, or economically, procured. Robust manufacturing processes that can exploit recycled materials when possible, but can substitute virgin material when necessary, can alleviate these problems.

11.4 COMPOSITE WASTE STREAMS

The advanced composites industry was surveyed in 1991 (Reference 11.2.1(a)) and 1995 (Reference 11.2.1(b)) to determine the type, quantity, and current disposal methods of composite waste. As shown in Figure 11.4(a), for waste generated at the manufacturing source, 66% was in the form of unused prepreg material. Approximately 18% was in the form of cured parts, 14% was trimmings, and one or two percent was comprised of finished parts and bonded honeycomb. Pre-consumer advanced composite waste, therefore, consists of approximately two-thirds prepreg scrap and one-third trimmings and cured parts.

Because of the long service life of many military and civilian platforms containing advanced composite materials, it is difficult to predict when the composite components contained within those platforms will enter the composite waste stream at the end-of-service-life. A study (Reference 11.2.1(b)) of the composites contained within many military vehicles shows the kind, and in some cases, the quantity of various types of composite materials that will require recycling or disposal at some point in time. The composites in military vehicles are largely comprised of carbon fiber/epoxy, aramid fiber/epoxy, and carbon/carbon composites as shown in Figure 11.4(b).

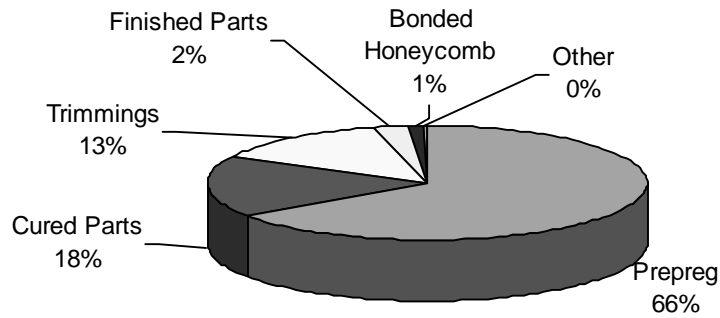
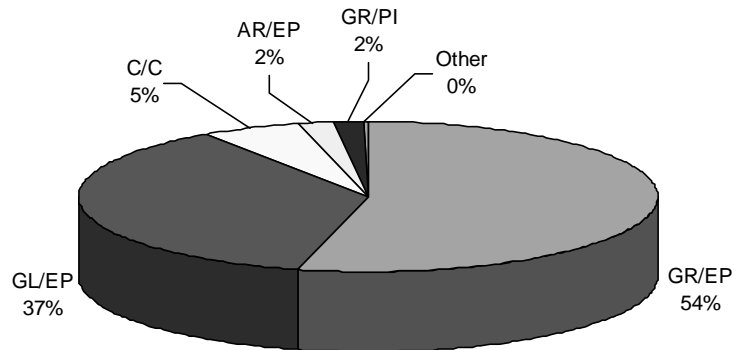


FIGURE 11.4(a) *The reported distribution of advanced composite manufacturing waste by type of material.*



GL/EP	-- Glass/Epoxy	AR/EP	-- Aramid/Epoxy
GR/EP	-- Graphite/Epoxy	GR/PI	-- Graphite/Polyimide
C/C	-- Carbon/C		

FIGURE 11.4(b) *The distribution of advanced composite materials in 1995 by matrix and fiber.*

11.4.1 Process waste

Because of the nature of most current advanced composite manufacturing processes, process wastes comprise a significant fraction of the overall composite waste stream. They are also the portion of the waste stream that must be disposed during production, rather than at the end of service, and so present immediate handling issues.

Prepreg comprises the largest fraction of process waste, as shown in Figure 11.4(a), and is, therefore, the most important target of source reduction and recycling efforts. Unused fibers, curing agents, and resins also contribute to process waste. After minimization by careful inventory control strategies (Section 11.5), these materials can often be reallocated or exchanged (Section 11.7.2).

11.4.2 Post consumer composite waste

Perhaps the greatest challenge for recycling of composite materials is finding a viable approach to collecting, sorting, processing and reusing post consumer composite wastes. Materials that have gone into service are likely to be dispersed geographically, may have picked up contaminants, require disassembly, and may contain fiber and matrix types that are not documented. The date of retirement from service for composite components may be decades after their production, making the logistics of planning for recyclability difficult, and of low priority. Nevertheless, addressing the issue of post-consumer composite recycling is essential if composite materials are to compete in systems that mandate recycling.

The quantities of composite materials that are produced can be derived from fiber manufacturer's data. Another tracking method is to document the quantities and types of composites used in various vehicles and other applications, and then to monitor the procurement levels for those vehicles. A pie chart of the percentage distributions of actual usage of various types of advanced composite materials for 1995 is shown in Figure 11.4(b) (Reference 11.2.1(b)).

The greatest uncertainty in assessing the post consumer composite waste stream is in the dates of retirement of the systems containing the composite components, or, otherwise, the dates of failure or destruction of the composite components. Because many military and civilian craft remain in service for decades, while others are rapidly rendered obsolete, the extent and timing of the advanced composite waste stream is difficult to predict.

More reliable predictions can be made about the sheet molding compound and other composites used in automotive applications, since the life cycle of automobiles is less variable. Polymers and polymer composites currently comprise about 20% of the total weight of new automobiles and are steadily increasing. In contrast to the recyclability of the bulk of automobile constituents, these materials currently contribute to the generation of automotive shredder residue (ASR), a mixture of plastic, rubber, glass, and inorganic materials which is commonly landfilled. Efforts to develop recycling techniques for ASR are underway but are beyond the scope of this discussion. Recycling technologies for sheet molding compound are discussed in Sections 11.8.3.2 and 11.8.3.5.

11.5 COMPOSITE WASTE STREAM SOURCE REDUCTION

Reduction of the volume of waste materials is the best approach to environmental impact mitigation. Waste that is not created in the first place does not need to be paid for, recycled, or disposed. Efforts to reduce the production of waste materials should, therefore, be given the highest priority. Waste source reduction yields direct benefits in both decreased procurement costs and decreased recycling or disposal costs. Efforts should, therefore, be made to identify the sources of waste material and reduce or eliminate them. Approaches to the reduction of composite precursor waste are described below.

11.5.1 Just-in-time and just enough material delivery

Just-in-time inventory control systems have made a major impact on the production plans of manufacturers in recent years. The benefits of having materials arrive shortly before use, include reduced inventory and storage requirements, and more efficient production flow. For composites that are produced from prepreg with a limited shelf life and that require refrigeration, even greater benefits can be derived. Great care should, therefore, be taken to ensure that tight control is maintained over inventories of prepreg, resins, and any other material with limited shelf life.

Prepreg inventory can be effectively tracked by logging shipments of prepreg as they are received into a computer database and affixing a bar coded label before storage. The information in the database can be compared with production requirements to plan and time future procurements. The database system can also be set to flag materials that are in danger of reaching their expiration dates so that processing can be scheduled to avoid waste. In some cases, prepreg that has reached its expiration date can still be used if testing is performed to ensure that the quality of the components is not impaired. Prepreg that no longer meets the stringent requirements for primary structures can sometimes be reassigned to less demanding applications, or resold for use in non-critical structures. See Section 11.7 for information on materials exchange.

Procurement of excess quantities of material is also a significant source of waste. If arrangements can be made with the material supplier, obtaining the correct amount, with minimal excess, is an efficient means of reducing the generation of wastes.

11.5.2 Electronic commerce acquisition management

Electronic commerce is the process of specifying and procuring materials and components by digitally transmitting the required information, usually over the Internet. Composite precursor acquisition by electronic commerce can reduce inventory requirements and shipping lead-time. It can also interface directly with management of inventories to minimize waste.

11.5.3 Waste minimization guidelines

Guidelines for implementing procedures that minimize the production of composite and precursor waste are provided in this section.

11.5.3.1 Prepreg

Efficient use of prepreg is one of the most effective methods of waste minimization. Prepreg cutting waste typically amounts to 25-50% of the material. This waste adds to both procurement and disposal costs. Efforts to develop recycling methods for prepreg have been made (References 11.2.1(a) - (b), 11.5.3.1(a) - (c)), but most are not fully ready for implementation. Particular emphasis should, therefore, be given to efforts to optimize the nesting of patterns for cutting shapes out of prepreg materials. Computer programs are available to facilitate this task.

11.5.3.2 Resin

Uncured resin waste is classified as a hazardous waste material in the U.S., and must be handled and disposed of accordingly. Curing of resin for the purposes of disposal is considered to be processing of hazardous waste, which requires special permitting, even though the same shop cures resin on a routine basis for the purpose of composite production. Unless, and until, these requirements are eased or modified, it is doubly important to minimize the creation of waste resin. Careful planning of procurement and just-enough procurement of resins are tools for this minimization.

11.5.3.3 Fiber

This section is reserved for future use.

11.5.3.4 Curing agents

This section is reserved for future use.

11.5.3.5 Autoclaving materials

This section is reserved for future use.

11.5.3.6 *Packaging materials*

This section is reserved for future use.

11.5.4 **Lightweighting**

Reduction of the weight of composite components by careful design improves environmental management by reducing the amount of material consumed, and that must ultimately be recycled or landfilled. Although the primary motives for lightweighting are to improve structural efficiency, these additional benefits occur at no additional cost. Lightweighting of composite components should, therefore, be considered to be a part of any environmental management plan.

Overdesign of composite components commonly occurs because of uncertainties about the failure criteria, material properties, and behavior under complex in-service loading conditions. This overdesign reduces the performance benefits of composites in comparison with monolithic materials. As improved composite design capabilities are developed by ongoing efforts in this area, implementation of those capabilities will help to reduce waste generation.

11.6 **REUSE OF COMPOSITE COMPONENTS AND MATERIALS**

After reduction of waste generation, the next best approach to environmental management involves the reuse of systems, components, and constituents. The greatest value for a complete component can best be realized by reusing it in the same, or, possibly, in some similar application. This section provides information and ideas for reuse of composite components.

11.6.1 **Reuse of composite components**

By far the greatest part of the value derived from recycled automobiles comes from the reuse of serviceable or remanufacturable components that are removed and resold by a large network of automobile parts distributors. Used automobile parts are inventoried and shipped to buyers through a sophisticated, satellite-linked database network that exchanges information between buyers and sellers. Similar systems for reallocating composite components that are removed from damaged or decommissioned vehicles could avoid disposal costs and return the maximum value for the material.

11.6.2 **Machining to smaller components**

End-of-service or otherwise surplus composite components can sometimes be reconfigured for another application by machining. In this manner, sailboat spars have been produced from aircraft components, for instance. Because such reuse usually returns a greater value than recycling, consideration should be given to reconfiguration, or sale to a company that performs that function, before sending material to be recycled. The greatest difficulty in machining components to smaller sizes arises from finding matches in material and geometric requirements. Applications that allow some flexibility for the geometry are advantageous for this reason.

11.7 **MATERIALS EXCHANGE**

Materials exchange is a method of reducing waste and lowering acquisition costs by reallocating or reselling unused materials. This can be done either within an organization, or between organizations, often with the assistance of a broker. This section describes guidelines and techniques for exchange of composite precursors.

11.7.1 Reallocation of precursors

Excess precursor material that is maintained in properly documented, good condition can often be reallocated within a company. If some degradation has occurred, or if the material has passed its expiration date, sometimes applications that allow lower standards can be found. Although it is not a substitute for tight inventory control, the most common disposal method for uncured waste prepreg, other than land-filling, is fabrication into flat panels (Reference 11.2.1(b)).

11.7.2 Composite materials exchange services

Materials exchange services either buy surplus materials and resell them, or list materials that are available for sale and charge a fee for placing buyers and sellers in contact. A wide range of materials can be resold in this manner. Materials exchange services that specialize in exchange of composite precursors are available to assist in locating sources or users of composite precursors. These companies should be contacted for detailed, specific information about the requirements and opportunities for exchanging particular fibers, prepregs, and other precursors.

11.7.2.1 Care of unused materials

Unused materials must be maintained with the same care given to new material if they are to be resold to other manufacturers so that the components they are incorporated in will meet specifications. Thermoset prepreg material that requires refrigerated storage should be kept refrigerated so that its remaining shelf life will be well defined. Failure to refrigerate, or leaving the material at room temperature for unknown periods, is a common handling error that results in partial curing, lack of drape and tack quality, and material that is worthless for reuse. If such material is used in components because its condition was not known, serious safety hazards could result. Similar, appropriate care should be given to fibers, resins, and curing agents.

11.7.2.2 Packaging

Unused precursors should be returned to the original packaging and sealed to exclude moisture, air, and other contaminants. If the original packing materials are inappropriate, or too large to store the reduced volume of precursor, other packaging that will match the original protection quality should be used. Packages that are left unsealed can cause a significant degradation of material properties.

11.7.2.3 Documentation of care

Material property, constituents, care, etc. must be documented for the materials to be used for critical applications. This section describes some of the types of requirements for composite and precursor materials exchange. If proper care is taken of surplus precursors, but that care is not properly documented, the quality of the material cannot be guaranteed and it cannot be used with confidence. For thermoset prepreg materials, for instance, a tracking log should be maintained that records the duration of exposures to atmosphere and to non-refrigerated temperatures. This log should accompany the material when it is shipped to the materials exchange service or to other users.

11.7.2.4 Description of unused materials

A complete description of the nature of the unused materials should be transmitted together with them. The type of fiber(s), matrix, and any other information should be copied from the original procurement so that the exchange service or other users will be informed about the composition.

11.7.2.5 DOD resale restrictions

In many cases the DOD places restrictions on the disposal of unused materials from DOD-supported projects. Intended to prevent corruption, these restrictions can prevent the resale or transfer of unused

materials until they have negligible residual value. Organizations attempting to exchange composite precursors should be aware of any conflicting legal and contractual stipulations.

11.8 RECYCLING OF COMPOSITE MATERIALS

If reuse or reconfiguration of composite components or materials is not possible, recycling provides the next highest value returned from the recyclable composite or precursor. This section provides guidelines to facilitate recycling and designing in recyclability.

11.8.1 Design for disassembly and recycling

Design for disassembly and recycling can greatly facilitate the recycling process for end-of-service-life components and systems. Component designers are already constrained by numerous requirements such as weight, envelope, strength, and toughness, so including the additional factors of recyclability may be difficult to implement in some cases. If design is performed while keeping in mind factors that either enhance or hinder disassembly and recycling, then better choices can be made at various decision points in the design process.

11.8.1.1 Fasteners

The choice of fastener can have a major impact on the ease of disassembly and recycling. Where possible, metal fastener inserts should be avoided, as they are difficult to remove during processing and present a source of contamination. Currently, adequate substitutes for metal fasteners do not exist for many applications. Research to develop such fasteners is required. These inserts should, ideally, be made from the same material as the rest of the composite component or at least material that is compatible with the matrix digestion process.

11.8.1.2 Adhesives

Whenever possible, adhesives for thermoplastic matrices should be selected that are compatible with the resins they are bonding after the melting and mixing operations involved in recycling. Many adhesives for thermoplastics are not compatible and would seriously degrade the properties of the recycled plastic or composite.

Compatibilizers have been developed that can allow some otherwise incompatible combinations of thermoplastics to be recycled in mixed form. It may be feasible to develop systems of adhesives, matrices, and compatibilizers that would expand the available range of recyclable adhesives and their properties.

Various welding processes are available as alternative bonding techniques that do not introduce foreign material and so produce bonds that are inherently recyclable.

11.8.1.3 Hybrid composites

Composite materials that use more than one type of fiber, such as aramid/carbon fiber structures, are far more difficult to shred and recycle than composites made with a single fiber type. After shredding and matrix digestion, the mix of fibers that results is difficult to reuse and so of much lower value than a single type of fiber would be. The use of hybrid composites should be avoided unless it is necessary to yield significant design advantages.

11.8.2 Recycling logistics

The logistics of recycling are of great importance for ensuring both the economic viability and quality of the properties of recycled materials that are produced. If the logistics of the recycle collections sys-

tem are inefficient or place an undue burden on those performing the collection, the process will probably fail.

11.8.2.1 Collection and transportation

Efficient collection of materials for recycling is an essential component of any economically successful recycling program.

Collection and recycling of pre-consumer waste, that is, seconds, overruns, and other scrap generated in-plant has a major recycling advantage because of the relative ease of collection, sorting, and quality control. Components that cannot be used because they do not meet specifications have the recycling advantages of containing a known matrix, a known fiber, and a known processing history. They are also available with minimal to no shipping costs. The case for in-plant recycling can be made to the manufacturer of composite materials that they have paid for the material in rejects and other waste, and should, therefore, seek uses for that material, rather than paying again for its disposal.

Shredded or ground reject components makes a particularly attractive filler or core material because it is made from an identical matrix and fibers as the rest of the components (References 11.8.2.1(a) - (c)). For the fiberglass boat industry, for instance, manufacturers collect the hatches and other cut outs, shred it, and use it as a replacement for wood core material.

11.8.2.2 Identification of fibers and matrices

Recycling of polymers is greatly facilitated by keeping the polymer waste streams separate. Mixed plastics usually have no value as structural materials because incompatibility of different polymers results in negligible mechanical strength. Keeping waste streams separate is generally easier than separating mixed waste streams.

Similar considerations apply in many cases to recycling of composites. If the waste stream has become mixed, containing vinyl ester/fiberglass and carbon fiber/epoxy, for instance, the process conditions required for shredding and digesting the different matrices will be less efficient, and the value of the reclaimed fibers will be greatly reduced by admixture. Although some types of fibers can be readily, visually distinguished, different types of carbon fibers are not distinguishable without elaborate and costly tests. It is strongly advised that the composite waste streams be kept separate throughout the collection, storage, and recycling processes.

11.8.2.2.1 Fourier transform infrared spectroscopy

Fourier transform infrared spectroscopy (FTIR) has been used as an identification tool for polymers sortation systems. The reflected infrared spectra of polymer containers, for instance, are acquired and correlated with stored spectra for the different classes of polymers that are recycled. The best match is found and each container is routed to the appropriate storage bin. Similar techniques could be applied to composite materials to identify their matrix material. Surface coatings such as paint or radar absorbing materials make FTIR more difficult. These surfaces must be removed before testing.

11.8.2.2.2 Densitometry

Density differences can be utilized as a simple, efficient means for segregating certain types of polymers and composite materials. For polymer separation, for instance, passage along a simple water trough can be used to separate polyethylene from other plastics. Similar processes with the fluid density increased by addition of a salt may be applicable to efficient sortation of polymer composites with different fiber and matrix densities.

11.8.2.2.3 *Coding of components*

Sortation of common plastics is facilitated by a coding system in which classifications are embossed on polymer containers. The system is comprised of seven classifications of polymer, such as polyethylene, polypropylene, PVC, and so forth. After consumer use, containers may be sorted by simply reading these numbers. Implementation of a similar classification system in which composites consisting of compatible fibers and matrices are placed in defined categories may be a useful approach to facilitating the eventual recycling of post-consumer composite products.

11.8.2.2.4 *Routing of waste streams*

This section is reserved for future use.

11.8.3 **Processing of composite recyclate**

This section describes some of the processes that have been developed for recycling of cured composite materials. Techniques for recycling or using waste prepreg materials are discussed in Section 11.7.4.

11.8.3.1 *Size reduction*

Components that are to be recycled, rather than reused, must usually be subjected to size reduction by shredding or grinding as a first process step. Steel knife shredders are commercially available that can rapidly and efficiently cut most composite materials into small pieces that are more convenient for shipping, storage, and subsequent processing. Sheet molding compound is often further reduced in size by grinding to form a filler powder. This powder is substituted for mineral fillers to produce new sheet molding compound with properties that meet the full specification requirements. The low cost of mineral filler, however, means that composite recycled in this manner is of very low value. Achieving higher value in the recyclate requires that the fibers be left with sufficient fiber length/diameter ratio to provide significant reinforcement.

After size reduction, recycled composite can be directly incorporated into new material to replace plywood, foams, or honeycomb cores. New composite can also be made by using shredded composite chips with new matrix material to produce a chipboard-like material.

11.8.3.2 *Matrix removal*

To recover fibers for reuse, they must generally be separated from the matrix material. Both thermoset and thermoplastic matrices can be readily digested by thermal, chemical, or thermochemical means without substantial fiber degradation. This section describes the current state of efforts to develop matrix removal processes.

Four matrix removal techniques have been used in attempts to develop recycling methods specifically for composite materials. These include catalytic conversion, reverse gasification, pyrolysis with indirect heating, and pyrolysis in fluidized beds. There are problems with each of these techniques, but refinement may make any of them technically and commercially viable.

Catalytic conversion of composite matrices is a technique that has been developed to remove matrix material at low temperatures (References 11.5.3.1(a) - (c), 11.8.3.2(a) - (d)). The process converts the matrix to a low molecular weight gas, which is removed for further processing or used as fuel. Because of the presence of a proprietary catalyst, matrix is removed at a relatively low processing temperature, on the order of 482°F (250°C), and fiber strength retention is likely to be good. Low temperatures also help to keep energy and reactor costs down, improving the chances of commercial viability. The technique has successfully decomposed epoxy matrix composites and other polymer materials, but was less effective with PEEK and PMR-15 matrices. The current implementation of this process involves a continuous

feed reactor capable of processing 5 - 10 kg/hour of scrap composite. Efforts are being made to transition the process to a pilot plant scale operation.

Reverse gasification has been applied to composite recycling by the University of Missouri at St. Louis working under a grant from the Department of Energy (References 11.2.1(b) and 11.2.2(c)). Waste composites and oxygen are fed into a reactor that operates at a high temperature to yield separated fibers and a combustible gas. The high temperatures required have the disadvantage of necessitating an expensive reactor and high energy costs, however, the method has an advantage in that it can be applied to any organic matrix material.

Fluidized bed combustion has been applied at the University of Nottingham, UK, in an effort to recover glass fibers from polyester sheet molding compound. The SMC was crushed and sized to <25 mm and fluidized by air. The fibers were subsequently recovered with a cyclone separator. The tensile strength of the fibers was found to be approximately 50% of that of the virgin fibers, and was found to be a function of bed temperature.

11.8.3.3 *Fiber reuse*

Fibers extracted from recycled composite materials represent the highest value and, therefore, the greatest potential economic driver for the process. The high cost of carbon fibers, which is not likely to go below \$5/Lb in the foreseeable future, and their limited supply, provides a high value, reliable market for recycle, a prime requisite for any successful recycling operation.

The mechanical properties of composites fabricated from recycled fibers are influenced by their strength and length distributions, and by their interfacial bonding. Degradation of fiber tensile strength by processing induced defects is a particular concern because very small surface defects can have a significant impact, and some of the potential matrix removal methods may have an effect on the fiber surface.

A potential application for recycled fibers is their combination with recycled polymers derived from other sources to produce a low cost composite material (References 11.8.3.3(a) - (b)). The fibers may help to mitigate the effects of mixed polymers, or of other contaminants by providing reinforcement.

11.8.3.4 *Products of matrix removal*

The composition of the products of matrix decomposition depends on the process used in their removal. Low temperature catalytic conversion primarily produces low molecular weight hydrocarbons in the form of a gas (References 11.2.2(a), 11.5.3.1(a) - (c), and 11.8.3.2(a) - (d)). This material may be distilled for use as a chemical feedstock or used as a fuel. The makeup of the hydrocarbons is somewhat dependent on the composition of the matrix material.

Matrix removal by reverse gasification yields a burnable gas when the process parameters are properly controlled (Reference 11.2.2(b)). This gas may be used for energy to drive the process, or compressed and stored for later use.

Matrix decomposition by fluidized bed combustion oxidizes the matrix in the bed, yielding energy and oxidation products. With sheet molding compounds (SMC) containing calcium carbonate fillers, the composite may be combusted along with coal to result in reduced emissions of sulfur oxides.

11.8.3.5 *Other recycling and processing methods*

Waste composite materials can also be recycled by grinding, or used in waste-to-energy incinerators to recover their value as an energy source. These techniques do not yield as much value from the composite as the methods that recover fibers intact, but may be appropriate for low value composites such as fiberglass and SMC.

Grinding has been used to recycle process waste SMC for a number of years (References 11.8.3.5(a) - (g)). Because glass fibers are inexpensive, it is necessary for recycled glass fibers to be recovered at very low cost for a fiber recovery-type recycling process to be economically viable for that material. Grinding is a less expensive operation than current fiber recovery methods. The products of grinding, however, have very low value because they are used as a substitute for the inorganic fillers in SMC, which are very low cost materials.

Waste-to-energy incineration is a relatively simple process that may be the most economically viable disposal technique for some kind of composite materials. Toxic emissions can be generated from some kinds of matrices, however, and so emission control scrubbers are required. It is also possible for carbon fibers to escape through exhaust flues, travel long distances, and short out electrical transmission wires. Waste-to-energy conversion is not considered to be a recycling process, although it is sometimes referred to as "quaternary recycling," but is at least preferable to landfilling if done properly.

An assessment of various techniques for processing glass fiber reinforced plastic has been made (Reference 11.8.3.5(h)) in an effort to quantitatively determine the economic viability of different techniques.

11.8.4 Recycling of waste prepreg

Prepreg materials constitute a major portion of the waste composite material generated by composite manufacturers, over 65% according to one survey. In 1995 approximately 1.9 million pounds of waste carbon fiber prepreg was generated (Reference 11.2.1(b)).

Most waste prepreg material is generated as a result of nesting inefficiency during composite lay-up. Approaches to reducing the generation of this waste are described in Section 11.5.3.1. This section describes methods that have been applied to the reuse or recycling of prepreg scraps.

The highest value can be obtained from waste prepreg by reusing it to fabricate composite components. Waste prepreg at its source contains the correct proportions of uncured matrix and virgin fibers of known composition and processing characteristics. For the additional effort of assembling the prepreg into components and curing it, composite components can be produced and waste disposal rendered unnecessary.

Matrix removal by catalytic conversion has been successfully applied to prepreg material (Reference 11.2.2(a) - (b), 11.3(b)), completely removing the matrix and yielding fibers with high residual tensile strength. The technique worked in spite of the presence of silicone-treated release layers, making their removal unnecessary. A tendency of the prepreg to jam at the system's intake was noted.

An effort to recycle waste prepreg by shredding it to produce a sheet-molding compound was investigated by McDonnell Douglas Corporation (Reference 11.2.2(a)). Other efforts to develop methods to recycle (Reference 11.8.4(a)) or reuse (Reference 11.8.4(b)) scrap prepreg are underway.

REFERENCES

- 11.2.1(a) Composite Prepreg Scrap Reclamation Program, McDonnell Douglas Corporation, MDC 95P0078, Final Report, Contract Number N00014-90-CA-0002 for Great Lakes Composites Consortium, 1995.
- 11.2.1(b) Unser, J.F., "Advanced Composites Recycling/Reuse Program," Final Report, WL-TR-95-7014, Wright Laboratory, Armament Directorate, Eglin AFB, FL, April 1995.
- 11.2.2(a) Allred, R.E., and Salas, R.M., "Chemical Recycling of Scrap Composites," Proc. AIA, SACMA, and NASA Joint Conference on Environmental, Safety, and Health Considerations, - Composite Materials in the Aerospace Industry, Phoenix, AZ, Oct. 20-21, 1994.
- 11.2.2(b) Eriksson, P.-A., Albertsson, A.-C., Boyde, P., Prautzsch, G., Manson, J.-A.E., Prediction of Mechanical Properties of Recycled Fiberglass Reinforced Polyamide 66, Polymer Composites, Vol. 17, No. 6, Dec. 1996, pp. 830-839.
- 11.2.2(c) Unser, J.F., Staley, T., and Larsen, D., "Advanced Composites Recycling," SAMPE Journal, Vol. 32, No. 5, Sept./Oct. 1996, pp. 52-57.
- 11.2.2(d) Allred, R.E., and Salas, R.M., Recycling Process for Aircraft Plastics and Composites, Final Report, Contract F08635-93-C-0109, December 1993, AT-93-5133-FR-001.
- 11.3(a) Thayer, A. "Plastics Recycling Up, but End Markets Down," Chemical & Engineering News, June 8, 1992, pp. 6.
- 11.3(b) Alexander, M., "The Challenge of Markets: The Supply of Recyclables is Larger than the Demand," EPA Journal, July/Aug. 1992, pp. 29-33.
- 11.5.3.1(a) Allred, R.E., Salas, R.M., and Gordon, B.W., "Tertiary Recycling Process for Plastics, Composites, and Electronic Materials," Proc. 40th Intl. SAMPE Symp. and Exhib., Anaheim, CA, May 8-11, 1995, pp. 1794-1805.
- 11.5.3.1(b) Allred, R.E., "Recycling Process for Scrap Composites and Prepregs," Proc. 41th Intl. SAMPE Symp. and Exhib., Anaheim, CA, March 24-28, 1996, pp. 21-31.
- 11.5.3.1(c) Allred, R.E., Coons, A.B., and Simonson, R., "Properties of Carbon Fibers Reclaimed from Composite Manufacturing Scrap by Tertiary Recycling," Proc. 28th Intl. SAMPE Tech. Conf., Seattle, WA, Nov. 4-7, 1996, pp. 139-150.
- 11.8.2.1(a) Pettersson, J. "Recycled Reinforced Plastics as Replacement for Coremat and Plywood Cores in Sandwich Laminate: A Comparison of Mechanical Properties," SPI 1996.
- 11.8.2.1(b) McDermott, J., "Fiberglass Recycling: Earning Respect," Composite Fabrication, May 1996.
- 11.8.2.1(c) "Process for Separating Fibres from Composite Materials," International Patent Application, International Publications No: WO93/05883, Phoenix Fiberglass Inc., April 1, 1993.
- 11.8.3.2(a) Allred, R.E., Doak, T.J., Coons, A.B., Newmeister, G.C., and Cochran, R.C., "Tertiary Recycling of Cured Composite Aircraft Parts," Proc. Composites '97 Manufacturing and Tooling Conf., Society of Manufacturing Engineers, Dearborn, MI 1997, pp. EM97-110 to EM97-110-17.

Volume 3, Chapter 11 - Environmental Management

- 11.8.3.2(b) Allred, R.E., and Busselle, L.D., "Economical Recycling Process for Mixtures of Electronic Scrap," Proc. 1997 IEEE Int'l Symp. On Electronics and the Environment, IEEE, Piscataway, NJ, 1997, pp. 115-120.
- 11.8.3.2(c) Allred, R.E., Doak, T.J., Gordon, B.W., Harrah, L.A., and Hoyt, A.E., "Catalytic Conversion Process for Recycling Navy Shipboard Plastic Wastes," Polymeric Materials Science and Engineering, Vol. 76, American Chemical Society, Washington, DC, 1994, pp. 578-579.
- 11.8.3.2(d) Allred, R.E., Doak, T.J., and Coons, A.B., "Recycling Process for Automotive Plastics and Composites," Proc. 12th Annual Am. Society for Composites Tech. Conf., Dearborn, MI, Oct. 6-8, 1997.
- 11.8.3.3(a) Xanthos, M., Greci, J., Patel, S.H., Jacob, C., Dey, S., and Dagli, S.S., Thermoplastic Composites from Maleic Anhydride Modified Post-Consumer Plastics, Polymer Composites, June 1995, Vol. 16, No. 3, pp. 204-214.
- 11.8.3.3(b) Kimura, T., Takeuchi, M., and Nakanishi, K., Recyclability of Waste Cord of Synthetic Fibers as Matrix Material of Thermoplastic Hybrid Composites, Proceedings of Tenth International Conference on Composite Materials (ICCM – 10), 1996, Volume IV, pp. 373-380.
- 11.8.3.5(a) Recycled SMC Now in Appearance Parts," Plastics Technology, Oct. 1993, pp. 94.
- 11.8.3.5(b) Etterson, J., and Nilsson, P., "Recycling of SMC and BMC in Standard Process Equipment," J. of Thermoplastic Composite Materials, Vol. 7, Jan. 1994.
- 11.8.3.5(c) Inoh, T, et. al., "SMC Recycling Technology," J. of Thermoplastic Composite Materials, Vol. 7, Jan. 1994.
- 11.8.3.5(d) Mapleston, P. Auto Sector's Recycling Goals Keep Plastics on Hot Seat, Modern Plastics, May 1995, pp. 48-56.
- 11.8.3.5(e) Allred, R.E., Recycling Process for Automotive Plastics and Composites, Project Title: Tertiary Recycling Process for Polymer-Based Automotive Components, SBIR Phase I Final Report, NSF Award Number DMI-9660673, 1997.
- 11.8.3.5(f) Update on Recycling Automotive Plastics, Automotive Engineering, August 1997, pp. 41-44.
- 11.8.3.5(g) Design for Recycling, Automotive Engineering, August 1997, pp. 46-48.
- 11.8.3.5(h) Fiber Reinforced Plastics: Planning for Profitable Reuse, Recycling Feasibility Final Report, for Minnesota Technology, Inc. funded by and available from Minnesota Office of Environmental Assistance, 520 Lafayette Rd. St. Paul, MN 55155, 1993.
- 11.8.4(a) Michaeli, W., and Oelgarth, A., New Technologies for Processing of Non-Cured Prepreg Waste – Preparation of High-Strength DMC, Proceedings, 41st International SAMPE Symposium, March, 1996, pp. 1551-1562.
- 11.8.4(b) Unser, J., Reuse of Scrap Prepreg, Proceedings of 42nd International SAMPE Symposium, May 4-8, 1997, pp. 216-224.

CHAPTER 12 LESSONS LEARNED

12.1 INTRODUCTION

The focus of much of what is in this handbook concentrates on establishing proper techniques for development and utilization of composite material property data. The motivation prompting specific choices is not always evident. This chapter provides a depository of knowledge gained from a number of involved contractors, agencies, and businesses for the purpose of disseminating lessons learned to potential users who might otherwise repeat past mistakes. Many of the contractors involved in developing the lessons learned are aerospace oriented. Thus, the lessons learned may have a decidedly aerospace viewpoint.

The chapter starts with a discussion of some of the characteristics of composite materials that makes them different from metals. These characteristics are the primary cause for establishing the methods and techniques contained in the handbook.

Specific lessons learned are defined in later sections. They contain the specific "rule of thumb" and the reason for its creation or the possible consequence if it is not followed. The lessons learned are organized into six different categories for convenience.

12.2 UNIQUE ISSUES FOR COMPOSITES

Composites are different from metals in several ways. These include their largely elastic response, their ability to be tailored in strength and stiffness, their damage tolerance characteristics, and their sensitivity to environmental factors. These differences force a different approach to analysis and design, processing, fabrication and assembly, quality control, testing, and certification.

12.2.1 Elastic properties

The elastic properties of a material are a measure of its stiffness. This property is necessary to determine the deformations that are produced by loads. In composites, the stiffness is dominated by the fibers; the role of the matrix is to prevent lateral deflections of the fibers and to provide a mechanism for shearing load from one fiber to another. Continuous fiber composites are transversely isotropic and in a two-dimensional stress state require four elastic properties to characterize the material:

- Modulus of elasticity parallel to the fiber, E_1
- Modulus of elasticity perpendicular to the fiber, E_2
- Shear modulus, G_{12}
- Major Poisson's ratio, ν_{12}

In general, material characterization may require additional properties not defined above. A thorough discussion of this subject is given in Section 5.3.1. Only two elastic properties are required for isotropic materials, the modulus of elasticity and Poisson's ratio.

The stress-strain response of commonly used fiber-dominated orientations of composite materials is almost linear to failure although some glasses and ceramics have nonlinear or bilinear behavior. This is contrasted to metals that exhibit nonlinear response above the proportional limit and eventual plastic deformation above the yield point. Many composites exhibit very little, if any, yielding in fiber dominated behavior. Toughened materials and thermoplastics can show considerable yielding, particularly in matrix dominated directions. This factor requires composites to be given special consideration in structural details where there are stress risers (holes, cutouts, notches, radii, tapers, etc.). These types of stress risers in metal are not a major concern for static strength analysis (they do play a big role in durability and damage tolerance analysis, however). In composites they must be considered in static strength analysis.

Volume 3, Chapter 12 - Lessons Learned

In general, if these stress risers are properly considered in design/analysis of laminated parts, fatigue loadings will not be critical.

Another unique characteristic of composite material elastic response is its orthotropy. When metals are extended in one direction, they contract in the perpendicular direction in an amount equal to the Poisson's ratio times the longitudinal strain. This is true regardless of which direction is extended. In composites, an extension in the longitudinal (1 or x) direction produces a contraction in the transverse direction (2 or y) equal to the "major" Poisson's ratio, ν_{xy} , times the longitudinal extension. If this is reversed, an extension in the transverse direction produces a much lower contraction in the longitudinal direction. In fiber dominated laminates, Poisson's ratio can vary from <0.1 to >0.5 .

The most unusual characteristic of composites is the response produced when the lay-up is unbalanced and/or unsymmetric. Such a laminate exhibits anisotropic warping characteristics. In this condition an extension in one direction can produce an in-plane shear deformation. It can also cause an out-of-plane bending or torsional response. All these effects are sometimes observed in one laminate. This type of response is generally undesirable because of warping or built-in stresses that occur. Hence, most laminate configurations are balanced and symmetric.

Classical lamination theory is used to combine the individual lamina properties to predict the linear elastic behavior of arbitrary laminates. Lamination theory requires the definition of lamina elastic properties, their orientation within the laminate, and their stacking position. The process assumes plane sections remain-plane and enforces equilibrium. Lamination theory will solve for the loads/stresses/strains for each lamina within the laminate at a given location for a given set of applied loads. This combined with appropriate failure theory will predict the strength of the laminate (empirically modified input ply properties are often necessary).

12.2.2 Tailored properties and out-of-plane loads

The properties of a composite laminate depend on the orientation of the individual plies. This provides the engineer with the ability to tailor a laminate to fit a particular requirement. For high axial loads predominantly in one direction, the laminate should have a majority of its plies oriented parallel to that loading direction. If the laminate is loaded mostly in shear, there should be a high percent of $\pm 45^\circ$ pairs. For loads in multi-directions, the laminate should be quasi-isotropic. An all 0° laminate represents the maximum strength and stiffness that can be attained in any given direction, but is impractical for most applications since the transverse properties are so weak that machining and handling can cause damage. Fiber-dominated, balanced and symmetric, laminate designs that have a minimum of 10% of the plies in each of the 0° , $+45^\circ$, -45° , and 90° directions are most commonly used.

Tailoring also means an engineer is not able to cite a strength or stiffness value for a composite laminate until he knows the laminate's ply percentages in each direction. Carpet plots of various properties vs. the percent of plies in each direction are commonly used for balanced and symmetric laminates. An example for stiffness is shown in Figure 12.2.2. Similar plots for strength can also be developed.

Out-of-plane loads can also be troublesome for composites. These loads cause interlaminar shear and tension in the laminate. Interlaminar shear stress can cause failure of the matrix or the fiber-matrix interphase region. Interlaminar shear and tensile stresses can delaminate or disbond a laminate. Such loading should be avoided if possible. Design situations that tend to create interlaminar shear loading include high out-of-plane loads (such as fuel pressure), buckling, abrupt changes in cross-section (such as stiffener terminations), ply drop-offs, and in some cases laminate ply orientations that cause unbalanced or unsymmetric lay-ups. Interlaminar stresses will arise at any free edge. Interlaminar stresses will arise between plies of dissimilar orientation wherever there is a gradient in the components of in-plane stress.

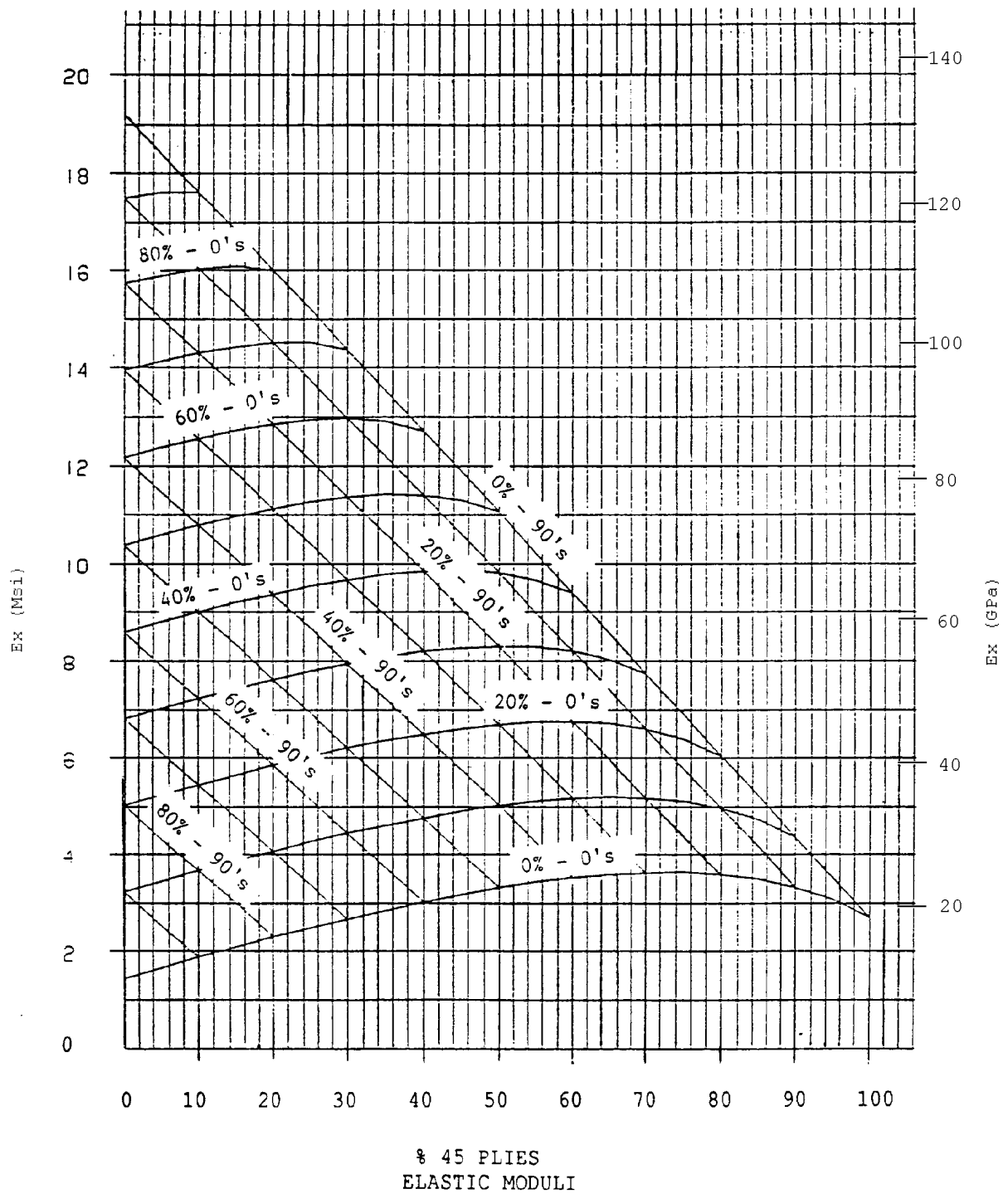


FIGURE 12.2.2 Sample carpet plot.

12.2.3 Damage tolerance

Damage tolerance is the measure of the structure's ability to sustain a level of damage or presence of a defect and be able to perform its operating functions. The concern is with the damaged structure having adequate residual strength and stiffness to continue in service safely: 1) until the damage can be detected by scheduled maintenance inspection and repaired, or 2) if the damage is undetected, for the remainder of the aircraft's life. Thus, safety is the primary goal of damage tolerance. Both static load and durability related damage tolerance must be interrogated experimentally because there are few, if any, accurate analytical methods.

There are basically two types of damage that are categorized by their occurrence during the fabrication and use of the part, i.e., damage occurring during manufacturing or damage occurring in service. It is hoped that the occurrence of the majority of manufacturing associated damage, if beyond specification limits, will be detected by routine quality inspection. Nevertheless, some "rogue" defects or damage beyond specification limits may go undetected. Consequently, their occurrence must be assumed in the design procedure and subsequent testing (static and fatigue) performed to verify the structural integrity.

Service damage concerns are similar to those for manufacturing. Types of service damage include edge and surface gouges and cuts or foreign object collision and blunt object impact damage caused by dropped tools or contact with service equipment. A level of non-detectable damage should be established and verified by test that will not endanger the normal operation of the aircraft structure for two lifetimes. A certain level (maximum allowed) damage that can be found by inspection should be defined such that the vehicle can operate for a specified number of hours before repair or replacement at loads not exceeding design limit. This damage should also be tested (statically and in fatigue) to verify the structural integrity.

Delaminations can also be critical defects. However, unless they are very large, historically more than 2 inches (50 mm) in diameter, the problem is mostly with thin laminates. Effects of manufacturing defects such as porosity and flawed fastener holes that are slightly in excess of the maximum allowable are usually less severe. They are generally accounted for by the use of design allowable properties that have been obtained by testing specimens with stress concentrations, e.g., notches. Most commonly these are specimens with a centered hole. Open holes are typically used for compression specimens while either open or filled holes (holes with an installed fastener) are used for tension testing. (Open holes are more critical than filled holes for compression. Filled holes may be more critical in tension, especially for laminates with ply orientations with a predominate number of plies in the load direction.) Consequently, the design allowables thus produced may be used to account for a nominal design stress concentration caused by an installed or missing fastener, at least to a 0.25 inch (6.4 mm) diameter, as well as accounting for many other manufacturing defects. This is sometimes called the "rogue flaw" approach to laminate design, see Reference 12.2.3.

12.2.4 Durability

Durability of a structure is its ability to maintain strength and stiffness throughout the service life of the structure. A structure must have adequate durability when subjected to the expected service loads and environment spectra to prevent excessive maintenance, repair, or modification costs over the service life. Thus, durability is primarily an economic consideration.

Metallic structure can be very sensitive to durability issues; major factors limiting life are corrosion and fatigue. Metal fatigue is dictated by the number of load cycles required to start a crack (crack initiation) and the number of load cycles for the crack to grow to its critical length, reaching catastrophic failure (crack growth). Crack/damage growth rate is very dependent on the concentration of stress around the crack.

In composites, it has been demonstrated that one of the most common damage growth mechanisms is intercracking (delamination). This makes composites most sensitive to compression-dominated fatigue loading. A second common fatigue failure mode is fastener hole wear caused by high bearing stresses.

Volume 3, Chapter 12 - Lessons Learned

In this failure mode the hole gradually elongates. The most serious damage to composite parts is low velocity impact damage which can reduce static strength, fatigue strength, or residual strength after fatigue. Again, testing is a must!

The strain level of composites in most actual vehicle applications to date has been held to relatively low values. Composites under in-plane loads have relatively flat stress-life (S-N) curves with high fatigue thresholds (endurance limits). These two factors combined have resulted in insensitivity to fatigue for most load cases. However, the greater variability found with composites requires an engineer to still characterize the composite's fatigue life to failure to correctly characterize its fatigue scatter.

12.2.5 Environmental sensitivity

When a composite with a polymeric matrix is placed in a wet environment, the matrix will absorb moisture. The moisture absorption of most fibers used in practice is negligible; however, aramid fibers (e.g., Kevlar) absorb significant amounts of moisture when exposed to high humidity. The absorption of moisture at the interface of glass/quartz fibers is a well-known degrading phenomena.

When a composite has been exposed to moisture and sufficient time has elapsed, the moisture concentration throughout the matrix will be uniform. A typical equilibrium moisture content for severe humidity exposure of common epoxy composites is 1.1 to 1.3 percent weight gain. The principal strength degrading effect is related to a change in the glass transition temperature of the matrix material. As moisture is absorbed, the temperature at which the matrix changes from a glassy state to a viscous state decreases. Thus, the strength properties decrease with increasing moisture content. Current data indicate this process is reversible. When the moisture content is decreased, the glass transition temperature increases and the original strength properties return. With glass/quartz fibers there is additional degradation at the interface with the matrix. For aramid fibers there is additional degradation at the interface with the matrix and, also, in the fibers.

The same considerations also apply for a temperature rise. The matrix, and therefore the lamina, loses strength and stiffness when the temperature rises. This effect is primarily important for the matrix-dominated properties. Temperature rise also worsens the fiber/matrix interface degradation for glass/quartz fibers and aramid fibers. The aramid fiber properties are also degraded by a rise in temperature.

The approach for design purposes is to assume a worst case. If the material is assumed to be fully saturated and at the maximum temperature, material allowables can be derived for this extreme. This is a conservative approach, since typical service environments do not generate full saturation for most complex structures. Once the diffusivity of a composite material is known, the moisture content and through the thickness distribution can be accurately predicted by Fickian equations. This depends on an accurate characterization of the temperature-humidity service environment.

Thermal expansion characteristics of common composites, like carbon/epoxy, are quite different from metals. In the (0 or 1) longitudinal direction, the thermal expansion coefficient of carbon/epoxy is almost zero. Transverse to the fiber (90 or 2 direction), the thermal expansion is the same magnitude as aluminum. This property gives composites the ability to provide a dimensionally stable structure throughout a wide range of temperatures.

Another feature of composites that is related to environment is resistance to corrosion. Polymer matrix composites (with the exception of some carbon/bismaleimides) are immune to salt water and most chemical substances as far as corrosion sensitivity. One precaution in this regard is galvanic corrosion. Carbon fiber is cathodic (noble); aluminum and steel are anodic (least noble). Thus carbon in contact with aluminum or steel promotes galvanic action which results in corrosion of the metal. Corrosion barriers (such as fiberglass and sealants) are placed at interfaces between composites and metals to prevent metal corrosion. Another precaution regards the use of paint strippers around most polymers. Chemical paint strippers are very powerful and attack the matrix of composites very destructively. Thus, chemical paint stripping is forbidden on composite structure.

Other environmental effects worth noting include the effect of long term exposure to radiation. Ultra-violet rays from the sun can degrade epoxy resins. This is easily protected by a surface finish such as a coat of paint. Another factor is erosion or pitting caused by high speed impact with rain or dust particles. This is likely to occur on unprotected leading edges. There are surface finishes such as rain erosion coats and paints for preventing surface wear. Lightning strike is also a concern to composites. A direct strike can cause considerable damage to a laminate. Lightning strike protection in the form of conductive surfaces is applied in susceptible areas. In cases where substructure is also composite, the inside end of attachment bolts may need to be connected with each other and to ground by a conducting wire.

12.2.6 Joints

12.2.6.1 Mechanically-fastened joints

Successful joint design relies on knowledge of potential failure modes. Failure modes depend on joint geometry and laminate lay-up for one given material. The type of fastener used can also influence the occurrence of a particular failure mode. Different materials will give different failure modes.

Net-section tensile/compressive failures occur when the bolt diameter is a sufficiently large fraction of the strip width. For most successful designs, this fraction (D/W) is about one-quarter or more for near-isotropic lay-ups in carbon/epoxy systems that have a D/E of one-third or less.

Shear-out and shear-out delamination failures occur because the bolt is too close to the edge of the laminate. Such a failure can be triggered when there is only a partial net-section tension or bearing failure. D/t ratios should be 0.75 to 1.25.

In some instances the bolt head may be pulled through the laminate after the bolt is bent and deformed. This mode is frequently seen with countersunk fasteners and is highly dependent on the particular fastener used.

Bearing strength is a function of joint geometry, fastener and member stiffnesses. For a $0/\pm 45/90$ family of laminates with 20-40% of 0° plies and 40-60% of $\pm 45^\circ$ plies, plus a minimum (10%) of 90° plies, the bearing strength is relatively constant. Fastener characteristics such as clamp-up force and head configuration have a significant effect. However, for a specific laminate family, a specific fastener, and equal thickness laminate joining members, the parameter with the greatest influence is D/t .

Composite joints require smaller D/W and D/E ratios than do metals to get bearing failures.

Composite joint strength characteristics differ from metals because the strength is influenced by the bypass load going around the joint. This occurs when two or more fasteners are arranged in a line to transfer the load through a joint. Since not all of the load is reacted by one fastener, some of the load by-passes it. The by-pass effects become prominent once the ratio of by-pass to fastener bearing load exceeds 20%.

Titanium fasteners are the most common means of mechanical attachment in composites. This is because titanium is non-corrosive in the galvanic atmosphere created by the dissimilar materials. Titanium is closer to carbon on the cathodic scale.

12.2.6.2 Problems associated with adhesive bonding to peel-ply composite surfaces

There are two schools of thought in regard to the adhesive bonding of fibrous composite laminates. One demands light but thorough mechanical abrasion, such as by low-pressure grit blasting, because the only such bonds never to fail prematurely were made to abraded surfaces on completely dry laminates. The other permits bonding directly to surfaces created by stripping off peel plies, with or without a drying requirement, using the justification that there is "adequate" initial strength, even though some of these joints have failed prematurely in service. It is also significant that no ultrasonic inspection technique has

Volume 3, Chapter 12 - Lessons Learned

been able to distinguish between bonded joints which will fail in service and those which will not. In addition, most traveler specimens do not represent the same cure conditions as experienced by adjacent large parts and, therefore, mechanical testing also often fails to identify defective bonding. One must depend on process control of techniques which can be relied upon 100 percent of the time and on thorough validation of the processes before committing them to production.

Consider a surface, created by stripping off a peel ply, which is then bonded as part of an adhesive joint. The resulting adhesive bond "sticks" well enough to pass all inspections; however, may fail prematurely at the interface between the laminate and the adhesive. All premature bond failures, other than those caused by incomplete cure, occur at the interface between the adhesive and the resin in the laminate. Structurally sound bonds either fail outside the joint area, cohesively within the layer of adhesive, or interlaminarly in the resin matrix between the surface fibers and the adhesive layer. These premature failures can occur either when uncured adhesive is bonded to precured laminates, or when uncured prepreg is cured against cured adhesive films used to stabilize honeycomb cores and the like.

There are several ways in which peel plies can create surfaces on which reliable durable bonds are not possible.

- The peel ply can be coated with a release agent, which transfers to the cured laminate when the peel ply is stripped off.
- The surface of the peel ply's fibers must be sufficiently inert that the ply can be removed without damaging the laminate. The grooves left in the laminate (or glue layer) by stripping off the peel ply may retain enough inert surface that the resin which is subsequently cured onto it may simply fail to adhere. Adhesion requires more than cleanliness; surface tension is also critical. In the absence of cohesion at the interface, a bonded joint relies only on mechanical interlocking, which is far weaker in peel than it is in shear.
- The peel-ply surface in the laminate consists of innumerable short grooves separated by sharp edges where the resin between the filaments in the peel ply fractured as the peel ply was stripped off. Moisture on (or in) the adhesive or the laminate can be trapped in these grooves. If this moisture cannot escape during the curing of the adhesive (or of a co-cured face sheet), the trapped moisture will result in a slick bond when examined microscopically after failure.

It should be noted that the latter two mechanisms function without any contamination.

One aircraft company's process specification has, for decades, required that any peel-ply surface to be bonded must first be thoroughly abraded to remove all traces of the texture of the peel ply. In the absence of the ridges between the grooves, it is presumed that moisture could escape, as it turned to steam during cure, unless the part was too large and too poorly ventilated. Using these requirements, this aircraft company has had no disbonds in those secondarily bonded composite structures which were grit blasted before bonding. The same cannot be claimed for bonds made to unabraded (or only scuff-sanded) peel-ply surfaces. In two instances, on different aircraft types, disbonds were traced to transfer of release agents from silicone-coated peel plies, the use of which is now banned throughout all documents, not only the approved materials lists.

On another aircraft type, interfacial failures on peel-ply surfaces appear to be the result of prebond moisture, the exact origin of which has yet to be established. An accident with one test panel during process qualification by a supplier revealed the consequences of condensate on adhesive film (the roll of adhesive had not been properly sealed when returned to the freezer after the previous use). There was absolutely no adhesion between the resin and the adhesive, even though the lap-shear numbers seemed to be acceptable. Microscopic examination of the surfaces clearly showed perfect imprints of the peel ply texture on both surfaces, with the surface in all grooves as smooth as glass and all of the resin on one surface and all of the adhesive on the other. However, with thicker-than-normal (0.123 inch (3.2 mm)) adherends of the same unidirectional carbon/epoxy, bonds made with the same nonreleased peel ply and the same kind of adhesive achieved cohesive failure of the bond at the same strength level attained by

metal-to-metal bonding (6,000 psi (40 MPa) or so). With normal thickness composite adherends, only half this strength was reached, because the resin between the surface fibers and adhesive layer then failed in peel, leaving resin clearly covering both surfaces. This problem can be minimized by maintaining very tight time limits between making parts and bonding them together, with a requirement to thoroughly dry everything before bonding if the time constraints are exceeded. Careful scheduling can avoid this added drying step. The same high-strength cohesive bond failures had previously been achieved by another supplier of composite structures using grit-blasted surfaces and 0.080 inch (2.0 mm) thick unidirectional laminates.

In considering adhesive bond strength, it is vital to note that the specimen testing *validates the process, NOT the part*. There is no requirement for the specimen to look like the actual part. Indeed, in a properly designed bonded joint, the bond will not fail first. Consequently, the use of specimens which are "similar" to the part and which are evaluated in terms of the "adequacy" of the load carried in relation to the stresses in the part, is not sufficient to ensure the integrity of the bonded composite structure. This issue is complicated because, only with unidirectional tape laminates is it possible to develop sufficient load to fail a high-strength adhesive bond cohesively. Therefore, only such specimens can provide any assurance that the part they are intended to substantiate has been bonded properly. However, in real parts made from woven-fabric laminates, failures within bundles of fibers at 90° to the applied load will trigger interlaminar failures before such bond strengths can be attained.

In all cases, the one condition which can be detected visually on test specimens and failed parts alike which is a guaranteed indicator of a defective bond is an interfacial failure with all of the resin on one side and all of the adhesive on the other, with a clear imprint of the peel ply texture on both surfaces.

12.2.7 Design

The design of composite structure is complicated by the fact that every ply must be defined. Drawings or design packages must describe the ply orientation, its position within the stack, and its boundaries. This is straightforward for a simple, constant thickness laminate. For complex parts with tapered thicknesses and ply build-ups around joints and cutouts, this can become extremely complex. The need to maintain relative balance and symmetry throughout the structure increases the difficulty.

Composites can not be designed without concurrence. Design details depend on tooling and processing as does assembly and inspection. Parts and processes are so interdependent it could be disastrous to attempt sequential design and manufacturing phasing.

Another factor approached differently in composite design is the accommodation of thickness tolerances at interfaces. If a composite part must fit into a space between two other parts or between a substructure and an outer mold line, the thickness requires special tolerances. The composite part thickness is controlled by the number of plies and the per-ply-thickness. Each ply has a range of possible thicknesses. When these are laid up to form the laminate they may not match the space available for assembly within other constraints. This discrepancy can be handled by using shims or by adding "sacrificial" plies to the laminate (for subsequent machining to a closer tolerance than is possible with nominal per-ply-thickness variations). The use of shims has design implications regarding load eccentricities. Another approach is to use closed die molding at the fit-up edges to mold to exact thickness needed.

The anisotropy of special laminates, while more complicated, enables a designer to tailor a structure for desired deflection characteristics. This has been applied to some extent for aeroelastic tailoring of wing skins.

Composites are most efficient when used in large, relatively uninterrupted structures. The cost is also related to the number of detail parts and the number of fasteners required. These two factors drive designs towards integration of features into large cocured structures. The nature of composites enables this possibility. Well designed, high quality tooling will reduce manufacturing and inspection cost and rejection rate and result in high quality parts.

12.2.8 Handling and storage

Epoxy resins are the most common form of matrix material used in composites. Epoxies are perishable. They must be stored below freezing temperature and even then have limited shelf life. Once the material is brought out of storage there is limited time it can be used to make parts (30 days is common). For very complex parts with many plies, the material's permissible out-time can be a controlling factor. If the material is not completely used, it may be returned to storage. An out-time record should be kept. In addition, freezer storage of these materials is usually limited by the vendor to 6 to 12 months. Overage material will produce laminates with a high level of porosity.

The perishability of the material also requires that it be shipped refrigerated from the supplier. Upon arrival at the contractor's facility, there must be provisions to prevent it being left on-dock for long periods of time.

Tack is another composite material characteristic that is unique. Tack is "stickiness" of the prepreg. It is both an aid and a hindrance. Tack is helpful to maintain location of a ply once it is placed in position. It also makes it difficult to adjust the location once the ply has been placed.

12.2.9 Processing and fabrication

Composite parts are fabricated by successive placement of plies one after the other. Parts are built-up rather than machined down. Many metal fabrication steps require successive removal of material starting from large ingots, plates, or forgings. Prepreg "tape" material typically comes in rolls of relatively thin strips (0.005-0.015 inches or 0.13 - 0.38 mm). These strips are a variety of widths: 3", 6", and 36". Prepreg "fabric" is usually thicker than tape (0.007-0.020 inches or 0.18 - 0.51 mm) and usually comes in 36-inch (0.9 m) wide rolls.

Fabrication of a detail part requires the material to be taken out of the freezer in a sealed bag and allowed to come to room temperature prior to any operations. Placement of the prepreg on the tool (if not automated) requires care. The plies must be aligned properly to the desired angle and stacked in the prescribed sequence. Prepreg plies come with a backing material to keep them from sticking together on the rolls. This backing material must be removed to prevent contamination of the laminate. Care must be exercised when handling the material to prevent splinters from piercing the hands.

Part lay-up (particularly when done by hand) can lead to air entrapment between plies. This creates difficulty when the part is cured because the air may not escape, causing porosity. Thus, thick parts are normally pre-compacted using a vacuum periodically during the lay-up.

Some prepreg materials contain an excess of resin. This excess is expected to be "bled" away during cure. Bleeder plies are placed under the vacuum bag to soak up the excess resin. However, most current prepreg materials are "net resin" so no bleeding is required.

Composite processing requires careful attention to tool design. The tools must sustain high pressures under elevated temperature conditions. The composite material has different expansion characteristics than most tooling materials, thus thermal stresses are created in the part and in the tool. Tool surfaces are treated with a release agent to facilitate removal of the part after cure. Tools must also be pressure tight because autoclave processing requires application of a vacuum on the laminate as well as positive autoclave pressure. Lastly, tool design must account for the rate of manufacture and the number of parts to be processed.

Prepreg material is not fully cured. Curing requires application of heat and pressure that is usually performed in the autoclave. Autoclaves typically apply 85 psi (590 kPa) pressure up to 350°F (180°C). They can go beyond these values if required for other materials (such as polyimides), but they must be qualified for higher extremes. Autoclave size may limit the size of a part to be designed and manufactured. Very large autoclaves are available, but they are expensive and costly to run. Common problems

Volume 3, Chapter 12 - Lessons Learned

that occur in autoclave operations include blown vacuum bags, improper heat-up rates, and loss of pressure.

Once the part is cured it may still require drilling, trimming and machining. Drilling of composites requires very sharp bits, careful feed and speed, and support of the back face to prevent splintering. Water-jet cutters are very useful for trimming. Machining produces a fine dust that requires protection for the operator's safety.

12.2.9.1 Quality control

The quality control function for composite materials starts at a much earlier phase than for metals. There is much coordination and interaction occurring between the material supplier and the user before the material is ever shipped. These controls are defined by the material and process specifications and in some cases design allowables requirements. The supplier is often required to perform chemical and mechanical tests on the material prior to shipment. These involve the individual material constituents, the prepreg, and cured laminates.

Material processing and handling must be monitored throughout the various manufacturing phases. Receiving inspections are performed on the prepreg and cured laminates when the material first comes in. From this time on the material is tracked to account for its shelf life and out-time.

Quality control activities include verification of the ply lay-up angle, its position in the stack, the number of plies, and the proper trim. During lay-up it is necessary to ensure all potential contaminants and foreign materials are not allowed to invade the material.

The curing process is monitored to ensure proper conformance to time-temperature-pressure profiles. These records are maintained for complete traceability of the parts.

After the part is cured, there are a number of methods to verify its adequacy. One of the most common is Through-Transmission-Ultrasonics (TTU). Parts with high porosity or delaminations can not transmit sound as well as unflawed parts. Thus ultrasound transmission is attenuated in a flawed part. Other techniques used to verify part quality include traveler specimens, specimens cut from excess material on the part, tracer yarns within the laminate, and in some cases proof loading. Visual inspections, thickness measurements, and tap testing also serve to interrogate composite parts.

One of the most crucial aspects of quality control is information on the effect of defects. It is not enough to discover a flaw or suspected non-conformity. There must also be sufficient information to evaluate the impact of that rejection. The quality control function in its entirety includes the dispositioning of exposed non-conformances. Dispositioning includes acceptance as-is, repair or rework, and scrap-page. If proper dispositioning is not possible because of a lack of knowledge about the effect of defects, an inordinate expense will be incurred scrapping or reworking affected parts.

12.3 LESSONS LEARNED

12.3.1 Design and analysis

<u>LESSON</u>	<u>REASON OR CONSEQUENCE</u>
A-1."Concurrent Engineering", whereby a new product or system is developed jointly and concurrently by a team composed of designers, stress analysts, materials and processes, manufacturing, quality control, and support engineers, (reliability, maintainability, survivability), as well as cost estimators, has become the accepted design approach.	To improve the quality and performance and reduce the development and production costs of complex systems
A-2.In general, design large cocured assemblies. Large assemblies must include consideration for handling and repair.	Lower cost due to reduced part count and assembly time. If the assembly requires overly complex tooling, the potential cost savings can be negated.
A-3.Structural designs and the associated tooling should be able to accommodate design changes associated with the inevitable increases in design loads.	To avoid scab-on reinforcements and similar last minute disruptions.
A-4.Not all parts are suited to composite construction. Material selection should be based on a thorough analysis that includes consideration of performance, cost, schedule, and risk.	The type of material greatly influences performance characteristics as well as producibility factors.
A-5.Uniwoven and bi-directional woven fabric should be used only when justified by trade studies (reduced fabrication costs). If justified, woven fabric may be used for 45° or 0°/90° plies.	Fabric has reduced strength and stiffness properties and the prepreg material costs more than tape. Fabric may be necessary for complex shapes and some applications may require the use of fabric for its drapability.
A-6.Whenever possible, mating surfaces should be tool surfaces to help maintain dimensional control. If this is not possible, either liquid shims or, if the gap is large, a combination of precured and liquid shims should be used.	To avoid excessive out-of-plane loads that can be imposed if adjoining surfaces are forced into place. Large gaps may require testing.
A-7.Part thickness tolerance varies directly with part thickness; thick parts require larger tolerance.	Thickness tolerance is a function of the number of plies and the associated per-ply-thickness variation.
A-8.Carbon fibers must be isolated from aluminum or steel by using an adhesive layer and/or a thin glass-fiber ply at faying surfaces.	Galvanic interaction between carbon and aluminum or steel will cause corrosion of the metal.

Volume 3, Chapter 12 - Lessons Learned

- | | |
|---|---|
| A-9. The inspectability of structures, both during production and in-service, must be considered in the design. Large defects or damage sizes must be assumed to exist when designing composite structures if reliable inspection procedures are not available. | There is a much better chance that problems will be found if a structure is easily inspected. |
| A-10. In Finite Element Analysis (FEA) a fine mesh must be used in regions of high stress gradients, such as around cut-outs and at ply and stiffener drop-offs. | Improper definition or management of the stresses around discontinuities can cause premature failures. |
| A-11. Eliminate or reduce stress risers whenever possible. | Composite (fiber-dominated) laminates are generally linear to failure. The material will not yield locally and redistribute stresses. Thus, stress risers reduce the static strength of the laminate. |
| A-12. Avoid or minimize conditions which cause peel stresses such as excessive abrupt laminate terminations or cocured structures with significantly different flexural stiffnesses (i.e., $EI_1 \gg EI_2$). | Peel stresses are out-of-plane to the laminate and hence, in its weakest direction. |
| A-13. Buckling or wrinkling is permissible in thin composite laminates provided all other potential failure modes are properly accounted for. In general, avoid instability in thick laminates. | Significant weight savings are possible with postbuckled design. |
| A-14. Locating 90° and $\pm 45^\circ$ plies toward the exterior surfaces improves the buckling allowables in many cases. Locate 45° plies toward the exterior surface of the laminate where local buckling is critical. | Increases the load carrying capability of the structure. |
| A-15. When adding plies, maintain balance and symmetry. Add between continuous plies in the same direction. Exterior surface plies should be continuous. | Minimizes warping and interlaminar shear. Develops strength of plies. Continuous surface plies minimize damage to edge of ply and help to prevent delamination. |
| A-16. Never terminate plies in fastener patterns. | Reduces profiling requirements on substructure. Prevents delamination caused by hold drilling. Improves bearing strength. |
| A-17. Stacking order of plies should be balanced and symmetrical about the laminate midplane. Any unavoidable unsymmetric or unbalanced plies should be placed near the laminate midplane. | Prevents warpage after cure. Reduces residual stresses. Eliminates "coupling" stresses. |

Volume 3, Chapter 12 - Lessons Learned

- | | |
|--|--|
| A-18. Use fiber dominated laminate wherever possible. The $[0^\circ/\pm 45^\circ/90^\circ]$ orientation is recommended for major load carrying structures. A minimum of 10% of the fibers should be oriented in each direction. | Fibers carry the load; the resin is relatively weak. This will minimize matrix and stiffness degradation. |
| A-19. When there are multiple load conditions, do not optimize the laminate for only the most severe load case. | Optimizing for a single load case can produce excessive resin or matrix stresses for the other load cases. |
| A-20. If the structure is mechanically fastened, an excess of 40% of the fibers oriented in any one direction is inadvisable. | Bearing strength of laminate is adversely affected. |
| A-21. Whenever possible maintain a dispersed stacking sequence and avoid grouping similar plies. If plies must be grouped, avoid grouping more than 4 plies of the same orientation together. | Increases strength and minimizes the tendency to delaminate. Creates a more homogeneous laminate. Minimizes interlaminar stresses. Minimizes matrix microcracking during and after service. |
| A-22. If possible, avoid grouping 90° plies. Separate 90° plies by a 0° or $\pm 45^\circ$ plies where 0° is direction of critical load. | Minimizes interlaminar shear and normal stresses. Minimizes multiple transverse fracture. Minimizes grouping of matrix critical plies. |
| A-23. Two conflicting requirements are involved in the pairing or separating of $\pm\theta^\circ$ plies (such as $\pm 45^\circ$) in a laminate. Laminate architecture should minimize interlaminar shear between plies and reduce bending/twisting coupling. | Separating $\pm\theta^\circ$ plies reduces interlaminar shear stresses between plies. Grouping $\pm\theta^\circ$ plies together in the laminate reduces bending/twisting coupling. |
| A-24. Locate at least one pair of $\pm 45^\circ$ plies at each laminate surface. A single ply of fabric will suffice. | Minimizes splintering when drilling. Protects basic load carrying plies. |
| A-25. Avoid abrupt ply terminations. Try not to exceed dropping more than 2 plies per increment. The plies that are dropped should not be adjacent to each other in the laminate. | Ply drops create stress concentrations and load path eccentricities. Thickness transitions can cause wrinkling of fibers and possible delaminations under load. Dropping non-adjacent plies minimizes the joggle of other plies. |
| A-26. Ply drop-offs should not exceed 0.010 inch (0.25mm) thick per drop with a minimum spacing of 0.20 inch (0.51 mm) in the major load direction. If possible, ply drop-offs should be symmetric about the laminate midplane with the shortest length ply nearest the exterior faces of the laminate. Shop tolerance for drop-offs should be 0.04 inch (1 mm). | Minimizes load introduction into the ply drop-off creating interlaminar shear stresses. Promotes a smooth contour. Minimizes stress concentration. |

Volume 3, Chapter 12 - Lessons Learned

- | | |
|--|---|
| A-27. Skin ply drop-offs should not occur across the width of spars, rib, or frame flange. | Provides a better load path and fit-up between parts. |
| A-28. In areas of load introduction there should be equal numbers of $+45^\circ$ and -45° plies on each side of the mid-plane. | Balanced and symmetric pairs of $\pm 45^\circ$ plies are strongest for in-plane shear loads which are common at load introduction points. |
| A-29. A continuous ply should not be butt-spliced transverse to the load direction. | Introduces a weak spot in the load path. |
| A-30. A continuous ply may be butt-spliced parallel to the load direction if coincident splices are separated by at least four plies of any orientation. | Eliminates the possibility of a weak spot where plies are butted together. |
| A-31. The butt joint of plies of the same orientation separated by less than four plies of any direction must be staggered by at least 0.6 inch (15 mm). | Minimizes the weak spot where plies are butted together. |
| A-32. Overlaps of plies are not permitted. Gaps should not exceed 0.08 inch (2 mm). | Plies will bridge a gap, but must joggle over an overlap. |

12.3.1.1 Sandwich design

- | | |
|---|--|
| B-1. Facesheets should be designed to minimize people induced damage during handling or maintenance of component. | Thin skin honeycomb structure is very susceptible to damage by harsh handling. |
| B-2. When possible avoid laminate buildup on the core side of the laminate. | Minimizes machining of the core. |
| B-3. Core edge chamfers should not exceed 20° (from the horizontal plane). Larger angles may require core stabilization. Flex core is more sensitive than rigid core. | Prevents core collapse during cure cycle. |
| B-4. Use only non-metallic or corrosion resistant metal honeycomb core in composite sandwich assemblies. | Prevents core corrosion |
| B-5. Choice of honeycomb core density should satisfy strength requirements for resisting the curing temperature and pressure during bonding or cocuring involving the core. 3.1 PCF (50 g/m^3) is a minimum for non-walking surfaces. | Prevents crushing of the core. |

Volume 3, Chapter 12 - Lessons Learned

B-6. For sandwich structure used as a walking surface, a core density of 6.1 PCF (98 g/m³) is recommended.

3.1 PCF (50 g/m³) core density will result in heel damage to the walking surface.

B-7. Do not use honeycomb core cell size greater than 3/16 inch (4.8 mm) for cocuring sandwich assemblies (1/8 inch (3.2 mm) cell size preferred).

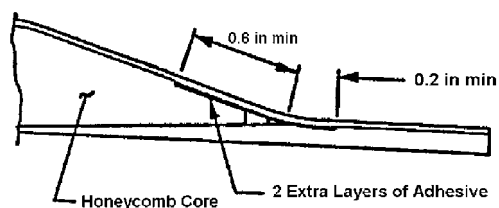
Prevents dimpling of face sheets.

B-8. When core is required to be filled around bolt holes, etc., this should be done using an approved filler to a minimum of 2D from the bolt center.

Prevents core crushing and possible laminate damage when bolt is installed.

B-9. Two extra layers of adhesive should be applied to the inner moldline at the core run out (edge chamfer). This should be applied a minimum of 0.6 in. (15 mm) from the intersection of the inner skin and edge band up the ramp and a minimum of 0.2 in. (5 mm) from that point into the edge band.

Curing pressures tend to cause the inner skin to "bridge" in this area creating a void in the adhesive (skin to core bond).



B-10. The use of honeycomb sandwich construction must be carefully evaluated in terms of its intended use, environment, inspectability, repairability, and customer acceptance.

Thin skin honeycomb is susceptible to impact damage, water intrusion due to freeze/thaw cycles, and is difficult to repair.

12.3.1.2 Bolted joints

C-1. Design the joints first and fill in the basic structure afterwards.

Optimizing the "basic" structure first compromises the joint design and results in low overall structural efficiency.

C-2. Joint analysis should include the effects of shimming to the limits permitted by drawings.

Shimming can reduce joint strength.

C-3. Design joints to accommodate the next larger fastener size.

To accommodate routine MRB and repair activities.

C-4. Bolted joint strength varies far less with percentage of 0° plies in fiber pattern than does unnotched laminate strength.

The stress concentration factor, K_t , is highly dependent on 0° plies.

C-5. Optimum single-row joints have approximately three-fourths of the strength of optimum four-row joints.

Optimum single-row joints operate at higher bearing stress than the most critical row in an optimized multi-row joint.

Volume 3, Chapter 12 - Lessons Learned

- | | |
|---|---|
| C-6. Common errors in composite bolted joints are to use too few bolts, space them too far apart, and to use too small a diameter. | Does not maximize the strength of the laminate. |
| C-7. Rated shear strength of fasteners does not usually control the joint design. | Bolt diameter is usually governed by the need not to exceed the allowable bearing stress in the laminate. |
| C-8. The peak hoop tensile stress around bolt holes is roughly equal to the average bearing stress. | Keeping the laminate tensile strength high requires keeping the bearing stress low. |
| C-9. Maximum torque values should be controlled, particularly with large diameter fasteners. | Avoids crushing the composite. |
| C-10. Bolt bending is much more significant in composites than for metals. | Composites tend to be thicker (for a given load) and more sensitive to non-uniform bearing stresses (because of brittle failure modes). |
| C-11. Optimum w/d ratio for multi-row bolted joints varies along length of joint. w/d = 5 at first row to minimize load transfer, w/d = 3 at last row to maximize transfer, w/d = 4 for intermediate bolts. | Maximizes joint strength. |
| C-12. Stainless steel fasteners in contact with carbon should be permanent and installed wet with sealant. | Prevents galvanic corrosion. |
| C-13. Use a layer of fiberglass or Kevlar (0.005 inch (0.13 mm) minimum) or adhesive with serim on faying surfaces of carbon epoxy panels to aluminum. | Prevents corrosion of aluminum. |
| C-14. Bolt stresses need careful analysis, particularly for the effects of permissible manufacturing parameters, for example, hole perpendicularity ($\pm 10^\circ$), shimming, loose holes. | Bolt failures are increasingly becoming the "weak link" with current high strength composite materials. |
| C-15. Bolted joint data bases should include the full range of all permitted design features. | Establishes that failure modes remain consistent and that there are no detrimental interaction effects between design parameters. |
| C-16. The design data base should be sufficient to validate all analysis methods over the entire range permitted in design. | For proper verification of analytical accuracy. |

Volume 3, Chapter 12 - Lessons Learned

- | | |
|--|---|
| C-17. Mechanical joint data bases should contain information pertaining to durability issues such as clamp-up, wear at interfaces, and hole elongation. Manufacturing permitted anomalies such as hole quality, edge finish, and fiber breakout also need to be evaluated. | Practical occurrences can affect strength and durability. |
| C-18. Use drilling procedures that prevent fiber break out on the back side of the component. | Improper back side support or drilling procedures can damage surface plies on the back side. |
| C-19. Splice plate stresses should be lower than the stresses in skins to prevent delaminations. | Splice plates see less clamp up than the skin sandwiched in between, because of bolt bending. |
| C-20. The best bolted joints can barely exceed half the strength of unnotched laminates. | The strength reduction is caused by stress concentrations around the hole for the fastener. |
| C-21. Laminate percentages for efficient load transfer: $0^\circ = 30\text{-}50\%$; $\pm 45^\circ = 40\text{-}60\%$; $90^\circ = \text{minimum of } 10\%$. | Best range for bearing and by-pass strength. |
| C-22. Countersink depths should not exceed 70% of laminate thickness. | Deep countersinks result in degraded bearing properties and increased hole wear. |
| C-23. Fastener edge distance and pitch: Use 3.0D edge distance in direction of major load; use $2.5D + 0.06$ side distance. (D is diameter of fastener.) | Maximizes joint strength. |
| C-24. Gap between attached parts should not exceed 0.03 inch (0.8 mm) for non-structural shim. | Large gaps cause excessive bolt bending, non-uniform bearing stresses, and eccentric load path. |
| C-25. Any gap in excess of 0.005 inch should be shimmed. | Minimizes interlaminar stresses due to clamp-up. |
| C-26. Use "form-in-place" gaskets on carbon/epoxy doors over anodized aluminum substructure. Allow for a seal thickness of 0.010 ± 0.005 inch (-0.25 ± 0.13 mm) minimum. | Prevents corrosion of aluminum. |
| C-27. Use only titanium, A286, PH13-8 MO, monel or PH17-4 stainless steel fastener with carbon/epoxy. | Prevents galvanic corrosion. |
| C-28. Do not buck rivets in composite structure. | The bucking force can damage the laminate. |

Volume 3, Chapter 12 - Lessons Learned

- | | |
|---|---|
| C-29. The use of interference fit fasteners should be checked before permitting their use in design. | Installation of interference-fit fasteners can damage laminates if a loose-fit sleeve is not installed first. |
| C-30. Fastener-to-hole size tolerance for primary structure joints must be assessed and controlled. | Tight fitting fastener promotes uniform bearing stress in a single fastener hole, and promotes proper load sharing in a multi-fastener joint. |
| C-31. Squeeze rivets can be used if washer is provided on tail side. | Washer helps protect the hole. |
| C-32. For blind attachments to composite substructure, use fastener with large blind side footprint of titanium or A286. | Prevents damage to composite substructure by locking collars of fasteners. |
| C-33. Tension head fasteners are preferred for most applications. Shear head fasteners may be used in special applications only with stress approval. | Shear head fasteners. |
| C-34. Avoid putting fastener threads in bearing against the laminate. | Fastener threads can gouge and damage the laminate. |
| C-35. Tapered splice plates should be used to tailor the load transfer, row by row, to minimize the bearing stress at the most critical row. | Multi-row bolted joints between uniformly thick members will have high peak bearing loads in outermost rows of fasteners. |

12.3.1.3 Bonded joints

- | | |
|---|--|
| D-1. Use secondary adhesive bonding extensively for thin, lightly loaded, composite structures, restricting the use of mechanical fastening to thicker, more heavily loaded structures. | Reduces cost. Reduces the number of holes in composite components. Reduces weight by eliminating build-ups for fastener countersinking and bearing strength. |
| D-2. Never design for an adhesive bond to be the weak link in a structure. The bonds should always be stronger than the members being joined. | Maximizes the strength of the structure. The bond could act as a weak-link fuse and unzip catastrophically from a local defect. |
| D-3. Thick bonded structures need complex stepped-lap joints to develop adequate efficiency. | Large loads require many steps to transfer the load and assure that adhesive develops the strength of the adherends. |
| D-4. Anticipate bolted repairs for thick structures by reducing strain levels. | Thick structures are impractical to repair by bonding, except for one-shot and throwaway structures. |

Volume 3, Chapter 12 - Lessons Learned

- | | |
|---|--|
| D-5. When there is no need for repair, as in missiles and unmanned aircraft, bonding permits extremely high structural efficiencies to be obtained, even on thick structures. | Load transfer is performed without drilling holes for fasteners. |
| D-6. Proper surface preparation is a "must" - beware of "cleaning" solvents and peel plies. Mechanical abrasion is more reliable. | Maintaining joint strength in service is very dependent on the condition of the surfaces to be bonded. |
| D-7. Laminates must be dried before performing bonded repairs. | Heat applied to the laminates during repair can cause any moisture present to vaporize and cause blisters. |
| D-8. Adherend overlaps must not go below specified minimums. | Key to durability of bonded joints is that some of the adhesive must be lightly stressed to resist creep. |
| D-9. Bonded overlaps are usually sized to survive hot/wet environmental conditions. | Elevated temperature and moisture degrade the strength and stiffness of the adhesive. |
| D-10. Bonded joint strength can also be degraded by cold environment where adhesive is brittle. | The brittleness of the adhesive limits joint strength. |
| D-11. Taper ends of bonded overlaps down to 0.020 inch (0.51 mm) thick with a 1-in-10 slope. | Minimizes induced peel stresses that would cause premature failures. |
| D-12. Adhesives work best in shear, are poor in peel, but composites are even weaker in interlaminar tension. | Joint must be designed to minimize out-of-plane stresses. |
| D-13. Design of simple, uniformly thick (for near quasi-isotropic carbon/epoxy) bonded splices is very simple. Use 30 t overlap in double shear, 80 t overlap for single-lap joints, 1-in-50 slope for scarf joint. | Provides a bonded joint with good strength capability. |
| D-14. Design of stepped-lap joints for thick structure needs a nonlinear analysis program. | Complex stress states in stepped-lap joints. Nonlinear adhesive characteristics. |
| D-15. Adhesives are well characterized by thick-adherend test specimen, generating complete nonlinear shear stress-strain curve. | This test provides ample data for analysis of joints critical in shear. |
| D-16. For highly loaded bonded joints a co-cured, multiple step, double sided lap is preferred. | Very efficient joint design. |

Volume 3, Chapter 12 - Lessons Learned

D-17. Never design a bonded joint such that the adhesive is primarily loaded in either peel or cleavage.	Adhesive peel strength is very poor and unpredictable.
D-18. Ductile adhesives are preferred over brittle ones.	Ductile adhesives are more forgiving.
D-19. Film adhesives are preferred over paste adhesives for large area bonds.	Provides more uniform bond line, easier to contain when heated.
D-20. Balanced adherend stiffnesses improve joint strength.	Reduces peel stresses.
D-21. Minimize joint eccentricities.	Reduces peel stresses.
D-22. Use adherends of similar coefficients of thermal expansion.	Reduces residual stresses.
D-23. Insure the bonded joint configuration is 100% visually inspectable.	Improves reliability and confidence. Need to emphasize process control.

12.3.1.4 Composite to metal splice joints

E-1. Bonding composites to titanium is preferred; steel is acceptable; aluminum is not recommended.	Minimizes differences in thermal expansion coefficient.
E-2. Bonded step joints preferred over scarf joints.	Better fit, higher strength.
E-3. Where possible, 45° plies (primary load direction) should be placed adjacent to the bondline; 0° plies are also acceptable. 90° plies should never be placed adjacent to the bondline unless it is also the primary load direction.	Minimizes the distance between the bondline and the plies that carry the load. Prevents failure of surface ply by "rolling log" mechanism.
E-4. For a stepped joint, the metal thickness at the end step should be 0.030 inch (0.76 mm) minimum and the step no longer than 0.375 in (9.5 mm).	Prevents metal failure of end step.
E-5. If possible, have $\pm 45^\circ$ plies end on first and last step of bonded step joint.	Reduces peak interlaminar shear stresses at end steps.
E-6. If possible, do not end more than two 0° plies (not more than 0.014 inch (0.36 mm) maximum thickness) on any one step surface. For 0° plies ending on last step (longest 0° ply) serrated edges have been shown to reduce stress concentration.	Reduces stress concentration at end of joint.

Volume 3, Chapter 12 - Lessons Learned

- | | |
|---|---|
| E-7. or 90° plies should butt up against the first step of a step joint. | Reduces magnitude of interruption in load path. |
| E-8. Tension and peel stresses should be avoided in adhesive bonded joints. | Minimum strength direction of adhesive. |

12.3.1.5 Composite to metal continuous joints

- | | |
|---|---|
| F-1. Bonding composites to titanium preferred, steel is acceptable. | Minimizes differences in thermal expansion coefficient. |
| F-2. No composite to aluminum structural adhesive bond except for corrosion resistant aluminum honeycomb core and lightly loaded secondary structure. | Minimizes interlaminar shear stress due to large difference in thermal expansion coefficient between composites and aluminum. |

12.3.1.6 Composite to composite splice joints

- | | |
|---|---|
| G-1. Scarfed joints are never preferred over stepped joints, except for repairs of thin structures. | Improves strength of joint. |
| G-2. Cocured joints are preferred over pre-cured joints if there are fit-up problems. | Less sensitive to tolerance mismatches. |
| G-3. For pre-cured parts, machined scarfs are preferred over layed up scarfs. | For improved fit. |
| G-4. Use of cocured bonded subassemblies should be evaluated in terms of supportability. | Reduces ply count and assembly time, but increases rework cost. |
| G-5. Bonded repairs are not acceptable for thick laminates. | Taper ratio requirement makes bonded repair impractical. |

12.3.2 Materials and processes**LESSON****REASON OR CONSEQUENCE**

- | | |
|---|---|
| H-1. Materials selection forms the foundation for structural and manufacturing development and supportability procedures. | The material selected influences critical issues, how parts are fabricated, inspected, and assembled, and how much previous data/learning is available. |
| H-2. Material selection must be based on a thorough analysis and occur early in the process. | Various materials have various advantages. Specific applications should use materials that best fit the needs of the application. |

Volume 3, Chapter 12 - Lessons Learned

H-3. Imide-based polymer composites should consider galvanic degradation.	Some of these materials have exhibited galvanic corrosion in the presence of salt water.
H-4. Net-resin prepregs improve quality at reduced cost.	Minimizes (eliminates) bleeding of prepreg during cure.
H-5. Composite material applications must have a margin between the wet T_g and the use temperature (usually 50°F).	To prevent the material from operating in an environment where its properties become greatly decreased and widely scattered.
H-6. Specific issues impacting materials selection/use: Fluid/solvent degradation High residual thermal stresses Mechanical performance Out-time/tack time Effects of defects Sensitivity to processing variations OSHA/EPA requirements Cost (Procurement, Manufacturing, Quality) Environmental degradation Cocure compatibility with other composites and adhesives.	Ignoring key material features could result in an inferior product.

12.3.3 Fabrication and assembly

<u>LESSON</u>	<u>REASON OR CONSEQUENCE</u>
I-1. Highly integral cocured structures are weight and cost effective, however, they place a high burden on tooling design.	Integrally cured structure eliminates parts and fasteners. The tools to perform the fabrication are complex and greatly influence the quality of the part.
I-2. Machining/drilling must be rigorously controlled; this includes feeds, speeds, lubrication, and tool replacement.	Backside breakout is a major nonconformance on all programs. Composite to metal drilling must avoid chip scoring. Highly directionally stacked laminates tend to gouge during drilling in the stacked areas.
I-3. Waterjet trimming of cured laminates has been shown to be highly successful.	Produces a clean, smooth edge very rapidly.
I-4. Sanding/trimming must consider out-of-plane damage. Tool rotation must be in the same plane as the laminate.	These operations tend to produce forces in the weakest direction of the laminate.

Volume 3, Chapter 12 - Lessons Learned

- | | |
|--|---|
| I-5. Waterjet prepreg cutting can fray prepreg edges. Frequent nozzle replacement may be necessary. | Produces acceptable cuts. |
| I-6. Lay-up shop temperature/humidity directly impacts handleability. | Tack and drapeability are influenced by temperature and moisture in the prepreg. |
| I-7. Unauthorized hand creams can lead to extensive porosity and contamination. The use of gloves can prevent this risk. | Some hand creams contain ingredients that are contaminants. |
| I-8. Irons and hot air guns used for ply locating and compaction must be calibrated. | Avoids ply damage due to overheating. |
| I-9. FOD control in the lay-up shop is absolutely necessary. | Can lead to foreign materials in the laminate. |
| I-10. Hand drills can cause significant damage. | Feed and speed are less precise. Hole perpendicularity may be imperfect. |
| I-11. Ply placement tolerances must be able to meet design requirements. | Strength/stiffness analysis is based on assumptions regarding angle of the plies and their location. |
| I-12. Assembly jigs must provide the dimensional rigidity necessary to meet assembly tolerances. | Composites are less tolerant of pull-up stresses imposed by poor fit. |
| I-13. Engineering drawings and specifications should be supplemented by fully illustrated planning documents or handbooks. | Drawings and specifications tend to be highly complex and detailed. They are not easy to follow on the factory floor. |
| I-14. Consider two-step curing process in bonding and cocuring operations. | Alleviates problems such as core slippage and crushing, skin movement, and ply wrinkling. |
| I-15. Fastener grip lengths should take into account actual thicknesses (including shims) at the fastener location. | A fastener with excessive grip length may not provide proper clamp-up. Too short a grip length may put threads in bearing or result in an improperly formed head. |
| I-16. Tolerance requirements have a big impact on selecting manufacturing and tooling processes and therefore cost. | Different processes produce varying tolerance control. |
| I-17. If possible, the mating surfaces should be tool surfaces. | Maintains the best possible dimensional control. |

Volume 3, Chapter 12 - Lessons Learned

- | | |
|---|--|
| I-18. The use of molded rubber and trapped rubber tools has had mixed success. Rubber can be used successfully in local areas as a pressure intensifier, such as inside radii on stiffeners of cocured structure. | Rubber tools are difficult to remove, tend to become entrapped. They do not wear well. |
| I-19. Analyses can be done to predict distortion or "spring back" of a part after it is removed from a tool. The problem is usually solved by trial and error methods through tool modifications. The "spring back" problem is generally more pronounced on metal tools than on CFRP tools. | Residual or curing stresses build up in composite laminates formed to various shapes. When the structure is removed from the tool, the residual stresses tend to relieve themselves causing "spring back". |
| I-20. Tool design, including tool material selection, must be an integral part of the overall design process. | Tool design is dependent on part size and configuration, production rate and quantity, and company experience. |
| I-21. Aluminum tools have been used successfully on small parts but are avoided on large parts and female molds. | Thermal expansion mismatch. |
| I-22. Invar is often used for production tooling. | Invar has good durability and low thermal expansion. |
| I-23. Electroformed nickel also produces a durable, high quality tool, but is less frequently used. | More expensive. |
| I-24. Steel or Invar tools are needed for curing high temperature resins such as polyimides and bismaleimides. | The thermal mismatch with other materials is magnified at the higher cure temperature of these resins. |
| I-25. Air bubbles in a silicone rubber tool will cause "bumps" in the cured laminate. | The tool fails to provide support for the laminate and apply uniform pressure. |
| I-26. Resin containment is essential to part thickness control. | Uncontained resin will cause resin rich and resin starved areas. |

12.3.4 Quality control**LESSON****REASON OR CONSEQUENCE**

- | | |
|--|--|
| J-1. Continuing process control and process monitoring are required during production. | Assures that neither the process nor the material is changing. |
|--|--|

Volume 3, Chapter 12 - Lessons Learned

- | | |
|---|--|
| J-2. Ultrasonic C-Scan is the most commonly used NDI technique. It may be supplemented by other techniques such as X-ray, shearography, and thermography. | Useful for detecting porosity, disbonds and delaminations. |
| J-3. Determine and understand the effect of defects on part performance. | Minimizes the cost of MRB activity. |
| J-4. There is no substitute for destructive, tear-down inspections of complex parts under development. | Not all discrepancies can be detected by NDI methods. |

12.3.5 Testing**LESSON****REASON OR CONSEQUENCE**

- | | |
|---|--|
| K-1. The testing of joints and demonstration of damage tolerance should include sufficient detail to adequately evaluate structural details and size effects. | Small details and size effects can have a large influence on the response of composite structure. In general, damage tolerance of composites exhibits size effects. Bolted and bonded joints, if properly designed, do not. |
| K-2. A well planned test program must include an accelerated approach for taking into account the effects of moisture, temperature, impact damage, etc. | Including moisture and elevated temperature on a real-time basis for full-scale testing is impractical for most components. |
| K-3. A finite element analysis should be performed prior to conducting a full-scale test. The analysis must accurately simulate the test article and the boundary conditions of the test fixture and loads applied during the test. | For a more accurate assessment of the internal loads and failure prediction of the test article. |
| K-4. Traceability of test specimens to batch, constituent material lots, autoclave run, panel, position in panel, and technicians is essential to data analysis. | If full traceability is not maintained and documented, the cause of outlier data points or unexpected failure modes may be difficult to identify. The result is that "bad" data, which might legitimately be discarded for cause, might be retained and add undesired variability to the data set. |
| K-5. Adequate instrumentation is essential for all design/development or concept validation testing. Placement of strain gages, LVDT's, etc., should be based on analysis. | A good understanding of local failure modes and correlation of test results with analysis will aid the design process. |

Volume 3, Chapter 12 - Lessons Learned

12.3.6 Certification**LESSON**

- L-1. The "building block" approach is an excellent method for developing and validating the details of the design.
- L-2. Component qualification is complicated by the fact that critical design conditions include hot, wet environments. This is often accomplished by overloading a test article that is in ambient conditions, or by analysis of failure modes coupled with strain measurements related back to subcomponent hot, wet tests.

REASON OR CONSEQUENCE

A wide variety of issues and details can be evaluated cost effectively. Hardware serves a dual purpose - engineering and manufacturing.

It is generally impractical to try to ingest moisture in full scale test articles and test them hot.

12.3.7 In-service and repair**LESSON**

- M-1. In spite of concerns about the sensitivity of composites to damage, experience in service has been good. Navy aircraft have not experienced any delamination failures in service. Most damage has occurred during assembly or routine service performed on the aircraft.
- M-2. Composite components located in the vicinity of engine exhaust are subject to thermal damage. At present there are no acceptable NDI methods for detecting thermal damage of matrix materials.
- M-3. Moisture ingestion is the biggest problem with honeycomb sandwich structure. The thin, stabilized skins that make honeycomb structurally efficient are also the reason they are damage prone. Panels get walked on and damaged.
- M-4. Aircraft are commonly painted and repainted. Paint stripping has been done with solvents. Solvents can damage epoxy matrices.

REASON OR CONSEQUENCE

Current design, fabrication, and certification procedures adequately prepare the structure to survive its intended environment.

Composite components exposed to engine exhaust or other heat sources should be shielded or insulated to keep temperatures down to an acceptable level.

Honeycomb design must be applied judiciously. Repair must account for the possibility of water in the core.

Increased use of water-based paints and solvent-less stripping of paint is desirable.

Volume 3, Chapter 12 - Lessons Learned

M-5. Records pertaining to MRB actions and in plant repairs of composite parts should be readily available to personnel responsible for in-service maintenance.

During routine maintenance checks, depot personnel sometimes find defects or discrepancies. In some cases they have been able to determine that the "defect" was in the part at delivery and considered acceptable.

M-6. Supportability and repair must be responsive to service environment.

It is necessary to account for equipment, facilities, and personnel capabilities.

REFERENCES

- 12.2.3 Grimes, G.C., "Tape Composite Material Allowables Application in Airframe Design/Analysis," *Composites Engineering*, Vol. 3, Nos. 7-8, pp. 777-804, 1993.

This page intentionally left blank

Volume 3, Index

Index

Abbreviations	Ch 1-2, 4, 8
Acronyms	Ch 1-10
Adherends	Ch 6-7, 18
Adhesive bonding	Ch 2-40, 50, 52, 64
Allowable	Ch 4-6, 16, 30
Alumina	Ch 2-8, 17, 18
Aramid	Ch 2-6, 7, 8, 12, 17, 26, 27, 29, 33, 34, 38, 50
Aramid fiber	Ch 2-10, 17, Ch 12-5
Autoclave cure	Ch 2-53
Bagging	Ch 8-44
Barely visible impact damage (BVID)	Ch 7-3, 8, 16
Bearing... Ch 7-1, 49, 50, 51, 53, 54, 56, 57, 58, 59, 60, 61, 62, 63, Ch 12-6, 12, 13, 15, 16, 17, 18, 23, 24	
Bearing/bypass	Ch 7-51, 58
Bending	Ch 6-22, 27, 30, 31, 34, 35, 36, 37, 38, 42, 50, 52, 53, 55, 56, 60, 61, 64, 66, 68, 70, 76, 78, 86, 88, 89, 93, 94
Beam	Ch 5-35
Bismaleimide	Ch 2-31
Bonding	Ch 2-7, 27, 35, 40, 49, 50, 51, 52, 64, 66
Boron	Ch 2-10, 15, 17
Boron fiber	Ch 2-15, 17, Ch 5-9
Boron/epoxy	Ch 5-10, 16
Braiding	Ch 1-15, 16, 18, 21, 24, Ch 2-9, 14, 47, 48
Buckling	Ch 6-1, 15, 17, 18, 31, 61, 63, 68, 70, 71, 72, 73, 74, 75, 76, 77, 78, 79, 86, 88, 89, 92, 93, 94, 114, 116
Stacking sequence effects	Ch 6-76
Building block approach	Ch 4-1, 3, 4, 29, 34, Ch 7-25
Carbon fiber	Ch 2-2, 6
Carbon/epoxy	Ch 5-11, 12, 32, 33, 35, 36, 39, 54, 56, 79, 81, 82, 85, 88, 89, Ch 6-5, 29, 30, 31, 35, 46
Carpet plot	Ch 5-55, Ch 12-2, 3
Certification	Ch 1-1
Characteristic damage state	Ch 7-65, 68, 69
Cobonding	Ch 2-51
Commercial Aircraft Composite Repair Committee (CACRC)	Ch 8-16
Composite cylinder assemblage (CCA)	Ch 5-4, 13
Compression after impact	Ch 6-68
Computer programs	Ch 5-86, 94
Coupon	Ch 4-35, 48, 49
Creep	Ch 6-1, 7, 8, 9, 55, 69
Crippling	Ch 6-70, 71, 72, 78, 79, 80, 83, 84, 86, 87, 88, 89, 90, 91, 92, 93
Damage	Ch 7-14, 20, 46, 49, 50, 52, 54, 56, 58, 60, 61, 62, 63, 69, 70, 71, 99, 121, 122, 135, Ch 8-35, 48
Damage resistance	Ch 7-71
Damage tolerance	Ch 7-52, 54, 58, 69, 70, 71, 84, Ch 8-1, 2, Ch 9-3, Ch 12-1, 4, 25
Defects	Ch 7-2, 3, 8, 16
Definitions	Ch 1-13, 35
Delamination	Ch 5-55, 58, 59, 60, 61, 62, 63, 66, 70, 71, 79, 92, 28, 36, 60, 114, Ch 12-4, 6, 12, 26

Volume 3, Index

Design	Ch 5-1 , 42, 43, 46, 48, 49, 50, 55, 60, 66, 68, 69, 71, 76, 78, 79, 88, 92, 94, Ch 6-1 , 2, 3, 5, 7, 8, 9, 10, 11, 16, 31, 39, 42, 45, 49, 50, 51, 59, 60, 61, 64, 64, Ch 7-1 , 2, 3, 4, 5, 6, 7, 8, Ch 8-1 , 2, 5, 6, 7, 8, 9, 11, 16, 21, 23, 29, Ch 12-1 , 2, 4, 5, 6, 8, 9, 10, 11, 12, 14, 15, 16, 18, 19, 20, 22, 23, 24, 25, 26
Design for repair	Ch 8-2
Design of experiments (DOE)	Ch 3-11
Design value	Ch 4-26
Destructive tests	Ch 3-6 , 7
Doublers	Ch 8-53
Durability	Ch 5-1 , 69, Ch 6-1 , 31, Ch 8-1 , 4, 17, 19, 24
Edge effects	Ch 5-56 , 61, 67
Effective elastic moduli	Ch 5-4
Effective elastic relations	Ch 5-3
Elastic properties	Ch 5-3 , 4, 6, 7, 9, 10, 12, 22, 32, 34, 35, 54, Ch 12-1 , 2
Engineering and manufacturing development (EMD)	Ch 4-15
Environment	Ch 6-61 , 63
Environmental effects	Ch 6-2 , 6
Epoxy	Ch 2-6 , 7, 9, 14, 17, 19, 20, 24, 25, 30, 31, 32, 33, 35, 51, 52, 55, 66, Ch 5-9 , 10, 11, 12, 16, 26, 32, 33, 35, 36, 39, 42, 46, 54, 56, 65, 79, 81, 83 88, 89, 98, Ch 12-5 , 6, 7, 9, 16, 17, 19, 26
Fabrication	Ch 12-1 , 4, 9, 11, 22, 67
Fabrics	Ch 2-6 , 8, 9, 11, 14, 21, 23, 27, 31, 32, 36, 37, 38, 39, 55
Factor-of-safety	Ch 9-2
Failure	
Lamina	Ch 5-21
Laminate	Ch 5-56 , Ch 10-1
Failure criteria	Ch 5-1 , 17, 18, 20, 21, 50, 51, 52, 55, 60, 64, 48, 59, 60, Ch 10-1 , 6, 19
Failure modes	Ch 5-17 , 18, 20, 61, 63, Ch 6-8 , 53, 59, 60, Ch 10-1
Fasteners	Ch 6-7 , 49, 50, 51, 60, 61, 63, Ch 12-4 , 6, 12, 15, 17, 18, 23
Fatigue	Ch 5-1 , 13, 50, 55, 70, 88, Ch 6-10 , 59, 60, 61, 62, 63, 64 Ch 9-2
Federal Aviation Administration (FAA)	Ch 4-28 , Ch 7-10
Federal Aviation Regulations (FAR)	Ch 4-29
Fiber failure	Ch 5-14 , 19, 52, 53, 61, 63, 64
Fiber placement	Ch 2-36 , 38, 40, 42
Finite element method	Ch 6-46 , 54, Ch 7-92
First ply failure	Ch 5-50 , 52
Fracture	Ch 7-84 , 86
Tensile	Ch 7-85 , 87
Generalized self consistent scheme (GSCS)	Ch 5-5
Glass	Ch 2-1 , 6, 7, 8, 9, 10, 11, 12, 13, 14, 19, 21, 26, 29, 31, 33, 34, 36, 38, 50, 58, 60
Glass fiber	Ch 5-9 , 16
Glass/epoxy	Ch 5-10 , 16
Graphite fiber	Ch 2-3
Homogeneity	Ch 5-2 , 34
Inspection	Ch 3-1 , 2, 4, 5, 6, 7, 8, 29, Ch 8-14 , 21, 22, 24, 26, 51, 52
Interlaminar stresses	Ch 5-49 , 55, 59, 66, 67, 88
Joint flexibility	Ch 6-50

Volume 3, Index

Joints.....	Ch 12-6, 8, 15, 16, 17, 18, 19, 20, 21, 25
Bolted	Ch 6-2, 49, 51, 61, 62
Bonded	Ch 6-2, 5, 7, 10, 11, 16, 31
Kevlar TM	Ch 2-6
Knitted fabrics	Ch 2-38
Lamina properties	Ch 5-1, 2, 21, 35, 40
Stress-strain relations	Ch 5-21
Laminate properties	Ch 5-31, 65, 71
Bending	Ch 5-34
Laminate stacking sequence	Ch 5-35, 42, 59, 60, 61, 68, 69, 76, 53, 82
Lamination theory	Ch 5-27, 29, 30, 35, 36, 44, 47, 50, 61, 77, Ch 12-2
Limit load.....	Ch 5-17, Ch 7-14, 18, Ch 9-1
Linearity	Ch 5-2
Load enhancement factor (LEF)	Ch 7-55, 56
Load sharing	Ch 6-49, 51
Loading mode	Ch 6-61, 62
Mechanically fastened joints	Ch 6-1, 2, 51, 60
Membrane stresses	Ch 5-31
Micromechanics	Ch 5-1, 2
Moisture conductivity	Ch 5-41
Moisture diffusion	Ch 5-12, 41, 42
Moisture diffusivity	Ch 5-13
Moisture expansion.....	Ch 5-40, 43, 63, 66
Netting analysis.....	Ch 5-45, 46, 49, 53
Nondestructive inspection (NDI)	Ch 3-5, Ch 8-21
Nonlinear stress analysis.....	Ch 5-49
Orthotropy	Ch 5-2
Out-of-plane loads	Ch 12-2, 11
PEEK	Ch 2-33
Peel stresses	Ch 6-2, 3, 5, 6, 9, 10, 17, 19, 20, 21, 22, 23, 26, 27, 28, 31, 34, 35, 36, 37, 39
PEKK	Ch 2-33
Phenolic	Ch 2-9, 30, 31, 35
Polyacrylonitrile (PAN)	Ch 2-4
Polyamide	Ch 2-6
Polyamideimide.....	Ch 2-34, 35
Polyarylate	Ch 2-34
Polyarylketone	Ch 2-33
Polyester	Ch 2-9, 30, 31, 32, 38, 51, 55
Polyether sulfone	Ch 2-34
Polyetherimide	Ch 2-34, 51
Polyethylene	Ch 2-26, 27, 32
Polyimide	Ch 2-19, 20, 26, 32
Polyphenylene sulfide	Ch 2-33, 34
Polyphenylene sulfide sulfone	Ch 2-34
Polyphenylsulfone.....	Ch 2-34
Polypropylene	Ch 2-33
Polystyrene	Ch 2-34
Polysulfone	Ch 2-34
Postbuckling.....	Ch 5-71, 79, 82, 86, 87, 88
Pressure vessels.....	Ch 5-46

Volume 3, Index

Probabilistic methods.....	Ch 9-5, 7
Process verification.....	Ch 3-2
Processing	Ch 10-1, 2, 4, Ch 12-1, 8, 9, 10, 22
Pull-thru strength.....	Ch 6-61
Quality assurance	Ch 3-2, 7
Quality control	Ch 12-1, 10, 11, 24
Quartz	Ch 2-21, 22, 23, 24, 25, 26, 33
Receiving	Ch 3-1, 2
Reliability.....	Ch 9-1, 2, 3, 4, 5, 6, 8
Repair.....	Ch 8-1, 7, 11, 15, 20, 27, 32, 33, Ch 12-4, 10, 11, 15, 16, 18, 21, 26
Analyses	Ch 8-37
Repair design.....	Ch 8-29, 34
Residual strength	Ch 6-61, 63
Residual stresses.....	Ch 5-2, 43, 52, 54, 63, 65, Ch 10-1
Resin	Ch 2-29, 60
Viscosity	Ch 2-60
Resin pressure.....	Ch 2-62
Resin transfer molding	Ch 2-30, 31, 55, 56
Response surface methodology (RSM).....	Ch 3-11
Rovings	Ch 2-6, 7, 8, 9, 13, 14, 21, 31, 36, 38, 39
Sandwich	Ch 8-20, Ch 12-14, 15, 26
Sandwich construction	Ch 2-40, 49, 60
Sandwich structure	Ch 8-42, 47, 50
Satin weave	Ch 2-36
Sequential ply failure	Ch 5-50
Shear-out	Ch 6-53, 59, Ch 12-6
Silicon carbide.....	Ch 2-19, 20
Silicone	Ch 2-9, 36
Specifications	Ch 3-1, 2, 4, 5
Stacking sequence.....	Ch 5-30, 31, 34, 35, 36, 37, 42, 43, 50, 55, 56, 58, 63, 64, 68, 71, 76, 79, 89, 93, 94
Stacking sequence effects	Ch 5-31, 37, 43, 56, 58, 68, 76, 79, 89, 94
Beam bending	Ch 5-35
Buckling.....	Ch 5-76
Delamination	Ch 5-60
Free edge effects.....	Ch 5-67
Hygroscopic analysis.....	Ch 5-42
Lamination theory.....	Ch 5-30
Notched strength.....	Ch 5-58
Thermal analysis	Ch 5-42
Vibration	Ch 5-94
Statistical process control (SPC)	Ch 3-8, 9
Strength.....	Ch 9-1, 2, 3, 5, 6, 7, 8
Compressive	Ch 5-16
Lamina.....	Ch 5-21
Laminate.....	Ch 5-56
Tensile	Ch 5-14
Stress concentration	Ch 6-1, 2, 3, 5, 7, 37, 49, 53, 54, 55
Stress concentrations	Ch 5-14, 52, 56
Stress-strain relations	Ch 5-21, Ch 12-1
Supportability	Ch 8-1, 7, 8, 9
Symbols	Ch 1-2, 4, 7, 8, Ch 5-72
Symmetric laminates.....	Ch 5-1, 27, 31, 34, 39, 42, 44, 45, 50

Tack.....	Ch 12-9, 22, 23
Terminology.....	Ch 1-13, 19
Test methods	
Thick-section	Ch 10-6
Testing.....	Ch 12-1, 4, 5, 7, 8, 10, 11, 25
Thermal conduction	Ch 5-12, 42
Thermal conductivity	Ch 5-3
Thermal expansion	Ch 5-2, 3, 9, 10, 11, 12, 38, 39, 40, 41, 45, 46, 54, 64, Ch 12-5
Thermoforming.....	Ch 2-33, 35, 59
Thermoplastic	Ch 2-6, 7, 8, 27, 32, 33, 34, 35, 36, 40, 52, 53, 59, 61
Amorphous	Ch 2-15, 32, 33, 34, 35, 52, 53
Condensation cure	Ch 2-32, 35
Semi-crystalline	Ch 2-32, 33, 34, 35
Thickness.....	Ch 6-2, 3, 4, 5, 8, 9, 10, 11, 12, 15, 17, 19, 20, 23, 26, 27, 28, 35, 36, 37, 39, 40, 41, 43, 44, 45, 49, 59, 61, 63
Thickness effects	Ch 5-65, 66
Thick-section	
Property prediction	Ch 10-21
Thick-section composites	Ch 10-1, 2, 6, 16, 23, 29
Three-dimensional analysis	Ch 10-2, 3, 29
Transverse tensile properties.....	Ch 5-67
UHMWPE.....	Ch 2-27, 29
Ultimate load	Ch 4-6, Ch 7-11, Ch 8-12, 18, 30, Ch 9-1
Unidirectional	Ch 5-7, 9, 17, 32, 33, 34, 36, 38, 39, 47, 66
Units	Ch 7-2, 12, 21, 26, 27, 32, 35
Conversion	Ch 1-12
Unsymmetric laminates	Ch 5-31, 41, 43, 50, 70
Vacuum assisted resin transfer molding	Ch 2-57
Vacuum bag molding	Ch 2-52
Vibration	Ch 5-1, 94, 95
Viscoelastic properties	Ch 5-3, 7, 9
X-ray inspection	Ch 8-6

This page intentionally left blank

CONCLUDING MATERIAL

Custodians:

Army - MR

Navy - AS

Air Force - 11

Preparing activity:

Army - MR

(Project CMPS-0173)

Review activities:

Army - AR, AT, AV, MI

Navy - SH

Air Force - 13

DLA-IS

STANDARDIZATION DOCUMENT IMPROVEMENT PROPOSAL

INSTRUCTIONS

1. The preparing activity must complete blocks 1, 2, 3, and 8. In block 1, both the document number and revision letter must be given.
2. The submitter of this form must complete blocks 4, 5, 6, and 7.

2. The preparing activity must provide a reply within 30 days from receipt of the form.

NOTE: This form may not be used to request copies of documents, nor to request waivers, or clarification of requirements on current contracts. Comments submitted on this form do not constitute or imply authorization to waive any portion of the referenced document(s) or to amend contractual requirements.

I RECOMMEND A CHANGE:

1. DOCUMENT NUMBER
MIL-HDBK-17-3F

2. DOCUMENT DATE (YYYYMMDD)
20020617

3. DOCUMENT TITLE

COMPOSITE MATERIALS HANDBOOK - VOLUME 3, Polymer Matrix Composites, Materials Usage, Design, and Analysis

4. NATURE OF CHANGE *(Identify paragraph number and include proposed rewrite, if possible. Attach extra sheets as needed)*

5. REASON FOR RECOMMENDATION

6. SUBMITTER

a. NAME (Last, First, Middle Initial)

b. ORGANIZATION

c. ADDRESS (Include Zip Code)

d. TELEPHONE (Include Area Code)
(1) Commercial
(2) DSN (If applicable)

7. DATE SUBMITTED
(YYYYMMDD)

8. PREPARING ACTIVITY

a. NAME

US Army Research Laboratory
Weapons & Materials Research Directorate

b. TELEPHONE (Including Area Code)

(1) Commercial (2) DSN
(410) 306-0725 458-0725

C. ADDRESS (Include Zip Code)

ARL/WMRD
ATTN: AMSRL-WM-MA
Aberdeen Proving Ground, MD 21005-5069

IF YOU DO NOT RECEIVE A REPLY WITHIN 45 DAYS, CONTACT:
Defense Standardization Program Office (DLSC-LM)
8725 John J. Kingman Road, Suite 2533, Fort Belvoir, VA 22060-6221
Telephone (703) 767-6888 DSN 427-6888